dc_840_14

MTA Doktori Pályázat
Rövid Értekezés

Az autofágia szerepe és szabályozása

Juhász Gábor

Eötvös Loránd Tudományegyetem

Budapest

2014/2015

TARTALOMJEGYZÉK

1 CÍMOLDAL

2 TARTALOMJEGYZÉK

3 RÖVIDÍTÉSJEGYZÉK

5 BEVEZETÉS

19 CÉLKITŰZÉSEK

20 ANYAGOK ÉS MÓDSZEREK

26 EREDMÉNYEK

42 DISZKUSSZIÓ

48 ÖSSZEFOGLALÁS

51 TOVÁBBI TERVEK ÉS EREDMÉNYEK

52 KÖSZÖNETNYILVÁNÍTÁS

53 IRODALOMJEGYZÉK

63 KÖZLEMÉNY ADATOK

RÖVIDÍTÉSJEGYZÉK

4E-BP	Eukaryotic Initiation Factor 4E-Binding Protein
AIM	Atg8 interacting motif
Atg	autophagy-related
CMA	chaperone-mediált autofágia
DFCP1	Double FYVE-containing protein 1
eIF2α	Eukaryotic Initiation Factor 2α
ER	endoplazmás retikulum
ESCRT	endosomal sorting complex required for transport
FIP200	FAK family kinase-interacting protein of 200 kDa
FKBP39	FK506-binding protein of 39 kDa
FOXO	Forkhead box O
FYVE	Fab1, YOTB, Vac1 and EEA1
Gadd34	growth arrest and DNA damage-inducible protein
GFP	green fluorescent protein
HOPS	homotypic vacuole fusion and protein sorting
HORMA	Hop1p, Rev7p and MAD2
Hsc70	heat shock cognate 70 kDa
JNK	c-Jun N-terminal kinase
Keap1	Kelch-like ECH-associated protein 1
KIR	Keap1 interacting region
LAMP-2A	lysosome-associated membrane protein 2A
LC3	light chain 3
LIR	LC3 interacting region
MTORC1	mechanistic target of rapamycin complex 1
Nrf2	Nuclear factor erythroid-derived 2-like 2
PAS	phagophore assembly site/pre-autophagosomal structure
PB1	Phox and Bem1
PE	foszfatidil-etanolamin
PERK	protein kinase RNA-like endoplasmic reticulum kinase
PI3K	foszfatidilinozitol 3-kináz
PI3P	foszfatidilinozitol 3-foszfát
QT-PCR	quantitative/real time polymerase chain reaction
Ref(2)P	Refractory to sigma P, más néven p62
RT-PCR	Reverse transcription polymerase chain reaction
S6K	S6 kinase
SENDA	Static encephalopathy of childhood with neurodegeneration in adulthood
SLC38A9	Solute Carrier Family 38, Member 9
SNAP-29	Synaptosomal-associated protein 29
SNARE	soluble NSF attachment protein receptor
SQSTM-1	sequestosome-1
Syx17	Syntaxin 17

TOR	Target of Rapamycin
TSC1/2	Tuberous Sclerosis Complex 1/2
UBA	ubiquitin-associated
ULK1/2	uncoordinated 51-like kinase
usnp	ubisnap, más néven SNAP-29
v-ATPáz	vacuolar-type H+ -ATPase
Vamp7	Vesicle-associated membrane protein 7
Vps	vacuolar protein sorting
WDR45	WD-repeat domain 45, más néven WIPI-4
WIPI4	WD Repeat Domain Phosphoinositide-Interacting Protein 4, más néven WDR45

BEVEZETÉS

Autofág lebontás az eukarióta sejtekben

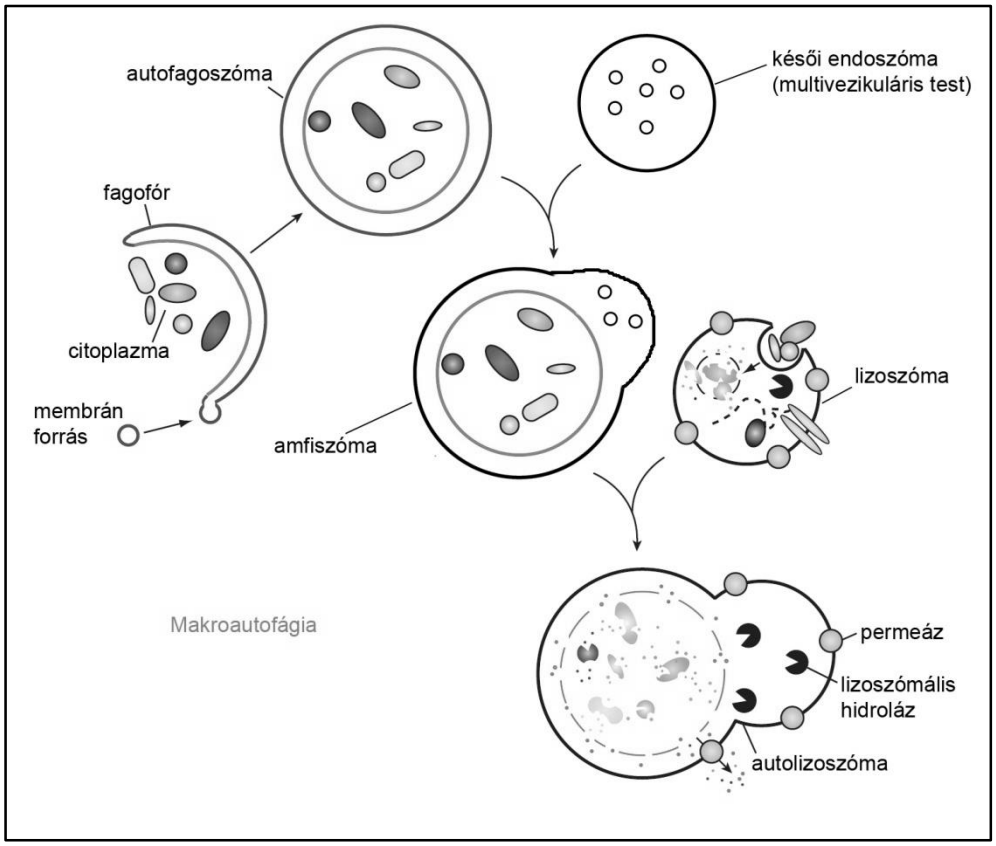
Minden sejt folyamatosan megújul, mivel a biológiai makromolekulák többsége állandó lebomlási és újraképződési ciklusokban vesz részt (kicserélődés, azaz turnover). Ennek során az időről időre károsodást szenvedő, funkcióképtelenné váló molekulák helyére mindig megfelelően működő új RNS, fehérje, lipid stb. molekula lép. Ezáltal a sejtek és szervezetek képesek megőrizni egyfajta belső állandóságot, azaz homeosztázist (bár talán a homeodinamika kifejezés megfelelőbb, hiszen dinamikus egyensúlyról van szó). Eukarióta sejtek esetén a folyamatos megújulás a sejtorganellumok szintjén is tetten érhető: nagyon fontos például a hibás, szétkapcsolódott elektron-transzport lánca miatt reaktív oxigén gyököket termelő mitokondriumok eltávolítása. A sejtorganellumok lebontása méretüket és összetett makromolekuláris felépítésüket tekintve bonyolultabb, mint egy egyszerű enzimreakció: ezt a lizoszómális önemésztés, azaz autofágia biztosítja.

Autofágia során a lebontandó anyagoknak a lizoszóma belsejébe kell kerülniük. Többféle autofág útvonalat különböztetünk meg annak alapján, hogy ez hogyan történik meg. A chaperone-mediált autofágia (CMA) során a Hsc70 dajkafehérje által letekert egyedi fehérjék a lizoszomális membránban található LAMP-2A (lysosome-associated membrane protein 2A) csatornán keresztül jutnak a lizoszómába, ahol a lizoszómális Hsc70 „fogadja” ezeket, majd lebontódnak a savas hidrolázok közreműködésével (Kaushik és Cuervo, 2012). A folyamat szelektivitását a KFERQ (vagy ehhez hasonló) aminosav szekvenciát hordozó fehérjék szelektív felismerése biztosítja a citoplazmában.

Mikroautofágia során a lizoszóma membránja befelé tűrődve felveszi a környező citoplazma egy részletét, majd a bekerült vezikula membránja a szállítmánnyal együtt a lizoszómában lebomlik (Mijaljica és mtsai, 2011). A folyamat ránézésre hasonlónak tűnhet az endocitózishoz, ezért fontos kiemelni, hogy a topológiája fordított, azaz ilyenkor nem a citoplazmába, hanem a külvilágnak tekinthető lizoszóma lumenébe kerül az anyag, és jelenlegi tudásunk szerint az endocitózisban szereplő fehérjék ehhez nem szükségesek. A mikroautofágia molekuláris mechanizmusa még kevéssé ismert, de genetikailag részben átfed a legfőbb útvonallal. A szállított anyag mennyisége már jóval több lehet, mint a CMA-nál: ezen az úton akár teljes organellumok, például peroxiszómák is bejuthatnak lizoszómába. A szelektív mikroautofág lebontás molekuláris háttere még jórészt ismeretlen.

A fő útvonal, a makroautofágia (a továbbiakban egyszerűen autofágia) során a citoplazmában megjelenik egy membráncisztema, amelyet fagofórnak (régebbi nevén izoláló membránnak) nevezünk. Ennek kialakulásában az autofág gének által kódolt fehérjék működnek közre (lásd később). A fagofór egyre növekedve bekeríti a citoplazma egy részletét, és így kettős membránnal határolt autofagoszómát képez (**1. ábra**). Ez a transzportvezikulum tartalmazhat szinte bármilyen sejtorganellumot: mitokondriumot, endoplazmás retikulumot, Golgi-készüléket, peroxiszómát stb. Az autofagoszóma ezek után

késői vagy multivezikuláris endoszómával egyesülhet, így egy amfiszómának nevezett átmeneti, pre-lizoszomális struktúra jön létre. Az autofagoszóma közvetlenül lizoszómával is egyesülhet bizonyos fajokban, például élesztőben (esetében a lizoszomális rendszernek megfelelő sejtszervecske a vakuólum). Az autofág folyamatok eredményeképpen képződő autolizoszómában az odaszállított anyagot (szállítmány, cargo) savas hidrolázok bontják le, amit a bomlástermékek - például fehérjék esetén az aminosavak - citoplazmába visszajutása és újrahasznosítása követ (Mizushima és Komatsu, 2011). Ennek köszönhetően az autofág lebontás különösen fontos szerepet játszik az éhezés során, amikor a sejtek nem jutnak elegendő tápanyaghoz: ilyenkor a keletkező bomlástermékek biztosítják az alapanyagokat az állandóan zajló bioszintetikus és energiatermelő folyamatokhoz.



1. ábra. *Az autofágia fő útvonala, a makroautofágia során először egy fagofór jön létre, mely egyre növekedve bekeríti a citoplazma egy részletét. A kettős membránnal határolt autofagoszóma ezután késői endoszómával egyesül, így egy átmeneti struktúrát, amfiszómát hoz létre. A lizoszómával történő fúziót követően képződő autolizoszómában történik meg az odaszállított anyagok lebontása. Ezután a bomlástermékek visszajutnak a citoplazmába, hogy ott újrahasznosuljanak (Juhász és mtsai, 2013).*

Az autofagoszómákat kialakító fagofór membrán eredete évtizedeken át vita tárgyát képezte, amit egy általam kezdeményezett összefoglaló cikkünkben mi is tárgyaltunk (Juhasz és Neufeld, 2006). Az autofágiában szereplő fehérjék sejten belüli mozgásának vizsgálata alapján mára már úgy tűnik, hogy több különféle sejtorganellum is szerepelhet mint membrán forrás, hiszen már demonstrálták az ER, mitokondriumok, Golgi-készülék, plazmamembrán és korai endoszómák ilyetén szerepét humán sejttenyészeti kísérletekben (Lamb és mtsai, 2013). Az endocitotikus út fontosságára utal az a tanszéki együttműködésben végzett munkánk is, miszerint a klatrin-mediált endocitotikus komplex tagja, az epsin *Drosophila* homológja szükséges az autofagoszómák kialakulásához (Csikos és mtsai, 2009). Egy élesztősejtek vizsgálatával foglalkozó tanulmány szerint akár a lizoszómális membrán is reciklizálódhat autofágia során (Yamamoto és mtsai, 2012). Ez különösen logikus lépés lenne a sejt részéről, hiszen így végülis az autofagoszómák lizoszómával fúzionáló külső membránja szolgálna a közvetlen közelben formálódó új autofagoszómák membránforrásaként. Megjegyzendő, hogy az autofagoszómák nemcsak élesztősejtekben képződnek általában a vakuólum (lizoszóma) közelében, hanem saját vizsgálataink alapján a *Drosophila* zsírtestben is (Nagy és mtsai, 2014b).

Az autofágia fő útvonala igen fontos szerepet játszik az ubikvitinált fehérjék lebontásában. Ezt megfelelő, szelektív autofág receptor fehérjék biztosítják. A plazmamembránban elhelyezkedő receptoroktól eltérően itt a receptor kifejezés arra utal, hogy ezek a molekulák képesek kétféle fehérjét összekapcsolni. Közülük az egyik rendszerint az ubikvitin, (poli-)ubikvitinált fehérjék formájában. A másik az Atg8/LC3 családba tartozó, ubikvitin-szerű fehérjék valamelyike. Ezen fehérjék interakcióinak az eredménye az lesz, hogy az ubikvitinált fehérjék és aggregátumok (a szállítmány) a képződő, Atg8-cal fedett fagofórhoz kötődnek a receptoron keresztül, majd együttesen a létrejött autofagoszóma belsejébe kerülnek. A legtöbbet vizsgált, Atg8-cal szelektíven kölcsönhatásba lépő fehérje a p62 (más néven SQSTM-1, sequestosome-1). A p62 az ubikvitinált fehérjéket UBA (ubiquitin-associated) doménje révén képes kötni, az Atg8/LC3-hoz pedig egy rövid peptidszakasz, az AIM/LIR motívum (Atg8 interacting motif/LC3 interacting region) révén köt. Ez egy körülbelül 8 aminosavas, általában rendezetlen fehérjerégióban elhelyezkedő szakasz. Az első három aminosav között gyakran fordul elő savas oldalláncú, a negyedik (0. pozíciónak tekintett) mindig egy aromás (triptofán, tirozin vagy fenilalanin), utána két savas vagy apoláros, végül pedig a 3. pozícióban egy apoláros oldalláncú (leucin, izoleucin vagy valin) aminosav helyezkedik el. Az UBA és AIM/LIR mellett a p62-ben szintén megtalálható PB1 (Phox and Bem1) domén is elengedhetetlen a megfelelő funkcióhoz, ugyanis ez biztosítja azt, hogy a p62 másik p62 fehérjével vagy egyéb, szintén PB1 domént hordozó proteinnel aggregálódni tudjon (Rogov és mtsai, 2014). Így jön létre az a szelektív receptorokat és ubikvitinált fehérjéket egyaránt tartalmazó aggregátum, ami köré tud nőni a képződő fagofór. Érdemes megemlíteni, hogy a Parkinson-kórt okozó egyik génhiba a Parkint érinti, ami egy ubikvitin ligáz. Jelenlegi tudásunk szerint a Parkin a mitokondrium külső membránjában található vagy ahhoz asszociált fehérjék ubikvitinálása révén jelöli ki a nem megfelelően működő mitokondriumokat szelektív autofág lebontásra.

Klasszikus, nagyrészt ultrastrukturális vizsgálatok

Az autofágia vizsgálatának kezdete 1959-re datálható, amikor Alex Novikoff vesesejtekről készült transzmissziós elektron mikroszkópos képein nemcsak felismerte, hanem helyesen is értelmezte az autofág struktúrákat (Novikoff, 1959). Ashford és Porter 1962-ben glukagon-perfundált patkány májsejtekben hasonló felfedezéseket tettet (Ashford és Porter, 1962), és Christian de Duve hamarosan kimutatta, hogy ez a folyamat a májsejtekben található lizoszómák pozíciójának megváltozásával jár (Deter és mtsai, 1967). Az autofágia elnevezést de Duve javasolta egy 1963-ban rendezett konferencián, majd pedig egy széles körben idézett összefoglalóban (De Duve és Wattiaux, 1966; de Reuck, 1963). Többek között a lizoszómák felfedezéséért de Duve 1974-ben Nobel-díjat kapott.

Már az 1960-as években publikáltak autofágiával kapcsolatos elektronmikroszkópos tanulmányokat rovarkutatók. Az első közlemények egyike 1963-ban demonstrálta, hogy a teljes átalakulást (metamorfózist) közvetlenül megelőzően a *Drosophila* lárvák zsírtest sejtjeiben hatalmas autolizoszómák láthatók, belsejükben még felismerhető ER-rel és mitokondriumokkal (von Gaudecker, 1963). Az autofágia ultrastruktúrájának egyik legrészletesebb morfológiai leírását 1965-ben publikálta Locke és Collins, akik egy lepkefaj, a *Calpodes ethlius* lárvális zsírtestét vizsgálták (Locke és Collins, 1965). A morfológiai leírások mellett Collins dekapitációs és ligációs kísérletek alapján már 1969-ben felismerte, hogy a rovarok vedlési hormonja (ekdizon) autofágiát indukál, de csak a juvenilis hormon alacsony szintje mellett (Collins, 1969), melyet később igazoltak más rovarfajokban, többek között *Drosophila*-ban is (Sass és Kovacs, 1975; Thomasson és Mitchell, 1972).

Az emlősökön és rovarokon végzett korai, szintén jórészt elektronmikroszkópos vizsgálatok részletekbe menő taglalásától a továbbiakban eltekintek, mivel nem lényegesek kutatási eredményeim jelentőségének értékeléséhez. Az eziránt érdeklődő olvasók egy társ-szenior szerzős összefoglalóm második fejezetében találhatnak további részleteket az autofágiával kapcsolatos korai kutatásokról; jómagam az első négy fejezetét írtam ennek a cikknek (Mulakkal és mtsai, 2014).

Az autofágia molekuláris mechanizmusa

Az autofágia kutatásának első 35-40 éve jórészt leíró jellegű közleményekből áll, mivel a folyamatban szereplő géntermékek mibenlétét ebben az időszakban még homály fedte. Az autofágiát vizsgáló kutatók az 1990-es évek környékén már használtak különféle hatóanyagokat a folyamat gátlására, mint például az autofagoszóma kialakulását megakadályozó 3-metiladenin (Seglen és Gordon, 1982), vagy az autofagoszóma-lizoszóma fúziót gátló bafilomicin A1 (Yamamoto és mtsai, 1998). Ezen gátlószerek alkalmazásának korlátait jól jelzi azonban in vivo toxicitásuk, valamint nem eléggé ismert hatásmechanizmusuk. Erre jó példa az elsősorban a lizoszómális protonpumpát, a v-ATPázt (vacuolar-type H+ -ATPase) gátló bafilomicin, hiszen általános az a nézet, hogy a lizoszóma savasodása valamiképpen szükséges a fúzióhoz (Yamamoto és mtsai, 1998). Azonban korábbi posztdoktori témavezetőmmel együttműködve nemrégiben kimutattuk, hogy nem a

lizoszómális protonpumpa hibája, hanem a bafilomicin egy másik célpontjának, az endoplazmás retikulum kalcium ATPáz fehérje funkciójának a kiesése okoz fúzió gátlást (Mauvezin és mtsai, 2015).

Az 1990-es évek közepén Yoshinori Ohsumi, Michael Thumm és Daniel J. Klionsky vezetésével három, egymástól függetlenül dolgozó kutatócsoport is publikált olyan genetikai szűrővizsgálatokat, amelyekben autofágia hibás élesztő mutánsokat izoláltak (Harding és mtsai, 1995; Thumm és mtsai, 1994; Tsukada és Ohsumi, 1993). Mivel ezeket a géneket kezdetben különféle nevekkel illették, a követhetőség érdekében 2003-ban egységes nevezéktant vezettek be élesztőben: azóta az összes, autofágiában szereplő gént általában *Atg* (autophagy-related) névvel és egy számmal jelölik (Klionsky és mtsai, 2003). Az autofágia jelensége és a folyamathoz szükséges gének többsége konzervált az eukarióta élőlények körében, így az élesztő *Atg* gének állati homológjait is gyakran hasonlóképpen nevezték el. Ezen gének egyikének *Drosophila* homológját, az *Aut1*-et (a génnek a fent említett, ámde később publikált egységes nómenklatúra szerinti neve *Atg3*) PhD tanulmányaim keretében vizsgáltam az akkoriban újdonságnak számító, transzgénikus RNS interferencia módszerrel (Juhász és mtsai, 2003). Ebben elsőként mutattam ki, hogy egy *Atg* gén állati szervezetben is szükséges az autofágiához. Mivel ez a publikáció képezte a 2004 márciusában megvédett PhD disszertációm alapját, ezeket az eredményeket jelen értekezésemben nem tárgyalom.

Az egyes *Atg* génekről átíródó fehérjék kölcsönhatásai alapján több fehérjekomplexet, működési egységet különíthetünk el:

A. Atg1 (emlősökben ULK1/2 [uncoordinated 51-like kinase]) protein kináz komplex
B. harmadik osztályú (class III) foszfatidilinozitol 3-kináz (PI3K), azaz lipid kináz komplex (Vps34 kináz komplexnek is nevezik a katalitikus alegység neve alapján)
C. Vps34 kináz effektorok, melyek foszfatidilinozitol 3-foszfátot (PI3P-t) kötnek, mint például az Atg18 és a DFCP1 (Double FYVE-containing protein 1), és ezek kötőpartnerei
D. Atg9, az egyetlen transzmembrán fehérje az Atg géntermékek között
E. ubikvitin-szerű konjugációs rendszerek. Az itt szereplő Atg8 és Atg12 fehérjék térszerkezete igen hasonló az ubikvitinéhez. Az enzimreakciók során az Atg8 C-terminális glicinje kovalensen kapcsolódik egy foszfatidil-etanolamin (PE) molekulához, és így membránkötött lesz. Autofágia kutatások során leggyakrabban az Atg8 és homológjainak intracelluláris pöttyszerű, autofagoszomális elhelyezkedését, és western blot kísérletekben a lipidált, fagofór- és autofagoszóma-asszociált Atg8 szintjét vizsgálják.

Ezek az élesztő genetikai kutatások mérföldkőnek tekinthetők az autofágia területén, mert lehetővé tették, hogy a modern molekuláris biológia eszköztárát alkalmazó mechanisztikus, azaz ok-okozati viszonyokat feltáró kutatásokat végezzünk eukarióta élőlényekben. A különféle modellállatok tanulmányozása és a genomléptékű asszociációs vizsgálatok rávilágítottak arra, hogy az autofágia hibája valószínűleg sokféle emberi betegséggel is kapcsolatba hozható.

Az autofágia jelentősége

Az éhezés túlélésének biztosítása

Az autofágia legősibb feladata az lehet, hogy segítse a tápanyaghiányos időszakok (éhezés) átvészelését. Ennek bizonyítékaként már a legelső, autofágiára képtelen élesztő-mutáns vizsgálatakor észrevették, hogy ezek a sejtek különösen érzékenyek az éhezésre (Tsukada és Ohsumi, 1993). Teljes éhezés, vagy csak cukrot tartalmazó diéta alkalmazásával autofág gén mutáns *Drosophila* lárvák és kifejlett legyek esetén is megfigyelhető, hogy ilyen körülmények között a vad típusú állatoknál hamarabb elpusztulnak (Juhasz és mtsai, 2007a; Scott és mtsai, 2004). Mindezekkel összhangban vannak a későbbiekben egereken végzett kutatási eredmények. Létrehoztak olyan génkiütött egereket, melyekben az ubikvitin-szerű konjugációs rendszer tagjait kódoló gének valamelyike vagy az *Atg9* hiányzik. Ezen egér mutánsok mindegyikére igaz az, hogy a születést követően nem sokkal elpusztulnak, mert a köldökzsinóron keresztül történő tápanyagellátás megszakadása után fellépő neonatális éhezést nem élik túl (Jiang és Mizushima, 2014). Kimutatták azt is, hogy már a megtermékenyítés autofágiát vált ki az így létrejövő zigótában, ami igen fontos a fejlődő korai embrió túléléséhez, hiszen az anyai szervezetből tápanyagokhoz csak a beágyazódást követően juthat (Tsukamoto és mtsai, 2008).

Az autofágia szerepe a programozott sejthalálban

Néhány évtizeddel ezelőtt általános nézet volt, hogy az autofágia tulajdonképpen egy, az apoptózistól morfológiailag elkülönülő sejthalál típus (Clarke, 1990). Ezt azokra a mikroszkópos vizsgálatokra alapozták, melyek során pusztuló sejtekben autofagoszómák és autolizoszómák nagy számban történő megjelenését látták. Az utóbbi 10 év során végzett, *Atg* géncsendesített vagy mutáns sejteket, vagy *Atg* génkiütött állatokat tanulmányozó vizsgálatok többségében viszont azt tapasztalták, hogy az autofágia hibája nem akadályozza meg a sejtpusztulást. Egyes vezető kutatók még azt is felvetették, hogy nem létezik autofág sejthalál (Kroemer és Levine, 2008; Levine és Yuan, 2005). Ez a kijelentés azonban valószínűleg túlzás, hiszen még ugyanezen kutatók is találtak autofág sejthalálra példát későbbi vizsgálataikban (Liu és mtsai, 2013). Ilyen szempontból is nagy jelentőségű volt az a megfigyelésünk, hogy az Atg1 kináz túltermeltetése révén lehetséges genetikai úton túlaktiválni az autofágiát, és ez mind a poliploid, mind pedig a diploid sejtekben kiváltja az apoptotikus kaszpázok aktiválódását, ami a sejtmagi DNS fragmentálódásához és a sejtek eliminációjához vezet. Az ezt bemutató, széles körben idézett cikkünk világosan demonstrálta, hogy a túlságosan magas autofág aktivitás igenis okozhat sejthalált (Scott és mtsai, 2007). Az mindenesetre elmondható, hogy az autofágia rendszerint a sejtek túlélését, nem pedig elpusztításukat szolgálja.

Az autofágia és az apoptózis mechanizmusa között is találni közös szabályozó elemeket. Erre talán a legjobban ismert példa az anti-apoptotikus Bcl-2 fehérje autofágiát is

gátló szerepe, mivel az élesztő Atg6 emlős homológjához, a Beclin-1-hez kötve megakadályozza annak autofág funkcióját (Pattingre és mtsai, 2005). Én is kimutattam egyik munkámban, hogy *Drosophila*-ban a diploid sejtekben proapoptotikus funkciójú *Hid* gén túltermeltetése poliploid sejtekben autofágiát indukál (Juhasz és Sass, 2005). Ez a fajta kettős szerep persze korántsem igaz minden apoptózisban szereplő fehérje esetén. Leírtuk, hogy az *Apaf-1* (*dark*) mutáns *Drosophila* lárvális nyálmirigy metamorfózis során történő hisztolízise gátolt ugyan, viszont az ebben az időszakban bekövetkező autofág indukció megtörténik (Akdemir és mtsai, 2006). Az Apaf-1 a mitokondriális úton indukált apoptózisban játszik kulcsszerepet, mivel az effektor kaszpázok aktiválásához szükséges apoptoszóma nem alakul ki nélküle. Tehát az apoptózis és az autofágia a nyálmirigyben egymással párhuzamosan működnek, vagy esetleg az autofágia az apoptózisnál korábban (upstream) hat.

Az autofágia és a neurodegenerációs betegségek

Az autofágia sejteket védő (citoprotektív) hatását támasztják alá a különféle neurodegenerációs betegségekről eddig gyűjtött adatok. Bizonyos kórképek (pl. Huntington-kór) esetén egyes fehérjékben egy poliglutamin szekvencia kiterjedése figyelhető meg, és az így létrejövő kóros fehérjék aggregátumokat képeznek az idegsejtekben. Az autofágia farmakológiai fokozása csökkenti az aggregátumok számát és a neurodegenerációs tüneteket sejtes, *Drosophila* és egér modellekben is (Ravikumar és mtsai, 2002; Ravikumar és mtsai, 2004). A Parkinson-kór esetén az egyik középagyi mozgásszabályozó központ (substantia nigra) dopamint termelő idegsejtjei válnak először működésképtelenné. *Drosophila* kísérletek mutattak rá arra, hogy az emberi betegség öröklődő formáit okozó egyes mutáns gének (pl. parkin) megfelelő muslica homológjának kiesése esetén nemcsak idegsejtpusztulás és mozgászavarok lépnek fel, hanem már a tüneteket megelőzően abnormális mitokondriumok jelennek meg a mutáns állatok izomsejtjeiben (Greene és mtsai, 2003). Mára már igen sok adat utal a parkin fehérje szerepére a sérült, nem megfelelően működő mitokondriumok szelektív autofág lebontásában, amit mitofágiának nevezünk (Narendra és mtsai, 2012). Feltehetően ennek a folyamatnak a hibája fontos szerepet játszik az emberi betegség kialakulása során.

Sajnos a leggyakoribb humán neurodegenerációs betegségek (mint például az Alzheimer-kór) megismerésében és kezelésében igazi áttörést nem sikerült elérni. Mivel a szórványosan kialakuló eseteknél a pontos genetikai elváltozások és az esetleges környezeti kiváltó hatások mibenlétét még nem ismerjük eléggé, így igazán jó állati modelleket is nehéz alkotni, pedig ezek vizsgálata segíthetne a pathomechanizmusok megértésében. A *Drosophila* retina is egy közkedvelt modell a neurodegenerációs betegségek kutatásában. Ezeket az autofágiával és neurodegenerációval kapcsolatos publikációkat részletesen tárgyaljuk egy meghívásra írt összefoglalónkban (Lorincz és mtsai, 2015).

Megjegyzendő, hogy eddig egyetlen központi *Atg* gént érintő mutációt azonosítottak, ami bizonyítottan emberi betegséget okoz (és nem csupán hajlamosít arra), mint a gyulladásos bélbetegség egyik rizikófaktoraként ismert, Atg16L1 fehérje T300A aminosavcserét hordozó allélje. Az élesztő *Atg18* gén egyik humán homológját, a *WDR45/WIPI4* (*WD-repeat domain*

45/WD Repeat Domain Phosphoinositide-Interacting Protein 4) gént érintő különféle de novo mutációk ugyanis a fehérjeszint csökkentése révén a SENDA-nak (Static encephalopathy of childhood with neurodegeneration in adulthood) nevezett neurodegenerációs betegség kialakulásához vezetnek (Saitsu és mtsai, 2013).

Az autofágia véd a fertőzések során

Az autofágia előnye a különféle fertőzések esetén is megmutatkozik, hiszen megfelelő felismerő mechanizmusok biztosítják a sejtekben szaporodó patogének (vírusok, baktériumok) szelektív autofág lebontását. A korábban említett parkin ugyanis nemcsak a hibás mitokondriumok, hanem a sejtbe jutó idegen baktériumok autofág eltávolítását (xenofágia) is elősegíti, mind *Drosophila,* mind pedig egér esetén (Manzanillo és mtsai, 2013). Ez a megfigyelés magyarázhatja, hogy Parkinson-kórban szenvedő betegek körében miért gyakoribb például a tuberkulózis.

Az autofágiának szintén fontos szerepe van az autoimmunitás megelőzésében. Az autofágia gátlása a csecsemőmirigy hámsejtjeiben ugyanis megakadályozza azt, hogy ezek a sejtek a citoplazmás auto-antigéneket prezentálják az érőfélben levő T-limfocitáknak, így az autoreaktív sejtek eliminálása nem történik meg (Nedjic és mtsai, 2008).

Természetesen számos további példát lehetne hozni az autofágia fertőzések és immunválasz során játszott szerepére, melyek taglalásától most eltekintek. A téma iránt érdeklődő olvasók figyelmét szeretném felhívni néhány kiváló összefoglalóra (Jiang és Mizushima, 2014; Randow és mtsai, 2013).

Az autofágia ellentmondásos szerepe a tumorigenezisben

A fenti, jórészt előnyös hatásokkal ellentétben az autofágia ellentmondásos szerepet játszik a rák kialakulása és növekedése során. A növekedési jelátviteli utak, mint például az inzulin-szerű növekedési faktorok által aktivált első osztályú (class I.) PI3K, valamint a TOR (Target of Rapamycin) kináz rendszerek a sejtnövekedést és a sejtosztódást serkentik, míg az autofágiát gátolják (Chang és mtsai, 2009). Ez biztosítja azt, hogy a sejt igényeinek megfelelően koordinálódjék az anabolikus és katabolikus folyamatok egyensúlya. Ismert, hogy az élesztő *Atg6* emlős homológja, a *Beclin-1* egy haploinszufficiens tumor szuppresszor, az *Atg7* gén májspecifikus deléciója pedig jóindulatú tumorok kialakulását eredményezi (Jiang és Mizushima, 2014). Feltételezések szerint az autofágia hiányában a károsodott, reaktív oxigéngyököket termelő mitokondriumok nem bomlanak le, ami a DNS hibák számának növekedése miatt rákot kiváltó mutációkhoz vezethet (White, 2012). Emellett autofágia hiányában a p62 szintje is drasztikusan megemelkedik a sejtekben. A p62 fehérjében az LC3 kötőhely (LIR) mellett található egy másik peptidszakasz, amelyet KIR-nek neveznek (Keap1 interacting region). Ebből már kitalálható, hogy a p62 ennek révén képes kötni a Keap1 (Kelch-like ECH-associated protein 1) fehérjét. A Keap1 egy intracelluláris oxidációs stressz szenzor. Alapesetben feladata az Nrf2 (Nuclear factor

erythroid-derived 2-like 2) kötése és proteaszómális lebontásának elősegítése. Oxidációs vagy elektrofil stressz hatására, azaz amikor például a reaktív oxigéngyökök koncentrációja megnő, a Keap1 megfelelő cisztein oldalláncai révén ezt érzékeli, és a folyamat eredményeképpen disszociál az Nrf2-től. Az Nrf2 ennek hatására egyrészt stabilizálódik, a fehérje szintje megnő, másrészt szabadon képes bejutni a sejtmagba, ahol az antioxidáns enzimeket kódoló célgének transzkripcióját aktiválja. Tehát autofágia gátlásakor megnő az antioxidáns válasz, ami valamilyen úton-módon szintén serkentheti a tumor kialakulását (White, 2012).

Fontos azonban megjegyezni, hogy az autofágia szintje gyakran viszonylag magas a már kialakult, agresszív, metasztatizáló ráksejtekben. Ennek sokféle oka lehet. Egyrészt, az autofágia fontos szerepet játszik a szolid tumorok belsejében található, tápanyag- és oxigénhiánynak kitett ráksejtek túlélésének biztosításában. Hasonló lehet a helyzet kemoterápiás, citotoxikus kezelés során. Másrészt, az autofágia a nélkülözhető sejtalkotók lebontása révén a bioszintetikus és energiatermelő folyamatok alapanyagigényéhez is hozzájárul, ami igen fontos lehet az aerob oxidációs metabolizmust (ún. Warburg effektus) folytató ráksejtek esetén. Ezzel összhangban mind kísérleti állatokban, mind pedig a klinikumban sikerrel alkalmazzák a klorokvin nevű, lizoszómális lebontást (és ezzel autofágiát is) gátló szert rákellenes kezelések során. Vagyis az autofágia a rák kialakulásának kezdeti lépéseit feltehetően gátolja, míg a már kialakult tumor túlélését és növekedését serkenti (Cheong és mtsai, 2012; White, 2012).

Autofágia és öregedés

A gerincteleneken végzett genetikai vizsgálatokhoz hasonlóan emlősök esetén is feltételezik azt, hogy az autofágia megfelelő szintje késlelteti az öregedés folyamatát. Ez igen nagy jelentőségű lehet, hiszen a sok embert érintő problémák (rák vagy neurodegenerációs betegségek) is jellemzően idős korban alakulnak ki. Gerinctelen és patkány kísérletek alapján ismert, hogy az autofágia szintje és a lebontó kapacitás egyre csökken az élet során. Az autofágiát indukáló kalorikus restrikció (azaz a korlátozás nélküli evéssel járó kalóriabevitel mintegy 60%-a) megnöveli az élethosszt mind gerinctelen, mind pedig rágcsáló modellekben. Fontos kiemelni azt, hogy ezekben a kísérletekben az állatok jóval tovább egészségesek is maradtak (Vellai és mtsai, 2009). Ezt humán epidemiológiai adatok is alátámasztják: a nem éhező, de szerényen táplálkozó és sok egészségesnek tartott növényi táplálékot fogyasztó embercsoportok (mint például az Okinawa szigetén élő japánok) különösen hosszú várható élettartammal rendelkeznek. Beth Levine kutatócsoportjának egyik legújabb, a napilapok hasábjaira is felkerült eredményei alapján a testmozgás (a vizsgált egerek esetében a mókuskerékben futás) autofágiát indukál (He és mtsai, 2012). Azt tapasztalták, hogy a testedzés hatására a Bcl-2 fehérje három meghatározott aminosav-oldalláncán foszforilálódik, és ez a kölcsönhatás destabilizálja a Bcl-2 Beclin-1-gyel (az Atg6 emlős homológjával) alkotott komplexét. Így a Beclin-1 felszabadul a Bcl-2 gátlás alól, ami hozzájárul a testedzés során megnövekvő autofágiához. Létrehoztak egy mutáns egértörzset ennek a vizsgálatára olyan genetikai módosítással (knock-in), amelyben az endogén Bcl2 fehérje normálisan az edzés hatására foszforilációdó három aminosavát alaninra cserélték. Így az egerek minden

vizsgált tekintetben (például éhezéssel indukált autofágia) vad típusra jellemző fenotípust mutattak, de testedzés során kevesebb autofagoszóma keletkezett a váz- és szívizomszövetben. Ezek az egerek cukorbetegségre és elhízásra hajlamosak, és a rendszeres testedzés nem javítja állapotukat (He és mtsai, 2012). Természetesen túlzás lenne minden életmódbeli változás öregedésre vagy egészségre gyakorolt jótékony hatását az autofágiára visszavezetni, de az talán már állítható, hogy a folyamat megfelelő működése fontos szerepet játszik az életünkben.

Kiemelném azokat a kutatásokat amelyekben kimutatták azt, hogy egy poliamin típusú vegyület, a spermidin fogyasztása jelentősen megnöveli különféle élőlények élethosszát (köztük a legyekét is), méghozzá autofágia-függő módon, ugyanis *Atg7* mutánsokra nem hat a spermidin etetés (Eisenberg és mtsai, 2009). A spermidin autofágia-indukáló és egyéb hatásait feltehetően a globális hiszton-acetiláció befolyásolásával fejti ki (Morselli és mtsai, 2011). A hiszton-acetiláció autofágiában és élethosszban betöltött szerepének fontosságát legújabb tanulmányunk is alátámasztja, amelyben külföldi együttműködő partnereinket segítve kimutattuk, hogy az acetil-koenzim A sejten belüli szintje szabályozza az autofágiát és az élethosszt különféle élőlényekben (Eisenberg és mtsai, 2014). Az acetil-koenzim A szintemelkedése feltehetően hiszton-acetilációs változások révén csökkenti az élethosszt és az *Atg* gének átírásának mértékét élesztő sejtekben, de ezek a hatások kivédhetők az acetil-koenzim A szintézis gátlásával. Ezzel összhangban azt találtuk, hogy *Drosophila* esetén az acetil-koenzim A szintáz idegsejt-specifikus csendesítése megnöveli a sejtek autofág lebontó aktivitását és az állatok élethosszát (Eisenberg és mtsai, 2014).

Az autofágia szerepe további emberi betegségekben

Az autofágia számos egyéb élettani és patológiás folyamatban játszik fontos szerepet. A teljesség igénye nélkül ezek közé tartoznak a különféle miopátiák, a gyulladásos bélbetegség, a lizoszomális raktározási betegségek, az elhízás, a cukorbetegség és a vérképzés zavarai (Jiang és Mizushima, 2014). Összességében elmondható, hogy az autofág aktivitás terápiás célú módosítása számos új gyógymódhoz vezethet a jövőben. Emiatt nem meglepő, hogy gőzerővel zajlik a minél specifikusabban autofágiát gátló vagy serkentő szerek fejlesztése mind akadémiai, mind pedig gyógyszeripari kutatólaboratóriumokban (Cheong és mtsai, 2012; Rubinsztein és mtsai, 2012).

Az autofágia iránt érdeklődő olvasók figyelmét szeretném felhívni egy elektronikus tankönyvre, amelyet kollégáimmal közösen készítettünk MSc hallgatók részére. Ebből én a 7-12. számú fejezeteket írtam (Juhász és mtsai, 2013). Ezekben szintén bemutattam az autofágia molekuláris mechanizmusait, a folyamat tanulmányozására felhasználható különféle vizsgálómódszereket, valamint az autofágia emberi betegségekben játszott szerepét.

Az autofágia szabályozása

Először élesztő kísérletekben írták le azt, hogy a TOR kináz gátolja az autofágiát (Noda és Ohsumi, 1998). Későbbi mentorom, Thomas Neufeld csoportja bizonyította az inzulin/PI3K jelátvitel és TOR jelátviteli utak autofágiát gátló hatását *Drosophila*-ban (Scott és mtsai, 2004). Posztdoktorként kapcsolódtam be az Atg1 kináz szerepét firtató vizsgálatokba, melyekben azt tapasztaltuk, hogy az Atg1 túltermeltetése nemcsak autofágiát (majd végül apoptózist) indukál, hanem a sejtnövekedést is gátolja (Scott és mtsai, 2007). Ez a hatás részben a TOR aktivitásának Atg1 általi gátlásával valósul meg, ugyanis az Atg1 túltermelés csökkenti az S6 kináz (S6K) 398-as treoninon történő, TOR általi foszforilációját. A későbbiekben más kutatók igazolták, hogy az Atg1/ULK kináz emberi sejtekben is gátolja a TOR-t, tehát ez egy evolúciósan konzervált, gátló visszacsatolási lépés (Jung és mtsai, 2011). Ezzel összhangban az *Atg1* mutáns zsírtest sejtek viszonylagos növekedési előnnyel rendelkeznek a környező kontroll sejtekhez képest, ami a hosszabb távú, 2 napos éhezés esetén mutatkozik meg (Scott és mtsai, 2007). A TOR kináz és az autofágia kölcsönösen egymásra ható kapcsolatát a saját és szakirodalmi adatok tükrében egy összefoglaló cikkben is elemeztük (Chang és mtsai, 2009).

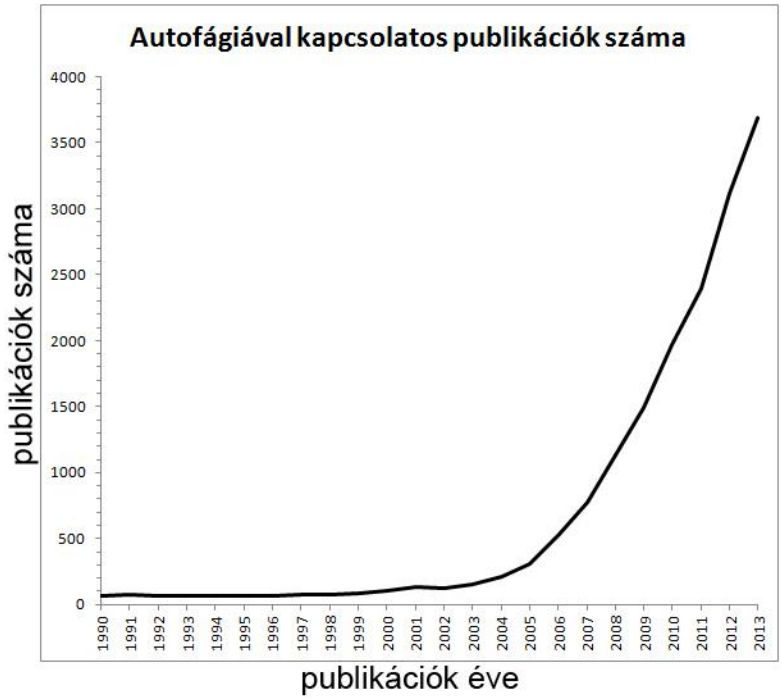
A TOR és az autofágia vizsgálatokhoz kapcsolódik az az ELTE Anatómiai Tanszéken dolgozó munkatársaimmal közösen végzett kísérletsorozat is, amelyben kimutattuk, hogy az AMPK szükséges a vándorló állatok zsírtestében megfigyelhető fejlődési autofágiához (Lippai és mtsai, 2008). Az AMPK kétféle úton is aktiválhatja az autofágiát (Wong és mtsai, 2013). Egyrészt a TSC1/2 komplexet foszforilálja és aktiválja, így ez a komplex serkenti a Rheb fehérje GTP-bontó aktivitását (melynek eredményeképp a Rheb inaktív lesz). Mivel a Rheb a TOR kritikus aktivátora, így az AMPK a TOR aktivitását gátolja, és így vehet részt az autofágia indukcióban. Másrészt az AMPK képes az Atg1/ULK1 kinázt direkt foszforiláció révén aktiválni.

Sokáig nem volt világos az sem, hogy az ekdizon milyen úton váltja ki a teljes átalakulással fejlődő rovarok metamorfózisa kezdetén megfigyelhető, ún. fejlődési autofágiát. Mivel a sejtnövekedési jelátviteli utak szabályozzák az autofágiát, ezért feltételeztük, hogy ez a szteroid hormon az inzulin/egyes típusú PI3K út gátlása révén fejti ki autofágiát indukáló hatását. Ez a hipotézis a későbbi, norvég partnereinkkel együttműködésben végzett vizsgálataink során beigazólódott. Bizonyítottuk, hogy az inzulin/PI3K jelátvitel aktivitása ekdizon hatására lecsökken a vándorló, metamorfózisra készülő lárvák zsírtestében, és az ekdizon receptor gátlása sejt-autonóm módon megakadályozza az autofágiát (Rusten és mtsai, 2004).

Természetesen az autofágiát számos egyéb jelátviteli út aktivitása is szabályozza, gyakran sejt- vagy szövetspecifikus módon. Ezek részletes tárgyalásától azonban eltekintek, mivel ez túlmutatna a jelen értekezés keretein.

Az autofágia vizsgálata

Az autofágia kutatásának népszerűsége az elmúlt évek, évtized során egyre növekedett, ami a témával kapcsolatos publikációk számának alakulásában is tetten érhető (**2. ábra**).



***2. ábra**. Az autofágiával kapcsolatos (keresési terminus: autophag*) publikációk évenkénti számának alakulása a PubMed adatbázis alapján (Takats és mtsai, 2014a).*

Ennek következménye az is, hogy sok, akár már egy másik terület kutatásában hírnevet szerzett kutatócsoport fogott autofágia vizsgálatokba. Sajnos gyakran előfordul még manapság is, hogy bizonyos kutatók egyetlen teszt (például az Atg8/LC3 pozitív struktúrák száma vagy a lipidált Atg8/LC3 mennyisége) alapján igyekeznek valamilyen autofágiára vonatkozó következtetést levonni. Talán a legfontosabb tanács az autofágia kutatók részére (is), hogy a kísérletekben elengedhetetlen több, módszertanilag különböző tesztet alkalmazni. Az autofágia vizsgálata egy adott módszerrel azért sem lehetséges, mert a folyamat több lépésből áll: az aktuális autofagoszóma-szám például a képződési és lebontási ráta függvénye. Tehát még ha sikerül is többféle módszer alkalmazásával kimutatni az autofagoszómák megnövekedett számát, ennek két oka is lehet: a keletkezés ütemének fokozódása, vagy az autofagoszómák lizoszómákkal történő fúziójának vagy lebontásának a gátlása. Emiatt az évek során egyre nagyobb hangsúlyt kapott az autofág flux meghatározása, tehát hogy mennyi anyag bomlik le adott idő alatt az autofág-lizoszomális úton. Ez az egyik fő üzenete annak a 2012-ben közlésre került, általános irányelveket megfogalmazó cikknek, amely az autofágiával foglalkozó kutatók konszenzusos véleményét igyekezett megfogalmazni (Klionsky és mtsai, 2012). Ennek köszönhetően a publikációnak 1269 szerzője lett, én a cikk

68-69. oldalán található *Drosophila* rész első felét írtam. A 2000-es években még viszonylag kevés kutató foglalkozott az autofágiával, így természetes volt az, hogy a *Drosophila* zsírtestben akkoriban alkalmazható néhány módszer részletes leírására minket kértek fel posztdoktori témavezetőmmel (Juhasz és Neufeld, 2008b). Szeretném megemlíteni, hogy a Methods folyóirat autofágia kutatással foglalkozó 2015-ös különszámába már én kaptam meghívást, hogy a *Drosophila*-ban mára elérhetővé vált vizsgálómódszereket részletesen mutassam be (Nagy és mtsai, 2015). A szóba jöhető technikákat az Anyagok és módszerek fejezetben sorolom fel.

A *Drosophila* (ecetmuslica, gyümölcslégy) mint modellállat

A bevezető végén szeretnék néhány általam lényegesnek gondolt tudnivalót megemlíteni az egész eddigi szakmai pályafutásom középpontjában álló kísérleti állatról. A *Drosophila melanogaster* egy genetikai, sejt- és fejlődésbiológiai kutatásokra több mint egy évszázada használt, jól bevált és még ma is népszerű modellállat. *Drosophila*-val foglalkozó kutatásokért már számos orvosi és élettani Nobel-díjat adtak: Thomas H. Morgan a rekombináció és az X kromoszómához kapcsolt öröklődés felfedezéséért 1933-ban, Hermann J. Muller a Röntgen-sugárzás indukálta mutagenezis felfedezéséért 1946-ban, Edward B. Lewis, Christine Nüsslein-Volhard és Eric F. Wieschaus a korai embrionális fejlődés genetikájának vizsgálatáért 1995-ben, míg 2011-ben Jules A. Hoffmann (megosztva) a veleszületett immunitás aktivációjának tanulmányozásáért részesült ebben az elismerésben.

A *Drosophila* egyik legfőbb erénye, hogy a genetikai vizsgálómódszerek állatok körében talán legszélesebb tárháza áll rendelkezésünkre, amelyek lehetővé teszik a mutáns, RNS interferencia (RNSi) vagy túltermeltetéses vizsgálatok elvégzését. Különösen fontos, hogy a funkcióvesztéses és funkciónyeréses kísérletek térben és időben kontrollált módon végezhetőek, tehát gyakorlatilag bármikor bármely szövetben vagy sejtben lehetséges célzott génmanipulációs változtatásokat eszközölni genetikai mozaik állatokban. Fontos megemlíteni, hogy mozaik állatokban a genetikailag módosított sejt fenotípusát rendszerint a szomszédos vad típusú, kontroll sejtekéhez lehet hasonlítani, ami egészen enyhe elváltozások kimutatását is lehetővé teszi az állatok között megfigyelhető biológiai variabilitás kiküszöbölése révén. Továbbá ennek köszönhetően akár a korai embriogenezishez szükséges gének funkciója is vizsgálható mozaikos lárvák vagy adultok sejtjeiben és szöveteiben.

A gyümölcslégy testfelépítése is nagyfokú hasonlóságokat mutat az emberével. Agyát százezer idegsejt - és ezek bonyolult hálózatokba szerveződő kapcsolatrendszere - alkotja, amelyek a létfenntartáshoz szükséges funkciók mellett irányítják például a hím muslicák párzási táncát, az alvás és ébrenlét ciklusát, és az emlékezést (Chiang és mtsai, 2011). A legyek vesesejtjeiben is található ultraszűrő membrán, melynek molekuláris felépítése szinte megegyezik az emberi podociták nyúlványai között elhelyezkedő, hasonló szerepű résmembránnal (Weavers és mtsai, 2009). Végül de nem utolsósorban, a kifejlett legyek bélhámja az emberéhez hasonlóan folyamatosan megújul, amit a bélőssejtek megfelelő ütemű, toxinok vagy fertőzések hatására felgyorsuló osztódása és differenciálódása biztosít (Lemaitre és Miguel-Aliaga, 2013). A fenti előnyöknek és hasonlóságoknak köszönhetően a *Drosophila*

genetikai analízise révén már számos esetben betekintést nyertünk emberi szempontból igen fontos élettani és patológiás folyamatok molekuláris mechanizmusába.

A modellélőlényeken végzett kutatások sebességének egyik meghatározó eleme az adott élőlény életciklusa. *Drosophila* esetén a szokásos, 25°C-on végzett kísérletek esetén a tenyészidő mintegy 10 nap, mely morfológiailag könnyen elkülöníthető stádiumokra oszlik. Az embrionális fejlődést követő három lárvastádium a táplálkozás és növekedés időszaka. Amikor a harmadik stádiumos lárvák már elég nagyra nőttek, megkezdik vándorló viselkedésüket. Ezt egy kisebb vedlési hormon (ekdizon) csúcs váltja ki, a juvenilis hormon alacsony szintje mellett (Riddiford, 1993). A vándorlás során a lárva elhagyja addigi táplálkozásának helyszínét (rothadó gyümölcs vagy mesterséges táptalaj), és megfelelően száraz helyet keres az előbáb (puparium) kialakításához. A tulajdonképpeni lárva-báb vedlés csak néhány órával később, a megkeményedett és megbarnult előbáb belsejében történik meg, a leendő felnőtt állat kültakaróját, lábait és szárnyait kialakító, ún. imágókorongok kifordulásával. A metamorfózis átlagosan 4-5 napot vesz igénybe, ami alatt a poliploid, ún. lárvális szövetek többsége lebomlik, és a diploid sejtek osztódva és differenciálódva létrehozzák az imágót. A bábból kikelő legyek igen szaporák: egy fiatal, jó kondícióban levő nőstény muslica akár száz petét is rakhat naponta.

A gyümölcslegyek hely- és táplálékigénye csekély, így viszonylag gyorsan és olcsón igen nagy számú utód vizsgálható, és az eredmények statisztikai értékeléséhez szükséges mintaszám könnyen elérhető . Ez azért is fontos szempont, mert ma gyakran azon múlik egy kutatócsoport sikere vagy akár puszta fennmaradása, hogy milyen gyorsan tud minél több és érdekesebb kísérleti eredményt produkálni és publikálni.

CÉLKITŰZÉSEK

Pályafutásom során célom mindvégig az autofágia molekuláris mechanizmusának és szerepének minél alaposabb felderítése volt egy népszerű gerinctelen modellállat, a *Drosophila melanogaster* genetikai, molekuláris, sejt- és fejlődésbiológiai módszereken alapuló vizsgálatával. Az ez irányban tett erőfeszítéseim során a PhD fokozatom megszerzését követően első vagy utolsó szerzőként publikált cikkeim fő célkitűzéseit az alábbiakban foglalom össze:

1. Az autofág géntermékek szerepének és transzkripciójának vizsgálata az autofág indukció során *Drosophila*-ban

2. Az autofágia szerepének vizsgálata az ubikvitinált fehérjék és a p62 lebontásában, valamint az állatok mozgásképességében és élethosszában

3. A Myc transzkripciós faktor és az autofágia viszonyának vizsgálata *Drosophila*-ban

4. Az autofagoszóma-lizoszóma fúzióban szereplő SNARE fehérjék és a pányvázó komplex azonosítása és vizsgálata *Drosophila*-ban

5. Annak elemzése, hogy a lizoszómális lebontás hibája hogyan hat a TOR kináz aktivitásán keresztül az autofagoszómák kialakulására

ANYAGOK ÉS MÓDSZEREK

Rekombináns DNS technikák

Kutatócsoportomban rutinszerűen végezzük a klasszikus, restrikciós endonukleáz emésztéssel (opcionálisan ezt megelőző PCR-rel - polymerase chain reaction), ligálással és *E. coli* sejtek transzformálásával történő klónozást, mivel ebben PhD és posztdoktori vizsgálataim során igen nagy gyakorlatot szereztem. A restrikciós helyek analízisét és primer tervezést rendszerint a Biology Workbench (http://workbench.sdsc.edu/) honlap segítségével végezzük. Emellett az Invitrogen által kifejlesztett Gateway klónozó rendszert is használjuk. Az elmúlt évek során több száz rekombináns plazmidot állítottunk elő, amelyeket transzgénikus legyek előállítására, rekombináns fehérjék létrehozására, és sejttenyészetben immunprecipitációs vizsgálatokra használtunk. Az általunk létrehozott DNS konstrukciók leírása a megfelelő publikációinkban megtalálható (Juhasz és mtsai, 2008; Juhasz és mtsai, 2007b; Nagy és mtsai, 2014a; Nagy és mtsai, 2014b; Takats és mtsai, 2013; Takats és mtsai, 2014b).

Drosophila genetika és kezelések

Rutinszerűen alkalmazzuk az alapvető *Drosophila* genetikai vizsgálómódszereket, azaz balancer kromoszómák és domináns mutációk révén bonyolult, több recesszív mutációt, illetve transzgént hordozó állatokat generálunk. Új mutánsokat a széleskörben alkalmazott transzpozon remobilizáció során keletkező pontatlan kivágódási események PCR vagy Western blot alapú azonosításával hozunk létre. Mozaik állatokat csak bizonyos sejteket és szöveteket érintő génmanipuláció révén generálunk. A felhasznált genetikai technikák és tenyészkörülmények (éhezés, csak cukrot tartalmazó diéta, neomicin, paraquat vagy hidrogén-peroxid kezelés, mászási/negatív geotaxis reflex vizsgálatok) részletes leírása a megfelelő publikációinkban megtalálható (Juhasz és mtsai, 2007a; Juhasz és mtsai, 2008; Juhasz és mtsai, 2007b; Low és mtsai, 2013; Nagy és mtsai, 2014a; Nagy és mtsai, 2014b; Nagy és mtsai, 2013; Takats és mtsai, 2013; Takats és mtsai, 2014b).

Fluoreszcens mikroszkópia

Rendszerint kiboncolt *Drosophila* szöveteket vizsgálunk, a preparátumot adott hullámhosszú fénnyel gerjesztve az aktiválódó molekulák által kibocsátott, megnövekvő hullámhosszú fényt fluoreszcens kutatómikroszkóppal detektálva. Az esetek többségében a kék, zöld és piros színcsatornákban fluoreszkáló jeleket rögzítünk, de sikerrel alkalmaztunk már ezekkel együtt egy negyedik, távoli piros színcsatornát is. A több színcsatorna felhasználásával válik vizsgálhatóvá különféle fehérjék kolokalizációja. Genetikai mozaik állatokban az eltérő genotípusú sejteket a zöld vagy piros (GFP vagy RFP) fehérje expressziója (vagy annak hiánya) alapján azonosítjuk. A fluoreszcens fényt gyakran riporter fehérje, illetve Lysotracker festéses kísérletekben a vitális festék bocsátja ki, ami lehetővé teszi az élő szövetek közvetlen

vizsgálatát. A bonyolultabb genotípusú törzsek létrehozásához, vagy épp a vizsgálni kívánt megfelelő genotípusú (például GFP-vel jelölt balancer kromoszómát nem hordozó) állatok kiválogatásához fluoreszcens sztereomikroszkópot használunk. Autofágia vizsgálatára rendszerint a zsírtestben viszonylag specifikusan autolizoszómákat jelölő Lysotracker Red vitális festéket, és GFP-vel vagy mCherry-vel jelölt Atg8a fúziós fehérje riportert használunk. Fontos különbség e kettő között, hogy előbbi döntően autofagoszómákat jelöl mivel a GFP inaktiválódik a lizoszómába jutva, míg az utóbbi az autofagoszómák mellett az autolizoszómákat is kijelöli, köszönhetően annak, hogy az mCherry a lizoszómában fluoreszcens marad és ott felhalmozódik. Ezt a különbséget aknázza ki a tandem, mCherry-vel és GFP-vel is jelölt Atg8a riporter, melynek segítségével megkülönböztethetőek a GFP+ mCherry+ autofagoszómák a csak mCherry+ autolizoszómáktól. A transzgénikus riportereink, valamint a felhasznált mikroszkópok részletes specifikációi a publikációinkban megtalálhatók (Juhasz és mtsai, 2007a; Juhasz és mtsai, 2008; Juhasz és Neufeld, 2008b; Nagy és mtsai, 2015; Nagy és mtsai, 2013; Takats és mtsai, 2013; Takats és mtsai, 2014b).

Indirekt immunfluoreszcencia

A vizsgálni kívánt fehérjék elleni ellenanyag felhasználásával kémiai rögzítőszerrel fixált és permeabilizált *Drosophila* szöveteket jelölünk, majd az elsődleges ellenanyagra specifikus, fluoreszcensen jelölt másodlagos ellenanyag révén tesszük láthatóvá az adott fehérje mikroszkópikus lokalizációját. Az ilyen kísérletekben jellemően az endogén p62-t tartalmazó fehérjeaggregátumok, valamint az endogén Atg8a-pozitív autofagoszómák intracelluláris szintjének és eloszlásának vizsgálatát végezzük. Az Atg8a- és a p62-pozítív struktúrák száma rendszerint ellentétes irányban változik a sejtekben, mivel a p62 autofágia révén bomlik le. Ez alól kivétel ha az autofagoszóma-lizoszóma fúzió gátolt, hiszen ekkor Atg8a-pozitív vezikulák jelenlétében is felhalmozódik a p62. Az általunk használt festési protokoll részletes leírása a cikkeinkben olvasható (Juhasz és mtsai, 2008; Nagy és mtsai, 2014b; Pircs és mtsai, 2012; Takats és mtsai, 2013).

TUNEL esszé

A programozott sejthalál során megfigyelhető sejtmagi DNS fragmentációt TUNEL (terminal deoxynucleotidyl transferase-mediated dUTP nick end labeling) esszével végeztük, a piros fluoreszcens jelet produkáló kit-et gyártó Roche leírása alapján (Juhasz és mtsai, 2007a; Takats és mtsai, 2013).

Elektronmikroszkópia

A kiboncolt *Drosophila* szöveteket kémiai rögzítőszerrel fixáljuk, majd ozmium-tetroxidos utófixálást követően műgyantába ágyazzuk. A megszilárdult blokkokban található anyag kifaragását követően ultravékony metszetet készítünk, és elektronmikroszkóppal vizsgáljuk a

minta ultrastruktúráját. A részletes protokoll a publikációinkban többször is leírásra került (Juhasz és mtsai, 2007a; Juhasz és mtsai, 2008; Takats és mtsai, 2013). A blokkokból félvékony metszetek is készíthetőek, amelyeket rendszerint valamilyen hisztológiai festés (például toluidinkék) felhasználásával értékelünk ki (Juhasz és mtsai, 2007a). Itt jegyzem meg, hogy a *Drosophila* szempigmentek vizsgálatakor nem feltétlenül kell festési lépést beiktatnunk (Lorincz és mtsai, 2015).

Immun-arany jelölés

Laborunkban a mintában található fehérjék ultrastrukturális elhelyezkedését ún. posztembedding módszerrel mutatjuk ki, azaz a műgyantába ágyazást követően. Ehhez az aralditba (ami jobb ultrastruktúrát ad, de nagyon csökkenti az immunogenitást) vagy LR White-ba (ami kicsit rosszabb ultrastruktúra mellett sokkal jobban megőrzi az epitópokat) ágyazott mintából készült ultravékony metszeteket inkubáljuk az elsődleges ellenanyaggal, majd ezt 5, 10 vagy 20 nanométeres aranyszemcsével konjugált másodlagos antitesttel tesszük elektron-mikroszkópos szinten láthatóvá. Különféle méretű aranyszemcsékkel jelölt másodlagos ellenanyagok felhasználásával ezt a módszert még kolokalizációs vizsgálatokra is fel tudjuk használni. További módszertani részletek a megfelelő cikkeinkben találhatók (Juhasz és mtsai, 2007a; Nagy és mtsai, 2014a; Takats és mtsai, 2013).

Ellenanyag termeltetés

Az endogén fehérjék mikroszkópos és western blot alapú vizsgálatához elengedhetetlen, hogy specifikus ellenanyagokat hozzunk létre, mivel *Drosophila* esetén a kereskedelmi forgalomban vagy kutató kollégáktól beszerezhető antitestek száma csekély. Sokat próbálkoztunk kereskedelmi szolgálatóknál kémiailag szintetizált peptidek elleni ellenanyagok termeltetésével, azonban 13 esetből csak egyszer koronázta siker a pénzbeli erőfeszítéseinket. Többszöri nekifutásra végül sikerült a *Drosophila* p62 (vagy más néven Ref(2)P) ellen egy affinitás-tisztított poliklonális nyúl ellenanyagot létrehozni a Genscript cég segítségével. A p62 az autofágia kutatások egyik leggyakrabban vizsgált fehérjéje, mivel szintje fordított arányban áll az autofág lebontással, így ez a teszt gyakran érzékenyebb, mint az Atg8/LC3 vizsgálata. Az ellenanyagunkat és magát a p62-alapú autofág aktivitás mérési módszert *Drosophila*-ban egy gyakran idézett cikkünkben publikáltuk (Pircs és mtsai, 2012). Különösen fontos az, hogy ebből az affinitás-tisztított ellenanyagból szinte korlátlan mennyiség áll rendelkezésünkre, mivel a korábban (az 1990-es években) leírt hasonló reagens már nem hozzáférhető.

A peptid-alapú ellenanyag termeltetés viszonylagos sikertelensége miatt rekombináns fehérjéket használtunk a további ellenanyagaink előállításához. Ezeket patkányokba és tengerimalacokba injektáltuk Freund-féle adjuváns felhasználásával, illetve néhány fehérje esetén neonatális FcR-t túltermelő transzgénikus nyulakat immunizált számunkra az Immunogenes Kft. Így sikerült a *Drosophila* Atg1 (patkány), Atg8a (patkány és nyúl), Atg9

(patkány), Atg13 (patkány), Atg14 (patkány), Atg16 (a fehérje különböző régióit felismerő kétféle patkány), FIP200 (FAK family kinase-interacting protein of 200 kDa)/Atg17 (patkány), TOR (patkány), Syx17 (patkány és tengerimalac), és usnp (patkány) fehérjékre a zárójelben jelölt gazdaállatban termeltetett ellenanyagokat előállítanunk, amelyek western blotra alkalmasak, valamint a patkány anti-Atg8a és anti-Syx17 immunfestésre is beváltak. Emellett anti-GFP és anti-mCherry ellenanyagokat is előállítottunk patkányokban, továbbá szegedi kollégáinkkal együttműködve tengerimalacokban is (Nagy és mtsai, 2014b; Takats és mtsai, 2013).

Rekombináns fehérjék előállítása

Az ellenanyag termeltetésre szánt rekombináns fehérjéket kódoló DNS szakaszt hagyományos vagy Gateway klónozás révén bakteriális expressziós vektorba helyezzük, majd Rosetta típusú *E. coli* sejtekben expresszáljuk. Általában a His-cimkével ellátott rekombináns fehérjét inszolubilis, inklúziós test formájában állítjuk elő, melyet ureában oldunk fel, nikkel oszlopon tisztítunk, majd dializálunk. Emellett több esetben is előállítottunk natív, szolubilis rekombináns fehérjéket, amelyeket szintén nikkel oszlopon tisztítottunk. Végül a kész fehérjepreparátumokat immunizálásra használjuk (Nagy és mtsai, 2014b; Takats és mtsai, 2013).

Western blot

A lárvális vagy adult *Drosophila* fehérjemintákat vagy immunprecipitációkat poliakrilamid gélelektroforézis után PVDF membránra visszük át. Ezt követi az elsődleges, majd a rendszerint alkalikus foszfatázzal konjugált másodlagos ellenanyaggal való inkubáció. Végül kemilumineszcens vagy látható csapadékot adó alkalikus foszfatáz szubsztrát segítségével tesszük láthatóvá a kimutatni kívánt fehérjét. A különféle genotípusú (vad típusú, mutáns stb) és kondícióknak kitett (jól táplált, éhező, vándorló lárva, vagy adult) állatok esetén leggyakrabban a szelektív autofágia révén lebomló p62/Ref(2)P szintjét, és az autofagoszóma-asszociált, lipidált Atg8a szintjét vizsgáljuk. Emellett szintén alkalmazzuk az autofág lebontás követésére a GFP-p62 vagy mCherry-Atg8a fehérjékből autolizoszómákban részleges proteolízissel keletkező, szabad GFP vagy mCherry sáv megjelenését anti-GFP vagy anti-mCherry ellenanyagok felhasználásával végzett western blot kísérleteinkben (ezek a fluoreszcens fehérjék ugyanis globuláris térszerkezetük miatt sokáig ellenállnak a lizoszómális lebontásnak). További részletek a cikkeinkben találhatók (Juhasz és mtsai, 2007a; Nagy és mtsai, 2014a; Nagy és mtsai, 2014b; Nagy és mtsai, 2015; Nagy és mtsai, 2013; Takats és mtsai, 2013; Takats és mtsai, 2014b).

Sejttenyésztés

Embrionális *Drosophila* vérsejt eredetű, szérumfüggetlen D.mel-2 (Invitrogen) sejteket a forgalmazó instrukciói alapján tenyésztünk. Az UAS-promóterrel kontrollált plazmidokat és az ezek expresszióját réz-szulfát hatására kiváltó metallothionein-Gal4 plazmidot a TransIT-2020 (Mirus) transzfekciós reagenssel juttatjuk be a sejtekbe. A transzfekció után 2-3 nappal, egy éjszakán át történő fehérje kifejeződést követően dolgozzuk fel a sejteket immunprecipitációra (Hegedus és mtsai, 2014; Nagy és mtsai, 2014a; Nagy és mtsai, 2014b; Nagy és mtsai, 2013; Takats és mtsai, 2013; Takats és mtsai, 2014b).

Immunprecipitáció

Rendszerint sejttenyészetben együttesen túltermeltetett, valamilyen peptid-cimkével (HA, FLAG, vagy myc) ellátott fehérjék kölcsönhatását vizsgáljuk a cimkére specifikus ellenanyagot hordozó agaróz gyöngy felhasználásával. A kísérleti körülmények részletes leírása a megfelelő publikációinkban található. Emellett többször is sikerült endogén fehérjék közötti kölcsönhatást kimutatnunk, az adott fehérjére specifikus ellenanyag és Protein A/G-t hordozó agaróz gyöngy segítségével (Hegedus és mtsai, 2014; Nagy és mtsai, 2014a; Nagy és mtsai, 2014b; Nagy és mtsai, 2013; Takats és mtsai, 2013; Takats és mtsai, 2014b).

Génexpressziós vizsgálatok

Az egyes génekről átíródó RNS-ek szintjét a megfelelő primerek megtervezése és legyártatása után RT-PCR-rel (reverse transcription polymerase chain reaction) vagy QT-PCR-rel (quantitative/real time polymerase chain reaction) végezzük (Erdi és mtsai, 2012; Hegedus és mtsai, 2014; Juhasz és mtsai, 2007a; Juhasz és mtsai, 2008; Low és mtsai, 2013; Takats és mtsai, 2015). A genomszintű génexpressziós változások vizsgálatát az MTA SZBK Funkcionális Genomika csoportjával együttműködésben, az Agilent által forgalmazott, teljes *Drosophila* transzkriptómot lefedő 4X44K oligonukleotid microarray-k segítségével végeztük (Erdi és mtsai, 2012). A teljes adatsor a www.ebi.ac.uk/arrayexpress honlapcímen, az E-MEXP-3352 elérési szám alapján megtekinthető.

Statisztikai kiértékelés

A mikroszkópos képek kiértékelését ImageJ (National Institutes of Health) programmal végezzük, melyet az adatok rendszerint SPSS (IBM) programcsomaggal való kiértékelése követ. Ennek során az összehasonlítani kívánt adatsorok számának és eloszlásának megfelelő statisztikai próbát alkalmazunk (Nagy és mtsai, 2014b; Nagy és mtsai, 2013; Takats és mtsai, 2013; Takats és mtsai, 2014b). Az állat szintjén jelentkező fenotípusok esetén (például az élethossz, a paraquat-kezelés túlélése vagy a negatív geotaxis reflex analízise során) szintén

SPSS vagy STATISTICA programcsomagot használtunk (Juhasz és mtsai, 2007a; Nagy és mtsai, 2013).

Publikált ábrák megszerkesztése

A cikkeinkben található ábrák elkészítéséhez az Adobe Photoshop programját használtuk, a megfelelő képrészletek kivágása és feliratozása mellett az egyes színcsatornák fényerejének és kontrasztjának beállítását is így végeztük. Minden efféle utólagos változtatást a teljes képre alkalmaztunk.

EREDMÉNYEK

1. Az autofagoszómák kialakulását az autofág géntermékek hierarchikus hálózata kontrollálja *Drosophila*-ban, melyek transzkripciója fokozódik autofág indukció során

Atg1 kináz komplex (alegységei: Atg1, Atg13, FIP200/Atg17, Atg101) szerepe az autofágia során

Az autofágia kezdeti lépése rendszerint a leginkább upstream ható Atg1/ULK1 kináz komplex aktiválódása, melyet az Atg1 túltermeltetés autofágiát indukáló hatása is jelez (Scott és mtsai, 2007). Egy korábbi, élesztősejteket vizsgáló cikk szerzői kémiai gátlószeren alapuló eredményeik alapján azt feltételezték, hogy az Atg1 kináz aktivitása nem szükséges az autofágia indukciójához (Abeliovich és mtsai, 2003). Ezt a hipotézist a kutatóközösség szkeptikusan fogadta. Kísérleteinkben mi is azt tapasztaltuk, hogy a *Drosophila* Atg1 fehérje pontmutáns, kináz inaktív változatát túltermeltetve nemhogy autofágia indukciót nem látunk, de még az éhezésre adott autofág válasz is gátlódik ezekben a sejtekben (Scott és mtsai, 2007).

Saját kutatólaborom megalapítása után is folytattuk a *Drosophila Atg* gének vizsgálatát. Azt találtuk, hogy az Atg1 kináz komplex egy másik alegysége, a FIP200/Atg17 túltermeltetése is fokozza az autofág aktivitást, bár kevésbé hatékonyan mint ami az Atg1 esetén tapasztalható (Nagy és mtsai, 2014b). Ez molekulárisan az Atg1 kináz komplex központi alegységének, az Atg13-nak az Atg1-függő hiperfoszforilációjában is tetten érhető. Atg1 és FIP200/Atg17 kiesésekor viszont nagymértékben csökkent az Atg13 foszforilációja. Eredményeink alapján tehát elmondható, hogy éhezés hatására az Atg13 Atg1- és FIP200-függő módon hiperfoszforilálódik, míg jól táplált állatokban az Atg13 hiperfoszforilációját Atg1 vagy FIP200 túltermeltetéssel is elérhetjük (Nagy és mtsai, 2014b).

Ebben a projektben létrehoztunk *FIP200/Atg17* null mutáns legyeket és kimutattuk, hogy a lárválís zsírtestükben mind az alapszintű, mind az éhezési, mind pedig a fejlődési autofágia gátolt: a szelektív autofág szállítmány p62 felhalmozódik a sejtekben, nem alakulnak ki Lysotracker- és mCherry-Atg8a-pozitív autofág struktúrák, és elektronmikroszkóppal vizsgálva mind az autofagoszómák, mind pedig az autolizoszómák hiányoznak (Nagy és mtsai, 2014b). Ezen felül a mutánsok nyálmirigyének metamorfózis során történő hisztolízise, és a lárválís bél eliminálása is zavart szenvednek (Nagy és mtsai, 2014b). Transzgénikus FIP200/Atg17-GFP expressziójával menekíteni tudtuk a mutánsunk autofágia hibáját és késői báb letalitását, és arra is figyelmesek lettünk, hogy a FIP200/Atg17 fehérje éhezés során a lizoszómák körül található autofág szállítmány, a p62 fehérje aggregátumaival kolokalizál. Ez különösen érdekes abból a szempontból, hogy élesztőben a fagofór kialakulása mindig a vakuólum (lizoszóma) felszínén, egy élesztőre jellemző szelektív autofág szállítmány, a pro-Ape1 aggregátumain történik (Scott és mtsai, 2000), hiszen így az

autofagoszóma képződés helye és mikéntje is evolúciósan konzervált lehet, még ha a konkrét molekuláris lépések némileg különböznek is.

Végezetül immunprecipitációs kísérletekben térképeztük az Atg1, Atg13 és FIP200/Atg17 fehérjék kölcsönhatásait. Azt találtuk, hogy az Atg13 erősen köti mindkét partnerét: C-terminálisa az Atg1-hez, míg feltehetően több régiója is a FIP200/Atg17-hez asszociál. Ezzel szemben az Atg1 és FIP200/Atg17 kölcsönhatása ezekben a kísérleteinkben alig volt kimutatható (Nagy és mtsai, 2014b).

Az Atg1 kináz negyedik alegységét, az Atg101-et is vizsgáltuk kutatócsoportommal. Kimutattuk, hogy az *Atg101* gén csendesítése szintén megakadályozza az éhezéssel kiváltott autofágiát a gátolt autolizoszómális Lysotracker festődés, továbbá az endogén Atg8a által jelölt autofagoszómák hiánya alapján, melyet elektron mikroszkópos vizsgálataink is igazoltak (Hegedus és mtsai, 2014). Emellett a p62 is felhalmozódik az *Atg101* RNS interferenciás sejtekben, jelezve a szelektív autofágia hibáját.

Az Atg101 fehérje és az Atg1 kináz komplex többi tagja közötti potenciális kölcsönhatásokat immunprecipitációs kísérletekben térképeztük. Azt találtuk, hogy az Atg1 több régiója is köthet az Atg101-hez, míg az Atg13 fehérje N-terminális HORMA (Hop1p, Rev7p and MAD2) doménje mutatott erős kölcsönhatást az Atg101-gyel. Mivel a HORMA domének dimerizálódni képesek, ezért bioinformatikai módszerekkel próbáltuk megjósolni az Atg101 fehérje térszerkezetét, ami a várakozásainknak megfelelően szintén HORMA doménnek mutatkozott (Hegedus és mtsai, 2014). Ezt a predikciónkat azóta kristályszerkezeti vizsgálatokkal kísérletesen igazolták, mindkét cikkben idézve a mi munkánkat (Michel és mtsai, 2015; Suzuki és mtsai, 2015).

A Vps34 lipid kináz szerepe az autofágia során

Az autofág indukció során a Vps34 lipid kináz komplex (alegységei a Vps34, Vps15, Atg6/Beclin-1, és az Atg14 vagy az UVRAG fehérjék) aktivációja kulcsfontosságú. Ez a fehérjekomplex azonban az endoszómák érésében és a lizoszómába irányuló bioszintetikus transzportfolyamatokban is szerepet játszik (Kihara és mtsai, 2001). Ugyanakkor egy humán sejttenyészeti munkában leírták, hogy a Vps34 szükséges a TOR kináz aminosavak általi aktivációjához is, ami igen meglepő felfedezés volt (Nobukuni és mtsai, 2005). Ez utóbbi megfigyelés motiválta arra poszdoktori témavezetőmet, hogy a Vps34 szerepét *Drosophila*-ban vizsgáljuk, mivel ő a sejtnövekedésben és sejtosztódásban szereplő jelátviteli utak tanulmányozását követően kezdett autofágia vizsgálatokba, és a TOR kináz aktivációjának szabályozását hosszú ideje kutatta akkor már (Zhang és mtsai, 2000).

Kísérleteinket *Vps34* null mutáns, és domináns-negatív Vps34-et túltermelő állatok létrehozásával kezdtük. Igazoltuk, hogy ezekben a funkcióvesztéses sejtekben a Vps34 terméke, a foszfatidil inozitol 3-foszfát (PI3P) nem mutatható ki a széleskörben erre a célra használt GFP-2xFYVE (Fab1, YOTB, Vac1 and EEA1) doménből álló riporterrel (Juhasz és mtsai, 2008). Kimutattuk, hogy a Vps34 szükséges az autofagoszómák kialakulásához, mivel

hiányában nem alakultak ki GFP-Atg8a-pozitív autofagoszómák és Lysotracker-pozitív autolizoszómák éhezéskor, amit ultrastrukturális vizsgálatokkal is megerősítettünk. A komplex egy másik alegységének, a *Vps15*-nek egy korábban leírt mutációja szintén gátolta az autofágiát (Juhasz és mtsai, 2008).

Felmerült a kérdés, hogy a Vps34 vajon az endocitózisban játszott szerepe révén szükséges-e az autofagoszómák kialakulásához. Hipotetikusan a Vps34 hiányában megrekedő endoszóma érés okozhatná azt, hogy a képződő autofagoszómák nem kapnak membránt az endoszómák felől. Ezt úgy vizsgáltuk, hogy a késői, multivezikuláris endoszómák kialakulásához szükséges ESCRT (endosomal sorting complex required for transport) komplexek működését gátoltuk *Vps28* és *Vps25* mutációk révén. Az ESCRT-hiányos sejtekben viszont felhalmozódtak az autofagoszómák GFP-Atg8a és ultrastrukturális vizsgálatok alapján, ami arra utalt, hogy a Vps34 más, specifikus szerepet játszik az autofagoszóma kialakulásban (Juhasz és mtsai, 2008). Meglepetésünkre a *Vps34-ESCRT* kettős mutáns sejtekben is találtunk autofagoszómákat. Ennek oka az lehet, hogy Vps34 hiányában is képződhet valamennyi autofagoszóma, ami az ESCRT hibájakor nem tud amfiszómává, illetve autolizoszómává alakulni. Persze az is elképzelhető, hogy egyszerűen az anyai géntermék az ESCRT alegységek esetében hamarabb elfogy, mint a Vps34 esetében. Ezt a feltevést sajnos megfelelő ellenyagok hiányában nem tudtuk vizsgálni.

A Vps34 lipid kináz enzim terméke, a PI3P foszfolipid nemcsak autofagoszómákon hanem endoszómákon is jelen van élesztő és emlős sejtekben. Ezzel összhangban azt láttuk, hogy a Vps34 szükséges az endocitózissal felvett, Texas Red-jelölt avidint hordozó endoszómák éréséhez, valamint a *Vps34* mutáns szemdiszkusz sejtekben a Notch receptor felhalmozódik, mivel gátolt az endolizoszomális lebontása (Juhasz és mtsai, 2008). Bemutattuk, hogy a jelenlegi tudásunk szerint egymástól jórészt függetlenül kialakuló, ám PI3P-re pozitív endoszómák (amiken a Rab5-GFP is kimutatható) és autofagoszómák (amiken a GFP-Atg8a is kimutatható) keletkezése jól követhető a lárvális *Drosophila* zsírtestben: jól táplált állatokban főleg endoszómákat látni, méghozzá jellemzően a sejtmag körül, míg éhezéskor a citoplazmában elszórtan jelennek meg az autofagoszómák (Juhasz és mtsai, 2008). Ez arra utal, hogy a Vps34 aktivitás helye megváltozik éhezés hatására.

Megjegyzendő, hogy az élesztő adatokhoz hasonlóan *Drosophila* sejtek esetén is azt tapasztaltuk, hogy a lizoszómákon lokalizálódó vagy azokon keresztül transzportálódó fehérjék eloszlása is megváltozik Vps34 hiányában. Például a LAMP1-GFP riporter a *Vps34* mutáns sejtek perifériáján halmozódik, és a spinster fehérje normálisan főleg plazmamembránban látható lokalizációja intracelluláris vezikulák irányába tolódik el (Juhasz és mtsai, 2008).

PI3P effektorok és kölcsönható partnereik szerepe az autofágia során

Kutatócsoportommal folytattuk a PI3P autofágiában játszott szerepének megértését célzó vizsgálatokat. A Vps34 termékéhez, a PI3P-hez több fehérje is képes kötni. A legjobban ismert ilyen foszfolipid effektor az Atg18, mely élesztőben az Atg2-vel együtt szabályozza az

Atg9 transzmembrán fehérje transzportját (Mizushima és mtsai, 2011). Az Atg18 egy WD40 ismétlődéseket hordozó, béta-propeller szerkezetű domént tartalmazó fehérjecsaládba tartozik. Az Atg18 homológjai emlősökben a WIPI1-4 fehérjék. *Drosophila*-ban is három élesztő Atg18-hoz hasonló fehérje található, és ezek egyikéről, a *Drosophila* Atg18a-ról leírták, hogy szükséges az éhezési és a fejlődési autofágiához (Berry és Baehrecke, 2007; Scott és mtsai, 2004).

Érdekes módon azt tapasztaltuk, hogy a *Drosophila Atg18a* mutánsok fenotípusai különböznek az *Atg2* mutánsokétól, mivel Atg8a-pozitív struktúrák csak az utóbbiak esetében alakulnak ki (Nagy és mtsai, 2014a). A későbbiekben ultrastrukturális vizsgálatokkal igazoltuk, hogy ezek a struktúrák fagofórok, amelyek nem képesek autofagoszómává záródni Atg2 hiányában (Nagy és mtsai, 2015). Az Atg9 fehérje is csak *Atg2* (és *Atg7* vagy *Atg8a*) mutánsokban halmozódik fel a p62 aggregátumokon, *Atg18a* vagy *Vps34* mutáns állatokban nem (Nagy és mtsai, 2014a). Eredményeinkkel részben átfedő fenotípusokról számoltak be férgekkel és humán sejtekkel foglalkozó kutatók is (Lu és mtsai, 2011; Polson és mtsai, 2010). Mindezek alapján elmondható, hogy az Atg18 csak élesztő esetén tölt be az Atg2-hez hasonló szerepet az autofagoszóma képződése során.

Ubikvitin-szerű protein konjugációs rendszerek szerepe az autofágia során

Az autofágiában szereplő ubikvitin-szerű fehérjék (Atg8a, Atg12, valamint az Atg5 melynek két ilyen doménje is van) és a kovalens konjugációjukhoz szükséges enzimkaszkád (Atg4, Atg7, Aut1/Atg3, Atg10, Atg16) közül többet is vizsgáltunk. Talán nem meglepő az eddig leírtak alapján, hogy az *Atg7, Atg8a* és *Atg3* mutációja, és az *Atg8a* vagy az *Atg16* gének csndesítése is az autofágia gátlását okozta az eddigiekben használt tesztjeinkben (Juhasz és mtsai, 2007a; Pircs és mtsai, 2012; Scott és mtsai, 2007). Az autofagoszómák kialakulásához fontos az Atg8 családba tartozó fehérjék lipidációja, azaz foszfatidil-etanolaminhoz (PE) történő kovalens konjugációja. Ennek első lépése az, hogy az Atg4 cisztein proteáz levágja az Atg8 C-terminusán található néhány aminosavat. Ezzel a limitált proteolízissel kerül a fehérje C-terminusára a további konjugációs lépésekben (E1: Atg7, E2: Atg3, E3: Atg5-12-16 komplex, és végül a PE molekula) részt vevő glicin. Szeretném e helyütt megemlíteni, hogy fiatal kutatócsoport-vezetőként még időm nagy részét a laborban dolgozva töltöttem, és sikerrel hoztam létre az Atg4 domináns-negatív transzgént túltermelő legyeket. Ennek az overexpressziója meggátolta az autofágiát Lysotracker festés, p62 felhalmozódás és ultrastrukturális vizsgálatok alapján (Pircs és mtsai, 2012).

Az autofág mutánsok és fehérje-lokalizációk vizsgálata során egyik említésre méltó megfigyelésünk az volt, hogy a bizonyos gének elveszésekor felhalmozódó, feltehetően fejlődésükben megrekedt autofág struktúrákon bizonyos, általunk korai, azaz upstream működésűnek gondolt fehérjék felhalmozódnak. Ez ugyan nem egy klasszikus episztázis analízis, azonban az autofágia kutatók körében gyakran használt és elismert módszer. Például az *Atg7* vagy *Atg8a* mutáns sejtekben szembetűnő a FIP200/Atg17 felhalmozódása a szelektív autofág szállítmány p62 aggregátumain (Nagy és mtsai, 2014b).

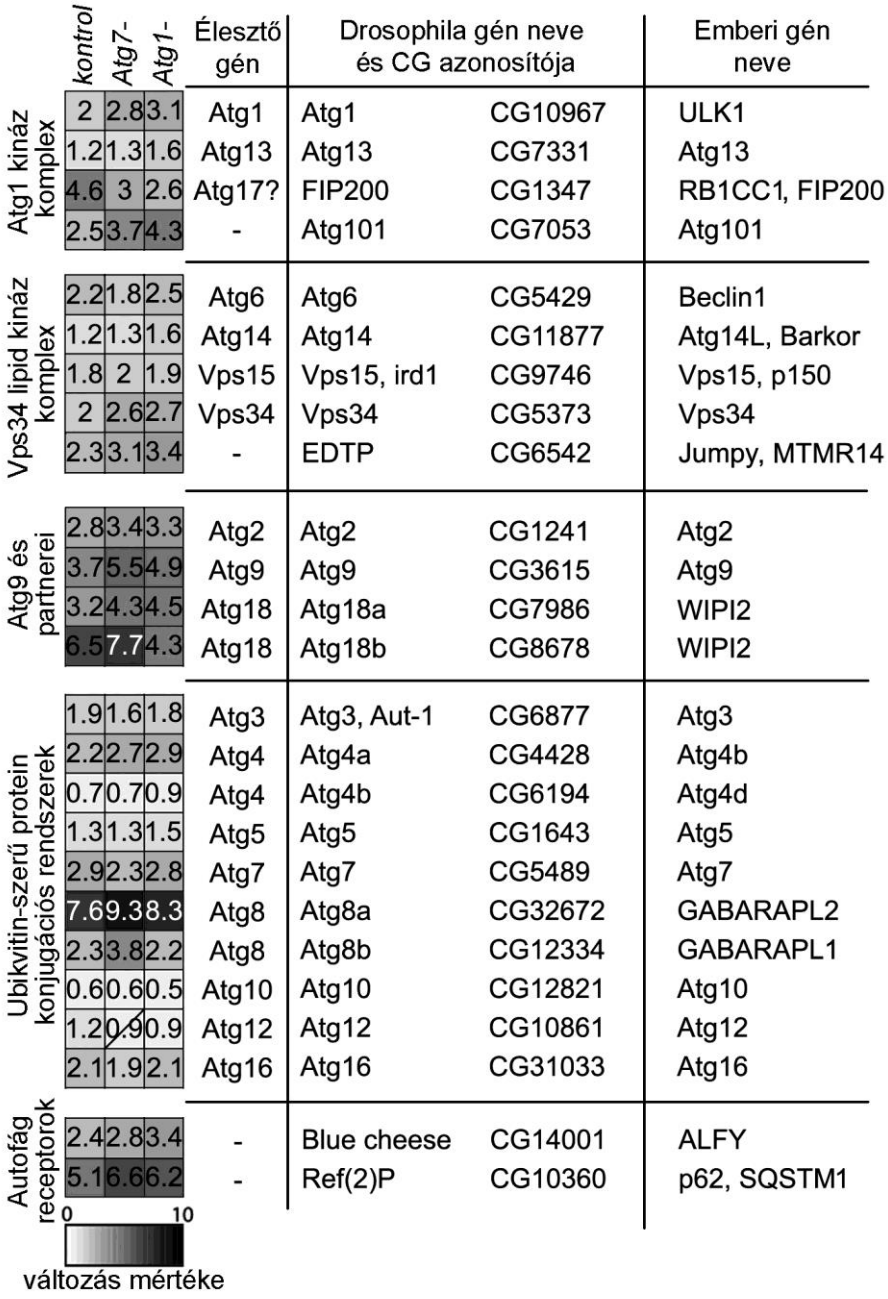
Az autofágiában szereplő gének átírása fokozódik autofágia során

Az autofágia szabályozása kapcsán sokan még ma is főként az Atg fehérjék poszttranszlációs módosításaira (pl. foszforiláció) fókuszálnak, pedig egyre inkább világossá válik, hogy ezen gének transzkripciója is jelentősen megváltozhat különböző hatásokra (Fullgrabe és mtsai, 2014). PhD disszertációm részét képezte az a szegedi kollégákkal közösen végzett nagyléptékű génexpressziós vizsgálat, melyben táplálkozó és vándorló lárvák zsírtest mintáit hasonlítottuk össze. Mivel az mRNS szintváltozásokat ott részletesen taglaltam, itt most csak annyit említek meg, hogy vándorláskor jónéhány *Atg* gén (például az *Atg8a*) átírása fokozódik a zsírtestben.

A Forkhead transzkripciós faktor családba tartozó FOXO (Forkhead box O) fehérjéket akut mieloid leukémia és rhabdomioszarkóma betegek kromoszomális transzlokációinak vizsgálata során írtak le először. Később kiderült, hogy az emlősökben redundáns *FOXO* gének *Caenorhabditis* (*DAF-16*) és *Drosophila* (*Foxo*) homológja kritikus szerepet játszik az élethossz szabályozásában: a PI3K sejtnövekedési út hibája esetén megfigyelhető élethossz növekedéshez a Foxo elengedhetetlen férgek és legyek esetén is (Kenyon és mtsai, 1993; Yamamoto és Tatar, 2011). Egyesült Államokban végzett posztdoktori vizsgálataim során fedeztem fel a Foxo autofágia indukcióban betöltött kritikus szerepét. A vándorló zsírtestben represszálódó *FKBP39 (FK506-binding protein of 39 kDa)* gén termékének túltermeltése gátolja az autofágiát Lysotracker és elektron mikroszkópos tesztek alapján, és egyúttal éhezéskor megakadályozza a Foxo transzlokációját a citoplazmából a sejtmagba. Ezek az adatok azt sugallták, hogy a Foxo szerepet játszhat az autofágia indukciójában. Valóban azt találtam, hogy *Foxo* mutáns *Drosophila* lárvákban az éheztetéssel indukált autofág válasz gátolt, míg a Foxo túltermeltetése önmagában is elég az autofágia indukciójához a zsírtestben autolizoszómákat kimutató Lysotracker festések alapján (Juhasz és mtsai, 2007b).

A Foxo autofág szerepéről szóló cikkem sikerén felbuzdulva első önálló kutatási pályázatom, egy posztdoktori OTKA projekt keretében szegedi kollégáinkkal ismét végeztünk egy - most már a teljes genomra kiterjedő - génexpressziós vizsgálatot. Azt tapasztaltuk, hogy éhezés hatására is megnő az autofágiában szereplő gének többségének mRNS szintje, mind vad típusú, mind pedig *Atg1* vagy *Atg7* mutáns lárvákban (Erdi és mtsai, 2012). Ez a változás leginkább az ubikvitin-szerű *Atg8a* és *Atg8b*, valamint az *Atg9* transzmembrán fehérjét és kölcsönható partnereit kódoló gének esetén szembeötlő (**3. ábra**). Érdekes módon azt találtuk, hogy az *Atg1* és az *Atg7* mutáns lárvákban a DNS replikációban szereplő gének expressziója csökken a vad típusú kontrollhoz képest, ami arra utal, hogy autofágia hiányában éhezéskor gátlódik a sejtosztódás, illetve poliploidizáció. Természetesen az éhezés során rengeteg gén transzkripciója megváltozik, nem csak az *Atg* géneké. Ezen, feltehetően autofágiától független változások részletezésétől itt most eltekintek, elemzésük a cikkünkben olvasható (Erdi és mtsai, 2012). A génexpressziós vizsgálatokat követő kísérletek során bizonyítottuk az indukálódó gének egyikáról, a *Rack1*-ről (receptor of activated protein kinase C 1), hogy az éhezéssel kiváltott megfelelő autofág válaszhoz szükséges Lysotracker festés és ultrastrukturális vizsgálatok alapján. Ezzel összhangban kimutattuk, hogy a Rack1 fehérje a

korai autofág struktúrákon megtalálható: kolokalizál a GFP-Atg8a-val és immun-arany jelölés alapján jelen van a fagofórokon és autofagoszómákon. Ezen felül azt találtuk, hogy a Rack1 a cukoroldatban történő éheztetés során képződő glikogénszemcsék kialakulásában is szerepet játszik (Erdi és mtsai, 2012).



3. ábra. *Az autofágia központi mechanizmusában részt vevő gének mRNS szintjének változása éhezés hatására vad típusú, Atg7 mutáns és Atg1 mutáns Drosophila lárvákban. További magyarázat a szövegben és a kapcsolódó cikkünkben olvasható (Erdi és mtsai, 2012).*

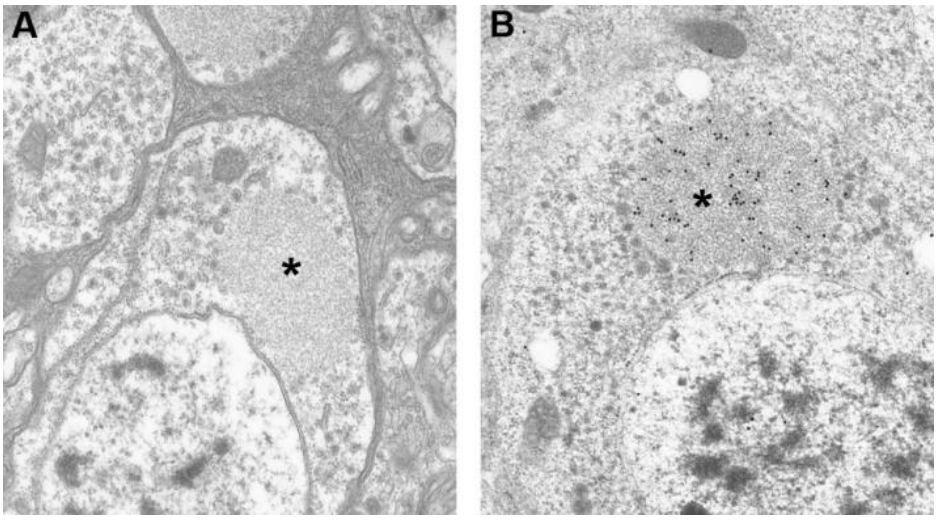
2. Az autofágia szükséges az ubikvitinált fehérjéket és p62-t tartalmazó aggregátumok lebontásához, és hibája mozgásképtelenséget és rövid élethosszt okoz *Drosophila*-ban

A metamorfózis során az autofágia nagymértékű indukciója figyelhető meg a lárva testtömegének többségét adó poliploid sejtekben. Feltételezések szerint ez a folyamat azt szolgálja, hogy a poliploid sejtekben felgyülemlett biomassza és energia a kifejlett imágót kialakító diploid sejtekbe helyeződjön át (Mulakkal és mtsai, 2014). Ennek fényében roppant meglepő volt az a felfedezésem, hogy az általam létrehozott *Atg7* null mutáns legyek életképesek: csupán a metamorfózis mintegy 4 napos időtartamához adódik hozzá 4 óra (Juhasz és mtsai, 2007a). Itt jegyzem meg, hogy null mutánst csak másodszori nekifutásra tudtam izolálni, ugyanis poszdoktori témavezetőmmel teljes mértékben meg voltunk győződve arról, hogy a gén hiánya letális lesz. Mivel erre a feltételezett letális fenotípusra támaszkodtam (volna) a mutáns vonalak keresése során, így csak a szomszédos, szekrécióhoz nélkülözhetetlen *Sec6* gént, vagy mindkét gént (*Sec6* és *Atg7*) érintő delécióakat tudtam azonosítani. Szerencsére ez nem tántorított el a további, immáron sikeres próbákozástól. Ez jó tanulságként szolgált a további, immár kutatócsoport-vezetőként irányított munkákban is, hiszen az elmúlt években sikerrel hoztunk létre homozigóta életképes null mutánsokat további *Drosophila* központi autofág gének esetén: az *Atg3*, *Atg5*, *Atg9* és az *Atg16* gének deléciója sem okoz letalitást, bár a kikelő imágók életképessége már igen változó: az *Atg3* mutáns állatok például gyakran pusztulnak el a bábállapot végén, a kikelés során. Ezen új mutánsaink vizsgálata jelenleg folyamatban van, még nem publikáltuk egyiket sem.

Mint már korábban említettem, az Atg7 egy ubikvitin-aktiváló E1 enzimhez hasonló fehérje. Az Atg7 mindkét kisméretű, ubikvitin-szerű fehérje (Atg8 és Atg12) konjugációjának aktivációs lépésében szerepel, ezért választottam posztdoktori kutatásaim alanyának. Természetesen az Atg7 hiányában mind az éhezés indukálta, mind pedig a fejlődési autofágia gátlását láttuk az autofagoszómális GFP-Atg8a és az autolizoszómális Lysotracker jel hiánya, valamint ultrastrukturális vizsgálatok alapján (Juhasz és mtsai, 2007a). Érdekes módon azt láttuk, hogy a lárválisbél metamorfózis során megfigyelhető zsugorodásához az Atg7 nem igazán szükséges, ami szintén egy nem várt megfigyelés volt, tekintve hogy az autofágia poliploid lárválisszervek eliminációjában játszott potenciális szerepét feltételezni lehetett.

Az *Atg7* mutáns imágók életképessége megkönnyítette vizsgálatukat, hiszen olyan teszteket is el tudtunk végezni amikhez adult legyek szükségesek. Az imágók éhezés hatására a kontrol állatokhoz képest hamarabb elpusztultak, és a különféle oxidációs károsodásokat okozó kezeléseket (parakvat, hidrogén-peroxid) is kevésbé tolerálták, ami az Atg7-függő autofágia jótékony hatásaira utal. Ezen felül a mutánsok élethossza is jelentősen csökkent: az állatok fele átlagosan már 31 napos korukra elpusztult, míg a vad típusú kontrol esetén ez az érték 43 napnak adódott. A mutánsok 30 napos korukra (ami nagyjából középkorúnak tekinthető) már igen rosszul teljesítettek a neuromuszkuláris rendszer állapotát felmérő negatív geotaxis reflexet vizsgáló, ún. mászási tesztekben. Ekkor az idegsejtek többsége már pusztulófélben volt, mivel sejtmagi DNS állományuk fragmentálódott, ami megmagyarázza, hogy miért nem képesek már mászni ezek az állatok (Juhasz és mtsai, 2007a).

Kimutattuk továbbá az *Atg7* mutáns imágók neuronjaiban az ubikvitinált fehérjéket tartalmazó aggregátumok felhalmozódását mind western blot kísérletben, mind pedig ultrastrukturális szinten immun-arany jelöléssel (**4. ábra**) (Juhasz és mtsai, 2007a). Feltehetően az abnormális, lebontásra kijelölt fehérjék akkumulációja ok-okozati viszonyban van a neuronok funkcióvesztésével és pusztulásával.



4. ábra. *Az ubikvitinált fehérjék lebontásához szükséges az autofágia.* ***A*** *Atg7 mutáns legyek idegsejtjeiben az ultrastrukturális kép alapján homogén szürkének látszó fehréjeaggregátumok halmozódnak fel (csillaggal jelölve).* ***B*** *Ezek az inklúziós testek ubikvitinált fehérjéket tartalmaznak az anti-ubikvitin elsődleges és 10 nm átmérőjű aranyszemcsékkel jelölt másodlagos ellenanyagokkal végzett immun-arany kimutatás alapján (fekete pöttyök a csillaggal jelölt aggregátum területén) (Juhasz és mtsai, 2007a).*

Vizsgálataink az akkortájt közölt, neuronspecifikus *Atg7* és *Atg5* génkiütött egerekről szóló publikációkkal együtt nemcsak megalapozták az alapszintű autofágia evolúciósan konzervált neuroprotektív hatását, hanem arra is rámutattak, hogy az autofágia az ubikvitinált fehérjék lebontásához nélkülözhetetlen, tehát ezt a feladatot a proteaszóma önmagában nem képes ellátni (Hara és mtsai, 2006; Komatsu és mtsai, 2006). A két fehérjebontó rendszer szoros kapcsolatával összhangban a kutatócsoportomban végzett későbbi vizsgálatainkban azt tapasztaltuk, hogy a proteaszóma genetikai inaktiválása - emlős sejtekhez hasonlóan - *Drosophila*-ban is kompenzáló autofágiát indukál (Korolchuk és mtsai, 2010; Low és mtsai, 2013).

Mind az autofág, mind pedig a proteaszomális lebontás gátlásakor a sejtekben felszaporodnak az ubikvitinált fehérjéket tartalmazó aggregátumok. Ezekben az inklúziós testekben az evolúciósan konzervált p62 fehérje is megtalálható, melyet emlősökben SQSTM-1, *Drosophila*-ban pedig Ref(2)P (Refractory to sigma P) névvel is illetnek. Az autofágia

gátlásakor felhalmozódó p62 szintjének mérése igen gyorsan az egyik leggyakrabban használt tesztté vált tenyésztett emlős sejtekben (Bjorkoy és mtsai, 2009). Emiatt nem volt meglepő, hogy az általunk előállított *Drosophila* p62 ellenanyaggal legyekben is kiválóan tudtuk követni az autofágia hibáját western blot és indirekt immunfluoreszcenciás jelölést követő mikroszkópos kísérleteinkben (Pircs és mtsai, 2012). Ezen módszerek alapvető fontosságának és a kiváló reagensünknek köszönhetően p62 ellenanyagunkat kérések alapján eddig több mint 50 kutatócsoportnak küldtük el, és természetesen minden ezt követően publikált kísérletes cikkünkben használtuk.

Szakirodalmi adatok alapján tudtuk, hogy p62 hiányában *Atg* mutáns sejtekben nem alakulnak ki ubikvitinált fehérjeaggregátumok sem *Drosophila*, sem pedig emlősök esetén (Komatsu és mtsai, 2007; Nezis és mtsai, 2008). Megfigyeléseink szerint a p62 az Atg8a mellett egyéb Atg fehérjékkel is kölcsönhatásba léphet. Feltehetően ennek köszönhető amit a kutatócsoportomban végzett kísérleteinkben tapasztaltuk: azt láttuk ugyanis, hogy a genetikailag később, downstream ható *Atg* génekre mutáns sejtekben a fagofór képződésben ismereteink szerint korábban, azaz upstream ható Atg fehérjék a p62 aggregátumokon halmozódnak fel, az Atg9 transzmembrán fehérjét hordozó vezikulumokkal együtt. Ezt mind fluoreszcens mikroszkópos kolokalizációs, mind pedig immun-arany jelölést követő ultrastrukturális eredményeink is alátámasztják (Nagy és mtsai, 2014a; Nagy és mtsai, 2014b; Nagy és mtsai, 2015). Ez felveti annak a lehetőségét, hogy ezek a p62-t és ubikvitinált fehérjéket tartalmazó aggregátumok az autofagoszóma képződés helyeként (platform) szolgálhatnak, tehát egy abnormális, fejlődésében megrekedt és ezért óriásira növekvő autofagoszóma összeszerelődési helynek tekinthetők.

A későbbiekben részletesen tárgyalt autofagoszóma-lizoszóma fúzióhoz szükséges fehérje, a Syntaxin 17 hiányában szintén a lebontatlan p62 felhalmozódását láttuk, valamint mozgásképtelenség alakul ki és drasztikusan lerövidül az állatok élethossza (Takats és mtsai, 2013), összhangban a központi *Atg* géneket érintő mutációk hatásával.

3. Az ER stressz-indukált autofágia szükséges a Myc túltermeltetés által fokozott sejtnövekedéshez Drosophila-ban

Új, autofágiát szabályozó gének azonosítása egy nagyléptékű genetikai szűrővizsgálatban

2009 őszén kezdtünk el egy nagy léptékű genetikai szűrővizsgálatot, amelyet az önálló laborom megalapítását támogató Wellcome Trust finanszírozott. A projekt során a konzervált genom több mint 90%-át teszteltük, tehát az egyértelmű humán homológgal rendelkező *Drosophila* gének nagy részét megvizsgáltuk abból a szempontból, hogy RNS interferenciával történő csendesítésük befolyásolja-e az éheztetéssel indukált autofágiát. Ezt a széleskörben használt és már jól bevált klonális analízis segítségével teszteltük, tehát GFP-vel jelölt RNSi sejtek fenotípusát hasonlítottuk a szomszédos kontroll sejtekéhez, mCherry-Atg8a

riporter felhasználásával. Mivel a közel 8000 tesztelt RNSi vonal közül mintegy 1000 esetében láttuk az mCherry-Atg8a jel szám-, méret- vagy intenzitásbeli csökkenését vagy növekedését, ezért ezeken a potenciális jelölteken további teszteket végeztünk. Többek között vizsgáltuk a zsírtestben autolizoszómákat jelölő Lysotracker Red festődést, a fehérjeaggregátumok számát anti-p62 immunjelöléssel, valamint az autofág flux teszthez széleskörben használt riporter, az mCherry-GFP-Atg8a fehérje eloszlását (Kimura és mtsai, 2007). Az endogén Atg8a ugyanis az autofagoszómák belső membránjához is köt, ezért fúziót követően az autolizoszómában lebomlik. A fúziós riporter-fehérje esetén az mCherry viszonylag hosszú ideig fluoreszcens marad a lizoszómák belsejére jellemző savas pH-n és ellenáll a hidrolázoknak is, ezért autofágia során az autolizoszómákban felhalmozódik. Ezzel ellentétben a GFP savas pH-n gyorsan inaktiválódik, így egy kettős, tandem fúziós riporterrel vizsgálva kontroll sejtekben az autofagoszómák GFP és mCherry pozitívak, míg az autolizoszómák mCherry pozitívak és GFP negatívak lesznek. A különféle tesztek során készült mikroszkópos képek kiértékelése minden esetben úgy történt, hogy a párhuzamosan értékelő három doktorandusz hallgatóm nem ismerte sem az adott genotípust, sem pedig a társai által adott pontszámokat. Az ebben a szűrővizsgálatban azonosított gének (mint például a *Myc*, *Syx17*, *usnp*, *Vamp7*, és a HOPS pányvázó komplex alegységeinek génjei) analízise már jónéhány cikkünk alapjául szolgált, amelyeket a következő fejezetekben részletesebben tárgyalok.

A Drosophila Myc szükséges az autofágiához

Nagy léptékű genetikai szűrővizsgálatunkban azt találtuk, hogy a *Myc* gén csendesítése gátolja az éhezéssel kiváltott autofágiát a lárvális zsírtestben. A Myc-Max komplex egy heterodimer transzkripciós faktor, és a sejtnövekedésben szerepet játszó gének transzkripcióját fokozza a promóter régiókban található E-box szekvenciához kötődve. Ezt a hatást a transzkripciós represszorként működő Mad-Max komplex képes antagonizálni. További vizsgálatainkban kimutattuk, hogy *Myc* RNS interferenciával történő gátlása, vagy a Mad overexpressziója gátolja az alapszintű és az éhezés-indukálta autofágiát anti-p62, Lysotracker és anti-Atg8a festések alapján. Ezt *Myc* null mutáns állatok vizsgálatával is megerősítettük, szintén Lysotracker és ultrastrukturális vizsgálatokkal (Nagy és mtsai, 2013).

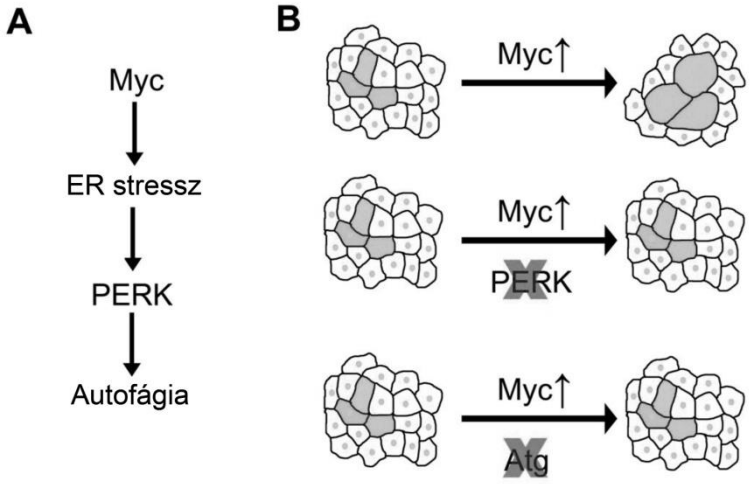
A Myc ER stressz kiváltása révén fokozza az autofág aktivitást

Mivel a *Myc* humán homológja egy onkogén és túlműködése a rák kialakulásának az egyik leggyakoribb kiváltó oka, ezért funkciónyeréses vizsgálatokat is végeztünk. Ismert volt, hogy a *Drosophila* Myc overexpressziója látványosan fokozza mind a poliploid, mind pedig a diploid sejtek növekedését (Pierce és mtsai, 2004). Mi azt tapasztaltuk, hogy a Myc túltermeltetése mindkét sejttípusban autofágiát indukál a megnövekvő Lysotracker és anti-Atg8a festés, valamint mCherry-Atg8a riporter pöttyök megjelenése alapján. A mechanizmus felderítését keresve kimutattuk, hogy Myc túltermelés hatására a feltehetően nem megfelelő térszerkezetű fehérjék endoplazmás retikulumban történő felhalmozódása ER stresszt vált ki,

melyet a PERK kináz szubsztrátjának, az eIF2α-nak (Eukaryotic Initiation Factor 2α) a foszforilációja jelez. Ez mind western blot, mind pedig immunjelöléses mikroszkópos vizsgálatainkban egyértelmű volt (Nagy és mtsai, 2013). Az ER stressz szignalizációban szereplő PERK (protein kinase RNA-like endoplasmic reticulum kinase) gén csendesítése, vagy a kináz aktivitását antagonizáló Gadd34 (growth arrest and DNA damage-inducible protein) foszfatáz túltermeltetése valóban megakadályozta a Myc-indukált autofágiát az mCherry-Atg8a riporter pöttyszerű eloszlásának gátlása alapján.

A Myc-indukált ER stressz-autofágia útvonal szükséges a fokozott sejtnövekedéshez

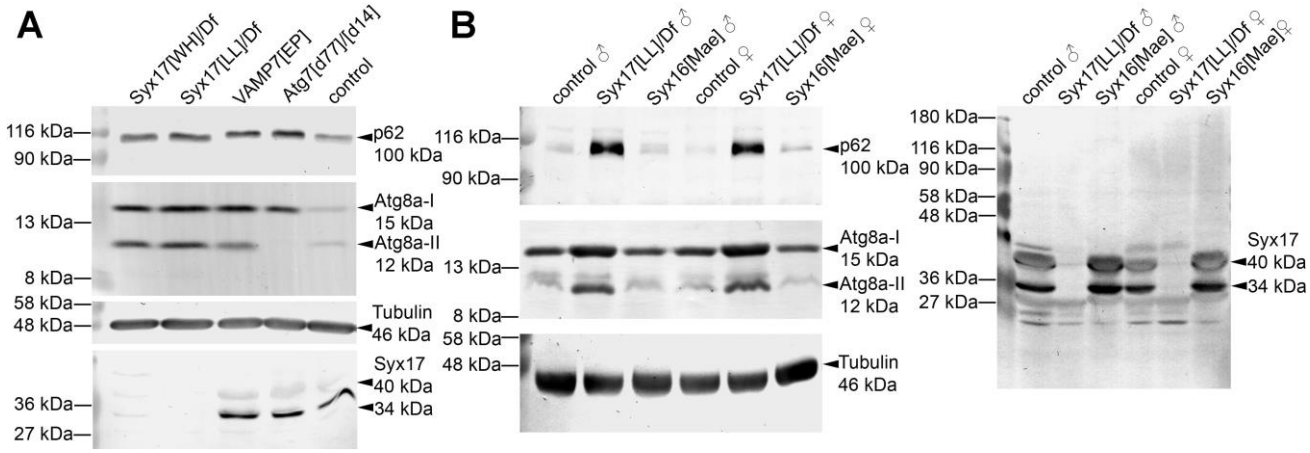
Amennyiben a PERK-eIF2α jelátvitelt gátoltuk, az megakadályozta a Myc-indukált sejtnövekedést (Nagy és mtsai, 2013). RNS interferencia kísérletek és mutánsok, valamint a klinikai terápiában is használt lizoszomális lebontást gátló drog (klorokvin) felhasználásával kimutattuk, hogy az autofágia gátlásakor a Myc sem a poliploid, sem pedig a diploid sejtek növekedését nem képes fokozni. Ugyanakkor az autofágia vagy a PERK-eIF2α útvonal gátlása a normál sejtek növekedését nem változtatta meg számottevően. Ezekből a kísérletekből azt a következtetést vontuk le, hogy az ER stressz jelátvitel és az autofágia szükségesek a Myc-indukált túlnövekedéshez, azonban a vad típusú sejtek növekedését nem befolyásolják (Nagy és mtsai, 2013). Kísérleteink eredményeinek sematikus összefoglalását az **5. ábra** mutatja be.



5. ábra. *A Myc és az autofágia kapcsolata.* ***A*** *Myc túltermelés ER stresszhez vezet, ami a PERK kináz aktiválódása révén autofágiát indukál.* ***B*** *A PERK és az autofágia (Atg gének) szükségesek a Myc-indukált túlnövekedéshez: a Myc túltermelése mozaik állatokban fokozza a sejtnövekedést (szürke színnel kitöltött, megnagyobbodó sejtek a képpanel felső sorának jobb oldalán), ez a hatás azonban a PERK vagy Atg gének gátlásakor elmarad (Nagy és mtsai, 2013).*

4. Az autofagoszóma-lizoszóma fúzióban egy Syntaxin 17-tartalmú SNARE komplex és a HOPS pányvázó komplex vesznek részt

A nagyszabású genetikai szűrővizsgálatunkban azonosított RNSi vonalak között volt egy olyan csoport, amelynél igen érdekes fenotípust láttunk: minden általunk használt teszt alapján arra lehetett következtetni, hogy kialakulnak ugyan az autofagoszómák, ám nem képesek lizoszómákkal fúzionálni és emiatt felhalmozódnak a zsírtestsejtekben. Ugyanis éheztetést követően nem láttunk Lysotracker-pozitív autolizoszómákat a géncsendesített sejtekben, és az mCherry-Atg8a struktúrák száma megnőtt ugyan, de ezek lényegesen kisebbek és halványabbak mint a környező kontrol sejtekben. Három SNARE (soluble NSF attachment protein receptor) fehérjét kódoló gén került ebbe a csoportba: a *Syx17* (*Syntaxin 17),* az *usnp/SNAP-29 (ubisnap/Synaptosomal-associated protein 29)* és a *Vamp7 (Vesicle-associated membrane protein 7)* (Takats és mtsai, 2013). A SNARE fehérjék rendszerint membránfúziót katalizálnak, így feltételeztük, hogy a fenti három fehérje által alkotott komplex az autofagoszómák késői endoszómával vagy lizoszómával történő egyesülésében szerepel. A *Syntaxin 17* és *Vamp7* mutáns állatok is az RNSi sejtekhez hasonló autofágia defektust mutattak, amit a Syx17 esetében vad típusú transzgén visszaadásával helyre tudtunk állítani. Az autofagoszómák felhalmozódását és az autolizoszómák hiányát ultrastrukturális vizsgálatokkal és western blot kísérletekben is megerősítettük (**6. ábra**).



6. ábra. *A Syx17 szükséges az autofagoszóma-lizoszóma fúzióhoz.* ***A*** *A Syx17 különböző mutáns allélkombinációi (WH vagy LL jelű transzpozon inszerció/deficiencia) és a Vamp7 mutációja az Atg7 null mutánsokhoz hasonló mértékű p62 felhalmozódáshoz vezet éhező lárvákban a vad típusú,* kontrol *lárvákhoz képest western blot kísérletekben. Jól látható a lipidált, autofagoszóma-asszociált Atg8a-II felhalmozódása is a Syx17 és Vamp7 mutáns lárvákban. Természetesen ez az izoforma az Atg7 mutánsoknál hiányzik. A Syx17 fehérje expressziója gátolt mindkét Syx17 mutánsban.* ***B*** *Adult állatokban még egyértelműbb a Syx17*

hiányában történő p62 és autofagoszóma-asszociált Atg8a-II felhalmozódás a vad típusú, vagy a további kontrolként használt Syx16 mutáns állatokhoz képest.

Azt is kimutattuk, hogy ezek a SNARE fehérjék a p62 és az Atg8a-pozitív autofagoszómák jól táplált állatokban is látható felhalmozódása alapján az alapszintű autofágiához, valamint a vándorló lárvák zsírtestének Lysotracker-rel és mCherry-Atg8a-val történő vizsgálata alapján a fejlődési autofágiához is esszenciálisak (Takats és mtsai, 2013).

Immunprecipitációs kísérletekkel igazoltuk, hogy ez a három SNARE fehérje valóban egy komplexet alkot. Tenyésztett *Drosophila* sejtekben overexpresszált, tag-elt fehérjéket használva azt láttuk, hogy a Syx17 mind az usnp-vel, mind a Vamp7-tel kölcsönhat, valamint hogy az usnp jelenléte erősíti a Syx17 és a Vamp7 kölcsönhatását (Takats és mtsai, 2013). Ezek az eredmények teljes mértékben egybevágnak a SNARE komplexek összeszerelődésével kapcsolatos tudásunkkal, hiszen a Syx17 egy Qa SNARE, az usnp-nek Qb és Qc doménjei is vannak, míg a Vamp7 egy R SNARE (a Q és R betűk a SNARE domén közepén, az ún. nulladik rétegben található aminosav egybetűs kódjára utalnak, ami glutamin vagy arginin). Ugyanis pontosan ez a négy SNARE domén található meg egy működőképes, fuzogén SNARE komplexben. Természetesen fontos volt igazolni azt is, hogy ez a komplex in vivo létezik, azaz hogy endogén fehérjék szintjén is látható kölcsönhatás. Ezt a Syx17 és az usnp fehérjék esetén sikerült kimutatnunk az általunk létrehozott ellenanyagokkal mind adult legyek, mind pedig tenyésztett sejtek lizátumában: a Syx17 immunprecipitációban jelent volt az usnp, és fordítva, az usnp immunprecipitációjával a Syx17-et is detektálni tudtuk (Takats és mtsai, 2013).

Kolokalizációs eredményeink pedig arra engedtek következtetni, hogy a Syntaxin 17 az a SNARE fehérje, ami egyelőre még nem ismert módon az autofagoszómákra kerül: az endogén Syx17 jelen volt a GFP-Atg8a- illetve endogén Atg8a-pozitív autofagoszómák egy részén. Ezt immun-arany jelölést követő elektronmikroszkópos vizsgálatokkal is megerősítettük (Takats és mtsai, 2013). Tehát az autofagoszómák a Syx17 odatoborzásával válnak kompetenssé a késői endoszómákkal vagy lizoszómákkal való egyesülésre.

A *Syntaxin 17* mutáns állatok a korábban említett *Atg7* mutánsokhoz hasonlóan életképesnek bizonyultak, ámbár a metamorfózis sikeres befejeztével kikelő imágók többsége 3-4 napon belül elpusztul. A mutánsok agyában döbbenetes mértékű autofagoszóma felhalmozódást láttunk endogén Atg8a jelölés és ultrastrukturális vizsgálatok alapján, és - a feltehetően ennek következtében kialakuló idegsejt-működési zavarok miatt - ezek az állatok igen rosszul teljesítenek a neuromuszkuláris funkciót mérő mászási tesztekben (Takats és mtsai, 2013). Némi apoptotikus kaszpáz aktivációt és sejtmagi DNS fragmentációt is megfigyeltünk a mutáns állatok neuronjaiban, azonban az apoptózis gátlása (kaszpáz inhibitor fehérjék túltermeltetésével) nem menekítette a mászáshibát, ellentétben a vad típusú transzgén visszaadásával. Ezért feltételezzük, hogy a Syx17 hiányában felhalmozódó autofagoszómák és p62 megzavarja az idegsejtek (és talán szintén az izomsejtek) normális működését.

Élesztőben az autofagoszóma-lizoszóma fúzióhoz szükséges a HOPS (homotypic vacuole fusion and protein sorting) pányvázó (tethering) komplex. A HOPS-szal autofagoszóma-vakuólum fúzió során kölcsönható SNARE fehérjék (Vam3, Vam7, Vti1) közül azonban az első kettőnek nincsen állati homológja (Wang és mtsai, 2002). Emlős és *Drosophila* sejtekben a HOPS autofágiában betöltött szerepe némileg kérdéses volt, különösen mivel eredményeink alapján teljesen más SNARE fehérjék szerepelnek a fúzióban. RNS interferencia-alapú genetikai szűrővizsgálatunkban a HOPS komplex mind a hat *Drosophila* alegységét (car, dor, lt, Vps11, Vps16A és Vps39) az autofagoszóma-lizoszóma fúzióban hibás csoport tagjaiként azonosítottuk, éheztetett mozaikos lárvák zsírtestének Lysotracker festése és az mCherry-Atg8 riporter megváltozott eloszlása alapján. Ezt igazoltuk *Vps16A* és *Vps11* mutánsok létrehozásával illetve karakterizálásával, továbbá korábban már leírt *car, dor* és *lt* mutánsok vizsgálatával: az autofagoszóma-asszociált endogén Atg8a és a p62 aggregátumok mikroszkópos és western blot kísérletekben felhalmozódtak. Az autofagoszómák akkumulációja és az autolizoszómák kialakulásának gátlása a *Vps16A, Vps11* és *lt* mutánsok zsírtestében szintén egyértelműen látszott az elektronmikroszkópos kísérleteinkben. Az ebben a munkában létrehozott *Vps16A* mutáns esetén pedig a vad típusú transzgén visszaadásával genetikai menekítő vizsgálatokban igazoltuk, hogy a látott fenotípusokat ténylegesen ennek a génnek a deléciója okozza (Takats és mtsai, 2014b).

Kolokalizációs kísérletekben a Vps16A fehérjét ki tudtuk mutatni az Atg8a- és Syx17-pozitív autofagoszómákon, és immunprecipitációs eredményeink szerint a HOPS komplex köt a Syntaxin 17 fehérjéhez: a car, dor és Vps16A esetén sejttenyészetben overexpresszált fehérjék, és a car esetében az endogén fehérjék közti kölcsönhatást is detektáltuk. Csonkolt Syx17 fehérjédarabokat használva pedig kimutattuk, hogy a HOPS leginkább a Syx17 SNARE doménjéhez köt, különösen a Syx17 transzmembrán doménjeinek jelenlétében (Takats és mtsai, 2014b).

Már ismert volt, hogy a HOPS komplex szerepel a késői endoszómák lizoszómákkal történő fúziójában és a lizoszómába irányuló bioszintetikus transzportban is. Az endocitotikus folyamat hibáját a fejlődő szemdiszkuszon végzett immunfestési kísérleteinkben a Notch és a Boss (endocitózissal lebomló, transzmembrán doménnal rendelkező jelátviteli molekulák) akkumulációja igazolta *car, dor, Vps16A* és *lt* mutánsok esetén. A lizoszómák biogenezise is zavart szenvedett a HOPS hiányában, amit lizoszómális fehérjék (LAMP, katepszin D) western blot kísérletekben látott felhalmozódása mellett a kifejlett muslica imágó szemének piros színét adó, lizoszóma-szerű pigment granulumok kialakulásának hibájaként is detektálni tudtuk. Mivel azt találtuk, hogy az endocitotikus és lizoszómális bioszintetikus folyamatok *Syntaxin 17* mutáns állatokban normálisan zajlanak, ezért arra a következtetésre jutottunk, hogy a HOPS Syntaxin 17-tel való kölcsönhatása autofágia-specifikus, tehát az endoszóma-lizoszóma fúzióban és a lizoszómába irányuló bioszintetikus transzportban nyilvánvalóan egy másik Qa SNARE fehérje szerepel (Takats és mtsai, 2014b).

Egy másik projektben kimutattuk, hogy a kis GTPáz Rab11 az éhezés hatására képződő autofagoszómákra vándorol az endoszómákról, és a késői endoszómákkal és lizoszómákkal történő fúziójukat serkenti (Szatmari és mtsai, 2014). Ebben a munkában az ELTE Anatómia Tanszékén dolgozó kollégákat segítve, főként tanácsokkal és akkor még nem publikált

reagenseink és módszereink biztosításával vettem részt, ezért az eredmények részletes tárgyalásától most eltekintek.

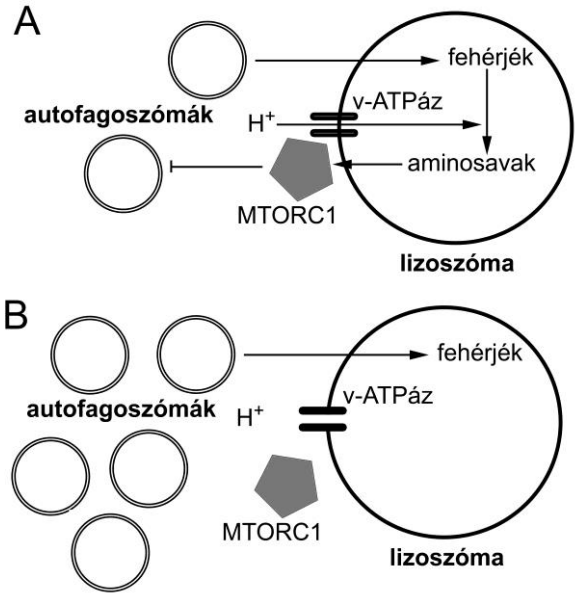
5. A lizoszómális lebontás hibájakor lecsökkenő TOR aktivitás miatt több autofagoszóma alakul ki

Az utóbbi évek igen fontos felfedezése volt, hogy a TOR a lizoszómákhoz kapcsolódva aktiválódik, ami a lizoszómán elhelyezkedő ún. Ragulator komplex és a Rag kis GTP-áz fehérjék kötése révén valósul meg (Sancak és mtsai, 2010). Ehhez szükséges még az is, hogy a lizoszómák belsejében a szabad aminosavak megfelelő koncentrációban legyenek jelen, azaz hogy a lizoszóma fehérjéket bontson le a savas pH-t biztosító lizoszómális proton pumpa, a v-ATPáz közreműködésével (Zoncu és mtsai, 2011). A legújabb eredmények alapján az SLC38A9 (Solute Carrier Family 38, Member 9) nevű lizoszómális aminosav-transzporter az a fehérje, ami valamiképpen jelez a TOR kináznak a lizoszómális aminosavak megfelelő szintjéről (Rebsamen és mtsai, 2015; Wang és mtsai, 2015).

Ezek az eredmények azért lényegesek az értekezésem szempontjából, mert az autofágiát sejttenyészetben kutatók többsége rutinszerűen alkalmaz lizoszomális lebontást gátló szereket az autofág flux meghatározására, azaz annak megállapítására, hogy időegység alatt mennyi autofág szállítmány degradálódik (Mizushima és mtsai, 2010). Ilyen gátlószerek például a korábban már említett bafilomicin A1 és a klorokvin. Ez utóbbi egy lizoszomotróp ágens amit a savas beltartalmú lizoszóma felvesz, és az ezt követő protonáció révén az intralizoszómális pH megemelkedik. A flux vizsgálatok bevett módja az Atg8 egyik emlős homológjának, az LC3-nak a lipidált, autofagoszóma-asszociált mennyiségének meghatározása western blot segítségével, vagy az LC3 sejten belüli eloszlásának (az LC3-pozitív pöttyök számát) vizsgálata gátlószer nélkül és gátlószer jelenlétében. E kettő különbségéből szokás az autofág lebontó aktivitásra következtetni. Arra azonban senki sem gondolt, hogy a lizoszomális lebontás gátlása a TOR aktivitását csökkentheti, és így a gátlószer kezelés serkentheti az autofagoszóma képződést és emiatt meghamisíthatja a flux vizsgálatok eredményét (**7. ábra**). Ezt az elméletet egy önálló, egyszerzős publikációmban fogalmaztam meg, ami egy minor revíziót követően szinte rögtön publikálásra került (Juhasz, 2012). Ebben a fenti ötlet kifejtése mellett leírtam, hogy a lizoszómális lebontást gátló szerek alkalmazásakor fontos a TOR kináz aktivitását is meghatározni, például az általa foszforilált 4E-BP (eukaryotic Initiation Factor 4E-Binding Protein) vagy S6K (S6 kinase) vizsgálatával.

Természetesen ezt a felvetést kísérletesen is meg szerettük volna vizsgálni, különösen mivel a Syx17 és HOPS analízisekor egyértelműen láttuk, hogy a HOPS hiányában jóval több autofagoszóma halmozódik fel, mint a *Syx17* mutáns állatokban. Ezt csak úgy tudtuk magyarázni, hogy a HOPS mutánsokban valamilyen okból több autofagoszóma keletkezik, hiszen a Syx17 hiányában is teljes mértékben gátolt az autofagoszóma-lizoszóma fúzió. A HOPS lizoszómába irányuló bioszintetikus és endocitotikus transzportban játszott szerepe alapján azt vártuk, hogy az autofagoszóma képződés fokozódását a lizoszóma-asszociált TOR

kináz csökkent aktivitása okozza. Ezt sikerült is kimutatnunk anti-foszfo-S6K western blot és anti-foszfo-4E-BP immunfestési kísérleteinkben. Ez utóbbi eredményeink a doktori cselekményem megindításakor már rendelkezésünkre álltak, ezért bátorkodom a dolgozatomban utalni rájuk. Időközben - azaz a doktori értekezésem átdolgozásáig - a kapcsolódó publikációnk is megszületett, melyben számos e helyütt nem részletezett további eredményt közöltünk a fentiek alátámasztására (Takats és mtsai, 2015).



7. ábra. *A TOR aktivitás és az autofág lebontás összefüggése.* ***A*** *Az éhezés során autofágia révén keletkező aminosavak reaktiválják a v-ATPáz protonpumpa komplexhez kötődő TOR kinázt (a képen MTORC1, azaz mechanistic target of rapamycin complex 1 néven jelölve), ami az autofagoszóma keletkezést gátolja.* ***B*** *Autofág/lizoszomális lebontást gátló szerek alkalmazásakor a TOR reaktiválódása és lizoszomális transzlokációja zavart szenved, aminek hatására az* ***A*** *panelen jelölthöz képest több autofagoszóma keletkezhet*

DISZKUSSZIÓ

1. Az autofagoszómák kialakulását az autofág géntermékek hierarchikus hálózata kontrollálja *Drosophila*-ban, melyek transzkripciója fokozódik autofág indukció során

Az autofág géntermékek aznosítását és funkcionális komplexekbe sorolását követően több kutatócsoport is megkísérelte az episztázis viszonyok felderítését. Kezdetben egyfajta lineáris sorba próbálták rendezni ezeket, rendszerint az Atg1 protein kináz komplexet említve elsőnek, másodiknak a Vps34 lipid kináz komplex került, majd ezt követte a lipid kináz effektor Atg18 és kötőpartnerei: az Atg2, valamint az egyetlen transzmembrán Atg fehérje, az Atg9, végül pedig az ubikvitinszerű protein konjugációs rendszerek. Élesztőben Dr. Yoshinori Ohsumi, az első autofág géneket felfedező kutatócsoport vezetője az Atg fehérjék a pro-Ape1 szelektív autofág szállítmány által kijelölt PAS-hoz (phagophore assembly site/pre-autophagosomal structure) történő lokalizációját vizsgálta különféle *Atg* mutáns háttereken. Az adataikat igen nehéz volt azonban értelmezni, ezek alapján végül arra a következtetésre jutottak, hogy az Atg9 már jóval hamarabb, az Atg1 komplex szintjén szerepel, és hogy az Atg2-Atg18 komplex az Atg8-Atg12 konjugációs rendszerekkel párhuzamosan hathat. Az efféle hierarchia-vizsgálatok másik fontos kutatója Dr. Noboru Mizushima csoportja, aki a fent leírt, egyszerűsített modellhez hasonló eredményekről számolt be kezdetben (Itakura és Mizushima, 2010). Egy újabb publikációjukban azonban leírták, hogy az autofág géntermékek kapcsolatai jóval bonyolultabbak egy egyszerű, lineáris sornál. Azt találták, hogy ugyan az Atg1/ULK1 protein komplex aktiválódik elsőként éhezés során emlős sejtekben, azonban az ezt követő Vps34 lipid kináz komplex aktiváció erre visszahat, mintegy megerősíti a kezdeti lépést (Koyama-Honda és mtsai, 2013). Megjegyzendő, hogy Dr. Terje Johansen kutatócsoportja, aki a p62 autofág szerepének felfedezéséről híres (Bjorkoy és mtsai, 2005; Pankiv és mtsai, 2007), kimutatta hogy az Atg1/ULK1 protein kináz komplex alegységei kötik az Atg8 családba tartozó fehérjéket funkcionális LIR motívumok révén (Alemu és mtsai, 2012). Ez világosan mutatja, hogy az Atg1/ULK1 kináz a lipidációja révén fagofórba horgonyzott Atg8-szerű fehérjékhez kötve fejtik ki aktivitásukat, tehát az Atg8/LC3 is visszahat a tőlük upstream funkcionáló komplexekre.

A vezetésemmel végzett *Drosophila* kutatásaink során az *Atg* gének homológjainak többségét már vizsgáltuk. Kezdetben én is igen lelkesem vágtam bele ezen gének hierarchiájának felderítésébe, azonban a saját és fent említett szakirodalmi adatok, valamint a Dr. Mizushimával és Ohsumival konferenciákon időről időre zajló egyeztetések kapcsán világossá vált, hogy ez a fajta analízis ma már nem feltétlenül kecsegtet kiemelkedő publikációkkal. Emellett meggyőződésemmé vált, hogy a *Drosophila* modell fő előnye az, hogy az autofágia szerepét sokféle, az emberéhez hasonló funkciójú sejtben, szövetben, szervben, és egy teljes állatban tudjuk vizsgálni. Emiatt az utóbbi években tudatosan elfordultunk az ilyenfajta kísérletektől, bár több korábban megkezdett projektünket sikerült publikációval lezárnunk az elmúlt néhány évben. Mint azt az Eredmények fejezetben

kifejtettem, mi is azt találtuk, hogy az Atg1 kináz komplex tagjai, azaz az Atg1 és a FIP200/Atg17 viszonylag upstream helyezkednek el. Fontos megfigyelésünknek tartom azt is, hogy autofágia gátlás esetén a szelektív szállítmány p62 aggregátumain - az élesztő pro-Ape1-hez hasonlóan - felhalmozódnak az autofág géntermékek, mint például a FIP200/Atg17 és az Atg9 (Nagy és mtsai, 2014a; Nagy és mtsai, 2014b).

Az autofágia és az endocitózis kapcsolata igen bonyolult és sokrétű. Feltehetően ennek köszönhető az, hogy a *Drosophila* Vps34-gyel kapcsolatos eredményeink széleskörben ismertek és idézettek. Posztdoktori kutatásaim során bizonyítottuk, hogy a Vps34 mind az autofagoszóma képződésben mind pedig az endoszóma érésben fontos szerepet játszik, sőt, még a lizoszómális fehérjék sejten belüli célbajuttatásához is hozzájárul. A *Vps34* mutáns sejtek autofágoszóma képződési hibájával ellentétben a lebontásra szánt receptorokat osztályozó multivezikuláris endoszómák kialakításához szükséges ESCRT (endosomal sorting complex required for transport) mutánsokban - másokkal összhangban (Rusten és mtsai, 2007) - azt láttuk, hogy autofagoszómák normálisan képződnek (sőt felhalmozódnak, mivel nem képesek lebontó autolizoszómává alakulni), tehát a Vps34 autofág szerepe az endocitózisban játszott funkciójától független (Juhasz és mtsai, 2008). Más megfogalmazásban autofágia során az ESCRT mutáns fenotípus episztatikus a *Vps34*-hez képest, azaz kettős mutáns sejtekben az ESCRT elvesztésének hatása érvényesül.

Az autofág géntermékek viszonyai, az autofágia során játszott szerepük kapcsán a szakirodalom döntő része a poszt-transzlációs szabályozási módokat boncolgatja, a gének kifejeződését és annak regulációját csak elvétve vizsgálják. Az *Atg* gének autofágia során általunk *Drosophila*-ban leírt transzkripciós indukciója világosan mutatja, hogy még jócskán van mit kutakodnunk az autofágia transzkripciós szabályozása kapcsán (Erdi és mtsai, 2012). Ennek kapcsán említem meg, hogy elsőként mutattam ki a Foxo transzkripciós faktor kulcsszerepét autofág indukció során (Juhasz és mtsai, 2007b), amit nem sokkal ezután emlős sejtekben is igazoltak, idézve az én munkámat (Mammucari és mtsai, 2007; Zhao és mtsai, 2007).

2. Az autofágia szükséges az ubikvitinált fehérjéket és p62-t tartalmazó aggregátumok lebontásához, és hibája mozgásképtelenséget és rövid élethosszt okoz Drosophila-ban

Posztdoktori kutatásaim egyik legfontosabb eredménye az *Atg7* null mutáns legyek létrehozása és vizsgálata volt. Az egyik legmeglepőbb felfedezésem az, hogy az Atg7-függő autofágia nem szükséges az életképességhez, azonban a kifejlett legyek agyában található neuronok funkciójának fenntartásában, az ubikvitinált fehérjék lebontásában, és a neurodegeneráció következtében kialakuló mozgásképtelenség és rövid élethossz elkerülésében kulcsszerepet játszik. Az eredményeim jelentőségét jelzi, hogy a cikkünk online megjelenésének napján kaptunk egy megkeresést a Cell szerkesztőitől, és így a Cell „Leading edge" rovatában megjelent egy, a munkánkat taglaló rövid leírás, valamint az Autophagy szaklap főszerkesztőjének felkérésére a cikkhez kapcsolódó és további *Atg7* mutáns

fenotípusokat bemutató önkommentárt is írtunk (Anonymous, 2007; Juhasz és Neufeld, 2008a). A későbbiekben neuromuszkuláris defektust és megrövidült élethosszt mutattunk ki a *Syntaxin 17* mutáns állatokban is, összhangban azzal, hogy nemcsak az autofagoszómák kialakulása hanem a megfelelő lebontásuk is igen fontos (Takats és mtsai, 2013).

Fent leírt megfigyeléseink tökéletesen egybevágnak a neuron-specifikus *Atg* génkiütött egerekben leírt fenotípusokkal (Hara és mtsai, 2006; Komatsu és mtsai, 2006). Ezek a publikációk - az én cikkemmel együtt - alapozták meg az autofágia ubikvitinált fehérjék lebontásában, valamint a neurodegeneráció elkerülésében játszott alapvető, evolúciósan konzervált szerepét. Mint az már közismert, ehhez az aggregátumok létrejöttét és autofág lebontását elősegítő p62 működése szükséges mind emlősök, mind pedig *Drosophila* esetén (Komatsu és mtsai, 2007; Nezis és mtsai, 2008).

Egy másik munkában azt is kimutatták, hogy a *Drosophila* Atg8a neuron-specifikus túltermeltetése megnöveli a legyek élethosszát (Simonsen és mtsai, 2008), feltételezhetően az autofágia fokozásával (bár ezt kísérletesen nem igazolták az említett publikációban). Ez összhangban van azzal az elmélettel, miszerint az autofágia fokozása – sok más dolog mellett - hozzájárulhat a hosszú és egészséges élethez (Vellai és mtsai, 2009). Ezt a bevezetésben tárgyalt csökkent kalóriabevitel vagy sportolás, vagy esetleg megfelelő hatóanyag (mint például a spermidin) fogyasztásával el lehet érni.

Persze azt is érdemes megjegyezni, hogy egy adott *Atg* gén deléciója nem feltétlenül jelenti azt, hogy az autofágia teljes mértékben gátolt. A Bevezetésben tárgyalt egyéb autofág lebontó útvonalak (mikroautofágia, chaperone-mediált autofágia) működése mellett ismertek szövet-specifikus különbségek az autofágia fő útvonalának szabályozásában. Nagy visszhangot kapott az a néhány éve megjelent cikk, amelyben leírtak egy ubikvitinszerű protein konjugációs rendszertől, azaz például az Atg5-től és Atg7-től független alternatív autofág utat (Nishida és mtsai, 2009). Ugyan ennek az eredménynek a jelentősége mindmáig nem igazán ismert, a közelmúltban hasonló megfigyeléseket tettek *Drosophila*-ban is. Azt találták, hogy ugyan éhezéskor a lárválís zsírtestben a nem-redundáns *Atg* gének szükségesek az autofágiához, ez a megfigyelés már nem igaz a metmorfózis kezdetén a lárválís középbél zsugorodásáért felelős fejlődési autofágiára (Xu és mtsai, 2015). Véleményem szerint ezek az adatok nagyon fontosak, hiszen így ha egy adott *Atg* gén hiánya nem befolyásolja a vizsgált fenotípust, akkor ez nem feltétlenül jelenti azt, hogy a folyamathoz az autofágia nem szükséges. Ebben az izgalmasnak tűnő kutatási irányban kutatócsoportomban jelenleg is végzünk kísérleteket.

3. Az ER stressz-indukált autofágia szükséges a Myc túltermeltetése által fokozott sejtnövekedéshez Drosophila-ban

A Myc transzkripciós faktor egy igen sokat vizsgált potenciális rákgyógyszer-célpont, de sajnos mivel nincs egy meghatározott aktív zsebe, mint például a katalitikus aktivitással

rendelkező enzimeknek, ezért nehéznek bizonyult ellene megfelelő gátlószert kifejleszteni. A Myc többféle effektor útvonalon át fejti ki hatását, ilyen például a megnövekedett riboszomális RNS szintézis (Gabay és mtsai, 2014). Feltételezték, hogy létezhetnek olyan onkogén-aktivált effektor folyamatok, melyek szükségesek a rákos sejtnövekedéshez, de a normál, vad típusú sejtekben nélkülözhetőek (ún. nem-onkogén addikciós útvonalak: non-oncogene addiction pathways) (Luo és mtsai, 2009). Óriási jelentőségű lenne a gyógyszerfejlesztés szempontjából, ha az ilyen effektor-útvonalakat gátló hatóanyagokat a humán rákgyógyászatban alkalmazni lehetne. Adataink alapján feltételezhető, hogy az ER stressz-indukált autofágia egy ilyen potenciális nem-onkogén addikciós útvonal a Myc túlműködése során, hiszen az ebben szereplő PERK jelátvitel vagy a központi autofág gének genetikai, vagy az autofágia farmakológiai gátlása megakadályozza a Myc-indukált túlnövekedést. Szeretném hangsúlyozni, hogy ezek a genetikai manipulációk a normál, Myc-et nem túltermelő sejtek növekedését nem befolyásolják, ami szintén a potenciális gyógyászati felhasználásra utal.

A mi *Drosophila* kutatásainktól függetlenül, velünk párhuzamosan dolgozó kutatók tenyésztett emlős sejtekben és egerekben szintén kimutatták, hogy az ER stressz-autofágia tengely kiesése (*PERK* vagy *Atg* génkiütés vagy klorokvin kezelés révén) gátolja a Myc által kiváltott tumorigenezist (Hart és mtsai, 2012). Az is igazolásra került, hogy a Myc tenyésztett emberi sejtekben is szükséges az autofágiához (Toh és mtsai, 2013). Meglepő módon azt találták, hogy autofág indukció során fontos a JNK (c-Jun N-terminal kinase) jelátvitel Myc-függő módon történő megnövekedése. Ez megmagyarázza azt, hogy miért nem láttuk az autofágiában szereplő gének transzkripciójának megváltozását a Myc genetikai manipulációja során végrehajtott kísérleteinkben, pedig sok ilyen irányú tesztet végeztünk (bár ezeket a negatív adatainkat végül nem vettük bele a publikációnkba).

Ezek az emlős sejteken elért eredmények teljes mértékben alátámasztják azt, hogy *Drosophila* adataink potenciálisan humán gyógyászati szempontból is jelentősek lehetnek.

4. Az autofagoszóma-lizoszóma fúzióban egy Syntaxin 17-tartalmú SNARE komplex és a HOPS pányvázó komplex vesznek részt

Véleményem szerint az autofagoszóma-lizoszóma fúzióban szereplő SNARE fehérjék azonosítása hasonló horderejű felfedezés, mint a központi autofág gének leírása volt az 1990-es években. Ezen cikkünk Dr. Qing Zhong javaslata alapján - jelentőségére való tekintettel - bekerült a Faculty of 1000 által javasolt, kiemelt publikációk közé. Eredményeink jelentőségét az is mutatja, hogy kéziratunk revíziója közben két cikk is megjelent, amelyekben a Syntaxin 17 autofágiában betöltött szerepét humán sejttenyészetben vizsgálták géncsendesítés segítségével (Hamasaki és mtsai, 2013; Itakura és mtsai, 2012). Meglepő módon a két cikk végkövetkeztetése egymásnak ellentmondó: a Cell cikkben - a mi munkánkhoz hasonlóan - a Syntaxin 17 autofagoszóma-lizoszóma fúzióban játszott kulcsszerepét írták le, míg a Nature cikkben - jóval felületesebb analízis alapján - azt

sugallták, hogy *Syntaxin 17* géncsendesítés hatására nem képződnek autofagoszómák. Tulajdonképpen ez az ellentmondás, továbbá az hogy mi egy teljes állatban vizsgáltuk a Syntaxin 17 hiányának a hatását, még segítette is a munkánk publikálását. Cikkünk megjelenését követően az Autophagy szaklap főszerkesztője, Dr. Daniel J. Klionsky felkérésére nemcsak a cikkhez kapcsolódó önkommentárt írtunk, hanem egy külső bírálók által lektorált összefoglalót is, melyben a fenti három cikk eredményeit kritikusan elemezzük (Hegedus és mtsai, 2013; Takats és Juhasz, 2013). A Nature cikkben leírták, hogy a Syntaxin 17 köt a Vps34 lipid kináz komplex Atg14 alegységéhez, ami az egyik legfőbb érv volt ezen SNARE autofagoszóma képződésben játszott szerepére. Fontos megemlíteni egy azóta született publikációt, amelyben leírták, hogy az Atg14 autofagoszóma kialakulásban valóban Vps34 kináz komplex alegységként tölti be szerepét, azonban önállóan dimerizálódni is képes. Az Atg14 dimer pedig vezikula-pányvázó aktivitással rendelkezik, és ekkor a Syntaxin 17-et kötve serkenti az autofagoszóma-lizoszóma fúziót (Diao és mtsai, 2015).

Az egy még nem ismert és igen fontos kérdés, hogy vajon miért szükséges két pányvázó faktor az autofagoszómák késői endoszómákkal és lizoszómákkal történő fúziójához. A HOPS komplex szükségessége ugyanis vitathatatlan ebben a folyamatban: szerepét a fúzióban saját kutatócsoportommal mi *Drosophila*-ban, valamint egy japán laboratórium tenyésztett emlős sejtekben is minden kétséget kizáróan demonstrálta. Itt jegyzem meg, hogy cikkünk publikálását a Dr. Noboru Mizushima vezette kutatócsoporttal koordináltuk, így a hasonló eredményeket *Drosophila*-ban és humán sejttenyészetben leíró két cikk ugyanazon újságban, egyszerre jelent meg (Jiang és mtsai, 2014; Takats és mtsai, 2014b).

A két külön pányvázó faktor létezésének egyik magyarázata lehet, hogy az autofagoszómák késői endoszómákkal és lizoszómákkal történő fúziójában esetleg előfordulhatnak szövetspecifikus különbségek, mint ahogy az a központi autofág gének esetén is valószínűsíthető. Ennek vizsgálatára a *Drosophila melanogaster* egy kiváló modell lehet, ezért az Atg14 dimerizációját és ezáltal csak a vezikula-pányvázó aktivitását specifikusan gátló mutációkat hordozó légymodell létrehozásán jelenleg is dolgozunk.

5. A lizoszómális lebontás hibájakor lecsökkenő TOR aktivitás miatt több autofagoszóma alakul ki

Az autofág flux meghatározása kapcsán, azaz hogy mennyi anyag bomlik le autofágia révén adott időegység alatt, igen fontossá vált az ezt mérni hivatott kísérletek elvégzése. Mivel az autofágia kutatásában születő cikkek döntő többsége tenyésztett humán (esetleg egér) sejteken zajlik, ezért magától értetődő volt, hogy a már ismert lebontást gátló szereket használja mindenki. Ezek általában a bafilomicin A1 vagy a klorokvin. Ezt jelzi, hogy a PubMed adatbázisban a „bafilmycin autophag*” vagy a „chloroquine autophag*” kifejezésekkel végzett keresések közel 500, illetve 800 publikációt azonosítanak. Ez a gyakorlat mit sem változott annak felfedezésével, hogy az autofágiát gátló TOR kináz aktiválódásának egyik fő helye az aminosavakat tartalmazó, tehát emésztő lizoszóma felszíne.

Fontosnak éreztem, hogy a fenti lizoszómális lebontást gátló hatóanyagok potenciálisan TOR kináz aktivitást és ezáltal fokozott autofagoszóma kialakulást kifejtő hatására felhívjam a kutatóközösség figyelmét. Ez egy meglepően könnyen elfogadott, önálló, egyszerzős cikk keretében sikerült is (Juhasz, 2012).

A későbbiekben ezt a feltevést kísérletesen is igazolta több független kutatócsoport humán sejttenyészeti kísérletekben, idézve az én cikkemet (Li és mtsai, 2013; Musiwaro és mtsai, 2013). Mi is kimutattuk, hogy a HOPS komplex hiányában több autofagoszóma keletkezik a lecsökkenő TOR aktivitás miatt mint vad típusú vagy *Syntaxin 17* mutáns állatokban, amit feltehetően a lizoszómába irányuló endocitotikus és bioszintetikus transzport hibája okoz (Takats és mtsai, 2013; Takats és mtsai, 2014b; Takats és mtsai, 2015). A HOPS hiányában lecsökkenő TOR aktivitást élesztősejteket vizsgáló kutatók is kimutatták (Kingsbury és mtsai, 2014). Ezen eredményeink alapján a *Syntaxin 17* gén mutációja vagy RNS interferenciával történő csendesítése nagyon is alkalmas teszt lehet az autofág flux vizsgálatára *Drosophila*-ban, hiszen egy teljes állatban a gátlószerek alkalmazása nehézkes. Azt tapasztaltuk ugyanis nem publikált kísérleteinkben, hogy a bafilomicin A1 kezelés egy órán belül a lárvák halálát okozza, míg a klorokvin esetén többórás kezelés szükséges a kívánt hatás eléréséhez, ami a TOR szisztémás, az állat egészére kiterjedő gátlása miatt valószínűleg befolyásolja a vizsgálni kívánt autofág lebontásra vonatkozó adatokat. Ezzel szemben a *Syntaxin 17* gén expressziójának genetikai úton történő gátlásával specifikusan, a TOR jelátvitel befolyásolása nélkül lehet blokkolni az autofág lebontást. Sőt, mozaik állatok felhasználásával ezt sejt-autonóm módon is megtehetjük, így kizárva a teljes állatra kiterjedő gátlás esetleges indirekt hatásait. Ezt a hipotézist a Syntaxin 17 szerepéről írt összefoglalónkban fogalmaztuk meg először, részben az akkor már meglevő kísérletes eredményeinkre támaszkodva (Hegedus és mtsai, 2013).

ÖSSZEFOGLALÁS

Doktori értekezésemet az általam posztdoktori kutatásaim során publikált elsőszerzős cikkeim egy részére, valamint a kutatócsoport-vezetőként utolsó szerzőként jegyzett cikkeim egy részére alapoztam. Elsőszerzős publikációimban a kísérletek döntő részét én magam terveztem meg és hajtottam végre, és ezeket a cikkeimet egyetlen kivétellel (Vps34) teljes egészében én írtam. Laborvezetőként én irányítottam és finanszíroztam a munkatársaim munkáját azokban a cikkekben ahol utolsó szerzőként szerepelek, és mindegyiket én magam írtam. A kutatócsoportom által kivitelezett munka önállóságát mutatja, hogy szenior szerzős kísérletes cikkeimben csak egy alkalommal szerepel egy külföldi szerző, és rendszerint saját csoportom tagjai végezték az összes kísérletet.

Az ezekre a cikkekre alapuló leglényegesebb eredményeinket röviden összefoglalva kimutattuk, hogy:

1. Az autofagoszómák kialakulását az autofág géntermékek hierarchikus hálózata kontrollálja *Drosophila*-ban, melyek transzkripciója fokozódik autofág indukció során. Ezt az állítást azokra a megfigyeléseinkre alapozom, miszerint: I. az Atg1 protein kináz komplexhez tartozó FIP200/Atg17 és az Atg9 az ubikvitinszerű protein konjugációs rendszereknél korábban (upstream) hatnak, *Atg7* és *Atg8a* mutánsokban a p62 aggregátumokon felhalmozódnak, amihez Atg9 esetén a Vps34 lipid kináz és effektora, az Atg18a is szükségesek (Nagy és mtsai, 2014a; Nagy és mtsai, 2014b). II. a Vps34 lipid kináz komplex az ESCRT fehérjéktől eltérően hat autofágia során, és autofagoszóma kialakulásban játszott szerepe független az endocitotikus funkciójától (Juhasz és Neufeld, 2008a). III. éhezéskor az *Atg* gének többségéről átíródó mRNS-ek szintje megnő (Erdi és mtsai, 2012). IV. a Foxo transzkripciós faktor szükséges a megfelelő autofág válaszhoz (Juhasz és mtsai, 2007b).

2. Az autofágia szükséges az ubikvitinált fehérjéket és p62-t tartalmazó aggregátumok lebontásához, és hibája mozgásképtelenséget és rövid élethosszt okoz *Drosophila*-ban. Ezt az állítást azokra a megfigyeléseinkre alapozom, miszerint: I. *Atg7* null mutánsok neuronjaiban ubikvitinált fehérjéket tartalmazó aggregátumok halmozódnak fel, ami feltehetően kiváltja az állatokban látott neurodegenerációt és ennek következtében mozgásképtelenséget és megrövidült élethosszt eredményez (Juhasz és mtsai, 2007a). II. az *Atg7* és további központi *Atg* gének funkcióvesztése az ubikvitinált fehérjék aggregációját és lebontását biztosító szelektív autofág szállítmány, a p62 akkumulációjához vezet (Pircs és mtsai, 2012). III. az autofagoszómális SNARE fehérje, a Syntaxin 17 hiánya szintén p62 felhalmozódást, neuromuszkuláris problémákat és megrövidült élethosszt eredményez, ámbár ebben az esetben a megfigyelt fenotípusokat nem a neuronok tömeges pusztulása okozza (Takats és mtsai, 2013).

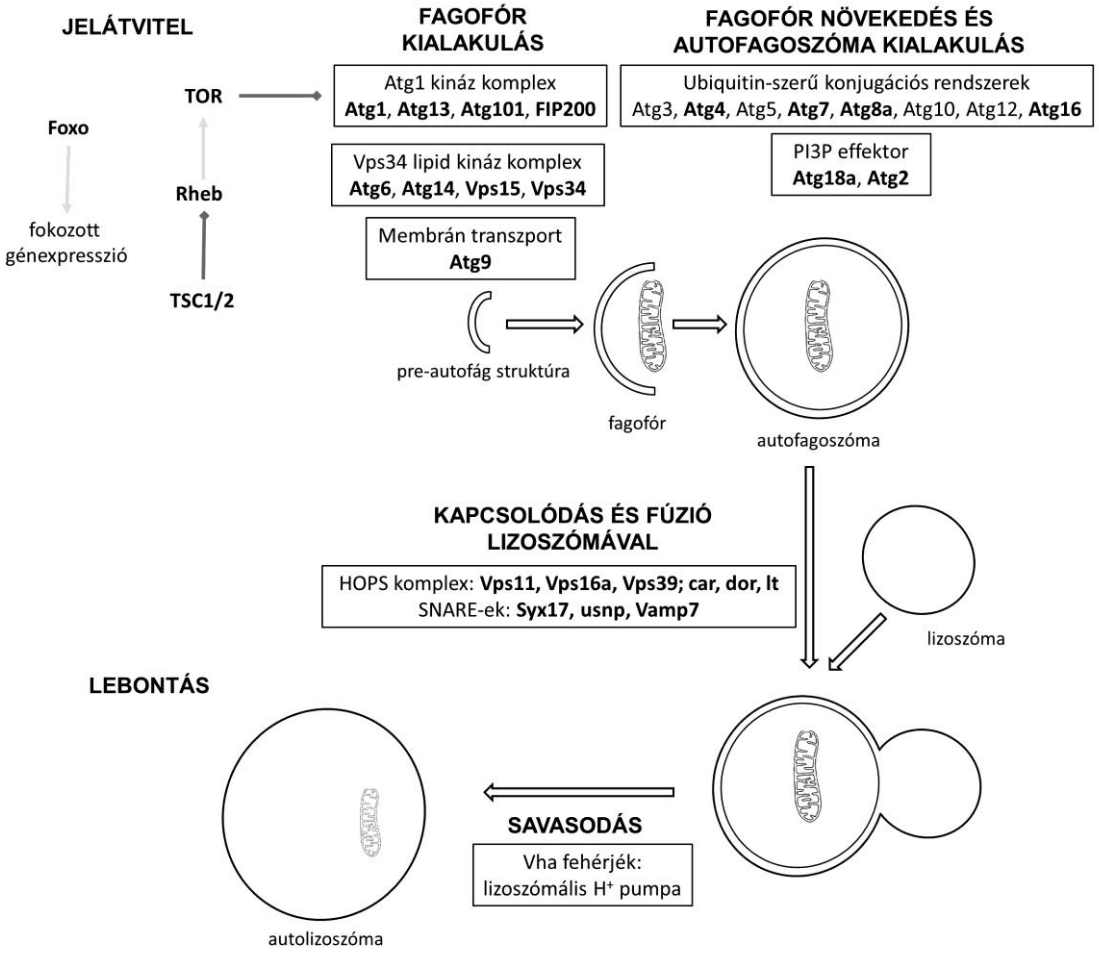
3. Az ER stressz-indukált autofágia szükséges a Myc túltermeltetés által fokozott sejtnövekedéshez *Drosophila*-ban. Ezt az állítást azokra a megfigyeléseinkre alapozom, miszerint: I. a Myc transzkripciós faktor hiányában elmarad a megfelelő autofág válasz (Nagy

és mtsai, 2013). II. a Myc túltermeltetése az ER stressz jelátvitel PERK útvonalának aktivációja révén autofágiát indukál (Nagy és mtsai, 2013). III. a PERK jelátvitel vagy az autofágia gátlása megakadályozza a Myc-indukált túlnövekedést (Nagy és mtsai, 2013).

4. Az autofagoszóma-lizoszóma fúzióban egy Syntaxin 17-tartalmú SNARE komplex és a HOPS pányvázó komplex vesznek részt. Ezt az állítást azokra a megfigyeléseinkre alapozom, miszerint: I. bizonyítottuk, hogy a Syntaxin 17, usnp/SNAP-29 és Vamp7 fehérjék által alkotott SNARE komplex szükséges az autofagoszómák késői endoszómával vagy lizoszómával történő fúziójához (Takats és mtsai, 2013). II. kimutattuk, hogy a HOPS pányvázó komplex mind a hat alegysége szükséges az autofagoszómák késői endoszómával vagy lizoszómával történő fúziójához, feltehetően a Syntaxin 17 kötése révén (Takats és mtsai, 2014b). III. bemutattuk, hogy a HOPS- Syntaxin 17 kölcsönhatás autofágiára specifikus, mivel az endocitotikus és lizoszóma biogenezis transzportfolyamatokhoz a HOPS-szal ellentétben a Syntaxin 17 nem szükséges (Takats és mtsai, 2014b).

5. A lizoszómális lebontás hibájakor lecsökkenő TOR aktivitás miatt több autofagoszóma alakul ki. Ezt az állítást arra alapozom, miszerint: I. az autofág flux vizsgálatok során rutinszerűen használt lizoszómális lebontást gátló szerek csökkentik a TOR aktivitást, ami így az autofagoszómák kialakulását serkentheti (Juhasz, 2012). II. a HOPS komplex hibája a TOR aktivitásának csökkenése miatt megnöveli az autofagoszóma kialakulás mértékét, feltehetően azért, mert a *Syntaxin 17* deléciójával ellentétben az összes lizoszómába irányuló transzportutat megzavarja (Hegedus és mtsai, 2013; Takats és mtsai, 2013; Takats és mtsai, 2014b; Takats és mtsai, 2015).

Egyre többet tudunk az autofágia fontosságáról és a folyamatot szabályozó útvonalakról. Kutatásainknak úttörő szerepe volt a **8. ábrán** bemutatott molekuláris mechanizmusok *Drosophila*-ban végzett feltárásában. Az ábrán félkövér betűtípussal kiemeltem azokat a géntermékeket, amelyek funkcionális vizsgálatáról fő szerzőként kutatási cikket közöltem.



8. ábra. *Az autofágiát szabályozó molekuláris mechanizmusok sematikus illusztrációja Drosophila példáján. Félkövér betűtípussal emeltem ki azokat a géntermékeket, amelyek funkcionális analíziséről első vagy utolsó szerzőként cikket közöltem a PhD fokozatom megszerzése óta. A Foxo transzkripciós faktor szükséges az éhezés-indukálta autofágiához. A TSC1/2 (Tuberous Sclerosis Complex 1/2) komplex a Rheb gátlásával inaktiválja a TOR kinázt. A TOR az Atg1-et közvetlenül foszforilálva akadályozza meg az autofágia kezdeti, iniciációs lépését. A fagofór kialakulásához a Vps34 lipid kináz komplex és az Atg9 transzmembrán fehérje is szükségesek. A fagofór növekedését és autofagoszómává záródását lipid kináz effektorok és ubikvitin-szerű konjugációs rendszerek segítik elő. Az autofagoszóma lizoszómával (vagy késői endoszómával) egyesül, amihez szükség van a HOPS pányvázó komplexre és a Syntaxin 17 (Syx17), usnp (SNAP-29) és Vamp7 SNARE fehérjékre. Az így létrejött autolizoszómában zajlik az odaszállított anyagok lebontása. Ebben a folyamatban savas hidrolázok és a működésükhöz megfelelő pH-t biztosító, Vha fehérje alegységekből álló protonpumpa játszanak főszerepet.*

TOVÁBBI TERVEK ÉS EREDMÉNYEK

Bízom benne, hogy folytatódó saját kutatásaink és erősödő együttműködéseink révén továbbra is hozzá tudunk járulni a szakterület fejlődéséhez (Juhasz és mtsai, 2013). Ennek kapcsán abban a különleges helyzetben vagyok, hogy már némi fejleményekre is tudok utalni, ugyanis az eredetileg 2014. júniusában befejezett doktori értekezésemet a Magyar Tudományos Akadémia Doktori Tanácsának javaslatára újraírtam a kifogásolt formai és tartalmi hiányosságok orvoslása céljából. Publikációs aktivitásunk töretlen: 2015-ben eddig, azaz augusztusig hat darab lektorált folyóiratcikkünk jelent meg az autofágia témakörében összesen több mint 40 impakt faktor értékben, amiből három esetben szenior szerzőként szerepelek (Kim és mtsai, 2015; Lorincz és mtsai, 2015; Maruzs és mtsai, 2015; Mauvezin és mtsai, 2015; Nagy és mtsai, 2015; Takats és mtsai, 2015). Természetesen mivel ezek a cikkek a doktori eljárásom megindítása után születtek, ezért a bírálat során nem veendők figyelembe. Részletesen nem is kerülnek ismertetésre a dolgozatomban, bár néhányukra bátorkodtam röviden utalni, mivel szorosan kapcsolódnak az értekezésemhez.

Kutatócsoportom felépítése is átalakulóban van. A 2009-es kezdést követő két évet a genomszintű genetikai szűrővizsgálattal töltöttük, ami a teljes labor munkaidejét nagyrészt igénybe vette. Kezdő kutatócsoport-vezetőként sok ihletet merítettem a Kenneth H. Blanchard nevével fémjelzett vállalatirányítási könyvekből. Ugyanis egy kutatócsoport vezetése a publikálj vagy pusztulj (publish or perish) elveknek való megfelelés kényszere miatt sokban hasonlít egy kis cég irányításához. A publikációkat egyfajta termékként kell „eladni”, azaz minél nívósabb szaklapokban leközölni, mert erre alapozva lehet újabb kutatási pályázatot nyerni. Ez esetemben különösen fontos, hiszen a kollégáim többségének fizetését (valamint teljes egészében a saját magamét is) laborom indítása óta pályázati pénzből teremtem elő. Ez igen sok tervezést igényelt: például az első 5-6 évben nemcsak a projekteket, hanem az összes molekuláris klónozási stratégiát és a szükséges primereket is én magam terveztem meg, és a laboromban zajló többi kísérletet szintén hasonló alapossággal felügyeltem. Jó és rossz döntéseim közül kiváló döntésnek bizonyult, hogy Nagy Péter Myc iránti érdeklődését, valamint Takáts Szabolcs autofagoszóma-lizoszóma fúzióval kapcsolatos ötleteit támogattam, hiszen ezekből születtek önálló kutatócsoportom talán legfontosabb publikációi. Mára már számos olyan kollégámra támaszkodhatok, akik sokéves vagy akár évtizedes rutinjuknak köszönhetően kutatásaikat egyre önállóbban végzik, szakdolgozó és doktorandusz hallgatóink munkáját felügyelik. A csoport fejlődését jól jelzi az is, hogy tanítványaim közül 2014-ben Hegedűs Krisztina, majd 2015-ben Nagy Péter posztdoktori OTKA pályázatot nyertek. Remélem *Drosophila* autofágia kutatócsoportunk működése hosszú távon is fenntarthatónak és eredményesnek bizonyul majd.

KÖSZÖNETNYILVÁNÍTÁS

Köszönöm feleségemnek, Marcsinak és gyermekeinknek, Máténak és Zsófinak, hogy megértéssel és türelemmel viselik a megszállott kutatói létemmel járó hátrányokat.

Köszönöm mentoraim, Sass Miklós és Tom Neufeld hosszú évek óta tartó támogatását és tanácsait.

Köszönöm laborom tagjainak, hogy lelkesedéssel, ötletekkel és becsülettel dolgozva oroszlánrészt vállaltak az elmúlt évek sikereiben. A közös célok érdekében végzett munkából, az értekezésemben bemutatott eredmények alapján Érdi Balázs, Kárpáti Manuéla, Nagy Péter, Pircs Karolina és Varga Ágnes témavezetésemmel PhD fokozatot szereztek, és Takáts Szabolcs és Varga Kata doktoranduszhallgatóim fokozatszerzési eljárása is folyamatban van. Külön köszönöm Pálfia Zsoltné Sárinak, hogy páratlan módszertani tudásával immáron 8 éve segíti munkánkat laborasszisztensként. Köszönöm Kovács Attila Lajosnak, hogy több évtizedes elektronmikroszkópos tapasztalatára építhettünk néhány munkánkban. Szeretném megköszönni munkatársaim oktatásban nyújtott segítségét is, például az autofágiáról szóló tankönyvrészletem ábraanyagának elkészítését, és hogy bekapcsolódtak az általam tanított tárgyak vizsgáztatásába és a zárthelyi dolgozatok javításába.

Köszönöm jelenlegi tanszékvezetőmnek, Lőw Péternek, hogy maximálisan támogatja és segíti munkánkat, és hogy munkatársként részt vett egyik projektünkben. Köszönöm az ELTE Anatómiai, Sejt- és Fejlődésbiológiai Tanszékén és az ELTE Biológiai Intézetben dolgozó kollégáknak, hogy biztosították a kutatásainkhoz szükséges feltételeket.

Köszönöm Dr. Papp Lászlónak az értekezés formai és tartalmi felépítésének kapcsán nyújtott útmutatását.

Végezetül hálásan köszönöm a Magyar Tudományos Akadémia (BO/00712/07, BO/00552/11, LP2014-2, és Bolyai plakett), az Országos Tudományos Kutatási Alap (PD72095, K83509) és a Wellcome Trust (WT087518) munkámhoz, kutatócsoportom működéséhez biztosított anyagi támogatását.

IRODALOMJEGYZÉK

Abeliovich, H., C. Zhang, W.A. Dunn, Jr., K.M. Shokat, and D.J. Klionsky. 2003. Chemical genetic analysis of Apg1 reveals a non-kinase role in the induction of autophagy. *Mol. Biol. Cell*. 14:477-490.

Akdemir, F., R. Farkas, P. Chen, G. Juhasz, L. Medved'ova, M. Sass, L. Wang, X. Wang, S. Chittaranjan, S.M. Gorski, A. Rodriguez, and J.M. Abrams. 2006. Autophagy occurs upstream or parallel to the apoptosome during histolytic cell death. *Development*. 133:1457-1465.

Alemu, E.A., T. Lamark, K.M. Torgersen, A.B. Birgisdottir, K. Bowitz Larsen, A. Jain, H. Olsvik, A. Overvatn, V. Kirkin, and T. Johansen. 2012. ATG8 Family Proteins Act as Scaffolds for Assembly of the ULK Complex: Sequence Requirements for LC3-Interacting Region (LIR) Motifs. *J. Biol. Chem.* 287:39275-39290.

Anonymous. 2007. Adults need autophagy too. *Cell*. 131:1209-1211.

Ashford, T.P., and K.R. Porter. 1962. Cytoplasmic components in hepatic cell lysosomes. *J. Cell Biol.* 12:198-202.

Berry, D.L., and E.H. Baehrecke. 2007. Growth arrest and autophagy are required for salivary gland cell degradation in Drosophila. *Cell*. 131:1137-1148.

Bjorkoy, G., T. Lamark, A. Brech, H. Outzen, M. Perander, A. Overvatn, H. Stenmark, and T. Johansen. 2005. p62/SQSTM1 forms protein aggregates degraded by autophagy and has a protective effect on huntingtin-induced cell death. *The Journal of Cell Biology*. 171:603-614.

Bjorkoy, G., T. Lamark, S. Pankiv, A. Overvatn, A. Brech, and T. Johansen. 2009. Monitoring autophagic degradation of p62/SQSTM1. *Methods Enzymol.* 452:181-197.

Chang, Y.Y., G. Juhasz, P. Goraksha-Hicks, A.M. Arsham, D.R. Mallin, L.K. Muller, and T.P. Neufeld. 2009. Nutrient-dependent regulation of autophagy through the target of rapamycin pathway. *Biochem. Soc. Trans.* 37:232-236.

Cheong, H., C. Lu, T. Lindsten, and C.B. Thompson. 2012. Therapeutic targets in cancer cell metabolism and autophagy. *Nat. Biotechnol.* 30:671-678.

Chiang, A.S., C.Y. Lin, C.C. Chuang, H.M. Chang, C.H. Hsieh, C.W. Yeh, C.T. Shih, J.J. Wu, G.T. Wang, Y.C. Chen, C.C. Wu, G.Y. Chen, Y.T. Ching, P.C. Lee, H.H. Lin, H.W. Hsu, Y.A. Huang, J.Y. Chen, H.J. Chiang, C.F. Lu, R.F. Ni, C.Y. Yeh, and J.K. Hwang. 2011. Three-dimensional reconstruction of brain-wide wiring networks in Drosophila at single-cell resolution. *Current biology : CB*. 21:1-11.

Clarke, P.G. 1990. Developmental cell death: morphological diversity and multiple mechanisms. *Anat Embryol (Berl)*. 181:195-213.

Collins, J.V. 1969. The hormonal control of fat body development in Calpodes ethlius (Lepidoptera, Hesperiidae). *J Insect Physiol.* 15:341-352.

Csikos, G., M. Lippai, T. Lukacsovich, G. Juhasz, L. Henn, M. Erdelyi, P. Maroy, and M. Sass. 2009. A novel role for the Drosophila epsin (lqf): involvement in autophagy. *Autophagy*. 5:636-648.

De Duve, C., and R. Wattiaux. 1966. Functions of lysosomes. *Annu. Rev. Physiol.* 28:435-492.

de Reuck, A.V.S., Cameron, M.P. 1963. *Ciba Foundation Symposium on Lysosomes.* London: J.A. Churchill Ltd.

Deter, R.L., P. Baudhuin, and C. De Duve. 1967. Participation of lysosomes in cellular autophagy induced in rat liver by glucagon. *J. Cell Biol.* 35:C11-16.

Diao, J., R. Liu, Y. Rong, M. Zhao, J. Zhang, Y. Lai, Q. Zhou, L.M. Wilz, J. Li, S. Vivona, R.A. Pfuetzner, A.T. Brunger, and Q. Zhong. 2015. ATG14 promotes membrane tethering and fusion of autophagosomes to endolysosomes. *Nature*.

Eisenberg, T., H. Knauer, A. Schauer, S. Buttner, C. Ruckenstuhl, D. Carmona-Gutierrez, J. Ring, S. Schroeder, C. Magnes, L. Antonacci, H. Fussi, L. Deszcz, R. Hartl, E. Schraml, A. Criollo, E. Megalou, D. Weiskopf, P. Laun, G. Heeren, M. Breitenbach, B. Grubeck-Loebenstein, E. Herker, B. Fahrenkrog, K.U. Frohlich, F. Sinner, N. Tavernarakis, N. Minois, G. Kroemer, and F. Madeo. 2009. Induction of autophagy by spermidine promotes longevity. *Nat. Cell Biol.* 11:1305-1314.

Eisenberg, T., S. Schroeder, A. Andryushkova, T. Pendl, V. Kuttner, A. Bhukel, G. Marino, F. Pietrocola, A. Harger, A. Zimmermann, T. Moustafa, A. Sprenger, E. Jany, S. Buttner, D. Carmona-Gutierrez, C. Ruckenstuhl, J. Ring, W. Reichelt, K. Schimmel, T. Leeb, C. Moser, S. Schatz, L.P. Kamolz, C. Magnes, F. Sinner, S. Sedej, K.U. Frohlich, G. Juhasz, T.R. Pieber, J. Dengjel, S.J. Sigrist, G. Kroemer, and F. Madeo. 2014. Nucleocytosolic depletion of the energy metabolite acetyl-coenzyme a stimulates autophagy and prolongs lifespan. *Cell Metab.* 19:431-444.

Erdi, B., P. Nagy, A. Zvara, A. Varga, K. Pircs, D. Menesi, L.G. Puskas, and G. Juhasz. 2012. Loss of the starvation-induced gene Rack1 leads to glycogen deficiency and impaired autophagic responses in Drosophila. *Autophagy*. 8:1124-1135.

Fullgrabe, J., D.J. Klionsky, and B. Joseph. 2014. The return of the nucleus: transcriptional and epigenetic control of autophagy. *Nat Rev Mol Cell Biol*. 15:65-74.

Gabay, M., Y. Li, and D.W. Felsher. 2014. MYC Activation Is a Hallmark of Cancer Initiation and Maintenance. *Cold Spring Harb Perspect Med*. 4.

Greene, J.C., A.J. Whitworth, I. Kuo, L.A. Andrews, M.B. Feany, and L.J. Pallanck. 2003. Mitochondrial pathology and apoptotic muscle degeneration in Drosophila parkin mutants. *Proc. Natl. Acad. Sci. USA*. 100:4078-4083.

Hamasaki, M., N. Furuta, A. Matsuda, A. Nezu, A. Yamamoto, N. Fujita, H. Oomori, T. Noda, T. Haraguchi, Y. Hiraoka, A. Amano, and T. Yoshimori. 2013. Autophagosomes form at ER-mitochondria contact sites. *Nature*. 495:389-393.

Hara, T., K. Nakamura, M. Matsui, A. Yamamoto, Y. Nakahara, R. Suzuki-Migishima, M. Yokoyama, K. Mishima, I. Saito, H. Okano, and N. Mizushima. 2006. Suppression of basal autophagy in neural cells causes neurodegenerative disease in mice. *Nature*. 441:885-889.

Harding, T.M., K.A. Morano, S.V. Scott, and D.J. Klionsky. 1995. Isolation and characterization of yeast mutants in the cytoplasm to vacuole protein targeting pathway. *The Journal of cell biology*. 131:591-602.

Hart, L.S., J.T. Cunningham, T. Datta, S. Dey, F. Tameire, S.L. Lehman, B. Qiu, H. Zhang, G. Cerniglia, M. Bi, Y. Li, Y. Gao, H. Liu, C. Li, A. Maity, A. Thomas-Tikhonenko,

A.E. Perl, A. Koong, S.Y. Fuchs, J.A. Diehl, I.G. Mills, D. Ruggero, and C. Koumenis. 2012. ER stress-mediated autophagy promotes Myc-dependent transformation and tumor growth. *J. Clin. Invest.* 122:4621-4634.

He, C., M.C. Bassik, V. Moresi, K. Sun, Y. Wei, Z. Zou, Z. An, J. Loh, J. Fisher, Q. Sun, S. Korsmeyer, M. Packer, H.I. May, J.A. Hill, H.W. Virgin, C. Gilpin, G. Xiao, R. Bassel-Duby, P.E. Scherer, and B. Levine. 2012. Exercise-induced BCL2-regulated autophagy is required for muscle glucose homeostasis. *Nature*. 481:511-515.

Hegedus, K., P. Nagy, Z. Gaspari, and G. Juhasz. 2014. The Putative HORMA Domain Protein Atg101 Dimerizes and Is Required for Starvation-Induced and Selective Autophagy in Drosophila. *BioMed Res Int.* 2014:470482.

Hegedus, K., S. Takats, A.L. Kovacs, and G. Juhasz. 2013. Evolutionarily conserved role and physiological relevance of a STX17/Syx17 (syntaxin 17)-containing SNARE complex in autophagosome fusion with endosomes and lysosomes. *Autophagy*. 9:1642-1646.

Itakura, E., C. Kishi-Itakura, and N. Mizushima. 2012. The hairpin-type tail-anchored SNARE syntaxin 17 targets to autophagosomes for fusion with endosomes/lysosomes. *Cell*. 151:1256-1269.

Itakura, E., and N. Mizushima. 2010. Characterization of autophagosome formation site by a hierarchical analysis of mammalian Atg proteins. *Autophagy*. 6:764-776.

Jiang, P., and N. Mizushima. 2014. Autophagy and human diseases. *Cell Res*. 24:69-79.

Jiang, P., T. Nishimura, Y. Sakamaki, E. Itakura, T. Hatta, T. Natsume, and N. Mizushima. 2014. The HOPS complex mediates autophagosome-lysosome fusion through interaction with syntaxin 17. *Mol. Biol. Cell*. 25:1327-1337.

Juhasz, G. 2012. Interpretation of bafilomycin, pH neutralizing or protease inhibitor treatments in autophagic flux experiments: novel considerations. *Autophagy*. 8:1875-1876.

Juhász, G., G. Csikós, R. Sinka, M. Erdélyi, and M. Sass. 2003. The Drosophila homolog of Aut1 is essential for autophagy and development. *FEBS Lett.* 543:154-158.

Juhasz, G., B. Erdi, M. Sass, and T.P. Neufeld. 2007a. Atg7-dependent autophagy promotes neuronal health, stress tolerance, and longevity but is dispensable for metamorphosis in Drosophila. *Genes Dev.* 21:3061-3066.

Juhasz, G., J.H. Hill, Y. Yan, M. Sass, E.H. Baehrecke, J.M. Backer, and T.P. Neufeld. 2008. The class III PI(3)K Vps34 promotes autophagy and endocytosis but not TOR signaling in Drosophila. *J. Cell Biol.* 181:655-666.

Juhász, G., A.L. Kovács, L. Lászlo, and P. Lőw. 2013. Az önemésztés, sejtpusztulás és megújulás molekuláris sejtbiológiája. *Egyetemi tankönyv, szerkesztő: Lőw Péter*.

Juhasz, G., and T.P. Neufeld. 2006. Autophagy: a forty-year search for a missing membrane source. *PLoS Biol*. 4:e36.

Juhasz, G., and T.P. Neufeld. 2008a. Drosophila Atg7: required for stress resistance, longevity and neuronal homeostasis, but not for metamorphosis. *Autophagy*. 4:357-358.

Juhasz, G., and T.P. Neufeld. 2008b. Experimental control and characterization of autophagy in Drosophila. *Methods Mol. Biol.* 445:125-133.

Juhasz, G., R. Puertollano, S. Shimizu, and M.I. Vaccaro. 2013. Autophagy researchers. *Autophagy*. 9:815-818.

Juhasz, G., L.G. Puskas, O. Komonyi, B. Erdi, P. Maroy, T.P. Neufeld, and M. Sass. 2007b. Gene expression profiling identifies FKBP39 as an inhibitor of autophagy in larval Drosophila fat body. *Cell Death Differ*. 14:1181-1190.

Juhasz, G., and M. Sass. 2005. Hid can induce, but is not required for autophagy in polyploid larval Drosophila tissues. *Eur. J. Cell Biol.* 84:491-502.

Jung, C.H., M. Seo, N.M. Otto, and D.H. Kim. 2011. ULK1 inhibits the kinase activity of mTORC1 and cell proliferation. *Autophagy*. 7:1212-1221.

Kaushik, S., and A.M. Cuervo. 2012. Chaperone-mediated autophagy: a unique way to enter the lysosome world. *Trends Cell Biol*. 22:407-417.

Kenyon, C., J. Chang, E. Gensch, A. Rudner, and R. Tabtiang. 1993. A C. elegans mutant that lives twice as long as wild type. *Nature*. 366:461-464.

Kihara, A., T. Noda, N. Ishihara, and Y. Ohsumi. 2001. Two distinct Vps34 phosphatidylinositol 3-kinase complexes function in autophagy and carboxypeptidase Y sorting in Saccharomyces cerevisiae. *J. Cell Biol.* 152:519-530.

Kim, M., I. Semple, B. Kim, A. Kiers, S. Nam, H.W. Park, H. Park, S.H. Ro, J.S. Kim, G. Juhasz, and J.H. Lee. 2015. Drosophila Gyf/GRB10 interacting GYF protein is an autophagy regulator that controls neuron and muscle homeostasis. *Autophagy*:0.

Kimura, S., T. Noda, and T. Yoshimori. 2007. Dissection of the autophagosome maturation process by a novel reporter protein, tandem fluorescent-tagged LC3. *Autophagy*. 3:452-460.

Kingsbury, J.M., N.D. Sen, T. Maeda, J. Heitman, and M.E. Cardenas. 2014. Endolysosomal membrane trafficking complexes drive nutrient-dependent TORC1 signaling to control cell growth in Saccharomyces cerevisiae. *Genetics*. 196:1077-1089.

Klionsky, D.J., F.C. Abdalla, H. Abeliovich, R.T. Abraham, A. Acevedo-Arozena, K. Adeli, L. Agholme, M. Agnello, P. Agostinis, J.A. Aguirre-Ghiso, H.J. Ahn, O. Ait-Mohamed, S. Ait-Si-Ali, T. Akematsu, S. Akira, H.M. Al-Younes, M.A. Al-Zeer, M.L. Albert, R.L. Albin, J. Alegre-Abarrategui, M.F. Aleo, M. Alirezaei, A. Almasan, M. Almonte-Becerril, A. Amano, R. Amaravadi, S. Amarnath, A.O. Amer, N. Andrieu-Abadie, V. Anantharam, D.K. Ann, S. Anoopkumar-Dukie, H. Aoki, N. Apostolova, P. Auberger, M. Baba, S.K. Backues, E.H. Baehrecke, B.A. Bahr, X.Y. Bai, Y. Bailly, R. Baiocchi, G. Baldini, W. Balduini, A. Ballabio, B.A. Bamber, E.T. Bampton, G. Banhegyi, C.R. Bartholomew, D.C. Bassham, R.C. Bast, Jr., H. Batoko, B.H. Bay, I. Beau, D.M. Bechet, T.J. Begley, C. Behl, C. Behrends, S. Bekri, B. Bellaire, L.J. Bendall, L. Benetti, L. Berliocchi, H. Bernardi, F. Bernassola, S. Besteiro, I. Bhatia-Kissova, X. Bi, M. Biard-Piechaczyk, J.S. Blum, L.H. Boise, P. Bonaldo, D.L. Boone, B.C. Bornhauser, K.R. Bortoluci, I. Bossis, F. Bost, J.P. Bourquin, P. Boya, M. Boyer-Guittaut, P.V. Bozhkov, N.R. Brady, C. Brancolini, A. Brech, J.E. Brenman, A. Brennand, E.H. Bresnick, P. Brest, D. Bridges, M.L. Bristol, P.S. Brookes, E.J. Brown, J.H. Brumell, N. Brunetti-Pierri, U.T. Brunk, D.E. Bulman, S.J. Bultman, G. Bultynck, L.F. Burbulla, W. Bursch, és mtsai. 2012. Guidelines for the use and interpretation of assays for monitoring autophagy. *Autophagy*. 8:445-544.

Klionsky, D.J., J.M. Cregg, W.A. Dunn, Jr., S.D. Emr, Y. Sakai, I.V. Sandoval, A. Sibirny, S. Subramani, M. Thumm, M. Veenhuis, and Y. Ohsumi. 2003. A unified nomenclature for yeast autophagy-related genes. *Dev. Cell*. 5:539-545.

Komatsu, M., S. Waguri, T. Chiba, S. Murata, J. Iwata, I. Tanida, T. Ueno, M. Koike, Y. Uchiyama, E. Kominami, and K. Tanaka. 2006. Loss of autophagy in the central nervous system causes neurodegeneration in mice. *Nature*. 441:880-884.

Komatsu, M., S. Waguri, M. Koike, Y.S. Sou, T. Ueno, T. Hara, N. Mizushima, J. Iwata, J. Ezaki, S. Murata, J. Hamazaki, Y. Nishito, S. Iemura, T. Natsume, T. Yanagawa, J. Uwayama, E. Warabi, H. Yoshida, T. Ishii, A. Kobayashi, M. Yamamoto, Z. Yue, Y. Uchiyama, E. Kominami, and K. Tanaka. 2007. Homeostatic levels of p62 control cytoplasmic inclusion body formation in autophagy-deficient mice. *Cell*. 131:1149-1163.

Korolchuk, V.I., F.M. Menzies, and D.C. Rubinsztein. 2010. Mechanisms of cross-talk between the ubiquitin-proteasome and autophagy-lysosome systems. *FEBS Lett.* 584:1393-1398.

Koyama-Honda, I., E. Itakura, T.K. Fujiwara, and N. Mizushima. 2013. Temporal analysis of recruitment of mammalian ATG proteins to the autophagosome formation site. *Autophagy*. 9:1491-1499.

Kroemer, G., and B. Levine. 2008. Autophagic cell death: the story of a misnomer. *Nat Rev Mol Cell Biol*. 9:1004-1010.

Lamb, C.A., T. Yoshimori, and S.A. Tooze. 2013. The autophagosome: origins unknown, biogenesis complex. *Nat Rev Mol Cell Biol*. 14:759-774.

Lemaitre, B., and I. Miguel-Aliaga. 2013. The digestive tract of Drosophila melanogaster. *Annu. Rev. Genet.* 47:377-404.

Levine, B., and J. Yuan. 2005. Autophagy in cell death: an innocent convict? *J. Clin. Invest.* 115:2679-2688.

Li, M., B. Khambu, H. Zhang, J.H. Kang, X. Chen, D. Chen, L. Vollmer, P.Q. Liu, A. Vogt, and X.M. Yin. 2013. Suppression of Lysosome Function Induces Autophagy via a Feedback Downregulation of MTORC1 Activity. *The Journal of biological chemistry*.

Lippai, M., G. Csikos, P. Maroy, T. Lukacsovich, G. Juhasz, and M. Sass. 2008. SNF4Agamma, the Drosophila AMPK gamma subunit is required for regulation of developmental and stress-induced autophagy. *Autophagy*. 4:476-486.

Liu, Y., S. Shoji-Kawata, R.M. Sumpter, Jr., Y. Wei, V. Ginet, L. Zhang, B. Posner, K.A. Tran, D.R. Green, R.J. Xavier, S.Y. Shaw, P.G. Clarke, J. Puyal, and B. Levine. 2013. Autosis is a Na+,K+-ATPase-regulated form of cell death triggered by autophagy-inducing peptides, starvation, and hypoxia-ischemia. *Proc. Natl. Acad. Sci. USA.* 110:20364-20371.

Locke, M., and J.V. Collins. 1965. The Structure and Formation of Protein Granules in the Fat Body of an Insect. *The Journal of cell biology*. 26:857-884.

Lorincz, P., S. Takats, M. Karpati, and G. Juhasz. 2015. iFly: The eye of the fruit fly as a model to study autophagy and related trafficking pathways. *Exp. Eye Res.*

Low, P., A. Varga, K. Pircs, P. Nagy, Z. Szatmari, M. Sass, and G. Juhasz. 2013. Impaired proteasomal degradation enhances autophagy via hypoxia signaling in Drosophila. *BMC Cell Biol*. 14:29.

Lu, Q., P. Yang, X. Huang, W. Hu, B. Guo, F. Wu, L. Lin, A.L. Kovacs, L. Yu, and H. Zhang. 2011. The WD40 repeat PtdIns(3)P-binding protein EPG-6 regulates progression of omegasomes to autophagosomes. *Dev. Cell*. 21:343-357.

Luo, J., N.L. Solimini, and S.J. Elledge. 2009. Principles of cancer therapy: oncogene and non-oncogene addiction. *Cell*. 136:823-837.

Mammucari, C., G. Milan, V. Romanello, E. Masiero, R. Rudolf, P. Del Piccolo, S.J. Burden, R. Di Lisi, C. Sandri, J. Zhao, A.L. Goldberg, S. Schiaffino, and M. Sandri. 2007. FoxO3 controls autophagy in skeletal muscle in vivo. *Cell Metab.* 6:458-471.

Manzanillo, P.S., J.S. Ayres, R.O. Watson, A.C. Collins, G. Souza, C.S. Rae, D.S. Schneider, K. Nakamura, M.U. Shiloh, and J.S. Cox. 2013. The ubiquitin ligase parkin mediates resistance to intracellular pathogens. *Nature*. 501:512-516.

Maruzs, T., P. Lorincz, Z. Szatmari, S. Szeplaki, Z. Sandor, Z. Lakatos, G. Puska, G. Juhasz, and M. Sass. 2015. Retromer ensures the degradation of autophagic cargo via maintaining lysosome function in Drosophila. *Traffic*.

Mauvezin, C., P. Nagy, G. Juhasz, and T.P. Neufeld. 2015. Autophagosome-lysosome fusion is independent of V-ATPase-mediated acidification. *Nat Commun*. 6:7007.

Michel, M., M. Schwarten, C. Decker, L. Nagel-Steger, D. Willbold, and O.H. Weiergraber. 2015. The mammalian autophagy initiator complex contains two HORMA domain proteins. *Autophagy*:0.

Mijaljica, D., M. Prescott, and R.J. Devenish. 2011. Microautophagy in mammalian cells: revisiting a 40-year-old conundrum. *Autophagy*. 7:673-682.

Mizushima, N., and M. Komatsu. 2011. Autophagy: renovation of cells and tissues. *Cell*. 147:728-741.

Mizushima, N., T. Yoshimori, and B. Levine. 2010. Methods in mammalian autophagy research. *Cell*. 140:313-326.

Mizushima, N., T. Yoshimori, and Y. Ohsumi. 2011. The role of Atg proteins in autophagosome formation. *Ann. Rev. Cell Dev. Biol.* 27:107-132.

Morselli, E., G. Marino, M.V. Bennetzen, T. Eisenberg, E. Megalou, S. Schroeder, S. Cabrera, P. Benit, P. Rustin, A. Criollo, O. Kepp, L. Galluzzi, S. Shen, S.A. Malik, M.C. Maiuri, Y. Horio, C. Lopez-Otin, J.S. Andersen, N. Tavernarakis, F. Madeo, and G. Kroemer. 2011. Spermidine and resveratrol induce autophagy by distinct pathways converging on the acetylproteome. *The Journal of cell biology*. 192:615-629.

Mulakkal, N.C., P. Nagy, S. Takats, R. Tusco, G. Juhasz, and I.P. Nezis. 2014. Autophagy in Drosophila: From Historical Studies to Current Knowledge. *BioMed Res Int*. 2014:273473.

Musiwaro, P., M. Smith, M. Manifava, S.A. Walker, and N.T. Ktistakis. 2013. Characteristics and requirements of basal autophagy in HEK 293 cells. *Autophagy*. 9:1407-1417.

Nagy, P., K. Hegedus, K. Pircs, A. Varga, and G. Juhasz. 2014a. Different effects of Atg2 and Atg18 mutations on Atg8a and Atg9 trafficking during starvation in Drosophila. *FEBS Lett.* 588:408-413.

Nagy, P., M. Karpati, A. Varga, K. Pircs, Z. Venkei, S. Takats, K. Varga, B. Erdi, K. Hegedus, and G. Juhasz. 2014b. Atg17/FIP200 localizes to perilysosomal Ref(2)P aggregates and promotes autophagy by activation of Atg1 in Drosophila. *Autophagy*. 10:453-467.

Nagy, P., A. Varga, A.L. Kovacs, S. Takats, and G. Juhasz. 2015. How and why to study autophagy in Drosophila: It's more than just a garbage chute. *Methods*. 75:151-161.

Nagy, P., A. Varga, K. Pircs, K. Hegedus, and G. Juhasz. 2013. Myc-Driven Overgrowth Requires Unfolded Protein Response-Mediated Induction of Autophagy and Antioxidant Responses in Drosophila melanogaster. *PLOS Genetics*. 9:e1003664.

Narendra, D., J.E. Walker, and R. Youle. 2012. Mitochondrial quality control mediated by PINK1 and Parkin: links to parkinsonism. *Cold Spring Harb Perspect Biol*. 4.

Nedjic, J., M. Aichinger, J. Emmerich, N. Mizushima, and L. Klein. 2008. Autophagy in thymic epithelium shapes the T-cell repertoire and is essential for tolerance. *Nature*. 455:396-400.

Nezis, I.P., A. Simonsen, A.P. Sagona, K. Finley, S. Gaumer, D. Contamine, T.E. Rusten, H. Stenmark, and A. Brech. 2008. Ref(2)P, the Drosophila melanogaster homologue of mammalian p62, is required for the formation of protein aggregates in adult brain. *J. Cell Biol.* 180:1065-1071.

Nishida, Y., S. Arakawa, K. Fujitani, H. Yamaguchi, T. Mizuta, T. Kanaseki, M. Komatsu, K. Otsu, Y. Tsujimoto, and S. Shimizu. 2009. Discovery of Atg5/Atg7-independent alternative macroautophagy. *Nature*. 461:654-658.

Nobukuni, T., M. Joaquin, M. Roccio, S.G. Dann, S.Y. Kim, P. Gulati, M.P. Byfield, J.M. Backer, F. Natt, J.L. Bos, F.J. Zwartkruis, and G. Thomas. 2005. Amino acids mediate mTOR/raptor signaling through activation of class 3 phosphatidylinositol 3OH-kinase. *Proc. Natl. Acad. Sci. USA*. 102:14238-14243.

Noda, T., and Y. Ohsumi. 1998. Tor, a phosphatidylinositol kinase homologue, controls autophagy in yeast. *J. Biol. Chem.* 273:3963-3966.

Novikoff, A.B. 1959. The proximal tubule cell in experimental hydronephrosis. *J Biophys Biochem Cytol*. 6:136-138.

Pankiv, S., T.H. Clausen, T. Lamark, A. Brech, J.A. Bruun, H. Outzen, A. Overvatn, G. Bjorkoy, and T. Johansen. 2007. p62/SQSTM1 binds directly to Atg8/LC3 to facilitate degradation of ubiquitinated protein aggregates by autophagy. *J. Biol. Chem.* 282:24131-24145.

Pattingre, S., A. Tassa, X. Qu, R. Garuti, X.H. Liang, N. Mizushima, M. Packer, M.D. Schneider, and B. Levine. 2005. Bcl-2 antiapoptotic proteins inhibit Beclin 1-dependent autophagy. *Cell*. 122:927-939.

Pierce, S.B., C. Yost, J.S. Britton, L.W. Loo, E.M. Flynn, B.A. Edgar, and R.N. Eisenman. 2004. dMyc is required for larval growth and endoreplication in Drosophila. *Development*. 131:2317-2327.

Pircs, K., P. Nagy, A. Varga, Z. Venkei, B. Erdi, K. Hegedus, and G. Juhasz. 2012. Advantages and limitations of different p62-based assays for estimating autophagic activity in Drosophila. *PLoS One*. 7:e44214.

Polson, H.E., J. de Lartigue, D.J. Rigden, M. Reedijk, S. Urbe, M.J. Clague, and S.A. Tooze. 2010. Mammalian Atg18 (WIPI2) localizes to omegasome-anchored phagophores and positively regulates LC3 lipidation. *Autophagy*. 6:506-522.

Randow, F., J.D. MacMicking, and L.C. James. 2013. Cellular self-defense: how cell-autonomous immunity protects against pathogens. *Science*. 340:701-706.

Ravikumar, B., R. Duden, and D.C. Rubinsztein. 2002. Aggregate-prone proteins with polyglutamine and polyalanine expansions are degraded by autophagy. *Hum. Mol. Genet.* 11:1107-1117.

Ravikumar, B., C. Vacher, Z. Berger, J.E. Davies, S. Luo, L.G. Oroz, F. Scaravilli, D.F. Easton, R. Duden, C.J. O'Kane, and D.C. Rubinsztein. 2004. Inhibition of mTOR induces autophagy and reduces toxicity of polyglutamine expansions in fly and mouse models of Huntington disease. *Nat. Genet.* 36:585-595.

Rebsamen, M., L. Pochini, T. Stasyk, M.E. de Araujo, M. Galluccio, R.K. Kandasamy, B. Snijder, A. Fauster, E.L. Rudashevskaya, M. Bruckner, S. Scorzoni, P.A. Filipek, K.V. Huber, J.W. Bigenzahn, L.X. Heinz, C. Kraft, K.L. Bennett, C. Indiveri, L.A. Huber, and G. Superti-Furga. 2015. SLC38A9 is a component of the lysosomal amino acid sensing machinery that controls mTORC1. *Nature*. 519:477-481.

Riddiford, L.M. 1993. Hormone receptors and the regulation of insect metamorphosis. *Receptor*. 3:203-209.

Rogov, V., V. Dotsch, T. Johansen, and V. Kirkin. 2014. Interactions between Autophagy Receptors and Ubiquitin-like Proteins Form the Molecular Basis for Selective Autophagy. *Mol. Cell*. 53:167-178.

Rubinsztein, D.C., P. Codogno, and B. Levine. 2012. Autophagy modulation as a potential therapeutic target for diverse diseases. *Nature reviews. Drug discovery*. 11:709-730.

Rusten, T.E., K. Lindmo, G. Juhasz, M. Sass, P.O. Seglen, A. Brech, and H. Stenmark. 2004. Programmed autophagy in the Drosophila fat body is induced by ecdysone through regulation of the PI3K pathway. *Dev. Cell*. 7:179-192.

Rusten, T.E., T. Vaccari, K. Lindmo, L.M. Rodahl, I.P. Nezis, C. Sem-Jacobsen, F. Wendler, J.P. Vincent, A. Brech, D. Bilder, and H. Stenmark. 2007. ESCRTs and Fab1 regulate distinct steps of autophagy. *Curr. Biol.* 17:1817-1825.

Saitsu, H., T. Nishimura, K. Muramatsu, H. Kodera, S. Kumada, K. Sugai, E. Kasai-Yoshida, N. Sawaura, H. Nishida, A. Hoshino, F. Ryujin, S. Yoshioka, K. Nishiyama, Y. Kondo, Y. Tsurusaki, M. Nakashima, N. Miyake, H. Arakawa, M. Kato, N. Mizushima, and N. Matsumoto. 2013. De novo mutations in the autophagy gene WDR45 cause static encephalopathy of childhood with neurodegeneration in adulthood. *Nat. Genet.* 45:445-449, 449e441.

Sancak, Y., L. Bar-Peled, R. Zoncu, A.L. Markhard, S. Nada, and D.M. Sabatini. 2010. Ragulator-Rag complex targets mTORC1 to the lysosomal surface and is necessary for its activation by amino acids. *Cell*. 141:290-303.

Sass, M., and J. Kovacs. 1975. Ecdysterone and an analogue of juvenile hormone on the autophagy in the cells of fat body of mamestra brassicae. *Acta Biol Acad Sci Hung*. 26:189-196.

Scott, R.C., G. Juhasz, and T.P. Neufeld. 2007. Direct induction of autophagy by atg1 inhibits cell growth and induces apoptotic cell death. *Curr. Biol.* 17:1-11.

Scott, R.C., O. Schuldiner, and T.P. Neufeld. 2004. Role and regulation of starvation-induced autophagy in the Drosophila fat body. *Dev. Cell*. 7:167-178.

Scott, S.V., D.C. Nice, 3rd, J.J. Nau, L.S. Weisman, Y. Kamada, I. Keizer-Gunnink, T. Funakoshi, M. Veenhuis, Y. Ohsumi, and D.J. Klionsky. 2000. Apg13p and Vac8p are part of a complex of phosphoproteins that are required for cytoplasm to vacuole targeting. *J. Biol. Chem.* 275:25840-25849.

Seglen, P.O., and P.B. Gordon. 1982. 3-Methyladenine: specific inhibitor of autophagic/lysosomal protein degradation in isolated rat hepatocytes. *Proc Natl Acad Sci U S A.* 79:1889-1892.

Simonsen, A., R.C. Cumming, A. Brech, P. Isakson, D.R. Schubert, and K.D. Finley. 2008. Promoting basal levels of autophagy in the nervous system enhances longevity and oxidant resistance in adult Drosophila. *Autophagy*. 4:176-184.

Suzuki, H., T. Kaizuka, N. Mizushima, and N.N. Noda. 2015. Structure of the Atg101-Atg13 complex reveals essential roles of Atg101 in autophagy initiation. *Nat Struct Mol Biol*. 22:572-580.

Szatmari, Z., V. Kis, M. Lippai, K. Hegedus, T. Farago, P. Lorincz, T. Tanaka, G. Juhasz, and M. Sass. 2014. Rab11 facilitates cross-talk between autophagy and endosomal pathway through regulation of Hook localization. *Mol. Biol. Cell*. 25:522-531.

Takats, S., and G. Juhasz. 2013. A genetic model with specifically impaired autophagosome-lysosome fusion. *Autophagy*. 9:1251-1252.

Takats, S., P. Nagy, and G. Juhasz. 2014a. Az autofágia szerepének és szabályozásának vizsgálata Drosophila modellen. *Biokémia*. 38:17-29.

Takats, S., P. Nagy, A. Varga, K. Pircs, M. Karpati, K. Varga, A.L. Kovacs, K. Hegedus, and G. Juhasz. 2013. Autophagosomal Syntaxin17-dependent lysosomal degradation maintains neuronal function in Drosophila. *J. Cell Biol.* 201:531-539.

Takats, S., K. Pircs, P. Nagy, A. Varga, M. Karpati, K. Hegedus, H. Kramer, A.L. Kovacs, M. Sass, and G. Juhasz. 2014b. Interaction of the HOPS complex with Syntaxin 17 mediates autophagosome clearance in Drosophila. *Mol. Biol. Cell*. 25:1338-1354.

Takats, S., A. Varga, K. Pircs, and G. Juhasz. 2015. Loss of Drosophila Vps16A enhances autophagosome formation through reduced TOR activity. *Autophagy*:0.

Thomasson, W.A., and H.K. Mitchell. 1972. Hormonal control of protein granule accumulation in fat bodies of Drosophila melanogaster larvae. *J Insect Physiol*. 18:1885-1899.

Thumm, M., R. Egner, B. Koch, M. Schlumpberger, M. Straub, M. Veenhuis, and D.H. Wolf. 1994. Isolation of autophagocytosis mutants of Saccharomyces cerevisiae. *FEBS Lett.* 349:275-280.

Toh, P.P., S. Luo, F.M. Menzies, T. Rasko, E.E. Wanker, and D.C. Rubinsztein. 2013. Myc inhibition impairs autophagosome formation. *Hum. Mol. Genet.* 22:5237-5248.

Tsukada, M., and Y. Ohsumi. 1993. Isolation and characterization of autophagy-defective mutants of Saccharomyces cerevisiae. *FEBS Lett.* 333:169-174.

Tsukamoto, S., A. Kuma, M. Murakami, C. Kishi, A. Yamamoto, and N. Mizushima. 2008. Autophagy is essential for preimplantation development of mouse embryos. *Science*. 321:117-120.

Vellai, T., K. Takacs-Vellai, M. Sass, and D.J. Klionsky. 2009. The regulation of aging: does autophagy underlie longevity? *Trends Cell Biol*. 19:487-494.

von Gaudecker, B. 1963. Uber den Formwechsel einiger Zellorganelle bei der Bildung der Reservestoffe in Fettkorper von Drosophila-larven. *Z. Zellforsch.* 61:56-95.

Wang, C.W., P.E. Stromhaug, J. Shima, and D.J. Klionsky. 2002. The Ccz1-Mon1 protein complex is required for the late step of multiple vacuole delivery pathways. *J. Biol. Chem.* 277:47917-47927.

Wang, S., Z.Y. Tsun, R.L. Wolfson, K. Shen, G.A. Wyant, M.E. Plovanich, E.D. Yuan, T.D. Jones, L. Chantranupong, W. Comb, T. Wang, L. Bar-Peled, R. Zoncu, C. Straub, C. Kim, J. Park, B.L. Sabatini, and D.M. Sabatini. 2015. Metabolism. Lysosomal amino acid transporter SLC38A9 signals arginine sufficiency to mTORC1. *Science*. 347:188-194.

Weavers, H., S. Prieto-Sanchez, F. Grawe, A. Garcia-Lopez, R. Artero, M. Wilsch-Brauninger, M. Ruiz-Gomez, H. Skaer, and B. Denholm. 2009. The insect nephrocyte is a podocyte-like cell with a filtration slit diaphragm. *Nature*. 457:322-326.

White, E. 2012. Deconvoluting the context-dependent role for autophagy in cancer. *Nature Rev Cancer*. 12:401-410.

Wong, P.M., C. Puente, I.G. Ganley, and X. Jiang. 2013. The ULK1 complex: sensing nutrient signals for autophagy activation. *Autophagy*. 9:124-137.

Xu, T., S. Nicolson, D. Denton, and S. Kumar. 2015. Distinct requirements of Autophagy-related genes in programmed cell death. *Cell Death Differ*.

Yamamoto, A., Y. Tagawa, T. Yoshimori, Y. Moriyama, R. Masaki, and Y. Tashiro. 1998. Bafilomycin A1 prevents maturation of autophagic vacuoles by inhibiting fusion between autophagosomes and lysosomes in rat hepatoma cell line, H-4-II-E cells. *Cell Struct. Funct.* 23:33-42.

Yamamoto, H., S. Kakuta, T.M. Watanabe, A. Kitamura, T. Sekito, C. Kondo-Kakuta, R. Ichikawa, M. Kinjo, and Y. Ohsumi. 2012. Atg9 vesicles are an important membrane source during early steps of autophagosome formation. *J. Cell Biol.* 198:219-233.

Yamamoto, R., and M. Tatar. 2011. Insulin receptor substrate chico acts with the transcription factor FOXO to extend Drosophila lifespan. *Aging Cell*. 10:729-732.

Zhang, H., J.P. Stallock, J.C. Ng, C. Reinhard, and T.P. Neufeld. 2000. Regulation of cellular growth by the Drosophila target of rapamycin dTOR. *Genes Dev.* 14:2712-2724.

Zhao, J., J.J. Brault, A. Schild, P. Cao, M. Sandri, S. Schiaffino, S.H. Lecker, and A.L. Goldberg. 2007. FoxO3 coordinately activates protein degradation by the autophagic/lysosomal and proteasomal pathways in atrophying muscle cells. *Cell Metab.* 6:472-483.

Zoncu, R., L. Bar-Peled, A. Efeyan, S. Wang, Y. Sancak, and D.M. Sabatini. 2011. mTORC1 senses lysosomal amino acids through an inside-out mechanism that requires the vacuolar H(+)-ATPase. *Science*. 334:678-683.

KÖZLEMÉNY ADATOK

Az értekezésben tárgyalt, PhD óta 2014. májusáig publikált, lektorált folyóiratcikkek

Cikkek száma 2014. májusáig: 27 (ebből 9 társszerzős, 6 elsőszerzős, 1 egyedüli szerzős, 11 utolsó szerzős [amiből egy megosztott utolsó szerzős])

Impakt faktoraik összege 2014. májusáig: 205.5

A nevem melletti * jel azokat a publikációkat jelzi, ahol levelező szerzőként szerepelek.

Rusten TE, Lindmo K, Juhasz G, Sass M, Seglen PO, Brech A, Stenmark H
Programmed autophagy in the Drosophila fat body is induced by ecdysone through regulation of the PI3K pathway
DEVELOPMENTAL CELL 7: pp. 179-192. (2004)
IF: 15.434

*Juhasz G, Sass M
Hid can induce, but is not required for autophagy in polyploid larval Drosophila tissues
EUROPEAN JOURNAL OF CELL BIOLOGY 84: pp. 491-502. (2005)
IF: 2.195

Akdemir F, Farkas R, Chen P, Juhasz G, Medvedova L, Sass M, Wang L, Wang XD, Chittaranjan S, Gorski SM, Rodriguez A, Abrams JM
Autophagy occurs upstream or parallel to the apoptosome during histolytic cell death
DEVELOPMENT 133:(8) pp. 1457-1465. (2006)
IF: 7.764

*Juhasz G, Neufeld TP
Autophagy: A Forty-year Search For a Missing Membrane Source
PLOS BIOLOGY 4:(2) pp. 161-164. (2006)
IF: 14.101

Juhasz G, Erdi B, Sass M, Neufeld TP
Atg7-dependent autophagy promotes neuronal health, stress tolerance, and longevity but is dispensable for metamorphosis in Drosophila.
GENES & DEVELOPMENT 21:(23) pp. 3061-3066. (2007)
IF: 14.795

*Juhasz G, Puskas LG, Komonyi O, Erdi B, Maroy P, Neufeld TP, Sass M
Gene expression profiling identifies FKBP39 as an inhibitor of autophagy in larval Drosophila fat body
CELL DEATH AND DIFFERENTIATION 14:(6) pp. 1181-1190. (2007)
IF: 8.254

Scott RC, Juhasz G, Neufeld TP
Direct induction of autophagy by Atg1 inhibits cell growth and induces apoptotic cell death
CURRENT BIOLOGY 17: pp. 1-11. (2007)
IF: 10.539

Juhasz G, Neufeld TP
Experimental control and characterization of autophagy in Drosophila
METHODS IN MOLECULAR BIOLOGY 445: pp. 125-133. (2008)
Autophagosome and Phagosome. (ISBN 978-1-58829-853-9)

Juhasz G, Hill JH, Yan Y, Sass M, Baehrecke EH, Backer JM, Neufeld TP
The class III PI(3)K Vps34 promotes autophagy and endocytosis but not TOR signaling in Drosophila.
JOURNAL OF CELL BIOLOGY 181:(4) pp. 655-666. (2008)
IF: 9.120

Lippai M, Csikos G, Maroy P, Lukacsovich T, Juhasz G, Sass M
SNF4Agamma, the Drosophila AMPK gamma subunit is required for regulation of developmental and stress-induced autophagy.
AUTOPHAGY 4:(4) pp. 476-486. (2008)
IF: 5.479

Chang YY, Juhasz G, Goraksha-Hicks P, Arsham AM, Mallin DR, Muller LK, Neufeld TP
Nutrient-dependent regulation of autophagy through the target of rapamycin pathway
BIOCHEMICAL SOCIETY TRANSACTIONS 37:(1) pp. 232-236. (2009)
IF: 3.378

Csikós G, Lippai M, Lukácsovich T, Juhász G, Henn L, Erdélyi M, Maróy P, Sass M
A novel role for the Drosophila epsin (lqf): involvement in autophagy
AUTOPHAGY 5:(5) pp. 636-648. (2009)
IF: 6.829

*Juhasz G
Interpretation of bafilomycin, pH neutralizing or protease inhibitor treatments in autophagic flux experiments: Novel considerations
AUTOPHAGY 8:(12) pp. 1875-1876. (2012)
IF: 12.042

Erdi B, Nagy P, Zvara A, Varga A, Pircs K, Menesi D, Puskas LG, *Juhasz G
Loss of the starvation-induced gene Rack1 leads to glycogen deficiency and impaired autophagic responses in Drosophila
AUTOPHAGY 8:(7) pp. 1124-1135. (2012)
IF: 12.042

Pircs K, Nagy P, Varga A, Venkei Z, Erdi B, Hegedus K, *Juhasz G
Advantages and Limitations of Different p62-Based Assays for Estimating Autophagic Activity in Drosophila
PLOS ONE 7:(8) Paper e44214. 11 p. (2012)
IF: 3.730

[1269 szerző], Klionsky DJ, Abdalla FC, Bánhegyi G, Fésüs L, Juhász G, Kovács AL, Lõw P, Sass M, Takács-Vellai K, Vellai T, Zuckerbraun B
Guidelines for the use and interpretation of assays for monitoring autophagy
AUTOPHAGY 8:(4) pp. 445-544. (2012)
IF: 12.042

Low P, Varga A, Pircs K, Nagy P, Szatmari Z, Sass M, *Juhasz G
Impaired proteasomal degradation enhances autophagy via hypoxia signaling in Drosophila.
BMC CELL BIOLOGY 14:(1) Paper 29. (2013)
IF: 2.808

Nagy P, Varga A, Pircs K, Hegedus K, *Juhasz G
Myc-Driven Overgrowth Requires Unfolded Protein Response-Mediated Induction of Autophagy and Antioxidant Responses in Drosophila melanogaster.
PLOS GENETICS 9:(8) p. e1003664. (2013)
IF: 8.517

Takats S, Nagy P, Varga A, Pircs K, Karpati M, Varga K, Kovacs AL, Hegedus K, *Juhasz G
Autophagosomal Syntaxin17-dependent lysosomal degradation maintains neuronal function in Drosophila.
JOURNAL OF CELL BIOLOGY 201:(4) pp. 531-539. (2013)
IF: 10.822

Hegedus K, Takats S, Kovacs AL, *Juhasz G
Evolutionarily conserved role and physiological relevance of a STX17/Syx17 (syntaxin 17)-containing SNARE complex in autophagosome fusion with endosomes and lysosomes.
AUTOPHAGY 9:(10) pp. 1642-1646. (2013)
IF: 12.042

Eisenberg T, Schroeder S, Andryushkova A, Pendl T, Kuttner V, Bhukel A, Marino G, Pietrocola F, Harger A, Zimmermann A, Moustafa T, Sprenger A, Jany E, Buttner S, Carmona-Gutierrez D, Ruckenstuhl C, Ring J, Reichelt W, Schimmel K, Leeb T, Moser C, Schatz S, Kamolz LP, Magnes C, Sinner F, Sedej S, Frohlich KU, Juhasz G, Pieber TR, Dengjel J, Sigrist SJ, Kroemer G, Madeo F
Nucleocytosolic depletion of the energy metabolite acetyl-coenzyme a stimulates autophagy and prolongs lifespan.
CELL METABOLISM 19:(3) pp. 431-444. (2014)
IF: 14.619

Hegedus K, Nagy P, Gaspari Z, *Juhasz G
The Putative HORMA Domain Protein Atg101 Dimerizes and Is Required for Starvation-Induced and Selective Autophagy in Drosophila
BIOMED RESEARCH INTERNATIONAL 2014: Paper 470482. 13 p. (2014)
IF: 2.880

Nagy P, Karpati M, Varga A, Pircs K, Venkei Z, Takats S, Varga K, Erdi B, Hegedus K, *Juhasz G
Atg17/FIP200 localizes to perilysosomal Ref(2)P aggregates and promotes autophagy by activation of Atg1 in Drosophila
AUTOPHAGY 10:(3) pp. 453-467. (2014)
IF: 12.042

Nagy P, Hegedus K, Pircs K, Varga A, *Juhasz G
Different effects of Atg2 and Atg18 mutations on Atg8a and Atg9 trafficking during starvation in Drosophila.
FEBS LETTERS 588: pp. 408-413. (2014)
IF: 3.582

Szatmari Z, Kis V, Lippai M, Hegedus K, Farago T, Lorincz P, Tanaka T, Juhasz G, Sass M
Rab11 facilitates crosstalk between autophagy and endosomal pathway through regulation of Hook localization.
MOLECULAR BIOLOGY OF THE CELL 25:(4) pp. 522-531. (2014)
IF: 4.803

Mulakkal N, Nagy P, Takats S, Tusco R, *Juhasz G, Nezis IP (társ-szenior szerzős publikáció)
Autophagy in Drosophila: from historical studies to current knowledge
BIOMED RESEARCH INTERNATIONAL 2014: Paper 273473. 24 p. (2014)
IF: 2.880

Takats S, Pircs K, Nagy P, Varga A, Karpati M, Hegedus K, Kramer H, Kovacs AL, Sass M, *Juhasz G
Interaction of the HOPS complex with Syntaxin 17 mediates autophagosome clearance in Drosophila
MOLECULAR BIOLOGY OF THE CELL 25:(8) pp. 1338-1354. (2014)
IF: 4.803

Az értekezés témakörében megjelent, PhD óta 2014. májusáig publikált, egyéb közlemények

Folyóiratcikk:Hozzászólás, helyreigazítás (főszerkesztői meghívásra írt, főszerkesztő által lektorált, nagy jelentőségűnek ítélt publikációhoz fűzött ön-kommentárok)

Juhasz G, Neufeld TP
Drosophila Atg7: required for stress resistance, longevity and neuronal homeostasis, but not for metamorphosis.
AUTOPHAGY 4:(3) pp. 357-358. (2008)

Takats S, *Juhasz G
A genetic model with specifically impaired autophagosome-lysosome fusion.
AUTOPHAGY 9:(8) pp. 1251-1252. (2013)

Felsőoktatási tankönyv

Juhász G, Kovács AL, László L, Lőw P
Lőw P (szerk.)
Az önemésztés, sejtpusztulás és megújulás molekuláris sejtbiológiája
Budapest: ELTE TTK, 2013.
http://elte.prompt.hu/sites/default/files/tananyagok/onemesztes/index.html
http://elte.prompt.hu/sites/default/files/tananyagok/onemesztes/book.pdf

Personalia, alkalmi megemlékezés

Juhasz G, Puertollano R, Shimizu S, Vaccaro MI
Autophagy researchers
AUTOPHAGY 9:(6) pp. 815-818. (2013)

Az értekezéshez közvetlenül nem kapcsolódó, PhD óta 2014. májusáig publikált, lektorált közlemények

Papp AM, Nyilas R, Szepesi Z, Lorincz ML, Takacs E, Abraham I, Szilagyi N, Toth J, Medveczky P, Szilagyi L, Juhasz G, Juhasz G
Visible light induces matrix metalloproteinase-9 expression in rat eye
JOURNAL OF NEUROCHEMISTRY 103:(6) pp. 2224-2233. (2007)
IF: 4.451

Kelemen-Valkony I, Kiss M, Csiha J, Kiss A, Bircher U, Szidonya J, Maroy P, Juhasz G, Komonyi O, Csiszar K, Mink M
Drosophila basement membrane collagen col4a1 mutations cause severe myopathy
MATRIX BIOLOGY 31:(1) pp. 29-37. (2012)
IF: 3.190

Venkei Z, Przewloka MR, Ladak Y, Albadri S, Sossick A, Juhasz G, Novak B, Glover DM
Spatiotemporal dynamics of Spc105 regulates the assembly of the Drosophila kinetochore.
OPEN BIOLOGY 2:(2) (2012)
IF: 3.625

Molnár I, Migh E, Szikora S, Kalmár T, Végh AG, Deák F, Barkó S, Bugyi B, Orfanos Z, Kovács J, Juhász G, Váró G, Nyitrai M, Sparrow J, Mihály J
DAAM is required for thin filament formation and sarcomerogenesis during muscle development in Drosophila
PLOS GENETICS 10:(2) Paper e1004166. 15 p. (2014)
IF: 8.517

Tudománymetriai adatok

Az MTMT adatbázis 2014. május 13-i zárásakor aktuális publikációs adataim:

Juhász Gábor tudományos és oktatási munkásságának összefoglalása
VIII. Biológiai Tudományok Osztálya (2014.06.02.)

Közlemény típusok	Száma		Hivatkozások[1]	
	Összesen	Részletezve	Független	Összes
I. Tudományos folyóiratcikk	33	---	---	---
teljes cikk[2], nemzetközi folyóiratban	---	31	1081	1235
teljes cikk, hazai idegen nyelvű folyóiratban	---	1	1	3
teljes cikk, magyar nyelvű folyóiratban	---	0	0	0
teljes cikk, rövid közlemény	---	0	0	0
Sokszerzős és/vagy csoportos szerzőségű cikk, szerzőként	---	1	99	322
II. Könyvek	1	---	---	---
a) Szakkönyv, tankönyv, szerzőként	1	---	---	---
Szakkönyv, kézikönyv, idegen nyelvű	---	0	0	0
Szakkönyv, kézikönyv, magyar nyelvű	---	0	0	0
Felsőoktatási tankönyv	---	1	0	0
b) Szakkönyv, szerkesztőként	0	---	---	---
Szakkönyv, kézikönyv, idegen nyelvű	---	0	---	---
Szakkönyv, kézikönyv, magyar nyelvű	---	0	---	---
Felsőoktatási tankönyv	---	0	---	---
III. Könyvfejezet	0	---	---	---
Könyvfejezet, idegen nyelvű	---	0	0	0
Könyvfejezet, magyar nyelvű	---	0	0	0
Felsőoktatási tankönyvekfejezet	---	0	0	0
IV. Konferenciaközlemény[3]	0	---	0	0
Tudományos és oktatási közlemények összesen (I-IV.)	34	---	1181	1560
V. Egyéb tudományos	3	---	---	---
Egyéb tudományos művek, ide értve a nem teljes folyóiratcikkeket és a nem ismert lektoráltságú folyóiratokban megjelent teljes folyóiratcikkeket is	---	1	0	0
Szerkesztőségi levelezés, hozzászólások, válaszok	---	2	13	13
VI. Absztrakt	3	---	0	0
Összesített impakt faktor	241,2	---	---	---
Idézettség száma[1]	---	---	1194	1573
Hirsch index[1]	13	---	---	---

Speciális tudománymetriai adatok	Adat
Első szerzős folyóiratcikkek száma (az összes %-ban)	9 (27,27%)
Utolsó szerzős tudományos cikkek száma (az összes %-ban)	11 (33,33%)
Első és utolsó szerzőségű folyóiratcikkek impakt faktorai	142,1
Hivatkozások nemzetközi adatbázisokban (WOS és/vagy Scopus), azonosítóval jelölve[4]	1427
Az utolsó tudományos fokozat (PhD) elnyerése utáni (2004 -) tudományos folyóiratcikkek összegzett impakt faktora és száma (zárójelben)	221,9 (30)
Az utolsó tudományos fokozat (PhD) elnyerése utáni (2004 -) tudományos folyóiratcikkek összegzett impakt faktora az összes %-ban	91,99%
Magyar nyelven megjelent tudományos teljes folyóiratcikkek száma	0
Az utolsó 10 év (2004-2014) tudományos teljes, lektorált folyóiratcikkeinek száma	31
impakt faktor összege	237,3
független hivatkozások száma	1119
Folyóiratcikkek, 15-nél több szerzővel	1

Az utolsó szerzős tudományos cikkeim számában, valamint az első és utolsó szerzős folyóiratcikkeim impakt faktoraiban megosztott szenior szerzős összefoglaló jellegű publikációmat (*BIOMED RES INT* 273473. 24 p. 2014, impakt faktor: 2,880) az MTMT nem vette figyelembe, mivel nem kezeli a megosztott szerzőséget.

A PhD fokozatom elnyerését követően, de ugyanabban az évben elfogadott és megjelent társszerzős cikkemet (*DEV CELL* 7: pp. 179-192. 2004, impakt faktor: 15,434) az MTMT nem vette figyelembe a PhD utáni tudományos folyóiratcikkeim összegzett impakt faktoránál és számánál, mivel a program csak a 2004 utáni publikációk alapján számol.

dc_840_14

MTA DOKTORI ÉRTEKEZÉS

KÖZLEMÉNYEK

JUHÁSZ GÁBOR

2014

dc_840_14

Juhász Gábor MTA Doktori értekezésének témakörében megjelent, PhD óta publikált, lektorált folyóiratcikkei

Cikkek száma: 27 (ebből 9 társszerzős, 6 elsőszerzős, 1 egyedüli szerzős, 11 utolsó szerzős [amiből egy megosztott utolsó szerzős])

Impakt faktoraik összege: 205.5

*A nevem melletti * jel azokat a publikációkat jelzi, ahol levelező szerzőként szerepelek.*

Rusten TE, Lindmo K, Juhasz G, Sass M, Seglen PO, Brech A, Stenmark H
Programmed autophagy in the Drosophila fat body is induced by ecdysone through regulation of the PI3K pathway
DEVELOPMENTAL CELL 7: pp. 179-192. (2004)
IF: 15.434

*Juhasz G, Sass M
Hid can induce, but is not required for autophagy in polyploid larval Drosophila tissues
EUROPEAN JOURNAL OF CELL BIOLOGY 84: pp. 491-502. (2005)
IF: 2.195

Akdemir F, Farkas R, Chen P, Juhasz G, Medvedova L, Sass M, Wang L, Wang XD, Chittaranjan S, Gorski SM, Rodriguez A, Abrams JM
Autophagy occurs upstream or parallel to the apoptosome during histolytic cell death
DEVELOPMENT 133:(8) pp. 1457-1465. (2006)
IF: 7.764

*Juhasz G, Neufeld TP
Autophagy: A Forty-year Search For a Missing Membrane Source
PLOS BIOLOGY 4:(2) pp. 161-164. (2006)
IF: 14.101

Juhasz G, Erdi B, Sass M, Neufeld TP
Atg7-dependent autophagy promotes neuronal health, stress tolerance, and longevity but is dispensable for metamorphosis in Drosophila.
GENES & DEVELOPMENT 21:(23) pp. 3061-3066. (2007)
IF: 14.795

*Juhasz G, Puskas LG, Komonyi O, Erdi B, Maroy P, Neufeld TP, Sass M
Gene expression profiling identifies FKBP39 as an inhibitor of autophagy in larval Drosophila fat body
CELL DEATH AND DIFFERENTIATION 14:(6) pp. 1181-1190. (2007)
IF: 8.254

Scott RC, Juhasz G, Neufeld TP
Direct induction of autophagy by Atg1 inhibits cell growth and induces apoptotic cell death
CURRENT BIOLOGY 17: pp. 1-11. (2007)
IF: 10.539

Juhasz G, Neufeld TP
Experimental control and characterization of autophagy in Drosophila
METHODS IN MOLECULAR BIOLOGY 445: pp. 125-133. (2008)
Autophagosome and Phagosome. (ISBN 978-1-58829-853-9)

Juhasz G, Hill JH, Yan Y, Sass M, Baehrecke EH, Backer JM, Neufeld TP
The class III PI(3)K Vps34 promotes autophagy and endocytosis but not TOR signaling in Drosophila.
JOURNAL OF CELL BIOLOGY 181:(4) pp. 655-666. (2008)
IF: 9.120

Lippai M, Csikos G, Maroy P, Lukacsovich T, Juhasz G, Sass M
SNF4Agamma, the Drosophila AMPK gamma subunit is required for regulation of developmental and stress-induced autophagy.
AUTOPHAGY 4:(4) pp. 476-486. (2008)
IF: 5.479

Chang YY, Juhasz G, Goraksha-Hicks P, Arsham AM, Mallin DR, Muller LK, Neufeld TP
Nutrient-dependent regulation of autophagy through the target of rapamycin pathway
BIOCHEMICAL SOCIETY TRANSACTIONS 37:(1) pp. 232-236. (2009)
IF: 3.378

Csikós G, Lippai M, Lukácsovich T, Juhász G, Henn L, Erdélyi M, Maróy P, Sass M
A novel role for the Drosophila epsin (lqf): involvement in autophagy
AUTOPHAGY 5:(5) pp. 636-648. (2009)
IF: 6.829

*Juhasz G
Interpretation of bafilomycin, pH neutralizing or protease inhibitor treatments in autophagic flux experiments: Novel considerations
AUTOPHAGY 8:(12) pp. 1875-1876. (2012)
IF: 12.042

Erdi B, Nagy P, Zvara A, Varga A, Pircs K, Menesi D, Puskas LG, *Juhasz G
Loss of the starvation-induced gene Rack1 leads to glycogen deficiency and impaired autophagic responses in Drosophila
AUTOPHAGY 8:(7) pp. 1124-1135. (2012)
IF: 12.042

Pircs K, Nagy P, Varga A, Venkei Z, Erdi B, Hegedus K, *Juhasz G
Advantages and Limitations of Different p62-Based Assays for Estimating Autophagic Activity in Drosophila
PLOS ONE 7:(8) Paper e44214. 11 p. (2012)
IF: 3.730

[1269 szerző], Klionsky DJ, Abdalla FC, Bánhegyi G, Fésüs L, Juhász G, Kovács AL, Lõw P, Sass M, Takács-Vellai K, Vellai T, Zuckerbraun B
Guidelines for the use and interpretation of assays for monitoring autophagy
AUTOPHAGY 8:(4) pp. 445-544. (2012)
IF: 12.042

Low P, Varga A, Pircs K, Nagy P, Szatmari Z, Sass M, *Juhasz G
Impaired proteasomal degradation enhances autophagy via hypoxia signaling in Drosophila.
BMC CELL BIOLOGY 14:(1) Paper 29. (2013)
IF: 2.808

Nagy P, Varga A, Pircs K, Hegedus K, *Juhasz G
Myc-Driven Overgrowth Requires Unfolded Protein Response-Mediated Induction of Autophagy and Antioxidant Responses in Drosophila melanogaster.
PLOS GENETICS 9:(8) p. e1003664. (2013)
IF: 8.517

Takats S, Nagy P, Varga A, Pircs K, Karpati M, Varga K, Kovacs AL, Hegedus K, *Juhasz G
Autophagosomal Syntaxin17-dependent lysosomal degradation maintains neuronal function in Drosophila.
JOURNAL OF CELL BIOLOGY 201:(4) pp. 531-539. (2013)
IF: 10.822

Hegedus K, Takats S, Kovacs AL, *Juhasz G
Evolutionarily conserved role and physiological relevance of a STX17/Syx17 (syntaxin 17)-containing SNARE complex in autophagosome fusion with endosomes and lysosomes.
AUTOPHAGY 9:(10) pp. 1642-1646. (2013)
IF: 12.042

Eisenberg T, Schroeder S, Andryushkova A, Pendl T, Kuttner V, Bhukel A, Marino G, Pietrocola F, Harger A, Zimmermann A, Moustafa T, Sprenger A, Jany E, Buttner S, Carmona-Gutierrez D, Ruckenstuhl C, Ring J, Reichelt W, Schimmel K, Leeb T, Moser C, Schatz S, Kamolz LP, Magnes C, Sinner F, Sedej S, Frohlich KU, Juhasz G, Pieber TR, Dengjel J, Sigrist SJ, Kroemer G, Madeo F
Nucleocytosolic depletion of the energy metabolite acetyl-coenzyme a stimulates autophagy and prolongs lifespan.
CELL METABOLISM 19:(3) pp. 431-444. (2014)
IF: 14.619

Hegedus K, Nagy P, Gaspari Z, *Juhasz G
The Putative HORMA Domain Protein Atg101 Dimerizes and Is Required for Starvation-Induced and Selective Autophagy in Drosophila
BIOMED RESEARCH INTERNATIONAL 2014: Paper 470482. 13 p. (2014)
IF: 2.880

Nagy P, Karpati M, Varga A, Pircs K, Venkei Z, Takats S, Varga K, Erdi B, Hegedus K, *Juhasz G
Atg17/FIP200 localizes to perilysosomal Ref(2)P aggregates and promotes autophagy by activation of Atg1 in Drosophila
AUTOPHAGY 10:(3) pp. 453-467. (2014)
IF: 12.042

Nagy P, Hegedus K, Pircs K, Varga A, *Juhasz G
Different effects of Atg2 and Atg18 mutations on Atg8a and Atg9 trafficking during starvation in Drosophila.
FEBS LETTERS 588: pp. 408-413. (2014)
IF: 3.582

Szatmari Z, Kis V, Lippai M, Hegedus K, Farago T, Lorincz P, Tanaka T, Juhasz G, Sass M
Rab11 facilitates crosstalk between autophagy and endosomal pathway through regulation of Hook localization.
MOLECULAR BIOLOGY OF THE CELL 25:(4) pp. 522-531. (2014)
IF: 4.803

Mulakkal N, Nagy P, Takats S, Tusco R, *Juhasz G, Nezis IP (társ-szenior szerzős publikáció)
Autophagy in Drosophila: from historical studies to current knowledge
BIOMED RESEARCH INTERNATIONAL 2014: Paper 273473. 24 p. (2014)
IF: 2.880

Takats S, Pircs K, Nagy P, Varga A, Karpati M, Hegedus K, Kramer H, Kovacs AL, Sass M, *Juhasz G
Interaction of the HOPS complex with Syntaxin 17 mediates autophagosome clearance in Drosophila
MOLECULAR BIOLOGY OF THE CELL 25:(8) pp. 1338-1354. (2014)
IF: 4.803

Developmental Cell, Vol. 7, 179–192, August, 2004, Copyright ©2004 by Cell Press
dc_840_14

Programmed Autophagy in the *Drosophila* Fat Body Is Induced by Ecdysone through Regulation of the PI3K Pathway

Tor Erik Rusten,[1] Karine Lindmo,[1] Gábor Juhász,[3] Miklós Sass,[3] Per O. Seglen,[2] Andreas Brech,[1] and Harald Stenmark[1,*]
[1]Department of Biochemistry
[2]Department of Cell Biology
The Norwegian Radium Hospital
Montebello, N-0310 Oslo
Norway
[3]Department of General Zoology
Eotvos Lorand University
Pazmany setany 1/C
Budapest H-1117
Hungary

Summary

Eukaryotic cells catabolize their own cytoplasm by autophagy in response to amino acid starvation and inductive signals during programmed tissue remodeling and cell death. The Tor and PI3K signaling pathways have been shown to negatively control autophagy in eukaryotes, but the mechanisms that link these effectors to overall animal development and nutritional status in multicellular organisms remain poorly understood. Here, we reveal a complex regulation of programmed and starvation-induced autophagy in the *Drosophila* fat body. Gain-of-function genetic analysis indicated that ecdysone receptor signaling induces programmed autophagy whereas PI3K signaling represses programmed autophagy. Genetic interaction studies showed that ecdysone signaling downregulates PI3K signaling and that this represents the effector mechanism for induction of programmed autophagy. Hence, these studies link hormonal induction of autophagy to the regulatory function of the PI3K signaling pathway in vivo.

Introduction

Macroautophagy (lysosomal degradation of cytoplasm, hereafter referred to as autophagy) plays important roles in regulating organelle turnover, growth, aging, cell death, and the mobilization of amino acids upon starvation (Baehrecke, 2002; Klionsky and Emr, 2000; Levine and Klionsky, 2004; Melendez et al., 2003). Impairment of this process has been implicated in a number of human diseases such as neurodegeneration, myopathy, and cancer (Edinger and Thompson, 2003; Klionsky, 2004). During autophagy, cytoplasmic components are enclosed by a cisternal isolation membrane, which in yeast derives from a distinct cellular region called the preautophagosomal structure (PAS, Figure 1A) (Klionsky and Emr, 2000; Noda et al., 2002; Seglen et al., 1990). Upon closure of the isolation membrane, a double membrane-enclosed autophagosome is formed which eventually fuses with the lysosome (Fengsrud et al., 2000). In the resulting autolysosome, the inner membrane with its contents is ultimately degraded. A thorough understanding of autophagy at the molecular level requires identification of the central molecular machinery responsible for the formation and maturation of autophagosomes as well as the signaling pathways that control the process (Codogno and Meijer, 2004; Møller et al., 2004).

Many essential components of the molecular machinery for autophagy have been identified and characterized using yeast genetics (Klionsky et al., 2003). Two ubiquitin-like conjugation systems are essential for the initiation and progression of autophagy (Noda et al., 2002). Atg12, a small ubiquitin-like protein, is covalently attached to Atg5, forming an Atg12-Atg5 conjugate (Mizushima et al., 1998). Atg8, a second small ubiquitin-like protein, is conjugated to the lipid, phosphatidylethanolamine (PE), possibly allowing its membrane localization (Ichimura et al., 2000; Kirisako et al., 2000). Genetic analysis has revealed that the Atg5-Atg12 conjugate is needed for Atg8 localization to the PAS and that both conjugates are necessary for progression of autophagy (Suzuki et al., 2001). Importantly, the Atg5-Atg12 conjugation process and its requirement for autophagy are conserved from yeast to mammals (Mizushima et al., 2001). Analysis of *atg5*-deficient mouse embryonic stem cells revealed that Atg5 is necessary for membrane elongation and autophagosome formation. Consistent with a role of Atg5 and Atg8 in autophagy, both proteins locate to nascent autophagic membrane structures in yeast and mammals. Ultrastructural analysis shows that both yeast Atg5, Atg8, and their mammalian homologs Atg5 and LC3 (Microtubule associated protein 1-light chain 3) localize to the isolation membranes (Kabeya et al., 2000; Kirisako et al., 1999; Mizushima et al., 2001). Upon closure of the membrane, Atg5 is lost from the newly formed autophagosome while LC3 is still attached (Kabeya et al., 2000; Mizushima et al., 2001). Upon fusion with the lysosome, GFP-LC3 from the inner autophagosomal membrane is still observable in the lysosomal lumen, making GFP-LC3 a useful marker for the autophagy process (Mizushima et al., 2003).

The control of autophagy is nutritionally, hormonally, and developmentally regulated through multiple signaling pathways (Codogno and Meijer, 2004; Levine and Klionsky, 2004). As in yeast, mammalian cells can initiate autophagy upon starvation, both in cell culture and in the intact organism (Kovacs et al., 1981a, 1981b; Mizushima et al., 2001, 2003). This starvation response is potently reversed by the presence of amino acids (Gordon et al., 1985; Kovacs et al., 1981b). The macrolide antibiotic, rapamycin, is able to induce autophagy even in the presence of a good nitrogen source (Blommaart et al., 1995; Noda and Ohsumi, 1998). The target of rapamycin (Tor) is an evolutionarily conserved kinase that is central in regulating several starvation responses, including the control of cell cycle progression, growth, transcription, and protein translation (Miron and Sonenberg, 2001; Oldham and Hafen, 2003).

Another central regulator of nutrient signaling is the

*Correspondence: stenmark@ulrik.uio.no

dc_840_14

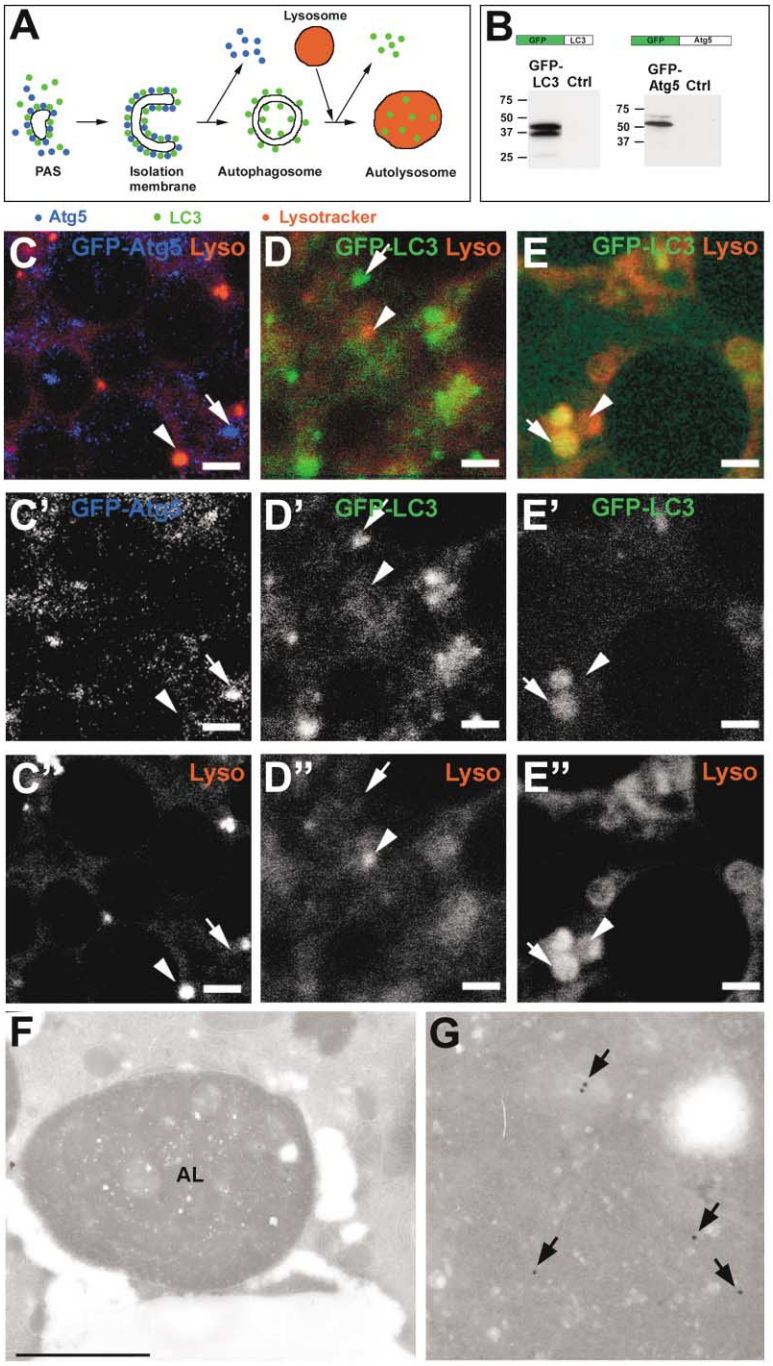


Figure 1. Lysotracker and GFP Fusions of Atg5 or LC3 as Markers for Autophagic Activity

Different stages of the autophagic process (A) can be visualized in the fat body of transgenic animals using the tub-Gal4 driver. Fly larvae carrying inducible fusion transgenes encoding human LC3 (green) or Atg5 (blue) (B) were observed by confocal microscopy (C–E) or electron microscopy (F and G).

(B) Western blot analysis detecting fusion proteins using anti-GFP antibodies in whole wandering L3 larvae. tub-Gal4>GFP-LC3 larvae display one band at 43 kDa corresponding to GFP-LC3-I and another band at 36 kDa probably corresponding to GFP-LC3-II (Kabeya et al., 2000; Mizushima et al., 2003). A weaker band at 27 kDa that probably represents GFP alone is also seen (Mizushima et al., 2003). None of the bands are observed in control larva (w^{1118}). tub-Gal4>GFP-Atg5-expressing animals display a 58 kDa band corresponding to GFP-Atg5 and a less mobile band possibly reflecting GFP-Atg5 with conjugated Atg12 (expected size of 71 kDa) (Mizushima et al., 1998).

(C–C″) In mid-feeding L3 larvae expressing GFP-Atg5, distinct 0.5 μm-sized structures (arrow) do not colocalize with lysotracker (arrowhead) and probably represent early autophagic structures (PAS and isolation membranes).

(D–D″) Similar structures are observed in GFP-LC3-expressing larvae at the same stage, in which small structures (arrow) do not colocalize with lysotracker (arrowhead).

(E–E″) In wandering L3 larvae, larger 2–5 μm-sized structures, representing autolysosomes (arrow), are colabeled by GFP-LC3 (arrows) and lysotracker (arrowhead).

(F and G) Immuno-gold electron microscopy images from a similarly staged larva as in (E) show enriched immunoreactivity within autolysosomes (AL). (G) shows a higher magnification of (F). Gold particles are labeled with arrows in (G).

Size bars 2 μm (C–E) and 1 μm (F).

class I phosphoinositide (PI) 3-kinase (PI3K) which catalyzes the formation of phosphatidylinositol-3,4,5-*tris*-phosphate (PIP_3) (Britton et al., 2002; Simonsen et al., 2001). PI3K is a downstream component of tyrosine kinase receptors, including the insulin signaling pathway known to be a potent repressor of autophagy in mammalian cells and *Caenorhabditis elegans* (Melendez et al., 2003; Seglen and Bohley, 1992). In HT-29 cells, activation of the class-I PI3K pathway by the cytokine interleukin-13 is able to inhibit autophagy (Petiot et al., 2000). Generation of PIP_3 at the cell membrane recruits the effectors Akt/PKB and PDK1 through their plextrin homology (PH) domains (Oldham and Hafen, 2003). Consistently, expression of Akt/PKB in human colon cancer cells is also able to inhibit autophagy (Arico et al., 2001). The level of PIP_3 is negatively controlled by PTEN (phosphatase and tensin homolog deleted from chromosome 10), which specifically dephosphorylates the 3′ position of PIP_3. Expression of a lipid phosphatase-deficient form of PTEN leads to inactivation of autophagy due to a failure to antagonize the inhibitory effect by the PI3K pathway (Arico et al., 2001).

Developmentally programmed autophagy and subsequent cell death occur in mammalian luteal cell regression and in tissue remodeling during insect metamorphosis (Baehrecke, 2002; Juhász et al., 2003; Thummel, 2001). This form of programmed autophagy is likely to be controlled by hormones. In holometabolous insects,

dc_840_14

the main hormone regulating global synchronization and progression of developmental stages, 20-hydroxyecdysone (ecdysone), is the best candidate for this control (Riddiford, 1993). Programmed autophagy in the midgut and fat body during the last larval stage of *Pieris brassicae* and *Mamestra brassicae* can be prematurely induced by administration of ecdysone (Komuves et al., 1985; Sass and Kovacs, 1975, 1977).

To begin to understand the regulation, molecular mechanisms, and role of autophagy in a multicellular animal, we have chosen the *Drosophila* fat body as a model system. Using a microscope-based autophagy assay, we first show that starvation and Tor and PI3K signaling control autophagy in this system. We then demonstrate that programmed autophagy in the *Drosophila* fat body is controlled by ecdysone and effected through inhibition of PI3K signaling.

Results

Visualizing Autophagy with GFP-Atg5, GFP-LC3, and Lysotracker

In order to initiate studies of autophagy in *Drosophila*, we sought to establish molecular markers and an assay for the process. The fly genome contains two putative homologs of Atg8 (CG32672, CG12334) and one homolog of Atg5 (CG1634) (Baehrecke, 2002; Juhász et al., 2001). We established several transgenic fly lines expressing LC3 and *Drosophila* Atg5 as fusion proteins with green fluorescent protein (GFP) under control of the Gal4-UAS system (Brand and Perrimon, 1993). Western blotting of extracts from stage 3 (L3) larvae confirmed expression of the transgenes. Animals ubiquitiously expressing GFP-LC3 or GFP-Atg5 under tub-Gal4 control were viable and showed no obvious phenotypic defects or growth delay (Figure 1B and data not shown).

The membrane permeant dye, lysotracker, labels acidic organelles such as lysosomes and autolysosomes and has been used as a probe for autophagy (Munafó and Colombo, 2001). We reasoned that a combination of GFP fusion constructs and lysotracker should allow us to visualize the three compartments relevant for autophagy, i.e., the lysosomes (lysotracker-positive), the forming autophagosomes (GFP-Atg5- or GFP-LC3-positive), and the autolysosomes (lysotracker- and GFP-LC3-positive). In larval L3 stage, autophagy is active in the fat body (Butterworth and Forrest, 1984). As expected, by confocal microscopy of GFP-Atg5 larvae, we observed small punctate structures of 0.5 μm in size that did not overlap with the lysotracker probe, consistent with labeling PAS and early autophagosomal structures in this tissue (Figure 1C). Analysis of GFP-LC3 larvae revealed two populations of GFP-positive structures (Figures1D and 1E). One population consisted of 0.5 μm-sized lysotracker-negative profiles whereas the other population contained larger structures, typically ranging 1–5 μm in size and positive for both GFP-LC3 and lysotracker. To confirm that the LC3 fusion constructs indeed labeled autophagic structures, we carried out immunogold labeling and electron microscopic analysis of L3 larval fat bodies. As reported in yeast and mammalian cells, tagged LC3 was enriched in autolysosomes as opposed to the general diffuse labeling in the cytoplasm (Figures 1F and 1G) (Kabeya et al., 2000; Mizushima et al., 2001, 2003). We concluded that the three populations of structures observed in GFP-LC3-expressing flies (GFP-LC3-positive, lysotracker-positive, or GFP-LC3/lysotracker-positive) should allow us to follow the dynamics of autophagy in live and fixed tissue using a simple microscopy-based assay.

The *Drosophila* Fat Body Has Defined Stages of Progressive Programmed Autophagy

During insect metamorphosis, the salivary gland, fat body, and midgut undergo precisely timed periods of programmed autophagy before dying (Supplemental Figures S1A–S1L [http://www.developmentalcell.com/cgi/content/full/7/2/179/DC1]) (Butterworth et al., 1988; Butterworth and Forrest, 1984; Lee and Baehrecke, 2001; Lee et al., 2002a; von Gaudecker and Schmale, 1974). We chose the fat body as a model system for studying programmed and starvation-induced autophagy with GFP-LC3, GFP-Atg5, and lysotracker as reporters. Small feeding early L3 larvae (feL3, 72 hr after egg laying, AEL) contained small, 0.5 μm-sized GFP-Atg5 and GFP-LC3 structures (Figures 1C and 1D and Figure 2A). Few structures labeled with lysotracker, consistent with earlier findings that no autolysosomes were observed at this stage (Butterworth et al., 1988; Butterworth and Forrest, 1984). In large L3 feeding larvae (feeding late L3, flL3), small (0.5–1 μm) strongly acidic lysosomes were numerous and overlapped frequently with GFP-LC3, indicating the presence of autolysosomes (Figure 2B). Autophagy is known to be initiated at 108 hAEL, when autolysosomes, typically containing glycogen and mitochondria in various stages of degeneration, are present (Butterworth et al., 1988; Butterworth and Forrest, 1984). In both wandering stage L3 larvae and in white pupae, most of the cytoplasm contained large, 2–5 μm-sized structures colabeling weakly for GFP-LC3 and lysotracker (Figures 2C and 2D). This finding is consistent with earlier reports in which small acidic lysosomes display reduced acidity upon fusion with autophagosomes (Dunn, 1990).

Consistent with the idea that the small structures observed in early L3 larvae represent early autophagic structures, we also observed structures labeled with GFP-Atg5 (data not shown). Quantification of the three populations of structures, acidic structures (lysosomes and late endosomes), PAS/autophagosomes, and autolysosomes, revealed a dynamic progression of autophagy in the larval fat body during the L3 stage (Figure 2H). Initially, small early autophagosomes or preautophagosomal structures predominated, followed by an increased appearance of acidic lysosomes and autolysosomes. At the white prepupal stage, essentially all GFP-LC3 structures contained lysotracker and were thus likely to represent autolysosomes. It is worth noting that the lysosomes in fat body cells of wandering larvae and white prepupae were larger than at feeding L3 stages, consistent with the idea that several autophagosomes may fuse with the same autolysosome as development proceeds.

The relative paucity of structures labeling with lysotracker at early L3 stages of development was surprising. This could either be due to a predominance of inactive, nonacidic lysosomes or may simply indicate that

dc_840_14

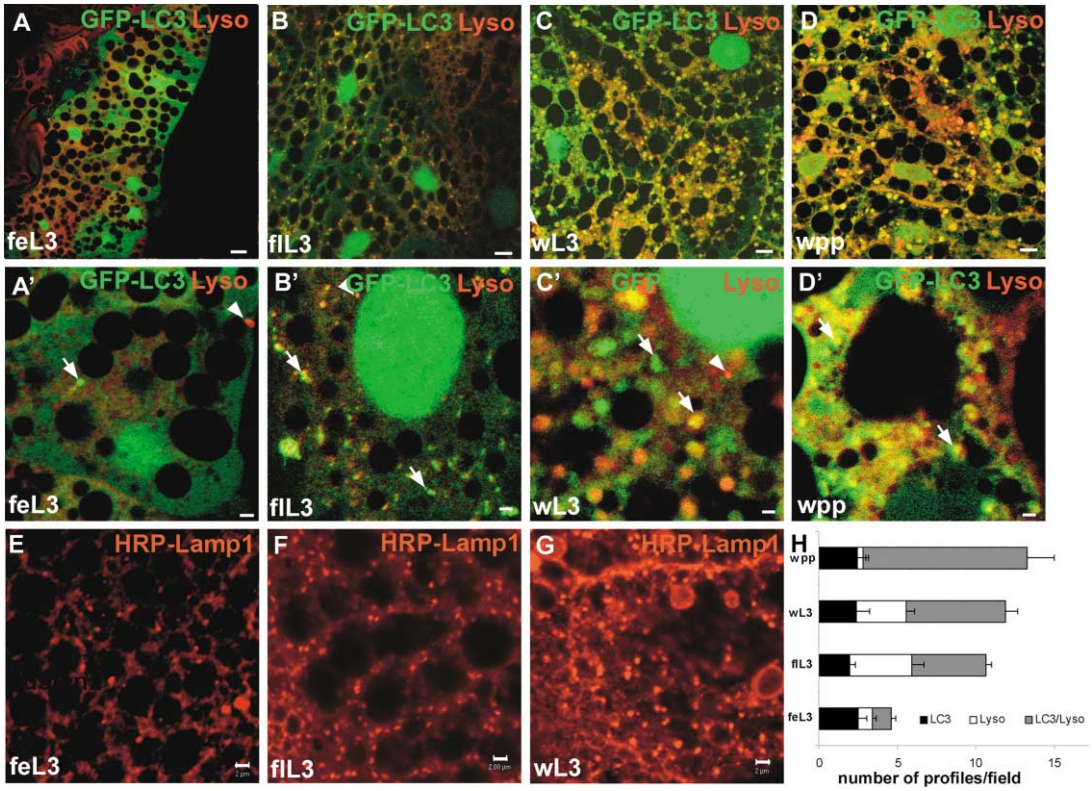


Figure 2. Progressive Programmed Autophagic Activity in the L3 Fat Body

The progress of programmed autophagy during the L3 stage and white prepupa (wpp) was followed in the fat body using lysotracker and GFP-LC3 in cg-Gal4>GFP-LC3 animals ([A]–[D], quantified in [H]). (A) Feeding early L3 (feL3) animals displayed little lysotracker staining (arrowhead [A′]) and small GFP-LC3 structures (arrow [A′]) indicative of early autophagic structures. (B–D) Increasing numbers and size of both GFP-LC3 (B′–D′)-, lysotracker (B′–D′)-, and GFP-LC3/lysotracker-positive structures were observed as the larval L3 stage proceeded into the early pupal stages (B–D). (E–G) The number of lysosomes as assayed by the lysosomal marker HRP-Lamp1 increased during the L3 stage in Adh-Gal4>HRP-Lamp1 animals. A dynamic and progressive development of early autophagic profiles (black, GFP-LC3), lysosomes (white, lysotracker), and autolysosomes (gray, GFP-LC3/lysotracker) can be observed (H). Feeding late L3 (flL3), wandering L3 (wL3), white prepupa (wpp). Arrows, GFP-LC3 or GFP-LC3/lysotracker; arrowheads, lysotracker. Size bars 10 μm (A–D) and 2 μm (A′–D′ and E–G).

lysosomes were fewer in number. To investigate this question, we used flies expressing a tagged version of the lysosomal membrane protein, Lamp1 (Lloyd et al., 2002). Larvae expressing HRP-Lamp1 under control of tub-Gal4 displayed a similar developmental profile as lysotracker staining during the different stages of larval development. This finding supports the idea that the biogenesis of acidic lysosomes in this tissue is developmentally regulated, perhaps in preparation for the tissue to undergo autophagy (Figures 2E–2G). The emergence of early GFP-LC3 and GFP-Atg5 structures and the later coappearance of GFP-LC3 with lysosomes meant that we could account for all three populations of the pathway, early autophagosomes, lysosomes, and autolysosomes, respectively.

We confirmed by electron and confocal microscopy that GFP-LC3 faithfully reports programmed autophagy also in salivary gland and midgut cells (Supplemental Figures S1A–S1L). Taken together, these results demonstrate that the dynamics of the autophagic process (earlier followed by electron microscopy) can indeed be visualized by confocal microscopy. This provides the opportunity to study the dynamics and progression of autophagy in live or fixed tissues.

Autophagy in the Fat Body Can Be Induced by Amino Acid Starvation, Ecdysone Signaling, and Rapamycin

Larvae fed on amino acid-deficient food display a quick starvation-induced response in the fat body, leading to the aggregation of storage vesicles (Britton et al., 2002; Colombani et al., 2003; Zhang et al., 2000). To investigate starvation-induced autophagy at different developmental stages in the fat body, we subjected L2 and early feeding L3 larvae with few GFP-LC3 structures and little lysotracker activity to 4 hr of starvation in an amino acid-deficient sucrose medium. As a control medium, the sucrose solution was supplemented with heat-killed yeast as an amino acid source. Confocal microscopy of live fat bodies showed that starvation resulted in an induction of structures labeled with GFP-Atg5, GFP-LC3, as well as GFP-LC3 overlapping with lysotracker (Figures 3A, 3B, 3D, and 3E). We then investigated the dynamics of autophagic induction during starvation, using the established assay. Animals were starved in sucrose for up to 4 hr. A rapid induction of GFP-LC3-positive structures was observed after 1 hr, and lysosomes increased both in number, acidity, and size over the duration of the experiment (Figure 3F). Similarly, the

dc_840_14

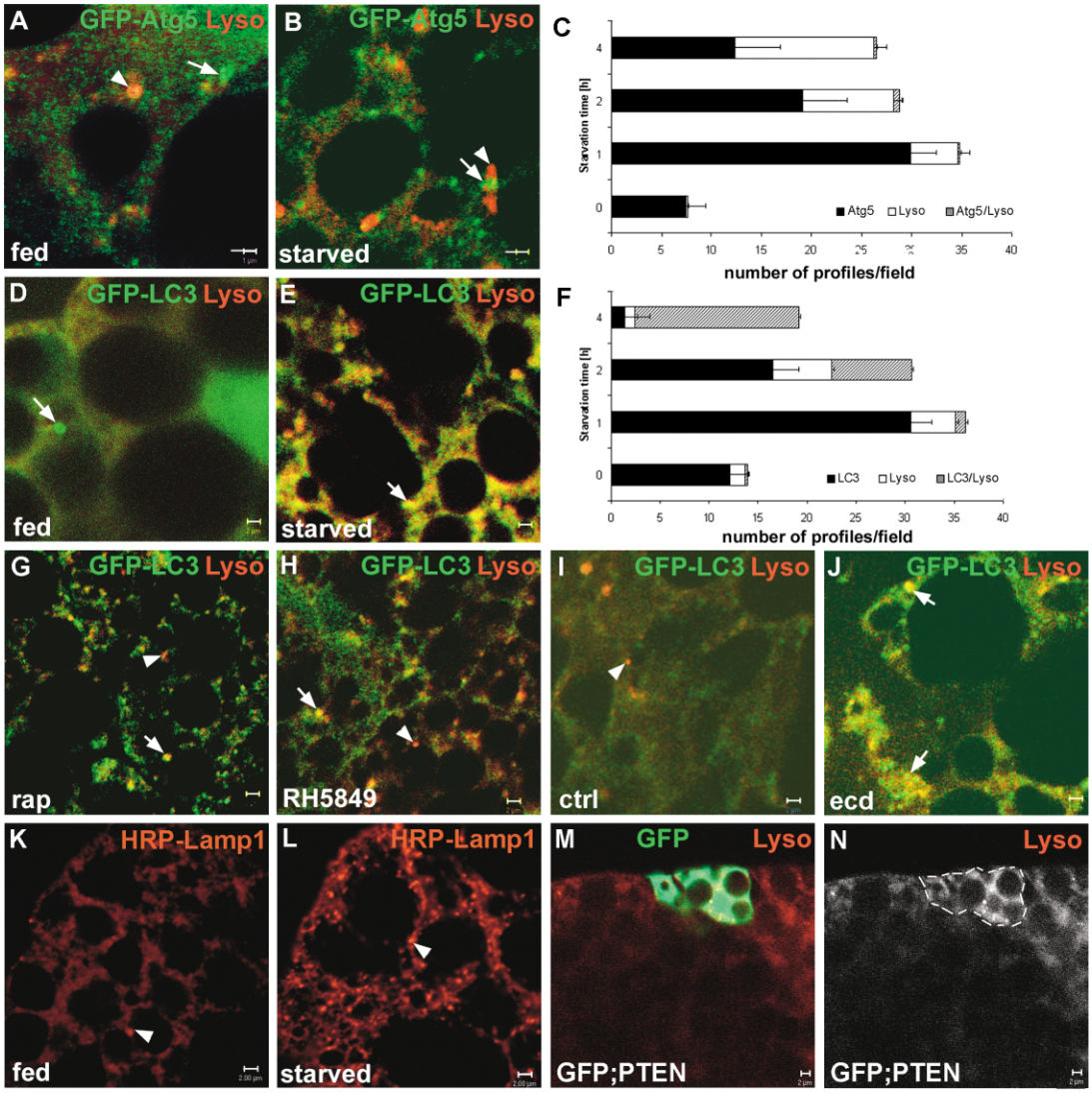


Figure 3. Autophagic Induction in the eL3 Fat Body

Early L3 larvae were challenged with amino acid starvation (see Experimental Procedures for details), rapamycin, or the ecdysone agonist RH5849. Amino acid starvation for 4 hr led to an increase in lysotracker-, GFP-LC3 (D and E)-, and GFP-Atg5 (A and B)-containing structures. The increase in early autophagosomal structures defined as GFP-LC3 or GFP-Atg5 positive alone increased after 1 hr of starvation and then decreased again as lysosotracker-positive structures appeared and fused with GFP-LC3 (C and F). The number of lysosomes as assayed by the lysosomal marker HRP-Lamp1 increased markedly after 3 hr of starvation ([L] compared with [K]). Both rapamycin (rap [G]) and RH5849 (H) were also able to induce GFP-LC3-, lysotracker-, and GFP-LC3/lysotracker-positive structures (compare with [D]). Fat body lobules from a larva with the genotype UAS-GFP-LC3/+; cg-Gal4/+ showed increased levels of lysotracker, GFP-LC3, and GFP-LC3/lysotracker structures when cultured with ecdysone (J) compared to control tissue (I). (M and N) Increased appearance of lysotracker-positive structures was seen in a PTEN-expressing clone (dashed line) in early L3 larvae of the genotype hsflp/+; Act>CD2>Gal4/+;UAS-PTEN/UAS-GFP. Size bar 2 μm. Arrows, GFP-LC3 or GFP-LC3/lysotracker; arrowheads, lysotracker (A, B, D, E, G–J) or HRP-Lamp1 (K and L).

number of GFP-Atg5 structures increased after 1 hr of starvation and then gradually declined as more lysosomes appeared (Figure 3C). The number of structures labeling with GFP-LC3 alone increased after 1 hr of starvation and then declined as more lysosomes and GFP-LC3/lysotracker structures appeared. These results can best be explained by a rapid induction of preautophagosomal structures and autophagosomes within 1 hr of starvation, followed by fusion with recently acidified lysosomes.

To investigate the dynamics of lysosome biogenesis upon starvation, we followed HRP-Lamp1 during a starvation period of 5 hr. A strong increase in the number of HRP-Lamp1 structures was observed during the starvation period (Figures 3K and 3L). We conclude that the formation of acidic lysosomes and autophagic activity can be induced by starvation at stages of development when autophagy is normally suppressed. Thus, the fat body has the capacity for both developmentally programmed and starvation-induced autophagy.

Rapamycin is a specific inhibitor of Tor and is frequently used to induce autophagy as it is generally assumed to phenocopy amino acid starvation. Addition of rapamycin to cells or to the food of feeding larvae leads to effects similar to those induced by mutations that inactivate *dTor* and phenocopies starvation (Oldham et

al., 2000; Zhang et al., 2000). We therefore asked whether rapamycin can induce autophagy in the fat body of feeding early L3 larvae. As expected, rapamycin led to effects similar to starvation, with fat bodies showing GFP-LC3/lysotracker overlap after 4 hr of stimulation (Figure 3G).

In the moth, *Mammestra brassicae*, ecdysone is able to induce autophagy before its normal onset (Sass and Kovacs, 1975, 1977). Autophagy in the fat body, followed by wandering behavior of larvae, is likely to be induced by a low but rising titer of ecdysone, which can be detected by radioimmune assay measurements (R. Farkas, personal communication). We noted that the developmental appearance of autolysosomes in the fat body correlated well with the rise in ecdysone concentration (Figure 2; see Discussion). To investigate if ecdysone is the responsible hormone inducing programmed autophagy in this tissue, we therefore challenged larvae for 4 hr with sucrose and yeast supplemented with the ecdysone agonist RH5849 (Wing, 1988). A rapid induction of lysotracker- and GFP-LC3/lysotracker-positive structures was observed, showing that the presence of an ecdysone agonist is indeed sufficient to induce autophagy (Figure 3H). Curiously, the appearance of acidic structures, presumably reflecting acidic lysosomes, could be stimulated in a similar manner by starvation, rapamycin treatment, or addition of the ecdysone agonist. Electron microscopy was used to verify that the fluorescent markers indeed reflected induction of autophagy and formation of autolysosomes. Highly increased numbers of autolysosomes were seen under all inducing conditions in comparison to the control-fed animals (Supplemental Figures S2A–S2H). To verify that RH5849 reflected a direct autophagy-inducing capacity of 20-hydroxyecdysone on the fat body, we performed in vitro organ culture experiments of the fat body (Sass and Kovacs, 1975, 1977). Fat body lobules from the same early feeding L3 larvae were cultured either in insect medium alone or supplemented with 20-hydroxyecdysone. A marked increase of autophagic activity was observed in the presence of 20-hydroxyecdysone (Figures 3I and 3J). Taken together, these results show that the *Drosophila* fat body can be induced to undergo starvation-, rapamycin-, and ecdysone-induced autophagy before the normal onset of programmed autophagy.

Effects of Ecdysone, PI3K, and Tor Signaling during Programmed Autophagy in the Fat Body

Next, we asked whether Tor, PI3K, and ecdysone signaling would have a regulatory role during the period of programmed autophagy in the fat body. For this purpose, we performed a gain-of-function genetic analysis using a fat body driver, Lsp-Gal4, that initiates expression at the mid-L3 transition (Cherbas et al., 2003). Amino acid sensing is suggested to exert its effects through inhibition of the Tor kinase complex (Colombani et al., 2003; Hara et al., 2002; Kim and Sabatini, 2004; Loewith et al., 2002; Scott et al., 2004). To investigate the effect of Tor inhibition during programmed autophagy, we expressed a dominant-negative version of Tor (Tor^{TED}) (Hennig and Neufeld, 2002). Expression of Tor^{TED} led to a marked increase in autolysosomal size, a 30% increase in the autophagic area (quantified by electron microscopy, not shown), a reduction of cytoplasmic area, and the disappearance of structures labeling for GFP-LC3 alone (Figures 4B and 4G). The autolysosomal structures were also less acidic than in the wild-type situation, possibly as a consequence of dilution of acidity due to more incoming autophagic material. Differential interference contrast microscopy showed the aggregation of fat droplets, a typical phenomenon observed during the starvation response (Colombani et al., 2003; Zhang et al., 2000). Giant autolysosomes up to 10 μm in size were frequent. Strong fluorescent structures were often observed within the autolysosomes, possibly representing recently fused autophagosomes (autophagic bodies) (Figure 4B′). These findings suggest that inhibition of Tor kinase activity increases the flux of autophagosomes into autolysosomes and that the Tor pathway is not completely inhibited during developmental autophagy in the fat body.

Both ecdysone and the ecdysone agonist RH5849 are potent inducers of autophagy at stages normally lacking autophagic structures (Figure 2 and 3H–3J). This strongly suggested that ecdysone is the bona fide inducer of programmed autophagy in this tissue. To directly test this hypothesis, we took advantage of the recently published dominant-negative versions of the ecdysone receptor, EcR^{F645A} and EcR^{W650A} (Cherbas et al., 2003; Hu et al., 2003). These mutant receptors are able to bind their heterodimeric partner (ultraspiracle) and DNA but produce strong dominant-negative effects on ecdysone signaling, both in cell culture and in vivo (Cherbas et al., 2003; Hu et al., 2003; Kozlova and Thummel, 2003; Riddiford et al., 2000). Overexpression of either EcR^{F645A} or EcR^{W650A} under Lsp-GAL4 control led to a strong reduction of both the number and size of GFP-LC3/lysotracker-positive structures relative to the control (Figures 4C and 4G). A strong accumulation of small 0.5–1 μm-sized GFP-LC3 structures, few small lysotracker-positive structures, and little detectable overlap between GFP-LC3 and lysotracker suggested that early autophagosomal structures were able to form but did not acidify, perhaps as a failure to fuse with lysosomes.

To investigate this possibility, we analyzed fat body tissue from Lsp-Gal4>EcR^{W650A} animals by electron microscopy (Figures 5C and 5D). At the wandering L3 stage of control animals, the cytoplasm was filled with autophagosomes and large 2–5 μm-sized autolysosomes with far-progressed degradation of internal structures and little visible organelle remnant material (Figures 5A–5B and 1F). In contrast, animals with decreased ecdysone signaling lacked large autolysosomes (Figure 5C) and instead contained numerous small, 0.2–0.5 μm-sized structures, probably representing aberrant autolysosome-related structures (Figures 5D, 5H, and 5I). Within these structures, tightly packed membrane material was found. The number of autolysosome-like structures observed by electron microscopy correlated closely with the numbers of GFP-LC3 structures observed by confocal microscopy, arguing that they are indeed the same structures (Figures 4G and 5I). The facts that (1) no large autolyosomes were observed, (2) the autophagic area was strongly reduced, and (3) many small nonacidic GFP-LC3-positive profiles yet few acidic structures occurred, indicate a strong inhibition of autophagy (Figure 5H).

In mammalian HT-29 cells, elevated PI3K signaling

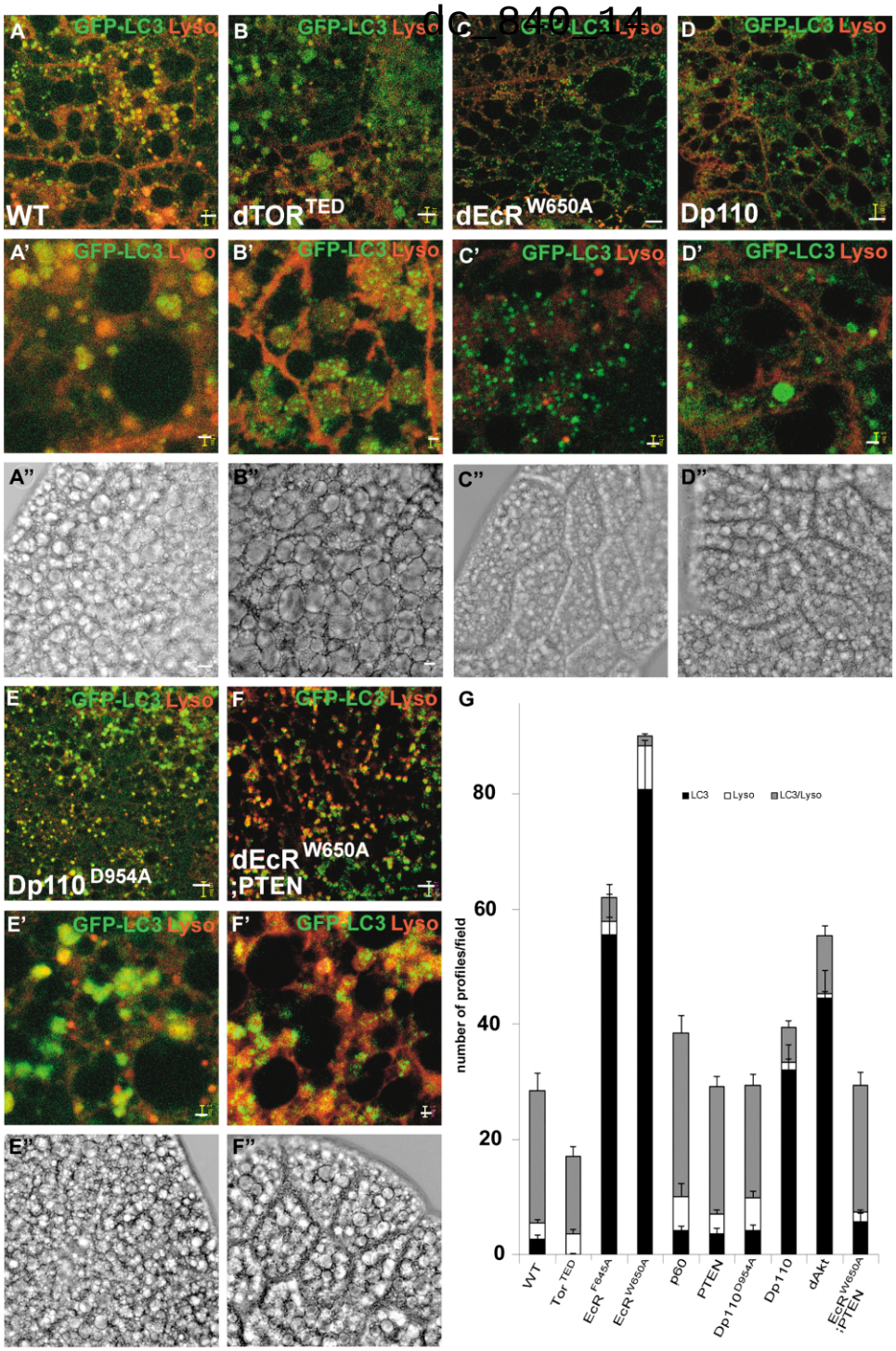


Figure 4. Inhibition of Ecdysone Signaling or Activation of the PI3K Pathway Blocks Programmed Autophagy

The progression of programmed autophagy was measured by GFP-LC3 and lysotracker in wL3 larvae by confocal microscopy ([A–F], enlarged in [A′]–[F′]), and fat droplet aggregation by Nomarski optics (A″–F″). Constructs affecting Tor, ecdysone, and PI3K signaling were expressed in the fat body under Lsp-Gal4 control at 29°C to achieve high expression levels.

(A–A″) Lsp-Gal4 control larvae showed extensive GFP-LC3/lysotracker overlap diagnostic of autolysosomes with a diameter of 2–5 μm.

(B–B″) Expression of a dominant-negative form of Tor (Lsp-Gal4>TOR^{TED} animals) resulted in an increase of autolysosomal size up to 10 μm, reduced acidity, reduced cytoplasmic area, and a relative loss of GFP-LC3 structures alone. Fat droplet aggregation was more pronounced than in control larvae ([B″] compare with [A″]).

(C–C″) Lsp-Gal4>UAS-EcR^{W650A} larvae, in which ecdysone signaling is blocked, displayed a dramatic accumulation of GFP-LC3 structures alone, reduced amounts of acidic vesicles, and few GFP-LC3/lysotracker-positive structures. A reduced fat droplet aggregation relative to control animals was observed.

(D–D″) Similar phenotypes were observed in Lsp-Gal4>Dp110 larvae in which PI3K signaling was activated, while no visible effects were observed in Lsp-Gal4>Dp110^{D954A} larvae, in which PI3K signaling was blocked (E–E″).

(F) Autophagy is restored by simultaneous expression of UAS-EcR^{W650A} and UAS-PTEN under Lsp-Gal4 control.

(G) GFP-LC3, lysotracker, and GFP-LC3/lysotracker structures were quantified in each genotype (see text for details). Size bars 10 μm (A–E) and 2 μm (A′–E′).

dc_840_14

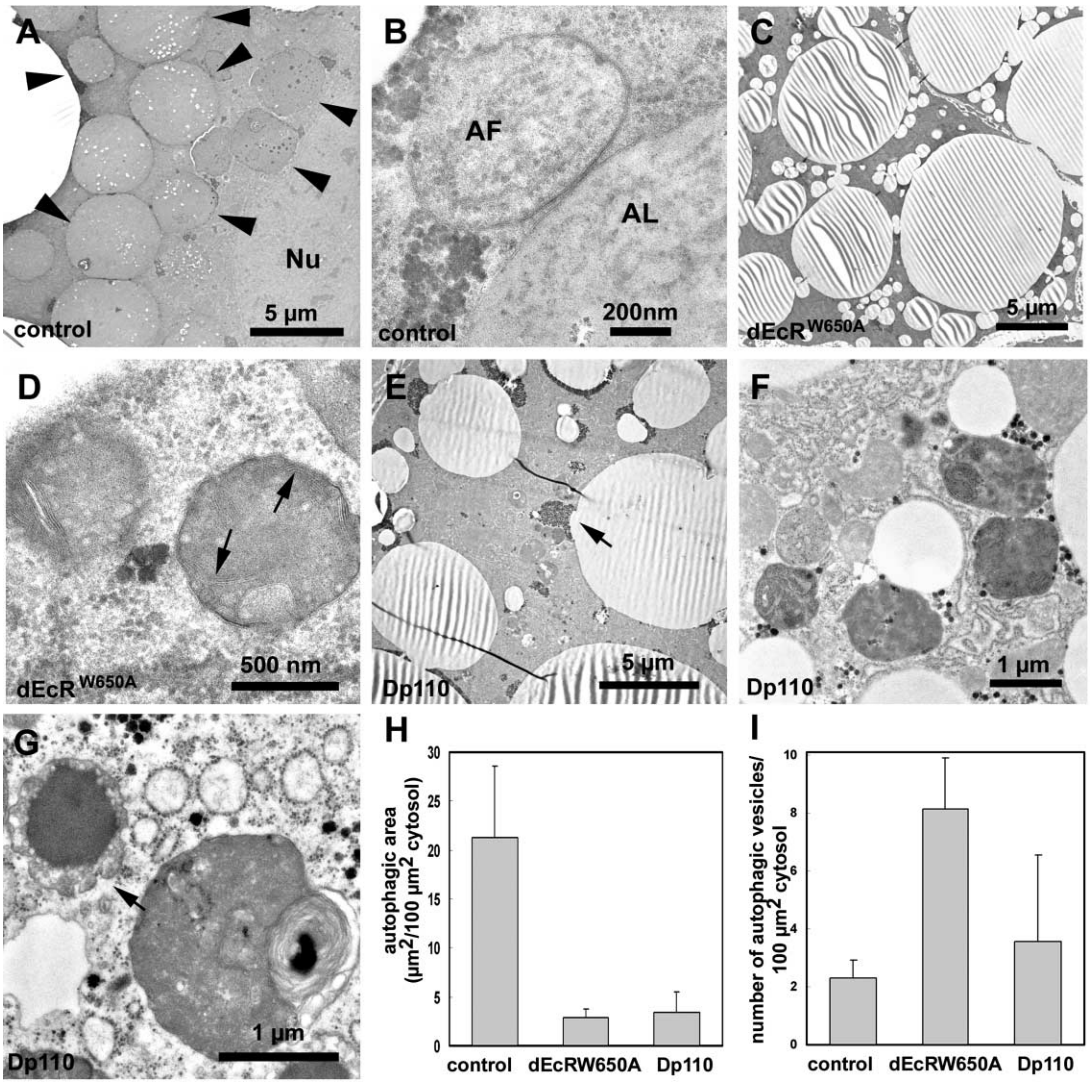


Figure 5. Block of Autophagic Activity by Increased PI3K and Reduced Ecdysone Signaling

Fat bodies from late-stage wandering L3 larvae of control Lsp-Gal4, Lsp-Gal>Dp110, and Lsp-Gal4>EcR^{W650A} were prepared for conventional EM as described in Experimental Procedures.

(A) In control larvae, the fat body contained numerous large autolysosomes (arrowheads). These vesicles were characterized by their content of more or less degraded ER and organelle remnants.

(B) Another prominent feature was the occurrence of double-membrane limited autophagosomes, mostly containing sequestered ER.

(C) The fat body of Lsp-Gal4>EcR^{W650A} larvae was devoid of large autolysosomal structures, but contained numerous large fat droplets (whose "striped" appearance is an EM artifact). In addition, the Gal4>EcR^{W650A} fat body contained many small, dense autolysosome-like vesicles, which often contained tightly packed matter forming characteristic layers (arrows in [D]).

(E) Lsp-Gal4>Dp110 cells were also characterized by the absence of large autolysosomes and showed a variety of autophagic and multilamellar vesicles and a striking accumulation of glycogen particles (arrows). At higher magnification, typical autophagosomes containing sequestered ER were observed (F), as well as multilamellar bodies and structures with a dense core and a multivesicular appearance around the vesicle periphery (arrow in [G]).

(H) A quantification of autophagic area showed a 5-fold decrease in Dp110- and EcR^{W650A}-expressing larvae (I). Conversely, the number of autophagic structures was strongly increased in dEcR^{W650A} larvae.

Abbreviations: Nu, nucleus; AF, autophagosome; AL, autolysosome.

can suppress autophagic activity (Petiot et al., 2000). The lipid product of PI3K, PIP_3, recruits the effectors Akt/PKB and PDK1 through their plextrin homology (PH) domains, and overexpression of Akt/PKB is able to inhibit autophagy (Arico et al., 2001; Oldham and Hafen, 2003). We investigated the effect of elevating PI3K signaling activity by expressing the catalytic subunit of PI3K, Dp110, or dAkt (Britton et al., 2002; Leevers et al., 1996; Verdu et al., 1999). Both Lsp-Gal4>UASDp110 and Lsp-Gal4>UASdAkt animals showed a strong reduction of GFP-LC3/lysotracker-positive structures, reminiscent of the effect of inhibiting ecdysone signaling (Figures 4D and 4G). In both cases, there was a noticeable absence of large autolysosomes (Figures 5E and 5F). Some larger GFP-LC3/lysotracker-positive structures were present, though, suggesting incomplete inhibiton (Figure 4D). The presence of these autolysosomes was confirmed by electron microscopy (Figures

5F and 5G). As observed when ecdysone signaling is blocked, the cytoplasm contained small autophagosomes and autolysosomes. A pronounced accumulation of glycogen was also observed in these animals, perhaps due to a failure of autophagy to degrade glycogen or an increased accumulation resulting from elevated PI3K signaling. As in Lsp-Gal4>EcR^{W650A} animals, the autophagic area was severely decreased compared to control animals, demonstrating a strong inhibition of autophagy (Figures 5H and 4G).

The level of PIP_3 is negatively controlled by the lipid phosphatase PTEN, which dephosphorylates the 3′ position of the inositol head group of PIP_3. Expression of a dominant-negative form of PTEN leads to a decrease in autophagic activity in colon carcinoma cells (HT-29) (Arico et al., 2001). Overexpression of PTEN, the regulatory subunit of PI3K (p60), and a dominant-negative version of the catalytic subunit of PI3K, $Dp110^{D954A}$ can each block PI3K signaling and prevent the cell growth effect of PI3K signaling (Britton et al., 2002; Gao et al., 2000; Leevers et al., 1996; Weinkove et al., 1999). However, Lsp-Gal4>$Dp110^{D954A}$, Lsp-Gal4>UASPTEN, and Lsp-Gal4>UASp60 animals did not show an obvious effect on the autophagic activity or the fat droplet aggregation in the larval fat body (Figures 4E and 4G and data not shown). This suggests that in the late wL3 larva, autophagy cannot be further increased by experimental suppression of PI3K signaling, as probably PI3K signaling is completely inhibited already. In contrast, clonal overexpression of PTEN before the onset of programmed autophagy did result in an increase of lysotracker positive structures, indicative of increased autophagy (Figures 3M and 3N). In conclusion, inhibition of ecdysone receptor activity or an increase in PI3K signaling can result in a severe inhibition of programmed autophagy.

PI3K Activity Is Regulated through Ecdysone Receptor Signaling in a Cell-Autonomous Fashion to Allow Programmed Autophagy

A constitutively active PI3K pathway or a decrease in ecdysone receptor activity leads to very similar inhibition of autophagy. We therefore investigated normal PI3K activity during the L3 stage using a GFP-PH domain fusion protein as a reporter for PI3K activity (Britton et al., 2002). The GFP-PH marker clearly reported the presence of PIP_3 at the cell membrane in early L3 larvae. This labeling gradually disappeared by the wandering L3 stage (Figures 6A–6C). The fact that no appreciable PIP_3 formation was observed in the fat body at the wL3 stage can explain the failure of overexpressed PTEN, p60, or $Dp110^{D954A}$ to cause any effect on autophagic activity, since no further downregulation of the pathway was possible. The correlation between a loss of PI3K signaling and the necessity and sufficiency of the ecdysone pulse for autophagic activity suggests that ecdysone exerts its effect through inhibition of PI3K signaling.

To directly test this hypothesis, we induced expression of EcR^{W650A} in clones of cells using the Flp-Gal4 technique and assayed for PI3K activity using the GFP-PH probe in both live and fixed tissue at the wandering L3 stage (Britton et al., 2002; Neufeld et al., 1998; Pignoni and Zipursky, 1997). Clones overexpressing EcR^{W650A} showed an indistinguishable phenotype from what was observed in all cells of the fat body in Lsp-Gal4>EcR^{W650A} animals (Figures 6E–6H, compare with Figures 4C–4C″). In live cells, the presence of the clonal marker GFP reports the cells expressing EcR^{W650A}. The EcR^{W650A}-expressing clones contained smaller and fewer acidic structures as well as more defined cell borders, and a different appearance of fat droplets compared to wild-type cells (Figures 6E–6H). This marked phenotypic difference between cells allowed an identification of cells expressing EcR^{W650A} and observation of PI3K activity using the GFP-PH probe in live cells. EcR^{W650A}-expressing clones had strong membrane localization of GFP-PH, indicating strong PI3K signaling compared to neighboring cells with low PI3K activity (Figures 6I–6L and 6C). To directly label the EcR^{W650A}-expressing clones, we performed the same experiment in fixed tissue in which the absence of the surface marker CD2 reports the expressing clone. Again, the membrane localization of GFP-PH was higher than in neighboring cells (Figures 6M and 6N), although the difference in GFP-PH membrane localization in fixed tissue was not as clear as in live cells, a phenomenon also observed by others (Britton et al., 2002; Colombani et al., 2003).

If the mechanism of autophagic regulation is governed through regulating the level of PI3K signaling and PIP_3 levels, then the presence of the ecdysone agonist RH5849 in the feeding medium would be predicted to promote PIP_3 downregulation. We therefore challenged feL3 larvae for 4 hr with RH5849 and observed the membrane localization of the GFP-PH probe. A significant reduction of plasma membrane localization of the GFP-PH probe was observed in the RH5849-treated animals in comparison to control animals (Figure 6D, compare with 6A). This indicates that ecdysone signaling can negatively regulate PI3K signaling.

If downregulation of PI3K signaling is the mechanism of autophagic induction by ecdysone signaling, then inhibition of the PI3K pathway should restore autophagic activity in animals with blocked ecdysone signaling. Indeed, larvae simultaneously expressing EcR^{W650A} and PTEN displayed a complete rescue of autophagic activity (Figures 4F and 4G). Taken together, the genetic data demonstrate that ecdysone signaling can downregulate PI3K signaling in a cell-autonomous fashion and that this downregulation is the only downstream requirement for developmental initiation of programmed autophagy.

Discussion

While the molecular machinery of autophagic progression is largely conserved from yeast to mammals, the control of autophagy in multicellular animals is necessarily more complex than in yeast as it is likely to be involved in functions other than the starvation response (Levine and Klionsky, 2004). For example, class I PI3K signaling (which is absent from *S. cerevisiae*) has been shown to suppress autophagy in mammalian cells and in *C. elegans*, but the context of its biological function in autophagic regulation is not known (Melendez et al., 2003; Petiot et al., 2000; Seglen and Bohley, 1992). In this work, we have used the *Drosophila* fat body as a model system to study the regulatory mechanisms of programmed autophagy. We found that PI3K signaling suppresses autophagy in the fat body and that this negative regulation is abolished during the last larval stage by

dc_840_14

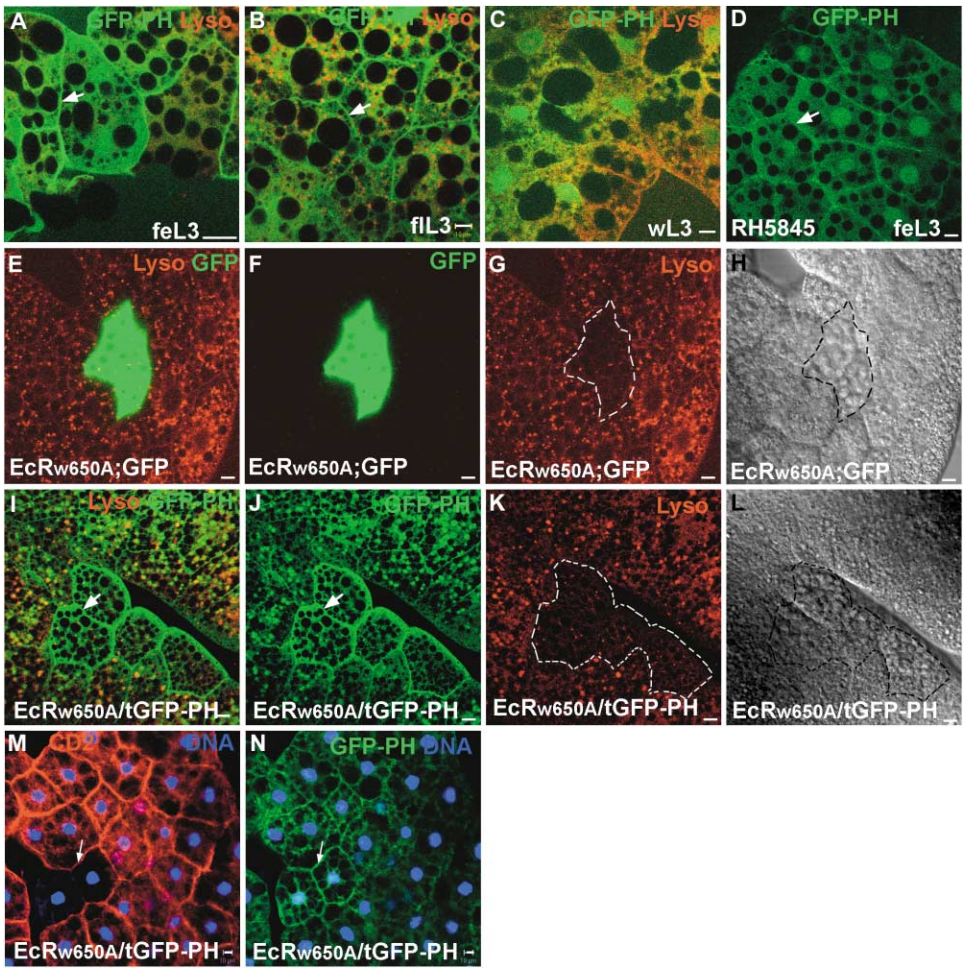


Figure 6. Ecdysone Signaling Cell-Autonomously Downregulates PI3K Activity in the Fat Body

The GFP-PH probe, which binds PIP_3 at the cell membrane, was used to assay PI3K signaling activity. (A–C) PI3K activity (arrow) was gradually reduced during the L3 stage in the fat body. (A and D) GFP-PH membrane localization (arrows) was reduced in eL3 larvae fed on 20% sucrose/yeast supplemented with RH5849 after 4 hr of incubation.

(E–H) Clones of live cells expressing EcR^{W650A} were recognized by GFP expression and showed a marked reduction of lysotracker staining (G), prominent cell outline, and failure of lipid aggregation observable by DIC microscopy (H).

(I–L) Cells expressing EcR^{W650A} displayed a prominent GFP-PH membrane localization.

(M–P) Clones expressing EcR^{W650A} were identified by the lack of the CD2 membrane marker in fixed tissue. More membrane localized GFP-PH was seen within the clone than in surrounding tissue.

Size bars 10 μm (A–L) and 20 μm (M and N).

ecdysone signaling, allowing programmed autophagy to take place.

Ecdysone Signaling Induces Programmed Autophagy in the Fat Body

The fat body is a primary nutrient-responsive tissue that emulates the functions of the liver and adipose tissue of vertebrates (Colombani et al., 2003). Fat body cells undergo programmed autophagy during the last larval stage (L3) preceding pupariation. We focused on the genetic regulation of programmed autophagy. Earlier findings in *Mamestra brassicae* demonstrated that autophagy could be induced by ecdysone (Sass and Kovacs, 1975, 1977). In *Drosophila*, autophagy is developmentally upregulated from mid-L3 stage in fat body cells (Butterworth and Forrest, 1984). Although previously the levels of ecdysone during the L3 stage of development in *Drosophila* have only been detected at low levels at the wandering-L3 stage and increase markedly before puparium formation in most studies (Richards, 1981; Riddiford, 1993), a small hormonal peak before the initiation of wandering has been reported (Berreur et al., 1984). We found that expression of dominant-negative ecdysone receptors from the mid-L3 stage under Lsp-Gal4 control resulted in a dramatic reduction of autophagy. The autophagic area was severely reduced, and fewer acidic structures were observed. Since we did not observe complete inhibiton of autophagy, we closely followed the timing of Lsp-Gal4 expression and found that it initiated reporter gene expression 20–30 min after programmed autophagy had been started (data not shown). Most likely, this latency of Lsp-Gal4 expression

dc_840_14

accounts for the incomplete penetrance of the phenotypes. In fact, driving expression of the dominant-negative EcR using a constitutive fat body Gal4 driver (cg-Gal4) (Asha et al., 2003), or placing a temperature-sensitive mutant of ecdysoneless (*ecd*^{1}) (Berreur et al., 1984) to restrictive temperature at the start of the L3 stage, led to a complete inhibition of autophagy (data not shown). This suggests that ecdysone has a regulatory role on programmed autophagy already at the early L3 stage and that the ecdysone titer at this stage of development is at the threshold of detection. The issue of ecdysone levels during larval development has recently been revisited: radioimmunoassay measurements detected low but continuously increasing levels of ecdysone during mid-L3 stage (R. Farkas, personal communication). Taken together, these results suggest that programmed autophagy is due to this low but rising level of ecdysone during the L3 stage of development.

Autophagic Regulation Downstream of Ecdysone Signaling

A simple explanation of ecdysone-induced programmed autophagy could be the initiation of wandering and therefore starvation-induced autophagy. This is not likely, however, for the following reasons. Developmental autophagy is initiated in fat bodies of late feeding animals at least 6 hr before the animals stop feeding and leave the food, and 12 hr before ingested food starts to disappear from the anterior part of the midgut (Lee et al., 2002a; Butterworth et al., 1988; this study). In addition, the autophagic response in fat body cells is uncoupled from the change in feeding behavior since expression of a dominant-negative ecdysone receptor cell autonomously inhibited programmed autophagy in late wandering L3 animals that ceased feeding 8 hr earlier.

PI3K signaling is able to regulate autophagy and is unlikely to be a part of the amino acid sensing mechanism during an acute starvation response, as amino acids and insulin have been shown to control autophagic proteolysis through different signaling pathways in rat hepatocytes (Kanazawa et al., 2004). This is supported by the fact that the presence of the PIP_3 binding probe, GFP-PH, at the cell membrane is not affected by amino acid deprivation in the fat body (Colombani et al., 2003). The loss of PI3K signaling was only observed after 24 hr of starvation, long after the acute starvation response of autophagy (Britton et al., 2002). This concurs with observations in cultured mammalian cells in which insulin signaling and PI3K activity do not respond to variations in nutrient levels (Shah et al., 2000).

What is then the physiological significance of PI3K signaling regulating autophagy? We modulated PI3K signaling in the fat body to see if it can influence the autophagic response to ecdysone. Elevation of PI3K signaling during the period of programmed autophagy prevented the biogenesis of autolysosomes. This epistatic regulation of PI3K signaling over ecdysone-induced programmed autophagy suggests that PI3K signaling is a part of the same pathway or a dominant repressor. A strong reduction and ultimately loss of PI3K signaling was observed in the fat body during the induction of programmed autophagy, suggesting that ecdysone downregulates PI3K signaling. In addition, a reduction in PI3K signaling failed to increase the autophagic activity during programmed autophagy, in line with the idea that it is in the same pathway and is already inhibited completely. In contrast, reducing Tor signaling in the fat body could further increase autophagic activity during developmental autophagy, suggesting that Tor is not inhibited completely, or not involved in programmed autophagy. Elucidating the role of Tor signaling during this process requires further studies.

Several lines of evidence support a role for PI3K signaling in ecdysone-induced programmed autophagy in the fat body: (1) Inhibition of ecdysone receptor activity or an increase in PI3K signaling produced very similar phenotypes, indicating that these pathways perform opposite regulatory roles on programmed autophagy. (2) Administration of the ecdysone analog RH5849 to feeding larvae promoted attenuation of PI3K signaling. (3) Clonal inactivation of ecdysone receptor signaling led to a failure of this attenuation. (4) Simultaneous downregulation of PI3K signaling and inhibiton of ecdysone receptor activity restored programmed autophagy to wild-type levels. Thus, ecdysone signaling is both necessary and sufficient for downregulation of the PI3K pathway during programmed autophagy. Taken together, these results suggest a model in which ecdysone receptor signaling has the ability to promote autophagy through the downregulation of PI3K signaling.

Experimental Procedures

Fly Strains

All transgenic lines were of the p[w+] variant except hs-FLP^{122}. w^{1118} (control in most experiments), y,w, hs-FLP^{122}; UAS-dTOR^{TED} (Hennig and Neufeld, 2002), w; UAS-EcR^{F645A}, and w; UAS-EcR^{W650A}(Cherbas et al., 2003), w; tub-Gal4/TM6b (Lee and Luo, 1999), w; Lsp2-Gal4 (Cherbas et al., 2003), w; Adh-Gal4 (Fischer et al., 1988), w; cg-Gal4 (Asha et al., 2003), w; UAS-dPTEN (Gao et al., 2000), y,w, hs-FLP^{122}; UAS-Dp110^{D945A}, and y,w, hs-FLP^{122}; UAS- Dp110(Leevers et al., 1996), y,w, hs-FLP^{122}; UAS- p60 (Weinkove et al., 1999), y,w, hs-FLP^{122}; UAS-dAkt (Verdu et al., 1999), Act>CD2>Gal4; tGPH (Britton et al., 2002), y, w, Act>Cd2>Gal4;UAS-GFP (Neufeld et al., 1998; Pignoni and Zipursky, 1997), w, UAS-GFP-LC3#10, w; UAS-GFP-Atg5#16.

Construction of GFP-LC3 and GFP-Atg5 Transgenes

Human LC3-B was PCR-amplified from a human brain cDNA library (Marathon ready, Clontech), and *Drosophila* Atg5 was PCR-amplified from a lambda-ZAP ovary cDNA library (Szabó et al., 2001). The PCR products were subcloned as in-frame fusions with eGFP into pUASp (Rørth, 1998). The resultant UAS-GFP-LC3 and UAS-GFP-Atg5 constructs were injected into w^{1118} embryos for transformation. A minimum of two independent transgenic lines on different chromosomes were established and tested in each case.

Electron Microscopy

Fat bodies for conventional plastic embedding were fixed in 2% glutaraldehyde in 0.1 M cacodylate buffer, pH 7.2. Samples were postfixed with 2% OsO_4 and 1.5% KFeCN in the same buffer, and 40–50 nm sections were observed in a Philips CM10 electron microscope. For cryo-immunocytochemistry, the fat body was fixed in 4.0% formaldehyde, 0.1% glutaraldehyde in 0.1 M Sørensen phosphate buffer (pH 7.4). The samples were washed in PBS, infiltrated with 2.3 M sucrose, mounted on sample stubs, and frozen in liquid nitrogen. Sectioning was done on a Leica FCS cryomicrotome. Sections were collected with a 1:1 mixture of 2% methyl cellulose and 2.3 M sucrose, transferred to formvar/carbon-coated grids and labeled with monoclonal mouse anti-GFP #Z378A (Promega) followed by a secondary rabbit anti-mouse bridging antibody (Dako) and

dc_840_14

Protein A-gold conjugate, essentially as described (Liou et al., 1996; Slot et al., 1991).

Lysotracker Assay

Larvae of the appropriate stage were dissected in PBS. The fat body was stained with LysoTracker Red DND-99 (Molecular Probes) diluted 1:1000 in PBS for 10 s either directly or after 3 min of fixation in 3% formaldehyde (Polysciences, Inc.) in PBS. Longer fixation compromises the lysotracker staining. Mounting was performed in 80% glycerol in PBS, and the samples were directly visualized by confocal microscopy.

Starvation, Rapamycin, and Ecdysone Agonist Experiments

Staged larvae were washed in PBS and starved in 20% sucrose in PBS as an amino acid-deficient starvation medium for 4 hr (Britton and Edgar, 1998). As feeding control, the 20% sucrose was supplemented with yeast paste boiled for a short while in a microwave oven. RH5849 (Wing, 1988) and Rapamycin (Sigma) were added to a final concentration of 0.01 μg/ml and 5 μM, respectively, to the feeding medium. Fat body lobules from the same animal were cultured in 1 X Grace's insect medium (GIBCO) with or without 10 μg/ml of 20-hydroxyecdysone (Sigma) for 4 hr.

Fluorescence Microscopy

Immunochemistry was performed using standard techniques. Anti-GFP mouse monoclonal antibody #Z378A was from Promega (1:1000), rabbit anti-HRP antibodies were from Sigma #P7899 (1:400), and rat CD2 mouse monoclonal antibodies #MCA154R from Serotec (1:200). Nuclei were visualized using TOTO-3 (Molecular Probes). Images were recorded using a Zeiss LSM 510 Meta confocal microscope and processed using Adobe Photohop 7.0.

Quantitative Analysis of Autophagy

A minimum of four samples from three independent animals of each genotype were obtained. The number of GFP-LC3, lysotracker, and GFP-LC3/lysotracker-structures were quantified from confocal image fields (1800 μm^2), using Adobe Photoshop. These results were expressed as mean values $\pm$ SEM. Quantification of the autophagic area in the fat body cytosol was performed on three different fat bodies for each experimental condition from electron microscopy pictures. 25–40 randomly chosen fields were photographed at 4600$\times$ magnification for control animals and at 10500$\times$ magnification for Lsp-Gal4>Dp110 and LspGAL4>EcR^{W650A} animals. The area occupied by autophagic vacuoles was determined by point counting with test lattices of appropriate length. Autophagic vacuoles were scored according to their morphology, comprising all structures that contained recognizable autophagocytosed material such as ER and mitochondria. The total cytosolic area quantified was 3600 μm^2 for control, 2650 μm^2 for Dp110, and 2875 μm^2 for EcR^{W650A}. These results were presented as mean values $\pm$ standard deviation.

Acknowledgments

We would like to thank H. Krämer and S. M. Cohen for providing fly strains, G. Jekely and P. Rørth for plasmids, A.M. Voie for assistance with generating transgenic flies, K. Pattni for critical reading of the manuscript, and M. Fengsrud and M.L. Sneve for comments during the course of the project. We are grateful to T. Neufeld and R. Scott for sharing unpublished information and tips on the lysotracker assay, and R. Farkas for sharing unpublished information. This work was supported by the Research Council of Norway, the Novo Nordisk Foundation and the Norwegian Cancer Society. M.S. was supported by grant 1/047, 2001, NKFP by the Hungarian Ministry of Education.

Received: February 7, 2004
Revised: June 30, 2004
Accepted: July 6, 2004
Published: August 9, 2004

References

Arico, S., Petiot, A., Bauvy, C., Dubbelhuis, P.F., Meijer, A.J., Codogno, P., and Ogier-Denis, E. (2001). The tumor suppressor PTEN positively regulates macroautophagy by inhibiting the phosphatidylinositol 3-kinase/protein kinase B pathway. J. Biol. Chem. *276*, 35243–35246.

Asha, H., Nagy, I., Kovacs, G., Stetson, D., Ando, I., and Dearolf, C.R. (2003). Analysis of Ras-induced overproliferation in *Drosophila* hemocytes. Genetics *163*, 203–215.

Baehrecke, E.H. (2002). How death shapes life during development. Nat. Rev. Mol. Cell Biol. *3*, 779–787.

Berreur, P., Porcheron, P., Moriniere, M., Berreur-Bonnenfant, J., Belinski-Deutsch, S., Busson, D., and Lamour-Audit, C. (1984). Ecdysteroids during the third larval instar in 1(3)ecd-1ts, a temperature-sensitive mutant of *Drosophila melanogaster*. Gen. Comp. Endocrinol. *54*, 76–84.

Blommaart, E.F., Luiken, J.J., Blommaart, P.J., van Woerkom, G.M., and Meijer, A.J. (1995). Phosphorylation of ribosomal protein S6 is inhibitory for autophagy in isolated rat hepatocytes. J. Biol. Chem. *270*, 2320–2326.

Brand, A.H., and Perrimon, N. (1993). Targeted gene expression as a means of altering cell fates and generating dominant phenotypes. Development *118*, 401–415.

Britton, J.S., and Edgar, B.A. (1998). Environmental control of the cell cycle in Drosophila: nutrition activates mitotic and endoreplicative cells by distinct mechanisms. Development *125*, 2149–2158.

Britton, J.S., Lockwood, W.K., Li, L., Cohen, S.M., and Edgar, B.A. (2002). *Drosophila*'s insulin/PI3-kinase pathway coordinates cellular metabolism with nutritional conditions. Dev. Cell *2*, 239–249.

Butterworth, F.M., and Forrest, E.C. (1984). Ultrastructure of the preparative phase of cell death in the larval fat body of *Drosophila melanogaster*. Tissue Cell *16*, 237–250.

Butterworth, F.M., Emerson, L., and Rasch, E.M. (1988). Maturation and degeneration of the fat body in the *Drosophila* larva and pupa as revealed by morphometric analysis. Tissue Cell *20*, 255–268.

Cherbas, L., Hu, X., Zhimulev, I., Belyaeva, E., and Cherbas, P. (2003). EcR isoforms in Drosophila: testing tissue-specific requirements by targeted blockade and rescue. Development *130*, 271–284.

Codogno, P., and Meijer, A.J. (2004). Signaling pathways in mammalian autophagy. In Autophagy, D.J. Klionsky, ed. (Georgetown, Texas: Landes Bioscience), pp. pp 26–47.

Colombani, J., Raisin, S., Pantalacci, S., Radimerski, T., Montagne, J., and Leopold, P. (2003). A nutrient sensor mechanism controls *Drosophila* growth. Cell *114*, 739–749.

Dunn, W.A., Jr. (1990). Studies on the mechanisms of autophagy: formation of the autophagic vacuole. J. Cell Biol. *110*, 1923–1933.

Edinger, A.L., and Thompson, C.G. (2003). Defective autophagy leads to cancer. Cancer Cell *4*, 422–424.

Fengsrud, M., Erichsen, E.S., Berg, T.O., Raiborg, C., and Seglen, P.O. (2000). Ultrastructural characterization of the delimiting membranes of isolated autophagosomes and amphisomes by freeze-fracture electron microscopy. Eur. J. Cell Biol. *79*, 871–882.

Fischer, J.A., Giniger, E., Maniatis, T., and Ptashne, M. (1988). GAL4 activates transcription in *Drosophila*. Nature *332*, 853–856.

Gao, X., Neufeld, T.P., and Pan, D. (2000). *Drosophila* PTEN regulates cell growth and proliferation through PI3K-dependent and -independent pathways. Dev. Biol. *221*, 404–418.

Gordon, P.B., Tolleshaug, H., and Seglen, P.O. (1985). Use of digitonin extraction to distinguish between autophagic-lysosomal sequestration and mitochondrial uptake of [14C]sucrose in hepatocytes. Biochem. J. *232*, 773–780.

Hara, K., Maruki, Y., Long, X., Yoshino, K., Oshiro, N., Hidayat, S., Tokunaga, C., Avruch, J., and Yonezawa, K. (2002). Raptor, a binding partner of target of rapamycin (TOR), mediates TOR action. Cell *110*, 177–189.

Hennig, K.M., and Neufeld, T.P. (2002). Inhibition of cellular growth and proliferation by dTOR overexpression in *Drosophila*. Genesis *34*, 107–110.

Hu, X., Cherbas, L., and Cherbas, P. (2003). Transcription activation by the ecdysone receptor (EcR/USP): identification of activation functions. Mol. Endocrinol. *17*, 716–731.

Ichimura, Y., Kirisako, T., Takao, T., Satomi, Y., Shimonishi, Y., Ishihara, N., Mizushima, N., Tanida, I., Kominami, E., Ohsumi, M., et al. (2000). A ubiquitin-like system mediates protein lipidation. Nature *408*, 488–492.

Juhász, G., Csikós, G.Y., and Sass, M. (2001). A possible approach to study autophagy in *Drosophila*. Acta Biol. Hung. *52*, 485–490.

Juhász, G., Csikós, G., Sinka, R., Erdélyi, M., and Sass, M. (2003). The *Drosophila* homolog of Aut1 is essential for autophagy and development. FEBS Lett. *543*, 154–158.

Kabeya, Y., Mizushima, N., Ueno, T., Yamamoto, A., Kirisako, T., Noda, T., Kominami, E., Ohsumi, Y., and Yoshimori, T. (2000). LC3, a mammalian homologue of yeast Apg8p, is localized in autophagosome membranes after processing. EMBO J. *19*, 5720–5728.

Kanazawa, T., Taneike, I., Akaishi, R., Yoshizawa, F., Furuya, N., Fujimura, S., and Kadowaki, M. (2004). Amino acids and insulin control autophagic proteolysis through different signaling pathways in relation to mTOR in isolated rat hepatocytes. J. Biol. Chem. *279*, 8452–8459.

Komuves, L., Sass, M., and Kovâacs, J. (1985). Autophagocytosis in the larval midgut cells of *Pieris brassicae* during metamorphosis. Cell Tissue Res. *240*, 215–221.

Kim, D.H., and Sabatini, D.M. (2004). Raptor and mTOR: subunits of a nutrient-sensitive complex. Curr. Top. Microbiol. Immunol. *279*, 259–270.

Kirisako, T., Baba, M., Ishihara, N., Miyazawa, K., Ohsumi, M., Yoshimori, T., Noda, T., and Ohsumi, Y. (1999). Formation process of autophagosome is traced with Apg8/Aut7p in yeast. J. Cell Biol. *147*, 435–446.

Kirisako, T., Ichimura, Y., Okada, H., Kabeya, Y., Mizushima, N., Yoshimori, T., Ohsumi, M., Takao, T., Noda, T., and Ohsumi, Y. (2000). The reversible modification regulates the membrane-binding state of Apg8/Aut7 essential for autophagy and the cytoplasm to vacuole targeting pathway. J. Cell Biol. *151*, 263–276.

Klionsky, D.J. (2004). Autophagy (Georgetown, Texas: Landes Bioscience).

Klionsky, D.J., and Emr, S.D. (2000). Autophagy as a regulated pathway of cellular degradation. Science *290*, 1717–1721.

Klionsky, D.J., Cregg, J.M., Dunn, W.A., Jr., Emr, S.D., Sakai, Y., Sandoval, I.V., Sibirny, A., Subramani, S., Thumm, M., Veenhuis, M., and Ohsumi, Y. (2003). A unified nomenclature for yeast autophagy-related genes. Dev. Cell *5*, 539–545.

Kovacs, A.L., Grinde, B., and Seglen, P.O. (1981a). Inhibition of autophagic vacuole formation and protein degradation by amino acids in isolated hepatocytes. Exp. Cell Res. *133*, 431–436.

Kovacs, A.L., Molnar, K., and Seglen, P.O. (1981b). Inhibition of autophagic sequestration and endogenous protein degradation in isolated rat hepatocytes by methylated adenosine derivatives. FEBS Lett. *134*, 194–196.

Kozlova, T., and Thummel, C.S. (2003). Essential roles for ecdysone signaling during Drosophila mid-embryonic development. Science *301*, 1911–1914.

Lee, C.Y., and Baehrecke, E.H. (2001). Steroid regulation of autophagic programmed cell death during development. Development *128*, 1443–1455.

Lee, C.Y., Cooksey, B.A., and Baehrecke, E.H. (2002a). Steroid regulation of midgut cell death during *Drosophila* development. Dev. Biol. *250*, 101–111.

Lee, T., and Luo, L. (1999). Mosaic analysis with a repressible cell marker for studies of gene function in neuronal morphogenesis. Neuron *22*, 451–461.

Leevers, S.J., Weinkove, D., MacDougall, L.K., Hafen, E., and Waterfield, M.D. (1996). The *Drosophila* phosphoinositide 3-kinase Dp110 promotes cell growth. EMBO J. *15*, 6584–6594.

Levine, B., and Klionsky, D.J. (2004). Development by self-digestion: molecular mechanisms and biological functions of autophagy. Dev. Cell *6*, 463–477.

Liou, W., Geuze, H.J., and Slot, J.W. (1996). Improving structural integrity of cryosections for immunogold labeling. Histochem. Cell Biol. *106*, 41–58.

Lloyd, T.E., Atkinson, R., Wu, M.N., Zhou, Y., Pennetta, G., and Bellen, H.J. (2002). Hrs regulates endosome membrane invagination and tyrosine kinase receptor signaling in *Drosophila*. Cell *108*, 261–269.

Loewith, R., Jacinto, E., Wullschleger, S., Lorberg, A., Crespo, J.L., Bonenfant, D., Oppliger, W., Jenoe, P., and Hall, M.N. (2002). Two TOR complexes, only one of which is rapamycin sensitive, have distinct roles in cell growth control. Mol. Cell *10*, 457–468.

Melendez, A., Talloczy, Z., Seaman, M., Eskelinen, E.L., Hall, D.H., and Levine, B. (2003). Autophagy genes are essential for dauer development and life-span extension in *C. elegans*. Science *301*, 1387–1391.

Miron, M., and Sonenberg, N. (2001). Regulation of translation via TOR signaling: insights from *Drosophila melanogaster*. J. Nutr. *131*, 2988S–2993S.

Mizushima, N., Noda, T., Yoshimori, T., Tanaka, Y., Ishii, T., George, M.D., Klionsky, D.J., Ohsumi, M., and Ohsumi, Y. (1998). A protein conjugation system essential for autophagy. Nature *395*, 395–398.

Mizushima, N., Yamamoto, A., Hatano, M., Kobayashi, Y., Kabeya, Y., Suzuki, K., Tokuhisa, T., Ohsumi, Y., and Yoshimori, T. (2001). Dissection of autophagosome formation using Apg5-deficient mouse embryonic stem cells. J. Cell Biol. *152*, 657–668.

Mizushima, N., Yamamoto, A., Matsui, M., Yoshimori, T., and Ohsumi, Y. (2003). In vivo analysis of autophagy in response to nutrient starvation using transgenic mice expressing a fluorescent autophagosome Marker. Mol. Biol. Cell. *15*, 1101–1111.

Munafó, D.B., and Colombo, M.I. (2001). A novel assay to study autophagy: regulation of autophagosome vacuole size by amino acid deprivation. J. Cell Sci. *114*, 3619–3629.

Møller, T.N., Samari, H.R., Holden, L., and Seglen, P.O. (2004). Regulation of mammalian autophagy by protein phosphorylation. In Autophagy, D.J. Klionsky, ed. (Georgetown, Texas: Landes Bioscience), pp. 48–59.

Neufeld, T.P., de la Cruz, A.F., Johnston, L.A., and Edgar, B.A. (1998). Coordination of growth and cell division in the *Drosophila* wing. Cell *93*, 1183–1193.

Noda, T., and Ohsumi, Y. (1998). Tor, a phosphatidylinositol kinase homologue, controls autophagy in yeast. J. Biol. Chem. *273*, 3963–3966.

Noda, T., Suzuki, K., and Ohsumi, Y. (2002). Yeast autophagosomes: de novo formation of a membrane structure. Trends Cell Biol. *12*, 231–235.

Oldham, S., and Hafen, E. (2003). Insulin/IGF and target of rapamycin signaling: a TOR de force in growth control. Trends Cell Biol. *13*, 79–85.

Oldham, S., Montagne, J., Radimerski, T., Thomas, G., and Hafen, E. (2000). Genetic and biochemical characterization of dTOR, the *Drosophila* homolog of the target of rapamycin. Genes Dev. *14*, 2689–2694.

Petiot, A., Ogier-Denis, E., Blommaart, E.F., Meijer, A.J., and Codogno, P. (2000). Distinct classes of phosphatidylinositol 3′-kinases are involved in signaling pathways that control macroautophagy in HT-29 cells. J. Biol. Chem. *275*, 992–998.

Pignoni, F., and Zipursky, S.L. (1997). Induction of *Drosophila* eye development by decapentaplegic. Development *124*, 271–278.

Richards, G. (1981). The radioimmune assay of ecdysteroid titres in *Drosophila melanogaster*. Mol. Cell. Endocrinol. *21*, 181–197.

Riddiford, L.M. (1993). Hormones and *Drosophila* development. In The Development of *Drosophila melanogaster*, B. Bate, and A. Martines Arias, eds. (New York: CSHL Press), pp. pp 899–939.

Riddiford, L.M., Cherbas, P., and Truman, J.W. (2000). Ecdysone receptors and their biological actions. Vitam. Horm. *60*, 1–73.

Rørth, P. (1998). Gal4 in the *Drosophila* female germline. Mech. Dev. *78*, 113–118.

Sass, M., and Kovacs, J. (1975). Ecdysterone and an analogue of

dc_840_14

juvenile hormone on the autophagy in the cells of fat body of *Mamestra brassicae*. Acta Biol. *26*, 189–196.

Sass, M., and Kovacs, J. (1977). The effect of ecdysone on the fat body cells of the penultimate larvae of *Mamestra brassicae*. Cell Tissue Res. *180*, 403–409.

Scott, R.C., Schuldiner, O., and Neufeld, T.P. (2004). Role and regulation of starvation-induced autophagy in the *Drosophila* fat body. Dev. Cell *7*, this issue, 167–178.

Seglen, P.O., and Bohley, P. (1992). Autophagy and other vacuolar protein degradation mechanisms. Experientia *48*, 158–172.

Seglen, P.O., Gordon, P.B., and Holen, I. (1990). Non-selective autophagy. Semin. Cell Biol. *1*, 441–448.

Shah, O.J., Anthony, J.C., Kimball, S.R., and Jefferson, L.S. (2000). 4E–BP1 and S6K1: translational integration sites for nutritional and hormonal information in muscle. Am. J. Physiol. Endocrinol. Metab. *279*, E715–E729.

Simonsen, A., Wurmser, A.E., Emr, S.D., and Stenmark, H. (2001). The role of phosphoinositides in membrane transport. Curr. Opin. Cell Biol. *13*, 485–492.

Slot, J.W., Geuze, H.J., Gigengack, S., Lienhard, G.E., and James, D.E. (1991). Immuno-localization of the insulin regulatable glucose transporter in brown adipose tissue of the rat. J. Cell Biol. *113*, 123–135.

Suzuki, K., Kirisako, T., Kamada, Y., Mizushima, N., Noda, T., and Ohsumi, Y. (2001). The pre-autophagosomal structure organized by concerted functions of APG genes is essential for autophagosome formation. EMBO J. *20*, 5971–5981.

Szabó, K., Jékely, G., and Rørth, P. (2001). Cloning and expression of *sprint*, a *Drosophila* homologue of RIN1. Mech. Dev. *101*, 259–262.

Thummel, C.S. (2001). Steroid-triggered death by autophagy. Bioessays *23*, 677–682.

Verdu, J., Buratovich, M.A., Wilder, E.L., and Birmbaum, M.J. (1999). Cell-autonomous regulation of cell and organ growth in *Drosophila* by Akt/PKB. Nat. Cell Biol. *1*, 500–506.

von Gaudecker, B., and Schmale, E.M. (1974). Substrate-histochemical investigations and ultrahistochemical demonstrations of acid phosphatase in larval and prepupal salivary glands of *Drosophila melanogaster*. Cell Tissue Res. *155*, 75–89.

Weinkove, D., Neufeld, T.P., Twardzik, T., Waterfield, M.D., and Leevers, S.J. (1999). Regulation of imaginal disc cell size, cell number and organ size by *Drosophila* class I(A) phosphoinositide 3-kinase and its adaptor. Curr. Biol. *9*, 1019–1029.

Wing, K.D. (1988). RH 5849, a nonsteroidal ecdysone agonist: effects on a *Drosophila* cell line. Science *241*, 467–469.

Zhang, H., Stallock, J.P., Ng, J.C., Reinhard, C., and Neufeld, T.P. (2000). Regulation of cellular growth by the *Drosophila* target of rapamycin dTOR. Genes Dev. *14*, 2712–2724.

dc_840_14
Available online at www.sciencedirect.com
SCIENCE DIRECT®
European Journal of Cell Biology 84 (2005) 491–502
European Journal of Cell Biology
www.elsevier.de/ejcb

Hid can induce, but is not required for autophagy in polyploid larval *Drosophila* tissues

Gábor Juhász*, Miklós Sass

Department of General Zoology, Eötvös Loránd University, H-1117 Pázmány sétány 1/C, Budapest, Hungary

Received 6 August 2004; received in revised form 2 November 2004; accepted 4 November 2004

Abstract

The major cell death pathways are apoptosis and autophagy-type cell death in *Drosophila*. Overexpression of proapoptotic genes in developing imaginal tissues leads to the activation of caspases and apoptosis, but most of them show no effect on the polytenic cells of the fat body during the last larval stage. Surprisingly, overexpression of Hid induces caspase-independent autophagy in the fat body, as well as in most other larval tissues tested. Hid mutation results in inhibition of salivary gland cell death, but the disintegration of the larval midgut is not affected. Electron microscopy shows that autophagy is normally induced in fat body, midgut and salivary gland cells of homozygous mutant larvae, suggesting that Hid is not required for autophagy itself. Constitutive expression of the caspase inhibitor p35 produces identical phenotypes. Our results show that the large, post-mitotic larval cells do not react or activate autophagy in response to the same strong apoptotic stimuli that trigger apoptosis in small, mitotically active imaginal disc cells.
© 2005 Elsevier GmbH. All rights reserved.

Keywords: Apoptosis; Autophagy; Cell death; *Drosophila*; Fat body; Hid

Introduction

Programmed cell death is used to selectively remove unwanted or dangerous cells in multicellular animals. On the basis of the morphology, two major forms can be recognized: apoptosis and autophagy-type cell death. Apoptosis serves as a targeted elimination of individual cells during physiological circumstances, followed by endocytosis of cellular remnants by macrophages and subsequent degradation in lysosomes. Autophagy is basically a self-defense reaction that ensures survival of the cells or organism in case of nitrogen starvation, by turning over most of the cytoplasm including organelles for re-use in synthetic processes. During autophagy, a membrane sac of uncertain origin called the isolation membrane engulfs portions of the cytoplasm and finally forms a double-membrane-layered initial autophagic vacuole (often referred to as autophagosome). After fusion with a lysosome, a degrading autophagic vacuole (often referred to as autolysosome) is formed, where the sequestered material is digested by lysosomal hydrolases (Ohsumi, 2001; Rusten et al., 2004). In multicellular animals, autophagy was integrated to multitudinous cell death events to cope with the mass of cytoplasm to be degraded in a short time, thereby lowering the need for macrophages to clear up the corpses (Baehrecke, 2002;

*Corresponding author. Present address: Department of Genetics, Cell Biology, and Development, University of Minnesota, 6-160 Jackson Hall, 321 Church Street S.E., Minneapolis, MN 55455, USA. Tel.: +1 612 626 5217; fax: +1 612 626 5652.
E-mail address: juhas001@umn.edu (G. Juhász).

0171-9335/$ - see front matter © 2005 Elsevier GmbH. All rights reserved.
doi:10.1016/j.ejcb.2004.11.010

Gozuacik and Kimchi, 2004). The regulation of apoptosis and autophagic cell death can involve common, "upstream" factors that mediate the actual death stimulus, and possibly different, "downstream" factors that are involved in the decision how to die.

During apoptosis, the activation of caspases (cysteine aspartyl proteases) rapidly results in selective cleavage of many intracellular proteins like lamin or actin, ultimately leading to chromatin margination in the nucleus, cytoskeletal collision, membrane blebbing and subsequent phagocytosis of emerging apoptotic bodies (Kaufmann and Hengartner, 2001). But this generalized picture is only true for some, but not all systems (Lockshin and Zakeri, 2002, 2004). For example, in case of the now classical apoptosis model *Caenorhabditis elegans*, cells eliminated during normal development share the above-mentioned morphological and molecular features (Horvitz, 2001), like dying embryonic and imaginal disc cells of *Drosophila*, as well as mammalian lymphocytes in tissue culture or in vivo (Baehrecke, 2002). However, in large, post-mitotic, often polyploid cells like larval insect tissues usually autophagy is induced, often as an early step of cell death which is sometimes considered the preparative phase (Butterworth and Forrest, 1984). The advantage of this is that self-material is delivered into lysosomes to ensure the degradation of cytoplasm that could otherwise overload macrophages, or that nutrients can be stored in these cells until needed by developing tissues, when cell death releases the reusable and pre-degraded components, as seen in case of the larval fat body of insects (Baehrecke, 2002; Lockshin and Zakeri, 2002; Neufeld, 2003). Autophagic cell death is independent of caspase activity, and is clearly different from the morphology of apoptosis: cytoskeleton is maintained, the cytoplasm retains its synthetic capacity but most of it is sequestered into autophagic vacuoles for lysosomal breakdown (Gozuacik and Kimchi, 2004). Of course, the process of autophagy is also caspase-independent, as its involvement in certain cell death events is only one of its many roles (Neufeld, 2003; and this study).

Often both types can be observed in the same cell, like in case of several neurodegenerative diseases (Yuan et al., 2003), or certain larval tissues of metamorphosing insects, in which autophagy is observed during the preparative phase of cell death, but the last phase involves caspase activation and apoptotic features (Lockshin and Zakeri, 2002, 2004; Neufeld, 2003).

A large amount of data is available on the regulation of apoptosis. The central proteases, caspases are tightly controlled to prevent accidental activation that would lead to catastrophic events. Inhibitor of apoptosis proteins (IAPs) bind to and inactivate caspases by targeting them to proteasomal degradation (Palaga and Osborne, 2002). Both extra- and intracellular signals can culminate in caspase activation (i.e. through inhibition of IAP function) and apoptosis. Extracellular signals triggering activation of caspase-8 and apoptosis include tumor necrosis factor (TNF), interferon-gamma and FasL. Intracellular changes that can lead to cell death are the activation of p53 in response to DNA damage, or mitochondrial dysfunction resulting in the release of several proapoptotic proteins into the cytoplasm. These include cytochrome c and Apaf-1 (apoptosis activating factor 1), the components of the apoptosome where the activation of caspase-9 takes place, and Smac/DIABLO, that binds to IAPs and deliberates caspases this way (see Kaufmann and Hengartner, 2001 for a more detailed review). The molecular mechanisms outlined above are fully conserved in *Drosophila*, making it an excellent model system for these studies (Aravind et al., 2001).

Recently, the core components and most important regulators of autophagy were also identified. Two, ubiquitin-like protein conjugation systems are necessary for the formation of autophagic vacuoles (Ohsumi, 2001). Autophagy is activated by reduced phosphatidylinositol 3-kinase and Tor kinase signaling (see Neufeld, 2003 for a review). However, very little is known about the regulation of autophagic cell death. So far, only death-associated protein kinase (DAPk), the DAPk-related protein 1 (DRP-1), the hypoxia inducible protein BNIP-3 and the transmembrane protein Spin are known to induce this form of cell death when overexpressed in cancer cell lines, and their mode of action is not yet described (Gozuacik and Kimchi, 2004).

How is autophagy induced during autophagy-type cell death? Possible hypotheses are that different signaling molecules are activated in different cell death processes, or there are signaling molecules capable of inducing apoptosis in one cell type and autophagy in the other, regardless of the last step that can be caspase activation and apoptosis finally, or the excess of autophagy leading to the death of the cell (as reviewed in Gozuacik and Kimchi, 2004).

Most papers dealing with cell death concentrate on relatively small, mitotically active cells like tissue culture systems or embryonic or imaginal disc cells in case of *Drosophila* (Lockshin and Zakeri, 2002). However, large, post-mitotic cells like adult neurons or muscle cells, or in *Drosophila*, polytenic larval tissues usually react differently to similar stimuli (Lee et al., 2003). To characterize the role of well-known proapoptotic genes in these large, post-mitotic larval cells, we undertook a gain-of-function study. We chose the fat body (the functional equivalent of the human liver) as a model tissue, because of its enormous autophagic capacity. No autophagic vacuoles can be identified during the first half of the last larval stage. However, by the end of this

stage, degrading autophagic vacuoles fill the cytoplasm of each cell (usually more than 20 vacuoles are seen in cross-sections containing the nucleus), making the fat body a very convenient model system: essentially a plus–minus response can be evaluated, as the area occupied by autophagic structures (isolation membranes, initial and degrading autophagic vacuoles) rises from 0% to 11% of the cytoplasm (Butterworth and Forrest, 1984). The hormonal control of the process is also known: the elevation of the 20-hydroxy-ecdysone level in mid-third instar at a low concentration of juvenile hormone induces autophagy, and also leads to wandering behavior of the larvae (Sass and Kovacs, 1975). Four to six hours before the onset of wandering and developmental autophagy in fat body, autophagy can be effectively induced by ectopic 20-hydroxy-ecdysone administration (Rusten et al., 2004). Starvation or rapamycin treatment (a drug that is widely used for induction of autophagy) are also very potent inducers of the process in this tissue (Rusten et al., 2004). Interestingly, larval fat body histolysis is delayed, as more than half of the cells die only on the first day following the eclosion of the adult fly, approximately 4 days after the induction of autophagy (Butterworth and Forrest, 1984). In contrast, autophagy is also induced in the larval midgut and salivary gland preceding metamorphosis, like in fat body, but all these cells die within 24 h in a caspase-dependent manner (Baehrecke, 2002; Rusten et al., 2004). As fat body cells represent the primary nutrient and energy reservoir of larvae and pupae, their final phase of death is delayed and not synchronous, probably in order to continuously provide all the necessary components for successful metamorphosis and eclosion.

The main question of our work is: how do those polyploid larval *Drosophila* cells react to direct apoptotic stimuli that are developmentally programmed for autophagy before dying, or as a way of cell death? Overexpression of key signaling molecules in these cells at a time when they normally show no sign of degeneration can lead to three different, but not mutually exclusive theoretical outcomes: (1) apoptosis is observed like in case of dividing cells, as the same signaling pathway operates in these cells also, but autophagy is induced (perhaps by a different stimulus) during normal development; (2) no effect is observed, as the apoptotic signaling molecule being tested is not functional or the pathway is suppressed in these cells; (3) autophagy is induced, as probably it is the primary reaction of that particular cell type to cell-death inducing stimuli, or because autophagy always precedes and is required for the actual death of these cells (due to the widespread expression of these genes in our system that leads to organismal lethality, we can not distinguish between these two different theories). Our results support version 2 in nearly all cases, showing that these cells are surprisingly resistant to apoptotic signals. However, Hid induces autophagy in most larval tissues tested, suggesting that autophagy may be the default degradatory pathway activated first in these cells (see below).

Overexpression of the caspase Dronc, p53, or the functional counterparts of Smac/DIABLO (Reaper, Hid, Grim and Sickle) was evaluated in the fat body. Only one of these, Hid produced any detectable effect on fat body cells (trophocytes), namely, the strong induction of autophagy. Overexpression of Hid also induced autophagy in most other polyploid larval tissues tested. Further studies showed that this effect is caspase independent, similar to naturally occurring developmental autophagy, unlike its mode of action during apoptosis. Careful examination of a Hid mutant suggested that the gene is not required for normally occurring autophagy in larval *Drosophila* tissues, or its function is redundant. In conclusion, we have shown that the same proapoptotic stimulus leads to strikingly different effects in larval post-mitotic and imaginal tissues.

Materials and methods

Fly strains

The Gal4 drivers hs-Gal4, act-Gal4, cg-Gal4, GMR-Gal4, tub-Gal4 and UAS-Rpr, two independent UAS-p35 and two independent hs-Hid transgenic lines and the lines l(3)05014, Df(3L)Cat were obtained from the Bloomington Stock Center. UAS-Hid, UAS-Grim, UAS-Sickle and UAS-DIAP1 were kindly provided by John R. Nambu; UAS-p53 was a gift of Imre Boros; UAS-Dronc was kindly provided by John M. Abrams. Fly crosses were set up in vials containing standard fly food at 25 °C. Heat shocks were applied by immersing the vials in a water bath at 37 °C for 1 h, followed by a 3.5-h incubation at 25 °C before sample preparation. For the scoring of larval genotypes, we used the dominant mutant phenotype of Bc (Black cells; located on the second chromosome) in case of CyO hsHid. For the third chromosome, we scored Tb (Tubby), located on the TM6B balancer chromosome in case of act-Gal4, tub-Gal4, TM3 hsHid, l(3)05014 and Df(3L)Cat. The Bc mutation causes the emergence of black hemocytes in larvae (visible through the cuticle), whereas the Tb mutation leads to an abnormally short larval body. After the crosses, in the first generation, all non-marked (non-Bc or non-Tb) larvae carry the chromosome of interest. All other insertions are homozygous viable. All of the Gal4-responsive UAS lines were crossed to the eye-specific GMR-Gal4 line as a control and expected phenotypes were seen.

Histology and transmission electron microscopy

Dissected tissues were fixed overnight at 4 °C in 0.1 N Na-cacodylate (Sigma) buffer, pH = 7.4, containing 3.2% paraformaldehyde (TAAB), 0.5% glutaraldehyde (TAAB), 1% sucrose (Sigma), and 40 mM $CaCl_2$ (Reanal) and embedded in Araldyte (Fluka). Semi-thick sections (500 nm) were processed for silver impregnation according to standard procedures. Ultrathin sections (80 nm) were post-contrasted by immersing the grids in lead citrate (Reanal) and observed with a JEOL CM-II 100 transmission electron microscope. Samples from three different animals at least were evaluated for each genotype.

Results

Hid, but not Grim, Sickle, Reaper, Dronc, or p53, induces autophagy in larval *Drosophila* tissues

Heat shock-mediated overexpression of Hid, Grim, Reaper, Sickle, p53, and the caspase Dronc in the larval fat body were evaluated by transmission electron microscopy. In case of Grim, Reaper, Sickle, p53, and Dronc, no effects were observed in trophocytes, similarly to control animals overexpressing green fluorescent protein (GFP) (Fig. 1a and not shown). However, Hid induced a very strong autophagic response in all fat body cells (more than 10 autophagic structures in all cells in cross-sections that contain the nucleus, Fig. 1b). Three different genotypes of Hid-overexpressing larvae (see Materials and methods) were examined and found to give indistinguishable results. To further characterize the autophagy-inducing effect of this gene, we analyzed its effect on other larval tissues. Overexpression of Hid also strongly induced autophagy in the larval epidermis (Fig. 1c and d), midgut, salivary gland (Fig. 1e–h), Malpighian tubules, trachea epithelium, but autophagic structures were scarcely observed in somatic and visceral muscle cells (not shown). As expected, overexpression of Hid resulted in apoptosis of imaginal disc cells and brain neurons exhibiting condensed chromatin in the nucleus and dark cytoplasm without the emergence of autophagic structures (Fig. 2a–d).

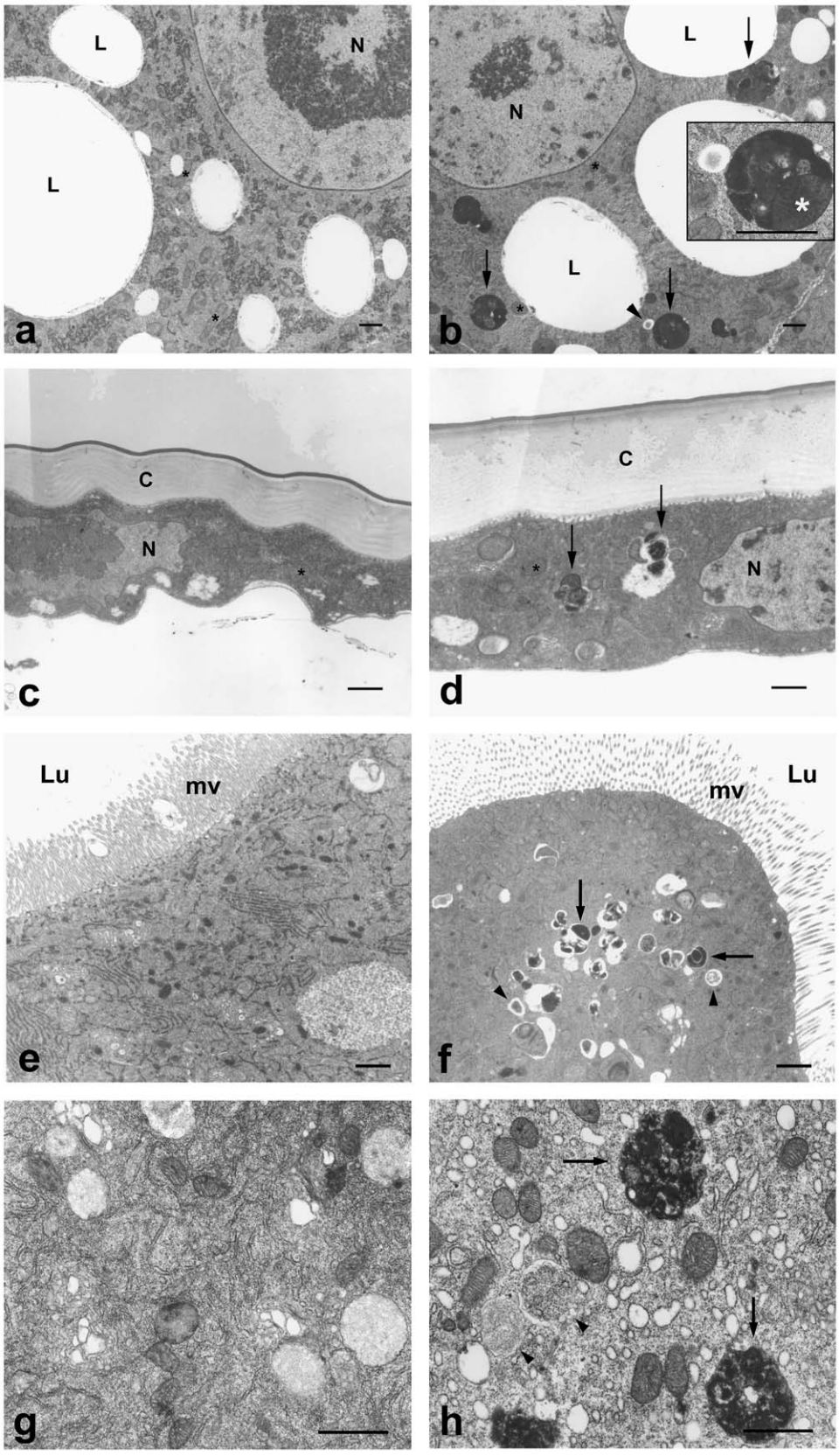
Hid-induced autophagy in fat body is independent of caspase activity

Caspases are the most important mediators of apoptosis, and overexpression of Hid in imaginal disc cells also results in caspase-dependent cell death (Grether et al., 1995). To gain further insight in the possible mechanism of Hid-mediated induction of autophagy in larval tissues, we studied the effect of Hid overproduction in animals that express the pan-caspase inhibitor p35 (Hay et al., 1994) in the fat body (Fig. 3a and b). The same strong effect was seen in all cells as without the presence of caspase inhibitors. As a control, we expressed the oncogenic Ras^{V12} mutant protein, which is a powerful inhibitor of Hid activity (Kurada and White, 1998; Bergmann et al., 2002). Expression of the constitutively active Ras form did indeed block the autophagy-inducing effect of Hid (Fig. 3c and d). Expression of the oncogenic mutant alone had no effect on developmental or starvation-induced autophagy (not shown).

Hid is not required for developmental autophagy

As Hid is required for the apoptosis of many cells during normal development (Grether et al., 1995), we wanted to examine its potential involvement in autophagy. A hypomorphic Hid mutation caused by the insertion of a transposon in the first intron of the gene in line l(3)05014 (Peterson et al., 2002) was used for our studies. These Hid mutant flies of the genotype l(3)05014/f(3L)Cat die during the prepupal and pupal stages. In wild-type controls, larval midgut and salivary gland tissue undergoes histolysis during metamorphosis (Jiang et al., 1997). The destruction of the larval midgut can be illustrated by the disappearance of gastric caeca at 5 h after puparium formation (apf), and by the shortening of the midgut (Fig. 4a and b). In the Hid mutant, the larval midgut exhibits the wild-type changes including the scheduled disappearance of gastric caeca ($n = 21/21$, Fig. 4c). However, the salivary glands that

Fig. 1. Overexpression of Hid induces autophagy in larval fat body and epidermis, midgut and salivary gland cells. Similarly to the wild-type situation, no autophagy is observed in the larval fat body during the feeding period in a green fluorescent protein-expressing animal (a). Overexpression of Hid strongly induces autophagy in the larval fat body, leading to the appearance of initial (arrowheads) and degrading autophagic vacuoles (arrows) (b); inset is an enlargement of (b) showing a degrading autophagic vacuole that contains a still recognizable mitochondrion. In the larval epidermis, autophagy is never observed (c), whereas overexpression of Hid also leads to the emergence of autophagic structures (d). No autophagy is observed in larval midgut (e) and salivary gland cells (g) during the first half of the last larval stage in the control animals. Overexpression of Hid induces autophagy in both midgut (f) and salivary gland cells (h). Cuticle (C), lipid droplets (L), midgut lumen (Lu), microvilli (mv), mitochondria (*), and nuclei (N) are marked. Arrowheads indicate initial, whereas arrows mark degrading autophagic vacuoles. Bars equal 1 μm.


L
N
L
a
L
N
L
b
C
N
c
C
N
d
Lu
mv
e
mv
Lu
f
g
h

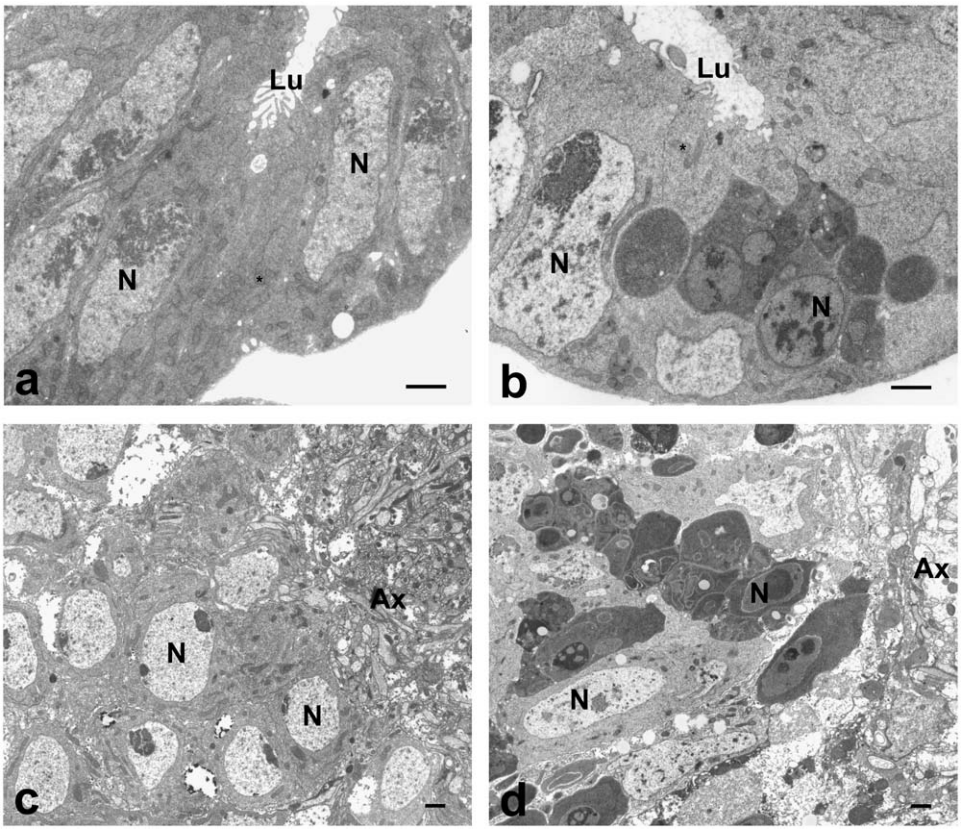


Fig. 2. Overexpression of Hid leads to apoptosis of imaginal disc and brain cells. Part of the wild-type eye-antenna disk (a) and the brain (c) is shown here. Note that overexpression of Hid during the first half of the last larval stage induces apoptosis (cells with dark cytoplasm and condensed chromatin) in the eye-antenna disk (b) and in the brain (d), but no autophagy is observed in these cells. Axons (Ax), lumen (Lu), mitochondria (*), microvilli (mv), and nuclei (N) are marked. Bars equal 1 μm.

normally disappear at 14–16 h apf (Fig. 4e and f) persist in Hid mutants even at 24 h apf ($n = 8/24$, Fig. 4(g). Only the animals that normally underwent head eversion at 12–14 h apf were scored.

We analyzed autophagy in larval tissues by transmission electron microscopy again. Hid mutant animals exhibited wild-type autophagy in larval fat body (Fig. 5b, compare to Fig. 5a), larval and prepupal midgut (Fig. 5e, compare to Fig. 5d) and pupal salivary gland cells (Fig. 5g).

Developmental autophagy is also caspase independent

As caspases are the major mediators of Hid, we examined the effect of the constitutive expression of the caspase inhibitor p35, mediated by the constitutive promoters of actin or tubulin. While tub-Gal4 mediated expression of p35 resulted in embryonic lethality due to the inhibition of essential embryonic cell death events (not shown), act-Gal4-mediated expression of p35 allows proper larval development and results in late prepupal-pupal lethality. Interestingly, act-Gal4-mediated constitutive expression of p35 nearly completely phenocopied the Hid mutation in case of larval midgut and salivary gland destruction. The larval and prepupal midgut displays wild-type changes ($n = 23/23$, Fig. 4d) whereas salivary gland cell death is blocked ($n = 21/22$, Fig. 4h). Again, autophagy was normally induced in larval fat body (not shown, see Fig. 5c) and larval and prepupal midgut, as well as in pupal salivary gland (Fig. 5f and h). Higher-level expression of p35 or DIAP1 (Hay et al., 1995) (using a heat shock-responsive promoter and heat shocks or the fat body and hemocyte-specific cg-Gal4 driver (Asha et al., 2003)) did not affect developmental or starvation-induced autophagy in the larval fat body either (Fig. 5c showing sections of fat body cells expressing p35 driven by cg-Gal4, and not shown).

Discussion

Programmed cell death became a popular research field in the last two decades, with many groups showing the important role of this process during normal

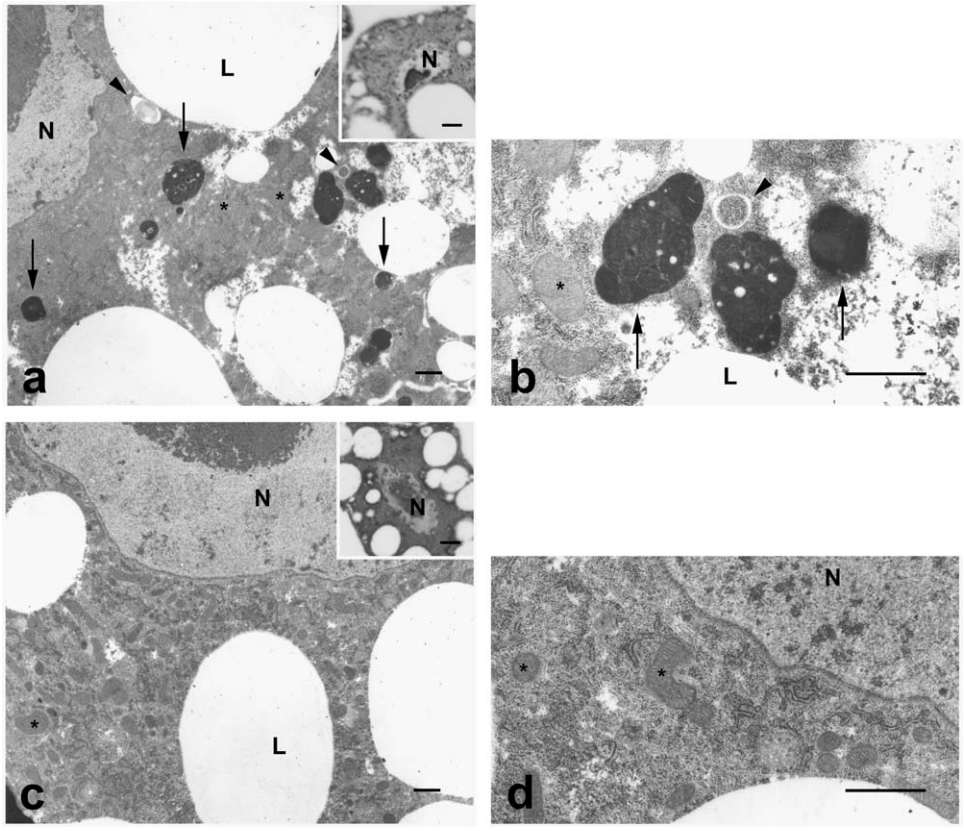


Fig. 3. Expression of the caspase inhibitor p35 does not inhibit Hid-induced autophagy, whereas expression of the hyperactive Ras mutant (V12) does. Expression of the pan-caspase inhibitor p35 in the larval fat body does not interfere with the autophagy-inducing effect of Hid overexpression (a, b is an enlargement of a), whereas expression of the constitutively active Ras mutant (Ras^{V12}) strongly inhibits Hid-induced autophagy (c, d is an enlargement of c). Insets show light microscopic images of the same samples; note the presence of small granules that correspond to Hid-induced autophagic vacuoles in the cytoplasm of the fat body cell expressing p35 (a, inset). These structures are absent from hyperactive Ras-expressing cells (c, inset). Initial (arrowheads) and degrading autophagic vacuoles (arrows), lipid droplets (L), mitochondria (*), and the nucleus (N) are marked. Bars equal 1 μm for electron microscopic and 10 μm for light microscopic images.

development, tumorigenesis, neurodegeneration diseases, and in response to stress stimuli like hypoxia or irradiation (Baehrecke, 2002; Kaufmann and Hengartner, 2001; Yuan et al., 2003). As the morphology and molecular mechanism of the process can be different in case of various research objects, several different terms were suggested to describe the phenomenon (Lockshin and Zakeri, 2002). The two major pathways of programmed cell death are apoptosis and autophagy-type cell death (see Introduction for details). Usually, the apoptotic morphology is caused by the activation of caspases, while autophagic cell death is independent of caspase activity, although exceptions were reported (see Baehrecke, 2002; Lockshin and Zakeri, 2002, 2004 for reviews).

Experimental inhibition of caspase activity can also lead to activation of a different pathway, resulting in the appearance of cells with necrotic morphology (Chautan et al., 1999), or in cells unable to activate caspases to apoptotic stimuli, the activation of the lysosomal system or autophagy can occur (Lockshin and Zakeri, 2004). Interestingly, a recent paper identified caspase-8 as a suppressor of autophagic cell death in L929 fibroblast cells as well as different macrophage lineages (Yu et al., 2004). The in vivo importance of this pathway awaits further characterization, but the fact that caspase-8-deficient cell lines can be established (Varfolomeev et al., 1998) suggests cell type-specific differences again.

Often the features of both apoptosis and autophagy can be observed in the very same cell, like in case of neurodegeneration diseases or dying *Drosophila* salivary glands (Baehrecke, 2002). Inhibition of caspase activity is sufficient to block these cell death events, but autophagy is normally induced in this case also. Unfortunately, at the moment no direct evidence is available about the importance of autophagy in these cases. Transcriptional profiling of salivary gland cell death identified many lysosomal hydrolases that can be involved in the process indeed (Lee et al., 2003; Gorski et al., 2003). Atg8 is a well-known marker of the major

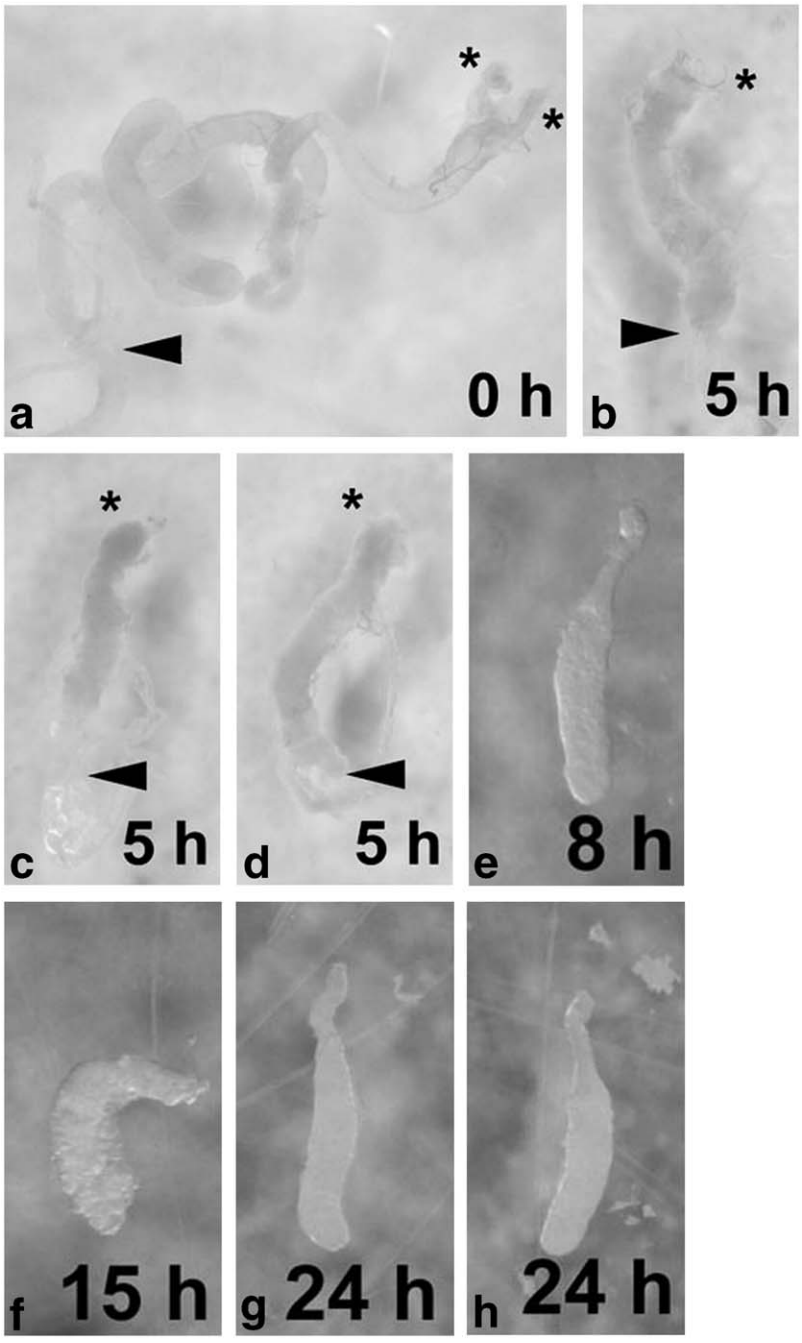


Fig. 4. Mutation of Hid or expression of the caspase inhibitor p35 block salivary gland cell death, but do not affect the destruction of the larval midgut. The scheduled destruction of the larval midgut is characterized by the disappearance of gastric caeca (asterisks in a), and the shortening of the organ (from gastric caeca to the proximal part of Malpighian tubules located between the thicker midgut and thinner hindgut regions [arrowhead in a–d]). The changes are apparent between the time of puparium formation (a) and 5 h after puparium formation (apf) (b). Larval midgut is normally destroyed in Hid mutants (c) and in animals expressing the pan-caspase inhibitor p35 (d) at 5 h apf. Asterisks mark the anterior part of the midgut lacking gastric caeca in (b–d). The larval salivary gland persists through the puparial stage (e), and the histolysis of the organ occurs at 14–16 h apf (f). Destruction of the larval salivary gland is blocked in Hid mutants (g) and in animals expressing p35 (h). Numbers in the bottom right corner refer to the age of the animal apf.

autophagy pathway (Ohsumi, 2001). Its homologs are upregulated during autophagy in starving yeast cells (Klionsky and Emr, 2000) and *Drosophila* larvae (Zinke et al., 2002), as well as in case of developmental autophagy in *Drosophila* larval fat body (manuscript in preparation). However, *Drosophila* homologs of Atg8 were not induced during salivary gland cell death (Lee et al., 2003; Gorski et al., 2003), and transgenic

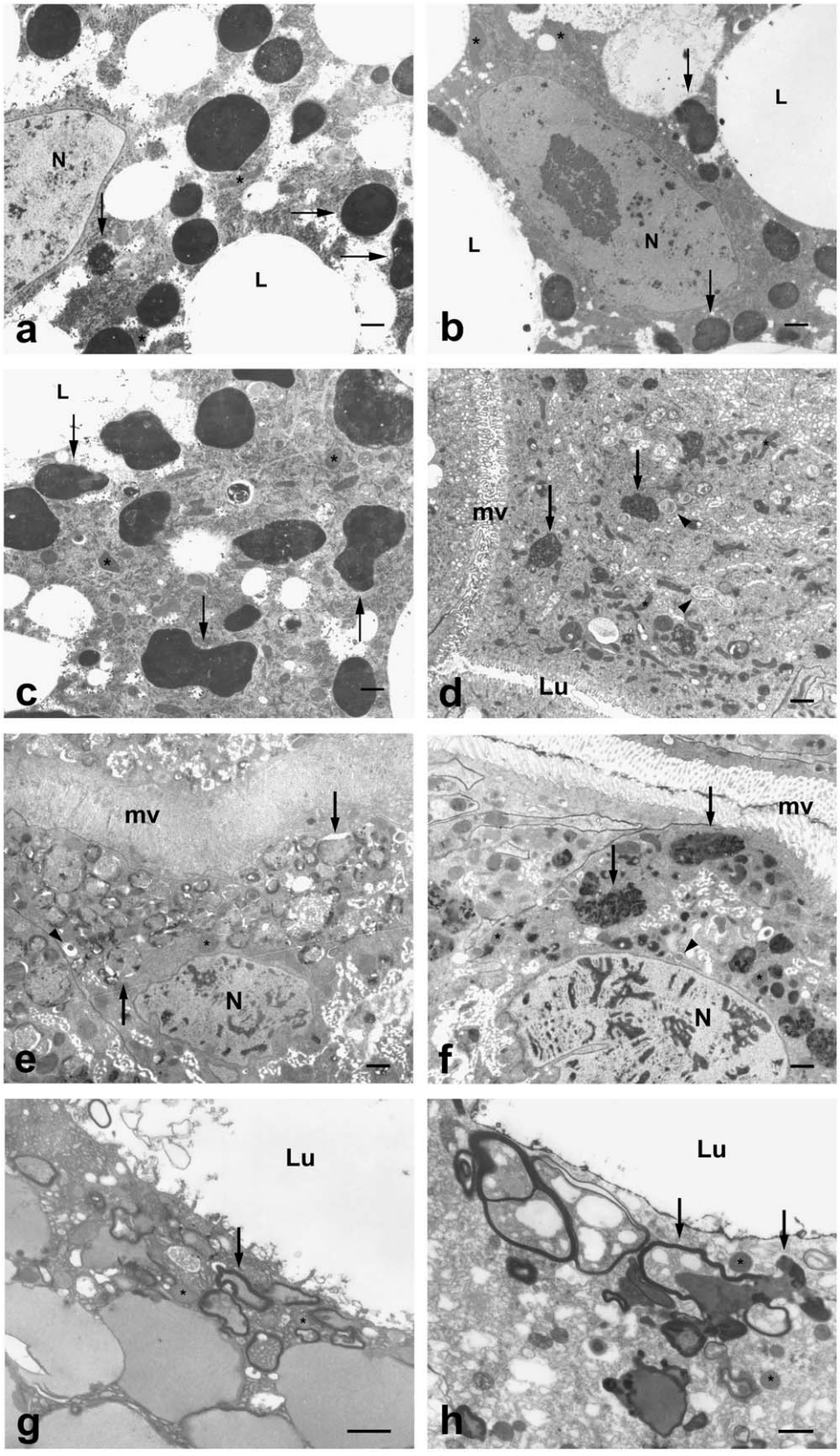
animals carrying a GFP fusion transgene of human Atg8 rarely show GFP-positive structures in dying salivary gland cells (Rusten et al., 2004), questioning the role of the major pathway of autophagy during the destruction of this tissue. Although lysosomal degradation can be readily observed in dying salivary gland cells, as well as in case of Hid mutation or inhibition of caspase activity, it can be due to a different mechanism than the classical pathway of autophagy, like lysosomal wrapping, when lysosomes directly engulf portions of the cytoplasm (see Fig. 5g and h) (Sakai et al., 1989). In other systems, lysosomal hydrolases were also shown to contribute to the activation of caspases and apoptosis (Lockshin and Zakeri, 2004).

To address the complicated question of possibly existing common regulators of apoptosis and autophagy, we tested the effect of many apoptosis-inducing proteins in larval *Drosophila* fat body. These cells proved highly resistant to apoptosis-inducing stimuli, at least before pupariation. Overexpression of p53, Reaper, Grim, Sickle and the caspase Dronc has no effect on these cells. The possible reason for this is that other, perhaps hormonal factors are necessary for them to reach the competence to die, as it was already shown in case of dying salivary gland cells (Lee and Baehrecke, 2001) — an attractive hypothesis that needs further testing. To our surprise, Hid was a very potent inducer of autophagy in larval fat body cells, and also in case of most other larval tissues investigated here.

The apoptosis-inducing ability of Hid was shown to mostly rely on activation of caspases (Grether et al., 1995). In our test, inhibiting caspase activity did not influence the autophagy-inducing ability of Hid in larval fat body, unlike direct inhibition of Hid by elevated Ras signaling.

As the genes Reaper, Hid, Grim and Sickle are usually grouped together on the basis of their shared amino-terminal IAP-interacting motif, it is intriguing that only Hid is capable of inducing autophagy in the larval fat body. One apparent difference is the presence of a homologous GH3 domain in Reaper, Grim and Sickle, that is also able to induce apoptosis but is absent from Hid (Claveria et al., 2002). The expression of these proapoptotic genes usually foreshadows cell death events, except for Hid, which is also expressed in cells not destined to die during development (Bangs et al., 2000). The activity of Hid is modulated by growth factor signaling, acting through the Ras pathway, which can inhibit Hid both transcriptionally and posttranslationally through phosphorylation (Kurada and White, 1998; Bergmann et al., 2002). Thus, cells expressing Hid undergo cell death only in the absence of growth factor signaling. Further differences are also seen with certain gain-of-function mutations of DIAP1. One class of mutations suppresses killing by ectopically expressed Reaper and Grim, but has no effect on killing by Hid. The other class of DIAP1 mutations instead suppresses killing by ectopically expressed Hid, but has no appreciable impact on Reaper or Grim killing (Lisi et al., 2000). Although locating the autophagy-inducing motif inside the Hid protein requires further experiments, this ability clearly reflects previously described differences in sequence, expression and in the ways of inducing apoptosis between Hid and the other three members of this group.

To test the potential involvement of Hid in developmental autophagy, we studied the hypomorphic Hid mutant l(3)05014 (Peterson et al., 2002). Dissection of prepupae revealed that the degeneration of larval midgut tissue occurs normally, but salivary gland cell death is blocked in animals that otherwise normally underwent head eversion, which occurs just before salivary gland cell death. A very recent study using RNA interference to reduce Hid expression similarly reported that downregulation of Hid is able to inhibit salivary gland cell death, but influences midgut degeneration only if it is combined with loss of Reaper expression (Yin and Thummel, 2004). Inhibition of caspases, the major components of apoptosis by constitutive expression of the caspase inhibitor p35 resulted in completely identical phenotypes. This is slightly contradicting with the reports of Jiang et al. (1997), showing that heat shock-mediated expression of p35 is capable of inhibiting midgut cell death. In our system, p35 is expressed at a relatively low level in both salivary gland and midgut cells as assayed by reporter gene analysis (not shown). As salivary gland cell death is completely blocked by this expression level, we conclude that the difference seen in case of midgut might originate from the very high level of p35 combined with possible developmental abnormalities induced by subsequent heat shocks used in the other study. Electron microscopic analysis of larval fat body and larval and prepupal midgut as well as pupal salivary gland cells reveals that developmental autophagy is normally induced in both Hid mutants and p35-expressing animals. Although it is possible that a minor remaining amount of Hid is enough for autophagy, or there is some residual caspase activity in spite of p35 expression, the clear effects on salivary gland cell death and organismal lethality support our hypothesis in both cases. Similarly, in a parallel study, no caspase activity was detected during autophagy in the fat body of the tobacco hornworm (*Manduca sexta*) (Muller et al., 2004). Further support for the different regulation of autophagy and apoptosis is provided by evaluating autophagy in E93 mutants. E93 is a transcription factor that is required for the induction of proapoptotic genes in dying larval tissues. E93 expression foreshadows larval cell death events during metamorphosis (Baehrecke, 2002). However, autophagy is normally induced in fat body and midgut cells of wandering stage E93 null


N
L
a
L
L
N
b
L
c
mv
Lu
d
mv
N
e
mv
N
f
Lu
g
Lu
h

mutant larvae (kindly provided by Eric H. Baehrecke; our unpublished results).

In conclusion, we have shown that although one of the tested apoptosis regulators, i.e. Hid, is a potent inducer of autophagy in larval *Drosophila* tissues, it is most likely not required for developmental autophagy, based on the mutant phenotype. These results can be ascribed to an overexpression artifact, or simply reflect functional redundancy that compensates for the loss of Hid function, as it was shown in case of Hid and Reaper in the degenerating midgut (Yin and Thummel, 2004). Further studies are necessary to address this question. Nevertheless, the autophagy-inducing effect of Hid does not rely on caspase activation, as is the case for developmental autophagy. Thus, the same cell death-inducing stimulus can lead to the markedly different effects of caspase-dependent apoptosis and caspase-independent autophagy, depending on the cell type examined in the experiments even in the same animal.

Acknowledgements

We would like to thank our colleagues listed in the Materials and methods section for providing fly strains. We also thank Emese Léder, Sarolta Pálfia, Mariann Saródy and Károlyné Válóczy for excellent technical assistance. This work was supported by the Hungarian Ministry of Education under Grant MEDICHEM 1/047 NKFP provided to M. Sass.

References

Aravind, L., Dixit, V.M., Koonin, E.V., 2001. Apoptotic molecular machinery: vastly increased complexity in vertebrates revealed by genome comparisons. Science 291, 1279–1284.

Asha, H., Nagy, I., Kovacs, G., Stetson, D., Ando, I., Dearolf, C.R., 2003. Analysis of Ras-induced overproliferation in *Drosophila* hemocytes. Genetics 163, 203–215.

Baehrecke, E.H., 2002. How death shapes life during development. Nat. Rev. Mol. Cell Biol. 3, 779–787.

Bangs, P., Franc, N., White, K., 2000. Molecular mechanisms of cell death and phagocytosis in *Drosophila*. Cell Death Differ. 7, 1027–1034.

Bergmann, A., Tugentman, M., Shilo, B.Z., Steller, H., 2002. Regulation of cell number by MAPK-dependent control of apoptosis: a mechanism for trophic survival signaling. Dev. Cell 2, 159–170.

Butterworth, F.M., Forrest, E.C., 1984. Ultrastructure of the preparative phase of cell death in the larval fat body of *Drosophila melanogaster*. Tissue Cell 16, 237–250.

Chautan, M., Chazal, G., Cecconi, F., Gruss, P., Golstein, P., 1999. Interdigital cell death can occur through a necrotic and caspase-independent pathway. Curr. Biol. 9, 967–970.

Claveria, C., Caminero, E., Martinez-Arias, C., Campuzano, S., Torres, M., 2002. GH3, a novel proapoptotic domain in *Drosophila* Grim, promotes a mitochondrial death pathway. EMBO J. 21, 3327–3336.

Gorski, S.M., Chittaranjan, S., Pleasance, E.D., Freeman, J.D., Anderson, C.L., Varhol, R.J., Coughlin, S.M., Zuyderduyn, S.D., Jones, S.J., Marra, M.A., 2003. A SAGE approach to discovery of genes involved in autophagic cell death. Curr. Biol. 13, 358–363.

Gozuacik, D., Kimchi, A., 2004. Autophagy as a cell death and tumor suppressor mechanism. Oncogene 23, 2891–2906.

Grether, M.E., Abrams, J.M., Agapite, J., White, K., Steller, H., 1995. The head involution defective gene of *Drosophila melanogaster* functions in programmed cell death. Genes Dev. 9, 1694–1708.

Hay, B.A., Wolff, T., Rubin, G.M., 1994. Expression of baculovirus P35 prevents cell death in *Drosophila*. Development 120, 2121–2129.

Hay, B.A., Wassarman, D.A., Rubin, G.M., 1995. *Drosophila* homologs of baculovirus inhibitor of apoptosis proteins function to block cell death. Cell 83, 1253–1262.

Horvitz, H.R., 2001. Genetic control of programmed cell death in *C. elegans*. Sci. World J. 1 (Suppl. 3), 137.

Jiang, C., Baehrecke, E.H., Thummel, C.S., 1997. Steroid regulated programmed cell death during *Drosophila* metamorphosis. Development 124, 4673–4683.

Kaufmann, S.H., Hengartner, M.O., 2001. Programmed cell death: alive and well in the new millennium. Trends Cell Biol. 11, 526–534.

Klionsky, D.J., Emr, S.D., 2000. Autophagy as a regulated pathway of cellular degradation. Science 290, 1717–1721.

Kurada, P., White, K., 1998. Ras promotes cell survival in *Drosophila* by downregulating hid expression. Cell 95, 319–329.

Lee, C.Y., Baehrecke, E.H., 2001. Steroid regulation of autophagic programmed cell death during development. Development 128, 1443–1455.

Lee, C.Y., Clough, E.A., Yellon, P., Teslovich, T.M., Stephan, D.A., Baehrecke, E.H., 2003. Genome-wide analyses of

Fig. 5. Developmental autophagy is not affected by mutation of Hid or expression of the caspase inhibitor p35. Developmental autophagy is induced in the larval fat body during the wandering period of the last larval stage (a) (compare to Fig. 1a). In Hid mutants (b), and in animals expressing the pan-caspase inhibitor p35 (c), degrading autophagic vacuoles (arrows) are also obvious. The strong induction of autophagy is observed in degenerating larval midgut cells, shown here in wild-type control animals at 5 h after puparium formation (apf) (d). Similarly, many autophagic structures appear in midgut cells of the Hid mutant (e) and the pan-caspase inhibitor p35-expressing animals (f) of the same age. Persisting salivary gland cells in Hid mutant (g) and p35-expressing animals (h) also exhibit signs of lysosomal degradation at 24 h apf. Lipid droplets (L), lumen (Lu), microvilli (mv), mitochondria (*), and nuclei (N) are marked, arrows point to degrading autophagic vacuoles, arrowheads mark double-membrane layered initial autophagic vacuoles. Bars equal 1 μm.

steroid- and radiation-triggered programmed cell death in *Drosophila*. Curr. Biol. 13, 350–357.

Lisi, S., Mazzon, I., White, K., 2000. Diverse domains of THREAD/DIAP1 are required to inhibit apoptosis induced by REAPER and HID in *Drosophila*. Genetics 154, 669–678.

Lockshin, R.A., Zakeri, Z., 2002. Caspase-independent cell deaths. Curr. Opin. Cell Biol. 14, 727–733.

Lockshin, R.A., Zakeri, Z., 2004. Caspase-independent cell death? Oncogene 23, 2766–2773.

Muller, F., Adori, C., Sass, M., 2004. Autophagic and apoptotic features during programmed cell death in the fat body of the tobacco hornworm (*Manduca sexta*). Eur. J. Cell Biol. 83, 67–78.

Neufeld, T.P., 2003. Role of autophagy in developmental cell growth and death: insights from *Drosophila*. In: Klionsky, D.J. (Ed.), Autophagy. Landes Bioscience, Georgetown, TX, pp. 224–232.

Ohsumi, Y., 2001. Molecular dissection of autophagy: two ubiquitin-like systems. Nat. Rev. Mol. Cell Biol. 2, 211–216.

Palaga, T., Osborne, B., 2002. The 3D's of apoptosis: death, degradation and DIAPs. Nat. Cell Biol. 4, E149–E151.

Peterson, C., Carney, G.E., Taylor, B.J., White, K., 2002. Reaper is required for neuroblast apoptosis during *Drosophila* development. Development 129, 1467–1476.

Rusten, T.E., Lindmo, K., Juhasz, G., Sass, M., Seglen, P.O., Brech, A., Stenmark, H., 2004. Programmed autophagy in the *Drosophila* fat body is induced by ecdysone and effected through the PI3K pathway. Dev. Cell 7, 179–192.

Sakai, M., Araki, N., Ogawa, K., 1989. Lysosomal movements during heterophagy and autophagy: with special reference to nematolysosome and wrapping lysosome. J. Electron Microsc. Tech. 12, 101–131.

Sass, M., Kovacs, J., 1975. Ecdysterone and an analogue of juvenile hormone on the autophagy in the cells of fat body of *Mamestra brassicae*. Acta Biol. 26, 189–196.

Varfolomeev, E.E., Schuchmann, M., Luria, V., Chiannilkulchai, N., Beckmann, J.S., Mett, I.L., Rebrikov, D., Brodianski, V.M., Kemper, O.C., Kollet, O., Lapidot, T., Soffer, D., Sobe, T., Avraham, K.B., Goncharov, T., Holtmann, H., Lonai, P., Wallach, D., 1998. Targeted disruption of the mouse caspase 8 gene ablates cell death induction by the TNF receptors, Fas/Apo1, and DR3 and is lethal prenatally. Immunity 9, 267–276.

Yin, V.P., Thummel, C.S., 2004. A balance between the diap1 death inhibitor and reaper and hid death inducers controls steroid-triggered cell death in *Drosophila*. Proc. Natl. Acad. Sci. USA 101, 8022–8027.

Yu, L., Alva, A., Su, H., Dutt, P., Freundt, E., Welsh, S., Baehrecke, E.H., Lenardo, M.J., 2004. Regulation of an ATG7-beclin 1 program of autophagic cell death by caspase-8. Science 304, 1500–1502.

Yuan, J., Lipinski, M., Degterev, A., 2003. Diversity in the mechanisms of neuronal cell death. Neuron 40, 401–413.

Zinke, I., Schutz, C.S., Katzenberger, J.D., Bauer, M., Pankratz, M.J., 2002. Nutrient control of gene expression in *Drosophila*: microarray analysis of starvation and sugar-dependent response. EMBO J. 21, 6162–6173.

Development ePress online publication date 15 March 2006

dc_840_14

Development 133, 1457-1465 (2006) doi:10.1242/dev.02332

Autophagy occurs upstream or parallel to the apoptosome during histolytic cell death

Fatih Akdemir[1], Robert Farkaš[2], Po Chen[1], Gabor Juhasz[3], Lucia Medved'ová[2,4], Miklos Sass[5], Lai Wang[6], Xiaodong Wang[6], Suganthi Chittaranjan[7], Sharon M. Gorski[7], Antony Rodriguez[8] and John M. Abrams[1,*]

Histolysis refers to a widespread disintegration of tissues that is morphologically distinct from apoptosis and often associated with the stimulation of autophagy. Here, we establish that a component of the apoptosome, and pivotal regulator of apoptosis, is also required for histolytic cell death. Using in vivo and ex vivo assays, we demonstrate a global apoptogenic requirement for *dark*, the fly ortholog of Apaf1, and show that a required focus of *dark*$^{-}$ organismal lethality maps to the central nervous system. We further demonstrate that the Dark protein itself is a caspase substrate and find that alterations of this cleavage site produced the first hypermorphic point mutation within the Apaf1/Ced-4 gene family. In a model of 'autophagic cell death', *dark* was essential for histolysis but dispensable for characteristic features of the autophagic program, indicating that the induction of autophagy occurs upstream or parallel to histolytic cell death. These results demonstrate that stimulation of autophagy per se is not a 'killing event' and, at the same time, establish that common effector pathways, regulated by the apoptosome, can underlie morphologically distinct forms of programmed cell death.

KEY WORDS: Autophagy, Apoptosis, *Drosophila*, Histolysis, *dark*

INTRODUCTION

Apical and effector caspases lie at the core of the apoptotic program (Danial and Korsmeyer, 2004). Upon interaction with adaptor molecules, apical caspases are stimulated to activate effector caspases by proteolysis. *dark*, the *Drosophila* homolog of nematode Ced-4 and mammalian Apaf1, is thought to regulate the apical caspase *Dronc* (*Nc* – FlyBase), through interactions involving respective caspase recruitment domains (CARD) (reviewed by Mills et al., 2005). As in mammalian systems, fly caspases are also subject to negative regulation by IAP proteins (Danial and Korsmeyer, 2004), and, among *Drosophila* members of this family, Diap1 (Thread – FlyBase) is known to exert important control over apoptosis (Goyal, 2001; Wang et al., 1999). This protein binds *Dronc* and the effector caspase *Drice* (*Ice* – FlyBase), inhibiting the activity of each via multiple mechanisms (Ditzel et al., 2003; Hays et al., 2002; Martin, 2002; Meier et al., 2000; Ryoo et al., 2002; Wilson et al., 2002; Wing et al., 2002b). Diap1 itself is under tight regulation and is effectively antagonized by proapoptotic proteins [*reaper* (*rpr*), *grim*, *hid* (also known as *Wrinkled*) and *skl*] encoded in the *reaper* region (Chai et al., 2003; Christich et al., 2002; Silke et al., 2004; Wing et al., 2002a; Wing et al., 2002b; Wing et al., 2001; Wu et al., 2001; Yoo et al., 2002; Zachariou et al., 2003). Together, these linked genes specify virtually all programmed cell death (PCD) in the fly embryo, as the combined deletion of these eliminates PCD at this stage (Abrams, 1999).

Three broadly conserved protein families, represented by Ced-9/Bcl2, Ced-4/Apaf1 and Ced-3/Caspase 9, define fundamental components in pathways of caspase control. However, a unified mechanism for their action in cell death remains elusive, as analogous physical interactions seen between nematode Ced-9 and Ced-4 do not occur among orthologous mammalian counterparts (Moriishi et al., 1999). Instead, mammalian Bcl2 proteins indirectly engage Apaf1 by controlling the mitochondrial release of cytochrome c, which promotes the formation of a multimeric complex referred to as the apoptosome (Danial and Korsmeyer, 2004; Spierings et al., 2005). Although the fly counterparts of these genes add provocative clues, particularly with respect to the negative regulators of caspase activity (Salvesen and Abrams, 2004), they also complicate the picture, as cytochrome c appears dispensable for *Drosophila* Apaf1 (*Dark*)-dependent cell death, despite the conservation of a WD domain thought to be necessary for cytochrome c binding and regulation (Adrain et al., 1999; Dorstyn et al., 2004; Hu et al., 1998; Rodriguez et al., 1999; Zimmermann et al., 2002). Previous data from us, and from others, on viable hypomorphic alleles (Kanuka et al., 1999; Rodriguez et al., 1999; Zhou et al., 1999) have established that *Dark* shares functional properties with its counterparts in *C. elegans*, where Ced-4 is required for all PCD, and in the mouse, where context-specific apoptogenic requirements for Apaf1 are seen. However, central questions, approachable only with a null allele, remained open.

Here, we isolate a single-gene null mutation at *dark* and demonstrate a general requirement for this gene in PCD and stress-induced apoptosis. The role for *dark* in PCD was not absolute, however, as rare cell deaths were observed. We show that a required focus of *dark*$^{-}$ organismal lethality maps to the central nervous system and also describe the first hypermorphic allele within the Apaf1/Ced-4 gene family. In a model of tissue histolysis, *dark* was essential for cell death but dispensable for characteristic features of the autophagic program, indicating that the stimulation of autophagy

[1]Department of Cell Biology, UT Southwestern Medical Center, Dallas, TX 75390, USA. [2]Institute of Experimental Endocrinology, Slovak Academy of Sciences, Vlarska 3, 83306 Bratislava–Kramare, Slovakia. [3]Department of Genetics, Cell Biology and Development, University of Minnesota, 6-160 Jackson Hall, 321 Church Street SE, Minneapolis, MN 55455, USA. [4]Department of Genetics, Faculty of Science, Comenius University, 84215 Bratislava, Slovakia. [5]Department of General Zoology, Lorand Eotvos University, Pazmany setany 1/C, H-1117 Budapest, Hungary. [6]Department of Biochemistry, UT Southwestern Medical Center, Dallas, TX 75390, USA. [7]Genome Sciences Centre, BC Cancer Research Centre, 675 West 10th Avenue, Vancouver, BC V5Z 1L3, Canada. [8]Wellcome Trust, Sanger Institute, Genome Campus, Cambridge CB10 1SA, UK.

*Author for correspondence (e-mail: John.Abrams@utsouthwestern.edu)

Accepted 17 February 2006

per se is not the mechanism of cell killing but lies upstream, or parallel to *dark*. These data establish that common effector pathways, regulated by the apoptosome, specify apoptotic and histolytic forms of PCD.

MATERIALS AND METHODS

Mutagenesis

To isolate deletions that eliminate *dark* without compromising the function of adjacent neighboring genes, a P insertion associated with $dark^{CD4}$ (Rodriguez et al., 1999) was remobilized and candidates were tested in trans to existing alleles and against lethal mutations in flanking genes. Promising 'hits' were screened by PCR. $dark^{82}$ failed to complement $dark^{CD4}$, but complements adjacent lethal alleles in the neighboring genes, RhoGEF and a new lethal P mutation in CG8963 that we fortuitously obtained in our first round of mutagenesis. Genomic PCR across the deletion junction and RT-PCR were used to validate the mutation and define the $dark^{82}$ lesion. *yw* was the parental wild-type strain for molecular analysis and for ex vivo hemocyte studies. RNA extraction and QRT-PCR were conducted as described by Gorski et al. (Gorski et al., 2003). Ages at 25°C were normalized from 18°C (Park et al., 1996). Genomic PCR and RT-PCR were performed as described by Chew et al. (Chew et al., 2004), with relevant gene-specific primers.

Transgenic 'rescue' and genetic manipulation

Full-length *dark* with 8×His-tags at the N terminus and 3×Myc-tags at the C terminus was cloned into the *Bam*HI/*Xho*I sites of the pFastBac1 vector (Invitrogen). The *Bam*HI/*Xho*I insert was then subcloned into the pUAST vector to produce pUAST-$dark^{WT}$. pUAST-$dark^{V}$ was generated by changing Aspartate 1292 to Alanine using a QuikChange Site-Directed Mutagenesis Kit (Stratagene). The pUAST constructs were injected into fly embryos following standard procedures to obtain transformants. Independent transgenic lines were mapped and crossed to the $dark^{82}$ background. For rescue experiments, $dark^{82}$*/CyO, actin-GFP;UAS-*$dark^{WT}$ or $dark^{82}$*/CyO, actin-GFP;UAS-*$dark^{V}$ flies were crossed to $dark^{82}$*/CyO, actin-GFP; Tub-Gal4/TM3, Sb* flies (or other drivers). The number of homozygous $dark^{82}$*; UAS-dark/Tub-Gal4* progeny and number of heterozygous $dark^{82}$*/CyO, actin-GFP; UAS-dark/Tub-Gal4* progeny were counted. The percent of rescue was calculated by dividing the number of rescued $dark^{82}$ homozygotes by the Mendelian value expected if $dark^{82}$ homozygotes were fully viable. Similar crosses were used to obtain $dark^{82}$*; UAS-dark/Hml-Gal4* L3 larvae for hemocyte isolation. *c81-Gal4, c833-Gal4* and *Hml-Gal4* strains (Drapeau et al., 2003; Goto et al., 2003; Hrdlicka et al., 2002; Manseau et al., 1997) were obtained from the Bloomington Stock Center.

Germline clones and AO staining

The $dark^{82}$ allele was recombined onto the $FRT^{2R\text{-}G13}$ chromosome. To generate $dark^{82}$ maternal-null embryos, the Dominant Female Sterile (DFS) technique was used, as described previously (Chou and Perrimon, 1996). *hs-Flp/+; OvoD* $FRT^{2R\text{-}G13}$/$dark^{82}$ $FRT^{2R\text{-}G13}$ females were crossed with $dark^{82}$*/CyO, actin-GFP* males to generate maternal and zygotic *dark*-null embryos. To detect cell death, Acridine Orange (AO) staining was carried out (Abrams et al., 1993).

Ex vivo hemocyte analyses

Wandering L3 instar larvae were prepared as described by Chew et al. (Chew et al., 2004), with the following modifications. Hemolymph was collected from six larvae and agents were added after media addition. Membrane blebbing, a characteristic feature of apoptosis, was used to quantify apoptosis. At ~6 hours post-treatment, cells were stained with a fluorescent membrane dye, 10 uM CellTracker (Molecular Probes) in DMSO, to facilitate the visualization of apoptotic membrane blebbing (without fluorescent labeling it was difficult to assess membrane blebbing owing to the phagocytic nature of hemocytes).

Immunohistochemistry and western blotting

Immunohistochemistry on dissected salivary glands was conducted as described by Farkas and Mechler (Farkas and Mechler, 2000). For actin counterstaining, fluorescein-conjugated phalloidin (1:200; Molecular Probes), or AlexaFluor488-Phalloidin or AlexaFluor546-Phalloidin (Molecular Probes) was used; for nuclear counterstaining, 0.5 μg/ml Hoechst 33258 (Calbiochem) or 1 μg/ml OliGreen (Molecular Probes); and for caspase activity, rabbit anti-cleaved caspase-3 antibody (1:500; Cell Signaling Technology). Optical sections (0.5 μm thick) were collected using a Zeiss LSM-510 Meta laser confocal microscope equipped with a 40× planapochromat oil objective. Recombinant Dark protein was prepared as described previously (Yu et al., 2005). Transgenic Dark protein was detected in extracts from adult heads, with an anti-Myc antibody at a dilution of 1:2000. Anti-Dark polyclonal antibody was used at a dilution of 1:3000.

Electron microscopy

Samples were prepared and processed for electron microscopy as described previously (Juhasz and Sass, 2005).

Visualization of MDC and GFP-LC3

Transgenic flies containing UAS-GFP-LC3 were kindly provided by the Harald Stenmark Laboratory (Rusten et al., 2004) and crossed to flies containing the salivary gland driver D59-Gal4 (Gustafson and Boulianne, 1996) (kindly provided by Carl Thummel). Salivary glands of the progeny were dissected in *Drosophila* Schneider's medium (Invitrogen) and transferred to the same medium with MDC (0.1 mM) for 30 minutes at room temperature. Samples were then rinsed once and mounted (both in Schneider's medium). Salivary glands were analyzed by fluorescence microscopy using a Zeiss Axioplan 2 microscope.

RESULTS

$dark^{82}$ is null allele

To investigate the molecular genetic properties of the *Drosophila* apoptosome, and to illuminate possible 'non-death' roles for the *dark* gene in development, we recovered a null mutation at *dark* in a screen for excision derivatives of an existing P insertion (Rodriguez et al., 1999). $dark^{82}$ is a 6.3-kb deletion spanning the entire open-reading frame and nearly the entire transcription unit (Fig. 1A-C). Animals homozygous for this allele arrest as late pupae and often present a characteristic dark blister located centrally along the midline. The mutation fails to complement all existing hypomorphic *dark* alleles, but complements flanking genes (see Materials and

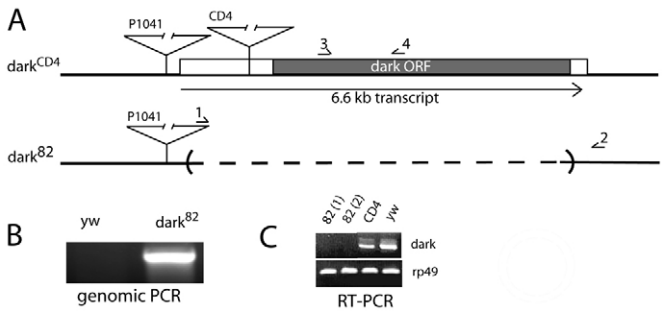


Fig. 1. Generation of a $dark^{82}$ null mutation. (**A**) Schematized view of the genomic structure of the *dark* locus, relevant alleles and the $dark^{82}$ null mutation. The *dark* transcript spans 6.6 kb. $dark^{82}$ is a 6324 bp deletion (dashed line) generated by imprecise excision of the indicated P-element in the $dark^{CD4}$ strain (Rodriguez et al., 1999). The allele was mapped by sequencing a 1.3 kb genomic PCR fragment (see **B**) using a primer pair (designated 1 and 2) spanning the junctional interval. In $dark^{82}$, sequences from –1277 bp (upstream of the translation start codon) to 19 bp downstream of the stop codon are absent such that the entire *dark* ORF and part of the untranslated first exon are missing. Note that 396 bp of sequence from the CD4 transposon remain at this junction. (**C**) RT-PCR with primer pair 3 and 4, using total RNA from prepupae, confirms complete loss of the *dark* transcript in the $dark^{82}$ allele. Two different isolates of $dark^{82}$ from the screen were assayed here, 82 (1) and 82 (2). rp49 is a control.

DEVELOPMENT

Table 1. Tissue-specific rescue by wild-type *dark* and a hypermorphic allele

	Driver	Percentage of rescued $dark^{82}$ homozygous flies
UAS-$dark^{WT}$.H4	No	0% (27)
UAS-$dark^{WT}$.B6	No	0% (24)
UAS-$dark^{V}$.C8	No	33% (18)
UAS-$dark^{V}$.G6	No	23% (30)
UAS-$dark^{WT}$.H4	Tubulin-Gal4	100% (27)
UAS-$dark^{WT}$.B6	Tubulin-Gal4	95% (38)
UAS-$dark^{V}$.C8	Tubulin-Gal4	92% (25)
UAS-$dark^{V}$.G6	Tubulin-Gal4	97% (30)
UAS-$dark^{WT}$.H4	Dal-Gal4	100% (34)
UAS-$dark^{WT}$.B6	Dal-Gal4	96% (25)
UAS-$dark^{V}$.C8	Dal-Gal4	103% (35)
UAS-$dark^{V}$.G6	Dal-Gal4	95% (29)
UAS-$dark^{WT}$.H4	Hml-Gal4	0% (22)
UAS-$dark^{WT}$.B6	Hml-Gal4	0% (33)
UAS-$dark^{V}$.C8	Hml-Gal4	29% (35)
UAS-$dark^{V}$.G6	Hml-Gal4	18% (29)
UAS-$dark^{WT}$.H4	pCNS-Gal4 (c81)	16% (62)
UAS-$dark^{WT}$.B6	pCNS-Gal4 (c81)	18% (80)
UAS-$dark^{WT}$.H4	c833-Gal4	0% (23)
UAS-$dark^{WT}$.B6	c833-Gal4	0% (25)

Data from transgenic rescue experiments is summarized. Reversal of $dark^{82}$ lethality was scored in contexts where tissue-specific expression of a wild-type transgene (UAS-$dark^{WT}$) or a *dark* variant transgene (UAS-$dark^{V}$) were tested. The left-hand column indicates the transgene tested in combination with the tissue 'driver' listed in the middle column. In each case, a single dose of the *dark* transgene and driver are tested. The right-hand column indicates the percentage of rescued animals relative to the expected Mendelian value, listed in parentheses. Note that, for each transgene, at least two independent lines were tested (H4 and B6 for UAS-$dark^{WT}$, and C8 and G6 for UAS-$dark^{V}$). $dark^{82}$ lethality is fully rescued if UAS-$dark^{WT}$ is driven by Tubulin-Gal4 or by Dal-Gal4, which both confer ubiquitous expression. By contrast, no rescue is observed if UAS-$dark^{WT}$ is combined with an embryonic CNS/larval disc driver (c833-Gal4) or a hemocyte-specific driver (Hml-Gal4). However, substantial rescue of $dark^{82}$ lethality occurs when expression of UAS-$dark^{WT}$ is restored in the post-embryonic CNS using the pCNS-Gal4 driver, also called c81-Gal4 and expressed diffusely throughout brain lobes, but not in embryos, egg chambers or imaginal discs (Drapeau et al., 2003; Manseau et al., 1997). Surprisingly, in the absence of any Gal4 driver, 'leaky' expression of $dark^{V}$ partially rescued $dark^{82}$ lethality, but wild-type *dark* did not.

methods). Homozygous $dark^{82}$ animals were rescued to viability using a transgene containing a full-length *dark* cDNA (see Table 1). Hence, $dark^{82}$ is a lethal, single-gene null mutation.

Elimination of maternal and zygotic *dark*

Because animals homozygous for $dark^{82}$ survive to pupation, we used the Dominant Female Sterile technique to examine the phenotypes of animals lacking maternally supplied *dark* (see Materials and methods). We found normal PCD patterns in embryos that retained zygotic, but lacked maternal, *dark* (Fig. 2A,B). By contrast, embryos devoid of both maternal and zygotic *dark* were almost entirely cell death defective, with rare cell deaths noticeable in later-staged animals (Fig. 2C,D). These observations demonstrate a global need for *dark* in PCD. However, the requirement is not absolute, as occasional apoptotic cell deaths did occur in the complete absence of *dark* function. Embryos lacking maternal and zygotic *dark* failed to hatch and were also defective for head involution, similar to cell-death defective mutations in the *Reaper* region (Grether et al., 1995; White et al., 1994) and *dronc* (Chew et al., 2004). At the same time, gastrulation, segmental patterning and extension of the germ band appeared grossly normal in the absence of *dark*. Hence, to the extent that these events involve migration and/or movement, we note that the proposed role for *dark* in cell motility evidently does not generalize to these morphogenic processes (Geisbrecht and Montell, 2004). We also tested larval

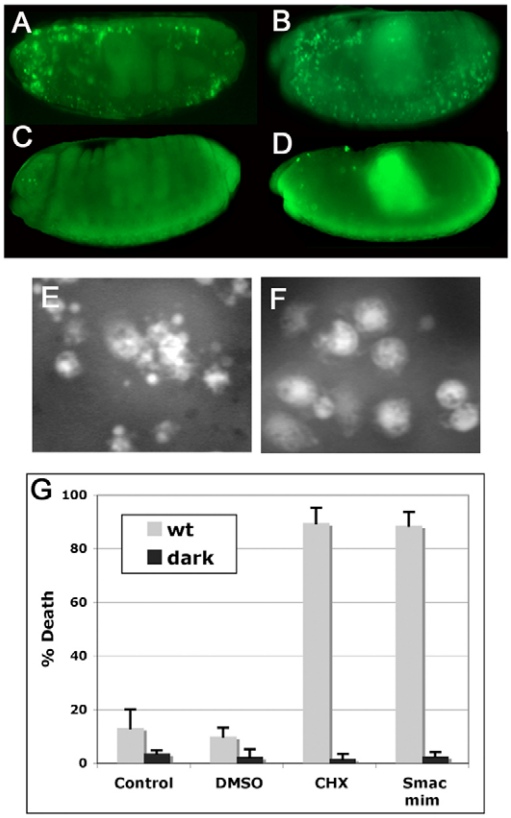


Fig. 2. *dark* is essential for programmed and unprogrammed apoptosis. (**A-D**) Maternal and zygotic sources of *dark* were removed using a Dominant Female Sterile strategy (see Materials and methods). The resulting embryos lacked nearly all PCD, shown here by Acridine Orange (AO) staining (green). A and B show mid-staged embryos eliminated for maternal *dark* but heterozygous for zygotic *dark*; C and D show comparably staged embryos lacking both maternal and zygotic *dark*. Note that without a source of *dark*, embryos are head involution defective with only few AO-positive cells (C,D). (**E-G**) Requirement for *dark* in models of stress-induced cell death. Hemocyte aspirates from $dark^{82}$ and wild-type (wt) wandering third instar larvae were treated with chemical stressors ex vivo and stained with CellTracker (see Materials and methods). Induction of apoptosis in wild-type (E) but not $dark^{82}$ (F) hemocytes is exemplified here with micrographs taken 6 hours after Cycloheximide (CHX) treatment. (G) Quantification of apoptosis 6 hours after challenge with either CHX or a Smac mimetic (Li et al., 2004) are plotted as the incidence of cell death in percentages. Error bars indicate s.d.

hemocytes in ex vivo models of stress-induced cell killing (Fig. 2E-G). In contrast to wild-type counterparts, $dark^{-}$ hemocytes were completely resistant to a Smac mimetic, which antagonizes inhibitor of apoptosis proteins (IAPs) and is thought to simulate the action of *reaper* proteins (Li et al., 2004; Salvesen and Abrams, 2004). Likewise, $dark^{-}$ cells were completely insensitive to the apoptogenic effects of cycloheximide, a protein synthesis inhibitor. Together, these data establish a central role for the action of *dark* in programmed and unprogrammed apoptosis.

Tissue-specific restoration in the CNS reverses $dark^{-}$ lethality

To confirm and extend these studies, we restored *dark* using a transgene (designated UAS-$dark^{WT}$) that places a full-length cDNA under the control of the yeast-derived UAS promoter, which permits

dc_840_14

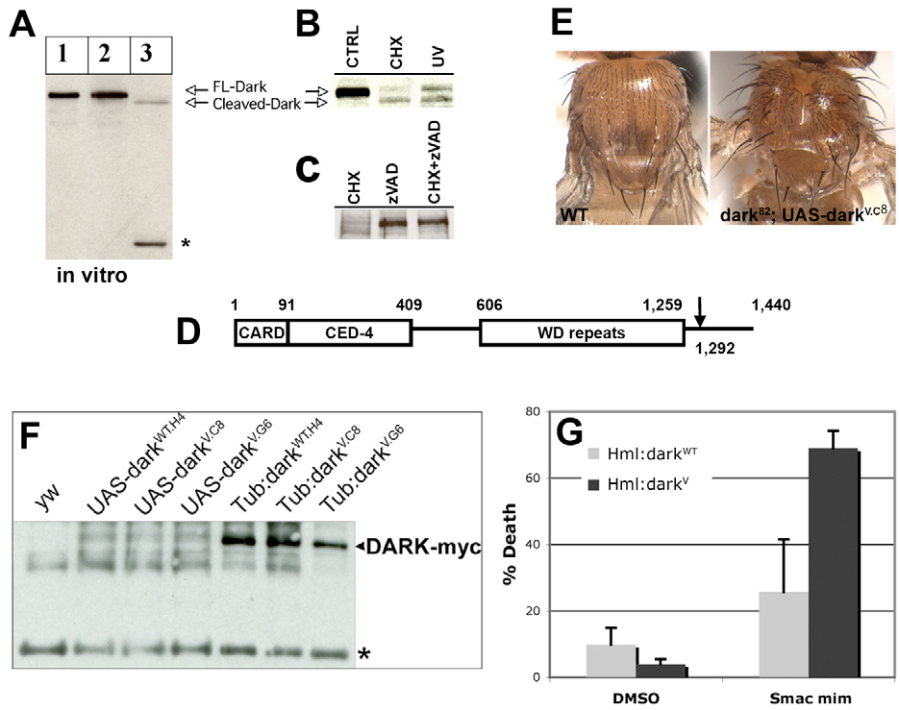


Fig. 3. Alteration of a caspase cleavage site produces a hypermorphic Dark variant. (**A**) Recombinant Dark protein (lane 1) was incubated with cytosolic S20 fractions prepared from control S2 cells (lane 2) or cycloheximide (CHX)-treated S2 cells (lane 3). Asterisk denotes the small Dark C-terminal fragment after cleavage. (**B**) Consistent with in vitro studies (A), stimulus-dependent cleavage of Dark is detected here in *Drosophila* S2 cells. Samples from unchallenged (Ctrl) S2 cells or cells treated with 20 μM Cycloheximide (CHX) or 200 mJ/cm^2 UV were harvested after 4 hours. (**C**) Cleavage of Dark as seen in panel B with CHX treatment, is reversed by the caspase inhibitor z-VAD (100 μM), shown here 5 hours post-treatment. In A,B and C, Dark was visualized with an anti-Dark polyclonal antibody. (**D**) The cleavage site, detected in vitro at residue 1292, is shown (arrow) in the schematized domain structure of the Dark protein. (**E**) Illustration of the defective anatomy of *dark*^{82} flies rescued by leaky expression of UAS-dark^{V}, which mutates the caspase site mapped in D. The notum of a *dark*^{82} homozygote rescued to viability by UAS-dark^{V}, shown here next to a wild-type fly notum (left), exhibits a 'split thorax' phenotype and bristle abnormalities. (**F**) Levels of transgenic Dark protein in various UAS-dark transgenic lines in the absence of any driver or under Tubulin-Gal4 were examined by immunoblot using an anti-Myc antibody. Arrowhead denotes Dark-myc; asterisk indicates an irrelevant cross-reacting band showing equal loading on each lane. Note that the levels of wild-type Dark and Dark^{V} are comparable when expressed from the Tubulin-Gal4 driver or when examined for basal expression. (**G**) Hemocyte aspirates from dark^{82}; Hml-Gal4:UAS-dark^{WT} (Hml:dark^{WT}) and dark^{82}; Hml-Gal4:UAS-dark^{V} (Hml:dark^{V}) L3 larvae were treated with DMSO or the Smac mimetic (Li et al., 2004), a potent apoptotic inducer. Expression of UAS-dark^{WT} in dark^{82} hemocytes only mildly restored apoptosis after Smac mimetic treatment. However, UAS-dark^{V} almost completely restored this apoptotic response to dark^{82} hemocytes.

conditional expression when combined with tissue-specific Gal4-driver strains. Table 1 shows that, in two independently transformed lines, ubiquitous expression of wild-type *dark*, using either Tubulin-Gal4 or Daughterless-Gal4 drivers, completely rescued *dark*^{82} lethality. In parallel studies, the expression of UAS-dark^{WT} in mutant hemocytes (via the Hml-Gal4 driver) did not rescue viability, but did partially restore sensitivity to Smac mimetic killing to these cells (Fig. 3G). Surprisingly, exclusive restoration of *dark* to the post-embryonic central nervous system using pCNS-Gal4 (also called c81-Gal4) reversed *dark*^{82} lethality, but restoration of *dark* to the embryonic CNS and imaginal discs (c833-Gal4 driver) did not. Although we cannot exclude the possibility that maternal *dark* is depleted in the CNS earlier than in other tissues, these results demonstrate that, at minimum, expression of *dark* in the post-embryonic CNS is necessary to reverse organismal lethality and to produce a viable adult. We also note here that male and female adults rescued by pCNS-Gal4 driven *dark* were sterile. However, in DAPI-stained preparations, no associated defects in germ line formation were detected at the gross morphological level.

A caspase cleavage site in Dark confers hypermorphic gene activity when mutated

Exploratory in vitro studies with recombinant Dark identified a putative caspase cleavage site that was mapped to Asp1292 (Fig. 3A,D). Consistent with this, studies using *Drosophila* S2 cells detected a cleavage of Dark that matched predictions from in vitro studies (Fig. 3B) and was caspase dependent, as it was prevented by the caspase inhibitor ZVAD (Fig. 3C). To examine the biological effects of this site in vivo, we tested a variant *dark*^{v} (see Materials and methods) that substitutes Ala for Asp at position 1292. Like wild-type transformants, ubiquitous restoration of this *dark* variant (UAS-dark^{v}) reversed the lethality caused by *dark*^{82} (Table 1). However, in the absence of any Gal4 driver, 'leaky' expression of UAS-dark^{v} also rescued *dark*^{82} lethality but, surprisingly, wild-type *dark* did not (Table 1). Therefore, dark^{v} exhibits hypermorphic gene action relative to wild-type *dark*. In fact, adult flies rescued to viability with *dark*^{v} displayed split thorax phenotypes and bristle abnormalities in the notum (Fig. 3E) that resemble *dark*^{cd4} homozygotes (Rodriguez et al., 1999). Together, these observations indicate that leaky expression of dark^{V} restores gene function to null animals, not to the wild-type level but, instead, to levels comparable to those seen in *dark*^{cd4}. Hypermorphic properties related to dark^{v} were also noted in ex vivo hemocyte assays. Expression of the wild-type cDNA in dark^{82} hemocytes only mildly restored stimulus-dependent apoptosis after treatment with a Smac mimetic. However, dark^{V} almost completely restored this apoptotic response to dark^{82} hemocytes (Fig. 3G). We considered the possibility that altered expression of UAS-dark^{v} might explain the hypermorphic properties conferred by dark^{V} but, as shown in Fig. 3F, the expression levels of wild-type and variant transgenes were equal. Therefore, in studies of organismal viability and hemocyte apoptosis, dark^{V} conferred striking hypermorphic gene activity without detectable effects upon steady-state expression. These results are consistent with negative-feedback models whereby the action of the Dark protein may be directly repressed by effector caspases, thereby setting an apoptotic threshold in cells that are specified for death.

dc_840_14

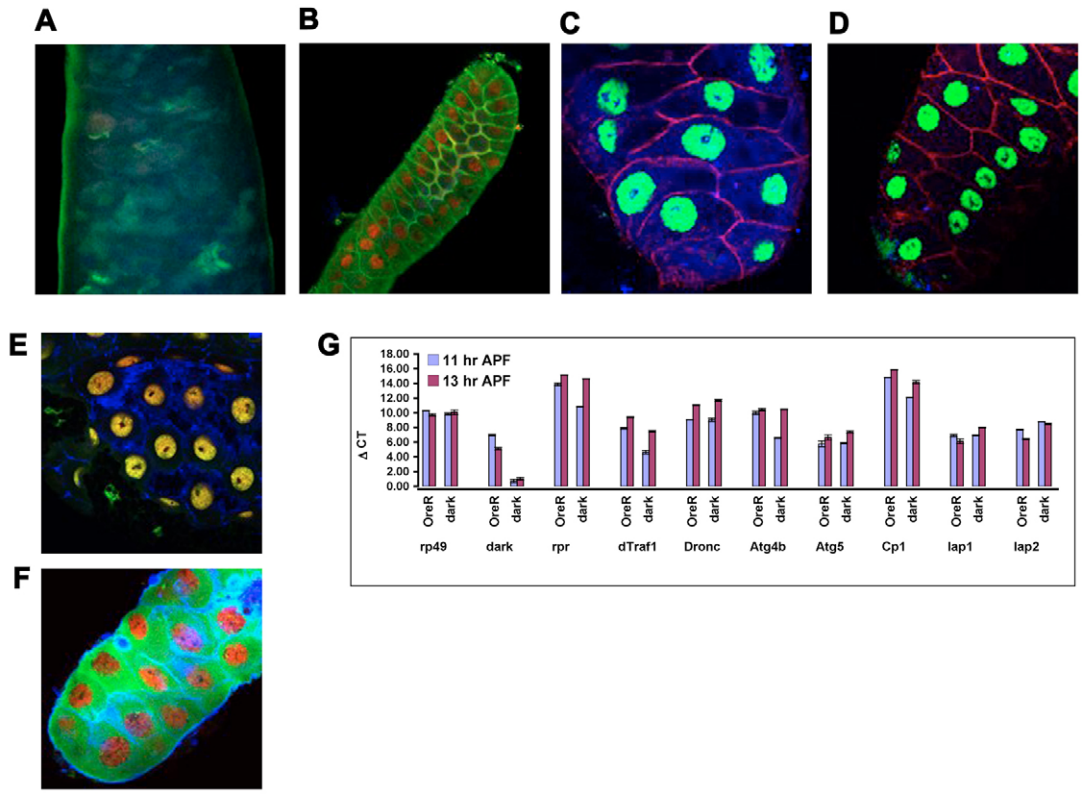


Fig. 4. *dark*^{82} salivary glands are defective for histolysis. (**A**,**B**) Confocal micrographs of salivary glands from wild-type (A) and dark^{82} (B) animals at 16 hours APF stained for a cytoplasmic protein, p127 (green), and a nuclear protein, BR-C (red). Head eversion, which marks the prepupal-pupal transition, has occurred in these animals. In wild type, larval salivary glands are completely histolysed, but in dark^{82} animals the glands persist and structural integrity is maintained. (**C**,**D**) Confocal micrographs showing immunohistochemical staining of salivary glands for anti-cleaved caspase 3 (blue), a marker for active DRICE (Yu et al., 2002), together with anti-actin, (red) and OliGreen, a nuclear stain (green). (C) Caspase activity (blue) in wild-type salivary glands is shown here at 12 hours APF, ~4 hours before final histolysis. (D) Caspase activity is starkly reduced in salivary glands of dark^{82} animals, shown here at 16 hours APF. (**E-G**) Ecdysone signaling and expression of death-related genes are unperturbed in *dark* mutant salivary glands. Immunohistochemical staining (E,F) shows nuclear accumulation of ecdysone-responsive transcription factors in persisting *dark* salivary glands at 16 hours APF. The confocal image in E shows coincident nuclear accumulation of Ecdysone Receptor (EcR, red) and BFTZ-F1 (green), counterstained for actin (blue). Overlapping stains for EcR and BFTZ-F1 produces a robust yellow signal in gland cell nuclei. In F, nuclear accumulation of E74A (red) is shown, with counterstaining for actin (blue) and the cytoplasmic protein Rab11 (green). (G) Pre-death expression profiles for the genes indicated were determined using real-time quantitative RT-PCR on RNA prepared from salivary glands dissected from wild-type (OreR) and dark^{82} animals at 11 hours and 13 hours APF (normalized from 18°C). The gene set analyzed here is a surrogate for profiles of pre-histolytic gene expression (Gorski et al., 2003). Expression levels are represented by ΔC_t values, where $\Delta C_t = C_t$ of no template control (set at 38 PCR cycles) – C_t of sample. C_t, or threshold cycle, is the PCR cycle at which a statistically significant increase in fluorescent signal can be detected above background. *Drosophila* rp49, used here as a control, showed no significant differences in expression. *dark* transcripts were not detected in mutant salivary glands, but, in all other respects, profiles between wild-type and dark glands were highly comparable.

Elimination of *dark* prevents salivary gland histolysis

To determine whether *dark* might function in autophagic cell death, we examined larval salivary glands, which normally histolyse at 16 hours after puparium formation (APF), manifesting vesicular features that are morphologically distinct from apoptosis (see Fig. 4A, Fig. 5A) (Lee and Baehrecke, 2001; Thummel, 2001). In *dark* mutants, these organs did not histolyse and, instead, persisted intact, even in 36-hour APF animals (Fig. 4B). Wild-type and *dark* glands were also stained for immunoreactivity with anti-cleaved caspase 3, an antibody that detects effector caspase activity in *Drosophila* tissues (Yu et al., 2002). In early pupariation stages (4 and 8 hours APF), wild-type salivary glands show little or no immunoreactivity (data not shown), but, four hours later (12 hours APF), widespread staining with anti-cleaved caspase 3 can be observed in the cytoplasm of these cells (Fig. 4C). By contrast, levels of anti-cleaved caspase 3 staining in *dark*$^{-}$ glands were starkly attenuated for reactivity at comparable stages and later (Fig. 4D).

These defects could reflect specific functional requirements for *dark* in histolysis or, alternatively, could result from a more generalized arrest in prepupal development. We can exclude the latter possibility, as persisting glands were always sampled from animals that had passed through the ‘head eversion stage’ into pupation (Ashburner, 1989) and numerous associated landmarks also proceeded on schedule (see below). Like many changes that occur during metamorphosis, salivary gland histolysis is tightly controlled by ecdysone and, hence, failure to histolyse might formally derive from a disruption of this hormonal axis (Yin and Thummel, 2005). To address this possibility, we examined

ecdysone-dependent signaling events known to occur during the period from 3 to 9 hours prior to histolysis (7-13 hours APF). For example, without *dark* function, ecdysone receptor (EcR) and other regulatory factors, such as BFTZ-f1 (Fig. 4E), E74A (Fig. 4F) and *Kruppel homolog* (not shown), accumulated in the nucleus of salivary gland cells. Likewise, in a survey of transcripts that anticipate salivary gland histolysis (Gorski et al., 2003; Lee et al., 2003), gene expression profiles from wild-type and $dark^{82}$ glands were highly comparable (see Fig. 4G). As an indicator of developmental progression, equivalent expression profiles (Fig. 4G) offer considerable statistical power, as a bulk analysis of 20-30 pairs of glands is represented at each time point. Therefore, by each criterion examined, hormonal signaling and associated target responses were unperturbed in *dark* animals. Together, these observations establish a specific requirement for the action of *dark* in salivary gland cell death and exclude generalized arrest or developmental delay as an explanation for defective histolysis.

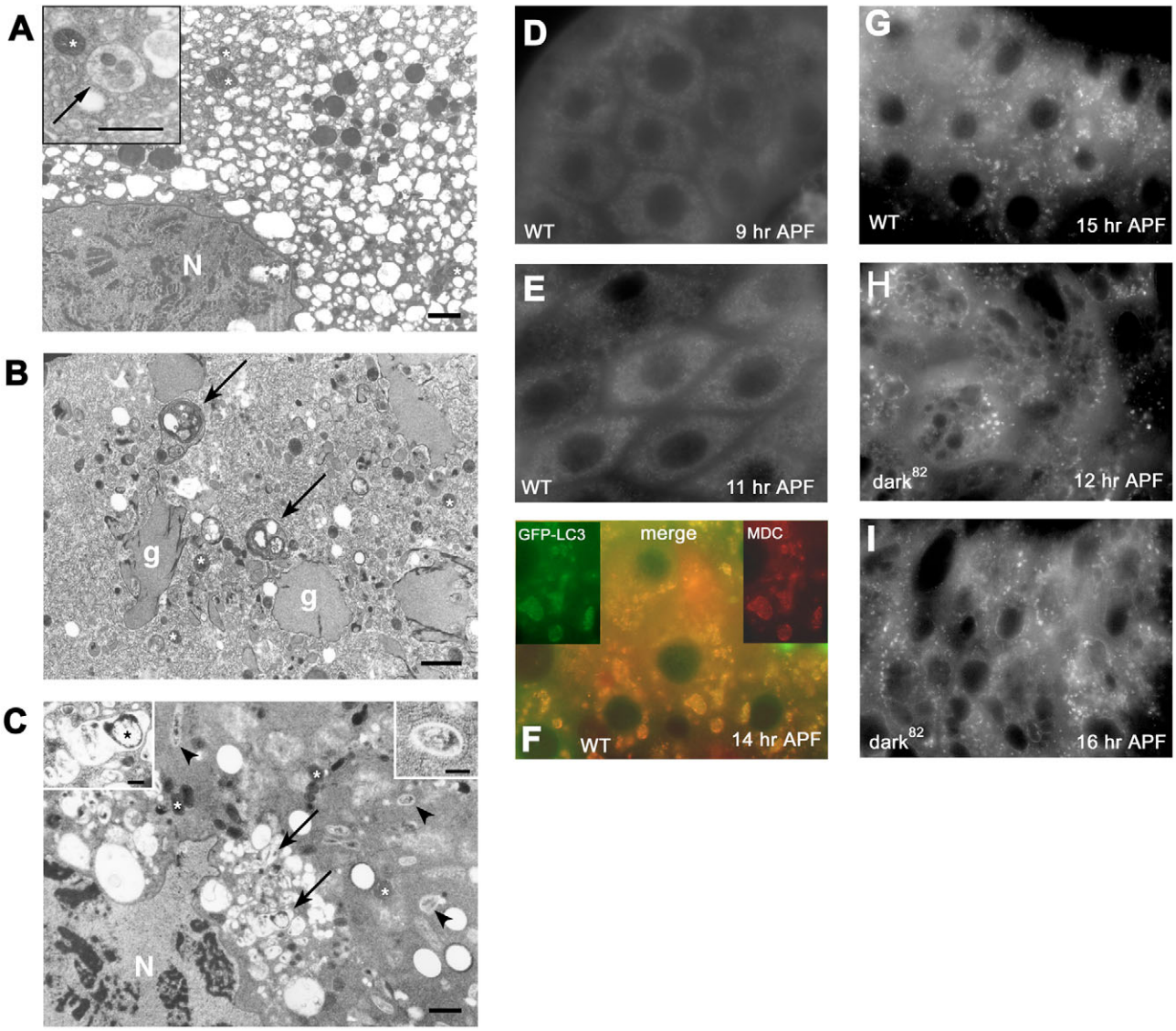


Fig. 5. Autophagy proceeds normally in *dark* mutant salivary glands. (**A-C**) Transmission EM of salivary gland cells. (A) A cytoplasm saturated with small vesicles and an electron dense nucleus (N) are indicative of ongoing cell death in wild-type cells at 14 hours APF. By contrast, salivary gland cells appear healthy in 14-hour APF $dark^{82}$ (B) and 24-hour APF $dark^{82}$ (C), showing no sign of cell death (compare the appearance of the nucleus in C with the nucleus in A). Arrows indicate autolysosomes in A-C, demonstrating that *dark* is not required for autophagy. Insets in panel C show enlargements of representative autophagosomes (top right corner) and autolysosomes (top left corner) seen in mutant glands. N, nucleus; g, secretory granule; asterisks indicate mitochondria. Scale bars: 1 μm; 250 nm for the insets. Arrowheads in C indicate autophagosomes. (**D-I**) Salivary glands dissected at the indicated time points (25°C) and stained with the acidic marker monodansylcadaverine (MDC) to detect autolysosomes (Munafo and Colombo, 2001). F shows a merged image of MDC staining (red) and detection of GFP-LC3 (green) (Rusten et al., 2004), a transgenic GFP marker for autophagosomes and autolysosomes in wild-type salivary glands (14 hours APF). At this stage, prior to histolysis, the overlap between MDC and GFP-LC3 is extensive, indicating an abundance of autolysosomes. (D-G) Time course of MDC staining in wild-type salivary glands. (D) At 9 hours APF, MDC staining is barely detectable. (E) At 11 hours APF, some punctate MDC-positive staining can be observed. However, by 14 hours APF (F) and in 15-hour APF glands (G), large MDC-positive structures are very conspicuous. Likewise, in comparably staged mutant glands, prominent MDC-positive vesicles are seen, shown here at 12 hours APF (H) and in persisting salivary glands 4 hours later (I).

Stimulation of autophagy occurs normally in persisting *dark* glands

We performed a series of histological and ultrastructural studies of mutant glands, with the goal of determining how *dark* might function in the histolysis of this organ. Two hours prior to histolysis of wild-type glands, the nucleus becomes electron dense, polytene chromosomes lose definition, vesicles saturate the cytoplasm and autolysosomes are prominent (Fig. 5A) (Farkas and Sutakova, 1998; Jiang et al., 1997; Juhasz and Sass, 2005). By stark contrast, comparably aged *dark* glands show no signs of vesicular saturation (Fig. 5B). Similarly, pre-histolytic changes that otherwise occur in the nucleus are not seen (Fig. 5C) and, instead, features characteristic of earlier-staged nuclei are retained. Like wild-type counterparts, however, numerous autolysosomes were evident in *dark* glands (Fig. 5B,C), indicating that *dark* function is not required for autophagy per se. To extend this analysis, we confirmed that monodansylcadaverine (MDC), an acidic marker that detects autolysosomes (Munafo and Colombo, 2001), overlapped with the signal derived from GFP-LC3 (Rusten et al., 2004), a transgenic marker of autophagy (Fig. 5F). Next, we established that, in wild-type salivary glands, dramatic accumulation of MDC staining anticipates PCD several hours prior to overt histolysis (Fig. 5D-G). We applied this methodology in *dark* animals and, likewise, observed a comparable abundance of MDC-stained structures in mutant glands (Fig. 5H,I), indicating that stimulation of autophagy, which normally anticipates histolysis, is not dependent on *dark* activity. Therefore, in this tissue, the action of *dark* in histolysis functions downstream of, or parallel to, an autophagic program.

DISCUSSION

Here, we show that *dark* encodes generalized functions in PCD. Loss of maternal and zygotic product caused profound defects, abolishing nearly all apoptotic deaths in the embryo. Likewise, elimination of zygotic *dark* prevented the histolytic death of salivary gland cells and also reversed drug-induced killing of hemocytes. These results establish widespread functions for *dark* in distinct models of programmed and stress-induced cell death. Moreover, because both apoptotic and histolytic forms of cell death were affected, it is clear that common effector pathways regulated by the apoptosome can specify apoptotic and non-apoptotic forms of PCD. The role for *dark* in PCD is not absolute, however, as rare apoptotic cell deaths were observed in animals lacking both the maternal and zygotic product. Although reminiscent of phenotypes associated with complete deletions in the *Reaper* region, loss of *dark* did not appear to perfectly phenocopy these, as occasional apoptotic cell deaths were observed. To substantiate this idea, we carefully compared the incidence of *dark*-independent cell deaths to the rare cell deaths that occur in H99 homozygous embryos. Among animals lacking both maternal and zygotic *dark*, an average of 8.9±2.0 cell deaths were found in late embryonic stages. However, only 3.1±2.1 cell deaths were found in comparably staged H99 embryos. Hence, in this respect, animals devoid of *dark* emulate cell death defects seen in animals lacking *dronc* (Xu et al., 2005). Together, these observations establish that, for a small population of embryonic cells, apoptotic activators in the *reaper* region can specify apoptosis without engaging the fly apoptosome. Similar pathways might occur in post-embryonic stages, but we caution against deriving firm conclusions in unaffected larval tissues, given the caveats relating to perdurance of maternally derived product.

Unlike its counterparts in the worm or the mouse, genetic elimination of *dark* produced a strictly lethal phenotype. Because ubiquitous and 'driver-specific' expression of a *dark* transgene complemented this phenotype, it was possible to map the focus of genetic activity responsible for restoring viability. We found that $dark^{82}$ lethality was reversed when expression was restored to cells of the post-embryonic CNS, but that complementation failed if *dark* was restored to hemocytes or imaginal discs. These results highlight essential functions for zygotic *dark* in the post-embryonic CNS and suggest that the action of this gene within other tissues may not be necessary for viability. Transgenic complementation also proved to be an effective means for distinguishing the wild-type gene action from that of derivatives with altered activities. By this approach, we determined that $dark^{v}$ encodes striking hypermorphic activity without affecting transgenic expression levels. As $dark^{v}$ is mutated at a caspase cleavage site (Fig. 3A-D), the data are consistent with negative-feedback models whereby the action of Dark is directly repressed by effector caspases, perhaps setting an apoptotic threshold in cells that are specified to die. These findings describe the first hypermorphic point mutation among all known alleles in the ced-4/Apaf1 gene family, and raise intriguing possibilities for investigating how life histories and stress responses might be impacted in adults with excessive apoptosomal activity. It is worth noting that, unlike cultured cell models, where full-length *dark* exhibits mild killing activity (Rodriguez et al., 1999), we found no evidence of dominant phenotypes associated with the forced overexpression of either the wild-type or the variant transgenes in tissues presented here (Fig. 3), or in other tissues, such as the eye (not shown). The different effects seen in culture cells versus transgenic animals might reflect authentic context-specific variance, or, alternatively, there may be a mild killing activity that does not manifest as a gross phenotype in the animal. Nevertheless, at least for most tissues and cells, it is unlikely that the levels of *Dark* protein alone qualify as a determinant of apoptosome activity. This inference, together with studies that exclude a fundamental requirement for *Drosophila* cytochrome c in formation of the apoptosome (Yu et al., 2005) or in models of apoptosis (Dorstyn et al., 2004; Zimmermann et al., 2002), suggests that, to function properly, *Dark* must be activated through an unknown mechanism.

Regression of *Drosophila* salivary glands in pupal development is a classic model of histolytic cell death, and dying cells in this gland appear morphologically distinct from cells undergoing apoptosis, indicating that novel cell death pathways may control forms of histolytic cell death (reviewed by Thummel, 2001). We assessed morphological, ultrastructural and molecular indicators to establish that, without *dark*, developmental progression was unperturbed, histolytic regression of this organ failed and salivary gland cells remained morphologically intact. Our results clearly establish a requisite function for Dark in the histolysis of salivary gland cells, despite the fact that PCD of these cells appears dissimilar from classical apoptosis. These observations are consistent with effects produced by p35, a broad-spectrum caspase inhibitor (Jiang et al., 1997; Lee and Baehrecke, 2001; Martin and Baehrecke, 2004), and with animals mutated for the apical caspase *dronc* (Daish et al., 2004). Because apoptotic and histolytic forms of cell death are similarly impacted by the same mutation, we conclude that common effector pathways, regulated by the apoptosome, underlie morphologically distinct forms of PCD.

The induction of autophagy that anticipates salivary gland histolysis may act as part of a novel killing mechanism in these cells (Lee and Baehrecke, 2001; Myohara, 2004; Thummel, 2001), and in mammalian cell death models as well (Shimizu et al., 2004; Yu et

al., 2004). However, in other circumstances, 'self-digestion' clearly promotes survival when apoptosis in prevented (Lum et al., 2005), and, consequently, it is important to understand how links between autophagy and cell death may instruct cell fates (Levine and Klionsky, 2004). As *dark*^{82} organs do not regress like their wild-type counterparts, *dark*^{82} animals afford a unique opportunity to dissect the relationship between histolysis and autophagy. Because the stimulation of autophagy continued in glands that failed to histolyse, we suggest that induced autophagy per se is not the 'lethal event' mediating histolysis of this organ. Instead, the epistasis experiments described here demonstrate that the induction of autophagy lies upstream of, or parallel to, the apoptosome in this model of histolytic cell death.

We gratefully acknowledge support to J.M.A. from the NIH (GM072124), and VEGA (2/3025/23) and APVT (51-027402) grants to R.F., and an NKFP grant (1/a/005/04) to M.S. We are also grateful to Kathleen Galindo for germ line transformations, to T. E. Rusten and H. Stenmark for GFP-LC3 flies, and to Margaret Hickson for administrative support.

References

Abrams, J. M. (1999). An emerging blueprint for apoptosis in Drosophila. *Trends Cell Biol.* **9**, 435-440.
Abrams, J. M., White, K., Fessler, L. and Steller, H. (1993). Programmed cell death during *Drosophila* embryogenesis. *Development* **117**, 29-44.
Adrain, C., Slee, E. A., Harte, M. T. and Martin, S. J. (1999). Regulation of apoptotic protease activating factor-1 oligomerization and apoptosis by the WD-40 repeat region. *J. Biol. Chem.* **274**, 20855-20860.
Ashburner, M. (1989). *Drosophila: A Laboratory Handbook*. Cold Spring Harbor: Cold Spring Harbor Laboratory Press.
Chai, J., Yan, N., Huh, J. R., Wu, J. W., Li, W., Hay, B. A. and Shi, Y. (2003). Molecular mechanism of Reaper-Grim-Hid-mediated suppression of DIAP1-dependent Dronc ubiquitination. *Nat. Struct. Biol.* **10**, 892-898.
Chew, S. K., Akdemir, F., Chen, P., Lu, W. J., Mills, K., Daish, T., Kumar, S., Rodriguez, A. and Abrams, J. M. (2004). The apical caspase dronc governs programmed and unprogrammed cell death in Drosophila. *Dev. Cell* **7**, 897-907.
Chou, T. B. and Perrimon, N. (1996). The autosomal FLP-DFS technique for generating germline mosaics in Drosophila melanogaster. *Genetics* **144**, 1673-1679.
Christich, A., Kauppila, S., Chen, P., Sogame, N., Ho, S. I. and Abrams, J. M. (2002). The Damage-responsive drosophila gene sickle encodes a novel IAP binding protein similar to but distinct from reaper, grim, and hid. *Curr. Biol.* **12**, 137-140.
Daish, T. J., Mills, K. and Kumar, S. (2004). Drosophila caspase DRONC is required for specific developmental cell death pathways and stress-induced apoptosis. *Dev. Cell* **7**, 909-915.
Danial, N. N. and Korsmeyer, S. J. (2004). Cell death: critical control points. *Cell* **116**, 205-219.
Ditzel, M., Wilson, R., Tenev, T., Zachariou, A., Paul, A., Deas, E. and Meier, P. (2003). Degradation of DIAP1 by the N-end rule pathway is essential for regulating apoptosis. *Nat. Cell Biol.* **5**, 467-473.
Dorstyn, L., Mills, K., Lazebnik, Y. and Kumar, S. (2004). The two cytochrome c species, DC3 and DC4, are not required for caspase activation and apoptosis in Drosophila cells. *J. Cell Biol.* **167**, 405-410.
Drapeau, M. D., Radovic, A., Wittkopp, P. J. and Long, A. D. (2003). A gene necessary for normal male courtship, yellow, acts downstream of fruitless in the Drosophila melanogaster larval brain. *J. Neurobiol.* **55**, 53-72.
Farkas, R. and Sutakova, G. (1998). Ultrastructural changes of Drosophila larval and prepupal salivary glands cultured in vitro with ecdysone. *In Vitro Cell. Dev. Biol. Anim.* **34**, 813-823.
Farkas, R. and Mechler, B. M. (2000). The timing of drosophila salivary gland apoptosis displays an l(2)gl-dose response. *Cell Death Differ.* **7**, 89-101.
Geisbrecht, E. R. and Montell, D. J. (2004). A role for Drosophila IAP1-mediated caspase inhibition in Rac-dependent cell migration. *Cell* **118**, 111-125.
Gorski, S. M., Chittaranjan, S., Pleasance, E. D., Freeman, J. D., Anderson, C. L., Varhol, R. J., Coughlin, S. M., Zuyderduyn, S. D., Jones, S. J. and Marra, M. A. (2003). A SAGE approach to discovery of genes involved in autophagic cell death. *Curr. Biol.* **13**, 358-363.
Goto, A., Kadowaki, T. and Kitagawa, Y. (2003). Drosophila hemolectin gene is expressed in embryonic and larval hemocytes and its knock down causes bleeding defects. *Dev. Biol.* **264**, 582-591.
Goyal, L. (2001). Cell death inhibition: keeping caspases in check. *Cell* **104**, 805-808.
Grether, M. E., Abrams, J. M., Agapite, J., White, K. and Steller, H. (1995). The *head involution defective* gene of *Drosophila melanogaster* functions in programmed cell death. *Genes Dev.* **9**, 1694-1708.
Gustafson, K. and Boulianne, G. L. (1996). Distinct expression patterns detected within individual tissues by the GAL4 enhancer trap technique. *Genome* **39**, 174-182.
Hays, R., Wickline, L. and Cagan, R. (2002). Morgue mediates apoptosis in the Drosophila melanogaster retina by promoting degradation of DIAP1. *Nat. Cell Biol.* **4**, 425-431.
Hrdlicka, L., Gibson, M., Kiger, A., Micchelli, C., Schober, M., Schock, F. and Perrimon, N. (2002). Analysis of twenty-four Gal4 lines in Drosophila melanogaster. *Genesis* **34**, 51-57.
Hu, Y. M., Ding, L. Y., Spencer, D. M. and Nunez, G. (1998). WD-40 repeat region regulates Apaf-1 self-association and procaspase-9 activation. *J. Biol. Chem.* **273**, 33489-33494.
Jiang, C., Baehrecke, E. H. and Thummel, C. S. (1997). Steroid regulated programmed cell death during Drosophila metamorphosis. *Development* **124**, 4673-4683.
Juhasz, G. and Sass, M. (2005). Hid can induce, but is not required for autophagy in polyploid larval Drosophila tissues. *Eur. J. Cell Biol.* **84**, 491-502.
Kanuka, H., Sawamoto, K., Inohara, N., Matsuno, K., Okano, H. and Miura, M. (1999). Control of the cell death pathway by Dapaf-1, a Drosophila Apaf-1/CED-4-related caspase activator. *Mol. Cell* **4**, 757-769.
Lee, C. Y. and Baehrecke, E. H. (2001). Steroid regulation of autophagic programmed cell death during development. *Development* **128**, 1443-1455.
Lee, C. Y., Clough, E. A., Yellon, P., Teslovich, T. M., Stephan, D. A. and Baehrecke, E. H. (2003). Genome-wide analyses of steroid- and radiation-triggered programmed cell death in Drosophila. *Curr. Biol.* **13**, 350-357.
Levine, B. and Klionsky, D. J. (2004). Development by self-digestion: molecular mechanisms and biological functions of autophagy. *Dev. Cell* **6**, 463-477.
Li, L., Thomas, R. M., Suzuki, H., De Brabander, J. K., Wang, X. and Harran, P. G. (2004). A small molecule Smac mimic potentiates TRAIL- and TNFalpha-mediated cell death. *Science* **305**, 1471-1474.
Lum, J. J., Bauer, D. E., Kong, M., Harris, M. H., Li, C., Lindsten, T. and Thompson, C. B. (2005). Growth factor regulation of autophagy and cell survival in the absence of apoptosis. *Cell* **120**, 237-248.
Manseau, L., Baradaran, A., Brower, D., Budhu, A., Elefant, F., Phan, H., Philp, A. V., Yang, M., Glover, D., Kaiser, K. et al. (1997). GAL4 enhancer traps expressed in the embryo, larval brain, imaginal discs, and ovary of Drosophila. *Dev. Dyn.* **209**, 310-322.
Martin, D. N. and Baehrecke, E. H. (2004). Caspases function in autophagic programmed cell death in Drosophila. *Development* **131**, 275-284.
Martin, S. J. (2002). Destabilizing influences in apoptosis. Sowing the seeds of IAP destruction. *Cell* **109**, 793-796.
Meier, P., Silke, J., Leevers, S. J. and Evan, G. I. (2000). The Drosophila caspase DRONC is regulated by DIAP1. *EMBO J.* **19**, 598-611.
Mills, K., Daish, T. and Kumar, S. (2005). The function of the Drosophila caspase DRONC in cell death and development. *Cell Cycle* **4**, 744-746.
Moriishi, K., Huang, D. C. S., Cory, S. and Adams, J. M. (1999). Bcl-2 family members do not inhibit apoptosis by binding the caspase activator Apaf-1. *Proc. Natl. Acad. Sci. USA* **96**, 9683-9688.
Munafo, D. B. and Colombo, M. I. (2001). A novel assay to study autophagy: regulation of autophagosome vacuole size by amino acid deprivation. *J. Cell Sci.* **114**, 3619-3629.
Myohara, M. (2004). Real-time observation of autophagic programmed cell death of Drosophila salivary glands in vitro. *Dev. Genes Evol.* **214**, 99-104.
Park, M., Wu, X., Golden, K., Axelrod, J. D. and Bodmer, R. (1996). The wingless signaling pathway is directly involved in Drosophila heart development. *Dev. Biol.* **177**, 104-116.
Rodriguez, A., Oliver, H., Zou, H., Chen, P., Wang, X. D. and Abrams, J. M. (1999). Dark is a Drosophila homologue of Apaf-1/CED-4 and functions in an evolutionarily conserved death pathway. *Nat. Cell Biol.* **1**, 272-279.
Rusten, T. E., Lindmo, K., Juhasz, G., Sass, M., Seglen, P. O., Brech, A. and Stenmark, H. (2004). Programmed autophagy in the Drosophila fat body is induced by ecdysone through regulation of the PI3K pathway. *Dev. Cell* **7**, 179-192.
Ryoo, H. D., Bergmann, A., Gonen, H., Ciechanover, A. and Steller, H. (2002). Regulation of Drosophila IAP1 degradation and apoptosis by reaper and ubcD1. *Nat. Cell Biol.* **4**, 432-438.
Salvesen, G. S. and Abrams, J. M. (2004). Caspase activation–stepping on the gas or releasing the brakes? Lessons from humans and flies. *Oncogene* **23**, 2774-2784.
Shimizu, S., Kanaseki, T., Mizushima, N., Mizuta, T., Arakawa-Kobayashi, S., Thompson, C. B. and Tsujimoto, Y. (2004). Role of Bcl-2 family proteins in a non-apoptotic programmed cell death dependent on autophagy genes. *Nat. Cell Biol.* **6**, 1221-1228.
Silke, J. H., Kratina, T., Ekert, P. G., Pakusch, M. and Vaux, D. L. (2004). Unlike Diablo/smac, grim promotes global ubiquitination and specific degradation of XIAP and neither cause apoptosis. *J. Biol. Chem.* **279**, 4313-4321.
Spierings, D., McStay, G., Saleh, M., Bender, C., Chipuk, J., Maurer, U. and Green, D. R. (2005). Connected to death: the (unexpurgated) mitochondrial pathway of apoptosis. *Science* **310**, 66-67.

Thummel, C. S. (2001). Steroid-triggered death by autophagy. *BioEssays* **23**, 677-682.
Wang, S. L., Hawkins, C. J., Yoo, S. J., Muller, H. A. J. and Hay, B. A. (1999). The Drosophila caspase inhibitor DIAP1 is essential for cell survival and is negatively regulated by HID. *Cell* **98**, 453-463.
White, K., Grether, M., Abrams, J. M., Young, L., Farrell, K. and Steller, H. (1994). Genetic control of programmed cell death in *Drosophila*. *Science* **264**, 677-683.
Wilson, R., Goyal, L., Ditzel, M., Zachariou, A., Baker, D. A., Agapite, J., Steller, H. and Meier, P. (2002). The DIAP1 RING finger mediates ubiquitination of Dronc and is indispensable for regulating apoptosis. *Nat. Cell Biol.* **4**, 445-450.
Wing, J. P., Schwartz, L. M. and Nambu, J. R. (2001). The RHG motifs of Drosophila Reaper and Grim are important for their distinct cell death-inducing abilities. *Mech. Dev.* **102**, 193-203.
Wing, J. P., Karres, J. S., Ogdahl, J. L., Zhou, L., Schwartz, L. M. and Nambu, J. R. (2002a). Drosophila sickle is a novel grim-reaper cell death activator. *Curr. Biol.* **12**, 131-135.
Wing, J. P., Schreader, B. A., Yokokura, T., Wang, Y., Andrews, P. S., Huseinovic, N., Dong, C. K., Ogdahl, J. L., Schwartz, L. M., White, K. et al. (2002b). Drosophila Morgue is an F box/ubiquitin conjugase domain protein important for grim-reaper mediated apoptosis. *Nat. Cell Biol.* **4**, 451-456.
Wu, J. W., Cocina, A. E., Chai, J. J., Hay, B. A. and Shi, Y. G. (2001). Structural analysis of a functional DIAP1 fragment bound to grim and hid peptides. *Mol. Cell* **8**, 95-104.
Xu, D., Li, Y., Arcaro, M., Lackey, M. and Bergmann, A. (2005). The CARD-carrying caspase Dronc is essential for most, but not all, developmental cell death in Drosophila. *Development* **132**, 2125-2134.
Yin, V. P. and Thummel, C. S. (2005). Mechanisms of steroid-triggered programmed cell death in Drosophila. *Semin. Cell Dev. Biol.* **16**, 237-243.
Yoo, S. J., Huh, J. R., Muro, I., Yu, H., Wang, L., Wang, S. L., Feldman, R. M., Clem, R. J., Muller, H. A. and Hay, B. A. (2002). Hid, Rpr and Grim negatively regulate DIAP1 levels through distinct mechanisms. *Nat. Cell Biol.* **4**, 416-424.
Yu, L., Alva, A., Su, H., Dutt, P., Freundt, E., Welsh, S., Baehrecke, E. H. and Lenardo, M. J. (2004). Regulation of an ATG7-beclin 1 program of autophagic cell death by caspase-8. *Science* **304**, 1500-1502.
Yu, S. Y., Yoo, S. J., Yang, L., Zapata, C., Srinivasan, A., Hay, B. A. and Baker, N. E. (2002). A pathway of signals regulating effector and initiator caspases in the developing Drosophila eye. *Development* **129**, 3269-3278.
Yu, X., Wang, L., Acehan, D., Wang, X. and Akey, C. W. (2005). Three-dimensional structure of a double apoptosome formed by the Drosophila Apaf-1 related killer. *J. Mol. Biol.* **355**, 577-589.
Zachariou, A., Tenev, T., Goyal, L., Agapite, J., Steller, H. and Meier, P. (2003). IAP-antagonists exhibit non-redundant modes of action through differential DIAP1 binding. *EMBO J.* **22**, 6642-6652.
Zhou, L., Song, Z. W., Tittel, J. and Steller, H. (1999). HAC-1, a Drosophila homolog of APAF-1 and CED-4 functions in developmental and radiation-induced apoptosis. *Mol. Cell* **4**, 745-755.
Zimmermann, K. C., Ricci, J. E., Droin, N. M. and Green, D. R. (2002). The role of ARK in stress-induced apoptosis in Drosophila cells. *J. Cell Biol.* **156**, 1077-1087.

OPEN ACCESS Freely available online

PLoS BIOLOGY

Unsolved Mystery

dc_840_14

Autophagy: A Forty-Year Search for a Missing Membrane Source

Gabor Juhasz*, Thomas P. Neufeld

Autophagy is the major self-degradative process in eukaryotic cells, with fundamental roles in cellular and organismal homeostasis, and is involved in many developmental and pathological situations. Structures targeted for autophagic destruction are sequestered into newly emerging double-membrane vesicles called autophagosomes, and delivered for lysosomal degradation. Despite recent advances in understanding the molecular mechanisms of autophagy, a long-standing question concerning the source of the autophagic membrane remains unresolved. Two major alternatives can be considered: the membrane may be derived from a pre-existing cytoplasmic organelle such as the endoplasmic reticulum (maturation model), or assembled from constituents at its site of genesis (assembly model).

Introduction

The stability of all biological systems—from single cells to ecological communities—is based on the continuous turnover of individual units. Just as new organisms are born to replace dying ones, turnover of constituents within a cell ensures that old or damaged macromolecules and organelles are replaced by newly synthesized ones. This constant replacement underlies the adaptability of biological systems, for example allowing cells to rapidly change their metabolism in response to a changing environment. Cellular homeostasis (the ability to maintain a stable condition inside the cell) is therefore based on the proper balance of synthesis and destruction.

In eukaryotic cells, various specialized cytoplasmic enzymes are responsible for the specific degradation of proteins (the ubiquitin-proteasome pathway), lipids, ribonucleic acids, sugars etc.; these degradation events can be crucial to the execution of cellular signaling and metabolic pathways. In contrast, nonspecific degradation of these materials occurs through autophagy ("self-eating" in Greek; in this case at a subcellular level) [1]. This process plays several important roles in the life of a cell. During times of starvation, autophagy ensures survival by randomly degrading bulk cytoplasm including organelles to provide breakdown products that can be used for energy and synthetic processes [2]. In response to a change in available nutrients, autophagy is also used to specifically eliminate obsolete metabolic organelles in several yeast species [3]. In multicellular organisms, autophagy is tightly controlled through several signaling pathways [4,5], and has been integrated into various developmental and physiological events, such as the remodeling of cells, tissues, organs, or even the entire body. To take an extreme example, nearly all of the larval tissues of a metamorphosing insect are self-digested inside the pupal case, making room and providing nutrients for the cells that will eventually give rise to the adult insect [6]. In mammals, autophagy occurs in virtually all cells at a basal rate, and has been shown to be required for the elimination of old and nonfunctional organelles and protein complexes [7]. Growth-promoting hormones such as insulin inhibit autophagy [8], whereas glucagon, synthesized in response to low blood sugar levels, induces this process [9]. Autophagy has been suggested to play a protective role during aging, cell death, defense against intracellular pathogens, neurodegenerative diseases, and tumorigenesis, emphasizing the biological and medical importance of autophagy [2,10].

Unsolved Mysteries discuss a topic of biological importance that is poorly understood and in need of research attention.

The Morphology of Autophagy

During autophagy, large membrane-bound portions of the cytoplasm are delivered for destruction to lysosomes, organelles loaded with various acidic hydrolases specialized for rapid and effective degradation of cellular and extracellular material. As early as the 1960s, the morphology of the major pathway of autophagy, macroautophagy (simply referred to as autophagy hereafter), was established by electron microscopic studies [1,9]. Upon induction of autophagy, a membrane cisterna (fold of membrane) known as the isolation membrane (IM; sometimes referred to as phagophore in mammals [11]) appears and curves around part of the cytoplasm. Sealing of the edges of the IM results in a unique double membrane vesicle, the autophagosome. Soon after forming, autophagosomes fuse with a lysosome, where degradation of the delivered material for recycling takes place (Figure 1A and 1B). The membranes of IMs and autophagosomes differ from other membranes in the cell in having few intramembrane proteins, evident by electron microscopy [12–14].

The dynamic membrane rearrangements of autophagy are also unique in that topologically intracellular material (cytoplasm) becomes converted into topologically

Citation: Juhasz G, Neufeld TP (2006) Autophagy: A forty-year search for a missing membrane source. PLoS Biol 4(2): e36.

Copyright: © 2006 Juhasz and Neufeld. This is an open-access article distributed under the terms of the Creative Commons Attribution License, which permits unrestricted use, distribution, and reproduction in ay medium, provided the original author and source are credited.

Abbreviations: Atg, autophagy-related gene; ER, endoplasmic reticulum; IM, isolation membrane; PAS, preautophagosomal structure

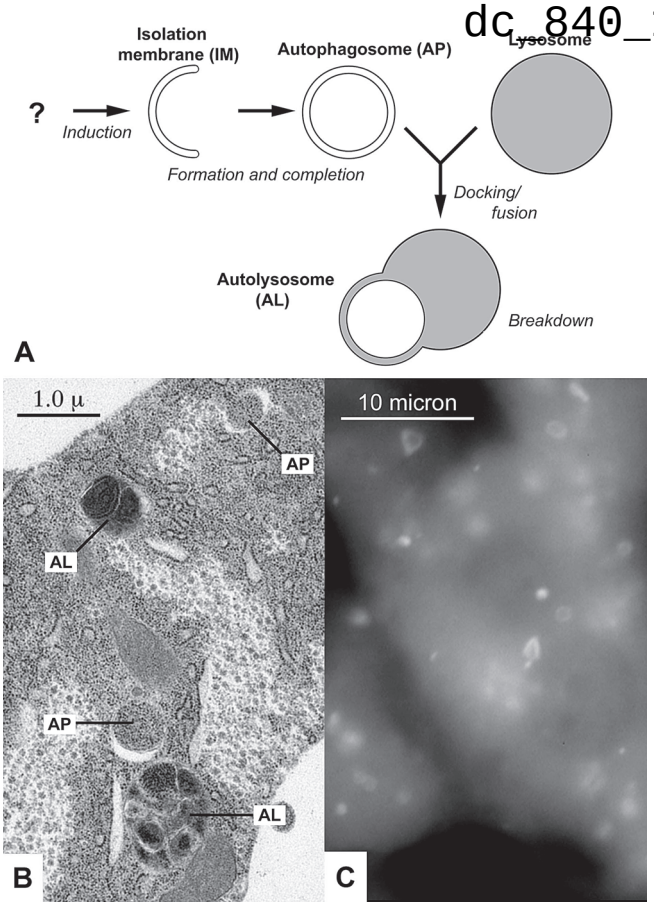
Gabor Juhasz and Thomas P. Neufeld are in the Department of Genetics, Cell Biology, and Development, University of Minnesota, Minneapolis, Minnesota, United States of America

Competing Interests: The authors have declared that no competing interests exist.

* To whom correspondence should be addressed. E-mail: juhas001@umn.edu (GJ); neufeld@med.umn.edu (TPN)

DOI: 10.1371/journal.pbio.0040036

dc_840_14



DOI: 10.1371/journal.pbio.0040036.g001

Figure 1. The Dynamic Membrane Events Involved in Autophagy

(A) Upon induction of autophagy, a membrane sac called the isolation membrane (IM) forms and engulfs portions of the cytoplasm. Sealing of its edges gives rise to the double-membrane bound autophagosome. Fusion of the outer membrane with a lysosome results in formation of an autolysosome, in which the inner autophagosomal membrane and its contents are degraded.

(B) Starvation-induced autophagosomes (AP) and autolysosomes (AL) in the fat body (the functional analogue of the liver) of a fruit fly larva. Note that APs contain intact cytoplasm, whereas the contents of ALs show various stages of degradation.

(C) Liver cells of starved mice carrying a fluorescently tagged LC3 transgene, labeling cup-shaped and ring-shaped structures that correspond to IMs and autophagosomes, respectively.

Images courtesy of Ryan Scott (B) and Dr. Noboru Mizushima (C).

extracellular (the lumen of lysosomes) without crossing a membrane barrier [15]. In contrast, material delivered to the lysosome by other routes either remains extracellular, in the case of endocytosis (formerly referred to as heterophagy [1]), or crosses a membrane, as in the case of lysosomal enzyme synthesis.

Identification of Genes Involved in Autophagy

Yeasts, like humans, alter their metabolism to meet the amount and type of available nutrients. And, unlike humans, they are much easier to study genetically. Little was known about the molecular mechanisms of autophagy until the last decade, when yeast genetic screens revealed ~27 autophagy-related genes (Atg), whose products are necessary for autophagy [16]. Most Atg proteins localize at least transiently to a single well-defined spot in the cytoplasm known as the preautophagosomal structure (PAS), a site from which the IM forms upon induction of autophagy. Atg proteins form three main multiprotein complexes: an autophagy-specific phosphatidyl-inositol 3-kinase (PI3K) complex, the Atg1 kinase complex, and two closely linked ubiquitin-like protein conjugation systems. Current research is aimed at understanding how these complexes interact to promote autophagy.

Multicellular organisms harbor homologs of most of the yeast Atg genes, reflecting the evolutionary conservation of autophagy and its molecular components. There are also some important differences. For example, IMs in yeast bud from the single PAS, whereas in mammalian cells, IMs are formed throughout the cytoplasm, and no definitive PAS is observed. The presence of multiple homologs of some Atg genes also suggests an as-yet unknown complexity of the process in metazoans.

One of the ubiquitin-like proteins, Atg8 (called LC3 in mammals), appears to be associated with IMs and autophagosomes through a lipid anchor [17], and therefore represents the first known protein covalently attached to these membranes. Atg8/LC3 fused to a fluorescent tag is now commonly used as a light microscopic marker to follow the formation of early autophagic structures (Figure 1C) [18].

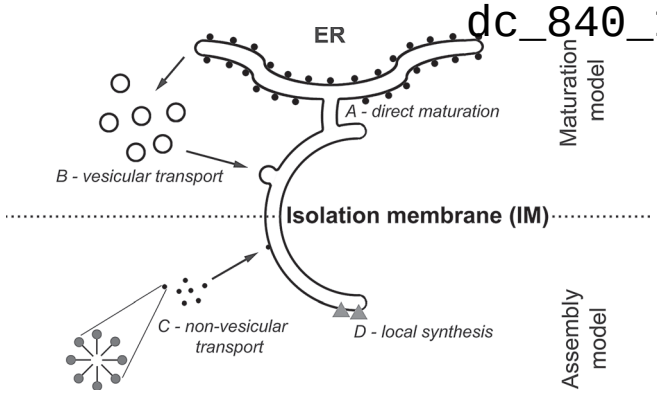
Potential Membrane Sources of the IM

Despite the recent advancement of autophagy research, one fundamental question remains unanswered: how does the autophagic membrane form? The membranes of IMs and autophagosomes are of the thin type (6–7 nm), like the membranes of the endoplasmic reticulum (ER), cis-Golgi, nuclear envelope, and inner and outer membranes of mitochondria. In contrast, membranes of the plasma membrane, lysosomes, and most of the Golgi are thick (9–10 nm), due to their different lipid composition (e.g., more cholesterol) and higher protein content. A review article written nearly 40 years ago by de Duve and Wattiaux [1] already mentioned that the source of the sequestering membrane "has given rise to many speculations," including the ER, Golgi complex, and de novo formation. Below we consider the evidence relating to two general models of autophagic membrane formation.

The Maturation Model

All cellular membrane is generally thought to derive from the ER. Membrane from the ER is transported through the secretory pathway by a continuous cycle of vesicular budding and fusion. Based on these observations, one model posits that the IM is derived from the ER or another pre-existing organelle upon induction of autophagy. For example, a portion of the ER may become cleared of ribosomes and fold onto itself to form the IM (Figure 2A); alternatively, vesicles may bud off from the ER and fuse together to form the IM (Figure 2B). This theory is supported by the similar membrane thickness of these organelles (see earlier), by the putative identification of ER proteins in IMs and autophagosomes in mammalian cells [19] (but see also [20] for an extended discussion of this point), and also by the observation that IMs are often observed between parallel ER cisternae in secretory cells [13]. In yeast, recent molecular genetic studies showed that genes necessary for ER trafficking are required for autophagy [21]. These data are consistent with a membrane contribution from the ER, although they

dc_840_14



DOI: 10.1371/journal.pbio.0040036.g002

Figure 2. Possible Membrane Sources of the IM

Some of the possible scenarios for IM formation are illustrated here. According to the maturation model, upon induction of autophagy, membrane may be directly derived from the ER by folding (A), or in the form of vesicular transport (B). In the assembly model, membrane may be assembled de novo at the site of IM formation, originating from nonvesicular transport, such as micellar, as shown in (C), or local synthesis (D). See text for further details.

may instead simply reflect a genetic requirement for one or more proteins synthesized in the ER.

The Assembly Model

Recent real-time studies have revealed that newly forming IMs continue to elongate until the final sealing of the autophagosome [22]. This observation is difficult to reconcile with the direct maturation of an existing organelle into an IM. An alternative model posits that the IM is assembled de novo. In this model, nonvesicular transport (Figure 2C) or local synthesis (Figure 2D) of lipids supplies the material for the growing membrane. Currently, support for this model comes mostly in the form of negative results, namely the lack of convincing identification of vesicles or membrane cisternae fusing to the IM, despite numerous transmission and freeze-fracture electron microscopic studies. Similarly, conventional vesicular structures have not been observed by electron microscopy at the PAS in yeast, although retrograde transport of some Atg proteins has recently been demonstrated, presumably involving a vesicular mechanism [23]. Interestingly, the cytoplasm in the area of the PAS largely excludes free ribosomes that normally fill the cytosol [24], consistent with a high lipid content or membranaceous barrier in this region.

In many cell types, induction of autophagy can be remarkably robust, resulting in a rapid appearance of numerous autophagosomes throughout the cell. Whether local synthesis or nonvesicular transport of lipids and their assembly into membranes could be efficient enough to generate sufficient amounts of membrane in a short time is unclear. It is also possible that multiple membrane pools contribute to the IM. The distinct steps of IM formation—nucleation, assembly, and elongation—may also rely on different membrane sources [10].

Toward a Solution

The unique molecular makeup of the autophagic membrane—rich in lipid, poor in protein—has likely hindered attempts to identify its source using traditional proteocentric cellular and molecular approaches. A definitive answer to this elusive question is thus likely to spring from new technologies, such as improved in vivo lipid labeling methods capable of specifically marking different cell membranes in live cells [25]. In addition, the recent and ongoing identification of the Atg proteins, many of which specifically localize to the PAS and IM, provides a powerful new set of tools to address this problem. This list is likely to grow as additional factors are identified, perhaps based on their co-localization with known Atg proteins, and through genetic screens in other organisms. Among the most promising of the known factors is Atg9, the sole known integral membrane protein involved in IM formation. Atg9 cycles through the PAS and other unidentified punctate structures [23,26]. As this protein is presumably membrane-bound from its inception, live tracking of Atg9 is likely to identify at least a subset of the contributing membrane. These reagents, in conjunction with standard cell biology approaches, thus represent novel means of investigating the membrane source. For example, a specific pool of lipids or Atg proteins en route to the forming and growing IM could be followed by photobleaching recovery or pulse-chase methods [27,28]. In addition, these tools will allow researchers to delve further into this mysterious puzzle, addressing a number of closely related fundamental questions: As new membrane is added to the growing IM, is it recruited to the tips, center or entire surface? How is this membrane targeted to the IM? Does induction of autophagy stimulate membrane production, or are pre-existing stores of lipid sufficient? Are the known Atg proteins directly involved in membrane recruitment or synthesis, and if so what are the mechanisms involved? A new generation of tools and a plate full of questions is attracting new researchers to this expanding field, leading to an accelerated pace of discovery. Future work will provide plenty of new information to ingest. ■

References

1. De Duve C, Wattiaux R (1966) Functions of lysosomes. Annu Rev Physiol 28: 435–492.
2. Levine B, Klionsky DJ (2004) Development by self-digestion: Molecular mechanisms and biological functions of autophagy. Dev Cell 6: 463–477.
3. Bellu AR, Kiel JA (2003) Selective degradation of peroxisomes in yeasts. Microsc Res Tech 61: 161–170.
4. Rusten TE, Lindmo K, Juhasz G, Sass M, Seglen PO, et al. (2004) Programmed autophagy in the Drosophila fat body is induced by ecdysone through regulation of the PI3K pathway. Dev Cell 7: 179–192.
5. Scott RC, Schuldiner O, Neufeld TP (2004) Role and regulation of starvation-induced autophagy in the Drosophila fat body. Dev Cell 7: 167–178.
6. Neufeld TP (2004) Role of autophagy in developmental cell growth and death: Insights from *Drosophila*. In: Klionsky DJ, editor. Autophagy. Georgetown: Landes Bioscience. pp. 224–232.
7. Komatsu M, Waguri S, Ueno T, Iwata J, Murata S, et al. (2005) Impairment of starvation-induced and constitutive autophagy in Atg7-deficient mice. J Cell Biol 169: 425–434.
8. Pfeifer U (1978) Inhibition by insulin of the formation of autophagic vacuoles in rat liver. A morphometric approach to the kinetics of intracellular degradation by autophagy. J Cell Biol 78: 152–167.
9. Ashford TP, Porter KR (1962) Cytoplasmic components in hepatic cell lysosomes. J Cell Biol 12: 198–202.
10. Reggiori F, Klionsky DJ (2005) Autophagosomes: Biogenesis from scratch? Curr Opin Cell Biol 17: 415–422.
11. Seglen PO (1987) Regulation of autophagic protein degradation in isolated liver cells. In: Glaumann H, Ballard FJ, editors. Lysosomes: Their role in protein breakdown. London: Academic Press. pp. 369–414.
12. Rez G, Meldolesi J (1980) Freeze-fracture of drug-induced autophagocytosis in the mouse exocrine pancreas. Lab Invest 43: 269–277.
13. Kovacs AL, Rez G, Palfia Z, Kovacs J (2000) Autophagy in the epithelial cells of murine seminal vesicle in vitro. Formation of large sheets of nascent isolation membranes, sequestration of the nucleus and inhibition by wortmannin and 3-methyladenine. Cell Tissue Res 302: 253–261.
14. Fengsrud M, Erichsen ES, Berg TO, Raiborg C, Seglen PO (2000) Ultrastructural characterization of the delimiting membranes of isolated autophagosomes and amphisomes by freeze-fracture electron microscopy. Eur J Cell Biol 79: 871–882.

dc_840_14

15. Stromhaug PE, Klionsky DJ (2001) Approaching the molecular mechanism of autophagy. Traffic 2: 524–531.
16. Klionsky DJ, Cregg JM, Dunn WA Jr, Emr SD, Sakai Y, et al. (2003) A unified nomenclature for yeast autophagy-related genes. Dev Cell 5: 539–545.
17. Ichimura Y, Kirisako T, Takao T, Satomi Y, Shimonishi Y, et al. (2000) A ubiquitin-like system mediates protein lipidation. Nature 408: 488–492.
18. Mizushima N, Yamamoto A, Matsui M, Yoshimori T, Ohsumi Y (2004) In vivo analysis of autophagy in response to nutrient starvation using transgenic mice expressing a fluorescent autophagosome marker. Mol Biol Cell 15: 1101–1111.
19. Dunn WA (1994) Autophagy and related mechanisms of lysosome-mediated protein degradation. Trends Cell Biol 4: 139–143.
20. Fengsrud M, Sneve ML, Overbye A, Seglen PO (2004) Structural aspects of mammalian autophagy. In: Klionsky DJ, editor. Autophagy. Georgetown (Texas): Landes Bioscience. pp. 11–25.
21. Ishihara N, Hamasaki M, Yokota S, Suzuki K, Kamada Y, et al. (2001) Autophagosome requires specific early Sec proteins for its formation and NSF/SNARE for vacuolar fusion. Mol Biol Cell 12: 3690–3702.
22. Mizushima N, Yamamoto A, Hatano M, Kobayashi Y, Kabeya Y, et al. (2001) Dissection of autophagosome formation using Apg5-deficient mouse embryonic stem cells. J Cell Biol 152: 657–668.
23. Reggiori F, Tucker KA, Stromhaug PE, Klionsky DJ (2004) The Atg1-Atg13 complex regulates Atg9 and Atg23 retrieval transport from the pre-autophagosomal structure. Dev Cell 6: 79–90.
24. Kirisako T, Baba M, Ishihara N, Miyazawa K, Ohsumi M, et al. (1999) Formation process of autophagosome is traced with Apg8/Aut7p in yeast. J Cell Biol 147: 435–446.
25. Kuerschner L, Ejsing CS, Ekroos K, Shevchenko A, Anderson KI, et al. (2005) Polyene-lipids: A new tool to image lipids. Nat Methods 2: 39–45.
26. Noda T, Kim J, Huang WP, Baba M, Tokunaga C, et al. (2000) Apg9p/Cvt7p is an integral membrane protein required for transport vesicle formation in the Cvt and autophagy pathways. J Cell Biol 148: 465–480.
27. Lippincott-Schwartz J, Altan-Bonnet N, Patterson GH (2003) Photobleaching and photoactivation: Following protein dynamics in living cells. Nat Cell Biol (Suppl): S7–S14.
28. Gaietta G, Deerinck TJ, Adams SR, Bouwer J, Tour O, et al. (2002) Multicolor and electron microscopic imaging of connexin trafficking. Science 296: 503–507.

Downloaded from www.genesdev.org on December 4, 2007 - Published by Cold Spring Harbor Laboratory Press

RESEARCH COMMUNICATION

Atg7-dependent autophagy promotes neuronal health, stress tolerance, and longevity but is dispensable for metamorphosis in *Drosophila*

Gábor Juhász,[1,2] Balázs Érdi,[2] Miklós Sass,[2] and Thomas P. Neufeld[1,3]

[1]Department of Genetics, Cell Biology, and Development, University of Minnesota, Minneapolis, Minnesota 55455, USA; [2]Department of Anatomy, Cell and Developmental Biology, Eötvös Loránd University, Budapest H-2120, Hungary

Autophagy, a cellular process of cytoplasmic degradation and recycling, is induced in *Drosophila* larval tissues during metamorphosis, potentially contributing to their destruction or reorganization. Unexpectedly, we find that flies lacking the core autophagy regulator Atg7 are viable, despite severe defects in autophagy. Although metamorphic cell death is perturbed in *Atg7* mutants, the larval–adult midgut transition proceeds normally, with extended pupal development compensating for reduced autophagy. *Atg7*$^{-/-}$ adults are short-lived, hypersensitive to nutrient and oxidative stress, and accumulate ubiquitin-positive aggregates in degenerating neurons. Thus, normal levels of autophagy are crucial for stress survival and continuous cellular renewal, but not metamorphosis.

Supplemental material is available at http://www.genesdev.org.

Received August 3, 2007; revised version accepted October 12, 2007.

Autophagy is a general term for the degradation of self-material in lysosomes. During the course of the main pathway, macroautophagy (hereafter referred to as autophagy), an isolation membrane appears that envelops random portions of the cytoplasm. Sealing of the edges results in a unique double-membrane vesicle called an autophagosome, which will then fuse with a lysosome to deliver its contents for degradation and reuse. This process is controlled by a core group of ~20 conserved autophagy-related (Atg) genes first identified in yeast (Klionsky et al. 2003). Among these, the ubiquitin-related proteins Atg8 and Atg12 and their E1- and E2-like processing enzymes are essential for autophagosome formation.

As in yeast, targeted disruption of Atg genes in mouse and *Drosophila* models results in a block of starvation-induced autophagy and causes an accelerated loss of viability under starvation conditions (Scott et al. 2004; Komatsu et al. 2005; Hara et al. 2006). In addition, Atg gene knockouts in these animal models have been shown to result in post-embryonic lethality even in the presence of optimal nutrients, suggesting that in higher eukaryotes, autophagy has evolved to serve additional functions beyond starvation survival. Indeed, recent reports showed that basal autophagy plays an essential role in protein quality control in mammals, by continuously degrading misfolded or damaged proteins (Komatsu et al. 2005, 2006; Hara et al. 2006), and prevents metabolic stress-induced genome instability and tumor progression (Mathew et al. 2007). During development, high levels of autophagy may also contribute to some forms of programmed cell death, as in the case of degenerating larval tissues during insect metamorphosis (Butterworth and Forrest 1984; Neufeld 2004; Penaloza et al. 2006).

We previously reported that mutations in *Drosophila Atg1* cause a strong inhibition of autophagy and result in lethality at the pupal stage of development (Scott et al. 2004, 2007). However, because Atg1 homologs in other species have been found to participate in nonautophagic processes (Tomoda et al. 2004; Ogura and Goshima 2006; Zhou et al. 2007), it is unclear whether the lethality of these mutants stems from defects in autophagy or whether this may reflect other functions of Atg1. Here we report the generation of null mutations in *Atg7*, which encodes the single E1-like enzyme required for activation of both Atg8 and Atg12. Surprisingly, despite severely reduced levels of autophagy, *Atg7* mutant flies are fully viable and fertile, and no major morphological defects are observed during metamorphosis. Emerging mutant adults are hypersensitive to stress and have a reduced life span, potentially due to accumulation of ubiquitin-positive aggregates in degenerating neurons.

Results and Discussion

Generation of Atg7 deletions

Several *P*-element insertions are available in the genomic region of *Atg7*, located in the intron between exons 6 and 7, and upstream of or downstream from the gene (Fig. 1A; data not shown). All of these lines yielded viable adults when crossed to the deletion-bearing line *Df(2R)Pu66*, and none of them showed a noticeable effect on starvation-induced autophagy (data not shown).

As previously identified mutations in *Drosophila* Atg genes with a strong autophagy-defective phenotype were lethal (Scott et al. 2004), we initially screened for lethal lines after remobilization of the *P*-element *Atg7*^{EY10058}, located 73 bases upstream of the predicted *Atg7* transcription start site. Of the lethal lines recovered, two groups of deletions could be identified. The first contained deletions extending from the original *P*-element insertion site into a neighboring gene, *Sec6* (data not shown). Lines in the second group had deletions extending into both *Atg7* and *Sec6*, as in the case of *Atg7*^{d14} (Fig. 1A), which removes the transcription and translation start sites and the majority of the Atg7 coding region, resulting in a presumptive null allele. As existing *Sec6* mutations described earlier were lethal (Murthy et al. 2005), we concluded that the lethality of these deletion lines could be ascribed to lack of Sec6 function. Our failure to identify any *Atg7*-specific events among these

[*Keywords*: Autophagy; Atg7; *Drosophila*; longevity; metamorphosis; neurodegeneration]
[3]Corresponding author.
E-MAIL neufeld@ahc.umn.edu; FAX (612) 626-7031.
Article is online at http://www.genesdev.org/cgi/doi/10.1101/gad.1600707.

Downloaded from www.genesdev.org on December 4, 2007 - Published by Cold Spring Harbor Laboratory Press

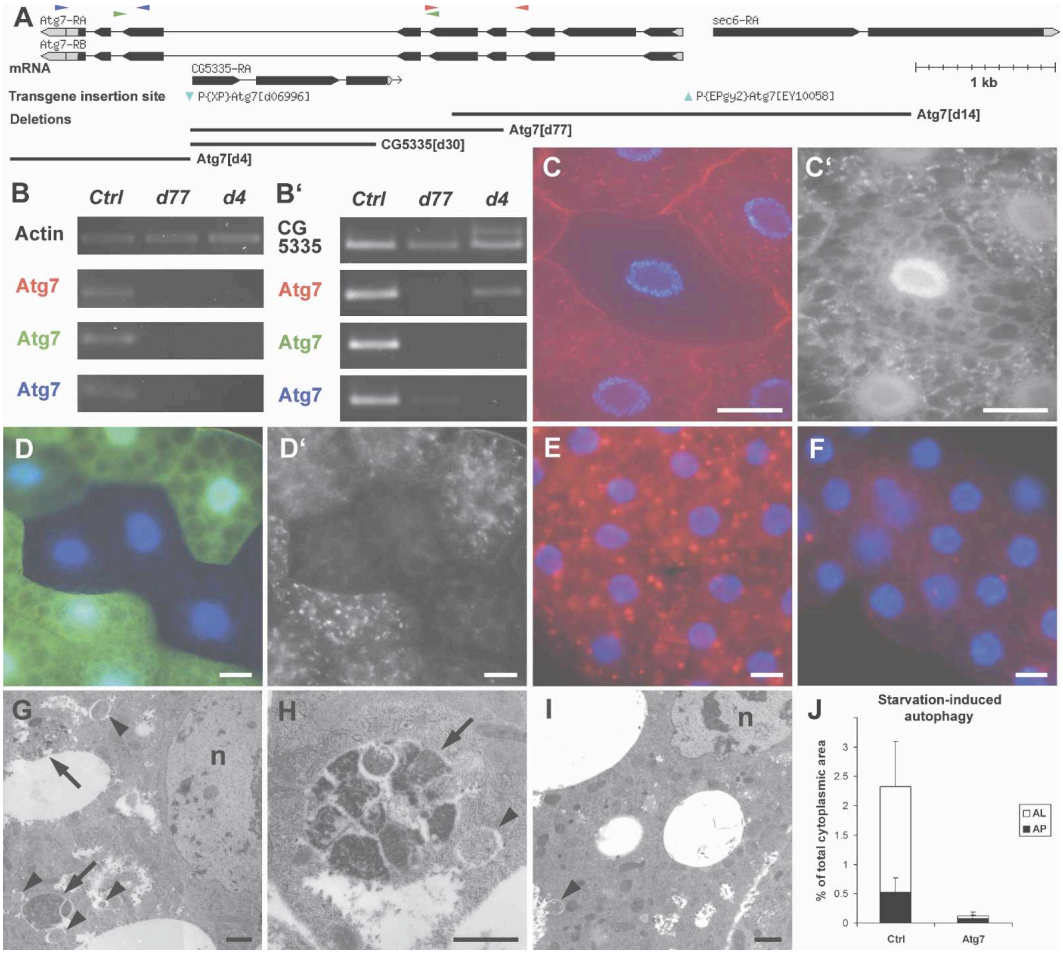


Figure 1. Atg7 is required for starvation-induced autophagy in the fat body. (*A*) The genomic region of *Atg7*. The two *P*-element insertions used to generate deletions (blue arrowheads), and four deletions are shown. (*B*,*B*′) *Atg7* mRNA expression was analyzed by RT–PCR in control and mutant third instar larvae. (*B*) No product is seen after 25 amplification cycles in *Atg7* mutants, indicating strongly reduced *Atg7* expression. (*B*′) Thirty cycles reveal the expression of C-terminal Atg7 sequences in $Atg7^{d77}$ and N-terminal sequences in $Atg7^{d4}$ larvae. As expected, deleted parts are not expressed in the mutants. See *A* for *Atg7* primer locations. (*C*–*D*′) Starvation-induced autophagy is severely impaired in $Atg7^{d4}$ mutant fat body clones, as shown by GFP-Atg8a labeling (*C*′) and Lysotracker Red staining (*D*′). Mutant cells are marked by lack of myrRFP (red, *C*) and GFP (green, *D*) expression, respectively. (*E*–*J*) $Atg7^{d77}$ larval fat bodies show a strongly reduced autophagy in response to starvation. Very little Lysotracker staining is seen in $Atg7^{d77}$ mutant fat bodies (*F*), while controls accumulate numerous Lysotracker-positive dots (*E*). Transmission EM reveals many autophagosomes (arrowheads) and autolysosomes (arrows) in control (*G*,*H*), but not in $Atg7^{d77}$ fat body cells following a 3-h starvation (*I*). *J* shows a morphometric evaluation of EM images. (AP) Autophagosome; (AL) autolysosome. Error bars represent standard deviation. Bars: *C*–*F*, 10 µm; *G*–*I*, 1 µm. (*B*,*E*,*G*,*H*,*J*) Control: $CG5335^{d30}/Atg7^{d14}$. (*B*) $Atg7^{d4}$: $Atg7^{d4}/Atg7^{d14}$. (*B*,*F*,*I*,*J*) $Atg7^{d77}$: $Atg7^{d77}/Atg7^{d14}$. (*C*) *FRT42D* $Atg7^{d4}$*/CgGAL4 UAS-GFP-Atg8a FRT42D UAS-myrRFP*. (*D*) *FRT42D* $Atg7^{d4}$*/UAS-2XeGFP FRT42D fb-GAL4*.

lethal deletions suggested that *Atg7* might not be an essential gene. This was confirmed by remobilization of a second *P*-element located in the intron between exons 6 and 7 of *Atg7*. None of the recovered 54 lines that lost this element were lethal. We identified three groups of deletions based on sequence data. The first group, represented by $Atg7^{d4}$, removed the last three exons of *Atg7*; the second group included deletions that removed most of *CG5335*, a gene located in the intron of *Atg7* as in the case of $CG5335^{d30}$; the third group consisted of deletions that completely removed *CG5335* and part of *Atg7*, as in the case of $Atg7^{d77}$, which lacks exons 5 and 6 and most of exon 4 (Fig. 1A). As these exons code for the E1-like domain of Atg7 that is required for its enzymatic activity, we concluded that $Atg7^{d77}$ is a likely null allele. As expected, the $Atg7^{d77}$ and $Atg7^{d4}$ deletions very strongly interfered with *Atg7* expression. No product could be detected by RT–PCR for the sequences removed by these deletions, respectively, and mRNA levels for the remaining portions were also very strongly reduced in both cases (Fig. 1B).

In the experiments below, we refer to $Atg7^{d77}/Atg7^{d14}$ animals as $Atg7^{d77}$ or simply *Atg7* mutants (homozygous mutant for *Atg7*, heterozygous for *Sec6* and *CG5335*), and we use flies of the genotype $CG5335^{d30}/Atg7^{d14}$ as control (heterozygous for *Atg7*, *Sec6*, and *CG5335*). Most tests were repeated using flies of the genotypes $Atg7^{d77}$*/Df(2R)Pu66* and $CG5335^{d30}$*/Df(2R)Pu66*, with similar results (Supplementary Table 1).

Atg7 is required for starvation-induced autophagy

To assess the role of fly Atg7 in autophagy, we stained larval fat bodies with Lysotracker Red, a vital dye used for the detection of acidic organelles including autolyso-

Downloaded from www.genesdev.org on December 4, 2007 - Published by Cold Spring Harbor Laboratory Press

somes. We also monitored the intracellular localization of GFP-Atg8a, a widely used marker of autophagosomes. In control animals, starvation leads to accumulation of both Lysotracker Red-positive vesicles and GFP-Atg8a-positive punctate structures (Scott et al. 2004). The number of such structures was severely reduced in $Atg7^{d4}$ homozygous mutant fat body cell clones (Fig. 1C,D). Similarly, starvation failed to induce punctate Lysotracker staining in fat bodies of $Atg7^{d77}$ mutant larvae (Fig. 1E,F).

We used transmission electron microscopy (EM) to quantify the autophagy defect seen in $Atg7^{d77}$ mutants. Following 3 h of starvation, many autophagosomes and autolysosomes were observed in control larval fat body cells (Fig. 1G,H). *Atg7* mutants exhibited a strong reduction of these autophagic structures (Fig. 1I). Morphometric analysis revealed that autophagosomes occupied 0.53% and autolysosomes 1.79% of the cytoplasm in controls, whereas the volume ratio was 0.08% and 0.04% in *Atg7* mutant fat body cells, respectively (Fig. 1J). Together, these results indicate that cells lacking Atg7 function are severely impaired in their ability to induce autophagy in response to starvation.

Atg7 is required for developmental autophagy in the larval midgut

At the onset of metamorphosis, autophagy is induced to high levels in larval tissues including the fat body, midgut, and salivary glands, and has been suggested to participate in the elimination of these tissues by programmed cell death events that take place during metamorphosis (Butterworth and Forrest 1984; Neufeld 2004; Penaloza et al. 2006). Accordingly, we observed numerous GFP-Atg8-positive punctate structures in the midgut gastric caeca of control larvae at the wandering stage, just prior to the onset of pupariation (Fig. 2A). *Atg7* mutant gastric caeca showed a strong decrease of GFP-Atg8 dots (Fig. 2B), confirming that Atg7 is required for developmental as well as starvation-induced autophagy. Our EM studies also showed numerous autophagosomes and autolysosomes in control larval midguts, and the number and size of these structures were strongly reduced in mutant cells (Fig. 2C,D). Morphometric analysis revealed that autophagosomes occupied 0.95% and autolysosomes 3.22% of the cytoplasm in controls, whereas the volume ratio was 0.17% and 0.42% in *Atg7* mutant midgut cells, respectively (Fig. 2E).

Loss of autophagy delays the death of larval midgut cells but causes no major developmental defects

We next asked whether the reduced autophagy in *Atg7* mutant midguts influences their elimination during metamorphosis. During the prepupal stage, the larval midgut shrinks and is shed into the lumen of the forming adult midgut. We observed neither major defects in adult epithelium formation nor elimination of the larval mid-

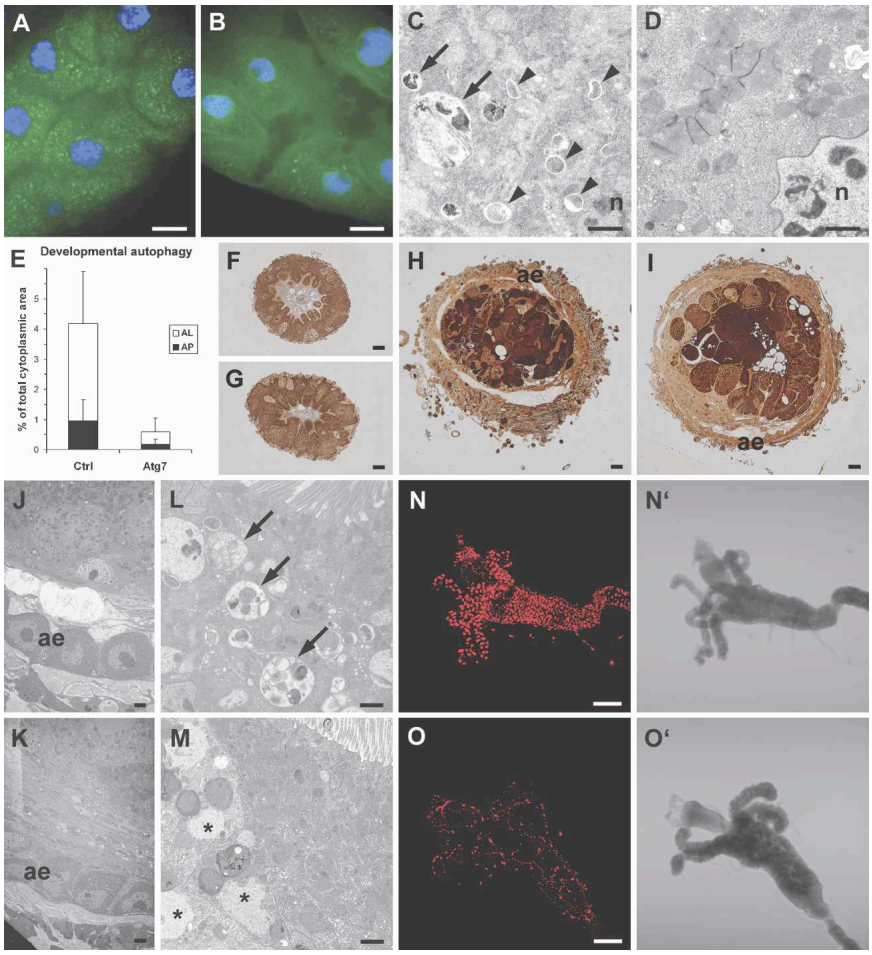


Figure 2. Atg7 is required for developmental autophagy and apoptotic DNA fragmentation in the midgut. (*A–E*) Developmental autophagy defects in $Atg7^{d77}$ mutant larval midguts. (*A*) Developmental autophagy results in punctate GFP-Atg8a localization in control midguts. (*B*) $Atg7^{d77}$ mutant midguts show a more uniform GFP-Atg8a signal with very few dots. Ultrastructural analysis reveals numerous autophagosomes and autolysosomes in control (*C*), but not in mutant midguts (*D*). *E* shows a morphometric evaluation of EM images; labels as in Figure 1. (*F–M*) Adult epithelium is formed normally in $Atg7^{d77}$ mutants during metamorphosis. (*F,G*) The larval midgut is composed mostly of large, polyploid cells, with intercalated small, diploid imaginal cells in control and mutant animals at the time of puparium formation (white prepupal stage). (*H–K*) The adult epithelium is formed from proliferating imaginal cells by 5 h RPF, accompanied by shortening and thickening of the entire midgut (note increased diameter in cross-section between *F–H* or *G–I*), and shedding of the larval cell layer into the lumen (dark cell masses in *H,I*). (*I*) Although appearing less condensed at this time, larval cells of *Atg7* mutants are also shed into the lumen. (*J,K*) Formation of the adult midgut epithelium (ae) proceeds normally in both control and mutant animals. Aberrant structures reminiscent of protein aggregates were seen in the apical area of mutant midgut cells at 5 h RPF (*M*), in the region where control cells accumulated numerous large autolysosomes (*L*). TUNEL staining of white prepupal midguts reveals defects in DNA fragmentation in dying $Atg7^{d77}$ larval cells (*O*), when compared with the robust nuclear staining seen in controls (*N*). Bars: *A,B,F–I*, 10 µm; *C,D,J–M*, 1 µm; *N,O*, 200 µm. (*A,C,E,F,H,J,L,N*) Control: $CG5335^{d30}/Atg7^{d14}$. (*B,D,E,G,I,K,M,O*) $Atg7^{d77}$: $Atg7^{d77}/Atg7^{d14}$.

Downloaded from www.genesdev.org on December 4, 2007 - Published by Cold Spring Harbor Laboratory Press

gut in *Atg7* mutants (Fig. 2F–K; see also Supplementary Fig. 1). Shrinkage and elimination of gastric caeca were similar in control and *Atg7* animals, and shedding of degenerating larval epithelium into the lumen of the forming adult midgut was completed by 16 h RPF (relative to puparium formation) as well (Supplementary Fig. 1). Interestingly, aberrant structures reminiscent of protein aggregates were observed in the apical region of mutant midgut cells at 5 h RPF, in the area where control cells accumulated numerous large autolysosomes (Fig. 2L,M).

Despite the apparently normal progression of midgut remodeling during metamorphosis, DNA fragmentation indicative of cell death that is readily detected in control midguts at the time of puparium formation was greatly reduced in *Atg7* mutants (Fig. 2N,O). In addition, we observed an ~4-h increase in the average time required to complete metamorphosis in *Atg7* mutants (Fig. 3A). Although modest, this extension of the pupal period was highly significant ($P < 10^{-20}$). We therefore conclude that normal levels of autophagy contribute to the timely progression through metamorphosis but are not essential for the extensive cell elimination and remodeling that occurs at this important stage of development.

Atg7 *mutants are hypersensitive to nutrient and oxidative stress and have a reduced life span*

As Atg7 mutants were fully viable (Supplementary Fig. 2A), we were able to investigate the role of autophagy in adult functions such as stress responses and aging. Under conditions of complete starvation or a sugar-only diet, *Atg7* mutants displayed an accelerated lethality compared with control flies (Fig. 3B,C), consistent with a conserved role for autophagy in promoting starvation survival by recycling cytoplasmic constituents. Previous studies in cultured mammalian cells have suggested that autophagy may protect against oxidative damage by targeting damaged macromolecules and organelles for elimination (Cuervo et al. 2005). To test whether autophagy contributes to oxidative stress resistance in an organismal context, we measured the survival of age-matched *Atg7* mutant and control flies treated with agents that induce oxidative stress. *Atg7* mutants were hypersensitive to paraquat treatments, dying at a two-fold faster rate than controls (Fig. 3D). Similar results were observed using hydrogen peroxide (Supplementary Fig. 2B). In addition, loss of *Atg7* resulted in a reduced life span under normal conditions (Fig. 3E; see Supplementary Table 2 for detailed statistical analysis of survival curves). *Atg7* mutant flies also displayed a significant age-dependent decline in climbing performance tests (Fig. 3F), an established measure of nervous system function (Martinez et al. 2007). Together, these results indicate the importance of autophagy in stress survival and longevity, potentially through elimination and recycling of damaged cellular components generated in response to induced oxidative stress or during normal aging, thus promoting constant cellular renewal.

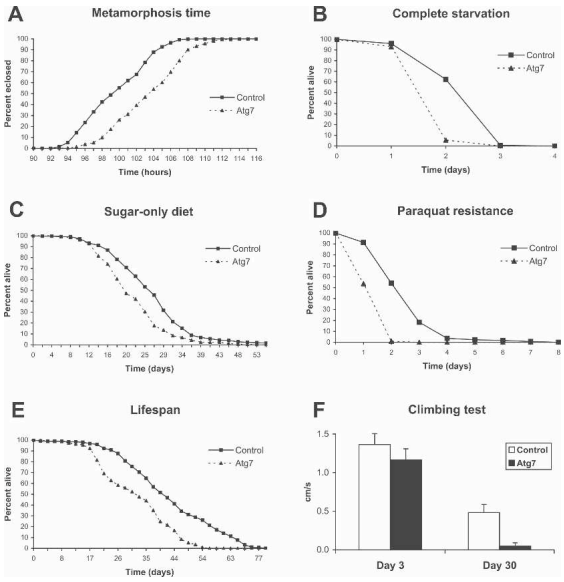


Figure 3. *Atg7* mutants show delayed metamorphosis, shorter life span, and stress sensitivity. $Atg7^{d77}$ mutants eclose later than age-matched controls (*A*), and emerging adults die faster than control flies on complete starvation (*B*) or if fed a sugar-only diet (*C*). (*D*) Including 30 mM paraquat in the medium to induce oxidative stress also kills mutants faster than controls. $Atg7^{d77}$ mutants show a reduced life span (*E*), and 30-d-old mutant flies score poorly in a climbing test relative to controls (–90.4% change, $P < 10^{-15}$), while they perform almost as well as control flies at day 3 (–14.6% change, $P = 0.00004$) (*F*). (All panels) Control: $CG5335^{d30}/Atg7^{d14}$; $Atg7^{d77}$: $Atg7^{d77}/Atg7^{d14}$.

Progressive neuronal degeneration in Atg7 *mutants*

The age-related decline of nervous system function in *Atg7* mutants suggested that the loss of autophagy in these flies leads to a neurodegenerative phenotype. Previous studies of *Atg5* and *Atg7* mutant mice reported an accumulation of ubiquitinated proteins and progressive neurodegeneration in these animals (Hara et al. 2006; Komatsu et al. 2006). We found that ubiquitinated proteins also accumulated in aged *Atg7* mutant fly head extracts, suggesting that protein aggregates form in the CNS (Fig. 4A). Ultrastructural analysis confirmed the presence of inclusion bodies in neurons of mutant, but not control fly brains (Fig. 4B,C). Immunoelectron microscopy further revealed that these aberrant structures are ubiquitin positive (Fig. 4D). The number of inclusion bodies increased over time in neurons of *Atg7* mutant brains: Larval neurons never contained such structures, whereas they were readily observed in 3-d-old adults, with the highest numbers in 30-d-old adults (Fig. 4E). Accumulation of these ubiquitin-positive aggregates was associated with a progressive neurodegeneration, as dead neurons were readily identified in *Atg7* mutant brains (Fig. 4F). Also, most brain cells of aged *Atg7* mutants showed extensive DNA fragmentation (Fig. 4H,J), whereas we observed no TUNEL labeling in controls (Fig. 4G,I). Neurodegeneration was also revealed by moderate vacuolization of 30-d-old mutant brains, compared with controls (Fig. 4K,L). As expected, we detected no DNA fragmentation in control or *Atg7* mutant brains at 3 d after eclosion (data not shown), but the presence of inclusion bodies in mutants may account for the slight decrease in climbing performance at this time. Interestingly, other tissues like indirect flight muscles were largely unaffected by the mutation, and overall ommatidial morphology was also similar to controls (Supplementary Fig. 3).

In conclusion, our findings indicate that normal levels

Downloaded from www.genesdev.org on December 4, 2007 - Published by Cold Spring Harbor Laboratory Press

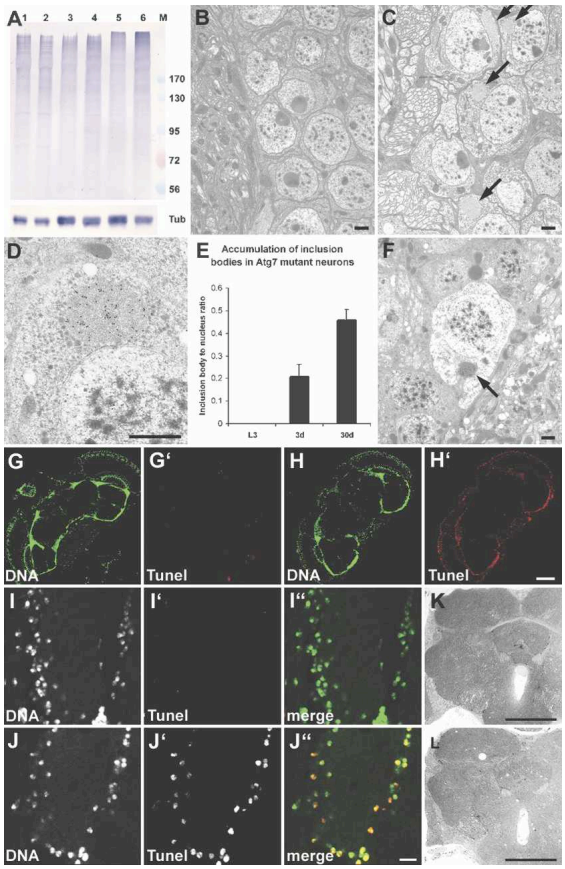


Figure 4. Ubiquitinated proteins accumulate in *Atg7* mutant brains, associated with progressive neurodegeneration. (*A*) A Western blot shows accumulation of ubiquitinated high-molecular-weight proteins in aging $Atg7^{d77}$ fly heads. No difference is seen between control (lane *1*) and mutant (lane *2*) late L3 larval samples. Accumulation of ubiquitinated proteins is already visible in 3-d-old $Atg7^{d77}$ adult head extracts (lane *4*, cf. control in lane *3*), and becomes very obvious by day 30 (lane *6*, cf. control in lane *5*). Numbers next to the marker (M) refer to molecular weights in kilodaltons. β-Tubulin is shown as a loading control. (*B–F*) Electron micrographs reveal the presence of inclusion bodies in 30-d-old $Atg7^{d77}$ (arrows in *C*), but not in control neurons (shown in *B*). (*D*) Immunoelectron microscopy confirms that these inclusion bodies contain ubiquitinated proteins. *E* shows progressive accumulation of aberrant protein aggregates in $Atg7^{d77}$ mutants: No inclusion bodies are seen in late third instar larval brains, while they appear in neurons of 3-d-old males, and further accumulate by age 30 d. (*F*) Dead neurons are readily identified in 30-d-old mutant brains, many still containing ubiquitin-positive inclusion bodies in the degenerating cytoplasm (arrow). (*G–J*) TUNEL staining of horizontal brain sections shows widespread DNA fragmentation in $Atg7^{d77}$ brains. (*H,J*) Most cells show DNA fragmentation in 30-d-old $Atg7^{d77}$ brains, (*G,I*) while no staining is seen in controls. Moderate vacuolization is seen in 30-d-old $Atg7^{d77}$ mutant brains (*L*), while no sign of degeneration is observed in controls (*K*). Bars: *B–F*, 1 µm; *I,J*, 10 µm; *G,H,K,L*, 150 µm. (*B,G,I,K*) Control: $CG5335^{d30}/Atg7^{d14}$. (*C,D,F,H,J,L*) $Atg7^{d77}$: $Atg7^{d77}/Atg7^{d14}$.

of autophagy are not required for viability in *Drosophila* and that the massive induction of autophagy that takes place during metamorphosis is not a prerequisite for the complex tissue rearrangements characteristic of this stage of development. These results also imply that lethality of previously described mutations in other *Drosophila* autophagy-related genes may stem from their roles in other essential processes. Consistent with this, we recently showed that the lethality of Atg1 mutants can be partially rescued by expression of a kinase-defective form of the Atg1 protein that inhibits starvation-induced autophagy (Scott et al. 2007), suggesting that one or more essential functions of Atg1 may be independent of autophagy. The identification of viable mutations in *Drosophila Atg8a* also supports this conclusion (Scott et al. 2007). Alternatively, the viability of *Atg7* mutants may reflect a less severe disruption or a qualitative difference in autophagy compared with other Atg mutants. Analysis of null mutations in additional Atg genes will further clarify this issue.

The role of autophagy in cell death has not been fully resolved. Although autophagy is generally considered a prosurvival cellular defense pathway, elevated levels of autophagy have been shown to cause cell death, at least under certain experimental conditions (Kroemer and Jaattela 2005; Pattingre et al. 2005; Scott et al. 2007). Our results provide in vivo evidence supporting a dual role for autophagy in cell death. During metamorphosis, extremely high autophagic activity in larval tissues such as the midgut epithelium precedes DNA fragmentation and cell death. Mutation of *Atg7* results in a marked decrease of autophagy and an inhibition of DNA fragmentation, suggesting that autophagy contributes to the normal cell death process in this case. As reported earlier, this cell death defect does not interfere with adult midgut epithelial development, which drives morphogenetic events during midgut reconstruction in *Drosophila* (Lee et al. 2002). In contrast to the case in these larval tissues, loss of Atg7 activity in the adult brain leads to DNA fragmentation and neuronal cell death, suggesting that autophagy acts to maintain neuronal health and prevent cell death in these cells. Our findings thus suggest that the net effect of autophagy on cell survival in vivo is dependent on both cell type and level of autophagic induction. Better understanding of the regulation of autophagy and identification of relevant substrates may provide new insight into neurodegenerative diseases and aging.

Materials and methods

P-element excisions and mutant fat body cell clones were generated as described earlier (Scott et al. 2007). Three- to five-day-old males were treated as follows: For complete starvation and the sugar-only diet, a paper towel soaked in water or 20% sucrose solution was placed in vials. Additional liquid was added as needed, and dead flies were counted daily. Paraquat or H_2O_2 was stirred into the food at a final concentration of 30 mM or 1%, respectively, and dead flies were counted daily. For life-span analysis, newly eclosed males were transferred to fresh food every 2–3 d, and dead flies were counted. Climbing assays were performed as described (Martinez et al. 2007). See the Supplemental Material for additional procedures.

Acknowledgments

We thank Sarolta Pálfia and Mariann Saródy for the excellent technical help, and BDSC and DSHB for providing flies and reagents. This work was supported by grants NIH RO1 GM62509 (to T.P.N.), MEDICHEM 1/047 NKFP, and RKC-06/OMFB-00598/2007 (to M.S.). G.J. is a Bólyai Fellow.

References

Butterworth, F.M. and Forrest, E.C. 1984. Ultrastructure of the preparative phase of cell death in the larval fat body of *Drosophila melanogaster*. *Tissue Cell* **16:** 237–250.

Downloaded from www.genesdev.org on December 4, 2007 - Published by Cold Spring Harbor Laboratory Press

Cuervo, A.M., Bergamini, E., Brunk, U.T., Droge, W., Ffrench, M., and Terman, A. 2005. Autophagy and aging: The importance of maintaining 'clean' cells. *Autophagy* **1:** 131–140.

Hara, T., Nakamura, K., Matsui, M., Yamamoto, A., Nakahara, Y., Suzuki-Migishima, R., Yokoyama, M., Mishima, K., Saito, I., Okano, H., et al. 2006. Suppression of basal autophagy in neural cells causes neurodegenerative disease in mice. *Nature* **441:** 885–889.

Klionsky, D.J., Cregg, J.M., Dunn Jr., W.A., Emr, S.D., Sakai, Y., Sandoval, I.V., Sibirny, A., Subramani, S., Thumm, M., Veenhuis, M., et al. 2003. A unified nomenclature for yeast autophagy-related genes. *Dev. Cell* **5:** 539–545.

Komatsu, M., Waguri, S., Ueno, T., Iwata, J., Murata, S., Tanida, I., Ezaki, J., Mizushima, N., Ohsumi, Y., Uchiyama, Y., et al. 2005. Impairment of starvation-induced and constitutive autophagy in Atg7-deficient mice. *J. Cell Biol.* **169:** 425–434.

Komatsu, M., Waguri, S., Chiba, T., Murata, S., Iwata, J., Tanida, I., Ueno, T., Koike, M., Uchiyama, Y., Kominami, E., et al. 2006. Loss of autophagy in the central nervous system causes neurodegeneration in mice. *Nature* **441:** 880–884.

Kroemer, G. and Jaattela, M. 2005. Lysosomes and autophagy in cell death control. *Nat. Rev. Cancer* **5:** 886–897.

Lee, C.Y., Simon, C.R., Woodard, C.T., and Baehrecke, E.H. 2002. Genetic mechanism for the stage- and tissue-specific regulation of steroid triggered programmed cell death in *Drosophila*. *Dev. Biol.* **252:** 138–148.

Martinez, V.G., Javadi, C.S., Ngo, E., Ngo, L., Lagow, R.D., and Zhang, B. 2007. Age-related changes in climbing behavior and neural circuit physiology in *Drosophila*. *Dev. Neurobiol.* **67:** 778–791.

Mathew, R., Kongara, S., Beaudoin, B., Karp, C.M., Bray, K., Degenhardt, K., Chen, G., Jin, S., and White, E. 2007. Autophagy suppresses tumor progression by limiting chromosomal instability. *Genes & Dev.* **21:** 1367–1381.

Murthy, M., Ranjan, R., Denef, N., Higashi, M.E., Schupbach, T., and Schwarz, T.L. 2005. Sec6 mutations and the *Drosophila* exocyst complex. *J. Cell Sci.* **118:** 1139–1150.

Neufeld, T.P. 2004. Role of autophagy in developmental cell growth and death: Insights from *Drosophila*. In *Autophagy* (ed. D.J. Klionsky), pp. 224–232. Landes Bioscience, Georgetown, TX.

Ogura, K. and Goshima, Y. 2006. The autophagy-related kinase UNC-51 and its binding partner UNC-14 regulate the subcellular localization of the Netrin receptor UNC-5 in *Caenorhabditis elegans*. *Development* **133:** 3441–3450.

Pattingre, S., Tassa, A., Qu, X., Garuti, R., Liang, X.H., Mizushima, N., Packer, M., Schneider, M.D., and Levine, B. 2005. Bcl-2 antiapoptotic proteins inhibit Beclin 1-dependent autophagy. *Cell* **122:** 927–939.

Penaloza, C., Lin, L., Lockshin, R.A., and Zakeri, Z. 2006. Cell death in development: Shaping the embryo. *Histochem. Cell Biol.* **126:** 149–158.

Scott, R.C., Schuldiner, O., and Neufeld, T.P. 2004. Role and regulation of starvation-induced autophagy in the *Drosophila* fat body. *Dev. Cell* **7:** 167–178.

Scott, R.C., Juhasz, G., and Neufeld, T.P. 2007. Direct induction of autophagy by atg1 inhibits cell growth and induces apoptotic cell death. *Curr. Biol.* **17:** 1–11.

Tomoda, T., Kim, J.H., Zhan, C., and Hatten, M.E. 2004. Role of Unc51.1 and its binding partners in CNS axon outgrowth. *Genes & Dev.* **18:** 541–558.

Zhou, X., Babu, J.R., da Silva, S., Shu, Q., Graef, I.A., Oliver, T., Tomoda, T., Tani, T., Wooten, M.W., and Wang, F. 2007. Unc-51-like kinase 1/2-mediated endocytic processes regulate filopodia extension and branching of sensory axons. *Proc. Natl. Acad. Sci.* **104:** 5842–5847.

dc_840_14 Cell Death and Differentiation (2007), 1–10
© 2007 Nature Publishing Group All rights reserved 1350-9047/07 $30.00
www.nature.com/cdd

Gene expression profiling identifies FKBP39 as an inhibitor of autophagy in larval *Drosophila* fat body

G Juhász*[,1,2], LG Puskás[3], O Komonyi[4], B Érdi[1], P Maróy[4], TP Neufeld[2] and M Sass[1]

In *Drosophila*, the fat body undergoes a massive burst of autophagy at the end of larval development in preparation for the pupal transition. To identify genes involved in this process, we carried out a microarray analysis. We found that mRNA levels of the homologs of Atg8, the coat protein of early autophagic structures, and lysosomal hydrolases were upregulated, consistent with previous results. Genes encoding mitochondrial proteins and many chaperones were downregulated, including the inhibitor of eIF2alpha kinases and the peptidyl-prolyl *cis–trans* isomerase FK506-binding protein of 39 kDa (FKBP39). Genetic manipulation of FKBP39 expression had a significant effect on autophagy, potentially through modulation of the transcription factor Foxo. Accordingly, we found that Foxo mutants cannot properly undergo autophagy in response to starvation, and that overexpression of Foxo induces autophagy.
Cell Death and Differentiation advance online publication, 16 March 2007; doi:10.1038/sj.cdd.4402123

Autophagy is the degradation of self material by lysosomes. As a primary cellular defense response, it is activated by nitrogen or amino-acid starvation from yeast to mammals, and promotes the survival of the cell or organism by recycling dispensable cellular constituents for re-use in synthetic processes. The morphology of the major pathway is well known for decades by electron microscopical studies.[1] In response to starvation or other stimuli, a membranous sac called isolation membrane forms and engulfs portions of the cytosol. After sealing of its edges, the emerging double-membrane organelle is referred to as an autophagosome. Upon fusion with a lysosome an autolysosome is formed, where degradation of the sequestered material takes place. The process of autophagy is remarkably similar in all eukaryotic organisms, suggesting the involvement of an evolutionary conserved set of genes. Indeed, functional homologs of most *Atg* (autophagy-related) genes required for autophagy in yeast were found in multiple species including plants, worms, flies, and mammals.[2] Despite the conservation of the core mechanism, there must be changes in the regulation of autophagy among different phyla, as it is involved in various cellular processes in multicellular animals. In addition to its fundamental role in starvation survival, autophagy is thought to be involved in cell death, neurodegeneration diseases, aging, immunity, growth, and cancer.[1,3,4]

In *Drosophila* and other insects undergoing complete metamorphosis, the larval fat body acts as a store of proteins and other materials, which are released through autophagy to provide energy and nutrients during metamorphosis and early adulthood.[5–8] The fat body, an analog of the human liver, is a polytenic tissue that grows in mass approximately 200-fold in feeding *Drosophila* larvae during the larval stages. After reaching an optimal mass, mature larvae stop eating and wander away from the food to find a suitable place for pupariation. At this time, the fat body undergoes a massive induction of autophagy, known as developmental autophagy. These changes are induced by the insect molting hormone ecdysone at a low concentration of juvenile hormone.[9] Recent results showed that ecdysone induces autophagy through downregulation of phosphatidyl-inositol 3-kinase (PI3K) signaling.[10]

A central regulator of cell growth and autophagy is target of rapamycin (Tor) kinase. Inhibition of Tor activity rapidly results in growth arrest and induction of autophagy, which involves multiple phosphorylation and dephosphorylation events.[11–13] In yeast, the phosphorylation state of a number of Atg proteins is rapamycin-sensitive, and the activity of the kinase Atg1 is regulated by Tor signaling.[14] Another regulatory mechanism is the induction of genes necessary for autophagy, or repression of genes that normally inhibit the process. It is known that the gene encoding Atg8, a ubiquitin-like coat protein for autophagosomes, is upregulated in starved yeast cells[15] and *Drosophila* larvae.[16]

To search for genes regulated during developmental autophagy, we carried out a microarray analysis by comparing the transcriptional profiles of fat bodies dissected from feeding and wandering third instar larvae. This analysis both demonstrated evolutionary conservation and identified additional genes with previously unknown roles in autophagy. Further

[1]Department of General Zoology, Eötvös Loránd University, Budapest, Hungary; [2]Department of Genetics, Cell Biology, and Development, University of Minnesota, Minneapolis, MN, USA; [3]Laboratory of Functional Genomics, Biological Research Center, Szeged, Hungary and [4]Department of Genetics and Molecular Biology, University of Szeged, Szeged, Hungary
*Correspondening author: G Juhász, Department of GCD, University of Minnesota, 6-160 Jackson Hall 321 Church Street S.E., Minneapolis, MN 55455, USA. Tel: +612 626 5217; Fax: +612 626 5652; E-mail: juhas001@umn.edu
Keywords: autophagy; *Drosophila*; FKBP39; foxo; microarray
Abbreviations: dIPK, *Drosophila* inhibitor of protein kinases; FKBP39, FK506-binding protein of 39 kDa; JNK, Jun N-terminal kinase; PI3K, phosphatidyl-inositol 3-kinase; Ppiase, peptidyl-prolyl *cis-trans* isomerase; QRT-PCR, quantitative real-time polymerase chain reaction; RT-PCR, reverse transcription polymerase chain reaction; Tor, target of rapamycin
Received 03.11.05; revised 18.1.07; accepted 08.2.07; Edited by E Baehrecke

characterization of a selected subset of genes in transgenic animals identified FK506-binding protein of 39 kDa (FKBP39) as an inhibitor of autophagy, which effect is likely mediated through modulation of the transcription factor Foxo.

Results

Microarray analysis of transcriptional changes during developmental autophagy. To assess gene expression changes during developmental autophagy in *Drosophila* larvae, we manually dissected fat bodies before and after the developmental induction of autophagy from feeding (60 h after hatching from the egg, Figure 1a) and wandering (84 h after hatching from the egg, Figure1b and e) larvae.[6,7] Samples were processed and cDNAs were hybridized to a microarray containing 3200 annotated *Drosophila* cDNAs.[17] About 1941 of the 3200 genes investigated were expressed in the fat body. Table 1 shows the 57 genes induced by 1.65-fold or greater (estimated *P*-value <0.025) during autophagy. The mRNA level of the eye pigment biosynthesis gene *Hn* was increased, consistent with the known role of the fat body in that process during the wandering stage.[18] A gene encoding Fbp2, a storage protein, was also induced; together these results provide a control for the proper developmental timing of our sample collection. Genes encoding putative lysosomal hydrolases (α-EST2, cathD, CG5932, CG1827, CG10992, CG1774) were upregulated, consistent with the expansion of the lysosomal compartment during autophagy. Ten of the 16 fly *Atg* gene homologs were represented on our chip, and only *CG32672/Atg8a* was induced significantly, in accordance with yeast and previous fly data.[1,16] A gene encoding another ubiquitin-like protein of unknown function (CG7224) was also upregulated.

The expression of 39 genes was significantly downregulated. Among them, two main subgroups could be identified: genes encoding mitochondrial proteins (CG17896, CG9140, ND42, CG6459, TRAP1, CG10664, Hsc70-5, CG2249, mRpL24, Marf) and cellular chaperones (CG8286/ *Drosophila* inhibitor of protein kinases (dIPK), CG4164, TRAP1, Hsc70-5, FKBP39). The expression level of *Baldspot*, encoding a transmembrane protein, also strongly decreased (Table 2).

Quantitation of expressional changes for a selected subset of genes. A subset of genes potentially involved in autophagy was selected for further analysis by quantitative real-time polymerase-chain reaction (QRT-PCR) to confirm and more precisely quantitate the changes in mRNA expression levels. We also analyzed expression of a few genes not represented on our chip, including *Tor*, *CG12334/Atg8b*, and *CG15283*, which encodes a ubiquitin-like protein highly similar to CG7224.

As shown in Table 3, these data well correlated with the results of the microarray analysis, and further confirmed the strong upregulation of both Atg8 homologs (*CG32672/Atg8a*: 6.96 $\times$ and *CG12334/Atg8b*: 3.53 $\times$) and cathepsin D (*CG1548*: 2.14 $\times$), a well-known lysosomal hydrolase. The two ubiquitin-related genes we tested were also induced (*CG7224*: 3.73 $\times$ and *CG15283*: 4.62 $\times$). Tor mRNA level did not change, whereas genes encoding the cellular chaperones FKBP39,[19] CG8286/dIPK,[20] and Baldspot[21] were strongly repressed (*FKBP39*: 6.73 $\times$, *CG8286/dIPK*: 4.92 $\times$, and *Baldspot*: 9.91 $\times$ repression).

Analysis of candidate autophagy-related genes in transgenic animals identified FKBP39 as an inhibitor of autophagy. To establish the role of selected genes regulated in autophagy, we carried out overexpression studies using the Gal4-UAS system. Overexpression of most genes we tested (cathD, Atg8a, Baldspot, and dIPK) produced various phenotypes with different Gal4 drivers (Supplementary Table 1), but neither induced nor inhibited autophagy (not shown).

In contrast to these results, fat body-specific overexpression of FKBP39, a peptidyl-prolyl *cis–trans* isomerase (PPiase) had a dramatic effect on developmental autophagy.

Figure 1 Overexpression of FKBP39 inhibits developmental and starvation-induced autophagy, whereas loss of *FKBP39* function leads to higher than wild-type induction of autophagy. (**a–c**) Lysotracker staining of fat bodies. No Lysotracker staining is seen in feeding early third instar larvae (**a**), whereas Lysotracker-positive granules (shown in red) accumulate in fat body cells of wandering late third instars (**b**). Overexpression of FKBP39 in the fat body inhibits the formation of Lysotracker-positive granules (**c**), and leads to an inhibition of cell growth. This effect is best seen by cortical actin staining (red) of fat bodies clonally overexpressing FKBP39, marked by co-overexpression of nuclear GFP (green) (**d**, top panel). Lower panel shows DNA staining. Note that the nuclei of FKBP39-overexpressing cells (green arrows) are of the same size but contain less DNA than surrounding wild-type cells (blue arrows). (**e** and **f**) Electron microscopic images show fat body cells of late third instar larvae. Developmental autophagy results in the accumulation of large autolysosomes in wild-type larvae (arrow in **e**; cytoplasmic dark blue granules in the inset), whereas only small autolysosomes are seen in FKBP39-overexpressing fat body cells of the same age (arrows in **f**). Note the greatly enlarged nucleolus (asterisk) in the nucleus (N) in **f**, also caused by the overexpression of FKBP39. Insets show toluidine blue staining of semi-thick sections. Again, note the greatly enlarged nucleoli (dark blue) in nuclei (arrowheads) in (**f**). (**g**) Quantitation of Lysotracker data on developmental autophagy is shown. Asterisk marks a significant change ($P<0.001$). (**h–j**) Lysotracker staining of fat bodies. Autophagy in fat body cells of early third instar larvae, induced by a 4-h starvation (**h**, compare to **a**). Fat body-specific overexpression of FKBP39 also blocks this starvation response (**i**). Co-overexpression of PTEN restores autophagy inhibited by FKBP39 (**j**). (**k**) Quantitation of Lysotracker data is shown. Asterisk and double asterisks mark significant differences ($P<0.001$ for columns 1-2, 2-3, 1-3). (**l**) RT-PCR of fat body samples dissected from control feeding larvae (lane 1), $FKBP39^{5\text{-}HA-2440}$ mutants (lane 2), and a precise excision line $FKBP39^{exA3}$ (lane 3). *FKBP39* expression is reduced in larval fat bodies of the mutants, but precise excision of the P-element restores wild-type mRNA expression (top panel). Bottom panel shows RT-PCR for actin as a control. (**m–o**) Lysotracker staining of fat bodies. Short, 80-min starvation induces higher levels of autophagy in fat bodies of $FKBP39^{5\text{-}HA-2440}$ mutant larvae than in wild-type controls (**n**, compare with **m**). Starvation response is restored to wild-type levels in the precise excision line $FKBP39^{exA3}$ (**o**). (**p**) Quantitation of the results is shown. Asterisk marks a significant change ($P=0.006$ for columns 1 and 2, $P<0.001$ for columns 2 and 3, $P=0.27$ for columns 1–3). Panels a–d, h–j and m–o are of the same magnification ($\times$ 200). Panels e and f are of the same magnification and bars equal 1 μm for electron microscopical images, 10 μm for insets. Error bars represent standard deviation in panels g, k and p. Genotypes: UASFKBP39/+ (**a**, **b**, **e**, **h**), cgGal4/UASFKBP39 (**c**, **f**, **i**), hsFLP; UASFKBP39/+; Act>CD2>Gal4, UASGFPnls/+ (**d**), cgGal4/UASFKBP39, UASPTEN (**j**), Df(3R)Exel6194/TM6 (**m**), $FKBP39^{5\text{-}HA-2440}$/Df(3R)Exel6194 (**n**), $FKBP39^{exA3}$/Df(3R)Exel6194 (**o**). For panel l, genotypes are identical to panels m–o, respectively

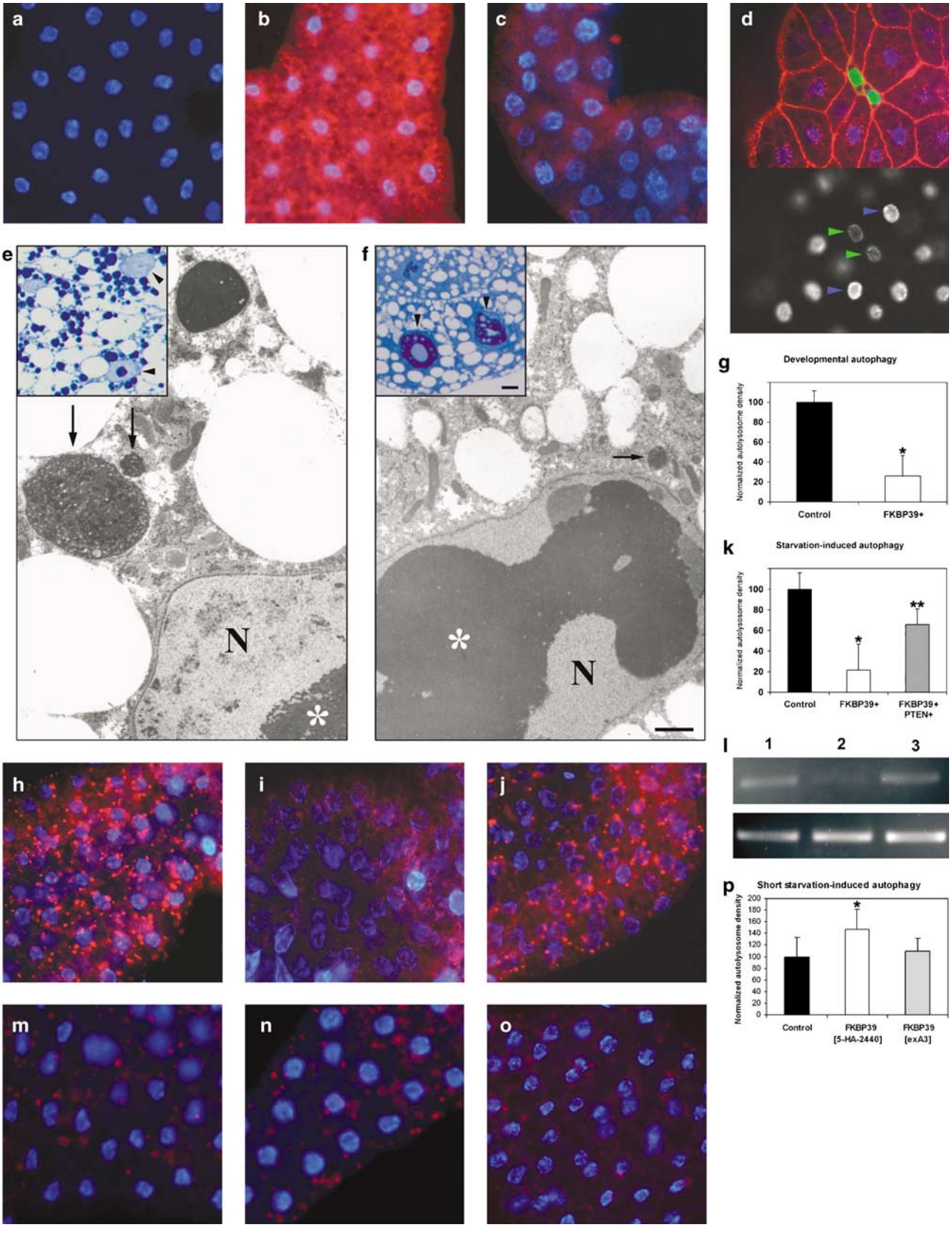

a
b
c
d
e
f
N
N
g
Developmental autophagy
Normalized autolysosome density
Control
FKBP39+
k
Starvation-induced autophagy
Normalized autolysosome density
Control
FKBP39+
FKBP39+ PTEN+
l
1
2
3
h
i
j
m
n
o
p
Short starvation-induced autophagy
Normalized autolysosome density
Control
FKBP39 [5-HA-2440]
FKBP39 [exA3]

Table 1 Genes upregulated during developmental autophagy in the *Drosophila* larval fat body

Gene name	Fold change	Function/family/domains	*P*-value
Cyp9f2	3.95	Oxidoreductase (cytochrome P450)	<0.0001
Cutlet	3.54	Serine-type endopeptidase	<0.0001
Fbp2	3.08	Nutrient reservoir; oxidoreductase	<0.0001
Alpha-Est2	2.77	Carboxylesterase	<0.0001
CG7224	2.73	Ubiquitin-like	<0.0001
Gs1	2.53	Glutamate synthase	0.0002
CG12262	2.52	Acyl-CoA dehydrogenase	0.0002
CathD	2.29	Cathepsin D	0.0007
Reg-2	2.28	Haloacid dehydrogenase-like hydrolase	0.0007
CG9431	2.16	Immunoglobulin-like	0.0014
CG6440	2.16	Neuropeptide hormone	0.0014
Syt	2.16	Calcium-dependent phospholipid binding	0.0015
CG18418	2.14	Membrane carrier	0.0016
CG6957	2.14	Glucoseamine-6-phosphate deaminase	0.0017
Cyp4d2	2.12	Oxidoreductase (cytochrome P450)	0.0018
CG7523	2.12	Unknown	0.0018
l(2)k09913	2.11	Unknown	0.0019
Hn	2.06	Eye pigment biosynthesis	0.0026
CG15309	2.06	Yippee-like protein	0.0026
CG12428	2.02	Acetyltransferase	0.0034
CG5932	1.99	Triacylglycerol lipase	0.0039
Cry	1.97	G-protein coupled photoreceptor activity	0.0045
CG1827	1.97	Aminohydrolase	0.0046
CG13603	1.94	Unknown	0.0053
CG30053	1.91	Unknown	0.0061
CG12323	1.91	Endopeptidase (proteasome b5 subunit)	0.0061
CG9813	1.90	Unknown	0.0065
CG7221	1.90	Oxidoreductase	0.0066
CG18787	1.89	Unknown	0.0069
CG4600	1.89	Acetyl-CoA acyltransferase	0.0071
Paip2	1.88	Translational repression	0.0073
CG8252	1.88	Unknown	0.0075
Atg8a	1.86	Coat protein for autophagosomes	0.0083
CG2767	1.86	Alcohol dehydrogenase	0.0084
Keren	1.84	Epidermal growth factor	0.0094
CG12292	1.84	Unknown	0.0095
CG5738	1.84	RNA polymerase II transcription factor	0.0097
Pdh	1.83	Photoreceptor dehydrogenase	0.0101
CG17597	1.82	Acyl-CoA C-acyltransferase	0.0108
CG4669	1.77	Unknown	0.014
CG10007	1.77	Unknown	0.0144
CG1236	1.76	Phosphoglycerate dehydrogenase	0.0149
CG9286	1.76	Unknown	0.015
Trn-SR	1.74	Nuclear import	0.0163
FucT6	1.73	Fucosyltransferase	0.0178
CG10992	1.73	Cathepsin B	0.0179
CG7789	1.72	Phosphatidylinositol phosphatase	0.0182
CG10433	1.72	Defense response	0.0187
CG32698	1.71	Carbonate dehydratase	0.0191
CG12428	1.71	Acetyltransferase	0.0194
CG8449	1.71	Unknown	0.0196
Ote	1.71	L-amino-associated polypeptide 2	0.02
CG14629	1.70	Unknown	0.0202
Fng	1.70	Glycosyltransferase	0.0202
CG1774	1.70	Lipid hydrolase	0.0206
CG12063	1.69	Endoglin/CD105 antigen, PAN domains	0.0215
CG5721	1.68	Unknown	0.023

The genes upregulated by at least 1.65-fold during developmental autophagy, are shown with an estimated *P*-value of <0.025. In the first column, gene names are listed as in Flybase (21); second column shows fold induction relative to early third instars (before the onset of autophagy); and third column shows the function, family or known domains of the genes listed

Very few autolysosomes were observed in fat body cells of wandering larvae overexpressing FKBP39, and these were also smaller than in wild-type animals (Figure 1c, f and g). Interestingly, FKBP39 overexpression also inhibited cell growth. The average size of fat body cells overexpressing FKBP39 was $43\pm21\%$ of wild-type neighboring cells (Figure 1d). The overexpressing cells also had a lower DNA content, suggesting a delay in endoreduplication. The fact that nuclei were about the same size as nuclei of wild-type cells is probably owing to the greatly enlarged nucleolus (Figure 1d and f).

We next tested if overexpression of FKBP39 had an effect on starvation-induced autophagy. Starving feeding larvae for 4 h in sucrose solution results in strong accumulation of Lysotracker-positive autolysosomes in larval fat body cells[13] (Figure 1h). Overexpression of FKBP39 in the fat body greatly

Table 2 Genes downregulated during developmental autophagy in the *Drosophila* larval fat body

Gene name	Fold change	Function/family/domains	*P*-value
Baldspot	−4.69	Transmembrane protein	<0.0001
CG17896	−2.73	Methylmalonate-semialdehyde dehydrogenase	<0.0001
CG3835	−2.71	Oxidoreductase	<0.0001
CG14683	−2.56	Methyltransferase	0.0001
CG5171	−2.37	Trehalose-phosphatase	0.0003
CG9140	−2.37	NADH dehydrogenase (ubiquinone)	0.0003
Nop56	−2.15	Small nuclear ribonucleoprotein complex subunit	0.0011
CG8286	−2.15	*Drosophila* inhibitor of protein kinases (dIPK)	0.0011
CG4164	−2.10	Hsp40	0.0015
CG10340	−2.08	Possibly involved in protein complex assembly	0.0017
ND42	−2.08	NADH dehydrogenase (ubiquinone)	0.0017
CG6459	−2.00	Mitochondrial glycoprotein	0.0027
CG3136	−1.97	Basic leucine zipper (bZIP) transcription factor	0.0033
TRAP1	−1.95	Mitochondrial Hsp90	0.0038
CG6164	−1.92	Unknown	0.0044
CG9249	−1.92	Methyltransferase	0.0045
CG18316	−1.89	Unknown	0.0055
CG10664	−1.89	Cytochrome-*c* oxidase	0.0055
Ate1	−1.87	Arginyltransferase	0.0062
Yip7	−1.86	Serine-type endopeptidase	0.0065
CG8732	−1.85	Acetate-CoA ligase	0.0069
Hsc70-5	−1.82	Mitochondrial Hsp70	0.0083
CG15771	−1.81	Unknown	0.0087
CG11597	−1.80	Protein serine/threonine phosphatase (PP2A-like)	0.0092
CG3358	−1.78	Nuclease	0.0104
CG2249	−1.77	Cytochrome-*c* oxidase	0.0107
Tm1	−1.76	Tropomyosin	0.0114
Sc2	−1.75	Unknown	0.0123
CG17278	−1.74	Protease inhibitor	0.0126
CG8664	−1.73	Unknown	0.0137
Jon65Aiii	−1.71	Serine-type endopeptidase	0.0151
mRpL24	−1.69	Mitochondrial large ribosomal subunit	0.017
Marf	−1.69	GTPase and dynamin domains	0.0172
CG3902	−1.69	Acyl-CoA dehydrogenase	0.0175
Cyp310a1	−1.68	Oxidoreductase (cytochrome p450)	0.0186
His2Av	−1.68	DNA binding (histone)	0.0187
EIF-4G	−1.67	Translation initiation factor	0.0198
FKBP39	−1.66	Peptidyl-prolyl *cis–trans* isomerase (PPiase)	0.0208
CkIIalpha	−1.66	Caseine kinase	0.021

The list of genes downregulated by at least 1.65-fold during developmental autophagy with an estimated *P*-value of <0.025 (see legend of Table 1 for details)

Table 3 Quantitative real-time PCR analysis of the expression of a selected set of genes during developmental autophagy

Gene	Microarray	QRT-PCR
Atg8a	1.86	6.96
CG15283	Not on chip	4.62
CG7224	2.73	3.73
Atg8b	Not on chip	3.53
CathD	2.29	2.14
Tor	Not on chip	No change
CG8286/dIPK	−2.15	−4.92
FKBP39	−1.66	−6.73
Baldspot	−4.69	−9.91

QRT-PCR analysis was used to confirm and further quantitate the expression changes seen in the microarray experiment, and also to analyze genes not physically represented on our chip. Gene names are listed in the first column; second column shows fold change based on the microarray experiment; and third column shows fold change based on QRT-PCR. See text for details

inhibited the induction of autophagy in starved animals (Figure 1i and k), similar to the case of developmental autophagy.

As a final verification, we then tested how loss of *FKBP39* function influences autophagy using the hypomorphic mutant lines $FKBP39^{5\text{-}HA-2440}$ and $FKBP39^{5\text{-}HA-2590}$, isolated in the DrosDel project.[22] Both lines harbor a P-element insertion 49 nucleotides upstream of the translation start codon, in the 5′ non-translated region of *FKBP39*.[21] As expected from the insertion data, these two mutant lines behaved indistinguishable in all of our tests, therefore only data on $FKBP39^{5\text{-}HA-2440}$ is shown here (see Supplementary Figure 1 for data on $FKBP39^{5\text{-}HA-2590}$). Mutant larvae exhibited a strong reduction of *FKBP39* expression, as analyzed by reverse transcription-polymerase chain reaction (RT-PCR) in dissected larval fat bodies (Figure 1l) and in whole adult flies (Supplementary Figure 1a). The mutants are viable and fertile, and show no obvious developmental abnormality or delay. Although we were unable to observe ectopic induction of autophagy in different larval tissues of these animals (not shown), we found that mutant larvae displayed a significantly higher level of autophagy than wild-type controls in response to a short, 80-min starvation (Figure 1m, n and p). Precise excision of the P-element ($FKBP39^{exA3}$) restored wild-type mRNA levels in larval fat bodies (Figure 1l) and in whole adult flies (Supplementary Figure 1a), and reverted the autophagy phenotype seen in the mutants (Figure 1o).

Co-overexpression of PTEN restores autophagy inhibited by FKBP39. To identify the signal transduction pathway FKBP39 may act through, we tested several signaling cascades that were previously reported to be

influenced by FKBPs.[23,24] Modulation of Ras (by overexpressing wild-type, hyperactive or dominant-negative Ras or wild-type Raf), protein kinase A (by overexpressing wild-type PKAc or its inhibitors PKI or mutant PKAr), or S6 kinase (by overexpressing hyperactive S6K) signaling had no effect on developmental autophagy, and did not restore autophagy in FKBP39-overexpressing fat bodies, as analyzed by Lysotracker staining (not shown). As Ras signaling was suggested to be involved in the induction of autophagy in other systems, and FKBP39 inhibited the Ras-mediated activation of MAPK (Supplementary Figure 2a), we analyzed autophagy by generating loss of function somatic clones of a *Ras* null mutation in the fat body. Although slightly smaller than surrounding wild-type cells, these cells showed normal induction of developmental autophagy (Supplementary Figure 2b), proving that Ras itself is not required for autophagy in this tissue.

In contrast to the above results, overexpression of PTEN, a phosphatase that antagonizes class I PI3K signaling, partially restored starvation-induced autophagy in FKBP39-expressing fat body cells (Figure 1j and k). Unfortunately, we could not test developmental autophagy in this case, as simultaneous expression of these two genes in the fat body led to a prolonged third instar stage and ultimately lethality, potentially owing to the cumulative growth-inhibiting effects of the two proteins.

The autophagy-inhibiting effect of FKBP39 is likely mediated by inhibition of Foxo, a novel regulator of autophagy. The above results suggested that FKBP39 may inhibit autophagy through activation of PI3K, a potent inhibitor of both starvation-induced and developmental autophagy.[10,13] To test this, we analyzed the level of PI3K signaling in FKBP39-overexpressing clones. GFP-pleckstrin homology (PH) domain fusion proteins are well-established markers of PI3K activity.[25] In cells with high levels of PI3K activity, accumulation of the membrane lipid phosphatidylinositol-3,4,5-phosphate results in localization of the GFP-PH marker to the cell membrane. We found that FKBP39 overexpression led to a reduction of membrane *versus* cytoplasmic ratio of the signal compared to surrounding wild-type cells (Figure 2a). This result indicates that PI3K activity is reduced in FKBP39-overexpressing cells, thus discounting the possibility that FKBP39 inhibits autophagy by upregulating PI3K signaling.

As another potential measure of PI3K signaling, we also examined the localization of the transcription factor Foxo in FKBP39 overexpressing clones. Elevated PI3K signaling results in phosphorylation of Foxo by the serine/threonine kinase Akt.[26] In response to this phosphorylation event, Foxo changes its intracellular localization: the nuclear pool translocates to the cytoplasm.[26] Wild-type mid-third instar fat body cells displayed a moderate level of nuclear Foxo.

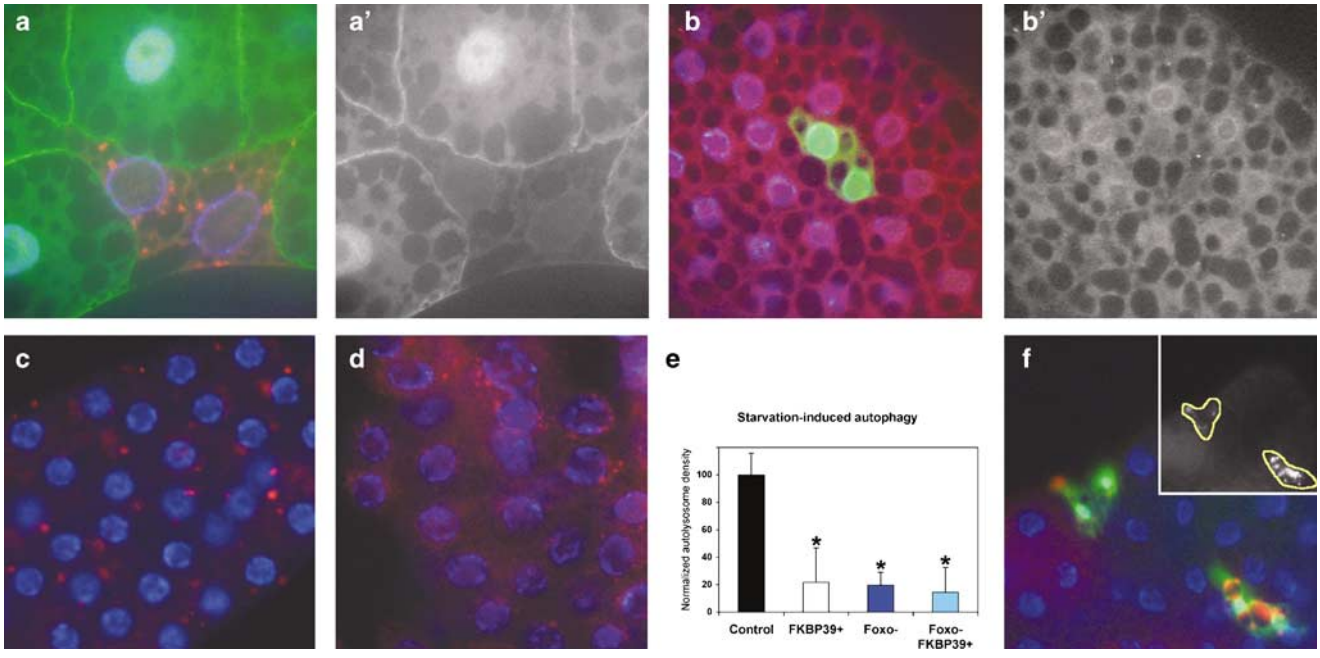


Figure 2 The autophagy-inhibiting effect of FKBP39 overexpression is potentially mediated by inhibition of Foxo. (**a**) The membrane localization of a probe used as an indicator of PI3K activity (GFP-PH, green) is greatly reduced compared to the cytoplasmic signal in fat body cells of feeding larvae that clonally overexpress FKBP39 (marked by punctate myrRFP expression, red). (**a′**) shows the green channel separately. (**b**) Foxo staining (red) in fat bodies of wild-type mid-third instar larvae shows both nuclear and cytoplasmic labeling. In cells overexpressing FKBP39 (and GFP, green), the nuclear pool of Foxo is completely abolished, and only cytoplasmic signal is seen. (**b′**) shows the red channel separately. (**c**) Null mutation of *Foxo* ($Foxo^{21}/Foxo^{25}$) strongly decreases starvation-induced autophagy in the larval fat body, as shown by Lysotracker staining (red) (compare to Figure 1h). (**d**) Overexpression of FKBP39 in a *Foxo* null mutant background results in a reduction similar to that seen in case of *Foxo* mutation or FKBP39 overexpression alone, also shown by quantitation of Lysotracker data in panel e. Asterisks mark significant changes ($P<0.001$ for columns 1–2, 1–3, 1–4, $P>0.2$ for columns 2–3, 2–4, 3–4). (**f**) Overexpression of an activated form of Foxo, Foxo™ strongly induces autophagy in fat body cells of feeding larvae. Inset shows the red channel (Lysotracker staining) in the overexpressing cells (delineated by a yellow line). Magnification is $\times$ 300 for panel a and $\times$ 200 for panels b–d and f. Error bars represent standard deviation in panel e. Genotypes: hsFLP; UASFKBP39/UASmyrRFP; Act > CD2 > Gal4, tGPH/+ (**a**), hsFLP; UASFKBP39/+; Act > CD2 > Gal4, UASGFPnls/+ (**b**), $Foxo^{21}/Foxo^{25}$ (**c**), cgGal4/UASFKBP39; $Foxo^{21}/Foxo^{25}$ (**d**), hsFLP; UASFoxo™/+; Act > CD2 > Gal4, UASGFPnls/+ (**f**)

Overexpression of FKBP39 led to nearly complete exclusion of Foxo from the nucleus (Figure 2b), despite the reduced level of PI3K signaling in these cells, suggesting that the autophagy-inhibiting effect of FKBP39 may be mediated through inhibition of Foxo.

To test this hypothesis, we carried out overexpression of FKBP39 in a *Foxo* null mutant background. Null mutation of *Foxo* alone strongly interfered with starvation-induced autophagy, indicating for the first time a role for Foxo in this process (Figure 2c and e). Overexpression of FKBP39 in a *Foxo* null mutant background failed to further suppress autophagy compared to mutation of *Foxo* or overexpression of FKBP39 alone (Figure 2d and e), suggesting that the autophagy-inhibiting effect of FKBP39 is at least partly mediated by inhibition of Foxo.

Finally, we also expressed an activated version of Foxo (Foxo$^{™}$)[26] in fat body cells of feeding larvae. We found that Foxo$^{™}$ expression was sufficient to strongly induce autophagy, further confirming the important role of Foxo in regulating autophagy (Figure 2f). Together, our results indicate that Foxo is necessary and sufficient for proper induction of autophagy, and they identify Foxo as a relevant target of FKBP39 action.

Discussion

We have used microarrays to identify genes that are regulated at the time of developmental autophagy in the larval fat body. Upregulated genes whose protein products likely function in developmental autophagy included various lysosomal hydrolases like cathepsin D and cathepsin B, and the ubiquitin-like coat proteins for autophagosomes, Atg8a and Atg8b. Expansion of the lysosomal system is usually observed during autophagy, and the upregulation of hydrolase genes is consistent with the demand for increased degrading capacity during massive induction of autophagy. Of the fly homologs of yeast autophagy genes, *Atg8a* and *Atg8b* showed induction, similarly to starved yeast cells or *Drosophila* larvae.[1,16] Genes of two additional small ubiquitin-like proteins, *CG7224* and *CG15283*, were also strongly upregulated. Although the potential role of these genes in autophagy requires further studies, it is interesting to note that they share a strongly conserved human homolog, *LOC135154*.

Genes encoding various mitochondrial proteins were downregulated, which is consistent with the observation that a large number of mitochondria are degraded during developmental autophagy.[5–7] mRNA levels of many cellular chaperones also decreased, as reported earlier (see below).

Gene expression profiling analyses under a variety of experimental conditions or developmental transitions in which induction of autophagy is observed have been reported previously.[16,27,28] Although it is impossible to isolate autophagy from the numerous other cellular processes with which cells respond to environmental or developmental conditions that also induce autophagy, careful comparison of our results and the results from these studies enabled us to identify the most promising candidate genes that may play a common role during autophagy. Of the genes we identified as being induced during developmental autophagy in the larval fat body, several were previously found to be also upregulated in response to sucrose or no-sugar starvation, conditions that provoke a strong autophagic response in most polyploid larval tissues. These included *CG7224*, *CG15309*, *CG13603*, *PAIP2*, *Atg8a* and *CG10992/cathepsin B*.[16] Moreover, all but one of these genes were also identified as upregulated during salivary gland cell death that likely involves autophagy.[27,28] The expression of Atg8, the coat protein for autophagosomes, which was identified as a rate-limiting factor for the main pathway of autophagy in yeast,[15] showed only a slight induction in these studies. It may suggest that apart from the main pathway of autophagy, other forms of lysosomal degradation are potentially involved in salivary gland cell death. In fact, studies of *Drosophila* null mutants for *dark*, the fly homolog of the apoptosis gene *Apaf-1*, suggest that autophagy is not affected in mutant salivary glands that fail to undergo histolysis,[29] similar to hypomorphic *Hid* mutants or to flies overexpressing the caspase inhibitor p35.[30]

The expression of the genes *Nop56*, *CG8286/dIPK*, *CG4164/Hsp40*, *CG6459*, *Hsc70-5*, *CG3902*, *His2Av* and *FKBP39* was also reduced both during developmental autophagy and in response to sucrose or no-sugar starvation.[16] Three of these, *CG8286/dIPK*, *CG4164/Hsp40* and *Hsc70-5* were also downregulated in dying salivary glands.[27,28]

In this work, we chose three downregulated genes for detailed analysis. Overexpression of dIPK, a cellular chaperone, and Baldspot, a transmembrane protein, did not inhibit autophagy in our tests. However, it is important to note that overexpression of Atg8a or cathD had no effect on autophagy either, despite their well-established role during autophagy. Indeed, the hypomorphic *Baldspot* mutation *l(3)02281* results in darker than usual body color.[21] As pigment granules are lysosome-related organelles, it may suggest that Baldspot normally inhibits the biogenesis of these pigment granules, and its mutation results in generation of more granules.

CG8286/dIPK is a cellular chaperone containing a heat shock protein DnaJ domain, a tetratricopeptide repeat that mediates protein–protein interactions, and a protein prenyltransferase domain. The human ortholog of dIPK is the 58 kDa inhibitor of protein kinases (p58IPK), which strongly inhibits eIF2alpha protein kinases PKR and PERK.[31,32] These kinases function in mediating various stress signals such as the presence of double-stranded RNA viruses, interferon gamma, endoplasmic reticulum stress or starvation.[33,34] p58IPK was shown to inhibit virus- or TNFα-induced cell death by both eIF2alpha kinase-dependent and independent mechanisms.[35] The yeast eIF2alpha kinase GCN2 is required for starvation-induced autophagy, and *PKR* null or non-phosphorylatable eIF2alpha mutant murine embryonic fibroblasts are defective in virus-induced autophagy.[36] In our system, overexpression of dIPK did not interfere with autophagy, suggesting that eIF2alpha kinase signaling is not the major pathway functioning during this process in *Drosophila*. Co-overexpression of dIPK partially rescued the phenotypes caused by expression of the proapoptotic protein reaper or the caspase dronc (G.J. unpublished), proving the evolutionary conserved anti-apoptotic function of dIPK.

FKBP39 belongs to the family of PPiases with 21 members in *Drosophila*.[21] PPiases catalyze the isomerization of the peptide bond between a proline and a bulky residue like

phosphoserine or phosphothreonine. This motif is generated through the action of proline-directed kinases, the best characterized examples of which are kinases downstream of Ras. FKBPs are also the intracellular receptors of the immunosuppressive drugs rapamycin and FK506. The FKBP12-rapamycin complex binds to Tor and inhibits cell growth and induces autophagy. Physiological roles of FKBPs are diverse and not fully characterized yet, but FKBP12 is known to bind to various receptor kinases and the phosphatase calcineurin and inhibit their activity. FKBP12 also binds to ER-resident calcium channels, modulating calcium release regulation by protein kinase A and calcineurin.[23]

We identified *FKBP39* as a downregulated gene during developmental autophagy in *Drosophila*, suggesting that FKBP39 is an inhibitor of autophagy. Indeed, overexpression of FKBP39 led to a strong inhibition of both developmental and starvation-induced autophagy in the larval fat body, whereas loss of *FKBP39* function resulted in a higher than wild-type induction of autophagy in response to a short starvation.

PI3K signaling is a major regulator of cell growth and autophagy, and it was recently shown that during developmental reprogramming of the fat body preceding metamorphosis, ecdysone induces autophagy in part by downregulating PI3K signaling.[10] In that study, expression of a dominant-negative ecdysone receptor inhibited developmental autophagy, and co-overexpression of PTEN, the phosphatase that antagonizes PI3K activity, reversed this effect. We identified FKBP39 as a potential physiological inhibitor of autophagy, its overexpression causing effects similar to inhibition of ecdysone signaling. Co-overexpression of PTEN also reversed the inhibitory effect of FKBP39 overexpression on autophagy. However, in a more direct test of PI3K activity, we found that overexpression of FKBP39 decreased the membrane localization of a probe that reflects PI3K activity. These results indicate that autophagy is inhibited in FKBP39-overexpressing cells despite a reduction in PI3K signaling. Further, they suggest that the small size of these cells may be due in part to decreased PI3K activity.

Interestingly, overexpression of FKBP39 resulted in nuclear exclusion of Foxo, suggesting that FKBP39 may inhibit autophagy through inhibition of Foxo. Foxo is a Forkhead family transcription factor activated by decreased PI3K or increased stress signaling, and has been shown to be required for growth inhibition, increased stress resistance, and lifespan extension provoked by modulation of these signaling pathways, respectively.[37,38] Mutation of *Foxo* caused a similar reduction of starvation-induced autophagy as overexpression of FKBP39, and overexpression of activated Foxo was sufficient to induce autophagy in feeding larvae, demonstrating that Foxo is indeed involved in the regulation of autophagy. Overexpression of FKBP39 in a *Foxo* mutant background did not significantly decrease autophagy compared to cells in which *Foxo* was mutated or FKBP39 was overexpressed alone. This result suggests that at least part of the effect of FKBP39 overexpression on autophagy is mediated by its inhibition of Foxo, as one would expect additive effects of autophagy inhibition in case of independent signaling pathways. Other effects caused by overexpression of FKBP39 (enlarged nucleolus and larval-prepupal lethality) were not affected by the *Foxo* mutant background.

Given the known targets of PPiases, the effect of FKBP39 on Foxo localization is probably indirect. In *Drosophila*, Foxo localization and activity has been shown to be regulated through phosphorylation by PI3K/Akt and Jun N-terminal kinase (JNK) signaling.[26,38] On the basis of our results, PI3K signaling is unlikely to mediate the effects of FKBP39 overexpression on Foxo localization, although it remains possible that FKBP39 may affect Akt independently of PI3K. Therefore, JNK signaling is a promising candidate for mediating at least some of the effects of FKBP39 overexpression,[24] especially considering the strong effect of FKBP39 overexpression on kinases downstream of Ras that are closely related to JNK family kinases. This issue clearly warrants future studies.

In summary, we have identified numerous genes regulated during developmental autophagy in larval *Drosophila* fat body, and we have shown that *FKBP39*, a gene downregulated during the process, encodes a relevant physiological inhibitor of autophagy. We have also identified Foxo as a novel regulator of autophagy, potentially mediating the inhibitory effect of FKBP39 on autophagy.

Materials and methods

***Drosophila* lines and methods.** The following *Drosophila* lines were used in our study: *EP362* (Atg8a), *EP2151* (cathD) (Szeged Stock Center, Hungary), *UASmyrRFP*, *hsGal4*, *cgGal4*, *GMRGal4*, *actGal4*, *tubGal4*, *eyGal4, Df(3R)Exel6174* (Bloomington Stock Center, IN, USA), $FKBP39^{5\text{-}HA-2440}$ and $FKBP39^{5\text{-}HA-2590}$ (kindly provided by Gunther Reuter), $FRT82B\ Ras^{c40b}$ (kindly provided by Celeste Berg), *hsFLP, Act>CD2>Gal4, UASGFPnls* and *Act>CD2>Gal4, tGPH* (kindly provided by Bruce A. Edgar), $Foxo^{25}$ and $Foxo^{21}$ (kindly provided by Heinrich Jasper and Ernst Hafen), and *UASFoxo*™ (kindly provided by Marc Tatar). Fruit flies were maintained at room temperature (23–25°C). Heat shocks were carried out by immersing vials in a 37°C water bath for 1 h. Gain of function clones in the fat body were spontaneously generated by the leaky expression of FLP recombinase in *hsFLP; Act>CD2>Gal4, UASGFPnls/UASFKBP39* animals.[25] We generated *Ras* null mutant clones in the fat body by heat-shocking 0–8 h old embryos of the genotype *hsFLP; cgGal4/+; FRT82B, UASGFP/FRT82B,* Ras^{c40b}. As expected, no *Ras* null mutant cells were recovered in the eyes of *eyFLP; FRT82B, M(3)95A/FRT82B,* Ras^{c40b} animals. For P element excision experiments, transposase was reintroduced to $FKBP39^{5\text{-}HA-2440}$ and $FKBP39^{5\text{-}HA-2590}$ animals (both lines have a P element inserted at the same place in the 5′ UTR of *FKBP39*, 49 bases upstream of the translation start codon). Multiple clean excision lines were identified by PCR and analyzed for each mutant as described in Theopold *et al.*[29] $FKBP39^{exA3}$ is a revertant for $FKBP39^{5\text{-}HA-2440}$, and $FKBP39^{exB1}$ is a revertant for $FKBP39^{5\text{-}HA-2590}$.

Molecular cloning and establishment of transgenic lines. Full-length cDNAs encoding Baldspot, dIPK and FKBP39 (EST# GH11554, LD25575 and LD30817, kindly provided by Miklós Erdélyi) were cloned into the pUAST fly transformation vector using EcoRI and XhoI restriction sites. The resulting plasmids were sequenced and injected into fruit fly embryos using standard microinjection techniques. Multiple transgenic lines were established and analyzed for each construct with similar results.

Microarrays, probe preparations, hybridizations, scanning, data analysis. Construction and use of microarrays were performed as described.[39] Briefly, 3200 amplified cDNA inserts from *Drosophila melanogaster* were purified with MultiScreen-PCR plate (Millipore), resuspended in 50% dimethylsulfoxide/water, and arrayed on amino-silanized slides (Sigma-Aldrich, Germany) by using a MicroGrid Total Array System (BioRobotics, Genomic Solutions Ltd., UK) spotter with 16 pins with a 4×4 format. All clones were spotted in duplicate. Before to hybridization, the slides were blocked in $1 \times$ SSC, 0.2% SDS, 1% BSA for 30 min at 42°C, washed with water and dried with high pressure air. Fat bodies were manually dissected from 150 to 200 carefully staged feeding and wandering animals. All tissues except the embedded gonad disks were dissected away before freezing fat

bodies in liquid nitrogen. Fifteen microgram of total RNA from each sample was amplified by a linear antisense RNA amplification method, and labeled with Cy3 or Cy5 fluorescent dye during reverse transcription as described previously.[40] Probes were mixed, reconstituted in 12 μl hybridization buffer (50% formamide, 5 $\times$ SSC, 0.1% SDS, 100 mg/ml salmon sperm DNA) and applied onto the array after denaturation by heating for 1 min at 90°C. The slide was covered and incubated at 42°C for 20 h in a humid hybridization chamber. After hybridization the arrays were washed by submersion and agitation for 10 min in 1 $\times$ SSC with 0.1% SDS, for 10 min in 0.1% $\times$ SSC with 0.1% SDS and for 10 min in 0.1 $\times$ SSC at room temperature, then rinsed briefly in deionized water and dried. Each array was scanned under a green laser (532 nm) (for Cy3 labeling) and under a red laser (660 nm) (for Cy5 labeling) by using a ScanArray Lite (GSI Lumonics, UK) scanning confocal fluorescent scanner with 10 μm resolution. Scanned output files were analyzed using the GenePix Pro 3.0 software (Axon Instruments Inc, Foster City, CA, USA). Each spot was defined by automatic positioning of a grid of circles over the image. The average and median pixel intensity ratios calculated from both channels and the local background of each spot were determined. An average expression ratio (MeaR, denotes the average of local background corrected pixel intensity ratios) was determined for each spot. Data analysis was done by the significance analysis of microarrays (SAM) method and visualization of scatter images were performed with the Microsoft EXCEL software.

Quantitative real-time PCR and reverse transcription PCR. QRT-PCR was performed on a RotorGene 2000 instrument (Corbett Research, Australia) with gene-specific primers and SybrGreen protocol to confirm the gene expression changes observed by using microarrays. Twenty micrograms of total RNA from each pool was reverse-transcribed in the presence of poly(dT) sequences in a total volume of 20 μl. After dilution of the mix with 80 μl of water, 2 μl of this mix was used as template in the QRT-PCR reaction. Relative expression ratios were normalized to actin. For RT-PCR, total RNA was isolated from fat bodies dissected from feeding L3 larvae or from whole adult flies, using RNAlater and RNeasy Micro Kit (Qiagen, Germany). cDNA synthesized with RevertAid First Strand cDNA Synthesis Kit (Fermentas, Lithuania) was used in RT-PCR reactions with a control primer pair specific for actin, and three different primer pairs for FKBP39 that gave identical results. We performed 25 amplification cycles in these reactions to avoid reaching saturation phase. PCR primer sequences used in this study are available upon request. All PCRs were performed in triplicates.

Histology. Lysotracker red staining of dissected larval fat bodies, cortical actin-phalloidin staining and electron microscopy was done as described previously.[8,10,13] Anti-Foxo antibody[26] was used at a dilution of 1 : 300. Student's *t*-test was used to determine probability values in quantification experiments.

Western blots. Western blots were carried out as described in Juhasz *et al.*[8] using an antibody specific to di-phosphorylated MAPK (Sigma) at a dilution of 1 : 1000.

Acknowledgements. We thank Zsoltné Pálfia, Mariann Saródy and Emese Léder for the excellent technical assistance, our colleagues listed in the Materials and Methods section for providing reagents, and our anonymous reviewers for their helpful comments. This work was supported by NIH grant RO1 GM62509 provided to TPN and by the Hungarian Ministry of Education grant MEDICHEM 1/047 NKFP provided to MS.

1. Klionsky DJ, Emr SD. Autophagy as a regulated pathway of cellular degradation. *Science* 2000; **290**: 1717–1721.
2. Klionsky DJ, Cregg JM, Dunn Jr WA, Emr SD, Sakai Y, Sandoval IV *et al.* A unified nomenclature for yeast autophagy-related genes. *Dev Cell* 2003; **5**: 539–545.
3. Levine B, Klionsky DJ. Development by self-digestion: molecular mechanisms and biological functions of autophagy. *Dev Cell* 2004 Apr; **6**: 463–477.
4. Mizushima N. The pleiotropic role of autophagy: from protein metabolism to bactericide. *Cell Death Differ* 2005 Nov; **12** (Suppl 2): 1535–1541.
5. Sass M, Kovacs J. The effect of ecdysone on the fat body cells of the penultimate larvae of Mamestra brassicae. *Cell Tissue Res* 1977; **180**: 403–409.
6. Butterworth FM, Forrest EC. Ultrastructure of the preparative phase of cell death in the larval fat body of *Drosophila melanogaster*. *Tissue Cell* 1984; **16**: 237–250.
7. Butterworth FM, Emerson L, Rasch EM. Maturation and degeneration of the fat body in the *Drosophila* larva and pupa as revealed by morphometric analysis. *Tissue Cell* 1988; **20**: 255–268.
8. Juhasz G, Csikos G, Sinka R, Erdelyi M, Sass M. The *Drosophila* homolog of Aut1 is essential for autophagy and development. *FEBS Lett* 2003; **543**: 154–158.
9. Sass M, Kovacs J. Ecdysterone and an analogue of juvenile hormone on the autophagy in the cells of fat body of mamestra brassicae. *Acta Biol Acad Sci Hung* 1975; **26**: 189–196.
10. Rusten TE, Lindmo K, Juhasz G, Sass M, Seglen PO, Brech A *et al.* Programmed autophagy in the *Drosophila* fat body is induced by ecdysone through regulation of the PI3K pathway. *Dev Cell* 2004 Aug; **7**: 179–192.
11. Noda T, Kim J, Huang WP, Baba M, Tokunaga C, Ohsumi Y *et al.* Apg9p/Cvt7p is an integral membrane protein required for transport vesicle formation in the Cvt and autophagy pathways. *J Cell Biol* 2000 Feb 7; **148**: 465–480.
12. Blommaart EF, Luiken JJ, Blommaart PJ, van Woerkom GM, Meijer AJ. Phosphorylation of ribosomal protein S6 is inhibitory for autophagy in isolated rat hepatocytes. *J Biol Chem* 1995; **270**: 2320–2326.
13. Scott RC, Schuldiner O, Neufeld TP. Role and regulation of starvation-induced autophagy in the *Drosophila* fat body. *Dev Cell* 2004 Aug; **7**: 167–178.
14. Kamada Y, Funakoshi T, Shintani T, Nagano K, Ohsumi M, Ohsumi Y. Tor-mediated induction of autophagy via an Apg1 protein kinase complex. *J Cell Biol* 2000; **150**: 1507–1513.
15. Kirisako T, Baba M, Ishihara N, Miyazawa K, Ohsumi M, Yoshimori T *et al.* Formation process of autophagosome is traced with Apg8/Aut7p in yeast. *J Cell Biol* 1999; **147**: 435–446.
16. Zinke I, Schutz CS, Katzenberger JD, Bauer M, Pankratz MJ. Nutrient control of gene expression in *Drosophila*: microarray analysis of starvation and sugar-dependent response. *EMBO J* 2002; **21**: 6162–6173.
17. Szuperak M, Zvara A, Erdelyi M. Identification of germ plasm-enriched mRNAs in *Drosophila* melanogaster by the cDNA microarray technique. *Gene Exp Patterns* 2005 Jun; **5**: 717–723.
18. Tearle R. Tissue specific effects of ommochrome pathway mutations in *Drosophila* melanogaster. *Genet Res* 1991 Jun; **57**: 257–266.
19. Theopold U, Dal Zotto L, Hultmark D. FKBP39, a *Drosophila* member of a family of proteins that bind the immunosuppressive drug FK506. *Gene* 1995 Apr 24; **156**: 247–251.
20. Melville MW, Katze MG, Tan SL. P58IPK, a novel cochaperone containing tetratricopeptide repeats and a J-domain with oncogenic potential. *Cell Mol Life Sci* 2000 Feb; **57**: 311–322.
21. Drysdale RA, Crosby MA. FlyBase: genes and gene models. *Nucleic Acids Res* 2005 Jan 1; **33**: D390–D395.
22. Ryder E, Blows F, Ashburner M, Bautista-Llacer R, Coulson D, Drummond J *et al.* The DrosDel collection: a set of P-element insertions for generating custom chromosomal aberrations in *Drosophila* melanogaster. *Genetics* 2004 Jun; **167**: 797–813.
23. Harrar Y, Bellini C, Faure JD. FKBPs: at the crossroads of folding and transduction. *Trends Plant Sci* 2001 Sep; **6**: 426–431.
24. Klettner A, Baumgrass R, Zhang Y, Fischer G, Burger E, Herdegen T *et al.* The neuroprotective actions of FK506 binding protein ligands: neuronal survival is triggered by *de novo* RNA synthesis, but is independent of inhibition of JNK and calcineurin. *Brain Res Mol Brain Res* 2001 Dec 16; **97**: 21–31.
25. Britton JS, Lockwood WK, Li L, Cohen SM, Edgar BA. *Drosophila*'s insulin/PI3-kinase pathway coordinates cellular metabolism with nutritional conditions. *Dev Cell* 2002; **2**: 239–249.
26. Hwangbo DS, Gersham B, Tu MP, Palmer M, Tatar M. *Drosophila* dFOXO controls lifespan and regulates insulin signalling in brain and fat body. *Nature* 2004 Jun 3; **429**: 562–566.
27. Lee CY, Clough EA, Yellon P, Teslovich TM, Stephan DA, Baehrecke EH. Genome-wide analyses of steroid- and radiation-triggered programmed cell death in *Drosophila*. *Curr Biol* 2003 Feb 18; **13**: 350–357.
28. Gorski SM, Chittaranjan S, Pleasance ED, Freeman JD, Anderson CL, Varhol RJ *et al.* A SAGE approach to discovery of genes involved in autophagic cell death. *Curr Biol* 2003 Feb 18; **13**: 358–363.
29. Akdemir F, Farkas R, Chen P, Juhasz G, Medved'ova L, Sass M *et al.* Autophagy occurs upstream or parallel to the apoptosome during histolytic cell death. *Development* 2006 Apr; **133**: 1457–1465.
30. Juhasz G, Sass M. Hid can induce, but is not required for autophagy in polyploid larval *Drosophila* tissues. *Eur J Cell Biol* 2005 Apr; **84**: 491–502.
31. Yan W, Frank CL, Korth MJ, Sopher BL, Novoa I, Ron D *et al.* Control of PERK eIF2alpha kinase activity by the endoplasmic reticulum stress-induced molecular chaperone P58IPK. *Proc Natl Acad Sci USA* 2002 Dec 10; **99**: 15920–15925.
32. Tan SL, Gale Jr MJ, Katze MG. Double-stranded RNA-independent dimerization of interferon-induced protein kinase PKR and inhibition of dimerization by the cellular P58IPK inhibitor. *Mol Cell Biol* 1998 May; **18**: 2431–2443.
33. Pain VM. Translational control during amino acid starvation. *Biochimie* 1994; **76**: 718–728.
34. Williams BR. PKR; a sentinel kinase for cellular stress. *Oncogene* 1999 Nov 1; **18**: 6112–6120.
35. Tang NM, Korth MJ, Gale Jr M, Wambach M, Der SD, Bandyopadhyay SK *et al.* Inhibition of double-stranded RNA- and tumor necrosis factor alpha-mediated apoptosis by tetratricopeptide repeat protein and cochaperone P58(IPK). *Mol Cell Biol* 1999 Jul; **19**: 4757–4765.

36. Talloczy Z, Jiang W, Virgin HWt, Leib DA, Scheuner D, Kaufman RJ *et al.* Regulation of starvation- and virus-induced autophagy by the eIF2alpha kinase signaling pathway. *Proc Natl Acad Sci USA* 2002 Jan 8; **99**: 190–195.
37. Junger MA, Rintelen F, Stocker H, Wasserman JD, Vegh M, Radimerski T *et al.* The *Drosophila* Forkhead transcription factor FOXO mediates the reduction in cell number associated with reduced insulin signaling. *J Biol* 2003; **2**: 20.
38. Wang MC, Bohmann D, Jasper H. JNK extends life span and limits growth by antagonizing cellular and organism-wide responses to insulin signaling. *Cell* 2005 Apr 8; **121**: 115–125.
39. Puskas LG, Zvara A, Hackler Jr L, Micsik T, van Hummelen P. Production of bulk amounts of universal RNA for DNA microarrays. *Biotechniques* 2002 Oct; **33**: 898–900, 902, 904..
40. Puskas LG, Zvara A, Hackler Jr L, Van Hummelen P. RNA amplification results in reproducible microarray data with slight ratio bias. *Biotechniques* 2002 Jun; **32**: 1330–1334, 1336, 1338, 1340.

Supplementary Information accompanies the paper on Cell Death and Differentiation website (http://www.nature.com/cdd)

Current Biology *17*, 1–11, January 9, 2007 ©2007 Elsevier Ltd All rights reserved DOI 10.1016/j.cub.2006.10.053

dc_840_14

Article

Direct Induction of Autophagy by Atg1 Inhibits Cell Growth and Induces Apoptotic Cell Death

Ryan C. Scott,[1] Gábor Juhász,[1] and Thomas P. Neufeld[1,*]
[1] Department of Genetics, Cell Biology, and Development
University of Minnesota
Minneapolis, Minnesota 55455

Summary

Background: To survive starvation and other forms of stress, eukaryotic cells undergo a lysosomal process of cytoplasmic degradation known as autophagy. Autophagy has been implicated in a number of cellular and developmental processes, including cell-growth control and programmed cell death. However, direct evidence of a causal role for autophagy in these processes is lacking, resulting in part from the pleiotropic effects of signaling molecules such as TOR that regulate autophagy. Here, we circumvent this difficulty by directly manipulating autophagy rates in *Drosophila* through the autophagy-specific protein kinase Atg1.
Results: We find that overexpression of Atg1 is sufficient to induce high levels of autophagy, the first such demonstration among wild-type Atg proteins. In contrast to findings in yeast, induction of autophagy by Atg1 is dependent on its kinase activity. We find that cells with high levels of Atg1-induced autophagy are rapidly eliminated, demonstrating that autophagy is capable of inducing cell death. However, this cell death is caspase dependent and displays DNA fragmentation, suggesting that autophagy represents an alternative induction of apoptosis, rather than a distinct form of cell death. In addition, we demonstrate that Atg1-induced autophagy strongly inhibits cell growth and that Atg1 mutant cells have a relative growth advantage under conditions of reduced TOR signaling. Finally, we show that Atg1 expression results in negative feedback on the activity of TOR itself.
Conclusions: Our results reveal a central role for Atg1 in mounting a coordinated autophagic response and demonstrate that autophagy has the capacity to induce cell death. Furthermore, this work identifies autophagy as a critical mechanism by which inhibition of TOR signaling leads to reduced cell growth.

Introduction

Under starvation conditions, eukaryotic cells recover nutrients via autophagy, a lysosome-mediated process of bulk cytoplasmic degradation. Through autophagy, long-lived proteins, organelles, and other components of the cytoplasm are nonselectively engulfed within specialized double-membraned vesicles known as autophagosomes. Subsequent fusion of the outer autophagosomal membrane with the lysosome results in a structure known as the autolysosome, in which the inner membrane and its cytoplasmic cargo are degraded. Breakdown products released from the autolysosome supply the cell with an internal source of nutrients that can support essential metabolic processes during starvation [1]. Approximately 20 *ATG* (autophagy-related) genes specifically required for autophagy have been discovered in *Saccharomyces cerevisiae* [2–4], and many of these genes have functional homologs in metazoans [1, 5].

In addition to survival of starvation, autophagy has been implicated in many aspects of health and development, including aging, programmed cell death, pathogenic infection, stress responses, neurodegenerative and muscle disorders, cellular remodeling, cancer, and cell growth [1, 6]. As in many of these processes, evidence for a role of autophagy in cell-growth control is largely correlative. Autophagy is promoted by several tumor suppressor genes including PTEN, TSC1 and 2, and beclin 1, and it is inhibited by growth-promoting pathways such as type I PI3K and target of rapamycin (TOR) signaling [5, 7–10]. A variety of conditions that stimulate cell growth, such as growth factor addition, partial hepatectomy, and refeeding after starvation, also inhibit autophagy, while growth-suppressive signals, such as contact inhibition and substrate detachment, induce autophagy [11]. Together, these correlative findings are consistent with a model in which the catabolic effects of autophagy act as a brake on cell growth during development. However, this issue is complicated by the pleiotropic nature of the signaling pathways that regulate autophagy. For example, in addition to inhibiting autophagy, the TOR pathway controls cell metabolism and biosynthesis by promoting ribosome biogenesis, protein synthesis, and nutrient uptake [12]. The relevant contribution of each of these downstream effector pathways to net cell growth is poorly understood.

Autophagy is also known to be involved in programmed cell death and distinguishes Type II (autophagic) from Type I (apoptotic) cell death. Autophagic cell death is characterized by an abundance of autophagosomes and autolysosomes in the dying cell and differs from apoptotic cell death in that dying cells are degraded by their own lysosomal enzymes, rather than by phagocytosis [13]. It has been difficult, however, to establish whether autophagy plays a causal role in Type II cell death or represents a failed attempt at cell survival in cells undergoing programmed cell death. Death signals often induce features of both apoptosis and autophagy, and mutations that disrupt autophagy have been shown to suppress cell death in some cases [14–16] and hasten it in others [2, 17]. Thus, as in the case for cell growth, much of the support for a direct role for autophagy in cell death rests on correlative evidence.

One approach to addressing the potential role of autophagy in functions such as cell death and growth would be to induce autophagy directly, independent of the signaling pathways that normally control it. In yeast,

*Correspondence: neufeld@ahc.umn.edu

dc_840_14

multiple signaling pathways, including TOR, AMPK, and Ras/PKA, converge on the Ser-Thr kinase Atg1 to regulate autophagy [18–20]. In addition, Atg1 interacts with multiple components of the autophagic machinery, through direct association, through phosphorylation, and/or through effects on intracellular localization [18, 21, 22]. Thus, Atg1 may represent a nodal point for controlling multiple steps in the autophagic process in response to various inductive cues.

Interestingly, the role of Atg1 kinase activity in yeast is the subject of some debate, and studies from different groups that used ATP analog-sensitive and kinase-defective Atg1 mutants have reached conflicting conclusions. One study reported that Atg1 kinase activity is required for the autophagy-related biosynthetic cytoplasm to vacuole targeting (CVT) pathway but not for autophagy, and concluded that Atg1 plays a structural role in autophagy [23]. However, other studies with similar reagents found a requirement for Atg1 kinase activity in both CVT and autophagy [18, 24].

We have previously shown that the *Drosophila melanogaster* homolog of Atg1 is required for autophagy in the larval fat body, an organ analogous to the vertebrate liver with roles in nutrient storage and mobilization [5]. Here, we investigate the effects of *Drosophila* Atg1 loss of function and overexpression on autophagy induction, cell-growth control, and cell death. Our findings indicate that Atg1 expression is sufficient to effect a full autophagic response, resulting in a marked inhibition of cell growth and a rapid induction of apoptotic cell death.

Results

Overexpression of Atg1 Induces Autophagy

Null mutation of *Atg1* results in a severe block of starvation-induced autophagy and leads to fully penetrant lethality by the late pupal stage [5]. To test the effects of Atg1 overexpression, we generated multiple transgenic lines expressing wild-type Atg1 under GAL4/UAS control. We also used an independently generated line (GS10797), in which UAS regulatory sequences have been inserted upstream of the endogenous *Atg1* gene. In control experiments, weak expression of UAS-Atg1 was sufficient to partially rescue *Atg1* null mutants to adult viability (34% of expected progeny; see Figure S1A in the Supplemental Data available online) and partially rescued the autophagy defect of these mutants, as measured by Lysotracker Red staining, an effective marker of autolysosomes in fat body tissue [5, 25]. Similar to wild-type larvae, *Atg1* mutants rescued by UAS-Atg1 showed no Lysotracker staining when fed normally (Figures S1B and S1G) but regained some capability to induce autophagy under starvation conditions (Figures S1C and S1G).

To address whether Atg1 overexpression is sufficient to induce autophagy in fed animals, we expressed high levels of transgenic Atg1 via the heat shock-inducible Hsp70-GAL4 driver. Ultrastructural analysis showed that heat shock alone does not increase the abundance of autophagic structures in fat body cells of normally fed larvae (Figure 1A). In contrast, heat shock-induced overexpression of Atg1 resulted in the formation of autophagosomes and autolysosomes throughout fat body cells of fed animals (Figure 1B). These autophagic structures were indistinguishable from those generated by starvation [5], with readily identifiable cytoplasmic components in various stages of degradation. Robust induction of autophagy in response to heat shock-induced Atg1 overexpression was also evident by Lysotracker staining in live fat body tissue from fed larvae (compare Figures 1C and 1D; Figure 1I). Punctate Lysotracker staining was also observed in response to constitutive expression of Atg1 throughout the fat body (see below), in fat body cell clones (Figure S1E), and in eye and wing imaginal disc cells (data not shown). In addition, we occasionally observed localization of autolysosomes to the perinuclear region by TEM and Lysotracker staining (Figures S1E and S3G and data not shown). This is consistent with recent observations that mammalian Atg9, a potential marker of the membrane source of autophagosomes, is recruited from the perinuclear trans-Golgi network in response to starvation in an Atg1-dependent manner [26]. Accumulation of Atg1-induced autolysosomes in the perinuclear region may therefore represent an early site of autolysosome formation.

To determine whether autophagy induced by Atg1 overexpression utilizes the same molecular components as starvation-induced autophagy, we first examined the localization of GFP-Atg8a and GFP-Atg8b, specific markers of the autophagosomal membrane [5, 27, 28]. As previously described, GFP-Atg8b was distributed uniformly in control fat body cells from fed animals (Figure 1E). In contrast, heat shock-induced overexpression of Atg1 resulted in redistribution of GFP-Atg8b to a punctate pattern (Figure 1F), similar to the effects of starvation [5]. In costaining experiments, GFP-Atg8-labeled punctae were often observed adjacent to or overlapping with Lysotracker-positive spots (Figure 1G), as previously observed in starved wild-type animals [5]. Expression of Atg1 in the developing retinal cells behind the morphogenetic furrow of the eye imaginal disc with GMR-GAL4 also resulted in punctate localization of GFP-Atg8a in normally fed animals, as compared to control cells ahead of the furrow (Figure S2C). Interestingly, Atg1 overexpression also led to a marked increase in abundance of GFP-Atg8a and GFP-Atg8b in both eye and wing imaginal discs. In these experiments, Atg1 was overexpressed in the posterior region of eye or wing discs with GMR-GAL4 or en-GAL4, respectively, causing increased levels of hsp70-driven GFP-Atg8 relative to the anterior regions of these discs (compare Figures S2A and S2B, and data not shown). An increase in GFP-Atg8b levels was also observed in Atg1-overexpressing eye and wing discs by immunoblot analysis (Figure S2E and data not shown). GFP-Atg8 expression is regulated by heterologous promoter and UTR sequences in these lines [5], and Atg1 overexpression did not affect the abundance of GFP alone nor of a control GFP fusion (data not shown), so we conclude that Atg1 has a posttranslational effect on GFP-Atg8 levels, perhaps through stabilization of GFP-Atg8 protein. Thus, Atg8 levels are increased under autophagy-inducing conditions, both transcriptionally [27, 29] (G.J., L.G. Puskás, O. Komonyi, B. Érdi, P. Maróy, T.P.N., and M. Sass, unpublished data) and posttranscriptionally.

To further explore the requirement for known components of the autophagic machinery, we tested whether mutations in other Atg genes affect the ability of Atg1

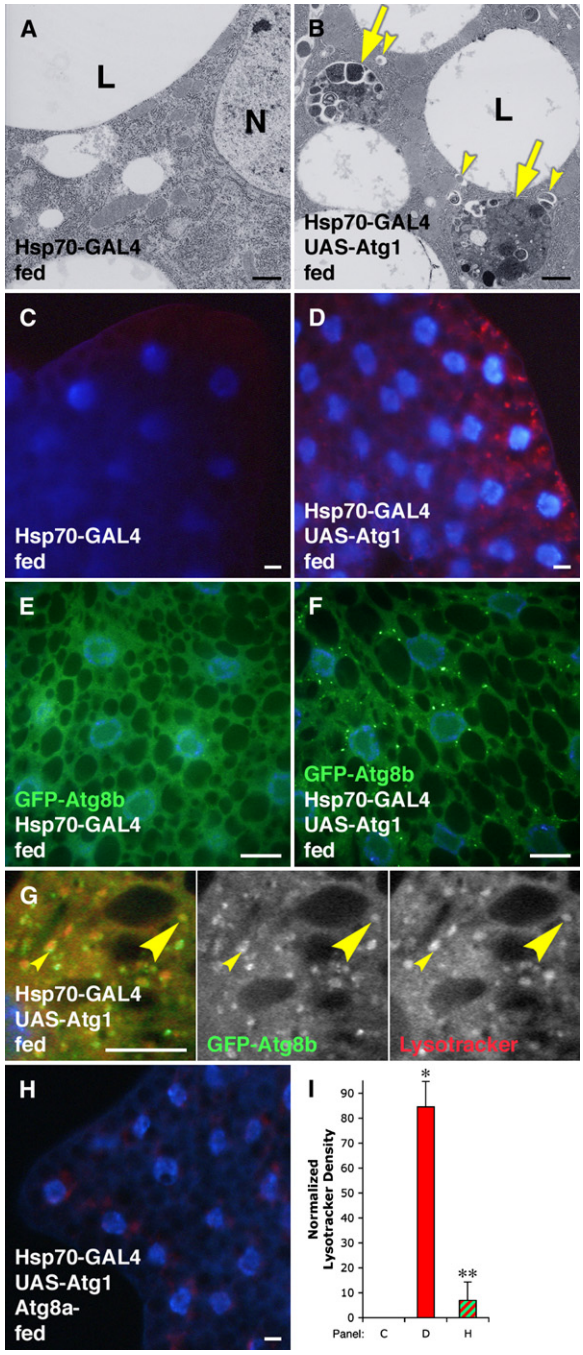


Figure 1. Overexpression of Atg1 Induces Autophagy

(A–G) Induction of autophagy by heat shock-induced overexpression of Atg1. TEM showing no induction of autophagy in the fat body of normally fed animals by heat shock alone (A), whereas heat shock-induced overexpression of Atg1 (B) results in the accumulation of autolysosomes (arrows) and autophagosomes (arrowheads). Heat shock alone shows no Lysotracker staining (C), while heat shock-induced Atg1 overexpression results in punctate Lysotracker staining (red) (D). Induction of Atg1 overexpression leads to a redistribution of GFP-Atg8b (green) from uniform staining (E) to a punctate pattern (F). Many GFP-Atg8-positive punctae are found either adjacent to (small arrowheads) or overlapping with (large arrowheads) Lysotracker-labeled structures (G). N indicates the nucleus in (A); L indicates a lipid droplet in (A) and (B).

(H) Mutation of *Atg8a* disrupts Atg1-induced Lysotracker staining.

(I) Quantitation of Lysotracker staining. Single asterisk indicates a significant difference from wild-type: $p < 0.0001$; double asterisk indicates a significant difference from Atg1 overexpression alone: $p = 0.0001$. Error bars indicate standard deviation (SD).

Scale bars represent 1 μm in (A) and (B) and 10 μm in (C)–(H). Nuclei are marked in blue in (C)–(H).

Genotypes: (A, C) *Hsp70-GAL4/+*. (B, D) *Hsp70-GAL4/UAS-Atg1*^{9}. (E) *Hsp70-GFP-Atg8b*^{6B}*/Hsp70-GFP-Atg8b*^{6B}; *Hsp70-GAL4/TM6B*. (F, G) *Hsp70-GFP-Atg8b*^{6B}*/Hsp70-GFP-Atg8b*^{6B}; *Hsp70-GAL4/UAS-Atg1*^{6B}. (H) *Atg8a*^{KG07569}*/Y*; *Hsp70-GAL4/UAS-Atg1*^{6B}. (I) As in (C), (D), and (H).

overexpression to induce autophagy. We identified a P element insertion in the coding region of *Atg8a* and generated a deletion in the *Atg3* locus, previously shown to be required for autophagy in *Drosophila* through RNAi analysis [30]. Each of these mutations caused a significant decrease in starvation-induced autophagy (compare Figure S3A to S3B and S3E; Figure S3K), which could be rescued by transgenic expression of the respective wild-type gene (Figure S3C, S3F, and S3K) and by excision of the P insertion from *Atg8a* (Figures S3D and S3K). Importantly, each mutation also caused a significant inhibition of Atg1-induced autophagy (Figures 1H and 1I; Figures S3G, S3H, and S3K). Together, these results indicate that Atg1 is both necessary and sufficient to induce a complete autophagic response and that Atg1-induced autophagy engages at least some of the same molecular machinery as starvation-induced autophagy.

Atg1-Dependent Autophagy Restricts Cell Growth

Inhibition of autophagy is strongly correlated with the cell-growth effects of TOR signaling, suggesting that as a catabolic process, autophagy may inhibit growth. To determine whether the increased level of autophagy in TOR pathway mutants contributes to their reduced rate of cell growth, we first examined the growth properties of mitotic clones in the wing imaginal disc. We found that clones of cells with a null mutation in *Pdk1*, a positive regulator of the TOR pathway [12], were reduced in size by 78% as compared with their wild-type twin spot (Figures 2A and 2E). Clones doubly mutant for *Pdk1* and *Atg1* showed no significant difference in size from *Pdk1* mutant clones (Figures 2B and 2E), indicating that while loss of *Pdk1* induces autophagy [5], this does not contribute significantly to the reduced growth rate of *Pdk1* null mutant cells. This result is consistent with our previous finding that RNAi-mediated inhibition of autophagy does not alleviate the growth defect of *Tor* null mutant cells [5].

We reasoned that the severe block to TOR signaling in *Pdk1* and *Tor* null mutants may lead to metabolic changes that mask the potential growth effects of autophagy. For example, the reduction of nutrient import in *Tor* null mutant cells [31] may engender a requirement for nutrients generated by autophagy, and thus the potential growth-suppressive effects of autophagy may be balanced or outweighed by its metabolic benefits under these severe conditions. To test the potential growth effects of autophagy under conditions of more moderately reduced TOR signaling, we treated larvae with a concentration of rapamycin that causes a 2-fold delay in larval development. In normally fed animals, the size of *Atg1* null mutant clones did not differ significantly from their twin spot controls (Figures 2C and 2E). In

dc_840_14

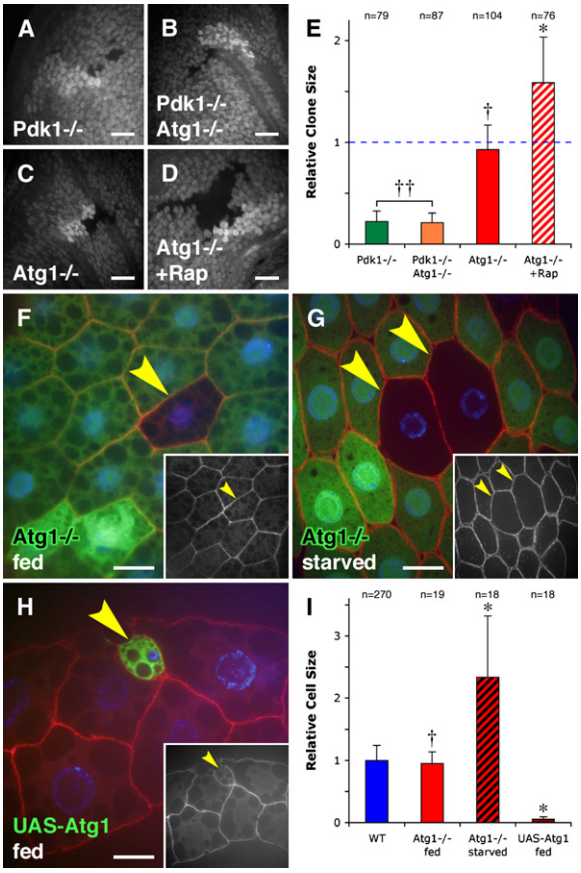


Figure 2. Atg1 Expression Leads to Reduced Cell Size

(A–D) Growth effects of *Atg1* loss of function in wing disc clones. *Pdk1* mutant clones (loss of GFP) display decreased clone size relative to the wild-type twin spot (increased GFP) (A). Simultaneous loss of *Atg1* (B) fails to rescue this reduction in size. *Atg1* mutant clones do not display a growth phenotype when grown on normal medium (C), but growth on medium containing 2 μM rapamycin gives the Atg1 mutant clones a relative growth advantage over wild-type (D).

(E) Quantitation of relative clone size in wing discs. Mean clone size normalized to wild-type twin spot within the same image. Dotted line indicates a 1:1 ratio (no growth phenotype). Double dagger indicates no significant difference from *Pdk1* mutant clones: p = 0.44; single dagger indicates an insignificant difference from wild-type twin spot: p = 0.28; asterisk indicates a significant difference from wild-type twin spot: p = 0.016. n indicates clone number.

(F–H) Cell size effects of Atg1 in the fat body. Clonal loss of *Atg1* function (loss of GFP, arrowheads) has no effect on fat body cell size in normally fed animals (F), but results in a relative growth advantage in animals starved of all nutrients for 45 hr (G). Clonal overexpression of Atg1 (GFP-positive cells, arrowhead) (H) results in a marked reduction in cell size. Actin cytoskeleton (red) is labeled with phalloidin (F and G) or α-spectrin antibody (H); nuclei are marked in blue. DNA channel in (H) shows two representative confocal sections. Insets show phalloidin (or α-spectrin) channels of respective images.

(I) Quantitation of relative cell size in fat body. Mean cell size normalized to wild-type (homozygous and heterozygous) cells within the same image. Wild-type column includes cells from both fed and starved animals. Dagger indicates no significant difference from wild-type: p = 0.54; asterisk indicates a significant difference from wild-type: p < 0.0001. n indicates cell number.

Scale bars represent 10 μm. Error bars indicate SD.

Genotypes: (A) *hsflp/+; Pdk1^{5} FRT80B/Ubi-GFP FRT80B*. (B) *hsflp/+; Pdk1^{5} Atg1$^{\Delta 3D}$ FRT80B/Ubi-GFP FRT80B*. (C, D) *hsflp/+; Atg1$^{\Delta 3D}$ FRT80B/Ubi-GFP FRT80B*. (E) As in (A)–(D). (F, G) *hsflp/+; Cg-GAL4/+; Atg1$^{\Delta 3D}$ FRT80B/UAS-2x eGFP FRT80B*. (H) *hsflp/+; Act>CD2>GAL4 UAS-GFP/UAS-Atg1^{6B}*. (I) As in (F)–(H).

contrast, addition of rapamycin to the media gave *Atg1* mutant clones a significant growth advantage over wild-type cells, resulting in a 59% larger average clone size compared to the wild-type twin spot (Figures 2D and 2E).

To test the growth functions of autophagy under more physiological conditions, we examined the effects of starvation on the relative size of wild-type and *Atg1* mutant cells in the larval fat body. We found that, as in wing discs, *Atg1* mutant cells did not show a significant difference in size relative to neighboring wild-type cells in normally fed animals (Figures 2F and 2I), consistent with the low rates of autophagy observed under these conditions. Prolonged starvation, however, gave *Atg1* mutant cells a 2.3-fold growth advantage over their wild-type neighbors (Figures 2G and 2I). Similar results were observed in cells expressing an RNAi construct targeting Atg5 (data not shown). We conclude that under physiological conditions that reduce TOR signaling, induction of autophagy is partially responsible for the observed reduced rates of cell growth. These results are consistent with recent findings that autophagy is required for starvation-induced size reduction of mouse embryonic fibroblasts, via a tetracycline-regulated Atg5 expression system [32].

As a complement to these genetic loss-of-function studies, we tested the growth effects of autophagy induced by UAS-Atg1 expression. Clonal overexpression of Atg1 caused a striking inhibition of fat body cell growth, resulting in a 94% decrease in cell area (Figures 2H and 2I). A corresponding decrease in nuclear size and DNA content was also observed in Atg1-expressing cells (Figure 2H; see also below), indicating that high levels of autophagy inhibit the endoreplicative cell cycle of these cells. Constitutive expression of Atg1 throughout the fat body, or in the eye or wing imaginal disc, also resulted in a marked reduction in size of these organs (see below, Figure S2G, and data not shown). Together, these results indicate that autophagy is necessary for normal growth inhibition in response to reduced TOR signaling and is sufficient to inhibit cell growth independent of upstream signaling.

High Levels of Autophagy Lead to Apoptotic Cell Death

Autophagy and cell death are correlated in a number of contexts, but the causal relationships are unclear. To test the potential role of autophagy in promoting cell death, we induced clones of GFP-marked wing imaginal disc cells overexpressing Atg1 and assayed the percentage of GFP-positive cells at successive intervals after induction. Although this approach does not monitor individual cells in real time, it allowed us to make strong inferences about their survival by assaying large numbers of cells across multiple time points. We found that, in contrast to control cells expressing GFP alone, most cells overexpressing Atg1 were eliminated within 36 hr of induction (Figures 3A–3C). Reduced cell numbers were noticeable by 12 hr after induction, the earliest time point at which we could identify GFP expression.

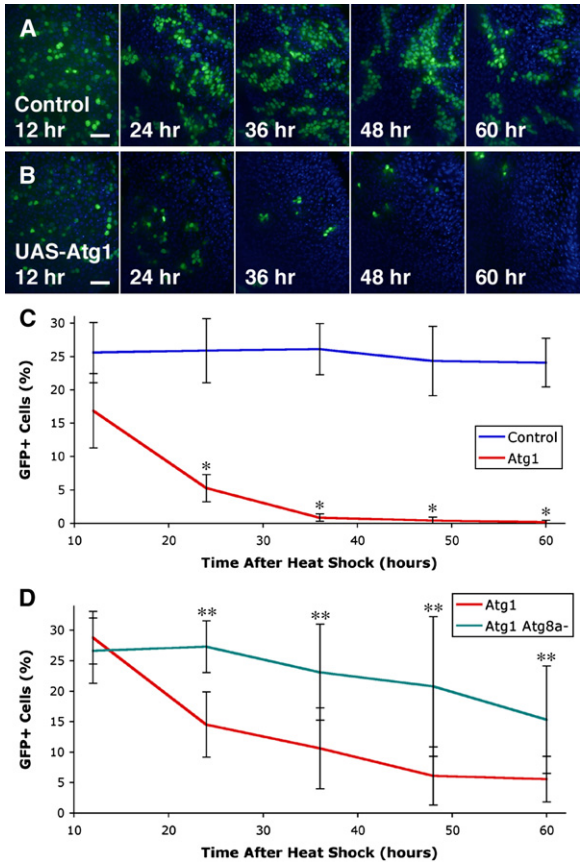


Figure 3. Overexpression of Atg1 Leads to Cell Elimination

(A–C) Elimination of Atg1-overexpressing clones in the wing disc. Wild-type controls show consistent numbers of GFP-positive cells at 12, 24, 36, 48, and 60 hr after induction by heat shock (A). Cells overexpressing Atg1 (GFP-positive cells) are abundant 12 hr after heat shock, but are eliminated over time (B). Mean numbers of GFP-positive cells, expressed as a percentage of total cells (C). Asterisk indicates a significant difference from the wild-type control: $p < 0.0001$.

(D) Mutation of *Atg8a* delays elimination of Atg1-overexpressing cells. Mean numbers of GFP-positive cells are expressed as a percentage of total cells. Double asterisk indicates a significant difference from Atg1 overexpression alone: $p < 0.03$.

Scale bars represent 10 μm. Nuclei are marked in blue. Error bars indicate SD.

Genotypes: (A) *hsflp/+*; *Act>CD2>GAL4 UAS-GFP/+*. (B) *hsflp/+*; *Act>CD2>GAL4 UAS-GFP/UAS-Atg1^{6B}*. (C) As in (A) and (B). (D) Atg1: *hsflp/Y*; *tub>CD2>GAL4/+*; *UAS-Atg1^{6B}/+*. Atg1 Atg8a-: *hsflp Atg8a^{KG07569}/Y*; *tub>CD2>GAL4/+*; *UAS-Atg1^{6B}/+*.

Elimination of Atg1-overexpressing cells was significantly reduced in an *Atg8a* mutant background (Figure 3D), suggesting that cell death resulted directly from increased autophagy.

Cells undergoing autophagic cell death have been observed to display signs of apoptosis [33, 34]. We therefore examined Atg1-overexpressing cells for caspase activity and DNA fragmentation, hallmark features of apoptotic cells. We found that 20% of wing disc cells clonally overexpressing Atg1 displayed caspase activation, as shown by active Caspase-3 antibody staining (Figure 4A). Similarly, terminal uridine nick end labeling (TUNEL) revealed DNA fragmentation in 22% of Atg1-overexpressing cells (Figure 4B). Consistent with these observations, coexpression of the caspase inhibitor p35 was sufficient to delay the death of Atg1-overexpressing cells, although these cells were also eventually eliminated (Figure 4C). Similar effects on Caspase-3 activation and TUNEL staining were observed in fat body cells clonally overexpressing Atg1 (Figures 4D and 4E). We also observed that Atg1 overexpression resulted in reduced or absent filamentous actin staining at the periphery of these cells and that they often became fragmented and/or engulfed by neighboring wild-type cells (Figures 4F and 4G).

Constitutive expression of Atg1 throughout the fat body (see Figure 5C) also resulted in substantial apoptosis (13% positive for caspase activation, 17% for TUNEL; Figure S3I), and this cell death was reduced by 94% in *Atg3* mutants ($p < 0.0001$; Figure S3J). TUNEL and active Caspase-3 staining resulting from clonal Atg1 overexpression were also reduced by 33% and 35%, respectively, in *Atg8a* mutants, consistent with their partial reduction in Atg1-induced Lysotracker staining (see Figure 1H) and elimination (see Figure 3D). These results indicate that the apoptosis observed in Atg1-overexpressing cells is due to high levels of autophagy.

The reduced eye size resulting from Atg1 overexpression (compare Figures S2F and S2G) also appears to be due in part to apoptosis, because coexpression of the caspase inhibitors DIAP1 or p35 resulted in a partial suppression of this phenotype (Figure S2H and data not shown). Finally, we found that Atg1 overexpression mediated by GMR-GAL4 led to a decrease in adult viability and that this was suppressed by coexpression of p35 or DIAP1 (Figure S2D).

Together, these results indicate that constitutive overexpression of Atg1 leads to a form of cell death that is both caspase and autophagy dependent, with features typical of apoptosis, such as DNA and cytoskeletal fragmentation. We therefore conclude that, in addition to promoting cell survival, autophagy has the capacity to promote cell death when induced to high levels.

Atg1-Dependent Phenotypes Are Modulated by the TOR Pathway

In yeast, suppression of autophagy by TOR signaling is transduced to the core Atg machinery in part through regulation of the assembly and activity of a multiprotein complex containing Atg1, Atg13, and Atg17. Under growth-promoting conditions, TOR-dependent hyperphosphorylation of Atg13 reduces its affinity for Atg1, resulting in dissociation of Atg13 from the complex and decreased kinase activity of Atg1. Upon TOR inactivation, dephosphorylation of Atg13 increases its affinity for Atg1, leading to increased Atg1 kinase activity and induction of autophagy [18]. Whether these aspects of Atg1 regulation by TOR signaling are conserved in higher eukaryotes is unclear, because homologs of Atg13 or Atg17 have not been identified in animals.

To investigate the connection between TOR and Atg1 in *Drosophila*, we tested whether increased TOR activity affected the ability of Atg1 overexpression to induce autophagy. As described above, heat shock-driven overexpression of Atg1 led to induction of autophagy in the fat body of normally fed larvae (Figures 5A and 5E). However, we found that in animals mutant for *Tsc2* (a negative regulator of TOR), induction of autophagy by heat

dc_840_14

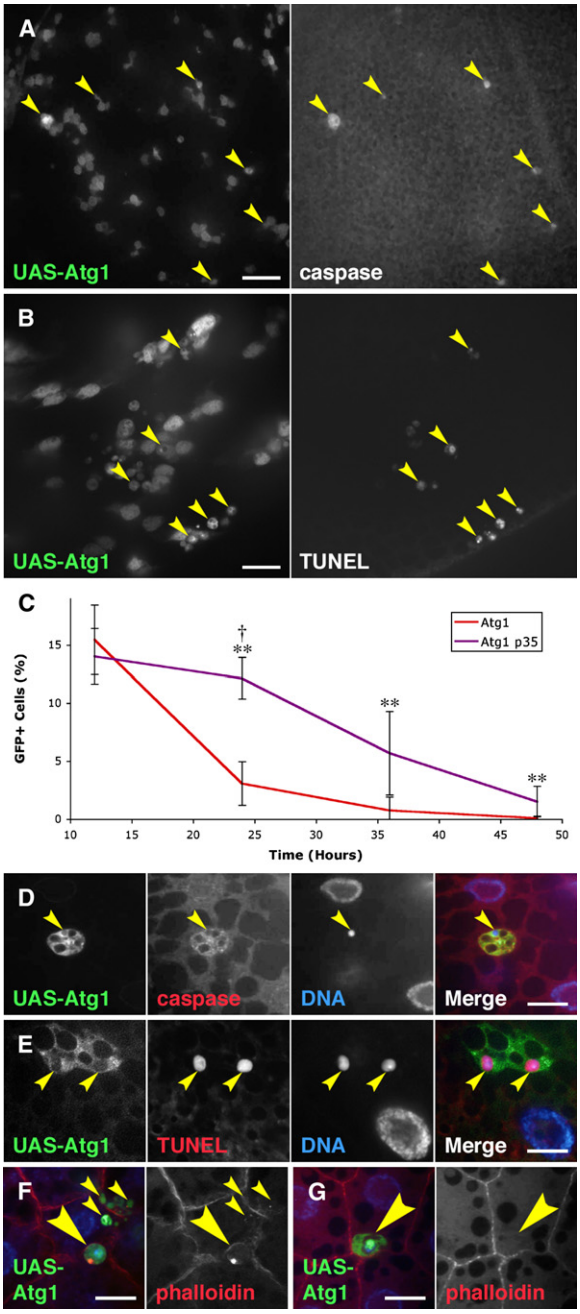


Figure 4. Atg1 Overexpression Induces Apoptosis

(A) Wing discs display active caspase 3 staining (arrowheads) in 20% (±15%, p = 0.007) of cells overexpressing Atg1 (GFP-positive cells).

(B) Wing discs show DNA fragmentation in 22% (±6%, p = 0.0002) of Atg1-overexpressing cells (GFP-positive cells) by TUNEL staining (arrowheads).

(C) Coexpression of p35 reduces elimination of Atg1-overexpressing cells. Mean numbers of GFP-positive cells are expressed as a percentage of total cells. Double asterisk indicates a significant difference from Atg1 overexpression alone: p < 0.020; dagger indicates no significant difference from the wild-type control: p = 0.63.

(D–G) Fat body cells overexpressing Atg1 die by apoptosis.

(D) An Atg1-overexpressing cell (arrowhead) staining for active caspase 3.

(E) Atg1-overexpressing cells (arrowheads) staining positive for TUNEL. TUNEL and DNA channels show two representative confocal sections.

shock-induced Atg1 overexpression was significantly reduced (Figures 5B and 5E). Similarly, induction of autophagy and inhibition of cell growth by constitutive expression of Atg1 throughout the fat body (Figure 5C) was strongly suppressed by coexpression of the small GTPase Rheb, an upstream activator of TOR signaling (Figure 5D). Overexpression of Rheb also significantly delayed the elimination of wing disc cells caused by Atg1 overexpression (Figure 5F). These results are consistent with the idea that TOR signaling in *Drosophila* may inhibit Atg1 activity as in yeast, although they do not rule out parallel, opposing inputs to autophagy by Atg1 and TOR.

Atg1 Negatively Feeds Back on TOR Signaling

Although studies in yeast indicate that Atg1 is directly associated with multiple components of the autophagic machinery, the effects of Atg1 overexpression on cell growth and autophagy in *Drosophila* could in principle be indirect, for example through modulation of signaling pathways that regulate autophagy, such as PI3K and TOR. To address this possibility, we examined the effect of Atg1 overexpression on cellular and biochemical markers of PI3K and TOR activity. The intracellular localization of the transcription factor FOXO serves as an in vivo readout of PI3K activity, because it resides in the nucleus under conditions of low PI3K activity and relocalizes to the cytoplasm in response to PI3K-dependent phosphorylation by Akt [35]. FOXO itself has also been shown to induce autophagy (G.J., L.G. Puskás, O. Komonyi, B. Érdi, P. Maróy, T.P.N., and M. Sass, unpublished data). However, we found that FOXO localization was unchanged by overexpression of Atg1 in fat body cells (Figure 6A), indicating that overexpression of Atg1 does not induce autophagy by affecting PI3K signaling upstream of Akt.

As a measure of TOR activity, we examined the effect of Atg1 overexpression on S6K phosphorylation. TOR specifically phosphorylates *Drosophila* S6K at Thr398, homologous to Thr389 of S6K1 in mammals [12]. Western blot analysis showed that while total S6K levels increased slightly in fat body from larvae overexpressing Atg1, phosphorylation of S6K at Thr398 was strongly reduced (Figure 6E). Rheb overexpression increased the level of S6K phosphorylation as expected and restored S6K phosphorylation when co-overexpressed with Atg1. These results suggest that Atg1 overexpression leads to a downregulation of TOR activity. While this effect alone could, in theory, account for the effect of Atg1 overexpression on autophagy and cell size, several observations suggest that this is not the case. *Tor* mutant fat body cells show constitutive autophagy [5]

(F) Atg1-overexpressing cells with aberrant actin staining (large arrowhead) or that have fragmented and been absorbed into neighboring cells (small arrowheads).

(G) A cell overexpressing Atg1 (arrowhead) has lost most peripheral actin staining and has been completely engulfed by a neighboring fat body cell.

Scale bars represent 10 μm. Nuclei are marked in blue. Error bars indicate SD.

Genotypes: (A, B, D–G) *hsflp/+; Act>CD2>GAL4 UAS-GFP/UAS-Atg1^{6B}*. (C) Control: *hsflp/+; Act>CD2>GAL4 UAS-GFP/+*. Atg1: *hsflp/+; Act>CD2>GAL4 UAS-GFP/UAS-Atg1^{6B}*. Atg1 p35: *hsflp/+; Act>CD2>GAL4 UAS-GFP/UAS-Atg1^{6B} UAS-p35*.

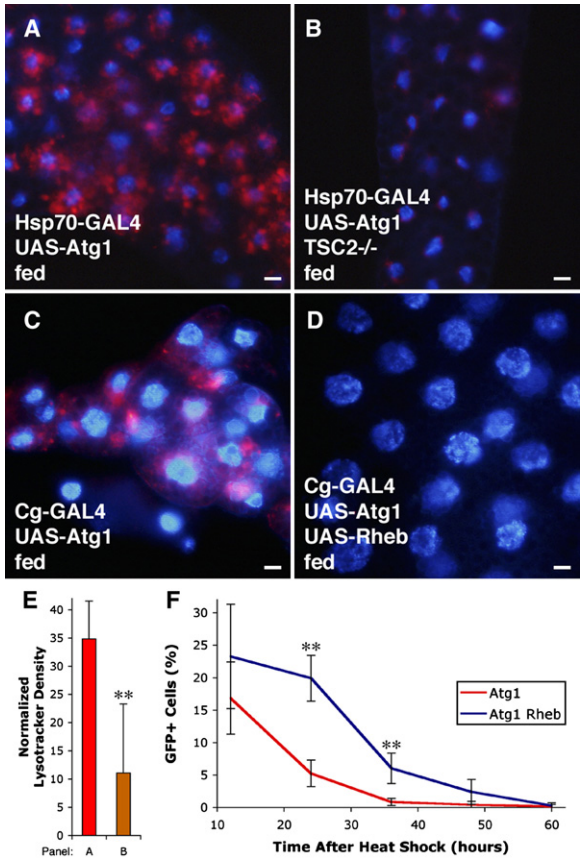


Figure 5. Regulation of Atg1 by TOR Signaling

(A–D) Atg1-induced autophagy is suppressed by activation of the TOR pathway. Heat shock-induced overexpression of Atg1 (A) induces autophagy as shown by Lysotracker staining (red), but mutation of TSC2 inhibits this induction (B). Overexpression of Rheb rescues Atg1-overexpression phenotypes. Overexpression of Atg1 throughout the fat body (C) results in variable reduction in cell size and induction of autophagy. Simultaneous overexpression of Rheb (D) rescues these effects.

(E) Quantitation of Lysotracker staining. Double asterisk indicates a significant difference from Atg1 overexpression alone: $p = 0.0051$.

(F) Coexpression of Rheb delays elimination of Atg1-overexpressing cells. Mean numbers of GFP-positive cells are expressed as a percentage of total cells. Double asterisk indicates a significant difference from Atg1 overexpression alone: $p < 0.002$.

Scale bars represent 10 μm. Nuclei are marked in blue. Error bars indicate SD.

Genotypes: (A) *Hsp70-GAL4/UAS-Atg1^{6B}*. (B) *Hsp70-GAL4 gig^{192}/UAS-Atg1^{6B} gig^{109}*. (C) *Cg-GAL4/+; UAS-Atg1^{GS10797}/+*. (D) *Cg-GAL4/+; UAS-Atg1^{GS10797}/UAS-Rheb$^{EP50.084\text{-}loxP}$*. (E) As in (A) and (B). (F) Atg1: *hsflp/+; Act>CD2>GAL4/UAS-Atg1^{6B}*. Atg1 Rheb: *hsflp/+; Act>CD2>GAL4/UAS-Atg1^{6B} UAS-Rheb^{AV4}*.

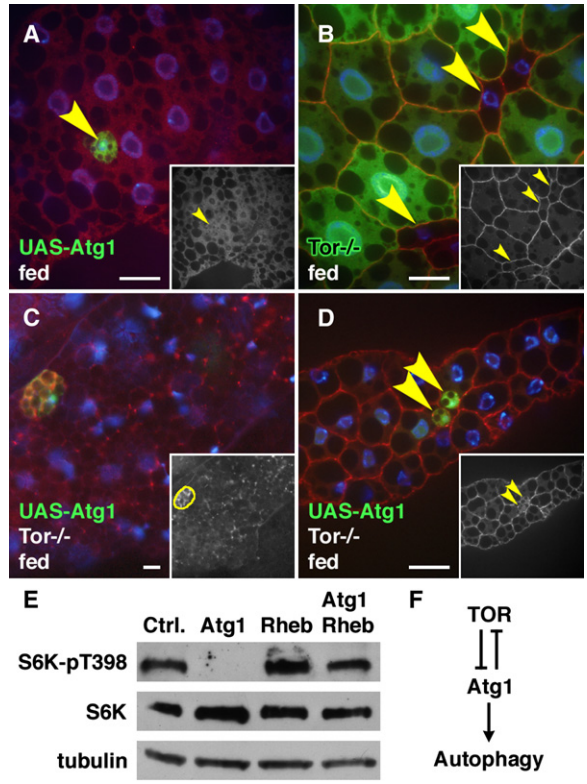


Figure 6. Feedback by Atg1 on TOR

(A) Atg1 overexpression (GFP-positive cell) does not cause FOXO (red) to localize to the nucleus (arrowhead). Inset shows FOXO channel.

(B) *Tor* null cells (loss of GFP, arrowheads) are 70% smaller than surrounding wild-type cells; $p < 0.0001$. Inset shows phalloidin channel.

(C and D) Overexpression of Atg1 in a *Tor* mutant background. In *Tor* null animals, cells overexpressing Atg1 (GFP-positive cells) show increased Lysotracker staining (C) and a 58% reduction in size (D); $p = 0.0003$. DNA channel in (D) shows three representative confocal sections. Inset in (C) shows Lysotracker channel with clonal boundaries outlines in yellow. Inset in (D) shows phalloidin channel; arrowheads indicate Atg1-overexpressing cells.

(E) Western blot showing a decrease in S6K phosphorylation in fat body from larvae overexpressing Atg1, but not from animals overexpressing both Atg1 and Rheb.

(F) Inhibitory feedback by Atg1.

Scale bars represent 10 μm. Nuclei are marked in blue.

Genotypes: (A) *hsflp/+; Act>CD2>GAL4 UAS-GFP/UAS-Atg1^{6B}*. (B) *hsflp; Tor$^{\Delta P}$ FRT40A/UAS-2x eGFP FRT40A fb-GAL4*. (C) *hsflp; Tor$^{\Delta P}$/Tor$^{\Delta P}$; Act>CD2>GAL4 UAS-GFP UAS-Atg1^{GS10797}/+*. (D) *hsflp; Tor$^{\Delta P}$/Tor$^{\Delta P}$; Act>CD2>GAL4 UAS-GFP/UAS-Atg1^{6B}*. (E) Control: *Hsp70-GAL4/+*. Atg1: *Hsp70-GAL4/UAS-Atg1^{6B}*. Rheb: *Hsp70-GAL4/UAS-Rheb$^{EP50.084\text{-}loxP}$*. Atg1 Rheb: *Hsp70-GAL4/UAS-Atg1^{6B} UAS-Rheb$^{EP50.084\text{-}loxP}$*.

and are reduced in size (Figure 6B). However, we found that overexpression of Atg1 in *Tor* null mutant animals led to a further increase in autophagy (Figure 6C) and a further decrease in cell size (Figure 6D), indicating that these effects are largely independent of TOR. Moreover, the growth reduction of Atg1-overexpressing cells is significantly more severe than that of *Tor* null mutant cells (94% versus 70%; $p < 0.0001$; compare Figures 2H and 6B), further indicating that the size reduction in Atg1-expressing cells is at least partially TOR independent. Thus, downregulation of TOR activity by Atg1 overexpression does not fully account for its effects on autophagy and cell size. Rather, these data are best described by a model whereby Atg1 overexpression negatively feeds back on TOR (Figure 6F), leading to a further activation of autophagy and reduced cell growth.

The Kinase Domain of Atg1 Is Essential for Induction of Autophagy

As described above, it is unclear whether the kinase activity of Atg1 is required for proper induction of autophagy in yeast. To address this issue, we generated

dc_840_14

a kinase-negative mutant of *Drosophila* Atg1 (Atg1^{K38Q}) through site-directed mutagenesis of lysine 38, in the ATP binding site of the kinase domain. This residue is homologous to lysine 54 of yeast Atg1, which has been shown to be required for normal kinase activity [18].

We found that expression of Atg1^{K38Q} did not lead to increased autophagy in the fat body of normally fed animals (Figure 7A), nor was it able to rescue the autophagy defect in *Atg1* null mutants (Figures S1D and S1G). Consistent with these results, clonal expression of Atg1^{K38Q} in the wing imaginal disc did not result in cell elimination, caspase activation, or DNA fragmentation (Figure 7F and data not shown), unlike wild-type Atg1. Interestingly, we found that expression of Atg1^{K38Q} was sufficient to inhibit starvation- or rapamycin-induced autophagy when expressed in clones (Figure 7B and Figure S1F) or throughout the fat body (compare Figures 7C and 7D; Figure 7E), suggesting that kinase-defective Atg1 interferes with the function of wild-type Atg1, acting as a dominant-negative mutant. Similarly, expression of Atg1^{K38Q} in the eye partially rescued the lethality and reduced adult eye size caused by Atg1 overexpression, but had no effect on eye morphology when expressed alone (Figures S2D, S2I, and S2J, respectively).

Expression of Atg1^{K38Q} was not completely without effect, however. We observed that it leads to a partial reduction in TOR activity (Figure 7G), as well as a modest decrease in cell size (see Figures 7A and 7B). These findings imply an as yet undetermined function of Atg1 that does not rely on its kinase activity. Indeed, the fact that Atg1^{K38Q} was able to rescue a low percentage of *Atg1* mutant flies to adulthood (Figure S1A) implies that Atg1 has a kinase-independent function outside regulation of autophagy. We therefore conclude that while Atg1 appears to have undetermined kinase-independent function, the kinase activity of Atg1 is essential for its ability to promote autophagy in *Drosophila*.

Discussion

Regulation of Autophagy by Atg1

Delivery of cytoplasmic components to the lysosome through autophagy involves multiple distinct steps including nucleation, expansion and closure of the autophagosome, and its subsequent fusion with the lysosome. These membrane-trafficking events require the recruitment and subsequent retrieval of a large number of autophagy-specific Atg proteins, as well as general factors involved in vesicle trafficking. Given this complexity, the finding that overexpression of a single Atg protein is sufficient to accomplish all essential steps in this process is striking. Autophagy occurs constitutively at a basal rate in most eukaryotic cells [6], so acceleration of a single rate-limiting step by overexpression of Atg1 may be sufficient to increase the overall rate of autophagy. Alternatively, the interaction of Atg1 with multiple Atg proteins suggests that Atg1 may function at multiple steps in the autophagic process. Identification of the relevant in vivo substrates of Atg1 will help to clarify this issue. A recent yeast proteomic microarray study identified a number of in vitro substrates of Atg1, including Atg8 and Atg18, which function in autophagosomal expansion and retrieval of components of the

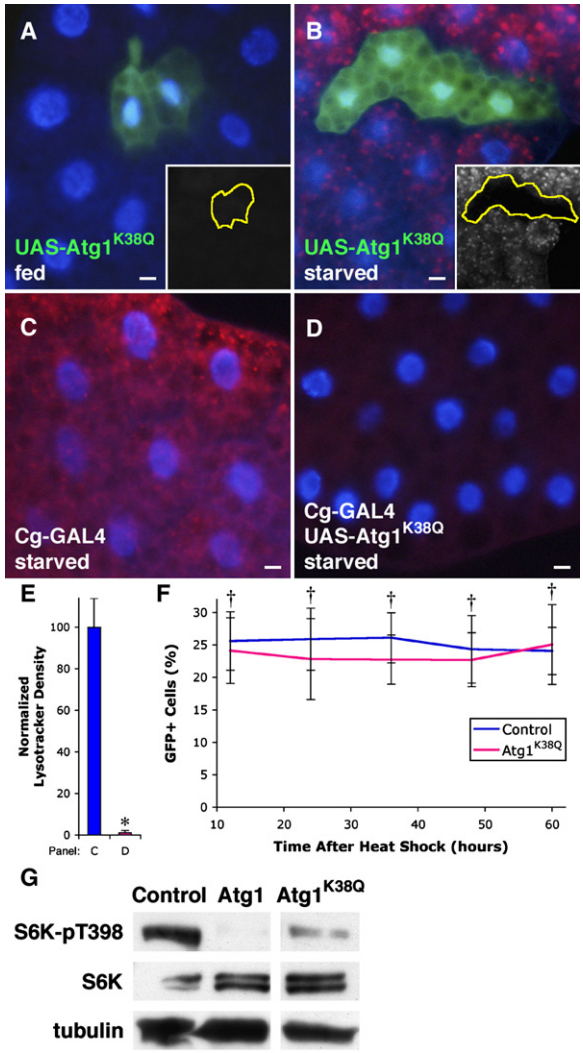


Figure 7. Induction of Autophagy Requires Atg1 Kinase Activity

(A–D) Expression of kinase-defective Atg1 inhibits autophagy. Atg1^{K38Q} expression has no effect on autophagy in fed animals (A) but cell autonomously inhibits induction of autophagy in the fat body of starved animals (B). Tissue-wide induction of autophagy by starvation (C) is inhibited by expression of kinase inactive Atg1 (D). Insets show the Lysotracker channel of the respective images, with clonal boundaries outlined in yellow.

(E) Quantitation of Lysotracker staining. Asterisk indicates a significant difference from wild-type: $p < 0.0001$.

(F) Wing disc cells overexpressing kinase-defective Atg1 are not eliminated. Mean numbers of GFP-positive cells are expressed as a percentage of total cells. Dagger indicates no significant difference from the wild-type control: $p > 0.1$.

(G) Kinase-defective Atg1 leads to a modest reduction in TOR signaling. Nonconsecutive lanes are shown from the same western blot.

Scale bars represent 10 μm. Nuclei are marked in blue. Error bars indicate SD.

Genotypes: (A, B) *hsflp/+; Act>CD2>GAL4 UAS-GFP/UAS-Atg1^{KQ13A}*. (C) *Cg-GAL4/+*. (D) *Cg-GAL4/+; UAS-Atg1^{KQ13A}/+*. (E) As in (C) and (D). (F) Control: *hsflp/+; Act>CD2>GAL4 UAS-GFP/+*. Atg1^{K38Q}: *hsflp/+; Act>CD2>GAL4 UAS-GFP/UAS-Atg1^{KQ13A}*. (G) Control: *Hsp70-GAL4/+*. Atg1: *Hsp70-GAL4/UAS-Atg1^{6B}*. Atg1^{K38Q}: *Hsp70-GAL4/UAS-Atg1^{KQ13A}*.

autophagic machinery, respectively, as well as general factors involved in vesicle transport and vacuolar function [21].

The role of the kinase activity of yeast Atg1 in regulating autophagy is the matter of some debate, and different groups have drawn conflicting conclusions. A consensus view, however, may be that autophagy and the CVT pathway require different levels of Atg1 kinase activity or that Atg1 has different substrates under differing nutrient conditions. In higher eukaryotes, the role of Atg1 kinase activity may differ from that in yeast, but the CVT pathway has not been observed in metazoan cells. Consistent with the findings of Ohsumi and colleagues [18, 24], however, our results indicate that the kinase domain of *Drosophila* Atg1 is required for autophagy, as indicated by the fact that the kinase-inactive $Atg1^{K38Q}$ mutant failed to restore starvation-induced autophagy to *Atg1* mutants and was unable to induce autophagy when overexpressed. However, the partial reduction in size and TOR activity observed upon expression of $Atg1^{K38Q}$, as well as its partial rescue of *Atg1* mutants, indicate that Atg1 may have other, kinase-independent functions beyond regulating autophagy.

The mechanisms by which upstream signaling pathways regulate Atg1 are also likely to differ between yeast and multicellular organisms, because essential components of the TOR-regulated Atg1 complex such as Atg13 and Atg17 are not readily identifiable in animal genomes. Nonetheless, our results are consistent with a similar negative regulation of Atg1 by TOR, as indicated by the fact that activation of TOR signaling by Rheb overexpression or *Tsc2* mutation suppressed the ability of Atg1 to induce autophagy. Increased Atg1 activity in response to loss of TOR signaling is likely to be critical for cell homeostasis and survival, as shown by the fact that animals doubly mutant for *Atg1* and *Tor* show a synthetic embryonic lethal phenotype [5]. In addition, our results demonstrate an unexpected mode of signaling from Atg1 to TOR, in which increased Atg1 levels lead to downregulation of TOR kinase activity. It is unclear whether this reflects a direct effect of Atg1 on the activity of TOR or an upstream regulator, or an indirect consequence of the high level of autophagy in these cells, perhaps through increased turnover of TOR-signaling components. The finding that a pool of TOR protein resides on intracellular vesicles [31, 36] and that TOR signaling is reduced in endocytic mutants [31] suggests that TOR activity may respond to rates of vesicular trafficking, such as autophagy. Regardless of mechanism, these results suggest the existence of a self-reinforcing feedback loop, whereby increased Atg1 levels lead to downregulation of TOR activity, resulting in further activation of Atg1. In contrast, we have shown previously that induction of autophagy in response to loss of TOR signaling is dampened by the resultant inactivation of S6K, which is required for normal autophagy [5]. Thus, TOR-mediated regulation of autophagy involves both positive and negative feedback.

Autophagy as a Negative Effector of Cell Growth

Autophagy is a catabolic process that inversely correlates with cell growth, suggesting that increased levels of autophagy observed in growth-restricted cells may contribute to their reduced growth rate. The results presented here provide genetic support for this model. Our data indicate that clones of autophagy-defective cells have a growth advantage over wild-type cells under physiological conditions that normally induce autophagy, including starvation and rapamycin treatment. These results are confirmed by the marked size reduction of cells overexpressing Atg1, further supporting the role of autophagy as a negative effector of growth in TOR signaling. Thus, autophagy is partly responsible for the growth restriction resulting from physiological inhibition of TOR signaling and is capable of inhibiting growth independent of TOR signaling.

In contrast to the growth advantage we observed in autophagy-defective cells, previous studies with yeast or cultured mammalian cells reported that inhibition of autophagy results in rapid cell death in response to starvation [2, 17]. This difference is likely due to the mosaic nature of our experiments, in which clones of *Atg1* mutant cells are surrounded by autophagy-competent wild-type cells and may in effect parasitize nutrients liberated through the autophagic activity of their neighbors. This is likely to be particularly evident in fat body cells, which are specialized for nutrient storage and mobilization. We note that this genetic mosaicism is similar to the situation facing tumor cells within wild-type tissues. Thus, the increased growth capacity resulting from disruption of autophagy may contribute to the tumorigenicity of cells mutant for tumor suppressors such as PTEN, TSC1 and 2, beclin 1/Atg6 [5, 7, 8], and possibly LC3/Atg8 and Atg7 [37].

Whereas autophagy had an inhibitory effect on cell growth under physiological conditions, this was not the case in cells with severely disrupted TOR signaling, such as in cells with null mutations in *Pdk1* (this report) or *Tor* [5], despite the strong correlation of reduced cell growth and increased autophagy in these cells. Disruption of autophagy had no effect on the growth of *Pdk1* null cells and actually led to a further decrease in cell size of *Tor* mutants. In the complete absence of TOR signaling, nutrient uptake is severely curtailed [31], and under these extreme conditions, the metabolic benefits of nutrients liberated by autophagy may outweigh its potential growth-inhibitory catabolic effect. We conclude that autophagy has context-dependent effects on cell growth, providing for a rudimentary level of metabolism and growth under conditions of severe nutrient deprivation, acting as a net inhibitor of growth under conditions of reduced TOR signaling, and strongly inhibiting cell growth when induced to high levels. These findings add autophagy to the growing list of effector pathways and cellular processes through which TOR signaling controls cell growth, including translation, transcription, nutrient import, and endocytosis.

Autophagy and Cell Death

Previous studies in a number of experimental systems indicate that the role of autophagy in cell death is also likely to be context dependent. For example, autophagy has been found to protect against cell death in cases of growth factor withdrawal, starvation, and neurodegeneration [17, 38, 39] but to be required for some cases of autophagic cell death [14–16, 40]. Thus, observations of autophagic structures in dying cells are equally consistent with a causal, neutral, or even inhibitory role of

dc_840_14

autophagy in cell death. The ability to induce autophagy through Atg1 overexpression has enabled us to directly test the potential role of autophagy in promoting cell death. Our results indicate that induction of autophagy is sufficient to induce cell death. We find that death resulting from Atg1-induced autophagy is suppressed by caspase inhibition and is associated with caspase activation, DNA fragmentation, and cytoskeletal disruption, suggesting that high levels of autophagy result in apoptotic cell death. The connection between apoptosis and autophagy is further supported by the recent demonstration that overexpression of the antiapoptotic protein Bcl-2 can inhibit autophagy by interacting with the Atg6 homolog Beclin 1 [41]. Mutant versions of Beclin 1 that are unable to bind Bcl-2 stimulate autophagy and promote cell death, similar to the effects of Atg1.

By what mechanisms might autophagy lead to cell death? The observation that starvation-induced autophagy is reversible and does not normally result in cell elimination suggests that starvation conditions may be protective against autophagy-induced death. Induction of autophagy is tolerated or even beneficial in cells with reduced biosynthetic activity, but may be detrimental in cells whose resources are devoted to continued growth. Self-limiting mechanisms also serve to prevent starvation-induced autophagy from proceeding at continuously high levels [5, 41]. During autophagic cell death, alternate activation of the autophagic machinery may circumvent these feedback mechanisms, resulting in high levels of sustained autophagy that are destructive to the cell. In addition, the level of *Atg1* gene expression may be critical; it is not upregulated under starvation conditions [27], but its levels peak at the beginning of the *Drosophila* pupal stage [42], when autophagic cell death is induced. Autophagic cell death may also result from the selective degradation of specific survival-promoting or death-inhibiting factors. In this regard, it was recently shown that the caspase-inhibitor zVAD results in targeted autophagic degradation of catalase, leading to accumulation of radical oxygen species and death [16].

Concluding Remarks

In summary, our results demonstrate that constitutive induction of autophagy inhibits cell growth and leads to cell death, highlighting the importance of physiological mechanisms that restrain this process. In addition, the finding that Atg1 expression is sufficient to induce autophagy provides a new tool for experimental or therapeutic manipulation of autophagy. Compounds that target the kinase activity of Atg1 may lead to novel therapies for the wide range of diseases linked to autophagy.

Experimental Procedures

GFP-marked overexpression clones in the fat body were generated through heat shock-independent induction as described [43] and in the wing disc by means of 1 hr heat shock at 37°C, 36–48 hr after hatching (elimination studies) or 30–60 min heat shock at 37°C, 24–52 hr after hatching (staining). Mutant clones in the fat body were generated by FLP/FRT mitotic recombination [44] by means of 2 hr heat shock at 37°C, 0–8 hr after egg laying. Cell elimination was quantitated with 5 images of each genotype; an average of 208 cells were quantitated. Because Ubi-GFP was found to have variable expression in the fat body, UAS-GFP driven by fb-GAL4 or Cg-GAL4 was used as a marker in that tissue. Mutant clones in the wing disc were generated with 2 hr heat shock at 37°C, 24–28 hr after hatching. 72–96 hr after hatching, untreated larvae containing mutant clones were dissected immediately (fed) or starved for 45 hr on PBS (starved). Rapamycin-treated larvae were raised on 2 μM rapamycin in fly medium from hatching and were dissected 192–196 hr after hatching. Hsp70-GAL4-driven overexpression of Atg1 was induced by 2 hr (1 hr in Figure 5) heat shock at 37°C, 48–72 hr after hatching, followed by 6 hr recovery at room temperature. Significance was determined in all experiments by two-tailed p values from unpaired t test. See Supplemental Data for additional procedures.

Supplemental Data

Supplemental Data include three figures and Supplemental Experimental Procedures and can be found with this article online at http://www.current-biology.com/cgi/content/full/17/1/1/DC1/.

Acknowledgments

We thank members of the Neufeld lab for helpful discussions and comments on the manuscript. This work was supported by National Institutes of Health grant RO1 GM62509.

Received: June 6, 2006
Revised: October 20, 2006
Accepted: October 26, 2006
Published: January 8, 2007

References

1. Levine, B., and Klionsky, D.J. (2004). Development by self-digestion: molecular mechanisms and biological functions of autophagy. Dev. Cell *6*, 463–477.
2. Tsukada, M., and Ohsumi, Y. (1993). Isolation and characterization of autophagy-defective mutants of *Saccharomyces cerevisiae*. FEBS Lett. *333*, 169–174.
3. Thumm, M., Egner, R., Koch, B., Schlumpberger, M., Straub, M., Veenhuis, M., and Wolf, D.H. (1994). Isolation of autophagocytosis mutants of *Saccharomyces cerevisiae*. FEBS Lett. *349*, 275–280.
4. Klionsky, D.J., Cregg, J.M., Dunn, W.A., Jr., Emr, S.D., Sakai, Y., Sandoval, I.V., Sibirny, A., Subramani, S., Thumm, M., Veenhuis, M., et al. (2003). A unified nomenclature for yeast autophagy-related genes. Dev. Cell *5*, 539–545.
5. Scott, R.C., Schuldiner, O., and Neufeld, T.P. (2004). Role and regulation of starvation-induced autophagy in the *Drosophila* fat body. Dev. Cell *7*, 167–178.
6. Shintani, T., and Klionsky, D.J. (2004). Autophagy in health and disease: a double-edged sword. Science *306*, 990–995.
7. Arico, S., Petiot, A., Bauvy, C., Dubbelhuis, P.F., Meijer, A.J., Codogno, P., and Ogier-Denis, E. (2001). The tumor suppressor PTEN positively regulates macroautophagy by inhibiting the phosphatidylinositol 3-kinase/protein kinase B pathway. J. Biol. Chem. *276*, 35243–35246.
8. Liang, X.H., Jackson, S., Seaman, M., Brown, K., Kempkes, B., Hibshoosh, H., and Levine, B. (1999). Induction of autophagy and inhibition of tumorigenesis by beclin 1. Nature *402*, 672–676.
9. Petiot, A., Ogier-Denis, E., Blommaart, E.F., Meijer, A.J., and Codogno, P. (2000). Distinct classes of phosphatidylinositol 3′-kinases are involved in signaling pathways that control macroautophagy in HT-29 cells. J. Biol. Chem. *275*, 992–998.
10. Noda, T., and Ohsumi, Y. (1998). Tor, a phosphatidylinositol kinase homologue, controls autophagy in yeast. J. Biol. Chem. *273*, 3963–3966.
11. Neufeld, T.P. (2004). Role of autophagy in developmental cell growth and death: insights from *Drosophila*. In Autophagy, D.J. Klionsky, ed. (Georgetown: Landes Bioscience), pp. 224–232.
12. Wullschleger, S., Loewith, R., and Hall, M.N. (2006). TOR signaling in growth and metabolism. Cell *124*, 471–484.
13. Clarke, P.G. (1990). Developmental cell death: morphological diversity and multiple mechanisms. Anat. Embryol. (Berl.) *181*, 195–213.

14. Shimizu, S., Kanaseki, T., Mizushima, N., Mizuta, T., Arakawa-Kobayashi, S., Thompson, C.B., and Tsujimoto, Y. (2004). Role of Bcl-2 family proteins in a non-apoptotic programmed cell death dependent on autophagy genes. Nat. Cell Biol. *6*, 1221–1228.
15. Veneault-Fourrey, C., Barooah, M., Egan, M., Wakley, G., and Talbot, N.J. (2006). Autophagic fungal cell death is necessary for infection by the rice blast fungus. Science *312*, 580–583.
16. Yu, L., Wan, F., Dutta, S., Welsh, S., Liu, Z., Freundt, E., Baehrecke, E.H., and Lenardo, M. (2006). Autophagic programmed cell death by selective catalase degradation. Proc. Natl. Acad. Sci. USA *103*, 4952–4957.
17. Lum, J.J., Bauer, D.E., Kong, M., Harris, M.H., Li, C., Lindsten, T., and Thompson, C.B. (2005). Growth factor regulation of autophagy and cell survival in the absence of apoptosis. Cell *120*, 237–248.
18. Kamada, Y., Funakoshi, T., Shintani, T., Nagano, K., Ohsumi, M., and Ohsumi, Y. (2000). Tor-mediated induction of autophagy via an Apg1 protein kinase complex. J. Cell Biol. *150*, 1507–1513.
19. Wang, Z., Wilson, W.A., Fujino, M.A., and Roach, P.J. (2001). Antagonistic controls of autophagy and glycogen accumulation by Snf1p, the yeast homolog of AMP-activated protein kinase, and the cyclin-dependent kinase Pho85p. Mol. Cell. Biol. *21*, 5742–5752.
20. Budovskaya, Y.V., Stephan, J.S., Deminoff, S.J., and Herman, P.K. (2005). An evolutionary proteomics approach identifies substrates of the cAMP-dependent protein kinase. Proc. Natl. Acad. Sci. USA *102*, 13933–13938.
21. Ptacek, J., Devgan, G., Michaud, G., Zhu, H., Zhu, X., Fasolo, J., Guo, H., Jona, G., Breitkreutz, A., Sopko, R., et al. (2005). Global analysis of protein phosphorylation in yeast. Nature *438*, 679–684.
22. Reggiori, F., Tucker, K.A., Stromhaug, P.E., and Klionsky, D.J. (2004). The Atg1-Atg13 complex regulates Atg9 and Atg23 retrieval transport from the pre-autophagosomal structure. Dev. Cell *6*, 79–90.
23. Abeliovich, H., Zhang, C., Dunn, W.A., Jr., Shokat, K.M., and Klionsky, D.J. (2003). Chemical genetic analysis of Apg1 reveals a non-kinase role in the induction of autophagy. Mol. Biol. Cell *14*, 477–490.
24. Kabeya, Y., Kamada, Y., Baba, M., Takikawa, H., Sasaki, M., and Ohsumi, Y. (2005). Atg17 functions in cooperation with Atg1 and Atg13 in yeast autophagy. Mol. Biol. Cell *16*, 2544–2553.
25. Rusten, T.E., Lindmo, K., Juhász, G., Sass, M., Seglen, P.O., Brech, A., and Stenmark, H. (2004). Programmed autophagy in the *Drosophila* fat body is induced by ecdysone through regulation of the PI3K pathway. Dev. Cell *7*, 179–192.
26. Young, A.R., Chan, E.Y., Hu, X.W., Kochl, R., Crawshaw, S.G., High, S., Hailey, D.W., Lippincott-Schwartz, J., and Tooze, S.A. (2006). Starvation and ULK1-dependent cycling of mammalian Atg9 between the TGN and endosomes. J. Cell Sci. *119*, 3888–3900.
27. Kirisako, T., Baba, M., Ishihara, N., Miyazawa, K., Ohsumi, M., Yoshimori, T., Noda, T., and Ohsumi, Y. (1999). Formation process of autophagosome is traced with Apg8/Aut7p in yeast. J. Cell Biol. *147*, 435–446.
28. Kabeya, Y., Mizushima, N., Ueno, T., Yamamoto, A., Kirisako, T., Noda, T., Kominami, E., Ohsumi, Y., and Yoshimori, T. (2000). LC3, a mammalian homologue of yeast Apg8p, is localized in autophagosome membranes after processing. EMBO J. *19*, 5720–5728.
29. Zinke, I., Schutz, C.S., Katzenberger, J.D., Bauer, M., and Pankratz, M.J. (2002). Nutrient control of gene expression in *Drosophila*: microarray analysis of starvation and sugar-dependent response. EMBO J. *21*, 6162–6173.
30. Juhász, G., Csikós, G., Sinka, R., Erdélyi, M., and Sass, M. (2003). The *Drosophila* homolog of Aut1 is essential for autophagy and development. FEBS Lett. *543*, 154–158.
31. Hennig, K.M., Colombani, J., and Neufeld, T.P. (2006). TOR coordinates bulk and targeted endocytosis in the *Drosophila melanogaster* fat body to regulate cell growth. J. Cell Biol. *173*, 963–974.
32. Hosokawa, N., Hara, Y., and Mizushima, N. (2006). Generation of cell lines with tetracycline-regulated autophagy and a role for autophagy in controlling cell size. FEBS Lett. *580*, 2623–2629.
33. Debnath, J., Mills, K.R., Collins, N.L., Reginato, M.J., Muthuswamy, S.K., and Brugge, J.S. (2002). The role of apoptosis in creating and maintaining luminal space within normal and oncogene-expressing mammary acini. Cell *111*, 29–40.
34. Martin, D.N., and Baehrecke, E.H. (2004). Caspases function in autophagic programmed cell death in *Drosophila*. Development *131*, 275–284.
35. Puig, O., Marr, M.T., Ruhf, M.L., and Tjian, R. (2003). Control of cell number by *Drosophila* FOXO: downstream and feedback regulation of the insulin receptor pathway. Genes Dev. *17*, 2006–2020.
36. Kunz, J., Schneider, U., Howald, I., Schmidt, A., and Hall, M.N. (2000). HEAT repeats mediate plasma membrane localization of Tor2p in yeast. J. Biol. Chem. *275*, 37011–37020.
37. Jin, S. (2006). Autophagy, mitochondrial quality control, and oncogenesis. Autophagy *2*, 80–84.
38. Hara, T., Nakamura, K., Matsui, M., Yamamoto, A., Nakahara, Y., Suzuki-Migishima, R., Yokoyama, M., Mishima, K., Saito, I., Okano, H., et al. (2006). Suppression of basal autophagy in neural cells causes neurodegenerative disease in mice. Nature *441*, 885–889.
39. Komatsu, M., Waguri, S., Chiba, T., Murata, S., Iwata, J., Tanida, I., Ueno, T., Koike, M., Uchiyama, Y., Kominami, E., et al. (2006). Loss of autophagy in the central nervous system causes neurodegeneration in mice. Nature *441*, 880–884.
40. Yu, L., Alva, A., Su, H., Dutt, P., Freundt, E., Welsh, S., Baehrecke, E.H., and Lenardo, M.J. (2004). Regulation of an ATG7-beclin 1 program of autophagic cell death by caspase-8. Science *304*, 1500–1502.
41. Pattingre, S., Tassa, A., Qu, X., Garuti, R., Liang, X.H., Mizushima, N., Packer, M., Schneider, M.D., and Levine, B. (2005). Bcl-2 antiapoptotic proteins inhibit Beclin 1-dependent autophagy. Cell *122*, 927–939.
42. Arbeitman, M.N., Furlong, E.E., Imam, F., Johnson, E., Null, B.H., Baker, B.S., Krasnow, M.A., Scott, M.P., Davis, R.W., and White, K.P. (2002). Gene expression during the life cycle of *Drosophila melanogaster*. Science *297*, 2270–2275.
43. Britton, J.S., Lockwood, W.K., Li, L., Cohen, S.M., and Edgar, B.A. (2002). *Drosophila*'s insulin/PI3-kinase pathway coordinates cellular metabolism with nutritional conditions. Dev. Cell *2*, 239–249.
44. Xu, T., and Rubin, G.M. (1993). Analysis of genetic mosaics in developing and adult *Drosophila* tissues. Development *117*, 1223–1237.

8

Experimental Control and Characterization of Autophagy in Drosophila

Gabor Juhasz and Thomas P. Neufeld

Summary

Insects such as the fruit fly *Drosophila melanogaster*, which fundamentally reorganize their body plan during metamorphosis, make extensive use of autophagy for their normal development and physiology. In the fruit fly, the hepatic/adipose organ known as the fat body accumulates nutrient stores during the larval feeding stage. Upon entering metamorphosis, as well as in response to starvation, these nutrients are mobilized through a massive induction of autophagy, providing support to other tissues and organs during periods of nutrient deprivation. High levels of autophagy are also observed in larval tissues destined for elimination, such as the salivary glands and larval gut. Drosophila is emerging as an important system for studying the functions and regulation of autophagy in an in vivo setting. In this chapter we describe reagents and methods for monitoring autophagy in Drosophila, focusing on the larval fat body. We also describe methods for experimentally activating and inhibiting autophagy in this system and discuss the potential for genetic analysis in Drosophila to identify novel genes involved in autophagy.

Key Words: Atg8; autophagy; Drosophila; GFP; TEM; LysoTracker Red; somatic clones.

1. Introduction

Autophagic structures in insect tissues were first described nearly 40 years ago in larval cells preparing for metamorphosis (reviewed in **ref. *1***). More recent analyses in Drosophila have focused on the interactions of autophagic and apoptotic processes ***(2–9)***, the regulation of autophagy by nutrient and hormonal signaling pathways ***(9–12)***, and its role in neurodegeneration ***(13)***. As Drosophila has emerged as a genetically amenable system to analyze

From: *Methods in Molecular Biology, vol. 445: Autophagosome and Phagosome*
Edited by: V. Deretic © Humana Press, Totowa, NJ

autophagy in vivo, a description of currently used methods for manipulating and monitoring autophagy in this system may be of use. Here we describe a number of approaches applicable to the study of autophagy in Drosophila.

2. Materials

2.1. Drosophila Stocks

For clonal expression of transgenes, we cross UAS lines of interest carrying X-linked hsp70-FLP to a Act>CD2>GAL4 UAS-GFP strain. For loss of function mosaic studies, mutations of interest are recombined with FRT inserts at the base of the proper chromosome arm, then crossed with fb-GAL4 FRT UAS-GFP lines. Alternatively, clones can be marked using UAS-dsRed or UAS-RFP, which allows GFP-Atg8 to be used as an autophagy indicator in this system.

2.2. Larval Cultures and Starvation

1. Standard cornmeal-molasses-agar fly food.
2. 20% sucrose in water.

2.3. Dissection and Staining of Fat Bodies with LysoTracker Red

1. PBS (phosphate-buffered saline), pH = 7.4.
2. DAPI (4′,6-diamidino-2-phenylindole dihydrochloride; Sigma, St. Louis, MO) dissolved in water to obtain a 1 m*M* (1000x) stock solution, which can be stored in a dark vial at 4°C.
3. LysoTracker Red DND-99 (Molecular Probes, Eugene, OR) diluted in PBS to obtain a 20 m*M* (200x) stock solution, which is stable in a dark vial at 4°C for a few weeks.

2.4. Fixation for Confocal Microscopy

1. Formaldehyde (Fluka, Milwaukee, WI).
2. Vectashield (Vectorlabs, Burlingame, CA).

2.5. Fixation and Embedding for Transmission Electron Microscopy (TEM)

1. Paraformaldehyde, glutaraldehyde, OsO_4, Polybed 812 (Polysciences, Warrington, PA).

dc_840_14

3. Methods

3.1. Experimental Regulation of Autophagy in the Larval Fat Body

This section discusses approaches for experimentally inducing or inhibiting autophagy in the Drosophila larval fat body, using manipulations of culture conditions and genetic expression.

3.1.1. Nutrient Control

The larval fat body is exquisitely sensitive to nutrient conditions, and thus autophagy is readily induced by a simple starvation regimen. Induction of autophagy can first be detected within 1–2 h of starvation, and by 4 h after food withdrawal a robust response is consistently observed.

3.1.1.1. Pretreatment

Due to the high sensitivity of the fat body to nutrient levels, preincubation of larvae in fresh media under uncrowded conditions is recommended to prevent chronic induction of autophagy, which can diminish the acute response to starvation. We generally transfer 10–20 late second-instar larvae to vials containing fresh fly food supplemented with live yeast paste, 16–24 h prior to starvation.

3.1.1.2. Induction by Starvation

Larvae can be conveniently floated out of fly food media by pouring several mL of a 20% sucrose solution onto the culture; the high density of this solution causes the larvae to float to the surface. Larvae are then transferred by forceps to vials or small dishes containing fresh 20% sucrose and incubated at room temperature for the duration of the starvation period, generally 4 h. Alternatively, larvae can be transferred to vials containing a strip of filter paper saturated with PBS. Following the starvation period, larvae are dissected and immediately processed as described in section 3.2.2.

3.1.1.3. Induction by Rapamycin

The autophagic response to starvation in the larval fat body appears to result largely from inhibition of the target of rapamycin (TOR) signaling pathway ***(14)***. As an alternative to starvation, direct inhibition of TOR by the drug rapamycin results in a robust autophagic response. Following pretreatment as above, larvae are transferred to fresh fly food containing rapamycin at a concentration of 1 μ*M*. Weak induction is observed by 4 h, with a much stronger response occurring by 24 h.

3.1.2. Developmental Control

During the final 24 h of the larval period, rising titers of the steroid hormone ecdysone result in a developmentally programmed induction of autophagy in the larval fat body ***(12,15)***. This developmentally regulated autophagy can be readily observed by comparing autophagy markers in early vs. late third-instar larvae under fed conditions. Premature induction can be achieved by exposure of dissected fat body to ecdysone in culture. Such methods have been described previously ***(15)*** and are not detailed here.

3.1.3. Genetic Control

A major advantage of Drosophila is the ease with which genetic function can be manipulated in this system. Gene expression can be readily induced or inhibited in vivo, either singly or in multiple combinations, and at precise times and locations during development. An important component of this control is the ability to alter gene expression using a mosaic approach, in which marked clones of cells differ in their genetic makeup from their wild-type neighbors **(Fig. 1A,B)**. The principal advantage of this approach is that experimental and control cells are subject to the same environmental and developmental conditions, and thus subtle phenotypic differences can be more readily detected than in animal-to-animal comparisons. This technique is especially applicable to studies of autophagy, which vary with developmental and culture conditions.

The method of choice for both loss and gain of function mosaic experiments in Drosophila is the Flippase (FLP)-Flippase Recombinase Target (FRT) system of mitotic recombination. In this system, FLP-induced exchange between heterozygous sister chromatids causes loss of heterozygosity for a given chromosomal arm. Alternatively, FLP-induced expression of the GAL4 transcription factor can be used to clonally activate UAS-controlled transgenes. As these methods have been extensively reviewed elsewhere ***(16,17)***, we will focus our comments on their application in the larval fat body.

3.1.3.1. Loss of Function Clones

The induction of FLP-mediated, green fluorescent protein (GFP)–marked loss of function clones in the fat body requires two modifications of the general protocols developed for imaginal tissues. First, because this procedure works only in mitotically active cells, clones must be induced during the first 8 h of embryonic development, after which time the fat body enters an endoreduplicative (nonmitotic) cell cycle. We typically perform 6- to 8-h embryo collections, followed immediately by a 1- to 2-hour heat shock at 37°C to activate expression of the hsp70-driven FLP gene. This typically gives rise to several

dc_840_14

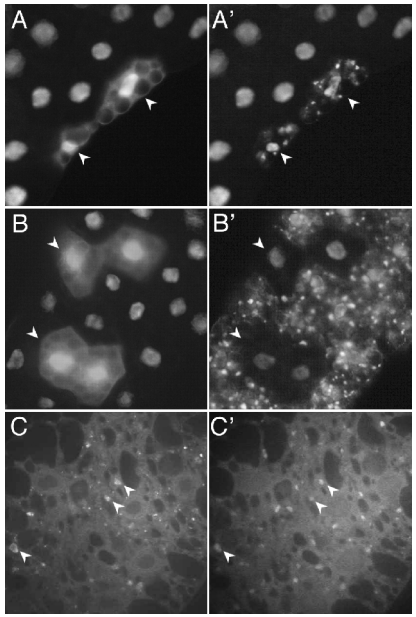


Fig. 1. Autophagy in the larval fat body. Examples of Lysotracker Red–stained samples are shown. (**A, A′**) In fed animals, clonal overexpression of Tsc1 and Tsc2, negative regulators of the TOR signaling pathway, causes a punctate pattern of LysoTracker Red staining (**A′**) exclusively within the transgene-expressing cells, which are marked by cytoplasmic GFP expression in (**A**) and indicated by arrowheads. Nuclei are stained with DAPI. (**B, B′**) In response to a 4-h starvation treatment, wild-type control cells display strong punctate LysoTracker Red staining (**B′**). In contrast, LysoTracker Red staining is blocked in cells expressing high levels of Rheb, an upstream activator of TOR signaling. Cells overexpressing Rheb are marked by cytoplasmic GFP expression in (**B**) and indicated by arrowheads. Nuclei are stained with DAPI. (**C, C′**) Fat body dissected from 4-h starved larvae expressing GFP-Atg8 (**C**) and stained with LysoTracker Red (**C′**). Large punctate structures positive for both GFP-Atg8 and LysoTracker Red represent autolysosomes (indicated by arrowheads), whereas smaller structures marked solely by GFP-Atg8 represent autophagosomes.

one- to two-cell clones per fat body lobe. Second, we find that the commonly used GFP marker lines driven by the ubiquitin promoter display nonuniform expression levels in the fat body, which can confound efforts to identify clones by GFP expression. As a remedy, we use Upstream Activating Sequence (UAS)-

driven GFP under the control of strong fat body GAL4 lines such as fb- or Cg-GAL4 ***(9,18)***. These transgenes are recombined onto chromosomes bearing centromere-proximal FRT sites prior to use. A final note is that, unlike in imaginal tissues, fat body cells mix extensively during development, which often results in considerable separation of clones from their sister twinspots.

3.1.3.2. Clonal Expression of Transgenes

A unique feature of the fat body makes it especially amenable to FLP-mediated clonal induction of transgene expression. Britton et al. ***(19)*** described heat shock–independent spontaneous induction of "flip-out" clones in the fat body and midguts of hsp70-FLP Act>CD2>GAL4-bearing larvae. Presumably these tissues are more sensitive than others to low levels of leaky expression of FLP early in their development. Induction of FLP later in development is not practical in the fat body, as it tends to result in ubiquitous transgene expression throughout the fat body, likely due to the polyploid nature of this tissue. **Figure 1** displays examples of spontaneously induced clones of GFP-marked cells overexpressing Tsc1 and Tsc2 (A), which induce autophagy by inhibiting TOR, or Rheb (B), which suppresses starvation-induced autophagy by maintaining TOR activation.

3.1.3.3. Forward Genetic Approaches to Identifying Autophagy Regulators

It is perhaps obvious to point out that the genetic approaches discussed above can easily be adapted for use as tools in gene discovery. The development of comprehensive collections of UAS-regulated lines allowing induction of overexpression or RNA interference will undoubtedly lead to identification of novel regulators and effectors of autophagy. In addition, newly available collections of FRT-linked lethal P insertions provide a valuable resource for loss of function mosaic studies.

3.2. Monitoring Autophagy in the Larval Fat Body

Here we describe three independent methods for assaying autophagy in the fat body. LysoTracker Red stains acidic organelles in fixed and living cells and is usually confined to the late endosomal and lysosomal compartments. Under fed conditions, the larval fat body displays virtually no punctate LysoTracker Red staining. Starvation causes a robust induction of staining, which is severely inhibited in autophagy mutants. Thus, LysoTracker Red can be considered a reliable indicator of starvation-induced autophagy in this tissue. Examples of LysoTracker Red staining are shown in **Fig. 1**. Greater specificity can be achieved by following the localization of GFP-Atg8, which becomes conjugated

dc_840_14

to autophagosomal membranes. Lines expressing GFP fused to both human and fly homologs of Atg8 have been described ***(10,12)*** and are available. The combination of LysoTracker Red staining and GFP-Atg8 fluorescence allows distinction between autophagosomes (green signal only) and autolysosomes (both green and red signal) **(Fig. 1C)**. Finally, we include a brief protocol for analysis by TEM.

3.2.1. Larval Cultures and Starvation

1. Set up fly crosses with 5–10 females and a similar number of males. Do a 24-h egg collection.
2. Forty-eight hours after finishing egg collection, transfer approximately 20 L2-stage larvae to a fresh vial to reduce crowding. Add yeast paste or dry yeast to make sure all larvae have plenty of food to eat.
3. On the next day, collect larvae to examine (fed), or transfer 8–10 larvae into 20% sucrose for 3 h (starved).

3.2.2. Dissection and Staining of Fat Bodies with LysoTracker Red

1. Wash larvae thoroughly in water or PBS.
2. Transfer three to five larvae into a drop of PBS. Cut them in half using a sharp blade, and turn the carcasses inside out using forceps.
3. Separate fat body lobes and transfer them to staining solution (1× LysoTracker Red + DAPI, prepared fresh daily) for 2 min.
4. Transfer fat body pieces into a drop of PBS or 50% glycerol-PBS on a slide. Cover with a cover slip and evaluate immediately using a fluorescent microscope.

3.2.3. Fixation for Confocal Microscopy

1. Follow the above steps, but dissect in PBS and fix in freshly prepared 3.7% formaldehyde in PBS for 20 min to overnight at 4°C.
2. Wash two times in PBS.
3. Mount in Vectashield mounting medium.
4. Seal preparations by applying nail polish around the edges of cover slips and store at 4°C.

3.2.4. Fixation and Embedding for TEM

1. Follow the steps described earlier, but dissect in PBS and fix overnight at 4°C in 2% paraformaldehyde, 4% glutaraldehyde, 2% sucrose, 100 m*M* phosphate buffer.
2. Rinse in 3% sucrose in 100 m*M* PBS.
3. Postfix in 2% OsO_4 in 100 m*M* phosphate buffer overnight.
4. Dehydrate in ethanol and embed into Polybed 812 following the manufacturer's recommendations.

4. Notes

1. All experiments are performed at 25°C except as otherwise noted.
2. With sufficient numbers of females, egg-collection times can be shortened to as little as an hour, resulting in a more synchronous larval culture.
3. Turning carcasses inside-out requires skill and practice. An alternative is to simply tear larvae open and dissect out the fat body instead.
4. To speed up the LysoTracker Red staining procedure, it is acceptable to dissect larvae directly in staining solution.
5. It is important that the appropriate amount of liquid be used when mounting fat body lobes. Too little liquid will result in crushing cells when the cover slip is applied, whereas in too much liquid, the fat body will not be flat enough for good photographs.
6. LysoTracker Red bleaches very rapidly, so it is essential to minimize exposure time when using this dye. It can be useful to first find the proper focal plane using the UV/DAPI channel.
7. LysoTracker Red fixes poorly in larval tissues, and in most cases its signal is gone by 5 min of 3.7% formaldehyde fixation. If you need to work with a fixed tissue (e.g., more time is needed for imaging, or you have a GFP-Atg8 signal also), reduce fixation time to a few seconds to 2 min. LysoTracker signal will be very weak, but you can use an antibleaching agent that way. Another option is to analyze LysoTracker Red staining and GFP-Atg8 signal in different animals using live and fixed tissue, respectively.
8. For TEM, alternate methods of fixation have also been used successfully. Dissected tissues can be fixed in 3.2% paraformaldehyde, 0.5% glutaraldehyde, 1% sucrose, 40 m*M* $CaCl_2$ in 0.1 *N* pH 7.4 sodium-cacodylate overnight, rinsed twice in 0.1 *N* sodium-cacodylate, postfixed in 0.5% OsO_4 in 0.1 *N* sodium-cacodylate for 1 h at room temperature, dehydrated in ethanol and embedded in Araldyte (Fluka) following the manufacturer's recommendations.

References

1. Neufeld, T. P. (2004) Role of autophagy in developmental cell growth and death: insights from *Drosophila*, in *Autophagy* (Klionsky, D. J., ed.), Landes Bioscience, Georgetown, pp. 224–232.
2. Velentzas, A. D., Nezis, I. P., Stravopodis, D. J., Papassideri, I. S., and Margaritis, L. H. (2007) Mechanisms of programmed cell death during oogenesis in Drosophila virilis. *Cell Tissue Res.* **327,** 399–414.
3. Akdemir, F., Farkas, R., Chen, P., et al. (2006) Autophagy occurs upstream or parallel to the apoptosome during histolytic cell death. *Development* **133,** 1457–1465.
4. Juhasz, G., and Sass, M. (2005) Hid can induce, but is not required for autophagy in polyploid larval Drosophila tissues. *Eur. J Cell Biol.* **84,** 491–502.
5. Martin, D. N., and Baehrecke, E. H. (2004) Caspases function in autophagic programmed cell death in Drosophila. *Development* **131,** 275–284.

dc_840_14

6. Gorski, S. M., Chittaranjan, S., Pleasance, E. D., et al. (2003) A SAGE approach to discovery of genes involved in autophagic cell death. *Curr. Biol.* **13,** 358–363.
7. Lee, C. Y., and Baehrecke, E. H. (2001) Steroid regulation of autophagic programmed cell death during development. *Development* **128,** 1443–1455.
8. Lee, C. Y., Clough, E. A., Yellon, P., Teslovich, T. M., Stephan, D. A., and Baehrecke, E. H. (2003) Genome-wide analyses of steroid- and radiation-triggered programmed cell death in Drosophila. *Curr. Biol.* **13,** 350–357.
9. Scott, R. C., Juhasz, G., and Neufeld, T. P. (2007) Direct induction of autophagy by Atg1 inhibits cell growth and induces apoptotic cell death. *Curr. Biol* .**17,** 1–11.
10. Scott, R. C., Schuldiner, O., and Neufeld, T. P. (2004) Role and regulation of starvation-induced autophagy in the Drosophila fat body. *Dev. Cell* **7,** 167–178.
11. Lindmo, K., Simonsen, A., Brech, A., Finley, K., Rusten, T. E., and Stenmark, H. (2006) A dual function for Deep orange in programmed autophagy in the Drosophila melanogaster fat body. *Exp. Cell Res.* **312,** 2018–2027.
12. Rusten, T. E., Lindmo, K., Juhasz, G., et al. (2004) Programmed autophagy in the Drosophila fat body is induced by ecdysone through regulation of the PI3K pathway. *Dev. Cell* **7,** 179–192.
13. Ravikumar, B., Vacher, C., Berger, Z., et al. (2004) Inhibition of mTOR induces autophagy and reduces toxicity of polyglutamine expansions in fly and mouse models of Huntington disease. *Nat. Genet.* **36,** 585–595.
14. Scott, P. H., Brunn, G. J., Kohn, A. D., Roth, R. A., and Lawrence, J. C., Jr. (1998) Evidence of insulin-stimulated phosphorylation and activation of the mammalian target of rapamycin mediated by a protein kinase B signaling pathway. *Proc. Natl. Acad. Sci. USA* **95,** 7772–7777.
15. Sass, M., and Kovacs, J. (1977) The effect of ecdysone on the fat body cells of the penultimate larvae of Mamestra brassicae. *Cell Tissue Res.* **180,** 403–409.
16. McGuire, S. E., Roman, G., and Davis, R. L. (2004) Gene expression systems in Drosophila: a synthesis of time and space. *Trends Genet.* **20,** 384–391.
17. Theodosiou, N. A., and Xu, T. (1998) Use of FLP/FRT system to study Drosophila development. *Methods* **14,** 355–365.
18. Hennig, K. M., Colombani, J., and Neufeld, T. P. (2006) TOR coordinates bulk and targeted endocytosis in the Drosophila melanogaster fat body to regulate cell growth. *J. Cell. Biol.* **173,** 963–974.
19. Britton, J. S., Lockwood, W. K., Li, L., Cohen, S. M., and Edgar, B. A. (2002) Drosophila's insulin/PI3-kinase pathway coordinates cellular metabolism with nutritional conditions. *Dev. Cell* **2,** 239–429.

dc_840_14

Published May 12, 2008

dc_840_14

The class III PI(3)K Vps34 promotes autophagy and endocytosis but not TOR signaling in *Drosophila*

Gábor Juhász,[1,2] Jahda H. Hill,[3] Ying Yan,[4] Miklós Sass,[2] Eric H. Baehrecke,[3,5] Jonathan M. Backer,[4] and Thomas P. Neufeld[1]

[1]Department of Genetics, Cell Biology, and Development, University of Minnesota, Minneapolis, MN 55455
[2]Department of Anatomy, Cell and Developmental Biology, Eötvös Loránd University, Budapest, H-2120 Hungary
[3]Center for Biosystems Research, University of Maryland Biotechnology Institute, College Park, MD 20742
[4]Department of Molecular Pharmacology, Albert Einstein College of Medicine, Bronx, NY 10461
[5]Department of Cancer Biology, University of Massachusetts Medical School, Worcester, MA 01605

Degradation of cytoplasmic components by autophagy requires the class III phosphatidylinositol 3 (PI(3))–kinase Vps34, but the mechanisms by which this kinase and its lipid product PI(3) phosphate (PI(3)P) promote autophagy are unclear. In mammalian cells, Vps34, with the proautophagic tumor suppressors Beclin1/Atg6, Bif-1, and UVRAG, forms a multiprotein complex that initiates autophagosome formation. Distinct Vps34 complexes also regulate endocytic processes that are critical for late-stage autophagosome-lysosome fusion. In contrast, Vps34 may also transduce activating nutrient signals to mammalian target of rapamycin (TOR), a negative regulator of autophagy. To determine potential in vivo functions of Vps34, we generated mutations in the single *Drosophila melanogaster Vps34* orthologue, causing cell-autonomous disruption of autophagosome/autolysosome formation in larval fat body cells. Endocytosis is also disrupted in $Vps34^{-/-}$ animals, but we demonstrate that this does not account for their autophagy defect. Unexpectedly, TOR signaling is unaffected in *Vps34* mutants, indicating that Vps34 does not act upstream of TOR in this system. Instead, we show that TOR/Atg1 signaling regulates the starvation-induced recruitment of PI(3)P to nascent autophagosomes. Our results suggest that Vps34 is regulated by TOR-dependent nutrient signals directly at sites of autophagosome formation.

Introduction

Engulfment of cytoplasmic material into specialized double-membrane vesicles known as autophagosomes is the defining feature of a process referred to as macroautophagy or simply autophagy. Subsequent fusion of autophagosomes with the endolysosomal network leads to hydrolytic degradation of the sequestered material. This process provides eukaryotic cells with a mechanism for cytoplasmic renewal by which they can rid themselves of defective organelles and protein complexes (Yorimitsu and Klionsky, 2005). In addition, nonselective autophagy can be induced to high levels by starvation, providing an internal source of nutrients on which cells can survive extended periods of nutrient deprivation. Conversely, under some circumstances autophagy may be used as a killing mechanism, acting as an alternative or augmentation to apoptotic cell death (Neufeld and Baehrecke, 2008). As autophagy has been implicated in several physiological and pathological conditions, including neurodegeneration, tumorigenesis, and aging (Huang and Klionsky, 2007), better understanding of the molecular mechanisms controlling autophagy and identification of pharmacological regulators of this process are important goals.

Wortmannin and 3-methyladenine are well established inhibitors of autophagy. These compounds are broad-spectrum phosphatidylinositol 3 (PI(3))–kinase inhibitors that disrupt autophagy by inhibiting Vps34 (Petiot et al., 2000), the enzymatic component of a multiprotein complex which also includes Vps15, Beclin1/Atg6, UVRAG, and Bif-1 in mammals and Vps15, Atg6, and Atg14 in yeast (Mari and Reggiori, 2007). Localized production of PI(3) phosphate (PI(3)P) by Vps34 can act to recruit proteins containing FYVE and PX domains to specific membrane compartments (Lindmo and Stenmark, 2006). In yeast, this Vps34 complex is critical for recruiting autophagy-related (Atg) proteins to the preautophagosomal structure, the yeast-specific site of autophagosome formation (Suzuki et al., 2007). The role

Correspondence to Thomas P. Neufeld: neufe003@umn.edu

Abbreviations used in this paper: dsRNA, double-stranded RNA; ESCRT, endosomal sorting complex required for transport; PI(3), phosphatidylinositol 3; PI(3)P, PI(3) phosphate; TOR, target of rapamycin; TR, Texas red.

The online version of this paper contains supplemental material.

© 2008 Juhász et al.
The Rockefeller University Press $30.00
J. Cell Biol. Vol. 181 No. 4 655–666
www.jcb.org/cgi/doi/10.1083/jcb.200712051

Supplemental Material can be found at:
http://jcb.rupress.org/cgi/content/full/jcb.200712051/DC1

THE JOURNAL OF CELL BIOLOGY

Downloaded from jcb.rupress.org on February 16, 2009

Published May 12, 2008

of PI(3)P in autophagosome biogenesis is less well understood in higher eukaryotes, and whether it functions at the autophagosomal, the donor, or another membrane has not been determined (Pattingre et al., 2007).

Vps34 is also required more broadly for several vesicular trafficking processes that may have indirect impacts on autophagy. These include sorting of hydrolytic enzymes to the lysosome/vacuole and early steps in the endocytic pathway (Lindmo and Stenmark, 2006). In mammalian cells, autophagosomes have been shown to fuse with early or late endosomes before fusion with lysosomes, resulting in intermediate structures known as amphisomes (Eskelinen, 2005). Recently, mutations in components of the endosomal sorting complex required for transport (ESCRT) complex, which is required for the transition from early to late (multivesicular) endosomes, have been shown to block autophagy by inhibiting autophagosome-endosome fusion (Nara et al., 2002; Lee et al., 2007; Rusten et al., 2007). Thus, the effect of PI(3)-kinase inhibitors on autophagy may be due, in part, to these more general trafficking functions of Vps34.

Recent work has shown that Vps34 can also function in a nutrient-sensing pathway upstream of the target of rapamycin (TOR) in several mammalian cell lines (Byfield et al., 2005; Nobukuni et al., 2005). Disruption of Vps34 activity with blocking antibodies or siRNA was found to inhibit activation of TOR by insulin, amino acids, and glucose (Byfield et al., 2005; Nobukuni et al., 2005). As TOR signaling inhibits autophagy, these findings are at odds with the conserved role of Vps34 in promoting autophagy under starvation conditions, suggesting that distinct complexes or pools of Vps34 may be subject to different modes of regulation.

In this paper, we address how these multiple potential roles of Vps34 are coordinated to regulate autophagy in an intact organism, the fruit fly *Drosophila melanogaster*. Our findings suggest that despite a critical role for Vps34 in endocytic uptake and recycling, its primary function in autophagy in vivo is limited to its direct role at the nascent autophagosome. We further show that Vps34 is not required for TOR activity in this system and that starvation results in a TOR/Atg1-dependent recruitment of Vps34 activity to the autophagosomal membrane.

Results

Generation of null and hypomorphic *Vps34* mutants

A single representative of each of the three classes of PI(3)-kinase is present in *D. melanogaster*. The class III PI(3)-kinase orthologue (referred to previously as Pi3K_59F and herein as Vps34) shows greatest similarity to human Vps34 (hVps34) in the kinase domain, with an overall identity of 37 and 57% to Vps34 proteins in yeast and human (Linassier et al., 1997). Previous work has shown that *D. melanogaster* Vps34 displays substrate specificity for PtdIns, with high sensitivity to wortmannin and nonionic detergent as is characteristic of this class (Linassier et al., 1997). *Vps34* transcripts are expressed widely during development and in adult flies, with expression in the larval fat body and relative enrichment in neuronal and gut tissues (Chintapalli et al., 2007).

To generate loss-of-function mutations in the *Vps34* gene, we established isogenic homozygous-viable stocks of the *P* element line NP1626 (Hayashi et al., 2002) inserted in the *Vps34* 5′ untranslated region. Transposase-mediated excision of this element generated several lines that displayed hemizygous larval lethality in trans to a deficiency for this region, Df(2R)bw5. By PCR analysis, we identified an excision line that contains a deletion extending 3,349 bases downstream of the *P* element insertion site (Fig. 1 A). In this line, *Δm22*, the entire *Vps34* coding region is eliminated, thus resulting in a presumptive null allele. In addition, other lines displaying full or partially penetrant lethality were found to contain partial remnants of the excised *P* element (Fig. 1 A) and likely represent hypomorphic *Vps34* alleles, as in the case of *ex32*. As expected, *Vps34* transcripts were undetectable by RT-PCR in *Δm22* mutants and were reduced in *ex32* animals (Fig. 1 B). To confirm that these lesions specifically affect the *Vps34* locus, we used the GAL4–UAS system to ubiquitously express a wild-type *Vps34* transgene in mutant animals, resulting in a complete rescue of lethality (unpublished data).

The activity of Vps34 can be monitored in vivo by examining the intracellular localization of FYVE domain–containing proteins (Gillooly et al., 2000). To assay Vps34 function in mutant cells, we used a transgenic UAS line expressing EGFP fused to two tandem copies of the FYVE domain from the early endosomal protein Hrs (GFP-2xFYVE) (Wucherpfennig et al., 2003). For these experiments, we assayed GFP-2xFYVE distribution in FLP-FRT–generated clones of *Vps34* mutant cells, which are marked by the loss of a UAS-driven dsRed marker. This system allows side-by-side comparison of mutant and wild-type cells within the same animal. In wild-type fat body cells, GFP-2xFYVE localized primarily to vesicular structures in the perinuclear region, with additional punctate staining occurring at low levels throughout the cytoplasm and at the cell periphery (Fig. 1, C and D). In contrast, GFP-2xFYVE staining was diffuse in *Δm22* mutant cells, with no perinuclear localization and few or no apparent punctate structures (Fig. 1 C). Collectively, these results indicate that the *Δm22* deletion specifically eliminates *Vps34* expression, resulting in a cell-autonomous loss of function.

As a complement to these mutations in the endogenous *Vps34* gene, we also generated UAS-regulated transgenic lines that express *D. melanogaster* Vps34 containing point mutations in conserved residues of the kinase domain (referred to as $Vps34^{KD}$). Analogous mutations in yeast and mammalian Vps34 result in a kinase-defective protein with dominant-inhibitory properties (Row et al., 2001). Coexpression of $Vps34^{KD}$ with GFP-2xFYVE in FLP-FRT–generated fat body clones (Britton et al., 2002) resulted in diffuse GFP-2xFYVE localization similar to the deletion mutant (Fig. 1 E), which is consistent with a disruption of Vps34 activity in $Vps34^{KD}$-expressing cells. Incubation of dissected fat body with the PI(3)K inhibitor 3-methyladenine also caused a similar defect in GFP-2xFYVE localization (Fig. S1, available at http://www.jcb.org/cgi/content/full/jcb.200712051/DC1).

Although Vps34 has been localized to several distinct subcellular compartments in different cell types and experimental systems, its highest levels of activity are typically found in the early endosome, and GFP-2xFYVE is commonly used as an

Downloaded from jcb.rupress.org on February 16, 2009

Published May 12, 2008

dc_840_14

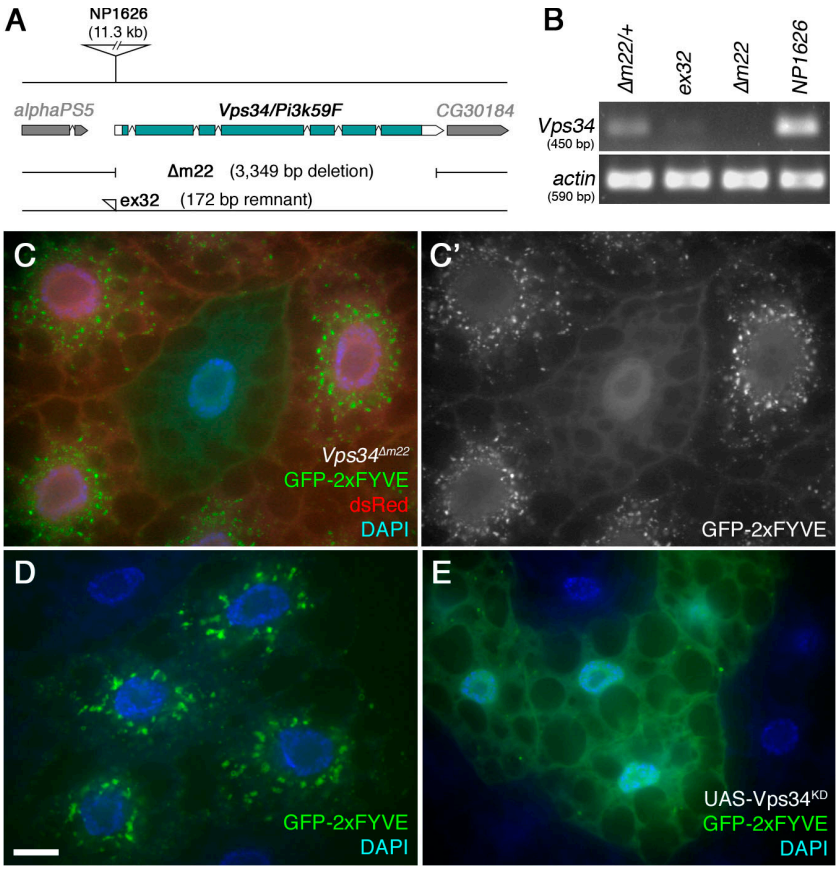


Figure 1. **Reagents to disrupt and monitor Vps34 function in *D. melanogaster*.** (A) Map of the *Vps34* locus, showing the location and extent of the *Δm22* deletion. (B) RT-PCR analysis of *Vps34* mRNA expression in control and mutant third instar larvae. *Vps34* transcript levels are strongly reduced in *ex32* animals and undetectable in the *Δm22* mutant. (C–E) Disruption of Vps34 function causes mislocalization of the PI(3)P reporter GFP-2xFYVE. In wild-type fat body cells (C and D), GFP-2xFYVE accumulates at the perinuclear endosomal compartment. This pattern of localization is lost in $Vps34^{\Delta m22}$ clones (C; mutant cell marked by lack of dsRed) or in response to expression of $Vps34^{KD}$ (E). Bar, 10 µm. Genotypes: (C) *hsflp; FRT42D UAS-GFP-2xFYVE* $Vps34^{\Delta m22}$*/Cg-GAL4 FRT42D UAS-GFP-2xFYVE UAS-dsRed*, (D) *hsflp; UAS-GFP-2xFYVE/+; Act>CD2>GAL4/+*, and (E) *hsflp; UAS-GFP-2xFYVE/+ ; Act>CD2>GAL4 / UAS-*$Vps34^{KD}$.

early endosomal marker (Gillooly et al., 2000). To test whether the perinuclear localization of GFP-2xFYVE in the fat body reflects the early endosomal compartment in this cell type, we examined the localization of other early endosomal markers. Both Hrs and Rab5-GFP displayed a similar perinuclear pattern which overlapped with GFP-2xFYVE or myc-2xFYVE and which was disrupted in *Δm22* mutant cells and in cells expressing $Vps34^{KD}$ (Fig. S1). We also found that the GFP-2xFYVE–labeled compartment was readily accessible to the endocytic tracer Texas Red (TR) avidin (see subsequent sections). In contrast, no colocalization was observed between GFP-2xFYVE and the Golgi marker p120 nor the late endosomal/lysosomal marker Lamp1 (Fig. S2). We conclude that Vps34 activity is concentrated in a perinuclear endosomal compartment in larval fat body cells. Disruption of GFP-2xFYVE, Hrs, and Rab5 localization in *Vps34* mutant cells indicates either that Vps34 activity is necessary for the recruitment or stable association of these markers or that the perinuclear endosomal compartment itself is disrupted in the mutant cells.

Vps34 is required for early steps of autophagosome formation

The fat body is specialized for a robust autophagic response to starvation, acting as a reserve source of nutrients for other critical tissues (Neufeld, 2004). Starvation results in an autophagy-dependent expansion and acidification of the lysosomal system, and thus the fluorescent Lysotracker dyes can be used to assay progression to late stages of autophagy in this tissue (Rusten et al., 2004; Scott et al., 2004). Starvation-induced formation of Lysotracker-positive structures was severely inhibited in clones of *Vps34* mutant cells and in cells expressing $Vps34^{KD}$ (Fig. 2, A and B), which is consistent with a requirement for *Vps34* in autophagy induction or progression. Overexpression of wild-type Vps34 was not sufficient to induce Lysotracker-positive structures under fed conditions (Fig. 2 C) but did result in a more robust response to starvation (Fig. 2 D). To examine earlier stages of autophagy, we determined the localization of the autophagosomal marker GFP-Atg8/LC3 in wild-type and *Vps34* mutant cells. Starvation-induced accumulation of GFP-Atg8 punctae was strongly curtailed in both *Vps34* mutant and $Vps34^{KD}$-expressing cells (Fig. 2, E–G), indicating an essential cell-autonomous role for Vps34 in autophagosome biogenesis. Expression of $Vps34^{KD}$ also blocked the starvation-induced accumulation of preautophagosomal membranes labeled with GFP-Atg5 (Fig. S3, available at http://www.jcb.org/cgi/content/full/jcb.200712051/DC1). Disruption of autophagosome and autolysosome formation was also evident by ultrastructural analysis of starved *Vps34* loss-of-function larvae (Fig. 2, H–J). Morphometric analysis revealed that the percent volume of cytoplasm occupied by autophagosomes and autolysosomes was reduced by more than 10-fold in both $Vps34^{\Delta m22}$ mutants and in animals overexpressing kinase-dead Vps34 in the fat body, relative to controls ($P < 0.0001$; Fig. 2 K).

We previously found that a hypomorphic *P* element allele of *D. melanogaster Atg6/beclin 1* results in a moderate

Downloaded from jcb.rupress.org on February 16, 2009

Published May 12, 2008

dc_840_14

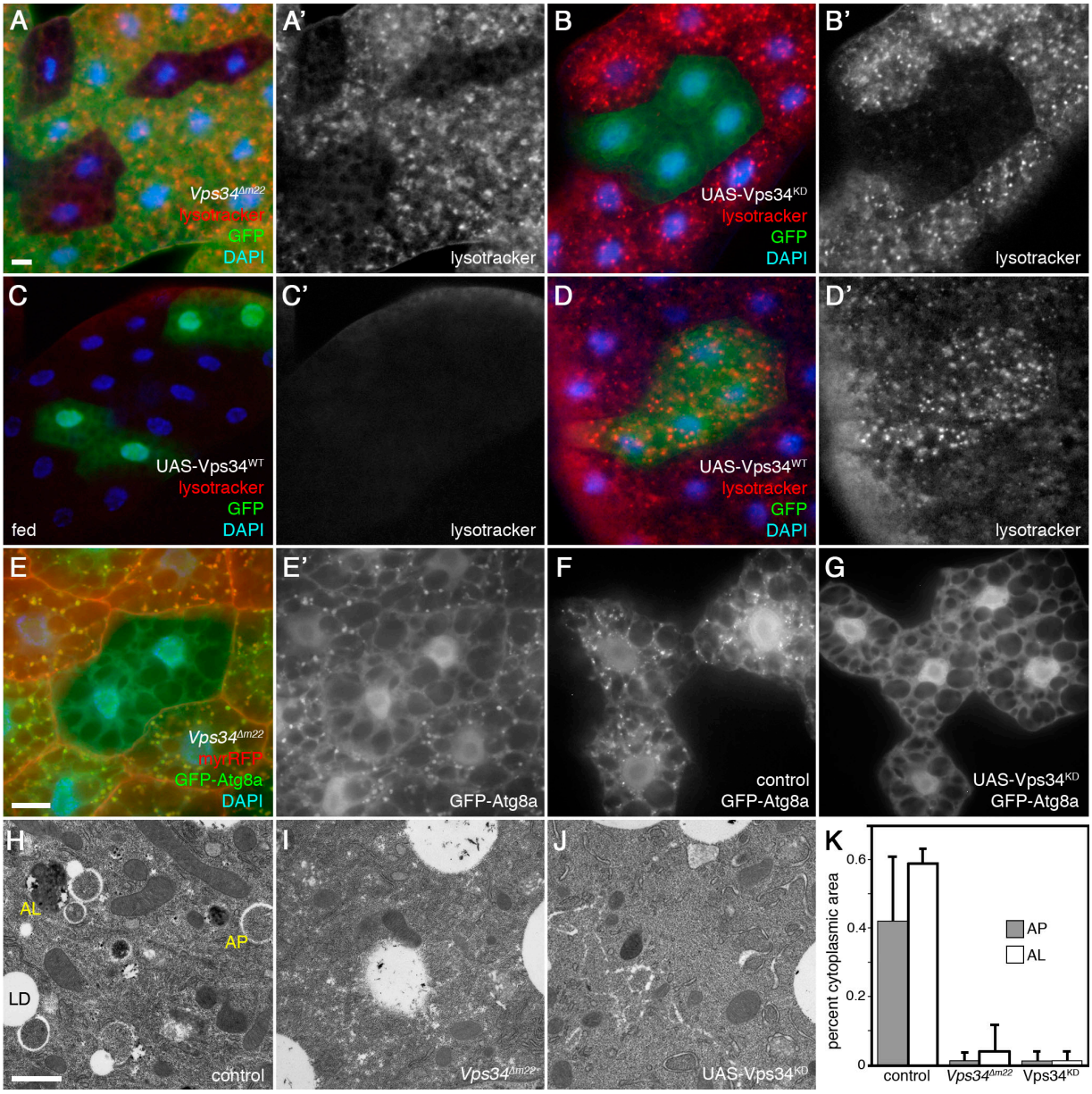


Figure 2. **Starvation-induced autophagy in the larval fat body requires Vps34.** All images depict live fat body tissue dissected from fed (C) or 4-h starved animals (all other panels). (A) *Vps34*$^{\Delta m22}$ loss-of-function clones (marked by lack of GFP) fail to accumulate autolysosomes (labeled by punctate Lysotracker Red staining) after starvation. (B) Vps34^{KD}-expressing cells (GFP positive) fail to accumulate punctate Lysotracker Red staining under starvation conditions. (C and D) Clonal expression of wild-type Vps34 (GFP-positive cells) does not induce autophagy under fed conditions (C) but increases the response to starvation (D). (E) *Vps34*$^{\Delta m22}$ loss-of-function clones (marked by lack of myrRFP) fail to accumulate autophagosomes (marked by punctate GFP-Atg8) in response to starvation. (F and G) Starvation-induced accumulation of GFP-Atg8a punctae is observed in controls (F) but not in animals expressing Vps34^{KD} (G). (H–K) TEM images reveal abundant autophagosomes (AP) and autolysosomes (AL) in control animals (H) but not *Vps34*$^{\Delta m22}$ mutants (I) nor animals expressing Vps34^{KD} (J). LD, lipid droplet. The graph in K shows autophagosome and autolysosome area ratios calculated from electron micrographs of five animals per genotype. Error bars show SD from the mean. P-values (Mann-Whitney *U* test): control versus *Vps34*$^{\Delta m22}$, AP, 1.45e-11 and AL, 3.9e-9; and control versus Vps34^{KD}, AP, 2.9e-11 and AL, 1.5 e-11. Bars: (A–G) 10 µm; (H–J) 1 µm. Genotypes: (A) *hsflp; FRT42D Vps34*$^{\Delta m22}$*/UAS-2xeGFP FRT42D fb-GAL4*, (B) *hsflp; Act>CD2>GAL4 UAS-GFP/UAS-Vps34*^{KD}, (C and D) *hsflp; Act>CD2>GAL4 UAS-GFP/UAS-Vps34*^{WT}, (E) *hsflp; FRT42D Vps34*$^{\Delta m22}$*/Cg-GAL4 UAS-GFP-Atg8a FRT42D UAS-myrRFP*, (F) *hsflp; Act>CD2>GAL4 UAS-GFP-Atg8a/+*, (G) *hsflp; Act>CD2>GAL4 UAS-GFP-Atg8a/UAS-Vps34*^{KD}, (H) *Vps34*$^{\Delta m22}$*/CyO-GFP*, (I) *Vps34*$^{\Delta m22/\Delta m22}$, (J) *Cg-GAL4 UAS-Vps34*^{KD}*/Cg-GAL4 UAS-Vps34*^{KD}, and (K) as in H–J.

defect in starvation-induced autophagy (Scott et al., 2004), and we also find that mutations in the Vps15 homologue *Ird1* result in a severe autophagy block (Fig. S3). To determine whether Vps34 functions in a complex containing these proteins, we first tested for physical association between epitope-tagged versions of Vps34, Vps15, and Atg6. We found that Atg6 could readily be precipitated with anti-Vps34 antibodies from larval extracts containing overexpressed myc-Atg6, Vps15-FLAG, and Vps34-TAP (Fig. 3 A). Consistent with findings in mammalian cells (Byfield et al., 2005), this association was observed under both fed and starved conditions, although starvation usually led to increased coprecipitation. Similar interactions were observed between Vps34-TAP and Vps15-FLAG (unpublished data).

Downloaded from jcb.rupress.org on February 16, 2009

Published May 12, 2008

To determine whether these physical associations are functionally relevant, we tested for genetic interactions between *Vps34*, *Vps15*, and *Atg6*. GAL4/UAS-mediated expression of Vps34-TAP resulted in a moderate statistically insignificant induction of GFP-Atg8a punctae formation under fed conditions (Fig. 3 B). Although expression of Atg6 or Vps15 also had little effect on their own, coexpression of these proteins with Vps34-TAP resulted in a significant increase in GFP-Atg8a punctae formation (Fig. 3 B). Thus, overexpression of Vps34 complexes promotes formation of GFP-Atg8a–labeled autophagosomes, but not Lysotracker-labeled autolysosomes, under fed conditions (Fig. 3 B and Fig. S3), suggesting that Vps34 activity is sufficient to drive early, but not later, steps of autophagy. Collectively, our findings suggest that *D. melanogaster* Vps34 is required for early events in autophagosome formation, at least in part via a conserved complex containing Vps34, Vps15, and Atg6.

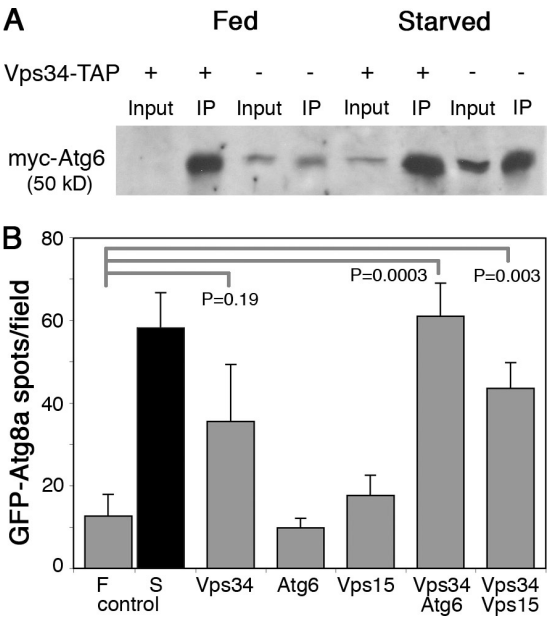


Figure 3. **Physical and genetic interactions between *D. melanogaster* Vps34, Vps15, and Atg6.** (A) Epitope-tagged Atg6 and Vps34 coimmunoprecipitate from larval extracts. myc-Atg6 and Vps15-FLAG were coexpressed with and without Vps34-TAP during larval development by heat shock–dependent GAL4 induction of UAS transgenes under either fed or starved conditions. Immunoprecipitation of larval extracts with hVps34 antibodies coprecipitates myc-Atg6. Levels of coprecipitated myc-Atg6 are higher in extracts from larvae overexpressing Vps34-TAP (lanes 2 and 6) than from larvae expressing only endogenous Vps34 (lanes 4 and 8). (B) Coexpression of Vps34-TAP with Atg6 or Vps15 results in cooperative induction of GFP-Atg8a–labeled autophagosomes under fed conditions. Number of GFP-Atg8a–positive spots per field in fat body of fed (F) and starved (S) control animals and in fed transgenic animals is indicated. Data represent mean ± SE of 10 animals per genotype. P-values were determined by two-tailed Student's *t* test.

Vps34 function in the endocytic pathway is distinct from its role in autophagy

Given the localization of Vps34 activity to the endosomal compartment and its role in formation of and localization to multivesicular bodies in mammalian cells (Gillooly et al., 2000; Futter et al., 2001), we next asked whether the loss of autophagy in *Vps34* mutants could be attributed in part to its role in the endocytic pathway. Consistent with recent studies (Rusten et al., 2007), we found that mutations in components of ESCRT-I (*Vps25*), -II (*Vps28*), or -III (*Vps32*) disrupted starvation-induced lysotracker staining in the larval fat body (Fig. 4 A; Fig. S4, available at http://www.jcb.org/cgi/content/full/jcb.200712051/DC1; and not depicted). In contrast to the lack of autophagosomes in *Vps34* mutants (Fig. 4 C), mutations in these ESCRT subunits led to an accumulation of GFP-Atg8a–labeled autophagosomes under fed conditions (Fig. 4 B and Fig. S4), which is consistent with a block in autophagosome-endosome fusion, as previously reported (Lee et al., 2007; Rusten et al., 2007). This difference between *Vps34* and ESCRT phenotypes suggests that these mutations disrupt distinct steps of autophagy progression.

To investigate this further, we generated clones of fat body cells mutant for both *Vps34* and *25* or *Vps34* and *28*. In these double mutant cells, GFP-Atg8a punctae still accumulated under fed conditions, albeit at somewhat reduced levels (Fig. 4 D and Fig. S4). Accumulation of autophagosomes was also evident in transmission electron micrographs of eye imaginal discs doubly mutant for *Vps34* and *25* (Fig. S5). This finding that autophagosomes accumulate in *Vps34-Vps25* and *Vps34-Vps28* double mutants, but not in *Vps34* single mutants, indicates that deletion of *Vps34* has a more severe kinetic effect on autophagosome formation than on autophagosome-lysosome fusion, such that the early steps in autophagosome formation become rate limiting. With additional mutation of *Vps25* or *Vps28*, autophagosome-lysosome fusion becomes rate limiting and autophagosomes accumulate. Thus, the ESCRT-dependent step required for autophagy is at least partially functional in cells lacking *Vps34*.

As reported previously (Vaccari and Bilder, 2005), loss of *Vps25* leads to accumulation of ubiquitin-positive punctae in cells of the developing eye (Fig. 4 E). Similar ubiquitin accumulation was observed in *Vps34-Vps25* mutant cells, but not in *Vps34* single mutants (Fig. 4, F and G), further indicating that the ESCRT pathway is not disrupted in *Vps34* mutants. The ubiquitin-containing structures in *Vps34-Vps25* mutant cells largely colocalized with the endosomal marker Hrs and were often adjacent to GFP-Atg8a–labeled punctae (Fig. S5). Similarly, immuno-EM analysis of *Vps25* and *Vps34-Vps25* mutant eye discs revealed accumulation of ubiquitin in tubulovesicular compartments but not in autophagosomes (Fig. S5). Thus, the ubiquitinated structures in *Vps25* and *Vps34-Vps25* mutant cells likely represent stalled intermediates in the endocytic pathway.

Despite the relatively normal progression of ESCRT-dependent processes in *Vps34* mutants, we found that they were severely defective in fluid-phase endocytosis. *Vps34* mutant clones in the larval fat body failed to incorporate the endocytic tracer TR-avidin beyond the cortical region of the cell, where it often accumulated to high levels (Fig. 5 A). A similar disruption was observed in *Vps34-Vps25* double mutant fat body cells (Fig. S4). Mutation of *Vps34* or expression of $Vps34^{KD}$ also inhibited TR-avidin uptake in the highly endocytic Garland cells (Fig. 5, B–E). In addition, we observed accumulation of Notch in *Vps34* mutant cells of the eye imaginal disc (Fig. 5 F), which is consistent with defective endocytic recycling (Vaccari and Bilder, 2005). Finally, loss of Vps34 dramatically altered the distribution of GFP-Lamp1 and Spin-GFP (Fig. S2), markers which localize to

Downloaded from jcb.rupress.org on February 16, 2009

Published May 12, 2008

dc_840_14

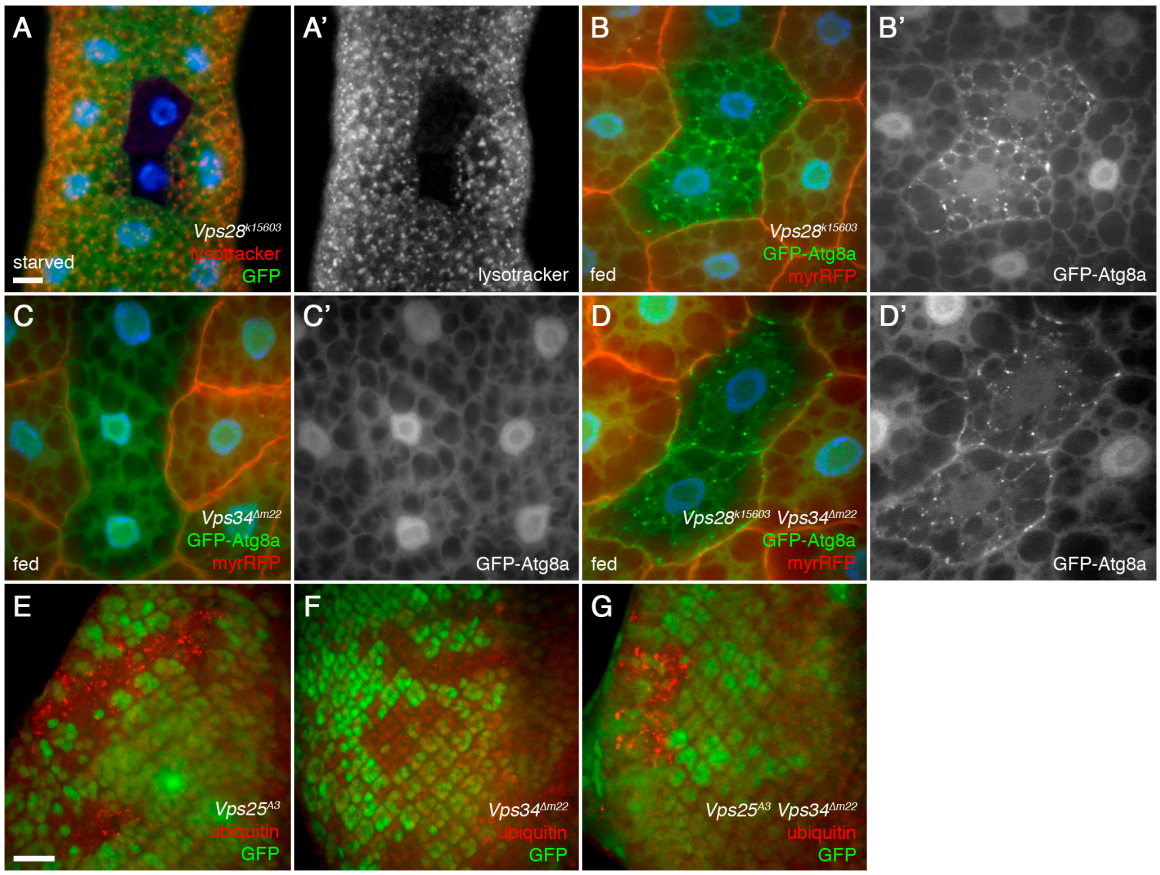


Figure 4. **Vps34 and ESCRT components are required for distinct steps in autophagy.** (A) Mutation of the ESCRT-II component Vps28 (mutant clone marked by lack of GFP) disrupts formation of Lysotracker Red punctae in response to 4-h starvation. Bar, 10 µm. (B–D) GFP-Atg8a–marked autophagosomes accumulate in clones of *Vps28* mutant (B) and *Vps34 Vps28* double mutant (D) cells but not in *Vps34* mutant cells (C). Mutant clones are marked by lack of myrRFP. (E–G) Mosaic eye imaginal discs showing accumulation of ubiquitin-positive punctae in *Vps25* (E) and *Vps25 Vps34* (G) mutant clones but not in *Vps34* mutant clones (F). Lack of GFP marks mutant clones. Bar, 10 µm (B–G). Genotypes: (A) *hsflp; FRT42D Vps28^{k15603}/UAS-2xeGFP FRT42D fb-GAL4*, (B) *hsflp; FRT42D Vps28^{k15603}/Cg-GAL4 UAS-GFP-Atg8a FRT42D UAS-myrRFP*, (C) *hsflp; FRT42D Vps34$^{\Delta m22}$/Cg-GAL4 UAS-GFP-Atg8a FRT42D UAS-myrRFP*, (D) *hsflp; FRT42D Vps28^{k15603} Vps34$^{\Delta m22}$/Cg-GAL4 UAS-GFP-Atg8a FRT42D UAS-myrRFP*, (E) *hsflp; FRT42D Vps25^{A3}/FRT42D Ubi-GFPnls*, (F) *hsflp; FRT42D Vps34$^{\Delta m22}$/FRT42D Ubi-GFPnls*, and (G) *hsflp; FRT42D Vps25^{A3} Vps34$^{\Delta m22}$/FRT42D Ubi-GFPnls*.

or transit through late endosomes and lysosomes. Collectively, these findings indicate that *D. melanogaster* Vps34 has an essential role in the endocytic pathway but that this role is distinct from ESCRT-dependent endocytic processes and does not constitute a rate-limiting step for its function in autophagy.

Vps34 is not required for nutrient-dependent signaling to TOR

In *D. melanogaster* and other systems, a hallmark of TOR signaling is its stimulation of cell growth and proliferation (Arsham and Neufeld, 2006). Down-regulation of this pathway in fat body cells through *Tor* mutation (Scott et al., 2007), RNAi-mediated inhibition of *Tor* expression (Fig. 6, A and L), or overexpression of the TOR inhibitors Tsc1 and 2 (Fig. 6, B and L) results in a significant reduction in cell size. In contrast, cells mutant for *Vps34* or expressing Vps34^{KD} were similar in size to wild-type cells (Fig. 6, C, D, and L). Similarly, in the eye imaginal disc, which is comprised of mitotically active diploid cells, mutations in *Tor* cause a strong proliferative disadvantage (Zhang et al., 2000), whereas *Vps34* mutant cells proliferate at a rate similar to that of control cells (Fig. 6, E and F). The normal rate of growth and proliferation suggests that TOR signaling is not appreciably compromised in *Vps34* mutant cells.

To ask whether a role for Vps34 in TOR signaling might be apparent only at higher or lower than normal levels of TOR activity, we induced clones of cells with altered expression of Rheb (a TOR activator) or Tsc1 and 2 in control or *Vps34*-deficient backgrounds. Cells overexpressing Rheb reached a larger size than neighboring cells, as previously reported (Saucedo et al., 2003), and coexpression of Rheb and Vps34^{KD} resulted in a similar cell enlargement (Fig. 6, G and H). Conversely, overexpression of Tsc1 and 2 inhibited cell growth to a similar extent in *Vps34* mutant and control animals (Fig. 6, I and J). Expression of wild-type or kinase-defective Vps34 also had no effect on cell size in starved animals or animals that were allowed to recover on normal media after 48 h of starvation (unpublished data). We also tested for loss-of-function genetic interactions between *Vps34* and components of the TOR pathway. Heterozygous mutation of *Tor* or *S6k* dominantly suppresses the lethality of *Tsc1* homozygous mutant animals (Radimerski et al., 2002; Zhang et al., 2006), presumably by restraining the abnormally high levels of TOR signaling caused by loss of *Tsc1*.

Downloaded from jcb.rupress.org on February 16, 2009

Published May 12, 2008

In contrast, *Vps34* mutants had no effect on the development or viability of *Tsc1* mutant animals (unpublished data).

To more directly assess the requirement for Vps34 in TOR activation, we examined the phosphorylation of S6K-Thr398, a direct substrate of the rapamycin-sensitive TOR complex I, as well as Akt-Ser505, which is phosphorylated by TOR complex II. Although the phosphorylation status of these sites is highly sensitive to the levels of Tsc1 or Rheb (Hennig et al., 2006; Scott et al., 2007), ubiquitous overexpression of UAS-driven wild-type or kinase-deficient Vps34 had no effect on the phosphorylation of these sites in whole larval extracts (Fig. 6 K). Fat body–specific expression of these transgenes also failed to alter the phosphorylation of these sites in extracts from dissected fat body tissue (unpublished data). Collectively, these results indicate that in contrast to the case in cultured mammalian cells, *D. melanogaster* Vps34 does not play a critical role in TOR activation in vivo.

Recruitment of Vps34 activity to autophagosomal membranes is regulated by TOR/Atg1-dependent nutrient signaling

Although Vps34 is required for starvation-induced autophagy, it remains uncertain whether and how the PI(3)-kinase enzymatic activity of autophagy-specific Vps34 complexes is regulated by nutrient conditions. For example, some studies have reported an increase in Beclin 1–associated PI(3)-kinase activity in response to starvation (Byfield et al., 2005; Nobukuni et al., 2005), whereas others report a decrease (Tassa et al., 2003; Takahashi et al., 2007). Comparison of GFP-2xFYVE localization in fed and starved animals revealed that starvation induced a relative shift from a perinuclear concentration of this marker to a more widely dispersed pattern (Fig. 7, A–D and F). This did not reflect a disruption of the early endosome itself, as the TR-avidin–accessible compartment remained in the perinuclear region in starved larvae (Fig. 7, A and B). Rab5-GFP also remained associated with the perinuclear early endosome under starvation conditions (Fig. 7, C and D), and the accumulation of peripheral GFP-2xFYVE punctae was not associated with decreased perinuclear localization (Fig. 7 F).

These findings suggest that starvation causes recruitment of Vps34 activity to peripheral locations throughout the cell, presumably nascent autophagosomes. This was confirmed by the observation that the nonendosomal myc-2xFYVE punctae induced by starvation displayed a nearly complete overlap with the autophagosomal marker GFP-Atg8a (Fig. 7 E). Thus, autophagy-inducing signals result in mobilization of Vps34 activity directly to the autophagosomal membrane. Although we were unable to detect endogenous Vps34 protein in vivo, UAS-driven Vps34 did not appear to be concentrated at the early endosome nor on autophagosomes, and its localization was not affected by starvation (unpublished data). Thus, the mobilization of Vps34 activity may reflect activation of preexisting Vps34 protein at distinct cellular locations. Alternatively, the high levels of UAS-driven expression may mask more subtle changes in the distribution of endogenous protein.

TOR signaling plays a critical role in conveying nutrient status to the autophagic machinery and may directly regulate the activity of the Ser-Thr kinase Atg1 (Kamada et al., 2000; Scott et al., 2007). To determine whether this pathway is involved in regulation of Vps34, we examined its effect on nutrient-dependent relocalization of GFP-2xFYVE. In clones of cells mutant for *Tsc2* or overexpressing Rheb, both of which result in constitutive TOR

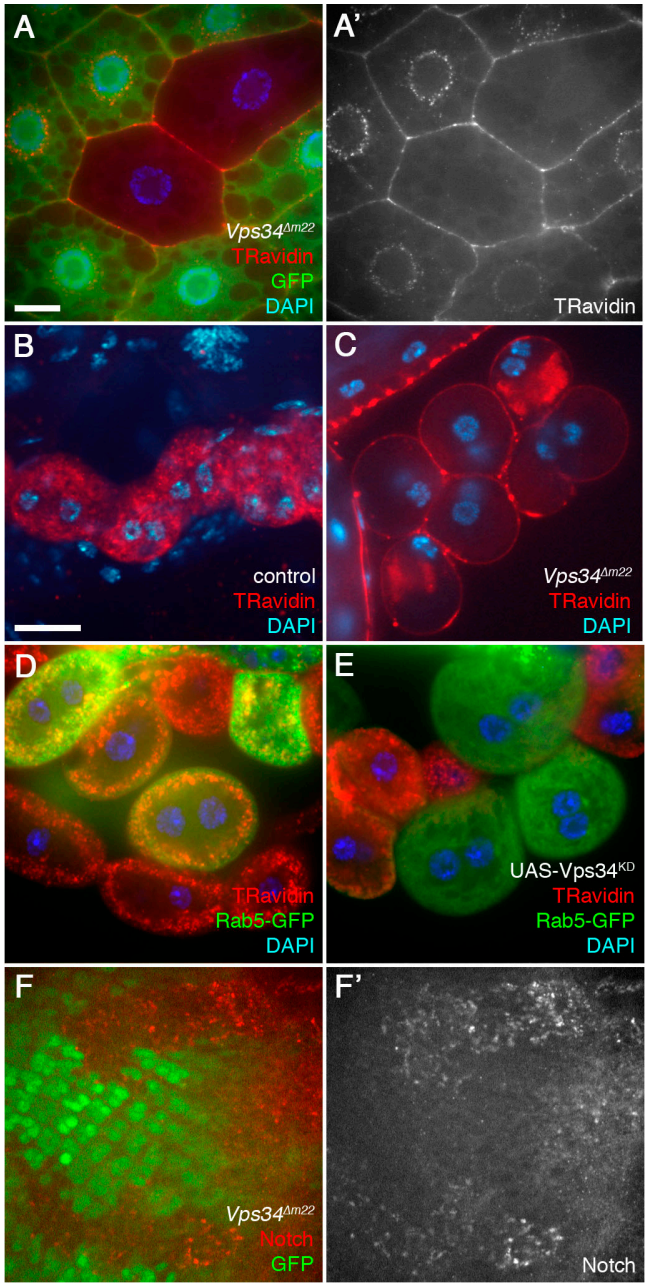


Figure 5. **Vps34 is required for endocytosis.** (A) *Vps34*$^{\Delta m22}$ loss-of-function fat body clones (marked by lack of GFP) fail to incorporate the endocytic tracer TR avidin into the perinuclear early endosome (20-min pulse followed by 10-min chase). (B and C) TR avidin accumulates in Garland cells of heterozygous controls (B) but not *Vps34*$^{\Delta m22}$ homozygous mutants (C; 2-min pulse followed by 20-min chase). (D and E) Mosaic larvae expressing Rab5-GFP (D) or Rab5-GFP and Vps34^{KD} (E) in a subset of Garland cells. TR avidin uptake and cortical localization of Rab5-GFP are disrupted in Vps34^{KD}-expressing cells (15-min pulse, no chase). Bar, 10 µm (B–E). (F) Clonal loss of *Vps34* (marked by lack of GFP) in the eye imaginal disc results in accumulation of Notch-positive punctae. Bar, 10 µm (A and F). Genotypes: (A) *hsflp; FRT42D Vps34*$^{\Delta m22}$*/UAS-2xeGFP FRT42D fb-GAL4*, (B) *Vps34*$^{\Delta m22}$*/CyO-GFP*, (C) *Vps34*$^{\Delta m22/\Delta m22}$, (D) *hsflp; Act>CD2>GAL4 UAS-Rab5-GFP/+*, (E) *hsflp; Act>CD2>GAL4 UAS-Rab5-GFP/UAS-Vps34*^{KD}, and (F) *hsflp; FRT42D Vps34*$^{\Delta m22}$*/FRT42D Ubi-GFPnls*.

Downloaded from jcb.rupress.org on February 16, 2009

Published May 12, 2008

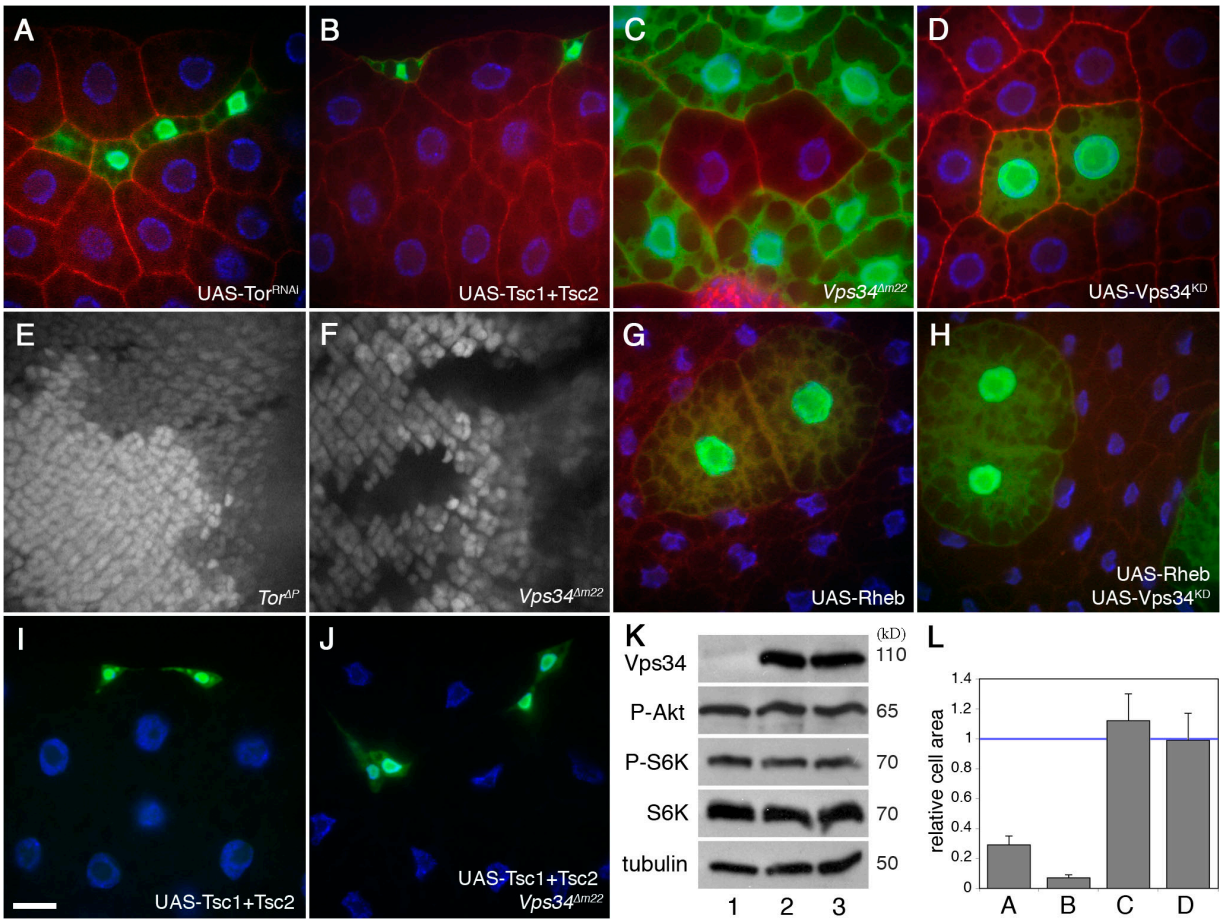


Figure 6. **Vps34 does not influence TOR signaling or function.** Transgene-expressing cells are marked by coexpression of GFP in A, B, D, and G–J. Loss-of-function mutant clones are marked by lack of GFP in C, E, and F. All images are from fed larvae except G and H, which are from 48-h starved animals. (A and B) Inhibition of TOR signaling by expression of *Tor* double-stranded RNA (dsRNA; A) or overexpression of Tsc1 and 2 (B) results in a reduction in fat body cell size. (C and D) Fat body cells lacking *Vps34* (C) or expressing Vps34^{KD} (D) are normal in size. (E and F) In the eye imaginal disc, cells mutant for *Tor* (E; GFP negative) proliferate more slowly than their wild-type "twin spot" control cells (two copies of GFP). *Vps34*$^{\Delta m22}$ homozygous mutant cells (F) proliferate at a rate similar to that of twin spot controls. (G and H) Overexpression of Rheb activates TOR and increases cell growth both in the absence (G) or presence (H) of coexpressed kinase-defective Vps34. (I and J) Inhibition of TOR signaling by cooverexpression of Tsc1 and 2 reduces cell growth in control (I) and *Vps34*$^{\Delta m22}$ (J) animals. (K) Ubiquitous hsGAL4-driven overexpression of wild-type Vps34 (lane 2) or kinase-defective Vps34 (lane 3) does not affect TOR-dependent phosphorylation of S6K-Thr398 or Akt-Ser505 relative to control extracts (lane 1). (L) Quantitation of the area of mutant or transgene-expressing cells in A–D relative to wild-type cells from the same tissue. Data represent mean ± SEM of 7–10 animals per genotype. Bar: 10 µm. Genotypes: (A) *hsflp; Act>CD2>GAL4 UAS-GFP/UAS-TOR*$^{dsRNA5092R-2}$, (B) *hsflp; Act>CD2>GAL4 UAS-GFP/UAS-Tsc1 UAS-Tsc2*, (C) *hsflp; FRT42D Vps34*$^{\Delta m22}$*/UAS-2xeGFP FRT42D fb-GAL4*, (D) *hsflp; Act>CD2>GAL4 UAS-GFP/UAS-Vps34*^{KD}, (E) *hsflp; Tor*$^{\Delta P}$ *FRT40A/Ubi-GFPnls FRT40A*, (F) *hsflp; FRT42D Vps34*$^{\Delta m22}$*/FRT42D Ubi-GFPnls*, (G) *hsflp; Act>CD2>GAL4 UAS-GFP UAS-Rheb*$^{EP50.084}$*/+*, (H) *hsflp; Act>CD2>GAL4 UAS-GFP UAS-Rheb*$^{EP50.084}$*/UAS-Vps34*^{KD}, (I) *hsflp; Act>CD2>GAL4 UAS-GFP/UAS-Tsc1 UAS-Tsc2*, and (J) *hsflp; Vps34*$^{\Delta m22}$*/Vps34*$^{\Delta m22}$*; Act>CD2>GAL4 UAS-GFP/UAS-Tsc1 UAS-Tsc2*.

activation, formation of GFP-2xFYVE cytoplasmic punctae in response to starvation was greatly diminished (Fig. 8 A and not depicted). Similar results were observed in cells lacking Atg1 (Fig. 8 B). Thus, signaling through TOR and Atg1 is necessary for proper nutrient-responsive recruitment of Vps34 activity to autophagosomes. Accordingly, down-regulation of TOR signaling by cooverexpression of Tsc1 and 2 led to autophagy induction in control animals, but not in *Vps34* mutants (Fig. 8, C and D), which is consistent with Vps34 functioning downstream of TOR-dependent nutrient signaling.

Discussion

Previous work in mammalian and yeast systems has identified a wide range of vesicle trafficking processes regulated by Vps34, including autophagy, endocytosis, endosome maturation, and both anterograde and retrograde trafficking between the Golgi and lysosome (Lindmo and Stenmark, 2006). Our findings indicate that despite these activities, the in vivo role of Vps34 in autophagy is largely limited to its function at the autophagosome. Although fluid-phase endocytosis, endocytic recycling of Notch, and trafficking of lysosomal proteins were disrupted by mutation of *Vps34*, our results suggest that events subsequent to autophagosome formation, including fusion between autophagosomes and endosomes or lysosomes and subsequent lysosomal degradation, are not rate limiting in the absence of Vps34. Why does endocytic disruption lead to autophagosome fusion defects in ESCRT mutants but not in *Vps34* mutants? Accumulation of endocytic tracer at the periphery of *Vps34* mutant cells suggests that Vps34 functions at an early step of endocytosis,

Downloaded from jcb.rupress.org on February 16, 2009

Published May 12, 2008

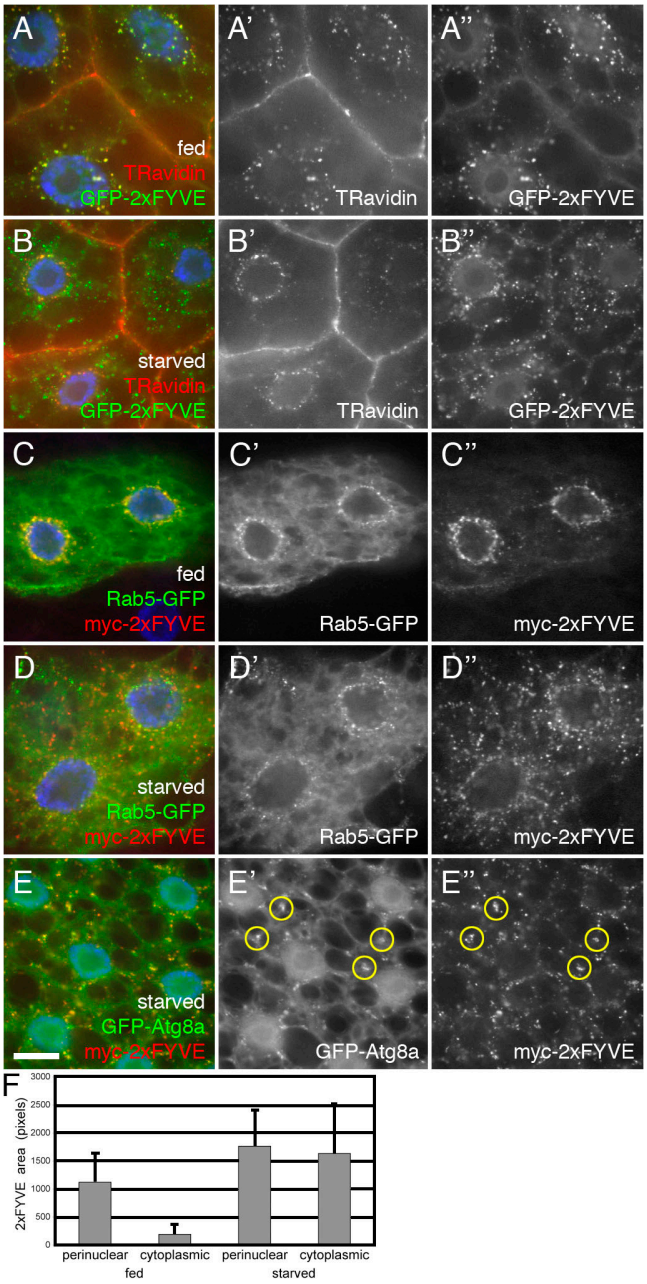


Figure 7. **Recruitment of PI(3)P from early endosomes to autophagosomes in response to TOR/Atg1-dependent nutrient signaling.** (A and B) Internalized TR avidin colocalizes with GFP-2xFYVE under fed conditions (A) but not after 4-h starvation (B). (C and D) Starvation causes dispersion of myc-2xFYVE but not Rab5-GFP. (E) Under starvation conditions, myc-2xFYVE displays extensive colocalization with GFP-Atg8a. Yellow circles in E′ and E′′ show overlap between GFP-Atg8a and myc-2xFYVE label. Bar, 10 µm. (F) Quantitation of the myc-2xFYVE–labeled compartment area in a 2-µm ring surrounding the nucleus (perinuclear) and the remaining peripheral cell area (cytoplasmic). Genotypes: (A and B) *Cg-GAL4/UAS-GFP-2xFYVE*, (C and D) *hsflp; Act>CD2>GAL4 UAS-Rab5-GFP/UAS-myc-2xFYVE*, and (E) *Cg-GAL4 UAS-GFP-Atg8a/UAS-myc-2xFYVE*.

and apparently this event, as well as normal endocytic flux is not essential for fusion of autophagosomes with elements of the endosomal-lysosomal compartment. Interestingly, the accumulation of autophagosomes in ESCRT/*Vps34* double mutants indicates that loss of Vps34 does not completely prevent autophagosome formation. Similarly, the lack of autophagosome

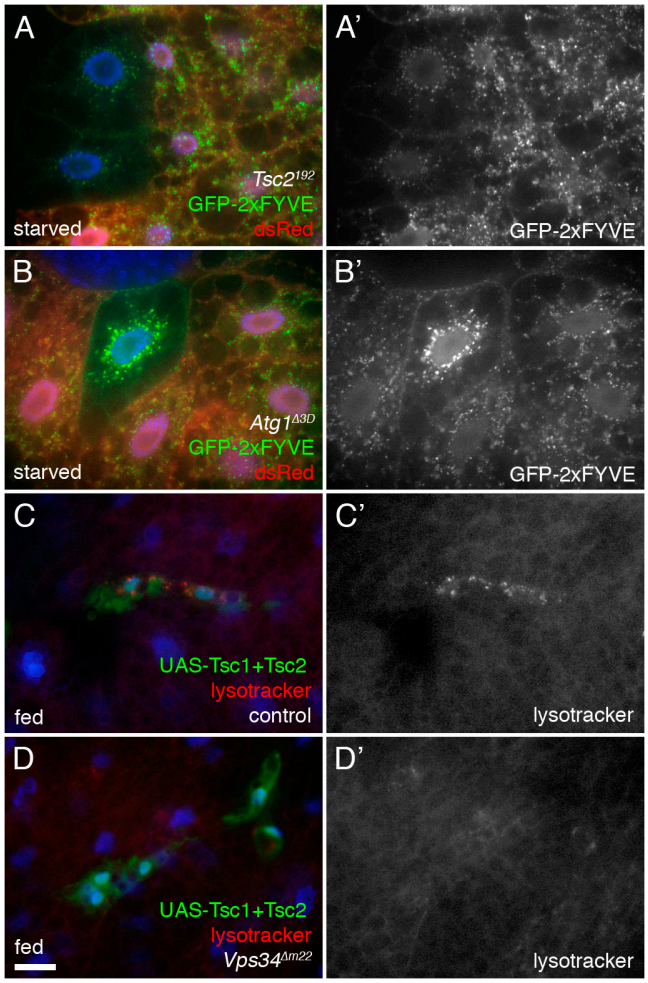


Figure 8. **Vps34 functions downstream of TOR signaling.** (A and B) Starvation-induced redistribution of Vps34 activity requires TOR-Atg1 signaling. 4-h starvation causes relocalization of GFP-2xFYVE in control cells but not in *Tsc2* homozygous mutant cells (A) nor in cells mutant for *Atg1* (B). Mutant clones are marked by lack of dsRed. Note also the changes in GFP-2xFYVE levels in the mutant cells. (C and D) Cooverexpression of Tsc1 and 2 in GFP-marked clones induces formation of autolysosomes under fed conditions in control (C) but not *Vps34* mutant (D) animals. Bar: (A and B) 10 µm; (C and D) 25 µm. Genotypes: (A) *hsflp; Cg-GAL4 UAS-GFP-2xFYVE/+; Tsc2^{192} FRT80B/UAS-dsRed FRT80B*, (B) *hsflp; Cg-GAL4 UAS-GFP-2xFYVE/+; Atg1$^{\Delta 3D}$ FRT80B/UAS-dsRed FRT80B*, (C) *hsflp; Vps34$^{\Delta m22}$/+; Act>CD2>GAL4 UAS-GFP/UAS-Tsc1 UAS-Tsc2*, and (D) *hsflp; Vps34$^{\Delta m22}$/Vps34$^{\Delta m22}$; Act>CD2>GAL4 UAS-GFP/UAS-Tsc1 UAS-Tsc2*.

accumulation in *Vps34* single mutants indicates that ESCRT complexes are at least partially functional in the absence of Vps34. Thus, PI(3)P may not be absolutely essential for these processes, or perhaps sufficient levels of PI(3)P are generated independently of Vps34 by the class II PI(3) kinase or by PI(3,4)P or PI(3,5)P phosphatases. As ESCRT components are required for multivesicular body formation but not autophagy in yeast (Reggiori et al., 2004), it will be interesting to determine whether the requirement for ESCRT complexes in autophagy in higher eukaryotes reflects their role in multivesicular body formation or an alternate function.

The cellular compartment in which Vps34 acts to promote autophagy and the mechanisms by which it is regulated by nutrient signals have remained unresolved. In mammalian cells,

Downloaded from jcb.rupress.org on February 16, 2009

Published May 12, 2008

Beclin1/Atg6 has been reported to localize to the trans-Golgi network, ER, and mitochondria (Kihara et al., 2001; Pattingre et al., 2005). It was recently shown that Beclin1–Vps34 complexes can be inhibited by the antiapoptotic factor Bcl-2 in a nutrient-dependent manner (Pattingre et al., 2005). Bcl-2 mutants that are targeted to the ER, but not to mitochondria, retain their capacity to inhibit starvation-induced autophagy, suggesting that the ER is an important site of Beclin1-Vps34 regulation. However, it is unknown how these organelles contribute to the formation of autophagosomes, and recent studies suggest that rather than budding off a preexisting compartment, the autophagosomal membrane is likely to form de novo from small lipid transport vesicles or lipoprotein complexes (Juhasz and Neufeld, 2006; Kovacs et al., 2007). Our finding that myc-2xFYVE is recruited to GFP-Atg8a–positive structures under starvation conditions indicates that Vps34 activity is targeted directly to autophagosomes in a TOR/Atg1-dependent manner. Although these results do not distinguish between a role for TOR/Atg1 signaling in regulating Vps34 activity versus providing a platform on which Vps34 complexes can assemble, together with these previous studies they indicate that Vps34 is likely to promote autophagy by different mechanisms from multiple cellular locations.

How the TOR signaling pathway senses intracellular levels of nutrients, such as amino acids, has been poorly understood despite considerable work in yeast, mammalian, and other model systems. The recent identification of Vps34 as a transducer of this signal in mammalian cells thus represents a significant new insight into this issue (Byfield et al., 2005; Nobukuni et al., 2005). However, further work is necessary to determine the extent to which this mechanism is generally conserved, as starvation appears to have opposing effects on Vps34 activity in different cell types (Tassa et al., 2003; Nobukuni et al., 2005; Takahashi et al., 2007). The results presented here fail to support this model in *D. melanogaster*, as mutation of *Vps34* did not appear to influence TOR-dependent phenotypes nor to disrupt TOR-dependent signaling. This may reflect a fundamental difference in signaling mechanisms between the fly and mammalian systems. The makeup of Vps34 complexes has diverged significantly between yeast and metazoans, and perhaps components of this complex, such as Ambra1 (Fimia et al., 2007), that appear to be unique to vertebrates may confer functions not found in flies. It is also possible that production of PI(3)P by Vps34-independent mechanisms is more efficient in *D. melanogaster* than in mammalian cells and, thus, a role for Vps34 in TOR signaling may be obscured by these other sources. The continued ESCRT function and basal level of autophagy in *Vps34* null mutants are consistent with this possibility. Alternatively, our findings may reflect important differences between the roles of TOR and Vps34 in vivo versus in cultured cells as well as the experimental paradigms of these systems. For example, although complete starvation is commonly used to inactivate TOR in cell culture studies, such experiments may not accurately mimic physiologically relevant events, given the inherent capacity of intact organisms to buffer changes in nutrient levels. Additional studies in an in vivo mammalian system will be helpful to clarify these issues.

Materials and methods

Fly stocks and culture

Flies were raised at 25°C on standard cornmeal/molasses/agar media. The following *D. melanogaster* stocks were used: *P[GawB]NP1626* (Kyoto stock center), *Df(2R)bw5* and UAS-YFP-Rab5 (Bloomington stock center), UAS-GFP-2xFYVE, UAS-myc-2xFYVE, and UAS-Rab5-GFP (gifts of M. Gonzalez-Gaitan, Max Planck Institute, Dresden, Germany), UAS-HRP-Lamp1, UAS-GFP-Lamp1, and *FRT42D Vps28[k16503]* (gifts of H. Kramer, University of Texas Southwestern Medical Center, Dallas, TX), UAS-spin-GFP (gift of G. Davis, University of California, San Francisco, San Francisco, CA), *Ird1[3]* and UAS-Vps15 (gifts of L. Wu, University of Maryland, College Park, MD), *FRT42D Vps25[A3]* (gift of D. Bilder, University of California, Berkeley, Berkeley, CA), *FRTG13 Vps32/shrb[4]* (gift of F.-B. Gao, Gladstone Institute, San Francisco, CA), UAS-Tor dsRNA line *5092R-2* (National Institute of Genetics), UAS-Tsc1 and UAS-Tsc2 (gifts of N. Tapon, London Research Institute, London, UK), *Rheb[EP50.084]* (gift of E. Hafen, Institute for Molecular Systems Biology, Zürich, Switzerland), *Tsc2[192] FRT80B* (gift of N. Ito, Massachussetts General Hospital, Charlestown, MA), *Tor[ΔP]* (Zhang et al., 2000), *Tor[R97C]* (Zhang et al., 2006), and *Atg1[Δ3D]* (Scott et al., 2007).

Null and hypomorphic alleles of *Vps34* were generated as previously described (Scott et al., 2004) through imprecise excision of P[GawB]NP1626 (Hayashi et al., 2002), inserted after base 13 of the annotated *PI3K_59F* transcript (Flybase ID FBtr0072064). Excision events were characterized by PCR amplification of the *Vps34* locus using the primers 5′-GCTGGAGGAGCACAGATCCGAGACG-3′ and 5′-CAGCAGCTCCATCATCTTGAACAGGAACC-3′.

RT-PCR of wild-type and mutant animals

Total RNA was isolated from 5 mg of larvae per genotype using RevertAid Total RNA Isolation kit (Fermentas). cDNA was synthetized using a First Strand cDNA Synthesis kit (Fermentas) with random primers and used in PCR reactions with the Vps34-specific primers 5′-GGTGTTCAACCA-GGGCAGAC-3′ and 5′-GTCCGACATACGCTTTTCGC-3′, with primers 5′-GTCGCTTAGCTCAGCCTCG-3′ and 5′-TAACCCTCGTAGATGGG-CAC-3′ specific to actin as control.

Construction of transgenic *D. melanogaster* lines

All *P* element constructs were injected into *w*− embryos according to standard procedures.

UAS-GFP-Atg8a. A NotI–XbaI fragment containing the GFP-Atg8a coding region was excised from pCasper-HS-GFP-Atg8a (Scott et al., 2004) and ligated into NotI–XbaI-digested pUAST.

UAS-Atg6. Atg6/CG5429 EST LD35669 was cloned from the vector pOT2 into pUAST using XhoI and EcoRI restriction sites.

UAS-Myc-Atg6. The Atg6 coding region was PCR amplified from EST LD35669 using the primers 5′-CACCATGAGTGAGGCGGAA-3′ and 5′-TCACGGTGACACAAACTGTG-3′, cloned into pENTR/D-TOPO, and then recombined into the *D. melanogaster* Gateway vector pTMW using LR clonase.

UAS-Vps34. The *D. melanogaster* Vps34/PI3K_59F ORF was PCR amplified from EST GH13170 and ligated into the pUAST vector. A kinase-defective version of this construct (UAS-Vps34^{KD}) with D805→A and N810→I substitutions was generated by site-directed mutagenesis of pUAST-Vps34 and confirmed by sequencing.

UAS-Vps34-TAP. TOPO-TA cloning was used to clone the *D. melanogaster* Vps34/PI3K_59F ORF using the primers 5′-GGGGTACCCCAAAAAT-GGACC-3′ (introducing a 5′ KpnI site) and 5′-CTAGGATTACTCGCTCCTCC-3′ for N-terminal fusion and 5′-GCAGATCTGATATCATCGCC-3′ and 5′-GGG-TACCCTTCCGCCAGTAT-3′ (introducing a 3′ KpnI site) for C-terminal fusion. To generate N-terminal UAS-TAP-Vps34, Vps34 was cloned from TOPO-Vps34(N) into pUAST-NTAP (obtained from A. Veraksa, University of Massachussetts, Boston, MA) using KpnI and XbaI restriction sites. C-terminal UAS-Vps34-TAP was generated by cloning Vps34 from TOPO-Vps34(C) into pUAST-CTAP using EcoRI and KpnI restriction sites.

Histology and imaging

Clonal analysis of fat body tissue and lysotracker staining were performed essentially as previously described (Scott et al., 2007), except that LysoTracker Red DND-99 (Invitrogen) was used at 100 nM. TR avidin uptake was performed as previously described (Hennig et al., 2006), with pulse and chase times as indicated. For immunohistochemistry, the following antibodies were used: mouse monoclonal anti–myc (9E10; 1:1,000; gift of

Downloaded from jcb.rupress.org on February 16, 2009

Published May 12, 2008

M. Stewart, North Dakota State University, Fargo, ND); mouse anti–*D. melanogaster* Golgi (p120; 1:150; EMD); rabbit anti-hVps34 (1:300; Siddhanta et al., 1998); chicken anti-Avl (1:1,000; gift of D. Bilder); chicken anti-ubiquitin (1:200; eBioscience); and mouse monoclonal anti-Notch extracellular domain (F461.3B; 1:10; Developmental Studies Hybridoma Bank). Images of live lysotracker-stained fat bodies were obtained on an epifluorescence microscope (Axioscope-2; Carl Zeiss, Inc.) with a Plan-Neofluar 40× 0.75 NA objective, coupled to a digital camera (DXM1200; Nikon) controlled by ACT-1 acquisition software (Nikon). Confocal images were acquired on a microscope (Axioplan-2; Carl Zeiss, Inc.) with a Plan-Apochromat 63× 1.4 NA objective, equipped with a CARV spinning disc confocal system and a digital camera (ORCA-ER; Hamamatsu). Axiovision software (Carl Zeiss, Inc.) was used for acquisition, and images were further processed using Photoshop CS2 (Adobe).

GFP-Atg8 quantification

24-h collections of larvae carrying hs-GFP-Atg8a, Lsp2-GAL4, and UAS transgenes were raised to third instar, heat shocked for 1 h at 37°C, and incubated at 25°C for 3 h under feeding or starvation conditions. For starvation experiments, incubations were done in a dish with a wet kimwipe. For feeding experiments, feeding larvae were scooped, along with food, into a dish for incubations. Larval fat body was dissected in phosphate-buffered saline 3 h after completion of heat shock and mounted in SlowFade Gold antifade reagent (Invitrogen). Fat body samples were imaged with a confocal laser scanning microscope (LSM510; Carl Zeiss, Inc.) using a 40× objective. For each genotype, three fields in each of 10 animals were imaged and GFP-positive spots were counted.

Transmission EM

Tissues were dissected and fixed overnight at 4°C in 3.2% PFA, 1% glutaraldehyde, 1% sucrose, and 0.028% $CaCl_2$ in 0.1 N sodium cacodylate, pH 7.4, thoroughly washed in 0.1 N sodium cacodylate, pH 7.4, postfixed in 0.5% osmium tetroxide for 1 h, and embedded in Durcupan resin (Sigma-Aldrich) according to the manufacturer's recommendations. 70-nm sections were cut, stained in Reynolds lead citrate, and viewed on a transmission electron microscope (CM-II 100; JEOL). Immuno-EM was performed as described in Juhasz et al. (2007).

TEM morphometry and statistics

Five images per section were taken randomly at a magnification of 2,700 from five larvae per genotype (25 pictures). The area of autophagosomes, autolysosomes, and total cytoplasm was calculated using Photoshop by manually encircling relevant structures. Values are given as percent of total cytoplasm ± SD. Significance values were calculated by STATISTICA software (StatSoft) using Mann-Whitney U probes.

Immunoprecipitation and Western blot

After 1-h heat shock and 3-h 25°C recovery incubation, larvae were homogenized in lysis buffer (50 mM Hepes, pH 7.4, 150 mM KCl, 6.5% glycerol, 0.5 mM DTT, 0.1% Triton X-100, and complete protease inhibitor tablet [Roche]) and incubated on ice for 15 min. Samples were spun at 10,000 *g* for 10 min at 4°C to collect protein, which was stored at −80°C. For each IP, 300 µg of protein was precleared with 50 µl of protein A Sepharose 4B 50% slurry (Invitrogen) on ice for 1 h. Precleared lysate was incubated with 2 µg of antibody (rabbit anti-hVps34 #243 [Siddhanta et al., 1998]) at 4°C for 1 h. 50 µl of protein A Sepharose was added, followed by an additional 1-h incubation at 4°C. Beads were collected by centrifugation at 10,000 *g* for 30 s, washed with lysis buffer, and resuspended in 25 µl of Laemmli buffer. Antigen–antibody complexes were released from beads with a 10-min incubation at 95°C, followed by centrifugation at 10,000 *g* for 5 min at 4°C. Protein was separated by SDS-PAGE on a 7.5% acrylamide gel and transferred to an Immobilon-P PVDF membrane (Millipore). Membranes were blocked in 3% milk/TBST for 1 h at room temperature and washed three times for 10 min each in TBST. Blots were incubated with primary antibody (anti–c-Myc [1:200] in 2% BSA/TBST) for 1 h at room temperature, followed by three 10-min washes in TBST. Blots were incubated in goat anti–rabbit-HRP secondary antibody and diluted 1:2,000 in 3% milk/TBST for 1 h at room temperature. Blots were washed in TBST and then incubated with ECL reagent (GE Healthcare) and exposed with Hyperfilm ECL (GE Healthcare).

Online supplemental material

Fig. S1 displays the localization of early endosomal markers in wild-type and *Vps34* mutant cells. Fig. S2 shows the effect of Vps34 on additional cellular markers. Fig. S3 shows the effects of *Vps34* and *15* on markers of autophagy. Fig. S4 displays endocytic and autophagic phenotypes of *Vps25-Vps34* mutants. Fig. S5 includes TEM and confocal analysis of *Vps25-Vps34* single and double mutants. Online supplemental material is available at http://www.jcb.org/cgi/content/full/jcb.200712051/DC1.

We thank David Bilder, Graeme Davis, Marcos Gonzalez-Gaitan, Fen-Biao Gao, Ernst Hafen, Naoto Ito, Helmut Kramer, Mary Stewart, Nicolas Tapon, Louisa Wu, and Jun Zhang for gifts of fly strains and antibodies, Laura Muller for cell size quantitation, Balázs Érdi for preparing RNAs and cDNAs, and Sarolta Pálfia, Gáborné Komjáti, and Mariann Saródy for technical assistance with EM.

This work was supported by National Institutes of Health grants GM59136 (E.H. Baehrecke), DK070679 (J.M. Backer), and GM62509 (T.P. Neufeld). G. Juhász is a Bólyai Fellow.

Submitted: 10 December 2007
Accepted: 22 April 2008

References

Arsham, A.M., and T.P. Neufeld. 2006. Thinking globally and acting locally with TOR. *Curr. Opin. Cell Biol.* 18:589–597.

Britton, J.S., W.K. Lockwood, L. Li, S.M. Cohen, and B.A. Edgar. 2002. *Drosophila's* insulin/PI3-kinase pathway coordinates cellular metabolism with nutritional conditions. *Dev. Cell.* 2:239–249.

Byfield, M.P., J.T. Murray, and J.M. Backer. 2005. hVps34 is a nutrient-regulated lipid kinase required for activation of p70 S6 kinase. *J. Biol. Chem.* 280:33076–33082.

Chintapalli, V.R., J. Wang, and J.A. Dow. 2007. Using FlyAtlas to identify better *Drosophila melanogaster* models of human disease. *Nat. Genet.* 39:715–720.

Eskelinen, E.L. 2005. Maturation of autophagic vacuoles in Mammalian cells. *Autophagy.* 1:1–10.

Fimia, G.M., A. Stoykova, A. Romagnoli, L. Giunta, S. Di Bartolomeo, R. Nardacci, M. Corazzari, C. Fuoco, A. Ucar, P. Schwartz, et al. 2007. Ambra1 regulates autophagy and development of the nervous system. *Nature.* 447:1121–1125.

Futter, C.E., L.M. Collinson, J.M. Backer, and C.R. Hopkins. 2001. Human VPS34 is required for internal vesicle formation within multivesicular endosomes. *J. Cell Biol.* 155:1251–1264.

Gillooly, D.J., I.C. Morrow, M. Lindsay, R. Gould, N.J. Bryant, J.M. Gaullier, R.G. Parton, and H. Stenmark. 2000. Localization of phosphatidylinositol 3-phosphate in yeast and mammalian cells. *EMBO J.* 19:4577–4588.

Hayashi, S., K. Ito, Y. Sado, M. Taniguchi, A. Akimoto, H. Takeuchi, T. Aigaki, F. Matsuzaki, H. Nakagoshi, T. Tanimura, et al. 2002. GETDB, a database compiling expression patterns and molecular locations of a collection of Gal4 enhancer traps. *Genesis.* 34:58–61.

Hennig, K.M., J. Colombani, and T.P. Neufeld. 2006. TOR coordinates bulk and targeted endocytosis in the *Drosophila melanogaster* fat body to regulate cell growth. *J. Cell Biol.* 173:963–974.

Huang, J., and D.J. Klionsky. 2007. Autophagy and human disease. *Cell Cycle.* 6:1837–1849.

Juhasz, G., B. Erdi, M. Sass, and T.P. Neufeld. 2007. Atg7-dependent autophagy promotes neuronal health, stress tolerance, and longevity but is dispensable for metamorphosis in *Drosophila*. *Genes Dev.* 21:3061–3066.

Juhasz, G., and T.P. Neufeld. 2006. Autophagy: a forty-year search for a missing membrane source. *PLoS Biol.* 4:e36.

Kamada, Y., T. Funakoshi, T. Shintani, K. Nagano, M. Ohsumi, and Y. Ohsumi. 2000. Tor-mediated induction of autophagy via an Apg1 protein kinase complex. *J. Cell Biol.* 150:1507–1513.

Kihara, A., Y. Kabeya, Y. Ohsumi, and T. Yoshimori. 2001. Beclin-phosphatidylinositol 3-kinase complex functions at the trans-Golgi network. *EMBO Rep.* 2:330–335.

Kovacs, A.L., Z. Palfia, G. Rez, T. Vellai, and J. Kovacs. 2007. Sequestration revisited: integrating traditional electron microscopy, de novo assembly and new results. *Autophagy.* 3:655–662.

Lee, J.A., A. Beigneux, S.T. Ahmad, S.G. Young, and F.B. Gao. 2007. ESCRT-III dysfunction causes autophagosome accumulation and neurodegeneration. *Curr. Biol.* 17:1561–1567.

Linassier, C., L.K. MacDougall, J. Domin, and M.D. Waterfield. 1997. Molecular cloning and biochemical characterization of a *Drosophila* phosphatidylinositol-specific phosphoinositide 3-kinase. *Biochem. J.* 321:849–856.

Lindmo, K., and H. Stenmark. 2006. Regulation of membrane traffic by phosphoinositide 3-kinases. *J. Cell Sci.* 119:605–614.

Mari, M., and F. Reggiori. 2007. Shaping membranes into autophagosomes. *Nat. Cell Biol.* 9:1125–1127.

Downloaded from jcb.rupress.org on February 16, 2009

Published May 12, 2008

Nara, A., N. Mizushima, A. Yamamoto, Y. Kabeya, Y. Ohsumi, and T. Yoshimori. 2002. SKD1 AAA ATPase-dependent endosomal transport is involved in autolysosome formation. *Cell Struct. Funct.* 27:29–37.

Neufeld, T.P. 2004. Role of autophagy in developmental cell growth and death: insights from *Drosophila. In* Autophagy. D.J. Klionsky, editor. Landes Bioscience, Georgetown. 224-232.

Neufeld, T.P., and E.H. Baehrecke. 2008. Eating on the fly: function and regulation of autophagy during cell growth, survival and death in *Drosophila*. *Autophagy*. http://www.landesbioscience.com/journals/3/article/5782 (accessed April 30, 2008).

Nobukuni, T., M. Joaquin, M. Roccio, S.G. Dann, S.Y. Kim, P. Gulati, M.P. Byfield, J.M. Backer, F. Natt, J.L. Bos, et al. 2005. Amino acids mediate mTOR/raptor signaling through activation of class 3 phosphatidylinositol 3OH-kinase. *Proc. Natl. Acad. Sci. USA.* 102:14238–14243.

Pattingre, S., A. Tassa, X. Qu, R. Garuti, X.H. Liang, N. Mizushima, M. Packer, M.D. Schneider, and B. Levine. 2005. Bcl-2 antiapoptotic proteins inhibit Beclin 1-dependent autophagy. *Cell.* 122:927–939.

Pattingre, S., L. Espert, M. Biard-Piechaczyk, and P. Codogno. 2007. Regulation of macroautophagy by mTOR and Beclin 1 complexes. *Biochimie.* 90:313–323.

Petiot, A., E. Ogier-Denis, E.F. Blommaart, A.J. Meijer, and P. Codogno. 2000. Distinct classes of phosphatidylinositol 3′-kinases are involved in signaling pathways that control macroautophagy in HT-29 cells. *J. Biol. Chem.* 275:992–998.

Radimerski, T., J. Montagne, M. Hemmings-Mieszczak, and G. Thomas. 2002. Lethality of *Drosophila* lacking TSC tumor suppressor function rescued by reducing dS6K signaling. *Genes Dev.* 16:2627–2632.

Reggiori, F., C.W. Wang, U. Nair, T. Shintani, H. Abeliovich, and D.J. Klionsky. 2004. Early stages of the secretory pathway, but not endosomes, are required for Cvt vesicle and autophagosome assembly in *Saccharomyces cerevisiae*. *Mol. Biol. Cell.* 15:2189–2204.

Row, P.E., B.J. Reaves, J. Domin, J.P. Luzio, and H.W. Davidson. 2001. Overexpression of a rat kinase-deficient phosphoinositide 3-kinase, Vps34p, inhibits cathepsin D maturation. *Biochem. J.* 353:655–661.

Rusten, T.E., K. Lindmo, G. Juhasz, M. Sass, P.O. Seglen, A. Brech, and H. Stenmark. 2004. Programmed autophagy in the *Drosophila* fat body is induced by ecdysone through regulation of the PI3K pathway. *Dev. Cell.* 7:179–192.

Rusten, T.E., T. Vaccari, K. Lindmo, L.M. Rodahl, I.P. Nezis, C. Sem-Jacobsen, F. Wendler, J.P. Vincent, A. Brech, D. Bilder, and H. Stenmark. 2007. ESCRTs and Fab1 regulate distinct steps of autophagy. *Curr. Biol.* 17:1817–1825.

Saucedo, L.J., X. Gao, D.A. Chiarelli, L. Li, D. Pan, and B.A. Edgar. 2003. Rheb promotes cell growth as a component of the insulin/TOR signalling network. *Nat. Cell Biol.* 5:566–571.

Scott, R.C., O. Schuldiner, and T.P. Neufeld. 2004. Role and regulation of starvation-induced autophagy in the *Drosophila* fat body. *Dev. Cell.* 7:167–178.

Scott, R.C., G. Juhasz, and T.P. Neufeld. 2007. Direct induction of autophagy by Atg1 inhibits cell growth and induces apoptotic cell death. *Curr. Biol.* 17:1–11.

Siddhanta, U., J. McIlroy, A. Shah, Y. Zhang, and J.M. Backer. 1998. Distinct roles for the p110α and hVPS34 phosphatidylinositol 3′-kinases in vesicular trafficking, regulation of the actin cytoskeleton, and mitogenesis. *J. Cell Biol.* 143:1647–1659.

Suzuki, K., Y. Kubota, T. Sekito, and Y. Ohsumi. 2007. Hierarchy of Atg proteins in pre-autophagosomal structure organization. *Genes Cells.* 12:209–218.

Takahashi, Y., D. Coppola, N. Matsushita, H.D. Cualing, M. Sun, Y. Sato, C. Liang, J.U. Jung, J.Q. Cheng, J.J. Mul, et al. 2007. Bif-1 interacts with Beclin 1 through UVRAG and regulates autophagy and tumorigenesis. *Nat. Cell Biol.* 9:1142–1151.

Tassa, A., M.P. Roux, D. Attaix, and D.M. Bechet. 2003. Class III phosphoinositide 3-kinase–Beclin1 complex mediates the amino acid-dependent regulation of autophagy in C2C12 myotubes. *Biochem. J.* 376:577–586.

Vaccari, T., and D. Bilder. 2005. The *Drosophila* tumor suppressor vps25 prevents nonautonomous overproliferation by regulating notch trafficking. *Dev. Cell.* 9:687–698.

Wucherpfennig, T., M. Wilsch-Brauninger, and M. Gonzalez-Gaitan. 2003. Role of *Drosophila* Rab5 during endosomal trafficking at the synapse and evoked neurotransmitter release. *J. Cell Biol.* 161:609–624.

Yorimitsu, T., and D.J. Klionsky. 2005. Autophagy: molecular machinery for self-eating. *Cell Death Differ.* 12:1542–1552.

Zhang, H., J.P. Stallock, J.C. Ng, C. Reinhard, and T.P. Neufeld. 2000. Regulation of cellular growth by the *Drosophila* target of rapamycin dTOR. *Genes Dev.* 14:2712–2724.

Zhang, Y., C.J. Billington Jr., D. Pan, and T.P. Neufeld. 2006. *Drosophil*a target of rapamycin kinase functions as a multimer. *Genetics.* 172:355–362.

Downloaded from jcb.rupress.org on February 16, 2009

[Autophagy 4:4, 1-11; 16 May 2008]; ©2008 Landes Bioscience

dc_840_14

Research Paper

SNF4Aγ, the Drosophila AMPK γ subunit is required for regulation of developmental and stress-induced autophagy

Mónika Lippai,[1] György Csikós,[1] Péter Maróy,[2] Tamás Lukácsovich,[3,4] Gábor Juhász[1] and Miklós Sass[1,*]

[1]Department of Anatomy, Cell and Developmental Biology; Eötvös Lóránd University; Budapest, Hungary; [2]Department of Genetics and Molecular Biology; University of Szeged; Szeged, Hungary; [3]Department of Developmental and Cell Biology; [4]Developmental Biology Center; University of California Irvine; Irvine, California USA

Abbreviations: AMPK, AMP-activated protein-kinase; 20-OHE, 20-hydroxyecdysone; PCR, polymerase chain reaction; RNAi, RNA interference; RT, room temperature

Key words: Drosophila, larval fat body, autophagy, AMPK, SNF4Aγ, ecdysone, P-element

This manuscript has been published online, prior to printing.Once the issue is complete and page numbers have been assigned, the citation will change accordingly.

In holometabolous insects including *Drosophila melanogaster* a wave of autophagy triggered by 20-hydroxyecdysone is observed in the larval tissues during the third larval stage of metamorphosis. We used this model system to study the genetic regulation of autophagy. We performed a genetic screen to select P-element insertions that affect autophagy in the larval fat body. Light and electron microscopy of one of the isolated mutants (l(3)S005042) revealed the absence of autophagic vesicles in their fat body cells during the third larval stage. We show that formation of autophagic vesicles cannot be induced by 20-hydroxyecdysone in the tissues of mutant flies and represent evidence demonstrating that the failure to form autophagic vesicles is due to the insertion of a P-element into the gene coding SNF4Aγ, the Drosophila homologue of the AMPK (AMP-activated protein kinase) γ subunit. The ability to form autophagic vesicles (wild-type phenotype) can be restored by remobilization of the P-element in the mutant. Silencing of *SNF4Aγ* by RNAi suppresses autophagic vesicle formation in wild-type flies. We raised an antibody against SNF4Aγ and showed that this gene product is constitutively present in the wild-type larval tissues during postembryonal development. SNF4Aγ is nearly absent from the cells of homozygous mutants. SNF4Aγ translocates into the nuclei of fat body cells at the onset of the wandering stage concurrently with the beginning of the autophagic process. Our results demonstrate that SNF4Aγ has an essential role in the regulation of autophagy in Drosophila larval fat body cells.

Introduction

Autophagy—"self-digestion"—is a basic, general function of the cell and is an evolutionarily conserved process that occurs in virtually all eukaryotic cell types from yeast to mammals. In the mature organism, so-called macroautophagy is a catabolic mechanism, which works at a very low level in each cell to maintain the normal turnover of the cytosol and organelles by eliminating damaged, unfunctioning or defective cellular organelles and long-lived proteins. During macroautophagy, portions of the cytoplasm are sequestered in a double-membrane structure, giving rise to autophagosomes, which in turn fuse with lysosomes. Upon the fusion, inside the formed autolysosomes, the engulfed material is digested by lysosomal enzymes and recycled for synthetic and energy-producing processes.[1-3] Although there are at least three distinct autophagic pathways: macroautophagy, microautophagy and chaperone-mediated autophagy, we will focus on macroautophagy and use the term autophagy. For many years until recently, autophagy has been considered as type II programmed cell death, beside type I programmed cell death (apoptosis).[4,5] Later, autophagy was also described as a mechanism of self-defense against starvation, hypoxia or physical and chemical influences.[6-11] During the last few years, accumulating data prove that autophagy is involved in many other physiological processes such as remodeling, aging, cell growth control, innate immunity, and defense against invading microorganisms.[12-19]

The genetic regulation and molecular machinery of autophagy has been originally described in yeast.[20-23] Using genetic screens that allow identification of genes involved in autophagy, about 30 genes were characterized in unicellular fungal systems. Since then, a considerable amount of work focused on the cellular functions of the homologs of yeast autophagy-related (*Atg*) genes in higher organisms. More than half of them have proven to possess the same or similar roles in autophagy in plants, nematodes, flies and mammals.[24]

Insect metamorphosis represents one of the most extreme examples for this process, since in most larval tissues a mass of autophagic vesicles is observable before and during the destruction of the epidermis,[25] salivary gland,[26] larval midgut,[27,28] Malpighian tubes,[29] prothoracic glands[30] and fat body.[31,32] These vesicles appear in a well determined time of the postembryonal development and their appearance is under the control of the insect molting hormone.[33]

Genome-wide microarray and SAGE analyses have been performed in the larval salivary gland[34,35] and in the fat body[36] to identify genes involved in hormone induced metamorphotic changes, including autophagy, but much additional work is necessary to find out which of the up- or downregulated genes are related directly to autophagic processes.

*Correspondence to: Miklós Sass; Eötvös Loránd University; Department of Anatomy, Cell and Developmental Biology; Pázmány Péter sétány 1/c; Budapest, Pest 1117 Hungary; Tel.: 36.1.2090555/8127; Fax: 36.1.3812184; Email: msass@elte.hu

Submitted: 10/08/07; Revised: 02/06/08; Accepted: 02/13/08

Previously published online as an *Autophagy* E-publication:
http://www.landesbioscience.com/journals/autophagy/article/5719

©2008 Landes Bioscience. Do not distribute.

dc_840_14

In the present work, we used a powerful forward genetic approach to select and identify autophagy genes in *Drosophila melanogaster*. By this method, the direct effect of a P-element induced loss-of-function mutation can be observed at the phenotypic level and can be followed experimentally in developing Drosophila larvae.

Among the identified genes found to contribute to the regulation of the autophagic process, one encodes the *SNF4A*γ gene, which is the Drosophila orthologue of the mammalian AMPK (AMP-activated protein kinase) γ subunit. At the cellular and whole body level, the AMPK complex is responsible for the maintenance of the energy balance through regulation of various anabolic and catabolic pathways, hence we became interested in studying its role in autophagy.

Results

Identification of loss-of-function autophagy genes in P-element-generated mutant collections. Lines with late larval lethal phenotype were selected from 2nd (Bloomington) and 3rd [44] chromosome P-insertion mutant collections to identify mutations with a fat body phenotype. Altogether, 400 late larval lethal lines are registered in the two collections, and 315 of them were tested at our laboratory. In the first screen, those in which the acidic acridine orange, neutral red and/or LysoTracker Red-stained granules were absent from the fat body or the number, size or distribution of the granules were strongly different from those of the wild-type larvae (50 lines) were considered as positive hits. These observations were also verified by electron microscopy. Larvae from all of these lines were treated with 20-hydroxyecdysone (20-OHE). Those mutants which were able to form granules after the hormonal administration were separated for further studies (9 lines). The remaining 41 lines were crossed with appropriate deletions. Formation of the granules was inhibited in 32 hemizygotes. We could restore the original, wild-type phenotype in 21 lines by remobilization of the P-element. One of our 21 remaining hits was the 1(3)S005042 line. In the present paper we describe in detail our results concerning this mutant.

Morphology of the larval fat body cells. During the feeding period of the last larval stage (L3F), in wild-type (Oregon) animals the isodiametric, large fat body cells were filled with several huge lipid droplets. The droplet-free cytoplasm and the nucleus were situated generally in the central part of the cell. In this developmental phase, there were no autophagosomes, autolysosomes, protein granules or multivesicular bodies in the trophocytes (Fig. 1A, D and G).

In the wild-type at the late larval (wandering, L3W) period, many acridine orange/LysoTracker-positive acidic granules were formed in the trophocytes of the wild-type animals, corresponding mainly to autophagic vesicles. At the ultrastructural level, a mass of autophagosomes, huge autolysosomes (30–50/cell), some multivesicular bodies and protein storage granules could be seen in the cytoplasm (Fig. 1B, E and H).

In the 1(3)S005042 mutant line, the total absence of neutral red/acridine orange-positive structures was the first phenotypic sign of the defect in autophagy. Our ultrastrucural observations revealed that the fat body cells were essentially unable to form autophagosomes, lysosomes or autolysosomes, and only 1–2 autophagic structures/cell section were present in the trophocytes of the mutant larvae during the wandering and prepupal period. The number and size of the lipid droplets and the size of the glycogen areas were normal; the structure of the nucleus, mitochondria and Golgi areas did not show any alterations relative to the controls (Fig. 1C, F and I).

The larval fat body cells of l(3)S005042 did not respond to 20-hydroxyecdysone treatment. Since autophagy is 20-OHE dependent, we tested if it takes place following hormone treatment in the fat body cells of l(3)S005042 mutants. Wild-type and l(3)S005042 homozygous animals were treated with the hormone during the feeding period of the last larval stage. In controls, autophagic structures appear in the fat body (Fig. 2A), while in mutants the morphological signs of autophagy could not been observed (Fig. 2B).

Impaired starvation-induced autophagy in l(3)S005042 mutant fat bodies. Next, we wanted to test if the mutant fat body cells have the capability to build the structures seen in autophagy. To examine this we chose amino acid starvation, which results in massive autophagic activity in the fat body. Four hours of amino acid deprivation of the L3F larvae resulted in intense acridine orange staining in the wild-type (Fig. 3A). However, the same treatment had no effect in the accumulation of autophagic vesicles in the fat body cells of homozygous l(3)S005042 larvae (Fig. 3B).

l(3)S005042 mutant flies carry a P-element insertion in the *SNF4A*γ gene. The P-element was localized to cytological position 93C1–C5 in the third chromosome, uncovered by the eN19(93B,94) and the eR1(93B,93D) deficiency.

Inverse PCR on l(3)S005042 genomic DNA was used to localize the insertion site of the P-element. The P-element is inserted in the sixteenth intron of the *SNF4A*γ gene, the γ-subunit of Drosophila AMP-activated protein kinase (AMPK). The *SNF4A*γ gene may encode a number of alternatively spliced transcripts (data from FlyBase), and the different mRNAs encode at least seven different protein isoforms, all sharing the same C terminus containing the so-called CBS domains responsible for the AMP-binding while varying in their N-terminal parts (Fig. 4).

The exact site of the insertion is 29 bp upstream of the transcription start site of the SNF4Aγ-RL transcript, which is very close (57 bp upstream) to the SNF4Aγ-RG start site. Since nine of the twelve transcripts contain the sixteenth intron, and the insertion may also affect the transcription of the SNF4Aγ-RG, SNF4Aγ-RL and/or SNF4Aγ-RI transcripts, almost all messages may be altered by the P-element.

We tested ten other P-element insertions in the SNF4Aγ region (Fig. 4). Only one of them (l(3)S012719, from the Szeged Stock Center) showed defective autophagy in homozygous late third instar larvae, with very similar phenotypic features to those observed in the l(3)S005042 mutants. l(3)S005042/l(3)S012719 transheterozygotes died before pupariation. The P-element in the l(3)S012719 strain inserted 53 bp upstream of the l(3)S005042 insertion site.

Interestingly, the two closest P-element insertions located upstream of the l(3)S005042 site (EP3015b and EP3310) caused lethality before the L3 stage. In contrast, flies homozygous for the EP648 insertion 24 bp downstream from the l(3)S005042 site (thus only 5 bp from the SNF4Aγ-RL transcription start site) are fully viable, without any signs of autophagy defects in late L3 larvae. This finding suggests that mutations in the genomic region ~20–500 bp upstream of the SNF4Aγ-RL transcription start site may affect the autophagy-related function of the SNF4Aγ gene.

SNF4Aγ-RG, -RL and -RI mRNA expression was analyzed by RT-PCR in wild-type and mutant third instar larvae. The RG and

©2008 Landes Bioscience. Do not distribute.

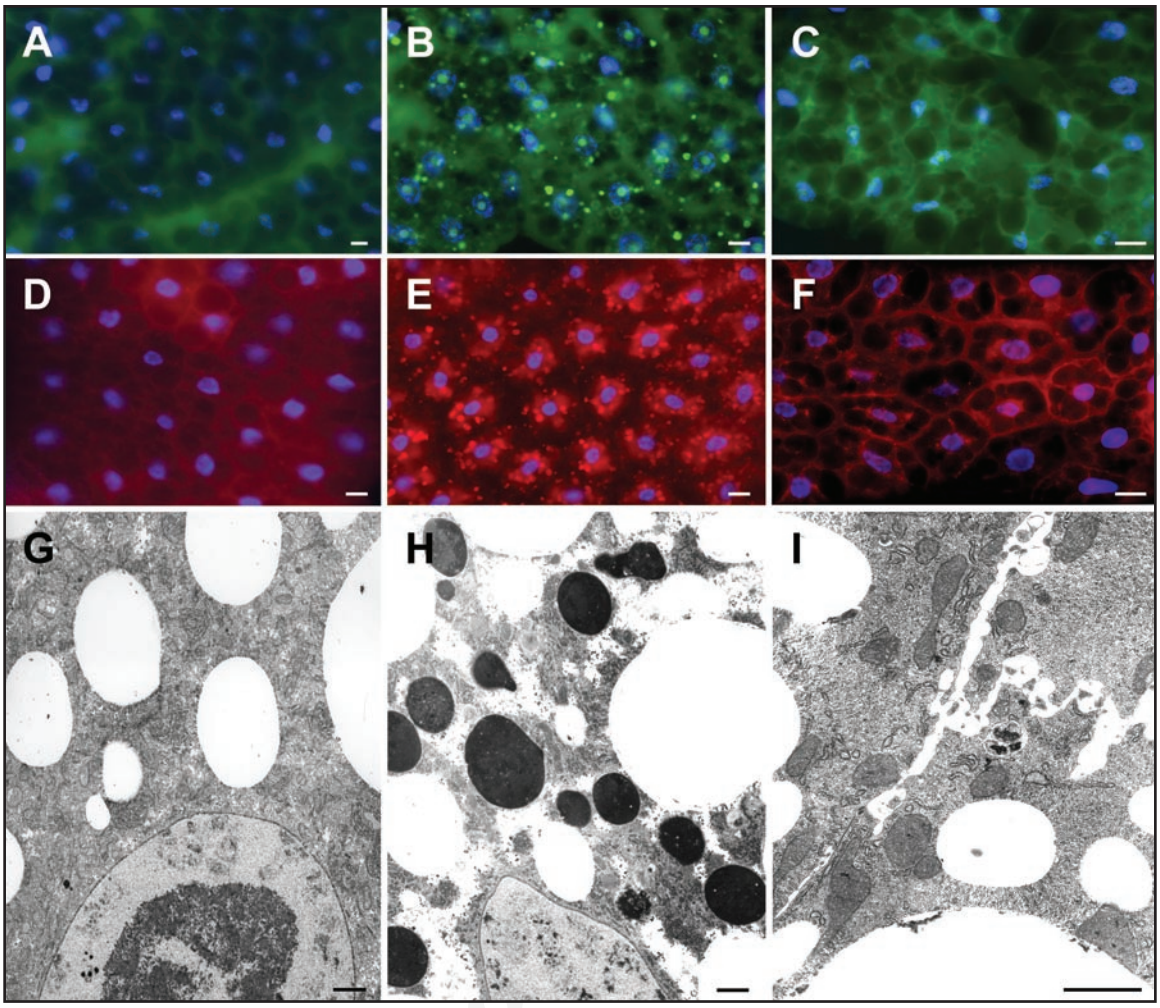


Figure 1. Acridine orange (A–C) and LysoTracker (D–F)-staining, and electron microscopy images (G–I) of whole-mount fat bodies of wild-type L3F, L3W and homozygous mutant larvae, respectively. DAPI stain was used for nuclei. (B and E) Acidic granules fill fat body cells of wild-type L3W larvae. These structures are missing in the early—L3F—stage (A and D) and the homozygous l(3)S005042 late third stage larval fat bodies (C and F). At the electron microscopy level, no autophagosomes or autolysosomes can be seen in feeding wild-type animals (G), whereas autophagic vesicles and protein granules accumulate in the cytoplasm during the L3W period (H). Fat bodies of homozygous l(3)S005042 larvae lack autophagic structures (I). Scale bar represents 25 μm for (A–F), and 1 μm for (G–I).

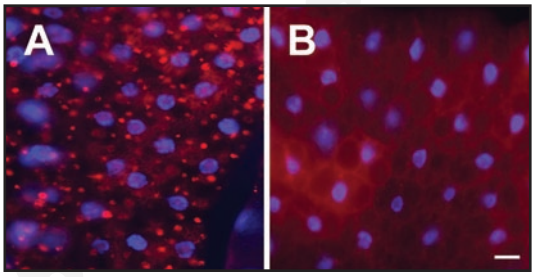


Figure 2. Effect of 20-OHE treatment on feeding wild-type and homozygous l(3)S005042 larvae, stained with LysoTracker and DAPI. (A) In control fat bodies, acidic vesicles were formed after the treatment, whereas mutant larval trophocytes did not respond to 20-OHE (B). Scale bar represents 25 μm.

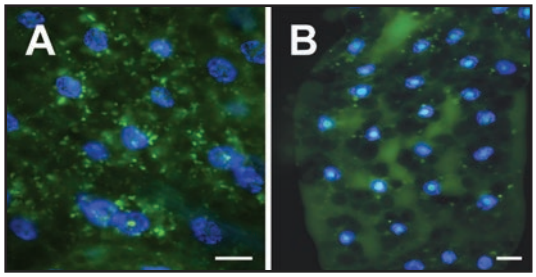


Figure 3. Acridine orange-stained whole-mount fat bodies of starved L3F wild-type and homozygous l(3)S005042 larvae. Nuclei were visualized with DAPI. (A) Acidic granules were present after 4 hours of starvation in wild-type fat body cells. (B) Larval fat bodies of the homozygotes did not show increase in the amount of acridine orange-positive granules. Scale bar represents 25 μm.

RL transcripts were nearly absent in mutant L3 larvae, and transcription of SNF4Aγ-RI was also strongly reduced (Fig. 5).

Autophagy is restored in revertants. To verify that the observed phenotype, the absence of the autophagic structures, is indeed caused by the insertion of the P-element into the SNF4Aγ gene, we remobilized it to see if it restores the wild-type phenotype. We established lines which showed reversion of the autophagy-defective phenotype. Several revertant lines were generated. All revertants

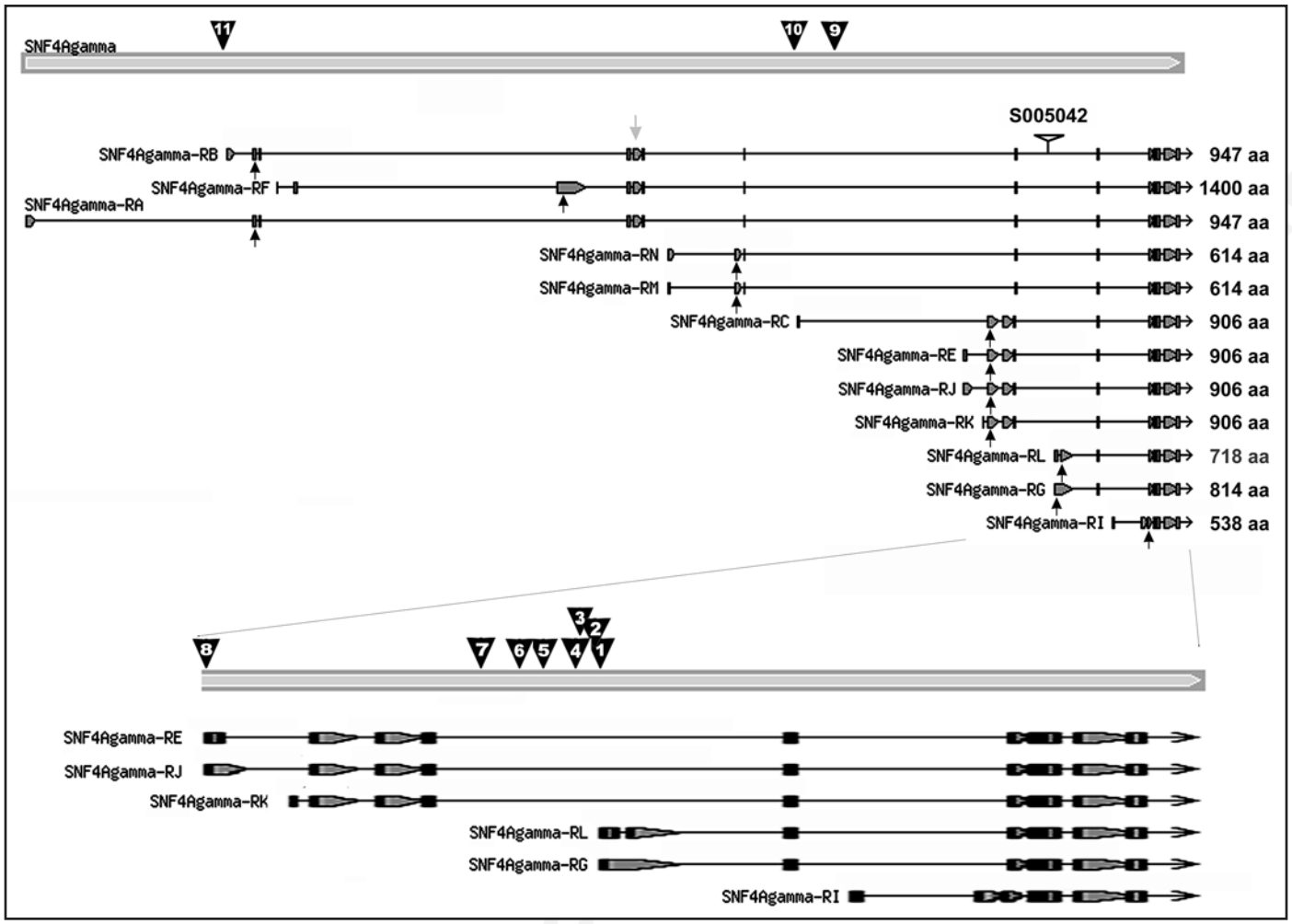


Figure 4. The genomic region adjacent to the P-element insertion site. The predicted exon-intron structures of the SNF4Aγ-RA to SNF4Aγ-RL transcripts are shown. Translational start codons are indicated by small arrows, and the predicted size of the translated protein by bold numbers. The grey arrow shows the exon used for antibody generation (see later). Large arrowheads indicate P-element insertions tested during this work, which are the following: (1) EP648 (Szeged); (2) l(3)S005042 (Szeged); (3) l(3)S012719 (Szeged); (4) EP3015b (Szeged); (5) EP3310 (Szeged); (6) EP3332 (Szeged); (7) EP3176 (Szeged); (8) KG10152 (Bloomington); (9) EP772 (Szeged); (10) KG00325 (Bloomington); (11) EY07066 (Bloomington). For better visibility, we magnified the 3' part of the genomic region containing most of the insertions.

were fully viable and fertile, and autophagy was normally induced. Acridine orange staining revealed huge amount of acidic vesicles in fat bodies of late third instar larvae (Fig. 6A), while numerous autophagic vesicles appeared between the lipid droplets in electron microscopy images (Fig. 6B). The precise excision of l(3)S005042 insertion restored the wild-type phenotype.

***SNF4Aγ* RNAi supresses autophagy in late larval fat body.** To check the biological consequences of the *SNF4Aγ* deficiency, we generated a Gal4 regulated transgene that contains an inverted repeat specific to the common 3' end of the transcripts (UAS-SNF4IR). To obtain directed SNF4Aγ silencing, lines carrying UAS-SNF4IR transgenes were crossed to the cg-Gal4 driver line. This driver expresses Gal4 in the fat body and in the hemocytes. In order to examine the effect of Gal4/UAS-induced SNF4Aγ inactivation specifically in L3W larvae, we used a temperature-sensitive Gal80 insertion. In this system, the activator function of the Gal4 protein is repressed by a ubiquitously expressed temperature-sensitive Gal80 protein (Gal80^{ts}) (functional at 18°C, non-functional at 32°C). When early L3 animals carrying only the cg-Gal4 driver and the

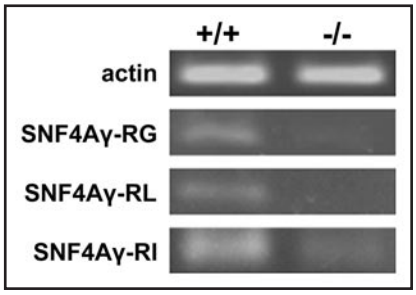


Figure 5. SNF4Aγ-RG, SNF4Aγ-RL and SNF4Aγ-RI mRNA expression was analyzed by RT-PCR in wild-type control (+/+) and homozygous mutant (-/-) third instar larvae. Expression of each of the three transcripts was decreased significantly in the mutants. Actin5C was used as a loading control.

tubulin(tub)—Gal80^{ts} gene were placed at 32°C for two days, we saw no change in the normal quantity of acidic granules in their fat body after the beginning of wandering (Fig. 7A). In contrast, restrictive temperature resulted in the absence of these structures during

dc_840_14

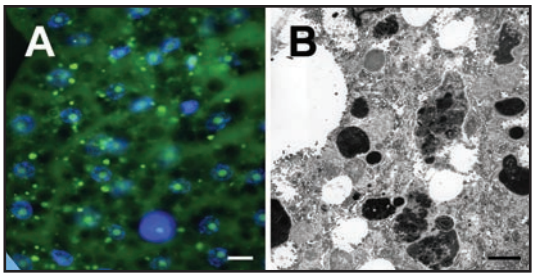


Figure 6. Late third instar larval fat bodies from revertant strains show complete restoration of the wild-type phenotype both at the light microscopy (acridine-orange and DAPI staining) (A) and electron microscopy level (B). Scale bar represents 25 μm in (A), and 1 μm in (B).

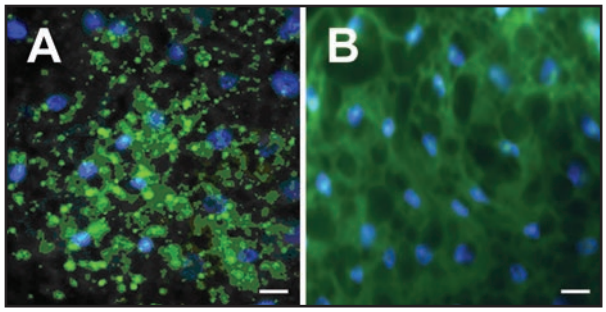


Figure 7. After RNAi induction, SFNF4IR suppresses the formation of acidic vesicles in late third instar larval fat body, suggesting inhibition of autophagic activity. (A) Trophocytes are filled with acidic vesicules in Gal80^{ts}/cgGal4; +/+ L3W larvae. (B) After induction of RNAi at the restrictive temperature, acidic structures did not appear in Gal80^{ts}/cgGal4; UAS-SNF4IR/+ L3W larvae. Scale bar represents 25 μm.

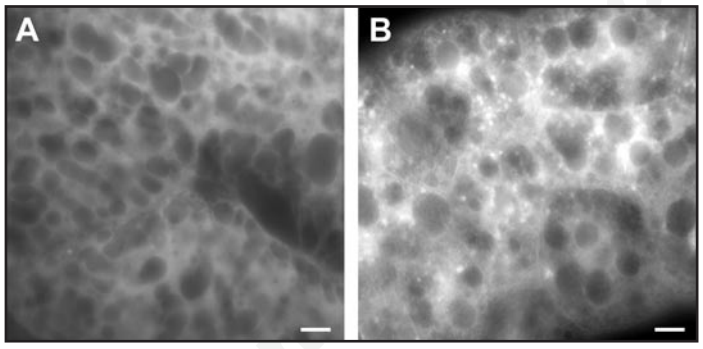


Figure 8. Heat-shock-induced overexpression of the wild-type SNF4Aγ-RG cDNA in homozygous mutant third instar larvae resulted in normal amount of LysoTracker-positive granules in their fat body cells (B), indicating restoration of autophagy. In contrast, larvae with the same genotype kept on room temperature did not show rescue of the mutant phenotype (A). Scale bar represents 25 μm.

wandering and led to a longer larval stage in animals also carrying the UAS-SNF4IR construct (Fig. 7B).

Partial rescue of the autophagy-defective phenotype of the l(3)S005042 mutants. We used again the UAS-Gal4 system to generate transgenic flies expressing the SNF4Aγ-RG cDNA under heat-shock control. Flies carrying the UAS-SNF4Aγ-RG cDNA were crossed to hs-Gal4 flies in the l(3)S005042 mutant background. Some of the offspring L3F larvae were heat-shocked (4 h, 32°C) to induce Gal4, and thus SNF4Aγ-RG expression. Homozygous mutant L3F larvae lacking the transgene construct served as a negative control (data not shown). In two hours, fat body cells of heat-shocked UAS-SNF4Aγ-RG carrying mutant larvae contained the normal amount of LysoTracker-positive granules (Fig. 8B), and these larvae were able to pupariate. Larvae with the same genotype kept at 21°C did not show restoration of the mutant phenotype, and died before pupariation (Fig. 8A). This result suggests that the overexpressed SNF4Aγ-RG cDNA was able to partially rescue the autophagy mutant phenotype of the l(3)S005042 strain.

Generation of the anti-SNF4Aγ antibody. SNF4Aγ antibody was raised against a protein corresponding to a shared exon of the SNF4Aγ-RA, SNF4Aγ-RB and SNF4Aγ-RF transcripts (ninth exon of the SNF4Aγ coding region, see Fig. 4; 194 amino acids). This exon was chosen for immunization because the SNF4Aγ-RF transcript was earlier described as loeI cDNA,[45] which, when mutated due to a P-element insertion, caused a neurodegenerative phenotype in Drosophila. Characterization of the recombinant protein expressed in *E. coli*, and fly SNF4Aγ is shown in Figure 9. Western blots performed with the anti-SNF4Aγ antibody detected a ~28 kDa band corresponding to the recombinant bacterial protein used for immunization, and a ~105 kDa protein in late third stage larvae, which presumably corresponds to the 947 amino acid SNF4Aγ-RA or SNF4Aγ-RB transcript.

SNF4Aγ expression during Drosophila development. After verifying that our SNF4Aγ antibody specifically recognizes its target protein, an analysis of SNF4Aγ protein expression during development of w^{1118} wild-type animals was performed. Western blot analysis of whole extracts showed one protein band with 105 kDa molecular weight. As shown in Figure 10, this 105 kDa SNF4Aγ protein was not detected in embryos, a weak expression was observed in first instar larvae, and a strong increase, and then a relatively uniform level of the protein was detected throughout the later larval and pupal stages. We did not find difference in the expression pattern of female and male L3 larvae (Fig. 11). These results are consistent with the idea that at least the SNF4Aγ-RA/RB transcript may have specific functions during the larval-pupal stages.

We tested our anti-SNF4Aγ antibody on western blots prepared from homozygous mutant third instar larvae. Expression of the 105 kDa SNF4Aγ protein was significantly reduced in L3F larvae, and was undetectable in L3W larvae (Fig. 12).

SNF4Aγ expression in SNF4Aγ-silenced wild-type flies. Western blot analysis was performed to confirm that the 105 kDa protein detected by our SNF4Aγ antibody truly corresponds to one of the SNF4Aγ translation products. We used the same Gal80^{ts}/Gal4 system to induce RNAi in L3W larvae (described above), except for the Gal4 driver, this time containing a ubiquitously expressed actin promoter to silence the SNF4Aγ gene in the whole larval body.

The level of the 105 kDa protein was markedly decreased in extracts from heat-shocked larvae containing the UAS-SNF4IR construct (Fig. 13, lane 1), whereas almost the same quantity was present in the heat-shocked control (same genotype without UAS-SNF4IR, Fig. 13, lane 2) and wild-type L3W larvae (Fig. 10).

SNF4Aγ localization in the larval fat body. We examined the expression of the SNF4Aγ protein in third instar larval fat body cells by immunohistochemistry. The protein showed uniform cytoplasmic

©2008 Landes Bioscience. Do not distribute.

dc_840_14

localization in fed early L3s, (Fig. 14A–A"), and a strong nuclear accumulation was observed later, in wandering larvae (Fig. 14B–B"). The same localization pattern was seen in L3F larvae after 4 h of starvation (Fig. 14C–C") or after 8 h of hypoxia (data not shown).

In fat body cells of homozygous mutant larvae, the antibody did not recognize any SNF4Aγ protein (Fig. 14D–D").

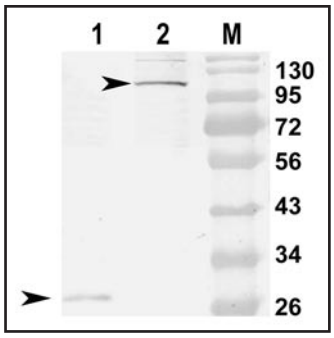


Figure 9. The SNF4Aγ antibody specifically recognizes its cognate protein, the recombinant partial SNF4Aγ in *E. coli* (lane 1) and the endogenous SNF4Aγ protein in Drosophila third stage larval extract (lane 2). Arrowheads show the 28 kDa band in lane 1 and the 105 kDa band in lane 2.

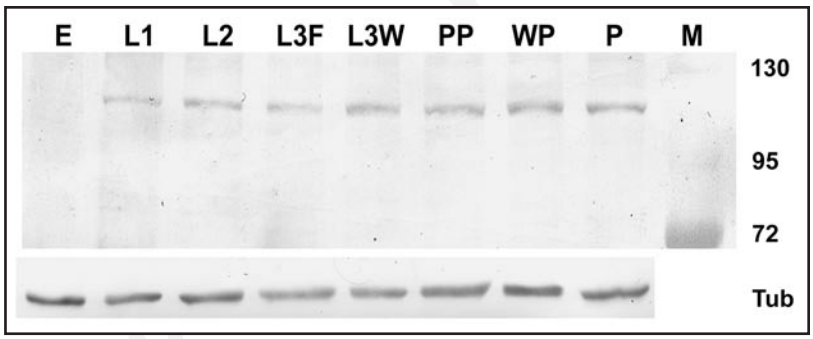


Figure 10. Expression of SNF4Aγ protein increases during development. Whole cell extracts were prepared from Drosophila embryos (E), larvae (L1-L3W), prepupae (PP), white pupae (WP) and pupae (P), and were probed for the SNF4Aγ protein by western blot analysis. α-tubulin was used as a loading control.

Discussion

In development and differentiation, autophagy is involved in morphogenetic changes during cell death, representing an integral part of normal development. Autophagic cell death is activated by a genetic program of development, when massive cell elimination is required in a tissue, organ or organ system. Extremely intensive formation and accumulation of autophagosomes and activation of the lysosomal system was observed in mammals, during the early development and differentiation of the pro- and mesonephros, Mullerian ducts, pharyngeal structures, limbs, heart and nervous system, and during the postembryonal development of the larval organs in amphibians and insects. These morphological and biochemical changes are in precise coincidence with the death and elimination of cells, tissues and even organs in developing systems.[7,46-48]

In insects it has been shown that 20-OHE stimulates autophagy in vivo and in vitro,[33,49-51] and this inductive effect can be inhibited at the transcriptional and translational level.[51,52] The 20-OHE-receptor complex acts as an activator of early genes encoding transcriptional factors which in turn stimulate late (effector) genes involved in the regulation of all metamorphotic changes in larval tissues including autophagy.[53-57] 20-OHE also has a strong influence in the regulation of the synthesis and activity of the lysosomal enzymes.[26,36,58-61]

The main aim of the present work was to select and identify autophagy-related genes in *Drosophila melanogaster*. Late larval lethal strains generated by P-element mutagenesis were screened to find mutants showing defects in the formation of autophagic structures (acidic granules identified by light and electron microscopy) in the larval fat body cells.

One of the candidate mutants is the l(3)S005042 strain, where the P-element is inserted in the *SNF4Aγ* gene. The SNF4Aγ protein is one of the regulatory subunits of the AMP-activated protein kinase (AMPK) complex in Drosophila. AMPK is an evolutionarily conserved master switch in the cellular energy balance activated by increases in AMP during metabolic stress. It inhibits anabolic processes (fatty acid, glycogen, protein synthesis, etc.) and stimulates catabolic pathways that generate ATP (fatty acid oxidation, glycolysis). AMPK also has a key role in the regulation of the whole body energy balance, initiating feeding behavior in response to hypoglycemia and causing an increase in the rate of breathing in response to hypoxia.[62] Its yeast homologue, the Snf1/Snf4 kinase complex is also activated by stress, most importantly by glucose limitation. Unlike AMPK, the Snf1/Snf4 complex is AMP-independent.[63]

AMPK is a heterotrimer, where the α subunit is responsible for the catalytic activity and the β and γ subunits have regulatory functions. The three subunits have a similar domain structure in all eukaryotes. The γ subunits contain variable N-terminal regions followed by four highly conserved repeat sequences at the C terminus, the CBS (cystathionine-b-synthase) domains that are important for the allosteric control of the α subunit by binding AMP.[64,65] The Drosophila genome contains single α, β and γ subunit genes,[66] in contrast to yeast and mammals, where multiple subunit isoforms are encoded by distinct genes. Therefore the Drosophila model provides a simpler tool to study evolutionarily conserved functions of AMPK.

Here we present molecular genetic and immunocytochemical data demonstrating that SNF4Aγ participates in the regulation of developmental and stress-induced autophagy in Drosophila. In the l(3)S005042 mutants, fat body cells are unable to undergo autophagy in response to 20-OHE treatments and starvation. These observations confirm the necessity and physiological role of the SNF4Aγ gene in autophagy. In order to collect further data on the function of the SNF4Aγ protein, a polyclonal antibody was developed. The antibody detected a ~105 kDa band constitutively present in all of the investigated larval and pupal extracts, presumably corresponding to the 947 amino acid SNF4Aγ-PA/PB proteins. The immunoblots showed that this gene product was nearly absent from homozygotes and gene silenced animals, suggesting that it is a prerequisite of autophagy, and that its presence is necessary for the process.

RT-PCR analysis confirmed strongly reduced expression of the SNF4Aγ-RG, SNF4Aγ-RL and SNF4Aγ-RI transcripts in mutant third instar larvae. On the other hand, overexpression of the SNF4Aγ-RG transcript resulted in partial rescue of the mutant

©2008 Landes Bioscience. Do not distribute.

dc_840_14

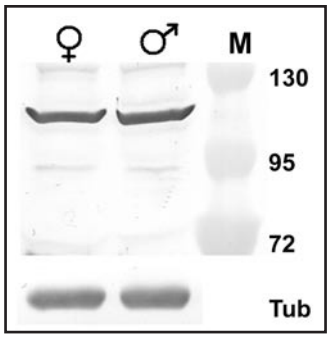


Figure 11. Expression of SNF4Aγ protein in third instar female and male larvae.

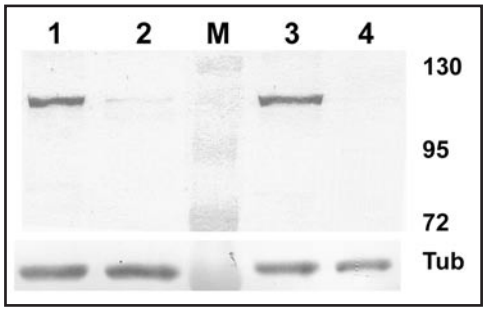


Figure 12. Compared with the wild-type L3F (lane 1) and L3W (lane 3) animals, the 105 kDa SNF4Aγ protein is very weakly expressed in homozygous mutant L3F (lane 2) and L3W larvae (lane 4).

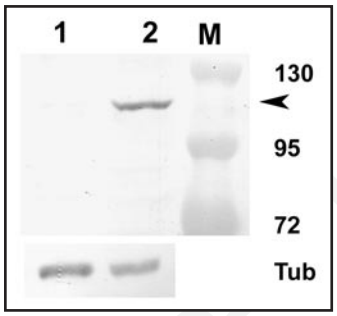


Figure 13. Induction of RNAi by heat-shock results in strong decrease in the quantity of the 105 kDa protein in Gal80^{ts}/actGal4; UAS-SNF4IR/+ L3W larvae (lane 1), in contrast with control Gal80^{ts}/actGal4; +/+ L3W animals (lane 2). The arrowhead marks the 105 kDa band.

phenotype in the homozygotes, suggesting that SNF4Aγ proteins really participate in the regulation of autophagy.

Inhibition of Tor-dependent signalling by rapamycin is known to stimulate autophagy.[12,51,67-68] Overexpression of tuberous sclerosis complex 1 and 2 (TSC1/2) in Drosophila fat body cells induces autophagy in fed larvae, whereas in TSC1 and TSC2 Drosophila mutants, starvation-induced autophagy was supressed.[12] The active TSC1/2 complex functions as an inhibitor of Rheb, the major positive regulator of Tor.[69] As TSC1/TSC2 is known to be activated by AMPK through phosphorylation,[64] AMPK is a possible negative regulator of Tor. (Fig. 15). Growing evidence suggests that, in this way, AMPK is also implicated in autophagy both in yeast and mammals. A yeast genetic screen revealed that Snf1 controls autophagy via Atg1 and Atg13,[70] whereas another yeast study found a direct connection between the prevention of the association of Atg1 and Atg13 due to Tor-induced Atg13 hyperphosphorylation and the repression of autophagy.[68] LKB1-AMPK pathway-dependent signaling permits mammalian cells to survive growth factor withdrawal and metabolic stress through autophagy.[72] Ischemia in the mouse heart also stimulates autophagy through an AMPK-dependent mechanism.[73] A recent study suggests that AMPK inhibits Tor and induces autophagy in nonstarved cells due to a rise in the free cytosolic Ca^{2+}, via the Ca^{2+}/calmodulin-dependent kinase kinase-β (CaMKK-β)-AMPK-TSC1/2-Rheb-Tor signaling pathway.[74]

Surprisingly, the SNF4Aγ protein recognized by our antibody translocated from the cytoplasm into the nuclei at the beginning of the formation of autophagic structures during normal development. This movement could be also induced by 20-OHE administration, starvation and hypoxia. Using PredictNLS,[75] we found a nuclear localization signal in the 8th exon of snf4aγ corresponding exclusively to the PA, PB and PF proteins. Although our finding about the translocation of SNF4Aγ was rather unexpected, there are some previous data supporting a nuclear role for AMPK. In yeast, there is an age-associated shift of the SNF4Aγ protein from the plasma membrane to the nucleus,[76] and in response to glucose limitation, the active kinase complex (containing the Gal83 β subunit) also accumulates in the nucleus.[77] In human skeletal muscle, exercise enhances the nuclear translocation of the AMPK complex containing the α2 subunit.[78,79] There are also some data concerning the nuclear function of the AMPK complex: it regulates nuclear proteins involved in gene transcription by direct phosphorylation.[80]

Our results suggest that SNF4Aγ can act in the nucleus, influencing gene regulatory processes during the induction of autophagy. Therefore, AMPK may regulate the autophagy process at multiple levels. Nuclear transport of the 105 kDa SNF4Aγ subunit may be needed to fulfill its role in the regulation of autophagy at the transcriptional level, whereas some SNF4Aγ proteins can reside in the cytoplasm completing the Tor-inhibiting effect of cytoplasmic AMPK, and to accomplish the canonical functions of AMPK.

During the past several years considerable advances have been achieved in determining the functions of autophagy-related (*Atg*) genes in yeast, and—using reverse genetic approaches—on the role of their orthologues in higher eukaryotes. Although, it is obvious to suppose that in highly organized animals more and different genes and regulatory pathways are involved in this process, our knowledge of the biology, regulation and molecular machinery of autophagy remains quite incomplete in multicellular organisms.

We performed a forward genetic screen in Drosophila to find genes associated with autophagy. The applicability and efficiency of our approach is proved by those hits (like the SNF4Aγ gene, presented here) which were also identified in two genome-wide analyses performed on dying Drosophila salivary gland.[34,35] Moreover, the involvement of AMPKγ in the regulation of autophagy in cultured mammalian cells has been suggested.[73,74] The similar results originating from the two different and independent sets of experiments emphasizes again that forward genetics is a proper and useful approach to identify autophagy genes. Furthermore, these findings have practical significance since genes and gene products regulating autophagy in multicellular organisms may represent new targets for

©Landes Bioscience. Do not distribute.

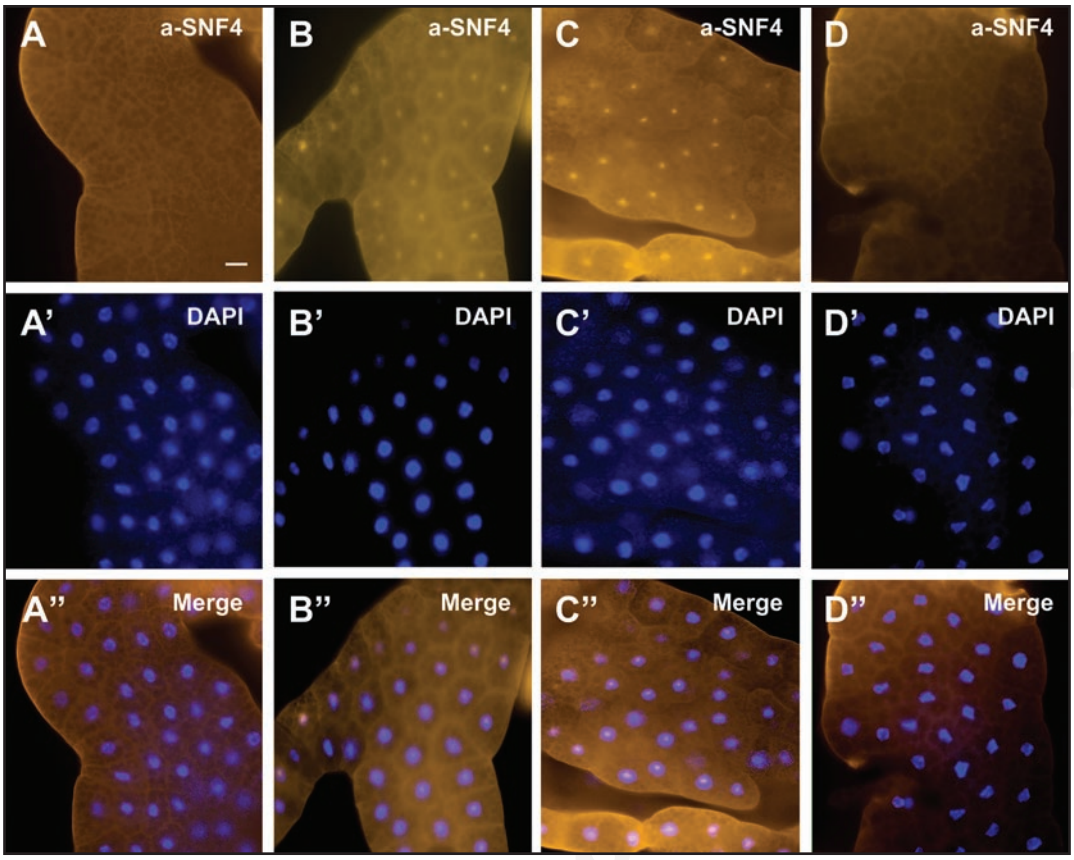


Figure 14. Pattern of SNF4Aγ protein localization in wild-type third instar larval fat body. In contrast with normally fed early L3 larvae (A–A"), the SNF4Aγ protein accumulated in the nucleus in the wandering period (B–B"), and in early L3 larvae during starvation (C–C"). No SNF4Aγ protein was detected in homozygous l(3)S005042 mutant larvae (D–D"). Scale bar in (A) represents 25 μm for all.

drug design and may help us to combat against widespread diseases such as strokes, neurondegenerative or developmental disorders.

Materials and Methods

Fly stocks. All Drosophila strains were maintained in a w^{1118} background, and all of the crosses and treatments were done at 25°C except where indicated.

For the revertant generation, the third chromosomal P-element was mobilized by crossing l(3)S005042/TM6,Tb flies to the TM3,Ser,delta2-3/Dr,delta2-3 strain.[37] The F1 l(3)S005042/TM3,Ser,delta2-3 males were crossed to the original P-element-carrying l(3)S005042/TM6,Tb females individually. The non-Tb, non-Ser, non-*white*-eyed viable progeny represented heterozygotes carrying the revertant third chromosome and were used to establish a stock.

Microinjection of the UAS-SNF4IR and the UAS-SNF4Aγ-RG construct (see below) into w^{1118} embryos was carried out by standard P-element-mediated germ line transformation.[38]

UAS-SNF4IR and tubulin-GAL80^{ts} [39] transgenes were combined in the same lines and crossed with the cg-Gal4 or the act-Gal4 line (Bloomington) which drives expression in fat body cells or in the whole body, respectively. Development was allowed to proceed at 18°C until the beginning of the third larval stage (84-hours after egg laying); individuals were then shifted to the restrictive temperature (32°C) for 48 hours.

For rescue experiments, a UAS-SNF4Aγ-RGCyO,hsGal4UAS-GFP; l(3)S005042/TM6Tb strain was generated (CyO,hsGal4UAS-GFP flies were obtained from Bloomington), and fat body cells of starved L3F larvae were examined with respect to autophagy induction.

Acridine orange and LysoTracker staining. Fat body from fed or starved larvae was dissected in phosphate-buffered saline (PBS), and then incubated for 5 min in 5 mg/ml acridine orange in PBS[40] or in 100 μM LysoTracker Red DND 99 (Molecular Probes), and 1 μg/ml DAPI (Sigma). Fat bodies were transferred to 80% glycerol in PBS on glass slides, covered and immediately photographed live on an OlympusBX-51 fluorescence microscope with FluoView digital imaging software.

Electron microscopy. Fat bodies were fixed in 2% glutaraldehyde in 0.1 M cacodylate buffer, pH 7.2. Samples were postfixed with 2% OsO_4 and 1.5% KFeCN in the same buffer, and 40–50 nm sections were observed in a JEOL CM-II 100 electron microscope.

Inverse PCR. Genomic DNA preparation was performed using standard methods. Inverse PCR[41] was performed using the recommended primers and restriction enzymes as described at http://www.fruitfly.org/about/methods/inverse.pcr.html for the *P{lacW}* transposon.

Reverse transcriptase PCR (RT-PCR). Total RNA from third instar larvae was extracted with RevertAid Total RNA Isolation Kit (Fermentas), and reversely transcribed using First Strand cDNA Synthesis Kit

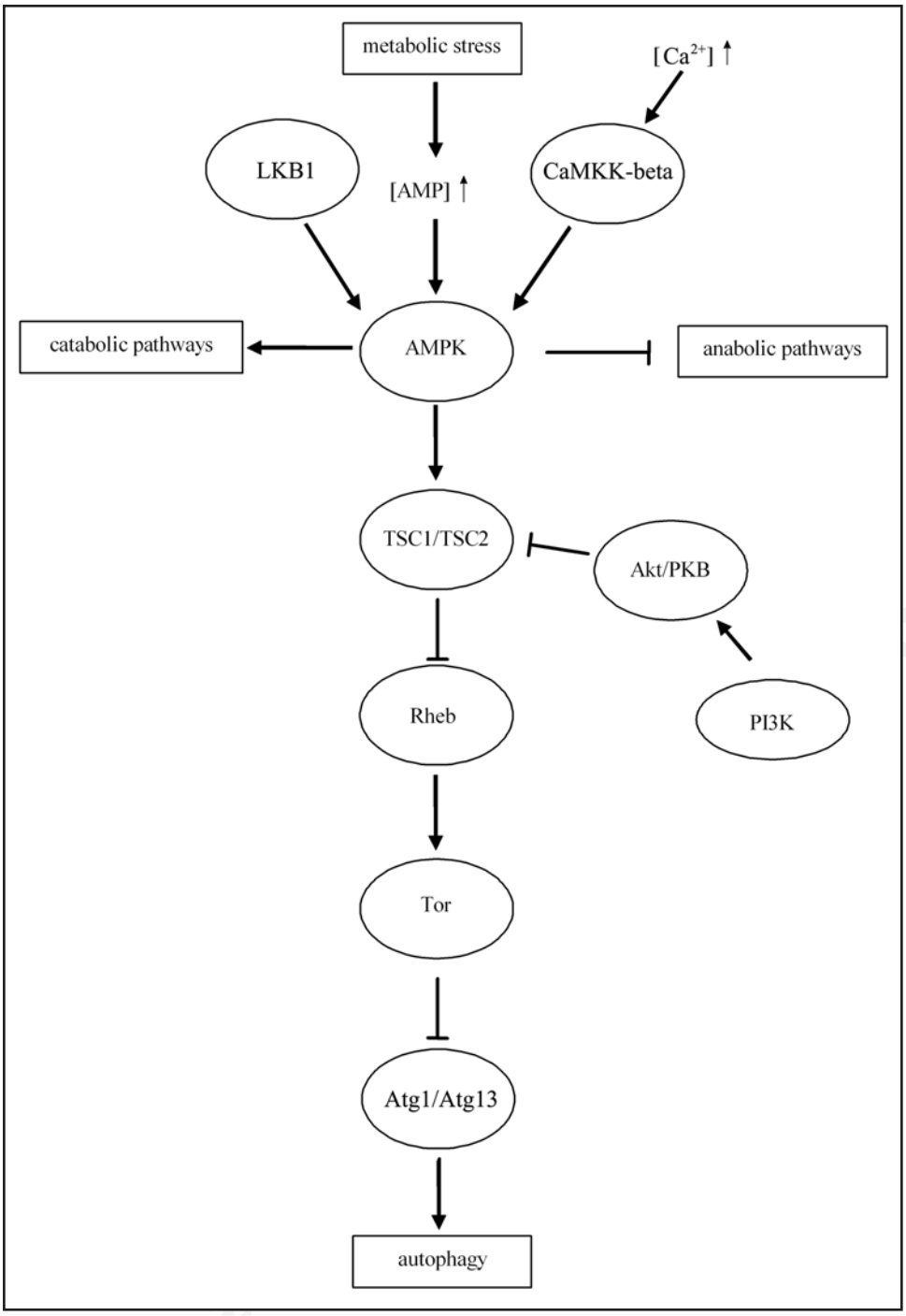


Figure 15. Possible role of AMPK in the regulation of autophagy via the Tor kinase pathway. In Drosophila and mammals, insulin-like receptor activation (via PI3K and Akt/PKB) and AMPK can act antagonistically to regulate TOR signaling through inhibitory and activating phosphorylation of TSC2, respectively. Arrows indicate activation, bars inhibition.

(Fermentas) with random primers. The following specific primers were used to amplify the three SNF4Aγ transcripts and the loading control Actin5C by PCR: 5'-CTTCTTCTTGAGTGCGCGGT-3' and 5'-GTCTTGTTTTTGCCGCTTGG-3' (SNF4Aγ-RG), 5'-CTGGCGCTCGCTAAACTCTT-3' and 5'-GTCTTGTTTTTGCCGCTTGG-3' (SNF4Aγ-RL), 5'-ACGGGCAGACGACACAAAAT-3' and 5'-AAGACAACCAACTTGGCGGA-3' (SNF4Aγ-RI) and 5'-GTCGCTTAGCTCAGCCTCG-3' and 5'-TAACCCTCGTAGATGGGCAC-3' (Actin5C).

Generation of the RNA interference construct. The SNF4Aγ RNA interference (RNAi) construct was created with a 0.7 kb PCR fragment of the common 3' terminal region using ExTaq DNA polymerase (Takara) and the primers 5'AATCTCGCCGCCGAGAAA3' and 5'GTCAGTGACTGGCCCAAA3' flanked with BglII and XhoI sites, respectively. The PCR fragment was subcloned into the Topo-TA PCR Cloning vector (Invitrogen), then the fragment was transferred into the modified pUAST vector pWizMod suitable for dsRNA generation (GenBank accession number AB186054; reviewed in ref. 42). In the first step, the fragment was inserted into the BglII-XhoI site of the pWizMod vector. In the second step, the same insert was cut out from Topo-TA by KpnI-XbaI double digestion and inserted in the opposite orientation into the KpnI-XbaI sites of the intermediate plasmid obtained from the first step. The resulting plasmid was named UAS-SNF4IR.

Generation of the rescue construct. To generate the UAS-SNF4Aγ-RG vector, the ORF coding for the SNF4Aγ-RG transcript was excised from the full-length cDNA clone LD30628 (obtained from Drosophila Genomics Resource Center, Bloomington) as an EcoRI-XhoI fragment and was ligated into the pUAST Drosophila transformation vector, and the resulting plasmid UAS-SNF4Aγ-RG was used for transformation.

Generation and purification of the recombinant SNF4Aγ partial protein. Molecular cloning techniques were performed according to standard procedures.[43] PCR amplification of the ninth SNF4Aγ exon was done using ExTaq DNA polymerase (Takara) with the primers 5' GAGGTCGGCTGACCCGCAGG 3' and 5'GGGGAATCTAGATTAACTAATTATTCG 3'. The PCR product was directly cloned into the pQE-UA bacterial expression vector (Qiagen), and a recombinant protein encoding the SNF4Aγ partial protein fused to an N-terminal hexahistidine tag was expressed in *E. coli* M15 cells. Protein purification was performed using the QIAexpressionist kit of Qiagen. Rabbits were immunized with the fusion peptide, and the obtained polyclonal antiserum was used for further investigation.

Preparation of protein extracts. Embryos, larvae and pupae were homogenized in 1x SDS electrophoresis running buffer supplemented with 2 mM Complete Proteinase Inhibitor Cocktail prepared from ready-to-use water soluble tablet (Roche) in a microcentrifuge tube

dc_840_14

using a pestle. The homogenate was centrifuged for 1 min at 13000 *g* at 4°C in a benchtop centrifuge, then the supernatant was collected, aliquoted and frozen.

Western blots. 1 mg of total proteins prepared from 0–4 h old Drosophila (w^{1118}) embryos, and each larval and pupal stage were subjected to SDS PAGE separation and transferred to nitrocellulose membrane for western blot analysis. Membranes were blocked in 5% milk prepared in TBS (10 mM Tris, pH 7.5, 100 mM NaCl), and hybridizations were carried out overnight at 4°C using 1:750 dilution of the SNF4Aγ antibody in 3% milk + TTBS (10 mM Tris, pH 7.5, 100 mM NaCl, 0.05% Tween). Membranes were washed three times (5 min each) in TTBS after hybridization. Alkaline-phosphatase-conjugated mouse anti-rabbit antibodies (Amersham) were used in 1:2000 dilution in 3% milk + TTBS, and the proteins were detected using NBT/BCIP (Sigma).

Prestained molecular weight marker (PageRuler™ Prestained Protein Ladder, Fermentas) served as the standard. Equal loading of samples was confirmed using an anti-α-tubulin antibody (DSHB AA4.3).

Immunocytochemistry. Immunocytochemistry was performed using standard techniques. Fat bodies from third instar larvae were dissected and fixed with 2% paraformaldehyde in PBS for 15 min at room temperature (RT). Samples were washed 2 x 5 min in PBS, then were incubated for 20 min in PBS + 0.1% Triton X-100. Following a 3 x 5 min wash with PBS, nonspecific binding sites were blocked by 1 hr incubation with 3% milk powder in PBS. Incubations with primary and secondary antibodies were performed in the blocking buffer overnight at 4°C and for 1 hr at RT respectively. Primary antibodies were used at a dilution of 1:100 (rabbit anti-SNF4Aγ; see above for preparation of SNF4Aγ antibodies). Anti-rabbit-Cy3 (Sigma; C-2306) secondary antibodies were used at a dilution of 1:400. An Olympus BX-51 fluorescence microscope with FluoView digital imaging software was used to image fluorescently labeled antibodies.

Acknowledgements

The authors thank Miklós Erdélyi and members of his laboratory for Drosophila embryo injections and Katalin Komjáti for the excellent technical help. This work was supported by grants from the OTKA (T048244) and the Hungarian National Research and Development Program (NKFP 1A/005/2004).

References

1. Dunn WA, Jr. Studies on the mechanisms of autophagy: formation of the autophagic vacuole. J Cell Biol 1990; 110:1923-33.
2. Dunn WA, Jr. Autophagy and related mechanisms of lysosome-mediated protein degradation. Trends Cell Biol 1994; 4:139-43.
3. Klionsky DJ, Emr SD. Autophagy as a regulated pathway of cellular degradation. Science 2000; 290:1717-21.
4. Clarke PGH. Developmental cell death-morphological diversity and multiple mechanisms. Anat Embryol (Berl) 1990; 181:195-213.
5. Edinger AL, Thompson CB. Death by design: apoptosis, necrosis and autophagy. Curr Opin Cell Biol 2004; 16:663-69.
6. Arstila AU, Trump BF. Autophagocytosis: origin of membrane and hydrolytic enzymes. Virchows Arch B Cell Pathol 1969; 2:85-90.
7. de Duve C, Wattiaux R. Functions of lysosomes. Annu Rev Physiol 1966; 28:435-92.
8. de Duve C. The peroxisome: a new cytoplasmic organelle. Proc R Soc Lond B Biol Sci 1969; 173:71-83.
9. Glinsmann WH, Ericsson JL. Observations on the subcellular organization of hepatic parenchymal cells. II. Evolution of reversible alterations induced by hypoxia. Lab Invest 1966; 15:762-77.
10. Réz G, Kovács J. Prevention of induced autophagocytosis by the protein-synthesis inhibitor emetine. Short communication. Acta Biol Acad Sci Hung 1973; 24:237-9.
11. Kovács J, Réz G, Kiss A. Vinblastine-induced autophagocytosis and its prevention by cycloheximide and emetine in mouse pancreatic acinar cells in vivo. Cytobiologie 1975; 11:309.
12. Scott RC, Schuldiner O, Neufeld TP. Role and regulation of starvation-induced autophagy in the Drosophila fat body. Dev Cell 2004; 7:167-78.
13. Neufeld TP. Role of autophagy in developmental cell growth and death: insights from Drosophila. In: Klionsky DJ, ed(s). Autophagy. Georgetown; Landes Bioscience, 2004: 224-32.
14. Scott RC, Juhász G, Neufeld TP. Direct induction of autophagy by Atg1 inhibits cell growth and induces apoptotic cell death. Curr Biol 2007; 17:1-11.
15. Melendez A, Tallóczy Z, Seaman M, Eskelinen EL, Hall DH, Levine B. Autophagy genes are essential for dauer development and life-span extension in *C. elegans*. Science 2003; 301:1387-91.
16. Nakagawa I, Amano A, Mizushima N, Yamamoto A, Yamaguchi H, Kamimoto T, Nara A, Funao J, Nakata M, Tsuda K, Hamada S, Yoshimori T. Autophagy defends cells against invading group A *Streptococcus*. Science 2004; 306:1037-40.
17. Gutierrez MG, Master SS, Singh SB, Taylor GA, Colombo MI, Deretic V. Autophagy is a defense mechanism inhibiting BCG and *Mycobacterium tuberculosis* survival in infected macrophages. Cell 2004; 119:753-66.
18. Levine B, Klionsky DJ. Development by self-digestion: molecular mechanisms and biological functions of autophagy. Dev Cell 2004; 6:463-77.
19. Levine B, Yuan J. Autophagy in cell death: an innocent convict? J Clin Invest 2005; 115:2679-88.
20. Tsukada M, Ohsumi Y. Isolation and characterization of autophagy-defective mutants of *Saccharomyces cerevisiae*. FEBS Lett 1993; 333:169-74.
21. Harding TM, Morano KA, Scott SV, Klionsky DJ. Isolation and characterization of yeast mutants in the cytoplasm to vacuole protein targeting pathway. J Cell Biol 1995; 131:591-602.
22. Ohsumi Y. Molecular dissection of autophagy: two ubiquitin-like systems. Nat Rev Mol Cell Biol 2001; 2:211-6.
23. Wang CW, Klionsky DJ. The molecular mechanism of autophagy. Mol Med 2003; 9:65-76.
24. Klionsky DJ, Cregg JM, Dunn WA Jr, Emr SD, Sakai Y, Sandoval IV, Sibirny A, Subramani S, Thumm M, Veenhuis M, Ohsumi Y. A unified nomenclature for yeast autophagy-related genes. Dev Cell 2003; 5:539-45.
25. Sedlak BJ, Gilbert LI. Epidermal cell development during the pupal-adult metamorphosis of *Hyalophora cecropia*. Tissue Cell 1976; 8:637-48.
26. Schin KS, Clever U. Lysosomal and free acid phosphatase in salivary glands of *Chironomus tentans*. Science 1965; 150:1053-5.
27. Judy KJ, Gilbert LI. Effects of juvenile hormone and molting hormone on rectal pad development in *Hyalophora cecropia* (L.). J Morphol 1970; 131:301-14.
28. Komuves LG, Sass, M, Kovács, J. Autophagocytosis in the larval midgut cells of *Pieris brassicae* during metamorphosis. Cell Tissue Res 1985; 240:215-21.
29. Ryerse JS. Developmental changes in Malpighian tubule cell structure. Tissue Cell 1979; 11:533-51.
30. Dai JD, Gilbert LI. Programmed cell death of the prothoracic glands of *Manduca sexta* during pupal-adult metamorphosis. Insect Biochem Mol Biol 1997; 27:69-78.
31. Butterworth FM, LaTendresse BL. Quantitive studies of cytochemical and sytological changes during cell death in the larval fat body of *Drosophila melanogaster*. J Insect Physiol 1973; 19:1487-500.
32. Sass M, Kovács J. Ultrastructural changes in the fat body cells of *Mamestra brassicae* (Noctuidae, Lepidoptera) during metamorphosis. Annales Univ Sci Budapest Rolando Eötvös, Sect Biol 1974; 16:189-205.
33. Sass M, Kovács J. Ecdysterone and an analogue of juvenile hormone on the autophagy in the cells of fat body of *Mamestra brassicae*. Acta Biol Acad Sci Hung 1975; 26:189-96.
34. Lee CY, Clough EA, Yellon P, Teslovich TM, Stephan DA, Baehrecke EH. Genome-wide analyses of steroid- and radiation-triggered programmed cell death in Drosophila. Curr Biol 2003; 13:350-57.
35. Gorski SM, Chittaranjan S, Pleasance ED, Freeman JD, Anderson CL, Varhol RJ, Coughlin SM, Zuyderduyn SD, Jones SJM, Marra MA. A SAGE approach to discovery of genes involved in autophagic cell death. Curr Biol 2003; 13:358-63.
36. Juhász G, Puskás LG, Komonyi O, Érdi B, Maróy P, Neufeld TP, Sass M. Gene expression profiling identifies FKBP39 as an inhibitor of autophagy in larval Drosophila fat body. Cell Death Differ 2007; 14:1181-90.
37. Robertson HM, Preston CR, Phillis RW, Johnson-Schlitz DM, Benz WK, Engels WR. A stable genomic source of P element transposase in *Drosophila melanogaster*. Genetics 1988; 118:461-70.
38. Rubin GM, Spradling AC. Genetic transformation of Drosophila with transposable element vectors. Science 1982; 218:348-53.
39. McGuire SE, Le PT, Osborn AJ, Matsumoto K, Davis RL. Spatiotemporal rescue of memory dysfunction in Drosophila. Science 2003; 302:1765-8.
40. Abrams JM, White K, Fessler LI, Steller H. Programmed cell death during Drosophila embryogenesis. Development 1993; 117:29-43.
41. Spradling AC, Stern D, Beaton A, Rhem EJ, Laverty T, Mozden N, Misra S, Rubin GM. The Berkeley Drosophila Genome Project gene disruption project: Single P-element insertions mutating 25% of vital Drosophila genes. Genetics 1999; 153:135-77.

©2008 Landes Bioscience. Do not distribute.

dc_840_14

42. Kurucz E, Márkus R, Zsámboki J, Folkl Medzihradszky K, Darula Z, Vilmos P, Udvardy A, Krausz I, Lukácsovich T, Gateff E, Zettervall CJ, Hultmark D, Andó I. Nimrod, a putative phagocytosis receptor with EGF repeats in Drosophila plasmatocytes. Curr Biol 2007; 17:649-54.
43. Sambrook J, Russel DW. Molecular Cloning. 3. Cold Spring Harbor, New York: Cold Spring Harbor Laboratory Press, 2001.
44. Deák P, Omar MM, Saunders RD, Pal M, Komonyi O, Szidonya J, Maróy P, Zhang Y, Ashburner M, Benos P, Savakis C, Siden Kiamos I, Louis C, Bolshakov VN, Kafatos FC, Madueno E, Modolell J, Glover DM. P-element insertion alleles of essential genes on the third chromosome of *Drosophila melanogaster*: correlation of physical and cytogenetic maps in chromosomal region 86E-87F. Genetics 1997; 147:1697-722.
45. Tschäpe JA, Hammerschmied C, Mühlig Versen M, Athenstaedt K, Daum G, Kretzschmar D. The neurodegeneration mutant löchrig interferes with cholesterol homeostasis and Appl processing. EMBO J 2002; 21:6367-76.
46. Schweichel JU, Merkel HJ. The morphology of various types of cell death in prenatal tissues. Teratology 1973; 7:253-66.
47. Lockshin RA, Zakeri Z. Apoptosis, autophagy, and more. Int J Biochem Cell Biol 2004; 36:2405-19.
48. Rubinsztein DC, DiFiglia M, Heintz N, Nixon RA, Qin ZH, Ravikumar B, Stefanis L, Tolkovsky A. Autophagy and its possible roles in nervous system diseases, damage and repair. Autophagy 2005; 1:11-22.
49. Sass M, Kovács J. The effect of ecdysone on the fat body cells of the penultimate larvae of *Mamestra brassicae*. Cell Tissue Res 1977; 180:403-9.
50. Dean RT. Lysosomes and membrane recycling. A hypothesis. Biochem J 1977; 168:603-5.
51. Rusten TE, Lindmo K, Juhász G, Sass M, Seglen PO, Brech A, Stenmark H. Programmed autophagy in the Drosophila fat body is induced by ecdysone through regulation of the PI3K pathway. Dev Cell 2004; 7:179-92.
52. Sass M, and Kovács, J. The effects of actinomycin-D, cycloheximide and puromycin on the 20-hydroxyecdysone induced autophagocytosis in larval fat-body cells of *Pieris brassicae*. J Insect Physiol 1980; 26:569.
53. Jiang C, Beahrecke EH, Thummel CS. Steroid regulated programmed cell death during Drosophila metamorphosis. Development 1997; 124:4673-83.
54. Lee CY, Baehrecke EH. Steroid regulation of autophagic programmed cell death during development. Development 2001; 128:1443-55.
55. Thummel CS. Steroid-triggered death by autophagy. Bioessays 2001; 23:677-82.
56. Lee CY, Cooksey BAK, Baehrecke EH. Steroid regulation of midgut cell death during Drosophila development. Dev Biol 2002; 250:101-11.
57. Baehrecke EH. Autophagic programmed cell death in Drosophila. Cell Death Differ 2003; 10:940-5.
58. van Pelt-Verkuil E. The induction of lysosomal enzyme activity in the fat body of *Calliphora erythrocephala*: Changes in internal environment. J Insect Physiol 1980; 26:91-101.
59. Ray AGD, Prasada Rao CD, Sridevi R, Ramamurty PS. Changes in acid phosphatase activity in *Spodoptera litura* (Lepidoptera-Noctuidae) during the postembryonic and adult development. Entomol 1984; 9:161-67.
60. Sass M, Komuves L, Csikós G, Kovács J. Changes in the activities of lysosomal enzymes in the fat body and midgut of two Lepidopteran insects (*Mamestra brassicae* and *Pieris brassicae*) during metamorphosis. Comp Biochem Physiol 1989; 92A:285-89.
61. Jones HE, Bowen ID. Acid phosphatase activity in the larval salivary glands of developing *Drosophila melanogaster*. Cell Biol Int 1993; 17:305-15.
62. Hardie DG, Hawley SA, Scott JW. AMP-activated protein kinase—development of the energy sensor concept. J Physiol 2006; 574:7-15.
63. Mitchelhill KI, Stapleton D, Gao G, House C, Michell B, Katsis F, Witters LA, Kemp BE. Mammalian AMP-activated protein kinase shares structural and functional homology with the catalytic domain of yeast Snf1 protein kinase. J Biol Chem 1994; 269:2361-4.
64. Hardie DG, Carling D, Carlson M. The AMP-activated/SNF1 protein kinase subfamily: metabolic sensors of the eukaryotic cell? Annu Rev Biochem 1998; 67:821-55.
65. Adams J, Chen ZP, Van Denderen BJ, Morton CJ, Parker MW, Witters LA, Stapleton D, Kemp BE. Intrasteric control of AMPK via the γ1 subunit AMP allosteric regulatory site. Protein Sci 2004; 13:155-65.
66. Pan DA, Hardie DG. A homologue of AMP-activated protein kinase in Drosophila melanogaster is sensitive to AMP and is activated by ATP depletion. Biochem J 2002; 367:179-86.
67. Noda T, Ohsumi Y. Tor, a phosphatidylinositol kinase homologue, controls autophagy in yeast. J Biol Chem 1998; 273:3963-6.
68. Kamada Y, Funakoshi T, Shintani T, Nagano K, Ohsumi M, Ohsumi Y. Tor-mediated induction of autophagy via an Apg1 protein kinase complex. J Cell Biol 2000; 150:1507-13.
69. Garami A, Zwartkruis FJT, Nobukuni T, Joaquin M, Roccio M, Stocker H, Kozma SC, Hafen E, Bos JL, Thomas G. Insulin activation of Rheb, a mediator of mTOR/S6K/4E-BP signaling, is inhibited by TSC1 and 2. Mol Cell 2003; 11:1457-66.
70. Wang Z, Wilson WA, Fujino MA, Roach PJ. Antagonistic controls of autophagy and glycogen accumulation by Snf1p, the yeast homolog of AMP-activated protein kinase, and the cyclin-dependent kinase Pho85p. Mol Cell Biol 2001; 21:5742-52.
71. Meley D, Bauvy C, Houben Weerts JH, Dubbelhuis PF, Helmond MT, Codogno P, Meijer AJ. AMP-activated protein kinase and the regulation of autophagic proteolysis. J Biol Chem 2006; 281:34870-9.
72. Liang J, Shao SH, Xu ZX, Hennessy B, Ding Z, Larrea M, Kondo S, Dumont DJ, Gutterman JU, Walker CL, Slingerland JM, Mills GB. The energy sensing LKB1-AMPK pathway regulates p27(kip1) phosphorylation mediating the decision to enter autophagy or apoptosis. Nat Cell Biol 2007; 9:218-24.
73. Takagi H, Matsui Y, Hirotani S, Sakoda H, Asano T, Sadoshima J. AMPK mediates autophagy during myocardial ischemia in vivo. Autophagy 2007; 3:405-7.
74. Høyer-Hansen M, Bastholm L, Szyniarowski P, Campanella M, Szabadkai G, Farkas T, Bianchi K, Fehrenbacher N, Elling F, Rizzuto R, Mathiasen IS, Jäättelä M. Control of macroautophagy by calcium, calmodulin-dependent kinase kinase-β, and Bcl-2. Mol Cell. 2007; 25:193-205.
75. Cokol M, Nair R, Rost B. Finding nuclear localization signals. EMBO Rep 2000; 1:411-5.
76. Lin SS, Manchester JK, Gordon JI. Sip2, an N-myristoylated β subunit of Snf1 kinase, regulates aging in *Saccharomyces cerevisiae* by affecting cellular histone kinase activity, recombination at rDNA loci, and silencing. J Biol Chem 2003; 278:13390-7.
77. Vincent O, Townley R, Kuchin S, Carlson M. Subcellular localization of the Snf1 kinase is regulated by specific β subunits and a novel glucose signaling mechanism. Genes Dev 2001; 15:1104-14.
78. McGee SL, Howlett KF, Starkie RL, Cameron Smith D, Kemp BE, Hargreaves M. Exercise increases nuclear AMPK α2 in human skeletal muscle. Diabetes 2003; 52:926-8.
79. Steinberg GR, Watt MJ, McGee SL, Chan S, Hargreaves M, Febbraio MA, Stapleton D, Kemp BE. Reduced glycogen availability is associated with increased AMPKα2 activity, nuclear AMPK α2 protein abundance, and GLUT4 mRNA expression in contracting human skeletal muscle. Appl Physiol Nutr Metab 2006; 31:302-12.
80. Leff, T. AMP-activated protein kinase regulates gene expression by direct phosphorylation of nuclear proteins. Biochemical Society 2003; 31:224-7.

©2008 Landes Bioscience. Do not distribute.

dc_840_14

Nutrient-dependent regulation of autophagy through the target of rapamycin pathway

Yu-Yun Chang, Gábor Juhász, Pankuri Goraksha-Hicks, Andrew M. Arsham, Daniel R. Mallin, Laura K. Muller and Thomas P. Neufeld[1]

Department of Genetics, Cell Biology, and Development, University of Minnesota, Minneapolis, MN 55455, U.S.A.

Abstract

In response to nutrient deficiency, eukaryotic cells activate macroautophagy, a degradative process in which proteins, organelles and cytoplasm are engulfed within unique vesicles called autophagosomes. Fusion of these vesicles with the endolysosomal compartment leads to breakdown of the sequestered material into amino acids and other simple molecules, which can be used as nutrient sources during periods of starvation. This process is driven by a group of autophagy-related (Atg) proteins, and is suppressed by TOR (target of rapamycin) signalling under favourable conditions. Several distinct kinase complexes have been implicated in autophagic signalling downstream of TOR. In yeast, TOR is known to control autophagosome formation in part through a multiprotein complex containing the serine/threonine protein kinase Atg1. Recent work in *Drosophila* and mammalian systems suggest that this complex and its regulation by TOR are conserved in higher eukaryotes, and that Atg1 has accrued additional functions including feedback regulation of TOR itself. TOR and Atg1 also control the activity of a second kinase complex containing Atg6/Beclin 1, Vps (vacuolar protein sorting) 15 and the class III PI3K (phosphoinositide 3-kinase) Vps34. During autophagy induction, Vps34 activity is mobilized from an early endosomal compartment to nascent autophagic membranes, in a TOR- and Atg1-responsive manner. Finally, the well-known TOR substrate S6K (p70 ribosomal protein S6 kinase) has been shown to play a positive role in autophagy, which may serve to limit levels of autophagy under conditions of continuously low TOR activity. Further insight into these TOR-dependent control mechanisms may support development of autophagy-based therapies for a number of pathological conditions.

Introduction

The TOR proteins were identified in 1991 by Hall and colleagues as direct targets of an antifungal rapamycin–FKBP (FK506-binding protein) complex, and were shown to be essential for progression through the G_1-phase of the cell cycle [1]. Subsequent studies have identified a wide range of additional TOR (target of rapamycin)-dependent cellular processes, including cap-dependent translation, transcription, nutrient transport, endocytosis, glycogen accumulation and autophagy [2,3]. Studies over the last 10 years have led to the concept of TOR complexes acting as a critical nodal point in a signalling network that regulates multiple cellular processes in response to nutrient conditions and several other inputs. A central challenge in this field is to understand the different roles each of these processes play in mediating TOR-dependent effects on cell growth, metabolism and aging. In addition, we are only beginning to understand how these different processes interact and the molecular mechanisms of their regulation.

The degradative process known as autophagy is closely linked to the role of TOR in nutrient sensing and uptake [4,5]. Under nutrient-poor conditions, decreased TOR activity results in removal of nutrient transporters from the cell surface, leading to a further decrease in available nutrients [6]. This loss of external nutrient supply is compensated for by increased production of nutrients from intracellular stores via autophagy. This catabolic process proceeds at a basal rate in nearly all eukaryotic cells, providing a self-renewal function that appears to be especially important in long-lived highly active cells such as neurons [7]. Nutrient, oxidative and energetic stresses result in a marked induction of autophagy in most cell types, and this plays a key role in cell survival under stressful conditions. The central role of TOR as an autophagy regulator in response to these diverse inputs has led to keen interest in the mechanisms by which TOR signalling suppresses autophagy. Recent studies in this area have identified a number of key downstream targets, and have revealed a surprising level of complexity involving both positive- and negative-feedback signalling.

Induction of autophagosome formation by Atg1 (autophagy-related gene) 1/Ulk1 (Unc51-like kinase 1) complexes

Genetic studies in yeast have identified approx. 30 *Atg* genes, which play essential roles in autophagy and autophagy-related processes such as pexophagy and cytoplasm-to-vacuole targeting of vacuolar hydrolases [8,9]. The products

Key words: autophagy-related gene 1/Unc51-like kinase 1 (Atg1/Ulk1), autophagy, cell growth, *Drosophila*, target of rapamycin (TOR), vacuolar protein sorting 34 (Vps34).

Abbreviations used: Atg, autophagy-related gene; ESCRT, endosomal sorting complex required for transport; PI3K, phosphoinositide 3-kinase; S6K, p70 ribosomal protein S6 kinase; TOR, target of rapamycin; Ulk1, Unc51-like kinase 1; Vps, vacuolar protein sorting.

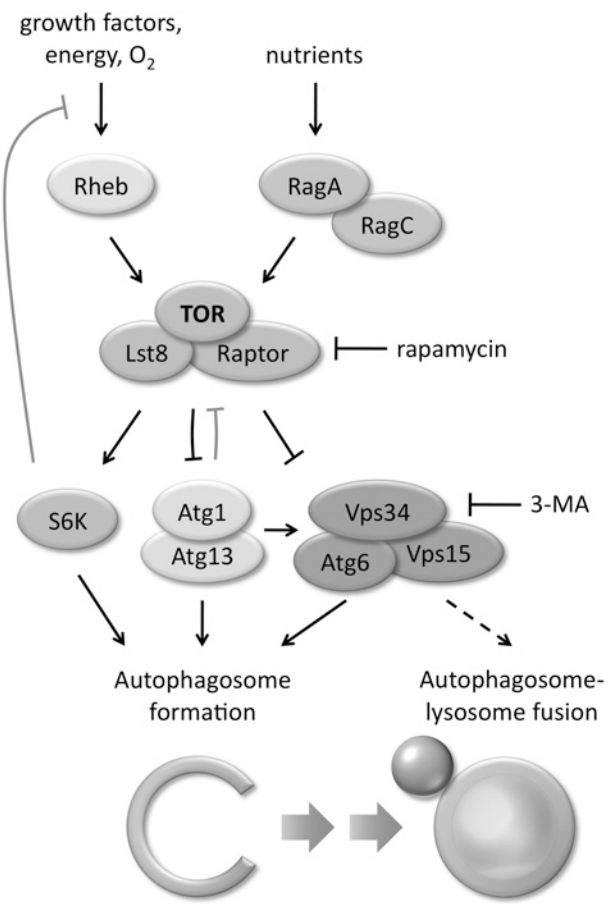
[1]**To whom correspondence should be addressed (email neufe003@umn.edu).**

©The Authors Journal compilation ©2009 Biochemical Society

dc_840_14

T1 **Figure 1 | The TOR pathway and autophagy regulation**

TOR complex 1, minimally comprising TOR, Lst8 and raptor (regulatory associated protein of TOR), regulates rapamycin-sensitive processes in response to upstream cues mediated by the Rheb and Rag family of small GTPases. TOR suppresses autophagy induction in part by inhibiting the activity of the serine/threonine protein kinase Atg1 and its partner Atg13, and by preventing recruitment of the class III PI3K Vps34 to autophagic membranes. Atg1 and Vps34 complexes are required for early steps of autophagosome nucleation and expansion. Vps34 also has an indirect role in subsequent vesicle fusion events (broken arrow), which is not rate-limiting for autophagy progression. Normal induction of autophagy also requires the serine/threonine protein kinase S6K, which is positively regulated through direct phosphorylation by TOR. Feedback signalling from S6K and Atg1 (grey arrows) result in self-limiting and amplifying effects respectively.



of these genes act at discrete steps in autophagosome formation. Among the earliest acting of the Atg components is a protein kinase complex consisting of Atg1, Atg13 and Atg17. Studies in *Saccharomyces cerevisiae* found that TOR-dependent phosphorylation of Atg13 prevents assembly of this complex under growth conditions [10–13]. Loss of TOR activity leads to dephosphorylation of Atg13, complex assembly and activation of Atg1 kinase activity. Interestingly, some Atg1 functions, such as recycling of certain Atg proteins, are independent of Atg1 kinase activity, implying an additional structural role for Atg1 [14,15].

Orthologues of Atg1 have also been shown be essential for autophagy induction in higher eukaryotes. Null mutations in the Drosophila *Atg1* gene cause a cell-autonomous defect in autophagosome formation in response to starvation, rapamycin treatment or developmental cues [16]. Similarly, dsRNA (double-stranded RNA)-mediated knockdown of the mammalian Atg1 orthologue Ulk1 (Unc51-like kinase 1) inhibits autophagy induction in human embryonic kidney cells [17]. Interestingly, autophagy is not disrupted in MEF (mouse embryonic fibroblast) cells harbouring a complete knockout of *Ulk1*, probably reflecting redundancy with the related *Ulk2* gene in some genetic backgrounds [18]. Expression of kinase-defective versions of Ulk1, Ulk2 or *Drosophila* Atg1 cause an autophagy block, presumably through a dominant-negative mechanism [16,17,19].

Given the conserved function of Atg1 orthologues, is the TOR-mediated regulation of these proteins conserved as well? Overexpression of *Drosophila* Atg1 leads to induction of autophagy in well-fed animals, indicating that high Atg1 levels can be sufficient to bypass TOR-dependent repressive signalling [20]. This function of Atg1 is inhibited by increased expression of Rheb or loss-of-function mutations in TSC2 (tuberous sclerosis 2), conditions that lead to TOR activation, consistent with the idea that TOR signalling suppresses Atg1 activity. Although characterization of Atg13 and Atg17 orthologues has not yet been reported, Mizushima and colleagues recently described the mammalian FAK (focal adhesion kinase)-interacting protein FIP200 as playing a role analogous to that of Atg17 [19]. This protein interacts with Ulk1 and promotes its stability and kinase activity. Atg13-related proteins have also recently been identified in metazoans [21], and we have found that the *Drosophila* orthologue is essential for autophagy induction downstream of TOR, and that it binds to and regulates the TOR-dependent phosphorylation and activity of Atg1 (Y.-Y. Chang and T.P. Neufeld, unpublished work). Thus the basic framework of signalling from TOR to Atg1 appears to have been largely retained from single to multicellular organisms, making this perhaps the most conserved output of TOR signalling identified to date.

Despite these similarities in signalling mechanisms, metazoan Atg1 proteins appear to have gained additional functions relative to their yeast counterparts. For example, overexpression of Atg1 has been shown to inhibit TOR signalling in *Drosophila* larvae, and disruption of Atg1 in *Drosophila* or mammalian cells leads to increased TOR activity, as measured by changes in S6K (p70 ribosomal protein S6 kinase) phosphorylation [20,22]. These effects of Atg1 are indicative of a self-reinforcing feedback loop between Atg1 and TOR, which may serve to amplify and stabilize initially small changes in nutrient signalling. To take another example, murine Ulk1 plays a role in neurite outgrowth through effects on Rab5-dependent endocytic trafficking [23]. Consistent with such an extra-autophagic function, *Drosophila Atg1* and *Atg13* mutant animals do not survive to adulthood, whereas fruitflies carrying mutations in other *Atg* genes that disrupt autophagy to a similar extent are viable [5,24]. Thus Atg1

©The Authors Journal compilation ©2009 Biochemical Society

dc_840_14

complexes may have adapted to provide increased regulation and other functions to meet the demands of multicellularity.

Vps (vacuolar protein sorting) 34: a PI3K (phosphoinositide 3-kinase) with multiple roles in autophagy

The class III PI3K Vps34 represents a second potential target for autophagy regulation by TOR. This kinase generates the monophosphorylated lipid PtdIns3*P*, which acts to recruit PX (Phox homology) and FYVE domain-containing proteins to membrane compartments [25,26]. The enzymatic activity of Vps34 is inhibited by the compound 3-methyladenine, a commonly used autophagy inhibitor. Vps34 potentially acts at a number of steps in autophagy. First, a complex comprising Vps34, Vps15, Atg6 and Atg14 in yeast (and Vp34, Vps15, the Atg6 orthologue Beclin1, the WD domain protein Ambra1 and the endophilin Bif-1 in mammals) is essential for an early nucleation step in autophagosome formation [4]. Secondly, a distinct Vps34 complex may function at a later step in the autophagy pathway in metazoan cells, in which autophagosomes must fuse with late endocytic vesicles to gain competency for lysosomal fusion [27]. Vps34 promotes the proper localization and assembly of components of the ESCRT (endosomal sorting complex required for transport), which acts in multivesicular endosome formation and is essential for autophagosome–lysosome fusion [28,29]. Thirdly, human Vps34 has been found to promote TOR activity in response to amino acid and calcium levels, which should lead to autophagy inhibition [30–32]. These conflicting roles of Vps34 suggest that distinct pools of Vps34 may be regulated in opposite ways by nutrients.

We recently addressed these potential Vps34 functions through genetic and biochemical studies in *Drosophila* [33]. Null mutations in *Vps34* were found to cause a strong block in starvation-induced autophagy in the larval fat body, resulting largely from a disruption of autophagosome biogenesis. In contrast, genetic disruption of the ESCRT leads to accumulation of autophagosomes, indicative of defective fusion. In cells doubly mutant for *Vps34* and ESCRT components, formation and fusion of autophagosomes are both deficient, resulting in their gradual accumulation under both fed and starved conditions. These and additional genetic results indicate the primary function of Vps34 in autophagy is early in autophagosome formation, probably in conjunction with Vps15 and Atg6/Beclin1, and that its endocytic functions are not rate-limiting for autophagy.

How is the activity of Vps34 linked to a cell's nutrient status to promote autophagy under appropriate conditions? In most cell types, Vps34 activity is concentrated at the early endocytic compartment. In *Drosophila* fat body cells, starvation causes a striking redistribution of PtdIns(3)*P* pools from Rab5-positive early endosomes to Atg8-positive nascent autophagosomes [33]. Interestingly, this starvation-induced shift in Vps34 activity requires both reduced TOR activity and wild-type Atg1 function, implicating Vps34 as a downstream target of TOR–Atg1 signalling.

In contrast with the case in cultured mammalian cells, *Vps34* mutants were found to have no effect on TOR activation *in vivo* in *Drosophila* [33]. Growth of *Drosophila Vps34* mutant cells is indistinguishable from that of wild-type, both in mitotic and endoreplicative tissues, and under both growth-promoting and -inhibitory conditions. Phosphorylation of the TOR-dependent site on dS6K (*Drosophila* S6K) is also unaffected by Vps34 activity. These results may point to fundamental differences in mechanisms of nutrient–TOR signalling between fruitflies and mammals, or may reflect differences in TOR activation in cultured cells compared with the case *in vivo*. Recent identification of Rag GTPases as transducers of nutrient signals to TOR in both *Drosophila* and mammalian systems indicates that this critical aspect of TOR activation is conserved [34,35].

S6K: putting on the brakes

Although autophagy is generally considered a beneficial process that promotes cell survival, high levels of autophagy are capable of causing cell death in some cases, e.g. in response to overexpression of Atg1 or activated Atg6/Beclin1. In *Drosophila*, starvation-induced autophagy peaks approx. 4 h after food withdrawal, and falls to a steady-state level that can be maintained for 2–3 weeks [16]. Similarly, Bax/Bak-deficient IL-3 (interleukin 3)-dependent cells can survive on intracellular nutrients generated through autophagy for several weeks [36]. What safeguards prevent autophagy from reaching harmful levels, while still allowing a sustained induction in response to starvation? Although the nutrients generated by autophagy potentially result in an intrinsic negative feedback, are there dedicated signalling mechanisms that function to keep this process in check even in the presence of inductive cues?

Findings from *Drosophila* and mammalian systems indicates that S6K may play such a role. Whereas S6K acts as positive mediator of TOR functions such as cell growth, its role in autophagy runs counter to that of the rest of the TOR pathway. Rather than inhibiting autophagy, S6K has been shown to be required for normal levels of starvation-induced autophagy. In *Drosophila*, S6K$^{-/-}$ fat body cells are deficient for autophagy induction in response to starvation or TOR mutation [16]. Similarly, simultaneous knockdown of mammalian S6K1 and S6K2 prevents autophagy induction [17]. One effect of this positive requirement for S6K is to limit the magnitude of autophagy in response to TOR down-regulation, due to the resulting down-regulation of S6K. In the *Drosophila* fat body, expression of activated S6K can increase the rate of autophagy in cells experiencing chronic TOR inactivation, but not in cells undergoing short-term starvation, indicating that S6K activity becomes limiting in the former case. By coupling a factor essential for autophagy to a negative regulator in this way, the chances of autophagy reaching damaging levels are reduced.

By what mechanisms does S6K promote autophagy? The requirement for S6K may simply reflect its role as a positive regulator of translation initiation, since protein synthesis is

©The Authors Journal compilation ©2009 Biochemical Society

dc_840_14

known to be required for normal expansion and maturation of autophagosomes [37,38]. Alternatively, S6K-dependent signalling to components of the Atg machinery or other signalling pathways may be required for a normal autophagic response. For example, S6K can negatively regulate insulin signalling through feedback phosphorylation of IRS1 (insulin receptor substrate 1) [39,40]. Induction of autophagy in response to TOR/S6K down-regulation may therefore be limited by a concomitant increase in insulin signalling, which inhibits autophagy induction. S6K may also participate directly in the regulation of more proximal autophagy regulators such as Atg1–Atg13 or Atg6–Vps34 complexes.

Perspectives and conclusions

Given the leading role TOR plays in autophagy regulation, and the important functions of autophagy in maintaining nutrient balance and cellular renewal, it is likely that autophagy makes a significant contribution to the physiological effects of TOR signalling. Indeed, the effects of rapamycin on cell growth and neurodegeneration have recently been shown to be partially dependent on autophagy [20,41]. Similarly, the beneficial effects of reduced TOR signalling on lifespan in *Caenorhabditis elegans* are prevented in autophagy mutants [42]. The identification of Atg6/Beclin1 as a haploinsufficient tumour-suppressor gene is also in keeping with autophagy contributing to the effects of TOR on cancer development and progression [43,44]. Although the ways in which autophagy influences these processes are poorly defined, these findings support the concept that autophagy represents a potential therapeutic target for a number of pathological conditions. In this regard, it may prove beneficial to develop treatments that directly modulate autophagy-related outputs of TOR signalling, while leaving other TOR outputs intact. Increased understanding of the signalling mechanisms underlying TOR-dependent autophagy regulation will aid in the development of such therapies. Q1

References

1 Heitman, J., Movva, N.R. and Hall, M.N. (1991) Targets for cell cycle arrest by the immunosuppressant rapamycin in yeast. Science **253**, 905–909
2 Arsham, A.M. and Neufeld, T.P. (2006) Thinking globally and acting locally with TOR. Curr. Opin. Cell Biol. **18**, 589–597
3 Wullschleger, S., Loewith, R. and Hall, M.N. (2006) TOR signaling in growth and metabolism. Cell **124**, 471–484
4 Pattingre, S., Espert, L., Biard-Piechaczyk, M. and Codogno, P. (2008) Regulation of macroautophagy by mTOR and Beclin 1 complexes. Biochimie **90**, 313–323
5 Melendez, A. and Neufeld, T.P. (2008) The cell biology of autophagy in metazoans: a developing story. Development **135**, 2347–2360
6 Edinger, A.L. (2007) Controlling cell growth and survival through regulated nutrient transporter expression. Biochem. J. **406**, 1–12
7 Mizushima, N., Levine, B., Cuervo, A.M. and Klionsky, D.J. (2008) Autophagy fights disease through cellular self-digestion. Nature **451**, 1069–1075
8 Xie, Z. and Klionsky, D.J. (2007) Autophagosome formation: core machinery and adaptations. Nat. Cell Biol. **9**, 1102–1109
9 Suzuki, K. and Ohsumi, Y. (2007) Molecular machinery of autophagosome formation in yeast, *Saccharomyces cerevisiae*. FEBS Lett. **581**, 2156–2161
10 Cheong, H., Yorimitsu, T., Reggiori, F., Legakis, J.E., Wang, C.W. and Klionsky, D.J. (2005) Atg17 regulates the magnitude of the autophagic response. Mol. Biol. Cell **16**, 3438–3453
11 Kabeya, Y., Kamada, Y., Baba, M., Takikawa, H., Sasaki, M. and Ohsumi, Y. (2005) Atg17 functions in cooperation with Atg1 and Atg13 in yeast autophagy. Mol. Biol. Cell **16**, 2544–2553
12 Kamada, Y., Funakoshi, T., Shintani, T., Nagano, K., Ohsumi, M. and Ohsumi, Y. (2000) Tor-mediated induction of autophagy via an Apg1 protein kinase complex. J. Cell Biol. **150**, 1507–1513
13 Scott, S.V., Nice, 3rd, D.C., Nau, J.J., Weisman, L.S., Kamada, Y., Keizer-Gunnink, I., Funakoshi, T., Veenhuis, M., Ohsumi, Y. and Klionsky, D.J. (2000) Apg13p and Vac8p are part of a complex of phosphoproteins that are required for cytoplasm to vacuole targeting. J. Biol. Chem. **275**, 25840–25849
14 Cheong, H., Nair, U., Geng, J. and Klionsky, D.J. (2008) The Atg1 kinase complex is involved in the regulation of protein recruitment to initiate sequestering vesicle formation for nonspecific autophagy in *Saccharomyces cerevisiae*. Mol. Biol. Cell **19**, 668–681
15 Reggiori, F., Tucker, K.A., Stromhaug, P.E. and Klionsky, D.J. (2004) The Atg1–Atg13 complex regulates Atg9 and Atg23 retrieval transport from the pre-autophagosomal structure. Dev. Cell **6**, 79–90
16 Scott, R.C., Schuldiner, O. and Neufeld, T.P. (2004) Role and regulation of starvation-induced autophagy in the *Drosophila* fat body. Dev. Cell **7**, 167–178
17 Chan, E.Y., Kir, S. and Tooze, S.A. (2007) siRNA screening of the kinome identifies ULK1 as a multidomain modulator of autophagy. J. Biol. Chem. **282**, 25464–25474
18 Kundu, M., Lindsten, T., Yang, C.Y., Wu, J., Zhao, F., Zhang, J., Selak, M.A., Ney, P.A. and Thompson, C.B. (2008) Ulk1 plays a critical role in the autophagic clearance of mitochondria and ribosomes during reticulocyte maturation. Blood **112**, 1493–1502
19 Hara, T., Takamura, A., Kishi, C., Iemura, S., Natsume, T., Guan, J.L. and Mizushima, N. (2008) FIP200, a ULK-interacting protein, is required for autophagosome formation in mammalian cells. J. Cell Biol. **181**, 497–510
20 Scott, R.C., Juhasz, G. and Neufeld, T.P. (2007) Direct induction of autophagy by Atg1 inhibits cell growth and induces apoptotic cell death. Curr. Biol. **17**, 1–11
21 Meijer, W.H., van der Klei, I.J., Veenhuis, M. and Kiel, J.A. (2007) ATG genes involved in non-selective autophagy are conserved from yeast to man, but the selective Cvt and pexophagy pathways also require organism-specific genes. Autophagy **3**, 106–116
22 Lee, S.B., Kim, S., Lee, J., Park, J., Lee, G., Kim, Y., Kim, J.M. and Chung, J. (2007) ATG1, an autophagy regulator, inhibits cell growth by negatively regulating S6 kinase. EMBO Rep. **8**, 360–365
23 Tomoda, T., Kim, J.H., Zhan, C. and Hatten, M.E. (2004) Role of Unc51.1 and its binding partners in CNS axon outgrowth. Genes Dev. **18**, 541–558
24 Juhász, G., Erdi, B., Sass, M. and Neufeld, T.P. (2007) Atg7-dependent autophagy promotes neuronal health, stress tolerance, and longevity but is dispensable for metamorphosis in *Drosophila*. Genes Dev. **21**, 3061–3066
25 Lindmo, K. and Stenmark, H. (2006) Regulation of membrane traffic by phosphoinositide 3-kinases. J. Cell Sci. **119**, 605–614
26 Backer, J.M. (2008) The regulation and function of Class III PI3Ks: novel roles for Vps34. Biochem. J. **410**, 1–17
27 Eskelinen, E.L. (2005) Maturation of autophagic vacuoles in mammalian cells. Autophagy **1**, 1–10
28 Rusten, T.E. and Simonsen, A. (2008) ESCRT functions in autophagy and associated disease. Cell Cycle **7**, 1166–1172
29 Futter, C.E., Collinson, L.M., Backer, J.M. and Hopkins, C.R. (2001) Human VPS34 is required for internal vesicle formation within multivesicular endosomes. J. Cell Biol. **155**, 1251–1264
30 Gulati, P., Gaspers, L.D., Dann, S.G., Joaquin, M., Nobukuni, T., Natt, F., Kozma, S.C., Thomas, A.P. and Thomas, G. (2008) Amino acids activate mTOR complex 1 via Ca^{2+}/CaM signaling to hVps34. Cell Metab. **7**, 456–465
31 Byfield, M.P., Murray, J.T. and Backer, J.M. (2005) hVps34 is a nutrient-regulated lipid kinase required for activation of p70 S6 kinase. J. Biol. Chem. **280**, 33076–33082
32 Nobukuni, T., Joaquin, M., Roccio, M., Dann, S.G., Kim, S.Y., Gulati, P., Byfield, M.P., Backer, J.M., Natt, F., Bos, J.L. et al. (2005) Amino acids mediate mTOR/raptor signaling through activation of class 3 phosphatidylinositol 3OH-kinase. Proc. Natl. Acad. Sci. U.S.A. **102**, 14238–14243
33 Juhász, G., Hill, J.H., Yang, Y., Sass, M., Baehrecke, E.H., Backer, J.M. and Neufeld, T.P. (2008) The class III PI(3)K Vps34 promotes autophagy and endocytosis but not TOR signaling in *Drosophila*. J. Cell Biol. **181**, 655–666

©The Authors Journal compilation ©2009 Biochemical Society

dc_840_14

34 Kim, E., Goraksha-Hicks, P., Li, L., Neufeld, T.P. and Guan, K.L. (2008) Regulation of TORC1 by Rag GTPases in nutrient response. Nat. Cell Biol. **10**, 935–945
35 Sancak, Y., Peterson, T.R., Shaul, Y.D., Lindquist, R.A., Thoreen, C.C., Bar-Peled, L. and Sabatini, D.M. (2008) The Rag GTPases bind raptor and mediate amino acid signaling to mTORC1. Science **320**, 1496–1501
36 Lum, J.J., Bauer, D.E., Kong, M., Harris, M.H., Li, C., Lindsten, T. and Thompson, C.B. (2005) Growth factor regulation of autophagy and cell survival in the absence of apoptosis. Cell **120**, 237–248
37 Lawrence, B.P. and Brown, W.J. (1993) Inhibition of protein synthesis separates autophagic sequestration from the delivery of lysosomal enzymes. J. Cell Sci. **105**, 473–480
38 Abeliovich, H., Dunn, Jr, W.A., Kim, J. and Klionsky, D.J. (2000) Dissection of autophagosome biogenesis into distinct nucleation and expansion steps. J. Cell Biol. **151**, 1025–1034
39 Harrington, L.S., Findlay, G.M., Gray, A., Tolkacheva, T., Wigfield, S., Rebholz, H., Barnett, J., Leslie, N.R., Cheng, S., Shepherd, P.R. et al. (2004) The TSC1–2 tumor suppressor controls insulin–PI3K signaling via regulation of IRS proteins. J. Cell Biol. **166**, 213–223
40 Shah, O.J., Wang, Z. and Hunter, T. (2004) Inappropriate activation of the TSC/Rheb/mTOR/S6K cassette induces IRS1/2 depletion, insulin resistance, and cell survival deficiencies. Curr. Biol. **14**, 1650–1656
41 Rubinsztein, D.C. (2006) The roles of intracellular protein-degradation pathways in neurodegeneration. Nature **443**, 780–786
42 Hansen, M., Chandra, A., Mitic, L.L., Onken, B., Driscoll, M. and Kenyon, C. (2008) A role for autophagy genes in the extension of lifespan by dietary restriction in *C. elegans*. PLoS Genet. **4**, e24
43 Qu, X., Yu, J., Bhagat, G., Furuya, N., Hibshoosh, H., Troxel, A., Rosen, J., Eskelinen, E.L., Mizushima, N., Ohsumi, Y. et al. (2003) Promotion of tumorigenesis by heterozygous disruption of the beclin 1 autophagy gene. J. Clin. Invest. **112**, 1809–1820
44 Yue, Z., Jin, S., Yang, C., Levine, A.J. and Heintz, N. (2003) Beclin 1, an autophagy gene essential for early embryonic development, is a haploinsufficient tumor suppressor. Proc. Natl. Acad. Sci. U.S.A. **100**, 15077–15082

Received 30 September 2008
doi:10.1042/BST037xxxx

©The Authors Journal compilation ©2009 Biochemical Society

[Autophagy 5:5, 1-13; 1 July 2009]; ©2009 Landes Bioscience dc_840_14

Research Paper

A novel role for the Drosophila epsin (lqf)

Involvement in autophagy

György Csikós,[1] Mónika Lippai,[1] Tamás Lukácsovich,[2] Gábor Juhász,[1] László Henn,[3] Miklós Erdélyi,[3] Péter Maróy[4] and Miklós Sass[1,*]

[1]Department of Anatomy; Cell and Developmental Biology; Eötvös Lóránd University; Budapest, Hungary; [2]Department of Developmental and Cell Biology; Developmental Biology Center; University of California Irvine; Irvine, CA USA; [3]Institute of Genetics; Biological Research Center of the Hungarian Academy of Science; Szeged, Hungary; [4]Department of Genetics; University of Szeged; Szeged, Hungary

Key words: liquid facets, endocytosis, autophagy, RNAi, immunolocalization

This manuscript has been published online, prior to printing. Once the issue is complete and page numbers have been assigned, the citation will change accordingly.

Screening P-element-induced mutant collections, 52 lines were selected as potentially defected ones in endocytosis or autophagy. After excluding those which were rescued by 20-hydroxyecdysone treatment, the exact position of the inserted P-element was determined in the remaining lines. In the case of *l(3)S011027* stock, that *liquid facets (lqf)* gene was affected which codes an epsin-homolog protein in Drosophila. We reveal that Lqf is essential to the receptor-mediated endocytosis of larval serum proteins (LSPs) in the larval fat body cells of Drosophila. In *l(3)S011027* line, lack of Lqf fails the formation of autophagosomes thus leading to the arrest of destroying of trophocytes. Transgenic larvae carrying Lqf-RNAi construct were unable to generate endocytic and autophagic vacuoles and led to a prolonged larval stage. On the other hand, Lqf protein showed an exclusive colocalization with the LysoTracker Red- or GFP-Atg8a labeled autophagosomes. By using the antiserum generated against the fifth exon of *lqf,* we demonstrated that prior to the onset of developmental autophagy the Lqf protein was present in the nucleus of fat body cell, but thereafter the protein was localized in the territory of endocytic and autophagic vacuoles. The fact that the inhibition of the target of rapamycin (TOR) did not restore the autophagic process and the normal development in the case of *lqf* mutant larvae points to that the Lqf is downstream to the TOR, the central kinase of the autophagy pathway.

Introduction

Autophagy is a basic cell biological process of self-digestion in eukaryotic cells that maintains homeostasis by cleaning up and recycling long-lived or damaged proteins and cellular organelles.[1] When the cells are challenged by different stress conditions such as hypoxia, cold or heat stress or starvation, autophagy provides monomers and energy for the survival of a cell or organism. Interestingly, autophagy also has been linked to programmed cell death, especially during postembryonal development of metamorphosing animals, which initiates a controversial discussion on how a suggested role of autophagy in cell suicide might meet with its survival function.[2-9]

Based on the mechanism of how cytoplasmic material is delivered to the lysosomal compartment, three types of autophagy have been established: chaperone-mediated autophagy, macroautophagy and microautophagy. During the course of the major pathway, macroautophagy (herein subsequently referred to as "autophagy"), part of the cytoplasm potentially including entire organelles is sequestered into double-membraned vesicles called autophagosomes, that subsequently fuse with lysosomes, thereby generating single-membraned autolysosomes in which degradation of the sequestered material takes place.[10-12]

The autophagic machinery is evolutionarily conserved from yeast to mammals including the genes and their products that control and/or execute it.[11,13,14] One of the central regulators of autophagy is the target of rapamycin (TOR) kinase, which inhibits autophagy under basal or nutrient-rich conditions.[15,16] TOR activity is stimulated by insulin-responsive phosphatidylinositol-3 kinase (PI3K)/Akt signaling, or by nutrients such as amino acids, and by high cellular energy levels.[17,18]

Downstream of TOR kinase, there are more than two dozen genes in yeast (known as the *Atg* genes) encoding proteins that are essential for the main steps of autophagy: initiation, vesicle formation (nucleation, expansion, completion, targeting, docking, fusion) and breakdown.[8,11,19]

Autophagy is an integral and essential part of insect metamorphosis. The forming of autophagosomes and autolysosomes in large numbers in larval tissues including the larval fat body is both temporally and spatially controlled in a precise way. The initiation of developmental autophagy is under exact hormonal regulation. 20-hydroxyecdysone (moulting hormone, 20-HE) not only triggers moultings in the course of postembryonic development but also stimulates autophagic activity in the larval tissues both in vivo and in vitro, while juvenile hormone inhibits it.[22-25] The increasing

*Correspondence to: Miklós Sass; Department of Anatomy; Cell and Developmental Biology; Eötvös Lóránd University; Budapest, Hungary; Email: msass@elte.hu

Submitted: 09/23/08; Revised: 02/12/09; Accepted: 02/16/09

Previously published online as an *Autophagy* E-publication:
http://www.landesbioscience.com/journals/autophagy/article/8168

©2009 LANDES BIOSCIENCE. DO NOT DISTRIBUTE.

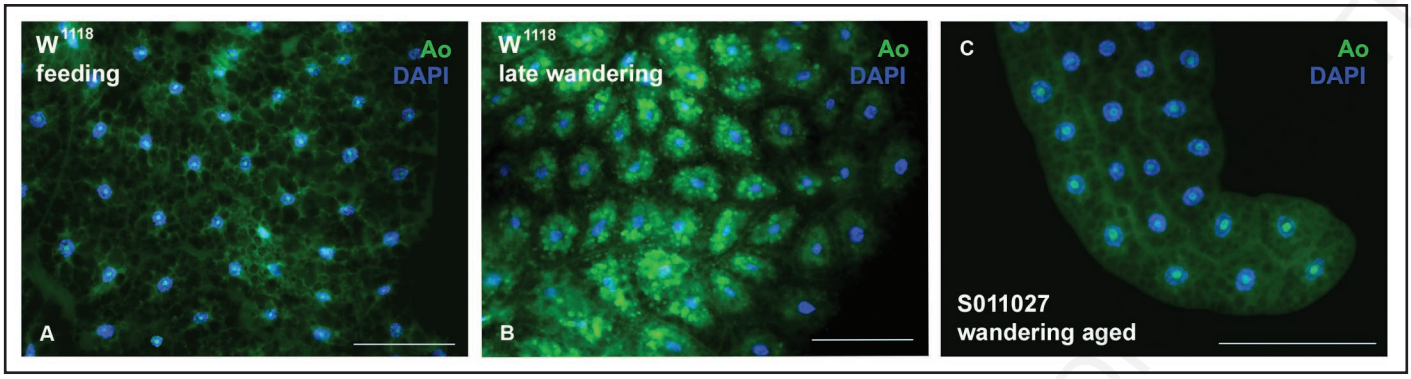


Figure 1. Acridine orange stained the whole mount fat body lobes of the feeding Oregon R larvae at 96–100 h AEL, (A) the late wandering Oregon R larvae at 114–120 h AEL, (B) and the wandering-aged homozygous l(3)S011027 larvae (C). Bars equal 100 μm. (A) The contours of the cells as well as the homogenous pale greenish colored cytoplasm can clearly be seen among the lipid droplets, although the granules have not appeared in it yet. The acridine orange only stained those particular nucleoli which occupied the central part of nuclei. (B) A strong granulation traces the accumulation of autophagic vacuoles, multivesicular bodies and protein granules in the trophocytes. (C) No granules can be observed in the cytoplasm of wandering-aged homozygous l(3)S011027 larvae.

titer of 20-HE stimulates the formation of autophagosomes and also the synthesis and activity of the lysosomal enzymes in larval tissues at the start of metamorphosis.[26] This hormone-induced developmental autophagy can be inhibited at both transcriptional and translational levels.[27]

The 20-hydroxyecdysone-receptor complex activates the immediate early genes that encode transcription factors, which then stimulate the expression of late genes responsible for the regulation of all metamorphotic changes including autophagy.[28-31] Genetic interaction studies revealed that ecdysone signaling downregulates the PI3K/Akt signaling pathway, forming a link between the hormonal induction of autophagy and the known regulatory function of the PI(3)K-AKT/PKB-TSC1/TSC2-Rheb-TOR signaling pathway in vivo.[25,31]

We conducted a forward genetic screen to isolate and identify genes regulating autophagy in the larval fat body cells of *Drosophila melanogaster*. Two P-element induced mutant collections were tested at first by light and electron miscroscopical methods for the lack of their ability to form autophagic structures.[32,33] One of the 21 identified loss-of-function mutations inhibiting the autophagic process was the *liquid facets (lqf),* a gene, which encodes the Drosophila homolog of vertebrate epsin.[34-36] *lqf*^{S011027} homozygous larvae could not activate autophagy or endocytosis prior to metamorphosis when these cell-biological processes are stimulated physiologically.

Using a combination of various genetic and molecular biology methods, we present our data to prove that the lqf is one of the candidate proteins which have essential roles in the regulation and molecular mechanisms of both endocytosis and autophagy in Drosophila.

Results

Identification of potential autophagy genes in P-element-induced mutant collections. As has been recently published, about 400 lines exhibiting late larval or early pupal lethal phenotype had been screened for aberration in the formation of protein granules in the fat body characteristic prior to metamorphosis.[37] The test included acridine orange and LysoTracker staining of the fat body dissected from wandering larvae. Fifty-two lines were identified exhibiting gross difference in either the formation of granules or in the number or the size, or the distribution of granules as compared to the wild-type situation. These observations were also verified at the ultrastructural level. To narrow the phenotype, if it is indeed not the result of arrested hormone-dependent development, homozygous mutant larvae were challenged with 20-HE. Those 43 mutant lines that were not able to form granules after the hormonal administration were studied further. As is well known, a good proportion of mutations induced by transposase activity carry background mutations as well. To identify if the fat body phenotype is indeed related to the P-element insertion, the lines were crossed to deletions uncovering the site of the transposone insertion. Formation of the granules was inhibited in 32 lines after crossing them with appropriate deletions. In most lines the P-element insertion was remobilized by transposase activity and tested if in the resulted white revertant larvae both the viability and the normal fat body pattern is restored. In this test the original, wild phenotype was restored in case of 21 lines. In the present paper we describe detailed results on the *l(3)S011027* line which represents one of these 21 hits.

Morphology of the larval fat body cells. Structural changes of control fat body cells during the last larval period. In wild-type (Oregon) animals, during the feeding period (72–104 h AEL) of the last larval stage huge lipid droplets gradually formed in the large, isodiametric fat body cells (trophocytes). The nuclei were located generally in the central part of cells. The functioning organelles were concentrated mainly around the nuclei and between the lipid droplets. In this developmental phase, there were no acidic acridine orange, neutral red and/or LysoTracker Red positive granules present in the trophocytes (Figs. 1A and 2A).

At the ultrastructural level, the cytoplasm of the fat body cells contained large lipid droplets and glycogen areas. The structure of the nuclei, mitochondria, RER and Golgi areas was normal. Occasionally some small multivesicular bodies could be seen (Fig. 4A).

©2009 LANDES BIOSCIENCE. DO NOT DISTRIBUTE.

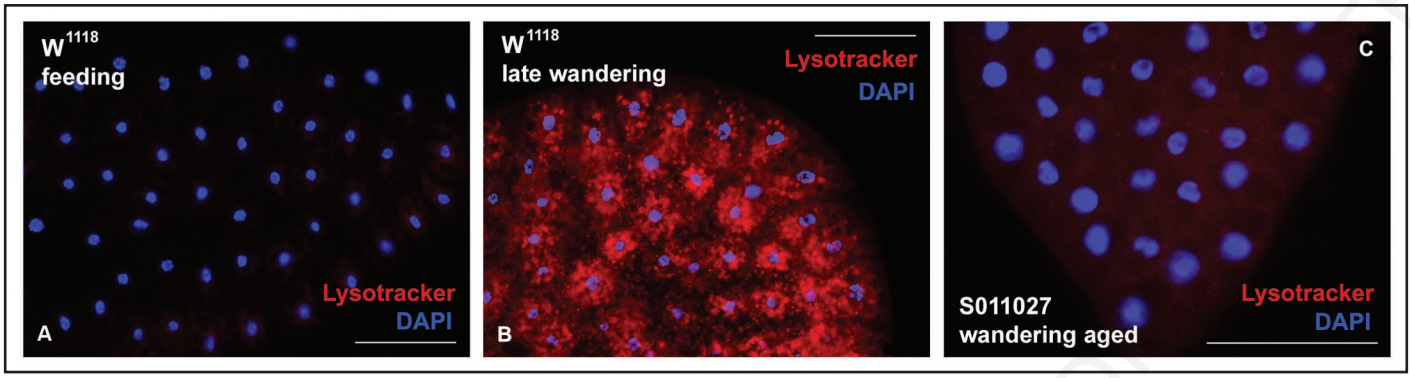


Figure 2. The LysoTracker Red stained fat body lobes of the feeding Oregon R larvae at 96–100 h AEL, (A); late wandering Oregon R larvae at 114–120 h AEL, (B) and wandering-aged homozygous l(3)S011027 larva (C). Bars equal 100 μm. (A) At this developmental stage, a very weak LysoTracker Red accumulation can be observed around the nuclei of the trophocytes. (B) At the time of wandering, a large amount of granules showing the LysoTracker Red positivity were accumulated in the wild-type fat body cells. (C) Very few small granules can be observed in the cytoplasm of the trophocytes of wandering-aged homozygous l(3)S011027 larvae. The size of the fat body cells of the mutant larvae was approximately similar to that of the adequate aged wild type larvae.

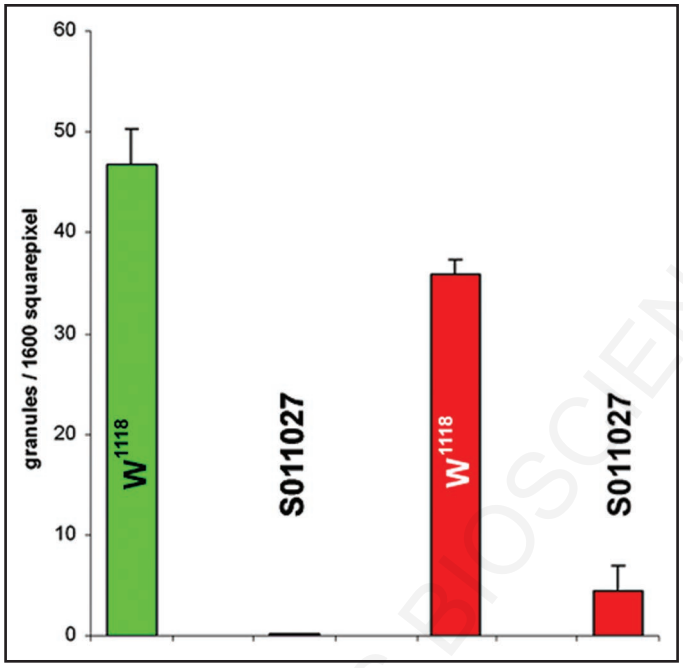


Figure 3. Relative quantity of the acridine orange-(green columns) and LysoTracke Red-positive (red columns) granules in the fat body cells of wild type and l(3)S011027 wandering larvae.

During the wandering period (approx. 110–120 h AEL), the formation of a mass of acridine orange, neutral red and LysoTracker Red positive granules could be observed. Approaching the time of pupariation, the number and size of these granules continuously grew and finally they became the dominant organelles of fat body cells (Figs. 1B and 2B).

At the ultrastructural level, large autolysosomes, protein storage granules and multivesicular bodies appeared and accumulated in the cytoplasm. The formation of autolysosomes seemed to be continuous in this period, since newly formed autophagosomes were also visible at the same time in the cells. Sometimes the fusion of autophagic and endocytotic vacuoles could be also observed. Before pupation, the functioning rought endoplasmic reticule (RER) areas and mitochondria were present only in the narrow, perinuclear part of the cytoplasm (Fig. 4B).

Structural changes of fat body cells of l(3)S011027 mutant larvae. The development of heterozygous *l(3)S011027*/+ larvae showed practically no differences compared to that of wild-type (Oregon) animals. The accumulation of acridine orange stained granules was clearly observed just prior to the pupariation in the trophocytes of *l(3)S011027*/+ larvae. (Data not shown).

There was no difference between the diameter of the trophocytes or their nucleus size between the homozygous mutant and age-matched wild-type larvae. In spite of these similarities the fat body of *l(3)S011027*/*S011027* larvae could not form any acridine orange or neutral red positive granules that correspond to the autophagic and/or endocytotic (heterophagic) vacuoles (Fig. 1C).

Using LysoTracker Red, lots of granules could be stained in the fat body cells of the *l(3)S011027*/+ heterozygous larvae (Data not shown). In the trophocytes of *l(3)S011027* homozygous mutant larvae only a few small LysoTracker Red positive granules (probably lysosomes) could be observed (Fig. 2C). Quantified data of light microscopic observations can be seen in Figure 3.

Our electron microscopic observations revealed that the fat body cells of *L(3)S011027* larvae were essentially unable to form large autophagosomes and autolysosomes. In spite of this, small lysosomes and autophagosomes could be observed in the cytoplasm of the trophocytes. Moreover, the multivesicular bodies and protein storage granules were also absent from the fat body cells of the mutant animals during the wandering period. Some other ultrastructural changes were also observed, potentially due to the mutation. The size of the lipid droplets and glycogen areas were smaller than in control animals and the RER was often fragmented into vesicles. The outer membrane of the mitochondria was thicker and more electron dense than those of the controls (Fig. 4C). The relative quantity of autophagosomes, autophag vacuoles, lysosomes and protein granules in the trophocytes of wild-type and *l(3)S011027* wandering larvae was presented in Figure 5.

©2009 LANDES BIOSCIENCE. DO NOT DISTRIBUTE.

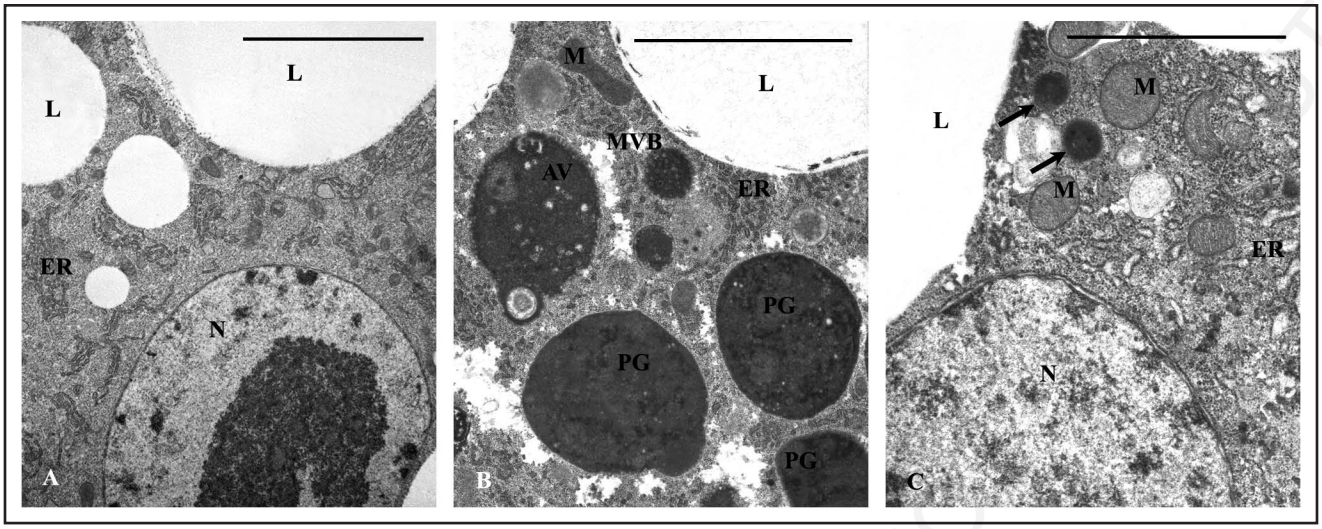


Figure 4. (A) The common organelles could be observed in the cytoplasm located around the nucleus of the trophocytes of Oregon R feeding larva at the electronmicroscopic level. Bar equals 5 μm. (B) By the time when the wild type larvae reach the late wandering stage, numerous autophagic vacuoles (AV), multivesicular bodies (MVB) and protein granules (PG) have already been accumulated in their trophocytes. Bar equals 10 μm. (C) Apart from some small autophagosomes (arrows), no sign of either endocytosis or autophagy can be detected in the electron micrographs of the fat body cells of homozygous l(3)S011027 wandering-aged larvae. Moreover, the multivesicular bodies and protein storage granules were also absent from the trophocytes. The endoplasmic reticulum (ER), however, was often fragmented into vesicles and the size of the lipid droplets (L) and glycogen areas became smaller. Bar equals 10 μm. Further abbreviations: nucleus (N), mitochondria (M).

20-HE treatment. As 20-HE is known to stimulate both autophagy and endocytosis in the course of normal development, it was necessary to verify that 20-HE signaling is properly working in *l(3)S011027* mutants. In the case of wild-type feeding larvae, a 4-hour 20-HE treatment was sufficient to induce autophagy. For the feeding *l(3)S011027* homozygous larvae, however, the 8-hours-long 20-HE treatment happened to be insufficient to elicit the formation of acridine orange-positive granules in their fat body cells. The same treatment however, resulted in a slight increase in the number of LysoTracker Red-positive granules (Fig. 6A and B).

***l(3)S011027* mutant flies carry a P-element insertion in the liquid facets (*lqf*) gene.** We performed inverse PCR on *l(3)S011027* genomic DNA to obtain a sequence tag that would precisely localize the insertion site of the P-element. We determined that the P-element is inserted at the 5' end of the *liquid facets* gene (*lqf*, CG8532, FBgn0028582). The exact site of the insertion is 32 bp downstream of the transcription start site of the *lqf* RC, RB, RE and RF transcripts. Therefore, all of these messages may be affected by this P-element insertion. The other two shorter transcripts reported on Flybase, lqf RA and RD are presumably also affected by the insertion.

Complementation test and heteroallelic combination. The P-element was localized by in situ hybridization to cytological position 66A4-66A5 on the left arm of the third chromosome. In order to test whether the fat body phenotype is really associated with the P-element insertion into the *lqf* gene, the *l(3)S011027* line was crossed with a deletion overlapping the insertion site. As expected, it failed to complement the deletion pbl-X1(65F, 66B), thus the *l(3)S011027* line had a lethal mutation within the break points of the deletion, which corresponded to the location of the P-element insertion.

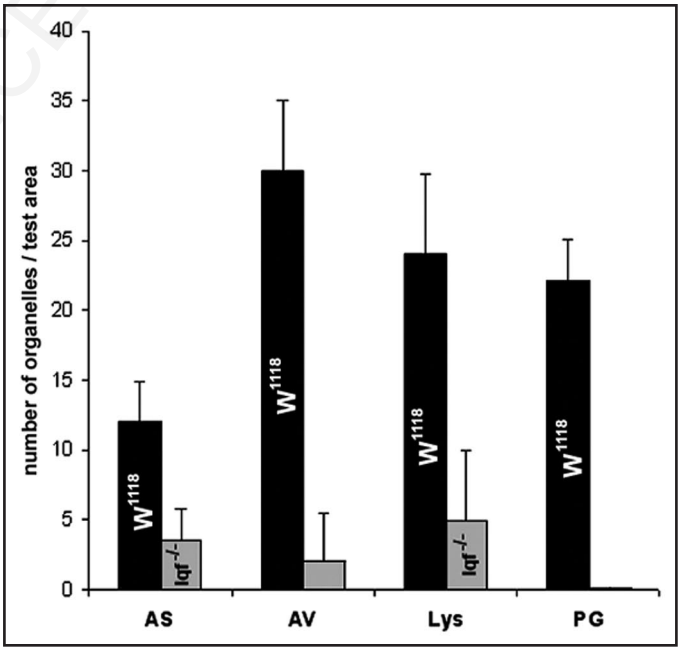


Figure 5. Relative quantity of autophagosomes, autophagy vacuoles, lysosomes and protein granules in the trophocytes of wild-type and l(3) S011027 wandering larvae.

To test that the observed phenotype was caused by a background mutation or not the viable *l(3)S011027/TM6b,* flies were crossed with either lqf^{ARI}/*TM6b* or lqf^{L71}/*TM6b* lines. The number of the homozygous larvae was less than 2% and all of them died before the onset of pupariation. Puparium formation occurred only in heterozygous animals. These results show that the observed

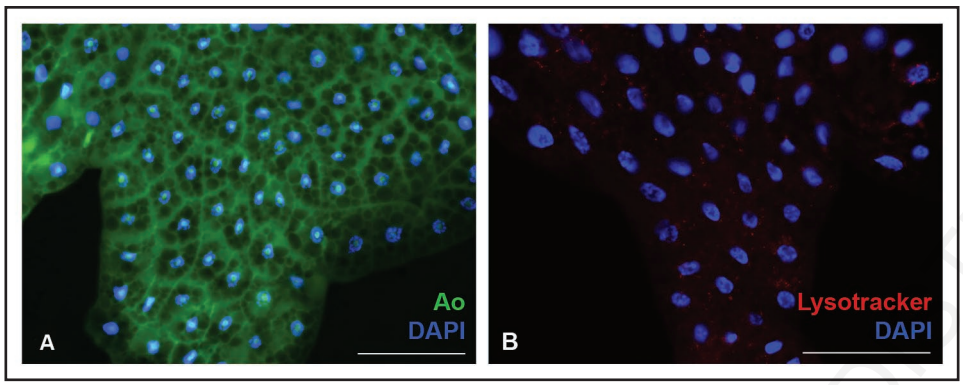


Figure 6. The treatment of homozygous l(3)S011027 wandering-aged larvae with 20-HE could not provoke the appearance of acridine orange-positive granules in their fat body cells (A). At the same time, however, the number of the LysoTracker Red-positive granules was slightly increased (B). Bar equals 100 μm.

Table 1 **The result of heteroallelic combination**

	Wild-type pupae	Tubby pupae
lqf^{ARI}/TM6b x S011027/TM6b	0	214
lqf^{L71}/TM6b x S011027/TM6b	0	131

phenotype was caused exclusively by the mutation of *lqf* gene (Table 1).

Analysis of mitotic clones. A line was created by crossing *hsFlp; cgGal4, UAS-GFP, FRT80B* virgins with lqf^{L71}*FRT80B/TM6b* males in which mitotic recombination was generated by a short heat shock during the embryonic development. The lqf^{L71} homozygous clones were unable to express GFP, whereas the flanking cells contained this fluorescent protein. The four-hour-long withdrawing of amino acids resulted strong accumulation of LysoTracker-positive granules in the trophocytes of 95–100 h AEL larvae, which have lqf^{71}/+ or +/+ genotype. At the same time no Lysotracker-positive granules were detected in the lqf^{L71} homozygous clones of fat body cells of the larvae aged 95–100 h AEL (Fig. 7).

Changes of the lqf transcript in mutant and transgenic lines. Experiments using the RT-PCR method were performed to test whether the *lqf* transcript is present in the $lqf^{S011027}$ larvae, and also to answer the question of whether the transcription level of the *lqf* gene was changed in w^{1118} larvae during the last larval instar (72–126 h AEL). A very small amount of *lqf* transcript was present in $lqf^{S011027}$ larvae at 115–120 h AEL, as compared to the wild-type control. This is, however, not surprising, because the mutations induced by the P-element insertion are frequently hypomorphic (Fig. 8A).

The aim of the second series of experiments was to reveal whether the *lqf* gene may contribute to the regulation of developmental autophagy, based on its expression pattern. It was clearly demonstrated that transcription of the *lqf* gene increased dramatically before the start of autophagy at 100–105 h AEL (Fig. 8B).

An increase of the *lqf* mRNA level could be also triggered by a 3-hour starvation in feeding wild-type larvae at 75–80 h AEL (Fig. 8C). In homozygous $lqf^{S011027}$ larvae, however, starvation failed to induce increased transcription of this gene (Data not shown).

lqf RNA interference in the larval fat body. Four transgenic lines carrying UAS-lqfIR (lqf^{6}, lqf^{7}, lqf^{10}, lqf^{12}) were generated in order to prove that the arrest of autophagy and endocytosis in $lqf^{S011027}$ larvae was caused by the insufficient expression of the *lqf* gene. In order to stimulate efficient RNA silencing, the UAS-lqfIR lines were crossed with *DCR2; hsGal4* transgenic line. The induction of RNAi against the *lqf* gene in early L2 larvae by shifting the animals from 18°C to 32°C for three days resulted in the absence of acridine orange-positive (Fig. 9A) or LysoTracker-positive (Fig. 10A) granules in wandering animals in all transgenic lines. This treatment led to a prolonged larval stage in case of animals that carry the UAS-lqfIR construct and resulted in the failure of metamorphosis. Without the heat treatment, the acridine orange-positive (Fig. 9B) and LysoTracker-positive (Fig. 10B) granules appeared in the trophocytes of these larvae and their development was unaffected.

Characterization of anti-Lqf antiserum on larval fat body samples. Lqf-antiserum was raised against a peptide corresponding to the fifth exon of the *lqf* gene encoding the Epsin N-terminal homology (ENTH) domain of the protein. Western blots performed with the anti-Lqf (fifth exon) antiserum cross-reacted only with a ~95 kDa protein in wild-type larvae at late third stage and in the prepupa. The size of the positive signal may be corresponding to a 824 or 831 amino acid protein, that can be translated from any of the putative transcripts of Lqf-RB, -RC, -RE and -RF or Lqf-RA/RD. On the other hand, expression of the 95 kDa Lqf protein was undetectable in homozygous $lqf^{S011027}$ L3 larvae (Fig. 11). In larvae in which the *lqf* RNA silencing was induced, the quantity of 95 kDa Lqf protein decreased with respect to the no heat-shocked controls or transgenic driver line (Fig. 12).

Localization of the Lqf protein in the larval fat body. In the larval fat body of wild-type feeding larvae, the Lqf protein showed a characteristic accumulation in the nuclear periphery of trophocytes, but no other compartments were labeled when 4% of paraformaldehide was used as fixative for 2 hours (Fig. 13A–C).

© Landes Bioscience. Do not distribute.

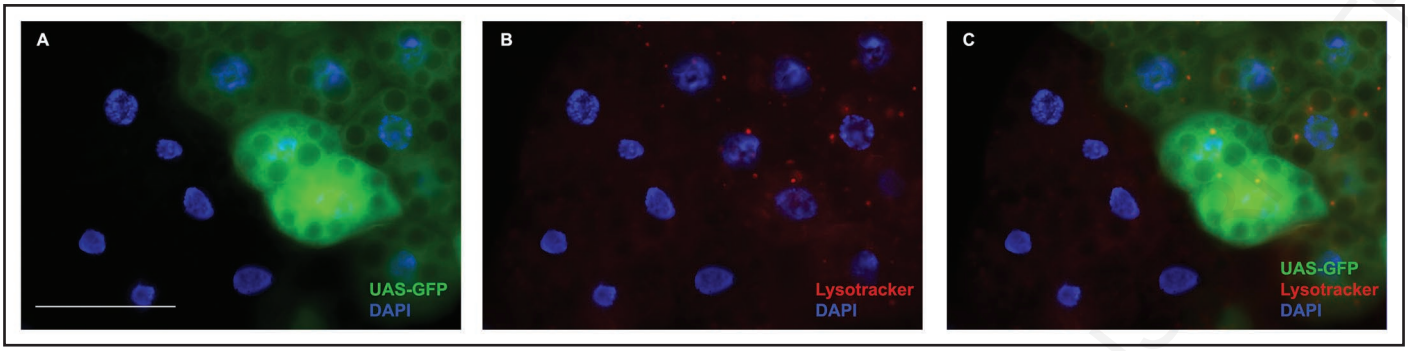


Figure 7. The four-hour-long starving led to the appearance of LysoTracker Red positive granules (B and C) in the GFP-expressing heterozygous (pale green) and the wild-type (strong green) fat body cells (A and C). However, there is no trace of the LysoTracker Red positive granules in the dark GFP negative lqf $^{-/-}$ clones of the trophocytes (A–C). Bar equal 100 μm.

At the beginning of the wandering stage, some newly formed Lqf-positive granules appeared in the cytoplasm of the fat body cells while the nuclei staining remained unchanged (Fig. 14A–C). Just before the prepupal stage, the localization pattern changed markedly because the cell nuclei became negative and the presence of Lqf protein was restricted to the territory of granules filling the cytoplasm (Fig. 15A–C).

The Lqf protein showed colocalization with Atg8 and lysotracker red. Since the Atg8 is the widely accepted marker for the autophagosomes and autophagic vacuoles, the colocalization of the Lqf protein with it may provide a strong evidence on the involvement of the *lqf* gene product in the formation of autophagic structures. The immunohistochemistry using the Lqf antiserum on *hsGFP-Atg8a* expressing fat body cells showed a strong colocalization of these two proteins (Fig. 16).

Since the LysoTracker Red dye is only ideal for unfixed tissues, a transgenic line bearing *UAS-GFP::Lqf* was created in order to identify whether those a-Lqf labeled vesicles also had lysoTracker-positivity. When the *UAS-GFP::Lqf* was expressed under the control of the *hsGal4* driver, the presence of the fusion protein was detected in the vacuolar compartment of the trophocytes of wandering larvae (Fig. 17A). The GFP-tagged protein also showed a strong and explicit colocalization with the LysoTracker Red-positive structures in these cells (Fig. 17B and C).

The CA07504 (Flytrap) line, in which the sequence of GFP was fused to the genomic *lqf* gene under the control of its endogenous promoter and enhancer elements, showed the same localization in the fat body cells (Fig. 18).

Lqf is also involved in receptor-mediated endocytosis of larval serum proteins. Larval serum proteins (LSPs) are synthesized and secreted into the hemolymph by the fat body cells during the first half of the last larval stage. Later on, LSPs are taken up from the hemolymph by the fat body cells and accumulate in the form of protein storage granules. Since LSPs are sequestered by receptor-mediated endocytosis, the fate of these proteins was investigated in *lqf*$^{\delta 011027}$ mutants. LSP2 specific western blot on the haemolymph from both *w*^{1118} and homozygous *lqf*$^{\delta 011027}$ late L3 larvae (115–120 h AEL) verified that the production and the secretion of LSP2 takes place in both lines equally. During the wandering period the trophocytes of wild-type larvae could take up LSPs from

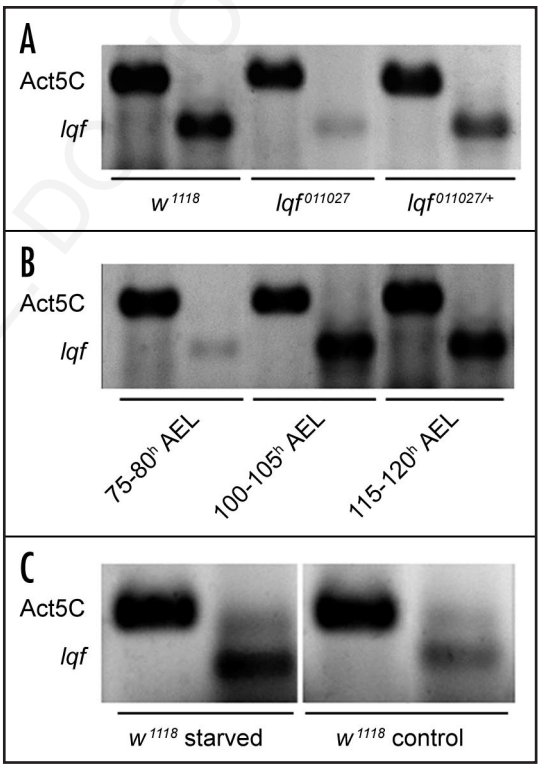


Figure 8. The quantity of the lqf transcript was strongly reduced in the wandering-aged homozygous l(3)S011027 larvae as compared to Oregon R or heterozygous l(3)S011027 larvae (A) The amount of the lqf transcript increased rapidly in wild type larvae during the first two-third of the last larval stage (B). Amino acid deprivation caused an increase of lqf mRNA levels in wild type larvae, but it did not change the amount of lqf transcript in the starved homozygous l(3)S011027 larvae (C).

the haemolymph, but the homozygous *lqf*$^{\delta 011027}$ larvae failed in the uptake (Fig. 19B). The protein content of the various samples on SDS PAGE was the same (Fig. 19A).

Effect of rapamycin treatment in vivo. In order to determine the position of Lqf relative to TOR, which is considered the central regulator of the autophagy pathway, *lqf*^{011027} homozygous wandering-aged larvae were treated with rapamycin, the widely-used inhibitor of TOR. Contrary to the trophocytes of the late

© 2008 LANDES BIOSCIENCE. DO NOT DISTRIBUTE.

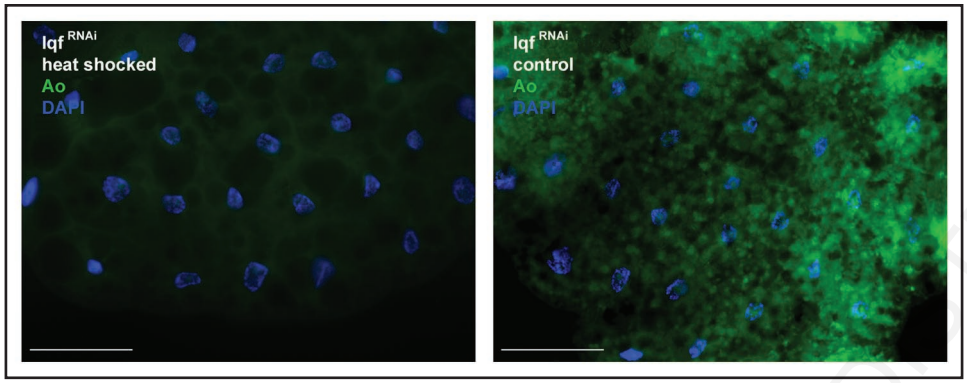


Figure 9. By silencing the lqf gene delayed the formation of acridine orange-positive granules in the UAS-lqfIR transgenic larvae (A) as compared to their siblings in which silencing was not turned on (B). Bar equals 100 μm.

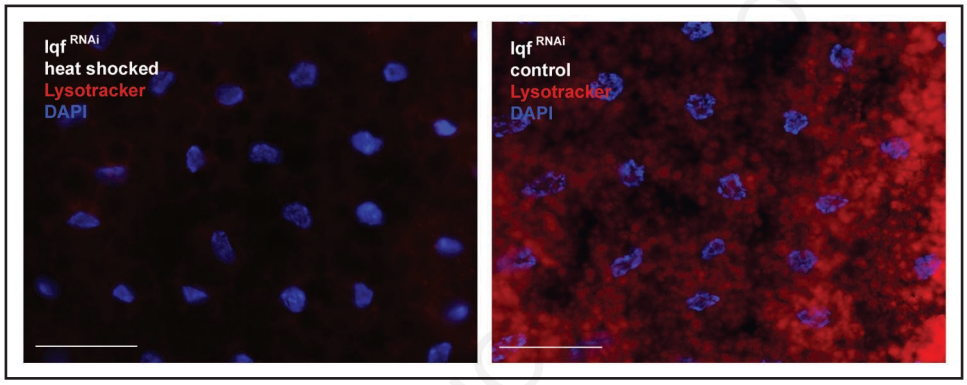


Figure 10. The formation of LysoTracker Red positive granules was completely inhibited by activation of lqf RNAi in the UAS-lqfIR transgenic larvae (A) while the trophocytes of their siblings were filled with granules (B). Bar equals 100 μm.

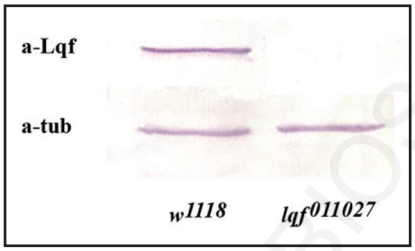


Figure 11. The Lqf protein was present in wild type larvae at the time of wandering, but it could not be determined in the case of homozygous l(3)S011027 wandering-aged larvae.

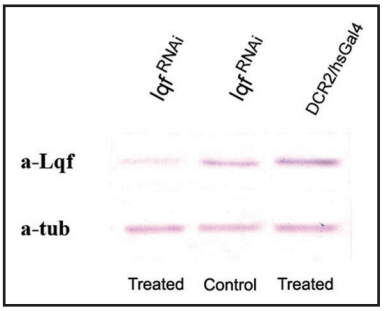


Figure 12. A decrease in the amount of Lqf protein was detected after silencing the lqf gene expression in the UAS-lqfIR transgenic larvae as compared to the case of the transgenic larvae in which the RNAi was not activated as well as the larvae carrying the driver constructions.

wandering wild-type (Fig. 20C) the fat body cells of those larvae that were fed with yeast paste containing 4 μM rapamycin for 6 hours, were absolutely free of LysoTracker Red-positive organelles (Fig. 20B) similar to those that were treated with yeast paste completed with the vehicle of rapamycin (Fig. 20A). Also, prolongation of the treatment did not result in the rescue of the late larval lethality.

Discussion

The genetic regulation and molecular machinery of autophagy has been first described in yeast.[14,38-41] Using genetic screens that allow identification of genes involved in autophagy, 27 autophagy-related (*atg*) genes were characterized in this unicellular organism.[14,42] Many of them are evolutionarily conserved, having the same or similar functions in *C. elegans*, in Drosophila, and even in mammals.[43-48] Now, on the basis of intensive reverse genetics-based research, it is clear that *ATG* genes have essential roles not only in the molecular mechanisms of autophagy, but also in other important biological functions, such as response to starvation, oxidative stress, cell growth, neuronal death, innate immunity and aging.[11,19] Therefore, it is quite obvious to suppose that in multicellular organisms more genes and different regulatory pathways are also involved in the control of autophagy.

©2009 LANDES BIOSCIENCE. DO NOT DISTRIBUTE.

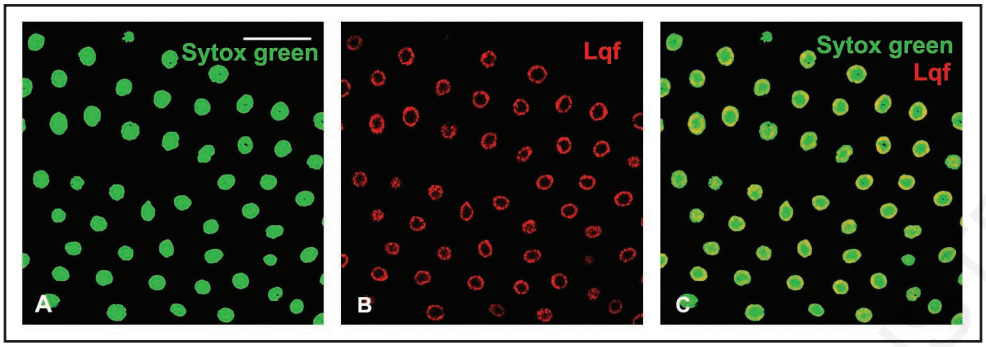


Figure 13. In the fat body cells of the wild type feeding larvae, the Lqf protein appeared in the peripheral region of nuclei in the trophocytes (A–C). Bar equal 100 μm.

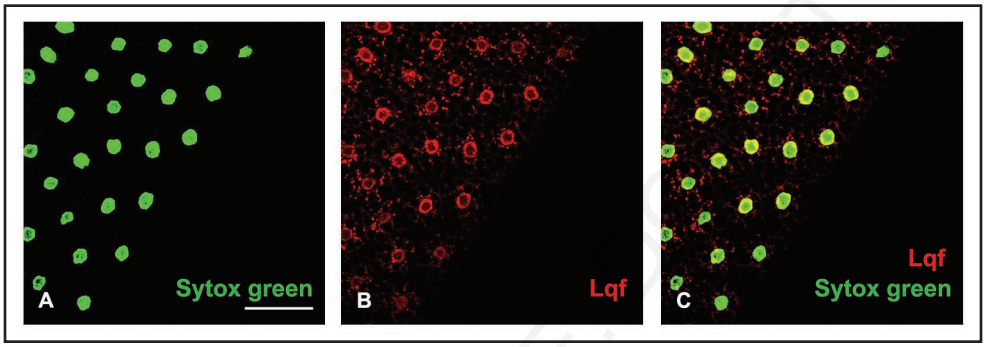


Figure 14. After the larvae have started to wander, the anti-Lqf antisera also reacted with the newly formed granules that appeared in the cytoplasm of fat body cells, while the nuclei, however, remained labeled (A–C). Bar equal 100 μm.

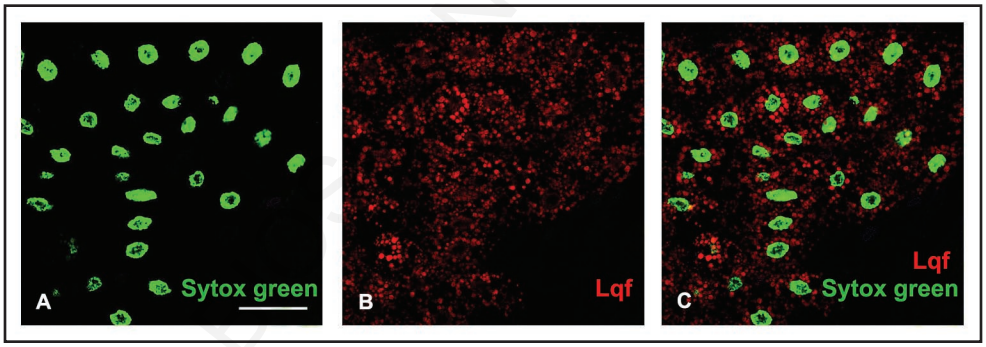


Figure 15. By the end of the wandering period, the localization pattern of Lqf protein changed remarkably, because the signal in the peripheral region of cell nuclei disappeared, and because the Lqf localization became restricted to the granules (A–C). Bar equal 100 μm.

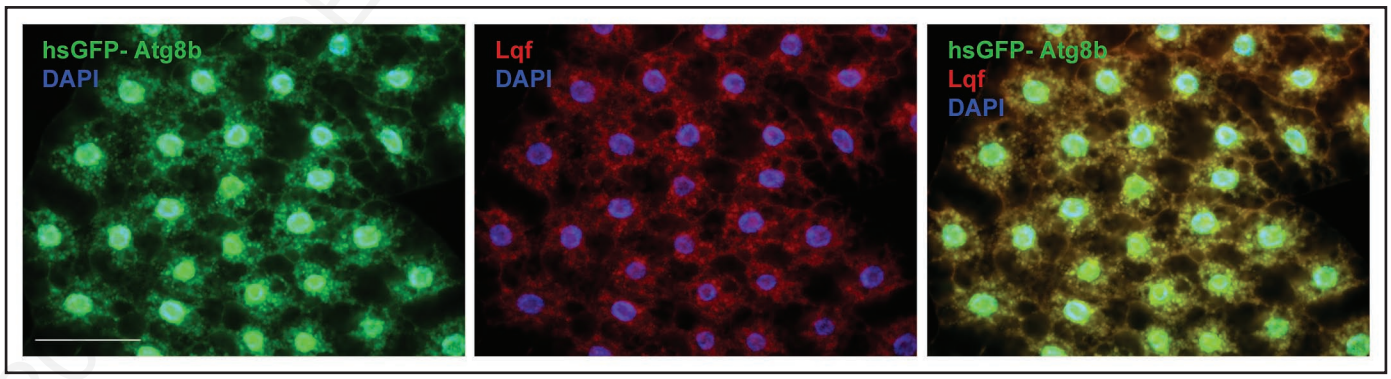


Figure 16. The Lqf protein showed a completely co-localization with the GFP-Atg8a containing granules (A–C). Bar equal 100 μm.

© 2014 Landes Bioscience. Do not distribute.

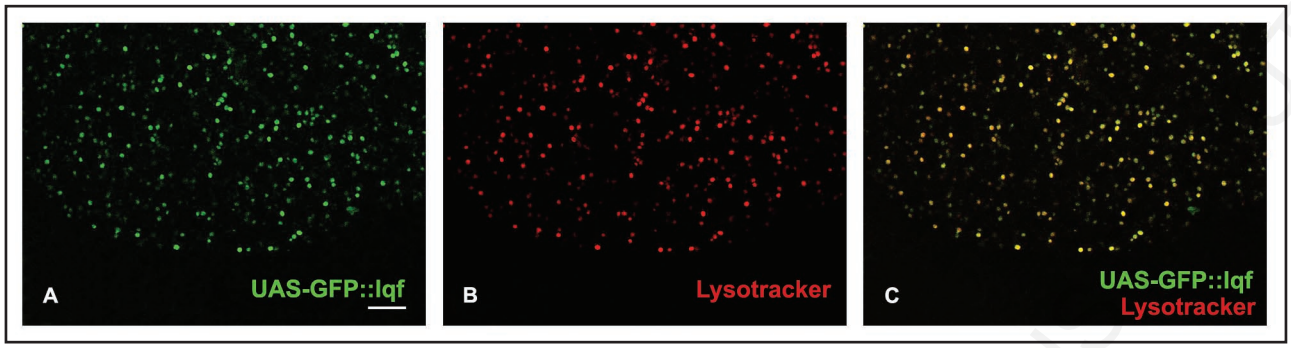


Figure 17. The GFP-tagged Lqf protein showed a clear co-localization with the LysoTracker Red-positive structures in the fat body cells of the transgenic wandering larvae (A–C). Bar equal 20 μm.

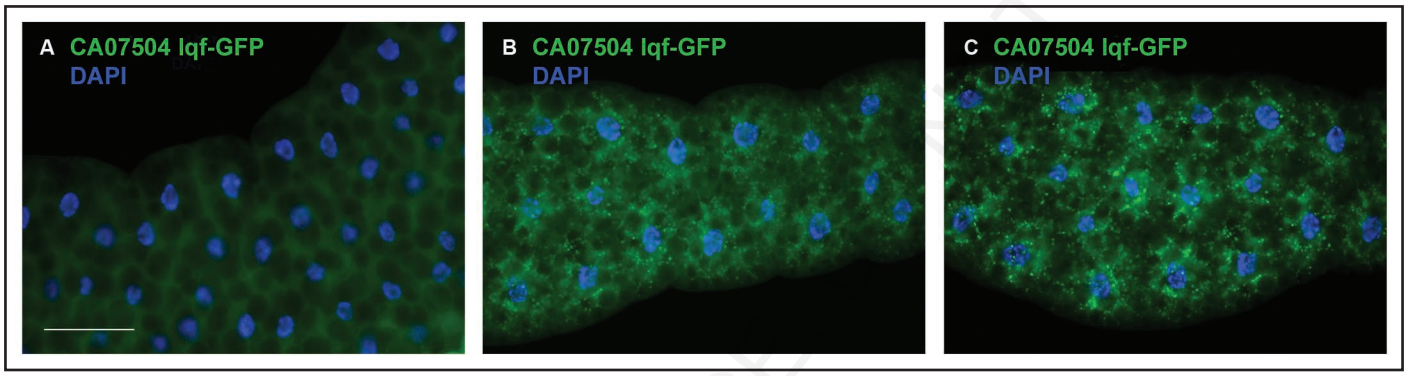


Figure 18. When the expression of GFP-labeled Lqf protein was under the control of endogenous promoter and the enhancer elements, the protein gradually appeared in the discrete granules as the larvae developed through the feeding (A) early wandering (B) and late wandering (C) stages.

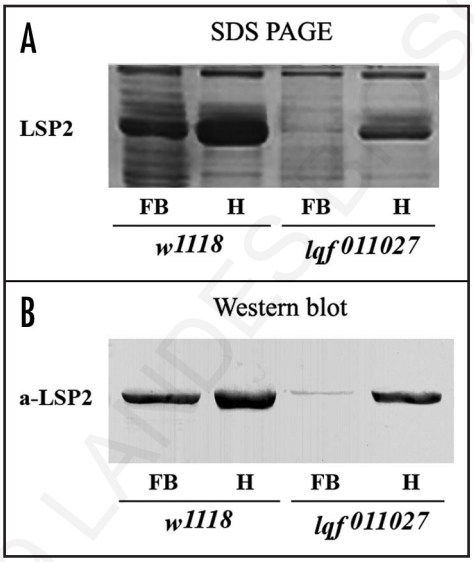


Figure 19. In spite of the fact that the trophocytes of homozygous l(3)S011027 larvae were able to synthesize and secrete LSP2 (larval serum protein 2) into the haemolymph, they were unable to re-uptake prior to metamorphosis (B) Apart from the accumulated LSPs the protein pattern were similar in both fat body or hemolymph samples came from wild type or l(3)S011027 larvae (A).

Our present work is based on a forward genetic approach. More than 300 P-element-induced, late larval lethal Drosophila mutants were screened to isolate and identify new genes regulating autophagy in multicellular animals. 21 of the tested mutants were unable to form autophagosomes and/or autolysosomes in the fat body. On the basis of this test system, regulatory function of SNF4A in autophagy has been recently published.[37]

In the present work we demonstrate our data on the l(3)S011027 P-element insertion line. In *l(3)S011027* mutant larvae, developmental autophagy was inhibited in both homozygotes and hemizygotes. Autophagy could not be induced by 20-hydroxyecdysone and by starvation or oxidative stress in mutants. Beyond the strong influence of this loss of function mutation on autophagy, the endocytotic uptake of larval storage proteins and the formation of protein granules were also inhibited in the fat body cells of wandering *l(3)S011027* larvae. It has been established that in the *l(3)S011027* mutant, a single P element was inserted into the first exon of the liquid facets (*lqf*) gene. The heteroallelic combination demonstrated that the phenotype was exclusively caused by the mutation of lqf gene itself. We also generated transgenic RNA interference animals to silence lqf expression, which severely impaired the formation of autophagic structures.

lqf encodes homolog of vertebrate epsin, a protein associated with the clathrin-mediated endocytosis complex.[34] Epsin has a modular structure: an epsin N-terminal homology (ENTH) domain, which binds phosphoinositides, ubiquitin interaction motifs (UIMs), and a long, flexible region that includes binding

©2009 LANDES SCIENCE. DO NOT DISTRIBUTE.

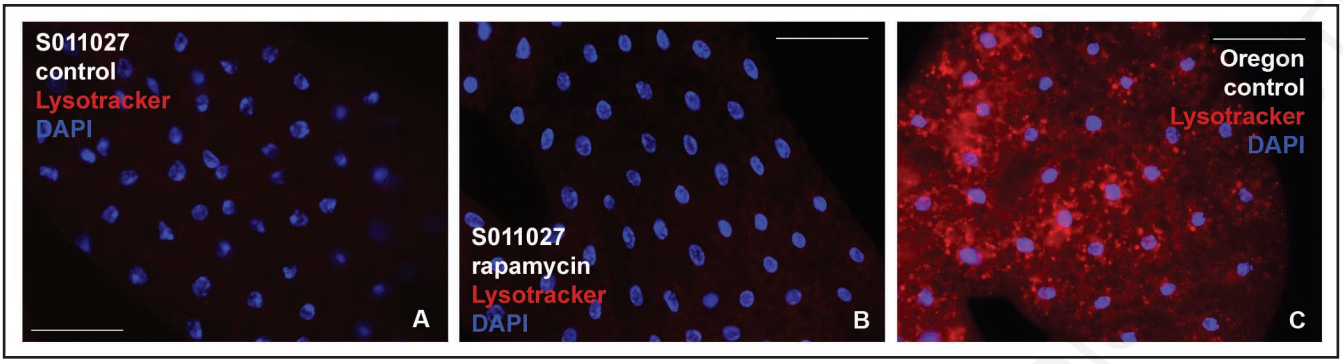


Figure 20. No sign of autophagy can be detected in the fat body cells of neither homozygous l(3)S011027 larvae following the treatment of rapamycin vehicle (A), nor after the rapamycin treatment (B) as compare to the trophocytes of wild-type wandering larva (C), Bar equals 100 μm.

sites for the clathrin adaptor AP-2, and EH domain-containing proteins such as Eps15, which is another UIM-containing endocytic adaptor.[50-53] The ENTH domain of epsins is one of the core components of the endocytic machinery evidenced by its dominant-negative effects on endocytosis in mammalian cells and ENTH also has an essential role in endocytosis in yeast cells.[54-56] Identification of the ubiquitin-interacting motifs (UIMs) in epsins has led to the suggestion that Epsins belong to a family of cargo-selective adapters.[50] It has been demonstrated that the Drosophila Epsin, *lqf*, is essential for endocytosis of delta (Dl) in the developing eye.[36]

Our observations agree well with all these data. In wild-type animals, LSP2 (larval serum protein 2) is synthesized by the fat body cells (trophocytes) and is secreted into the hemolymph from the beginning of the third larval stage, until pupariation.[57-59] During the wandering period, the LSPs are taken up from the hemolymph by the larval fat body cells.[60,61] These processes are under the control of 20-HE, the moulting hormone.[57,58,62]

The P-element mutation in *lqf* inhibits the endocytotic processes in the fat body. Although *l(3)S011027* mutant larvae are able to synthesize and secrete LSP2, they are unable to take up this storage protein from the hemolymph. As a consequence, LSP2 remains in the hemolymph until the death of the mutant larvae.

These results suggest that the mutation in the *lqf* gene may have a direct effect on both endocytosis and autophagy, since fat body cells can normally synthetise and secrete LPS2 during the last larval instar.

The localization of Lqf showed a markedly different pattern in the fat body cells of feeding and wandering wild-type larvae. It was present in the nuclei of the fat body cells during the feeding period. In mammals, most epsins are found in the cytosol by immunohistochemistry, even after overexpression.[54,63] However, it has been also reported that epsin1 is localized to the nucleus when overexpressed together with PLZF, and it was suggested that they take part in the regulation of specific gene expression.[64]

From the beginning of the wandering period (when autophagy and endocytosis are started in the fat body), the Lqf protein was found to be associated with the membrane of acidic organelles, similar to the distribution of the GFP-Lqf fusion protein. The association of proteins which contain an ENTH-domain like epsin1 and the huntingtin interacting protein1 (HIP1) to the membrane of endocytotic vacuoles was detected in different cell lines.[65-67] According to our interpretation Lqf might have the same function in the formation of curved membranes, as it has been reported for the formation of curved membranes of primary endocytotic vesicles.[68]

Autophagy and endocytosis represent two of the most important inputs of the lysosomal compartment. Still, there are only a few reports dissecting the possible cross-talk between the regulation of these two processes. It is well known that TOR kinase is the central regulator of autophagy.[69,70] It has been observed that LSP2 uptake was severely reduced in *Tor* mutant Drosophila larvae, demonstrating a role for TOR in endocytosis.[71] Biochemical studies in yeast found that TOR localizes to intracellular vesicles and cofractionates with endosomal markers which suggests again the endocytotic role of TOR.[72,73]

To find out the position of Lqf relative to Tor in the regulatory pathway of autophagy, $lqf^{S011027}$ larvae were treated with rapamycin. Rapamycin is a potent and specific inhibitor of TOR, and inhibition of TOR induces massive autophagy in wild-type animals.[44,74] In $lqf^{S011027}$ mutants, fat body cells were unable to form autophagic structures when treated with rapamycin. This observation suggests that *lqf* acts downstream to the TOR.

We recently demonstrated that, similar to other autophagy-related genes, *lqf* is also involved in aging. RNAi-mediated silencing of *lqf* in adult flies significantly shortened their lifespan.[48,77,76]

Taken together, our results suggest that Lqf, a Drosophila epsin, is required for both autophagy and endocytosis. Its function in autophagy is probably not due to its requirement for endocytosis, as is the case for ESCRT components, since mutation of ESCRTs inhibits endocytosis and as a result autophagosomes accumulate even in well-fed animals, a phenotype we have not seen in *lqf* mutants.[77,78] Another necessary component of the endocytotic machinery is the lipid kinase Vps34, and we have recently shown that it is required for the generation of autophagosomes independent of its endocytotic function.[78] Therefore, Vps34 mutant animals are defective in both endocytosis and autophagosome generation, so they do not accumulate autophagosomes unlike ESCRT mutant animals.[77,78] In this respect, the *lqf* phenotype is similar to that of Vps34 mutant flies: both endocytosis and

© LANDES BIOSCIENCE. DO NOT DISTRIBUTE.

autophagy are impaired, and no autophagosome accumulation is observed in the mutants. Further biochemical studies and genetic interaction tests are necessary to reveal the exact role of *lqf* in these processes.

Materials and Methods

Fly stocks. All Drosophila strains were maintained in a w^{1118} background. All of the crosses and treatments were done at 25°C except where otherwise indicated.

Acridine orange and LysoTracker staining. Fat bodies from feeding, wandering or starved third instar (L3) larvae were dissected in 100 µl phosphate-buffered saline (PBS), and then incubated for 5 min in 5 mg/ml acridine orange in PBS or in 100 µM LysoTracker Red DND 99 (Invitrogen-Molecular Probes), and 1 µg/ml DAPI (Sigma).[79] Following 3 washes in PBS, the fat bodies were transferred to 80% glycerol in PBS on glass slides, covered and immediately photographed live on an OlympusBX-51 fluorescence microscope with AnalySis digital imaging software.

Electron microscopy. Fat bodies were fixed in 2% glutaraldehyde in 0.1 M cacodylate buffer, pH 7.2. Samples were postfixed with 2% OsO_4 in the same buffer, embedded in Araldyte (Fluka) and 60–70 nm sections were investigated in a JEOL CM-II 100 electron microscope.

Treatments. 20-hydroxyecdysone treatment. Pure baker yeast was diluted with equal volume distilled water and boiled. After cooling, 10 µl of 20-hydroxyecdysone solution (5 mg hormone was dissolved in 1 ml nanopure water containing 5% ethanol) was added per ml of the yeast mixture and 100 µl was loaded into each well of a 24 well plate. Larvae at the late wandering stage were kept on the yeast mixture completed with hormone, while controls were put on the purely diluted yeast. After 12 hours the larvae were dissected, stained and investigated under light microscope.

Rapamycin treatment. Wandering aged $lqf^{k011027}$ larvae were kept in yeast mixture containing 4 µM rapamycin (Sigma) for 6 hours. The rapamycin was solved in PBS completed with 10% DMSO. After treatment the larvae were dissected and stained with LysoTracker Red.

Inverse PCR. Genomic DNA preparation was performed using standard methods. Inverse PCR was performed using the recommended primers and restriction enzymes as described at http://www.fruitfly.org/about/methods/inverse.pcr.html for the *P{lacW}* transposon.

Analysis of mitotic clones. The virgins of *hsFlp; cgGal4, UAS-GFP, FRT80B* line (courtesy of Thomas Neufeld) were crossed with $lqf^{4.71}$*FRT80B/TM6b* males (courtesy of Janice Fischer) and the freshly laid eggs (till 8 h AEL) were heat shocked for 30 min at 32°C. During the subsequent developmental period the larvae were kept at 25°C. Followed the 4 hour-long starving in 20% sucrose solution the 95–100 h AEL larvae were dissected and stained with LysoTracker Red and their fat body lobes were investigated under fluorescent microscope.

Generation of the RNA interference construct. The pWizMod vector used for the RNAi experiment carries the 1.2 kb long third intron of the *wg* gene inserted into the polycloning site of pUAST plasmid.[80] The vector has unique restriction sites on both sides of the intron (BglII and XhoI sites upstream and SpeI, KpnI and XbaI sites downstream of it in the given order) for cloning the same fragment of the targeted cDNA in opposite orientation. After expressing the entire artificial transcript, the intron is spliced out by the splicing machinery of the fly cell and the parts of the inverted repeats bind to form a hairpin. (Genebank accession number: AB186054 describes a specific application of the vector).

The *lqf* RNAi construct contains a 605 bp long piece of the fifth exon (FBgn0028582:6) which was amplified by PCR from Drosophila genomic DNA. The following two primers were used for the PCR amplification:

forward:
5'GGA TCC AGC GAG ATA GCG GAA CTC ACC3'
reverse:
5'CTC GAG TCA CTT GAA ATC CTG CTC ACT C3'

The resulting fragment was inserted into PCR cloning vector Topo-TA (Invitrogen, catalog number: K4600). First, the *lqf* fragment was excised using its flanking BamHI and XhoI restriction sites (shown in lower case on the primer sequences) and cloned into a BglII, XhoI digested pWizMod vector. In the second cloning step, the same insert was excised from Topo-TA by KpnI, XbaI double digestion (using vector specific flanking sites this time) and inserted into KpnI, XbaI sites of the intermediate plasmid obtained from the first step resulting in the desired inverted repeat arrangement of the insert at opposite side of the intron. The resulting plasmid was named UAS-LqfIR.

Microinjection of the UAS-LqfIR into w^{1118} embryos was carried out by standard P-element mediated germ line transformation (Spradling, 1986).

The *DCR2; hsGal4* (courtesy of William Ja) driver was used for the expression of UAS-lqfIR. Development was allowed to proceed at 18°C until the beginning of second larval stage (48 hours after egg laying, (AEL)); individuals were then shifted to the restrictive temperature (32°C) for 72 hours.

Creation of the construct coding GFP-Lqf fusion protein. First, the GFP-tagging cassette was prepared by subcloning a BamHI-BglII fragment containing GFP-sequence from pRSET/EmGFP (Invitrogen) into pUAST vector. The original GFP ORF was amplified from the pRSET/EmGFP using primers that were completed by BamHI and BglII site at their flanking regions (shown in lower case on the primer sequences). The following two primers were used for the PCR amplification:

forward:
5'ATT GGA TCC ATG GTG AGC AAG GGC GAG3'
reverse:
5'CTT AGA CTC CTT GTA CAG CTC GTC CAT3'

Then the fragments were cloned into a BglII-digested pUAST vector in-frame in front of the multi cloning site (pUAST-GFP). Second, the full length *lqf* cDNA GH27912 in a pOT2 vector (from Berkeley Drosophila Genome Project, BDGP) was amplified by primers bearing artificially formed BglIIand XhoI sites (shown

© 2009 LANDES BIOSCIENCE. DO NOT DISTRIBUTE.

in lower case on the primer sequences) at their endings. The primers which were used in this step were:

forward:
5'AGA TCT ATG GAT CCG GTA TCG GCG AAC3'
reverse:
5'CTC GAG CGA CAA AAA CGG ATT TGT TGC3'

Finally, these fragments were gel-purified, digested with BglII and XhoI and ligated into pUAST-GFP vector in-frame behind the GFP. The resulted plasmid named pUAST-GFP::Lqf was injected into w^{1118} embryos according to standard techniques.[81]

Generation and purification of the recombinant Lqf partial protein. Molecular cloning techniques were performed according to standard procedures. PCR amplification of the fifth exon (FBgn0028582:6) of *lqf* gene was done using ExTaq DNA polymerase (Takara) with the primers 5'GGA TCC CCA AAA CTT CCG CCT CCC GT3' and 5'CTG CAG TTC CAG CTT GCA GTT GGC CG3'. The forward and reverse primer was completed with BamHI and PstI site, respectively, which was shown in lower case on the primer sequences. The PCR product was directly cloned into the pQE-UA bacterial expression vector (Qiagen), and the recombinant partial LQF protein fused to an N-terminal hexahistidine tag was expressed in *E. coli* M15 cells. Protein purification was performed using the QIAexpressionist kit (Qiagen). Mice were immunized with the fusion peptide, and the obtained polyclonal antiserum was used for further investigations.

Preparation of protein extracts. Embryos, larvae and pupae were homogenized in Eppendorf tubes using a pestle in 2 mM Complete Proteinase Inhibitor Cocktail prepared from ready-to-use water soluble tablet (Roche). The homogenate was completed with 2x SDS electrophoresis running buffer then centrifuged for 2 min at 13,000 *g* at 4°C in a benchtop centrifuge. The supernatant was collected, aliquoted and frozen.

Western blots. 10 μg of total protein prepared from each larval and pupal stage was subjected to SDS-PAGE separation and transferred to nitrocellulose membrane (BioRad) for western blot analysis. Membranes were blocked in 5% milk prepared in TBS (10 mM Tris, 100 mM NaCl, pH 7.5), and hybridizations were carried out overnight at 4°C using 1:750 dilution of the Lqf antibody in 3% milk in TTBS (10 mM Tris, 100 mM NaCl, 0.05% Tween, pH 7.5). Membranes were washed three times (5 min each) in TTBS after hybridization. Alkaline-phosphatase-conjugated anti-mouse (goat) antibodies (Sigma) were used in 1:2,000 dilution in 3% milk + TTBS, and the proteins were detected using NBT/BCIP (Sigma).

Prestained molecular weight marker (PageRuler™ Prestained Protein Ladder, Fermentas) served as standard. Equal loading of samples was confirmed using an anti-α-tubulin antibody (Sigma, DM 1/A clone).

Immuncytochemistry. Immuncytochemistry was performed using standard techniques. Fat bodies from third instar larvae were dissected and fixed with 2% paraformaldehyde in PBS for 15 min at room temperature (RT). Samples were washed 2 x 5 min in PBS then were incubated for 20 min in PBS + 0.1% Triton X-100. Following 3 x 5 min wash with PBS, nonspecific binding sites were blocked by incubation with 3% milk powder in PBS for 1 hr. Incubations with primary and secondary antibodies were performed in the blocking buffer overnight at 4°C and for 1 hr at RT respectively. Primary antibodies were used at a dilution of 1:100 (rabbit anti-Lqf; see above for preparation of Lqf antiserum). Anti-mouse-Alexa488 (Invitrogen) secondary antibodiy was used at a dilution of 1:400. An Olympus IX-81 View 500 confocal microscope with Fluoview digital imaging software was used to image fluorescently labeled antibodies.

Semi-quantitative analysis of *lqf* mRNA abundance. Total RNA was isolated from w^- (w^{1118})—control—and $lqf^{5011027}$ larvae using QIAeasy RNA isolation kit (Qiagen). The RNA for Revers Transcriptase PCR (RT-PCR) was treated with RNAse free DNAse (Fermentas) prior to the synthesis of first-strand cDNA by RevertAid kit (Fermentas). The RT-PCR reaction was performed in 28 cycles with Ex-Taq polymerase (TaKaRa), using the *lqf* second exon-specific forward 5' GGC AAA GGA AAG ATT CGC CC 3' and reverse 5' CCA TGC CAG GTC CAA GAG CT 3' primers as well as Drosophila actin Act5C specific primers as control. The products were analyzed in a 1% agarose gel containing SybrSafe (Invitrogen) dye.

Acknowledgements

The authors thank Mariann Saródy and Eszter Tóth for the excellent technical help.

This work was supported by grants from OTKA (T048744) and the RET-06/2006 provided by National Office for Research and Technology.

References

1. Klionsky DJ, Emr SD. Autophagy as a regulated pathway of cellular degradation. Science 2000; 290:1717-21.
2. Bursch W. The autophagosomal-lysosomal compartment in programmed cell death. Cell Death Diff 2001; 8:569-81.
3. Edinger AL, Thompson CB. Death by design: apoptosis, necrosis and autophagy. Curr Opin Cell Biol 2004; 16:663-69.
4. Lockshin RA, Zakeri Z. Apoptosis, autophagy, and more. International Journal of Biochemistry Cell Biology 2004; 36:2405-19.
5. Shintani T, Klionsky DJ. Autophagy in health and disease: A double-edged sword. Science 2004; 306:990-95.
6. Lum JJ, DeBerardinis RJ, Thompson CB. Autophagy in metazoans: cell survival in the land of plenty. Mol Cell Biol 2005; 6:439-48.
7. Levine B, Yuan J. Autophagy in cell death: an innocent convict? J Clin Invest 2005; 115:2679-88.
8. Mizushima N, Klionsky D. Protein turnover via autophagy: implications for metabolism. Annu Rev Nutr 2007; 27:19-40.
9. Juhász G, Erdi B, Sass M, Neufeld TP. Atg7-dependent autophagy promotes neuronal health, stress tolerance, and longevity but is dispensable for metamorphosis in Drosophila. Genes Dev 2007; 21:3061-66.
10. Codogno P, Meijer AJ. Signaling pathways in mammalian autophagy. In: Klionsky D, ed. Autophagy. Georgetown Texas, USA: Landes Bioscience and Austin Texas, USA: Eurekah.com, 2004:26-47.
11. Levine B, Klionsky DJ. Development by self-digestion: molecular mechanisms and biological functions of autophagy. Dev Cell 2004; 6:463-77.
12. Yoshimori T. Autophagy: a regulated bulk degradation process inside cells. Biochem. Biophys. Res Commun 2004; 313:453-58.
13. Reggiori F, Klionsky DJ. Autophagy in the eukaryotic cell. Eukaryot Cell 2002; 1:11-21.
14. Wang CW, Klionsky DJ. The molecular mechanism of autophagy. Mol Med 2003; 9:65-76.
15. Noda T, Ohsumi Y. Tor, a phosphatidylinositol kinase homologue, controls autophagy in yeast. J Biol Chem 1998; 273:3963-66.
16. Schmelzle T, Hall MN. TOR, a central controller of cell growth. Cell 2000; 103:253-62.
17. Martin DE, Hall MN. The expanding TOR signaling network. Curr Opin Cell Biol 2005; 17:158-66.

© 2008 LANDES BIOSCIENCE. DO NOT DISTRIBUTE.

18. Sarbassov, DD, Ali SM, Sabatini DM. Growing roles for the mTOR pathway. Curr Opin Cell Biol 2005; 17:596-603.
19. Levine B, Kroemer G. Autophagy in the pathogenesis of Disease Cell, 2008, 132, 27-42.
20. Sass M, Kovacs J. Ecdysterone and an analogue of juvenile hormone on the autophagy in the cells of fat body of Mamestra brassicae. Acta Biol 1975; 26:189-96.
21. Sass M, Kovacs J. The effect of ecdysone on the fat body cells of the penultimate larvae of Mamestra brassicae. Cell Tissue Res 1977; 180:403-9.
22. Dean RL. The induction of autophagy in isolated insect fat body by B-ecdysone. J. Insect Physiol 1978; 24:439-47.
23. Lee CY, Baehrecke EH. Steroid regulation of autophagic programmed cell death during development. Development 2001; 128:1443-55.
24. Thummel CS. Steroid-triggered death by autophagy. Bioessays 2001; 8:677-82. Review
25. Rusten TE, Lindmo K, Juhasz G, Sass M, Seglen PO, Brech A, et al. Programmed autophagy in the Drosophila fat body is induced by ecdysone through regulation of the PI3K pathway. Dev Cell 2004; 7:179-92.
26. Sass M, Kömüves L, Csikós G, Kovács J. Changes in the activities of lysosomal enzymes in the fat body and mid gut of two Lepidopteran insects during metamorphosis. Comp. Biochem. Physiol. 1989, 92A, 285-289
27. Sass M, Kovács J. The effects of actinomycin D, cycloheximide and puromycin on the 20-hydroxyecdysone induced autophagocytosis in larval fat body cells of Pieris brassicae. J Insect Physiol 1980; 26:569-73.
28. Ashburner M. Patterns of puffing activity in the salivary gland chromosomes of Drosophila. Chromosoma 1967; 21:398-428.
29. Thummel CS. Flies on steroids—Drosophila metamorphosis and the mechanisms of steroid hormone action. Trend Genet 1996; 12:306-10. Review
30. Jiang C, Beahrecke EH, Thummel CS. Steroid regulated programmed cell death during Drosophila metamorphosis. Development 1997; 124:4673-83.
31. Berry LB, Baehrecke EH. Growth arrest and autophagy are required for salivary gland cell degradation in Drosophila. Cell 2007; 131:1137-48.
32. Török T, Tick G, Alvarado M, Kiss I. P-lacWinsertional mutagenesis on the second chromosome of Drosophila melanogaster: isolation of lethals with different overgrowth phenotypes. Genetics 1993; 135:71-80.
33. Deák P, Omar MM, Saunders RD, Pal M, Komonyi O, Szidonya J, et al. P-element insertion alleles of essential genes on the third chromosome of Drosophila melanogaster: correlation of physical and cytogenetic maps in chromosomal region 86E-87F. Genetics 1997; 147:1697-722.
34. Cadavid ALM, Ginzel A, Fischer JA. The function of the Drosophila Fat facets deubiquitinating enzyme in limiting photoreceptor cell number is intimately associated with endocytosis. Development 2000; 127:1727-36.
35. Chen X, Zhang B, Fischer JA. A specific protein substrate for a deubiquitinating enzyme: Liquid facets is the substrate of Fat facets. Genes Dev 2002; 16:289-94.
36. Overstreet E, Chen X, Wendland B, Fischer JA. Either part of a Drosophila epsin protein, divided after the ENTH domain, functions in endocytosis of delta in the developing eye. Curr Biol 2003; 13:854-60.
37. Lippai M, Csikós G, Maróy P, Lukácsovich T, Juhász G, Sass M. SNF4Agamma, the Drosophila AMPK gamma subunit is required for regulation of developmental and stress-induced autophagy. Autophagy 2008; 4:476-86.
38. Tsukada M, Ohsumi Y. Isolation and characterization of autophagy-defective mutants of Saccharomyces cerevisiae. FEBS Lett 1993; 333:169-74.
39. Harding TM, Morano KA, Scott SV, Klionsky DJ. Isolation and characterization of yeast mutants in the cytoplasm to vacuole protein targeting pathway. J Cell Biol 1995; 131:591-602.
40. Ohsumi Y. Molecular dissection of autophagy: two ubiquitin-like systems. Nat Rev Mol Cell Biol 2001; 2:211-16. Review
41. Klionsky DJ, Cregg JM, Dunn WA Jr, Emr SD, Sakai Y, Sandoval IV, et al. A unified nomenclature for yeast autophagy-related genes. Dev Cell 2003; 4:539-45.
42. Suzuki K, Ohsumi Y. Molecular machinery of autophagosome formation in yeast, Saccharomyces cerevisiae. FEBS Lett 2007; 581:2156-61.
43. Juhász G, Csikós G, Sinka R, Erdélyi M, Sass M. The Drosophila homolog of Aut1 is essential for autophagy and development. FEBS Lett 2003; 543:154-58.
44. Neufeld TP. Genetic analysis of TOR signaling in Drosophila. Curr Top Microbiol Immunol. 2004; 279:139-52. Review
45. Neufeld TP, Baehrecke EH. Eating on the fly: Function and regulation of autophagy during cell growth, survival and death in Drosophila. Autophagy 2008; 4:557-62.
46. Mizushima N, Levine B, Cuervo AM, Klionsky DJ. Autophagy fights disease through cellular self-digestion. Nature 2008; 451:1069-75. Review
47. Scott RC, Juhász G, Neufeld TP. Direct induction of autophagy by Atg1 inhibits cell growth and induces apoptotic cell death. Curr Biol 2007; 17:1-11.
48. Tóth ML, Sigmond T, Borsos E, Barna J, Erdélyi P, Takács-Vellai K, et al. Longevity pathways converge on autophagy genes to regulate life span in Caenorhabditis elegans. Autophagy 2008; 4:330-38.
49. Winslow AR, Rubinsztein DC. Autophagy in neurodegeneration and development. Biochim Biophys Acta 2008; 1782:723-9.
50. Wendland B. Epsins: adaptors in endocytosis? Nat Rev Mol Cell Biol 2002; 3:971-7.
51. De Camilli P, Chen H, Hyman J, Panepucci E, Bateman A, Brunger AT. The ENTH domain. FEBS Lett 2002; 20: 513:11-8. Review
52. Polo S, Confalonieri S, Salcini AE, Di Fiore PP. EH and UIM: endocytosis and more. Sci STKE. 2003; 2003:re17. Review.
53. Hofmann K, Falquet L. A ubiquitin-interacting motif conserved in components of the proteasomal and lysosomal protein degradation systems. Trends Biochem Sci 2001; 26:347-50.
54. Chen H, Fre S, Slepnev VI, Capua MR, Takei K, Butler MH, et al. Epsin is an EHdomain-binding protein implicated in clathrin-mediated endocytosis. Nature 1998; 394:793-97.
55. Ford MGJ, Mills IG, Peter BJ, Vallis Y, Praefcke GJK, Evans PR, et al. Curvature of clathrin Coated pits driven by epsin. Nature 2002; 419:361-66.
56. Wendland B, Steece KE, Emr SD. Yeast epsins contain an essential N-terminal ENTH domain, bind clathrin and are required for endocytosis. EMBO J 1999; 18:4384-93.
57. Lepesant JA, Levine M, Garen A, Lepesant-Kejzlarvoa J, Rat L, Somme-Martin G. Developmentally regulated gene expression in Drosophila larval fat bodies. J Mol Appl Genet 1982; 1:371-83.
58. Powell D, Sato JD, Brock HW, Roberts DB. Regulation of synthesis of the larval serum proteins of Drosophila melanogaster. Dev Biol 1984; 102:206-15.
59. Benes H, Spivey DW, Miles J, Neal K, Edmondson RG. Fat-body-specific expression of the Drosophila Lsp-2 gene. SAAS Bull Biochem Biotechnol 1990; 3:129-33.
60. Tojo S, Kiguchi K, Kobazashi M. Hormonal control of the storage protein synthesis and uptake by the fat body in the silkworm Bombyx mori. J Insect Physiol 1981; 27:491-7.
61. Levenbook L, Bauer AC. The fate of the larval storage protein calliphorin during adult development of Calliphora vicina. Insect Biochem 1984; 14:77-86.
62. Wolfe J, Akam ME, Roberts DB. Biochemical and immunological studies on larval serum protein 1, the major haemolymph protein of Drosophila melanogaster third-instar larvae. Eur. J. Biochem. 1977; 79:47-53.
63. Rosenthal JA, Chen H, Slepnev VI, Pellegrini L, Salcini AE, Di Fiore PP, et al. The epsins define a family of proteins that interact with components of the clathrin coat and contain a new protein module. J Biol Chem 1999; 274:33959-65.
64. Hyman J, Chen H, Di Fiore PP, De Camilli P, Brunger AT. Epsin 1 undergoes nucleocytosolic shuttling and its eps15 interactor NH(2)-terminal homology (ENTH) domain, structurally similar to Armadillo and HEAT repeats, interacts with the transcription factor promyelocytic leukemia Zn(2)+ finger protein (PLZF). J Cell Biol 2000; 149:537-46.
65. Drake MT, Downs MA, Traub LM. Epsin binds to clathrin by associating directly with the clathrin-terminal domain. Evidence for cooperative binding through two discrete sites. J Biol Chem 2000; 9:6479-89.
66. Waelter S, Scherzinger E, Hasenbank R, Nordhoff E, Lurz R, Goehler H, et al. The huntingtin interacting protein HIP1 is a clathrin and alpha-adaptin-binding protein involved in receptor-mediated endocytosis. Hum Mol Genet 2001; 10:1807-17.
67. Hawryluk MJ, Keyel PA, Mishra SK, Watkins SC, Heuser JE, Traub LM. Epsin 1 is a polyubiquitin-selective clathrin-associated sorting protein. Traffic 2006; 7:262-81.
68. Horvath CA, Vanden Broeck D, Boulet GA, Bogers J, De Wolf MJ. Epsin: inducing membrane curvature. Int J Biochem Cell Biol 2007; 39:1765-70. Review
69. Inoki K, Ouyang H, Li Y, Guan KL. Signaling by target of rapamycin proteins in cell growth control. Microbiol Mol Biol Rev 2005; 69:79-100. Review.
70. Pattingre S, Espert L, Biard-Piechaczyk M, Codogno P. Regulation of macroautophagy by mTOR and Beclin 1 complexes. Biochimie 2008; 90:313-23.
71. Hennig KM, Colombani J, Neufeld TP. TOR coordinates bulk and targeted endocytosis in the Drosophila melanogaster fat body to regulate cell growth. J Cell Biol 2006; 173:963-74.
72. Kunz J, Schneider U, Howald I, Schmidt A, Hall MN. HEAT repeats mediate plasma membrane localization of Tor2p in yeast. J Biol Chem 2000; 275:37011-20.
73. Chen EJ, Kaiser CA. LST8 negatively regulates amino acid biosynthesis as a component of the TOR pathway. J Cell Biol 2003; 161:333-47.
74. Zhang H, Stallock JP, Ng JC, Reinhard C, Neufeld TP. Regulation of cellular growth by the Drosophila target of rapamycin dTOR. Genes Dev 2000; 14:2712-24.
75. Partridge L. Some highlights of research on aging with invertebrates. Aging Cell 2008; 7:605-8.
76. Meléndez A, Neufeld TP. The cell biology of autophagy in metazoans: a developing story. Development 2008; 135:2347-60.
77. Rusten TE, Vaccari T, Lindmo K, Rodahl LM, Nezis IP, Sem-Jacobsen C, et al. ESCRTs and Fab1 regulate distinct steps of autophagy. Curr Biol 2007; 17:1817-25.
78. Juhász G, Hill JH, Yan Y, Sass M, Baehrecke EH, Backer JM, et al. The class III PI(3)K Vps34 promotes autophagy and endocytosis but not TOR signaling in Drosophila. J Cell Biol. 2008,181:655-66.
79. Canonico PG, Bird JWC. The use of acridine orange as a lysosomal marker in rat skeletal muscle. J Cell Biol 1969; 43:367-71.
80. Brand AH, Perrimon N. Targeted gene expression as a means of altering cell fates and generating dominant phenotypes. Development 1993; 118:401-15.
81. Spradling A. P element-mediated transformation. In: Roberts Db, ed. Drosophila: A Practical Approach. Oxford, Washington DC:IRL Press, 1986:175-97.

© Landes Bioscience. Do not distribute.

Autophagy 8:12, 1-2; December 2012; © 2012 Landes Bioscience

dc_840_14

Interpretation of bafilomycin, pH neutralizing or protease inhibitor treatments in autophagic flux experiments

Novel considerations

Gábor Juhász

Department of Anatomy, Cell and Developmental Biology; Eötvös Loránd University; Budapest, Hungary

Recent publications showed that the kinase MTOR localizes to lysosomes and its activation depends on amino acids inside the lysosomal lumen, implying that autophagic protein degradation is a positive regulator of MTOR in this setting. Since decreased MTOR activity results in autophagy induction, drug treatments that block autolysosomal degradation (a commonly used technique to estimate autophagic flux) may actually interfere not only with lysosomal breakdown, but also increase autophagosome generation through impaired MTOR signaling.

Autophagy ensures the autophagosome-mediated transport of cytoplasmic material to lysosomes for degradation and re-use. By now it has become widely accepted that analyzing the number of autophagy-related structures alone is an inadequate measure of autophagic degradation activity (flux), as increased autophagosome numbers can reflect both their accelerated generation or decreased clearence. Similarly, the number and size of autolysosomes depend on both 'input': material delivered by autophagosomes, and 'output': material degraded and recycled back to the cytoplasm for re-use. The levels of activated, lipidated Atg8/MAP1LC3 family proteins (mostly referred to as Atg8-II or LC3-II) are increased during autophagy induction which can be easily followed in western blot experiments, but since Atg8 molecules linked to the inner autophagosomal membrane are subject to degradation in autolysosomes, their levels also depend on both activation (i.e. autophagy induction) and degradation (i.e. breakdown in autolysosomes).[1]

One popular method for the estimation of autophagic flux is to carry out experiments in the absence and presence of lysosomal protease inhibitors (such as leupeptin), intralysosomal pH neutralizing agents (such as chloroquine), or drugs that inhibit the vacuolar type H^+-ATPase (v-ATPase) complex necessary for lysosomal acidification (such as bafilomycin A_1). These treatments block autophagic degradation at a step downstream of autophagosome formation, allowing one to make a direct comparison of autophagosome numbers or lipidated Atg8/LC3 levels with experiments done without using these drugs.[1]

MTOR (mechanistic target of rapamycin) is a serine/threonine kinase that integrates multiple signals such as growth factor abundance with intracellular amino acid and ATP levels to coordinate cell growth and autophagy. MTOR promotes translation in a number of ways including the activation of RPS6KB1/2 (ribosomal protein S6 kinase, 70 kDa, polypeptide 1/2) and inhibition of EIF4EBP1 (eukaryotic translation initiation factor 4E binding protein 1) and blocks autophagy by inhibiting the Atg1/ULK1 (unc-51-like kinase 1) kinase complex.[2] MTOR is rapidly inactivated upon starvation that results in autophagy induction typically peaking at 2–4 h depending on the experimental system. Recent papers showed that autophagy is required for the re-activation of MTOR and repression of autophagy during prolonged starvation, and that amino acids inside lysosomes

Keywords: Atg8, autophagy, bafilomycin A_1, chloroquine, LC3, leupeptin, lysosome, MTOR, TOR, v-ATPase

Submitted: 06/25/12

Revised: 07/17/12

Accepted: 07/19/12

http://dx.doi.org/10.4161/auto.21544

Correspondence to: Gábor Juhász;
Email: szmrt@elte.hu

©2012 Landes Bioscience. Do not distribute.

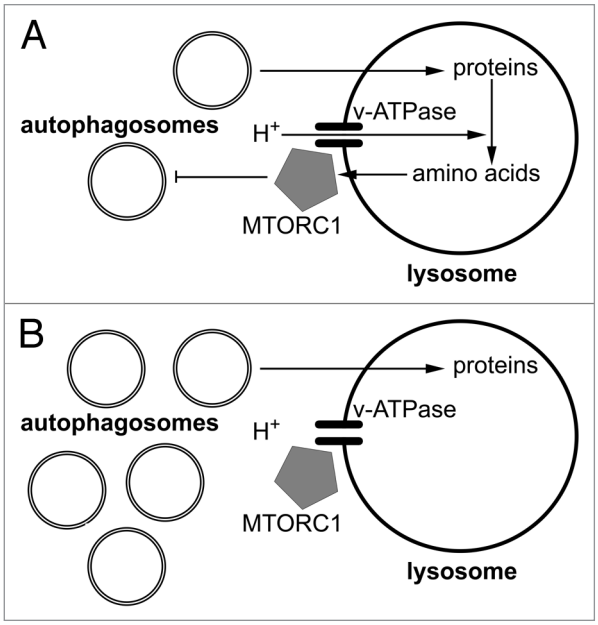


Figure 1. Schematic representation of the connection between autophagy and MTOR signaling mediated by lysosomes. (A) Induction of autophagy results in autophagosome-mediated delivery of proteins to lysosomes. The v-ATPase complex ensures optimal acidic pH for lysosomal proteases that break down proteins into amino acids, which in turn activate MTOR complex 1 associated with the v-ATPase complex. MTORC1 activation then results in feedback inhibition of autophagosome generation. (B) Inhibition of the v-ATPase proton pump, neutralization of lysosomal acidity or block of lysosomal proteases decreases autophagic protein degradation and intralysosomal amino acid levels, likely leading to MTORC1 inactivation and increased formation of autophagosomes.

are necessary for MTOR activity.[3,4] Also, the ragulator complex required for amino acid-induced MTOR activation recruits MTOR complex 1 to the v-ATPase complex and ensures the localization of active MTOR on lysosomes (**Fig. 1A**).[5]

In light of these new results, we may need to re-evaluate the use of inhibitors that block lysosomal protein degradation for autophagic flux. Bafilomycin, chloroquine and protease inhibitor treatments are very likely to interfere with MTOR activity, potentially resulting in further acceleration of autophagosome formation unless MTOR is already completely inactive in the experimental setting (**Fig. 1B**). Therefore, estimating MTOR activity by looking at phospho-RPS6KB1/2 and phospho-EIF4EBP1 levels should be an essential part of flux assays that involve these drug treatments. Along these lines, finding of a drug or genetic mutation that specifically blocks only the fusion of autophagosomes with endosomes or lysosomes and not other vesicle fusion events would provide a useful tool for the autophagy community.

Acknowledgments

Work in the author's lab is funded by the Wellcome Trust (087518/Z/08/Z) and the Hungarian Scientific Research Fund (OTKA K83509).

References

1. Klionsky DJ, Abdalla FC, Abeliovich H, Abraham RT, Acevedo-Arozena A, Adeli K, et al. Guidelines for the use and interpretation of assays for monitoring autophagy. Autophagy 2012; 8:445-544; http://dx.doi.org/10.4161/auto.19496.
2. Neufeld TP. TOR-dependent control of autophagy: biting the hand that feeds. Curr Opin Cell Biol 2010; 22:157-68; PMID:20006481; http://dx.doi.org/10.1016/j.ceb.2009.11.005.
3. Yu L, McPhee CK, Zheng L, Mardones GA, Rong Y, Peng J, et al. Termination of autophagy and reformation of lysosomes regulated by mTOR. Nature 2010; 465:942-6; PMID:20526321; http://dx.doi.org/10.1038/nature09076.
4. Zoncu R, Bar-Peled L, Efeyan A, Wang S, Sancak Y, Sabatini DM. mTORC1 senses lysosomal amino acids through an inside-out mechanism that requires the vacuolar H(+)-ATPase. Science 2011; 334:678-83; PMID:22053050; http://dx.doi.org/10.1126/science.1207056.
5. Sancak Y, Bar-Peled L, Zoncu R, Markhard AL, Nada S, Sabatini DM. Ragulator-Rag complex targets mTORC1 to the lysosomal surface and is necessary for its activation by amino acids. Cell 2010; 141:290-303; PMID:20381137; http://dx.doi.org/10.1016/j.cell.2010.02.024.

©2012 Landes Bioscience. Do not distribute.

Autophagy 8:7, 1124–1135; July 2012; © 2012 Landes Bioscience
dc_840_14

Loss of the starvation-induced gene Rack1 leads to glycogen deficiency and impaired autophagic responses in Drosophila

Balázs Érdi,[1†] Péter Nagy,[1†] Ágnes Zvara,[2] Ágnes Varga,[1] Karolina Pircs,[1] Dalma Ménesi,[2] László G. Puskás[2] and Gábor Juhász[1,*]

[1]Department of Anatomy, Cell and Developmental Biology; Eötvös Loránd University; Budapest, Hungary; [2]Laboratory of Functional Genomics; Biological Research Center; Tzeged, Hungary

[†]These authors contributed equally to this work.

Keywords: antimicrobial peptides, Atg8, autophagy, Drosophila, fat body, glycogen, GSK-3B, microarray, Rack1, starvation

Autophagy delivers cytoplasmic material for lysosomal degradation in eukaryotic cells. Starvation induces high levels of autophagy to promote survival in the lack of nutrients. We compared genome-wide transcriptional profiles of fed and starved control, autophagy-deficient *Atg7* and *Atg1* null mutant Drosophila larvae to search for novel regulators of autophagy. Genes involved in catabolic processes including autophagy were transcriptionally upregulated in all cases. We also detected repression of genes involved in DNA replication in autophagy mutants compared with control animals. The expression of *Rack1* (receptor of activated protein kinase C 1) increased 4.1- to 5.5-fold during nutrient deprivation in all three genotypes. The scaffold protein Rack1 plays a role in a wide range of processes including translation, cell adhesion and migration, cell survival and cancer. Loss of *Rack1* led to attenuated autophagic response to starvation, and glycogen stores were decreased 11.8-fold in *Rack1* mutant cells. Endogenous Rack1 partially colocalized with GFP-Atg8a and early autophagic structures on the ultrastructural level, suggesting its involvement in autophagosome formation. Endogenous Rack1 also showed a high degree of colocalization with glycogen particles in the larval fat body, and with Shaggy, the Drosophila homolog of glycogen synthase kinase 3B (GSK-3B). Our results, for the first time, demonstrated the fundamental role of Rack1 in autophagy and glycogen synthesis.

Introduction

The proper balance of anabolic and catabolic processes ensures cellular and organism-wide homeostasis under physiological conditions. Major intracellular catabolic pathways include the ubiquitin-proteasome system, responsible for the regulated degradation of selected proteins and autophagy, capable of degrading all intracellular macromolecules and even whole organelles. The major pathway of autophagy utilizes double-membrane vesicles called autophagosomes to deliver cytoplasmic cargo for degradation in lysosomes.[1] Basal levels of autophagy are required to prevent the accumulation of abnormal protein aggregates that are detrimental for cell function and survival, especially in long-lived cells such as neurons.[2-5] Autophagic activity is tightly controlled in all cells: factors increasing cell growth rate usually decrease, while nutrient or growth factor deprivation dramatically increases the levels of autophagy.[1]

A set of about 20 evolutionarily conserved genes required for autophagy has been identified in yeast. These *Atg* (autophagy-related) gene products orchestrate the formation of early autophagic structures where autophagosome generation takes place.[6] The Atg1 protein kinase complex is directly controlled by TOR (target of rapamycin), a kinase that coordinates growth-promoting stimuli with the availability of nutrients, ATP and oxygen. Inactivation of TOR rapidly activates the Atg1 complex, resulting in autophagy induction.[7] Autophagy also requires a specific phosphatidylinositol-3-kinase (PtdIns3K) complex, the transmembrane protein Atg9 and factors involved in its cycling from cellular reservoirs to phagophore assembly sites, and two ubiquitin-like protein conjugation systems that ensure lipidation and membrane association of the ubiquitin-like protein Atg8. Atg8 is associated with the surface of autophagosomes similar to a coat protein. Atg8 needs to be cleaved off from the outer membrane to allow the fusion of autophagosomes with lysosomes and endosomes, while the Atg8 pool associated with the inner membrane is degraded along with sequestered cargo in autolysosomes.[8,9] This way, half of these Atg8 protein molecules are broken down in each autophagosomal cycle.[10]

Yeast studies found that the levels of Atg8 can become rate-limiting during autophagy, and that upregulation of this gene is normally observed during induction.[1] In higher eukaryotes, increased transcription from *Atg8* homologs and other *Atg* genes has been documented in certain settings, for example in murine muscles, or in Drosophila fat body and salivary gland cells at the

*Correspondence to: Gábor Juhász; Email: szmrt@elte.hu
Submitted: 09/14/11; Revised: 03/19/12; Accepted: 03/19/12
http://dx.doi.org/10.4161/auto.20069

onset of metamorphosis, but not in all cases of autophagy induction.[11-15] Basal levels of Atg proteins and the extent of autophagy induction must together determine if transcriptional upregulation of these genes is necessary during the response. The presence of multiple homologs of a single yeast gene may also supply enough proteins to support autophagy induction. Interestingly, the *Atg8* gene family has expanded in higher eukaryotes, for example there are two members in Drosophila (*Atg8a* and *Atg8b*), and five in mammals with specialized functions during autophagosome formation (*GABARAP*, *GABARAPL1*, *GABARAPL2*, *GABARAPL3* and *MAP1LC3*—this latter gene also produces four different protein isoforms).[6,16]

Drosophila is an excellent model for autophagy studies, as polyploid tissues like the fat body grow rapidly during the larval stages, and store nutrients to support metamorphosis later on. Therefore, low levels of autophagy are observed during the feeding period in larval stages L1 (approximately 24–48 h after egg laying—AEL), L2 (48–72 h AEL) and most of L3 (72–120 h AEL). Larvae leave the food at around 108 h AEL (the onset of the wandering period) to find a proper, dry place for pupariation, which is observed around 120 h AEL. Robust induction of autophagy is seen in the larval fat body and midgut in wandering larvae, or in response to starvation during earlier stages.[17,18]

We have previously used transcription profiling to search for gene expression changes in dissected fat bodies of feeding and wandering animals. By following the expression levels of 3,200 genes, we found that Atg8 homologs were upregulated, and we have successfully shown that the downregulated gene *FKBP39* (FK506-binding protein of 39 kD) is an inhibitor of autophagy. FKBP39 likely acts by inhibiting the transcription factor Foxo, and we found for the first time that Foxo is an important positive regulator of autophagy.[15] Since then, Foxo-dependent transcriptional upregulation of *Atg8* homologs during autophagy has been described in murine muscles.[11,12]

We reasoned that a similar strategy could be applied by looking at gene expression changes during starvation. An earlier study reported a whole-genome analysis of starvation responses in 48 h AEL (L2 stage) larvae, and found the transcriptional induction of only *Atg8a* (annotated as *CG1534* at that time) and *Atg9* of all the autophagy genes.[19] We decided to use a more sensitive newer generation microarray platform to test 86 h AEL (L3 stage) larvae as these are used in most cases for studies on starvation-induced autophagy. In addition, this time point is after the developmental milestone known as the '70 h change.' This simply refers to the observation that all larvae before 70 h AEL die in a few days upon complete starvation, while a fraction of the larvae past 70 h AEL (near the L2- to L3-molt) that have presumably accumulated appropriate nutrient stores to sustain metamorphosis are able to pupariate and give rise to small adults.[20]

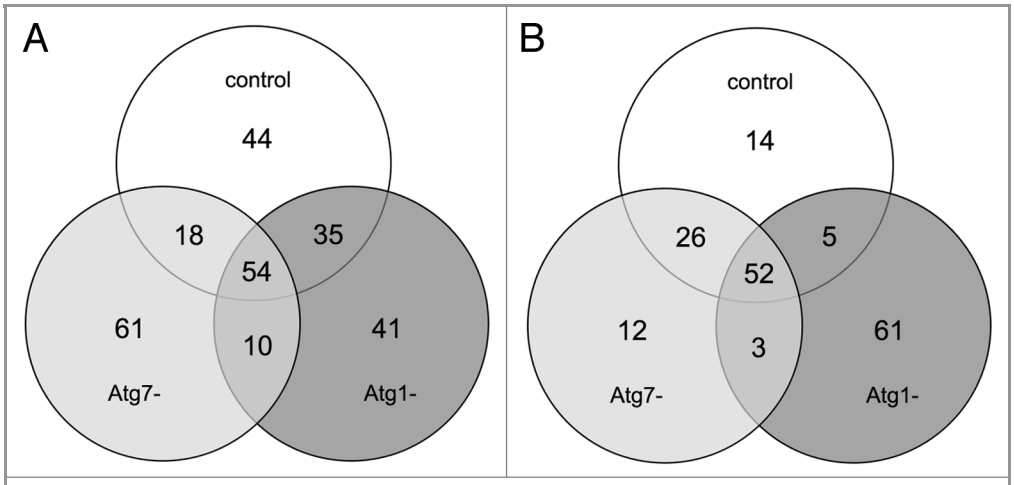
Results

Microarray analysis of starvation-induced autophagy in Drosophila larvae. We compared genome-wide expression changes of 86 h AEL control larvae subjected to a 4-h complete starvation to their well-fed siblings. We have also analyzed previously described autophagy-deficient null mutants for *Atg7* (on a similar genetic background with control larvae) and *Atg1* (from a distinct genetic background), with the purpose of finding gene networks that are specifically regulated in starved autophagy mutants.[3,21] Genes that showed at least a two-fold induction or repression with a p value < 0.05 were considered regulated. We found that the expression of 2,819 vs. 3,690 and 3,971 of 13,613 genes (represented by unique FBgn identifiers)[22] was starvation-regulated in controls, *Atg7* and *Atg1* mutants, respectively. Please see **Table S1** for detailed results.

Genes encoding antimicrobial peptides such as Drosomycin and IM10 (immune-induced molecule 10) were among the most highly upregulated genes in all three genotypes (**Table S2**). Growth/insulin signaling is inhibited in response to starvation, which activates the transcription factor Foxo (forkhead box, subgroup O).[15] Induction of these immune effector molecules is directly controlled by Foxo.[23] The FoxA/Forkhead transcription factor target gene *CG6770* which is transcriptionally induced upon inhibition of TOR was also induced 37- to 95-fold.[19,24] Another highly upregulated gene was *CG7224,* encoding a small, 118-amino acid protein. As it was transcriptionally induced 19.5- to 30.5-fold in the different genotypes, we named this gene *Sirup* (starvation-upregulated protein). Interestingly, expression of *Sirup* and its paralog *CG15283* was also induced during developmental autophagy of the fat body.[15]

Of the 20 genes showing the strongest downregulation, only two were found in all three genotypes: *CG15615* encoding an oxidoreductase (36- to 61-fold repression) and *CG15155* encoding a transferase that transfers acyl groups other than amino-acyl groups (30- to 60-fold repression; **Table S3**). The biological processes in which these gene products are involved are not known, and no phenotypic data are available for these genes.

We performed gene ontology (GO) analysis of the significantly regulated genes in the three different genotypes (**Fig. 1A and B**; **Tables S4 and S5** for details). The analysis revealed that genes belonging to 10 enriched GO categories were specifically induced in autophagy mutants (please see **Table S6** for a list of induced genes in these 10 Atg mutant-specific enriched GO categories). Some of these GO categories that are high in the hierarchy of GO terms (such as GO0009056: catabolic process) included genes that were also present in other, more specific GO groups enriched in all three genotypes, which is a clear limitation of GO analyses. Nevertheless, these groups include genes involved in the metabolism of purine nucleotides and in various catabolic processes, such as *CG9363* encoding an enzyme involved in the breakdown of tyrosine and L-phenylalanine. Numerous genes encoding members of the ubiquitin-dependent protein catabolic process were also found here, including *CHIP*, *CG1950*, *CG4661*, *CG18341* and *Ubc84D*.[22] Only 3 enriched GO terms were specific for autophagy mutants among repressed genes (please see **Table S7** for a list of repressed genes in these 3 Atg mutant-specific enriched GO categories). Genes in these categories encode proteins involved in DNA metabolism, amplification and replication, such as DNA polymerases CG8142, DNA polymerase α 73 kD and 180 kD, DNA polymerase delta, and essential DNA replication factors Mcm5



C

	control	Atg7	Atg1	Yeast Name	Drosophila Name	Drosophila CG number	Human Name
Atg1 complex	2	2.8	3.1	Atg1	Atg1	CG10967	ULK1
	1.2	1.3	1.6	Atg13	Atg13	CG7331	Atg13
	4.6	3	2.6	Atg17?	FIP200	CG1347	RB1CC1, FIP200
	2.5	3.7	4.3	-	Atg101	CG7053	Atg101
PI3P signaling	2.2	1.8	2.5	Atg6	Atg6	CG5429	Beclin1
	1.2	1.3	1.6	Atg14	Atg14	CG11877	Atg14L, Barkor
	1.8	2	1.9	Vps15	Vps15, ird1	CG9746	Vps15, p150
	2	2.6	2.7	Vps34	Vps34, PI3K59F	CG5373	Vps34, PIK3C3
	2.3	3.1	3.4	-	EDTP	CG6542	Jumpy, MTMR14
Pre-autophagosomal cycling complex	2.8	3.4	3.3	Atg2	Atg2	CG1241	Atg2
	3.7	5.5	4.9	Atg9	Atg9	CG3615	Atg9
	3.2	4.3	4.5	Atg18	Atg18a	CG7986	WIPI2
	6.5	7.7	4.3	Atg18	Atg18b	CG8678	WIPI2
Ubiquitin-like conjugation systems	1.9	1.6	1.8	Atg3	Atg3, Aut-1	CG6877	Atg3
	2.2	2.7	2.9	Atg4	Atg4a	CG4428	Atg4b
	0.7	0.7	0.9	Atg4	Atg4b	CG6194	Atg4d
	1.3	1.3	1.5	Atg5	Atg5	CG1643	Atg5
	2.9	2.3	2.8	Atg7	Atg7	CG5489	Atg7
	7.6	9.3	8.3	Atg8	Atg8a	CG32672	GABARAPL2
	2.3	3.8	2.2	Atg8	Atg8b	CG12334	GABARAPL1
	0.6	0.6	0.5	Atg10	Atg10	CG12821	Atg10
	1.2	0.9	0.9	Atg12	Atg12	CG10861	Atg12
	2.1	1.9	2.1	Atg16	Atg16	CG31033	Atg16
Cargo selection	2.4	2.8	3.4	-	Blue cheese	CG14001	ALFY
	5.1	6.6	6.2	-	Ref(2)P, p62	CG10360	p62, SQSTM1

0 10
fold change

D

QTPCR	
4.1	Atg1
3	Atg13
3.1	FIP200
2.2	Atg101
5.2	Atg6
4.6	Atg14
6	Vps15, ird1
5.7	Vps34
6.5	EDTP
24	Atg2
15	Atg9
11	Atg18a
35	Atg18b
3.7	Atg3, Aut-1
23	Atg4a
8.4	Atg4b
7.6	Atg5
3.2	Atg7
169	Atg8a
118	Atg8b
N/A	Atg10
55	Atg12
7.2	Atg16
10	Blue cheese
4.8	Ref(2)P

Figure 1. Transcriptional analysis of starvation responses. The number of gene ontology (GO) terms enriched ($p < 0.05$) among the significantly upregulated (A) and downregulated (B) genes (minimum two-fold change in expression level during the 4-h complete starvation, $p < 0.05$) in control, *Atg7* and *Atg1* mutant larvae. See text and **Tables S4 and S5** for details. (C) lists starvation-induced transcriptional changes (gene expression levels in starved animals relative to the expression levels detected in fed animals) for Drosophila homologs of yeast and human *Atg* genes, involved in the core mechanism of autophagy. *Atg8a* encoding a ubiquitin-like protein showed the highest induction during starvation. Interestingly, the highest average upregulation was observed for genes encoding members of the Atg9 cycling complex. (D) Quantitative real-time (QT) PCR analysis of fat bodies dissected from fed and starved control larvae. Numbers represent fold change values, and nonsignificant changes are crossed out in (C and D).

(Minichromosome maintenance 5), Mcm10, disc proliferation abnormal, replication factor C subunits RfC3 and RfC38, double parked, DNA ligase I, SuUR (suppressor of under-replication), mus209/PCNA (proliferating cell nuclear antigen) and origin recognition complex subunit 2.[22]

Interestingly, we detected many more genes significantly regulated upon a 4-h complete starvation when compared with an earlier study.[19] Zinke et al. reported 369 and 279 genes significantly induced or repressed, respectively, while we found that 1,584 and 1,235 genes were significantly up- or down-regulated in control larvae, respectively. Comparing the list of hits revealed that 170 genes were found induced and 134 repressed in both studies (please see **Tables S8 and S9** for a list of these genes), which is almost half of all genes identified by Zinke et al. While some of these differences are likely due to the different genetic backgrounds and larval stages tested, we are convinced that our approximately 4.3-fold higher discovery rate is mostly due to the use of a different, more sensitive microarray. This is further supported by a previous study that compared different microarray technologies and found that the long oligonucleotide platform (such as in the case of our study utilizing arrays printed with 60-mer oligos) is more sensitive and produces lower levels of technical variability when compared with cDNA-based systems (used by Zinke et al.).[25]

Most autophagy genes are transcriptionally induced during starvation. Several GO terms that include *Atg* genes (such as GO0048102: autophagic cell death) were found enriched among the upregulated genes in all three genotypes. To focus more on autophagy, we looked at the expression of *Atg* gene homologs. Many of these genes showed increased induction in autophagy mutants compared with controls (**Fig. 1C**). Expression from the *Atg7* and *Atg1* loci was still observed in the mutants; since these alleles had been previously characterized as genetic nulls, presumably truncated versions of wild-type transcripts were detected.[3,21]

Of the genes encoding members of the Atg1 kinase complex, *Atg1*, *FIP200* and *Atg101* showed a moderate induction, while the levels of *Atg13* did not change. This is in agreement with recent findings that Atg13 is continuously degraded by the ubiquitin-proteasome system, and it is stabilized by the binding of Atg101 during autophagy induction.[26,27] Therefore, Atg13 protein levels appear to be mainly regulated on the post-translational level. It is important to note that *Atg101* showed the highest upregulation in this group (on average 3.5-fold in the 3 different genotypes), but it was mostly due to its stronger induction in autophagy mutants. In controls, *FIP200* shows the highest induction in this group (4.6-fold).

Genes encoding members of the autophagy-specific PtdIns3K complex (Vps34, Vps15, Atg6, Atg14) showed an even milder response: only *Vps34* that codes for the lipid kinase itself was upregulated in all three genotypes. To our surprise, *EDTP* (Egg-derived tyrosine phosphatase) showed the highest average induction in this lipid signaling group: 2.9-fold. This gene encodes the Drosophila homolog of the lipid phosphatase Jumpy, a potent antagonist of the autophagy-promoting activity of Vps34 in mammals.[28] The upregulation of a potential inhibitor of autophagy may represent a negative feedback loop that acts to prevent hyperactivation. Elucidation of this hypothetical mechanism needs further studies.

Interestingly, genes encoding members of the pre-autophagosomal cycling complex showed the strongest average induction, between 3.2- and 6.2-fold. Atg9 is the only transmembrane protein among *Atg* gene products, and it has been shown to cycle between early autophagic structures and potential intracellular membrane sources to ensure membrane transport to forming autophagosomes. Atg2 and Atg18 are required for the cycling of Atg9 in yeast.[29]

Half of the genes (5/10) encoding members of the ubiquitin-like protein conjugation systems did not even show an upregulation. *Atg4a*, *Atg7*, *Atg8b* and *Atg16* were moderately induced, while the highest upregulation of all the *Atg* genes was detected for *Atg8a*, 8.4-fold on average.

Atg8a itself is a specific cargo selectively degraded during autophagy. Additional substrates have also been described, such as p62/Ref(2)P, which is an intracellular receptor of ubiquitinated proteins for selective autophagy, in addition to its scaffolding roles in multiple signaling pathways. p62 binds to Atg8 homologs, so it is continuously degraded during autophagy.[30] We found that *p62* is transcriptionally induced 6-fold during starvation, potentially in part to compensate for its accelerated rate of degradation during increased autophagy. A more moderate upregulation was detected for *Blue cheese/Alfy*, whose protein product is involved in the selective degradation of cytosolic protein aggregates.[31]

Next we sought to expand on our findings obtained by microarray analysis of starved whole larvae by focusing on the fat body. We followed the expression of selected genes by quantitative real-time PCRs, comparing fat bodies dissected from starved vs. fed control larvae (**Fig. 1D**). These QT-PCR experiments further supported our most important findings: among the genes encoding members of the Atg1 kinase and lipid kinase complexes *EDTP* showed the highest upregulation (6.5-fold), which is still moderate when compared with genes that showed the strongest induction. *Atg8a* was by far the most highly upregulated gene (169-fold), and all members of the membrane transport group were strongly induced (11- to 35-fold). The expression of *Sirup* also increased 60.4-fold. There were also important differences, such as in the case of *Atg5* that showed a 7.6-fold upregulation in fat bodies while no significant change was detected in whole larvae, as it was probably masked by other tissues.

Rack1 is required for a full autophagic response to starvation. We selected a set of genes for further studies that were starvation-regulated in all three genotypes, and no autophagic function had been assigned to these in spite of having been already characterized to some extent. For example, *Rack1* transcription increased 4.1-, 5.5- and 4.1-fold in controls, *Atg7* and *Atg1* mutants, respectively. QT-PCR analysis also showed that *Rack1* was upregulated 21.6-fold in the fat body upon starvation.

Silencing of *Rack1* expression reduced autophagy based on mCherry-Atg8a (**Fig. 2A and N**), Lysotracker Red staining and Lamp-GFP, a reporter for lysosomes.[32] Numerous small, presumably inactive Lamp-GFP positive lysosomes were seen in

fat body cells of well-fed control larvae, which were not strongly acidic as revealed by lack of Lysotracker Red labeling (**Fig. 2B**). In contrast, large Lamp-GFP and Lysotracker-positive autolysosomes were formed during starvation (**Fig. 2C**). Silencing of *Rack1* reduced the number and size of Lysotracker and Lamp-GFP positive autolysosomes formed during starvation (**Fig. 2D**, see also **Fig. 2O–Q** for statistics).

To expand on these RNAi studies we have also analyzed a previously described null mutant *Rack1[1.8]*.[33] Using the same mCherry-Atg8a and Lysotracker assays, we observed again a strong reduction of autophagy in *Rack1* mutants compared with heterozygous controls (**Fig. 2E–H**; see also **Fig. 2N and O** for statistics). As a final proof for the role of Rack1 in autophagy, we have generated transgenic animals expressing Rack1 with a C-terminal FLAG-HA tag by using a DNA construct from the ongoing Drosophila proteomics project. Heat shock-mediated expression of Rack1 in mutant larvae partially rescued their autophagy defect (**Fig. 2I and O**). To avoid a possible effect of the heat shock on autophagy, all genotypes were heat shocked in these Lysotracker and electron microscopy experiments (see below).

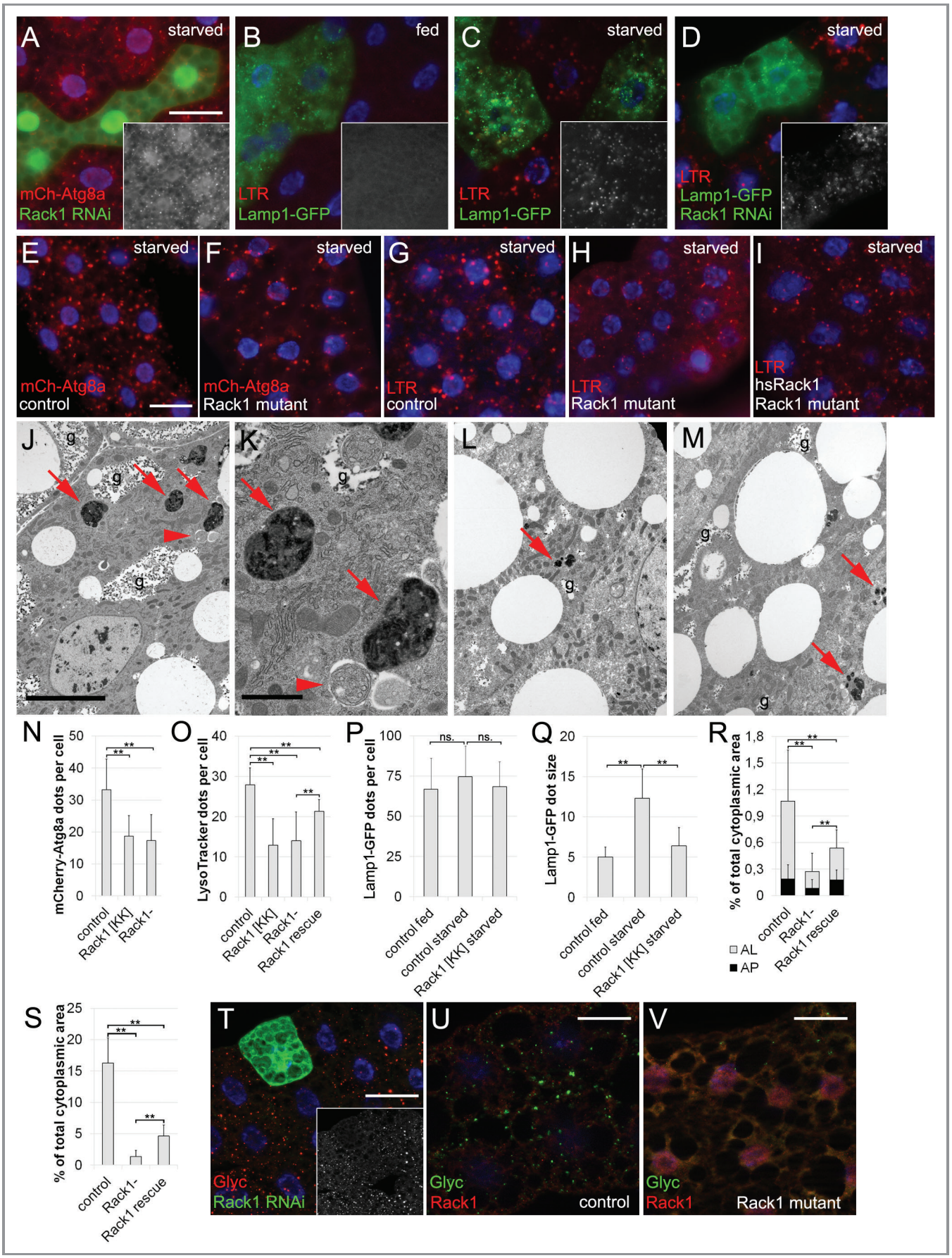
Similar to the above findings, ultrastructural analysis showed that while numerous autophagosomes and large autolysosomes were observed in heterozygous controls, the cumulative area of these structures was decreased in cross-sections of *Rack1* mutant fat body cells, and heat shock-mediated expression of Rack1 in mutant larvae again showed a partial rescue (**Fig. 2J–M**; see **Fig. 2R** for statistics). The partial rescue effect may reflect insufficient expression levels, or more likely it may be caused by the C-terminal tag interfering with full protein activity. Still, the reduction of autophagosome area was completely rescued in these experiments ($p = 0.02$ for mutant and rescue, and $p = 0.84$ for control and rescue sample pairs, respectively), suggesting that Rack1 is required for efficient autophagosome formation (**Fig. 2L**).

Interestingly, we found that Rack1 was dispensable for developmental autophagy induced in fat body and midgut cells prior to metamorphosis in late L3 stage wandering animals (**Fig. S1C and S1D**). In contrast, p62 aggregates accumulated in Rack1 RNAi cells in well-fed early L3 stage animals (**Fig. S1E and S1F**). This finding suggests that Rack1 is also involved in basal autophagy, as the ubiquitin- and Atg8-binding protein p62 is continuously degraded by autophagy along with aggregated ubiquitinated proteins.[30]

Rack1 is involved in glycogen synthesis. Glycogen stores are normally present in fat body, midgut and muscle cells in Drosophila larvae. A striking phenotype of these *Rack1* mutant fat body cells was the 11.8-fold reduction of glycogen particle area compared with heterozygous controls in electron micrographs, and this effect was also partially rescued by Rack1 expression (**Fig. 2J–M**; see **Fig. 2S** for statistics). Reduced glycogen stores were most likely caused by defects in glycogen synthesis induced by the 4 h starvation in 20% sucrose rather than accelerated degradation, as no glycogen particles could be observed in fat bodies of well-fed control or *Rack1* mutant larvae (**Fig. S1A and S1B**). In these latter cases, the lack of glycogen was probably due to the high-protein diet that we routinely feed larvae before starving them, by supplementing the medium with live yeast paste. Taking advantage of a monoclonal antibody specific for glycogen, we were also able to show that silencing of *Rack1* decreased glycogen stores in a cell-autonomous manner in larvae fed a high sugar-high protein diet, that is, medium supplemented with live yeast paste prepared in 20% sugar; similar phenotypes were observed in mutants (**Fig. 2T–V**).

Endogenous Rack1 localizes to early autophagic structures and glycogen. Immunofluorescence analysis revealed that Rack1 is present in numerous cytoplasmic particles in most tissues. Knockdown of *Rack1* expression reduced staining both in fat body and midgut cells (**Fig. 3A and B**). To assess the potential role of Rack1 in autophagy, we performed colocalization experiments. Atg8a fusion proteins are the best characterized fluorescent reporters for autophagosome generation. We found that endogenous Rack1 colocalized with GFP-Atg8a in 5.8% of the cases (n = 10/171 dots) (**Fig. 3C**). Vice versa, 6.1% of GFP-Atg8a particles colocalized with Rack1 (n = 11/181 dots). In contrast, not a single case of colocalization was observed between endogenous Rack1 and the lysosome reporter Lamp1-GFP (**Fig. 3D**). We next used immunogold labeling of endogenous Rack1 to localize it on the ultrastructural level. We found that Rack1 was associated with 7.7% of pre-autophagosomal phagophores and autophagosomes (n = 17/221) (**Fig. 3E**; see also **Fig. 3G**). Again, no labeling of lysosomes was seen.

Figure 2 (See opposite page). Rack1 is required for the full autophagic response to starvation, and for efficient glycogen synthesis. (A) Knockdown of *Rack1* results in reduction of autophagy in response to starvation. Please compare the number of mCherry-positive dots in RNAi cells vs. control cells in each panel (red; the red channel is also shown in greyscale in insets). RNAi expressing cells are marked by coexpression of GFP (green). Cell nuclei are labeled with DAPI (blue). (B) Numerous small Lamp1-GFP dots are seen in fat body cells of well-fed control larvae, which are not co-labeled by Lysotracker Red. (C) In contrast, large Lamp1-GFP and Lysotracker-positive autolysosomes are formed during starvation. (D) Silencing of *Rack1* strongly reduces the number of Lysotracker particles that are formed during starvation; note that the size of Lamp1-GFP dots is also more similar to fed control cells. (E and F) The number of starvation-induced mCherry-Atg8a dots is reduced in *Rack1* null mutant fat bodies compared with controls. (G and H) Similarly, the number of Lysotracker-positive autolysosomes is reduced in *Rack1* mutants compared with controls. (I) Starvation-induced autophagy is rescued by heat shock-mediated expression of a *Rack1* transgene in *Rack1* null mutant animals. (J) Transmission electron microscopy shows the presence of large glycogen stores (g), numerous double-membrane autophagosomes (arrowheads) and autolysosomes (arrows) in fat body cells of control animals starved for 4 h in 20% sucrose. (K) A portion of (J) is shown enlarged. (L) Fewer autophagic structures and glycogen particles are detected in *Rack1* mutants. (M) Heat-shock mediated expression of a *Rack1* transgene in *Rack1* null mutant animals partially rescues the reduced autophagy and glycogen accumulation phenotypes of the mutants. (N–S) Statistical analyses of mutant and RNAi phenotypes on autophagy and glycogen stores. Graphs represent dots/cell (N–P), average dot size (Q) and normalized cytoplasmic area (R and S), $^{**}p < 0.01$ (two-tailed, two-sample unequal variance Student's t-test). (T) Knockdown of *Rack1* expression cell-autonomously decreases glycogen stores. (U and V) No specific Rack1 labeling is observed in *Rack1* mutants, and glycogen stores are strongly decreased compared with heterozygous controls. Scale bars: 30 μm for all fluorescent images (indicated in A, E and T–V), 10 μm for (J, L and M, indicated in J) and 2 μm for (K).


A
starved
mCh-Atg8a
Rack1 RNAi
B
fed
LTR
Lamp1-GFP
C
starved
LTR
Lamp1-GFP
D
starved
LTR
Lamp1-GFP
Rack1 RNAi
E
starved
mCh-Atg8a
control
F
starved
mCh-Atg8a
Rack1 mutant
G
starved
LTR
control
H
starved
LTR
Rack1 mutant
I
starved
LTR
hsRack1
Rack1 mutant
J
K
L
M
g
N
mCherry-Atg8a dots per cell
control
Rack1 [KK]
Rack1-
O
LysoTracker dots per cell
control
Rack1 [KK]
Rack1-
Rack1 rescue
P
Lamp1-GFP dots per cell
ns.
control fed
control starved
Rack1 [KK] starved
Q
Lamp1-GFP dot size
control fed
control starved
Rack1 [KK] starved
R
% of total cytoplasmic area
AL
AP
control
Rack1-
Rack1 rescue
S
% of total cytoplasmic area
control
Rack1-
Rack1 rescue
T
Glyc
Rack1 RNAi
U
Glyc
Rack1
control
V
Glyc
Rack1
Rack1 mutant

Immuno-electron microscopy analysis also identified that endogenous Rack1 localized in the periphery of, or immediately next to glycogen particles in fat body cells, in addition to being present in unidentified cytoplasmic clusters (**Fig. 3F and G**). In indirect immunofluorescence experiments most Rack1-positive dots localized next to or in the periphery of glycogen particles in laser scanning confocal microscopy as well (**Fig. 3H**). 77% of glycogen particles had associated Rack1 dots (n = 426/553), while 48% of Rack1 dots were associated with glycogen (n = 394/822).

The activity of glycogen synthase is a major determinant of glycogen levels. Phosphorylation of glycogen synthase by Shaggy, the Drosophila homolog of glycogen synthase kinase 3B (GSK-3B) promotes glycogen synthesis.[34] A physical interaction between the human homologs of Rack1 and GSK-3B was already reported.[35] In line with that, we found that 73.9% of endogenous Rack1 colocalized with endogenous Shaggy, and 39.4% of Shaggy positive dots were also positive for Rack1 (n = 82/111 and n = 82/208 dots, respectively) (**Fig. 3I**). In contrast, no colocalization was found between Shaggy and GFP-Atg8a (not shown).

Discussion

We have used whole-genome microarrays to identify genes regulated during the starvation response in Drosophila, and also compared gene expression changes between control, *Atg7* and *Atg1* mutant larvae. Based on a gene ontology analysis, genes involved in catabolic processes such as proteasomal degradation and amino acid catabolism were more significantly upregulated in starved autophagy mutants, which is likely a compensatory reaction. On the other hand, genes required for DNA replication were specifically downregulated. Mitotic tissues continue to grow and divide even in Drosophila larvae deprived of all nutrients.[36] Repression of genes required for DNA replication in autophagy mutants suggests that energy-consuming DNA replication processes are strongly inhibited in completely starved autophagy mutants, presumably because polyploid cells are not able to supply nutrients to support diploid cell divisions in the absence of autophagy.

We detected increased transcription of most *Atg* genes upon starvation, and an even higher upregulation was seen for most genes in fat bodies dissected from starved vs. fed animals. The most highly induced gene was *Atg8a* in all cases, in agreement with previous studies that showed the importance of *Atg8* induction during autophagy in various models.[1,12,15] It is important to note that *Atg8b* is mostly expressed in adult testis, and its very low level larval expression is restricted to the fat body.[37] In line with this, mutation of *Atg8a* completely blocks starvation-induced autophagy in the fat body confirming that *Atg8b* expression is unable to sustain autophagy in this setting, although *Atg8b* was also upregulated 118-fold during starvation in the fat body.[21] Induction of *Atg8a* is likely necessary to make up for the degradation of half of its protein products involved in each autophagosomal cycle. Members of the Atg9 cycling complex showed the strongest average upregulation of the functional groups of Atg proteins. We speculate that the sudden induction of autophagy in polyploid larval Drosophila tissues requires a lot of membrane to sustain the high level of autophagosome generation, explaining the increased transcription of genes whose products are required for membrane transport.

In this work we chose Rack1 (receptor of activated protein kinase C 1) for further analysis. *Rack1* was induced in whole animals and in dissected fat bodies during starvation, and loss of *Rack1* impaired both starvation-induced and basal autophagy, while it had no effect on developmentally programmed autophagy of the fat body. These findings indicate that Rack1 is involved in multiple but not all types of autophagy.

Autophagosomes generally have a short half-life of 5–10 min, which is the most likely explanation why basal levels of autophagy are very difficult to visualize in most tissues.[38] In contrast, autophagosomes appear in high numbers during starvation. The autophagosomal compartment was reduced in *Rack1* mutants which was rescued completely by transgenic expression of *Rack1*, and Rack1 was at least transiently associated with phagophore assembly sites and autophagosomes, altogether suggesting that Rack1 is required for efficient autophagosome formation. As we observed no defects in cell size/cell growth, DNA polyploidization or lipid droplet accumulation in *Rack1* loss of function cells, the autophagy defect seems to be a highly specific phenotype and not just a consequence of general problems with normal cellular functions.

Rack1 is an evolutionarily conserved guanine nucleotide-binding scaffold protein with a WD40-repeat: 77% (243/315) of the amino acid residues are identical and 87% (275/315) are similar between Drosophila Rack1 and human GNB2L1. A proteomic study of Atg complexes found that GNB2L1 interacts with human homologs of Atg1, Atg4, Atg14 and Atg18.[39] Although GNB2L1 was not classified as a high-confidence interacting partner, these data support our hypothesis that Rack1 may act as a scaffold, transiently binding multiple Atg proteins at phagophore assembly sites to promote maximal activity. In line with that, it is interesting to note that the potential interacting partners of human Rack1 include a member from all four Atg protein complexes. Further biochemical studies such as co-immunoprecipitation experiments are necessary to verify this hypothetical mechanism.

In addition, half of the Rack1-positive dots localized to glycogen particles, and loss of Rack1 prevented the proper formation of glycogen stores in larval fat body cells. The high degree of colocalization with GSK-3B strongly suggests that Rack1 is associated with a pool of GSK-3B that promotes glycogen synthesis. The known interacting partners of Rack1 include three subunits of AMPK (AMP-activated protein kinase): PRKAA1, PRKAA2 and PRKAB2. The β-subunit of AMPK has a glycogen-binding domain that targets a pool of this kinase to bind the surface of the glycogen particle. Activated AMPK turns on catabolic processes to generate ATP, and it also inhibits glycogen synthesis through direct phosphorylation of glycogen synthase.[40] We hypothesize that a signaling complex containing Rack1, GSK-3B and AMPK assembles on glycogen particles to regulate the rate of synthesis through phosphorylating different amino acid residues of glycogen synthase, with AMPK being responsible for targeting this complex to glycogen. In this scenario, the activity of

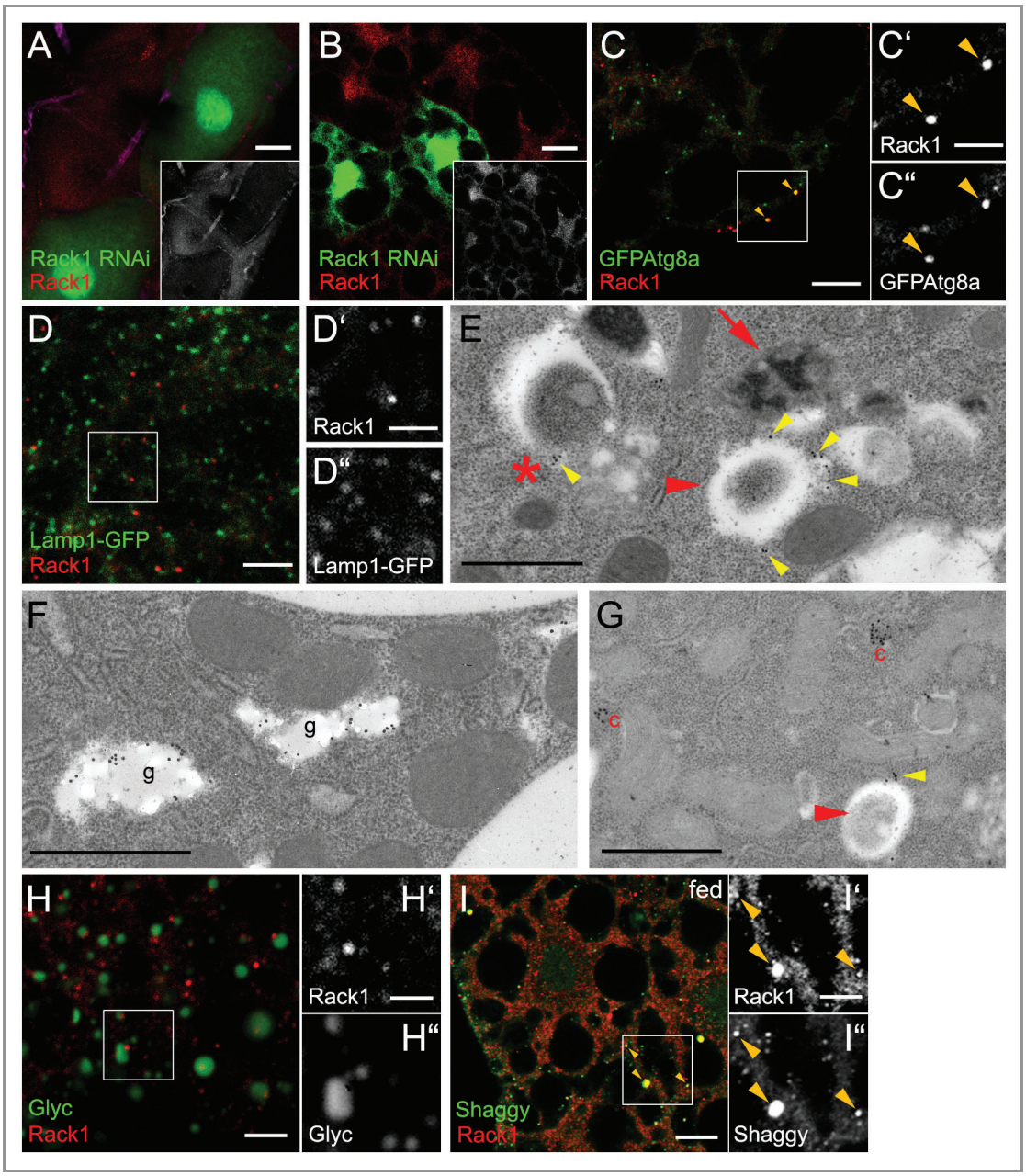


Figure 3. Localization of endogenous Rack1. (A and B) Knockdown of *Rack1* reduces anti-Rack1 immunostaining in both midgut and fat body cells in a cell-autonomous manner. (C) Rack1 shows a partial colocalization with the (pre-) autophagosome reporter GFP-Atg8a. (D) In contrast, no overlap was found between Rack1 and the lysosome reporter Lamp1-GFP. Boxed areas in (C and D) are shown enlarged. (E) Immunogold labeling of Rack1 is associated with a pre-autophagosomal phagophore near the growing edges (asterisk) and an autophagosome (red arrowhead). Please note the characteristic cleft (empty-looking space) between the two membrane sheets of phagophores and autophagosomes, which facilitates their recognition in glutaraldehyde-fixed samples. In contrast, no labeling of a lysosome is observed (arrow in E). Some of the gold particles are highlighted by yellow arrowheads. (F) Gold particles representing endogenous Rack1 are frequently associated with the peripheral parts of glycogen stores (g) in fat body cells. (G) Rack1 is also present in cytoplasmic clusters (c); an autophagosome (red arrowhead) is also labeled (yellow arrowhead). (H and I) Rack1 is closely associated with glycogen granules in the fat body, and it colocalizes with Shaggy, the Drosophila homolog of GSK-3B. Boxed areas of (A and B) are shown enlarged. Scale bars: 10 μm for (A–D, H and I), 5 μm for (C'–D" and H'–I") and 1 μm for (E–G). All colocalization experiments were performed using confocal laser scanning microscopy.

multiple kinases including AMPK and GSK-3B would determine the rate of glycogen synthesis. These interactions may be less relevant for Rack1's role in autophagy for a number of reasons. First, GSK-3B never colocalized with Atg8a, and overexpression of GSK-3B actually inhibits starvation-induced autophagy (our unpublished observation). Second, the exact role of AMPK in starvation-induced autophagy of the fat body is not clear: mutation of *SNF4Aγ* encoding a regulatory subunit of AMPK

has been shown to lead to impaired autophagic responses in mutants, but a more recent report suggested that AMPK mutants show a persistent starvation phenotype that may interfere with further induction of autophagy by additional experimental starvation.[41,42] In line with that, none of the more than 10 different transgenic RNAi and dominant-negative AMPK lines we tested showed any suppression of starvation-induced autophagy in clonal analysis (our unpublished observations), potentially supporting the hypothesis that the autophagy phenotype of AMPK mutants may not be cell autonomous in the Drosophila fat body.

Rack1 was originally described as a cytoplasmic receptor for activated protein kinase C (PKC). The structure of Rack1 resembles that of the β-subunit of heterotrimeric G proteins. The individual WD40 repeats can simultaneously bind to different proteins, making Rack1 a candidate platform for integrating several signaling pathways. Rack1 was shown to physically interact with β-integrin, various kinases including PKC, AMPK, GSK-3B and Src, protein phosphatase 2A, focal adhesion components, and even ribosomes. Indeed, Rack1 plays a role in a wide range of processes including cell adhesion and migration, cell survival and translation.[33,43] Recent findings showed that Rack1 promotes and is required for progression of several types of cancers, and its increased expression predicts poor clinical outcome for breast cancer patients.[44-48]

Here we have shown that Drosophila Rack1 is also involved in the autophagic response to starvation, potentially acting again as a scaffold protein during the formation of autophagosomes. In addition, Rack1 is necessary for the proper generation of glycogen particles in the larval fat body, likely through recruiting Shaggy/GSK-3B to promote glycogen synthesis. Taken together, we have demonstrated that novel roles in autophagy and glycogen synthesis must be added to the already diverse list of functions for Rack1.

Materials and Methods

Drosophila stocks and culture. Flies were raised at 25°C on standard cornmeal/agar media, at 60% humidity and a 12-h light/12-h dark daily cycle. The following stocks were used: *CG5335 [d30], Atg7[d77], Atg7[d14]*,[3] (d14 deletes the promoters and the first parts of both *Atg7* and *Sec6*, d77 deletes both *CG5335* and *Atg7,* and d30 deletes *CG5335* only; therefore, *d77/d14* animals are mutant for *Atg7* only and heterozygous for both *CG5335* and *Sec6*, while *d30/d14* are heterozygous for all three genes), *Atg1 [d3D]*,[21] *UAS-Lamp1-GFP, UAS-GFP-Atg8a*,[49] *hs-Flp; UAS-Dcr2; R4-mCherry-Atg8a, Act > CD2 > Gal4, UAS-GFPnls* (gift of Tom Neufeld), *Df(2L)rack1-mts, Rack1[1.8]*,[33] (the 1.8 allele carries a premature stop codon instead of the sixth amino acid; we used hemizygous animals in trans with the deficiency *Df(2L) rack1-mts* that deletes both *Rack1* and *mts* in all experiments), *hs-Gal4* (Bloomington Drosophila Stock Center, BDSC), and transgenic RNAi lines for *Rack1 KK104470* (designated as Rack1 RNAi throughout the text and figures), *HMS01173* (designated as Rack1 RNAi_2 in **Fig. S1F**) (provided by the Vienna Drosophila RNAi Center, VDRC and BDSC, respectively). Starvations were routinely performed by floating well-fed 72–96 h AEL (after egg laying) larvae on top of a 20% sucrose solution in an Eppendorf tube for 4 h. For complete starvations (no calorie), we placed well-fed animals onto filter papers soaked in PBS. Twenty to 30 larvae were transferred into a new vial amply supplemented with live yeast culture (high protein diet) 12–24 h before starvation to reduce crowding and make sure that all animals were well-fed at the onset of the starvation experiments, which is necessary for a proper autophagic response. For diet high in both protein and sugar, yeast paste was prepared in a 20% sucrose solution.

Microarray analysis. Our microarray experiments conformed to MIAME guidelines, and full data sets are available at www.ebi.ac.uk/arrayexpress under accession number E-MEXP-3352.

Four microarrays were used for analyzing each genotype: two independent fed and starved samples were collected (biological replica), and a dye swap was performed for each fed/starved sample pair (technical replica—please see below). Eighty-six ± 2 h AEL L3 stage larvae were allowed to feed on standard fly food supplemented with yeast (fed) or starved in PBS for 4 h (starved). Approximately 30 mg of larvae were collected and frozen immediately in liquid nitrogen in RNAlater (Sigma, R0901). Total RNA was purified using a NucleoSpin RNA II RNA isolation kit (Macherey-Nagel, 740955). RNA samples were stored at –80°C in the presence of 30 U Prime RNase inhibitor (Fermentas, EO0382). For probe preparation, 1 μg of total RNA were first reverse transcribed in 10 μl volume using Oligo(dT) Primer and ArrayScript enzyme, then the second cDNA strand was synthesized in 50 μl final volume using DNA polymerase and RNase H. Amino allyl modified aRNA were then synthesized by in vitro transcription using aaUTP and T7 Enzyme mix. All these steps were done using AminoAllyl MessageAmp™ II aRNA Amplification Kit (Ambion, AM1753). Six micrograms of amino allyl modified amplified RNA was labeled with either Cy5 or Cy3 dyes in 10 μl volume (GE Healthcare, PA23001, PA25001) and purified using RNA purification columns (Macherey Nagel, 740955). The specific activity and concentration of the labeled aRNA samples was checked by spectrophotometry (NanoDrop 3.1.0, Rockland). 4 × 44 k format Drosophila Gene Expression Microarrays (Agilent, G2519F-021791) were used to determine gene expression changes. 300 ng of Cy5 and Cy3 labeled aRNA in 19 μl volume, 5 μl 10 × blocking agent and 1 μl 25 × fragmentation buffer were mixed together and incubated at 60°C for 30 min. Twenty-five microliters 2× GEx hybridization fuffer was added to each sample to stop the fragmentation reaction. All these steps were done using gene expression hybridization kit (Agilent, 5188-5242). Forty-eight microliters of these mixes were used for the hybridization in microarray hybridization chambers (Agilent, G2534A). The chambers were then loaded into a hybridization rotator rack (~5 rpm) and incubated at 65°C for 17 h. After hybridization the slides were washed in wash buffer 1 (Agilent, 5188-5327) at room temperature for 1 min then in wash buffer 2 at 37°C for another 1 min before scanning. Each array was scanned at 543 nm (for Cy3 labeling) or at 633 nm (for Cy5 labeling) in Agilent Scanner using the built-in XDR (Extended Dynamic Range) function with 5 μm resolution. Output images were analyzed with the Feature

Extraction software from Agilent (ver.9.5.1.1.) using the two-color gene expression protocol (GE2_v5_95_Feb07) to get the raw data. All ratios were normalized using the Lowess normalization method. Two-tailed two-sample unequal variance Student's t-test with a two-fold change cut off was applied to determine which genes showed significantly altered expression levels ($p < 0.05$). Additionally, we applied multiple testing correction (Benjamini-Hochberg method; p value 2 in **Tables S1–S3**) using Genspring to estimate false discovery rate (corrected p value in supplemental tables) associated with such a large number of comparisons.

QT-PCR experiments. RNA samples were prepared from fat bodies dissected from fed and starved control larvae as described above. QT-PCR reactions were performed on 4 independently collected fed and 4 independently collected starved fat body samples. The reactions were performed on a RotorGene 3000 instrument (Corbett Research) with gene-specific primers and SybrGreen protocol to monitor gene expression. Two micrograms of total RNA was reverse transcribed using the High-Capacity cDNA Archive Kit (Applied Biosystems, 4322171) according to the manufacturer's instructions in a final volume of 30 μL. The temperature profile of the reverse transcription was the following: 10 min at room temperature, 2 h at 37°C, 5 min on ice and finally 10 min at 75°C for enzyme inactivation. After dilution with 30 μL of water, 1 μL of the diluted reaction mix was used as template in QT-PCR reactions, using FastStart SYBR Green Master mix (Roche, 04673484001) at a final primer concentration of 250 nM under the following conditions: 15 min at 95°C, 45 cycles of 95°C for 15 sec, 60°C for 25 sec and 72°C for 25 sec. Fluorescence intensity of SYBR Green was detected after each amplification step. Melting temperature analysis was done after each reaction to check the quality of the products. Relative expression ratios were calculated as normalized ratios to *GAPDH*. As an additional control, no significant change was observed in expression from the *Actin5C* locus. Nontemplate control sample was used for each PCR run to check the primer-dimer formation. The final relative gene expression ratios were calculated as ΔΔCt values. Primer sequences are available upon request. Two-tailed two-sample unequal variance Student's t-test was used to calculate p values.

Bioinformatic analysis. GO analysis was performed using DAVID Bioinformatics Resources 6.7 at http://david.niaid.nih.gov.[50] We selected unique FBgn identifiers of genes showing an at least two-fold expression change in response to starvation with $p < 0.05$ from all three genotypes. Separate lists of induced and repressed FBgn identifiers were uploaded, and the GO terms of biological processes functional annotation tool was used for functional annotation clustering with default options. We then compared the significantly enriched ($p < 0.05$) GO categories among the three genotypes. As most genes are represented by multiple 60-mer oligos on the whole-genome microarray, all $p < 0.05$ fold change values were collected for each gene of interest, averaged, and then visualized using JColorGrid for the expression analysis of individual *Atg* genes.[51] BLASTP searches were used to find homologous gene products in yeast, Drosophila and human, and the top-scoring hit is shown for each gene in **Figure 1C**.

Construction of UAS-Rack1 transgenic lines and genetic rescue experiments. The pUAST-Rack1-FLAG-HA clone UFO04269 was obtained from DGRC (Drosophila Genomics Resource Center). Following sequencing, standard PhiC31-mediated transformation procedures were used to obtain transgenic Drosophila lines carrying *UAS-Rack1* on a 65B2 platform chromosome (Bestgene). Expression of *UAS-Rack1* was induced with hs-Gal4 in a *Rack1* null mutant background by a 1 h heat shock at 37°C, followed by a 4 h starvation.

Histology and imaging. Clonal analysis in polyploid larval Drosophila tissues and Lysotracker stainings were performed as described previously.[21,49] For statistics, Lysotracker, mCherry-Atg8a and Lamp1-GFP puncta were manually counted in Photoshop. Two-tailed two-sample unequal variance Student's t-test was used to calculate p values. The following antibodies were used for immunostainings: rabbit polyclonal anti-Rack1 (1:500, gift from Julie Kadrmas),[33] mouse monoclonal anti-glycogen (1:20, gift from Otto Baba),[52] mouse monoclonal anti-Shaggy (4G1E11, 1:100, gift from Marc Bourouis),[34] mouse monoclonal anti-GFP (1:1,000, Invitrogen, A11120), Alexa488-conjugated goat anti-mouse (Invitrogen, A11001, 1:1,000), Alexa568-conjugated goat anti-rabbit (Invitrogen, A21069, 1:1,000). A Zeiss Axioimager M2 microscope equipped with an Apotome2 unit and a Plan-NeoFluar 40× 0.75 NA objective was used to capture images with Axiovision software using MinMax setting for automatically adjusting image levels. Confocal images were acquired on an Olympus FV500 laser scanning microscope with a 63× 1.45 NA oil-immersion objective in sequential scanning mode. Primary images were processed in Adobe Photoshop to produce final figures.

Transmission electron microscopy (TEM). Tissues were processed for TEM analysis as described previously.[49] For immuno-electron microscopy, rabbit polyclonal anti-Rack1 (1:50) was used as described previously.[3] Images were captured on a JEOL JEM-1011 transmission electron microscope using an Olympus Morada 11 megapixel camera and iTEM software (Olympus). For statistical analysis, four 5,000 × magnification images were taken randomly from four larvae in each genotype (16 images per genotype), and the area of autophagic structures and glycogen has been manually encircled in Photoshop to obtain area values. Relative cytoplasmic area values and two-tailed two-sample unequal variance Student's t-tests were calculated using Excel.

Disclosure of Potential Conflicts of Interest

No potential conflicts of interest were disclosed.

Acknowledgments

We thank Sarolta Pálfia for her excellent technical assistance, Otto Baba, Marc Bourouis and Julie Kadrmas for providing antibodies, Tom Neufeld and stock centers BDSC and VDRC for fly strains. This work was supported by the Wellcome Trust (087518/Z/08/Z), the Hungarian Scientific Research Fund (OTKA PD72095), the Hungarian Academy of Sciences (BO/00712/07, BO/00781/11, BO/00552/11) and the European Union and the European Social Fund contributed to the purchase of the electron microscope (TÁMOP 4.2.1./B-09/1/KMR-2010-0003).

Supplemental Materials

Supplemental materials may be found here:
www.landesbioscience.com/journals/autophagy/article/20069

References

1. Klionsky DJ, Emr SD. Autophagy as a regulated pathway of cellular degradation. Science 2000; 290:1717-21; PMID:11099404; http://dx.doi.org/10.1126/science.290.5497.1717
2. Hara T, Nakamura K, Matsui M, Yamamoto A, Nakahara Y, Suzuki-Migishima R, et al. Suppression of basal autophagy in neural cells causes neurodegenerative disease in mice. Nature 2006; 441:885-9; PMID:16625204; http://dx.doi.org/10.1038/nature04724
3. Juhász G, Erdi B, Sass M, Neufeld TP. Atg7-dependent autophagy promotes neuronal health, stress tolerance, and longevity but is dispensable for metamorphosis in Drosophila. Genes Dev 2007; 21:3061-6; PMID:18056421; http://dx.doi.org/10.1101/gad.1600707
4. Komatsu M, Waguri S, Chiba T, Murata S, Iwata J, Tanida I, et al. Loss of autophagy in the central nervous system causes neurodegeneration in mice. Nature 2006; 441:880-4; PMID:16625205; http://dx.doi.org/10.1038/nature04723
5. Simonsen A, Cumming RC, Brech A, Isakson P, Schubert DR, Finley KD. Promoting basal levels of autophagy in the nervous system enhances longevity and oxidant resistance in adult Drosophila. Autophagy 2008; 4:176-84; PMID:18059160
6. Klionsky DJ, Cregg JM, Dunn WA, Jr., Emr SD, Sakai Y, Sandoval IV, et al. A unified nomenclature for yeast autophagy-related genes. Dev Cell 2003; 5:539-45; PMID:14536056; http://dx.doi.org/10.1016/S1534-5807(03)00296-X
7. Hosokawa N, Hara T, Kaizuka T, Kishi C, Takamura A, Miura Y, et al. Nutrient-dependent mTORC1 association with the ULK1-Atg13-FIP200 complex required for autophagy. Mol Biol Cell 2009; 20:1981-91; PMID:19211835; http://dx.doi.org/10.1091/mbc.E08-12-1248
8. Nakatogawa H, Ishii J, Asai E, Ohsumi Y. Atg4 recycles inappropriately lipidated Atg8 to promote autophagosome biogenesis. Autophagy 2012; 8:177-86; PMID:22240591; http://dx.doi.org/10.4161/auto.8.2.18373
9. Tanida I, Sou YS, Ezaki J, Minematsu-Ikeguchi N, Ueno T, Kominami E. HsAtg4B/HsApg4B/autophagin-1 cleaves the carboxyl termini of three human Atg8 homologues and delipidates microtubule-associated protein light chain 3- and GABAA receptor-associated protein-phospholipid conjugates. J Biol Chem 2004; 279:36268-76; PMID:15187094; http://dx.doi.org/10.1074/jbc.M401461200
10. Orsi A, Polson HE, Tooze SA. Membrane trafficking events that partake in autophagy. Curr Opin Cell Biol 2010; 22:150-6; PMID:20036114; http://dx.doi.org/10.1016/j.ceb.2009.11.013
11. Mammucari C, Milan G, Romanello V, Masiero E, Rudolf R, Del Piccolo P, et al. FoxO3 controls autophagy in skeletal muscle in vivo. Cell Metab 2007; 6:458-71; PMID:18054315; http://dx.doi.org/10.1016/j.cmet.2007.11.001
12. Sandri M. Autophagy in skeletal muscle. FEBS Lett 2010; 584:1411-6; PMID:20132819; http://dx.doi.org/10.1016/j.febslet.2010.01.056
13. Lee CY, Clough EA, Yellon P, Teslovich TM, Stephan DA, Baehrecke EH. Genome-wide analyses of steroid- and radiation-triggered programmed cell death in Drosophila. Curr Biol 2003; 13:350-7; PMID:12593803; http://dx.doi.org/10.1016/S0960-9822(03)00085-X
14. Gorski SM, Chittaranjan S, Pleasance ED, Freeman JD, Anderson CL, Varhol RJ, et al. A SAGE approach to discovery of genes involved in autophagic cell death. Curr Biol 2003; 13:358-63; PMID:12593804; http://dx.doi.org/10.1016/S0960-9822(03)00082-4
15. Juhász G, Puskás LG, Komonyi O, Erdi B, Maróy P, Neufeld TP, et al. Gene expression profiling identifies FKBP39 as an inhibitor of autophagy in larval Drosophila fat body. Cell Death Differ 2007; 14:1181-90; PMID:17363962; http://dx.doi.org/10.1038/sj.cdd.4402123
16. Weidberg H, Shpilka T, Shvets E, Abada A, Shimron F, Elazar Z. LC3 and GATE-16 N termini mediate membrane fusion processes required for autophagosome biogenesis. Dev Cell 2011; 20:444-54; PMID:21497758; http://dx.doi.org/10.1016/j.devcel.2011.02.006
17. Rusten TE, Lindmo K, Juhász G, Sass M, Seglen PO, Brech A, et al. Programmed autophagy in the Drosophila fat body is induced by ecdysone through regulation of the PI3K pathway. Dev Cell 2004; 7:179-92; PMID:15296715; http://dx.doi.org/10.1016/j.devcel.2004.07.005
18. Scott RC, Schuldiner O, Neufeld TP. Role and regulation of starvation-induced autophagy in the Drosophila fat body. Dev Cell 2004; 7:167-78; PMID:15296714; http://dx.doi.org/10.1016/j.devcel.2004.07.009
19. Zinke I, Schütz CS, Katzenberger JD, Bauer M, Pankratz MJ. Nutrient control of gene expression in Drosophila: microarray analysis of starvation and sugar-dependent response. EMBO J 2002; 21:6162-73; PMID:12426388; http://dx.doi.org/10.1093/emboj/cdf600
20. Beadle G, Tatum EL, Clancy CW. Food level in relation to rate of development and eye pigmentation in Drosophila melanogaster. Biol Bull 1938; 75:447-62; http://dx.doi.org/10.2307/1537573
21. Scott RC, Juhász G, Neufeld TP. Direct induction of autophagy by Atg1 inhibits cell growth and induces apoptotic cell death. Curr Biol 2007; 17:1-11; PMID:17208179; http://dx.doi.org/10.1016/j.cub.2006.10.053
22. Tweedie S, Ashburner M, Falls K, Leyland P, McQuilton P, Marygold S, et al. FlyBase Consortium. FlyBase: enhancing Drosophila Gene Ontology annotations. Nucleic Acids Res 2009; 37 (Database issue):D555-9; PMID:18948289; http://dx.doi.org/10.1093/nar/gkn788
23. Becker T, Loch G, Beyer M, Zinke I, Aschenbrenner AC, Carrera P, et al. FOXO-dependent regulation of innate immune homeostasis. Nature 2010; 463:369-73; PMID:20090753; http://dx.doi.org/10.1038/nature08698
24. Bülow MH, Aebersold R, Pankratz MJ, Jünger MA. The Drosophila FoxA ortholog Fork head regulates growth and gene expression downstream of Target of rapamycin. PLoS One 2010; 5:e15171; PMID:21217822; http://dx.doi.org/10.1371/journal.pone.0015171
25. Yauk CL, Berndt ML, Williams A, Douglas GR. Comprehensive comparison of six microarray technologies. Nucleic Acids Res 2004; 32:e124; PMID:15333675; http://dx.doi.org/10.1093/nar/gnh123
26. Hosokawa N, Sasaki T, Iemura S, Natsume T, Hara T, Mizushima N. Atg101, a novel mammalian autophagy protein interacting with Atg13. Autophagy 2009; 5:973-9; PMID:19597335; http://dx.doi.org/10.4161/auto.5.7.9296
27. Mercer CA, Kaliappan A, Dennis PB. A novel, human Atg13 binding protein, Atg101, interacts with ULK1 and is essential for macroautophagy. Autophagy 2009; 5:649-62; PMID:19287211; http://dx.doi.org/10.4161/auto.5.5.8249
28. Vergne I, Roberts E, Elmaoued RA, Tosch V, Delgado MA, Proikas-Cezanne T, et al. Control of autophagy initiation by phosphoinositide 3-phosphatase Jumpy. EMBO J 2009; 28:2244-58; PMID:19590496; http://dx.doi.org/10.1038/emboj.2009.159
29. Mari M, Griffith J, Rieter E, Krishnappa L, Klionsky DJ, Reggiori F. An Atg9-containing compartment that functions in the early steps of autophagosome biogenesis. J Cell Biol 2010; 190:1005-22; PMID:20855505; http://dx.doi.org/10.1083/jcb.200912089
30. Pankiv S, Clausen TH, Lamark T, Brech A, Bruun JA, Outzen H, et al. p62/SQSTM1 binds directly to Atg8/LC3 to facilitate degradation of ubiquitinated protein aggregates by autophagy. J Biol Chem 2007; 282:24131-45; PMID:17580304; http://dx.doi.org/10.1074/jbc.M702824200
31. Simonsen A, Birkeland HC, Gillooly DJ, Mizushima N, Kuma A, Yoshimori T, et al. Alfy, a novel FYVE-domain-containing protein associated with protein granules and autophagic membranes. J Cell Sci 2004; 117:4239-51; PMID:15292400; http://dx.doi.org/10.1242/jcs.01287
32. Pulipparacharuvil S, Akbar MA, Ray S, Sevrioukov EA, Haberman AS, Rohrer J, et al. Drosophila Vps16A is required for trafficking to lysosomes and biogenesis of pigment granules. J Cell Sci 2005; 118:3663-73; PMID:16046475; http://dx.doi.org/10.1242/jcs.02502
33. Kadrmas JL, Smith MA, Pronovost SM, Beckerle MC. Characterization of RACK1 function in Drosophila development. Dev Dyn 2007; 236:2207-15; PMID:17584887; http://dx.doi.org/10.1002/dvdy.21217
34. Papadopoulou D, Bianchi MW, Bourouis M. Functional studies of shaggy/glycogen synthase kinase 3 phosphorylation sites in Drosophila melanogaster. Mol Cell Biol 2004; 24:4909-19; PMID:15143183; http://dx.doi.org/10.1128/MCB.24.11.4909-4919.2004
35. De Toni-Costes F, Despeaux M, Bertrand J, Bourogaa E, Ysebaert L, Payrastre B, et al. A New alpha5beta1 integrin-dependent survival pathway through GSK3beta activation in leukemic cells. PLoS One 2010; 5:e9807; PMID:20352103; http://dx.doi.org/10.1371/journal.pone.0009807
36. Britton JS, Edgar BA. Environmental control of the cell cycle in Drosophila: nutrition activates mitotic and endoreplicative cells by distinct mechanisms. Development 1998; 125:2149-58; PMID:9570778
37. Chintapalli VR, Wang J, Dow JA. Using FlyAtlas to identify better Drosophila melanogaster models of human disease. Nat Genet 2007; 39:715-20; PMID:17534367; http://dx.doi.org/10.1038/ng2049

38. Mizushima N, Yamamoto A, Matsui M, Yoshimori T, Ohsumi Y. In vivo analysis of autophagy in response to nutrient starvation using transgenic mice expressing a fluorescent autophagosome marker. Mol Biol Cell 2004; 15:1101-11; PMID:14699058; http://dx.doi.org/10.1091/mbc.E03-09-0704
39. Behrends C, Sowa ME, Gygi SP, Harper JW. Network organization of the human autophagy system. Nature 2010; 466:68-76; PMID:20562859; http://dx.doi.org/10.1038/nature09204
40. Hardie DG. Energy sensing by the AMP-activated protein kinase and its effects on muscle metabolism. Proc Nutr Soc 2011; 70:92-9; PMID:21067629; http://dx.doi.org/10.1017/S0029665110003915
41. Johnson EC, Kazgan N, Bretz CA, Forsberg LJ, Hector CE, Worthen RJ, et al. Altered metabolism and persistent starvation behaviors caused by reduced AMPK function in Drosophila. PLoS One 2010; 5:5; PMID:20862213; http://dx.doi.org/10.1371/journal.pone.0012799
42. Lippai M, Csikós G, Maróy P, Lukácsovich T, Juhász G, Sass M. SNF4Agamma, the Drosophila AMPK gamma subunit is required for regulation of developmental and stress-induced autophagy. Autophagy 2008; 4:476-86; PMID:18285699
43. Nilsson J, Sengupta J, Frank J, Nissen P. Regulation of eukaryotic translation by the RACK1 protein: a platform for signalling molecules on the ribosome. EMBO Rep 2004; 5:1137-41; PMID:15577927; http://dx.doi.org/10.1038/sj.embor.7400291
44. Bertrand J, Despeaux M, Joly S, Bourogaa E, Gallay N, Demur C, et al. Sex differences in the GSK3beta-mediated survival of adherent leukemic progenitors. Oncogene 2011; 31:694-705; PMID:21725365; http://dx.doi.org/10.1038/onc.2011.258
45. Wang F, Osawa T, Tsuchida R, Yuasa Y, Shibuya M. Down-regulation of RACK1 suppresses tumor growth by inhibiting tumor cell proliferation and tumor-associated angiogenesis. Cancer Sci 2011; 102:2007-13; PMID:21848913; http://dx.doi.org/10.1111/j.1349-7006.2011.02065.x
46. Cao XX, Xu JD, Liu XL, Xu JW, Wang WJ, Li QQ, et al. RACK1: A superior independent predictor for poor clinical outcome in breast cancer. Int J Cancer 2010; 127:1172-9; PMID:20020495; http://dx.doi.org/10.1002/ijc.25120
47. Cao XX, Xu JD, Xu JW, Liu XL, Cheng YY, Wang WJ, et al. RACK1 promotes breast carcinoma proliferation and invasion/metastasis in vitro and in vivo. Breast Cancer Res Treat 2010; 123:375-86; PMID:19946739; http://dx.doi.org/10.1007/s10549-009-0657-x
48. Nagashio R, Sato Y, Matsumoto T, Kageyama T, Satoh Y, Shinichiro R, et al. Expression of RACK1 is a novel biomarker in pulmonary adenocarcinomas. Lung Cancer 2010; 69:54-9; PMID:19892429; http://dx.doi.org/10.1016/j.lungcan.2009.09.015
49. Juhász G, Hill JH, Yan Y, Sass M, Baehrecke EH, Backer JM, et al. The class III PI(3)K Vps34 promotes autophagy and endocytosis but not TOR signaling in Drosophila. J Cell Biol 2008; 181:655-66; PMID:18474623; http://dx.doi.org/10.1083/jcb.200712051
50. Huang W, Sherman BT, Lempicki RA. Systematic and integrative analysis of large gene lists using DAVID bioinformatics resources. Nat Protoc 2009; 4:44-57; PMID:19131956; http://dx.doi.org/10.1038/nprot.2008.211
51. Joachimiak MP, Weisman JL, May BCh. JColorGrid: software for the visualization of biological measurements. BMC Bioinformatics 2006; 7:225; PMID:16640789; http://dx.doi.org/10.1186/1471-2105-7-225
52. Baba O. Production of monoclonal antibody that recognizes glycogen and its application for immunohistochemistry. Kokubyo Gakkai Zasshi 1993; 60:264-87; PMID:8345245; http://dx.doi.org/10.5357/koubyou.60.264

OPEN ACCESS Freely available online

dc_840_14

PLOS ONE

Advantages and Limitations of Different p62-Based Assays for Estimating Autophagic Activity in Drosophila

Karolina Pircs, Peter Nagy, Agnes Varga, Zsolt Venkei, Balazs Erdi, Krisztina Hegedus, Gabor Juhasz*

Department of Anatomy, Cell and Developmental Biology, Eotvos Lorand University, Budapest, Hungary

Abstract

Levels of the selective autophagy substrate p62 have been established in recent years as a specific readout for basal autophagic activity. Here we compared different experimental approaches for using this assay in Drosophila larvae. Similar to the more commonly used western blots, quantifying p62 dots in immunostained fat body cells of L3 stage larvae detected a strong accumulation of endogenous p62 aggregates in null mutants for Atg genes and S6K. Importantly, genes whose mutation or silencing results in early stage lethality can only be analyzed by microscopy using clonal analysis. The loss of numerous general housekeeping genes show a phenotype in large-scale screens including autophagy, and the p62 assay was potentially suitable for distinguishing bona fide autophagy regulators from silencing of a DNA polymerase subunit or a ribosomal gene that likely has a non-specific effect on autophagy. p62 accumulation upon RNAi silencing of known autophagy regulators was dependent on the duration of the knockdown effect, unlike in the case of starvation-induced autophagy. The endogenous p62 assay was more sensitive than a constitutively overexpressed p62-GFP reporter, which showed self-aggregation and large-scale accumulation even in control cells. We recommend western blots for following the conversion of overexpressed p62-GFP reporters to estimate autophagic activity if sample collection from mutant larvae or adults is possible. In addition, we also showed that overexpressed p62 or Atg8 reporters can strongly influence the phenotypes of each other, potentially giving rise to false or contradicting results. Overexpressed p62 aggregates also incorporated Atg8 reporter molecules that might lead to a wrong conclusion of strongly enhanced autophagy, whereas expression of an Atg8 reporter transgene rescued the inhibitory effect of a dominant-negative Atg4 mutant on basal and starvation-induced autophagy.

Citation: Pircs K, Nagy P, Varga A, Venkei Z, Erdi B, et al. (2012) Advantages and Limitations of Different p62-Based Assays for Estimating Autophagic Activity in Drosophila. PLoS ONE 7(8): e44214. doi:10.1371/journal.pone.0044214

Editor: Mel B. Feany, Brigham and Women's Hospital, Harvard Medical School, United States of America

Received May 17, 2012; **Accepted** July 30, 2012; **Published** August 31, 2012

Copyright: © 2012 Pircs et al. This is an open-access article distributed under the terms of the Creative Commons Attribution License, which permits unrestricted use, distribution, and reproduction in any medium, provided the original author and source are credited.

Funding: This work was supported by the Wellcome Trust (087518/Z/08/Z), the Hungarian Academy of Sciences (BO/00552/11), and the European Union and the European Social Fund contributed to the purchase of the electron microscope (TÁMOP 4.2.1./B-09/1/KMR-2010–0003). The funders had no role in study design, data collection and analysis, decision to publish, or preparation of the manuscript.

Competing Interests: The authors have declared that no competing interests exist.

* E-mail: szmrt@elte.hu

Introduction

Human p62/SQSTM1 (sequestosome-1) is a multidomain scaffold protein involved in various signaling pathways regulating a number of processes including apoptosis, stress responses, and cell growth. [1] Its single Drosophila homolog is also known as Ref(2)P (refractory to sigma P), based on its implicated roles in sigma rhabdovirus multiplication. [2] For simplicity, hereafter we refer to the Drosophila gene as p62. Its encoded protein product shows a similar domain structure to human p62, both containing an N-terminal PB1 domain required for self-oligomerization and binding to other PB1-domain proteins, a ZZ-type zinc finger domain, an LIR (LC3-interacting region) required for its interaction with Atg8/LC3 family members, and a C-terminal ubiquitin-binding UBA (ubiquitin-associated) domain. [3] The Atg8/LC3 interaction enables selective degradation of p62 by autophagy, and by acting as a specific adaptor protein it also ensures the targeting of ubiquitinated proteins for lysosomal degradation. Numerous human degenerative disorders are accompanied by the formation of cytoplasmic aggregates containing p62 and ubiquitinated proteins. [4] These abnormal aggregates also form in response to impaired autophagy, so p62 levels are thought to inversely correlate with dysregulation of basal autophagy. [5,6].

Different p62-based assays have been implemented in recent years in various experimental systems, including immunostaining of cultured cells or tissue samples, western blots, and GFP-tagged reporters. [7] Drosophila melanogaster is a key in vivo model organism, traditionally used as a tool for the discovery of genes and genetic interactions. Previous reports have already shown the progressive formation of p62/ubiquitin aggregates in adult brains, with greatly enhanced rates upon genetic inhibition of autophagy and in fly models of neurodegenerative disorders. [3,4,8,9] Here we set out to test different p62-based assays in the fat body or whole larvae in a quantitative manner, comparing the results and relative efficiency of the various experimental approaches. Our work has important implications for other model systems as well: we show that I. statistical analysis of p62-positive aggregates in immunostained cells and tissues is similarly effective as western blots for the estimation of basal autophagy levels, II. immunostaining of mosaic fat bodies allows for testing the specific role of genes with lethal phenotypes in basal autophagy, III. endogenous p62 provides a much more sensitive measure of autophagy levels than a constitutively overexpressed GFP-tagged reporter in microscopy, IV. the duration of efficient RNAi knockdown is

dc_840_14

very important for the p62 assay unlike in the case of induced autophagy, V. p62 and Atg8 reporters may strongly interact with each other, and hence ''autophagy phenotypes''.

Results

Given the importance of the p62 assay in characterizing autophagy phenotypes of selected mutants and RNAi treatments, we have generated polyclonal antibodies against endogenous Drosophila p62. The antibody recognized a single prominent band of about 100 kDa on western blots prepared form L3 stage larvae or adult heads (**Figure 1a**). The intensity of this band was reduced more than 10-fold relative to tubulin levels upon silencing of p62 in both cases of ubiquitously expressed different RNAi transgenes in L3 larvae. Null mutation of Atg8a resulted in a substantial increase of p62 levels in larvae and in adult heads, respectively, similar to Atg7 mutant heads. Expression of p62-GFP in the larval fat body gave rise to a slower mobility band of about 130 kDa, corresponding to the tagged version of this protein (**Figure 1a**). Interestingly, the presence of p62-GFP also increased the levels of endogenous p62 3.3-fold on an organismal level (probably much higher in case of the fat body, the tissue in which the tagged protein was expressed). This finding suggests that overexpression of a p62 reporter strongly drives aggregate formation, and that endogenous p62 may also be captured and stabilized in these structures.

Next we analyzed the distribution of p62 in larval fat body cells by immunostaining whole-mount tissues. We found that endogenous p62 formed numerous small cytoplasmic dots in these cells, and RNAi silencing of p62 using three different transgenes all strongly and significantly reduced the number of these dots (**Figure 1b–d**, see **Figure 1f** for statistics). As expected, expression of p62-GFP in fat body cell clones strongly promoted aggregate formation, resulting in a 9-fold increase in the number and 2.8-fold increase in the size of p62-positive structures, respectively (**Figure 1e, f**).

Since defective basal autophagy is known to enhance p62 aggregation, we analyzed previously described null mutants for selected genes involved in autophagy. Both the number and size of p62-positive dots were significantly increased in fat bodies dissected from L3 stage larvae mutant for the following core autophagy genes: Atg1 and Atg13 (encoding members of the Atg1 kinase complex), Vps34 (encoding the phosphatidyl-inositol 3-kinase), Atg2 and Atg18a (encoding binding partners of the transmembrane protein Atg9), Atg7 and Atg8a (encoding the E1-like enzyme and one of the ubiquitin-like proteins in the autophagy-specific protein conjugation systems) (**Figure 2a, b, d**, see also Figure S1 for additional images). S6 kinase is a physiologic substrate of TOR kinase (Target Of Rapamycin), a central regulator of autophagy and cell growth. Activation of TOR suppresses autophagy and results in phosphorylation of S6K. Based on these correlations, S6K was long considered as an inhibitor of autophagy. Therefore, the finding that Drosophila S6K was actually required for starvation-induced autophagy was surprising. [10,11] In line with those observations, we have also found that loss of S6K significantly increased the number (but in this case not the size) of p62 aggregates in larval fat body cells, consistent with its suggested positive role in autophagy (**Figure 2c**, compare to **Figure 2a**; see also **Figure 2d** for quantification).

We then evaluated how inactivation of known regulators of autophagy in somatic clones of mosaic animals affected p62 levels. RNAi silencing of Atg1 or Atg14 (the autophagy-specific subunit of the Vps34 complex) enhanced p62 aggregation, similar to overexpression of dominant-negative Vps34 (**Figure 3a, d**; see also Figure S2). Silencing of Atg2, Atg9 and Atg8a also promoted p62 dot formation. Enhancing TOR signaling by overexpression of its activator Rheb or knockdown of the Rheb inhibitor Tsc2 also increased p62 dot number, although in case of Rheb the phenotypes were so variable that the change was not statistically significant (**Figure 3b, d**; see also Figure S2). Silencing of Atg7 did not lead to increased p62 dots, consistent with the observation that this line had a weaker effect on starvation-induced autophagy relative to the other lines we used, potentially caused by either less efficient knockdown or by the kinetics of the Atg7 E1-like enzyme reaction, that is, lowered levels of Atg7 due to RNAi being potentially sufficient to support basal autophagy (data not shown).

Numerous genes are required for fundamental cellular processes such as transcription or translation. It is not so surprising that these genes are often identified as putative hits in various genome-wide RNAi screens, although their effect is likely indirect in most cases. While knockdown of many of these genes reduces cell size to an extent that evaluation of autophagy phenotypes becomes practically impossible, silencing of the genes coding for the RNA polymerase II. complex member Atms or the ribosomal subunit RpS8 strongly interfered with starvation-induced mCherry-Atg8 and Lysotracker puncta formation (Figure S3). On the other hand, these knockdowns did not enhance p62 aggregation as expected from a condition that indirectly interferes with autophagy induction through perturbing a fundamental cellular process and/or the expression of a transgenic marker (**Figure 3c, d**; see also Figure S2), suggesting that the p62 assay is potentially suitable for distinguishing specific regulators of autophagy (''hits'') from indirect effects (''noise'').

A GFP-tagged p62 reporter was previously used successfully in Drosophila to detect basal autophagy defects in Atg13 mutant cells. [12] We decided to investigate how phenotypes obtained by p62-GFP compare with those based on the endogenous protein. Expression of p62-GFP together with RNAi against Atg1, Atg7, Atg8a, Atg9, Atg14, Atg18a, Tsc2, Pten or with dominant-negative Vps34 were all found to decrease the number of GFP-positive aggregates (**Figure 3e–g**; see also Figure S4). In case of Pten and Tsc2 the size of GFP-positive aggregates increased significantly, while it did not change in most cases. Importantly, the number of these aggregates also decreased while their size increased in case of both RpS8 and Atms. As no clear conclusions could be drawn based on these results, we also looked at exposure times used during image acquisition. With this approach we could detect significantly increased GFP signal for Atg1, Atg8a, Atg9, Atg14, Atg18a, Pten RNAi and Vps34KD expressing cells, but not in the case of Atg7, Tsc2, RpS8 and Atms RNAi cells (**Figure 3e–h**; see also Figure S4). These results well agreed with the data obtained with the endogenous p62 antibody differing only in the case of Tsc2, although there was a several-fold difference for each positively scoring line in favor of the endogenous p62 assay.

While testing a large number of RNAi lines in our genome-wide RNAi screen (to be described elsewhere), one striking observation was that the p62 assay occasionally showed large differences in case of two different RNAi lines targeting the same gene. For example, two different transgenic RNAi lines for Atg18a had quantitatively different effects on p62 aggregation, potentially reflecting differences in knockdown efficiencies. Interestingly, one of two different RNAi lines against Atg16 (encoding a protein required for Atg8a lipidation) failed to enhance p62 aggregation, similar to the case of PTEN, inactivation of which strongly enhances insulin signaling to promote cell growth and suppress autophagy (**Figure 3d**; see also Figure S2). As both RNAi lines for Atg18a, Atg16 and PTEN very effectively blocked starvation-induced autophagy in L3 larvae, we decided to look for potential

dc_840_14

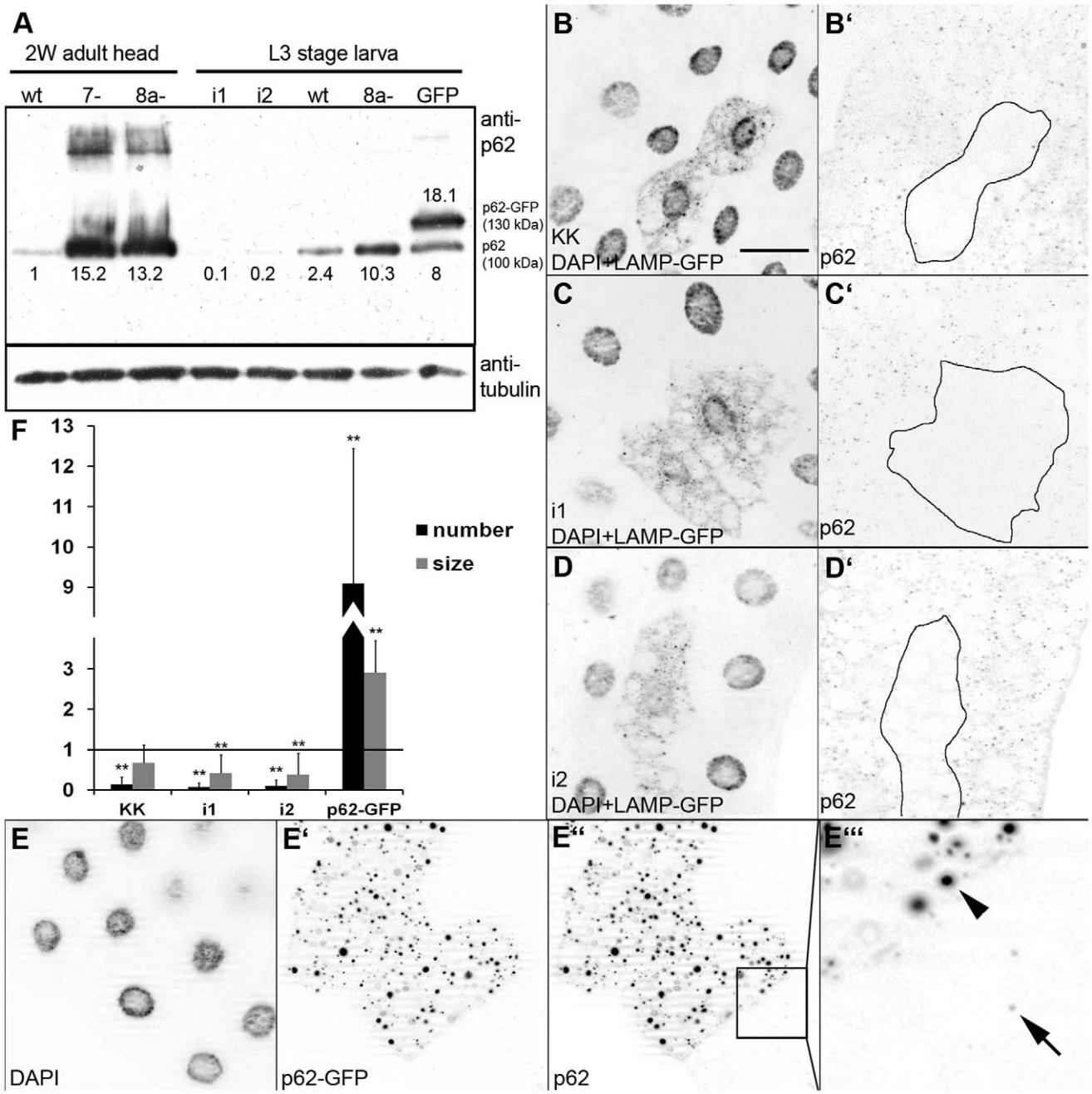


Figure 1. p62 levels in Atg mutants, p62 RNAi and p62 overexpression cells. A. Western blot analysis shows p62 accumulation in Atg8a and Atg7 mutant heads and in Atg8a mutant larvae. RNAi knockdowns of p62 (i1, i2) greatly decrease endogenous protein levels, while overexpression of p62-GFP increases endogenous p62 levels in addition to the appearance of the 130 kDa extra band corresponding to the tagged protein. Numbers refer to p62 protein level relative to tubulin loading control for each sample. B-D. RNAi knockdown of p62 in fat body cell clones (marked by expression of Lamp-GFP) strongly decreases p62 puncta formation. E. Expression of p62-GFP in cell clones increases aggregate formation. Arrowhead in E′ indicates a large aggregate in a p62-GFP expressing cell, arrow marks an endogenous p62 dot in a control cell. F. Statistical evaluation of the number and size of p62 dots for samples in panels B–E. ** indicates a very significant difference ($p<0.01$), based on two-tailed two-sample unequal Student's t tests. Scalebar in panel B equals 30 µm for panels B–E. *Genotypes are: (A) lane 1: w [1118], lane 2: Atg7[d77]/Atg7[d14], lane 3: Atg8a[d4], lane 4: UbiGal4/+; p62[HMS00551]/+, lane 5: UbiGal4/+; p62[HMS00938]/+, lane 6: w [1118], lane 7: Atg8a[d4], lane 8: cgGal4/UAS-p62-GFP; (B) hs-Flp; UAS-LampGFP/p62[KK108193]; Act>CD2>Gal4, UAS-Dcr2/+; (C) hs-Flp; UAS-LampGFP/+; Act>CD2>Gal4, UAS-Dcr2/p62[HMS00551]; (D) hs-Flp; UAS-LampGFP/+; Act>CD2>Gal4, UAS-Dcr2/p62[HMS00938]; (E) hsFlp; UAS-p62-GFP/+; Act>CD2>Gal4,UAS-Dcr2/+.*
doi:10.1371/journal.pone.0044214.g001

reasons of these discrepancies. Quantification of mCherry-Atg8a dots in starved fat bodies revealed that $Atg18a^{JF}$ showed better suppression than $Atg18a^{KK}$ in both L3 and L2 stage animals, likely explaining the quantitatively different p62 results (**Figure 4f–j**). In case of PTEN RNAi lines (**Figure 4k–o**), both showed a strong suppression of mCherry-Atg8a dot formation in L3 stage, while $PTEN^{KK}$ did not significantly inhibit starvation-induced autophagy in L2 animals, consistent with its failure to enhance p62 dot

dc_840_14

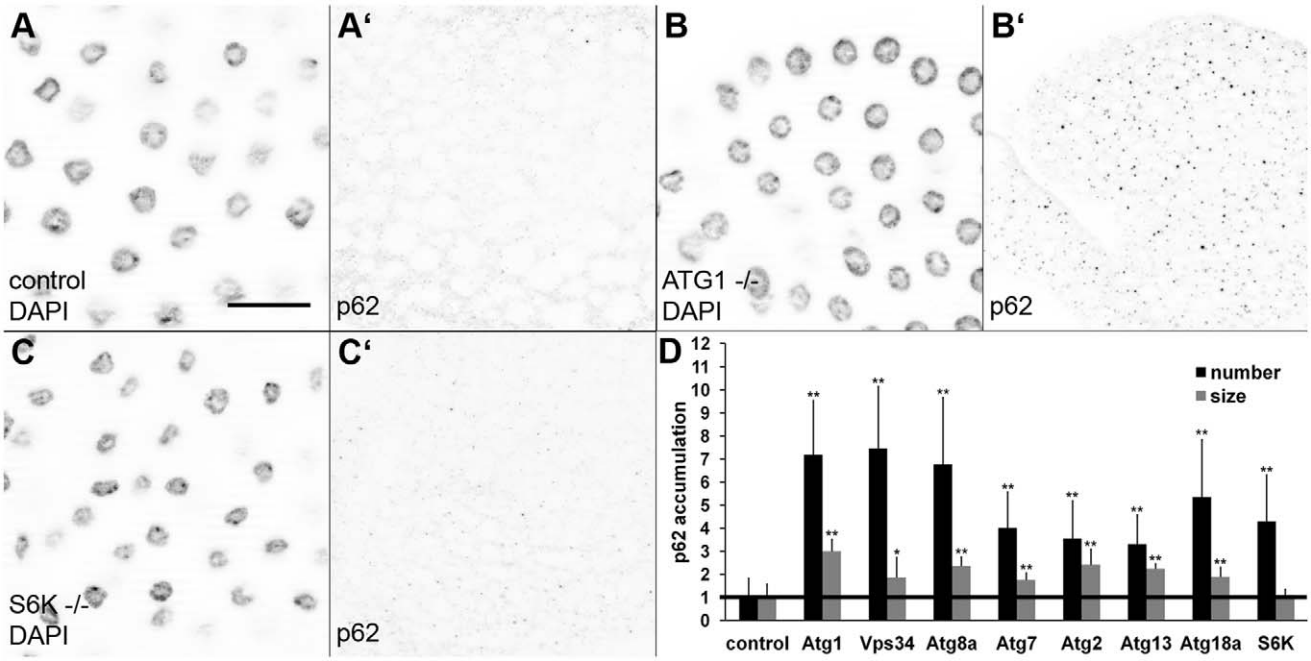


Figure 2. Endogenous p62 accumulates in Atg and S6K mutants. A. p62 immunostaining detects small dots scattered throughout the cytoplasm in fat body cells of wild-type larvae. B. p62 aggregates appear bigger and more numerous in Atg1 null mutants, while loss of S6K (C) only increases the number, but not the size of p62 aggregates. D. Statistical evaluation of p62 puncta in fat bodies of various Atg mutants and in S6K null animals. * indicates a significant difference ($p<0.05$), ** indicates a very significant difference ($p<0.01$), based on two-tailed two-sample unequal Student's t tests. Scalebar in panel A equals 30 µm for panels A–C. *Genotypes are: (A) w [1118]; (B) Atg1 [25]; (C) S6K[l–1].*
doi:10.1371/journal.pone.0044214.g002

formation. Interestingly, no differences could be seen in starved L3 stage animals between the two RNAi lines in case of Atg16. However, $Atg16^{HMS}$ reduced the size of dots 8-fold, while $Atg16^{KK}$ showed only a two-fold reduction in L2 stage (**Figure 4a–e**). Larger mCherry-Atg8a dots are thought to represent mature autolysosomes, and $Atg16^{HMS}$ had a stronger block on formation of these structures in L2 stage larvae. Lysotracker stainings further supported this hypothesis, as only $Atg16^{HMS}$ reduced the size of Lysotracker puncta statistically significantly in L2 stage animals (Figure S5). Altogether, these results suggest that differences seen in starvation-induced autophagy in the L2 stage and the progressive formation of p62 aggregates (analyzed in the L3 stage) may both reflect the knockdown efficiency of the given RNAi line in earlier stages (that is, L2).

Finally, we have evaluated the impact of overexpressed p62 and Atg8a reporters (which potentially create a gain of function condition) on autophagy phenotypes, as the possibility of genetic interactions could not be excluded. In fact, when p62-GFP was co-expressed with mCherry-Atg8a, large colocalizing GFP- and mCherry-positive aggregates were formed even in well-fed animals (**Figure 5a**). These aggregates were likely caused by the specific interaction of the two overexpressed proteins and represented an artefact and not bona fide autophagic structures, as Atg8a strongly binds to the LC3-interacting region of p62. In line with that, we did not detect an obvious increase in autophagy in p62-GFP expressing cells by Lysotracker staining and transmission electron microscopy (**Figure 5b, c**). Similarly, we saw no conversion of p62-GFP to free GFP in western blots of larvae coexpressing mCherry-Atg8a and p62-GFP in the fat body, suggesting that mCherry-Atg8a expression does not obviously enhance autophagic degradation of p62-GFP in well-fed L3 stage control animals. As expected, free GFP was readily detected after a 4-hour starvation or in wandering stage animals undergoing developmental autophagy. Expression of Atg1 RNAi or dominant-negative Vps34 strongly decreased starvation-induced conversion of p62-GFP, while Atg1 silencing showed only a weaker effect in wandering animals (**Figure 5d**).

Atg4 encodes a cysteine protease required for the cleavage of the C-terminal amino acids of Atg8a, which is necessary for its subsequent activation and conjugation to the membrane lipid phosphatidyl-ethanolamine. Atg8a needs to be delipidated after successful completion of an autophagosome to allow lysosomal fusion. A mutant form of human Atg4B with a substitution of cysteine 74 to alanine was shown to act in a dominant-negative fashion, inhibiting proper formation and clearence of autophagosomes. [13] We reconstituted this mutant in Drosophila, creating transgenic flies with inducible expression of $Atg4a^{C98A}$. Expression of dominant-negative Atg4a strongly suppressed Lysotracker staining in fat body cells of starved larvae, and also caused accumulation of p62 (**Figure 5e, Figure 3d**; see also Figure S2). As expression of mCherry-Atg8a in Atg8a null mutants could rescue the p62 accumulation phenotype (Figure S6a, b), we tested whether overexpressed mCherry-Atg8a can also rescue the effect of dominant-negative Atg4. Co-expression of mCherry-Atg8a with dominant-negative Atg4 restored both starvation-induced autophagy in starved animals and the normal turnover of p62 (**Figure 5f**; see also Figure S6c, d). Ultrastructural analysis further confirmed that expression of dominant-negative Atg4 strongly inhibited starvation-induced autophagy: no autolysosomes were seen in cross-sections of fat body cells, while small autophagosome-like structures were occasionally observed (**Figure 5g**). Coexpression of Atg8a with dominant-negative Atg4 restored starvation-induced autophagy, as numerous autolysosomes and autophagosomes were seen in all cells (**Figure 5h**), similar to previous findings in mammalian

dc_840_14

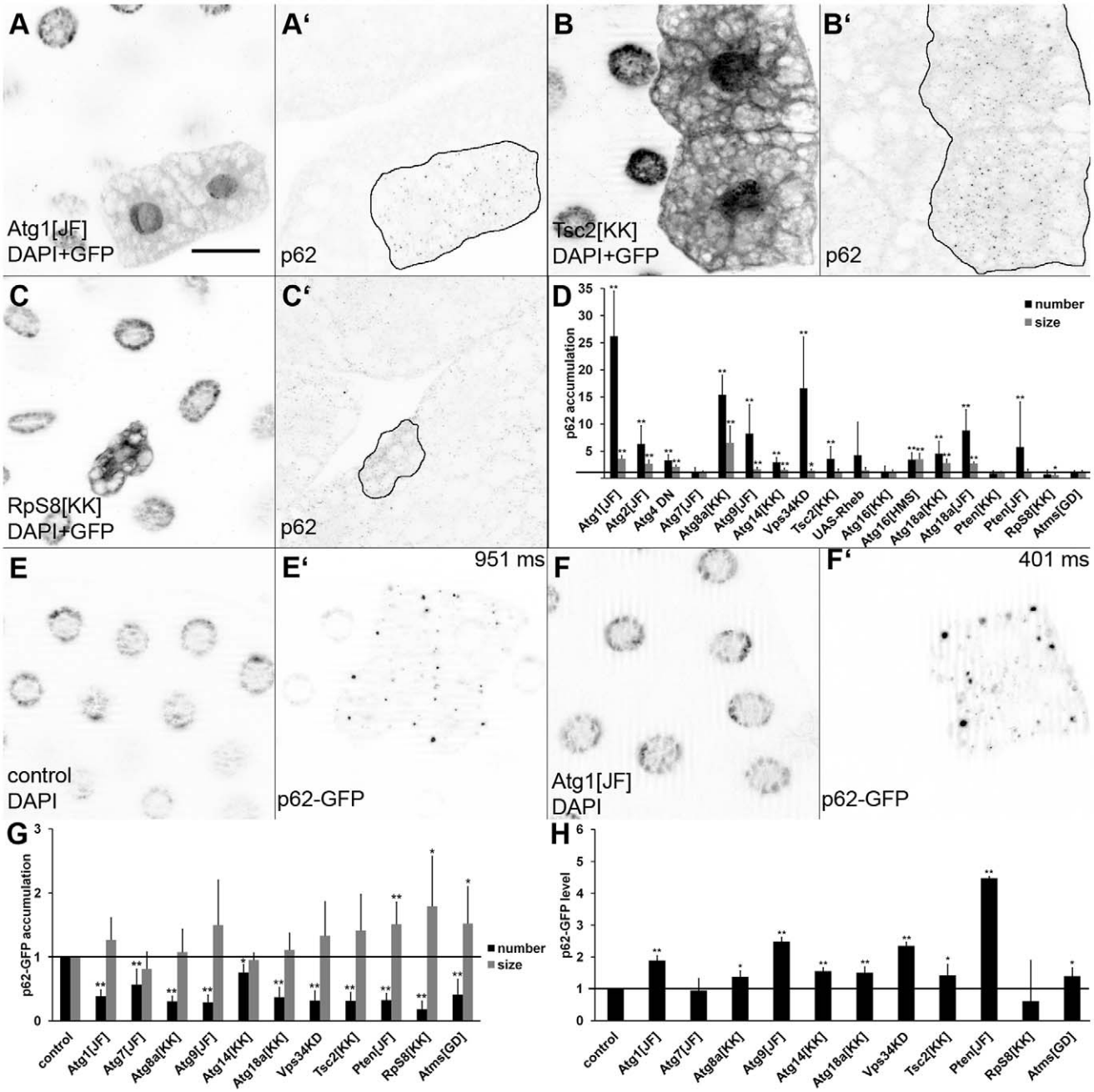
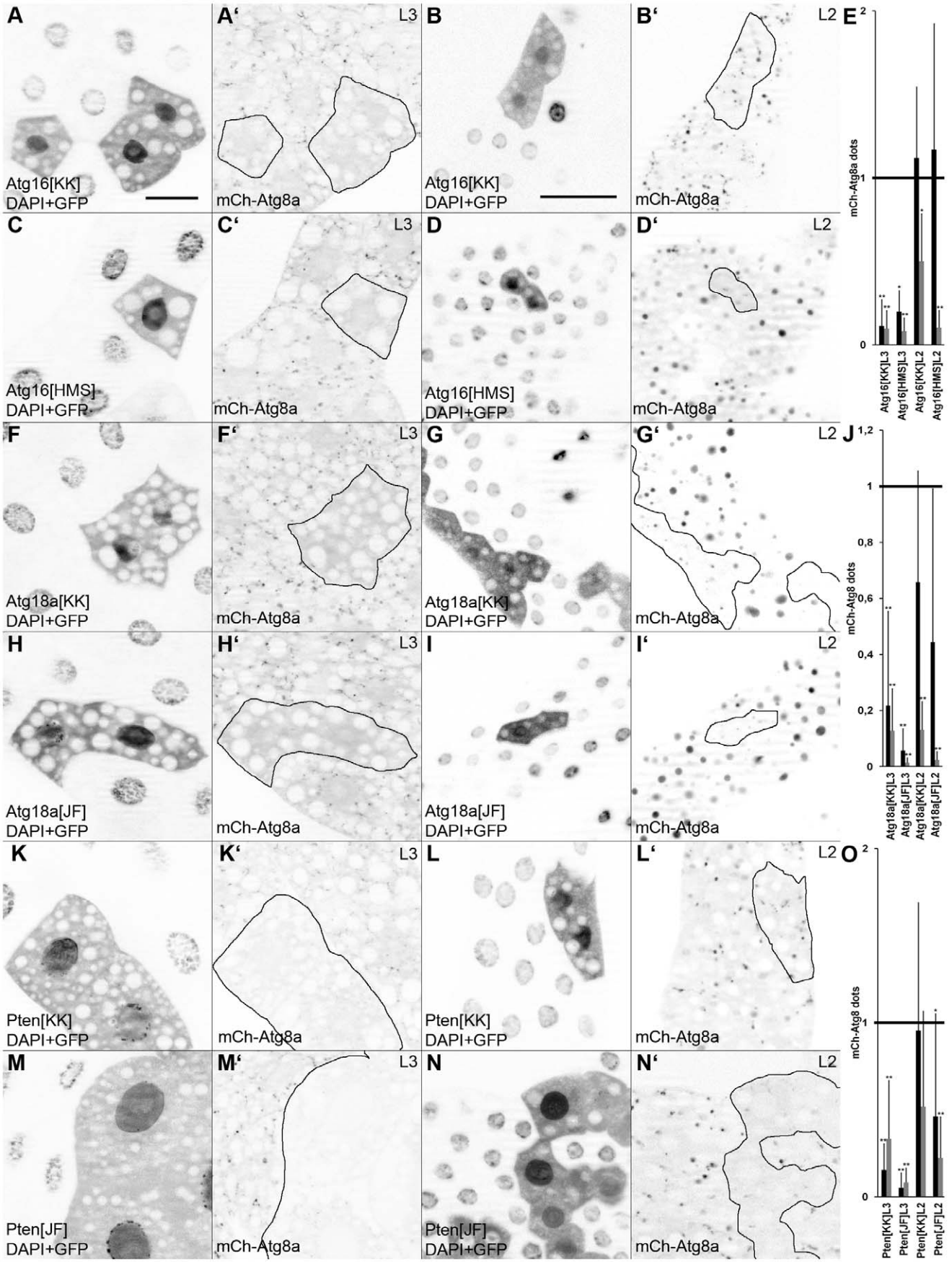


Figure 3. Loss of known autophagy regulators enhances p62 puncta formation cell-autonomously. Knockdown of Atg1 (A) or Tsc2 (B) increases p62 aggregate formation, while silencing of RpS8 results in a slight reduction of p62 dot number (C). Panel D shows statistical evaluation of the effect of RNAi and overexpression lines on p62 accumulation. Overexpressed p62-GFP forms multiple aggregates in control and Atg1 RNAi cells (panels E and F, respectively). Exposure times are indicated in the top right corner for panels E and F. Statistical evaluation of p62-GFP aggregate size and number in various RNAi and overexpression lines reveals changes that are difficult to interpret (G), but p62-GFP levels inferred from exposure times during image acquisition are qualitatively similar to data obtained with anti-p62 immunostaining (compare H to D). * indicates a significant difference ($p<0.05$), ** indicates a very significant difference ($p<0.01$), based on two-tailed two-sample unequal Student's t tests in panels D, G, H. Scalebar in panel A equals 30 μm for panels A–C and E–F. *Genotypes are: (A) hsFlp; UAS-Dcr2/+; Act>CD2>Gal4, UAS-GFPnls/Atg1[JF02273]; (B) hsFlp; UAS-Dcr2/TSC2[KK103417]; Act>CD2>Gal4, UAS-GFPnls/+; (C) hsFlp; UAS-Dcr2/RpS8[KK106835]; Act>CD2>Gal4, UAS-GFPnls/+; (E) hsFlp; UAS-p62-GFP/+; Act>CD2>Gal4, UAS-Dcr2/+ (F) hsFlp; UAS-p62-GFP/+; Act>CD2>Gal4, UAS-Dcr2/Atg1[JF02273].*
doi:10.1371/journal.pone.0044214.g003

cells. [13] Similarly, knockdown of Atg4a using the RNAi line $Atg4a^{KK}$ blocked starvation-induced Lysotracker staining and induced p62 accumulation in fat body cells but failed to inhibit mCherry-Atg8a dot formation (not shown), further supporting our hypothesis that partial loss of Atg4a function can be rescued by overexpression of Atg8a.

dc_840_14


A
A'
L3
B
B'
L2
E
Atg16[KK]
DAPI+GFP
mCh-Atg8a
mCh-Atg8a dots
C
C'
D
D'
Atg16[HMS]
F
F'
G
G'
J
Atg18a[KK]
mCh-Atg8 dots
H
H'
I
I'
Atg18a[JF]
K
K'
L
L'
O
Pten[KK]
M
M'
N
N'
Pten[JF]
Atg16[KK]L3
Atg16[HMS]L3
Atg16[KK]L2
Atg16[HMS]L2
Atg18a[KK]L3
Atg18a[JF]L3
Atg18a[KK]L2
Atg18a[JF]L2
Pten[KK]L3
Pten[JF]L3
Pten[KK]L2
Pten[JF]L2

dc_840_14

Figure 4. The effect of Atg16, Atg18a and Pten RNAi lines on starvation-induced autophagy in L3 and L2 larval stages. Both RNAi lines for Atg16 show a similar block of mCherry-Atg8a puncta formation in L3 (compare A to C), while the size of these dots is reduced more efficiently by $Atg16^{HMS}$ in L2 (compare B to D; see also panel E for statistics). Both RNAi lines for Atg18a strongly inhibit mCherry-Atg8a dot formation in L3 (compare F to H), while $Atg18a^{JF}$ shows a more complete block in L2, reducing both the size and number of puncta (compare G to I; see also panel J for statistics). Both RNAi lines for Pten strongly inhibit mCherry-Atg8a dot formation in L3 (compare K to M), while $Pten^{JF}$ shows a more complete block in L2, again reducing both the size and number of puncta (compare L to N; see also panel O for statistics). * indicates a significant difference ($p<0.05$), ** indicates a very significant difference ($p<0.01$), based on two-tailed two-sample unequal Student'st tests in panels E, J, O. Scalebar in panel A equals 30 µm for panels A, C, F, H, K, M, and scalebar in panel B equals 30 µm for panels B, D, G, I, L, N. *Genotypes are: (A, B) hsFlp; UAS-Dcr2/Atg16[KK105993]; Act>CD2>Gal4, UAS-GFPnls, r4-mCherry-Atg8a/+; (C, D) hsFlp; UAS-Dcr2/+; Act>CD2>Gal4, UAS-GFPnls, r4-mCherry-Atg8a/Atg16[HMS01347]; (F, G) hsFlp; UAS-Dcr2/Atg18a[KK105366]; Act>CD2>Gal4, UAS-GFPnls, r4-mCherry-Atg8a/+; (H, I) hsFlp; UAS-Dcr2/+; Act>CD2>Gal4, UAS-GFPnls, r4-mCherry-Atg8a/Atg18a[JF02898]; (K, L) hsFlp; UAS-Dcr2/Pten[KK101475]; Act>CD2>Gal4, UAS-GFPnls, r4-mCherry-Atg8a/+; (M, N) hsFlp; UAS-Dcr2/+; Act>CD2>Gal4, UAS-GFPnls, r4-mCherry-Atg8a/Pten[JF01987].*
doi:10.1371/journal.pone.0044214.g004

Discussion

Determining the levels of the specific autophagy substrate p62 is becoming a standard assay to estimate basal autophagy rates. [7] Western blots are the most widely used experimental setup to detect endogenous p62 levels with the possibility to distinguish soluble and aggregated forms using differential detergent extractions, but these experiments are simply not feasible in studies that involve genetic mosaic animals. Here we presented evidence that an immunostaining approach is similarly effective as western blots to detect even subtle changes of p62 aggregation in the larval fat body, and it can actually provide additional information compared with western blots, as the number, size and intracellular distribution of these aggregates are all detected this way. We recommend using a p62-specific antibody rather than a constitutively overexpressed GFP-tagged reporter as the latter led to extensive self-aggregation and also increased the level of the endogenous protein, because of which the size and number of p62 aggregates were no longer indicative of autophagic activity. Still, comparing GFP signal intensities may yield qualitatively similar information to data obtained by looking at endogenous p62 levels in some but not all cases. Endogenous p62 protein levels may also be influenced by changes unrelated to autophagy, which should not be a problem with a tagged reporter expressed from an artificial promoter. In addition to comparing fluorescence intensities of p62-GFP expressing cell clones, a probably more reliable approach is to follow the generation of free GFP produced by autolysosomal degradation in western blots of larvae expressing p62-GFP by a tissue-specific promoter. Alternatively, p62-GFP expression can be induced by a heat shock in mutant animals and the decay of the tagged protein followed in western blots or microscopy to measure tagged p62 half-life in a pulse-chase assay. This a very efficient method to determine flux during basal or starvation-induced autophagy in cultured cells. [7] Regarding endogenous p62 expression, we found that it is transcriptionally upregulated 4.8-fold in larval fat body cells in response to a 4-hour starvation, [14] and a similar starvation-induced upregulation is also obvious on western blots. Interestingly, starvation mainly increases soluble p62 levels and decreases the amount of the aggregated fraction. [4] This observation also suggests that evaluation of endogenous p62 aggregates is a reliable measure of autophagic flux.

In case of autophagy induced by a certain stimulus such as starvation, levels of proteins required for autophagy at the time of the stimulus and during the response are critical determinants of the magnitude of autophagy that follows. In contrast, p62 levels are also strongly influenced by basal autophagic activity, so formation of excess p62 aggregates is a progressive, time-dependent process. Therefore, duration of a certain treatment or effective gene silencing by RNAi has a major impact on this type of assay. In line with that, we have shown here that p62 levels may remain normal despite a strong block of starvation-induced autophagy if the onset of efficient gene knockdown is delayed during larval Drosophila development. Based on these observations, the perdurance of maternally supplied gene products during development may also account for some of the differences seen in p62 levels in different Atg mutants.

Additionally, certain problems may arise when using overexpressed reporter transgenes for autophagy. First, overexpressed Atg8a reporters were found to be captured in overexpressed p62 aggregates, giving a false impression of increased autophagy. Second, overexpression of an Atg8a reporter may genetically rescue the partial loss of a gene as seen in case of Atg4a, again complicating the interpretation of potentially contradicting results. While the examples shown here may be rare, we have seen several instances when inactivation of certain genes led to such a high accumulation of endogenous p62 aggregates that sequestered Atg8a reporter molecules, and overexpressed Atg8a reporters also seemed to genetically rescue the effect of a number of RNAi lines on autophagy.

Finally, although our experiments involved fat body cells of Drosophila larvae, we are convinced that the results and limitations presented here will be applicable to most cells and organisms used in autophagy research.

Methods

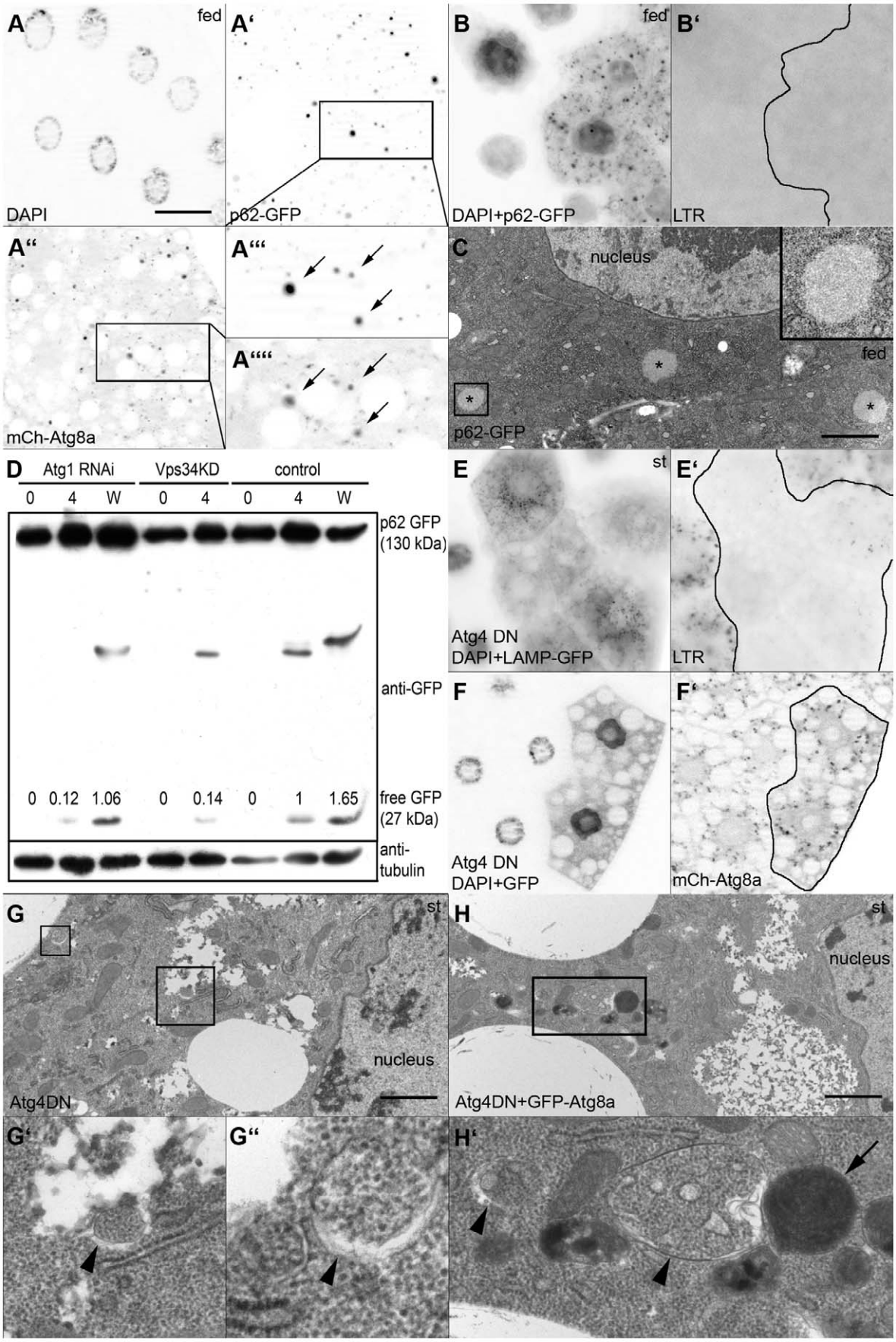
Fly Husbandry

Drosophila stocks were maintained on a standard cornmeal/sugar/agar medium at 25°C and 50% humidity on a 12 h light/12 h dark cycle. Thestocks used in this study were: *UAS-p62-GFP*, *Atg13[Δ81]*, [*12*] *p62[KK108193]*, *Atg8a[KK109654]*, *Atg18a[KK105366]*, *Atg14[KK108559]*, *Atg16[KK105993]*, *TSC2[KK103417]*, *Pten[KK101475]*, *RpS8[KK106835]*, *Atms[GD20876]*, [*15*] *Atg7[d77]/Atg7[d14]*, [*8*] *Vps34[Δm22]*, *UAS-Vps34[KD]*, [*16*] *p62[HMS00551]*, *p62[HMS00938]*, *Atg1[JF02273]*, *Atg18a[JF02898]*, *Atg9[JF02891]*, *Atg7[JF02787]*, *Atg16[HMS01347]*, *Atg2[JF02786]*, *Pten[JF01987]*, [*17*] *Atg2[EP3697]/Df(3L)BSC119]*, *Atg18a[KG03090]/Df(3L)Exel6112]*, *S6K[l-1]*, *UAS-Rheb[EP50.084cre(w-)]/TM6B*, *w [1118]*, [*11*] *Atg1 [25]*. [*18*]. The *Atg8a[d4]* mutant used in this study was generated by imprecise excision of the P element *KG07569* and harbors a deletion removing the first 25 codons of Atg8a and the first 53 codons of CG1826, a gene with an unknown function (kindly provided by Tom Neufeld). The mutants are homozygous viable and fertile with no gross morphological or developmental abnormalities. *UAS-Atg4[C98A]* transgenics were established as described below.

Molecular Cloning and Embryo Injections

The full-length coding sequence of Atg4a/CG4428 with a Cysteine 98 to Alanine mutation changing the coding triplet from TGC to GCC was chemically synthesized (Genscript), and

dc_840_14


A
fed
DAPI
A'
p62-GFP
A''
mCh-Atg8a
A'''
A''''
B
fed
DAPI+p62-GFP
B'
LTR
C
nucleus
fed
p62-GFP
D
Atg1 RNAi
Vps34KD
control
0 4 W 0 4 0 4 W
p62 GFP
(130 kDa)
anti-GFP
0 0.12 1.06 0 0.14 0 1 1.65
free GFP
(27 kDa)
anti-
tubulin
E
st
Atg4 DN
DAPI+LAMP-GFP
E'
LTR
F
Atg4 DN
DAPI+GFP
F'
mCh-Atg8a
G
st
nucleus
Atg4DN
G'
G''
H
st
nucleus
Atg4DN+GFP-Atg8a
H'

dc_840_14

Figure 5. The effect of p62 and Atg8a reporters on autophagy phenotypes. A. Coexpression of p62-GFP and mCherry-Atg8a results in formation of aggregates containing both tagged proteins in fed animals, potentially suggesting enhanced autophagy. B. Expression of p62-GFP fails to induce Lysotracker puncta in fed animals. C. p62-GFP expression leads to the appearance of protein aggregates in ultrastructural images of fat body cells (asterisks), but no autophagic structures are seen in the cytoplasm. Inset shows an enlarged aggregate to illustrate that these inclusion bodies are not membrane-bound. D. Western blot analysis using anti-GFP antibodies of larval extracts expressing mCherry-Atg8a and p62-GFP in the fat body. No generation of free GFP by autolysosomal degradation is seen in well-fed control larvae, it is only induced by a 4-hour starvation or in the wandering stage. Silencing of Atg1 or expression of dominant-negative Vps34 inhibits autophagy-mediated conversion of p62-GFP to free GFP. E, F. Expression of dominant-negative Atg4 blocks starvation-induced Lysotracker puncta formation, but it has no effect on overexpressed mCherry-Atg8a dots. G. Ultrastructural analysis of starved fat bodies reveal small autophagosomes (marked by arrowheads in G′ and G′), but no autolysosomes are seen. Coexpression of GFP-Atg8a with dominant-negative Atg4 rescues this inhibition: numerous autolysosomes (arrow) and autophagosomes (arrowheads) are seen in H, H′. Scalebar in panel A equals 30 μm for panels A, B, E, F and scalebars in panels C, G, H equal 2 μm. *Genotypes are: (A) hsFlp; UAS-p62-GFP/+; Act>CD2>Gal4, UAS-Dcr2/r4-mCherry-Atg8a; (B, C) hsFlp; UAS-p62-GFP/+; Act>CD2>Gal4, UAS-Dcr2/+; (D) lanes 1, 2, 3: cgGal4, UAS-p62-GFP/+; Atg1[JF02273]/+, lanes 4, 5, : cgGal4, UAS-Vps34[KD]/UAS-p62-GFP, lanes 6, 7, 8, : cgGal4, UAS-p62-GFP/+; (E, G) hs-Flp; UAS-Dcr2/+; Act>CD2>Gal4, UAS-GFPnls/UAS-Atg4[C98A]; (F, H) hs-Flp; UAS-Dcr2/+; Act>CD2>Gal4, UAS-GFPnls, r4-mCherry-Atg8a/UAS-Atg4[C98A].*
doi:10.1371/journal.pone.0044214.g005

cloned into pUAST using EcoRI and XhoI restriction sites. Drosophila embryo transformation was carried out according to standard methods (Bestgene).

Polyclonal Anti-p62 and Anti-GFP Antibodies and Western Blots

The polyclonal affinity-purified p62 antibody was raised in rabbits using the peptide antigene PRTEDPVTTPRSTQ corresponding to amino acids 297–311 (Genscript). Polyclonal anti-GFP antibodies were raised using standard procedures by immunizing rats with bacterially expressed His-tagged eGFP purified on Ni affinity columns (Sigma). Samples were separated by SDS-PAGE on an 8% acrylamide gel and transferred to Immobilon-P PVDF membrane (Millipore). Membranes were blocked in 3% milk/TBS for 1 h at room temperature and washed three times for 10 min each in TBST (TBS +0.1% Tween-20). Blots were incubated with primary antibodies: rabbit polyclonal anti-p62 [1:8,000], mouse monoclonal anti-tubulin AA4.3 (DSHB) [1:200], rat polyclonal anti-GFP [1:10,000] in 1.5% milk/TBST for 1 h at room temperature, followed by three 10-min washes in TBST. Blots were incubated in AP-conjugated goat anti-rat (Sigma), anti-rabbit or anti-mouse secondary antibody (Millipore) diluted 1:10,000 in 1.5% milk/TBST for 1 h at room temperature. Blots were washed for 3×10 min in TBST and then incubated with Immobilon Western Chemiluminescent AP Substrate (Millipore), followed by exposure to Super RX film (Fuji).

Histology and Imaging

Clonal analysis using the spontaneously activated Gal4/UAS system in the larval fat body was carried out as described previously. [11,12,16,19] Bisected third instar larvae were inverted and fixed with 3.7% paraformaldehyde in PBS overnight at 4°C. Next, samples were rinsed twice and washed for 2 hours in PBS, permeabilized for 15 minutes in PBTX-DOC (PBS with 0.1% Triton X-100 and 0.05% sodium deoxycholate) and blocked for 3 h in 3% goat serum in PBTX-DOC. Samples were then incubated overnight at 4°C with primary antibodies rabbit polyclonal anti-p62 [1:2,000] and mouse monoclonal anti-GFP [1:1,500] (Invitrogen) in 1% goat serum in PBTX-DOC. After 3×30 minutes washes in PBTX-DOC, samples were incubated with secondary antibodies goat anti-mouse Alexa 488 and goat anti-rabbit Alexa 568 [1:1,500] (Invitrogen) in 1% goat serum in PBTX-DOC for 4 hours at room temperature. Finally, after 3×15 minutes washes in PBTX-DOC and 1×15 minutes in PBS, fat bodies were dissected and mounted in 50% glycerol/PBS with 0.2 μM DAPI. For p62 staining of mCherry-Atg8a expressing cells Alexa 647-conjugated goat anti-rabbit antibody was used to avoid detection of signal from mCherry. Lysotracker stainings have been carried out as described previously. Images were captured on a Zeiss Axioimager M2 microscope equipped with an Apotome2 grid confocal unit, a Plan-NeoFluar 40×0.75 NA objective, Axiocam Mrm camera, and Axiovision software using a MinMax setting for automatically adjusting image levels. Lysotracker stainings were photographed in widefield mode, and single optical sections are shown for colocalisations and mCherry-Atg8a assays. For p62 stainings, 3 subsequent optical sections taken at 0.55 μm intervals were projected into a single plane using Maximum Intensity Projection.

Statistical Analysis

For western blots, the image of the scanned film was inverted in Adobe Photoshop, saved and loaded in ImageJ. The strongest band was selected first, and individual bands were measured (Analyze, Set measurements, Integrated density, Measure) using a selection area with the same width and height as for the strongest band. Mean p62 values were normalized to tubulin mean scores first, and then expression levels were calculated relative to the control sample (wt head, lane 1). For immunostainings, images were loaded in ImageJ, and the image type was changed from RGB Color to RGB Stack. In the case of mutants, a 300×300 dpi area was chosen randomly from the red channel, and the threshold was adjusted to select dots. Each selected area was analyzed (Analyze Particles, Show, Masks) and the count and average size (in pixel^2) were noted from the summary of masked images. At least 10 images were evaluated from 4–6 animals per genotype. The number/size data were summarized in Excel, and normalized to control (average dot number and size in control animals was set to 1). For clonal analysis, image type was again changed from RGB Color to RGB Stack. Then the threshold was adjusted for the adequte channel, and clone cells and neighbouring control cells were evaluated. First, randomly selected GFP-positive or control cells were manually encircled with the Freehand selection tool, and then the selected area was analyzed in the channel of interest (Analyze Particles, Show, Masks), and the count and average size (in pixel^2) were noted from the summary of masked images. At least 10 images from 4–6 animals were evaluated for each genotype. These number/size data were processed as in the case of mutants, except that GFP-positive cells were compared to controls cells in the same image, and data was also normalized to cell size. Two-tailed two-sample unequal Student's t test was used to estimate p values in all cases.

Transmission Electron Microscopy

Larvae of the genotypes hs-Flp; UAS-p62-GFP/+; Act>CD2>Gal4, UAS-Dcr2/+ or hs-Flp; UAS-Dcr2/+; Act>CD2>Gal4, UAS-GFPnls/UAS-Atg4[C98A] or hs-Flp; UAS-Dcr2/+; Act>CD2>Gal4, UAS-GFPnls, r4-mCherry-Atg8a/UAS-Atg4[C98A] were heat shocked for 1 hour at 37°C

dc_840_14

to activate Act>CD2>Gal4 expression by hs-Flp in all fat body cells. Larvae were processed for electron microscopy 24 hours later as described previously. [16] Ultrathin sections were prepared from two animals per genotype and images were captured using a JEOL JEM-1011 transmission electron microscope with an Olympus Morada 11 megapixel camera and iTEM software (Olympus).

Supporting Information

Figure S1 Endogenous p62 dots in Atg mutants. Loss of Atg2 (A), Atg7 (B), Atg8a (C), Atg13 (D), Atg18a (E) and Vps34 (F) all increase p62 aggregation. Scalebar in panel A equals 30 μm for all images. *Genotypes are: (A) Atg2[EP3697]/Df(3L)BSC119]; (B) Atg7[d77]/Atg7[d14]; (C) Atg8a[d4]; (D) Atg13[Δ81]; (E) Atg18a[KG03090]/Df(3L)Exel6112]; (F) Vps34[Δm22].*
(TIF)

Figure S2 The effect of additional RNAi and overexpression lines on p62 aggregation. The effect of overexpressed dominant-negative Atg4 (B), dominant-negative Vps34 (G), wild-type Rheb (H), and knockdown of Atg2 (A), Atg7 (C), Atg8a (D), Atg9 (E), Atg14 (F), Atg16 (I, J), Atg18a (K, L), Pten (M, N) and Atms (O) on p62 aggregation. Scalebar in panel A equals 40 μm for all images. *Genotypes are: (A) hsFlp; UAS-Dcr2/+; Act>CD2>Gal4, UAS-GFPnls/Atg2[JF02786]; (B) hsFlp; UAS-Dcr2/+; Act>CD2>Gal4, UAS-GFPnls/UAS-Atg4[C98A]; (C) hsFlp; UAS-Dcr2/+; Act>CD2>Gal4, UAS-GFPnls/Atg7[JF02787]; (D) hsFlp; UAS-Dcr2/Atg8a[KK109654]; Act>CD2>Gal4, UAS-GFPnls/+; (E) hsFlp; UAS-Dcr2/+; Act>CD2>Gal4, UAS-GFPnls/Atg9[JF02891]; (F) hsFlp; UAS-Dcr2/Atg14[KK108559]; Act>CD2>Gal4, UAS-GFPnls/+; (G) hsFlp; UAS-Dcr2/UAS-Vps34[KD]; Act>CD2>Gal4, UAS-GFPnls/+; (H) hsFlp; UAS-Dcr2/+; Act>CD2>Gal4, UAS-GFPnls/UAS-Rheb[EP50.084cre(w-)]; (I) hsFlp; UAS-Dcr2/Atg16[KK105993]; Act>CD2>Gal4, UAS-GFPnls/+; (J) hsFlp; UAS-Dcr2/+; Act>CD2>Gal4, UAS-GFPnls/Atg16[HMS01347]; (K) hsFlp; UAS-Dcr2/Atg18a[KK105366]; Act>CD2>Gal4, UAS-GFPnls/+; (L) hsFlp; UAS-Dcr2/+; Act>CD2>Gal4, UAS-GFPnls/Atg18a[JF02898]; (M) hsFlp; UAS-Dcr2/Pten[KK101475]; Act>CD2>Gal4, UAS-GFPnls/+; (N) hsFlp; UAS-Dcr2/+; Act>CD2>Gal4, UAS-GFPnls/Pten[JF01987]; (O) hsFlp; UAS-Dcr2/Atms[GD20876]; Act>CD2>Gal4, UAS-GFPnls/+.*
(TIF)

Figure S3 Knockdown of RpS8 or Atms inhibits starvation-induced mCherry-Atg8a and Lysotracker puncta formation. Silencing of RpS8 or Atms strongly interferes with starvation-induced mCherry-Atg8a dot formation (panels A and B, respectively) and blocks punctate Lysotracker staining (panels C and D, respectively). Scalebar in panel A equals 30 μm for all images. *Genotypes are: (A) hs-Flp; UAS-Dcr2/RpS8[KK106835]; Act>CD2>Gal4, UAS-GFPnls, r4-mCherry-Atg8a/+; (B) hs-Flp; UAS-Dcr2/Atms[GD20876]; Act>CD2>Gal4, UAS-GFPnls, r4-mCherry-Atg8a/+; (C) hs-Flp; UAS-LampGFP/RpS8[KK106835]; Act>CD2>Gal4, UAS-Dcr2; (D) hs-Flp; UAS-LampGFP/Atms[GD20876]; Act>CD2>Gal4, UAS-Dcr2.*
(TIF)

Figure S4 p62-GFP aggregation in additional RNAi and overexpression lines. Knockdown of Atg7 (A), Atg8a (B), Atg9 (C), Atg14 (D), Atg18a (E), Pten (G), Tsc2 (H), RpS8(I), Atms (J) and expression of dominant-negative Vps34 (F) in p62-GFP expressing cell clones. Exposure times are indicated in the top right corner for each image. Scalebar in panel A equals 30 μm for all images. *Genotypes are: (A) hsFlp; UAS-p62-GFP/+; Act>CD2>''' Gal4, UAS-Dcr2/Atg7[JF02787]; (B) hsFlp; UAS-p62-GFP/Atg8a[KK109654]; Act>CD2>Gal4, UAS-Dcr2/+; (C) hsFlp; UAS-p62-GFP/+; Act>CD2>Gal4, UAS-Dcr2/Atg9[JF02891]; (D) hsFlp; UAS-p62-GFP/Atg14[KK108559]; Act>CD2>Gal4, UAS-Dcr2/+; (E) hsFlp; UAS-p62-GFP/Atg18a[KK105366]; Act>CD2>Gal4, UAS-Dcr2/+; (F) hsFlp; UAS-p62-GFP/UAS-Vps34[KD]; Act>CD2>Gal4, UAS-Dcr2/+; (G) hsFlp; UAS-p62-GFP/+; Act>CD2>Gal4, UAS-Dcr2/Pten[JF01987]; (H) hsFlp; UAS-p62-GFP/TSC2[KK103417]; Act>CD2>Gal4, UAS-Dcr2/+; (I) hsFlp; UAS-p62-GFP/RpS8[KK106835]; Act>CD2>Gal4, UAS-Dcr2/+; (J) hsFlp; UAS-p62-GFP/Atms[GD20876]; Act>CD2>Gal4, UAS-Dcr2/+.*
(TIF)

Figure S5 The effect of Atg16 RNAi lines on starvation-induced punctate Lysotracker staining in L3 and L2 larval stages. Both RNAi lines for Atg16 show a similar block of Lysotracker puncta formation in L3 (panels A and C), while the size of these dots is only reduced significantly by $Atg16^{HMS}$ in L2 (compare D to B; see also panel E for statistics). * indicates a significant difference ($p<0.05$), ** indicates a very significant difference ($p<0.01$), based on two-tailed two-sample unequal Student's t tests. Scalebar in panel A equals 30 μm for panels A, C, and scalebar in panel B equals 30 μm for panels B, D. *Genotypes are: (A,B) hs-Flp; UAS-LampGFP/Atg16[KK105993]; Act>CD2>Gal4, UAS-Dcr2; (C,D) hs-Flp; UAS-LampGFP/+; Act>CD2>Gal4, UAS-Dcr3/Atg16[HMS01347].*
(TIF)

Figure S6 Overexpression of mCherry-Atg8a rescues the effect of Atg8a mutation or expression of dominant-negative Atg4 on p62 accumulation. Expression of mCherry-Atg8a reduces the size and number of p62 aggregates in Atg8a null mutants (A; see panel B for statistics). No accumulation of p62 dots is observed in fat body cells coexpressing mCherry-Atg8a and dominant-negative Atg4 relative to control cells (C; see panel D for statistics – no significant difference is seen). Scalebar in panel A equals 30 μm. *Genotypes are: (A)Atg8a[d4]; +/+; r4-mCherry-Atg8a/+; (B) hs-Flp; UAS-Dcr2/+; Act>CD2>Gal4, UAS-GFPnls, r4-mCherry-Atg8a/UAS-Atg4[C98A].*
(TIF)

Acknowledgments

We thank Sarolta Palfia for her excellent technical assistance, Tom Neufeld for stocks, sharing the unpublished Atg8a mutant, helpful discussions and critical reading of the manuscript, and stock centers BDSC, VDRC, and the TRiP at Harvard Medical School for providing fly strains used in this study.

Author Contributions

Conceived and designed the experiments: KP KH GJ. Performed the experiments: KP PN AV ZV BE KH GJ. Analyzed the data: KP GJ. Contributed reagents/materials/analysis tools: KP PN KH GJ. Wrote the paper: KP PN GJ.

References

1. Moscat J, Diaz-Meco MT (2009) p62 at the crossroads of autophagy, apoptosis, and cancer. Cell 137: 1001–1004.

2. Dezelee S, Bras F, Contamine D, Lopez-Ferber M, Segretain D, et al. (1989) Molecular analysis of ref(2)P, a Drosophila gene implicated in sigma rhabdovirus

dc_840_14

multiplication and necessary for male fertility. The EMBO journal 8: 3437–3446.
3. Nezis IP, Simonsen A, Sagona AP, Finley K, Gaumer S, et al. (2008) Ref(2)P, the Drosophila melanogaster homologue of mammalian p62, is required for the formation of protein aggregates in adult brain. J Cell Biol 180: 1065–1071.
4. Bartlett BJ, Isakson P, Lewerenz J, Sanchez H, Kotzebue RW, et al. (2011) p62, Ref(2)P and ubiquitinated proteins are conserved markers of neuronal aging, aggregate formation and progressive autophagic defects. Autophagy 7: 572–583.
5. Komatsu M, Waguri S, Chiba T, Murata S, Iwata J, et al. (2006) Loss of autophagy in the central nervous system causes neurodegeneration in mice. Nature 441: 880–884.
6. Hara T, Nakamura K, Matsui M, Yamamoto A, Nakahara Y, et al. (2006) Suppression of basal autophagy in neural cells causes neurodegenerative disease in mice. Nature 441: 885–889.
7. Bjorkoy G, Lamark T, Pankiv S, Overvatn A, Brech A, et al. (2009) Monitoring autophagic degradation of p62/SQSTM1. Methods in enzymology 452: 181–197.
8. Juhasz G, Erdi B, Sass M, Neufeld TP (2007) Atg7-dependent autophagy promotes neuronal health, stress tolerance, and longevity but is dispensable for metamorphosis in Drosophila. Genes Dev 21: 3061–3066.
9. Simonsen A, Cumming RC, Brech A, Isakson P, Schubert DR, et al. (2008) Promoting basal levels of autophagy in the nervous system enhances longevity and oxidant resistance in adult Drosophila. Autophagy 4: 176–184.
10. Klionsky DJ, Meijer AJ, Codogno P (2005) Autophagy and p70S6 kinase. Autophagy 1: 59–60; discussion 60–51.
11. Scott RC, Schuldiner O, Neufeld TP (2004) Role and regulation of starvation-induced autophagy in the Drosophila fat body. Dev Cell 7: 167–178.
12. Chang YY, Neufeld TP (2009) An Atg1/Atg13 complex with multiple roles in TOR-mediated autophagy regulation. Molecular Biology of the Cell 20: 2004–2014.
13. Fujita N, Hayashi-Nishino M, Fukumoto H, Omori H, Yamamoto A, et al. (2008) An Atg4B mutant hampers the lipidation of LC3 paralogues and causes defects in autophagosome closure. Molecular Biology of the Cell 19: 4651–4659.
14. Erdi B, Nagy P, Zvara A, Varga A, Pircs K, et al. (2012) Loss of the starvation-induced gene Rack1 leads to glycogen deficiency and impaired autophagic responses in Drosophila. Autophagy 8.
15. Dietzl G, Chen D, Schnorrer F, Su KC, Barinova Y, et al. (2007) A genome-wide transgenic RNAi library for conditional gene inactivation in Drosophila. Nature 448: 151–156.
16. Juhasz G, Hill JH, Yan Y, Sass M, Baehrecke EH, et al. (2008) The class III PI(3)K Vps34 promotes autophagy and endocytosis but not TOR signaling in Drosophila. J Cell Biol 181: 655–666.
17. Ni JQ, Liu LP, Binari R, Hardy R, Shim HS, et al. (2009) A Drosophila resource of transgenic RNAi lines for neurogenetics. Genetics 182: 1089–1100.
18. Toda H, Mochizuki H, Flores R, 3rd, Josowitz R, Krasieva TB, et al. (2008) UNC-51/ATG1 kinase regulates axonal transport by mediating motor-cargo assembly. Genes Dev 22: 3292–3307.
19. Juhasz G, Neufeld TP (2008) Experimental control and characterization of autophagy in Drosophila. Methods Mol Biol 445: 125–133.

Autophagy 8:4, 1–100; April 2012; © 2012 Landes Bioscience

Guidelines for the use and interpretation of assays for monitoring autophagy

Daniel J. Klionsky,[1,2,3,*] Fabio C. Abdalla,[4] Hagai Abeliovich,[5] Robert T. Abraham,[6] Abraham Acevedo-Arozena,[7] Khosrow Adeli,[8] Lotta Agholme,[9] Maria Agnello,[10] Patrizia Agostinis,[11] Julio A. Aguirre-Ghiso,[12] Hyung Jun Ahn,[13] Ouardia Ait-Mohamed,[14] Slimane Ait-Si-Ali,[14] Takahiko Akematsu,[15] Shizuo Akira,[16] Hesham M. Al-Younes,[17] Munir A. Al-Zeer,[18] Matthew L. Albert,[19] Roger L. Albin,[20,21] Javier Alegre-Abarrategui,[22] Maria Francesca Aleo,[23] Mehrdad Alirezaei,[24] Alexandru Almasan,[25] Maylin Almonte-Becerril,[26] Atsuo Amano,[27] Ravi Amaravadi,[28] Shoba Amarnath,[29] Amal O. Amer,[30,31] Nathalie Andrieu-Abadie,[32,33] Vellareddy Anantharam,[34] David K. Ann,[35] Shailendra Anoopkumar-Dukie,[36] Hiroshi Aoki,[37] Nadezda Apostolova,[38] Giuseppe Arancia,[39] John P. Aris,[40] Katsuhiko Asanuma,[41] Nana Y.O. Asare,[42] Hisashi Ashida,[43] Valerie Askanas,[44] David S. Askew,[45] Patrick Auberger,[46,47] Misuzu Baba,[48] Steven K. Backues,[1] Eric H. Baehrecke,[49] Ben A. Bahr,[50] Xue-Yuan Bai,[51] Yannick Bailly,[52] Robert Baiocchi,[53] Giulia Baldini,[54] Walter Balduini,[55] Andrea Ballabio,[56,57] Bruce A. Bamber,[58] Edward T.W. Bampton,[59] Gábor Bánhegyi,[60] Clinton R. Bartholomew,[1] Diane C. Bassham,[61] Robert C. Bast, Jr.,[62] Henri Batoko,[63] Boon-Huat Bay,[64] Isabelle Beau,[65] Daniel M. Béchet,[66] Thomas J. Begley,[67] Christian Behl,[68] Christian Behrends,[69] Soumeya Bekri,[70] Bryan Bellaire,[71] Linda J. Bendall,[72] Luca Benetti,[73] Laura Berliocchi,[74] Henri Bernardi,[75] Francesca Bernassola,[76] Sébastien Besteiro,[77] Ingrid Bhatia-Kissova,[78] Xiaoning Bi,[79] Martine Biard-Piechaczyk,[80] Janice S. Blum,[81] Lawrence H. Boise,[82] Paolo Bonaldo,[83] David L. Boone,[84] Beat C. Bornhauser,[85] Karina R. Bortoluci,[86] Ioannis Bossis,[87] Frédéric Bost,[46] Jean-Pierre Bourquin,[85] Patricia Boya,[88] Michaël Boyer-Guittaut,[89] Peter V. Bozhkov,[90] Nathan R. Brady,[91] Claudio Brancolini,[92] Andreas Brech,[93] Jay E. Brenman,[94] Ana Brennand,[95] Emery H. Bresnick,[96] Patrick Brest,[97] Dave Bridges,[1] Molly L. Bristol,[98] Paul S. Brookes,[99] Eric J. Brown,[100] John H. Brumell,[101] Nicola Brunetti-Pierri,[56,57] Ulf T. Brunk,[102] Dennis E. Bulman,[103] Scott J. Bultman,[104] Geert Bultynck,[105] Lena F. Burbulla,[106] Wilfried Bursch,[107] Jonathan P. Butchar,[108] Wanda Buzgariu,[109] Sergio P. Bydlowski,[110] Ken Cadwell,[111] Monika Cahová,[112] Dongsheng Cai,[113] Jiyang Cai,[114] Qian Cai,[115] Bruno Calabretta,[116] Javier Calvo-Garrido,[117] Nadine Camougrand,[118] Michelangelo Campanella,[119,120] Jenny Campos-Salinas,[121] Eleonora Candi,[122] Lizhi Cao,[123] Allan B. Caplan,[124] Simon R. Carding,[125,126] Sandra M. Cardoso,[127] Jennifer S. Carew,[128] Cathleen R. Carlin,[129] Virginie Carmignac,[130] Leticia A.M. Carneiro,[131] Serena Carra,[132,133] Rosario A. Caruso,[134] Giorgio Casari,[135] Caty Casas,[136] Roberta Castino,[137] Eduardo Cebollero,[138,139] Francesco Cecconi,[140,141] Jean Celli,[142] Hassan Chaachouay,[143] Han-Jung Chae,[144] Chee-Yin Chai,[145] David C. Chan,[146] Edmond Y. Chan,[147] Raymond Chuen-Chung Chang,[148] Chi-Ming Che,[149] Ching-Chow Chen,[150] Guang-Chao Chen,[151] Guo-Qiang Chen,[152] Min Chen,[153] Quan Chen,[154,155] Steve S.-L. Chen,[156] WenLi Chen,[157] Xi Chen,[158] Xiangmei Chen,[51] Xiequn Chen,[159] Ye-Guang Chen,[160] Yingyu Chen,[161] Yongqiang Chen,[162] Yu-Jen Chen,[163] Zhixiang Chen,[164] Alan Cheng,[165] Christopher H.K. Cheng,[166] Yan Cheng,[167,168] Heesun Cheong,[169] Jae-Ho Cheong,[170] Sara Cherry,[171] Russ Chess-Williams,[172] Zelda H. Cheung,[173] Eric Chevet,[174] Hui-Ling Chiang,[175] Roberto Chiarelli,[10] Tomoki Chiba,[176] Lih-Shen Chin,[177] Shih-Hwa Chiou,[178] Francis V. Chisari,[24] Chi Hin Cho,[179] Dong-Hyung Cho,[180] Augustine M.K. Choi,[181] DooSeok Choi,[182] Kyeong Sook Choi,[183] Mary E. Choi,[184] Salem Chouaib,[185] Divaker Choubey,[186] Vinay Choubey,[187] Charleen T. Chu,[188,189] Tsung-Hsien Chuang,[190] Sheau-Huei Chueh,[191] Taehoon Chun,[192] Yong-Joon Chwae,[193] Mee-Len Chye,[194] Roberto Ciarcia,[195] Maria R. Ciriolo,[141,196] Michael J. Clague,[197] Robert S.B. Clark,[198] Peter G.H. Clarke,[199] Robert Clarke,[200] Patrice Codogno,[201] Hilary A. Coller,[202] María I. Colombo,[203] Sergio Comincini,[204] Maria Condello,[39] Fabrizio Condorelli,[205] Mark R. Cookson,[206] Graham H. Coombs,[147] Isabelle Coppens,[207] Ramon Corbalan,[208] Pascale Cossart,[209,210] Paola Costelli,[211] Safia Costes,[212] Ana Coto-Montes,[213] Eduardo Couve,[214] Fraser P. Coxon,[215] James M. Cregg,[216] José L. Crespo,[217] Marianne J. Cronjé,[218] Ana Maria Cuervo,[219,220,221] Joseph J. Cullen,[222] Mark J. Czaja,[221,223] Marcello D'Amelio,[224] Arlette Darfeuille-Michaud,[225,226] Dipak K. Das,[227] Lester M. Davids,[228] Faith E. Davies,[229] Massimo De Felici,[230] John F. de Groot,[231] Cornelis A.M. de Haan,[232] Luisa De Martino,[233] Angelo De Milito,[234] Vincenzo De Tata,[235] Jayanta Debnath,[236] Alexei Degterev,[237] Benjamin Dehay,[238] Lea M.D. Delbridge,[239] Francesca Demarchi,[240] Yi Zhen Deng,[241] Jörn Dengjel,[242] Paul Dent,[243] Donna Denton,[244,245] Vojo Deretic,[246] Shyamal D. Desai,[247] Rodney J. Devenish,[248,249] Mario Di Gioacchino,[250] Gilbert Di Paolo,[251,252] Chiara Di Pietro,[253] Guillermo Díaz-Araya,[254] Inés Díaz-Laviada,[255] Maria T. Diaz-Meco,[256] Javier Diaz-Nido,[257] Ivan Dikic,[69,258] Savithramma P. Dinesh-Kumar,[259] Wen-Xing Ding,[260] Clark W. Distelhorst,[261,262,263,264,265] Abhinav Diwan,[266,267] Mojgan Djavaheri-Mergny,[268] Svetlana Dokudovskaya,[269] Zheng Dong,[270,271] Frank C. Dorsey,[272] Victor Dosenko,[273] James J. Dowling,[20,274] Stephen Doxsey,[275] Marlène Dreux,[276] Mark E. Drew,[30] Qiuhong Duan,[277] Michel A. Duchosal,[278] Karen Duff,[251,252] Isabelle Dugail,[279,280] Madeleine Durbeej,[130] Michael Duszenko,[281] Charles L. Edelstein,[282] Aimee L. Edinger,[283] Gustavo Egea,[284] Ludwig Eichinger,[285] N. Tony Eissa,[286] Suhendan Ekmekcioglu,[287] Wafik S. El-Deiry,[168,288] Zvulun Elazar,[289] Mohamed Elgendy,[290] Lisa M. Ellerby,[291] Kai Er Eng,[292] Anna-Mart Engelbrecht,[293] Simone Engelender,[294] Jekaterina Erenpreisa,[295] Ricardo Escalante,[117] Audrey Esclatine,[65] Eeva-Liisa Eskelinen,[296] Lucile Espert,[80] Virginia Espina,[297] Huizhou Fan,[298] Jia Fan,[299] Qi-Wen Fan,[300] Zhen Fan,[62] Shengyun Fang,[301,302] Yongqi Fang,[303] Manolis Fanto,[304] Alessandro Fanzani,[23] Thomas Farkas,[305] Jean-Claude Farré,[306] Mathias Faure,[307] Marcus Fechheimer,[308] Carl G. Feng,[309] Jian Feng,[310] Qili Feng,[311] Youji Feng,[312] László Fésüs,[313] Ralph Feuer,[314] Maria E. Figueiredo-Pereira,[315] Gian Maria Fimia,[316] Diane C. Fingar,[317] Steven Finkbeiner,[318] Toren Finkel,[319] Kim D. Finley,[320] Filomena Fiorito,[233] Edward A. Fisher,[321] Paul B. Fisher,[322] Marc Flajolet,[323] Maria L. Florez-McClure,[324] Salvatore Florio,[195] Edward A. Fon,[325] Francesco Fornai,[326] Franco Fortunato,[327] Rati Fotedar,[256] Daniel H. Fowler,[29] Howard S. Fox,[328] Rodrigo Franco,[329] Lisa B. Frankel,[330] Marc Fransen,[331] José M. Fuentes,[332] Juan Fueyo,[231] Jun Fujii,[333] Kozo Fujisaki,[334] Eriko Fujita,[335] Mitsunori Fukuda,[336] Ruth H. Furukawa,[308] Matthias Gaestel,[337] Philippe Gailly,[338] Matgorzata Gajewska,[339] Brigitte Galliot,[109] Vincent Galy,[340] Subramaniam Ganesh,[341] Barry Ganetzky,[342] Ian G. Ganley,[343] Fen-Biao Gao,[344] George F. Gao,[345] Jinming Gao,[346] Lorena Garcia,[347] Guillermo Garcia-Manero,[348] Mikel Garcia-Marcos,[349] Marjan Garmyn,[350] Andrei L. Gartel,[351] Evelina Gatti,[352] Mathias Gautel,[353] Thomas R. Gawriluk,[354] Matthew E. Gegg,[355] Jiefei Geng,[356] Marc Germain,[357] Jason E. Gestwicki,[1,3,358] David A. Gewirtz,[98] Saeid Ghavami,[359] Pradipta Ghosh,[360] Anna M. Giammarioli,[361] Alexandra N. Giatromanolaki,[362] Spencer B. Gibson,[363] Robert W. Gilkerson,[364] Michael L. Ginger,[365] Henry N. Ginsberg,[366] Jakub Golab,[367] Michael S. Goligorsky,[368] Pierre Golstein,[352] Candelaria Gomez-Manzano,[231,369] Ebru Goncu,[370] Céline Gongora,[371] Claudio D. Gonzalez,[372] Ramon Gonzalez,[373] Cristina González-Estévez,[374] Rosa Ana González-Polo,[332] Elena Gonzalez-Rey,[121] Nikolai V. Gorbunov,[375] Sharon Gorski,[376] Sandro Goruppi,[377] Roberta A. Gottlieb,[320] Devrim Gozuacik,[378] Giovanna Elvira Granato,[195] Gary D. Grant,[36] Kim N. Green,[379] Aleš Gregorc,[380] Frédéric Gros,[381] Charles Grose,[382] Thomas W. Grunt,[383] Philippe Gual,[46,47] Jun-Lin Guan,[162,317] Kun-Liang Guan,[384] Sylvie M. Guichard,[385] Anna S. Gukovskaya,[386] Ilya Gukovsky,[386] Jan Gunst,[387] Asa B. Gustafsson,[388] Andrew J. Halayko,[359,389] Amber N. Hale,[354] Sandra K. Halonen,[390] Maho Hamasaki,[391] Feng Han,[392] Ting Han,[1,317] Michael K. Hancock,[393] Malene Hansen,[256] Hisashi Harada,[394] Masaru Harada,[395] Stefan E. Hardt,[396] J. Wade Harper,[356] Adrian L. Harris,[397] James Harris,[398] Steven D. Harris,[399] Makoto Hashimoto,[400] Jeffrey A. Haspel,[181,401] Shin-ichiro Hayashi,[402] Lori A. Hazelhurst,[403] Congcong He,[404] You-Wen He,[405] Marie-Josée Hébert,[406] Kim A. Heidenreich,[407] Miep H. Helfrich,[215] Gudmundur V. Helgason,[408] Elizabeth P. Henske,[181] Brian Herman,[409] Paul K. Herman,[410] Claudio Hetz,[411] Sabine Hilfiker,[412] Joseph A. Hill,[413] Lynne J. Hocking,[215] Paul Hofman,[414] Thomas G. Hofmann,[415] Jörg Höhfeld,[416] Tessa L. Holyoake,[408] Ming-Huang Hong,[417] David A. Hood,[418] Gökhan S. Hotamisligil,[419] Ewout J. Houwerzijl,[420] Maria Høyer-Hansen,[421] Bingren Hu,[422] Chien-An A. Hu,[423] Hong-Ming Hu,[424] Ya Hua,[425] Canhua Huang,[426] Ju Huang,[101] Shengbing Huang,[427] Wei-Pang Huang,[428] Tobias B. Huber,[429] Won-Ki Huh,[430] Tai-Ho Hung,[431] Ted R. Hupp,[432] Gang Min Hur,[433] James B. Hurley,[434] Sabah N.A. Hussain,[435] Patrick J. Hussey,[436] Jung Jin Hwang,[437] Seungmin Hwang,[438] Atsuhiro Ichihara,[439] Shirin Ilkhanizadeh,[300] Ken Inoki,[440] Takeshi Into,[441] Valentina Iovane,[233] Juan L. Iovanna,[442] Nancy Y. Ip,[443] Yoshitaka Isaka,[444] Hiroyuki Ishida,[445] Ciro Isidoro,[137] Ken-ichi Isobe,[446] Akiko Iwasaki,[447] Marta Izquierdo,[257] Yotaro Izumi,[448] Panu M. Jaakkola,[449] Marja Jäättelä,[305] George R. Jackson,[450] William T. Jackson,[451] Bassam Janji,[452] Marina Jendrach,[453] Ju-Hong Jeon,[454] Eui-Bae Jeung,[455] Hong Jiang,[231] Hongchi Jiang,[456] Jean X. Jiang,[457] Ming Jiang,[458] Qing Jiang,[459] Xuejun Jiang,[460] Xuejun Jiang,[461] Alberto Jiménez,[462] Meiyan Jin,[1,2] Shengkan Jin,[463] Cheol O. Joe,[464] Terje Johansen,[465] Daniel E. Johnson,[466] Gail V.W. Johnson,[99] Nicola L. Jones,[467] Bertrand Joseph,[234] Suresh K. Joseph,[468] Annie M. Joubert,[469] Gábor Juhász,[470] Lucienne Juillerat-Jeanneret,[471] Chang Hwa Jung,[472] Yong-Keun Jung,[473] Kai Kaarniranta,[474] Allen Kaasik,[187] Tomohiro Kabuta,[475] Motoni Kadowaki,[476] Katarina Kagedal,[477] Yoshiaki Kamada,[478] Vitaliy O. Kaminskyy,[479] Harm H. Kampinga,[133] Hiromitsu Kanamori,[480] Chanhee Kang,[481] Khong Bee Kang,[482] Kwang Il Kang,[483] Rui Kang,[484] Yoon-A Kang,[96] Tomotake Kanki,[485] Thirumala-Devi Kanneganti,[486] Haruo Kanno,[487] Anumantha G. Kanthasamy,[34] Arthi Kanthasamy,[34] Vassiliki Karantza,[488] Gur P. Kaushal,[489] Susmita Kaushik,[219,220,221] Yoshinori Kawazoe,[490] Po-Yuan Ke,[156,491] John H. Kehrl,[492] Ameeta Kelekar,[493] Claus Kerkhoff,[494] David H. Kessel,[495] Hany Khalil,[496] Jan A.K.W. Kiel,[497] Amy A. Kiger,[498] Akio Kihara,[499] Deok Ryong Kim,[500] Do-Hyung Kim,[501] Dong-Hou Kim,[502] Eun-Kyoung Kim,[503] Hyung-Ryong Kim,[504] Jae-Sung Kim,[505] Jeong Hun Kim,[506] Jin Cheon Kim,[507] John K. Kim,[1,508] Peter K. Kim,[101,509] Seong Who Kim,[510] Yong-Sun Kim,[511,512] Yonghyun Kim,[513] Adi Kimchi,[514] Alec C. Kimmelman,[515] Jason S. King,[516] Timothy J. Kinsella,[517] Vladimir Kirkin,[518] Lorrie A. Kirshenbaum,[359,519] Katsuhiko Kitamoto,[520] Kaio Kitazato,[521] Ludger Klein,[522] Walter T. Klimecki,[523] Jochen Klucken,[524] Erwin Knecht,[525] Ben C.B. Ko,[526] Jan C. Koch,[527] Hiroshi Koga,[220,221] Jae-Young Koh,[528] Young Ho Koh,[511] Masato Koike,[529] Masaaki Komatsu,[530] Eiki Kominami,[531] Hee Jeong Kong,[532] Wei-Jia Kong,[533] Viktor I. Korolchuk,[534] Yaichiro Kotake,[535] Michael I. Koukourakis,[536] Juan B. Kouri Flores,[26] Attila L. Kovács,[470] Claudine Kraft,[537] Dimitri Krainc,[538] Helmut Krämer,[539] Carole Kretz-Remy,[540] Anna M. Krichevsky,[541] Guido Kroemer,[279,542] Rejko Krüger,[106] Oleg Krut,[543] Nicholas T. Ktistakis,[544] Chia-Yi Kuan,[545] Roza Kucharczyk,[546] Ashok Kumar,[547] Raj Kumar,[548] Sharad Kumar,[244,245] Mondira Kundu,[549] Hsing-Jien Kung,[550] Tino Kurz,[102] Ho Jeong Kwon,[551] Albert R. La Spada,[552,553] Frank Lafont,[554] Trond Lamark,[465] Jacques Landry,[555] Jon D. Lane,[556] Pierre Lapaquette,[557] Jocelyn F. Laporte,[558] Lajos László,[470] Sergio Lavandero,[347,413] Josée N. Lavoie,[555] Robert Layfield,[559] Pedro A. Lazo,[560] Weidong Le,[561,562] Laurent Le Cam,[371] Daniel J. Ledbetter,[354] Alvin J.X. Lee,[563] Byung-Wan Lee,[564] Gyun Min Lee,[464] Jongdae Lee,[360] Ju-Hyun Lee,[565] Michael Lee,[566] Myung-Shik Lee,[567] Sug Hyung Lee,[568] Christiaan Leeuwenburgh,[569] Patrick Legembre,[570] Renaud Legouis,[571] Michael Lehmann,[572] Huan-Yao Lei,[573] Qun-Ying Lei,[574] David A. Leib,[575] José Leiro,[576] John J. Lemasters,[577] Antoinette Lemoine,[578] Maciej S. Lesniak,[579] Dina Lev,[580] Victor V. Levenson,[581] Beth Levine,[404,582] Efrat Levy,[565,583] Faqiang Li,[584] Jun-Lin Li,[585] Lian Li,[177] Sheng Li,[562,586] Weijie Li,[587] Xue-Jun Li,[588] Yan-bo Li,[589] Yi-Ping Li,[590] Chengyu Liang,[591] Qiangrong Liang,[592] Yung-Feng Liao,[593] Pawel P. Liberski,[594] Andrew Lieberman,[358] Hyunjung J. Lim,[595] Kah-Leong Lim,[596] Kyu Lim,[597] Chiou-Feng Lin,[598] Fu-Cheng Lin,[599] Jian Lin,[600] Jiandie D. Lin,[1,317] Kui Lin,[601] Wan-Wan Lin,[150] Weei-Chin Lin,[286,602] Yi-Ling Lin,[156] Rafael Linden,[603] Paul Lingor,[527] Jennifer Lippincott-Schwartz,[604] Michael P. Lisanti,[605] Paloma B. Liton,[606] Bo Liu,[426] Chun-Feng Liu,[607] Kaiyu Liu,[608] Leyuan Liu,[609]

dc_840_14

Qiong A. Liu,[610] Wei Liu,[611] Young-Chau Liu,[612] Yule Liu,[160] Richard A. Lockshin,[613] Chun-Nam Lok,[149] Sagar Lonial,[82] Benjamin Loos,[293] Gabriel Lopez-Berestein,[62] Carlos López-Otín,[614] Laura Lossi,[615] Michael T. Lotze,[484] Peter Löw,[470] Binfeng Lu,[616] Bingwei Lu,[617] Bo Lu,[618] Zhen Lu,[62] Frédéric Luciano,[46,47] Nicholas W. Lukacs,[358] Anders H. Lund,[330] Melinda A. Lynch-Day,[1,2] Yong Ma,[456] Fernando Macian,[619] Jeff MacKeigan,[620] Kay F. Macleod,[621] Frank Madeo,[622] Luigi Maiuri,[623] Maria Chiara Maiuri,[279,542] Davide Malagoli,[624] May Christine V. Malicdan,[625] Walter Malorni,[361,626] Na Man,[627] Eva-Maria Mandelkow,[628] Stéphen Manon,[118] Irena Manov,[629] Kai Mao,[1,2] Xiang Mao,[630] Zixu Mao,[177,631] Philippe Marambaud,[632] Daniela Marazziti,[253] Yves L. Marcel,[633] Katie Marchbank,[634] Piero Marchetti,[635] Stefan J. Marciniak,[636] Mateus Marcondes,[4] Mohsen Mardi,[637] Gabriella Marfe,[76] Guillermo Mariño,[638] Maria Markaki,[639] Mark R. Marten,[513] Seamus J. Martin,[640] Camille Martinand-Mari,[641] Wim Martinet,[642] Marta Martinez-Vicente,[643] Matilde Masini,[644] Paolo Matarrese,[645] Saburo Matsuo,[646] Raffaele Matteoni,[253] Andreas Mayer,[647] Nathalie M. Mazure,[648] David J. McConkey,[580,649] Melanie J. McConnell,[650] Catherine McDermott,[651] Christine McDonald,[652] Gerald M. McInerney,[292] Sharon L. McKenna,[653] BethAnn McLaughlin,[654] Pamela J. McLean,[538] Christopher R. McMaster,[655] G. Angus McQuibban,[509] Alfred J. Meijer,[656] Miriam H. Meisler,[508] Alicia Meléndez,[613,657] Thomas J. Melia,[658] Gerry Melino,[59,659] Maria A. Mena,[660] Javier A. Menendez,[661] Rubem F. S. Menna-Barreto,[662] Manoj B. Menon,[337] Fiona M. Menzies,[663] Carol A. Mercer,[664] Adalberto Merighi,[615] Diane E. Merry,[665] Stefania Meschini,[39] Christian G. Meyer,[666] Thomas F. Meyer,[18] Chao-Yu Miao,[667] Jun-Ying Miao,[668] Paul A.M. Michels,[95] Carine Michiels,[669] Dalibor Mijaljica,[248] Ana Milojkovic,[670] Saverio Minucci,[290] Clelia Miracco,[671] Cindy K. Miranti,[672] Ioannis Mitroulis,[673] Keisuke Miyazawa,[674] Noboru Mizushima,[675] Baharia Mograbi,[676] Simin Mohseni,[677] Xavier Molero,[678] Bertrand Mollereau,[679] Faustino Mollinedo,[560] Takashi Momoi,[680] Iryna Monastyrska,[232] Martha M. Monick,[681] Mervyn J. Monteiro,[301,682] Michael N. Moore,[683] Rodrigo Mora,[684] Kevin Moreau,[663] Paula I. Moreira,[127] Yuji Moriyasu,[685] Jorge Moscat,[256] Serge Mostowy,[686] Jeremy C. Mottram,[687] Tomasz Motyl,[339] Charbel E.-H. Moussa,[688] Sylke Müller,[687] Sylviane Muller,[381] Karl Münger,[689] Christian Münz,[690] Leon O. Murphy,[691] Maureen E. Murphy,[692] Antonio Musarò,[693] Indira Mysorekar,[694] Eiichiro Nagata,[695] Kazuhiro Nagata,[696] Aimable Nahimana,[697] Usha Nair,[1] Toshiyuki Nakagawa,[698] Kiichi Nakahira,[181] Hiroyasu Nakano,[699] Hitoshi Nakatogawa,[700] Meera Nanjundan,[701] Naweed I. Naqvi,[241] Derek P. Narendra,[702] Masashi Narita,[703] Miguel Navarro,[412] Steffan T. Nawrocki,[128] Taras Y. Nazarko,[306] Andriy Nemchenko,[413] Mihai G. Netea,[704] Thomas P. Neufeld,[705] Paul A. Ney,[706] Ioannis P. Nezis,[93] Huu Phuc Nguyen,[707] Daotai Nie,[708] Ichizo Nishino,[709] Corey Nislow,[710] Ralph A. Nixon,[565] Takeshi Noda,[391] Angelika A. Noegel,[285] Anna Nogalska,[44] Satoru Noguchi,[709] Lucia Notterpek,[711] Ivana Novak,[712] Tomoyoshi Nozaki,[713] Nobuyuki Nukina,[714] Thorsten Nürnberger,[715] Beat Nyfeler,[691] Keisuke Obara,[499] Terry D. Oberley,[716] Salvatore Oddo,[717] Michinaga Ogawa,[718] Toya Ohashi,[719,720] Koji Okamoto,[721] Nancy L. Oleinick,[264,722,723] F. Javier Oliver,[121] Laura J. Olsen,[2] Stefan Olsson,[724] Onya Opota,[725] Timothy F. Osborne,[726] Gary K. Ostrander,[727] Kinya Otsu,[728] Jing-hsiung James Ou,[591] Mireille Ouimet,[633] Michael Overholtzer,[460] Bulent Ozpolat,[62] Paolo Paganetti,[729] Ugo Pagnini,[233] Nicolas Pallet,[730] Glen E. Palmer,[731] Camilla Palumbo,[76] Tianhong Pan,[732] Theocharis Panaretakis,[734] Udai Bhan Pandey,[733] Zuzana Papackova,[112] Issidora Papassideri,[734] Irmgard Paris,[735] Junsoo Park,[736] Ohkmae K. Park,[192] Jan B. Parys,[11] Katherine R. Parzych,[1,2] Susann Patschan,[737] Cam Patterson,[738] Sophie Pattingre,[371] John M. Pawelek,[739] Jianxin Peng,[740] David H. Perlmutter,[741] Ida Perrotta,[742] George Perry,[743] Shazib Pervaiz,[596,744] Matthias Peter,[745] Godefridus J. Peters,[746] Morten Petersen,[747] Goran Petrovski,[748] James M. Phang,[611] Mauro Piacentini,[141] Philippe Pierre,[352] Valérie Pierrefite-Carle,[749] Gérard Pierron,[750] Ronit Pinkas-Kramarski,[751] Antonio Piras,[752] Natik Piri,[753] Leonidas C. Platanias,[754] Stefanie Pöggeler,[755] Marc Poirot,[32,756] Angelo Poletti,[757] Christian Poüs,[758] Mercedes Pozuelo-Rubio,[759] Mette Prætorius-Ibba,[760] Anil Prasad,[761] Mark Prescott,[248] Muriel Priault,[118] Nathalie Produit-Zengaffinen,[762] Ann Progulske-Fox,[763] Tassula Proikas-Cezanne,[764] Serge Przedborski,[252,364,765] Karin Przyklenk,[766] Rosa Puertollano,[767] Julien Puyal,[199] Shu-Bing Qian,[768] Liang Qin,[769] Zheng-Hong Qin,[770] Susan E. Quaggin,[771] Nina Raben,[772] Hannah Rabinowich,[188] Simon W. Rabkin,[773] Irfan Rahman,[774] Abdelhaq Rami,[775] Georg Ramm,[248,776] Glenn Randall,[777] Felix Randow,[778] V. Ashutosh Rao,[779] Jeffrey C. Rathmell,[405,780] Brinda Ravikumar,[781] Swapan K. Ray,[782] Bruce H. Reed,[783] John C. Reed,[256] Fulvio Reggiori,[138] Anne Régnier-Vigouroux,[784] Andreas S. Reichert,[785] John J. Reiners, Jr.,[786] Russel J. Reiter,[409] Jun Ren,[787] José L. Revuelta,[462] Christopher J. Rhodes,[788] Konstantinos Ritis,[673] Elizete Rizzo,[789] Jeffrey Robbins,[790] Michel Roberge,[791] Hernan Roca,[792] Maria C. Roccheri,[10] Stephane Rocchi,[46,793] H. Peter Rodemann,[143] Santiago Rodríguez de Córdoba,[794] Bärbel Rohrer,[795] Igor B. Roninson,[796] Kirill Rosen,[655] Magdalena M. Rost-Roszkowska,[797] Mustapha Rouis,[798] Kasper M.A. Rouschop,[799] Francesca Rovetta,[23] Brian P. Rubin,[800] David C. Rubinsztein,[663] Klaus Ruckdeschel,[801] Edmund B. Rucker, III,[354] Assaf Rudich,[802] Emil Rudolf,[803] Nelson Ruiz-Opazo,[804] Rossella Russo,[805] Tor Erik Rusten,[93] Kevin M. Ryan,[516] Stefan W. Ryter,[181] David M. Sabatini,[806,807] Junichi Sadoshima,[808] Tapas Saha,[200] Tatsuya Saitoh,[16] Hiroshi Sakagami,[809] Yasuyoshi Sakai,[810] Ghasem Hoseini Salekdeh,[811] Paolo Salomoni,[812] Paul M. Salvaterra,[813] Guy Salvesen,[256] Rosa Salvioli,[814] Anthony M.J. Sanchez,[75] José A. Sánchez-Alcázar,[815] Ricardo Sánchez-Prieto,[816] Marco Sandri,[83,817,818] Uma Sankar,[819] Poonam Sansanwal,[820] Laura Santambrogio,[619,821] Shweta Saran,[822] Sovan Sarkar,[807] Minnie Sarwal,[820,823] Chihiro Sasakawa,[718] Ausra Sasnauskiene,[824] Miklós Sass,[470] Ken Sato,[825] Miyuki Sato,[825] Anthony H.V. Schapira,[355] Michael Scharl,[826] Hermann M. Schätzl,[827] Wiep Scheper,[828] Stefano Schiaffino,[818] Claudio Schneider,[240] Marion E. Schneider,[829] Regine Schneider-Stock,[830] Patricia V. Schoenlein,[831] Daniel F. Schorderet,[762,832] Christoph Schüller,[833] Gary K. Schwartz,[834] Luca Scorrano,[817,835] Linda Sealy,[836] Per O. Seglen,[837] Juan Segura-Aguilar,[838] Iban Seiliez,[839] Oleksandr Seleverstov,[840] Christian Sell,[841] Jong Bok Seo,[842] Duska Separovic,[843] Vijayasaradhi Setaluri,[844] Takao Setoguchi,[845] Carmine Settembre,[56,57] John J. Shacka,[846] Mala Shanmugam,[754] Irving M. Shapiro,[847] Eitan Shaulian,[848] Reuben J. Shaw,[849] James H. Shelhamer,[850] Han-Ming Shen,[851] Wei-Chiang Shen,[852] Zu-Hang Sheng,[853] Yang Shi,[854] Kenichi Shibuya,[855] Yoshihiro Shidoji,[856] Jeng-Jer Shieh,[857] Chwen-Ming Shih,[858] Yohta Shimada,[719] Shigeomi Shimizu,[859] Takahiro Shintani,[860] Orian S. Shirihai,[861] Gordon C. Shore,[862] Andriy A. Sibirny,[863] Stan B. Sidhu,[864] Beata Sikorska,[594] Elaine C.M. Silva-Zacarin,[4] Alison Simmons,[865] Anna Katharina Simon,[866] Hans-Uwe Simon,[867] Cristiano Simone,[868] Anne Simonsen,[869] David A. Sinclair,[870] Rajat Singh,[871] Debasish Sinha,[872] Frank A. Sinicrope,[427,873] Agnieszka Sirko,[546] Parco M. Siu,[874] Efthimios Sivridis,[362] Vojtech Skop,[875] Vladimir P. Skulachev,[876] Ruth S. Slack,[357] Soraya S. Smaili,[877] Duncan R. Smith,[878] Maria S. Soengas,[879] Thierry Soldati,[880] Xueqin Song,[881] Anil K. Sood,[882] Tuck Wah Soong,[596] Federica Sotgia,[116] Stephen A. Spector,[553,883] Claudia D. Spies,[884] Wolfdieter Springer,[885] Srinivasa M. Srinivasula,[886] Leonidas Stefanis,[887] Joan S. Steffan,[888] Ruediger Stendel,[889] Harald Stenmark,[93] Anastasis Stephanou,[890] Stephan T. Stern,[891] Cinthya Sternberg,[892] Björn Stork,[893] Peter Strålfors,[677] Carlos S. Subauste,[261,894] Xinbing Sui,[895] David Sulzer,[364,896] Jiaren Sun,[897] Shi-Yong Sun,[82] Zhi-Jun Sun,[898] Joseph J.Y. Sung,[899] Kuninori Suzuki,[900] Toshihiko Suzuki,[901] Michele S. Swanson,[902] Charles Swanton,[563] Sean T. Sweeney,[903] Lai-King Sy,[149] Gyorgy Szabadkai,[904] Ira Tabas,[366] Heinrich Taegtmeyer,[905] Marco Tafani,[906] Krisztina Takács-Vellai,[907] Yoshitaka Takano,[908] Kaoru Takegawa,[909] Genzou Takemura,[480] Fumihiko Takeshita,[910] Nicholas J. Talbot,[911] Kevin S.W. Tan,[912] Keiji Tanaka,[530] Kozo Tanaka,[913] Daolin Tang,[484] Dingzhong Tang,[914,915] Isei Tanida,[916] Bakhos A. Tannous,[538,917] Nektarios Tavernarakis,[639] Graham S. Taylor,[918] Gregory A. Taylor,[405,919] J. Paul Taylor,[920] Lance S. Terada,[404] Alexei Terman,[921] Gianluca Tettamanti,[922] Karin Thevissen,[923] Craig B. Thompson,[169] Andrew Thorburn,[924] Michael Thumm,[925] FengFeng Tian,[926] Yuan Tian,[323] Glauco Tocchini-Valentini,[253] Aviva M. Tolkovsky,[927] Yasuhiko Tomino,[41] Lars Tönges,[527] Sharon A. Tooze,[928] Cathy Tournier,[929] John Tower,[930] Roberto Towns,[162] Vladimir Trajkovic,[931] Leonardo H. Travassos,[932] Ting-Fen Tsai,[933] Mario P. Tschan,[934] Takeshi Tsubata,[935] Allan Tsung,[936] Boris Turk,[937] Lorianne S. Turner,[938] Suresh C. Tyagi,[939] Yasuo Uchiyama,[529] Takashi Ueno,[531] Midori Umekawa,[1] Rika Umemiya-Shirafuji,[334] Vivek K. Unni,[940] Maria I. Vaccaro,[372] Enza Maria Valente,[941] Greet Van den Berghe,[387] Ida J. van der Klei,[497] Wouter G. van Doorn,[942] Linda F. van Dyk,[943] Marjolein van Egmond,[944] Leo A. van Grunsven,[945] Peter Vandenabeele,[946] Wim P. Vandenberghe,[947] Ilse Vanhorebeek,[387] Eva C. Vaquero,[948] Guillermo Velasco,[949] Tibor Vellai,[907] Jose Miguel Vicencio,[904] Richard D. Vierstra,[584] Miquel Vila,[643,950] Cécile Vindis,[33,951] Giampietro Viola,[952] Maria Teresa Viscomi,[953] Olga V. Voitsekhovskaja,[954] Clarissa von Haefen,[884] Marcela Votruba,[955] Keiji Wada,[475] Richard Wade-Martins,[22] Cheryl L. Walker,[956] Craig M. Walsh,[957] Jochen Walter,[958] Xiang-Bo Wan,[959] Aimin Wang,[960] Chenguang Wang,[961] Dawei Wang,[456] Fan Wang,[962] Fen Wang,[609] Guanghui Wang,[770] Haichao Wang,[963] Hong-Gang Wang,[167,168] Horng-Dar Wang,[964] Jin Wang,[153] Ke Wang,[1,2] Mei Wang,[744] Richard C. Wang,[965] Xinlong Wang,[263] Xuejun Wang,[966] Ying-Jan Wang,[967] Yipeng Wang,[628] Zhen Wang,[968] Zhigang Charles Wang,[969] Zhinong Wang,[970] Derick G. Wansink,[971] Diane M. Ward,[972] Hirotaka Watada,[973] Sarah L. Waters,[634,728,974] Paul Webster,[975] Lixin Wei,[976] Conrad C. Weihl,[977] William A. Weiss,[300] Scott M. Welford,[722] Long-Ping Wen,[978] Caroline A. Whitehouse,[634] J. Lindsay Whitton,[24] Alexander J. Whitworth,[979] Tom Wileman,[980] John W. Wiley,[162] Simon Wilkinson,[981] Dieter Willbold,[982] Roger L. Williams,[778] Peter R. Williamson,[983] Bradly G. Wouters,[984] Chenghan Wu,[985] Dao-Cheng Wu,[986] William K.K. Wu,[899] Andreas Wyttenbach,[987] Ramnik J. Xavier,[988] Zhijun Xi,[989] Pu Xia,[990] Gengfu Xiao,[991] Zhiping Xie,[992] Zhonglin Xie,[993] Da-zhi Xu,[994] Jianzhen Xu,[995] Liang Xu,[996] Xiaolei Xu,[997] Ai Yamamoto,[252,364] Akitsugu Yamamoto,[998] Shunhei Yamashina,[999] Michiaki Yamashita,[1000] Xianghua Yan,[1001] Mitsuhiro Yanagida,[1002] Dun-Sheng Yang,[565] Elizabeth Yang,[1003] Jin-Ming Yang,[167,168] Shi Yu Yang,[1004] Wannian Yang,[1005] Wei Yuan Yang,[151] Zhifen Yang,[256] Meng-Chao Yao,[1006] Tso-Pang Yao,[780] Behzad Yeganeh,[359] Wei-Lien Yen,[1] Jia-jing Yin,[589] Xiao-Ming Yin,[1007] Ook-Joon Yoo,[1008] Gyesoon Yoon,[1009] Seung-Yong Yoon,[502] Tomohiro Yorimitsu,[1010] Yuko Yoshikawa,[1011] Tamotsu Yoshimori,[391] Kohki Yoshimoto,[1012] Ho Jin You,[1013] Richard J. Youle,[702] Anas Younes,[1014] Li Yu,[160] Long Yu,[1015] Seong-Woon Yu,[503] Wai Haung Yu,[251,252] Zhi-Min Yuan,[1016] Zhenyu Yue,[1017] Cheol-Heui Yun,[1018] Michisuke Yuzaki,[1019] Olga Zabirnyk,[1020] Elaine Silva-Zacarin,[4] David Zacks,[1021] Eldad Zacksenhaus,[1022] Nadia Zaffaroni,[1023] Zahra Zakeri,[613] Herbert J. Zeh, III,[1024] Scott O. Zeitlin,[1025] Hong Zhang,[1026] Hui-Ling Zhang,[770,1027] Jianhua Zhang,[846] Jing-Pu Zhang,[968] Lin Zhang,[1028] Long Zhang,[1029] Ming-Yong Zhang,[1030] Xu Dong Zhang,[1031] Mantong Zhao,[1,2] Yi-Fang Zhao,[898] Ying Zhao,[1032,1033] Zhizhuang J. Zhao,[1034] Xiaoxiang Zheng,[1035] Boris Zhivotovsky,[479] Qing Zhong,[1036] Cong-Zhao Zhou,[627] Changlian Zhu,[1037] Wei-Guo Zhu,[1033] Xiao-Feng Zhu,[1038] Xiongwei Zhu,[263] Yuangang Zhu,[915] Teresa Zoladek,[546] Wei-Xing Zong,[1039] Antonio Zorzano,[1040] Jürgen Zschocke[1041] and Brian Zuckerbraun[1042]

[1]Life Sciences Institute; University of Michigan; Ann Arbor, MI USA; [2]Department of Molecular, Cellular and Developmental Biology; University of Michigan; Ann Arbor, MI USA; [3]Department of Biological Chemistry; University of Michigan; Ann Arbor, MI USA; [4]Laboratory of Structural and Functional Biology; Federal University of São Carlos (UFSCar); Campus Sorocaba; São Paulo State, Brazil; [5]Department of Biochemistry and Food Science; Hebrew University; Rehovot, Israel; [6]Oncology Research Unit; Pfizer Worldwide Research and Development; Pearl River, NY USA; [7]MRC Mammalian Genetics Unit; Harwell, UK; [8]Research Institute; The Hospital for Sick Children; University of Toronto; Ontario, Canada; [9]Division of Geriatrics; Department of Clinical and Experimental Medicine; Faculty of Health Science; Linköping University; Linköping, Sweden; [10]Department of STEMBIO (Cell Biology); University of Palermo; Palermo, Italy; [11]Department of Molecular Cell Biology; Catholic University of Leuven; Leuven, Belgium; [12]Department of Medicine and Department of Otolaryngology; Tisch Cancer Institute at Mount Sinai; Mount Sinai School of Medicine; New York University; New York, NY USA; [13]Center for Theragnosis; Biomedical Research Institute; Korea Institute of Science and Technology; Seoul, South Korea; [14]Laboratoire Epigénétique et Destin Cellulaire; UMR7216; Centre National de la Recherche Scientifique (CNRS); Université Paris Diderot Sorbonne Paris Cité; Paris, France; [15]Department of Biology; York University; Toronto, Ontario Canada; [16]Laboratory of Host Defense; WPI Immunology Frontier Research Center, and Department of Host Defense; Research Institute for Microbial Diseases; Osaka University; Osaka, Japan; [17]Department of Biological Sciences; Faculty of Science; University of Jordan; Amman, Jordan; [18]Department of Molecular Biology; Max Planck Institute for Infection Biology; Berlin, Germany; [19]Laboratory of Dendritic Cell Biology; Department of Immunology; Institut Pasteur and INSERM U818; Paris, France; [20]Department of Neurology; University of Michigan; Ann Arbor, MI USA; [21]Geriatrics Research, Education,

©2012 Landes Bioscience. Do not distribute.

dc_840_14

and Clinical Center; VAAAHS; Ann Arbor, MI USA; [22]Oxford Parkinson's Disease Centre; Department of Physiology, Anatomy and Genetics; University of Oxford; Oxford, UK; [23]Department of Biomedical Sciences and Biotechnologies; School of Medicine; University of Brescia; Brescia, Italy; [24]Department of Immunology and Microbial Science; Scripps Research Institute; La Jolla, CA USA; [25]Department of Cancer Biology; Cleveland Clinic; Cleveland, OH USA; [26]Infectomic and Molecular Pathogenesis Departament; Centro de investigación y de Estudios avanzados del Instituto Politécnico Nacional (CINVESTAV-IPN); México City, México; [27]Department of Preventive Dentistry; Osaka University Graduate School of Dentistry; Osaka, Japan; [28]Department of Medicine; Perelman School of Medicine; University of Pennsylvania; Philadelphia, PA USA; [29]Experimental Transplantation and Immunology Branch; National Cancer Institute; National Institutes of Health; Bethesda, MD USA; [30]The Department of Microbial Infection and Immunity; the Department of Internal Medicine; Center for Microbial Interface Biology; The Ohio State University; Columbus, OH USA; [31]Davis Heart and Lung Research Institute; The Ohio State University; Columbus, OH USA; [32]INSERM UMR1037; University Paul Sabatier; Toulouse, France; [33]University Paul Sabatier; Toulouse, France; [34]Department of Biomedical Science; Iowa Center for Advanced Neurotoxicology; Iowa State University; Ames, IA USA; [35]Department of Molecular Pharmacology; Beckman Research Institute; City of Hope; Duarte, CA USA; [36]Griffith Health Institute and School of Pharmacy; Griffith University; Gold Coast, Australia; [37]Department of Neurosurgery; Brain Research Institute; Niigata University; Niigata, Japan; [38]Departamento de Farmacologia; Facultad de Medicina; Universitat de Valencia; Valencia, Spain; [39]Ultrastructural Methods for Innovative Cancer Therapies Unit; Technology and Health Department; Italian National Institute of Health; Rome, Italy; [40]Department of Anatomy and Cell Biology; University of Florida College of Medicine; Gainesville, FL USA; [41]Division of Nephrology; Department of Internal Medicine; Juntendo University Faculty of Medicine; Tokyo, Japan; [42]Department of Chemical Toxicology; Norwegian Institute of Public Health; Oslo, Norway; [43]Graduate School of Biostudies; Kyoto University; Kyoto, Japan; [44]Department of Neurology; USC Neuromuscular Center; University of Southern California Keck School of Medicine; Los Angeles, CA USA; [45]Department of Pathology & Laboratory Medicine; University of Cincinnati College of Medicine; Cincinnati, OH USA; [46]INSERM U895; Centre Mediterraneen de Medecine Moleculaire (C3M); University of Nice Sophia Antipolis; Nice, France; [47]University of Nice Sophia Antipolis; Nice, France; [48]Collaborative Open Research Center; Research Institute for Science and Technology; Kogakuin University; Tokyo, Japan; [49]Department of Cancer Biology; University of Massachusetts Medical School; Worcester, MA USA; [50]Biotechnology Research and Training Center; William C. Friday Laboratory; University of North Carolina Pembroke; Pembroke, NC USA; [51]Department of Nephrology; State Key Laboratory of Kidney Diseases; Chinese PLA General Hospital; Beijing, China; [52]Cytologie et Cytopathologie Neuronales; INCI - CNRS UPR 3212; Université de Strasbourg; Strasbourg, France; [53]Division of Hematology; The Ohio State University, Columbus; OH USA; [54]Department of Biochemistry and Molecular Biology; University of Arkansas for Medical Sciences; Little Rock, AR USA; [55]Department of Biomolecular Sciences; University of Urbino "Carlo Bo"; Urbino, Italy; [56]Telethon Institute of Genetics and Medicine (TIGEM); Federico II University; Naples, Italy; [57]Department of Pediatrics; Federico II University; Naples, Italy; and Jan and Dan Duncan Neurological Research Institute; Baylor College of Medicine; Houston, TX USA; [58]Department of Biological Sciences; University of Toledo; Toledo, OH USA; [59]MRC Toxicology Unit; University of Leicester; Lancaster Road; Leicester, UK; [60]Semmelweis University; Department of Biochemistry, Molecular Biology and Pathobiochemistry; Budapest, Hungary; [61]Department of Genetics, Development and Cell Biology, and Plant Sciences Institute; Iowa State University; Ames, IA USA; [62]Department of Experimental Therapeutics; MD Anderson Cancer Center; Houston, TX USA; [63]Catholic University of Louvain; Institute of Life Sciences; UCL/ ISV; Louvain-la-Neuve, Belgium; [64]Department of Anatomy; Yong Loo Lin School of Medicine; National University of Singapore; Singapore; [65]35 INSERM UMR-S984; and Université Paris Sud; Châtenay-Malabry, France; [66]INRA UMR 1019; Unité de Nutrition Humaine; and CRNH; Université d'Auvergne; Clermont-Ferrand, France; [67]College of Nanoscale Science and Engineering; University at Albany; SUNY; Albany, NY USA; [68]Institute for Pathobiochemistry; University Medical Center of the Johannes Gutenberg-University; Mainz, Germany; [69]Institute of Biochemistry II; Medical School Goethe University; Frankfurt, Germany; [70]Laboratoire de Biochimie Médicale; Rouen University Hospital and NeoVasc EA 4309; University of Rouen; Rouen, France; [71]Veterinary Microbiology and Preventive Medicine; Iowa State University; Ames, IA USA; [72]Westmead Millennium Institute; University of Sydney; Westmead Institute for Cancer Research; Westmead, NSW, Australia; [73]Vaccine Manufacturing Sciences and Commercialization; Merck Manufacturing Division; West Point, PA USA; [74]Department of Health Sciences; Magna Graecia University; Catanzaro, Italy; [75]INRA; UMR866 Dynamique Musculaire et Métabolisme; Université Montpellier 1; Montpellier, France; [76]Department of Experimental Medicine and Biochemical Sciences; University of Rome "Tor Vergata"; Rome, Italy; [77]DIMNP; UMR5235; CNRS; Université de Montpellier 2; Montpellier, France; [78]Department of Biochemistry; Comenius University; Bratislava, Slovak Republic; [79]Basic Medical Sciences; Western University of Health Sciences; Pomona, CA USA; [80]Centre d'études d'agents Pathogènes et Biotechnologies pour la Santé; CNRS UM1; UM2; Montpellier, France; [81]Department of Microbiology and Immunology; Indiana University School of Medicine; Indianapolis, IN USA; [82]Department of Hematology and Medical Oncology; Winship Cancer Institute; Emory University School of Medicine; Atlanta, GA USA; [83]Department of Biomedical Sciences; University of Padova; Padova, Italy; [84]Department of Medicine; University of Chicago; Chicago, IL USA; [85]Department of Oncology; University Children's Hospital; University of Zurich; Zurich, Switzerland; [86]Department of Biological Sciences and Cellular and Molecular Therapy Center - Universidade Federal de São Paulo; São Paulo, Brazil; [87]Department of Veterinary Medicine; University of Maryland; College Park, MD USA; [88]Department of Cell Proliferation and Development; Centro de Investigaciones Biológicas; CIB-CSIC; Madrid, Spain; [89]Université de Franche-Comté; Laboratoire de Biochimie; EA3922; "Estrogènes; Expression Génique et Pathologies du Système Nerveux Central"; IFR133; U.F.R. Sciences et Techniques; Besançon, France; [90]Department of Plant Biology and Forest Genetics; Uppsala BioCentre; Swedish University of Agricultural Sciences; Uppsala, Sweden; [91]Systems Biology of Cell Death Mechanisms; German Cancer Research Center (DKFZ); and Medical Faculty; University of Heidelberg; Heidelberg, Germany; [92]Dipartment Scienze Mediche e Biologiche; Università degli Studi di Udine; Udine, Italy; [93]Centre for Cancer Biomedicine; University of Oslo and Department of Biochemistry; Oslo University Hospital; Oslo, Norway; [94]Department of Cell and Developmental Biology; UNC School of Medicine; Chapel Hill, NC USA; [95]Research Unit for Tropical Diseases; de Duve Institute and Laboratory of Biochemistry; Université Catholique de Louvain; Brussels, Belgium; [96]Department of Cell and Regenerative Biology; Paul Carbone Cancer Center; University of Wisconsin School of Medicine and Public Health; Madison, WI USA; [97]University of Nice-Sophia Antipolis; Institute of Research on Cancer and Ageing of Nice (IRCAN); INSERM CNRS; Nice, France; CHU-Nice; Laboratoire de Pathologie Clinique et Expérimentale; IFR-50; Nice, France; ARC 9; Villejuif, France; [98]Virginia Commonwealth University; Departments of Pharmacology and Toxicology; Massey Cancer Center; Goodwin Research Laboratories; Richmond, VA USA; [99]Department of Anesthesiology; University of Rochester Medical Center; Rochester, NY USA; [100]Department of Microbial Pathogenesis; Genentech, Inc.; South San Francisco, CA USA; [101]Cell Biology Program; Hospital for Sick Children; Department of Molecular Genetics; University of Toronto; Ontario, Canada; [102]Division of Pharmacology; Faculty of Health Sciences; Linköping University; Linköping, Sweden; [103]Regenerative Medicine Program; Ottawa Hospital Research Institute; Ottawa, ON Canada; [104]Department of Genetics; University of North Carolina; Chapel Hill, NC USA; [105]Laboratory of Molecular and Cellular Signaling; Department of Molecular Cell Biology; Catholic University of Leuven; Leuven, Belgium; [106]Department of Neurodegenerative Diseases; Hertie-Institute for Clinical Brain Research; University of Tuebingen; and DZNE; German Center for Neurodegenerative Diseases; Tuebingen, Germany; [107]Department of Medicine I; Division of Oncology; Institute of Cancer Research; Medical University of Vienna; Vienna, Austria; [108]Department of Internal Medicine; Division of Pulmonary, Allergy, Critical Care & Sleep Medicine; The Ohio State University; Columbus, OH USA; [109]Department of Genetics and Evolution; University of Geneva; Geneva, Switzerland; [110]Laboratory of Genetics and Molecular Hematology; University of São Paulo School of Medicine; São Paulo, Brazil; [111]Skirball Institute of Biomolecular Medicine; Department of Microbiology; New York University School of Medicine; New York, NY USA; [112]Department of Metabolism and Diabetes; Institute of Clinical and Experimental Medicine; Prague, Czech Republic; [113]Department of Molecular Pharmacology; Albert Einstein College of Medicine; Bronx, NY USA; [114]Vanderbilt Eye Institute; Vanderbilt University; Nashville, TN USA; [115]Department of Cell Biology and Neuroscience; Rutgers University; Piscataway, NJ USA; [116]Department of Cancer Biology; Kimmel Cancer Center; Thomas Jefferson University; Philadelphia, PA USA; [117]Instituto de Investigaciones Biomédicas "Alberto Sols"; Consejo Superior de Investigaciones Científicas (CSIC) and Universidad Autónoma de Madrid (UAM); Madrid, Spain; [118]Team "Mitochondries, Stress et Morts Cellulaires"; Institut de Biochimie et de Génétique Cellulaires (IBGC); UMR5095; CNRS & Université Bordeaux-Ségalen; Bordeaux, France; [119]Royal Veterinary College; University of London; Consortium for Mitochondrial Research; University College London; London UK; [120]EBRI-Rita Levi Montalcini Foundation; Rome, Italy; [121]Institute of Parasitology and Biomedicine "Lopez-Neyra"-CSIC; Department of Cell Biology and Immunology; Granada, Spain; [122]Department of Biochemistry; University of Rome "Tor Vergata"; Rome, Italy; [123]Department of Pediatrics; Xiangya Hospital; Central South University; China; [124]Department of Plant, Soil, and Entomological Sciences; University of Idaho; Moscow, ID USA; [125]GI Tract Programme, Institute of Food Research; Norwich School of Medicine, The University of East Anglia; Faculty of Health; Norwich Research Park; Norwich, UK; [126]Department of Mucosal Immunology; Norwich School of Medicine; The University of East Anglia–Faculty of Health; Norwich Research Park; Norwich, UK; [127]Faculty of Medicine and Center for Neurosciences and Cell Biology; University of Coimbra; Coimbra, Portugal; [128]Department of Medicine; Division of Hematology/Oncology; University of Texas Health Science Center at San Antonio; San Antonio, TX USA; [129]Department of Molecular Biology and Microbiology; Case Western Reserve University; Cleveland, OH USA; [130]Muscle Biology Unit; Departement of Experimental Medical Science; Lund University; Lund, Sweden; [131]Instituto de Microbiologia; Universidade Federal do Rio de Janeiro; Rio de Janeiro, Brazil; [132]Department of Medical Biosciences; University of Modena and Reggio Emilia; Italy; [133]Department of Cell Biology; University Medical Center Groningen; Groningen, The Netherlands; [134]Department of Human Pathology; University of Messina; Messina, Italy; [135]Vita-Salute San Raffaele University & San Raffaele Scientific Institute; Milan, Italy; [136]Institute of Neuroscience; Department of Cell Biology, Physiology and Immunology; Universitat Autònoma de Barcelona; Barcelona, Spain; [137]Department of Health Sciences; Università del Piemonte Orientale "A. Avogadro"; Novara, Italy; [138]Department of Cell Biology and Institute of Biomembranes; University Medical Centre Utrecht; Utrecht, The Netherlands; [139]Department of Biochemistry and Cell Biology and Institute of Biomembranes; Utrecht University; Utrecht, The Netherlands; [140]Dulbecco Telethon Institute–IRCCS Santa Lucia Foundation; University of Rome Tor Vergata; Rome, Italy; [141]Department of Biology; University of Rome Tor Vergata; Rome, Italy; [142]Laboratory of Intracellular Parasites; Rocky Mountain Laboratories; National Institute of Allergy and Infectious Diseases; National Institutes of Health; Hamilton, MT USA; [143]Division of Radiation Biology & Molecular Environmental Research; Department of Radiation Oncology; University of Tuebingen; Tuebingen, Germany; [144]Department of Pharmacology and Cardiovascular Research Institute; Medical School; Chonbuk University; Chonbuk, Korea; [145]Department of Pathology; Kaohsiung Medical University Hospital; Kaohsiung, Taiwan; [146]Division of Biology; California Institute of Technology; Pasadena, CA USA; [147]Strathclyde Institute of Pharmacy and Biomedical Sciences; University of Strathclyde; Glasgow, Scotland UK; [148]Laboratory of Neurodegenerative Diseases; Department of Anatomy; Li Ka Shing Faculty of Medicine; The University of Hong Kong; Hong Kong, China; [149]Department of Chemistry; The University of Hong Kong; Hong Kong; [150]Department of Pharmacology; College of Medicine; National Taiwan University; Taipei, Taiwan; [151]Institute of Biological Chemistry; Academia Sinica; Taipei, Taiwan; [152]Key Laboratory of Cell Differentiation and Apoptosis of Chinese Ministry of Education; Shanghai Jiao Tong University School of Medicine; Shanghai, China; [153]Department of Pathology and Immunology; Baylor College of Medicine; Houston, TX USA; [154]State Key Laboratory of Membrane Biology; Institute of Zoology; Chinese Academy of Sciences; [155]College of Life Sciences; Nankai University; [156]Institute of Biomedical Sciences; Academia Sinica; Taipei, Taiwan; [157]MOE Key Laboratory of Laser Life Science & Institute of Laser Life Science; South China Normal University; Guangzhou, China; [158]The Children's Hospital; Zhejiang University School of Medicine; Hangzhou, China; [159]Department of Hematology; Xijing Hospital; Fourth Military Medical University; Xi'an, China; [160]School of Life Sciences; Tsinghua University; Beijing, China; [161]Department of Immunology; Peking University; Center for Human Disease Genomics; Beijing, China; [162]Department of Internal Medicine; University of Michigan Medical School; Ann Arbor, MI USA; [163]Department of Radiation Oncology; Mackay Memorial Hospital; Taipei, Taiwan; [164]Department of Botany and Plant Pathology; Purdue University; West Lafayette, IN USA; [165]Department of Biochemistry and Molecular Biology; University of Louisville; Louisville, KY USA; [166]School of Biomedical Sciences; The Chinese University of Hong Kong; Shatin, Hong Kong; [167]Department of Pharmacology; The Pennsylvania State University College of Medicine; Penn State Hershey Cancer Institute; Hershey, PA USA; [168]Penn State Hershey Cancer Institute; Hershey, PA USA; [169]Department of Cancer Biology and Genetics; Memorial Sloan-Kettering Cancer Center; New York, NY USA; [170]Department of Surgery; Yonsei University College of Medicine; Seoul, Korea; [171]Department of Microbiology; University of Pennsylvania; Philadelphia, PA USA; [172]Faculty of Health Sciences and Medicine; Bond University; Queensland, Australia; [173]Department of Biochemistry; Li Ka Shing Faculty of Medicine; The University of Hong Kong; Hong Kong, China; [174]INSERM U1053; and Université Bordeaux Segalen; Bordeaux, France; [175]Department of Cellular and Molecular Physiology; Penn State University College of Medicine; Hershey, PA USA; [176]Graduate School of Life and Environmental Sciences; University of Tsukuba; Ibaraki, Japan; [177]Department of Pharmacology; Emory University School of Medicine; Atlanta, GA USA; [178]Institute of Pharmacology; School of Medicine; National Yang-Ming University; Taipei, Taiwan; [179]School of Biomedical Sciences; The Chinese University of Hong Kong; Hong Kong, China; [180]Graduate School of East-West Medical Science; Kyung Hee University; Yongin, Korea; [181]Division of Pulmonary and Critical Care Medicine; Brigham & Women's Hospital; Harvard Medical School; Boston, MA USA; [182]Department of Obstetrics and Gynecology; Samsung Medical Center; Sungkyunkwan University School of Medicine; Seoul, Korea; [183]Institute for Medical Sciences; Ajou University School of Medicine; Suwon, Korea; [184]Renal Division; Department of Medicine; Brigham and Women's Hospital; Harvard Medical School; Boston, MA USA; [185]INSERM U753 PR1; Institut Gustave Roussy; Villejuif, France; [186]Department of Environmental Health; University of Cincinnati; Cincinnati, OH USA; [187]Department of Pharmacology; Tartu University; Tartu, Estonia; [188]Department of Pathology; University of Pittsburgh School of Medicine; Pittsburgh, PA USA; [189]Center for Neuroscience; University of Pittsburgh School of Medicine; Pittsburgh, PA USA; [190]Immunology Research Center; National Health Research Institutes; Miaoli County, Taiwan; [191]Department of Biochemistry; National Defense Medical Center; Taipei, Taiwan; [192]School of Life Sciences and Biotechnology; Korea University; Seoul, Korea; [193]Department of Microbiology; Ajou University School of Medicine; Suwon, Korea; [194]School of Biological Sciences; University of Hong Kong; Pokfulam, Hong Kong, China; [195]Department of Structures, Function and Biological Technologies; University of Naples "Federico II"; Naples, Italy; [196]IRCCS San Raffaele; Rome, Italy; [197]Physiological Laboratory; Institute of Translational Medicine; University of Liverpool; Liverpool, UK; [198]Safar Center for Resuscitation Research; Pittsburgh, PA USA; [199]Département de Biologie Cellulaire et de Morphologie; Université de Lausanne; Lausanne, Switzerland; [200]Department of Oncology; Lombardi Comprehensive Cancer Center; Georgetown University; Washington D.C. USA; [201]INSERM U984; University of Paris-South; Paris, France; [202]Department of Molecular Biology; Princeton University; Princeton, NJ USA; [203]Laboratorio de Biología Celular y Molecular-Instituto de Histología y Embriología; Universidad Nacional de Cuyo-CONICET; Mendoza, Argentina; [204]Department of Genetics and Microbiology; University of Pavia; Pavia, Italy; [205]Pharmacology; Faculty of Pharmacy; Università del Piemonte Orientale "A. Avogadro"; Novara, Italy; [206]Cell Biology and Gene Expression Section; Laboratory of Neurogenetics; National Institute on Aging; National Institutes of Health; Bethesda, MD USA; [207]Department of Molecular Microbiology and Immunology; Johns Hopkins University; Baltimore, MD USA; [208]Departamento Enfermedades Cardiovasculares; Facultad de Medicina; Pontificia Universidad Catolica de Chile; Santiago, Chile; [209]Institut Pasteur; Unité des Interactions Bactéries-Cellules; Paris, France; [210]INSERM; U604; INRA; USC2020; Paris, France; [211]Department of Experimental Medicine and Oncology; University of Torino; Torino, Italy; [212]Larry Hillblom Islet Research Center; David Geffen School of Medicine; University of California; Los Angeles, CA USA; [213]Departamento de Morfología y Biología Celular; Universidad de Oviedo; Oviedo, Spain; [214]Departamento de Biología y Cs Ambientales; Facultad de Ciencias; Universidad de Valparaíso; Valparaíso, Chile; [215]Division of Applied Medicine; University of Aberdeen; Aberdeen, UK; [216]Keck Graduate Institute of Applied Sciences; Claremont, CA USA; [217]Instituto de Bioquímica Vegetal y Fotosíntesis (CSIC-Universidad de Sevilla); Sevilla, Spain; [218]Department of Biochemistry; University of Johannesburg; Johannesburg, South Africa; [219]Department of Anatomy and Structural Biology; Albert Einstein College of Medicine; Bronx, NY USA; [220]Department of Developmental and Molecular Biology; Albert Einstein College of Medicine; Bronx, NY USA; [221]Marion Bessin Liver Research Center; Albert Einstein College of Medicine; Bronx, NY USA; [222]Department of Surgery; University of Iowa; Iowa City, IA USA; [223]Department of Medicine; Albert Einstein College of Medicine; Bronx, NY USA; [224]Experimental Neurology Unit; European Centre for Brain Research; Santa Lucia Foundation; Rome, Italy; [225]Pathogénie Bactérienne Intestinale USC-INRA 2018; Clermont-Ferrand, France; [226]JE2526 Université Auvergne; Clermont-Ferrand, France; [227]Cardiovascular Research Center; University of Connecticut School of Medicine; Farmington, CT USA; [228]Department of Human Biology; University of Cape Town; Cape Town, South Africa; [229]Division of Molecular Pathology; Cancer Therapeutics and Clinical Studies; Institute of Cancer Research and Royal Marsden Hosptial; Sutton, Surrey UK; [230]Department of Public Health and Cell Biology; University of Rome Tor Vergata; Rome, Italy; [231]Department of Neuro-Oncology; MD Anderson Cancer Center; University of Texas; Houston, TX USA; [232]Virology Division; Department of Infectious Diseases and Immunology; Utrecht University; Utrecht, The Netherlands; [233]Department of Pathology and Animal Health; University of Naples "Federico II"; Naples, Italy; [234]Cancer Center Karolinska; Department of Oncology-Pathology; Karolinska Institute; Stockholm, Sweden; [235]Department of Experimental Pathology; University of Pisa Medical School; Pisa, Italy; [236]Department of Pathology; University of California; San Francisco, CA USA; [237]Department of Biochemistry; Tufts University School of Medicine; Boston, MA USA; [238]CNRS UMR 5293; Institut des Maladies Neurodégénératives; Université Bordeaux Segalen; Bordeaux, France; [239]Department of Physiology; University of Melbourne; Parkville, Victoria Australia; [240]Laboratorio Nazionale Consorzio Interuniversitario Biotecnologie; Trieste, Italy; [241]Fungal Patho-Biology Group; Temasek Life Sciences Laboratory; National University of Singapore; Singapore; [242]Freiburg Institute for Advanced Studies (FRIAS); School of Life Sciences (LifeNet); Freiburg, Germany; [243]Department of Neurosurgery; VCU Institute of Moleular Medicine; VCU Massey Cancer Center; Virginia Commonwealth University; School of Medicine; Richmond, VA USA; [244]Centre for Cancer Biology; SA Pathology; University of Adelaide; SA, Australia; [245]School of Molecular and Biomedical Science; University of Adelaide; SA, Australia; [246]Department of Molecular Genetics and Microbiology; University of New Mexico Health Science Center; Albuquerque, NM USA; [247]Department of Biochemistry and Molecular Biology; Louisiana State University–Health Sciences Center-School of Medicine; New Orleans, LA USA; [248]Department of Biochemistry & Molecular Biology; Monash University; Clayton Campus; Melbourne, Victoria Australia; [249]ARC Centre of Excellence in Structural and Functional Microbial Genomics; Monash University; Clayton Campus; Melbourne, Victoria Australia; [250]Unit of Allergy and Immunotoxicology; Ageing Research Center (Ce.S.I.); Università G. d'Annunzio Foundation; Chieti, Italy;

dc_840_14

[251]Taub Institute for Alzheimer's Disease Research; Columbia University Medical Center; New York, NY USA; [252]Department of Pathology and Cell Biology; Columbia University Medical Center; New York, NY USA; [253]Institute of Cell Biology and Neurobiology; EMMA-CNR; Campus "A. Buzzati Traverso"; Rome, Italy; [254]Department of Pharmacological and Toxicological Chemistry; University of Chile; Santiago, Chile; [255]Department of Biochemistry and Molecular Biology; School of Medicine; University of Alcalá; Madrid, Spain; [256]Sanford-Burnham Medical Research Institute; La Jolla, CA USA; [257]Departamento de Biología Molecular; Centro de Biología Molecular Severo Ochoa (UAM-CSIC); Universidad Autonoma de Madrid; Madrid, Spain; [258]Molecular Signaling; Frankfurt Institute for Molecular Life Sciences; Frankfurt am Main, Germany; [259]Department of Plant Biology and The Genome Center; College of Biological Sciences; University of California; Davis, CA USA; [260]Department of Pharmacology, Toxicology and Therapeutics; The University of Kansas Medical Center; Kansas City, KS USA; [261]Department of Medicine; Case Western Reserve University; University Hospitals of Cleveland; Cleveland, OH USA; [262]Department of Pharmacology; Case Western Reserve University; University Hospitals of Cleveland; Cleveland, OH USA; [263]Department of Pathology; Case Western Reserve University; University Hospitals of Cleveland; Cleveland, OH USA; [264]Comprehensive Cancer Center; Case Western Reserve University; University Hospitals of Cleveland; Cleveland, OH USA; [265]University Hospitals of Cleveland; Cleveland, OH USA; [266]Center for Cardiovascular Research; Washington University School of Medicine; Saint Louis, MO USA; [267]Department of Internal Medicine; Washington University School of Medicine; Saint Louis, MO USA; [268]INSERM U916 VINCO; Université Bordeaux; Bordeaux, France; [269]CNRS UMR 8126; Université Paris-Sud 11; Institut Gustave Roussy; Villejuif, France; [270]Department of Cellular Biology and Anatomy; Georgia Health Sciences University; Charlie Norwood VA Medical Center; Augusta, GA USA; [271]Charlie Norwood VA Medical Center; Augusta, GA USA; [272]Lilly Research Laboratories; Eli Lilly and Company; Indianapolis, IN USA; [273]General and Molecular Pathophysiology Department; Bogomoletz Institute of Physiology; Kiev, Ukraine; [274]Department of Pediatrics and Communicable Diseases; University of Michigan Medical School; Ann Arbor, MI USA; [275]Department of Cell Biology; University of Massachusetts Medical School; Worcester, MA USA; [276]Department of Human Virology; INSERM U758; Ecole Normale Supèrieure de Lyon; Lyon, France; [277]Department of Biochemistry and Molecular Biology; Tongji Medical College; Huazhong University of Techology and Science; Wuhan, Hubei China; [278]Division of Hematology and Central laboratory of Hematology; Lausanne University Hospital; Lausanne, Switzerland; [279]Centre de Recherche des Cordeliers; INSERM; U872; Paris, France; [280]Université Pierre et Marie Curie; Paris, France; [281]Department of Biochemistry; University of Tuebingen; Tuebingen, Germany; [282]Division of Renal Diseases and Hypertension; University of Colorado at Denver; Aurora, CO USA; [283]Department of Developmental and Cell Biology; University of California; Irvine, CA USA; [284]Department of Biología Celular, Inmunología y Neurociencias; Facultad de Medicina; Universidad de Barcelona–IDIBAPS; Barcelona, Spain; [285]Institute of Biochemistry I; Medical Faculty; University of Cologne; Cologne, Germany; [286]Department of Medicine; Baylor College of Medicine; Houston, TX USA; [287]Department of Melanoma Medical Oncology; University of Texas; MD Anderson Cancer Center; Houston, TX USA; [288]Laboratory of Translational Oncology and Experimental Cancer Therapeutics; Department of Medicine (Hematology/Oncology); Penn State College of Medicine; Penn State Hershey Medical Center; Hershey PA USA; [289]Department of Biological Chemistry; The Weizmann Institute of Science; Rehovot, Israel; [290]European Institute of Oncology, and Department of Biomolecular Sciences and Biotechnologies; University of Milan; Milan, Italy; [291]Buck Institute for Research on Aging; Novato, CA USA; [292]Department of Microbiology, Tumor and Cell Biology; Karolinska Institutet; Stockholm, Sweden; [293]Department of Physiological Sciences; University of Stellenbosch; Stellenbosch, South Africa; [294]Department of Pharmacology; The B. Rappaport Faculty of Medicine; Technion-Israel Institute of Technology; Haifa, Israel; [295]Latvian Biomedical Research and Study Centre; Riga, Latvia; [296]Department of Biosciences; University of Helsinki; Helsinki, Finland; [297]Center for Applied Proteomics and Molecular Medicine; George Mason University; Manassas, VA USA; [298]Department of Physiology and Biophysics; University of Medicine and Dentistry of New Jersey-Robert Wood Johnson Medical School; Piscataway, NJ USA; [299]Liver Cancer Institute; Zhongshan Hospital; Fudan University; Shanghai, China; [300]Departments of Neurology, Pediatrics, Neurological Surgery and Brain Tumor Research Center; Helen Diller Family Comprehensive Cancer Center, University of California; San Francisco, CA USA; [301]Center for Biomedical Engineering and Technology (BioMET); University of Maryland, Baltimore; Baltimore, MD USA; [302]Department of Physiology; University of Maryland, Baltimore; Baltimore, MD USA; [303]The First Affiliated Hospital of Guangzhou University of Chinese Medicine; Guangzhou, China; [304]MRC Centre for Developmental Neurobiology; King's College London, UK; [305]Cell Death and Metabolism; Danish Cancer Society Research Center; Copenhagen, Denmark; [306]Section of Molecular Biology; Division of Biological Sciences; University of California; San Diego; La Jolla, CA USA; [307]INSERM U851; Université de Lyon, and the Université Lyon1; Lyon, France; [308]Department of Cellular Biology; University of Georgia; Athens, GA USA; [309]Immunobiology Section; Laboratory of Parasitic Diseases; National Institute of Allergy and Infectious Diseases; National Institutes of Health; Bethesda, MD USA; [310]Department of Physiology and Biophysics; State University of New York at Buffalo; Buffalo, NY USA; [311]Guangdong Provincial Key Lab of Biotechnology for Plant Development; School of Life Sciences; South China Normal University; Guangzhou, China; [312]Department of Obstetrics & Gynecology; Shanghai First People's Hospital; Shanghai Jiao Tong University; Shanghai, China; [313]Departments of Biochemistry and Molecular Biology, Apoptosis and Genomics Research Group of the Hungarian Academy of Sciences; Research Center for Molecular Medicine; University of Debrecen; Debrecen, Hungary; [314]Cell & Molecular Biology Joint Doctoral Program; Department of Biology; San Diego State University; San Diego, CA USA; [315]Department of Biological Sciences; Hunter College; City University of New York; New York, NY USA; [316]National Institute for Infectious Diseases IRCCS L. Spallanzani; Rome, Italy; [317]Department of Cell and Developmental Biology; University of Michigan Medical School; Ann Arbor, MI USA; [318]Gladstone Institutes; Taube-Koret Center for Huntington's Disease and the Hellman Alzheimer's Disease Program; University of California; San Francisco, CA USA; [319]Laboratory of Molecular Biology; National Heart, Lung, and Blood Institute; National Institutes of Health; Bethesda, MD USA; [320]Bioscience Center; San Diego State University; San Diego, CA USA; [321]Departments of Medicine and Cell Biology; Marc and Ruti Bell Program in Vascular Biology; New York University School of Medicine; New York, NY USA; [322]Department of Human and Molecular Genetics; VCU Institute of Molecular Medicine; VCU Massey Cancer Center; Virginia Commonwealth University; School of Medicine; Richmond, VA USA; [323]Laboratory of Molecular and Cellular Neuroscience; Rockefeller University; New York, NY USA; [324]Institute for Behavioral Genetics; University of Colorado; Boulder, CO USA; [325]McGill Parkinson Program; Department of Neurology & Neurosurgery; Montreal Neurological Institute; McGill University; Montreal, Quebec Canada; [326]Department of Human Morphology; University of Pisa and IRCCS Neuromed; Pisa, Italy; [327]University Hospital Heidelberg; Department of Surgery/Research Lab; Heidelberg, Germany; [328]Department of Pharmacology and Experimental Neuroscience; University of Nebraska Medical Center; Omaha, NE USA; [329]Redox Biology Center and School of Veterinary Medicine and Biomedical Sciences; University of Nebraska–Lincoln; Lincoln, NE USA; [330]Biotech Research and Innovation Centre; University of Copenhagen; Copenhagen, Denmark; [331]Department of Molecular and Cellular Medicine; University of Leuven; Leuven, Belgium; [332]Centro de Investigación Biomédica en Red de Enfermedades Neurodegenerativas (CIBERNED); Departamento Bioquímica y Biología Molecular y Genética; E.U. Enfermería; Universidad de Extremadura; Cáceres, Spain; [333]Department of Bacteriology; Graduate school of Medical Sciences; Kyushu University; Kagoshima, Japan; [334]Laboratory of Emerging Infectious Diseases; Department of Frontier Veterinary Medicine; Kagoshima University; Kagoshima, Japan; [335]Department of Pediatrics; Jichi Medical University; Tochigi, Japan; [336]Department of Developmental Biology and Neurosciences; Graduate School of Life Sciences; Tohoku University; Miyagi, Japan; [337]Institute of Physiological Chemistry; Hannover Medical School; Hannover, Germany; [338]Laboratory of Cell Physiology; University of Louvain; Brussels, Belgium; [339]Department of Physiological Sciences; Faculty of Veterinary Medicine; Warsaw University of Life Sciences; Warsaw, Poland; [340]UMR CNRS 7622; Biologie du Développement; Université Pierre et Marie Curie; Paris, France; [341]Department of Biological Sciences & Bioengineering; Indian Institute of Technology; Kanpur, India; [342]Laboratory of Genetics; University of Wisconsin; Madison, WI USA; [343]MRC Protein Phosphorylation Unit; College of Life Sciences; University of Dundee; Dundee, Scotland UK; [344]Department of Neurology; University of Massachusetts Medical School; Worcester, MA USA; [345]CAS Key Laboratory of Pathogenic Microbiology and Imuunology; Institute of Microbiology; Chinese Academy of Sciences (CAS); Beijing, China; [346]Oncology and Pharmacology; UT Southwestern Medical Center; Dallas, TX USA; [347]Centro Estudios Moleculares de la Celula; Facultad Ciencias Quimicas y Farmaceuticas; Universidad de Chile; Santiago, Chile; [348]Department of Leukemia; University of Texas; MD Anderson Cancer Center; Houston, TX USA; [349]Department of Biochemistry; School of Medicine; Boston University; Boston, MA USA; [350]Laboratory of Dermatology; Department of Oncology; University of Leuven; Leuven, Belgium; [351]Department of Medicine; University of Illinois at Chicago; Chicago, IL USA; [352]Center of Immunology of Marseille Luminy; Aix-Marseille Univ; INSERM U631; and CNRS UMR6102; Marseille, France; [353]Department of Molecular Cardiology; Randall Division for Cell and Molecular Biophysics and Cardiovascular Division; Kings College; London UK; [354]Department of Biology; University of Kentucky; Lexington, KY USA; [355]Department of Clinical Neurosciences; Institute of Neurology; University College London; London UK; [356]Department of Cell Biology; Harvard Medical School; Boston, MA USA; [357]Department of Cellular Molecular Medicine; University of Ottawa; Ottawa, Ontario Canada; [358]Department of Pathology; University of Michigan; Ann Arbor, MI USA; [359]Department of Physiology; Manitoba Institute of Child Health; University of Manitoba; Manitoba, Canada; [360]Department of Medicine; University of California San Diego School of Medicine; La Jolla, CA USA; [361]Department of Therapeutic Research and Medicine Evaluation; Istituto Superiore di Sanita; Rome, Italy;

[362]Department of Pathology; Democritus University of Thrace and University General Hospital of Alexandroupolis; Alexandroupolis, Greece; [363]Biochemistry and Medical Genetics; Manitoba Institute of Cell Biology; University of Manitoba; Winnipeg, Manitoba Canada; [364]Department of Neurology; Columbia University Medical Center; New York, NY USA; [365]School of Health and Medicine; Lancaster University; Lancaster UK; [366]Department of Medicine; Columbia University College of Physicians and Surgeons; New York, NY USA; [367]Department of Immunology; Medical University of Warsaw; Warsaw, Poland; [368]Renal Research Institute; New York Medical College; Valhalla, NY USA; [369]Department of Genetics; University of Texas MD Anderson Cancer Center; Houston, TX USA; [370]Biology Department; Faculty of Science; Ege University; Bornova, Izmir Turkey; [371]Institut de Recherche en Cancérologie de Montpellier; INSERM U896; Université Montpellier1; Montpellier, France; [372]Department of Pathophysiology; School of Pharmacy and Biochemistry; University of Buenos Aires; Buenos Aires, Argentina; [373]Instituto de Ciencias de la Vid y del Vino; CSIC-UR-CAR; Logroño, Spain; [374]Department of Developmental Genetics and Gene Control; Centre for Genetics and Genomics; The University of Nottingham; Queen's Medical Centre; Nottingham UK; [375]The Henry M. Jackson Foundation for the Advancement of Military Medicine; Uniformed Services University of the Health Sciences; Bethesda, MD USA; [376]Genome Sciences Center; BC Cancer Agency; Vancouver, BC Canada; [377]Molecular Cardiology Research Institute; Tufts Medical Center and Department of Medicine; Tufts University School of Medicine; Boston, MA USA; [378]Biological Sciences and Bioengineering Program; Sabancı University; Orhanlı-Tuzla, Istanbul, Turkey; [379]Department of Neurobiology and Behavior; University of California; Irvine, CA USA; [380]Agricultural Institute of Slovenia; Ljubljana, Slovenia; [381]University of Strasbourg; Immunologie et Chimie Thérapeutiques; CNRS; Strasbourg, France; [382]Department of Pediatrics; Children's Hospital; University of Iowa; Iowa City, IA USA; [383]Signaling Networks Program; Division of Oncology; Department of Medicine I; Comprehensive Cancer Center; Medical University Vienna & Ludwig Boltzmann Cluster Oncology; Vienna, Austria; [384]Department of Pharmacology and Moores Cancer Center; University of California San Diego; La Jolla, CA USA; [385]AstraZeneca; Cancer&Infection Research Area; Cheshire UK; [386]Department of Medicine; the David Geffen School of Medicine; University of California; Los Angeles, CA USA; [387]Department and Laboratory of Intensive Care Medicine; Katholieke Universiteit Leuven; Leuven, Belgium; [388]Skaggs School of Pharmacy and Pharmaceutical Sciences; University of California San Diego; San Diego, CA USA; [389]Department of Internal Medicine; Manitoba Institute of Child Health; University of Manitoba; Winnipeg, Manitoba Canada; [390]Department of Microbiology; Montana State University; Bozeman, MT USA; [391]Department of Genetics; Osaka University Graduate School of Medicine; Osaka, Japan; [392]Institute of Pharmacology, Toxicology and Biochemical Pharmaceutics; Zhejiang University; Hangzhou, China; [393]Discovery & ADMET-TOX Systems; Life Technologies; Madison, WI USA; [394]Department of Oral and Craniofacial Molecular Biology; Massey Cancer Center; Virginia Commonwealth University; Richmond, VA USA; [395]Third Department of Internal Medicine; School of Medicine; University Occupational and Environmental Health; Kitakyushu, Japan; [396]Department of Cardiology; Angiology and Pulmology; University of Heidelberg; Heidelberg, Germany; [397]Molecular Oncology Laboratories; Oxford University Department of Oncology; Weatherall Institute of Molecular Medicine; John Radcliffe Hospital; Oxford UK; [398]Immunology Research Centre; School of Biochemistry & Immunology; Trinity College Dublin; Dublin, Ireland; [399]Center for Plant Science Innovation; University of Nebraska-Lincoln; Lincoln, NE USA; [400]Division of Sensory and Motor Systems; Tokyo Metropolitan Institute of Medical Science; Tokyo, Japan; [401]VA Boston Healthcare System; Boston, MA USA; [402]Divison of Hypertension and Nephrology; National Cerebral and Cardiovascular Center; Osaka, Japan; and Department of Cell Signaling; Gifu University Graduate School of Medicine; Gifu, Japan; [403]Molecular Oncology; Moffitt Cancer Center; Tampa, FL USA; [404]Department of Internal Medicine; University of Texas Southwestern Medical Center; Dallas, TX USA; [405]Department of Immunology; Duke University Medical Center; Durham, NC USA; [406]Department of Nephrology; CRCHUM; Montréal, QB Canada; [407]Department of Pharmacology; University of Colorado School of Medicine; Aurora, CO USA; [408]College of Medical; Veterinary & Life Sciences; Institute of Cancer Sciences; University of Glasgow; Glasgow UK; [409]Department of Cellular and Structural Biology; University of Texas Health Science Center at San Antonio; San Antonio, TX USA; [410]Department of Molecular Genetics; The Ohio State University; Columbus, OH USA; [411]Biomedical Neuroscience Institute; ICBM; Faculty of Medicine; University of Chile; Santiago, Chile; [412]Department of Molecular Biology; Institute of Parasitology and Biomedicine "López-Neyra"; IPBLN-CSIC; Granada, Spain; [413]Division of Cardiology; University of Texas Southwestern Medical Center; Dallas, TX USA; [414]INSERM ERI 21/EA2319; and the Laboratoire de Pathologie Clinique et Expérimentale; IFR-50; Nice, France; [415]Cellular Senescence Group A210; German Cancer Research Center; DKFZ-ZMBH Alliance; Heidelberg, Germany; [416]Molecular Cell Biology; Institute for Cell Biology; University Bonn; Bonn, Germany; [417]GCP center; Cancer Center of Sun Yat-sen University; Guangzhou, China; [418]School of Kinesiology and Health Science; York University; Toronto; ON Canada; [419]Harvard University; School of Public Health; Boston, MA USA; [420]Department of Internal Medicine; University Medical Center Groningen; Groningen, The Netherlands; [421]Department of Molecular Biomedicine; LEO Pharma A/S; Ballerup, Denmark; [422]Neurology and Anesthesiology; Shock Trauma & Anesthesiology Research Center; University of Maryland School of Medicine; Baltimore, MD USA; [423]Department of Biochemistry and Molecular Biology; University of New Mexico School of Medicine; Albuquerque, NM USA; [424]Laboratory of Cancer Immunobiology; Earle A. Chiles Research Institute; Providence Portland Medical Center; Portland, OR USA; [425]Department of Neurosurgery; University of Michigan; Ann Arbor, MI USA; [426]The State Key Laboratory of Biotherapy; West China Hospital; Sichuan University; Chengdu, China; [427]Department of Medicine; Mayo Clinic and Mayo Cancer Center; Rochester, MN USA; [428]Department of Life Science and Institute of Zoology; National Taiwan University; Taipei, Taiwan; [429]Renal Division; University Hospital Freiburg; and BIOSS Centre for Biological Signalling Studies; Albert-Ludwigs-University; Freiburg, Germany; [430]School of Biological Sciences and Research Center for Functional Cellulomics; Seoul National University; Seoul, Korea; [431]Department of Obstetrics and Gynecology; Chang Gung Memorial Hospital at Taipei; Taipei, Taiwan; [432]Department of Experimental Cancer Research; University of Edinburgh; Institute of Genetics and Molecular Medicine; Cell Signalling Unit; Edinburgh UK; [433]Department of Pharmacology; Infection Signaling Network; Research Center; College of Medicine; Chungnam National University; Daejeon, Korea; [434]Department of Biochemistry; University of Washington; Seattle, WA USA; [435]Critical Care Department; McGill University; Montreal, QB Canada; [436]School of Biological and Biomedical Sciences; University of Durham; Durham UK; [437]Institute for Innovative Cancer Research; University of Ulsan College of Medicine; and Asan Medical Center; Seoul, Korea; [438]Department of Pathology and Immunology; Washington University School of Medicine; St. Louis, MO USA; [439]Department of Medicine II; Endocrinology and Hypertension; Tokyo Women's Medical University; Tokyo, Japan; [440]Department of Molecular and Integrative Physiology, and the Division of Nephrology; Department of Internal Medicine; University of Michigan Medical School; Ann Arbor, MI USA; [441]Department of Oral Microbiology; Division of Oral Infections and Health Sciences; Asahi University School of Dentistry; Mizuho, Japan; [442]INSERM U624 and University of Méditerranée; Marseille, France; [443]Division of Life Science and State Key Laboratory of Molecular Neuroscience; The Hong Kong University of Science and Technology; Hong Kong, China; [444]Department of Geriatric Medicine and Nephrology; Osaka University Graduate School of Medicine; Suita, Japan; [445]Department of Applied Plant Science; Graduate School of Agricultural Sciences; Tohoku University; Miyagi, Japan; [446]Department of Immunology; Nagoya University Graduate School of Medicine; Nagoya University; Nagoya, Japan; [447]Department of Immunobiology; Yale University School of Medicine; New Haven, CT USA; [448]Division of General Thoracic Surgery; School of Medicine; Keio University; Tokyo, Japan; [449]Centre for Biotechnology; University of Turku; Turku, Finland; [450]Department of Neurology; University of Texas Medical Branch; Galveston, TX USA; [451]Department of Microbiology and Molecular Genetics; Medical College of Wisconsin; Milwaukee, WI USA; [452]Laboratory of Experimental-Hemato-Oncology; Department of Oncology; Public Research Center for Health (CRP-Santé); Luxembourg City, Luxembourg; [453]Department of Neurology; University Medical School; Goethe University; Frankfurt/Main, Germany; [454]Department of Physiology; Seoul National University College of Medicine; Seoul, Korea; [455]Laboratory of Veterinary Biochemistry and Molecular Biology; College of Veterinary Medicine; Chungbuk National University; Cheongju, Korea; [456]Key Laboratory of Hepatosplenic Surgery; Department of General Surgery; the First Affiliated Hospital of Harbin Medical University; Harbin, China; [457]Department of Biochemistry; University of Texas Health Science Center; San Antonio, TX USA; [458]Department of Urologic Surgery; Vanderbilt University Medical Center; Nashville TN USA; [459]Department of Nutrition Science; Purdue University; West Lafayette, IN USA; [460]Department of Cell Biology; Memorial Sloan-Kettering Cancer Center; New York, NY USA; [461]State Key Laboratory of Mycology; Institute of Microbiology; Chinese Academy of Sciences; Beijing, China; [462]Departamento de Microbiología y Genética; Universidad de Salamanca; Salamanca, Spain; [463]Department of Pharmacology; University of Medicine and Dentistry of New Jersey-Robert Wood Johnson Medical School; Piscataway, New Jersey USA; [464]Department of Biological Sciences; Korea Advanced Institute of Science and Technology; Daejeon, South Korea; [465]Biochemistry Department; Institute of Medical Biology; University of Tromsø; Tromsø, Norway; [466]Department of Medicine; University of Pittsburgh; Pittsburgh, PA USA; [467]Cell Biology Program; Sickkids; Departments of Paediatrics and Physiology; University of Toronto; Toronto, ON Canada; [468]Department of Pathology and Cell Biology; Thomas Jefferson University; Philadelphia, PA USA; [469]Department of Physiology; University of Pretoria; Pretoria, South Africa; [470]Department of Anatomy, Cell and Developmental Biology; Eötvös Loránd University; Budapest, Hungary; [471]University Institute of Pathology; CHUV–University of Lausanne; Lausanne, Switzerland; [472]Functional Food Technology Research Group; Korea Food Research Institute; Korea; [473]Department of Biological Science; Seoul National University; Seoul, Korea; [474]Department of Ophthalmology;

dc_840_14

University of Eastern Finland and Kuopio University Hospital; Kuopio, Finland; [475]Department of Degenerative Neurological Diseases; National Institute of Neuroscience; National Center of Neurology and Psychiatry (NCNP); Tokyo, Japan; [476]Department of Applied Biological Chemistry; Niigata University; Niigata, Japan; [477]Experimental Pathology; Department of Clinical and Experimental Medicine; Faculty of Health Science; Linköping University; Linköping, Sweden; [478]Laboratory of Biological Diversity; National Institute for Basic Biology; Okazaki, Japan; [479]Institute of Environmental Medicine; Karolinska Institutet; Stockholm, Sweden; [480]Gifu University Graduate School of Medicine; Division of Cardiology; Gifu, Japan; [481]Howard Hughes Medical Institute; Division of Genetics; Brigham and Women's Hospital; Department of Genetics; Harvard Medical School; Boston, MA USA; [482]Division of Medical Sciences; Humphrey Oei Institute of Cancer Research; National Cancer Centre Singapore; Singapore; [483]Department of Chemistry and Biology; Korea Science Academy of KAIST; Busan, Korea; [484]The DAMP Laboratory; Department of Surgery; Hillman Cancer Center; University of Pittsburgh Cancer Institute; University of Pittsburgh; Pittsburgh, PA USA; [485]Department of Clinical Chemistry and Laboratory Medicine; Kyushu University Graduate School of Medical Sciences; Fukuoka, Japan; [486]Department of Immunology; St. Jude Children's Research Hospital; Memphis, TN USA; [487]Department of Orthopaedic Surgery; Tohoku University School of Medicine; Miyagi, Japan; [488]Division of Medical Oncology; Department of Internal Medicine; University of Medicine and Dentistry of New Jersey; Robert Wood Johnson Medical School; Piscataway; and The Cancer Institute of New Jersey; New Brunswick, NJ USA; [489]Central Arkansas Veterans Healthcare System and Department of Medicine; University of Arkansas for Medical Sciences; Little Rock, AR USA; [490]Division of Biochemistry; Institute for Chemical Research; Kyoto University; Kyoto, Japan; [491]Department of Biochemistry and Molecular Biology; College of Medicine; Chang Gung University; Taoyuan, Taiwan; [492]B cell Molecular Immunology Section; Laboratory of Immunoregulation; NIAID; National Institutes of Health; Bethesda, MD USA; [493]Department of Laboratory Medicine and Pathology; University of Minnesota Cancer Center; Minneapolis, MN USA; [494]Fraunhofer Group "Extracorporeal Immune Modulation (EXIM)"; Division of Nephrology; Department of Internal Medicine; Rostock, Germany; [495]Department of Pharmacology; Wayne State University School of Medicine; Detroit, MI USA; [496]Department of Molecular Biology; Genetic Engineering and Biotechnology Research Institute; Menoufiya University; El-Sadat City, Egypt; [497]Molecular Cell Biology; Groningen Biomolecular Sciences and Biotechnology Institute (GBB) & Kluyver Centre for Genomics of Industrial Fermentation; University of Groningen; Haren, The Netherlands; [498]Section of Cell and Developmental Biology; University of California, San Diego; La Jolla, CA USA; [499]Faculty of Pharmaceutical Sciences; Hokkaido University; Sapporo, Japan; [500]Department of Biochemistry and Institute of Health Sciences; Gyeongsang National University School of Medicine; JinJu, Korea; [501]Department of Biochemistry, Molecular Biology & Biophysics; University of Minnesota; Minneapolis, MN USA; [502]Cell Dysfunction Research Center (CDRC); Department of Anatomy and Cell Biology; University of Ulsan College of Medicine; Seoul, Korea; [503]Department of Brain Science; Daegu Gyeongbuk Institute of Science and Technology; Daegu, Korea; [504]Department of Dental Pharmacology; College of Dentistry; Wonkwang University; Chonbuk, South Korea; [505]Department of Surgery; University of Florida; Gainesville, FL USA; [506]Fight against Angiogenesis-Related Blindness (FARB) Laboratory; Clinical Research Institute; Seoul National University & Department of Ophthalmology; Seoul National University College of Medicine; Seoul, Korea; [507]Department of Surgery; University of Ulsan College of Medicine and Asan Medical Center; Seoul, Korea; [508]Department of Human Genetics; University of Michigan; Ann Arbor, MI USA; [509]Department of Biochemistry; University of Toronto; Toronto ON Canada; [510]Department of Biochemistry and Molecular Biology; University of Ulsan College of Medicine; Seoul, Korea; [511]Ilsong Institute of Life Science; College of Medicine; Hallym University; Anyang, Korea; [512]Department of Microbiology; College of Medicine; Hallym University; Anyang, Korea; [513]Department of Chemical Biochemical and Environmental Engineering; University of Maryland, Baltimore County; Baltimore, MD USA; [514]Department of Molecular Genetics; Weizmann Institute of Science; Rehovot, Israel; [515]Division of Genomic Stability and DNA Repair; Department of Radiation Oncology; Dana-Farber Cancer Institute; Harvard Medical School; Boston, MA USA; [516]Tumour Cell Death Laboratory; Beatson Institute for Cancer Research; Glasgow UK; [517]Brown University; Department of Radiation Oncology; Warren Alpert Medical School and Rhode Island Hospital; Providence, RI USA; [518]Merck Serono; Merck KGaA; Darmstadt, Germany; [519]University of Manitoba; Department of Pharmacology & Therapeutics; Institute of Cardiovascular Sciences; St. Boniface General Hospital Research Centre; Winnipeg, Manitoba Canada; [520]Department of Biotechnology; University of Tokyo; Tokyo, Japan; [521]Department of Molecular Miocrobiology and Immunology; Graduate School of Biomedical Sciences; Nagasaki University; Nagasaki, Japan; [522]Institute for Immunology; University of Munich; Munich, Germany; [523]Department of Pharmacology and Toxicology; University of Arizona; Tucson, AZ USA; [524]Division of Molecular Neurology; University Hospital; Erlangen, Germany; [525]Department of Cell Biology; Centro de Investigación Príncipe Felipe; Valencia, Spain; [526]Department of Anatomical and Cellular Pathology; The State Key Laboratory in Oncology in Southern China; The Chinese University of Hong Kong; Hong Kong, China; [527]Department of Neurology; University Medicine Göttingen; Göttingen, Germany; [528]Department of Neurology; University of Ulsan College of Medicine; Seoul, Korea; [529]Department of Cell Biology and Neuroscience; Juntendo University School of Medicine; Tokyo, Japan; [530]Protein Metabolism Project; Tokyo Metropolitan Institute of Medical Science; Tokyo, Japan; [531]Department of Biochemistry; Juntendo University School of Medicine; Tokyo, Japan; [532]Biotechnology Research Division; National Fisheries Research and Development Institute (NFRDI); Busan, Korea; [533]Department of Otorhinolaryngology; Union Hospital of Tongji Medical College; Huazhong Science and Technology University; Wuhan, China; [534]Institute for Ageing and Health; Newcastle University; Newcastle upon Tyne UK; [535]Graduate School of Biomedical Sciences; Hiroshima University; Hiroshima, Japan; [536]Department of Radiotherapy–Oncology; Democritus University of Thrace; Alexandroupolis, Greece; [537]Max F. Perutz Laboratories; University of Vienna; Vienna, Austria; [538]Massachusetts General Hospital; Harvard Medical School; Department of Neurology; MassGeneral Institute for Neurodegenerative Disease; Charlestown, MA USA; [539]Departments of Neuroscience and Cell Biology; University of Texas Southwestern Medical Center; Dallas, TX USA; [540]Centre de Génétique et de Physiologie Moléculaire et Cellulaire; CNRS-UMR5534; Université Lyon I; Villeurbanne; Université de Lyon; Lyon, France; [541]Department of Neurology; Brigham and Women's Hospital; Harvard Medical School; Boston, MA USA; [542]Faculty of Medicine of the University of Paris Descartes; Paris, France; [543]Institute for Medical Microbiology, Immunology and Hygiene; University of Cologne; Cologne, Germany; [544]Signaling Program; Babraham Institute; Cambridge UK; [545]Division of Developmental Biology; Cincinnati Children's Hospital Research Foundation; Cincinnati, OH USA; [546]Institute of Biochemistry and Biophysics; Polish Academy of Sciences; Warsaw, Poland; [547]Department of Anatomical Sciences and Neurobiology; University of Louisville School of Medicine; Louisville, KY USA; [548]Department of Basic Sciences; The Commonwealth Medical College; Scranton, PA USA; [549]Department of Pathology; St. Jude Children's Research Hospital; Memphis, TN USA; [550]Department of Biochemistry & Molecular Medicine; University of California, Davis Cancer Center; Sacramento, CA USA; [551]Department of Biotechnology; Yonsei University; College of Life Science & Biotechnology; Seoul, Korea; [552]Departments of Pediatrics, Cellular & Molecular Medicine, and Neurosciences; and the Institute for Genomic Medicine; University of California, San Diego; La Jolla, CA USA; [553]Rady Children's Hospital; San Diego, CA USA; [554]Center for Infection and Immunity of Lille; Institut Pasteur de Lille; CNRS UMR8204; INSERM U1019; University Lille Nord de France; Lille, France; [555]Laval University Cancer Research Center; Québec, Canada; [556]School of Biochemistry; University of Bristol; University Walk; Bristol UK; [557]Nuclear Organisation and Oncogenesis Unit; INSERM U993; Institut Pasteur; Paris, France; [558]Department of Translational Medecine; Institut de Génétique et de Biologie Moléculaire et Cellulaire (IGBMC); INSERM U964; CNRS UMR7104; Université de Strasbourg; Illkirch, France; [559]School of Biomedical Sciences; The University of Nottingham; Queen's Medical Centre; Nottingham UK; [560]Instituto de Biología Molecular y Celular del Cáncer; Consejo Superior de Investigaciones Científicas (CSIC); Universidad de Salamanca; Salamanca, Spain; [561]Institute of Health Sciences; Shanghai Jiao Tong University School of Medicine; Chinese Academy of Sciences; Shanghai, China; [562]Shanghai Institutes for Biological Sciences; Chinese Academy of Sciences; Shanghai, China; [563]Translational Cancer Therapeutics Laboratory; Cancer Research UK London Research Institute; London, England UK; [564]Department of Internal Medicine; Yonsei University College of Medicine; Seoul, Korea; [565]Department of Psychiatry; Nathan Kline Institute for Psychiatric Research; New York University School of Medicine; Orangeburg, NY USA; [566]Division of Life Sciences; University of Incheon; Incheon, Korea; [567]Department of Medicine; Samsung Medical Center; Seoul, Korea; [568]Department of Pathology; College of Medicine; The Catholic University of Korea; Seoul, South Korea; [569]Department of Aging and Geriatrics; Division of Biology of Aging; University of Florida; Gainesville, FL USA; [570]University of Rennes-1; IRSET; INSERM U1085; Team DRaTE; Rennes, France; [571]Centre de Génétique Moléculaire; CNRS UPR3404 Université Paris Sud; Gif-sur-Yvette, France; [572]Department of Biological Sciences; University of Arkansas; Fayetteville, AR USA; [573]Department of Microbiology and Immunology; College of Medicine; National Cheng Kung University; Tainan, Taiwan; [574]Biomedical Sciences Institute; and Departments of Biochemistry and Molecular Biology; Shanghai Medical College; Fudan University; Shanghai, China; [575]Department of Microbiology and Immunology; Dartmouth Medical School; Lebanon, NH USA; [576]Universidad de Santiago de Compostela; Laboratorio de Parasitología; Instituto de Investigación y Análisis Alimentarios; La Coruña, Spain; [577]Departments of Pharmaceutical & Biomedical Sciences and Biochemistry & Molecular Biology; Medical University of South Carolina; Charleston, SC USA; [578]Department of Biochemistry and Molecular Biology; APHP; University of Paris 11; Inserm U1004; Villejuif, France; [579]Department of Surgery and Cancer Biology; The University of Chicago; Chicago, IL USA; [580]Department of Cancer Biology; University of Texas; MD Anderson Cancer Center; Houston, TX USA; [581]Department of Radiation Oncology; Rush University Medical Center; Chicago, IL USA; [582]Department of Microbiology; Howard Hughes Medical Institute; University of Texas Southwestern Medical Center; Dallas, TX USA; [583]Department of Pharmacology; Nathan Kline Institute for Psychiatric Research; New York University School of Medicine; Orangeburg, NY USA; [584]Department of Genetics; University of Wisconsin; Madison, WI USA; [585]Department of General Surgery; The Central Hospital of Yongzhou City; Hunan, China; [586]Key Laboratory of Insect Developmental and Evolutionary Biology; Institute of Plant Physiology and Ecology; Shanghai, China; [587]Department of Chemistry; Hanshan Normal University; Chaozhou, China; [588]Department of Pharmacology; School of Basic Medical Sciences; Peking University; Beijing, China; [589]Department of Endocrinology; The First Affiliated Hospital of Harbin Medical University; Harbin, China; [590]Department of Integrative Biology and Pharmacology; University of Texas Health Science Center at Houston; Houston, TX USA; [591]Department of Molecular Microbiology & Immunology; University of Southern California; Keck School of Medicine; Los Angeles, CA USA; [592]Cardiovascular Health Research Center; Sanford Research; University of South Dakota; and University of South Dakota Sanford School of Medicine; Sioux Falls, SD USA; [593]Institute of Cellular and Organismic Biology; Academia Sinica; Taipei, Taiwan; [594]Department of Molecular Pathology and Neuropathology; Medical University Lodz; Lodz, Poland; [595]Department of Biomedical Science & Technology; Konkuk University; Seoul, Korea; [596]Department of Physiology; Yong Loo Lin School of Medicine; National University of Singapore; Singapore; [597]Department of Biochemistry; Cancer Research Institute and Infection Signaling Network Research Center; College of Medicine; Chungnam National University; Daejeon, Korea; [598]Institute of Clinical Medicine; College of Medicine; National Cheng Kung University; Tainan, Taiwan; [599]Biotechnology Institute; Zhejiang University; Hangzhou, China; [600]Beijing NMR Center; College of Chemistry and Molecular Engineering; Peking University; Beijing, China; [601]Department of Cancer Signaling; Genentech; South San Francisco, CA USA; [602]Department of Molecular and Cellular Biology; Baylor College of Medicine; Houston, TX USA; [603]Institute of Biophysics; Federal University of Rio de Janeiro; Rio de Janeiro, Brazil; [604]The Eunice Kennedy Shriver National Institute of Child Health and Development; National Institutes of Health; Bethesda, MD USA; [605]Department of Stem Cell Biology; Kimmel Cancer Center; Thomas Jefferson University; Philadelphia, PA USA; and Breakthrough Breast Cancer Research Unit; University of Manchester; Manchester UK; [606]Department of Ophthalmology; Duke University; Durham, NC USA; [607]Department of Neurology; Second Affiliated Hospital; and Institute of Neuroscience; Soochow University; Suzhou, China; [608]College of Life Science; Central China Normal University; Wuhan, China; [609]Center for Cancer and Stem Cell Biology; Institute of Biosciences and Technology; Texas A&M Health Science Center; Houston, TX USA; [610]Department of Biochemistry and Cell Biology; Stony Brook University; Stony Brook, NY USA; [611]Metabolism & Cancer Susceptibility Section; Basic Research Laboratory; Center for Cancer Research; NCI–Frederick; Frederick, MD USA; [612]Division of Natural Science; College of Liberal Education; Shu-Te University; Taiwan; [613]Department of Biology; Queens College and Graduate Center of CUNY; Flushing, NY USA; [614]Departamento de Bioquímica y Biología Molecular; Instituto Universitario de Oncología; Universidad de Oviedo; Oviedo, Spain; [615]University of Turin; Turin, Italy; [616]Department of Immunology; University of Pittsburgh; Pittsburgh, PA USA; [617]Department of Pathology; Stanford University School of Medicine; Stanford, CA USA; [618]Department of Radiation Oncology; Thomas Jefferson University & Hospitals; Philadelphia, PA USA; [619]Department of Pathology; Albert Einstein College of Medicine; Bronx, NY USA; [620]Laboratory of Systems Biology; Van Andel Research Institute; Grand Rapids, MI USA; [621]Ben May Department for Cancer Research; University of Chicago; Gordon Center for Integrative Sciences; Chicago, IL USA; [622]Institute for Molecular Biosciences; University of Graz; Graz, Austria; [623]European Institute for Research in Cystic Fibrosis; San Raffaele Scientific Institute; Milan, Italy; [624]Department of Biology; University of Modena and Reggio Emilia; Modena, Italy; [625]Medical Genetics Branch and UDP Translational Medicine; National Human Genome Research Institute; National Institutes of Health; Bethesda, MD USA; [626]San Raffaele Sulmona Institute; L'Aquila, Italy; [627]Hefei National Laboratory for Physical Sciences at Microscale; and School of Life Sciences; University of Science & Technology of China; Hefei, Anhui China; [628]DZNE (German Center for Neurodegenerative Diseases); and CAESAR Research Center; Bonn, Germany; [629]Pediatric Research and Electron Microscopy Unit; Ruth and Bruce Rappaport Faculty of Medicine; Technion-Israel Institute of Technology; Haifa, Israel; [630]Nanjing Agricultural University; College of Veterinary Medicine; Nanjing, China; [631]Department of Neurology; Emory University School of Medicine; Atlanta, GA USA; [632]The Feinstein Institute for Medical Research; Manhasset, NY USA; [633]University of Ottawa Heart Institute; Ottawa, ON Canada; [634]Department of Medical and Molecular Genetics; Kings College London; London UK; [635]Department of Endocrinology and Metabolism; University of Pisa; Pisa, Italy; [636]School of Clinical Medicine; Cambridge Institute for Medical Research (CIMR); University of Cambridge; Cambridge, UK; [637]Department of Genomics; Agricultural Biotechnology Research Institute of Iran; Karaj, Iran; [638]INSERM; U848; Institut Gustave Roussy; Villejuif (Paris), France; [639]Institute of Molecular Biology and Biotechnology; Foundation for Research and Technology-Hellas & Medical School; University of Crete; Heraklion, Crete Greece; [640]Department of Genetics; The Smurfit Institute; Trinity College; Dublin, Ireland; [641]University Montpellier 2; Institut des Sciences de l'Evolution; Montpellier, France; [642]Department of Pharmacology; University of Antwerp; Antwerp, Belgium; [643]Neurodegenerative Diseases Research Group; Vall d'Hebron Research Institute-CIBERNED; Barcelona, Spain; [644]Department of General Pathology; University of Pisa; Pisa, Italy; [645]National Institute of Health; Department of Therapeutic Research and Medicine Evaluation; Section of Cell Aging and Degeneration; Rome, Italy; [646]Laboratory of Toxicology; Osaka Prefecture University Graduate School of Life and Environmental Biosciences; Izumisano, Japan; [647]Department de Biochimie; Université de Lausanne; Lausanne, Switzerland; [648]Institute of Developmental Biology and Cancer Research; University of Nice; CNRS-UMR 6543; Centre Antoine Lacassagne; Nice, France; [649]Departments of Urology and Cancer Biology; University of Texas MD Anderson Cancer Center; Houston, TX USA; [650]Malaghan Institute of Medical Research; Wellington, New Zealand; [651]Department of Biomedical Science; Bond University; Robina, Queensland Australia; [652]Department of Pathobiology; Lerner Research Institute; Cleveland Clinic; Cleveland, OH USA; [653]Cork Cancer Research Centre; University College, Cork; Cork, Ireland; [654]Department of Neurology; Vanderbilt University; Nashville, TN USA; [655]Departments of Pediatrics and Biochemistry & Molecular Biology; The Atlantic Research Centre; Dalhousie University; Halifax, NS Canada; [656]Department of Medical Biochemistry; Academic Medical Center; Amsterdam, The Netherlands; [657]The Graduate Center of the City University of New York; New York, NY USA; [658]Department of Cell Biology; Yale University; New Haven, CT USA; [659]IDI-IRCCS Laboratory; University Tor Vergata; Rome, Italy; [660]Department of Neurobiology; Hospital Ramon y Cajal; Madrid, Spain; [661]Catalan Institute of Oncology (ICO); Girona Biomedical Research Institute (IDIBGi); Catalonia, Spain; [662]Laboratório de Biologia Celular; Instituto Oswaldo Cruz–FIOCRUZ; Rio de Janeiro, RJ Brasil; [663]Department of Medical Genetics; Cambridge Institute for Medical Research; University of Cambridge; Cambridge UK; [664]Department of Hematology/Oncology; University of Cincinnati; Cincinnati, OH USA; [665]Department of Biochemistry and Molecular Biology; Thomas Jefferson University; Philadelphia, PA USA; [666]Bernhard-Nocht-Institut für Tropenmedizin; Tropenmedizinische Grundlagenforschung; Hamburg, Germany; [667]Department of Pharmacology; Second Military Medical University; Shanghai, China; [668]Institute of Developmental Biology; School of Life Science; Shandong University; Jinan, China; [669]URBC-NARILIS; University of Namur–FUNDP; Namur, Belgium; [670]Department of Molecular Immunology and Gene Therapy; Max-Delbrück-Center for Molecular Medicine; Berlin, Germany; [671]Department of Human Pathology and Oncology; Section of Pathological Anatomy; University of Siena; Siena, Italy; [672]Lab of Integrin Signaling; Van Andel Research Institute; Grand Rapids, MI USA; [673]First Department of Internal Medicine; Democritus University of Thrace; Alexandroupolis, Greece; [674]Department of Biochemistry; Tokyo Medical University; Tokyo, Japan; [675]Department of Physiology and Cell Biology; Tokyo Medical and Dental University; Tokyo, Japan; [676]Institute of Research on Cancer and Ageing of Nice (IRCAN); INSERM; CNRS; Université de Nice-Sophia Antipolis; Faculté de Médecine; Nice, France; and Equipe Labellisée par l; Villejuif, France; [677]Department of Clinical and Experimental Medicine; Division of Cell Biology; Linköping University; Linköping, Sweden; [678]Grup de Recerca en Patologia Pancreatica; Institut de Recerca Hospital Universitari Vall d'Hebron; Barcelona, Spain; [679]Ecole Normale Supérieure de Lyon; Laboratory of Molecular Biology of the Cell; CNRS UMR 5239; Lyon; France; [680]Center for Medical Science; International University of Health and Welfare; Tochigi, Japan; [681]Department of Internal Medicine; University of Iowa; Iowa City, IA USA; [682]Department of Anatomy and Neurobiology; University of Maryland; Baltimore, MD USA; [683]Plymouth Marine Laboratory; Plymouth UK; [684]Systems Biology of Personalized Therapy; Virology Department; Faculty of Microbiology and Centro de Investigación en Estructuras Microscópicas CIEMIC; University of Costa Rica; Costa Rica; [685]Department of Regulatory Biology; Graduate School of Science and Engineering; Saitama University; Saitama, Japan; [686]Section of Microbiology; Centre for Molecular Microbiology and Infection; Imperial College London; London UK; [687]Wellcome Trust Centre for Molecular Parasitology; Institute of Infection; Immunity and Inflammation; College of Medical, Veterinary and Life Sciences; University of Glasgow; Glasgow UK; [688]Department of Neuroscience; Georgetown University Medical Center; Washington D.C. USA; [689]Division of Infectious Diseases; Brigham and Women's Hospital and Department of Medicine Harvard Medical School; Boston, MA USA; [690]Viral Immunobiology; Institute of Experimental Immunology; University of Zürich; Zürich, Switzerland; [691]Novartis Institutes for Biomedical Research; Cambridge, MA USA; [692]Molecular and Cellular Oncogenesis; The Wistar Institute; Philadelphia, PA USA; [693]DAHFMO-Unit of Histology and Medical Embryology; Sapienza University of Rome; Rome, Italy; [694]Department of Obstetrics and Gynecology; Washington University School of Medicine; St. Louis, MO USA; [695]Department of Neurology; Tokai University School of Medicine; Kanagawa, Japan; [696]Laboratory of Molecular and Cellular Biology; Faculty of Life Sciences; Kyoto Sangyo University; Kyoto, Japan; [697]Central Laboratory of Hematology;

© 2012 Landes Bioscience. Do not distribute.

doi: 10.4161/auto.19496

University Hospital of Lausanne; Lausanne, Switzerland; [698]Department of Neurobiology; Gifu University Graduate School of Medicine; Gifu, Japan; [699]Department of Immunology; Juntendo University School of Medicine; Tokyo, Japan; [700]Frontier Research Center; Tokyo Institute of Technology; Yokohama, Japan; [701]Department of Cell Biology, Microbiology, and Molecular Biology; University of South Florida; Tampa, FL USA; [702]Biochemistry Section; Surgical Neurology Branch; National Institute of Neurological Disorders and Stroke; National Institutes of Health; Bethesda, MD USA; [703]Cancer Research UK; Cambridge Research Institute; Li Ka Shing Centre; Cambridge UK; [704]Department of Medicine; Radboud University Nijmegen Medical Centre; Nijmegen, The Netherlands; [705]Department of Genetics, Cell Biology & Development; University of Minnesota; Minneapolis, MN USA; [706]Department of Cell & Molecular Biology; Lindsley F. Kimball Research Institute; New York Blood Center; New York, NY USA; [707]Department of Medical Genetics; University of Tuebingen; Tuebingen, Germany; [708]Department of Medical Microbiology, Immunology, and Cell Biology; Southern Illinois University School of Medicine; Simmons Cancer Institute; Springfield, IL USA; [709]Department of Neuromuscular Research; National Institute of Neuroscience; National Center of Neurology and Psychiatry (NCNP); Kodaira, Tokyo Japan; [710]Donnelly Centre; Banting and Best Department of Medical Research and the Department of Molecular Genetics; University of Toronto; Toronto; ON Canada; [711]Department of Neuroscience; College of Medicine; McKnight Brain Institute of the University of Florida; Gainesville, FL USA; [712]School of Medicine; University of Split; Split, Croatia; [713]Department of Parasitology; National Institute of Infectious Diseases; Tokyo, Japan; and University of Tsukuba; Ibaraki, Japan; [714]Laboratory for Structural Neuropathology; RIKEN Brain Science Institute; Wako, Saitama Japan; [715]Center for Plant Molecular Biology; Eberhard-Karls-University; Tübingen, Germany; [716]Departments of Pathology & Laboratory Medicine; University of Wisconsin; Madison; WI USA; [717]Department of Physiology; South Texas Research Facility; University of Texas Health Science Center; San Antonio, TX USA; [718]Department of Microbiology and Immunology; Institute of Medical Science; University of Tokyo; Tokyo, Japan; [719]Department of Gene Therapy; Institute of DNA Medicine; The Jikei University School of Medicine; Tokyo, Japan; [720]Department of Pediatrics; The Jikei University School of Medicine; Tokyo, Japan; [721]Laboratory of Mitochondrial Dynamics; Graduate School of Frontier Biosciences; Osaka University; Osaka, Japan; [722]Department of Radiation Oncology; Case Western Reserve University; Cleveland, OH USA; [723]Department of Biochemistry; and Environmental Health Sciences; Case Western Reserve University; Cleveland, OH USA; [724]University of Copenhagen; Department of Agriculture and Ecology; Frederiksberg C, Denmark; [725]Ecole Polytechnique Fédérale de Lausanne; School of Life Sciences; Global Health Institute; Lausanne, Switzerland; [726]Sanford-Burnham Medical Research Institute at Lake Nona; Orlando FL USA; [727]Pacific Biosciences Research Center; University of Hawaii; Honolulu, HI USA; [728]Cardiovascular Division; King's College London; London UK; [729]AC Immune SA; Ecole Polytechnique Fédérale de Lausanne (EPFL); Lausanne, Switzerland; [730]INSERM U775; Université Paris Descartes; Paris, France; [731]Department of Microbiology Immunology and Parasitology; Louisiana State University Health Sciences Center; School of Medicine; New Orleans, LA USA; [732]Department of Neurology; Baylor College of Medicine; Houston, TX USA; [733]Department of Genetics; Louisiana State University Health Sciences Center; New Orleans, LA USA; [734]Department of Cell Biology and Biophysics; University of Athens; Panepistimiopolis Zografou, Athens Greece; [735]Molecular & Clinical Pharmacology; Faculty of Medicine; University of Chile; Santiago, Chile; and Santo Tomas University; Viña del Mar, Chile; [736]Division of Biological Science and Technology; Yonsei University; Wonju, Korea; [737]Departmenet of Internal Medicine; University of Goettingen; Göttingen, Niedersachsen Germany; [738]UNC Mcallister Heart Institute; University of North Carolina at Chapel Hill; Chapel Hill, NC USA; [739]Department of Dermatology and the Yale Cancer Center; Yale School of Medicine; New Haven, CT USA; [740]Institute of Entomology; Central China Normal University; Wuhan, China; [741]Department of Pediatrics; University of Pittsburgh School of Medicine and Children's Hospital of Pittsburgh; Pittsburgh, PA USA; [742]Department of Ecology; University of Calabria; Rende (CS), Italy; [743]Department of Biology; College of Sciences; University of Texas at San Antonio; San Antonio, TX USA; [744]Cancer and Stem Cell Biology Program; Duke-NUS Graduate Medical School; Singapore; [745]Institute of Biochemistry; ETH Zurich; Zurich, Switzerland; [746]Department of Medical Oncology; VU University Medical Center; Amsterdam, The Netherlands; [747]Department of Biology; University of Copenhagen; Copenhagen, Denmark; [748]Departments of Ophthalmology and Biochemistry and Molecular Biology; University of Debrecen; Medical and Health Science Center; Debrecen, Hungary; [749]GéPITOs UMR 6235 CNRS; Faculté de Médecine; Université de Nice Sophia Antipolis; Nice, France; [750]CNRS; UMR 8122; Institut Gustave Roussy; Villejuif, France; [751]Department of Neurobiology; Tel-Aviv University; Ramat-Aviv, Tel-Aviv Israel; [752]Università degli Studi di Torino; Neuroscience Institute Cavalieri-Ottolenghi (NICO); Orbassano (TO), Italy; [753]Jules Stein Eye Institute; University of California Los Angeles; Los Angeles, CA USA; [754]Robert H. Lurie Comprehensive Cancer Center and Division of Hematology/Oncology; Northwestern University Medical School; Chicago, IL USA; [755]Institute of Microbiology and Genetics; Department Genetics of Eukaryotic Microorganisms; Georg-August-University; Goettingen, Germany; [756]University Toulouse III; CRCT; Institut Claudius Regaud; Toulouse, France; [757]Universita' degli Studi di Milano; Dipartimento di Endocrinologia; Fisiopatologia e Biologia Applicata; Centro di Eccellenza sulle Malattie Neurodegenerative; Universita' degli Studi di Milano; Milano, Italy; [758]EA4530; Dynamique des microtubules en physiopathologie; Université Paris-Sud 11; Chatenay-Malabry, France; [759]Centro Andaluz de Biología Molecular y Medicina Regenerativa; CSIC; Sevilla, Spain; [760]Department of Molecular and Cellular Biochemistry; The Ohio State University; Columbus, OH USA; [761]Division of Experimental Medicine; Beth Israel Deaconess Medical Center; Harvard Medical School; Boston, MA USA; [762]Institute for Research in Ophthalmology (IRO); Sion, Switzerland; [763]Center for Molecular Microbiology and Department of Oral Biology; University of Florida; Gainesville, FL USA; [764]Department of Molecular Biology; University of Tuebingen; Tuebingen, Germany; [765]Center for Motor Neuron Biology and Disease; Columbia University; New York, NY USA; [766]Cardiovascular Research Institute and Departments of Physiology & Emergency Medicine; Wayne State University School of Medicine; Detroit, MI USA; [767]Laboratory of Cell Biology; National Heart, Lung, and Blood Institute; National Institutes of Health; Bethesda, MD USA; [768]Division of Nutritional Sciences; Cornell University; Ithaca, NY USA; [769]Institute of Basic Medical Sciences & School of Basic Medicine; Chinese Academy of Medical Sciences and Peking Union Medical College; Departments of Physiology & Pathology; Beijing, China; [770]Department of Pharmacology; Soochow University School of Pharmaceutical Science; Suzhou, China; [771]The Samuel Lunenfeld Research Institute; University of Toronto; Toronto, ON Canada; [772]Arthritis and Rheumatism Branch; National Institute of Arthritis and Musculoskeletal and Skin Diseases; National Institutes of Health; Bethesda, MD USA; [773]Department of Medicine; University of British Columbia; Vancouver, BC Canada; [774]Department of Environmental Medicine; Lung Biology and Disease Program; University of Rochester Medical Center; Rochester, NY USA; [775]Institute of Cellular and Molecular Anatomy; Clinics of the JWG-University; Frankfurt, Germany; [776]Monash Micro Imaging; Monash University; Clayton Campus; Melbourne, Victoria; Australia; [777]Department of Microbiology; The University of Chicago; Chicago, IL USA; [778]MRC Laboratory of Molecular Biology; Cambridge UK; [779]Laboratory of Biochemistry; Center for Drug Evaluation and Research; Food and Drug Administration; Bethesda, MD USA; [780]Department of Pharmacology and Cancer Biology; Duke University Medical Center; Durham, NC USA; [781]Neurodegenerative Disease Research; EMD Serono Research Institute, Inc.; Billerica, MA USA; [782]Department of Pathology, Microbiology, and Immunology; University of South Carolina School of Medicine; Columbia, SC USA; [783]Department of Biology; University of Waterloo; Waterloo, ON Canada; [784]Division of Tumor Virology; German Cancer Research Center; Heidelberg and Department of Biology; University of Mainz; Mainz, Germany; [785]Mitochondrial Biology; Frankfurt Institute for Molecular Life Sciences; and Mitochondriale Biologie; Zentrum für Molekulare Medizin; Goethe Universität Frankfurt a m Main; Frankfurt am Main, Germany; [786]Institute of Environmental Health Sciences; Wayne State University; Detroit, MI USA; [787]Pharmacology; University of Wyoming College of Health Sciences; Laramie, WY USA; [788]Kovler Diabetes Center; University of Chicago; Chicago, IL USA; [789]Departamento de Morfologia; Universidade Federal de Minas Gerais; Minas Gerais, Brasil; [790]Department of Pediatrics; Cincinnati Children's Hospital; Cincinnati, OH USA; [791]Department of Biochemistry and Molecular Biology; University of British Columbia; Vancouver, BC Canada; [792]Department of Urology; Comprehensive Cancer Center; University of Michigan; Ann Arbor, MI USA; [793]Service de Dermatologie; Hôpital Archet II; CHU Nice, France; [794]Centro de Investigaciones Biológicas (CSIC) and Ciber de Enfermedades Raras; Madrid, Spain; [795]Ophthalmology, and Neurosciences Division; Medical University of South Carolina; Charleston, SC USA; [796]Department of Pharmaceutical and Biomedical Sciences; South Carolina College of Pharmacy; University of South Carolina; Columbia, SC USA; [797]Department of Animal Histology and Embryology; University of Silesia; Katowice, Poland; [798]Unité de Recherche 04; Vieillissement; Stress et Inflammation; Université Pierre et Marie Curie (UPMC); Paris, France; [799]Department of Radiation Oncology (Maastro Lab); GROW School for Oncology & Developmental Biology; Maastricht University; Maastricht, The Netherlands; [800]Departments of Molecular Genetics and Anatomic Pathology; Cleveland Clinic; Lerner Research Institute; Taussig Cancer Center; Cleveland, OH USA; [801]Institute for Medical Microbiology, Virology and Hygiene; University Medical Center Eppendorf; Hamburg, Germany; [802]Dearptment of Clinical Biochemistry and National Institute of Biotechnology Negev; Ben-Gurion University; Beer-Sheva, Israel; [803]Department of Medical Biology and Genetics; Faculty of Medicine in Hradec Králové; Charles University; Hradec Králové, Czech Republic; [804]Boston University; School of Medicine; Section of Molecular Medicine; Boston, MA USA; [805]Department of Pharmacobiology; University of Calabria; Arcavacata di Rende; Italy; [806]Department of Biology; Massachusetts Institute of Technology; Whitehead Institute; Cambridge, MA USA; [807]Whitehead Institute; Cambridge, MA USA; [808]Department of Cell Biology and Molecular Medicine; Cardiovascular Research Institute; University of Medicine and Dentistry of New Jersey–New Jersey Medical School; Newark, NJ USA; [809]Department of Diagnostic and Therapeutic Sciences; Meikai University School of Dentistry; Sakado, Japan; [810]Division of Applied Life Sciences; Graduate School of Agriculture; and Research Unit for Physiological Chemistry; the Center for the Promotion of Interdisciplinary Education and Research; Kyoto University; Kyoto, Japan; [811]Department of Systems Biology; Agricultural Biotechnology Research Institute of Iran; Karaj, Iran; [812]Samantha Dickson Brain Cancer Unit; UCL Cancer Institute; London UK; [813]Division of Neuroscience; Beckman Research Institute of the City of Hope; Duarte, CA USA; [814]Department of Hematology, Oncology and Molecular Medicine; Istituto Superiore di Sanità; Rome, Italy; [815]Centro Andaluz de Biología del Desarrollo (CABD); Universidad Pablo de Olavide-Consejo Superior de Investigaciones Cientificas-Junta de Andalucía; Sevilla, Spain; [816]Laboratorio de Oncologia Molecular; CRIB-PcyTA; Universidad de Castilla la Mancha; Albacete, Spain; [817]Dulbecco Telethon Institute; [818]Venetian Institue of Molecular Medicine; Padova, Italy; [819]Department of Pharmacology and Toxicology; James Graham Brown Cancer Center and Owensboro Cancer Research Program; University of Louisville; Louisville, KY USA; [820]Department of Pediatrics; Stanford University; Stanford, CA USA; [821]Department of Immunology and Microbiology; Albert Einstein College of Medicine; Bronx, NY USA; [822]Jawaharlal Nehru University; School of Life Sciences; New Delhi, India; [823]Departments of Immunology and Surgery; Stanford University; Stanford, CA USA; [824]Department of Biochemistry and Biophysics; Vilnius University; Vilnius, Lithuania; [825]Laboratory of Molecular Traffic; Institute for Molecular and Cellular Regulation; Gunma University; Maebashi, Gunma Japan; [826]Division of Gastroenterology and Hepatology; University Hospital Zürich; Zürich, Switzerland; [827]Departments of Veterinary Sciences and Molecular Biology; University of Wyoming; Laramie, WY USA; [828]Departments of Genome Analysis and Neurology; Academic Medical Center; Amsterdam, The Netherlands; [829]Sektion Experimentelle Anästhesiologie; Universitätsklinikum Ulm; Ulm, Germany; [830]Experimental Tumor Pathology; Institute of Pathology; University of Erlangen-Nürnberg; Erlangen, Germany; [831]Department of Cellular Biology and Anatomy; Medical College of Georgia; Augusta, GA USA; [832]Ecole Polytechnique Fédérale de Lausanne (EPFL); Lausanne, Switzerland; [833]DAGZ; Department of Applied Genetics and Cell Biology; University of Natural Resources and Life Sciences Vienna (BOKU); Vienna, Austria; [834]Memorial Hospital Research Laboratories; Memorial Sloan-Kettering Cancer Center; Medicine; New York, NY USA; [835]Department of Cell Physiology and Medicine; University of Geneva; Geneva, Switzerland; [836]Department of Molecular Physiology and Biophysics; and Department of Cancer Biology; Vanderbilt University School of Medicine; Nashville, TN USA; [837]Department of Cell Biology; Institute for Cancer Research; Rikshospitalet-Radiumhospitalet HF; Montebello, Oslo Norway; [838]Molecular & Clinical Pharmacology; Faculty of Medicine; University of Chile; Santiago, Chile; [839]INRA; UR1067 Nutrition Métabolisme et Aquaculture; Saint-Pée-sur-Nivelle, France; [840]Department of Surgery; St. Jude Children's Research Hospital; Memphis, TN USA; [841]Department of Pathology; Drexel University College of Medicine; Philadelphia, PA, USA; [842]Integrating Proteomics & Metabolomics Research Team; Korea Basic Science Institute; Seoul, Korea; [843]Department of Pharmaceutical Sciences; Wayne State University College of Pharmacy; Detroit, MI USA; [844]Department of Dermatology; University of Wisconsin School of Medicine & Public Health; Madison, WI USA; [845]The Near-Future Locomoter Organ Medicine Creation Course (Kusunoki Kai); Graduate School of Medical and Dental Science; Kagoshima University; Kagoshima, Japan; [846]Department of Pathology; University of Alabama at Birmingham; Birmingham, AL USA; [847]Department of Orthopaedic Surgery; Jefferson Medical College; Thomas Jefferson University; Philadelphia, PA USA; [848]Department of Biochemistry and Molecular Biology; IMRIC; The Hebrew University-Hadassah Medical School; Jerusalem, Israel; [849]Howard Hughes Medical Institute; Molecular and Cell Biology Laboratory; The Salk Institute for Biological Studies; La Jolla, CA USA; [850]Critical Care Medicine Department; Clinical Center; National Institutes of Health; Bethesda, MD USA; [851]Department of Epidemiology and Public Health; Yong Loo Lin School of Medicine; National University of Singapore; Singapore; [852]University of Southern California School of Pharmacy; Los Angeles, CA USA; [853]Synaptic Function Section; National Institute of Neurological Disorders and Stroke; National Institutes of Health; Bethesda, MD USA; [854]Division of Pediatric Surgery; Department of Surgery; Medical College of Wisconsin; Milwaukee, WI USA; [855]National Institute of Floricultural Science; National Agriculture and Food Research Organization (NARO); Tsukuba, Japan; [856]Laboratory of Molecular and Cellular Biology; Graduate School of Human Health Science; University of Nagasaki; Nagayo, Nagasaki Japan; [857]Institute of Biomedical Sciences; College of Life Sciences; National Chung Hsing University; Taichung, Taiwan; [858]Department of Biochemistry; School of Medicine; Taipei Medical University; Taipei, Taiwan; [859]Department of Pathological Cell Biology; Tokyo Medical and Dental University; Tokyo, Japan; [860]Laboratory of Bioindustrial Genomics; Graduate School of Agricultural Science; Tohoku University; Miyagi, Japan; [861]Department of Pharmacology and Experimental Therapeutics; Tufts University School of Medicine; Boston, MA USA; [862]Department of Biochemistry and Goodman Cancer Center; McGill University; Montreal, QB Canada; [863]Institute of Cell Biology; National Academy of Sciences of Ukraine; Lviv, Ukraine; and University of Rzeszow; Rzeszow, Poland; [864]Cancer Genetics; Kolling Institute of Medical Research; University of Sydney and Royal North Shore Hospital; New South Wales, Australia; [865]MRC Human Immunology Unit; Weatherall Institute of Molecular Medicine; University of Oxford; Oxford UK; [866]Nuffield Department of Medicine; Oxford, UK; [867]Institute of Pharmacology; University of Bern; Bern, Switzerland; [868]Laboratory of Signal-Dependent Transcription; DTP; Consorzio Mario Negri Sud; Santa Maria Imbaro (Ch); Italy; and IRCCS "Saverio de Bellis"; Castellana Grotte (Ba), Italy; [869]Department of Biochemistry; Institute of Basic Medical Sciences; University of Oslo; Oslo, Norway; [870]Department of Genetics; Harvard Medical School; Boston, MA USA; [871]Department of Medicine and Diabetes Research Center; Albert Einstein College of Medicine; Bronx, NY USA; [872]Wilmer Eye Institute; Johns Hopkins University School of Medicine; Baltimore, MD USA; [873]Division of Oncology; Mayo Clinic and Mayo Cancer Center; Rochester, MN USA; [874]Department of Health Technology and Informatics; Hong Kong Polytechnic University; Hung Hom; Kowloon, Hong Kong China; [875]Department of Biochemistry and Microbiology; Institute of Chemical Technology; Prague, Czech Republic; [876]A.N. Belozersky Institute of Physico-Chemical Biology; Moscow State University; Moscow, Russia; [877]Department of Pharmacology; Federal University of São Paulo; School of Medicine; São Paulo, Brazil; [878]Institute of Molecular Biosciences and Center for Emerging and Neglected Infectious Diseases; Mahidol University; Thailand; [879]Melanoma Laboratory; Spanish Cancer Research Centre; Madrid, Spain; [880]Department of Biochemistry; University of Geneva; Geneva, Switzerland; [881]Department of Neurology; The Second Hospital of Hebei Medical University; Institute of Cardiocerebrovascular Disease; and Neurological Laboratory of Hebei Province; Shijiazhuang, Hebei China; [882]Departments of Gynecologic Oncology and Cancer Biology; Center for RNA Interference and Non-Coding RNA; MD Anderson Cancer Center; Houston, TX USA; [883]Pediatric Infectious Disease; University of California, San Diego; La Jolla, CA USA; and Rady Children's Hospital; San Diego, CA USA; [884]Department of Anaesthesiology and Intensive Care Medicine; Campus Virchow-Klinikum and Campus Charité Mitte; Charité-Universitaetsmedizin Berlin; Berlin, Germany; [885]Department of Neuroscience; Mayo Clinic; Jacksonville, FL USA; [886]Laboratory of Immune Cell Biology; National Cancer Institute; National Institutes of Health; Bethesda, MD USA; [887]Laboratory of Neurodegenerative Diseases; Biomedical Research Foundation of the Academy of Athens; Athens, Greece; [888]Department of Psychiatry and Human Behavior; University of California, Irvine; Irvine, CA USA; [889]Department of Neurosurgery; Charité–University Medicine Berlin; Berlin, Germany; [890]Division of Medicine; University College London; UK; [891]Nanotechnology Characterization Laboratory; Advanced Technology Program; SAIC-Frederick, Inc.; NCI-Frederick; Frederick, MD USA; [892]Laboratory of Translational Research; Clinical Research; National Cancer Institute of Brazil; Rio de Janeiro, Brazil; [893]Institute of Molecular Medicine; Heinrich-Heine-University; Düsseldorf, Germany; [894]Departments of Ophthalmology and Medicine; Case Western Reserve University School of Medicine; Institute of Pathology; Cleveland, OH USA; [895]Department of Colorectal Surgery and Key Laboratory of Biotherapy of Zhejiang Province; Sir Run Run Shaw hospital; Zhejiang University; Hangzhou, Zhejiang China; [896]Department of Psychiatry; Columbia University Medical Center; New York, NY USA; [897]Department of Microbiol Immunology; University of Texas Medical Branch; Galveston, TX USA; [898]The State Key Laboratory Breeding Base of Basic Science of Stomatology (Hubei-MOST); Key Laboratory of Oral Biomedicine Ministry of Education; School & Hospital of Stomatology; Wuhan University; Wuhan, China; [899]Institute of Digestive Diseases; Li Ka Shing Institute of Health Science and Department of Medicine & Therapeutics; The Chinese University of Hong Kong; Hong Kong, China; [900]Bioimaging Center; Graduate School of Frontier Sciences; University of Tokyo; Chiba, Japan; [901]Department of Molecular Bacteriology and Immunology; Graduate School of Medicine; University of the Ryukyus; Okinawa, Japan; [902]Department of Microbiology and Immunology; University of Michigan; Ann Arbor, MI USA; [903]Department of Biology; University of York; Heslington, York UK; [904]Department of Cell & Developmental Biology; Consortium for Mitochondrial Research; University College London; London UK; [905]Division of Cardiology; Department of Medicine; The University of Texas Medical School at Houston; Houston, TX USA; [906]Department of Experimental Medicine; University of Rome "Sapienza"; Rome, Italy; [907]Department of Genetics; Eötvös Loránd University; Budapest, Hungary; [908]Laboratory of Plant Pathology; Graduate School of Agriculture; Kyoto University; Kyoto, Japan; [909]Department of Bioscience & Biotechnology; Kyushu University; Kyushu, Japan; [910]Department of Molecular Biodefense Research; Yokohama City University Graduate School of Medicine; Yokohama, Japan; [911]School of Biosciences; University of Exeter; Exeter UK; [912]Department of Microbiology; Yong Loo Lin School of Medicine; National University of Singapore; Singapore; [913]Department of Molecular Oncology; Institute of Development, Aging and Cancer; Tohoku University; Miyagi, Japan; [914]State Key Laboratory of Plant Cell and Chromosome Engineering; Chinese Academy of Sciences; Beijing, China; [915]Institute of Genetics and Developmental Biology; Chinese Academy of Sciences; Beijing, China; [916]Laboratory of Biomembranes; Department of Biochemistry and Cell Biology; National Institute of Infectious Diseases; Tokyo, Japan; [917]Laboratory of Experimental Therapeutics and Molecular Imaging; Neuroscience Center; Massachusetts General Hospital and

Copyright © Landes Bioscience. Do not distribute.

dc_840_14

Harvard Medical School; Charlestown, MA USA; [918]CRUK Institute for Cancer Studies; University of Birmingham; Birmingham UK; [919]Departments of Medicine; Molecular Genetics and Microbiology; Division of Geriatrics; and Center for the Study of Aging and Human Development; Duke University Medical Center; Durham, NC USA; and GRECC; VA Medical Center; Durham, NC USA; [920]Developmental Neurobiology; St. Jude Children's Research Hospital; Memphis, TN USA; [921]Department of Clinical Pathology and Cytology; Karolinska University Hospital in Huddinge; Stockholm, Sweden; [922]Department of Biotechnology and Life Sciences; University of Insubria; Varese, Italy; [923]Centre of Microbial and Plant Genetics (CMPG); Katholieke Universiteit Leuven; Leuven, Belgium; [924]Department of Pharmacology; University of Colorado School of Medicine; Denver, CO USA; [925]Department Biochemistry II; Georg-August-Universitaet; Goettingen, Germany; [926]Department of Neurology; Okayama University Medical School; Okayama City, Japan; [927]Department of Biochemistry; University of Cambridge; Cambridge UK; [928]Secretory Pathways Laboratory; Cancer Research UK London Research Institute; London, England UK; [929]Faculty of Life Sciences; University of Manchester; Manchester, Lancashire UK; [930]Molecular and Computational Biology Program; University of Southern California; Los Angeles, CA USA; [931]Institute of Microbiology and Immunology; School of Medicine; University of Belgrade; Belgrade, Serbia; [932]Laboratory of Respiratory Phisiology; Carlos Chagas Filho Biophysics Institute; Federal University of Rio de Janeiro; Rio de Janeiro, Brasil; [933]Department of Life Sciences and Institute of Genome Sciences; National Yang-Ming University; Taipei, Taiwan; [934]Experimental Oncology/Hematology; Departments of Clinical Research and Medical Oncology; Inselspital; Bern University Hospital; Bern, Switzerland; [935]Laboratory of Immunology; Graduate School of Biomedical Sciences; Tokyo Medical and Dental University; Tokyo, Japan; [936]Division of Transplantation and Division of Surgical Oncology; University of Pittsburgh Medical Center; Pittsburgh, PA USA; [937]Department of Biochemistry and Molecular and Structural Biology; J. Stefan Institute; Ljubljana, Slovenia; [938]Department of Biology; Francis Marion University; Florence, SC USA; [939]Department of Physiology and Biophysics School of Medicine; University of Louisville; Louisville, KY USA; [940]Department of Neurology; Jungers Center for Neurosciences Research; Oregon Health & Science University; Portland, OR USA; [941]IRCCS Casa Sollievo della Sofferenza; CSS-Mendel Laboratory; San Giovanni Rotondo; and University of Messina; Messina, Italy; [942]Mann Laboratory; Department of Plant Sciences; University of California; Davis, CA USA; [943]Microbiology and Immunology Departments; University of Colorado School of Medicine; Aurora, CO USA; [944]Departments of Molecular and Cell Biololgy and Immunology/Surgery; VU University Medical Center; Amsterdam, The Netherlands; [945]Liver Cell Biology Laboratory; Department of Cell Biology; Vrije Universiteit Brussel; Brussels, Belgium; [946]Molecular Signalling and Cell Death Unit; Department for Molecular Biomedical Research; VIB; Ghent University; Ghent, Belgium; [947]Department of Neurology; University Hospitals Leuven; Leuven, Belgium; [948]Hospital Clinic; Division of Gastroenterology; CiberEHD; Barcelona; Catalonia Spain; [949]Department of Biochemistry and Molecular Biology I; Complutense University; School of Biology; Madrid, Spain; [950]Department of Biochemistry and Molecular Biology; Autonomous University of Barcelona (UAB); and Catalan Institution for Research and Advanced Studies (ICREA); Barcelona, Spain; [951]INSERM U1048; Toulouse, France; [952]Department of Pediatrics; Laboratory of Oncohematology; University of Padova; Padova, Italy; [953]Experimental Neurorehabilitation Lab; IRCSS Santa Lucia Foundation; Rome, Italy; [954]Laboratory of Plant Ecological Physiology; Komarov Botanical Institute; Russian Academy of Sciences; St. Petersburg, Russia; [955]Visual Neuroscience & Molecular Biology Group; School of Optometry & Vision Sciences; Cardiff University; Cardiff UK; [956]Texas A&M Institute for Biosciences and Technology; Houston, TX USA; [957]Molecular Biology & Biochemistry; University of California, Irvine; Irvine, CA USA; [958]Department of Neurology; University of Bonn; Bonn, Germany; [959]Department of Medical Oncology; the 3rd Affiliated Hospital of Sun Yat-sen University; Guangzhou, China; [960]The Cleveland Clinic Foundation; Biomedical Engineering; Cleveland; OH USA; [961]Department of Stem Cell Biology & Regenerative Medicine; Thomas Jefferson University; Philadelphia, PA USA; [962]Department of Cell Biology; Duke University Medical Center; Durham, NC USA; [963]Department of Emergency Medicine; North Shore University Hospital; Manhasset, NY USA; [964]Institute of Biotechnology and Department of Life Science; National Tsing Hua University; HsinChu, Taiwan; [965]Department of Dermatology; University of Texas Southwestern Medical Center; Dallas, TX USA; [966]Protein Quality Control and Degradation Research Center; Division of Basic Biomedical Sciences; Sanford School of Medicine of the University of South Dakota; Vermillion, SD USA; [967]Department of Environmental and Occupational Health; National Cheng Kung University; Medical College; Tainan, Taiwan; [968]Institute of Medicinal Biotechnology; Chinese Academy of Medical Sciences & Peking Union Medical College; Beijing, China; [969]Department of Cancer Biology; Dana-Farber Cancer Institute; Harvard Medical School; Boston, MA USA; [970]Department of Cardiothoracic Surgery; Changzheng Hospital; The Second Military Medical University; Shanghai, China; [971]Department of Cell Biology; Nijmegen Centre for Molecular Life Sciences Radboud University Nijmegen Medical Centre; Nijmegen, The Netherlands; [972]Department of Pathology; University of Utah; School of Medicine; Salt Lake City, UT USA; [973]Juntendo University Graduate School of Medicine; Department of Metabolism and Endocrinology; Tokyo, Japan; [974]Randall Division for Cell and Molecular Biophysics; Kings College; London UK; [975]House Research Institute; Los Angeles, CA USA; [976]Tumor Immunology and Gene Therapy Center; Eastern Hepatobiliary Hospital; Second Military Medical University; Shanghai, China; [977]Department of Neurology; Washington University School of Medicine; Saint Louis, MO USA; [978]School of Life Science; University of Science & Technology of China; Hefei, Anhui China; [979]MRC Centre for Developmental and Biomedical Genetics; Department of Biomedical Science; University of Sheffield; Sheffield UK; [980]University of East Anglia; Faculty of Health; Biomedical Research Centre; Norwich, East Anglia UK; [981]Edinburgh CRUK Research Centre; Institute of Genetics and Molecular Medicine; University of Edinburgh; Edinburgh UK; [982]Institute of Physical Biology; Heinrich-Heine-Universität; Düsseldorf, Germany; and Institute of Complex Systems; ICS-6; Research Centre Jülich; Jülich, Germany; [983]Laboratory of Clinical Infectious Diseases; National Institute of Allergy and Infectious Diseases; National Institutes of Health; Bethesda, MD USA; [984]Hypoxia and Microenvironment Program; Ontario Cancer Institute/Princess Margaret Hospital; University Health Network; Departments of Radiation Oncology and Medical Biophysics; University of Toronto; ON Canada; [985]The Second Affiliated Clinical College of Fujian University of Traditional Chinese Medicine; Fuzhou, China; [986]Key Laboratory of Biomedical Information Engineering of Ministry of Education; School of Life Science and Technology; Xi'an Jiaotong University; Xi'an, China; [987]School of Biological Sciences; Life Sciences Building; Highfield Campus; University of Southampton; Southampton UK; [988]Center for Computational and Integrative Biology and Gastrointestinal Unit; Massachusetts General Hospital; Harvard Medical School; Boston, MA USA; [989]Department of Urology; Peking University First Hospital; Beijing, China; [990]Centenary Institute and Sydney Medical School University of Sydney; Sydney, Australia; [991]State Key Laboratory of Virology; Wuhan Institute of Virology; Chinese Academy of Sciences; Wuhan, China; [992]School of Medicine; Nankai University; Tianjin, China; [993]Section of Molecular Medicine; Department of Medicine; University of Oklahoma Health Sciences Center; Oklahoma City, OK US; [994]State Key Laboratory of Oncology in South China; Department of Gastric and Pancreatic Surgery; Cancer Center; Sun Yat-sen University; Guangzhou, China; [995]College of Bioengineering; Henan University of Technology; Zhengzhou, China; [996]Departments of Molecular Biosciences, Urology and Radiation Oncology; University of Kansas; Lawrence, KS USA; [997]Department of Biochemistry and Molecular Biology; Mayo Clinic College of Medicine; Rochester, MN USA; [998]Department of Cell Biology; Nagahama Institute of Bio-Science and Technology; Nagahama, Japan; [999]Department of Gastroenterology; Juntendo University School of Medicine; Tokyo, Japan; [1000]National Research Institute of Fisheries Science; Yokohama, Japan; [1001]College of Animal Sciences and Technology; Huazhong Agricultural University; Wuhan, China; [1002]OIST Promotion Corporaton; Okinawa, Japan; [1003]Department of Pediatrics; Vanderbilt Ingram Cancer Center; Vanderbilt University School of Medicine; Nashville, TN USA; [1004]Division of Surgery & Interventional Science; University College London; London UK; [1005]Weis Center for Research; Geisinger Clinic; Danville, PA USA; [1006]Institute of Molecular Biology; Academia Sinica; Taipei, Taiwan; [1007]Department of Pathology and Laboratory Medicine; Indiana University School of Medicine; Indianapolis, IN USA; [1008]BioMedical Research Center; Graduate School of Medical Science and Engineering; Korea Advanced Institute of Science and Technology; Daejeon, Korea; [1009]Department of Biochemistry; Ajou University School of Medicine; Suwon, Korea; [1010]Department of Life Sciences; Graduate School of Arts and Sciences; University of Tokyo; Tokyo, Japan; [10011]School of Food and Nutritional Sciences; University of Shizuoka; Shizuoka, Japan; [1012]RIKEN; Plant Science Center; Tsurumi-ku, Yokohama Japan; [1013]Department of Pharmacology; DNA Repair Research Center; Chosun University School of Medicine; Gwangju, Korea; [1014]Department of Lymphoma/Myeloma; MD Anderson Cancer Center; Houston, TX USA; [1015]State Key Laboratory of Genetics Engineering; School of Life Sciences; Fudan University; Shanghai, China; [1016]Department of Radiation Oncology; University of Texas Health Science Center San Antonio; San Antonio, TX USA; [1017]Department of Neurology & Neuroscience; Friedman Brain Institute; Mount Sinai School of Medicine; New York, NY USA; [1018]Protein Engineering and Comparative Immunology; Graduate School of Agricultural Biotechnology; Seoul National University; Seoul, Korea; [1019]Department of Neurophysiology; Keio University School of Medicine; Tokyo, Japan; [1020]Metabolism and Cancer Susceptibility Section; Laboratory of Comparative Carcinogenesis; Center for Cancer Research; NCI-Frederick; National Institutes of Health; Frederick, MD USA; [1021]Department of Ophthalmology and Visual Sciences; University of Michigan School of Medicine; Ann Arbor, MI USA; [1022]Division of Cell & Molecular Biology; Toronto General Research Institute–University Health Network; Toronto, ON Canada; [1023]Department of Experimental Oncology and Molecular Medicine; Fondazione IRCCS Istituto Nazionale Tumori; Milan, Italy; [1024]Department of Surgery; University of Pittsburgh; Pittsburgh, PA USA; [1025]Department of Neuroscience; University of Virginia; Charlottesville, VA USA; [1026]National Institute of Biological Sciences; Beijing, China; [1027]Laboratory of Cerebrovascular Pharmacology; College of Pharmaceutical Science; Soochow University; Suzhou, China; [1028]Department of Pharmacology and Chemical Biology; University of Pittsburgh School of Medicine; Pittsburgh, PA USA; [1029]Department of Molecular Cell Biology; Leiden University Medical Center; Leiden, The Netherlands; [1030]Key Laboratory of Plant Resources Conservation and Sustainable Utilization; South China Botanical Garden; Chinese Academy of Sciences; Guangzhou, China; [1031]School of Medicine and Public Health; University of Newcastle; New South Wales, Australia; [1032]Key Laboratory of Carcinogenesis and Translational Research (Ministry of Education); Peking University Health Science Center; Beijing, China; [1033]Department of Biochemistry and Molecular Biology; Peking University Health Science Center; Beijing, China; [1034]Department of Pathology; University of Oklahoma Health Sciences Center; Oklahoma City, OK USA; [1035]Qiushi Academy for Advanced Studies; Zhejiang University; Hangzhou, China; [1036]Department of Molecular and Cell Biology; University of California; Berkeley, CA USA; [1037]Center for Brain Repair and Rehabilitation; Institute of Neuroscience and Physiology; University of Gothenburg; Gothenburg, Sweden; [1038]State Key Laboratory of Oncology in South China; Department of Medical Oncology; Cancer Center; Sun Yat-sen University; Guangzhou, China; [1039]Department of Molecular Genetics & Microbiology; Stony Brook University; Stony Brook, NY USA; [1040]Institute for Research in Biomedicine; CIBERDEM; and Universitat de Barcelona; Barcelona, Spain; [1041]Max Planck Institute of Psychiatry; Munich, Germany; [1042]Department of General Surgery; University of Pittsburgh Medical Center and VA Pittsburgh Healthcare System; Pittsburgh, PA USA

Keywords: autolysosome, autophagosome, flux, LC3, lysosome, phagophore, stress, vacuole

Abbreviations: 3-MA, 3-methyladenine; AMPK, AMP-activated protein kinase; Ape1, aminopeptidase I; Atg, autophagy-related; AV, autophagic vacuole; CLEAR, coordinated lysosomal enhancement and regulation; CLEM, correlative light and electron microscopy; CMA, chaperone-mediated autophagy; Cvt, cytoplasm-to-vacuole targeting; DQ-BSA, dequenched bovine serum albumin; e-MI, endosomal microautophagy; EBSS, Earle's balanced salt solution; FACS, fluorescence-activated cell sorter; GFP, green fluorescent protein; IMP, intramembrane particle; LAMP2, lysosome-associated membrane protein 2; LAP, LC3-associated phagocytosis; LC3, microtubule-associated protein 1 light chain 3 (MAP1LC3); MDC, monodansylcadaverine; mRFP, monomeric red fluorescent protein; MTOR, mechanistic target of rapamycin; NVJ, nucleus-vacuole junction; RPS6KB2, ribosomal protein S6 kinase, 70kDa, polypeptide 2; PAS, phagophore assembly site; PE, phosphatidylethanolamine; PMN, piecemeal microautophagy of the nucleus; PtdIns3K, phosphatidylinositol 3-kinase; PtdIns3KC3, PtdIns3K class III; Rluc, *Renilla reniformis* luciferase; SD, standard deviation; SOD, superoxide dismutase; TEM, transmission electron microscopy; tfLC3, tandem fluorescent LC3; TORC1, TOR complex I; TR-FRET, time-resolved fluorescence resonance energy transfer; UPR, unfolded protein response

In 2008 we published the first set of guidelines for standardizing research in autophagy. Since then, research on this topic has continued to accelerate, and many new scientists have entered the field. Our knowledge base and relevant new technologies have also been expanding. Accordingly, it is important to update these guidelines for monitoring autophagy in different organisms. Various reviews have described the range of assays that have been used for this purpose. Nevertheless, there continues to be confusion regarding acceptable methods to measure autophagy, especially in multicellular eukaryotes. A key point that needs to be emphasized is that there is a difference between measurements that monitor the numbers or volume of autophagic elements (e.g., autophagosomes or autolysosomes) at any stage of the autophagic process vs. those that measure flux through the autophagy pathway (i.e., the complete process); thus, a block in macroautophagy that results in autophagosome accumulation needs to be differentiated from stimuli that result in increased autophagic activity, defined as increased autophagy induction coupled with increased delivery to, and degradation within, lysosomes (in most higher eukaryotes and some protists such as Dictyostelium) or the vacuole (in plants and fungi). In other words, it is especially important that investigators new to the field understand that the appearance of more autophagosomes does not necessarily equate with more autophagy. In fact, in many cases, autophagosomes accumulate because of a block in trafficking to lysosomes without a concomitant change in autophagosome biogenesis, whereas an increase in autolysosomes may reflect a reduction in degradative activity. Here, we present a set of guidelines for the selection and interpretation of methods for use by investigators who aim to examine macroautophagy and related processes, as well as for reviewers who need to provide realistic and reasonable critiques of papers that are focused on these processes. These guidelines are not meant to be a formulaic set of rules, because the appropriate assays depend in part on the question being asked and the system being used. In addition, we emphasize that no individual assay is guaranteed to be the most appropriate one in every situation, and we strongly recommend the use of multiple assays to monitor autophagy. In these guidelines, we consider these various methods of assessing autophagy and what information can, or cannot, be obtained from them. Finally, by discussing the merits and limits of particular autophagy assays, we hope to encourage technical innovation in the field.

Table of Contents

A. Methods for Monitoring Autophagy

1. Transmission electron microscopy 18
2. Atg8/LC3 detection and quantification 22
   a. Western blotting and ubiquitin-like protein conjugation systems 22

*Correspondence to: Daniel J. Klionsky; Email: klionsky@umich.edu
Submitted: 01/26/12; Accepted: 01/26/12
http://dx.doi.org/10.4161/auto.8.4.19496

dc_840_14

b. Turnover of LC3-II/Atg8–PE 26
c. GFP-Atg8/LC3 lysosomal delivery and proteolysis 28
d. GFP-Atg8/LC3 fluorescence microscopy 30
e. Tandem mRFP/mCherry-GFP fluorescence microscopy 35
f. Autophagic flux determination using flow and multispectral imaging cytometry 36
g. Immunohistochemistry 38
3. p62 and related LC3 binding protein turnover assays 39
4. MTOR, AMPK and Atg1/ULK1 40
5. Additional autophagy-related markers 43
a. Atg9 43
b. Atg12–Atg5 43
c. ATG14 43
d. ATG16L1 44
e. Atg18/WIPI family 44
f. BECN1/Atg6 44
g. DFCP1 45
h. DRAM 45
6. Transcriptional and translational regulation 45
7. Autophagic protein degradation 47
8. Selective types of autophagy 48
a. The Cvt pathway, mitophagy, pexophagy and piecemeal microautophagy of the nucleus in yeast 48
b. Reticulophagy and ribophagy 50
c. Vacuole import and degradation pathway 50
d. Mammalian mitophagy and peroxisome degradation 51
e. Aggrephagy 53
f. Xenophagy 54
g. Lipophagy 55
h. Zymophagy 55
i. Allophagy 55
9. Autophagic sequestration assays 55
10. Turnover of autophagic compartments 56
11. Autophagosome-lysosome colocalization and dequenching assay 56
12. Tissue fractionation 57
13. Analyses in vivo 58
14. Cell death 60
15. Chaperone-mediated autophagy 60
B. Comments on Additional Methods 63
1. Acidotropic dyes 63
2. Autophagy inhibitors and inducers 63
3. Basal autophagy 67
4. Experimental systems 67
5. Nomenclature 67
C. Methods and Challenges of Specialized Model Systems 67
1. *C. elegans* 68
2. Chicken B-lymphoid DT40 cells and retina 68
3. Chlamydomonas 68
4. Drosophila 68
5. Filamentous fungi 70
6. Honeybee 70
7. Human 70
8. Hydra 72
9. Large animals 72
10. Lepidoptera 73
11. Neotropical teleosts 73
12. Odontoblasts 74
13. Planarians 74

14. Plants 74
15. Protists 75
16. Rainbow trout 76
17. Sea Urchin 76
18. Ticks 76
19. Food biotechnology 76
20. Zebrafish 77
Conclusions and Future Perspectives 77
References 78
Glossary 99
Index 100

Introduction

Many researchers, especially those new to the field, need to determine which criteria are essential for demonstrating autophagy, either for the purposes of their own research, or in the capacity of a manuscript or grant review.[1] This is an important issue, particularly considering that each of us may have his/her own opinion regarding the answer. Unfortunately, the answer is in part a "moving target" as the field evolves,[2] and this can be extremely frustrating for researchers who may think they have met those criteria, only to find out that the reviewers of their paper have different ideas. Conversely, as a reviewer, it is tiresome to raise the same objections repeatedly, wondering why researchers have not fulfilled some of the basic requirements for establishing the occurrence of an autophagic process. In addition, drugs that potentially modulate autophagy are increasingly being used in clinical trials, and screens are being performed for new drugs that can modulate autophagy for therapeutic purposes. Clearly it is important to determine whether these drugs are truly affecting autophagy based on a set of accepted criteria. Accordingly, we describe here a basic set of contemporary guidelines that can be used by researchers to plan and interpret their experiments, by clinicians to evaluate the literature with regard to autophagy-modulating therapies, and by both authors and reviewers to justify or criticize an experimental approach.

Several fundamental points must be kept in mind as we establish guidelines for the selection of appropriate methods to monitor autophagy.[1] Importantly, there are no absolute criteria for determining autophagic status that are applicable in every biological or experimental context. This is because some assays are inappropriate, problematic or may not work at all in particular cells, tissues or organisms.[3-6] In addition, these guidelines are likely to evolve as new methodologies are developed and current assays are superseded. Nonetheless, it is useful to establish guidelines for acceptable assays that can reliably monitor autophagy in many experimental systems. It is important to note that in this set of guidelines the term "autophagy" generally refers to macroautophagy; other autophagy-related processes are specifically designated when appropriate.

For the purposes of this review, the autophagic compartments (**Fig. 1**) are referred to as the sequestering (pre-autophagosomal) phagophore (previously called the isolation or sequestration membrane[7,8]),[9] the autophagosome,[10] the amphisome (generated by the fusion of autophagosomes with endosomes, also referred to as an acidic late autophagosome[11]),[12] the autolysosome (generated by fusion of autophagosomes or amphisomes with a lysosome), and the autophagic body (generated by fusion and release of the internal autophagosomal compartment into the vacuole in fungi and plants; autophagic bodies are not formed within lysosomes/autolysosomes because these lytic organelles are typically smaller than autophagosomes[13]).[8,10] One critical point is that autophagy is a highly dynamic, multi-step process. Like other cellular pathways, it can be modulated at several steps, both positively and negatively. An accumulation of autophagosomes [measured by transmission electron microscopy (TEM) image analysis, a fluorescent GFP-MAP1LC3 (GFP-LC3) dots, or as LC3 lipidation on a western blot], could, for example, reflect induction of autophagy, reduction in autophagosome turnover,[14-16] or the inability of turnover to keep pace with increased autophagosome formation (**Fig. 1**).[17] For example, inefficient fusion with endosomes and/or lysosomes, respectively, or perturbation of the transport machinery,[18] would inhibit autophagosome maturation to amphisomes or autolysosomes, whereas decreased flux could also be due to inefficient degradation of the cargo once fusion has occurred.[19]

Accordingly, the use of autophagy markers such as LC3-II needs to be complemented by assays to estimate overall autophagic flux, or flow, to permit a correct interpretation of the results. That is, autophagic activity includes not just the increased synthesis or lipidation of Atg8/LC3 (LC3 is the mammalian homolog of yeast Atg8), or an increase in the formation of autophagosomes, but, most importantly, flux through the entire system, including lysosomes or the vacuole, and the subsequent release of the breakdown products. Therefore, autophagic substrates need to be monitored dynamically over time to verify that they have reached the lysosome/vacuole, and, when appropriate, are degraded. By responding to perturbations in the extracellular environment, cells tune autophagic flux to meet intracellular metabolic demands. The impact of autophagic flux on cell death and human pathologies therefore demands accurate tools to measure not only the current flux of the system, but also its capacity,[20] and its response time, when exposed to a defined insult.[21]

One approach is to measure the rate of general protein breakdown by autophagy.[8,22] Alternatively, it is possible to arrest the autophagic flux at a given point, and then record the

© 2012 Landes Bioscience. Do not distribute.
dc_840_14

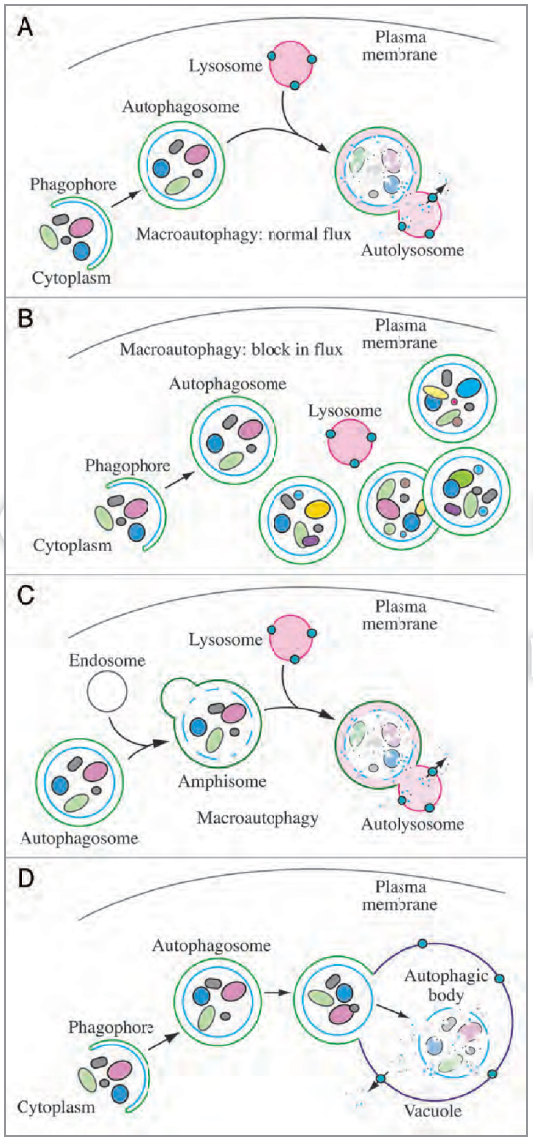


Figure 1. Schematic model demonstrating the induction of autophagosome formation when turnover is blocked vs. normal autophagic flux, and illustrating the morphological intermediates of macroautophagy. (A) The initiation of autophagy includes the formation of the phagophore, the initial sequestering compartment, which expands into an autophagosome. Completion of the autophagosome is followed by fusion with lysosomes and degradation of the contents, allowing complete flux, or flow, through the entire pathway. This is a different outcome than the situation shown in (B) where induction results in the initiation of autophagy, but a defect in autophagosome turnover due, for example, to a block in fusion with lysosomes or disruption of lysosomal functions will result in an increased number of autophagosomes. In this scenario, autophagy has been induced, but there is no or limited autophagic flux. (C) An autophagosome can fuse with an endosome to generate an amphisome, prior to fusion with the lysosome. (D) Schematic drawing showing the formation of an autophagic body in plants and fungi. The large size of the plant and fungal vacuole relative to autophagosomes allows the release of the single-membrane autophagic body within the vacuole lumen. In cells that lack vacuolar hydrolase activity, or in the presence of inhibitors that block hydrolase activity, intact autophagic bodies accumulate within the vacuole lumen and can be detected by light microscopy. The lysosome of most higher eukaryotes is too small to allow the release of an autophagic body.

time-dependent accumulation of an organelle, an organelle marker, a cargo marker or the entire cargo at the point of blockage; however, the latter assumes there is no feedback of the accumulating structure on its own rate of formation.,[23] Along the same lines, one can follow the time-dependent decrease of an autophagy-degradable marker (with the caveat that the potential contribution of other proteolytic systems needs to be experimentally addressed). In theory, this can be achieved by blocking autophagic sequestration at specific steps of the pathway (e.g., blocking further induction or nucleation of new phagophores) and by measuring the decrease of markers distal to the block point.[14,16,24] The key issue is to differentiate between the often transient accumulation of autophagosomes due to increased induction, from accumulation due to inefficient completion of autophagy by measuring both the levels of autophagosomes at static time points and by addressing changes in the rates of autophagic degradation of cellular components.[19] Both processes have been used to estimate "autophagy," but unless the experiments can relate changes in autophagosome numbers to a direct or indirect measurement for autophagic flux, they may be difficult to interpret.[25] A general caution regarding the use of the term "steady state" is warranted at this point. It should not be assumed that an autophagic system is at

steady-state in the strict biochemical meaning of this term, as this implies that the level of autophagosomes does not change with time, and the flux through the system is constant. In these guidelines, we use steady-state to refer to the baseline range of autophagic flux in a system that is not subjected to specific perturbations that increase or decrease that flux.

Autophagic flux refers to the entire process of autophagy including the delivery of cargo to lysosomes (via fusion of the latter with autophagosomes or amphisomes) and its subsequent breakdown and release of the resulting macromolecules back into the cytosol (this may be referred to as productive or complete autophagy). Thus, increases in the level of phosphatidylethanolamine (PE)-modified Atg8/LC3 (Atg8–PE/LC3-II), or even the appearance of autophagosomes are not measures of autophagic flux per se, but can reflect the induction of autophagic sequestration and/or inhibition of autophagosome or amphisome clearance. Also, it is important to realize that while formation of Atg8–PE/LC3-II appears to correlate with the induction of autophagy, we do not know, at present, the actual mechanistic relationship between Atg8–PE/LC3-II formation and the rest of the autophagic process; indeed, it may be possible to execute "self-eating" in the absence of LC3-II.[26] As a final note, we also recommend that researchers refrain from the use of the expression "percent autophagy" when describing experimental results, as in "The cells displayed a 25% increase in autophagy." In contrast, it is appropriate to indicate that the average number of GFP-Atg8/LC3 puncta per cell is increased or a certain percentage of cells display punctate GFP-Atg8/LC3 that exceeds a particular threshold (and this threshold should be clearly defined in the methods), or that there is a particular increase or decrease in the rate of degradation of long-lived proteins, as these are the actual measurements being quantified.

In the previous version of these guidelines,[1] the methods were separated into two main sections—steady-state and flux. In some instances, a lack of clear distinction between the actual methodologies and their potential uses made such a separation somewhat artificial. For example, fluorescence microscopy was initially listed as a steady-state method, although this approach can clearly be used to monitor flux as described in this article, especially when considering the increasing availability of new technologies such as microfluidics. Furthermore, the use of multiple time points and/or lysosomal fusion/degradation inhibitors can turn even a typically static method such as TEM into one that monitors flux. Therefore, although we maintain the importance of monitoring autophagic flux and not just induction, this revised set of guidelines does not separate the methods based on this criterion. Readers should be aware that this article is not meant to present protocols, but rather guidelines, including information that is typically not presented in protocol papers. For detailed information on experimental procedures we refer readers to various protocols that have been published elsewhere.[27-42]

Collectively, we propose the following guidelines for measuring various aspects of selective and nonselective autophagy in eukaryotes.

A. Methods for Monitoring Autophagy

1. *Transmission electron microscopy.* Autophagy was first detected by TEM in the 1950s (reviewed in ref. 8). The focal degradation of cytoplasmic areas sequestered by the phagophore, which matures into the autophagosome, is the morphological hallmark of autophagy. TEM can be used to monitor both selective and nonselective autophagy. In the case of selective autophagy, the cargo should correspond to the specific substrate being targeted for sequestration—bulk cytoplasm is essentially excluded. In contrast, during nonselective autophagy, the content of the autophagosome is morphologically identical to the cytoplasm, containing similar densities of ribosomes, and intact sequestered organelles are clearly identifiable. Therefore, the use of TEM is a valid and important method both for the qualitative and quantitative analysis of changes in various autophagic structures that sequentially form the phagophore, autophagosome, amphisome, autolysosome and autophagic body (**Fig. 1**).[43] The maturation from the phagophore through the autolysosome is a dynamic and continuous process,[44] and, thus, the classification of compartments into discrete morphological subsets can be problematic; however, some basic guidelines can be offered.

Autophagosomes (also referred to as initial autophagic vacuoles, AVi) have a double membrane that is usually at least partly visible as two parallel membrane bilayers separated by an electron-lucent cleft (**Fig. 2A**).[45,46] Autophagosomes contain cytosol and/or organelles that look morphologically intact, i.e. similar to the cytosol and organelles elsewhere in the cell.[43,47] Amphisomes[48] can sometimes be identified by the presence of small internal vesicles inside the autophagosome/autophagic vacuole (AV).[49] These internal vesicles are delivered into the lumen by fusion with multivesicular endosomes. Late/degradative autophagic vacuoles and autolysosomes (AVd) usually have only one limiting membrane, and contain cytoplasmic material and/or organelles at various stages of degradation (**Fig. 2A and B**).[43,47] It should be emphasized that not all vesicles containing electron-dense amorphous material are autolysosomes. The cytoplasmic origin of the contents must still be morphologically identifiable, if morphology is the only criterion that is being used for the identification of autolysosomes. For many biological and pathological situations, examination of both early and late autophagic structures yields valuable data regarding the overall autophagy/lysosomal status in the cells.[17] Along these lines, it is possible to use immunocytochemistry to follow particular cytosolic proteins such as CuZn superoxide dismutase (SOD) and carbonic anhydrase to determine the stage of autophagy; the former is much more resistant to lysosomal degradation.[50] In some autophagy-inducing conditions it is possible to observe multi-lamellar membrane structures in addition to the conventional double-membrane autophagosomes. The nature of these structures is not fully understood. They may indeed be multiple double layers of phagophores[51] and positive for LC3,[52] or mere artifacts of fixation.

TEM observations of platinum-carbon replicas obtained by the freeze fracture technique can also supply useful ultrastructural

doc 840.14

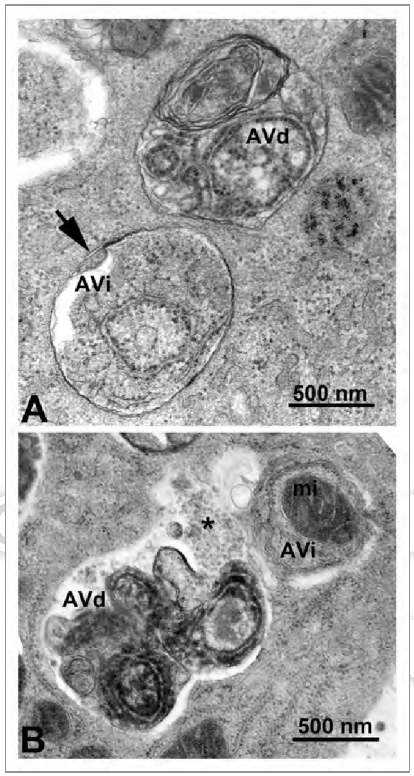


Figure 2. TEM images of autophagic vacuoles in isolated mouse hepatocytes. (A) One autophagosome or early autophagic vacuole (AVi) and one degradative autophagic vacuole (AVd) are shown. The AVi can be identified by its contents (morphologically intact cytoplasm, inlcuding ribosomes, and rough endoplasmic reticulum), and the limiting membrane that is partially visible as two bilayers separated by a narrow electron-lucent deft, i. e., as a double membrane (arrow). The AVd can be identified by its contents, partially degraded, electron-dense rough endoplasmic reticulum. The vesicle next to the AVd is an endosomal/lysosomal structure containing 5-nm gold particles that were added to the culture medium to trace the endocytic pathway. (B) One AVi, containing rough endoplasmic reticulum and a mitochondrion, and one AVd, containing partially degraded rough endoplasmic reticulum, are shown. Note that the limiting membrane of the AVi is not clearly visible, possibly because it is tangentially sectioned. However, the electron-lucent cleft between the two limiting membranes is visible and helps in the identification of the AVi. The AVd contains a region filled by small internal vesicles (asterisk), indicating that the AVd has fused with a multivesicular endosome. mi, mitochondrion. Image provided by E.-L. Eskelinen.

information on the autophagic process. In quickly frozen and fractured cells the fracture runs preferentially along the hydrophobic plane of the membranes, allowing characterization of the limiting membranes of the different types of autophagic vacuoles and visualization of their limited protein intramembrane particles (IMPs, or integral membrane proteins). Several studies have been performed using this technique on yeast,[53] as well as on mammalian cells or tissue, first on mouse exocrine pancreas,[54] then on mouse and rat liver,[55,56] mouse seminal vesicle epithelium[24,51] or cancer cell lines (e.g., breast cancer MDA-MB-231)[57] to investigate the various phases of autophagosome maturation, and to reveal useful details about the origin and evolution of their limiting membranes.[2,8,58-60]

The phagophore and the limiting membranes of autophagosomes contain few, or no detectable, IMPs (**Fig. 3A and B**), when compared with other cellular membranes and to the membranes of lysosomes. In subsequent stages of the autophagic process the fusion of the autophagosome with an endosome and a lysosome results in increased density of IMPs in the membrane of the formed autophagic compartments (amphisomes, autolysosomes; **Fig. 3C**).[8,24,53-56,61,62] Autolysosomes are generally delimited by a single membrane because, in addition to the engulfed material, the inner membrane is degraded by the lytic enzymes. Similarly, the limiting membrane of autophagic bodies in yeast and plants is also quickly broken down under normal conditions. Autophagic bodies can be stabilized, however, by the addition of phenylmethylsulphonylfluoride (PMSF) or genetically by the deletion of the yeast *PEP4* gene. Thus, another method to consider for monitoring autophagy in plants and yeast is to count autophagic bodies by TEM using at least two time points. The advantage of this approach is that it can provide accurate information on flux even when the autophagosomes are abnormally small.[63,64] Thus, although a high frequency of "abnormal" structures presents a challenge, TEM is still very helpful in analyzing autophagy.

Cautionary notes: Although TEM is one of the most widely used methodologies to monitor autophagy, it is also one of the most problematic due to misinterpretations mostly deriving from methodological artifacts.[45,46,65,66] Care in the choice of sample to be analyzed is critical to the success of TEM studies for autophagy. Whereas fixation of in vitro samples is relatively straightforward, fixation of excised tissues requires care to avoid sampling a nonrepresentative or uninformative section of tissue. For instance, if 95% of a tumor is necrotic, TEM analysis of the necrotic core may not be informative, and if the sampling is from the viable rim, this needs to be specified when reported. Ex vivo tissue should be fixed immediately and systematically across samples to avoid changes in autophagy that may occur simply due to elapsed time ex vivo. It is recommended that for tissue samples, perfusion fixation should be used when possible. For yeast, rapid freezing techniques such as high pressure freezing followed by freeze substitution (i.e., dehydration at low temperature) may be particularly useful.

Due to the high potential for sampling artifacts, careful selection of appropriate nonbiased methods of quantification



Figure 3. Different autophagic vesicles observed after freeze fracturing in cultured osteosarcoma cells after treatment with the autophagy inducer voacamine.[59] (A) Early autophagosome delimited by a double membrane. (B) Inner monolayer of an autophagosome membrane deprived of protein particles. (C) Autolysosome delimited by a single membrane rich in protein particles. In the cross-fractured portion (on the right) the profile of the single membrane and the inner digested material are easily visible. Images provided by S. Meschini, M. Condello and A. Giuseppe.

and morphometric/stereological analyses is essential.[67-69] Data obtained simply by scoring for the presence or absence of autophagic vacuoles (autophagosomes, autolysosomes) in the section of a cell leads to unreliable results due to variability in cell areas, and autophagic vacuole profiles in the sections. It is more reliable to quantify autophagosome (and/or autolysosome) profiles per total cytoplasmic or cellular area on sections, which still includes an unaccounted variability in the profile size of the autophagic element. The best approach is to estimate the volume occupied by autophagic structures (as percent of cytoplasmic or cellular volume, using volumetric morphometry/stereology) in at least 20 cell profiles per sample (the number needed should be dictated by some form of power analysis, which indicates that the data are significant).[20,65,68,70,71] During quantification it is important to make sure that each imaged cell profile is captured and scored at the same magnification, and that every cell profile in the thin section has an equal probability to be included in the counting.

The accurate identification of the autophagosome is a prerequisite for a valid analysis. An additional complication, however, is that maturation of metazoan autophagosomes involves a transition from a double-membrane compartment to single-membrane structures (i.e., amphisomes and autolysosomes).[72] In addition, not all double-membrane structures are autophagosomes. Thus, double membranes cannot be relied upon as the sole means for the ultrastructural identification of autophagy-related structures, and it is important to employ expert analysis to avoid misinterpretation of micrographs.[46,65,66] In some cases, it may be prudent to employ tomographic reconstructions of the TEM images to confirm that the autophagic compartments are spherical and are not being confused with endomembrane cisternae or damaged mitochondria with similar appearance in thin-sections (e.g., see ref.73), but this is obviously a time-consuming approach requiring sophisticated equipment. In addition, interpretation of tomographic images can be problematic. For example, starvation-induced autophagosomes should contain cytoplasm (i.e., cytosol and possibly organelles), but autophagosome-related structures involved in specific types of autophagy should show the selective cytoplasmic target, but may be relatively devoid of cytoplasm. Such processes include selective peroxisome or mitochondria degradation (pexophagy or mitophagy, respectively),[74,75] targeted degradation of pathogenic microbes (xenophagy),[76-81] as well as the yeast biosynthetic cytoplasm-to-vacuole targeting (Cvt) pathway.[82] Furthermore, some pathogenic microbes express membrane-disrupting factors during infection (e.g., phospholipases) that disrupt the normal double-membrane architecture of autophagosomes.[83] It is not even clear if the sequestering compartments used for specific organelle degradation or xenophagy should be termed autophagosomes or if alternate terms such as pexophagosome,[84] mitophagosome and xenophagosome should be used, even though the membrane and mechanisms involved in their formation may be identical to those for starvation-induced autophagosomes; for example, the double-membrane vesicle of the Cvt pathway is referred to as a Cvt vesicle.

It can also be difficult to determine whether material present within a phagosomal structure reflects self-eating, or is from a heterophagic (consumption of components from outside the cell) process. A prominent example is related to apoptosis. Apoptotic bodies from neighboring cells are readily phagocytosed by surviving cells of the same tissue.[85,86] Immediately after phagocytic uptake of apoptotic bodies, phagosomes have double limiting membranes. The inner one is from the plasma membrane of the apoptotic body and the outer one is that of the phagocytizing cell. The early heterophagic vacuole formed in this way may appear similar to an autophagosome or, in a later stage, an early autolysosome in that it contains recognizable cytoplasmic material. A major difference, however, is that the surrounding membranes are the thicker (plasma membrane type), rather than the thinner sequestration membrane type (9–10 nm, vs. 7–8 nm, respectively).[66] A good feature to distinguish between autophagosomes and double plasma membrane-bound structures is the lack of the distended empty space (characteristic for the sequestration membranes of autophagosomes) between the two membranes of the phagocytic vacuoles. In addition, engulfed apoptotic

dc 840 14

bodies usually have a larger average size than autophagosomes.[87] The problem of heterophagic elements interfering with the identification of autophagic ones is most prominent in cell types with particularly intense heterophagic activity (such as macrophages, and amoeboid or ciliate protists). Special attention has to be paid to this problem in cell cultures or in vivo treatments (e.g., with toxic or chemotherapeutic agents) causing extensive apoptosis.

To decide about the lytic nature of a vacuolar compartment, demonstration of the presence of lysosomal enzymes by traditional (enzyme) cytochemistry or immunocytochemistry is also feasible for identifying post-fusion autophagic compartments. However, when heterophagy and autophagy are going on in parallel, the fusion of secondary lysosomes from both sources happens without distinction. The result will be a mixture of degradative products that may be derived both from heterophagy and autophagy, making it impossible to determine the proportion derived from a single process.

There are numerous structures in cells that resemble, or can be confused with, autophagic vesicles. The most common organelles are mitochondria, and ER, and also (depending on their structure) plastids in plants. Due to the cisternal structure of the ER, double membrane-like structures surrounding mitochondria or other organelles are often observed after sectioning,[88] but these can also correspond to cisternae of the ER coming into and out of the section plane.[45] If there are ribosomes associated with these membranes they can help distinguish them from the ribosome-free double-membrane of the phagophore and autophagosome. Observation of a mixture of early and late autophagosomes that is modulated by time point of collection and/or brief pulses of bafilomycin A_1 (a V-ATPase inhibitor) to trap the cargo in a recognizable early state[41] increases the confidence that an autophagic process is being observed. Criteria for distinguishing specialized structures such as melanosomes containing electron dense pigment from autophagosomes should be specified prior to scoring and included in a methods section when reporting the results. Considering that swollen mitochondria can encompass most of the internal structure of small autophagosomes, the possibility exists for scoring errors in every study. To minimize the impact of such errors, exact specification of autophagic elements must be applied. Efforts should be made to clarify the nature of questionable structures by extensive preliminary comparison in many test areas. Elements that still remain questionable should be categorized into special groups and measured separately. Should their later identification become possible, they can be added to the proper category or, if not, kept separate.

Uncertainties of identification and special features of the autophagic process may be clarified by immuno-TEM with gold-labeling,[89,90] using antibodies, for example, to cargo proteins of cytoplasmic origin and to LC3 to verify the autophagic nature of the compartment. Although labeling of LC3 can be difficult, good antibodies exist to visualize the GFP moiety of GFP-LC3 reporter constructs.[91] Antibodies against an abundant cytosolic protein will result in high background labeling; however, organelle markers work well. Because there are very few characterized proteins that remain associated with the completed structure, the choices for confirmation of its autophagic nature are limited. Furthermore, autophagosome-associated proteins may be cell type-specific. At any rate, the success of this methodology depends on the quality of the antibodies and also on the TEM preparation and fixation procedures utilized. With immuno-TEM, authors should provide controls showing that labeling is specific. This may require a quantification of staining over different cellular compartments.

In addition, statistical information should be provided due to the necessity of showing only a selective number of sections. Again, we note that for quantitative data it is preferable to use proper volumetric analysis rather than just counting numbers of sectioned objects. On the one hand, it must be kept in mind that even volumetric morphometry/stereology only shows either steady-state levels, or a snapshot in a changing dynamic process. Such data by themselves are not informative regarding autophagic flux, unless performed over multiple time points. Alternatively, investigation in the presence and absence of flux inhibitors can reveal the dynamic changes in various stages of the autophagic process.[14,20,92,93] For example, if the turnover of autolysosomes is very rapid, a low number/volume will not necessarily be an accurate reflection of low autophagic activity. On the other hand, quantitative analyses indicate that autophagosome volume in many cases does correlate with the rates of protein degradation.[94-96] One potential compromise is to perform whole cell quantification of autophagosomes using fluorescence methods, with qualitative verification by TEM,[97] to show that the changes in fluorescent puncta reflect increases in autophagic structures.

One additional caveat with TEM, and to some extent with confocal fluorescence microscopy, is that the analysis of a single plane within a cell can be misleading and may make the identification of autophagic structures difficult. Confocal microscopy and fluorescence microscopy with deconvolution software (or with much more work, 3-dimensional TEM) can be used to generate multiple/serial sections of the same cell to reduce this concern; however, in some cases where there is sufficient structural resolution, analysis of a single plane with multiple cells can suffice given practical limitations. Newer EM technologies, including focused ion beam dual-beam EM, should make it much easier to apply three-dimensional analyses. An additional methodology to assess autophagosome accumulation is correlative light and electron microscopy, CLEM, which is helpful in confirming that fluorescent structures are autophagosomes.[98,99] Along these lines, the new mini Singlet Oxygen Generator (miniSOG) fluorescent flavoprotein, which is less than half the size of GFP, provides an additional means to genetically tag proteins for CLEM analysis under conditions that are particularly suited to subsequent TEM analysis.[100] Combinatorial assays using tandem mRFP-GFP-LC3 (see *Tandem mRFP/mCherry-GFP fluorescence microscopy*) along with static TEM images should help in the analysis of flux and the visualization of cargo structures.[101] Another technique that has proven quite useful for analyzing the complex membrane structures that participate in autophagy is three-dimensional electron tomography,[102,103] and cryoelectron microscopy (**Fig. 4**). Finally,

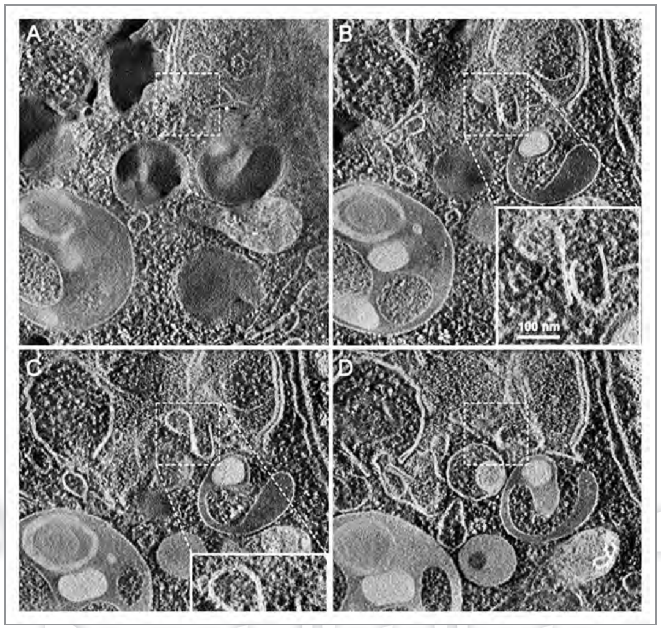


Figure 4. Cryoelectron microscopy can be used as a three-dimensional approach to monitor the autophagic process. Four computed sections of an electron tomogram of the autophagic vesicle-rich cytoplasm in a hemophagocyte of a semi-thin section after high-pressure freezing preparation. The dashed area is membrane-free (1A) but tomography reveals newly formed or degrading membranes with a parallel stretch (1B). In another computed section (1C) of the same tomogram, the parallel stretch of the two membranes shows only one membrane bilayer, and this membrane composition has disappeared in the computed section shown in (1D). Image published previously[104] and provided by M. Schneider and P. Walter.

although an indirect measurement, a comparison of the ratio of autophagosomes to autolysosomes by TEM can support alterations in autophagy identified by other procedures.[105] In this case it is important to always compare samples to the control of the same cell type and in the same growth phase, as the ratio of autophagosome/autolysosome varies in a cell context-dependent fashion, depending on their clearance activity. It may also be necessary to distinguish autolysosomes from telolysosomes/late secondary lysosomes (the former are actively engaged in degradation, whereas the latter have reached an end point in the breakdown of lumenal contents and are also referred to as residual bodies; see *Tissue fractionation*) because lysosome numbers generally increase when autophagy is induced.

With regard to immunohistochemistry using SOD1 as a marker to follow autophagy, it should be noted that a portion of the CuZn superoxide dismutase, SOD1, is also associated with various organelles, including the ER, mitochondria and peroxisomes. In addition, the wild-type SOD1 protein can be oxidized, and this form (SODox) is associated with sporadic cases of amyotrophic lateral sclerosis.[106] Thus, the oxidized form of SOD1 might interfere with autophagy, and, if so, it may not be a good choice for a marker to monitor steady-state autophagic flux.

Conclusion: EM can be an extremely informative method for monitoring autophagy; however, it must be performed with extreme caution and rigor to avoid bias, and to ensure correct identification and quantification of autophagic compartments. With TEM, immunogold labeling is strongly recommended as it generally provides the most unequivocal results. Whenever possible, EM should not be the sole method used to monitor autophagy, but rather should be complemented by additional assays as described in this article.

2. *Atg8/LC3 detection and quantification*. Atg8/LC3 is the most widely monitored autophagy-related protein. In this section we describe multiple assays that utilize this protein, separating the descriptions into several subsections for ease of discussion.

a. Western blotting and ubiquitin-like protein conjugation systems. The Atg8/LC3 protein is a ubiquitin-like protein that can be conjugated to PE (and possibly to phosphatidylserine[107]). In yeast

dc_840_14

and several other organisms, the conjugated form is referred to as Atg8–PE. The mammalian homologs of Atg8 constitute a family of proteins subdivided in two subfamilies: LC3 (microtubule-associated protein 1 light chain 3) and GABARAP ($GABA_A$ receptor-associated protein). The former is comprised of LC3A, B, B2 and C, whereas the latter family includes GABARAP, GABARAPL1/Atg8L/GEC1 ($GABA_A$ receptor-associated protein like 1/Glandular Epithelial Cell 1), GABARAPL2/GATE-16/GEF2 ($GABA_A$ receptor-associated protein like 2/Golgi-associated ATPase enhancer of 16 kDa/ganglioside expression factor 2) and GABARAPL3 ($GABA_A$ receptor-associated protein like 3).[108] The nonlipidated and lipidated forms are usually referred to as LC3-I and LC3-II, or GABARAP and GABARAP–PE, etc. The positions of both Atg8/LC3-I (approximately 18 kDa) and Atg8–PE/LC3-II (approximately 16 kDa) should be indicated on western blots whenever both are detectable.

The mammalian Atg8 homologs share from 29% to 94% sequence identity and have all, apart from GABARAPL3, been demonstrated to be involved in autophagosome biogenesis.[109] The LC3 proteins are involved in phagophore formation, with participation of GABARAP subfamily members in later stages of autophagosome formation, in particular phagophore elongation and closure.[110] Nevertheless, in most published studies, LC3 has been the primary Atg8 homolog examined in mammalian cells and the one that is typically characterized as an autophagosome marker per se, making this factor the most relevant for this discussion (note that although this protein is referred to as "Atg8" in many other systems, for simplicity we primarily refer to it here as LC3 to distinguish it from the yeast protein). LC3, like the other Atg8 homologs, is initially synthesized in an unprocessed form, proLC3, which is converted into a proteolytically processed form lacking amino acids from the C terminus, LC3-I, and is finally modified into the PE-conjugated form, LC3-II (**Fig. 5**). Atg8–PE/LC3-II is the only protein marker that is reliably associated with completed autophagosomes, but is also localized to phagophores. In yeast, Atg8 amounts increase at least 10-fold when autophagy is induced.[113] In mammalian cells, however, the total levels of LC3 do not necessarily change in a predictable manner, as there may be increases in the conversion of LC3-I to LC3-II, or a decrease in LC3-II relative to LC3-I if degradation of LC3-II via lysosomal turnover is particularly rapid. Both of these events can be seen sequentially in several cell types as a response to total nutrient and serum starvation. In cells of neuronal origin a high ratio of LC3-I to LC3-II is a common finding.[114] For instance, SH-SY5Y neuroblastoma cell lines display only a slight increase of LC3-II after nutrient deprivation, whereas LC3-I is clearly reduced. This is likely related to a high basal autophagic flux, as suggested by the higher increase in LC3-II when cells are treated with NH_4Cl,[115,116] although cell-specific differences in transcriptional regulation of LC3 may also play a role. The pattern of LC3-I to LC3-II conversion seems not only to be cell specific, but also related to the kind of stress to which cells are subjected. For example, the same SH-SY5Y cells display a strong increase of LC3-II when treated with the mitochondrial uncoupler CCCP, a well-known inducer of mitophagy. Thus, neither assessment of LC3-I consumption nor the evaluation of LC3-II levels would necessarily reveal a slight induction of autophagy (e.g., by rapamycin). Also, there is not always a clear precursor/product relationship between LC3-I and LC3-II, because the conversion of the former to the latter is cell type-specific and dependent on the treatment used to induce autophagy. Accumulation of LC3-II can be obtained by interrupting the autophagosome-lysosome fusion step (e.g., by depolymerizing acetylated microtubules with vinblastine, or by raising the lysosomal pH with the lysosomal proton pump inhibitor bafilomycin A_1) or by inhibiting lysosome-mediated proteolysis (e.g., with the cysteine protease inhibitor E-64d, the aspartic protease inhibitor pepstatin A, or chloroquine[117]). Western blotting can be used to monitor changes in LC3 amounts (**Fig. 5**);[25,118] however, even if the total amount of LC3 does increase, the magnitude of the response is generally less than that documented in yeast. It is worth noting that since the conjugated forms of the GABARAP subfamily members are usually undetectable without induction of autophagy in mammalian cells,[119] these proteins might be more suitable than LC3 to study and quantify subtle changes in the autophagic flux.

In most organisms, Atg8/LC3 is initially synthesized with a C-terminal extension that is removed by the Atg4 protease. Accordingly, it is possible to use this processing event to monitor Atg4 activity. For example, when GFP is fused at the C terminus of Atg8 (Atg8-GFP), the GFP moiety is removed in the cytosol to generate free Atg8 and GFP. This processing can be easily monitored by western blot.[120] It is also possible to use assays with an artificial fluorogenic substrate, or a fusion of LC3B to phospholipase A(2) that allows the release of the active phospholipase for a subsequent fluorogenic assay,[121] and there is a FRET-based assay utilizing CFP and YFP tagged versions of LC3B and GABARAPL2/GATE-16 that can be used for high-throughput screening.[122] Another method to monitor ATG4 activity in vivo uses the release of Gaussia luciferase from the C terminus of LC3 that is tethered to actin.[123] Note that there are four Atg4 homologs in mammals, and they have different activities with regard to the Atg8 subfamilies of proteins.[124] ATG4A is able to cleave the GABARAP subfamily, but has very limited activity toward the LC3 subfamily, whereas ATG4B is apparently active against most or all of these proteins. The ATG4C and ATG4D isoforms have minimal activity for any of the Atg8 homologs. In particular because a C-terminal fusion will be cleaved immediately by Atg4, researchers should be careful to correctly specify whether they are using GFP-Atg8/LC3 (an N-terminal fusion, which can be used to monitor various steps of autophagy) or Atg8/LC3-GFP (a C-terminal fusion, which can only be used to monitor Atg4 activity).[125]

Cautionary notes: There are several important caveats to using Atg8/LC3-II or GABARAP-II to visualize fluctuations in autophagy. First, changes in LC3-II amounts are tissue- and cell context-dependent.[112,126] Indeed, in some cases, autophagosome accumulation detected by TEM does not correlate well with the amount of LC3-II (Tallóczy Z, de Vries RLA, Sulzer D, unpublished results; Eskelinen E-L, unpublished results). This is particularly evident in those cells that show low levels of LC3-II

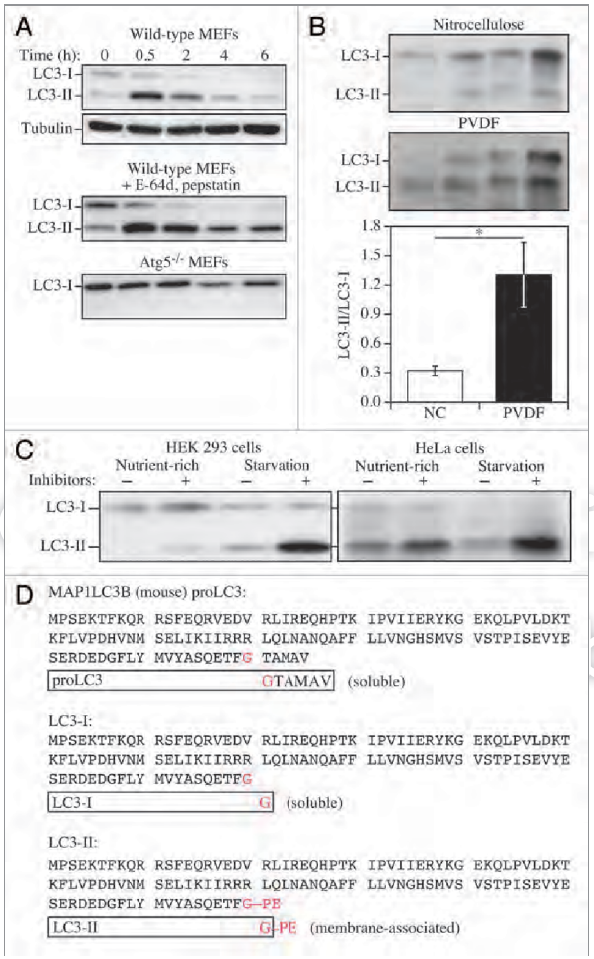


Figure 5. LC3-I conversion and LC3-II turnover. (A) Expression levels of LC3-I and LC3-II during starvation. *Atg5*$^{+/+}$ (wild-type) and *Atg5*$^{-/-}$ MEFs were cultured in DMEM without amino acids and serum for the indicated times, and then subjected to immunoblot analysis using anti-LC3 antibody and anti-tubulin antibody. E-64d (10 μg/ml) and pepstatin A (10 μg/ml) were added to the medium where indicated. Positions of LC3-I and LC3-II are indicated. The inclusion of lysosomal protease inhibitors reveals that the apparent decrease in LC3-II is due to lysosomal degradation as easily seen by comparing samples with and without inhibitors at the same time points (the overall decrease seen in the presence of inhibitors may reflect decreasing effectiveness of the inhibitors over time). Monitoring autophagy by following steady-state amounts of LC3-II without including inhibitors in the analysis can result in an incorrect interpretation that autophagy is not taking place (due to the apparent absence of LC3-II). Conversely, if there are high levels of LC3-II but there is no change in the presence of inhibitors this may indicate that induction has occurred but that the final steps of autophagy are blocked, resulting in stabilization of this protein. This figure was modified from data previously published in reference 25 and is reproduced by permission of Landes Bioscience, copyright 2007. (B) Lysates of 4 human adipose tissue biopsies were resolved on two 12% polyacrylamide gels, as described previously.[111] Proteins were transferred in parallel to either a PVDF or a nitrocellulose membrane, and blotted with anti-LC3 antibody, and then identified by reacting the membranes with an HRP-conjugated anti-rabbit IgG antibody, followed by ECL. The LC3-II/LC3-I ratio was calculated based on densitometry analysis of both bands. *$p < 0.05$. (C) HEK 293 and HeLa cells were cultured in nutrient-rich medium (DMEM containing10% FCS) or incubated for 4 h in starvation conditions (Krebs-Ringer medium) in the absence (-) or presence (+) of E-64d and pepstatin at 10 μg/ml each (Inhibitors). Cells were then lysed and the proteins resolved by SDS-PAGE. Endogenous LC3 was detected by immunoblotting. Positions of LC3-I and LC3-II are indicated. In the absence of lysosomal protease inhibitors, starvation results in a modest increase (HEK 293 cells) or even a decrease (HeLa cells) in the amount of LC3-II. The use of inhibitors reveals that this apparent decrease is due to lysosome-dependent degradation. This figure was modified from data previously published in reference ,112 and is reproduced by permission of Landes Bioscience, copyright 2005. (D) Sequence and schematic representation of the different forms of LC3B. The sequence for the nascent (proLC3) from mouse is shown. The glycine at position 120 indicates the cleavage site for ATG4. After this cleavage, the truncated LC3 is referred to as LC3-I, which is still a soluble form of the protein. Conjugation to PE generates the membrane-associated LC3-II (equivalent to Atg8–PE).

(based on western blotting) because of an intense autophagy flux that consumes this protein,[127] or in cell lines having high levels of LC3-II that are tumor-derived, such as MDA-MB-231.[112] Conversely, the detectable formation of LC3-II is not sufficient evidence for autophagy, without careful quantification. For example, homozygous deletion of *Becn1* does not prevent the formation of LC3-II in embryonic stem cells even though autophagy is substantially reduced, whereas deletion of *atg5* results in the complete absence of LC3-II (see **Fig. 5A** and Supplemental Data in ref.128). The same is true for the generation of Atg8–PE in yeast in the absence of *ATG6* (see **Fig. 7** in ref.129). Thus, it is important to remember that not all of the autophagy-related

dc_840_14

proteins are required for Atg8/LC3 processing, including lipidation.[129] Vagaries in the detection and amounts of LC3-I vs. LC3-II present technical problems. For example, LC3-I is very abundant in brain tissue, and the intensity of the LC3-I band may obscure detection of LC3-II, unless the polyacrylamide crosslinking density is optimized. Conversely, certain cell lines have much less visible LC3-I compared with LC3-II. In addition, tissues may have asynchronous and heterogeneous cell populations, and this may present challenges when analyzing LC3 by western blotting.

Second, LC3-II also associates with the membranes of non-autophagic structures. For example, some members of the γ-protocadherin family undergo clustering to form intracellular tubules that emanate from lysosomes.[130] LC3-II is recruited to these tubules, and appears to promote or stabilize membrane expansion. Furthermore, LC3 can be recruited directly to bacteria-containing phagosome membranes under certain immune activating conditions, for example, TLR-mediated stimulation, in a process designated LC3-associated phagocytosis (LAP)[131,132] and also to apoptotic cell-containing phagosome membranes,[133,134] macropinosomes,[133] and to single-membrane entotic vacuoles.[133] TEM analysis of murine macrophage-like RAW 264.7 cells infected with *Burkholderia pseudomallei* reveals that intracellular bacteria colocalize with GFP-LC3 puncta. However, the TEM analysis further shows that bacteria are either free in the cytosol, or sequestered in single-membrane phagosomes rather than within canonical double-membrane autophagosomes.[135] Therefore, in studies of infection of mammalian cells by bacterial pathogens the identity of the LC3-II labeled compartment as an autophagosome should be confirmed by a second method, such as TEM. It is also worth noting that autophagy induced in response to bacterial infection is not directed solely against the bacteria but can also be a response to remnants of the phagocytic membrane.[136] Similar cautions apply with regard to viral infection, as coronaviruses induce the formation of double-membrane vesicles that are coated with LC3-I, and this nonlipidated form of LC3 plays an autophagy-independent role in viral replication.[137] Along these lines, with herpes simplex virus infection, an LC3$^+$ autophagosome-like organelle derived from nuclear membranes is observed that contains viral proteins.[138]

Third, caution must be exercised in general when evaluating LC3 by western blotting, and appropriate standardization controls are necessary. For example, LC3-I may be less sensitive to detection by certain anti-LC3 antibodies. Moreover, LC3-I is more labile than LC3-II, being more sensitive to freezing-thawing and to degradation in SDS sample buffer, so fresh samples should be boiled and assessed as soon as possible and should not be subjected to repeated freeze-thaw cycles. A general point to consider when examining transfected cells concerns the efficiency of transfection. A western blot will detect LC3 in the entire cell population, including those that are not transfected. Thus, if transfection efficiency is too low, it may be necessary to use methods, such as fluorescence microscopy, that allow autophagy to be monitored in single cells. The critical point is that the analysis of the gel shift of transfected LC3 or GFP-LC3 can be employed to follow LC3 lipidation only in readily transfected cells.[139]

When dealing with animal tissues, western blotting of LC3 should be performed on frozen biopsy samples homogenized in the presence of general protease inhibitors (Isidoro C, personal communication; see also *Human*).[140] Caveats regarding detection of LC3 by western blotting have been covered in a review.[25] For example, PVDF membranes may result in a stronger LC3-II retention than nitrocellulose membranes, possibly due to a higher affinity for hydrophobic proteins (**Fig. 5B**; Kovsan J, Rudich A, personal communication), and Triton X-100 may not efficiently solubilize LC3-II in some systems.[141] Heating in the presence of 1% SDS, or analysis of membrane fractions,[142] may assist in the detection of this protein.

Another important issue concerns the quantification of changes in LC3-II. The previous version of these guidelines specifically stated that the levels of LC3-II should be compared with actin (and here we would modify this to include other appropriate "housekeeping" proteins) and not to that of LC3-I. As a general rule, this still holds true, but there are some exceptions. For example, in some cases actin levels decrease when autophagy is induced, so that it may be more appropriate to determine the ratio of LC3-II to LC3-I. Either method has its potential advantages and disadvantages. For example, if the amount of LC3-I is high relative to LC3-II (as in brain tissues, where the LC3-I signal can be overwhelming), it can be difficult to quantify the change in LC3-II relative to LC3-I. Conversely, by ignoring the level of LC3-I in favor of LC3-II the researcher may miss part of the overall picture of the cellular autophagic response.

Fourth, LC3 is expressed as four isoforms in mammalian cells, LC3A, LC3B, LC3B2 and LC3C,[143,144] which exhibit different tissue distributions, and it may be necessary to use different antisera or antibodies that distinguish among these isoforms. A point of caution along these lines is that the increase in LC3A-II vs. LC3B-II levels may not display equivalent changes in all organisms under autophagy-inducing conditions, and it should not be assumed that LC3B is the optimal protein to monitor.[145] This supports the important notion that the LC3 isoforms display different functions, but these are yet to be fully elucidated. The commercialized anti-LC3B antibodies also recognize LC3A, but do not recognize LC3C, which shares less sequence homology. It is important to note that LC3C possesses in its primary amino acid sequence the DYKD motif that is recognized with a high affinity by anti-FLAG antibodies. Thus, the standard anti-FLAG M2 antibody can detect and immunoprecipitate over-expressed LC3C, and caution has to be taken in experiments using FLAG-tagged proteins (Biard-Piechaczyk M, Espert L, personal communication).

In addition, it is important to keep in mind the presence of the other subfamily of Atg8 proteins, the GABARAP subfamily (see above).[109,146] Certain types of mitophagy induced by NIX/BNIP3L are highly dependent on GABARAP and less dependent on LC3 proteins.[147] Furthermore, commercial antibodies for GABARAPL1 also recognize GABARAP,[108] which might lead to misinterpretation of experiments, in particular those using immunohistochemical techniques. The problem with

cross-reactivity of the anti-GABARAPL1 antibody can be overcome when analyzing these proteins by western blot because they can be resolved during SDS-PAGE using high concentration (15%) gels, with GABARAP migrating faster than GABARAPL1 (Boyer-Guittaut M, personal communication). We therefore advise caution in choosing antibodies for western blotting and immunofluorescence experiments and in interpreting results based on stated affinities of antibodies unless these have been clearly determined. As with any western blot, proper methods of quantification must be used, which are, unfortunately, often not well disseminated, and the readers are referred to an excellent paper on this subject (see ref.148). Unlike the other members of the GABARAP family, almost no information is available on GABARAPL3, perhaps because it is not yet possible to differentiate between GABARAPL1 and GABARAPL3 proteins, which have 94% identity. As stated by the laboratory that described the cloning of the human *GABARAPL1* and *GABARAPL3* genes,[146] their expression patterns are apparently identical. It is worth noting that *GABARAPL3* is the only gene of the *GABARAP* subfamily that seems to lack an ortholog in mice.[146] *GABARAPL3* might therefore be considered as a pseudogene without an intron that is derived from *GABARAPL1*. Hence, until new data are published, *GABARAPL3* should not be considered as the fourth member of the *GABARAP* family.

Fifth, in non-mammalian species, the discrimination of Atg8–PE from the nonlipidated form can be complicated by their nearly identical SDS-PAGE mobilities and the presence of multiple isoforms (e.g., there are 9 in Arabidopsis). In yeast, it is possible to resolve Atg8 (the nonlipidated form) from Atg8–PE by including 6 M urea in the SDS-PAGE separating gel,[149] or by using a 15% resolving gel without urea (Reggiori F, personal communication). Similarly, urea combined with prior treatment of the samples with (or without) phospholipase D (that will remove the PE moiety) can often resolve the ATG8 species in plants.[150,151] It is also possible to label cells with radioactive ethanolamine, followed by autoradiography to identify Atg8–PE, and a C-terminal peptide can be analyzed by mass spectrometry to identify the lipid modification at the terminal glycine residue. Furthermore, Atg8–PE aberrantly migrates faster than unconjugated Atg8 during SDS-PAGE, even though the former has a larger molecular mass. Special treatments are not needed for the separation of mammalian LC3-I from LC3-II.

Finally, we would like to point out that one general issue with regard to any assay is that it could introduce some type of stress—for example, mechanical stress due to lysis, temperature stress due to heating or cooling a sample, or oxidative stress on a microscope slide, which could lead to potential artifacts including the induction of autophagy.[152] This point is not intended to limit the use of any specific methodology, but rather to note that there are no perfect assays; special care should be taken with cells in suspension, however, as the stress resulting from centrifugation can induce autophagy. Therefore, it is important to verify that the positive (e.g., treatment with rapamycin, torin1 or other inducers) and negative (e.g., inhibitor treatment) controls behave as expected in any assays being utilized. Similarly, plasmid transfection or nucleofection can result in the potent induction of autophagy (based on increases in LC3-II or p62 degradation). In some cell types, the amount of autophagy induced by transfection of a control empty vector may be so high that it is virtually impossible to examine the effect of enforced gene expression on autophagy (Levine B, personal communication). This effect is generally not observed with siRNA transfection; however, it is an issue for plasmid shRNA transfection and for plasmid expression constructs. The use of endotoxin-free DNA reduces, but does not eliminate, this problem. Finally, the precise composition of media components can have profound effects on basal autophagy levels and may need to be modified empirically depending on the cell lines being used.

Conclusion: Atg8/LC3 is often an excellent marker for autophagy; however, it must be kept in mind that there are multiple LC3 isoforms, there is a second family of mammalian Atg8-like proteins (GABARAPs), and antibody affinity (for LC3-I vs. LC3-II) and specificity (for example, for LC3A vs. LC3B) must be considered and/or determined.

b. Turnover of LC3-II/Atg8–PE. Autophagic flux can be measured by inferring LC3-II turnover by western blot (**Fig. 5C**)[112] in the presence and absence of lysosomal, or vacuolar degradation. The relevant parameter in this assay is the difference in the amount of LC3-II in the presence and absence of saturating levels of inhibitors, which can be used to examine the transit of LC3-II through the autophagic pathway; if flux is occurring, the amount of LC3-II will be higher in the presence of the inhibitor.[112] Lysosomal degradation can be prevented through the use of protease inhibitors (e.g., pepstatin A and E-64d), compounds such as bafilomycin A_1, chloroquine or NH_4Cl that neutralize the lysosomal pH,[18,114,153,154] or by treatment with agents that block fusion of autophagosomes with lysosomes (note that bafilomycin A_1 will ultimately cause a fusion block as well as neutralize the pH[155]).[156] Alternatively, knocking down or knocking out lysosome-associated membrane protein-2 (LAMP2) represents a genetic approach to block the fusion of autophagosomes and lysosomes [for example, inhibiting LAMP2 in myeloid leukemic cells results in a marked increase of GFP-LC3 dot formation and endogenous LC3-II protein compared with control cells upon autophagy induction during myeloid differentiation (Tschan MP, unpublished data)].[157] This approach, however, may be complicated by the compensatory upregulation of macroautophagy that occurs when chaperone-mediated autophagy is blocked,[158] unless the LAMP2B isoform is specifically knocked down.[159]

Generally, an increase in the levels of LC3-II observed with a particular treatment condition in the presence of bafilomycin A_1, compared with the treatment alone, is indicative of some degree of flux through the system (i.e., compound/drug treatment plus bafilomycin A_1 should result in a higher amount of LC3-II than compound/drug treatment alone); however, a treatment condition increasing LC3-II on its own that has no difference in LC3-II in the presence of bafilomycin A_1 compared with treatment alone may suggest a block in autophagy at the terminal stages.[6] This procedure has been validated with several autophagy modulators.[160] With each of these techniques, it is essential to avoid assay saturation. The duration of the

dc_840_14

bafilomycin A_1 treatment needs to be relatively short (1–2 h) to allow comparisons of the amount of LC3 that is lysosomally degraded over a given time frame under one treatment condition to another treatment condition. Positive control experiments using treatment with known autophagy inducers, along with bafilomycin A_1 vs. vehicle, are important to demonstrate the utility of this approach in each experimental context. The same type of assay monitoring the turnover of Atg8–PE can be used to monitor flux in yeast, by comparing the amount of Atg8 present in a wild-type vs. a *pep4*Δ strain following autophagy induction.[161]

An additional methodology for monitoring autophagy relies on the observation that a subpopulation of LC3-II exists in a cytosolic form (LC3-IIs) in some cell types.[162] The amount of cytosolic LC3-IIs and the ratio between LC3-I and LC3-IIs appears to correlate with changes in autophagy and may provide a more accurate measure of autophagic flux than ratios based on the total level of LC3-II.[162] The validity of this method has been demonstrated by comparing autophagic proteolytic flux in rat hepatocytes and hepatoma cells. One advantage of this approach is that it does not require the presence of autophagic or lysosomal inhibitors to block the degradation of LC3-II.

Finally, autophagic flux can be monitored based on the turnover of LC3-II, by utilizing a fluorescence-based assay. For example, a reporter assay based on the degradation of *Renilla reniformis* luciferase (Rluc)-LC3 fusion proteins is well suited for screening compounds affecting autophagic flux.[163] In this assay, Rluc is fused N-terminally to either wild-type LC3 (LC3wt) or a lipidation-deficient mutant of LC3 (G120A). Since Rluc-LC3wt, in contrast to Rluc-LC3-G120A, specifically associates with the autophagosomal membranes, Rluc-LC3wt is more sensitive to autophagic degradation. A change in autophagy-dependent LC3-turnover can thus be estimated by monitoring the change in the ratio of luciferase activities between the two cell populations expressing either Rluc-LC3wt or Rluc-LC3-G120A. In its simplest form, the Rluc-LC3-assay can be used to estimate autophagic flux at a single time point by defining the luciferase activities in cell extracts. Moreover, the use of a live cell luciferase substrate makes it possible to monitor changes in autophagic activity in living cells in real time. This method has been successfully used to identify positive and negative regulators of autophagy from cells treated with microRNA, siRNA and small molecule libraries.[163-166]

Cautionary notes: The main caveat regarding the measurement of LC3-IIs/LC3-I is that this method has only been tested in isolated rat hepatocytes and H4-II-E cells. Thus, it is not yet known whether it is generally applicable to other cell types, and a soluble form of LC3-II (i.e., LC3-IIs) is not observed in many standard cell types including HeLa, HEK 293 and PC12. In addition, the same concerns apply regarding detection of LC3-I by western blotting. It should be noted that the LC3-IIs/LC3-I ratio must be analyzed using the cytosolic fractions rather than the total homogenates. Furthermore, the same caveats mentioned above regarding the use of LC3 for qualitatively monitoring autophagy also apply to the use of this marker for evaluating flux.

The use of a radioactive pulse-chase analysis provides an alternative to lysosomal protease inhibitors,[113] although such inhibitors should still be used to verify that degradation is lysosome-dependent. In addition, drugs must be used at concentrations and for time spans that are effective in inhibiting fusion or degradation, but that do not provoke cell death. Thus, these techniques may not be practical in all cell types or in tissues from whole organisms where the use of protease inhibitors is problematic, and where pulse labeling requires artificial short-term culture conditions that may induce autophagy. Another concern when monitoring flux via LC3-II turnover may be seen in the case of a partial autophagy block; in this situation, agents that disrupt autophagy (e.g., bafilomycin A_1) will still result in an increase in LC3-II, which may be interpreted as the complete absence of a block resulting from the mutant or compound being tested. Thus, care is needed in interpretation. Furthermore, for characterizing new autophagy modulators, it is ideal to test autophagic flux at early (e.g., 4 h) and late (e.g., 24 h) time-points, since in certain instances, such as with calcium phosphate precipitates, a compound may increase or decrease flux at these two time-points, respectively.[167] Finally, many of the chemicals used to inhibit autophagy, such as bafilomycin A_1, NH_4Cl (see *Autophagy inhibitors and inducers* below) or chloroquine, also directly inhibit the endocytosis/uncoating of viruses (Smith DR, personal communication), and other endocytic events requiring low pH, as well as exit from the Golgi (Tooze S, personal communication) and as such should be used only with extreme caution in studies investigating autophagy-virus interactions.

One additional consideration is that it may not be absolutely necessary to follow LC3-II turnover if other substrates are being monitored simultaneously. For example, an increase in LC3-II levels in combination with the lysosomal (or ideally autophagy-specific) removal of an autophagic substrate (such as an organelle[168,169]) that is not a good proteasomal substrate provides an independent assessment of autophagic flux. However, due to the fact that LC3 might be coupled to endosomal membranes and not just autophagosomes, and the levels of well-characterized autophagosome substrates such as p62 can also be affected by proteasome inhibitors,[170] it is probably prudent to monitor both turnover of LC3-II and an autophagosome substrate in parallel.

Another issue relates to the use of protease inhibitors (see *Autophagy inhibitors and inducers* below). When using lysosomal protease inhibitors, it is of fundamental importance to assess proper conditions of inhibitor concentration and time of pre-incubation to ensure full inhibition of lysosomal cathepsins. In this respect, 1 h of pre-incubation with 10 μg/ml E-64d is sufficient in most cases, since this inhibitor is membrane permeable and rapidly accumulates within lysosomes. On the other hand, pepstatin A is membrane impermeable (ethanol or preferably DMSO must be employed as a vehicle) and requires a prolonged incubation (> 8 h) and a relatively high concentration (> 50 μg/ml) to fully inhibit lysosomal cathepsin D (**Fig. 6**). An incubation of this duration, however, can be problematic due to indirect effects (see *GFP-Atg8/LC3 lysosomal delivery and proteolysis*). Also, note that the relative amount of lysosomal cathepsins B and D is cell-specific and changes with

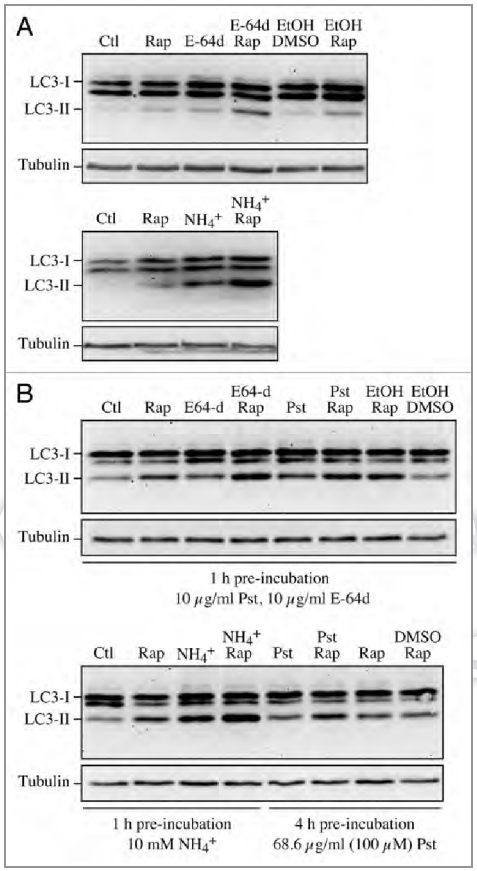


Figure 6. Effect of different inhibitors on LC3-II accumulation. SH-SY5Y human neuroblastoma cells were plated and allowed to adhere for a minimum of 24 h, then treated in fresh medium. Treatments were as follows: rapamycin (Rap), (A) 1 μM, 4 h or (B) 10 μM, 4 h; E-64d, final concentration 10 μg/ml from a 1 mg/ml stock in ethanol (ETOH); NH_4Cl (NH_4^+), final concentration 10 mM from a 1 M stock in water; pepstatin A (Pst), final concentration 10 μg/ml from a 1 mg/ml stock in ethanol, or 68.6 μg/ml from a 6.86 mg/ml stock in DMSO; ethanol or DMSO, final concentration 1%. Pre-incubations in (B) were for 1 or 4 h as indicated. Ten mM NH_4Cl (or 30 μM chloroquine, not shown) were the most effective compounds for demonstrating the accumulation of LC3-II. E-64d was also effective in preventing the degradation of LC3-II, with or without a preincubation, but ammonium chloride (or chloroquine) may be more effective. Pepstatin A at 10 μg/ml with a 1 h pre-incubation was not effective at blocking degradation, whereas a 100 μM concentration with 4 h pre-incubation had a partial effect. Thus, alkalinizing compounds are more effective in blocking LC3-II degradation, and pepstatin A must be used at saturating conditions to have any noticeable effect. Images provided by C. Isidoro. Note that the band running just below LC3-I at approximately 17.5 kDa may be a processing intermediate of LC3-I; it is detectable in freshly prepared homogenates, but is less visible after the sample is subjected to a freeze-thaw cycle.

culture conditions. In contrast to the protease inhibitors, chloroquine (10 μM) or bafilomycin A_1 (1–100 nM) can be added to cells immediately prior to autophagy induction.

Conclusion: It is important to be aware of the difference between monitoring the steady-state level of Atg8/LC3 and autophagic flux; the latter can be determined by following Atg8/LC3 in the absence and presence of autophagy inhibitors, and/or by examining the autophagy-dependent degradation of appropriate substrates. In particular, if there is any evidence of an increase in LC3-II (or autophagosomes), it is essential to determine whether this represents increased flux, or a block in fusion or degradation through the use of inhibitors such as chloroquine or bafilomycin A_1.

c. GFP-Atg8/LC3 lysosomal delivery and proteolysis. GFP-LC3B (hereafter referred to as GFP-LC3) has also been used to follow flux. First, when GFP-Atg8 or GFP-LC3 is delivered to a lysosome/vacuole the Atg8/LC3 part of the chimera is sensitive to degradation, whereas the GFP protein is relatively resistant to hydrolysis (note, however, that GFP fluorescence is quenched by low pH; see *GFP-Atg8/LC3 fluorescence microscopy* and *Tandem mRFP/mCherry-GFP fluorescence microscopy*). Therefore, the appearance of free GFP on western blots can be used to monitor lysis of the inner autophagosome membrane and breakdown of the cargo in metazoans (**Fig. 7A**),[161,171,173] or the delivery of autophagosomes to, and the breakdown of autophagic bodies within, the yeast and plant vacuole.[151,161,174] Reports on Dictyostelium and mammalian cells highlight the importance of lysosomal pH as a critical factor in the detection of free GFP that results from the degradation of fused proteins. In these cell types, free GFP fragments are only detectable in the presence of nonsaturating levels of lysosomotropic compounds (NH_4Cl or choroquine) or under conditions that attenuate lysosomal acidity; otherwise, the autophagic/degradative machinery appears to be too efficient to allow the accumulation of the proteolytic fragment (**Fig. 7B and C**).[36,172] Hence, a reduction in the intensity of the free GFP band may indicate reduced flux, but it may also be due to efficient turnover. Using a range of concentrations and treatment times of compounds that inhibit autophagy can be useful in distinguishing between these possibilities.[175] Since the pH in the yeast vacuole is higher than that in mammalian or Dictyostelium lysosomes, the levels of free GFP fragments are detectable in yeast without the necessity of using lysosomotropic compounds.[29] Additionally, in yeast the diffuse fluorescent haze from the released GFP moiety within the vacuole lumen can be observed by fluorescence microscopy.

dc—840-14

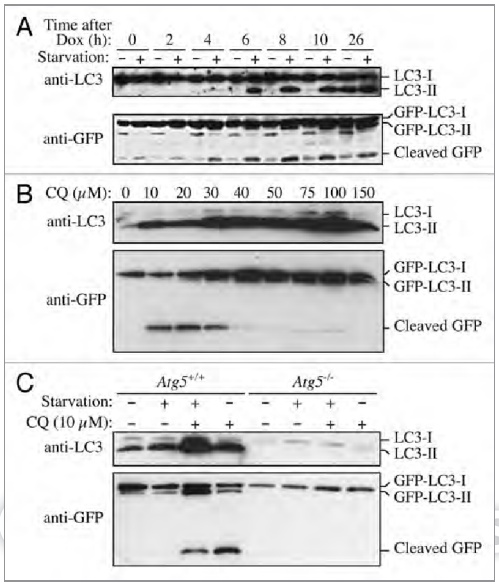


Figure 7. GFP-LC3 processing can be used to monitor delivery of autophagosomal membranes. (A) *Atg5*$^{-/-}$ MEFs engineered to express Atg5 under the control of the Tet-off promoter were grown in the presence of doxycyline (10 ng/ml) for one week to suppress autophagy. Cells were then cultured in the absence of drug for the indicated times, with or without a final 2 h starvation. Protein lysates were analyzed by western blot using anti-LC3 and anti-GFP antibodies. The positions of untagged and GFP-tagged LC3-I and LC3-II, and free GFP are indicated. This figure was modified from data previously published in reference 171, FEBS Letters, 580, Hosokawa N, Hara Y, Mizushima N, Generation of cell lines with tetracycline-regulated autophagy and a role for autophagy in controlling cell size, pp. 2623–2629, copyright 2006, with permission from Elsevier. (B) Differential role of unsaturating and saturating concentrations of lysosomal inhibitors on GFP-LC3 cleavage. HeLa cells stably transfected with GFP-LC3 were treated with various concentrations of chloroquine (CQ) for 6 h. Total lysates were prepared and subjected to immunoblot analysis. (C) CQ-induced free GFP fragments require classical autophagy machinery. Wild-type and *Atg5*$^{-/-}$ MEFs were first infected with adenovirus GFP-LC3 (100 viral particles per cell) for 24 h. The cells were then either cultured in regular culture medium with or without CQ (10 μM), or subjected to starvation in EBSS buffer in the absence or presence of CQ for 6 h. Total lysates were prepared and subjected to immunoblot analysis. Panel B and C are modified from the data previously published in reference 172.

The movement of GFP-LC3 to lysosomes also can be monitored by fluorescence microscopy, although, as mentioned above, the GFP fluorescent signal is more sensitive to acidic pH than other fluorophores (see *GFP-Atg8/LC3 fluorescence microscopy*). A time-course evaluation of the cell population showing GFP-LC3 puncta can serve to monitor the autophagy flux, since a constant increase in the number of cells accumulating GFP-LC3 puncta is suggestive of defective fusion of autophagosomes with lysosomes, and conversely a decline implies that GFP-LC3 is consumed within newly formed autolysosomes. In either case, it can be problematic to use GFP fluorescence to follow flux, as new GFP-LC3 is continuously being synthesized. A potential solution to this problem for following fluorescence is to use a photoactivatable version of the fluorescent protein,[176] which allows this assay to be performed essentially as a pulse/chase analysis. Another alternative is to follow flux using GFP-LC3 fluorescence by adding lysosomal protease or fusion inhibitors to cells expressing GFP-LC3 and monitoring changes in the number of puncta. In this case, the presence of lysosomal inhibitors should increase the number of GFP-LC3-positive structures, and the absence of an effect on the total number of GFP-LC3 puncta or on the percentage of cells displaying numerous puncta is indicative of a defect(s) in autophagic flux.[177] The combination of protease inhibitors (to prevent the degradation of GFP) or compounds that modify lysosomal pH such as NH_4Cl or chloroquine, or compounds such as bafilomycin A_1 or others that block fusion of autophagosomes with lysosomes (e.g., vinblastine) may be most effective in preventing lysosome-dependent decreases in GFP-LC3 puncta. However, because the stability of GFP is affected by lysosomal pH, we advise the use of protease inhibitors whether or not lysosomotropic compounds or fusion inhibitors are included (although lysosomotropic compounds should help stabilize GFP by neutralizing the pH in the lysosome they do not have an immediate effect on lysosomal hydrolase activity).

Cautionary notes: The GFP-Atg8 processing assay is used routinely to monitor autophagy in yeast. One caveat, however, is that this assay is not always performed in a quantitative manner (for example, western blot exposures need to be in the linear range). Accordingly, an enzymatic assay such as the Pho8Δ60 assay may be preferred (see *Autophagic protein degradation*),[178,179] especially when the differences in autophagic activity need to be precisely determined; however, appropriate caution must be used as with any enzyme assay regarding, for example, substrate concentrations and linearity (note that an equivalent assay has not been developed for higher eukaryotic cells).

The main limitation of the GFP-LC3 processing assay in mammalian cells is that it seems to depend on cell type and culture conditions (Hosokawa N, Mizushima N, unpublished data). Apparently, GFP is more sensitive to mammalian lysosomal hydrolases than to the degradative milieu of the yeast vacuole. Alternatively, the lower pH of lysosomes relative to that of the vacuole may contribute to differences in detecting free GFP. Under certain conditions [such as Earle's balanced salt solution (EBSS)-induced starvation] in some cell lines, when the lysosomal pH becomes particularly low, free GFP is undetectable because both the LC3-II and free GFP fragments are quickly degraded.[172] Therefore, if this method is used it should be accompanied by immunoblotting including controls to address the stability of nonlysosomal GFP such as GFP-LC3-I. It should also be noted that free GFP can be detected when cells are treated with nonsaturating doses of lysosomal inhibitors such as chloroquine, E-64d and bafilomycin A_1. The saturating concentrations of these lysosomal inhibitors vary in different cell lines, and it would be better to use a saturating concentration of lysosomal inhibitors when performing an autophagic flux assay.[172] Therefore, caution must be exercised in interpreting the data using this assay; it would be helpful to combine an analysis of GFP-LC3 processing with other assays such as the monitoring of endogenous LC3-II by western blot.

Along these lines, a caution concerning the use of the EGFP fluorescent protein for microscopy is that this fluorophore has a relatively neutral pH optimum for fluorescence,[180] so that its signal may diminish quickly during live cell imaging due to the acidic environment of the lysosome. It is possible to circumvent this latter problem by imaging paraformaldehyde-fixed cultures that are maintained in a neutral pH buffer, which retains EGFP fluorescence (Kleinman M, Reiners JJ, personal communication). Alternatively, it may be preferable to use a different fluorophore such as monomeric red fluorescent protein (mRFP) or mCherry, which retain fluorescence even at acidic pH.[181] On the one hand, a putative advantage of mCherry over mRFP is its enhanced photostability and intensity, which are an order of magnitude higher (and comparable to GFP), enabling acquisition of images at similar exposure settings as are used for GFP, thus minimizing potential bias in interpretation.[182] On the other hand, caution is required when evaluating the localization of mCherry fusion proteins during autophagy due to the persistence of the mCherry signal in acidic environments; all tagged proteins are prone to show enrichment in lysosomes during nonspecific autophagy of the cytoplasm, especially at higher expression levels. In addition, red fluorescent proteins (even the monomeric forms) can be toxic due to aggregation.[183] Dendra2 is an improved version of the green-to-red photoswitchable fluorescent protein Dendra, which is derived from the octocoral *Dendronephthya sp.*[184] Dendra2 is capable of irreversible photoconversion from a green to a red fluorescent form, but can be used also as normal GFP or RFP vector. This modified version of the fluorophore has certain properties including a monomeric state, low phototoxic activation and efficient chromophore maturation, which make it suitable for real-time tracking of LC3 and p62 (**Fig. 8**; Kaarniranta K, personal communication). Another alternative to mRFP or mCherry is to use the Venus variant of YFP, which is brighter than mRFP and less sensitive to pH than GFP.[186]

The pH optimum of EGFP is important to consider when using GFP-LC3 constructs, as the original GFP-LC3 marker[187] uses the EGFP variant, which may result in a reduced signal upon the formation of amphisomes or autolysosomes. An additional caveat when using the photoactivatable construct PA-GFP[180] is that the process of activation by photons may induce DNA damage, which could, in turn, elicit induction of autophagy. Also, GFP is relatively resistant to denaturation, and boiling for 5 min may be needed to prevent the folded protein from being trapped in the stacking gel during SDS-PAGE.

As noted above (see *Western blotting and ubiquitin-like protein conjugation systems*), Atg4 cleaves the residue(s) that follow the C-terminal glycine of Atg8/LC3 that will be conjugated to PE. Accordingly, it is critical that any chimeras be constructed with the fluorescent tag at the N-terminus of Atg8/LC3.

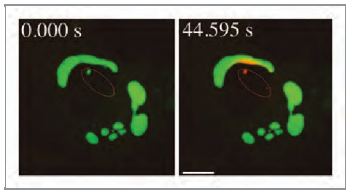


Figure 8. Movement of activated pDendra2-hp62 (orange) from the nucleus (middle) to the aggregate in ARPE-19 cells, revealed by confocal microscopy. Cells were exposed to 5 μM MG132 for 24 h to induce the formation of perinuclear aggregates.[185] The cells were then exposed to a UV pulse (the UV-induced area is shown by red lines that are inside of the nucleus) that converts Dendra2 from green to red, and the time shown after the pulse is indicated. p62 is present in a small nuclear aggregrate, and is shuttled from the nucleus to a perinuclear large protein aggregate (detected as red). Scale bar, 5 μm. Image provided by K. Kaarniranta.

Finally, lysosomal inhibition needs to be carefully controlled. Prolonged inhibition of lysosomal hydrolases (> 6 h) is likely to induce a secondary autophagic response triggered by the accumulated undigested autophagy cargo. This secondary autophagic response can complicate the analysis of the autophagy flux, making it appear more vigorous than it would in the absence of the lysosomal inhibitors.

Conclusion: The GFP-Atg8/LC3 processing assay (the generation of free GFP within the vacuole/lysosome) is a convenient way to monitor autophagy, but it does not work in all cell types, and is not as easy to quantify as enzyme-based assays.

d. GFP-Atg8/LC3 fluorescence microscopy. LC3B, or the protein tagged at its N terminus with a fluorescent protein such as GFP (GFP-LC3), has been used to monitor autophagy through indirect immunofluorescence or direct fluorescence microscopy (**Fig. 9**), measured as an increase in punctate LC3 or GFP-LC3.[187,188] The detection of GFP-LC3/Atg8 is also useful for in vivo studies using transgenic organisms such as *Caenorhabditis elegans*,[189] *Dictyostelium discoideum*,[190] filamentous ascomycetes,[191-195] *Ciona intestinalis*,[196] Drosophila *melanogaster*,[197-199] *Arabidopsis thaliana*,[200] *Leishmania major*[201-203] and mice.[126] It is also possible to use anti-LC3/Atg8 antibodies for immunocytochemistry or immunohistochemistry,[140,204-209] procedures that have the advantages of detecting the endogenous protein, obviating the need for transfection and or the generation of a transgenic organism, as well as avoiding potential artifacts resulting from overexpression (for example, high levels of overexpressed GFP-LC3 can result in its nuclear localization, although the protein can still relocate to the cytosol upon starvation), but we note that it is not always possible to detect endogenous Atg8/LC3. The use of imaging cytometry allows rapid and quantitative measures of the number of LC3 puncta and their relative number in individual or mixed cell types, using computerized assessment,

dc_840_14

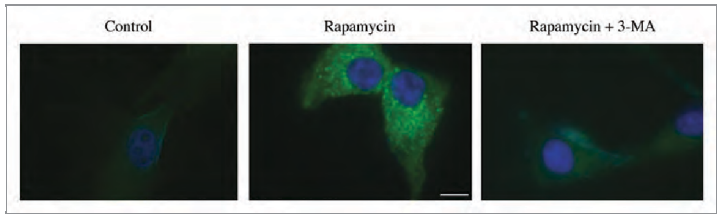


Figure 9. Changes in the detection and localization of GFP-LC3 upon the induction of autophagy. U87 cells stably expressing GFP-LC3 were treated with PBS, rapamycin (200 nM), or rapamycin in combination with 3-MA (2 mM) for 24 h. Representative fluorescence images of cells counterstained with DAPI (nuclei) are shown. Scale bar, 10 μm. This figure was modified from **Figure 6** published in Badr et al. Lanatoside C sensitizes glioblastoma cells to tumor necrosis factor–related apoptosis-inducing ligand and induces an alternative cell death pathway. Neuro-Oncology, 13:1213–24, 2011, by permission of Oxford University Press.

enumeration, and data display (e.g., see refs.142 and 210). In this respect, the alternative use of an automated counting system may be helpful for obtaining an objective number of puncta per cell. For this purpose, the WatershedCounting3D plug-in for ImageJ may be useful.[211,212]

Monitoring the endogenous protein, however, obviously depends on the ability to detect it in the system of interest. If the endogenous amount is below the level of detection, the use of an exogenous construct is warranted. In this case, it is important to consider the use of stable transformants vs. transient transfections. On the one hand, stable transformants may have reduced background resulting from the lower gene expression, and there is also the advantage of eliminating artifacts resulting from recent exposure to transfection reagents (see below). Furthermore, with stable transformants more cells can be easily analyzed because nearly 100% of the population will express tagged LC3. On the other hand, one disadvantage of stable transfectants is that the integration sites cannot always be predicted, and expression levels may not be optimal. Therefore, it is worth considering the use of stable episomal plasmids that avoid the problem of unsuitable integration.[181] An important advantage of transient transfection is that this approach is better for examining the immediate effects of the transfected protein on autophagy, although it restricts the length of time that the analysis can be performed, and consideration must be given to the induction of autophagy resulting from exposure to the transfection reagents (see below). In addition, a double transfection can be used (e.g., with GFP-LC3 and the protein of interest) to visually tag the cells that express the protein being examined. In conclusion, there is no simple rule for the use of stable vs. transient transfections. When stable transfections are utilized, it is worthwhile screening for clones that give the best signal to noise ratio, and when transient transfections are used, it is worthwhile optimizing the GFP-LC3 DNA concentration to give the best signal to noise ratio. In clones, the uniformity of expression of GFP-LC3 also makes "thresholding" when scoring puncta-positive cells (see below) much easier. However, there is also a need to beware of the frequent unrepresentative behavior of mammalian cell lines when selecting a single cell clone from a parental pool; therefore, it may be better to use a pool of multiple selected clones to avoid possible artifacts that can arise from the selection and propagation of individual clones from a single transfected cell (although the use of a pool is also problematic as its composition will change over time). Optimization, together with including the appropriate controls, will help overcome the effects of the inherent variability in these analyses.

An additional use of GFP-LC3 is to monitor colocalization with a target during autophagy-related processes such as organelle degradation or the sequestration of pathogenic microbes.[213-215] Preincubation of cells stably expressing GFP-LC3 with leupeptin can help stabilize the GFP-LC3 signal during fluorescence microscopy, especially under conditions of induced autophagic flux. Leupeptin is an inhibitor of lysosomal cysteine and serine proteases and will therefore inhibit degradation of membrane-conjugated GFP-LC3 that is present within autolysosomes.

Cautionary notes: Quantification of autophagy by measuring GFP-LC3 puncta (or LC3 by immunofluorescence) can be more tedious, depending on the method used (e.g., high-throughput image analysis can obviously be rapid and efficient), than monitoring LC3-II by western blot; however, the former may be more sensitive and quantitative. Ideally, it is preferable to include both assays and to compare the two sets of results. In addition, if GFP-LC3 is being quantified, it is better to determine the number of puncta corresponding to GFP-LC3 on a per cell basis (or per cell area basis if the cell population is in culture or the cell composition of the tissue is not homogenous, as well as in the case of plant cells, which tend to grow) rather than simply the total number of cells displaying puncta. This latter point is critical because even in nutrient-rich conditions, cells display some basal level of GFP-LC3 puncta, unless they are lacking autophagy-related genes (and even in the latter case it is possible to get puncta of GFP-LC3 depending on the specific conditions). There are, however, practical issues with counting puncta manually and reliably, especially if there are large numbers per cell [although this may be more accurate than relying on a software program, in which case it is important to ensure that only appropriate dots are being counted; applicable programs include ImageJ, Imaris, which may be more accurate (Ktistakis NT, personal communication), and the open-source software CellProfiler[216]]. Moreover, when autophagosome-lysosome fusion is blocked, larger autophagosomes are detected, possibly due to autophagosome-autophagosome fusion. Although it is possible to detect changes in the size of GFP-Atg8/LC3 puncta by fluorescence microscopy, it is not possible to correlate size with autophagy activity without additional assay methods. Size determinations can be problematic by fluorescence microscopy unless careful standardization is performed,[217] and size estimation is not recommended as a method for monitoring autophagy; however, it is possible to quantify the fluorescence intensity of GFP-Atg8/LC3 at specific puncta, which does provide a valid measure of protein recruitment.[218]

In addition to autophagosome size, the number of puncta visible to the eye will also be influenced by both the level of expression of GFP-LC3 in a given cell and by the exposure time of the microscope, if using widefield microscopy. In many cell types it may be possible to establish a cut-off value for the number of puncta per cell in conditions of "low" and "high" autophagy.[219] This can be tested empirically by exposing cells to autophagy-inducing and -blocking agents. Thus, cell populations showing significantly greater proportions of cells with autophagosome numbers higher than the cut-off in perturbation conditions compared with the control cells could provide quantitative evidence of altered autophagy. It is then possible to score the population as the percentage of cells displaying numerous autophagosomes. This approach will only be feasible if the background number of puncta is relatively low. For this method, it is particularly important to count a large number of cells and multiple representative sections of the sample (probably on the order of 50 or more, preferably in at least three different trials, depending on the particular system and experiment, but the critical point is that this determination should be based on statistical power analysis). Accordingly, high-content imaging analysis methods are extremely applicable to provide reliable values. Such methods enable quantification of GFP-LC3 puncta (or overall fluorescence intensity) in thousands of cells per sample (e.g., see refs.164,175 and 220). When using automated analysis methods, care must be taken to manually evaluate parameters used to establish background cutoff values for different treatment conditions and cell types. Another note of caution is that treatments affecting cell morphology, leading to the "rounding-up" of cells for example, can result in apparent changes in the number of GFP-LC3 puncta per cell. To avoid misinterpretation of results due to such potential artifacts, manual review of cell images is highly recommended.

To allow comparisons by other researchers attempting to repeat these experiments, it is critical that the authors also specify the baseline number of puncta that are used to define "normal" or "low" autophagy. Furthermore, the cells should also be counted using unbiased procedures (e.g., using a random start point followed by inclusion of all cells at regular intervals), and statistical information should be provided for both baseline and altered conditions, as these assays can be highly variable. One possible method to obtain unbiased counting of GFP-LC3 puncta in a large number of cells is to perform multispectral imaging flow cytometry (see *Autophagic flux determination using flow and multispectral imaging cytometry*).[221] This method can also be used for endogenous LC3, and, therefore, is useful for non-transfected primary cells.[222] Multispectral imaging flow cytometry allows characterization of single cells within a population by assessing a combination of morphology and immunofluorescence patterns, thereby providing statistically meaningful data.[223] For adherent cell cultures, one caution for flow cytometry is that the techniques necessary to produce single cell suspensions can cause significant injury to the cells, leading to secondary changes in autophagy. Therefore, staining for plasma membrane permeabilization (e.g., cell death) before vs. after isolation is an important control.

An important caveat in the use of GFP-LC3 is that this chimera can associate with aggregates, especially when expressed at high levels in the presence of aggregate-prone proteins, which can lead to a misinterpretation of the results.[224] Of note, GFP-LC3 can associate with ubiquitinated protein aggregates;[225] however, this does not occur if the GFP-LC3 is expressed at low levels (Rubinsztein DC, unpublished observations). These aggregates have been described in many systems, and are also referred to as Aggresome-Like Induced Structures or ALIS,[225-227] dendritic cell ALIS,[228] p62 bodies/sequestosomes[229] and inclusions. Inhibition of autophagy in vitro and in vivo leads to the accumulation of these aggregates, suggesting a role for autophagy in mediating their clearance.[225,226,230-232] One way to control for background levels of puncta is to determine fluorescence from untagged GFP.

The adaptor protein p62 is required for the formation of ubiquitinated protein aggregates in vitro (see *p62 and related LC3 binding protein turnover assays*).[229] In this case, the interaction of p62 with both ubiquitinated proteins and LC3 is thought to mediate delivery of these aggregates to the autophagy system.[233,234] Many cellular stresses can induce the formation of aggregates, including transfection reagents,[225] or the introduction of foreign DNA (especially if the DNA is not extracted endotoxin free). p62-positive aggregates are also formed by proteasome inhibition or puromycin treatment. Calcium phosphate transfection of COS7 cells or lipofectamine transfection of MEFs (Pinkas-Kramarski R, personal communication), primary neurons (La Spada AR, personal communication) or neuronal cells (Chu CT, personal communication) transiently increases basal levels of GFP-LC3 puncta and/or the amount of LC3-II. One solution is to examine GFP-LC3 puncta in cells stably expressing GFP-LC3; however, as transfection-induced increases in GFP-LC3 puncta and LC3-II are often transient, another approach is to use cells transfected with GFP, and cells subjected to a mock time-matched transfection as background (negative) controls. A lipidation-defective LC3 mutant where glycine 120 is mutated to alanine is targeted to these aggregates independently of autophagy (likely via its interaction with p62, see above) and as a result this mutant can serve as another valuable control.[225] When carrying out transfections it may be necessary to alter the protocol depending on the level of background fluorescence. For example, changing the medium and waiting 24 to 48 h after the transfection can help to reduce the background level of GFP-LC3 puncta that is due to the transfection reagent (Colombo MI, personal communication). Similarly, when using an mCherry-GFP-p62 double tag (see *Tandem mRFP/mCherry-GFP fluorescence microscopy*) in

dc_840_14

transient transfections it is best to wait 48 h after transfection to reduce the level of aggregate formation and potential inhibition of autophagy (Johansen T, personal communication). An additional consideration is that in addition to transfection, viral infection can activate stress pathways in some cells and possibly induce autophagy, again emphasizing the importance of appropriate controls, such as control viruses expressing GFP.[235]

Ubiquitinated protein aggregate formation and clearance appear to represent a cellular recycling process. Aggregate formation can occur when autophagy is either inhibited or when its capacity for degradation is exceeded by the formation of proteins delivered to the aggregates. In principle, formation of GFP-LC3-positive aggregates represents a component of the autophagy process. However, the formation of GFP-LC3-positive ubiquitinated protein aggregates does not directly reflect either the induction of autophagy (or autophagosome formation), or flux through the system. Indeed, formation of ubiquitinated protein aggregates that are GFP-LC3 positive can occur in autophagy-deficient cells.[225] Therefore, it should be remembered that GFP-LC3 puncta likely represent a mix of ubiquitinated protein aggregates in the cytosol, ubiquitinated protein aggregates within autophagosomes and more "conventional" phagophores and autophagosomes bearing other cytoplasmic cargo (this is one example where CLEM could help in resolving this question). In Dictyostelium, inhibition of autophagy leads to huge ubiquitinated protein aggregates containing p62 and GFP-Atg8, when the latter is co-expressed; the size of the aggregates and the typical presence of only one structure per cell make them easily distinguishable from autophagosomes. Saponin treatment has been used to reduce background fluorescence under conditions where no aggregation of GFP-LC3 is detected in hepatocytes, GFP-LC3 stably-transfected HEK 293[235] and human osteosarcoma cells, and in nontransfected cells;[236] however, treatment with saponin and other detergents can provoke artifactual GFP-LC3 puncta formation,[237] and controls need to be included in such experiments in light of these findings. In general, it is preferable to include additional assays that measure autophagy rather than relying solely on monitoring GFP-LC3. In addition, we recommend that researchers validate their assays by demonstrating the absence or reversal of GFP-LC3 puncta formation in cells treated with pharmacological or RNA interference-based autophagy inhibitors (**Table 1**). For example, 3-MA is commonly used to inhibit starvation- or rapamycin-induced autophagy,[256] but some data indicate that this compound can also have stimulatory effects (see *Autophagy inhibitors and inducers*).[257]

Another general limitation of the GFP-LC3 assay is that it requires a system amenable to the introduction of an exogenous gene. Accordingly, the use of GFP-LC3 in primary non-transgenic cells is more challenging. Here again, controls need to be included to verify that the transfection protocol itself does not artifactually induce GFP-LC3 puncta or cause LC3 aggregation. Furthermore, transfection should be performed with low levels of constructs, and the transfected cells should be followed to determine (1) when sufficient expression for detection is achieved, and (2) that during the time frame of the assay, basal GFP-LC3 puncta remain appropriately low. In addition, the demonstration of a reduction in the number of induced GFP-LC3 puncta under conditions of autophagy inhibition is helpful. For some primary cells, delivering GFP-LC3 to precursor cells by infection with recombinant lentivirus, retrovirus or adenovirus,[258] and subsequent differentiation into the cell type of interest, is a powerful alternative to transfection of the already differentiated cell type.[91]

To implement the scoring of autophagy via fluorescence microscopy, one option is to measure pixel intensity. Since the expression of GFP-LC3 may not be the same in all cells—as discussed above—it is possible to use specific imaging software to calculate the standard deviation (SD) of pixel intensity within the fluorescence image and divide this by the mean intensity of the pixels within the area of analysis. This will provide a ratio useful for establishing differences in the degree of autophagy between cells. Cells with increased levels of autophagic activity, and hence a greater number of autophagosomes in their cytosol, are associated with a greater variability in pixel intensity (i.e., a high SD). Conversely, in cells where autophagy is not occurring, GFP-LC3 is uniformly distributed throughout the cytosol and a variation in pixel intensity is not observed (i.e., a low SD) (Campanella M, personal communication).

Although LC3-II is primarily membrane-associated, it is not necessarily associated with autophagosomes as is often assumed; the protein is also found on phagophores, the precursors to autophagosomes, as well as on amphisomes and phagosomes (see *Western blotting and ubiquitin-like protein conjugation systems*).[132,259,260] Along these lines, yeast Atg8 can associate with the vacuole membrane independent of lipidation, so that a punctate pattern does not necessarily correspond to autophagic compartments.[261] Thus, the use of additional markers is necessary to specify the identity of an LC3-positive structure; for example, ATG12–ATG5-ATG16L1 would be present on a phagophore, but not an autophagosome. In addition, the site(s) of LC3 conjugation to PE is not definitively known and levels of Atg8–PE/LC3-II can increase even in autophagy mutants that cannot form autophagosomes.[262] One method that can be used to examine LC3-II membrane association is differential extraction in Triton X-114, which can be used with mammalian cells,[258] or western blot analysis of total membrane fractions following solubilization with Triton X-100, which is helpful in plants.[150,151] Another approach is to examine colocalization of LC3 with ATG5 (or other ATG proteins); the ATG12–ATG5 conjugate does not remain associated with autophagosomes, meaning that colocalized structures would correspond to phagophores. Importantly, we stress again that numbers of GFP-LC3 puncta, similar to steady-state LC3-II levels, reflect only a snapshot of the numbers of autophagy-related structures (e.g., autophagosomes) in a cell, and not autophagic flux.

Finally, we offer a general note of caution with regard to using GFP. First, the GFP tag is large, in particular relative to the size of LC3; therefore, it is possible that a chimera may behave differently from the native protein in some respects. Second, GFP is not native to most systems, and as such it may be recognized as an aberrant protein and targeted for degradation, which has obvious implications when studying autophagy. Third, some forms of GFP tend to oligomerize, which may interfere with protein function and/or localization. Fourth, EGFP inhibits polyubiquitination[263] and may cause defects in other cellular processes. Fifth, not all LC3 puncta represent LC3-II and correspond to autophagosomes.[137,264,265] Accordingly it would be prudent to complement any assays that rely on GFP fusions (to Atg8/LC3 or any protein) with additional methods that avoid the use of this fluorophore. Similarly, with the emergence of "super-resolution" microscopy methods such as photoactivated localization microscopy (PALM), new tags are being used (e.g., the EosFP green to red photoconvertible fluorescent protein, or the Dronpa GFP-like protein) that will need to be tested and validated.[266]

Table 1. Genetic and pharmacological regulation of autophagy†

Method	Comments
1. 3-methyladenine	A PtdIns3K inhibitor that effectively blocks an early stage of autophagy by inhibiting the class III PtdIns3K, but is not a specific autophagy inhibitor. 3-MA also inhibits the class I PtdIns3K and can thus, at suboptimal concentrations in long-term experiments, promote autophagy in some systems, as well as affect cell survival through AKT and other kinases.
2. 10-NCP	10-(4′-N-diethylamino)butyl)-2-chlorophenoxazine; an AKT inhibitor that induces autophagy in neurons.[238]
3. 17-AAG	An inhibitor of the HSP90-CDC37 chaperone complex, induces autophagy in certain systems (e.g., neurons), but impairs starvation-induced autophagy and mitophagy in others by promoting the turnover of ULK1.[239]
4. $ATG4^{C74A}$	An active site mutant of ATG4 that is defective for autophagy.[240]
5. Bafilomycin A_1	A V-ATPase inhibitor that causes an increase in lysosomal/vacuolar pH, and ultimately blocks fusion of autophagosomes with the vacuole.
6. Calcium	An autophagy activator that can be released from ER or lysosomal stores under stress conditions; however, calcium can also inhibit autophagy.[241]
7. Chloroquine, NH_4Cl	Lysosomotropic compounds that elevate/neutralize the lysosomal/vacuolar pH.
8. Deletion	This method provides the most direct evidence for the role of an autophagic component; however, more than one gene involved in autophagy should be targeted to avoid indirect effects.
9. E-64d	A membrane-permeable cysteine protease inhibitor that can block the activity of a subset of lysosomal hydrolases; should be used in combination with pepstatin A for inhibiting lysosomal protein degradation.
10. Knockdown	This method provides relatively direct evidence for the role of an autophagic component. However, the efficiency of knockdown varies, as does the stability of the targeted protein. In addition, more than one gene involved in autophagy should be targeted to avoid indirect effects.
11. KU-0063794	An MTOR inhibitor that binds the catalytic site and activates autophagy.[242,243]
12. Leupeptin	An inhibitor of cysteine, serine and threonine proteases that can be used in combination with pepstatin A and/or E-64d to block lysosomal protein degradation. Leupeptin is not membrane permeable, so its effect on cathepsins may depend on endocytic activity.
13. microRNA	Can be used to reduce the levels of target mRNA(s) or block translation.
14. NAADP-AM	Activates the lysosomal two pore channel and induces autophagy.[244]
15. NED-19	Inhibits the lysosomal two-pore channel and NAADP- induced autophagy.[244]
16. NVP-BEZ235	A dual inhibitor of p110 and the MTOR catalytic site that activates autophagy.[245,246]
17. Pathogen-derived ICP34.5. vBCL2, vFLIP, influenza M2, and HIV Nef	autophagy inhibitor transfection.
18. Pepstatin A	An aspartyl protease inhibitor that can be used to partially block lysosomal degradation; should be used in combination with other inhibitors such as E-64d. Pepstatin A is not membrane permeable.
19. Protease inhibitors	These chemicals inhibit the degradation of autophagic substrates within the lysosome/vacuole lumen. A combination of inhibitors (e.g., leupeptin, pepstatin A and E-64d) is needed for complete blockage of degradation.
20. Rapamycin	Inhibits MTOR by binding to RAPTOR, thus inducing autophagy, but only provides partial inhibition.
21. Resveratrol	A natural polyphenol that induces autophagy via activation of AMPK.[247,248]
22. RNAi	Can be used to inhibit gene expression.
23. RSVAs	Synthetic small-molecule analogs of resveratrol that potently activate AMPK and induce autophagy.[249]
24. Thapsigargin	An inhibitor of the sarcoplasmic/endoplasmic reticulum Ca^{2+} ATPase (SERCA) that inhibits autophagic sequestration through the depletion of intracellular Ca^{2+} stores;[250] however, thapsigargin may also block fusion of autophagosomes with endosomes by interfering with recruitment of RAB7, resulting in autophagosome accumulation.[251] Long-term thapsigargin treatment may induce ER stress and a secondary stimulation of autophagy.
25. Torin1	A catalytic MTOR inhibitor that induces autophagy and provides more complete inhibition than rapamycin (it inhibits all forms of MTOR).[252]
26. Trehalose	An inducer of autophagy that may be relevant for the treatment of different neurodegenerative diseases.[253,254]
27. Tunicamycin	A glycosylation inhibitor that induces autophagy due to ER stress.[255]
28. Vinblastine	A depolymerizer of both normal and acetylated microbtubles that interferes with autophagosome-lysosome fusion.[156]
29. Wortmannin	An inhibitor of PtdIns 3-kinase that blocks autophagy, but is not a specific inhibitor (see *3-MA* above).

†This table is not meant to be complete, as there are many compounds and genetic methods that regulate autophagy, and new ones are being discovered routinely.

dc_840_14

Conclusion: GFP-LC3 provides a marker that is relatively easy to use for monitoring autophagy induction (based on the appearance of puncta), or colocalization; however, it is not a preferred method for determining flux. In addition, it is recommended to use additional assays along with GFP-LC3 fluorescence microscopy to monitor autophagy.

e. **Tandem mRFP/mCherry-GFP fluorescence microscopy**. A fluorescence assay that is particularly designed to monitor flux relies on the use of a tandem monomeric RFP-GFP-tagged LC3 (tfLC3; **Fig. 10**).[181] The GFP signal is sensitive to the acidic and/or proteolytic conditions of the lysosome lumen, whereas mRFP is more stable. Therefore, colocalization of both GFP and mRFP fluorescence indicates a compartment that has not fused with a lysosome, such as the phagophore or an autophagosome. In contrast, an mRFP signal without GFP corresponds to an amphisome or autolysosome. Other fluorophores such as mCherry are also suitable instead of mRFP,[229] and an image-recognition algorithm has been developed to quantify flux of the reporter to acidified compartments.[242,267] One of the major advantages of the tandem mRFP/mCherry-GFP reporter method is that it enables simultaneous estimation of both the induction of autophagy and flux through autophagic compartments in essentially native conditions, without requiring any drug treatment. The use of more than one time point allows visualization of increased early autophagosomes followed by increases in late autophagosomes as an additional assurance that flux has been maintained.[268] In addition, this method can be used to monitor autophagy in high-throughput drug screening studies.[242] The quantification of "yellow only" and "red only" dots in a stable tandem-fluorescent LC3-reporter cell line can be automated by a Cellomics microscope that can be used to assess a huge population of cells (1,000 or more) over a large number of random fields of view. This can give rise to more accurate data than can be achieved by manual assessment of a few selected cells.[167,269]

An alternative dual fluorescence assay involves the Rosella biosensor. This assay monitors the uptake of material to the lysosome/vacuole and complements the use of the tandem mRFP/mCherry-GFP reporter. The assay is based upon the genetically encoded dual color-emission biosensor Rosella, a fusion between a relatively pH-stable fast-maturing RFP variant, and a pH-sensitive GFP variant. When targeted to specific cellular compartments or fused to an individual protein, the Rosella biosensor provides information about the identity of the cellular component being delivered to the vacuole/lysosome for degradation. Importantly, the pH-sensitive dual color fluorescence emission provides information about the environment of the biosensor during autophagy of various cellular components. In yeast, Rosella has been successfully used to monitor autophagy of cytosol, mitochondria (mitophagy) and the nucleus (nucleophagy).[270,271] Furthermore, the Rosella biosensor can be used as a reporter under various conditions including nitrogen depletion-dependent induction of autophagy.[270,271] The Rosella biosensor can also be expressed in mammalian cells to follow nonselective autophagy (cytoplasmic turnover), or mitophagy.[271]

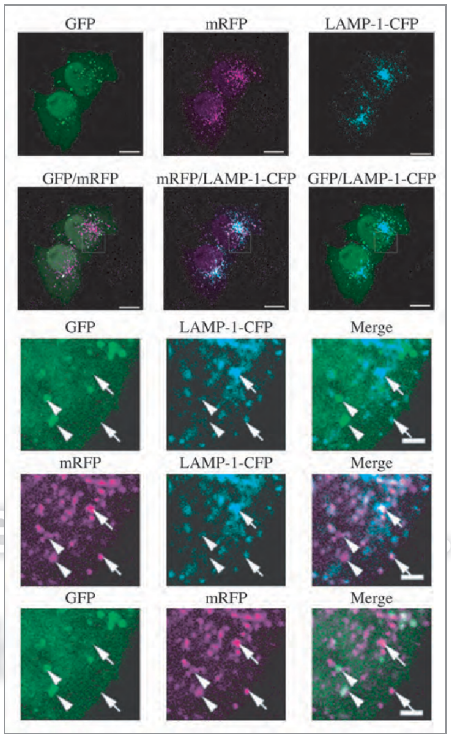


Figure 10. The GFP and mRFP signals of tandem fluorescent LC3 (tfLC3, mRFP-GFP-LC3) show different localization patterns. HeLa cells were cotransfected with plasmids expressing either tfLC3 or LAMP1-CFP. Twenty-four hours after the transfection, the cells were starved in Hanks' solution for 2 h, fixed and analyzed by microscopy. The lower panels are a higher magnification of the upper panels. Bar, 10 μm in the upper panels and 2 μm in the lower panels. Arrows in the lower panels point to (or mark the location of) typical examples of colocalized signals of mRFP and LAMP1. Arrowheads point to (or mark the location of) typical examples of colocalized particles of GFP and mRFP signals. This figure was previously published in reference ,181 and is reproduced by permission of Landes Bioscience, copyright 2007.

Cautionary notes: The use of tandem mRFP/mCherry-GFP-LC3/Atg8 reporters in live imaging experiments can be complicated by the motion of LC3/Atg8 puncta. As a consequence, conventional confocal microscopy may not allow visualization of colocalized mRFP/mCherry-GFP puncta. In this case, GFP or colocalized puncta represent newly formed autophagic structures whereas mRFP/mCherry-only puncta are ambiguous. Spinning disk confocal microscopy, or rapid acquisition times may be required for imaging tandem mRFP/mCherry-GFP proteins, although these techniques require a brighter fluorescent signal associated with what may be undesirably higher levels of transgene expression. One solution is to use the mTagRFP-mWasabi-LC3 chimera,[272] as mTagRFP is brighter than mRFP1 and mCherry, and mWasabi is brighter than EGFP (Lin J, personal communication). Another possibility is to use fixed cells; however, this presents an additional concern: The use of tandem mRFP/mCherry-GFP relies on the quenching of the GFP signal in the acidic autolysosome; however, fixation solutions are often neutral or weak bases, which will increase the pH of the entire cell. Accordingly, the GFP signal may be restored after fixation (**Fig. 11**), which would cause an underestimation of the amount of signal that corresponds only to RFP (i.e., in the autolysosome). Thus, the tissue or cell samples must be properly processed to avoid losing the acidic environment of the autolysosomes. In addition, there may be weak fluorescence of EGFP even in an acidic environment (pH between 4 and 5).[180,258] Therefore, it may be desirable to choose a monomeric green fluorescent protein that is more acid sensitive than EGFP for assaying autophagic flux.

Another caution in the interpretation of the tandem fluorescent marker is that colocalization of GFP and mRFP/mCherry might also be seen in the case of impaired proteolytic degradation within autolysosomes, or altered lysosomal pH. Finally, expression of tandem mRFP-GFP-LC3 is toxic to some cancer cell lines relative to GFP-LC3 or RFP-LC3 (K.S. Choi, personal communication). The cytotoxicity of DsRed and its variants such as mRFP1 is associated with downregulation of BCL2L1 (Bcl-x_L).[273] In contrast to mRFP-GFP-LC3, overexpression of mTagRFP-mWasabi-LC3 does not appear to be toxic to HeLa cells (Lin J, personal communication).

The Rosella assay has not been tested in a wide range of mammalian cell types. Accordingly, the sensitivity and the specificity of the assay must be verified independently until this method has been tested more extensively and used more widely.

Finally, it is ideal to capture the dynamic behavior of autophagy in real time, in order to generate data revealing the rate of formation and clearance of autophagosomes over time, rather than single data points. For example, by acquiring signals from two fluorescent constructs in real time, the rate of change in colocalization signal as a measure of the fusion rate and recycling rate between autophagosomes and lysosomes can be assessed. Importantly, due to the integral dynamic relationship of autophagic flux with the onset of apoptosis and necrosis it is advantageous to monitor cell death and autophagic flux parameters concomitantly over time, which FRET-based reporter constructs make possible.[274]

Conclusion: The use of tandem fluorescent constructs, which display different emission signals depending on the environment (in particular, GFP fluorescence is particularly sensitive to an acidic pH), provides a convenient way to monitor autophagy flux in many cell types.

f. Autophagic flux determination using flow and multispectral imaging cytometry. Whereas fluorescence microscopy, in combination with novel autophagy probes, has permitted single cell analysis of autophagic flux, automation for allowing medium- to high-throughput analysis has been challenging. A number of methods have been developed that allow the determination of autophagic flux using the fluorescence-activated cell sorter (FACS),[154,223,236,275-277] and commercial kits are now available for monitoring autophagy by flow cytometry. These approaches make it possible to capture high-content images of cells in flow (up to 1,000 cells/sec), and are particularly useful for cells that grow in suspension. Optimization of image analysis permits the study of cells with heterogeneous LC3 puncta, thus making it possible to quantify autophagic flux accurately in situations that might perturb normal processes (e.g., microbial infection).[277,278] Since EGFP-LC3 is a substrate for autophagic degradation, total fluorescence intensity of EGFP-LC3 can be used to indicate levels of autophagy in living mammalian cells.[275] When autophagy is induced, the decrease in total cellular fluorescence can be precisely quantified in large numbers of cells to obtain robust data. In another approach, soluble EGFP-LC3-I can be depleted from the cell by a brief saponin extraction so that the total fluorescence of EGFP-LC3 then represents that of EGFP-LC3-II alone (**Fig. 12A**).[235,236] Since EGFP-LC3 transfection typically results in high relative levels of EGFP-LC3-I, this treatment significantly reduces the background fluorescence due to non-autophagosome-associated reporter protein. By comparing treatments in the presence or absence of lysosomal degradation inhibitors, subtle changes in the flux rate of the GFP-LC3 reporter construct can be detected. If it is not desirable to treat cells with lysosomal inhibitors to determine rates of autophagic flux, a tandem mRFP-mCherry-EGFP-LC3 (or similar) construct can also be used for autophagic flux measurements in FACS experiments (see *Tandem mRFP/mCherry-GFP fluorescence microscopy*).[276]

These methods, however, require the cells of interest to be transfected with reporter constructs. Since the saponin extraction method can also be combined with intracellular staining for endogenous LC3 protein, subtle changes in autophagic flux can be measured without the need for reporter transfections (**Fig. 12B**). This enables investigations of autophagic flux in a wide variety of cell types and tissues.

Cautionary notes: Care must be taken when applying flow cytometry measurements to adherent cells, particularly neurons and other cells with interdigitated processes, as the preparation of single cell suspensions entails significant levels of plasma membrane disruption and injury that can secondarily induce autophagy.

Users of the saponin extraction method should carefully titrate saponin concentrations and times of treatment in order to ensure specific extraction of LC3-I in their systems. Also, it has been observed in some cell types that saponin treatment can lead to non-autophagic aggregation of LC3,[237] which should be controlled for in these assays (see *GFP-Atg8/LC3 fluorescence microscopy*).

Cell membrane permeabilization with digitonin and extraction of the nonmembrane-bound form of LC3 allows combined staining of membrane-associated LC3-II protein and any markers for detection of autophagy in relation to other cellular events/processes. Based on this approach a method for monitoring

dc_840_14

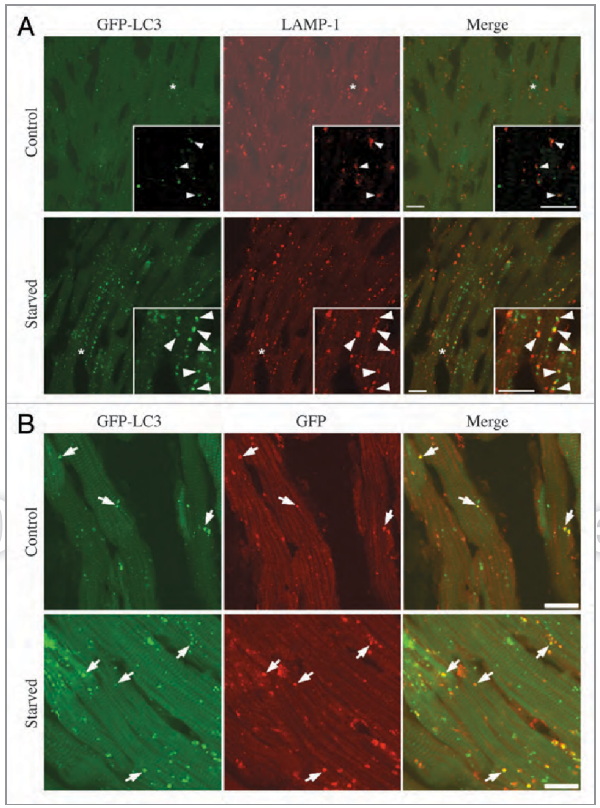


Figure 11. GFP fluorescence in the autolysosome can be recovered upon neutralization of the pH. (A) GFP-LC3 emits green fluorescence in the autolysosomes of post-mortem processed heart sections. Cryosections of 3.8% paraformaldehyde fixed ventricular myocardium from 3-week old GFP-LC3 transgenic mice at the baseline (control) or starved for 24 h (starved) were processed for immunostaining using a standard protocol (buffered at pH 7.4). Most of the GFP-LC3 puncta are positive for LAMP1, suggesting that the autolysosomes had recovered GFP fluorescence. (B) Colocalization between GFP-LC3 direct fluorescence (green) and indirect immunostaining for GFP (red). Sections processed as in (A) were immunostained for GFP using a red fluorescence-tagged secondary antibody, and the colocalization with GFP fluorescence was examined by confocal microscopy. Almost all of the red puncta emit green fluorescence. Images provided by X. Wang.

autophagy in different stages of the cell cycle was developed.[279] Thus, the presence of basal or starvation-induced autophagy is detected in G_1, S and G_2/M phases of the cell cycle in MEFs with doxycycline-regulated ATG5 expression. In these experiments cells were gated based on their DNA content, and the relative intensity of GFP-LC3-II and LC3-II expression. This approach might also be used for the detection of autophagic flux in different stages of the cell cycle or subG_1 apoptotic cell population by measuring accumulation of LC3-II in the presence or absence of lysosomal inhibitors.

Although GFP-LC3 can be used as a reporter for flow cytometry, it is more stable (which is not necessarily ideal for flux measurements) than GFP-p62 or GFP-NBR1 (NBR1 is a selective autophagic substrate with structural similarity to p62[280]); GFP-p62 displays the largest magnitude change following the induction of autophagy by amino acid deprivation or rapamycin

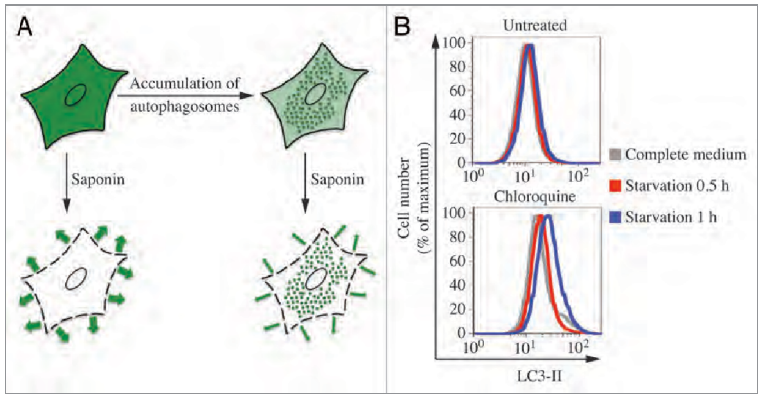


Figure 12. Saponin extraction allows quantification of LC3-II fluorescence by FACS. (A) Schematic diagram of the effects of the saponin wash. Due to the reorganization of the EGFP-LC3 reporter protein, induction of autophagosome formation does not change the total levels of fluorescence in EGFP-LC3-transfected cells. However, extraction of EGFP-LC3-I with saponin results in a higher level of fluorescence in cells with proportionally higher levels of EGFP-LC3-II-containing autophagosomes. This figure was previously published in reference.236 (B) Saponin extraction can also be used to measure flux of endogenous LC3 protein. Human osteosarcoma cells were starved of amino acids and serum by incubation in EBSS, for the indicated times in the presence or absence of a 1 h chloroquine (50 μM) treatment. Cells were then washed with PBS containing 0.05% saponin and processed for FACS analysis for endogenous LC3. These data are provided by K.E. Eng and G.M. McInerney.

treatment, and may thus be a better marker for following autophagic flux by this method (confirmed in SH-SY5Y neuronal cell lines stably expressing GFP-p62; Valente EM, personal communication).[281] However, p62 changes can be cell type and context specific. In some cell types, there is no change in overall p62 levels despite strong levels of autophagy induction, verified by the tandem mRFP/mCherry-GFP-LC3 reporter as well as Atg7- and lysosome-dependent turnover of cargo proteins (Chu CT, personal observation). In other contexts, a robust loss of p62 does not correlate with increased autophagic flux as assessed by a luciferase-based measure of flux.[166] Thus, appropriate positive and negative controls, and assessment of p62 mRNA levels, may be needed prior to the use of p62 as a flux indicator in a particular cellular context.

Conclusion: Medium- to high-throughput analysis of autophagy is possible using flow and multispectral imaging cytometry (**Fig. 13**). The advantage of this approach is that larger numbers of cells can be analyzed with regard to GFP-LC3 puncta, cell morphology and/or autophagic flux, and concomitant detection of surface markers can be included, potentially providing more robust data than is achieved with other methods.

g. **Immunohistochemistry**. Immunodetection of ATG proteins (particularly LC3 and BECN1) has been reported as a prognostic factor in various human carcinomas, including lymphoma,[140,282] breast carcinoma,[283] endometrial adenocarcinoma,[284,285] head and neck squamous cell carcinoma,[286,287] hepatocellular carcinoma,[288,289] gliomas,[290] non-small cell lung carcinomas,[291] pancreatic[292] and colon adenocarcinomas,[293-295] as well as in cutaneous and uveal melanomas.[296,297] Importantly, this kind of assay should be performed as recommended by the Reporting Recommendations for Tumor Marker Prognostic Studies (REMARK).[298] As we identify new drugs for modulating autophagy in clinical applications, this type of information may prove useful in the identification of subgroups of patients for targeted therapy.[299-301]

In mouse and rat tissues, endogenous LC3, ATG4B, and ATG9A have been detected by immnohistochemical analyses using both paraffin sections and cryosections.[208,302-304] When autophagosomes are absent, the localization pattern of LC3 in the cells of various tissues is diffuse and cytosolic. Moreover, intense fibrillary staining of LC3 is detectable along dendrites of intact neurons, whereas granular staining for LC3 appears mainly in the perikarya of neurons in cathepsin D- or cathepsins B- and L-deficient mouse brains.[208] In developing retinal tissue in chicken, BECN1 and AMBRA1 are detected by immunofluorescence.[305,306] Finally, in non-mammalian vertebrates, BECN1 was detected during follicular atresia in the ovary of three fish species using paraffin sections; a punctate immunostaining for BECN1 was scattered throughout the cytoplasm of the follicular cells when they were in intense phagocytic activity for yolk removal (Rizzo E, unpublished results).

Cautionary notes: One problem with immunohistochemistry for LC3 is that in some tissues this protein can be localized in structures other than autophagosomes. For example, in murine hepatocytes and cardiomyocytes under starved conditions, endogenous LC3 is detected not only in autophagosomes but also on lipid droplets.[307] In neurons in ATG7-deficient mice, LC3 is accumulated in ubiquitin- and p62-positive aggregates.[308] Thus, immunodetection of LC3 in cytoplasmic granules is not sufficient to monitor autophagy in vivo.

dc_840_14

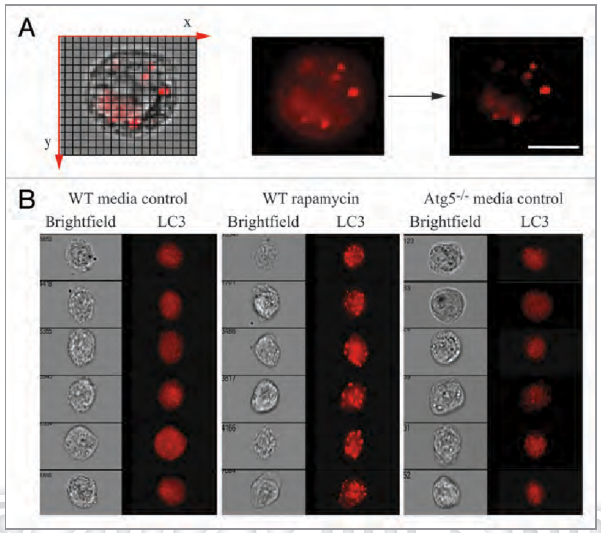


Figure 13. Assessing autophagy with multispectral imaging cytometry. (A) Bright Detail Intensity (BDI) measures the foreground intensity of bright puncta (that are three pixels or less) within the cell image. For each cell, the local background around the spots is removed before intensity calculation. Thus, autophagic cells with puncta have higher BDI values. (B) Media control (untreated wild type), rapamycin-treated wild-type and *Atg5*$^{-/-}$ MEFs were gated based on BDI. Representative images of cells with high or low BDI values. Scale bar, 10 μm. Images provided by M.L. Albert.

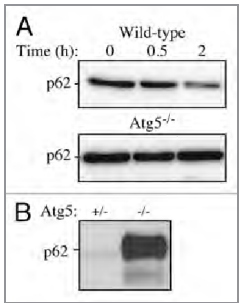


Figure 14. Regulation of the p62 protein during autophagy. (A) The level of p62 during starvation. *Atg5*$^{+/+}$ and *Atg5*$^{-/-}$ MEFs were cultured in DMEM without amino acids and serum for the indicated times, and then subjected to immunoblot analysis using anti-p62 antibody (Progen Biotechnik). This figure was previously published in reference 25 and is reproduced by permission of Landes Bioscience, copyright 2007. (B) The level of p62 in the brain of neural-cell specific Atg5 knockout mice. This image was generously provided by Dr. Taichi Hara (Tokyo Medical and Dental University).

© 2012 Landes Bioscience. Do not distribute.

Conclusion: It has not been clearly demonstrated that immunohistochemistry of ATG proteins in tissues corresponds to autophagy activity, and this area of research needs to be further explored before we can make specific recommendations.

3. *p62 and related LC3 binding protein turnover assays.* In addition to LC3, p62/SQSTM1, or other receptors such as NBR1, can also be used as a protein marker, at least in certain settings.[25,309] The p62 protein serves as a link between LC3 and ubiquitinated substrates.[98] p62 and p62-bound polyubiquitinated proteins become incorporated into the completed autophagosome and are degraded in autolysosomes, thus serving as a readout of autophagic degradation (**Fig. 14**). Inhibition of autophagy correlates with increased levels of p62 in mammals and Drosophila, suggesting that steady-state levels of this protein reflect the autophagic status.[304,310-315] Similarly, decreased p62 levels are associated with autophagy activation. The phosphorylation of p62 at Ser403 appears to regulate its role in the autophagic clearance of ubiquitinated proteins, and anti-phospho-p62 antibodies can be used to detect the modified form of the protein.[234]

Cautionary notes: p62 contains an LC3 interacting motif as well as a ubiquitin binding domain, and appears to act by linking ubiquitinated substrates with the autophagic machinery. Nonetheless, it would be prudent to keep in mind that p62 contains domains that interact with several signaling molecules,[316] and p62 may be part of the mechanistic target of rapamycin (MTOR) complex 1 (TORC1).[317] Thus, it may have additional functions that need to be considered with regard to its role in autophagy. In the context of autophagy as a stress response, the complexity of using p62 as an autophagy marker is underscored by its capacity to modulate the NRF2 anti-oxidant response pathway through a KEAP1 binding domain.[318] In fact, p62 may, itself, be transcriptionally induced by NRF2.[319] Furthermore, it is necessary to examine endogenous p62 because overexpression of this protein leads to the formation of protein inclusions. In fact, even endogenous p62 becomes Triton X-100-insoluble in the presence of protein aggregates and when autophagic degradation is inhibited; thus, results with this protein are often context-dependent. In addition, p62 participates in proteasomal degradation, and its level may also increase when the proteasome is inhibited.[320] Accordingly, the p62 degradation rate should be analyzed in the presence of an inhibitor such as epoxomicin or lactacystin to determine the contribution from the proteasome (see *Autophagy inhibitors and inducers* for potential problems with MG132).[321] p62 is also a substrate for caspases 6 and 8 (as well as calpain 1), which may confound its use in examining cell death and autophagy.[322] Another issue is that some phosphatidylinositol 3-kinase (PtdIns3K) inhibitors such as LY294002, and to a lesser extent wortmannin (but apparently not 3-MA)[256] can inhibit protein synthesis;[323] this might in turn affect the turnover of p62 and LC3, which could influence conclusions that are drawn from the status of these proteins regarding autophagy flux or aggresome-like induced structures (ALIS) formation. Accordingly, it may be advisable to measure protein synthesis and proteasome activity along with autophagy under inhibitory or activating conditions. With regard to protein synthesis, it is worth noting that this can be monitored through a nonradioactive method.[324] Finally, p62 may be transcriptionally upregulated under certain conditions,[227,325] further complicating the interpretation of results. For example, p62 upregulation, and at least transient increases in the amount of p62, is seen in some situations where there is an increase in autophagic flux.[326-328] Of interest, p62 hyperexpression at both gene and protein levels can be observed in muscle atrophy induced by cancer, though not by glucocorticoids, suggesting that the stimulus inducing autophagy may also be relevant to the differential regulation of autophagy-related proteins (Penna F, Costelli P, unpublished observations). One solution to problems relating to variations in p62 synthesis is to use a HaloTag®-p62 chimera.[329] The chimeric protein can be covalently labeled with HaloTag® ligands, and the loss of signal can then be monitored without interference by subsequent changes in protein synthesis. Similarly, a stable cell line expressing EGFP-tagged p62 under the control of in inducible promoter can be used to assess the rates of p62 degradation, taking into account the limitations outlined above (see *Autophagic flux determination using flow and multi-spectral imaging cytometry*).[281] Yet another solution is to employ a radioactive pulse-chase assay to measure the reates of p62 degradation.[330]

Western blot analysis using NP40 or Triton X-100 lysis in autophagic conditions typically shows a reduction in p62 levels. However, this does not necessarily indicate that p62 is degraded, because p62 aggregates are insoluble in these detergent lysis conditions.[227,331] Moreover, in some instances p62 levels do not change in the soluble fractions despite autophagic degradation, a finding that might be explained by simultaneous transcriptional induction of the gene encoding p62, since the soluble fraction accounts only for the diffuse or free form of p62. Accumulation of p62 in the Triton X-100-insoluble fraction can be observed when autophagy-mediated degradation is inhibited. Under conditions of higher autophagic flux, accumulation of p62 in Triton X-100-insoluble fractions may not be observed and p62 levels may be reduced or maintained. The simplest approach to circumvent many of these problems is by using lysis buffer that allows identification of the entire cellular pool of p62 (e.g., containing 1% SDS); however, additional assessment of both Triton X-100-soluble and -insoluble fractions will provide further information regarding the extent of p62 oligomerization.[308]

To conclusively establish p62 degradation by autophagy, p62 levels in both Triton X-100-soluble and -insoluble fractions need to be determined upon treatment with autophagy inducers in combination with autophagy inhibitors, such as those that inhibit the autolysosomal degradation steps (e.g., protease inhibitors, chloroquine or bafilomycin A_1, or genetically by knocking out or knocking down *LAMP2*). Additionally, an alteration in the levels of p62 may not be immediately evident with changes observed in autophagic flux upon certain chemical perturbations (Sarkar S, personal communication). Whereas LC3 changes may be rapid, clearance of autophagy substrates may require a longer time. Therefore, if LC3 changes are assessed at 6 h or 24 h after a drug treatment, p62 levels can be tested not only at the same time points, but also at later time points (24 h or 48 h) for determining the maximal impact on substrate clearance. An alternative method is immunostaining for p62 with and without autophagy inhibitors, which will appear as either a diffuse or punctate pattern. Experiments with autophagy inducers and inhibitors, in combination with western blot and immunostaining analyses, best establish autophagic degradation based on p62 turnover. A final point, however, is that empirical evidence suggests that the species-specificity of antibodies for detecting p62 must be taken into account. For example, some commercial antibodies recognize both human and mouse p62, whereas others detect the human, but not the mouse protein (see the *Autophagy Forum* at https://www.landesbioscience.com/journals/autophagy/forum/ for information pertaining to anti-p62 antibodies).[332] Another issue with detecting p62 in the context of human disease is that it can be mutated (e.g., in Paget disease of bone).[333] Thus, care should be taken to ensure that potential mutations are not affecting the epitopes that are recognized by anti-p62 antibodies when using western blotting to detect this protein.

Conclusion: There is not always a clear correlation between increases in LC3-II and decreases in p62. Thus, although analysis of p62 can assist in assessing the impairment of autophagy or autophagy flux, we recommend using p62 only in combination with other methods such as LC3-II turnover to monitor flux.

4. *TOR, AMPK and Atg1/ULK1.* Atg1/ULK1 are central components in autophagy that likely act at more than one stage of the process. There are multiple ULK isoforms in mammalian cells including ULK1, ULK2, ULK3, ULK4 and STK36.[334] ULK3 is a positive regulator of the Hedgehog signaling pathway,[335] and its overexpression induces both autophagy and senescence.[336] Along these lines, ectopic ULK3 displays a punctate pattern upon starvation-induced autophagy induction.[336] ULK3, ULK4 and STK36, however, lack the domain present on ULK1 and ULK2 that bind ATG13 and FIP200.[337] Thus, ULK3 may play a role that is restricted to senescence, and that is independent of the core autophagy machinery. ULK2 has a higher degree of identity with ULK1 than any of the other homologs, and they may have similar functions that are tissue specific; however, ULK1 may be the predominant isoform involved in autophagy, as knockdown of ULK2 does not affect movement of ATG9.[338] The stability and activation of ULK1, but not ULK2, is dependent on its interaction with the HSP90-CDC37 chaperone complex. Pharmacological or genetic inhibition of the chaperone complex increases proteasome-mediated turnover of ULK1, impairing its kinase activity and ability to promote both starvation-induced autophagy and mitophagy.[239]

AMP-activated protein kinase (AMPK) is a multimeric serine/threonine protein kinase comprising α- (catalytic), β- (scaffold), and γ- (regulatory) subunits. The enzyme activity of AMPK is

Do not distribute.

dc_840_14

absolutely dependent on phosphorylation of the α-subunit on Thr172,[339,340] and can, therefore, be conveniently monitored by western blotting with a phosphospecific antibody against this site. In some cells, Thr172 is phosphorylated by the Ca^{2+}-activated protein kinase CaMKKβ; in other cells by the constitutively active kinase LKB1, regulation of AMPK activity being performed primarily by Thr172-dephosphorylating protein phosphatases such as PP1 and PP2A.[341] Thr172 dephosphorylation is modulated by adenine nucleotides that bind competitively to regulatory sites in the γ-subunit. AMP and ADP inhibit dephosphorylation and promote AMPK activity, whereas Mg^{2+}-ATP has the opposite effect.[340] AMPK thus acts as a fine-tuned sensor of the overall cellular energy charge that regulates cellular metabolism to maintain energy homeostasis. Activation of AMPK is also associated with the phosphorylation of downstream enzymes involved in ATP-consuming processes, such as fatty acid (acetyl-CoA carboxylase) and cholesterol (hydroxymethylglutaryl-CoA dehydrogenase) biosynthesis.

The role of AMPK in autophagy is complex, and highly dependent on both cell type and metabolic conditions. In liver cells, AMPK suppresses autophagy at the level of cargo sequestration as indicated by the rapid sequestration-inhibitory effects of a variety of AMPK activators, whereas it appears to stimulate autophagy in many other cell types, including fibroblasts, colon carcinoma cells and skeletal muscle.[342-351] Autophagy-promoting effects of AMPK are most evident in cells cultured in a complete medium with serum and amino acids, where cargo sequestration is otherwise largely suppressed.[348] Presumably, AMPK antagonizes the autophagy-inhibitory effect of amino acids (at the level of phagophore assembly) by phosphorylating proteins involved in TORC1 signaling, such as TSC2[352] and RAPTOR[353] as well the TORC1 target ULK1 (see below).[354-356]

Compound C is an effective and widely used inhibitor of activated (phosphorylated) AMPK.[357] However, being a non-specific inhibitor of oxidative phosphorylation,[358,359] this drug has been observed to *inhibit* autophagy under conditions where AMPK is already inactive or knocked out,[360] and has even been shown to *stimulate* autophagy by an AMP-independent mechanism.[359,361] Compound C thus cannot be used as a stand-alone indicator of AMPK involvement.

TORC1 is an autophagy-suppressive regulator that integrates growth factor, nutrient and energy signals. In most systems, inhibition of MTOR leads to induction of autophagy, and AMPK activity is generally antagonistic toward MTOR function. TORC1 mediates the autophagy-inhibitory effect of amino acids, which stimulate the MTOR protein kinase through a Rag GTPase dimer. Insulin and growth factors activate TORC1 through upstream kinases including AKT (protein kinase B), and extracellular signal regulated kinase (ERK) when the energy supply is sufficient, whereas energy depletion may induce AMPK-mediated TORC1 inhibition and autophagy stimulation, for example, during glucose starvation. Amino acid starvation, on the other hand, can strongly induce autophagy even in cells completely lacking AMPK catalytic activity.[362]

AMPK and TORC1 regulate autophagy through coordinated phosphorylation of ULK1; under glucose starvation, AMPK promotes autophagy by directly activating ULK1 through phosphorylation, although the exact AMPK-mediated ULK1 phosphorylation site(s) remains unclear.[351,354-356] Under conditions of nutrient sufficiency, high TORC1 activity prevents ULK1 activation by phosphorylating alternate ULK1 residues and disrupting the interaction between ULK1 and AMPK. There are commercially available phospho-specific antibodies that recognize different forms of ULK1. For example, phosphorylation at Ser555, an AMPK site, is indicative of increased autophagy in response to nutrient stress, whereas Ser757 is targeted by MTOR to inhibit autophagy. Even the autophagy-suppressive effects of AMPK could, conceivably, be mediated through ULK1 phosphorylation, for example, at the inhibitory site Ser638.[363] AMPK inhibits MTOR by phosphorylating and activating TSC2.[364] Therefore, AMPK is involved in processes that synergize to activate autophagy, by directly activating ULK1, and indirectly impairing MTOR-dependent inhibition of ULK1. The identification of ULK1 as a direct target of TORC1 and AMPK represents a significant step toward the definition of new tools to monitor the induction of autophagy. However, further studies directed at identifying physiological substrates of ULK1 will be essential to understand how ULK1 activation results in initiation of the autophagy program. Along these lines, ULK1 phosphorylates AMBRA1,[365] and the MLCK-like protein Sqa,[366] as well as ATG13 and FIP200.[367-370] In addition, ULK1 binds to, and phosphorylates, RAPTOR, leading to inhibition of TORC1.[371] Furthermore, ULK1 itself appears to be able to mediate inhibitory AMPK phosphorylation to generate a negative feedback loop.[372]

TORC1 activity can be monitored by following the phosphorylation of its substrates, such as EIF4EBP1 (4E-BP1/PHAS-I) and RPS6KB2 (p70S6 kinase) or the latter's downstream target, the ribosomal protein S6, for which good commercial antibodies are available.[373-375] In mammalian cells, the analysis should focus on the phosphorylation of S6K1 at Thr389, and EIF4EBP1 at Thr37 and Thr46, which are directly phosphorylated by TORC1.[376] The TORC1-dependent phosphorylation of EIF4EBP1 can be detected as a molecular mass shift by western blot.[375] Examining the phosphorylation status of RPS6KB2 and EIF4EBP1 may be a better method for monitoring TORC1 activity than following the phosphorylation of proteins such as S6, because the latter is not a direct substrate of TORC1 (although S6 phosphorylation is a good readout for S6K1/2 activities, which are directly dependent on mTOR), and it can also be phosphorylated by other kinases such as RSK. Furthermore, the mechanisms that determine the selectivity as well as the sensitivity of TORC1 for its substrates seem to be dependent on the integrity and configuration of TORC1. For example, rapamycin strongly reduces S6K1 phosphorylation, whereas its effect on EIF4EBP1 is more variable. In the case of rapamycin treatment, EIF4EBP1 can be phosphorylated by TORC1 until rapamycin disrupts TORC1 dimerization and its integrity, whereas S6K1 phosphorylation is quickly reduced when rapamycin simply interacts with MTOR in TORC1 (see *Autophagy inhibitors and inducers* for information on catalytic MTOR inhibitors such as torin1).[376] Since it is likely that other inhibitors, stress, and stimuli may also affect the integrity of TORC1, a decrease or increase in the phosphorylation status of one TORC1 substrate does not necessarily correlate with changes in others, including ULK1. Therefore, reliable antiphospho-ULK1 antibodies should be used to directly examine the phosphorylation state of ULK1, along with additional experimental approaches to analyze the role of the MTOR complex in regulating autophagy.

Activation/assembly of the Atg1 complex in yeast (composed of at least Atg1-Atg13-Atg17-Atg29-Atg31) or the ULK1 complex in mammals (ULK1-FIP200-ATG13-ATG101) is one of the first steps of autophagy induction. Therefore, activation of this complex can be assessed to monitor autophagy induction. In yeast, dephosphorylation of Atg13 is associated with activation/assembly of the core complex, which can be assessed by immunoprecipitation or western blotting.[377-380] In addition, the autophosphorylation of Atg1 at Thr226 is required for its kinase activity and for autophagy induction; this can be detected using phospho-specific antibodies, by immunoprecipitation or western blotting (**Fig. 15**).[381,382] In mammalian cells, the phosphorylation status of ULK1 at the activating sites (Ser317, 777, 467, 555, 637, or Thr574) or dephosphorylation at inactivating sites (Ser638, 757) can be determined using phospho-specific antibodies,[355,356] or by western blotting.[383] In general, the core complex is stable in mammalian cells, although, as noted above, upstream inhibitors (MTOR) or activators (AMPK) may interact dynamically with it, thereby determining the status of autophagy.

One additional topic that bears on ULK1 concerns the process of LC3-associated phagocytosis. LAP is a type of phagocytosis in macrophages that involves the conjugation of LC3 to single-membrane pathogen-containing phagosomes, a process that promotes phagosome acidification and fusion with lysosomes.[131] Most of the core autophagy components are required for LAP, but the two processes can be distinguished by the presence or absence, respectively, of a double-membrane sequestering vesicle. ULK1 is not needed for LAP, which provides a more convenient means for distinguishing between the two processes.[134]

Cautionary notes: A decrease in TORC1 activity is a good measure for autophagy induction; however, TORC1 activity does not necessarily preclude autophagy induction because there are TOR-independent mechanisms that induce autophagy.[384-387] Along these lines, whereas in most systems inhibition of MTOR leads to the induction of autophagy, there are instances in commonly used cancer cell lines in which MTOR appears to be a positive effector.[388] Furthermore, in adult skeletal muscle, autophagy gene upregulation and autophagosome formation is independent of TORC1 but partially dependent on MTOR complex 2 (TORC2), as shown by the finding that autophagosome formation is increased by knockdown of RICTOR, a component of TORC2, but not TORC1.[346] In addition, TORC1 is downstream of AKT; however, oxidative stress inhibits MTOR, thus allowing autophagy, despite the concomitant activation of AKT.[115] Also, persistent autophagy induction can cause negative feedback that results in the reactivation of MTOR under conditions of ongoing starvation.[389] Thus, it is necessary to be cautious in deciding how to monitor the MTOR pathway, and to verify that the pathway being analyzed displays MTOR-dependent inhibition.

One problem in monitoring assembly of the ULK1 complex is the low abundance of endogenous ULK1 in many systems, which makes it difficult to detect phospho-ULK1 by western blot analysis. In addition, Atg1/ULK1 is phosphorylated by multiple kinases, and the amount of phosphorylation at different sites can increase or decrease during autophagy induction. Thus, although there is an increase in phosphorylation at the activating sites upon induction, the overall phosphorylation states of ULK1 and ATG13 are decreased under conditions that lead to induction of autophagy; therefore, monitoring changes in phosphorylation by following molecular mass shifts upon SDS-PAGE may not be informative. In addition, such phosphorylation/dephosphorylation events are expected to occur relatively early (1–2 h) in the signaling cascade of autophagy. Therefore, it is necessary to optimize treatment time conditions. Finally, in Arabidopsis and possibly other eukaryotes, the ATG1 and ATG13 proteins are targets of autophagy, which means that their levels may drop substantially under conditions that induce autophagic turnover.[174]

At present, the use of Atg1/ULK1 kinase activity as a tool to monitor autophagy is limited because only a few physiological substrates have been identified, and the importance of the Atg1/ULK1-dependent phosphorylation has not been determined. Nonetheless, Atg1/ULK1 kinase activity appears to increase when autophagy is induced, irrespective of the pathway leading to induction. As additional physiological substrates of Atg1/ULK1 are identified it will be possible to follow their phosphorylation in vivo as is done with analyses for MTOR. Nonetheless, it must be kept in mind that monitoring changes in the activity of Atg1/ULK1 is not a direct assay for autophagy, although such changes may correlate with autophagy activity. Furthermore, in some cells ULK1 has functions in addition to autophagy, such as in axonal transport and outgrowth, and its activity state may thus reflect its role in these processes.[390-395] Accordingly, other methods as described throughout these guidelines should also be used to follow autophagy directly.

Finally, there is not a complete consensus on the specific residues of ULK1 that are targeted by AMPK or MTOR. Similarly, apparently contradictory data have been published regarding the association of AMPK and MTOR with the ULK1 kinase complex under different conditions. Therefore, caution should be used in monitoring ULK1 phosphorylation or the status of ULK1 association with AMPK until these issues are resolved.

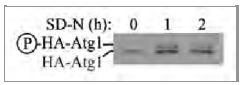


Figure 15. *S. cerevisae* cells transformed with a plasmid encoding HA-Atg1 were cultured to mid-log phase and shifted to SD-N (minimal medium lacking nitrogen that induces a starvation response). Immunoblotting was done with anti-HA antibody. The upper band corresponds to autophosphorylation of Atg1. This figure was modified from data previously published in reference ,381 and is reproduced by permission of the American Society for Cell Biology, copyright 2011.

dc 840_14
© Landes Bioscience. Do not distribute.

Conclusion: Assays for Atg1/ULK1 can provide detailed insight into the induction of autophagy, but are not a direct measurement of the process. Similarly, analysis of MTOR substrates such as S6K1 and EIF4EBP1 are not recommended readouts for autophagy, and need to be combined with other assays that directly monitor autophagy activity.

5. *Additional autophagy-related markers.* Although Atg8/LC3 has been the most extensively used protein for monitoring autophagy, other proteins can also be used for this purpose. Here, we discuss some of the more commonly used or better-characterized possibilities.

a. *Atg9.* Atg9 is the only integral membrane Atg protein that is essential for autophagosome formation. ATG9 displays partial colocalization with GFP-LC3.[396] Perhaps the most unique feature of Atg9, however, is that it localizes to multiple discrete puncta, whereas most Atg proteins are detected primarily in a single punctum or diffusely within the cytosol. Yeast Atg9 may cycle between the phagophore assembly site (PAS, also referred to as the phagophore assembly site) and peripheral reservoirs;[397] the latter correspond to tubulovesicular clusters that are precursors to the phagophore.[398] Anterograde movement to the PAS is dependent on Atg11, Atg23, Atg27 and actin. Retrograde movement requires Atg1-Atg13, Atg2-Atg18 and the PtdIns3K complex I.[399] Mutants such as *atg1*Δ accumulate Atg9 exclusively at the PAS, and this phenotype forms the basis of the transport of Atg9 after knocking out *ATG1* (TAKA) assay.[63] In brief, this is an epistasis analysis in which a double-mutant strain is constructed (one of the mutations being *atg1*Δ) that expresses Atg9-GFP. If the second mutated gene encodes a protein that is needed for Atg9 anterograde transport, the double mutant will display multiple Atg9-GFP puncta. In contrast, if the protein acts along with or after Atg1, all of the Atg9-GFP will be confined to the PAS. Monitoring the localization of ATG9 has not been used extensively in higher eukaryotes, but this protein displays the same type of dependence on Atg1/ULK1 for cycling as seen in yeast,[396,399] suggesting that it is possible to follow this protein as an indication of ULK1 and ATG13 function.[370]

b. Atg12–Atg5. ATG5, ATG12, and ATG16L1, associate with the phagophore and have been detected by fluorescence or immunofluorescence (**Fig. 16**).[400,401] Endogenous ATG5, ATG12 or ATG16L1 puncta formation can be followed to monitor autophagy upregulation. Under physiological conditions, the endogenous proteins are predominantly diffusely distributed throughout the cytoplasm. Upon induction of autophagy, for example during starvation, there is a marked increase in the proportion of cells with punctate ATG5, ATG12 and ATG16L1. Furthermore, inhibitors of autophagosome formation result in a block in this starvation-induced puncta formation, and this assay is very robust in mammalian cells.

Atg12–Atg5 conjugation has been used in some studies to measure autophagy. In Arabidopsis and some mammalian cells it appears that essentially all of the ATG5 and ATG12 proteins exist in the conjugated form and the expression levels do not change, at least during short-term starvation.[150,400-402] Therefore, monitoring ATG12–ATG5 conjugation per se may not be a useful method for following the induction of autophagy. It is worth noting, however, that in some cell lines free ATG5 can be detected,[403] suggesting that the amount of free ATG5 may be cell line-dependent. One final parameter that may be considered is that the total amount of the ATG12–ATG5 conjugate may increase following prolonged starvation as has been observed in hepatocytes and both mouse and human fibroblasts (Cuervo AM, personal communication; Sarkar S, personal communication).

c. ATG14. Yeast Atg14 is the autophagy-specific subunit of the Vps34 complex I,[404] and a human homolog, named ATG14 (ATG14L/BARKOR), has been identified.[405-408] ATG14 localizes primarily to phagophores. The C-terminal fragment of the protein is named the BATS domain (BARKOR/ATG14(L) autophagosome targeting sequence), and is able to direct GFP and BECN1 to autophagosomes in the context of a chimeric protein.[409] Currently, a good antibody that can be used to detect the endogenous ATG14 does not exist. ATG14-GFP or BATS-GFP detected by fluorescence microscopy or TEM can be used as a phagophore marker; however, ATG14 is not localized exclusively to phagophores, as it can also be detected on mature autophagosomes as well as the ER.[409,410] Accordingly, detection of ATG14 should be performed in combination with other phagophore and autophagosome markers.

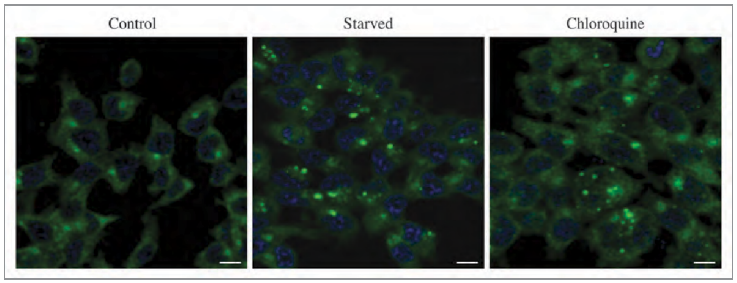


Figure 16. Confocal microscopy image of HCT116 cells immunostained with human-specific antibody to ATG12. Cells were starved for 8 h or treated with chloroquine (50 μM) for 3 h. Scale bar, 10 μm. Image provided by M. Llanos Valero, M.A de la Cruz and R. Sanchez-Prieto.

d. ATG16L1. ATG16L1 has been used to monitor the movement of plasma membrane as a donor for autophagy, and thus an early step in the process; ATG16L1 is located on phagophores, but not on completed autophagosomes.[269,411] ATG16L1 can be detected by immuno-TEM, by immunostaining of Flag epitope-tagged ATG16L1, and/or by the use of GFP-tagged ATG16L1.

e. Atg18/WIPI family. Yeast Atg18[412,413] and Atg21[262] (or the mammalian WIPI homologs[414]) are required for both macroautophagy (i.e., nonspecific sequestration of cytoplasm) and autophagy-related processes (e.g., the Cvt pathway,[415,416] specific organelle degradation,[74] and autophagic elimination of invasive microbes[77,78,80,81,417]).[412] These proteins bind phosphatidylinositol 3-phosphate (PtdIns3P) that is present at the phagophore and autophagosome[418,419] and also PtdIns(3,5)P_2. Human WIPI-1 and WIPI-2 function downstream of the phosphatidylinositol 3-kinase class III (PtdIns3KC3) complex I [PtdIns3KC3, BECN1, PIK3R4 (VPS15), ATG14] and upstream of both the ATG12 and LC3 ubiquitin-like conjugation systems.[418,420,421] Upon the initiation of the autophagic pathway, WIPI1 and WIPI2 bind PtdIns3P and accumulate at limiting membranes, such as those of the endoplasmic reticulum, where they participate in the formation of omegasomes and/or autophagosomes. On the basis of quantitative fluorescence microscopy, this specific WIPI protein localization has been used as an assay to monitor autophagy in human cells.[419] Using either endogenous WIPI1 or WIPI2, detected by indirect fluorescence microscopy or EM, or transiently or stably expressed tagged fusions of GFP to WIPI1 or WIPI2, basal autophagy can be detected in cells that display WIPI puncta at autophagosomal membranes. In circumstances of increased autophagic activity, such as nutrient starvation or rapamycin administration, the induction of autophagy is reflected by the elevated number of cells that display WIPI puncta when compared with the control setting. Also, in circumstances of reduced autophagic activity such as wortmannin treatment, the reduced number of WIPI puncta-positive cells reflects the inhibition of autophagy. Basal, induced and inhibited formation of WIPI puncta closely correlate with both the protein level of LC3-II and the formation of GFP-LC3 puncta.[419,421] Accordingly, WIPI puncta can be assessed as an alternative to LC3. Automated imaging and analysis of fluorescent WIPI-1 (**Fig. 17**) or WIPI2 puncta represents an efficient and reliable opportunity to combine the detection of WIPI proteins with other parameters. It should be noted that there are two isoforms of WIPI2 (2B and 2D),[421] and in *C. elegans* WIPI4 (EPG-6) has been identified as the WIPI homolog required for autophagy.[422] Thus, these proteins, along with the currently uncharacterized WIPI3, provide additional possibilities for monitoring phagophore and autophagosome formation.

Cautionary notes: With regard to detection of the WIPI proteins, endogenous WIPI1 puncta cannot be detected in many cell types,[418] and the level of transiently expressed GFP-WIPI1 puncta is cell context-dependent;[418,419] however, it has been used in human and mouse cell systems[348,419] and mCherry-Atg18 also works in transgenic Drosophila (Juhász G, personal communication), although one caution with regard to the latter is that GFP-Atg18 expression can induce autophagy in the fat body of fed larvae (Kiger A, unpublished observation). GFP-WIPI1 and GFP-WIPI2 have been detected on the completed (mature) autophagosome by freeze-fracture analysis,[60] but endogenous WIPI2 has not been detected on mRFP-LC3- or LAMP2-positive autophagosomes or autolysosomes using immunolabeling.[418] Accordingly, it may be possible to follow the formation and subsequent disappearance of WIPI puncta to monitor autophagy induction and flux using specific techniques. As with GFP-LC3, overexpression of WIPI1 or WIPI2 can lead to the formation of aggregates, which are stable in the presence of PtdIns3K inhibitors.

f. BECN1/Atg6. BECN1 (Atg6) and VPS34 are essential partners in the autophagy interactome that signals the onset of autophagy,[404,423,424] and many researchers use this protein as a way to monitor autophagy. BECN1 is inhibited by its binding to the anti-apoptotic protein BCL2.[425] Autophagy is induced by the release of BECN1 from BCL2 by pro-apoptotic BH3 proteins, phosphorylation of BECN1 by DAPK (at Thr119, located in the BH3 domain),[426] or phosphorylation of BCL2 by JNK1 (at Thr69, Ser70 and Ser87).[427,428] The relationship between BECN1 and BCL2 is more complex in developing cerebellar neurons as it appears that the cellular levels of BCL2 are, in turn, post-translationally regulated by an autophagic mechanism linked to a switch from immaturity to maturity.[429,430] It is important to be aware, however, that certain forms of macroautophagy are induced in a BECN1-independent manner, and are not blocked by PtdIns3K inhibitors.[97,431] Interestingly, caspase-mediated cleavage of BECN1 inactivates BECN1-induced autophagy and enhances apoptosis in several cell types,[432] emphasizing that the crosstalk between apoptosis and autophagy is complex.

Although a population of BECN1 may localize in proximity to the trans-Golgi network,[433] it is also present at the ER and mitochondria.[425] In keeping with these observations, in cerebellar organotypic cultures BECN1 co-immunoprecipitates with BCL2 that is primarily localized at the mitochondria and ER, and in a mouse model of neurodegeneration autophagic vacuoles in Purkinje neurons contain partially digested organelles that are immunoreactive for BCL2.[430,434] In addition, BECN1 and VPS34 can be present in multiple complexes, so caution must be exercised when monitoring localization. On induction of autophagy by various stimuli the presence of BECN1- and VPS34-positive macroaggregates can be detected in the region of the Golgi complex by immunofluorescence.[115,435] Thus, BECN1-GFP puncta detected by fluorescence microscopy or TEM may serve as an additional marker for autophagy induction;[436] however, as with any GFP chimeras there is a concern that the GFP moiety interferes with correct localization of BECN1. To demonstrate that BECN1 or PtdIns3K macroaggregates are an indirect indication of ongoing autophagy, it is mandatory to show their specific association with the process by including

dc 840 14

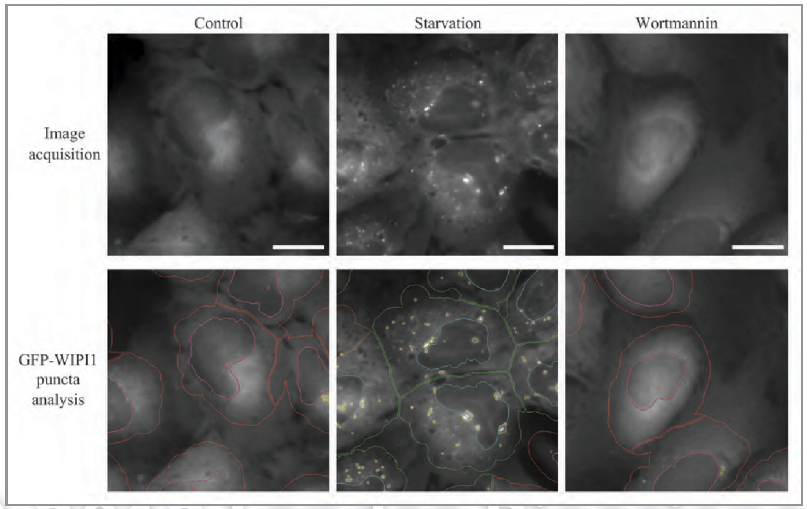


Figure 17. Automated WIPI1 puncta image acquisition and analysis monitors the induction and inhibition of autophagy. Stable U2OS clones expressing GFP-WIPI1 were selected using 0.6 μg/ml G418 and then cultured in 96-well plates. Cells were treated for 3 h with nutrient-rich medium (control), nutrient-free medium (EBSS), or with 233 nM wortmannin. Cells were fixed in 3.7% paraformaldehyde and stained with DAPI (5 μg/ml in PBS). An automated imaging and analysis platform was used to determine the number of both GFP-WIPI1 puncta-positive cells and the number of GFP-WIPI1 puncta per individual cell.[248] Cells without GFP-WIPI1 puncta are highlighted in red (cell detection) and purple (nuclei detection), whereas GFP-WIPI1 puncta-positive cells are highlighted in yellow (GFP-WIPI1 puncta detection), green (cell detection) and blue (nuclei detection). Bars, 20 μm. These images were provided by S. Pfisterer and T. Proikas-Cezanne.

© 2012 Landes Bioscience. Do not distribute.

appropriate controls with inhibitors (e.g., 3-MA) or autophagy gene silencing. When a BECN1-independent autophagy pathway is induced, such aggregates are not formed regardless of the fact that the cell expresses BECN1 (e.g., as assessed by western blotting) (Isidoro C, personal communication).

g. DFCP1. DFCP1 (double FYVE-containing protein 1) binds PtdIns3P that localizes to the ER and Golgi. The ER population of DFCP1 is involved in formation of the omegasome.[437] Starvation induces the translocation of DFCP1 to punctate structures on the ER. DFCP1 partially colocalizes with WIPI1 upon nutrient starvation,[421] and also with WIPI2.[418]

h. DRAM. DRAM (damage-regulated autophagic modulator) is a gene induced by activated p53 in response to different types of cellular stress, including DNA damage.[438,439] DRAM is a small hydrophobic protein with six transmembrane domains. It is detected as a subpopulation in the Golgi and cis-Golgi, colocalizing with giantin and GM130, and also in early and late endosomes and lysosomes, colocalizing with EEA1 and LAMP2.[439] The elimination of DRAM by siRNA blocks autophagy,[439,440] as effectively as elimination of BECN1, indicating it is an essential component for this process, although its mechanism of action is not known. The time course of autophagy as a consequence of DRAM activation can be monitored following the disappearance of the VRK1 protein, a direct target of this process, by immunoblot.[439] Detection of *DRAM* RNA is very easy by qRT-PCR during autophagy;[438,439] however, detection of the DRAM protein is very difficult because of its small size and hydrophobicity, which makes generation of specific antibodies a complicated process, and in general these have very low sensitivity.

Conclusion: Proteins other than Atg8/LC3 can be monitored to follow autophagy, and can be important tools to define specific steps of the process. For example, WIPI puncta formation can be used to monitor autophagy, but, similar to Atg8/LC3, should be examined in the presence and absence of inhibitors. Analysis of WIPI puncta should be combined with other assays because individual members of the WIPI family might also participate in additional, uncharacterized functions apart from their role in autophagy. At present, we caution against the use of changes in BECN1 localization as a marker of autophagy induction.

6. *Transcriptional and translational regulation*. The induction of autophagy in certain scenarios is accompanied by an increase in the mRNA levels of certain autophagy genes, such as *ATG8/Lc3*[441,442] and *Atg12*,[443] and an autophagy-dedicated microarray was developed as a high-throughput tool to simultaneously monitor the transcriptional regulation of all genes involved in, and related to, autophagy.[444] The gene that shows the greatest transcriptional regulation in the liver (in response to starvation and circadian signals) is *Ulk1*, but others also show more limited changes in mRNA levels including *Gabarapl1*, *Bnip3* and, to a minor extent, *Lc3B* (Lin JD, personal communication). In several mouse and human cancer cell lines, ER stress and hypoxia increase the transcription of *LC3*, *ATG5* and *ATG12* by a mechanism involving the unfolded protein response (UPR). Similarly, a stimulus-dependent increase in *LC3B* expression is detected in neutrophils undergoing autophagy induction.[445] Increased expression of *Atg5* in vivo after optic nerve axotomy in mice[446] and increased expression of *Atg7, Becn1* and *Lc3A* during neurogenesis at different embryonic stages in the mouse olfactory bulb are also seen.[447] LC3 and ATG5 are not required for the initiation of autophagy, but mediate phagophore expansion and autophagosome formation. In this regard, the transcriptional induction of *LC3* may be necessary to replenish the LC3 protein that is turned over during extensive ER stress- and hypoxia-induced autophagy.[443,448] Thus, assessing the mRNA levels of *LC3* and other autophagy-related genes by northern blot or qRT-PCR may provide correlative data relating to the induction of autophagy. It is not clear if these changes are sufficient to induce autophagy, however, and therefore these are not direct measurements.

Of note, large changes in *Atg* gene transcription just prior to Drosophila salivary gland cell death (that is accompanied by an increase in autophagy) are detected in *Atg2*, *Atg4*, *Atg5* and *Atg7*, whereas there is no significant change in *Atg8a* or *Atg8b*.[449,450] Autophagy is critical for Drosophila midgut cell death, which is accompanied by transcriptional upregulation of all of the *Atg* genes tested, including *Atg8a* (**Fig. 18**).[199,451] Similarly, in the silkworm (*B. mori*) larval midgut the occurrence of autophagy is accompanied by an upregulation of *Atg5*, *Atg6* and *Atg8* mRNA levels.[452] Transcriptional upregulation of Drosophila *Atg8a* and *Atg8b* is also observed in the fat body following induction of autophagy at the end of larval development,[453] *Atg5*, *Atg6*, *Atg8a* and *Atg18* are upregulated in the ovary of starved flies,[454] and an increase in Drosophila *Atg8b* is observed in cultured Drosophila *l(2)mbn* cells following starvation (Gorski S, personal communication). An upregulation of plant ATG8 may be needed during the adaptation to reproductive growth; a T-DNA inserted mutation of rice *ATG8b* blocked the change from vegetative growth to reproductive growth in both homozygous and heterozygous plant lines (Zhang M-Y, unpublished results).

Similarly, the upregulation of autophagy-related genes (*Lc3, Gabarapl1, Bnip3, Atg4b, Atg12l*) has been documented at the transcriptional and translational level in several other species (e.g., mouse, rat, trout, Arabidopsis and maize) under conditions of ER stress,[443] and diverse types of prolonged (several days) catabolic situations including cancer cachexia, diabetes mellitus, uremia and fasting.[151,346,455-457] Along these lines, *ATG9* and *ATG16L1* are transcriptionally upregulated upon influenza virus infection (Khalil H, personal communication), and in *C. elegans*, the FOXA transcription factor PHA-4 regulates the expression of several autophagy-related genes.[458] Such prolonged induction of the expression of *ATG* genes has been thought to allow the replenishment of critical proteins (e.g., LC3 and GABARAP) that are destroyed during autophagosome fusion with the lysosome.[459] The polyamine spermidine increases life span and induces autophagy in cultured yeast and mammalian cells, as well as in nematodes and flies; in aging yeast, spermidine treatment triggers epigenetic deacetylation of histone H3 through inhibition of histone acetyltransferases, leading to significant upregulation of various autophagy-related transcripts.[460]

In addition to the *ATG* genes, transcriptional upregulation of *VMP1* (a protein that is involved in autophagy regulation and that remains associated with the completed autophagosome) can be detected in mammalian cells subjected to rapamycin treatment or starvation, and in tissues undergoing disease-induced autophagy.[461] *VMP1* is an essential autophagy gene that is conserved from Dictyostelium to mammals,[232,462] and the VMP1 protein regulates early steps of the autophagic pathway.[420] VMP1 is poorly expressed in mammalian cells under nutrient-normal conditions, but is highly upregulated in cells undergoing autophagy, and the expression of VMP1 induces autophagosome formation.

A gene regulatory network, named CLEAR (coordinated lysosomal enhancement and regulation) that controls both lysosome

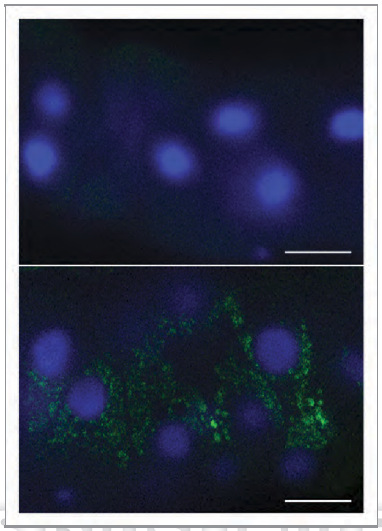


Figure 18. pGFP-Atg8a can be used to monitor autophagy in *Drosophila melanogaster*. The autophagosome marker pGFP-Atg8a, results in expression of Atg8a fused to GFP from the endogenous *Atg8a* promoter.[199] Live imaging of gastric ceca from *Drosophila melanogaster* midgut pGFP-Atg8a puncta (green) and Hoechst 33342 (blue). Midgut from early third instar larvae prior to the onset of cell death (top) and from dying midgut at 2 h after puparium formation (bottom). Bar, 25 μm. Figure provided by D. Denton and S. Kumar.

dc_840_14

and autophagosome biogenesis was identified using a systems-biology approach.[463-465] The basic helix-loop-helix transcription factor EB (TFEB) acts as a master gene of the CLEAR network and positively regulates the expression of both lysosomal and autophagy genes, thus linking the biogenesis of two distinct types of cellular compartments that cooperate in the autophagic pathway. TFEB activity is regulated by starvation and is controlled by ERK2-mediated phosphorylation at a specific serine residue,[463] and can thus serve as a new tool for monitoring transcriptional regulation connected with autophagy. Along these lines, the erythroid transcription factor GATA1 and its coregulator Friend of GATA1 induce the transcription of multiple genes encoding autophagy components; this developmentally regulated transcriptional response is coupled to increases in autophagosome number as well as the percent of cells that contain autophagosomes.[466] Finally, C/EBPβ is a transcription factor that regulates autophagy in response to the circadian cycle.[467]

Although less work has been done on post-transcriptional regulation, several studies implicate microRNAs in controlling the expression of proteins associated with autophagy.[164,468-470]

Cautionary notes: Most of the *ATG* genes do not show significant changes in mRNA levels when autophagy is induced. Even increases in *LC3* mRNA can be quite modest and are cell type- and organism-dependent.[471] In addition, it is generally better to follow protein levels because that is the ultimate readout that is significant with regard to the initiation and completion of autophagy, although ATG protein amounts do not always change significantly and the extent of increase is again cell type- and tissue-dependent. In some cases (e.g., yeast *ATG14*), increased transcription is not accompanied by increased protein levels, apparently due to changes in translation efficiency under starvation conditions (Abeliovich H, unpublished data). Finally, changes in autophagy protein levels are not sufficient evidence of autophagy induction, and must be accompanied by additional assays as described herein. Thus, monitoring changes in mRNA levels for either *ATG* genes or autophagy regulators may provide some evidence for autophagy induction, but should be used along with other methods.

Another general caution pertains to the fact that in any cell culture system different types of cells (for example, those undergoing autophagy or not) exist simultaneously. Therefore, only an average level of protein or mRNA expression can be evaluated with most methods. This means that the results regarding specific changes in autophagic cells could be hidden due to the background of the average data. Along these lines, experiments using single-cell real-time PCR to examine gene expression in individual cardiomyocytes with and without signs of autophagy revealed that the transcription of MTOR markedly and significantly increased in autophagic cells in intact cultures (spontaneously undergoing autophagy) as well as in cultures treated with proteasome inhibitors to induce autophagy (Dosenko V, personal communication). Finally, researchers need to realize that mammalian cell lines may have mutations that alter autophagy signaling or execution; this problem can be avoided by using primary cells.

Conclusion: Although there are changes in *ATG* gene expression that coincide with, and may be needed for, autophagy, this has not been carefully studied experimentally. Therefore, at the present time we do not recommend the monitoring of *ATG* gene transcription as a general readout for autophagy unless there is clear documentation that the change(s) correlates with autophagy activity.

7. *Autophagic protein degradation*. Protein degradation assays represent a well-established methodology for measuring autophagic flux, and they allow good quantification. The general strategy is first to label cellular proteins by incorporation of a radioactive amino acid (e.g., [^{14}C]-leucine, [^{14}C]-valine or [^{35}S]-methionine; although valine may be preferred over leucine due to the strong inhibitory effects of the latter on autophagy), preferably for a long time to achieve sufficient labeling of the long-lived proteins that best represent autophagic substrates, and then to follow this with a long cold-chase so that the assay starts well after labeled short-lived proteins are degraded (which occurs predominantly via the proteasome). Next, the time-dependent release of acid-soluble radioactivity from the labeled protein in intact cells or perfused organs is measured.[3,472,473] Note that the inclusion of the appropriate unlabeled amino acid (i.e., valine, leucine or methionine) in the starvation medium at a concentration equivalent to that of other amino acids in the chase medium is necessary; otherwise, the released [^{14}C]-amino acid is effectively re-incorporated into cellular proteins, which results in a significant underestimation of protein degradation. The turnover of specific proteins can also be measured in a pulse-chase regimen using the Tet-ON/OFF system and subsequent western blot analysis.[474,475]

In this type of assay a considerable fraction of the measured degradation will be non-autophagic, and thus it is important to also measure, in parallel, cell samples treated with autophagy-suppressive concentrations of 3-MA or amino acids, or obtained from mutants missing central ATG components (however, the latter assumes that non-autophagic proteolytic activity remains unchanged, which is unlikely); these values are then subtracted from the total. The complementary approach of using compounds that block other degradative pathways, such as proteasome inhibitors, may cause unexpected results and should generally be avoided due to crosstalk among the degradative systems. For example, blocking proteasome function may activate autophagy.[476-479] Thus, when using inhibitors it is critical to know whether the inhibitors being used alter autophagy in the particular cell type and context being examined. In addition, because 3-MA could have some autophagy-independent effects in particular settings it is advisable to verify that the 3-MA-sensitive degradation is also sensitive to general lysosomal inhibitors (such as NH_4Cl or leupeptin).

The use of stable isotopes, such as ^{13}C and ^{15}N, in quantitative mass spectrometry-based proteomics allows the recording of degradation rates of thousands of proteins simultaneously. These assays may be applied to autophagy-related questions enabling researchers to investigate differential effects in global protein or even organelle degradation studies.[480,481] SILAC (stable isotope labeling with amino acids in cell culture) can also provide comparative information between different treatment conditions, or between a wild type and mutant.

Another assay that could be considered relies on the limited proteolysis of a betaine homocysteine methyltransferase (BHMT) fusion protein. The 44-kDa full-length BHMT protein is cleaved in hepatocyte amphisomes in the presence of leupeptin to generate 32-kDa and 10-kDa fragments.[482-485] Accumulation of these fragments is time-dependent and is blocked by treatment with autophagy inhibitors. A modified version of this marker, GST-BHMT, can be expressed in other cell lines where it behaves similar to the wild-type protein.[486] Other substrates may be considered for similar types of assays. For example, the neomycin phosphotransferase II-GFP (NeoR-GFP) fusion protein is a target of autophagy.[487] Transfection of lymphoblastoid cells with a plasmid encoding NeoR-GFP followed by incubation in the presence of 3-MA leads to an accumulation of the NeoR-GFP protein as measured by flow cytometry.[488]

A similar western blot assay is based on the degradation of a cytosolic protein fused to GFP. This method has been used in yeast and Dictyostelium cells using GFP-PgkA and GFP-Tkt-1 (phosphoglycerate kinase and transketolase, respectively). In this case the relative amount of the free GFP and the complete fusion protein is the relevant parameter for quantification; although it may not be possible to detect clear changes in the amount of the full-length chimera, especially under conditions of limited flux.[29,36] As described above for the marker GFP-Atg8/LC3, nonsaturating levels of lysosomal inhibitors are also needed in Dictyostelium cells to slow down the autophagic degradation, allowing the accumulation and detection of free GFP. It should be noted that this method monitors bulk autophagy since it relies on the passive transit of a cytoplasmic marker to the lysosome. Consequently, it is important to determine that the marker is distributed homogeneously in the cytoplasm.

One of the most useful methods for monitoring autophagy in *S. cerevisiae* is the Pho8Δ60 assay. *PHO8* encodes the vacuolar alkaline phosphatase, which is synthesized as a zymogen before finally being transported to and activated in the vacuole.[489] A molecular genetic modification that eliminates the first 60 amino acids prevents the mutant (Pho8Δ60) from entering the endoplasmic reticulum, leaving the zymogen in the cytosol. When autophagy is induced, the mutant zymogen is delivered to the vacuole nonselectively inside autophagosomes along with other cytoplasmic material. The resulting activation of the zymogen can be easily measured by assays for alkaline phosphatase.[178] To minimize background activity, it is preferable to have the gene encoding cytosolic alkaline phosphatase (*PHO13*) additionally deleted (although this is not necessary when assaying certain substrates).

Cautionary notes: Measuring the degradation of long-lived proteins requires prior radiolabeling of the cells, and subsequent separation of acid-soluble from acid-insoluble radioactivity. The labeling can be done with relative ease both in cultured cells, and in live animals.[3] In cells, it is also possible to measure the release of an unlabeled amino acid by chromatographic methods, thereby obviating the need for prelabeling;[490] however, it is important to keep in mind that amino acid release is also regulated by protein synthesis, which in turn is modulated by many different factors. In either case, one potential problem is that the released amino acid may be further metabolized. For example, branched chain amino acids are good indicators of proteolysis in hepatocytes, but not in muscle cells where they are further oxidized (Meijer AJ, personal communication). In addition, the amino acid can be reincorporated into protein; for this reason, such experiments can be performed in the presence of cycloheximide, but this raises additional concerns (see *Turnover of autophagic compartments*). In the case of labeled amino acids, a nonlabeled chase is added where the tracer amino acid is present in excess (being cautious to avoid using an amino acid that inhibits autophagy), or by use of single pass perfused organs or superfused cells.[491,492] The perfused organ system also allows for testing the reversibility of effects on proteolysis and the use of autophagy-specific inhibitors in the same experimental preparation, which are crucial controls for proper assessment.

If the autophagic protein degradation is low (as it will be in cells in replete medium), it may be difficult to measure it reliably above the relatively high background of non-autophagic degradation. It should also be noted that the usual practice of incubating the cells under "degradation conditions," that is, in a saline buffer, indicates the potential autophagic *capacity* (maximal attainable activity) of the cells rather than the autophagic *activity* that prevails in vivo or under rich culture conditions. Finally, inhibition of a particular degradative pathway is typically accompanied by an increase in a separate pathway as the cell attempts to compensate for the loss of degradative capacity.[158,478,493] This compensation might interfere with control measurements under conditions that attempt to inhibit macroautophagy; however, as the latter is the major degradative pathway, the contributions of other types of degradation over the course of this type of experiment are most often negligible.

The Pho8Δ60 assay requires standard positive and negative controls (such as an *atg1*Δ strain), and care must be taken to ensure the efficiency of cell lysis. Glass beads lysis works well in general, provided that the agitation speed of the instrument is adequate. Instruments designed for liquid mixing with lower speeds should be avoided. We also recommend against holding individual sample tubes on a vortex, as it is difficult to maintain reproducibility; devices or attachments are available to allow multiple tubes to be agitated simultaneously.

Conclusion: Measuring the turnover of long-lived proteins is a good method for determining autophagic flux.

8. *Selective types of autophagy*. Although autophagy can be nonspecific, in particular during starvation, there are many examples of selective types of autophagy.

a. **The Cvt pathway, mitophagy, pexophagy and piecemeal microautophagy of the nucleus in yeast**. The precursor form of aminopeptidase I (prApe1) is the major cargo of the Cvt pathway in yeast, a biosynthetic autophagy-related pathway.[82] The propeptide of prApe1 is proteolytically cleaved upon vacuolar delivery, and the resulting shift in molecular mass can be monitored by western blot. Under starvation conditions, prApe1 can enter the vacuole through nonspecific autophagy, and thus

© Landes Bioscience. Do not distribute.

doi: 10.4161/auto.8.1.14840

has been used as a marker for both the Cvt pathway and autophagy. The yeast Cvt pathway is unique in that it is a biosynthetic route that utilizes the autophagy-related protein machinery, whereas other types of selective autophagy are degradative. The latter include pexophagy, mitophagy, reticulophagy, ribophagy and xenophagy, and each process has its own marker proteins, although these are typically variations of other assays used to monitor the Cvt pathway or autophagy. One common type of assay involves the processing of a GFP chimera similar to the GFP-Atg8/LC3 processing assay (see *GFP-Atg8/LC3 lysosomal delivery and proteolysis*). For example, yeast pexophagy utilizes the processing of Pex14-GFP and Pot1 (thiolase)-GFP,[494,495] whereas mitophagy can be monitored by the generation of free GFP from Om45-GFP, Idh1-GFP, Idp1-GFP or mito-DHFR-GFP.[496-500] Localization of these mitochondrially-targeted proteins (or specific MitoTracker dyes) or similar organelle markers such as those for the peroxisome [e.g., GFP-SKL with Ser-Lys-Leu at the C terminus that acts as a peroxisomal targeting signal, acyl-CoA oxidase 3 (Aox3-EYFP) that allows simultaneous observation of peroxisome-vacuole dynamics with the single FITC filter set, or GFP-catalase] can also be followed by fluorescence microscopy.[412,495,501-503] In addition, yeast mitophagy requires both the Slt2 and Hog1 signaling pathways; the activation and phosphorylation of Slt2 and Hog1 can be monitored with commercially available phospho-specific antibodies (**Fig. 19**).[381] It is also possible to monitor pexophagy in yeasts by the disappearance of activities of specific peroxisome markers such as catalase, alcohol oxidase or amine oxidase in cell-free extracts,[504] or permeabilized cell suspensions. Catalase activity, however, is a useful marker only when peroxisomal catalases are the only such enzymes present. In *S. cereviseae* there are two genes encoding catalase activity, and only one of these gene products is localized in peroxisomes. Plate assays for monitoring the activity of peroxisomal oxidases in yeast colonies are also available.[501,505] The decrease in the level of endogenous proteins such as alcohol oxidase or Pot1 can be followed by western blotting,[412,506-509] TEM,[510] fluorescence microscopy[412,511,512] or laser confocal scanning microscopy of GFP-labeled peroxisomes.[513,514]

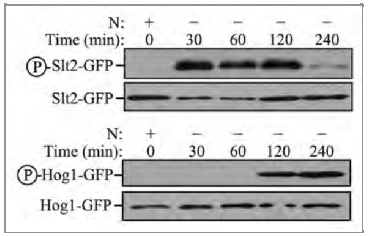


Figure 19. *S. cerevisae* cells were cultured to mid-log phase and shifted to SD-N for the indicated times. Samples were taken before (+) and at the indicated times after (–) nitrogen starvation. Immunoblotting was done with anti-phospho-Slt2 and anti-phospho-Hog1 antibody. This figure was modified from data previously published in reference,[381] and is reproduced by permission of the American Society for Cell Biology, copyright 2011.

In yeast, nonspecific autophagy can be induced by nitrogen starvation conditions, whereas degradative types of selective autophagy generally require a carbon source change or ER stress for efficient induction. For example, to induce a substantial level of mitophagy, cells need to be precultured in a nonfermentable carbon source such as lactate or glycerol to stimulate the proliferation of mitochondria. After sufficient mitochondria proliferation, shifting the cells back to a fermentable carbon source such as glucose will cause the autophagic degradation of superfluous mitochondria.[497] It should be noted that in addition to carbon source change, simultaneous nitrogen starvation is also required for efficient mitophagy induction. This is possibly because excessive mitochondria can be segregated into daughter cells by cell division if growth continues.[478]A similar carbon source change from oleic acid or methanol to ethanol or glucose (with or without nitrogen starvation) can be used to assay for pexophagy.[515] In addition, mitophagy can also be induced by culturing the cells in a nonfermentable carbon source to post-log phase. In this case, mitophagy may be induced because the energy demand is lower at post-log phase and the mitochondrial mass exceeds the cell's needs.[75,516,517] It has been suggested by several workers in the field that this type of mitophagy, also known as "stationary phase mitophagy," reflects a quality-control function that culls defective mitochondria that accumulate in nondividing, respiring cells.[518] Similar, pexophagy can be induced by culturing the cells in a peroxisome proliferation medium to post-log phase (Farré J-C, unpublished results). Along these lines, it should also be realized that selective types of autophagy continuously occur at a low level under noninducing conditions. Thus, organelles such as peroxisomes have a finite life span and are turned over at a slow rate by autophagy-related pathways.[519]

Piecemeal microautophagy of the nucleus (PMN, also micronucleophagy) is another selective autophagic subtype, which targets portions of the nucleus for degradation.[520-522] In *S. cerevisiae*, the nuclear outer membrane, which is continuous with the nuclear ER, forms contact sites with the vacuolar membrane. These nucleus-vacuole junctions (NVJs) are generated by interaction of the outer nuclear membrane protein Nvj1 with the vacuolar protein Vac8.[523] Nvj1 further recruits the ER-membrane protein Tsc13, which is involved in the synthesis of very-long-chain fatty acids (VLCFAs) and Osh1, a member of a family of oxysterol-binding proteins. Upon starvation the NVJs bulge into the vacuole and subsequently a PMN-vesicle pinches off into the vacuole. PMN vesicles thus contain nuclear material and are limited by three membranes with the outermost derived from the vacuole, and the two inner ones from the nuclear ER. It is not clear which nuclear components are removed by PMN, but since PMN is not a cell death mechanism per se, most likely superfluous material is recycled. During PMN the NVJs are selectively incorporated into the PMN vesicles and degraded. Accordingly, PMN can be monitored using the proteins that are associated with the NVJs as markers. To quantitatively follow PMN, an assay analogous to the above-described GFP-Atg8/LC3 processing assay has been established using either GFP-Osh1 or Nvj1-GFP. These GFP chimeras are, together with the PMN-vesicles, degraded in the vacuole. Thus, the formation of the relatively proteolysis-resistant GFP detected in western blots correlates with the PMN rate. In fluorescence microscopy, PMN can be visualized with the same constructs, and a chimera of mCherry fused to a nuclear localization signal (NLS-mCherry) can also be used. To assure that the measured PMN rate is indeed due to selective micronucleophagy, appropriate controls such as cells lacking Nvj1 or Vac8 should be included. Detailed protocols for the described assays are provided in ref.524

b. **Reticulophagy and ribophagy**. Activation of the UPR in the ER in yeast induces a type of selective macroautophagy of the ER.[525-527] This process is termed reticulophagy to be consistent with the terms pexophagy and mitophagy.[527] Reticulophagy-associated autophagosomes are lamellar-membraned structures that contain ER proteins. In theory, since reticulophagy is selective, it should be able to sequester parts of the ER that are damaged, and eliminate protein aggregates that cannot be removed in other ways. Reticulophagy may also serve to limit the UPR, by reducing the ER to a normal level after a particular stress condition has ended. Some of the mutated dysferlin protein, LGMB2B/Miyoshi type muscle dystrophy, which accumulates in the ER, is degraded by ER-stress mediated reticulophagy.[528] In addition to activation of the UPR, PtdIns3P and its binding proteins could be good markers for reticulophagy.[437] Autophagy is also used for the selective removal of ribosomes.[529] This process can be monitored by western blot, following the generation of free GFP from Rpl25-GFP or the disappearance of ribosomal subunits such as Rps3. Vacuolar localization of Rpl25-GFP can also be seen by fluorescence microscopy.

Cautionary notes: The Cvt pathway has been demonstrated to occur only in yeast. In addition, the sequestration of prApe1 is specific, even under starvation conditions, as it involves the recognition of the propeptide by a receptor, Atg19, which in turn interacts with the scaffold protein Atg11.[530,531] Thus, unless the propeptide is removed, prApe1 is recognized as a selective substrate. Overexpression of prApe1 saturates import by the Cvt pathway, and the precursor form accumulates, but is rapidly matured upon autophagy induction.[218] In addition, mutants such as *vac8*Δ and *tlg2*Δ accumulate prApe1 under rich conditions, but not during autophagy.[380,532]Accordingly, it is possible to monitor the processing of prApe1 when overexpressed, or in certain mutant strains to follow autophagy induction. However, even the latter conditions may be misleading, as they do not indicate the size of the autophagosome. The Cvt complex (prApe1 bound to Atg19) is smaller than typical peroxisomes or mitochondrial fragments that are subject to autophagic degradation. Accordingly, particular mutants may display complete maturation of prApe1 under autophagy-inducing conditions, but may still have a defect in other types of selective autophagy, as well as being unable to induce a normal level of nonspecific autophagy.[63] For this reason, it is good practice to evaluate autophagosome size and number by TEM. Actually, it is much simpler to monitor autophagic bodies (rather than autophagosomes) in yeast. First, the vacuole is easily identified, making the identification of autophagic bodies much simpler. Second, autophagic bodies can be accumulated within the vacuole, allowing for an increased sample size. It is best to use a strain background that is *pep4*Δ *vps4*Δ to prevent the breakdown of the autophagic bodies, and to eliminate confounding vesicles from the multivesicular body pathway. One caveat to the detection of autophagic bodies, however, is that they may coalesce in the vacuole lumen, making it difficult to obtain an accurate quantification.

In general, when working with yeast it is preferable to use strains that have the marker proteins integrated into the chromosome rather than relying on plasmid-based expression, because plasmid numbers can vary from cell to cell. The GFP-Atg8, or similar, processing assay is easy to perform and is suitable for analysis by microscopy as well as western blotting; however, particular care is needed to obtain quantitative data for GFP-Atg8, Pex14-GFP or Om45-GFP, etc. processing assays (see cautionary notes for *GFP-Atg8/LC3 lysosomal delivery and proteolysis*). An alternative is an organelle targeted Pho8Δ60 assay. For example, mitoPho8Δ60 can be used to quantitatively measure mitophagy.[498] In addition, for the GFP-Atg8 processing assay, 2 h of starvation is generally sufficient to detect a significant level of free (i.e., vacuolar) GFP by western blotting as a measure of nonselective autophagy. For selective types of autophagy, the length of induction needed for a clearly detectable free GFP band will vary depending on the rate of cargo delivery to degradation. Usually 6 h of mitophagy induction is needed to be able to detect free GFP (e.g., from Om45-GFP) by western blot under starvation conditions, whereas stationary phase mitophagy typically requires 3 d before a free GFP band is observed.

c. **Vacuole import and degradation pathway**. In yeast, gluconeogenic enzymes such as fructose-1,6-bisphosphatase (Fbp1, also called FBPase), malate dehydrogenase (Mdh2), isocitrate lyase (Icl1) and phosphoenolpyruvate carboxykinase (Pck1) constitute the cargo of the vacuole import and degradation (Vid) pathway.[533] These enzymes are induced when yeast cells are glucose starved (grown in a medium containing 0.5% glucose and potassium acetate). Upon replenishing these cells with fresh glucose (a medium containing 2% glucose), these enzymes are degraded in either the proteasome[534-536] or the vacuole[533,537] depending on the duration of starvation. Following glucose replenishment after 3 d glucose starvation, the gluconeogenic enzymes are delivered to the vacuole for degradation.[538] These enzymes are sequestered in specialized 30- to 50-nm vesicles called Vid vesicles.[539] Vid vesicles can be purified by fractionation and gradient centrifugation; western blotting analysis using antibodies against organelle markers and Fbp1, and the subsequent verification of fractions by EM facilitate their identification.[539] Furthermore, the amount of marker proteins in the cytosol compared with the Vid vesicles can be examined by differential centrifugation. In this case, yeast cells are lysed and subjected to differential centrifugation. The Vid vesicle-enriched pellet fraction and the cytosolic supernatant fraction are examined with antibodies against Vid24, Vid30, Sec28 and Fbp1.[540-542]

Vid/endosomes containing their cargo aggregate around endocytic vesicles forming on the plasma membrane and are released into the cytoplasm. The Vid/endosomes can be purified by

dc_840_14

fractionation and density gradient centrifugation.[543] The fractions containing purified Vid/endosomes can be identified by western blot analysis using antibodies against Vid24, Fbp1 and the endosomal marker Pep12. The distribution of Vid vesicles containing cargo destined for endosomes, and finally for the vacuole, can be examined using FM 4–64, a lipophilic dye that stains endocytic compartments and the vacuole limiting membrane.[544] In these experiments, starved yeast cells are replenished with fresh glucose and FM 4–64, and cells are collected at appropriate time points for examination by fluorescence microscopy.[541] The site of degradation of the cargo in the vacuole can be determined by studying the distribution of Fbp1-GFP, or other Vid cargo markers in wild-type and *pep4*Δ cells.[545] Cells can also be examined for the distribution of Fbp1 at the ultrastructural level by immuno-TEM.[543]

As actin patch polymerization is required for the delivery of cargo to the vacuole in the Vid pathway, distribution of Vid vesicles containing cargo and actin patches can be examined by actin staining (with phalloidin conjugated to rhodamine) using fluorescence microscopy.[543] The distribution of GFP tagged protein and actin is examined by fluorescent microscopy. GFP-Vid24, Vid30-GFP and Sec28-GFP colocalize with actin during prolonged glucose starvation and for up to 30 min following glucose replenishment in wild-type cells; however, colocalization is less obvious by the 60 min time point.[540,543]

d. **Mammalian mitophagy and peroxisome degradation**. There is no consensus at the present time with regard to the best method for monitoring mammalian mitophagy. As with any organelle-specific form of autophagy, it is necessary to demonstrate: i) increased levels of autophagosomes containing mitochondria, ii) maturation of these autophagosomes to culminate with mitochondrial degradation, which can be blocked by specific inhibitors of autophagy or of lysosomal degradation, and iii) whether the changes are due to selective mitophagy or increased mitochondrial degradation during generalized autophagy. Techniques to address each of these points have been reviewed.[41]

Ultrastructural analysis at early time points can be used to establish selective mitophagy, although a maturation inhibitor may be needed to trap early autophagosomes with recognizable cargo (**Fig. 20**). Depending on the use of specific imaging techniques, dyes for living cells or antibodies for fixed cells have to be chosen. In any case, transfection of the autophagosomal marker GFP-LC3 and visualization of mitochondria (independent of their mitochondrial membrane potential) makes it possible to determine the association of these two cellular components. This may appear as fluorescence colocalization or as rings of GFP-LC3 surrounding mitochondria in higher resolution images. For live cell imaging microscopy, a method that marks mitochondria independently of mitochondrial membrane potential, such as MitoTracker® Green FM or transfection with a matrix-targeted fluorescent protein, should be used to detect mitochondrial structures. Antibodies that specifically recognize mitochondrial proteins such as VDAC, TOM20 or complex IV subunit I may be used to visualize mitochondria in immunohistochemical experimental procedures.[546,547] Colocalization analyses of mitochondria and autophagosomes provide an indication of the degree of sequestration. TEM can be used to demonstrate the presence of mitochondria within autophagosomes (referred to as mitophagosomes during mitophagy), and this can be coupled with bafilomycin A_1 treatment to prevent fusion with the lysosome.[41]

The fusion process of mitophagosomes with hydrolase-containing lysosomes represents the next step in the degradation process. To monitor the amount of fused organelles via live cell imaging microscopy, MitoTracker® Green FM, as a mitochondrial marker without significant membrane potential dependence and LysoTracker® Red DND-99 may be used to visualize the fusion process (**Fig. 21**). Independent of the cell-type specific concentration used for both dyes, we recommend exchanging MitoTracker® Green FM with normal medium after incubation

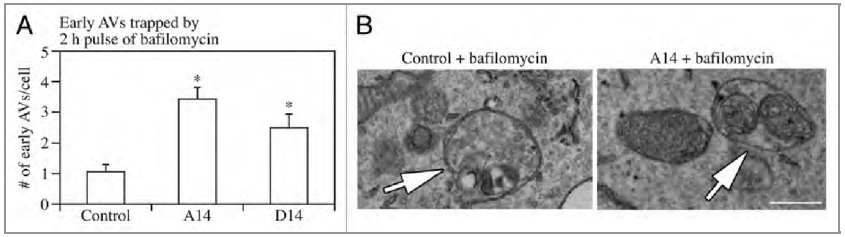


Figure 20. Autophagosomes with recognizable cargo are rare in cells. (A) To assess relative rates of autophagosome formation, the fusion inhibitor bafilomycin A_1 (10 nM) was applied for 2 h prior to fixation with 2% glutaraldehyde in order to trap newly formed autophagosomes. Two different PINK1 shRNA lines exhibit increased AV formation over 2 h compared with the control shRNA line. *$p > 0.05$ vs. Control. (B) Autophagosomes in bafilomycin A_1-treated control cells contain a variety of cytoplasmic structures (left, arrow), while mitochondria comprise a prominent component of autophagosomes in A14 bafilomycin A_1-treated (PINK1 shRNA) cells (right, arrow). Scale bar, 500 nm. These data indicate induction of selective mitophagy in PINK1-deficient cells. This figure was modified from **Figure 2** published in Chu CT. A pivotal role for PINK1 and autophagy in mitochondrial quality control: implications for Parkinson disease. *Human Molecular Genetics* 2010; 19:R28-R37.

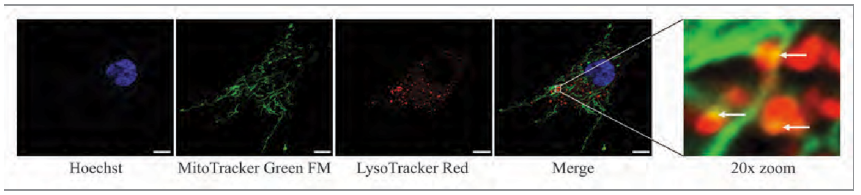


Figure 21. Human fibroblasts showing colocalization of mitochondria with lysosomes. The degree of colocalization of mitochondria with lysosomes in human fibroblasts was measured via live cell imaging microscopy at 37°C and 5% CO_2 atmosphere using the ApoTome® technique. LysoTracker® Red DND-99 staining was applied to mark lysosomal structures (red), and MitoTracker® Green FM to visualize mitochondria (green). Hoechst 33342 dye was used to stain nuclei (blue). A positive colocalization is indicated by yellow signals (merge) due to the overlap of LysoTracker® Red and MitoTracker® Green staining (white arrows). Scale bar, 10 µm. Statistical evaluation is performed by calculating the Pearson's coefficient for colocalizing pixels. Image provided by L. Burbulla and R. Krüger.

with the dye, whereas it is best to maintain the LysoTracker® Red staining in the incubation medium during the acquisition of images. For immuncytochemical experiments, antibodies specific for mitochondrial proteins and an antibody against the lysosomal-associated membrane protein 1 (LAMP1) can be used. Overlapping signals appear as a merged color and can be used as indicators for successful fusion of autophagosomes that contain mitochondria with lysosomal structures.[548] To measure the correlation between two variables by imaging techniques, such as the colocalization of two different stainings, we recommend some form of correlation analysis to assess the value correlating with the strength of the association. This may use, for example, ImageJ software, or other colocalization scores that can be derived from consideration not only of pixel colocalization, but also from a determination that the structures have the appropriate shape. During live-cell imaging, the two structures should move together in more than one frame. Mitophagy can also be quantitatively monitored using a mitochondria-targeted version of the pH-dependent Keima protein.[549] The peak of the excitation spectrum of the protein shifts from 440 nm to 586 nm when mitochondria are delivered to acidic lysosomes, which allows easy quantification of mitophagy (**Fig. 22**). However, it should be noted that long exposure times of the specimen to intense laser light lead to a similar spectral change.

The third and last step of the degradation process is the monitoring of the amount of remaining mitochondria by analyzing the mitochondrial mass. This final step provides the opportunity to determine the efficiency of degradation of dysfunctional, aged or impaired mitochondria. Mitochondrial mass can either be measured by a FACS technique using MitoTracker® Green FM or, on a single cell basis, by either live cell imaging or immuncytochemistry with use of MitoTracker® Green FM or MitoTracker® Red FM for the former, and antibodies specifically raised against different mitochondrial proteins for the latter.[1] Immunoblot analysis of the levels of mitochondrial proteins from different mitochondrial subcompartments is valuable for validating the data from FACS or microscopy studies. EM can also be used to verify loss of entire mitochondria, and PCR (or fluorescence microscopy) to quantify mitochondrial DNA.

In addition to monitoring the steady-state levels of different steps of mitophagy, investigation of the mitophagic flux is needed to decipher which steps within this process potentially fail to

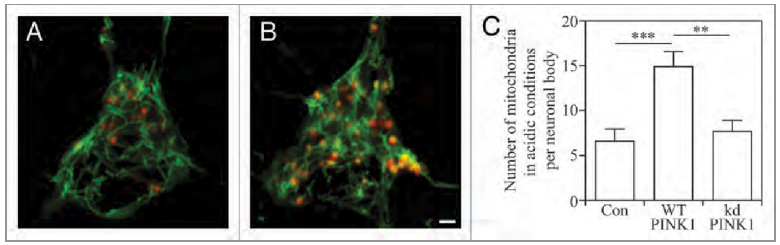


Figure 22. Detection of mitophagy in primary cortical neurons using mitochondria-targeted Keima. Neurons transfected with mito-Keima were visualized using 458 nm (green, mitochondria at neutral pH) and 561 nm (red, mitochondria in acidic pH) laser lines and 575 nm band pass filter. Compared with the control (A) wild-type PINK1 overexpression (B) increases the number of the mitochondria exposed to acidic conditions. Scale bar, 2 µm. (C) Quantification of red dots suggests increased mitophagy in wild-type PINK1 but not in the kinase dead $PINK1^{K219M}$-overexpressing neurons. Figure provided by V. Choubey and A. Kaasik.

dc_840_14

result in efficient mitochondrial degradation. Therefore, appropriate treatment may be applied to prevent mitochondrial degradation at distinct steps of the process.

Certain cellular models require stress conditions to measure the mitochondrial degradation capacity, as basal levels are too low to reliably assess organelle clearance. Hence, it may be useful to pretreat the cells with uncoupling agents, such as CCCP that stimulate mitochondrial degradation and allow measurements of mitophagic activity; however, it should be kept in mind that, although helpful to stimulate mitochondrial degradation, this treatment is not physiological. Another method to induce mitophagy is by expressing and activating a mitochondrially-localized fluorescent protein photosensitizer such as Killer Red.[550] The excitation of Killer Red results in an acute increase of superoxide that causes mitochondrial damage resulting in mitophagy (Kim PK, unpublished results). The advantage of using a genetically encoded photosensitizer is that it allows for both spatial and temporal control in inducing mitophagy.

Relatively little work has been done in the area of mammalian peroxisome degradation by autophagy, and at present it is not known if this is a selective process. Typically, peroxisomes are induced by treatment with hypolipidemic drugs such as clofibrate or dioctyl phthalate, and degradation is induced by drug withdrawal, although starvation without prior proliferation can also be used. Loss of peroxisomes can be followed enzymatically or by immunoblot, monitoring enzymes such as fatty acyl-CoA oxidase (note that this enzyme is sometimes abbreviated "AOX," but should not be confused with the enzyme alcohol oxidase that is frequently used in assays for yeast pexophagy) or catalase, and also by EM.[551,552] Finally, a HaloTag$^{®}$-PTS1 marker that is targeted to peroxisomes has been used to fluorescently label the organelle.[553]

Cautionary notes: There are many assays that can be used to monitor specific types of autophagy, but caution must be used in choosing an appropriate marker(s). It is best to monitor more than one protein, and to include an inner membrane or matrix component in the analysis. In particular, it is not sufficient to follow a single mitochondrial outer membrane protein because these can be degraded independently of mitophagy. Although the localization of PARK2 (PARKIN) to mitochondria as monitored by fluorescence microscopy is associated with the early stages of protonophore uncoupler (CCCP)-driven mitochondria degradation,[169] this by itself cannot be used as a marker for mitophagy, as these events can be dissociated.[554] PARK2 translocates to damaged mitochondria and ubiquitinates a wide range of outer membrane proteins including VDAC1, MFN1/2 and TOMM20 (TOM20).[547,555-557] This results in the preferential degradation of mitochondrial outer membrane proteins by the proteasome, while inner membrane proteins and mitochondrial DNA[558] remain intact. Monitoring loss of a single protein such as TOM20 by western blot or fluorescence microscopy to follow mitophagy may thus be misleading.[555] MitoTracker dyes are widely used to stain mitochondria and, when colocalized with GFP-LC3, they can function as a marker for mitophagy. However, staining with certain MitoTracker dyes depends on mitochondrial activity and membrane potential, so that damaged, or sequestered nonfunctional mitochondria may not be stained.

Although it is widely assumed that macroautophagy is the major mechanism for degradation of entire organelles, there are multiple mechanisms that may account for the disappearance of mitochondrial markers. These include proteasomal degradation of outer membrane proteins and/or proteins that fail to correctly translocate into the mitochondria, degradation due to proteases within the mitochondria, and reduced biosynthesis or import of proteins. In addition to mitophagy, mitochondria can be eliminated by extrusion from the cell (mitoptosis).[559] Thus, it is advisable to use a variety of complementary methods to monitor mitochondria loss including TEM, single cell analysis of LC3 fluorescent puncta, and western blot, in conjunction with flux inhibitors and specific inhibitors of autophagy induction compared with inhibitors of the other major degradation systems (see cautions in *Autophagy inhibitors and inducers*).

Likewise, although the mechanism(s) of peroxisome degradation in mammals awaits further elucidation, it can occur by both autophagic and proteasome-dependent mechanisms.[560] Thus, controls are needed to determine the extent of degradation that is due to the proteasome. Moreover, two additional degradation mechanisms have been suggested: the action of the peroxisome-specific Lon protease and the membrane disruption effect of 15-lipoxygenase.[561]

e. **Aggrephagy**. Aggrephagy is the selective removal of aggregates by macroautophagy.[562] This process can be followed in vitro (in cell culture) and in vivo (in mice) by monitoring the levels of an aggregate-prone protein such as an expanded polyglutamine (polyQ)-containing protein or mutant SNCA (α-synuclein). Levels are quantified by immunofluorescence or traditional immunoblot. Similarly, fluorescently tagged aggregated proteins such as polyQ80-CFP can be monitored via immunoblot and immunofluorescence. A polyQ80-luciferase reporter, which forms aggregates, can also be used to follow aggrephagy.[563] A nonaggregating polyQ19-luciferase or untagged full-length luciferase serves as a control. The ratio of luciferase activity from these two constructs can be calculated to determine autophagic flux.

Autophagic degradation of endogenous aggregates such as lipofuscin can in some cell types be monitored by fluorescence microscopy, utilizing the autofluorescence of lipofuscin particles. The amount of lipofuscin in primary human adipocytes can be reduced by activation of autophagy, and the amount of lipofuscin is dramatically reduced in adipocytes from patients with type 2 diabetes and chronically enhanced autophagy.[209]

Cautionary notes: Caution must be used when performing immunoblots of aggregated proteins, as many protein aggregates fail to enter the resolving gel and are retained in the stacking gel. In addition, the polyQ80-luciferase in the aggregated state lacks luciferase activity whereas soluble polyQ80-luciferase retains activity. Therefore, caution must be used when interpreting results with these vectors, as treatments that increase aggrephagy or enhance protein aggregation can lead to a decrease in luciferase activity.[564] Finally, soluble polyQ reporters can be degraded by the proteasome; thus, changes in the ratio of polyQ19-luciferase:polyQ80-luciferase may also reflect proteasomal effects and not just changes in autophagic flux.

f. ***Xenophagy***. The macroautophagy pathway has emerged as an important cellular factor in both innate and adaptive immunity. Many in vitro and in vivo studies have demonstrated that genes encoding macroautophagy components are required for host defense against infection by bacteria, parasites and viruses. Macroautophagy may be defective in human diseases such as inflammatory bowel disease, since genes encoding essential macroautophagy components have been linked to the disease. Xenophagy is often used as a term to describe autophagy of microbial pathogens, mediating their capture and delivery to lysosomes for degradation. Since xenophagy presents an immune defense, it is not surprising that microbial pathogens have evolved strategies to overcome it. The interactions of such pathogens with the autophagy system of host cells are complex and have been the subject of several excellent reviews.[76-81,565-570] Here we will make note of a few key considerations when studying interactions of microbial pathogens with the autophagy system.

LC3 is commonly used as a marker of macroautophagy. However, studies have established that LC3 can promote phagosome maturation independently of macroautophagy through LC3-associated phagocytosis (see cautionary notes in *Atg8/LC3 detection and quantification*). Other studies show that macroautophagy of *Salmonella* Typhimurium is dependent on Atg9, an essential macroautophagy gene, whereas LC3 recruitment to bacteria does not require Atg9.[571] In contrast, macroautophagy of these bacteria requires ubiquitination of target proteins (not yet identified) and recruitment of three ubiquitin-binding adaptor proteins, p62/SQSTM1,[572] NDP52[573] and OPTN.[574] Therefore, the currently available criteria to differentiate LAP from macroautophagy include: i) LAP involves LC3 recruitment to bacteria in a manner that requires reactive oxygen species production by an NADPH oxidase. It should be noted that most cells express at least one member of the NADPH oxidase (also known as NOX) family. Targeting expression of the common p22^{phox} subunit is an effective way to disrupt the NOX NADPH oxidases. Scavenging of reactive oxygen species by antioxidants such as resveratrol and α-tocopherol is also an effective way to inhibit LAP. In contrast, N-acetylcysteine, which raises cellular glutathione levels, does not inhibit LAP.[575] ii) Macroautophagy of bacteria requires Atg9, while LAP apparently does not.[571] iii) LAP involves single-membrane structures. For LAP, CLEM (with LC3 as a marker) is expected to show single-membrane structures that are LC3^{+} with LAP.[131] In contrast, macroautophagy is expected to generate double-membrane structures surrounding cargo (which may include single membrane phagosomes, giving rise to triple-membrane structures[571]). iv) Macroautophagy of bacteria requires protein ubiquitination and ubiquitin-binding adaptors (p62/SQSTM1, NDP52, OPTN, and possibly others), whereas LAP does not. It is anticipated that more specific markers of LAP will be identified as these phagosomes are further characterized.

Nonmotile *Listeria monocytogenes* can be targeted to double-membrane autophagosomes upon antibiotic treatment,[576] which indicates that macroautophagy serves as a cellular defense to microbes in the cytosol. However, subsequent studies have revealed that macroautophagy can also target pathogens within phagosomes, damaged phagosomes or the cytosol. Therefore, when studying microbial interactions by EM, many structures can be visualized, with any number of membranes encompassing microbes, all of which may be LC3^{+}.[577] As discussed above, single-membrane structures that are LC3^{+} may arise through LAP, and we cannot rule out the possibility that both LAP and macroautophagy may operate at the same time to target the same phagosome.

Viruses can also be targeted by autophagy, and in turn can act to inhibit autophagy. For example, infection of a cell by influenza and dengue viruses[578] or enforced expression of the hepatitis B virus C protein[579] have profound consequences for autophagy, as viral proteins such as NS4A stimulate autophagy and protect the infected cell against apoptosis, thus extending the time in which the virus can replicate. Conversely, the herpes simplex virus ICP34.5 protein inhibits autophagy by targeting BECN1.[580] While the impact of ICP34.5's targeting of BECN1 on virus replication in cultured permissive cells is minimal, it has a significant impact upon pathogenesis in vivo, most likely through interfering with activation of CD4^{+} T cells.[581,582] Care must be taken in determining the role of autophagy in virus replication, as some viruses such as vaccinia use double-membrane structures that form independently of the autophagy machinery.[583] Similarly, dengue virus replication, which appears to involve a double-membrane compartment, requires the ER rather than autophagosomes,[584] whereas coronaviruses use a non-lipidated version of LC3 (see *Atg8/LC3 detection and quantification*).[137] Yet another type of variation is seen with hepatitis C virus, which requires BECN1, ATG4B, ATG5 and ATG12 for initiating replication, but does not require these proteins once an infection is established.[585]

Finally, it is important to realize that there may be other macroautophagy-like pathways that have yet to be characterized. For example, in response to cytotoxic stress (treatment with etoposide), autophagosomes are formed in an ATG5- and ATG7-independent manner.[26] While this does not rule out involvement of other macroautophagy regulators/components in the formation of these autophagosomes, it does establish that the canonical macroautophagy pathway involving LC3 conjugation is not involved. In contrast, RAB9 is required for this alternative pathway, potentially providing a useful marker for analysis of these structures. Returning to xenophagy, *Mycobacterium tuberculosis* can be targeted to autophagosomes in an ATG5-independent manner.[586] Furthermore, up to 25% of intracellular *Salmonella typhimurium* are observed in multilamellar membrane structures resembling autophagosomes in *Atg5*$^{-/-}$ MEFs.[572] These findings indicate that an alternate macroautophagy pathway is relevant to host-pathogen interactions. Moreover, differences are observed that depend on the cell type being studied. *Yersinia pseudotuberculosis* is targeted to autophagosomes where they can replicate in bone marrow-derived macrophages,[587] whereas in RAW264.7 and J774 cells, bacteria are targeted both to autophagosomes, and

©2012 Landes Bioscience. Do not distribute
dc_840_14

LC3-negative, single-membrane vacuoles (Lafont F, personal communication).

g. ***Lipophagy***. The specific macroautophagic degradation of lipid droplets represents another type of selective autophagy.[588] Lipophagy requires the core autophagic machinery and can be monitored by following triglyceride content, or total lipid levels using BODIPY 493/503 or HCS LipidTOX neutral lipid stains with fluorescence microscopy, cell staining with Oil Red O, or ideally label-free techniques such as CARS or SRS microscopy. TEM can also be used to monitor lipid droplet size and number.

Cautionary notes: With regard to changes in the cellular neutral lipid content, the presence and potential activation of cytoplasmic lipases that are unrelated to lysosomal degradation must be considered.

h. ***Zymophagy***. Zymophagy is a protective mechanism induced during pancreatitis that results in the selective degradation of activated zymogen granules, which are deleterious for the pancreatic acinar cells.[589] This process can be monitored by TEM, identifying autophagosomes containing secretory granules, by following p62 degradation by western blot, and by examining the subcellular localization of VMP1-EGFP, which relocates to granular areas of the cell upon zymophagy induction. Colocalization of trypsinogen (which is packaged within zymogen granules) and LC3, or of GFP-ubiquitin (which is recruited to the activated granules) with RFP-LC3 can also be observed by indirect or direct immunofluorescence microscopy, respectively.

i. ***Allophagy***. In metazoans, mitochondria, and hence mitochondrial DNA, from the sperm is eliminated by an autophagic process. This process of allogeneic (nonself) organelle autophagy is termed "allophagy."[590,591] During allophagy in *C. elegans*, both paternal mitochondria and membranous organelles (a sperm-specific membrane compartment) are eliminated by the 16-cell stage (100–120 min post-fertilization).[592,593] The degradation process can be monitored in living embryos with GFP::ubiquitin, which appears in the vicinity of the sperm chromatin (labeled for example with mCherry-histone H2B) on the membranous organelles within 3 min after fertilization. GFP fusions and antibodies specific for LGG-1 and LGG-2 (Atg8/LC3 homologs), which appear next to the sperm DNA, membranous organelles and mitochondria (labeled with CMXRos or mitochondria-targeted GFP) within 15 to 30 min post-fertilization, can be used to verify the autophagic nature of the degradation. TEM can also be utilized to demonstrate the presence of mitochondria within autophagosomes in the early embryo.

Conclusion: There are many assays that can be used to monitor specific types of autophagy, but caution must be used in choosing an appropriate marker(s). The potential role of other degradative pathways for any individual organelle or cargo marker should be considered, and it is advisable to use more than one marker or technique.

9. *Autophagic sequestration assays*. Autophagic activity can also be monitored by the sequestration of autophagic cargo, using either an (electro)injected, inert cytosolic marker such as [^{3}H]raffinose,[594] or an endogenous cytosolic protein such as lactate dehydrogenase (LDH),[595] in the latter case along with treatment with a protease inhibitor (e.g., leupeptin) to prevent intralysosomal degradation of the protein marker. The assay simply measures the transfer of cargo from the soluble (cytosol) to the insoluble (sedimentable) cell fraction (which includes autophagic compartments), with no need for a sophisticated subcellular fractionation (a filtration assay would presumably work just as well as centrifugation, although it would be necessary to verify that the filtration membrane does not destroy the integrity of the postnuclear supernatant compartments). The cargo marker can be quantified by an enzymatic assay, or by western blotting. In principle, any intracellular component can be used as a cargo marker, but cytosolic enzymes having low sedimentable backgrounds are preferable. Membrane-associated markers are less suitable, and proteins such as LC3, which are part of the sequestering system itself, will have a much more complex relationship to the autophagic flux than a pure cargo marker such as LDH.

In yeast, sequestration assays are typically done by monitoring protease protection of an autophagosome marker or a cargo protein. For example, prApe1, and GFP-Atg8 have been used to follow completion of the autophagosome.[596] The relative resistance or sensitivity to an exogenous protease in the absence of detergent is an indication of whether the autophagosome (or other sequestering vesicle) is complete or incomplete, respectively. Thus, this method also distinguishes between a block in autophagosome formation vs. fusion with the vacuole. The critical issues to keep in mind involve the use of appropriate control strains and/or proteins, and deciding on the correct reporter protein. In addition to protease protection assays, sequestration can be monitored by fluorescence microscopy during pexophagy of methanol-induced peroxisomes, using GFP-Atg8 as a pexophagosome marker, and BFP-SKL to label the peroxisomes. The vacuolar sequestration process during micropexophagy can also be monitored by formation of the vacuolar sequestration membrane (VSM) stained with FM 4–64.[501,507]

Sequestration assays can be designed to measure flux through individual steps of the autophagy pathway. For example, intralysosomally degraded sequestration probes such as [^{14}C]-lactate or LDH will mark prelysosomal compartments in the absence of degradation inhibitors. Hence, their accumulation in such compartments can be observed when fusion with lysosomes is suppressed, for example, by a microtubule inhibitor such as vinblastine.[597] Furthermore, lactate hydrolysis can be used to monitor the overall autophagic pathway (autophagic lactolysis).[598] One caveat, however, is that inhibitors may affect sequestration indirectly, for example, by modifying the uptake and metabolism (including protein synthesis) of autophagy-suppressive amino acids (see *Autophagy inhibitors and inducers*).

A variation of this approach applicable to mammalian cells includes live cell imaging. Autophagy induction is monitored as the movement of cargo, such as mitochondria, to GFP-LC3-colocalizing compartments, and then fusion/flux is measured by delivery of cargo to lysosomal compartments.[258,599] In addition, sequestration of fluorescently tagged cytosolic proteins into membranous compartments can be measured, as fluorescent puncta become resistant to the detergent digitonin.[600] Use of multiple time points and monitoring colocalization of a particular cargo with GFP-LC3 and lysosomes can also be used to assess sequestration of cargo with autophagosomes as well as delivery to lysosomes.[601]

Cautionary notes: The electro-injection of radiolabeled probes is technically demanding, but the use of an endogenous cytosolic protein probe is very simple and requires no pretreatment of the cells other than with a protease inhibitor. Another concern with electro-injection is that it can affect cellular physiology, so it is necessary to verify that the cells behave properly under control situations such as amino acid deprivation. An alternate approach for incorporating exogenous proteins into mammalian cell cytosol is to use "scrape-loading," a method that works for cells that are adherent to tissue culture plates.[602] Finally, these assays work well with hepatocytes but may be problematic with other cell types, and it can be difficult to load the cell while retaining the integrity of the compartments in the post-nuclear supernatant (Tooze S, unpublished results). General points of caution to be addressed with regard to live cell imaging relate to photobleaching of the fluorophore, cell injury due to repetitive imaging, autofluorescence in tissues containing lipofuscin, and the pH sensitivity of the fluorophore.

There are several issues to keep in mind when monitoring sequestration by the protease protection assay in yeast.[596] First, as discussed in *Selective types of autophagy*, prApe1 is not an accurate marker for nonspecific autophagy; import of prApe1 utilizes a receptor (Atg19) and a scaffold (Atg11) that make the process specific. In addition, vesicles that are substantially smaller than autophagosomes can effectively sequester the Cvt complex. Another problem is that prApe1 cannot be used as an autophagy reporter for mutants that are not defective in the Cvt pathway, although this can be bypassed by using a *vac8*Δ background.[603] At present, the prApe1 assay cannot be used in any system other than yeast. The GFP-Atg8 protease protection assay avoids these problems, but the signal-to-noise ratio is typically substantially higher. In theory, it should be possible to use this assay in other cell types, but at present no publications report its use other than in yeast.

Conclusion: Sequestration assays present another valid method for monitoring autophagy, and in particular for discriminating between conditions where the autophagosome is complete (but not fused with the lysosome/vacuole) or open (i.e., a phagophore). These assays can also be modified to measure autophagic flux.

10. *Turnover of autophagic compartments*. Inhibitors of autophagic sequestration (e.g., amino acids, 3-MA or wortmannin) can be used to monitor the disappearance of autophagic elements (phagophores, autophagosomes, autolysosomes) to estimate their half-life by TEM morphometry/stereology. The turnover of the autophagosome or the autolysosome will be differentially affected if fusion or intralysosomal degradation is inhibited.[14,16,24,604] The duration of such experiments is usually only a few hours; therefore, long-term side effects or declining effectiveness of the inhibitors can be avoided. It should be noted that fluorescence microscopy has also been used to monitor the half-life of autophagosomes, monitoring GFP-LC3 in the presence and absence of bafilomycin A_1 or following GFP-LC3 after starvation and recovery in amino acid-rich medium (see *Atg8/LC3 detection and quantification*).[18,605]

Cautionary notes: The inhibitory effect must be strong and the efficiency of the inhibitor needs to be tested under the experimental conditions to be employed. Cycloheximide is sometimes used as an autophagy inhibitor, but this is problematic because of the many potential indirect effects. Cycloheximide inhibits translational elongation, and therefore protein synthesis. In addition, it decreases the efficiency of protein degradation in several cell types (Cuervo AM, personal communication) including hematopoietic cells (Edinger A, personal communication). Treatment with cycloheximide causes a potent increase in TORC1 activity, which can decrease autophagy in part as a result of the increase in the amino acid pool resulting from suppressed protein synthesis (Shen H-M, personal communication).[606,607] In addition, at high concentrations (in the millimolar range) cycloheximide inhibits complex I of the mitochondrial respiratory chain,[608,609] but this is not a problem, at least in hepatocytes, at low concentrations (10 -20 μM) that are sufficient to prevent protein synthesis (Meijer AJ, personal communication).

Conclusion: The turnover of autophagic compartments is valid, but less preferred method, for monitoring flux, and cycloheximide must be used in these experiments with caution.

11. *Autophagosome-lysosome colocalization and dequenching assay*. Another method to demonstrate the convergence of the autophagic pathway with a functional degradative compartment is to incubate cells with the bovine serum albumin derivative, dequenched (DQ)-BSA that has been labeled with the red-fluorescent BODIPY TR-X dye; this conjugate will accumulate in lysosomes. The labeling of DQ-BSA is so extensive that the fluorophore is self-quenched. Proteolysis of this compound results in dequenching and the release of brightly fluorescent fragments. Thus, DQ-BSA is useful for detecting intracellular proteolytic activity as a measure of a functional lysosome.[610]

Furthermore, DQ-BSA labeling can be combined with GFP-LC3 to monitor colocalization, and thus visualize the convergence, of amphisomes with a functional degradative compartment (DQ-BSA is internalized by endocytosis). This method can also be used to visualize fusion events in real-time experiments by confocal microscopy (live cell imaging). Along similar lines, other approaches for monitoring convergence are to follow the colocalization of RFP-LC3 and LysoSensor Green (Bains M, Heidenreich KA, personal communication), mCherry-LC3 and LysoSensor Blue,[259] or tagged versions of LC3 and LAMP1 (Macleod K, personal communication) or CD63[258] as a measure of the fusion of autophagosomes with lysosomes. It is also possible to trace autophagic events by visualizing the pH-dependent excitation changes of the coral protein Keima.[549] This quantitative technique is capable of monitoring the fusion of autophagosomes with lysosomes, that is, the formation of an autolysosome, and the assay does not depend on the analysis of LC3.

Cautionary notes: Some experiments require the use of inhibitors (e.g., 3-MA or wortmannin) or overexpression of proteins (e.g., RAB7 dominant negative mutants) that may also affect the

dc_840_14

endocytic pathway or the delivery of DQ-BSA to lysosomes (e.g., wortmannin causes the swelling of late endosomes[611]). In this case, the lysosomal compartment can be labeled with DQ-BSA overnight before treating the cells with the drugs, or prior to the transfection.

Conclusion: DQ-BSA provides a relatively convenient means for monitoring lysosomal protease function, and can also be used to follow the fusion of amphisomes with the lysosome. Colocalization of autophagosomes (fluorescently tagged LC3) with lysosomal proteins or dyes can also be monitored.

12. *Tissue fractionation.* The study of autophagy in the organs of larger animals, in large numbers of organisms with very similar characteristics, or in tissue culture cells provides an opportunity to use tissue fractionation techniques as has been possible with autophagy in rat liver.[34,48,612-617] Because of their sizes [smaller than nuclei but larger than membrane fragments (microsomes)], differential centrifugation can be used to obtain a subcellular fraction enriched in mitochondria and organelles of the autophagic-lysosomal system, which can then be subjected to density gradient centrifugation to enrich autophagosomes, amphisomes, autolysosomes and lysosomes.[34,48,617-621] Any part of such a fraction can be considered to be a representative sample of tissue constituents and used in quantitative biochemical, centrifugational and morphological studies of autophagic particle populations.

The simplest studies of the autophagic process take advantage of sequestered marker enzymes, changes in location of these enzymes, differences in particle/compartment size and differential sensitivity of particles of different sizes to mechanical and osmotic stress (for example, acid hydrolases are found primarily in membrane-bound compartments and their latent activities cannot be measured unless these membranes are lysed). Such a change in enzyme accessibility can be used to follow the time course of an exogenously induced, or naturally occurring, autophagic process.[612,614,616]

Quantitative localization of enzymatic activity (or any other marker) to specific cytoplasmic particle populations and changes in the location of such markers during autophagy can be performed using rate sedimentation ultracentrifugation (see *Autophagic sequestration assays*).[618] Similar results can be obtained with isopycnic centrifugation where particles enter a density gradient (sometimes made with sucrose but iso-osmotic media such as iodixanol, metrizamide and Nycodenz may be preferred as discussed below under *Cautionary notes*) and are centrifuged until they reach locations in the gradient where their densities are equal to those of the gradient.[618]

The fractionation of organelles can also be evaluated by protein-correlation-profiling (PCP), a quantitative mass spectrometry-based proteomics approach. Similar to the biochemical assays described above, gradient profiles of marker proteins can be recorded and compared with proteins of interest.[278] Compared with classical biochemical approaches, PCP allows the proteome-wide recording of protein gradient profiles.

Particle populations in subcellular fractions evaluated with quantitative biochemical and centrifugational approaches can also be studied with quantitative morphological methods. Detailed morphological study of the particle populations involved in the autophagic process usually requires the use of EM. The thin sections required for such studies pose major sampling problems in both intact cells[622] and subcellular fractions.[618] With the latter, 2,000,000 sections can be obtained from each 0.1 ml of pellet volume, so any practical sample size is an infinitesimally small subsample of the total sample.[618] However, through homogenization and resuspension, complex and heterogeneous components of subcellular fractions become randomly distributed throughout the fraction volume. Therefore, any aliquot of that volume can be considered a random sample of the whole volume. What is necessary is to conserve this property of subcellular fractions in the generation of a specimen that can be examined with the electron microscope. This can be done with the use of a pressure filtration procedure.[618,623] Because of the thinness of the sections, multiple sections of individual particles are possible so morphometric/stereological methods[622] must be used to determine the volume occupied by a given class of particles, as well as the size distribution and average size of the particle class. From this information the number of particles in a specific particle class can be calculated.[624] Examination of individual profiles gives information on the contents of different types of particles and their degree of degradation, as well as their enclosing membranes.[612,614]

Cautionary notes: When isolating organelles from tissues and cells in culture it is essential to use disruption methods that do not alter the membrane of lysosomes and autophagosomes, compartments that are particularly sensitive to some of those procedures. For example teflon/glass motor homogenization is suitable for tissues with abundant connective tissue, such as liver, but for circulating cells or cells in culture, disruption by nitrogen cavitation is a good method to preserve lysosomal membrane stability;[625] however, this method is not suitable for small samples and may not be readily available. Other methods, including "Balch" or "Dounce" homogenizers also work well.[626,627] During the isolation procedure it is essential to always use iso-osmotic solutions to avoid hypotonic or hypertonic disruption of the organelles. In that respect, because lysosomes are able to take up sucrose if it is present at high concentrations, the use of sucrose gradients for the isolation of intact lysosome-related organelles is strongly discouraged.

As with the isolation of any other intracellular organelle, it is essential to assess the purity of each preparation, as there is often considerable variability from experiment to experiment due to the many steps involved in the process. Correction for purity can be done through calculation of recovery (percentage of the total activity present in the homogenate) and enrichment (dividing by the specific activity in the homogenate) of enzymes or protein markers for those compartments (e.g., β-hexosaminidase is routinely used to assess lysosomal purity, but enzymes such as cathepsin B may also be used and may provide more accurate readouts).[625] Because of the time-consuming nature of quantitative morphological studies, such studies should not be performed until simpler biochemical procedures have established the circumstances most likely to give meaningful morphometric/stereological results.

Finally, it is worthwhile noting that not all lysosomes are alike. For example, there are differences among primary lysosomes, autolysosomes and telolysosomes. Furthermore, what we refer to as "lysosomes" are actually a very heterogeneous pool of organelles that simply fulfill five classical criteria, having a pH < 5.6, mature cathepsins, the presence of LAMP proteins, a single membrane, and the absence of endosomal and recycling compartment markers (e.g., the mannose-6-phosphate receptor or RAB5). But even applying those criteria we can separate lysosomes with clear differences in their proteome and other properties, and these distinct populations of lysosomes are likely to participate in different functions in the cell (see *Chaperone-mediated autophagy*).[628]

Conclusion: Considering the limited methods available for in vivo analysis of autophagy, tissue fractionation is a valid, although relatively laborious, method for monitoring autophagy. Care must be taken to ensure that sample analysis is representative.

13. *Analyses in vivo.* Monitoring autophagic flux in vivo or in organs is one of the least developed areas at present, and ideal methods relative to the techniques possible with cell culture may not exist. Importantly, the level of basal autophagy, time course of autophagic induction, and the bioavailabilty of autophagy-stimulating and -inhibiting drugs is likely tissue specific. Moreover, basal autophagy or sensitivity to autophagic induction may vary with animal age, sex or strain background. Therefore methods may need to be optimized for the tissue of interest. One method for in vivo studies is the analysis of GFP-LC3/Atg8 (see *GFP-Atg8/LC3 fluorescence microscopy* above). Autophagy can be monitored in tissue (e.g., skeletal muscle, liver and retina) in vivo in transgenic mice systemically expressing GFP-LC3,[126,446] or in other models by transfection with GFP-LC3 plasmids.[346] In addition, tissue-specific GFP-LC3 mice have been generated for monitoring cardiac myocytes.[629,630] In these settings, GFP fluorescent puncta are indicative of autophagic structures. In addition, cleavage of GFP-LC3 to generate free GFP can be evaluated. This has been successfully performed in mouse liver,[172,631] suggesting the GFP-LC3 cleavage assay may also be applied to in vivo studies. Alternatively, confocal laser scanning microscopy, which makes it possible to obtain numerous sections and substantial data about spatial localization features, can be a suitable system for studying autophagic structures (especially for whole mount embryo in vivo analysis).[632] In addition, this method can be used to obtain quantitative data through densitometric analysis of fluorescent signals.[633]

Another possibility is immunohistochemical staining, an important procedure that may be applicable to human studies as well considering the role of autophagy in neurodegeneration, myopathies and cardiac disease where samples may be limited to biopsy/autopsy tissue. Immunodetection of LC3 as definite puncta is possible in paraffin-embedded tissue sections and fresh frozen tissue, by either immunohistochemistry or immunofluorescence;[140,634-637] however, this methodology has not received extensive evaluation, and does not lend itself well to dynamic assays. Other autophagic substrates can be evaluated via immunohistochemistry and include p62, NBR1, ubiquitinated inclusions and protein aggregates. Similarly, autophagy can be evaluated by measuring levels of these autophagic substrates via traditional immunoblot; however, their presence or absence needs to be cautiously interpreted as some of these substrates can accumulate with either an increase or a decrease in autophagic flux (see *p62 and related LC3 binding protein turnover assays*). Bone marrow transfer has been used to document in vivo the role of autophagy in the reverse cholesterol transport pathway from peripheral tissues or cells (e.g., macrophages) to the liver for secretion in bile and for excretion,[638] and a study shows that transglutaminase type 2 protein levels decrease in mouse liver in vivo upon starvation in an autophagy-dependent manner (and in human cell lines in vitro in response to various stimuli; Piacentini M, personal communication), presenting additional possible methods for following autophagy activity.

It is also possible to analyze tissues ex vivo, and these studies can be particularly helpful in assessing autophagic flux as they avoid the risks of toxicity and bioavailabilty of compounds such as bafilomycin A_1 or other autophagy inhibitors. Along these lines, autophagic flux can be determined by western blot in retinas placed in culture for 4 h with protease inhibitors. This method could be used in tissues that can remain "alive" for several hours in culture such as the retina (Boya P, unpublished observations) and brain slices (Desai S, unpublished observations).

Several studies have demonstrated the feasibility of monitoring autophagic flux in vivo in skeletal muscle. Starvation is one of the easiest and most rapid methods for stimulating the autophagic machinery in skeletal muscles. Twelve h of fasting in mice may be sufficient to trigger autophagy in muscle,[639,640] but the appropriate time should be determined empirically. Data about the autophagic flux can be obtained by treating mice with, for example, chloroquine,[640] leupeptin[641] or colchicine[153] and then monitoring the change in accumulation of LC3 (see cautionary notes). This type of analysis can also be done with liver, by comparing the LC3-II level in untreated liver (obtained by a partial hepatectomy) to that following subsequent exposure to chloroquine (Skop V, Papackova Z, Cahová M, personal communication). Additional reporter assays to monitor autophagy flux in vivo need to be developed, including tandem fluorescent-LC3 transgenic mice, or viral vectors to express this construct in vivo in localized areas.

Some biochemical assays may be used to at least provide indirect correlative data relating to autophagy, in particular when examining the role of autophagy in cell death. For example, cellular viability is related to high cathepsin B activity and low cathepsin D activities.[642] Therefore, the appearance of the opposite levels of activities may be one indication of the initiation of autophagy (lysosome)-dependent cell death. The question of "high" vs. "low" activities can be determined by comparison to the same tissue under control conditions, or to a different tissue in the same organism, depending on the specific question.

With regard to living mammals, a minimally invasive method that may be used even in humans is to measure the arterio-venous amino acid exchange rate in the peripheral tissues as a measure of postabsorptive protein catabolism. In humans, the insulin- and amino acid-sensitive postabsorptive (autophagic) net protein catabolism in the peripheral (mostly skeletal muscle) tissue can

dc_840_14

©2012 Landes Bioscience. Do not distribute.

be measured by determining the amino acid exchange rate across the lower extremities, as defined by the difference between the plasma amino acid concentrations in the femoral artery and femoral vein multiplied by the blood flow.[643-645] Amino acid exchange studies show that the peripheral tissues take up amino acids during the post-prandial (fed) state and release amino acids in the postabsorptive (fasted) state, i.e., in a state with relatively low plasma insulin and amino acid levels. This post-absorptive release of amino acids is strongly inhibited by infusion of insulin or by exogenous supply of amino acids, suggesting that it is mainly mediated by a lysosomal/autophagic mechanism of protein catabolism.[643-650] However, the relative contribution of autophagy to the post-absorptive release of amino acids may be changed in disease states (see cautionary notes).

Cautionary notes: The major hurdle with in vivo analyses is the identification of autophagy-specific substrates and the ability to "block" autophagosome degradation with a compound such as bafilomycin A_1. Regardless, it is still essential to adapt the same rigors for measuring autophagic flux in vitro to measurements made with in vivo systems. Moreover, as with cell culture, in order to substantiate a change in autophagic flux it is not adequate to rely solely on the analysis of static levels or changes in LC3-II protein levels on western blot using tissue samples. To truly measure in vivo autophagic flux using LC3-II as a biomarker, it is necessary to block lysosomal degradation of the protein. Several studies have successfully done this in select tissues in vivo. Certain general principles need to be kept in mind: a) Any autophagic blocker, whether leupeptin, bafilomycin A_1, chloroquine or microtubule depolarizing agents such as colchicine or vinblastine must significantly increase basal LC3-II levels. The turnover of LC3-II or rate of basal autophagic flux is not known for tissues in vivo, and therefore short treatments (e.g., 4 h) may not be as effective as blocking for longer times (e.g., 12 to 24 h); b) the toxicity of the blocking agent needs to be considered (e.g., treating animals with bafilomycin A_1 for 2 h can be quite toxic) and food intake must be monitored. If long-term treatment is needed to see a change in LC3-II levels, then confirmation that the animals have not lost weight may be needed. Mice may lose a substantial portion of their body weight when deprived of food for 24 h, and starvation is a potent stimulus for the activation of autophagy. c) The bioavailability of the agent needs to be considered. For example, many inhibitors such as bafilomycin A_1 or chloroquine have relatively poor bioavailability to the central nervous system. To overcome this problem, intracerebroventricular injection can be performed.

When analyzing autophagic flux in vivo, one major limitation is the variability between animals. Different animals do not always activate autophagy at the same time. To improve the statistical relevance and avoid unclear results, these experiments should be repeated more than once and each experiment should include several animals. Induction of autophagy in a time-dependent manner by fasting mice for different times requires appropriate caution. Mice are nocturnal animals, so they preferentially move and eat during the night, while they mostly rest during daylight. Therefore, in such experiments it is better to start food deprivation early in the morning, in order to avoid the possibility that the animals have already been fasting for several hours. The use of chloroquine is technically easier, since it only needs one intraperitoneal injection per day, but the main concern is that chloroquine has some toxicity. Chloroquine suppresses the immunological response in a manner that is not due to its pH-dependent lysosomotropic accumulation (chloroquine interferes with lipopolysaccharide-induced TNF-α gene expression by a nonlysosmotropic mechanism),[651] as well as through its pH-dependent inhibition of antigen presentation.[652] Therefore, chloroquine treatment should be used for short times and at doses that do not induce severe collateral effects, which may invalidate the measurement of the autophagic flux, and care must be exercised in using chloroquine for studies on autophagy that involve immunological aspects. It is also important to have time-matched controls for in vivo analyses. That is, having only a zero hour time point control is not sufficient because there may be substantial diurnal changes in basal autophagy.[467] For example, variations in basal flux in the liver associated with circadian rhythm may be several fold, which can equal or exceed the changes due to starvation. Along these lines, in order to allow comparisons of a single time-point it is important to specify what time of day the measurement is taken, and the lighting conditions under which the animals are housed. It is also important that the replicate experiments are conducted at the same time of day. Controlling for circadian effects can greatly reduce the mouse-to-mouse variability in autophagy markers and flux (Haspel JA, Choi AMK, personal communication).

The amino acid exchange rate, which has been suggested as a minimal invasive marker for measuring autophagic flux in vivo should be used with special caution. Postprandial suppression of amino acid release by peripheral tissues is strongly mediated by insulin and amino acids and is therefore thought to be mediated by autophagy (see above). However, the ubiquitin-proteasome system likely confounds this investigation, as this pathway can also be inhibited by insulin and amino acids.[653] In addition, multiple disease states have been associated with an altered activity of the ubiquitin-proteasome system, further complicating the use of the amino acid exchange rate as a marker of autophagy.[654]

When analyzing basal autophagic level in vivo using GFP-LC3 transgenic mice,[126] one pitfall is that GFP-LC3 expression is driven by the cytomegalovirus enhancer and β-actin (CAG) promoter, so that the intensity of the GFP signal may not always represent the actual autophagic activity, but rather the CAG promoter activity in individual cells. For example, GFP-LC3 transgenic mice exhibit prominent fluorescence in podocytes, but rarely in tubular epithelial cells in the kidney,[126] but a similar GFP pattern is observed in transgenic mice carrying CAG promoter-driven non-tagged GFP.[655] Furthermore, proximal tubule-specific ATG5-deficient mice[656] display a degeneration phenotype earlier than podocyte-specific ATG5-deficient mice,[657] suggesting that autophagy, and hence LC3 levels, might actually be more prominent in the former.

One caution in using approaches that monitor ubiquitinated aggregates is that the accumulation of ubiquitin may indicate a block in autophagy, inhibition of proteasomal degradation, or may correspond to structural changes in the substrate proteins that hinder their degradation. In addition, only cytosolic and not nuclear ubiquitin is subject to autophagic degeneration. It is helpful to analyze aggregate degradation in an autophagy-deficient control strain, such as an autophagy mutant mouse, whenever possible to determine whether an aggregate is being degraded by an autophagic mechanism. This type of control will be impractical for some tissues such as those of the central nervous system because the absence of autophagy leads to rapid degeneration. Accordingly, the use of *Atg16l1* hypomorphs or *Becn1/becn1* heterozygotes may help circumvent this problem.

Conclusion: Although the techniques for analyzing autophagy in vivo are not as advanced as those for cell culture, it is still possible to follow this process (including flux) by monitoring, for example, GFP-LC3 by fluorescence microscopy, and p62 and NBR1 by immunohistochemistry and/or western blotting.

14. *Cell death*. In a limited number of cases, autophagy has been established as the cause of cell death;[97,199,658-664] although opposite results have been reported using analogous experimental settings.[665] Furthermore, many of the papers claiming a causative role of autophagy in cell death fail to provide adequate evidence.[666] Other papers suffer from ambiguous use of the term "autophagic cell death," which was coined in the 1970s[667] in a purely morphological context to refer to cell death with autophagic features (especially the presence of numerous secondary lysosomes); this was sometimes taken to suggest a role of autophagy in the cell death mechanism, but death-mediation was not part of the definition.[668] Unfortunately, the term "autophagic cell death" is now used in at least three different ways: a) autophagy-associated cell death (the original meaning); b) autophagy-mediated cell death (which could involve a standard mechanism of cell death such as apoptosis, but triggered by autophagy); c) a distinct mechanism of cell death, independent of apoptosis or necrosis. Clearly claim (b) is stronger than claim (a), and needs to be justified by proof that inhibiting autophagy, through either genetic or chemical means, prevents cell death.[669] Claim (c) is still stronger, because, even if the cell death is blocked by autophagy inhibition, proof needs to be provided that the cell death mechanism is not apoptosis or necrosis.[670] In view of the current confusion it may be preferable to replace the term "autophagic cell death" by other terms such as "autophagy-associated cell death" or "autophagy-mediated cell death," unless the criteria in claim (c) above have been satisfied. Along these lines, it is preferable to use the term "autophagy-dependent cell death" instead of "autophagy-mediated cell death" when it is proven that autophagy is a prerequisite for the occurrence of cell death, but it is not proven that autophagy mechanistically mediates the switch to cell death. A special caution should also be taken when describing developmental programmed cell death in plants, which is in most cases executed by the growing lytic vacuoles and therefore is referred to as "vacuolar cell death."[671] Although the morphology of vacuolar cell death resembles a combination of macro- and microautophagy, there is no genetic evidence yet that this death requires the core autophagic machinery. Finally, the relationship between autophagy and cell death may significantly differ as a function of the model system being studied. For example, upon induction by starvation of multicellular development in the protist Dictyostelium, autophagy (or at least Atg1) is required to protect against starvation-induced cell death, allowing vacuolar developmental cell death to take place instead.[672,673] Autophagy may be involved not only in allowing this death to occur, but also in the vacuolization process itself.[674]

Cautionary notes: In brief, rigorous criteria must be met in order to establish a death-mediating role of autophagy, as this process typically promotes cell survival. These include a clear demonstration of autophagic flux as described in this article, as well as verification that inhibition of autophagy prevents cell death [claim (b) above; if using a knockdown approach, at least two *ATG* genes should be targeted], and that other mechanisms of cell death are not responsible [claim (c) above]. As part of this analysis, it is necessary to examine the effect of the specific treatment, conditions or mutation on cell viability using several methods.[675] In the case of postmitotic cells such as neurons or retinal cells, cell death—and cell rescue by autophagy inhibition—can usually be established in vivo by morphological analysis,[676] and in culture by cell counts and/or measurement of the release of an enzyme such as LDH into the medium at early and late time points; however, a substantial amount of neuronal cell death occurs during neurogenesis, making it problematic to carry out a correct analysis in vivo or ex vivo.[677,678] In populations of rapidly dividing cells, the problems may be greater. A commonly used method is the 3-(4,5-dimethylthiazol-2-yl)-2,5-diphenyltetrazolium bromide (MTT) assay, or a related assay using a similar, or a water-soluble, tetrazolium salt. The main concern with the MTT assay is that it measures mitochondrial activity, but does not allow a precise determination of cellular viability or cell death, whereas methods that show cell death directly (e.g., trypan blue exclusion) fail to establish the viability of the remaining cell population.[679] Accordingly, a preferred alternative is to accurately quantify cell death by appropriate cytofluorometric or microscopy assays.[675] Moreover, long-term clonogenic assays should be employed when possible to measure the effective functional survival of cells.

Conclusion: In most systems, ascribing death to autophagy based solely on morphological criteria is insufficient; autophagic cell death can only be demonstrated as death that is suppressed by the inhibition of autophagy, through either genetic or chemical means.[669] In addition, more than one assay should be used to measure cell death.

15. *Chaperone-mediated autophagy*. The primary characteristic that makes chaperone-mediated autophagy (CMA) different from the other autophagic variants described in these guidelines is that it does not require formation of intermediate vesicular compartments (autophagosomes or microvesicles) for the import of cargo into lysosomes.[680,681] Instead, the CMA substrates are translocated across the lysosomal membrane through the action of HSPA8 (HSC70) located in the cytosol and lysosome lumen, and the lysosome membrane protein LAMP2A. To date, CMA has only been identified in mammalian cells, and accordingly this section refers only to studies in mammals.

The following methods are commonly utilized to determine if a protein is a CMA substrate (see ref.682 for experimental details): (a) Analysis of the amino acid sequence of the protein to

dc_840_14

identify the presence of a KFERQ-related motif that is an absolute requirement for all CMA substrates.[683] (b) Colocalization studies with lysosomal markers (typically LAMP2A and/or LysoTracker) to identify a fraction of the protein associated with lysosomes. The increase in association of the putative substrate under conditions that upregulate CMA (such as prolonged starvation) or upon blockage of lysosomal proteases (to prevent the degradation of the protein) helps support the hypothesis that the protein of interest is a CMA substrate. However, association with lysosomes is necessary but not sufficient to consider a protein an authentic CMA substrate, because proteins delivered by other pathways to lysosomes will also behave in a similar manner. A higher degree of confidence can be attained if the association is preferentially with the subset of lysosomes active for CMA (i.e., those containing HSPA8 in their lumen), which can be separated from other lysosomes following published procedures.[628] (c) Co-immunoprecipitation of the protein of interest with cytosolic HSPA8. Due to the large number of proteins that interact with this chaperone, it is usually better to perform affinity isolation with the protein of interest and then analyze the isolated proteins for the presence of HSPA8 rather than vice versa. (d) Co-immunoprecipitation of the protein of interest with LAMP2A.[684] Due to the fact that the only antibodies specific for the LAMP2A variant (the only one of the three LAMP2 variants involved in CMA[105,685]) are generated against the cytosolic tail of LAMP2A, where the substrate also binds, it is necessary to affinity isolate the protein of interest and then analyze for the presence of LAMP2A. Immunoblot for LAMP2A in the precipitate can only be done with the antibodies specific for LAMP2A and not just those that recognize the lumenal portion of the protein that is identical in the other LAMP2 variants. If the protein of interest is abundant inside cells, co-immunoprecipitations with LAMP2A can be done in total cellular lysates, but for low abundance cellular proteins, preparation of a membrane fraction (enriched in lysosomes) by differential centrifugation may facilitate the detection of the population of the protein bound to LAMP2A. (e) Selective upregulation and blockage of CMA to demonstrate that degradation of the protein of interest changes with these manipulations. Selective chemical inhibitors for CMA are not currently available. Note that general inhibitors of lysosomal proteases (e.g., bafilomycin A_1, NH_4Cl, leupeptin) also block the degradation of proteins delivered to lysosomes by other autophagic and endosomal pathways. The most selective way to block CMA is by knockdown of LAMP2A, which causes this protein to become a limiting factor.[105] The other components involved in CMA, including HSPA8, HSP90, GFAP, and eF1α are all multifunctional cellular proteins, making it difficult to interpret the effects of knockdowns. Overexpression of LAMP2A[684] is also a better approach to upregulate CMA than the use of chemical modulators. The two compounds demonstrated to affect degradation of long-lived proteins in lysosomes,[686] 6-aminonicotinamide and geldanamycin, lack selectivity, as they affect many other cellular processes. In addition, in the case of geldanamycin, the effect on CMA can be the opposite (inhibition rather than stimulation) depending on the cell type (this is due to the fact that the observed stimulation of CMA is actually a compensatory response to the blockage of HSP90 in lysosomes, and different cells activate different compensatory responses).[687] (f) The most conclusive way to prove that a protein is a CMA substrate is by reconstituting its direct translocation into lysosomes using a cell-free system.[682] This method is only possible when the protein of interest can be purified, and it requires the isolation of the population of lysosomes active for CMA. Internalization of the protein of interest inside lysosomes upon incubation with the isolated organelle can be monitored using protease protection assays (in which addition of an exogenous protease removes the protein bound to the cytosolic side of lysosomes, whereas it is inaccessible to the protein that has reached the lysosomal lumen; note that pre-incubation of lysosomes with lysosomal protease inhibitors before adding the substrate is required to prevent the degradation of the translocated substrate inside lysosomes).[688] The use of exogenous protease requires numerous controls (see ref.682) to guarantee that the amount of protease is sufficient to remove all the substrate outside lysosomes, but will not penetrate inside the lysosomal lumen upon breaking the lysosomal membrane. The difficulties in the adjustment of the amount of protease, has led to the development of a second method that is more suitable for laboratories that have no previous experience with these procedures. In this case, the substrate is incubated with lysosomes untreated or previously incubated with inhibitors of lysosomal proteases, and uptake is determined as the difference of protein associated with lysosomes not incubated with inhibitors (in which the only remaining protein will be the one associated with the cytosolic side of the lysosomal membrane) and those incubated with the protease inhibitors (which contain both the protein bound to the membrane and that translocated into the lumen).[689] Confidence that the lysosomal internalization is by CMA increases if the uptake of the substrate can be competed with proteins previously identified as substrates for CMA (e.g., glyceraldehyde-3-phosphate dehydrogenase or ribonuclease A, both commercially available as purified proteins), but is not affected by the presence of similar amounts of nonsubstrate proteins (such as ovalbumin or cyclophilin A). Blockage of uptake by pre-incubation of the lysosomes with antibodies against the cytosolic tail of LAMP2A also reinforces the hypothesis that the protein is a CMA substrate.

In other instances, rather than determining if a particular protein is a CMA substrate, the interest may be to analyze possible changes in CMA activity under different conditions or in response to different modifications. We enumerate here the methods, from lower to higher complexity that can be utilized to measure CMA in cultured cells and in tissues (see ref.682 for detailed experimental procedures). (a) Measurement of changes in the intracellular rates of degradation of long-lived proteins, when combined with inhibitors of other autophagic pathways, can provide a first demonstration in support of changes that are due to CMA. For example, CMA is defined as lysosomal degradation upregulated in response to serum removal but insensitive to PtdIns3K inhibitors. (b) Measurement of levels of CMA components is insufficient to conclude changes in CMA because this does not provide functional information, and changes in CMA components can also occur under other conditions.

However, analysis of the levels of LAMP2A can be used to support changes in CMA detected by other procedures. Cytosolic levels of HSPA8 remain constant and are not limiting for CMA, thus providing no information about this pathway. Likewise, changes in total cellular levels of LAMP2A do not have an impact on this pathway unless they also affect their lysosomal levels (i.e., conditions in which LAMP2A is massively overexpressed lead to its targeting to the plasma membrane where it cannot function in CMA). It is advisable that changes in the levels of these two CMA components are confirmed to occur in lysosomes, either by colocalization with lysosomal markers when using image-based procedures or by performing immunoblot of a lysosomal enriched fraction (purification of this fraction does not require the large amounts of cells/tissue necessary for the isolation of the subset of lysosomes active for CMA). (c) Tracking changes in the subset of lysosomes active for CMA. This group of lysosomes is defined as those containing HSPA8 in their lumen (note that LAMP2A is present in both lysosomes that are active and inactive for CMA, and it is the presence of HSPA8 that confers CMA capability). Immunogold or immunofluorescence against these two proteins (LAMP2A and HSPA8) makes it possible to quantify changes in the levels of these lysosomes present at a given time, which correlates well with CMA activity.[628] (d) Analysis of lysosomal association of fluorescent artificial CMA substrates. Two different fluorescent probes have been generated to track changes in CMA activity in cultured cells using immunofluorescence or FACS analysis.[628] These probes contain the KFERQ and context sequences in frame with photoswitchable or photoactivated fluorescent proteins. Activation of CMA results in the mobilization of a fraction of the cytosolic probe to lysosomes and the subsequent change from a diffuse to a punctate pattern. CMA activity can be quantified as the number of fluorescent puncta per cell or as the decay in fluorescence activity over time because of degradation of the artificial substrate. Because the assay does not allow measuring accumulation of the substrate (which must unfold for translocation), it is advisable to perform a time-course analysis to determine gradual changes in CMA activity. Antibodies against the fluorescent protein in combination with inhibitors of lysosomal proteases can be used to monitor accumulation of the probe in lysosomes over a period of time, but both the photoswitchable and the unmodified probe will be detected by this procedure.[690] As for any other fluorescence probe based on analysis of intracellular "puncta" it is essential to include controls to confirm that the puncta are indeed lysosomes (colocalization with LysoTracker or LAMPs and lack of colocalization with markers of cytosolic aggregation such as ubiquitin), and do not reach the lysosomes through other autophagic pathways (insensitivity to PtdIns3K inhibitors and sensitivity to LAMP2A knockdown are good controls in this respect). (e) Direct measurement of CMA using in vitro cell free assays. Although the introduction of the fluorescent probes should facilitate measurement of CMA in many instances, they are not applicable for tissue samples. In addition, because the probes measure binding of substrate to lysosomal membranes it is important to confirm that enhanced binding does not result from defective translocation. Lastly, the in vitro uptake assays are also the most efficient way to determine primary changes in CMA independently of changes in other proteolytic systems in the cells. These in vitro assays are the same ones described in the previous section on the identification of proteins as substrates of CMA, but are performed in this case with purified proteins previously characterized to be substrates for CMA. In this case the substrate protein is always the same and what changes is the source of lysosomes (from the different tissues or cells that are to be compared). As described in the previous section, binding and uptake can be analyzed separately using lysosomes previously treated or not with protease inhibitors. The analysis of the purity of the lysosomal fractions prior to performing functional analysis is essential to conclude that changes in the efficiency to take up the substrates results from changes in CMA rather than from different levels of lysosomes in the isolated fractions. Control of the integrity of the lysosomal membrane and sufficiency of the proteases are also essential to discard the possibility that degradation is occurring outside lysosomes because of leakage, or that accumulation of substrates inside lysosomes is due to enhanced uptake rather than to decreased degradation.

Cautionary notes: The discovery of a new selective form of protein degradation in mammals named endosomal-microautophagy (e-MI)[691] has made it necessary to reconsider some of the criteria that applied in the past for the definition of a protein as a CMA substrate. The KFERQ-like motif, previously considered to be exclusive for CMA, is also used to mediate selective targeting of cytosolic proteins to the surface of late endosomes. Once there, substrates can be internalized in microvesicules that form from the surface of these organelles in an ESCRT-dependent manner. HSPA8 has been identified as the chaperone that binds this subset of substrates and directly interacts with lipids in the late endosomal membrane, acting thus as a receptor for cytosolic substrates in this compartment. At a practical level, to determine if a KFERQ-containing protein is being degraded by CMA or e-MI the following criteria can be applied: (a) Inhibition of lysosomal proteolysis (for example with NH_4Cl and leupeptin) blocks degradation by both pathways. (b) Knockdown of LAMP2A inhibits CMA but not e-MI. (c) Knockdown of components of ESCRTI and II (e.g., VPS4 and TG101) inhibits e-MI but not CMA. (d) Interfering with the capability to unfold the substrate protein blocks its degradation by CMA, but does not affect e-MI of the protein. In this respect soluble proteins, oligomers and protein aggregates can undergo e-MI, but only soluble proteins can be CMA substrates. (e) In vitro uptake of e-MI substrates can be reconstituted using isolated late endosomes whereas in vitro uptake of CMA substrates can only be reconstituted using lysosomes.

Another pathway that needs to be considered relative to CMA is chaperone-assisted selective autophagy (CASA).[692] CASA is dependent on HSPA8 and LAMP2 (although it is not yet known if it is dependent solely on the LAMP2A isoform). Thus, a requirement for these two proteins is not sufficient to conclude that a protein is degraded by CMA.

Conclusion: One of the key issues with the analysis of CMA is verifying that the protein of interest is an authentic susbstrate. Methods for monitoring CMA that utilize fluorescent probes are

dc_840_14

available that eliminate the need for the isolation of CMA-competent lysosomes, one of the most difficult aspects of assaying this process.

B. Comments on Additional Methods

1. *Acidotropic dyes*. Among the older methods for following autophagy is staining with acidotropic dyes such as monodansylcadaverine (MDC),[693] acridine orange,[694] Neutral Red,[632] LysoSensor Blue[695] and LysoTracker Red.[198,696]

Cautionary notes: Although MDC was first described as a specific marker of autophagic vacuoles[697] subsequent studies have suggested that this, and other acidotropic dyes, are not specific markers for early autophagosomes,[258] but rather label later stages in the degradation process. For example, autophagosomes are not acidic, and MDC staining can be seen in autophagy-defective mutants[401] and in the absence of autophagy activation.[698] MDC may also show confounding levels of background labeling unless narrow bandpass filters are used. However, in the presence of vinblastine, which blocks fusion with lysosomes, MDC labeling increases, suggesting that under these conditions MDC can label late-stage autophagosomes.[699] Along these lines, cells that over-express a dominant negative version of RAB7 (the T22N mutant) show colocalization of this protein with MDC; in this case fusion with lysosomes is also blocked[700] indicating that MDC does not just label lysosomes. Finally, MDC labeling could be considered to be an indicator of autophagy when the increased labeling of cellular compartments by this dye is prevented by treatment with autophagy inhibitors such as wortmannin or 3-MA.

Overall, staining with MDC or its derivative monodansylamylamine (MDH)[693] is not, by itself, a sufficient method for monitoring autophagy. Similarly, LysoTracker Red, Neutral Red and acridine orange are not ideal markers for autophagy because they primarily detect lysosomes. These markers are, however, useful for monitoring selective autophagy when used in conjunction with protein markers or other dyes. For example, increased colocalization of mitochondria with both GFP-LC3 and LysoTracker can be used as evidence of autophagic cargo delivery to lysosomes. Moreover, LysoTracker Red has been used to provide correlative data on autophagy in *Drosophila melanogaster* fat body cells (**Fig. 23**).[197,198] However, additional assays, such as GFP-Atg8/LC3 fluorescence or EM, should be used to substantiate results obtained with acidotropic dyes whenever possible. One important caution when co-imaging with LysoTracker Red and a green-fluorescing marker (e.g., GFP-LC3 or MitoTracker Green) is that it is necessary to control for rapid red-to-green photoconversion of the LysoTracker, which can otherwise result in an incorrect interpretation of colocalization.[701]

Some of the confusion regarding the interpretation of results with these dyes stems in part from the nomenclature in this field. Indeed, the discussion of acidotropic dyes points out why it is advisable to differentiate between the terms "autophagosome" and "autophagic vacuole," although they are occasionally, and incorrectly, used interchangeably. The autophagosome is the sequestering compartment generated by the phagophore. The fusion of an autophagosome with an endosome or a lysosome generates an amphisome or an autolysosome, respectively. The early autophagosome is not an acidic compartment, whereas amphisomes and autolysosomes are acidic. Earlier names for these compartments are "initial autophagic vacuole (AVi)," "intermediate autophagic vacuole (AVi/d)" and "degradative autophagic vacuole (AVd)," respectively. Thus, acidotropic dyes can stain late autophagic vacuoles (in particular autolysosomes), but not the initial autophagic vacuole, the early autophagosome. With the above caveats in mind, the combined use of early and late markers of autophagy is highly encouraged, and when quantifying mammalian lysosomes, it is important to keep in mind that increases in both lysosome size and number are frequently observed. Finally, in order to avoid confusion with the plant and fungal vacuole, the equivalent organelle to the lysosome, we recommend the use of the term "autophagosome" instead of "autophagic vacuole," and the use of "autophagic compartment" when the specific nature of the structure is not known.

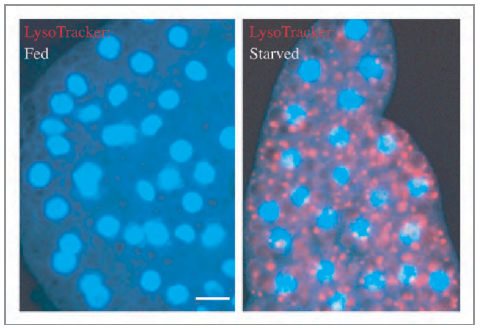


Figure 23. LysoTracker Red stains lysosomes and can be used to monitor autophagy in Drosophila. Live fat body tissues from Drosophila were stained with LysoTracker Red (red) and Hoechst 33342 (blue) to stain the nucleus. Tissues were isolated from fed (left) or 3 h starved (right) animals. Bar, 25 μm. This figure was modified from data presented in reference ,198 Developmental Cell, 7, Scott RC, Schuldiner O, Neufeld TP, Role and regulation of starvation-induced autophagy in the Drosophila fat body, pp. 167–78, copyright 2004, with permission from Elsevier.

Conclusion: Given the development of better techniques that are indicators of autophagy, the use of acidotropic dyes to study this process is discouraged, and relying entirely on such dyes is not acceptable.

2. *Autophagy inhibitors and inducers*. In many situations it is important to demonstrate an effect resulting from inhibition or stimulation of autophagy (see ref.702 for a partial listing of regulatory compounds), and a few words of caution are worthwhile in this regard. Most chemical inhibitors of autophagy are not entirely specific, and it is important to consider possible dose- and time-dependent effects. Accordingly, it is generally preferable to analyze specific loss-of-function *Atg* mutants. However, it must be kept in mind that some apparently specific *Atg* gene products may have autophagy-independent roles (e.g., ATG5 in cell death, and the VPS34-containing complexes—including BECN1—in apoptosis, endosomal function and protein trafficking).[403,432,703-706] Therefore, the experimental conditions of inhibitor application and their side effects must be carefully considered. In addition, it must be emphasized once again that autophagy, as a multistep process, can be inhibited at different stages. Sequestration inhibitors, including 3-MA, LY294002 and wortmannin, inhibit class I as well as class III PtdIns3Ks.[134,257,707] The class I enzymes generate products [PtdIns(3,4,5)P_3] that inhibit autophagic sequestration, whereas the class III product (PtdIns3P) generally stimulates autophagic sequestration. The overall effect of these inhibitors is typically to block autophagy because the class III enzymes that are required to activate autophagy act downstream of the negative regulatory class I enzymes, although cell death may ensue in cell types that are dependent upon high levels of AKT for survival. The effect of 3-MA (but not that of wortmannin) is further complicated by the fact that it has different temporal patterns of inhibition, causing a long-term suppression of the class I PtdIns3K, but only a transient inhibition of the class III enzyme. In cells incubated in a complete medium for extended periods of time, 3-MA may, therefore (particularly at suboptimal concentrations), promote autophagy by inhibition of the class I enzyme.[257] Thus, wortmannin may be considered as an alternative to 3-MA for autophagy inhibition.[257] However, wortmannin can induce the formation of vacuoles that may have the appearance of autophagosomes, although they are swollen late endocytic compartments.[611] Furthermore, studies have demonstrated that inhibition of autophagy with 3-MA or wortmannin can have effects on cytokine transcription, processing and secretion, particularly IL-1 family members,[708-710] but 3-MA also inhibits the secretion of some cytokines (e.g., TNF, IL-6) in an autophagy-independent manner (Harris J, unpublished observations). Thus, in studies where the effect of autophagy inhibition on specific cellular processes is being investigated, is is important to confirm results using other methods, such as RNA silencing. Due to these issues, it is of great interest that inhibitors with specificity for the class III PtdIns3Ks, and their consequent effects on autophagy, have been described.[165]

Cycloheximide, a commonly used protein synthesis inhibitor in mammals, is also an inhibitor of sequestration in vivo,[14-16,92,604,711-715] and in various cell types in vitro,[344,716] and it has been utilized to investigate the dynamic nature of the regression of various autophagic elements.[14-16,24,92,712,713] The mechanism of action of cycloheximide in short-term experiments is not clear, but it has no direct relation to the inhibition of protein synthesis.[344] This latter activity, however, may complicate certain types of analysis when using this drug.

A significant challenge for a more detailed analysis of the dynamic role of autophagy in physiological and pathophysiological processes, for instance with regard to cancer and cancer therapy, is to find more specific inhibitors of autophagy signaling which do not affect other signaling cascades. For example, in the context of cellular radiation responses it is well known that PtdIns3Ks (e.g., ATM, DNA-PKcs), in addition to signaling through the PtdIns3K-AKT pathway, have a major role in the regulation of DNA-damage repair.[717] However, 3-MA, which is a nonspecific inhibitor of class 3 PtdIns3Ks, can alter the function of other classes of this enzyme, which are involved in the DNA-damage repair response. This is of particular importance for investigations into the role of radiation-induced autophagy in cellular radiation sensitivity or resistance.[718,719]

Most other inhibitory drugs act at post-sequestration steps. These types of agents have been used in many experiments to both inhibit endogenous protein degradation and to increase the number of autophagic compartments. They cause the accumulation of sequestered material in either autophagosomes or autolysosomes, or both, because they allow autophagic sequestration to proceed. The main categories of these types of inhibitors include the vinca alkaloids (e.g., vinblastine) and other microtubule poisons that inhibit fusion, inhibitors of lysosomal enzymes (e.g., leupeptin, pepstatin A and E-64d), and compounds that elevate lysosomal pH (e.g., inhibitors of vacuolar-type ATPases such as bafilomycin A_1 and concanamycin A (another V-ATPase inhibitor), and weak base amines including methyl- or propylamine, chloroquine, and Neutral Red, some of which slow down fusion). Ammonia is a very useful agent for the elevation of lysosomal pH in short-term experiments, but has been reported to cause a stimulation of autophagy during long-term incubation of cells in a full medium,[720] under which conditions a good alternative might be methylamine or propylamine.[721] Along these lines, it should be noted that the half-life of glutamine in cell culture media is approximately two weeks due to chemical decomposition, which results in media with lowered glutamine and elevated ammonia concentrations that can affect the autophagic flux (either inhibiting or stimulating autophagy, depending on the concentration[722]). Thus, the use of freshly prepared cell culture media with glutamine is advised, to help reduce experimental variation. A special note of caution is also warranted in regard to chloroquine. Although this chemical is commonly used as an autophagy inhibitor, chloroquine may initially stimulate autophagy (Dorsey FC, personal communication; Franco R, personal communication).

Some data suggest that some nanomaterials may also be novel inhibitors of autophagy, by as yet unidentified mechanisms.[723] It is worth noting that lysosomal proteases fall into three general groups, cysteine, aspartic acid and serine proteases. Therefore, the fact that leupeptin, a serine and cysteine protease inhibitor, has little or no effect does not necessarily indicate that lysosomal degradation is not taking place; a combination of leupeptin, pepstatin A and E-64d may be a more effective treatment. However, it should also be pointed out that these protease inhibitors can exert inhibitory effects not only on lysosomal proteases, but also on cytosolic proteases, that is, degradation of proteins might be blocked through inhibition of cytosolic instead of lysosomal proteases. Conversely, it should be noted that MG132 (Z-leu-leu-leu-al) and its related peptide aldehydes are commonly used as proteasomal inhibitors, but they can also inhibit certain lysosomal hydrolases such as cathepsins and calpains.[724] Thus, any positive results using MG132 do not rule

dc_840_14
Landes Bioscience. Do not distribute.

out the possibility of involvement of the autophagy-lysosome system. Therefore, even if MG132 is effective, it is important to confirm the result using more specific proteasomal inhibitors such as lactacystin or epoxomicin. Finally, there are significant differences in cell permeability among protease inhibitors. For example, E-64d is membrane permeable, whereas leupeptin and pepstatin A are not (although there are derivatives that display greater permeability such as pepstatin A methyl ester).[725] Thus, when analyzing whether a protein is an autophagy substrate, caution should be taken in utilizing these protease inhibitors to block autophagy.

As with the PtdIns3K inhibitors, many autophagy-suppressive compounds are not specific. For example, okadaic acid[726] is a powerful general inhibitor of both type 1 (PP1) and type 2A (PP2A) protein phosphatases.[727] Bafilomycin A_1 and other compounds that raise the lysosomal pH may have indirect effects on any acidified compartments. Moreover, treatment with bafilomycin A_1 for extended periods (18 h) can cause significant disruption of the mitochondrial network in cultured cells (Gegg ME, personal communication), and either bafilomycin A_1 or concanamycin A cause swelling of the Golgi in plants,[728] and increase cell death by apoptosis in cancer cells (Rao VA, personal communication). Bafilomycin A_1 is often used at a final concentration of 100 nM, but much lower concentrations such as 1 nM may be sufficient to inhibit autophagic-lysosomal degradation and are less likely to cause indirect effects;[154,729,730] however, appropriate inhibitory concentrations should be empirically determined for each cell type.[6] One final caution with regard to bafilomycin A_1 is that activation of lysosomally localized TORC1 depends on an active V-ATPase.[364] This means that treatment with bafilomycin A_1 could elevate the autophagic flux through MTOR inhibition, while simultaneously interfering with flux by inhibiting fusion. Accordingly, other compounds may be preferred for flux measurements. Thus, although these various agents can inhibit different steps of the autophagic pathway, their potential side effects must be considered in interpretation of the secondary consequences of autophagy inhibition, especially in long-term studies. For example, lysosomotropic compounds can increase the rate of autophagosome formation by inhibiting TORC1.[731] Along these lines, chloroquine treatment may cause an apparent increase in the formation of autophagosomes possibly by blocking fusion with the lysosome (F.C. Dorsey and J.L. Cleveland, personal communication). This conclusion is supported by the finding that chloroquine reduces the colocalization of LC3 and LysoTracker despite the presence of autophagosomes and lysosomes (Simon AK, personal communication). Concanamycin A blocks sorting of vacuolar proteins in plant cells in addition to inhibiting vacuolar acidification.[732] Furthermore, in addition to causing the accumulation of autophagic compartments, many of these drugs seem to be stimulators of sequestration in many cell types, especially in vivo.[93,235,604,712,716,733-737] Although it is clear why these drugs cause the accumulation of autophagic compartments, it is not known why they stimulate sequestration. One possibility, at least for hepatocytes, is that the inhibition of protein degradation reduces the intracellular amino acid pool, which in turn upregulates sequestration. A time-course study of the changes in both the intra- and extracellular fractions may provide accurate information regarding amino acid metabolism. For these various reasons, it is important to include appropriate controls; along these lines, MTOR inhibitors such as rapamycin or amino acid deprivation can be utilized as positive controls for inducing autophagy. In many cell types, however, the induction of autophagy by rapamycin is relatively slow, or transient, allowing more time for indirect effects; thus, rapamycin may fail to activate autophagy in cultured primary neurons, despite its potent stimulation of autophagy in some cancer cell lines,[238,738,739] and, similarly, it does not induce autophagy in human neuroblastoma SH-SY5Y cells, which can differentiate into neuron-like cells (Diaz-Nido J, personal communication). Along these lines, glucose depletion may be much more efficient at inducing autophagy than rapamycin or amino acid starvation in neurons in culture (Germain M, Slack R, personal communication); although a number of compounds can also be quite efficient autophagy inducers in neurons including the calpain inhibitor calpeptin.[238,740,741] Several small molecule inhibitors, including torin1, PP242, KU-0063794, PtdIns-103 and NVP-BEZ235, have been developed that target the catalytic domain of MTOR in an ATP-competitive manner.[154,252,742-745] In comparison to rapamycin, these catalytic MTOR inhibitors are more potent, and hence are stronger autophagy agonists in most cell lines.[242,252,746] The use of these second-generation MTOR inhibitors may reveal that some reports of mTOR-independent autophagy may actually reflect the use of the relatively weak inhibitor rapamycin. Furthermore, the use of these compounds has revealed a role for TORC1 and TORC2 as independent regulators of autophagy.[747] Finally, a specialized class of compounds with α,β-unsaturated ketone structure tends to induce autophagic cell death, accompanied by changes in mitochondrial morphology; since the cytotoxic action of these compounds is efficiently blocked by *N*-acetyl-L-cysteine, the β-position in the structure may interact with an SH group of the targeted molecules.[748] Due to the potential pleiotropic effects of various drug treatments, it is incumbent upon the researcher to demonstrate that autophagy is indeed inhibited, by using the methodologies described herein. Accordingly, it is critical to verify the effect of a particular biochemical treatment with regard to its effects on autophagy induction or inhibition when using a cell line that was previously uncharacterized for the chemical being used. Similarly, cytotoxicity of the relevant chemical should be assessed.

The use of gene deletions/inactivations (e.g., in primary or immortalized *atg*$^{-/-}$ MEFs,[401] plant T-DNA or transposon insertion mutants,[200,749] or in vivo using transgenic knockout models[750,751] including Cre-lox based "conditional" knockouts[230,231]) or functional knockdowns (e.g., with RNAi against *ATG* genes) is the preferred approach when possible because these methods allow a more direct assessment of the resulting phenotype; however, different floxed genes are deleted with varying efficiency, and the proportion deleted must be carefully quantified (Hwang S, Virgin IV HW, personal communication). Studies also suggest that microRNAs may be used for blocking gene expression.[164,468,469,752] In certain contexts, it is advisable

when using a knockout or knockdown approach to examine multiple autophagy-related genes to exclude the possibility that the phenotype observed is due to effects on a non-autophagic function(s) of the corresponding protein, especially when examining the possibility of autophagic cell death (in contrast, if examining whether perturbation induces clearance of a substrate via autophagy, a single *Atg* gene knockout is probably sufficient). This is particularly the case in evaluating BECN1, which interacts with anti-apoptotic BCL2 family proteins,[425] or when low levels of a target protein are sufficient for maintaining autophagy as is the case with ATG5.[171] With regard to ATG5, a better approach may be to use a dominant negative (K130R) version.[706,753,754] Along these lines, and as stated above for the use of inhibitors, when employing a knockout or especially a knockdown approach, it is again incumbent upon the researcher to demonstrate that autophagy is actually inhibited, by using the methodologies described herein. Finally, we note that the long-term secondary consequences of gene knockouts or knockdowns are likely much more complex than the immediate effects of the actual autophagy inhibition. To overcome this concern, inducible knockout systems might be useful.[171,315] One additional caveat to knockdown experiments is that pathogen-associated molecular pattern (PAMP) recognition pathways can be triggered by double-stranded RNAs (dsRNA), like siRNA probes, or the viral vector systems that deliver shRNA.[755] Some of these, like TLR-mediated RNA recognition,[756] can influence autophagy by either masking any inhibitory effect or compromising autophagy independent of the knockdown probe. Therefore, nontargeting (scrambled) siRNA or shRNA controls should be used with the respective transfection or transduction methods in the experiments that employ ATG knockdown. Another strategy to specifically interfere with autophagy is to use dominant negative inhibitors. Delivery of these agents by transient transfection, adenovirus, or TAT-mediated protein transduction offers the possibility of their use in cell culture or in vivo.[753] However, since autophagy is an essential metabolic process for many cell types and tissues, loss of viability due to autophagy inhibition always has to be a concern when analyzing cell death-unrelated questions. In this respect it is noteworthy that some cell-types of the immune system such as dendritic cells[260] seem to tolerate loss of autophagy fairly well, whereas others such as T and B cells are compromised in their development and function after autophagy inhibition.[757,758]

In addition to pharmacological inhibition, RNA silencing, gene knockout and dominant negative RAB and ATG protein expression, pathogen-derived autophagy inhibitors can also be considered to manipulate autophagy. Along these lines ICP34.5, viral BCL2 homologs and viral FLIP of herpesviruses block autophagosome formation,[425,580,759] whereas M2 of influenza virus and HIV Nef block autophagosome degradation.[278,760] However, as with other tools discussed in this section, transfection or transduction of viral autophagy inhibitors should be used in parallel with other means of autophagy manipulation, because these proteins are used for the regulation of usually more than one cellular pathway by the respective pathogens.

There are fewer compounds that act as inducers of autophagy, but the initial characterization of this process was due in large part to the inducing effects of glucagon, which appears to act through indirect inhibition of MTOR via the activation of LKB1-AMPK.[615,616,761] Currently, the most commonly used inducer of autophagy is rapamycin, an allosteric inhibitor of TORC1, although one caution is that MTOR is a major regulatory protein that is part of the insulin signaling pathway, and it controls processes other than autophagy, so that rapamycin will ultimately affect many metabolic pathways.[379,762-764] In particular, the strong effects of MTOR on protein synthesis may be a confounding factor when analyzing the effects of rapamycin. MTOR-independent regulation can be achieved through lithium, sodium valproate and carbamazepine, compounds that lower the myo-inositol-1,4,5-triphosphate levels.[765] In vivo treatment of embryos with cadmium results in an increase in autophagy, probably to counter the stress, allowing cell survival through the elimination/recycling of damaged structures.[632] Autophagy may also be regulated by the release of calcium from the endoplasmic reticulum under stress conditions;[212,726,766] however, additional calcium signals from other stores such as the mitochondria and lysosomes could also play an important role in autophagy induction. The activation of the lysosomal two pore channel (TPC), by nicotinic acid adenine dinucleotide phosphate (NAADP) induces autophagy, which can selectively be inhibited by the TPC blocker NED-19, or by pre-incubation with BAPTA, showing that lysosomal calcium also modulates autophagy.[244]

Another way to induce autophagy, both in cultured cells and in vivo, is through transcriptional control. For example, this can be achieved either through overexpression or post-translational activation of the gene encoding TFEB (see *Transcriptional and translational regulation*), a transcriptional regulator of the biogenesis of both lysosomes and autophagosomes.[463,464] Similarly, adenoviral-mediated expression of the transcription factor C/EBPβ induces autophagy in hepatocytes.[467]

Relatively little is known about direct regulation via the ATG proteins, but there is some indication that tamoxifen acts to induce autophagy by increasing the expression of BECN1 in MCF7 cells.[767] However, in U87MG cells treated with tamoxifen BECN1 does not appear to be upregulated, whereas the levels of LC3-II and p62 are increased, while LAMP2B is downregulated and cathepsin D and L activities are almost completely blocked (Choi KS, personal communication). Thus, the effect of tamoxifen may differ depending on the cell type. Other data suggest that tamoxifen acts by blocking cholesterol biosynthesis, and that the sterol balance may determine whether autophagy acts in a protective vs. cytotoxic manner.[768,769] Finally, screens have identified small molecules that induce autophagy independently of rapamycin, and allow the removal of misfolded or aggregate-prone proteins,[770,771] suggesting that they may prove useful in therapeutic applications. However, caution should be taken because of the crosstalk between autophagy and the proteasomal system. For example, trehalose, an mTOR-independent autophagy inducer,[253] can compromise proteasomal activity in cultured primary neurons.[739]

Conclusion: Rapamycin is much less effective at inhibiting MTOR and inducing autophagy than catalytic inhibitors, and the latter should therefore be considered for use instead of rapamycin;

dc_840_14

however, it must be kept in mind that catalytic inhibitors also affect mTORC2. The main concern with pharmacological manipulations is pleiotropic effects of the compound being used. Accordingly, genetic confirmation is preferred whenever possible.

3. *Basal autophagy*. Basal levels of LC3-II or GFP-LC3 puncta may change according to the time after addition of fresh medium to cells, and this can lead to misinterpretations of what basal autophagy means. This is particularly important when comparing the levels of basal autophagy between different cell populations (such as knockout vs. wild-type clones). If cells are very sensitive to nutrient supply and display a high variability of basal autophagy, the best experimental condition is to monitor the levels of basal autophagy at different times after the addition of fresh medium. One example is the chicken lymphoma DT40 cells (see *Chicken B-lymphoid DT40 cells* below) and their knockout variant for all three inositol 1,4,5-trisphosphate receptor isoforms.[241,772,773] In these cells, no differences in basal levels of LC3-II can be observed up to 4 h after addition of fresh medium, but differences can be observed after longer times (Vicencio JM, Szabadkai G, personal communication). This concept should also be applied to experiments in which the effect of a drug upon autophagy is the subject of study. If the drugs are added after a time in which basal autophagy is already high, then the effects of the drug can be masked by the cell's basal autophagy, and wrong conclusions may be drawn. To avoid this, fresh medium should be added first in order to reduce and equilibrate basal autophagy in cells under all conditions, and then the drugs can be added. The basal autophagy levels of the cell under study must be identified beforehand in order to know the time needed to reduce basal autophagy.

A similar caution must be exercised with regard to cell culture density and hypoxia. When cells are grown in normoxic conditions at high cell density, HIF-1α is stabilized at levels similar to that obtained with low-density cultures under hypoxic conditions.[774] This results in the induction of BNIP3 and BNIP3L/NIX and "hypoxia"-induced autophagy, even though the conditions are theoretically normoxic.[775] Therefore, researchers need to be careful about cell density in order to avoid accidental induction of autophagy.

It should be realized that also in yeast species, medium changes can trigger a higher "basal" level of autophagy in the cells. In the methylotrophic yeast species *Pichia pastoris* and *Hansenula polymorpha* a shift of cells grown in batch from glucose to methanol results in stimulation of autophagy.[776,777] A shift to a new medium can be considered a stress situation. Thus, it appears to be essential to cultivate the yeast cells for a number of hours to stabilize the level of basal autophagy, before performing experiments intended to study levels of (selective) autophagy (e.g., pexophagy). Finally, plant root tips cultured in nutrient-sufficient medium display constitutive autophagic flux (i.e., a basal level), which is enhanced in nutrient-deprived medium.[696,778,779]

Conclusion: The levels of basal autophagy can vary substantially and can mask the effects of the experimental parameters being tested. Changes in media and growth conditions need to be examined empirically to determine affects on basal autophagy and the appropriate times for subsequent manipulations.

4. *Experimental systems*. Throughout these guidelines we have noted that it is not possible to state explicit rules that can be applied to all experimental systems. For example, some techniques may not work in particular cell types or organisms. In each case, efficacy of autophagy promotors, inhibitors and measurement technique must be empirically determined, which is why it is important to include appropriate controls. Differences may also be seen between in vivo or perfused organ studies and cell culture analyses. For example, insulin has no effect on proteolysis in suspended rat hepatocytes, in contrast to the result with perfused rat liver. The insulin effect reappears, however, when isolated hepatocytes are incubated in stationary dishes[780,781] or are allowed to settle down on the matrix (Häussinger D, personal communication). The reason for this might be that autophagy regulation by insulin and some amino acids requires volume sensing via integrin-matrix interactions and also intact microtubules.[782-784] Along these lines, the use of whole embryos makes it possible to investigate autophagy in multipotent cells, which interact among themselves in their natural environment, bypassing the disadvantages of isolated cells that are deprived of their normal network of interactions.[632] In general, it is important to keep in mind that results from one particular system may not be generally applicable to others.

Conclusion: Although autophagy is conserved from yeast to human, there may be tremendous differences in the specific details among systems. Thus, results based on one system should not be assumed to be applicable to another.

5. *Nomenclature*. In order to minimize confusion regarding nomenclature, we make the following notes: In general, we follow the conventions established by the nomenclature committees for each model organism whenever appropriate guidelines are available, and briefly summarize the information here using "ATG1" as an example for yeast and mammals. The standard nomenclature of autophagy-related genes, mutants and proteins for yeast is *ATG1*, *atg1* (or *atg1*Δ in the case of deletions) and Atg1, respectively, according to the guidelines adopted by the *Saccharomyces* Genome Database (http://www.yeastgenome.org/gene_guidelines.shtml). For mammals we follow the recommendations of the International Committee on Standardized Genetic Nomenclature for Mice (www.informatics.jax.org/mgihome/nomen/), which dictates the designations *Atg1*, *atg1* and ATG1 (for all rodents), respectively, and the guidelines for human genes established by the HUGO Nomenclature Committee (http://www.genenames.org/guidelines.html), which states that human gene symbols are in the form *ATG1*, and recommends that proteins use the same designation without italics, as with ATG1.

C. Methods and Challenges of Specialized Model Systems

There are now a large number of model systems being used to study autophagy. These guidelines cannot cover every detail, and this article is not meant to provide detailed protocols. Nonetheless, we think it is useful to briefly discuss what techniques can be used in these systems, and to highlight some of the specific concerns and/or challenges. We also refer readers to the three volumes of Methods in Enzymology that provide additional information for "nonstandard" model systems.[38-40]

1. *C. elegans*. *C. elegans* has a single ortholog of most yeast Atg proteins; however, two nematode homologs exist for Atg4 and Atg8.[785] Multiple studies have established *C. elegans* as a useful multicellular genetic model to delineate the autophagy pathway and associated functions (see for example refs.189, 462, 592, 593 and 786). The LGG-1/Atg8/LC3 reporter is the most commonly used tool to detect autophagy in *C. elegans*. Similar to Atg8, which is incorporated into the double membrane of autophagic vesicles during autophagy,[113,187,442] the *C. elegans* LGG-1 localizes into cytoplasmic puncta under conditions known to induce autophagy. Fluorescent reporter fusions of LGG-1/Atg8 with GFP, DsRED or mCherry have been used to monitor autophagosome formation in vivo, in the nematode. These reporters can be expressed either in specific cells and tissues or throughout the animal.[189,593,787,788] LGG-2 is the second LC3 homolog and is also a convenient marker for autophagy either fused to GFP,[789] especially when expressed from an integrated transgene to prevent its germline silencing,[592] or using specific antibodies.[592] The exact function of LGG-1 vs. LGG-2 remains to be addressed.

For observing autophagy by GFP-LC3 fluorescence in *C. elegans*, it is best to use integrated versions of GFP-LC3[592,593,790] (GFP::LGG-1 and GFP::LGG-2; **Fig. 24**) rather than extrachromosomal transgenic strains[189,789] because the latter show variable expression among different animals or mosaic expression (Kang C, personal communication; Galy V, personal communication). It is also possible to carry out indirect immunofluorescence microscopy using antibodies against endogenous LGG-1,[462,593] or LGG-2.[592] In addition, with the integrated version, or with antibodies directed against endogenous LGG-1, it is possible to perform a western blot analysis for lipidation, at least in embryos,[790] and in the whole animal,[593] respectively. Finally, we point out the increasing availability of instruments that are capable of "super-resolution" fluorescence microscopy, which will further enhance the value and possibilities afforded by this technology.[791,792]

2. Chicken B-lymphoid DT40 cells and retina. The chicken B-lymphoid DT40 cell line represents a suitable tool for the analysis of autophagic processes in a nonmammalian vertebrate system. In DT40 cells, foreign DNA integrates with a very high frequency by homologous recombination compared with random integration. This makes the cell line a very valuable tool for the generation of cellular gene knockouts. Generally, the complete knockout of autophagy-regulatory proteins is preferable compared with RNAi-mediated knockdown, since in some cases these proteins function normally when expressed at reduced levels.[171] Different Atg-deficient DT40 cell lines already exist, including *atg13*$^{-/-}$, *ulk1*$^{-/-}$, *ulk2*$^{-/-}$, *ulk1/2*$^{-/-}$,[793] *becn1*$^{-/-}$, and *fip200*$^{-/-}$ (Stork B, personal communication). Many additional non-autophagy-related gene knockout DT40 cell lines have been generated and are commercially available.[794]

DT40 cells are highly proliferative (the generation time is approximately 10 h) and knockout cells can be easily reconstituted with cDNAs by retroviral gene transfer for the mutational analysis of signaling pathways. DT40 cells mount an autophagic response upon starvation in EBSS,[793] and autophagy can be analyzed by a variety of assays in this cell line. Steady-state methods that can be used include TEM, LC3 western blotting and fluorescence microscopy; flux measurements include monitoring LC3-II turnover and tandem mRFP/mCherry-GFP-LC3 fluorescence microscopy. Using *atg13*$^{-/-}$ and *ulk1/2*$^{-/-}$ DT40 cells, it was shown that ATG13 and its binding capacity for FIP200 are mandatory for both basal and starvation-induced autophagy in this cell line, whereas ULK1/2 and in vitro-mapped ULK1-dependent phosphorylation sites of ATG13 appear to be dispensable for these processes.[793]

Another useful system is chick retina, which can be used for monitoring autophagy at different stages of development. For example, lipidation of LC3 is observed during starvation, and can be blocked with a short-term incubation with 3-MA.[305,306] LEP-100 antibody is commercially available for the detection of this lysosomal protein.

Cautionary notes: Since the DT40 cell line derives from chicken bursal lymphoma, not all ATG proteins and autophagy-regulatory proteins are detected by the commercially available antibodies produced against their mammalian orthologs. The chicken genome is almost completely assembled, which facilitates the design of targeting constructs. However, in the May 2006 chicken (*Gallus gallus*) v2.1 assembly 5% of the sequence has not been anchored to specific chromosomes, and this might also include autophagy regulatory genes. It is possible that there is some divergence within the signaling pathways between mammalian and nonmammalian model systems. One example might be the role of ULK1/2 in starvation-induced autophagy described above. Additionally, neither rapamycin nor torin1 seem to be potent inducers of autophagy in DT40 cells, although MTOR activity is completely repressed as detected by phosphorylated RPS6KB2 western blotting.[793] Finally, DT40 cells represent a transformed cell line, being derived from an avian leukosis virus (ALV)-induced bursal lymphoma. Thus, DT40 cells release ALV into the medium, and the 3'-long-terminal repeat has integrated upstream of the c-myc gene, leading to an increased c-myc expression.[795] Both circumstances might influence basal and starvation-induced autophagy.

3. Chlamydomonas. It is possible to detect Atg8 modification as well as an increase in the amount of the protein by western blotting in response to autophagy activation.[207] Detection of Atg8 by immunofluorescence microscopy assays is also a reliable method to study autophagy, although it is recommended that this be combined with western blot analysis.

4. Drosophila. Drosophila provides an excellent system for in vivo analysis of autophagy. In this case, the problem of animal-to-animal variability can be circumvented by the use of clonal mutant cell analysis, a major advantage of this model system. In this scenario, somatic clones of cells are induced that either overexpress the gene of interest, or silence the gene through expression of a transgenic RNA interference construct, or homozygous mutant cells are generated. These gain- or loss-of-function clones are surrounded by wild-type cells, which serve as an internal control for autophagy induction. In such an analysis,

dc 840-14

© Landes Bioscience. Do not distribute.

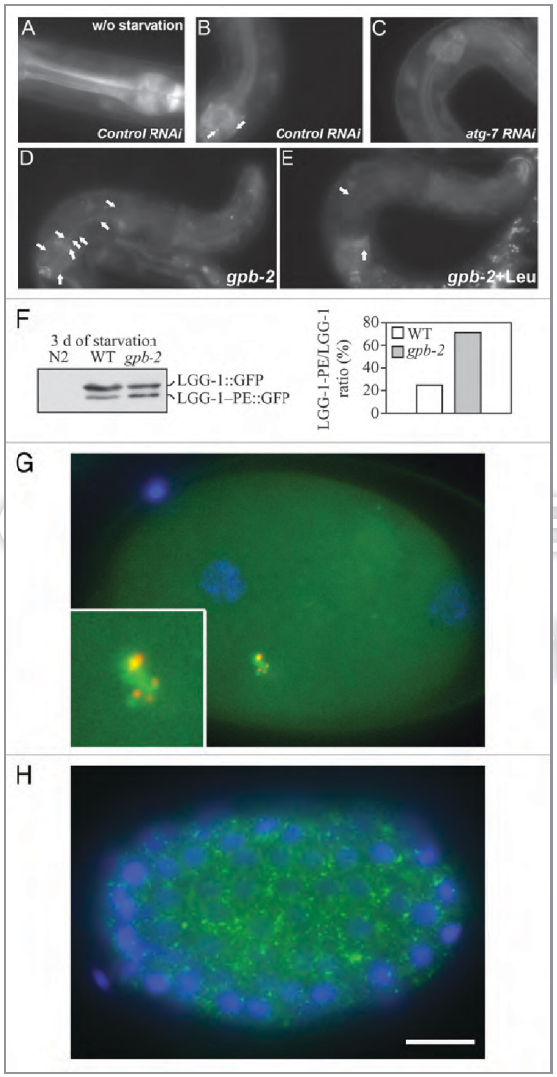


Figure 24. GFP::LGG-1 and GFP::LGG-2 are autophagy markers in *C. elegans*. (A–F) Animals were generated that carry an integrated transgene expressing a GFP-tagged version of *lgg-1*, the *C. elegans* ortholog of mammalian MAP1LC3. Representative green fluorescence images in the pharyngeal muscles of (A) control RNAi animals without starvation, (B) control RNAi animals after 9 d of starvation, (C) *atg-7* RNAi animals after 9 d of starvation, (D) starvation-hypersensitive *gpb-2* mutants without leucine after 3 d of starvation, and (E) *gpb-2* mutants with leucine after 3 d of starvation. The arrows show representative GFP::LGG-1-positive punctate areas that label pre-autophagosomal and autophagosomal structures. (F) The relative levels of PE-conjugated and unconjugated GFP::LGG-1 were determined by western blotting. These figures were modified from data previously published in Kang, C, Y.J. You, and L. Avery. 2007. Dual roles of autophagy in the survival of *Caenorhabditis elegans* during starvation. *Genes & Development*. 21:2161–71, Copyright © 2007, *Genes & Development* by Cold Spring Harbor Laboratory Press and Kang, C., and L. Avery. 2009. Systemic regulation of starvation response in *Caenorhabditis elegans*. *Genes & Development*. 23:12–7, Copyright © 2011, *Genes and Development* by Cold Spring Harbor Laboratory Press, www.genesdev.org. (G and H) GFP:LGG-2 serves as a marker for autophagosomes in early *C. elegans* embryos. (G) GFP::LGG-2 expressed in the germline from an integrated transgene reveal the formation of autophagosomes (green) around sperm inherited membranous organelles (red). DNA of the two pronuclei is stained (blue). (H) Later during development, GFP::LGG-2-positive structures are present in all cells of the embryo. Scale bar, 10 μm. Images provided by V. Galy.

autophagy in these genetically distinct cells is always compared with neighboring cells of the same tissue, thus eliminating most of the variability and also ruling out potential non-cell-autonomous effects that may arise in mutant animals. Along these lines, clonal analysis should be an integral part of in vivo Drosophila studies when possible.

LC3-II western blotting using antibodies against mammalian proteins does not work in Drosophila (Baehrecke E, Denton D, Kumar S, Neufeld T, unpublished results). Western blotting has been used successfully in Drosophila by monitoring flies expressing human GFP-LC3[101,197] or using an antibody directed against the endogenous Atg8 protein.[454,796] In addition, cultured Drosophila (S2) cells can be stably transfected with GFP fused to Drosophila Atg8a, which generates easily resolvable GFP-Atg8a and GFP-Atg8a–PE forms that respond to autophagic stimuli (Wilkinson S, personal communication). Similarly, cultured Drosophila cells (l(2)mbn or S2) stably transfected with EGFP-humanLC3B respond to autophagy stimuli (nutrient deprivation) and inhibitors (3-MA, bafilomycin A_1) as expected, and can be used to quantify GFP-LC3 puncta, which works best using fixed cells with the aid of an anti-GFP antibody.[797] However, in the Drosophila eye, overexpression of GFP-Atg8 results in a significant increase in Atg8–PE by western blot, and this occurs even in control flies in which punctate GFP-Atg8 is not detected by immunofluorescence (Fanto M, unpublished results), and in transfected Drosophila Kc167 cells, uninducible but persistent GFP-Atg8 puncta are detected (Kiger A, unpublished results). In contrast, expression of GFP-LC3 under the control of the rh1 promoter in wild-type flies did not result in the formation of LC3-II detectable by western blot, nor the formation of punctate staining; however, increased GFP-LC3 puncta by immunofluorescence or LC3-II by western blot were observed upon activation of autophagy (Mollereau B, unpublished results). Autophagy can also be monitored with mCherry-Atg18, which is displayed in punctate patterns that are very similar to mCherry-Atg8a (Juhász G, personal communication). Tandem fluorescence reporters have been established in Drosophila in vivo, where GFP-mCherry-Atg8a is expressed in the nurse cells of the developing egg chamber.[662] A Drosophila transgenic line (Ref(2)P-GFP) and a specific antibody against Ref(2)P, the Drosophila p62 homolog, are available to follow p62 expression and localization.[312,368]

5. Filamentous fungi. As in yeast, autophagy is involved in nutrient recycling during starvation.[193,194,798-801] In addition, macroautophagy seems to be involved in many normal developmental processes such as sexual and asexual reproduction, where there is a need for reallocation of nutrients from one part of the mycelium to another to supply the developing spores and spore-bearing structures.[194,798,799,801,802] Similarly, autophagy also affects conidial germination under nitrogen-limiting conditions.[194] In *Podospora anserina*, autophagy has been studied in relation to incompatibility reactions between mating strains where it seems to play a prosurvival role.[192,802] Of special interest to many researchers of autophagy in filamentous fungi has been the possible involvement of autophagy in plant pathogen infection and growth inside the host.[193,798,799,803-805] Autophagy also appears to be necessary for the development of aerial hyphae,[194,798,802,804] and for appresorium function in *Magnaporthe oryzae* and *Colletotrichum orbiculare*.[193,803,804] Some of these effects could be caused by the absence of autophagic processing of storage lipids (lipophagy) to generate glycerol for increasing turgor.[798,804,805]

Methods for functional analysis of autophagy have been covered in a review article.[806] Most studies on autophagy in filamentous fungi have involved deleting some of the key genes necessary for autophagy, followed by an investigation of what effects this has on the biology of the fungus. Most commonly, *ATG1* and/or *ATG8* has been deleted.[193,798,799,801,802,804] To confirm that the deletion(s) affects autophagy, the formation of autophagic bodies in the wild type and the mutant can be compared. In filamentous fungi the presence of autophagic bodies can be detected using MDC staining,[193,798] TEM[193,799] or fluorescence microscopy to monitor Atg8 tagged with a fluorescent protein.[194,801,802] This type of analysis is most effective after increasing the number of autophagic bodies by starvation, in combination with decreasing the degradation of the autophagic bodies through the use of the protease inhibitor PMSF,[193,799,801,802] or alternatively by adding the autophagy-inducing drug rapamycin.[194,798] In filamentous fungi it might also be possible to detect the accumulation of autophagic bodies in the vacuoles using differential interference contrast (DIC) microscopy.[801,802] Additional information regarding the timing of autophagy induction can be gained by monitoring transcript accumulation of *ATG1* and/or *ATG8* using qRT-PCR.[799]

6. Honeybee. The reproductive system of bees, or insects with meroistic polytrophic ovaries, with regard to the ovary developmental cycle can be a very useful tool to analyze and monitor physiological autophagy. Both queen and worker ovaries of Africanized *A. mellifera* display time-regulated features of cell death that are, however, linked to external stimuli.[807] Features of apoptosis and autophagy are frequently associated with the degeneration process in bee organs, but only more recently has the role of autophagy been highlighted in degenerating bee tissues. TEM is the primary method currently being used to monitor autophagy by following the formation of autophagosomes and autolysosomes. This can be combined with cytochemical and immunohistochemical detection of acid phosphatase as a marker for autolysosomes.[808,809] Acidotropic dyes can also be used to follow autophagy in bee organs, as long as the cautions noted in this article are followed. The honeybee genome has been sequenced, and differential gene expression has been used to monitor *Atg18* in bees parasitized by *Varroa destructor*.[810]

7. Human. Considering that much of the research conducted today is directed at understanding the functioning of the human body, in both normal and disease states, it is pertinent to include humans and primary human tissues and cells as important models for the investigation of autophagy. Although clinical studies are not readily amenable to these types of analyses, it should be kept in mind that the TORC1 inhibitor rapamycin is available as a clinically approved drug (e.g., sirolimus). Furthermore, fresh biopsies of some human tissues are possible to obtain. Blood, in particular, as well as samples of adipose and muscle tissues, can be obtained from needle biopsies or from elective surgery. For example, in a large study, adipocytes were isolated from pieces of adipose tissue (obtained during surgery) and examined for insulin signaling and autophagy. It was demonstrated that autophagy was strongly upregulated (based on LC3 flux, EM, and lipofuscin degradation) in adipocytes obtained from obese patients with type 2 diabetes compared with nondiabetic subjects.[209]

The major caveat of the work concerning autophagy on human tissue is the problem of postmortem times and fixation. Postmortem times are typically longer in autopsy material than when surgical biopsies are obtained. For tumors, careful sampling to avoid necrosis, hemorrhagic areas and non-neoplastic tissue is required. The problem of fixation is that it can diminish the antibody binding capability; in addition, especially in autopsies, material is not obtained immediately after death.[811,812] The possibilities of postmortem autolysis and fixation artifacts must always be taken into consideration when interpreting changes attributed to autophagy.[813] Analyses of these types of samples require not only special antigen retrieval techniques, but also histopathological experience to interpret autophagy studies by immunohistochemistry, immunofluorescence or TEM.

The situation is even worse with TEM, where postmortem delays can cause vacuolization. Researchers experienced in the

dc 840 14

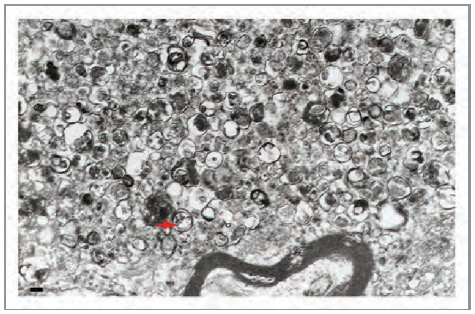


Figure 25. A large dystrophic neurite from a brain biopsy of a patient with Gerstmann-Sträussler-Scheinker (GSS) disease not unlike those reported for Alzheimer disease.[814] This structure is filled with innumerable autophagic vacuoles, some of which are covered by a double membrane. Electron dense lysosomal-like structures are also visible. The red arrow points to a double-membrane autophagic vacuole. Scale bar, 200 nm. Image provided by P. Liberski.

analysis of TEM images corresponding to autophagy should be able to identify these potential artifacts because autophagic vacuoles should contain cytoplasm. While brain biopsies may be usable for high quality TEM (**Figs. 25** and **26**), this depends upon proper handling at the intraoperative consultation stage, and such biopsies are performed infrequently except for brain tumor diagnostic studies. An analysis that examined liver and skeletal muscle from critically ill patients utilized tissue biopsies that were taken within 30 ± 20 min after death and were flash-frozen in liquid nitrogen followed by storage at -80°C.[815] Samples could subsequently be used for EM and western blot analysis.

A major limitation of studying patient biopsies is that only static measurements can be performed. This limitation does not apply, however, for dynamic experiments on tissue biopsies or cells derived from biopsies, as described above.[209] Multiple measurements over time, especially when deep (vital) organs are involved, are impossible and ethically not justifiable. Hence, quantitative flux measurements are virtually impossible in patients. To overcome these problems to the extent possible and to gain a more robust picture of the autophagic status, observational studies need to include two different aspects. First, a static marker for phagophore or autophagosome formation needs to be measured. This can be done by assessing ultrastructural changes with TEM and/or on the molecular level by measuring LC3-II protein levels. Second, accumulation of autophagy substrates, such as p62 and (poly)ubiquitinated proteins can provide information on the overall efficacy of the pathway and can be a surrogate marker of the consequences of altered autophagic flux, especially when autophagy is insufficient, although these changes can also be affected by the ubiquitin-proteasome system as mentioned above. In addition, and even more so when problems with specific pathways are suspected (e.g., mitophagy), specific substrates of these pathways should be determined. Again, none of these measurements on its own provides enough information on (the efficacy of) autophagy, because other processes may confound

©2012 Landes Bioscience. Do not distribute.

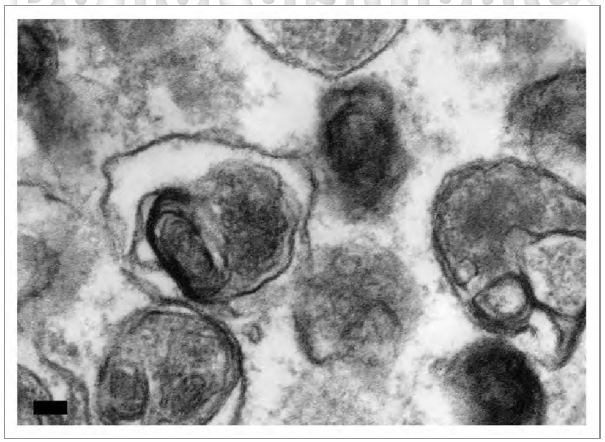


Figure 26. A high-power electron micrograph from a brain biopsy showing autophagic vacuoles in a case of ganglioglioma. Scale bar, 200 nm. Image provided by P. Liberski.

every single parameter. However, the combination of multiple analyses should be informative. Although still in its infancy with regard to autophagy, it is worth pointing out that mathematical modeling has the power to bridge whole body in vivo data with in vitro data from tissues and cells. The usefulness of so-called hierarchical or multilevel modeling has thus been demonstrated when examining the relevance of insulin signaling to glucose uptake in primary human adipocytes compared with whole-body glucose homeostasis.[816]

The amino acid exchange rate, which has been suggested as a minimal invasive marker for measuring autophagic flux in vivo should be used with special caution, as its utility is debatable in disease models (see *Analyses in vivo*).

A stepwise process can be proposed for linking changes in the autophagic pathway to changes in disease outcome. First, in an observational study, the changes in the autophagic pathway (see above) should be quantified and linked to changes in disease outcome. To prove causality, a subsequent autophagy-modifying intervention should be tested in a randomized study. Before an intervention study is performed in human patients, the phenotype of (in)active autophagy contributing to poor outcome should be established in a validated animal model of the disease. For the validation of the hypothesis in an animal model, a similar two-step process is suggested, with the assessment of the phenotype in a first stage, followed by a proof-of-concept intervention study (see *Large animals*).

8. Hydra. Hydra is a freshwater cnidarian animal that provides a unique model system to test autophagy either in the context of nutrient deprivation, as these animals easily survive several weeks of starvation,[817,818] or in the context of regeneration, because in the absence of protease inhibitors, bisection of the animals leads to an uncontrolled wave of autophagy; in the latter case, an excess of autophagy in the regenerating tip immediately after amputation is deleterious.[819-821] Most components of the autophagy and MTOR pathways are evolutionarily conserved in Hydra.[818] For steady-state measurements, autophagy can be monitored by western blot for ATG8/LC3, by immunofluorescence (using antibodies to ATG8/LC3, LBPA or RSK), or with dyes such as MitoFluor Red 589 and LysoTracker Red. Flux measurements can be made by following ATG8/LC3 turnover using lysosomal protease inhibitors (leupeptin and pepstatin A), or in vivo labeling using LysoTracker Red. It is also possible to monitor MTOR activity with phosphospecific antibodies to RPS6KB2 kinase and EIF4EBP1, or to examine gene expression by semiquantitative RT-PCR, using primers that are designed for Hydra. Autophagy can be induced by RNAi-mediated knockdown of *Kazal1*,[819,820] or with rapamycin treatment, and can be inhibited with wortmannin or bafilomycin A_1.[817,818]

9. Large animals. Assessment of autophagy (and, in particular, autophagic flux) in clinically relevant large animal models is critical in establishing its (patho)physiological role in multiple disease states. For example, evidence obtained in swine suggests that upregulation of autophagy may protect the heart against damage caused by acute myocardial infarction or "heart attack."[822] Autophagy also plays an important role in the development and remodeling of the bovine mammary gland. In vitro studies with the use of a three-dimensional culture model of bovine mammary epithelial cells (MECs) have shown that this process is involved in the formation of fully developed alveoli-like structures.[823] Earlier studies show that intensified autophagy is observed in bovine MECs at the end of lactation and during the dry period, when there is a decrease in the levels of lactogenic hormones, increased expression of auto/paracrine apoptogenic peptides, increased influence of sex steroids and enhanced competition between the intensively developing fetus and the mother organism for nutritional and bioactive compounds.[824,825] These studies were based on some of the methods described elsewhere in these guidelines, including GFP-Atg8/LC3 fluorescence microscopy, TEM, and western blotting of LC3 and BECN1. Creation of a specific GFP-LC3 construct by insertion of cDNA encoding bovine LC3 into the pEGFP-C1 vector makes it possible to observe induction of autophagy in bovine MECs in a more specific manner than can be achieved by immunofluoresce techniques, in which the antibodies do not show specific reactivity to bovine cells and tissues.[823,825] However, it is important to remember that definitive confirmation of cause-and-effect is challenging for studies on large animals, given the lack or poor availability of specific antibodies and other molecular tools, the frequent inability to utilize genetic approaches, and the often prohibitive costs of administering pharmacological inhibitors in these translational preparations.

In contrast with cell culture experiments, precise monitoring of autophagic flux is practically impossible in large animals. Theoretically, repetitive analyses of small tissue biopsies should be performed to study ultrastructural and molecular alterations over time in the presence or absence of an autophagy inhibitor (e.g., chloroquine). However, several practical problems impede applicability of this approach. First, repetitive sampling of small needle biopsies in the same animal (a major challenge by itself) could be assumed to induce artifacts following repetitive tissue destruction, especially when deep (vital) organs are involved. In addition, chemical inhibitors of autophagy have considerable side effects and toxicity, hampering their usage. Also, the general physical condition of an animal may confound results obtained with administration of a certain compound, for instance altered uptake of the compound when perfusion is worse.

Therefore, in contrast to cells, where it is more practical to accurately document autophagic flux, we suggest the use of a stepwise approach in animal models to provide a proof-of-concept with an initial evaluation of sequellae of (in)active autophagy and the relation to the outcome of interest.

First, prior to an intervention, the static ultrastructural and molecular changes in the autophagic pathway should be documented and linked to the outcome of interest (organ function, muscle mass or strength, survival, etc.). These changes can be evaluated by light microscopy, EM and/or by molecular markers such as LC3-II. In addition, the cellular content of specific substrates normally cleared by autophagy should be quantified, as such measurement, despite the static nature, could provide a clue about the results of altered autophagic flux in vivo. These autophagic substrates can include p62 and (poly) ubiquitinated substrates or aggregates, but also specific substrates such as damaged mitochondria. As noted above, measurement of

dc_840_14

these autophagic substrates is mainly informative when autophagic flux is prohibited/insufficient, and, individually, all have specific limitations for interpretation. As mentioned several times in these guidelines, no single measurement provides enough information on its own to reliably assess autophagy, and all measurements should be interpreted in view of the whole picture. In every case, both static measurements reflecting the number of autophagosomes (ultrastructural and/or molecular) and measurements of autophagic substrates as surrogate markers of autophagic flux need to be combined. Depending on the study hypothesis, essential molecular markers can further be studied to pinpoint at which stage of the process autophagy may be disrupted.

After having identified a potential role of autophagy in mediating an outcome in a clinically relevant animal model, an autophagy-modifying intervention should be tested. For this purpose, an adequately designed, randomized controlled study of sufficient size on the effect of a certain intervention on the phenotype and outcome can be performed in a large animal model. Alternatively, the effect of a genetic intervention can be studied in a small animal model with clinical relevance to the studied disease.

As mentioned above, exact assessment of autophagic flux requires multiple time points, which cannot be done in the same animal. Alternatively, different animals can be studied for different periods of time. Due to the high variability between animals, however, it is important to include a sufficiently high number of animals per time point. This thus limits feasibility and the number of time points that can be investigated. The right approach to studying autophagy in large animals likely differs depending on the question that is being addressed. Several shortcomings regarding the methodology, inherent to working with large animals, can be overcome by an adequate study design. As for every study question, the use of an appropriate control group with a sufficient number of animals is crucial in this regard.

10. Lepidoptera. Some of the earliest work in the autophagy field was performed in the area of insect metamorphosis.[667] Microscopy and biochemical research revealed autophagy during the metamorphosis of American silkmoths and the tobacco hornworm, *Manduca sexta*, and included studies of the intersegmental muscles, but they did not include molecular analysis of autophagy. Overall, these tissues cannot be easily maintained in culture, and antibodies against mammalian proteins do not often work. Accordingly, these studies were confined to biochemical measurements and electron micrographs. During metamorphosis, the bulk of the larval tissue is removed by autophagy and other forms of proteolysis.[826] *Bombyx mori* is now used as a representative model among Lepidoptera, for studying not only the regulation of autophagy in a developmental setting, but also the relations between autophagy and apoptosis. The advantages of this model are the large amount of information gathered on its developmental biology, physiology and endocrinology, the availability of numerous genetic and molecular biology tools, and a completely sequenced genome.[827] The basic studies of *B. mori* autophagy have been performed in four main larval systems: the silk gland, the fat body, the midgut and the ovary. The methods used for these studies are comparatively similar, starting from EM, which is the most widely used method to follow the changes of various autophagic structures and other features of the cytosol and organelles that are degraded during autophagy.[452,828-831] Immuno-TEM also can be used, when specific antibodies for autophagic markers are available. Acidotropic dyes such as MDC and LysoTracker Red staining have been used as markers for autophagy in silk moth egg chambers combined always with additional assays.[828,829] Acidic phosphatase also can be used as a marker for autolysosomal participation in these tissues.[452,830,832] Systematic cloning and analysis revealed that homologs of most of the *Atg* genes identified in other insect species such as Drosophila are present in *B. mori*, and 11 *Atg* genes have now been identified in the silkworm genome, as well as other genes involved in the MTOR signal transduction pathway.[833,834] Variations in the expression of several of these genes have been monitored not only in silkworm larval organs, where autophagy is associated with development,[452,833-835] but also in the fat body of larvae undergoing starvation.[833]

In the IPLB-LdFB cell line, derived from the fat body of the caterpillar of the gypsy moth *Lymantria dispar*, indirect immunofluorescence experiments have demonstrated an increased number of Atg8-positive dots in cells with increased autophagic activity; however, western blotting did not reveal the conversion of Atg8 into Atg8–PE. Instead, a single band with an approximate molecular mass of 42 kDa was observed that was independent of the percentage of cells displaying punctate Atg8 (Malagoli D, unpublished results). In contrast, with *B. mori* midgut, the use of an antibody specific for BmAtg8 makes it possible to monitor BmAtg8 processing to BmAtg8–PE by western blotting.[452] Thus, the utility of monitoring Atg8 in insects may depend on the particular organism and antibody.

11. Neotropical teleosts. In tropical environments, fish have developed different reproductive strategies, and many species have the potential for use as biological model in cell and molecular biology, especially for studying the mechanisms that regulate gametogenesis and embryo development. In these fish, the ovary is a suitable experimental model system for studying autophagy and its interplay with cell death programs due to the presence of postovulatory follicles (POFs) and atretic follicles (AFs), which follow different routes during ovarian remodeling after spawning.[836] In the fish reproductive biology, POFs are excellent morphological indicators of spawning, whereas AFs are relevant biomarkers of environmental stress. In addition, many freshwater teleosts of commercial value do not spawn spontaneously in captivity, providing a suitable model for studying the mechanisms of follicular atresia under controlled conditions.[837] When these species are subjected to induced spawning, the final oocyte maturation (resumption of meiosis) occurs, and POFs are formed and quickly reabsorbed in ovaries after spawning.[838] Assessment of autophagy in fish has been primarily made using TEM at different times of ovarian regression.[839] Due to the difficulty of obtaining antibodies specific for each fish species, immunodetection of ATG-proteins (mainly LC3 and BECN1) by immunohistochemistry associated with analyses by western blotting can be performed using antibodies that are commercially available for other vertebrates. Such studies suggest dual roles for autophagy in follicular cells;[836] however, evaluation of the autophagic flux in different conditions is critical for establishing its physiological role during follicular regression and ovarian remodeling after spawning. Given the ease of obtaining samples and monitoring them during development, embryos of these fish are also suitable models for studying autophagy that is activated in response to different environmental stressors, particularly in studies in vivo.

12. Odontoblasts. Odontoblasts are long-lived dentin-forming postmitotic cells, which evolved from neural crest cells early during vertebrate evolution. These cells are aligned at the periphery of the dental pulp and are maintained during the entire healthy life of a tooth. As opposed to other permanent postmitotic cells such as cardiac myocytes or central nervous system neurons, odontoblasts are significantly less protected from environmental insult, such as dental caries and trauma. Mature odontoblasts develop a well-characterized autophagic-lysosomal system, including a conspicuous autophagic vacuole that ensures turnover and degradation of cell components. Immunocytochemical and TEM studies make it possible to monitor age-related changes in autophagic activity in human odontoblasts.[840]

13. Planarians. Planarians are one of the favorite model systems in which to study regeneration and stem cell biology, and represent a unique model where it is possible to investigate autophagy in the context of regeneration, stem cells and growth. Currently the method used to detect autophagy is TEM. A detailed protocol adapted to planarians has been described.[841,842] However, complementary methods to detect autophagy are also needed, since TEM cannot easily distinguish between activation and blockage of autophagy, which would both be observed as an accumulation of autophagosomes. Detection of autophagy by other methods are being developed (González-Estévez C, personal communication), including immunohistochemistry and western blotting approaches for the planarian homolog of LC3. Several commercial antibodies against human LC3 have been tried for cross-reactivity without success (see the *Autophagy Forum* for details) and three planarian-specific antibodies have been generated. Some preliminary results show that LysoTracker Red can be a useful technique on whole-mount planarians. Interestingly, most of the components of the autophagy and MTOR signaling machinery are evolutionarily conserved in planarians, and an RNA interference screen is being performed. Whether autophagy genes vary at the mRNA level during starvation and after depletion of MTOR signaling components is also currently being investigated (González-Estévez C, personal communication).

14. Plants. The fluorophore of the red fluorescent protein shows a relatively high stability under acidic pH conditions. Thus, chimeric RFP fusion proteins that are sequestered within autophagosomes and delivered to the plant vacuole can be easily detected by fluorescence microscopy. Furthermore, fusion proteins with some versions of RFP tend to form intracellular aggregates, allowing the development of a visible autophagic assay for plant cells.[843] For example, fusion of cytochrome b5 and the original (tetrameric) RFP generate an aggregated cargo protein that displays cytosolic puncta of red fluorescence and, following vacuolar delivery, diffuse staining throughout the vacuolar lumen. This system allows autophagy to be monitored through fluorescence microscopy with minimum damage to intact plant cells. In addition, the size difference between the intact and processed cargo protein allows the quantification of autophagic degradation through the detection of RFP after separation of total protein by gel electrophoresis, similar to the GFP-Atg8/LC3 processing assay described for yeast and mammals.

Arabidopsis cells can be stably transfected with GFP fused to plant ATG8, and the lipidated and nonlipidated forms can be separated by SDS-PAGE.[150] Furthermore, the GFP-ATG8 processing assay is particularly robust in Arabidopsis and can be observed not only by western blotting but also by a diffuse fluorescent haze that appears in vacuoles together with punctate GFP fluorescence, which is presumed to represent free soluble GFP and GFP-ATG8–PE still bound to autophagic bodies, respectively.[151,174] Thus, as with other systems, autophagosome formation in plants can be monitored through the use of fluorescent protein fusions to ATG8, and by TEM (**Fig. 27**). A tandem fluorescence reporter system is also available in Arabidopsis.[844]

Furthermore, it is possible to use plant homologs of p62 and NBR1 (JOKA2 in tobacco[845] and NBR1 in Arabidopsis[844]) as markers for autophagy when constructed as fluorescent chimeras. It is worth noting that in some plant models including Arabidopsis[200,402] and somatic embryos of *Picea abies* (Norway spruce) (Minina A, Bozhkov PV, personal communication), the high turnover rate of Atg8-decorated autophagosomes precludes their detection in untreated cells using fluorescent markers (GFP/RFP-Atg8, MDC or LysoTracker) and necessitates pretreatment with concanamycin A. However, the latter treatment will increase vacuolar pH, which may subsequently interfere with its detection by MDC and LysoTracker.

In some systems, including fungi and plants, the size of the vacuole is sufficiently large such that fusion of the autophagosome

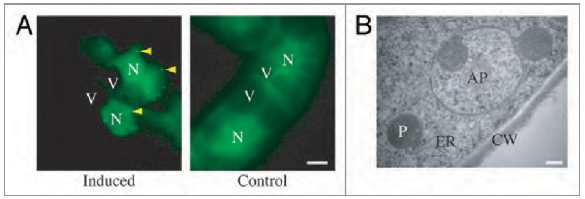


Figure 27. Detection of macroautophagy in tobacco BY-2 cells. (A) Induction of autophagosomes in tobacco BY-2 cells expressing YFP-NtAtg8 (shown in green for ease of visualization) under conditions of nitrogen limitation (Induced). Arrowheads indicate autophagosomes that can be seen as a bright green dot. No such structure was found in cells grown in normal culture medium (Control). Bar, 10 μm. N, nucleus; V, vacuole. (B) Ultrastructure of an autophagosome in a tobacco BY-2 cell cultured for 24 h without a nitrogen source. Bar, 200 μm. AP, autophagosome; P, plastid; CW, cell wall. This image was provided by Dr. Kiminori Toyooka, (RIKEN Plant Science Center).

doi: 10.4161/auto.8.4.19840

results in the release of the inner vesicle into the organelle lumen; the resulting single-membrane vesicle is termed an autophagic body (**Fig. 1**).[200,846] The accumulation of autophagic bodies can be detected by light microscopy in cells that lack vacuolar hydrolase activity (e.g., the *pep4*Δ yeast mutant) or in the presence of inhibitors that interfere with hydrolase activity (e.g., PMSF or concanamycin). Using Nomarski optics (differential interference contrast) it is easy to distinguish and quantify yeast vacuoles that lack autophagic bodies from those that have accumulated them, and the same is true for plants.

Other methods described throughout these guidelines can also be used in plants. For example, in tobacco cells cultured in sucrose starvation medium, the net degradation of cellular proteins can be measured by a standard protein assay; this degradation is inhibited by 3-MA and E-64c (an analog of E-64d), and is thus presumed to be due to autophagy.[847] In addition, the cytoplasm in tobacco cells that is present in transvacuolar strands that cross the large central vacuole can be seen by TEM to disappear during starvation-induced autophagy.[847]

Cautionary notes: Although the detection of vacuolar RFP can be applied to both plant cell lines and to intact plants, it is not practical to measure RFP fluorescence in intact plant leaves, due to the very high red fluorescence of chloroplasts. Furthermore, different autophagic induction conditions cause differences in protein synthesis rates; thus, special care should be taken to monitor the efficiency of autophagy by quantifying the intact and processed cargo proteins. With regard to autophagic body accumulation, it is difficult to quantify their number and/or volume, although their presence or absence can be examined by light microscopy or TEM. In addition, the accumulation of autophagic bodies requires the inhibition of vacuolar hydrolase activity. Therefore, to demonstrate turnover, the assay must be performed either in the absence and presence of appropriate inhibitors, or in both a wild-type strain and a strain with a mutation/deletion in a gene encoding a vacuolar hydrolase(s) (see *Selective types of autophagy*). Otherwise, accumulation of autophagic bodies could instead indicate a defect in the lysis/degradation step of autophagy. Finally, this method is not well suited for systems other than plants or fungi because lysosomes are too small for detection by standard (i.e., nonfluorescence) light microscopy, and fusion with autophagosomes does not generate autophagic bodies (**Fig. 1**).

15. Protists. An essential role of autophagy during the differentiation of parasitic protists (formerly called protozoa) is clearly emerging. Only a few of the known *ATG* genes are present in these organisms, which raises the question about the minimal system that is necessary for the normal functioning of autophagy. The reduced complexity of the autophagic machinery in many protists provides a simplified model to investigate the core mechanisms of autophagosome formation necessary for selective proteolysis, and will open a completely new area in autophagy research. Some of the standard techniques used in other systems can be applied to protists including indirect immunofluorescence using antibodies generated against ATG8, the generation of stable lines expressing mCherry- or GFP-fused ATG8 for live microscopy and immuno-TEM analyses. Extrachromosomal constructs of GFP-ATG8 also work well with lower eukaryotes,[201-203] as do other fluorescently-tagged ATG proteins including ATG5 and ATG12.

The unicellular amoeba *Dictyostelium discoideum* provides another useful system for monitoring autophagy.[848] The primary advantage of Dictyostelium is that it has a unique life cycle that involves a transition from a unicellular to a multicellular form. Upon starvation, up to 100,000 single cells aggregate by chemotaxis and form a multicellular structure that undergoes morphogenesis and cell-type differentiation. Development proceeds via the mound stage, the tipped aggregate and a motile slug and culminates with the formation of a fruiting body that is composed of a ball of spores supported by a thin, long stalk made of vacuolized dead cells. Development is dependent on autophagy and, at present, all of the generated mutants in Dictyostelium autophagy genes display developmental phenotypes of varying severity.[848,849] *D. discoideum* is also a versatile model to study infection with human pathogens and the role of autophagy in the infection process. The susceptibility of *D. discoideum* to microbial infection and its strategies to counteract pathogens are similar to those in higher eukaryotes.[850] Along these lines, Dictyostelium utilizes some of the proteins involved in autophagy that are not present in *S. cerevisiae* including Atg101, Uvrag and Vmp1, in addition to the core Atg proteins. Autophagy can be monitored in Dictyostelium by fluorescence microscopy of GFP-Atg8, by TEM and by western blot to detect free GFP or the loss of p62.[848]

One cautionary note with regard to the use of GFP-ATG8 in protists is that these organisms display some "nonclassical" variations in their ATG proteins. For example, Leishmania contains many apparent ATG8-like proteins (the number varying per species; e.g., up to 25 in *L. major*) grouped in four families, but only one labels true autophagosomes even though the others form puncta,[202] and ATG12 requires truncation to provide the C-terminal glycine before it functions in the canonical way. Unusual variants in protein structures also exist in other protists, including the malaria parasite *Plasmodium falciparum*, which expresses ATG8 with a terminal glycine not requiring cleavage to become functional in autophagy.[851] Thus, in each case care needs to be applied and the use of the protein to monitor autophagy validated. In addition, due to possible divergence in the upstream signaling kinases, classical inhibitors such as 3-MA, or inducers like rapamycin, which are not as potent for trypanosomes[852] or apicomplexan parasites as in mammalian cells or yeast, must be used with caution (Coppens I, personal communication);[201] however, RNAi knockdown of TORC1 (e.g., TOR1 or RAPTOR) is effective in inducing autophagy.

The scuticociliate *Philasterides dicentrarchi* has proven to be a good experimental organism for identifying autophagy-inducing drugs or for autophagy initiation by starvation-like conditions, since this process can be easily induced and visualized in this ciliate.[853] In scuticociliates, the presence of autophagic vacuoles can be detected by TEM, fluorescence microscopy or confocal laser scanning microscopy by using dyes such as MitoTracker Deep Red FM® and MDC.

Finally, a novel autophagy event has been found in *Tetrahymena thermophila*, which is a free-living ciliated protist. A remarkable, virtually unique feature of the ciliates is that they maintain spatially differentiated germline and somatic nuclear genomes within a single cell. The germline genome is housed in the micronucleus, while the somatic genome is housed in the macronucleus. These nuclei are produced during sexual reproduction (conjugation), which involves not only meiosis and mitosis of the micronucleus and its products, but also degradation of some of these nuclei as well as the parental old macronucleus. Hence, there should be a mechanism governing the degradation of these nuclei. The inhibition of PtdIns3Ks with wortmannin or LY294002 results in the accumulation of additional nuclei during conjugation.[854] During degradation of the parental old macronucleus, the envelope of the nucleus becomes MDC- and LysoTracker Red-stainable without sequestration of the nucleus by a double membrane and with the exposure of certain sugars and phosphatidylserine on the envelope.[855] Subsequently, lysosomes fuse only to the old parental macronucleus, but other co-existing nuclei such as developing new macro- and micronuclei are unaffected.[855] This evidence suggests that selective autophagy may be involved in the regulation of the degradation of nuclei during conjugation, but its mechanism apparently differs from the classical pathway. Indeed, no *ATG* genes homologous to those in yeast are characterized in this organism to date.

16. Rainbow trout. Salmonids (e.g., salmon, rainbow trout) experience long periods of fasting often associated with seasonal reductions in water temperature and prey availability or spawning migrations. As such, they represent an interesting model system for studying and monitoring the long-term induction of autophagy. Moreover, the rainbow trout (*Oncorhynchus mykiss*) displays unusual metabolic features that may allow us to gain a better understanding of the nutritional regulation of this degradative system (i.e., a high dietary protein requirement, an important use of amino acids as energy sources, and an apparent inability to metabolize dietary carbohydrates). It is also probably one of the most deeply studied fish species with a long history of research performed in physiology, nutrition, ecology, genetics, pathology, carcinogenesis and toxicology.[856] Its relatively large size compared with model fish such as zebrafish or medaka, makes rainbow trout a particularly well-suited alternative model to carry out biochemical and molecular studies on specific tissues or cells that are impossible to decipher in small fish models. The genomic resources in rainbow trout are now being extensively developed; a high-throughput DNA sequencing program of EST has been initiated associated with numerous transcriptomics studies,[857-860] and the full genome sequence is now available.

Most components of the autophagy and associated signaling pathways (AKT, TOR, AMPK, FOXO) are evolutionarily conserved in rainbow trout;[457,861-863] however, not all ATG proteins and autophagy-regulatory proteins are detected by the commercially available antibodies produced against their mammalian orthologs. Nonetheless, the expressed sequence transcript databases facilitate the design of targeting constructs. For steady-state measurement, autophagy can be monitored by western blot or by immunofluorescence using antibodies to ATG8/LC3.[863] Flux measurements can be made in a trout cell culture model (e.g., in primary culture of trout myocytes) by following ATG8/LC3 turnover in the absence and presence of bafilomycin A_1. It is also possible to monitor the mRNA levels of *ATG* genes by real-time PCR using primer sequences chosen from trout sequences available in the above-mentioned expressed sequence transcript database. A major challenge in the near future will be to develop for this model the use of RNAi-mediated gene silencing in order to analyze the role of some signaling proteins in the control of autophagy, and also the function of autophagy-related genes in this species.

17. Sea urchin. Sea urchin embryo is an appropriate model system for studying and monitoring autophagy and other defense mechanisms activated during physiological development and in response to stress.[632] This experimental model offers the possibility of detecting LC3 through both protein gel blot and immunofluorescence in situ analysis. Furthermore, in vivo staining of autolysosomes with acidotropic dyes can also be performed. Studies on whole embryos make it possible to obtain qualitative and quantitative data for autophagy and also to get information about spatial localization aspects in cells that interact among themselves in their natural environment. Cautionary notes include the standard recommendation that it is always preferable to combine molecular and morphological parameters to support the validity of the data.

18. Ticks. In the hard tick *Haemaphysalis longicornis*, endogenous autophagy-related proteins (Atg6 and Atg12) can be detected by western blotting and/or by immunohistochemical analysis of midgut sections.[864,865] It is also possible to detect endogenous Atg3 and Atg8 by western blotting using antibodies produced against the *H. longicornis* proteins (Umemiya-Shirafuji R, unpublished results). Commercial antibodies against mammalian ATG orthologs (ATG3, ATG5, and BECN1) can be also used for western blotting; however, when the tick samples include blood of a host animal, the animal species immunized with autophagy-related proteins should be checked before use to avoid nonspecific background cross-reactivity. In addition to these methods, TEM is recommended to detect autophagosomes and autolysosomes. Although acidotropic dyes can be useful as a marker for autolysosomes in some animals, careful attention should be taken when using the dyes in ticks. Since the midgut epithelial cells contain acidic organelles (e.g., lysosomes) that are related to blood digestion during blood feeding, this method may cause confusion. It is difficult to distinguish between autophagy (autolysosomes) and blood digestion (lysosomes) with acidotropic dyes. Another available monitoring method is to assess the mRNA levels of tick *ATG* genes by real-time PCR.[866] However, this method should be used along with other approaches such as western blotting, immunostaining, and TEM as described in this article. Unlike model insects, such as Drosophila, powerful genetic tools to assess autophagy are still not established in ticks. However, RNAi-mediated gene silencing is currently being developed to analyze the function of autophagy-related genes in ticks during nonfeeding periods (Umemiya-Shirafuji R, unpublished results).

19. Food biotechnology. Required for yeast cell survival under a variety of stress conditions, autophagy has the potential to contribute to the outcome of many food fermentation processes.

dc_840_14

For example, autophagy induction is observed during the primary fermentation of synthetic grape must,[867] and during sparkling wine production (secondary fermentation).[868] A number of genome-wide studies have identified vacuolar functions and autophagy as relevant processes during primary wine fermentation or for ethanol tolerance, based on gene expression data or cell viability of knockout yeast strains;[867,869-873] however, understanding the actual relevance of autophagy in yeast-driven food fermentation processes would require addressing this issue experimentally using some of the methods available for *S. cerevisiae* as described in these guidelines.

Autophagy is a target for some widespread food preservatives used to prevent yeast-dependent spoilage. For example, the effect of benzoic acid is exacerbated when concurrent with nitrogen starvation.[874] This opened the way to devise strategies to improve the usefulness of sorbic and benzoic acid, taking advantage of their combination with stress conditions that would require functional autophagy for yeast cell survival.[875] Practical application of these findings would also require extending this research to other relevant food spoilage yeast species, which would be of obvious practical interest.

In the food/health interface, the effect of some food bioactive compounds on autophagy in different human cell types has already attracted some attention.[876,877] Interpreting the results of this type of research, however, warrants two cautionary notes.[878] First, the relationship between health status and autophagic activity is obviously far from being direct. Second, experimental design in this field must take into account the actual levels of these molecules in the target organs after ingestion, as well as exposure time and their transformations in the human body. In addition, attention must be paid to the fact that several mechanisms might contribute to the observed biological effects. Thus, relevant conclusions about the actual involvement of autophagy on the health-related effect of food bioactive compounds would only be possible by assaying the correct molecules in the correct concentrations.

20. Zebrafish. Zebrafish have many characteristics that make them a valuable vertebrate model organism for the analysis of autophagy. For example, taking advantage of the transparency of embryos, autophagosome formation can be visualized in vivo during development using transgenic GFP-Lc3 and GFP-Gabarap fish. The addition of 1-phenyl-2-thiourea (PTU) to media inhibits melanogenesis allowing visualization of later-stage embryos. Lysosomes can also be readily detected in vivo by the addition of LysoTracker Red to fish media prior to visualization. Additionally, protocols have been developed to monitor Lc3 protein levels and conjugation to PE by western blot analysis using commercially available Lc3 antibodies.[35,879]

Because of their translucent character and external fertilization and development, this vertebrate has proved an exceptional choice for developmental research. In situ hydridization of whole embryos can be performed to determine expression patterns. Knockdown of gene function is performed by treatment with morpholinos; the core autophagy machinery protein Gabarap,[880] and regulatory proteins such as the phosphinositide phosphatase Mtmr14,[881] Raptor and Mtor,[882] have all been successfully knocked down by morpholino treatment. However, research is currently somewhat hampered by the deficiency of efficient methods for targeted gene mutations and deletions.

Zebrafish are ideal organisms for in vivo drug discovery and/or verification because of their relatively small size and aqueous habitat, and several chemicals have been identified that modulate zebrafish autophagy activity.[879] Many chemicals can be added to the media and are absorbed directly through the skin. Because of simple drug delivery and the onset of neurodegenerative disease phenotypes at the larval stage, zebrafish are a promising organism for the study of autophagy's role in neurodegenative disease. Along these lines, a zebrafish model of Huntington disease has been developed.[740]

Conclusions and Future Perspectives

There is no question that research on the topic of autophagy has expanded dramatically since the publication of the first set of guidelines.[1] To help keep track of the field we have published a glossary of autophagy-related molecules and processes,[883,884] and there are now databases that are specifically dedicated to autophagy including the Human Autophagy-dedicated Database (HADb; www.autophagy.lu) and the Autophagy Database (http://tp-apg.genes.nig.ac.jp/autophagy/).

With this continued influx of new researchers we think it is critical to try to define standards for the field. Accordingly, we have highlighted the uses and caveats of an expanding set of recommended methods for monitoring macroautophagy in a wide range of systems (**Table 2**). Importantly, investigators need to determine whether they are evaluating levels of early or late autophagic compartments, or autophagic flux. If the question being asked is whether a particular condition changes autophagic flux (i.e., the rate of delivery of autophagy substrates to lysosomes or the vacuole, followed by degradation), then assessment of steady-state levels of autophagosomes (e.g., by counting GFP-LC3 puncta, monitoring the amount of LC3-II without examining turnover, or by single time point electron micrographs) is not sufficient as an isolated approach. In this case it is also necessary to directly measure the flux of autophagosomes and/or autophagy cargo (e.g., in wild-type cells compared with autophagy-deficient cells, the latter generated by treatment with an autophagy inhibitor or resulting from *ATG* gene knockdowns). Collectively, we strongly recommend the use of multiple assays whenever possible, rather than relying on the results from a single method.

As a final reminder, we stated at the beginning of this article that this set of guidelines is not meant to be a formulaic compilation of rules, because the appropriate assays depend in part on the question being asked and the system being used. Rather, these guidelines are presented primarily to emphasize key issues that need to be addressed such as the difference between measuring autophagy components, and flux or substrate clearance; they are not meant to constrain imaginative approaches to monitoring autophagy. Indeed, it is hoped that new methods for monitoring autophagy will continue to be developed, and new findings may alter our view of the current assays. Similar to the process of autophagy, this is a dynamic field, and we need to remain flexible in the standards we apply.

©2008 Landes Bioscience. Do not distribute

Table 2. Recommended methods for monitoring autophagy

Method Description
1. Electron microscopy Quantitative electron microscopy, immuno-TEM; monitor autophagosome number, volume
2. Atg8/LC3 western blotting western blot. The analysis is performed in the absence and presence of lysosomal protease or fusion inhibitors to monitor flux; an increase in the LC3-II amount in the presence of the inhibitor is usually indicative of flux
3. GFP-Atg8/LC3 lysosomal delivery and western blot ± lysosomal fusion or proteolysis degradation inhibitors; the generation of free GFP indicates lysosomal/vacuolar delivery
4. GFP-Atg8/LC3 fluorescence microscopy Fluorescence microscopy, FACS to monitor vacuolar/lysosomal localization. Also, increase in punctate GFP-Atg8/LC3 or Atg18/WIPI
5. Tandem mRFP/mCherry-GFP fluorescence Flux can be monitored as a decrease in microscopy, Rosella green/red (yellow) fluorescence (phagophores, autophagosomes) and an increase in red fluorescence (autolysosomes)
6. p62 and related LC3 binding protein turnover The amount of p62 increases when autophagy is inhibited and decreases when autophagy is induced
7. MTOR, AMPK and Atg1/ULK1 kinase activity western blot, immunoprecipitation or kinase assays
8. WIPI fluorescence microscopy Quantitative fluorescence analysis using endogenous WIPI proteins, or GFP- or Myc-tagged versions. Suitable for high-throughput imaging procedures.
9. Transcriptional and translational regulation northern blot, or qRT-PCR, autophagy-dedicated microarray
10. Autophagic protein degradation Turnover of long-lived proteins to monitor flux
11. Pex14-GFP, GFP-Atg8, Om45-GFP, A range of assays can be used to monitor mitoPho8Δ60 selective types of autophagy. These typically involve proteolytic maturation of a resident enzyme or degradation of a chimera, which can be followed enzymatically or by western blot
12. Autophagic sequestration assays Lysosomal accumulation by biochemical or multilabel fluorescence techniques, and TEM with a maturation inhibitor
13. Turnover of autophagic compartments Electron microscopy with morphometry/stereology
14. Autophagosome-lysosome colocalization Fluorescence microscopy and dequenching assay
15. Sequestration and processing assays Chimeric RFP fluorescence and processing, in plants and light and electron microscopy
16. Tissue fractionation Centrifugation, western blot and electron microscopy
17. Degradation of endogenous lipofuscin Fluorescence microscopy

dc_840_14

Acknowledgments

In a rapidly expanding and highly dynamic field such as autophagy, it is possible that some authors who should have been included on this manuscript have been missed. D.J.K. extends his apologies to researchers in the field of autophagy who, due to oversight or any other reason, could not be included on this manuscript. This work was supported by National Institutes of Health Public Health Service grant GM53396 to D.J.K. Due to space and other limitations, it is not possible to include all other sources of financial support.

References

1. Klionsky DJ, Abeliovich H, Agostinis P, Agrawal DK, Aliev G, Askew DS, et al. Guidelines for the use and interpretation of assays for monitoring autophagy in higher eukaryotes. Autophagy 2008; 4:151-75; PMID: 18188003
2. Klionsky DJ. Autophagy: from phenomenology to molecular understanding in less than a decade. Nat Rev Mol Cell Biol 2007; 8:931-7; PMID:17712358; http://dx.doi.org/10.1038/nrm2245
3. Klionsky DJ, Cuervo AM, Seglen PO. Methods for monitoring autophagy from yeast to human. Autophagy 2007; 3:181-206; PMID:17224625
4. Mizushima N. Methods for monitoring autophagy. Int J Biochem Cell Biol 2004; 36:2491-502; PMID: 15325587; http://dx.doi.org/10.1016/j.biocel.2004.02.005
5. Mizushima N, Yoshimori T, Levine B. Methods in mammalian autophagy research. Cell 2010; 140:313-26; PMID:20144757; http://dx.doi.org/10.1016/j.cell.2010.01.028
6. Rubinsztein DC, Cuervo AM, Ravikumar B, Sarkar S, Korolchuk V, Kaushik S, et al. In search of an "autophagomometer". Autophagy 2009; 5:585-9; PMID: 19411822; http://dx.doi.org/10.4161/auto.5.5.8823
7. Klionsky DJ. The autophagosome is overrated! Autophagy 2011; 7:353-4; PMID:21258205; http://dx.doi.org/10.4161/auto.7.4.14730
8. Eskelinen E-L, Reggiori F, Baba M, Kovács AL, Seglen PO. Seeing is believing: the impact of electron microscopy on autophagy research. Autophagy 2011; 7:935-56; PMID:21566462; http://dx.doi.org/10.4161/auto.7.9.15760
9. Seglen PO. Regulation of autophagic protein degradation in isolated liver cells. In: Glaumann H and Ballard FJ, eds. Lysosomes: Their Role in Protein Breakdown. London: Academic Press, 1987:369-414.
10. De Duve C, Wattiaux R. Functions of lysosomes. Annu Rev Physiol 1966; 28:435-92; PMID:5322983; http://dx.doi.org/10.1146/annurev.ph.28.030166.002251
11. Dunn WA, Jr.. Autophagy and related mechanisms of lysosome-mediated protein degradation. Trends Cell Biol 1994; 4:139-43; PMID:14731737; http://dx.doi.org/10.1016/0962-8924(94)90069-8
12. Gordon PB, Seglen PO. Prelysosomal convergence of autophagic and endocytic pathways. Biochem Biophys Res Commun 1988; 151:40-7; PMID:3126737; http://dx.doi.org/10.1016/0006-291X(88)90556-6
13. Dice JF. Artophagy: the art of autophagy–macroautophagy. Interview by Daniel J. Klionsky. Autophagy 2010; 6:320-1; PMID:20118653; http://dx.doi.org/10.4161/auto.6.3.11263
14. Kovács J, Fellinger E, Kárpáti AP, Kovács AL, László L, Réz G. Morphometric evaluation of the turnover of autophagic vacuoles after treatment with Triton X-100 and vinblastine in murine pancreatic acinar and seminal vesicle epithelial cells. Virchows Arch B Cell Pathol Incl Mol Pathol 1987; 53:183-90; PMID: 2888237; http://dx.doi.org/10.1007/BF02890242
15. Kovács J, Fellinger E, Kárpáti PA, Kovács AL, László L. The turnover of autophagic vacuoles: evaluation by quantitative electron microscopy. Biomed Biochim Acta 1986; 45:1543-7; PMID:3579875
16. Kovács J, László L, Kovács AL. Regression of autophagic vacuoles in pancreatic acinar, seminal vesicle epithelial, and liver parenchymal cells: a comparative morphometric study of the effect of vinblastine and leupeptin followed by cycloheximide treatment. Exp Cell Res 1988; 174:244-51; PMID:3335225; http://dx.doi.org/10.1016/0014-4827(88)90158-9

17. Chu CT. Autophagic stress in neuronal injury and disease. J Neuropathol Exp Neurol 2006; 65:423-32; PMID:16772866; http://dx.doi.org/10.1097/01.jnen.0000229233.75253.be
18. Fass E, Shvets E, Degani I, Hirschberg K, Elazar Z. Microtubules support production of starvation-induced autophagosomes but not their targeting and fusion with lysosomes. J Biol Chem 2006; 281:36303-16; PMID:16963441; http://dx.doi.org/10.1074/jbc.M607031200
19. Kovács AL, Reith A, Seglen PO. Accumulation of autophagosomes after inhibition of hepatocytic protein degradation by vinblastine, leupeptin or a lysosomotropic amine. Exp Cell Res 1982; 137:191-201; PMID:7056284; http://dx.doi.org/10.1016/0014-4827(82)90020-9
20. Tóth S, Nagy K, Pálfia Z, Réz G. Cellular autophagic capacity changes during azaserine-induced tumour progression in the rat pancreas. Up-regulation in all premalignant stages and down-regulation with loss of cycloheximide sensitivity of segregation along with malignant transformation. Cell Tissue Res 2002; 309:409-16; PMID:12195297
21. Loos B, Engelbrecht AM. Cell death: a dynamic response concept. Autophagy 2009; 5:590-603; PMID: 19363298; http://dx.doi.org/10.4161/auto.5.5.8479
22. Seglen PO, Gordon PB, Grinde B, Solheim A, Kovács AL, Poli A. Inhibitors and pathways of hepatocytic protein degradation. Acta Biol Med Ger 1981; 40:1587-98; PMID:7342604
23. Ktistakis NT, Andrews S, Long J. What is the advantage of a transient precursor in autophagosome biogenesis? Autophagy 2011; 7:118-22; PMID: 20935487; http://dx.doi.org/10.4161/auto.7.1.13697
24. Kovács AL, Réz G, Pálfia Z, Kovács J. Autophagy in the epithelial cells of murine seminal vesicle in vitro. Formation of large sheets of nascent isolation membranes, sequestration of the nucleus and inhibition by wortmannin and 3-ethyladenine. Cell Tissue Res 2000; 302:253-61; PMID:11131136
25. Mizushima N, Yoshimori T. How to interpret LC3 immunoblotting. Autophagy 2007; 3:542-5; PMID: 17611390
26. Nishida Y, Arakawa S, Fujitani K, Yamaguchi H, Mizuta T, Kanaseki T, et al. Discovery of Atg5/Atg7-independent alternative macroautophagy. Nature 2009; 461:654-8; PMID:19794493; http://dx.doi.org/10.1038/nature08455
27. Kanki T, Kang D, Klionsky DJ. Monitoring mitophagy in yeast: the Om45-GFP processing assay. Autophagy 2009; 5:1186-9; PMID:19806021; http://dx.doi.org/10.4161/auto.5.8.9854
28. Grandér D, Kharaziha P, Laane E, Pokrovskaja K, Panaretakis T. Autophagy as the main means of cytotoxicity by glucocorticoids in hematological malignancies. Autophagy 2009; 5:1198-200; PMID: 19855186; http://dx.doi.org/10.4161/auto.5.8.10122
29. Welter E, Thumm M, Krick R. Quantification of nonselective bulk autophagy in *S. cerevisiae* using Pgk1-GFP. Autophagy 2010; 6:794-7; PMID: 20523132; http://dx.doi.org/10.4161/auto.6.6.12348
30. Raju D, Jones NL. Methods to monitor autophagy in *H. pylori* vacuolating cytotoxin A (VacA)-treated cells. Autophagy 2010; 6:138-43; PMID:19875940; http://dx.doi.org/10.4161/auto.6.1.10222
31. Geng J, Klionsky DJ. Determining Atg protein stoichiometry at the phagophore assembly site by fluorescence microscopy. Autophagy 2010; 6:144-7; PMID:20131413; http://dx.doi.org/10.4161/auto.6.1.10249
32. Swanlund JM, Kregel KC, Oberley TD. Investigating autophagy: quantitative morphometric analysis using electron microscopy. Autophagy 2010; 6:270-7; PMID:19923921; http://dx.doi.org/10.4161/auto.6.2.10439
33. Zhang J, Ney PA. Reticulocyte mitophagy: monitoring mitochondrial clearance in a mammalian model. Autophagy 2010; 6:405-8; PMID:20200480; http://dx.doi.org/10.4161/auto.6.3.11245
34. Seglen PO, Brinchmann MF. Purification of autophagosomes from rat hepatocytes. Autophagy 2010; 6:542-7; PMID:20505360; http://dx.doi.org/10.4161/auto.6.4.11272
35. He C, Klionsky DJ. Analyzing autophagy in zebrafish. Autophagy 2010; 6:642-4; PMID:20495344; http://dx.doi.org/10.4161/auto.6.5.12092
36. Calvo-Garrido J, Carilla-Latorre S, Mesquita A, Escalante R. A proteolytic cleavage assay to monitor autophagy in *Dictyostelium discoideum*. Autophagy 2011; 7:1063-8; PMID:21876387; http://dx.doi.org/10.4161/auto.7.9.16629
37. Xu F, Liu XH, Zhuang FL, Zhu J, Lin FC. Analyzing autophagy in *Magnaporthe oryzae*. Autophagy 2011; 7:525-30; PMID:21317549; http://dx.doi.org/10.4161/auto.7.5.15020
38. Klionsky DJ. Autophagy: Lower Eukaryotes and Non-Mammalian Systems, Part A. Amsterdam: Academic Press/Elsevier, 2008.
39. Klionsky DJ. Autophagy in Disease and Clinical Applications, Part C. Amsterdam: Academic Press/Elsevier, 2008.
40. Klionsky DJ. Autophagy in Mammalian Systems, Part B. Amsterdam: Academic Press/Elsevier, 2008.
41. Zhu J, Dagda RK, Chu CT. Monitoring mitophagy in neuronal cell cultures. Methods Mol Biol 2011; 793:325-39; PMID:21913110; http://dx.doi.org/10.1007/978-1-61779-328-8_21
42. http://www.landesbioscience.com/journals/autophagy/protocols/
43. Ylä-Anttila P, Vihinen H, Jokitalo E, Eskelinen E-L. Monitoring autophagy by electron microscopy in Mammalian cells. Methods Enzymol 2009; 452:143-64; PMID:19200881; http://dx.doi.org/10.1016/S0076-6879(08)03610-0
44. Eskelinen E-L. Maturation of autophagic vacuoles in Mammalian cells. Autophagy 2005; 1:1-10; PMID: 16874026; http://dx.doi.org/10.4161/auto.1.1.1270
45. Eskelinen E-L. To be or not to be? Examples of incorrect identification of autophagic compartments in conventional transmission electron microscopy of mammalian cells. Autophagy 2008; 4:257-60; PMID: 17986849
46. Eskelinen E-L, Kovács AL. Double membranes vs. lipid bilayers, and their significance for correct identification of macroautophagic structures. Autophagy 2011; 7:931-2; PMID:21642767; http://dx.doi.org/10.4161/auto.7.9.16679
47. Eskelinen E-L. Fine structure of the autophagosome. In: Deretic V, ed. Autophagosome and Phagosome. Totowa, NJ: Humana Press, 2008:11-28.
48. Berg TO, Fengsrud M, Strømhaug PE, Berg T, Seglen PO. Isolation and characterization of rat liver amphisomes. Evidence for fusion of autophagosomes with both early and late endosomes. J Biol Chem 1998; 273:21883-92; PMID:9705327; http://dx.doi.org/10.1074/jbc.273.34.21883
49. Eskelinen E-L. Macroautophagy in mammalian cells. In: Saftig P, ed. Lysosomes. Georgetown, TX: LandesBioscience/Eurekah.com, 2005.
50. Rabouille C, Strous GJ, Crapo JD, Geuze HJ, Slot JW. The differential degradation of two cytosolic proteins as a tool to monitor autophagy in hepatocytes by immunocytochemistry. J Cell Biol 1993; 120:897-908; PMID:8432730; http://dx.doi.org/10.1083/jcb.120.4.897
51. Kovács AL, Pálfia Z, Réz G, Vellai T, Kovács J. Sequestration revisited: integrating traditional electron microscopy, de novo assembly and new results. Autophagy 2007; 3:655-62; PMID:17603297
52. Gao W, Kang JH, Liao Y, Ding WX, Gambotto AA, Watkins SC, et al. Biochemical isolation and characterization of the tubulovesicular LC3-positive autophagosomal compartment. J Biol Chem 2010; 285:1371-83; PMID:19910472; http://dx.doi.org/10.1074/jbc.M109.054197
53. Baba M, Osumi M, Ohsumi Y. Analysis of the membrane structures involved in autophagy in yeast by freeze-replica method. Cell Struct Funct 1995; 20:465-71; PMID:8825067; http://dx.doi.org/10.1247/csf.20.465
54. Réz G, Meldolesi J. Freeze-fracture of drug-induced autophagocytosis in the mouse exocrine pancreas. Lab Invest 1980; 43:269-77; PMID:7401637
55. Punnonen E-L, Pihakaski K, Mattila K, Lounatmaa K, Hirsimäki P. Intramembrane particles and filipin labelling on the membranes of autophagic vacuoles and lysosomes in mouse liver. Cell Tissue Res 1989; 258:269-76; PMID:2582478; http://dx.doi.org/10.1007/BF00239447
56. Fengsrud M, Erichsen ES, Berg TO, Raiborg C, Seglen PO. Ultrastructural characterization of the delimiting membranes of isolated autophagosomes and amphisomes by freeze-fracture electron microscopy. Eur J Cell Biol 2000; 79:871-82; PMID:11152279; http://dx.doi.org/10.1078/0171-9335-00125
57. Rao VA, Klein SR, Bonar SJ, Zielonka J, Mizuno N, Dickey JS, et al. The antioxidant transcription factor Nrf2 negatively regulates autophagy and growth arrest induced by the anticancer redox agent mitoquinone. J Biol Chem 2010; 285:34447-59; PMID:20805228; http://dx.doi.org/10.1074/jbc.M110.133579
58. Krick R, Mühe Y, Prick T, Bredschneider M, Bremer S, Wenzel D, et al. Piecemeal microautophagy of the nucleus: genetic and morphological traits. Autophagy 2009; 5:270-2; PMID:19182523; http://dx.doi.org/10.4161/auto.5.2.7639
59. Meschini S, Condello M, Calcabrini A, Marra M, Formisano G, Lista P, et al. The plant alkaloid voacamine induces apoptosis-independent autophagic cell death on both sensitive and multidrug resistant human osteosarcoma cells. Autophagy 2008; 4:1020-33; PMID:18838862
60. Proikas-Cezanne T, Robenek H. Freeze-fracture replica immunolabelling reveals human WIPI-1 and WIPI-2 as membrane proteins of autophagosomes. J Cell Mol Med 2011; 15:2007-10; PMID:21564513; http://dx.doi.org/10.1111/j.1582-4934.2011.01339.x
61. Kovács J, Réz G, Kovács AL, Csák J, Zboray G. Autophagocytosis freeze-fracture morphology, effects of vinblastine and influence of transcriptional and translational inhibitors. Acta Biol Med Ger 1982; 41:131-5; PMID:7113544
62. Hirsimäki Y, Hirsimäki P, Lounatmaa K. Vinblastine-induced autophagic vacuoles in mouse liver and Ehrlich ascites tumor cells as assessed by freeze-fracture electron microscopy. Eur J Cell Biol 1982; 27:298-301; PMID:7117273
63. Cheong H, Yorimitsu T, Reggiori F, Legakis JE, Wang C-W, Klionsky DJ. Atg17 regulates the magnitude of the autophagic response. Mol Biol Cell 2005; 16:3438-53; PMID:15901835; http://dx.doi.org/10.1091/mbc.E04-10-0894
64. Xie Z, Nair U, Klionsky DJ. Atg8 controls phagophore expansion during autophagosome formation. Mol Biol Cell 2008; 19:3290-8; PMID:18508918; http://dx.doi.org/10.1091/mbc.E07-12-1292
65. Sigmond T, Fehér J, Balsa A, Pásti G, Pálfia Z, Takács-Vellai K, et al. Qualitative and quantitative characterization of autophagy in Caenorhabditis elegans by electron microscopy. Methods Enzymol 2008; 451:467-91; PMID:19185736; http://dx.doi.org/10.1016/S0076-6879(08)03228-X
66. Kovács AL, Vellai T, Müller F. Autophagy in *Caenorhabditis elegans*. In: Klionsky DJ, ed. Autophagy. Georgetown, Texas: Landes Bioscience, 2004:217-23.
67. Weibel ER. Practical Methods for Biological Morphometry. Academic Press, New York, 1979.
68. Williams MA. Quantitative methods in biology: Practical methods in electron microscopy. Amsterdam, New York, Oxford: North-Holland Publishing Company, 1977.
69. Howard V, Reed MG. Unbiased stereology: three dimensional measurement in microscopy. U Bios Scientific Publishers, 1998.
70. Punnonen EL, Reunanen H. Effects of vinblastine, leucine, and histidine, and 3-methyladenine on autophagy in Ehrlich ascites cells. Exp Mol Pathol 1990; 52:87-97; PMID:2307216; http://dx.doi.org/10.1016/0014-4800(90)90061-H
71. Kovács AL, László L, Fellinger E, Jakab A, Orosz A, Réz G, et al. Combined effects of fasting and vinblastine treatment on serum insulin level, the size of autophagic-lysosomal compartment, protein content and lysosomal enzyme activities of liver and exocrine pancreatic cells of the mouse. Comp Biochem Physiol B 1989; 94:505-10; PMID:2695284; http://dx.doi.org/10.1016/0305-0491(89)90189-2
72. Shelburne JD, Arstila AU, Trump BF. Studies on cellular autophagocytosis. The relationship of autophagocytosis to protein synthesis and to energy metabolism in rat liver and flounder kidney tubules in vitro. Am J Pathol 1973; 73:641-70; PMID: 4767257
73. Reyes FC, Chung T, Holding D, Jung R, Vierstra R, Otegui MS. Delivery of prolamins to the protein storage vacuole in maize aleurone cells. Plant Cell 2011; 23:769-84; PMID:21343414; http://dx.doi.org/10.1105/tpc.110.082156
74. Dunn WA, Jr., Cregg JM, Kiel JAKW, van der Klei IJ, Oku M, Sakai Y, et al. Pexophagy: the selective autophagy of peroxisomes. Autophagy 2005; 1:75-83; PMID:16874024; http://dx.doi.org/10.4161/auto.1.2.1737
75. Wang K, Klionsky DJ. Mitochondria removal by autophagy. Autophagy 2011; 7:297-300; PMID: 21252623; http://dx.doi.org/10.4161/auto.7.3.14502
76. Bélanger M, Rodrigues PH, Dunn WA, Jr., Progulske-Fox A. Autophagy: a highway for *Porphyromonas gingivalis* in endothelial cells. Autophagy 2006; 2:165-70; PMID:16874051
77. Birmingham CL, Brumell JH. Autophagy recognizes intracellular *Salmonella enterica* serovar Typhimurium in damaged vacuoles. Autophagy 2006; 2:156-8; PMID:16874057
78. Colombo MI, Gutierrez MG, Romano PS. The two faces of autophagy: *Coxiella* and *Mycobacterium*. Autophagy 2006; 2:162-4; PMID:16874070
79. Ogawa M, Sasakawa C. *Shigella* and autophagy. Autophagy 2006; 2:171-4; PMID:16874102
80. Vergne I, Singh S, Roberts E, Kyei G, Master S, Harris J, et al. Autophagy in immune defense against *Mycobacterium tuberculosis*. Autophagy 2006; 2:175-8; PMID: 16874111
81. Yoshimori T. Autophagy vs. Group A Streptococcus. Autophagy 2006; 2:154-5; PMID:16874113
82. Lynch-Day MA, Klionsky DJ. The Cvt pathway as a model for selective autophagy. FEBS Lett 2010; 584:1359-66; PMID:20146925; http://dx.doi.org/10.1016/j.febslet.2010.02.013
83. Birmingham CL, Canadien V, Gouin E, Troy EB, Yoshimori T, Cossart P, et al. *Listeria monocytogenes* evades killing by autophagy during colonization of host cells. Autophagy 2007; 3:442-51; PMID:17568179
84. Klionsky DJ. Protein transport from the cytoplasm into the vacuole. J Membr Biol 1997; 157:105-15; PMID: 9151652; http://dx.doi.org/10.1007/s002329900220
85. Dini L, Pagliara P, Carlà EC. Phagocytosis of apoptotic cells by liver: a morphological study. Microsc Res Tech 2002; 57:530-40; PMID:12112436; http://dx.doi.org/10.1002/jemt.10107
86. Kroemer G, El-Deiry WS, Golstein P, Peter ME, Vaux D, Vandenabeele P, et al & Nomenclature Committee on Cell Death. Classification of cell death: recommendations of the Nomenclature Committee on Cell Death. Cell Death Differ 2005; 12(Suppl 2):1463-7; PMID:16247491; http://dx.doi.org/10.1038/sj.cdd.4401724
87. Réz G, Pálfia Z, Fellinger E. Occurrence and inhibition by cycloheximide of apoptosis in vinblastine-treated murine pancreas. A role for autophagy? Acta Biol Hung 1991; 42:133-40; PMID:1844306
88. Giammarioli AM, Gambardella L, Barbati C, Pietraforte D, Tinari A, Alberton M, et al. Differential effects of the glycolysis inhibitor 2-deoxy-D-glucose on the activity of pro-apoptotic agents in metastatic melanoma cells, and induction of a cyto-protective autophagic response. Int J Cancer 2012; In press; PMID:21913183
89. Mayhew TM. Quantitative immunoelectron microscopy: alternative ways of assessing subcellular patterns of gold labeling. Methods Mol Biol 2007; 369:309-29; PMID:17656757; http://dx.doi.org/10.1007/978-1-59745-294-6_15
90. Mayhew TM, Lucocq JM, Griffiths G. Relative labelling index: a novel stereological approach to test for non-random immunogold labelling of organelles and membranes on transmission electron microscopy thin sections. J Microsc 2002; 205:153-64; PMID: 11879430; http://dx.doi.org/10.1046/j.0022-2720.2001.00977.x
91. Schmid D, Pypaert M, Münz C. Antigen-loading compartments for major histocompatibility complex class II molecules continuously receive input from autophagosomes. Immunity 2007; 26:79-92; PMID: 17182262; http://dx.doi.org/10.1016/j.immuni.2006.10.018
92. Kovács J. Regression of autophagic vacuoles in seminal vesicle cells following cycloheximide treatment. Exp Cell Res 1983; 144:231-4; PMID:6840208; http://dx.doi.org/10.1016/0014-4827(83)90460-3
93. Réz G, Csák J, Fellinger E, László L, Kovács AL, Oliva O, et al. Time course of vinblastine-induced autophagocytosis and changes in the endoplasmic reticulum in murine pancreatic acinar cells: a morphometric and biochemical study. Eur J Cell Biol 1996; 71:341-50; PMID:8980904
94. Kovács AL, Grinde B, Seglen PO. Inhibition of autophagic vacuole formation and protein degradation by amino acids in isolated hepatocytes. Exp Cell Res 1981; 133:431-6; PMID:7238609; http://dx.doi.org/10.1016/0014-4827(81)90336-0
95. Mortimore GE, Hutson NJ, Surmacz CA. Quantitative correlation between proteolysis and macro- and microautophagy in mouse hepatocytes during starvation and refeeding. Proc Natl Acad Sci U S A 1983; 80:2179-83; PMID:6340116; http://dx.doi.org/10.1073/pnas.80.8.2179
96. Mortimore GE, Lardeux BR, Adams CE. Regulation of microautophagy and basal protein turnover in rat liver. Effects of short-term starvation. J Biol Chem 1988; 263:2506-12; PMID:3257493
97. Zhu JH, Horbinski C, Guo F, Watkins S, Uchiyama Y, Chu CT. Regulation of autophagy by extracellular signal-regulated protein kinases during 1-methyl-4-phenylpyridinium-induced cell death. Am J Pathol 2007; 170:75-86; PMID:17200184; http://dx.doi.org/10.2353/ajpath.2007.060524
98. Bjørkøy G, Lamark T, Brech A, Outzen H, Perander M, Øvervatn A, et al. p62/SQSTM1 forms protein aggregates degraded by autophagy and has a protective effect on huntingtin-induced cell death. J Cell Biol 2005; 171:603-14; PMID:16286508; http://dx.doi.org/10.1083/jcb.200507002
99. Razi M, Tooze SA. Correlative light and electron microscopy. Methods Enzymol 2009; 452:261-75; PMID:19200888; http://dx.doi.org/10.1016/S0076-6879(08)03617-3
100. Shu X, Lev-Ram V, Deerinck TJ, Qi Y, Ramko EB, Davidson MW, et al. A genetically encoded tag for correlated light and electron microscopy of intact cells, tissues, and organisms. PLoS Biol 2011; 9:e1001041; PMID:21483721; http://dx.doi.org/10.1371/journal.pbio.1001041
101. Castillo K, Rojas-Rivera D, Lisbona F, Caballero B, Nassif M, Court FA, et al. BAX inhibitor-1 regulates autophagy by controlling the IRE1α branch of the unfolded protein response. EMBO J 2011; 30:4465-78; PMID:21926971; http://dx.doi.org/10.1038/emboj.2011.318
102. Ylä-Anttila P, Vihinen H, Jokitalo E, Eskelinen E-L. 3D tomography reveals connections between the phagophore and endoplasmic reticulum. Autophagy 2009; 5:1180-5; PMID:19855179; http://dx.doi.org/10.4161/auto.5.8.10274
103. Hayashi-Nishino M, Fujita N, Noda T, Yamaguchi A, Yoshimori T, Yamamoto A. Electron tomography reveals the endoplasmic reticulum as a membrane source for autophagosome formation. Autophagy 2010; 6:301-3; PMID:20104025; http://dx.doi.org/10.4161/auto.6.2.11134
104. Schneider EM, Lorezn M, Walther P. Autophagy as a hallmark of hemophagocytic diseases In: Gorbunov N, ed. Autophagy: Principles, Regulation and Roles in Disease: Nova Science Publishers, 2012.
105. Massey AC, Kaushik S, Sovak G, Kiffin R, Cuervo AM. Consequences of the selective blockage of chaperone-mediated autophagy. Proc Natl Acad Sci U S A 2006; 103:5805-10; PMID:16585521; http://dx.doi.org/10.1073/pnas.0507436103
106. Bosco DA, Morfini G, Karabacak NM, Song Y, Gros-Louis F, Pasinelli P, et al. Wild-type and mutant SOD1 share an aberrant conformation and a common pathogenic pathway in ALS. Nat Neurosci 2010; 13:1396-403; PMID:20953194; http://dx.doi.org/10.1038/nn.2660
107. Sou YS, Tanida I, Komatsu M, Ueno T, Kominami E. Phosphatidylserine in addition to phosphatidylethanolamine is an in vitro target of the mammalian Atg8 modifiers, LC3, GABARAP, and GATE-16. J Biol Chem 2006; 281:3017-24; PMID:16303767; http://dx.doi.org/10.1074/jbc.M508888200
108. Le Grand JN, Chakrama FZ, Seguin-Py S, Fraichard A, Delage-Mourroux R, Jouvenot M, et al. GABARAPL1 (GEC1): original or copycat? Autophagy 2011; 7:1098-107; PMID:21597319; http://dx.doi.org/10.4161/auto.7.10.15904
109. Kabeya Y, Mizushima N, Yamamoto A, Oshitani-Okamoto S, Ohsumi Y, Yoshimori T. LC3, GABARAP and GATE16 localize to autophagosomal membrane depending on form-II formation. J Cell Sci 2004; 117:2805-12; PMID:15169837; http://dx.doi.org/10.1242/jcs.01131
110. Weidberg H, Shvets E, Shpilka T, Shimron F, Shinder V, Elazar Z. LC3 and GATE-16/GABARAP subfamilies are both essential yet act differently in autophagosome biogenesis. EMBO J 2010; 29:1792-802; PMID: 20418806; http://dx.doi.org/10.1038/emboj.2010.74

dc 840_14
© Landes Bioscience. Do not distribute.

111. Kovsan J, Blüher M, Tarnovscki T, Klöting N, Kirshtein B, Madar L, et al. Altered autophagy in human adipose tissues in obesity. J Clin Endocrinol Metab 2011; 96:E268-77; PMID:21047928; http://dx.doi.org/10.1210/jc.2010-1681
112. Tanida I, Minematsu-Ikeguchi N, Ueno T, Kominami E. Lysosomal turnover, but not a cellular level, of endogenous LC3 is a marker for autophagy. Autophagy 2005; 1:84-91; PMID:16874052; http://dx.doi.org/10.4161/auto.1.2.1697
113. Huang W-P, Scott SV, Kim J, Klionsky DJ. The itinerary of a vesicle component, Aut7p/Cvt5p, terminates in the yeast vacuole via the autophagy/Cvt pathways. J Biol Chem 2000; 275:5845-51; PMID: 10681575; http://dx.doi.org/10.1074/jbc.275.8.5845
114. Cai Q, Lu L, Tian J-H, Zhu Y-B, Qiao H, Sheng Z-H. Snapin-regulated late endosomal transport is critical for efficient autophagy-lysosomal function in neurons. Neuron 2010; 68:73-86; PMID:20920792; http://dx.doi.org/10.1016/j.neuron.2010.09.022
115. Castino R, Fiorentino I, Cagnin M, Giovia A, Isidoro C. Chelation of lysosomal iron protects dopaminergic SH-SY5Y neuroblastoma cells from hydrogen peroxide toxicity by precluding autophagy and Akt dephosphorylation. Toxicol Sci 2011; 123:523-41; PMID: 21742779; http://dx.doi.org/10.1093/toxsci/kfr179
116. Michiorri S, Gelmetti V, Giarda E, Lombardi F, Romano F, Marongiu R, et al. The Parkinson-associated protein PINK1 interacts with Beclin1 and promotes autophagy. Cell Death Differ 2010; 17:962-74; PMID:20057503
117. Ahlberg J, Berkenstam A, Henell F, Glaumann H. Degradation of short and long lived proteins in isolated rat liver lysosomes. Effects of pH, temperature, and proteolytic inhibitors. J Biol Chem 1985; 260:5847-54; PMID:3988775
118. McLeland CB, Rodriguez J, Stern ST. Autophagy monitoring assay: qualitative analysis of MAP LC3-I to II conversion by immunoblot. Methods Mol Biol 2011; 697:199-206; PMID:21116969; http://dx.doi.org/10.1007/978-1-60327-198-1_21
119. Chakrama FZ, Seguin-Py S, Le Grand JN, Fraichard A, Delage-Mourroux R, Despouy G, et al. GABARAPL1 (GEC1) associates with autophagic vesicles. Autophagy 2010; 6:495-505; PMID: 20404487; http://dx.doi.org/10.4161/auto.6.4.11819
120. Kim J, Huang W-P, Klionsky DJ. Membrane recruitment of Aut7p in the autophagy and cytoplasm to vacuole targeting pathways requires Aut1p, Aut2p, and the autophagy conjugation complex. J Cell Biol 2001; 152:51-64; PMID:11149920; http://dx.doi.org/10.1083/jcb.152.1.51
121. Shu CW, Drag M, Bekes M, Zhai D, Salvesen GS, Reed JC. Synthetic substrates for measuring activity of autophagy proteases: autophagins (Atg4). Autophagy 2010; 6:936-47; PMID:20818167; http://dx.doi.org/10.4161/auto.6.7.13075
122. Li M, Chen X, Ye Q-Z, Vogt A, Yin X-M. A high-throughput FRET-based assay for determination of Atg4 activity. Autophagy 2012; 8; In press; PMID: 22302004
123. Ketteler R, Seed B. Quantitation of autophagy by luciferase release assay. Autophagy 2008; 4:801-6; PMID:18641457
124. Li M, Hou Y, Wang J, Chen X, Shao ZM, Yin X-M. Kinetics comparisons of mammalian Atg4 homologues indicate selective preferences toward diverse Atg8 substrates. J Biol Chem 2011; 286:7327-38; PMID: 21177865; http://dx.doi.org/10.1074/jbc.M110.199059
125. Klionsky DJ. For the last time, it is GFP-Atg8, not Atg8-GFP (and the same goes for LC3). Autophagy 2011; 7:1093-4; PMID:21993240; http://dx.doi.org/10.4161/auto.7.10.15492
126. Mizushima N, Yamamoto A, Matsui M, Yoshimori T, Ohsumi Y. In vivo analysis of autophagy in response to nutrient starvation using transgenic mice expressing a fluorescent autophagosome marker. Mol Biol Cell 2004; 15:1101-11; PMID:14699058; http://dx.doi.org/10.1091/mbc.E03-09-0704
127. Castino R, Lazzeri G, Lenzi P, Bellio N, Follo C, Ferrucci M, et al. Suppression of autophagy precipitates neuronal cell death following low doses of methamphetamine. J Neurochem 2008; 106:1426-39; PMID:18489716; http://dx.doi.org/10.1111/j.1471-4159.2008.05488.x
128. Matsui Y, Takagi H, Qu X, Abdellatif M, Sakoda H, Asano T, et al. Distinct roles of autophagy in the heart during ischemia and reperfusion: roles of AMP-activated protein kinase and Beclin 1 in mediating autophagy. Circ Res 2007; 100:914-22; PMID:17332429; http://dx.doi.org/10.1161/01.RES.0000261924.76669.36
129. Suzuki K, Kirisako T, Kamada Y, Mizushima N, Noda T, Ohsumi Y. The pre-autophagosomal structure organized by concerted functions of *APG* genes is essential for autophagosome formation. EMBO J 2001; 20:5971-81; PMID:11689437; http://dx.doi.org/10.1093/emboj/20.21.5971
130. Hanson HH, Kang S, Fernández-Monreal M, Oung T, Yildirim M, Lee R, et al. LC3-dependent intracellular membrane tubules induced by gamma-protocadherins A3 and B2: a role for intraluminal interactions. J Biol Chem 2010; 285:20982-92; PMID:20439459; http://dx.doi.org/10.1074/jbc.M109.092031
131. Sanjuan MA, Dillon CP, Tait SW, Moshiach S, Dorsey F, Connell S, et al. Toll-like receptor signalling in macrophages links the autophagy pathway to phagocytosis. Nature 2007; 450:1253-7; PMID: 18097416; http://dx.doi.org/10.1038/nature06421
132. Sanjuan MA, Milasta S, Green DR. Toll-like receptor signaling in the lysosomal pathways. Immunol Rev 2009; 227:203-20; PMID:19120486; http://dx.doi.org/10.1111/j.1600-065X.2008.00732.x
133. Florey O, Kim SE, Sandoval CP, Haynes CM, Overholtzer M. Autophagy machinery mediates macroendocytic processing and entotic cell death by targeting single membranes. Nat Cell Biol 2011; 13:1335-43; PMID:22002674; http://dx.doi.org/10.1038/ncb2363
134. Martínez J, Almendinger J, Oberst A, Ness R, Dillon CP, Fitzgerald P, et al. Microtubule-associated protein 1 light chain 3 alpha (LC3)-associated phagocytosis is required for the efficient clearance of dead cells. Proc Natl Acad Sci U S A 2011; 108:17396-401; PMID:21969579; http://dx.doi.org/10.1073/pnas.1113421108
135. Gong L, Cullinane M, Treerat P, Ramm G, Prescott M, Adler B, et al. The Burkholderia pseudomallei type III secretion system and BopA are required for evasion of LC3-associated phagocytosis. PLoS One 2011; 6:e17852; PMID:21412437; http://dx.doi.org/10.1371/journal.pone.0017852
136. Dupont N, Lacas-Gervais S, Bertout J, Paz I, Freche B, Van Nhieu GT, et al. Shigella phagocytic vacuolar membrane remnants participate in the cellular response to pathogen invasion and are regulated by autophagy. Cell Host Microbe 2009; 6:137-49; PMID:19683680; http://dx.doi.org/10.1016/j.chom.2009.07.005
137. Reggiori F, Monastyrska I, Verheije MH, Calì T, Ulasli M, Bianchi S, et al. Coronaviruses Hijack the LC3-I-positive EDEMosomes, ER-derived vesicles exporting short-lived ERAD regulators, for replication. Cell Host Microbe 2010; 7:500-8; PMID:20542253; http://dx.doi.org/10.1016/j.chom.2010.05.013
138. English L, Chemali M, Duron J, Rondeau C, Laplante A, Gingras D, et al. Autophagy enhances the presentation of endogenous viral antigens on MHC class I molecules during HSV-1 infection. Nat Immunol 2009; 10:480-7; PMID:19305394; http://dx.doi.org/10.1038/ni.1720
139. Plowey ED, Cherra SJ, 3rd, Liu YJ, Chu CT. Role of autophagy in G2019S-LRRK2-associated neurite shortening in differentiated SH-SY5Y cells. J Neurochem 2008; 105:1048-56; PMID:18182054; http://dx.doi.org/10.1111/j.1471-4159.2008.05217.x
140. Nicotra G, Mercalli F, Peracchio C, Castino R, Follo C, Valente G, et al. Autophagy-active beclin-1 correlates with favourable clinical outcome in non-Hodgkin lymphomas. Mod Pathol 2010; 23:937-50; PMID: 20473282; http://dx.doi.org/10.1038/modpathol.2010.80
141. Tanida I, Ueno T, Kominami E. LC3 and Autophagy. Methods Mol Biol 2008; 445:77-88; PMID:18425443; http://dx.doi.org/10.1007/978-1-59745-157-4_4
142. Chu CT, Plowey ED, Dagda RK, Hickey RW, Cherra SJ, 3rd, Clark RS. Autophagy in neurite injury and neurodegeneration: in vitro and in vivo models. Methods Enzymol 2009; 453:217-49; PMID:19216909; http://dx.doi.org/10.1016/S0076-6879(08)04011-1
143. He H, Dang Y, Dai F, Guo Z, Wu J, She X, et al. Post-translational modifications of three members of the human MAP1LC3 family and detection of a novel type of modification for MAP1LC3B. J Biol Chem 2003; 278:29278-87; PMID:12740394; http://dx.doi.org/10.1074/jbc.M303800200
144. Shpilka T, Weidberg H, Pietrokovski S, Elazar Z. Atg8: an autophagy-related ubiquitin-like protein family. Genome Biol 2011; 12:226; PMID:21867568; http://dx.doi.org/10.1186/gb-2011-12-7-226
145. Zois CE, Koukourakis MI. Radiation-induced autophagy in normal and cancer cells: towards novel cytoprotection and radio-sensitization policies? Autophagy 2009; 5:442-50; PMID:19164950; http://dx.doi.org/10.4161/auto.5.4.7667
146. Xin Y, Yu L, Chen Z, Zheng L, Fu Q, Jiang J, et al. Cloning, expression patterns, and chromosome localization of three human and two mouse homologues of GABA(A) receptor-associated protein. Genomics 2001; 74:408-13; PMID:11414770; http://dx.doi.org/10.1006/geno.2001.6555
147. Novak I, Kirkin V, McEwan DG, Zhang J, Wild P, Rozenknop A, et al. Nix is a selective autophagy receptor for mitochondrial clearance. EMBO Rep 2010; 11:45-51; PMID:20010802; http://dx.doi.org/10.1038/embor.2009.256
148. Gassmann M, Grenacher B, Rohde B, Vogel J. Quantifying Western blots: pitfalls of densitometry. Electrophoresis 2009; 30:1845-55; PMID:19517440; http://dx.doi.org/10.1002/elps.200800720
149. Kirisako T, Ichimura Y, Okada H, Kabeya Y, Mizushima N, Yoshimori T, et al. The reversible modification regulates the membrane-binding state of Apg8/Aut7 essential for autophagy and the cytoplasm to vacuole targeting pathway. J Cell Biol 2000; 151:263-76; PMID:11038174; http://dx.doi.org/10.1083/jcb.151.2.263
150. Chung T, Phillips AR, Vierstra RD. ATG8 lipidation and ATG8-mediated autophagy in Arabidopsis require ATG12 expressed from the differentially controlled ATG12A AND ATG12B loci. Plant J 2010; 62:483-93; PMID:20136727; http://dx.doi.org/10.1111/j.1365-313X.2010.04166.x
151. Chung T, Suttangkakul A, Vierstra RD. The ATG autophagic conjugation system in maize: ATG transcripts and abundance of the ATG8-lipid adduct are regulated by development and nutrient availability. Plant Physiol 2009; 149:220-34; PMID:18790996; http://dx.doi.org/10.1104/pp.108.126714
152. King JS, Veltman DM, Insall RH. The induction of autophagy by mechanical stress. Autophagy 2011; 7:1490-9; PMID:22024750; http://dx.doi.org/10.4161/auto.7.12.17924
153. Ju JS, Varadhachary AS, Miller SE, Weihl CC. Quantitation of "autophagic flux" in mature skeletal muscle. Autophagy 2010; 6:929-35; PMID: 20657169; http://dx.doi.org/10.4161/auto.6.7.12785
154. Degtyarev M, De Mazière A, Orr C, Lin J, Lee BB, Tien JY, et al. Akt inhibition promotes autophagy and sensitizes PTEN-null tumors to lysosomotropic agents. J Cell Biol 2008; 183:101-16; PMID:18838554; http://dx.doi.org/10.1083/jcb.200801099
155. Klionsky DJ, Elazar Z, Seglen PO, Rubinsztein DC. Does bafilomycin A_1 block the fusion of autophagosomes with lysosomes? Autophagy 2008; 4:849-50; PMID:18758232
156. Xie R, Nguyen S, McKeehan WL, Liu L. Acetylated microtubules are required for fusion of autophagosomes with lysosomes. BMC Cell Biol 2010; 11:89; PMID:21092184; http://dx.doi.org/10.1186/1471-2121-11-89
157. González-Polo RA, Boya P, Pauleau AL, Jalil A, Larochette N, Souquère S, et al. The apoptosis/autophagy paradox: autophagic vacuolization before apoptotic death. J Cell Sci 2005; 118:3091-102; PMID:15985464; http://dx.doi.org/10.1242/jcs.02447
158. Cuervo AM, Stefanis L, Fredenburg R, Lansbury PT, Sulzer D. Impaired degradation of mutant alpha-synuclein by chaperone-mediated autophagy. Science 2004; 305:1292-5; PMID:15333840; http://dx.doi.org/10.1126/science.1101738
159. Trincheri NF, Follo C, Nicotra G, Peracchio C, Castino R, Isidoro C. Resveratrol-induced apoptosis depends on the lipid kinase activity of Vps34 and on the formation of autophagolysosomes. Carcinogenesis 2008; 29:381-9; PMID:18048384; http://dx.doi.org/10.1093/carcin/bgm271
160. Sarkar S, Ravikumar B, Rubinsztein DC. Autophagic clearance of aggregate-prone proteins associated with neurodegeneration. Methods Enzymol 2009; 453:83-110; PMID:19216903; http://dx.doi.org/10.1016/S0076-6879(08)04005-6
161. Shintani T, Klionsky DJ. Cargo proteins facilitate the formation of transport vesicles in the cytoplasm to vacuole targeting pathway. J Biol Chem 2004; 279:29889-94; PMID:15138258; http://dx.doi.org/10.1074/jbc.M404399200
162. Karim MR, Kanazawa T, Daigaku Y, Fujimura S, Miotto G, Kadowaki M. Cytosolic LC3 ratio as a sensitive index of macroautophagy in isolated rat hepatocytes and H4-II-E cells. Autophagy 2007; 3:553-60; PMID:17617739
163. Farkas T, Høyer-Hansen M, Jäättelä M. Identification of novel autophagy regulators by a luciferase-based assay for the kinetics of autophagic flux. Autophagy 2009; 5:1018-25; PMID:19652534; http://dx.doi.org/10.4161/auto.5.7.9443
164. Frankel LB, Wen J, Lees M, Høyer-Hansen M, Farkas T, Krogh A, et al. microRNA-101 is a potent inhibitor of autophagy. EMBO J 2011; 30:4628-41; PMID: 21915098; http://dx.doi.org/10.1038/emboj.2011.331
165. Farkas T, Daugaard M, Jäättelä M. Identification of small molecule inhibitors of phosphatidylinositol 3-kinase and autophagy. J Biol Chem 2011; 286:38904-12; PMID:21930714
166. Szyniarowski P, Corcelle-Termeau E, Farkas T, Høyer-Hansen M, Nylandsted J, Kallunki T, et al. A comprehensive siRNA screen for kinases that suppress macroautophagy in optimal growth conditions. Autophagy 2011; 7:892-903; PMID:21508868; http://dx.doi.org/10.4161/auto.7.8.15770
167. Sarkar S, Korolchuk V, Renna M, Winslow A, Rubinsztein DC. Methodological considerations for assessing autophagy modulators: a study with calcium phosphate precipitates. Autophagy 2009; 5:307-13; PMID:19182529; http://dx.doi.org/10.4161/auto.5.3.7664
168. Iwata J, Ezaki J, Komatsu M, Yokota S, Ueno T, Tanida I, et al. Excess peroxisomes are degraded by autophagic machinery in mammals. J Biol Chem 2006; 281:4035-41; PMID:16332691; http://dx.doi.org/10.1074/jbc.M512283200
169. Narendra D, Tanaka A, Suen DF, Youle RJ. Parkin is recruited selectively to impaired mitochondria and promotes their autophagy. J Cell Biol 2008; 183:795-803; PMID:19029340; http://dx.doi.org/10.1083/jcb.200809125
170. Nogalska A, Terracciano C, D'Agostino C, King Engel W, Askanas V. p62/SQSTM1 is overexpressed and prominently accumulated in inclusions of sporadic inclusion-body myositis muscle fibers, and can help differentiating it from polymyositis and dermatomyositis. Acta Neuropathol 2009; 118:407-13; PMID: 19557423; http://dx.doi.org/10.1007/s00401-009-0564-6
171. Hosokawa N, Hara Y, Mizushima N. Generation of cell lines with tetracycline-regulated autophagy and a role for autophagy in controlling cell size. FEBS Lett 2006; 580:2623-9; PMID:16647067; http://dx.doi.org/10.1016/j.febslet.2006.04.008
172. Ni HM, Bockus A, Wozniak AL, Jones K, Weinman S, Yin XM, et al. Dissecting the dynamic turnover of GFP-LC3 in the autolysosome. Autophagy 2011; 7:188-204; PMID:21107021; http://dx.doi.org/10.4161/auto.7.2.14181
173. Gutierrez MG, Saka HA, Chinen I, Zoppino FC, Yoshimori T, Bocco JL, et al. Protective role of autophagy against *Vibrio cholerae* cytolysin, a pore-forming toxin from *V. cholerae*. Proc Natl Acad Sci U S A 2007; 104:1829-34; PMID:17267617; http://dx.doi.org/10.1073/pnas.0601437104
174. Suttangkakul A, Li F, Chung T, Vierstra RD. The ATG1/ATG13 protein kinase complex is both a regulator and a target of autophagic recycling in Arabidopsis. Plant Cell 2011; 23:3761-79; PMID: 21984698; http://dx.doi.org/10.1105/tpc.111.090993
175. Balgi AD, Fonseca BD, Donohue E, Tsang TC, Lajoie P, Proud CG, et al. Screen for chemical modulators of autophagy reveals novel therapeutic inhibitors of mTORC1 signaling. PLoS One 2009; 4:e7124; PMID:19771169; http://dx.doi.org/10.1371/journal.pone.0007124
176. Patterson GH, Lippincott-Schwartz J. Selective photolabeling of proteins using photoactivatable GFP. Methods 2004; 32:445-50; PMID:15003607; http://dx.doi.org/10.1016/j.ymeth.2003.10.006
177. Hamacher-Brady A, Brady NR, Gottlieb RA. Enhancing macroautophagy protects against ischemia/reperfusion injury in cardiac myocytes. J Biol Chem 2006; 281:29776-87; PMID:16882669; http://dx.doi.org/10.1074/jbc.M603783200
178. Noda T, Klionsky DJ. The quantitative Pho8Delta60 assay of nonspecific autophagy. Methods Enzymol 2008; 451:33-42; PMID:19185711; http://dx.doi.org/10.1016/S0076-6879(08)03203-5
179. Klionsky DJ. Monitoring autophagy in yeast: the Pho8Delta60 assay. Methods Mol Biol 2007; 390:363-71; PMID:17951700; http://dx.doi.org/10.1007/978-1-59745-466-7_24
180. Patterson GH, Knobel SM, Sharif WD, Kain SR, Piston DW. Use of the green fluorescent protein and its mutants in quantitative fluorescence microscopy. Biophys J 1997; 73:2782-90; PMID:9370472; http://dx.doi.org/10.1016/S0006-3495(97)78307-3
181. Kimura S, Noda T, Yoshimori T. Dissection of the autophagosome maturation process by a novel reporter protein, tandem fluorescent-tagged LC3. Autophagy 2007; 3:452-60; PMID:17534139
182. Shaner NC, Campbell RE, Steinbach PA, Giepmans BN, Palmer AE, Tsien RY. Improved monomeric red, orange and yellow fluorescent proteins derived from Discosoma sp. red fluorescent protein. Nat Biotechnol 2004; 22:1567-72; PMID:15558047; http://dx.doi.org/10.1038/nbt1037
183. Strack RL, Keenan RJ, Glick BS. Noncytotoxic DsRed derivatives for whole-cell labeling. Methods Mol Biol 2011; 699:355-70; PMID:21116992; http://dx.doi.org/10.1007/978-1-61737-950-5_17
184. Gurskaya NG, Verkhusha VV, Shcheglov AS, Staroverov DB, Chepurnykh TV, Fradkov AF, et al. Engineering of a monomeric green-to-red photoactivatable fluorescent protein induced by blue light. Nat Biotechnol 2006; 24:461-5; PMID:16550175; http://dx.doi.org/10.1038/nbt1191
185. Ryhänen T, Hyttinen JM, Kopitz J, Rilla K, Kuusisto E, Mannermaa E, et al. Crosstalk between Hsp70 molecular chaperone, lysosomes and proteasomes in autophagy-mediated proteolysis in human retinal pigment epithelial cells. J Cell Mol Med 2009; 13(9B):3616-31; PMID:19017362; http://dx.doi.org/10.1111/j.1582-4934.2008.00577.x
186. Rekas A, Alattia JR, Nagai T, Miyawaki A, Ikura M. Crystal structure of venus, a yellow fluorescent protein with improved maturation and reduced environmental sensitivity. J Biol Chem 2002; 277:50573-8; PMID: 12370172; http://dx.doi.org/10.1074/jbc.M209524200
187. Kabeya Y, Mizushima N, Ueno T, Yamamoto A, Kirisako T, Noda T, et al. LC3, a mammalian homologue of yeast Apg8p, is localized in autophagosome membranes after processing. EMBO J 2000; 19:5720-8; PMID:11060023; http://dx.doi.org/10.1093/emboj/19.21.5720
188. Badr CE, Wurdinger T, Nilsson J, Niers JM, Whalen M, Degtyarev A, et al. Lanatoside C sensitizes glioblastoma cells to tumor necrosis factor-related apoptosis-inducing ligand and induces an alternative cell death pathway. Neuro Oncol 2011; 13:1213-24; PMID: 21757445; http://dx.doi.org/10.1093/neuonc/nor067
189. Meléndez A, Tallóczy Z, Seaman M, Eskelinen E-L, Hall DH, Levine B. Autophagy genes are essential for dauer development and life-span extension in *C. elegans*. Science 2003; 301:1387-91; PMID:12958363; http://dx.doi.org/10.1126/science.1087782
190. Otto GP, Wu MY, Kazgan N, Anderson OR, Kessin RH. Macroautophagy is required for multicellular development of the social amoeba *Dictyostelium discoideum*. J Biol Chem 2003; 278:17636-45; PMID: 12626495; http://dx.doi.org/10.1074/jbc.M212467200
191. Liu XH, Liu TB, Lin FC. Monitoring autophagy in *Magnaporthe oryzae*. Methods Enzymol 2008; 451:271-94; PMID:19185727; http://dx.doi.org/10.1016/S0076-6879(08)03219-9
192. Pinan-Lucarré B, Paoletti M, Dementhon K, Coulary-Salin B, Clavé C. Autophagy is induced during cell death by incompatibility and is essential for differentiation in the filamentous fungus *Podospora anserina*. Mol Microbiol 2003; 47:321-33; PMID:12519185; http://dx.doi.org/10.1046/j.1365-2958.2003.03208.x
193. Veneault-Fourrey C, Barooah M, Egan M, Wakley G, Talbot NJ. Autophagic fungal cell death is necessary for infection by the rice blast fungus. Science 2006; 312:580-3; PMID:16645096; http://dx.doi.org/10.1126/science.1124550

© 2012 Landes Bioscience. Do not distribute

doi: 10.4161/auto.19496

194. Kikuma T, Ohneda M, Arioka M, Kitamoto K. Functional analysis of the ATG8 homologue Aoatg8 and role of autophagy in differentiation and germination in *Aspergillus oryzae*. Eukaryot Cell 2006; 5:1328-36; PMID:16896216; http://dx.doi.org/10.1128/EC.00024-06

195. Nolting N, Bernhards Y, Pöggeler S. SmATG7 is required for viability in the homothallic ascomycete *Sordaria macrospora*. Fungal Genet Biol 2009; 46:531-42; PMID:19351563; http://dx.doi.org/10.1016/j.fgb.2009.03.008

196. Baghdiguian S, Martinand-Mari C, Mangeat P. Using Ciona to study developmental programmed cell death. Semin Cancer Biol 2007; 17:147-53; PMID:17197195; http://dx.doi.org/10.1016/j.semcancer.2006.11.005

197. Rusten TE, Lindmo K, Juhász G, Sass M, Seglen PO, Brech A, et al. Programmed autophagy in the *Drosophila* fat body is induced by ecdysone through regulation of the PI3K pathway. Dev Cell 2004; 7:179-92; PMID:15296715; http://dx.doi.org/10.1016/j.devcel.2004.07.005

198. Scott RC, Schuldiner O, Neufeld TP. Role and regulation of starvation-induced autophagy in the *Drosophila* fat body. Dev Cell 2004; 7:167-78; PMID:15296714; http://dx.doi.org/10.1016/j.devcel.2004.07.009

199. Denton D, Shravage B, Simin R, Mills K, Berry DL, Baehrecke EH, et al. Autophagy, not apoptosis, is essential for midgut cell death in Drosophila. Curr Biol 2009; 19:1741-6; PMID:19818615; http://dx.doi.org/10.1016/j.cub.2009.08.042

200. Yoshimoto K, Hanaoka H, Sato S, Kato T, Tabata S, Noda T, et al. Processing of ATG8s, ubiquitin-like proteins, and their deconjugation by ATG4s are essential for plant autophagy. Plant Cell 2004; 16:2967-83; PMID:15494556; http://dx.doi.org/10.1105/tpc.104.025395

201. Besteiro S, Brooks CF, Striepen B, Dubremetz J-F. Autophagy protein Atg3 is essential for maintaining mitochondrial integrity and for normal intracellular development of *Toxoplasma gondii* tachyzoites. PLoS Pathog 2011; 7:e1002416; PMID:22144900; http://dx.doi.org/10.1371/journal.ppat.1002416

202. Williams RA, Tetley L, Mottram JC, Coombs GH. Cysteine peptidases CPA and CPB are vital for autophagy and differentiation in *Leishmania mexicana*. Mol Microbiol 2006; 61:655-74; PMID:16803590; http://dx.doi.org/10.1111/j.1365-2958.2006.05274.x

203. Williams RA, Woods KL, Juliano L, Mottram JC, Coombs GH. Characterization of unusual families of ATG8-like proteins and ATG12 in the protozoan parasite *Leishmania major*. Autophagy 2009; 5:159-72; PMID:19066473; http://dx.doi.org/10.4161/auto.5.2.7328

204. Elässer A, Vogt AM, Nef H, Kostin S, Möllmann H, Skwara W, et al. Human hibernating myocardium is jeopardized by apoptotic and autophagic cell death. J Am Coll Cardiol 2004; 43:2191-9; PMID:15193679; http://dx.doi.org/10.1016/j.jacc.2004.02.053

205. Knaapen MW, Davies MJ, De Bie M, Haven AJ, Martinet W, Kockx MM. Apoptotic versus autophagic cell death in heart failure. Cardiovasc Res 2001; 51:304-12; PMID:11470470; http://dx.doi.org/10.1016/S0008-6363(01)00290-5

206. Kostin S, Pool L, Elsässer A, Hein S, Drexler HC, Arnon E, et al. Myocytes die by multiple mechanisms in failing human hearts. Circ Res 2003; 92:715-24; PMID:12649263; http://dx.doi.org/10.1161/01.RES.0000067471.95890.5C

207. Pérez-Pérez ME, Florencio FJ, Crespo JL. Inhibition of target of rapamycin signaling and stress activate autophagy in *Chlamydomonas reinhardtii*. Plant Physiol 2010; 152:1874-88; PMID:20107021; http://dx.doi.org/10.1104/pp.109.152520

208. Koike M, Shibata M, Waguri S, Yoshimura K, Tanida I, Kominami E, et al. Participation of autophagy in storage of lysosomes in neurons from mouse models of neuronal ceroid-lipofuscinoses (Batten disease). Am J Pathol 2005; 167:1713-28; PMID:16314482; http://dx.doi.org/10.1016/S0002-9440(10)61253-9

209. Ost A, Svensson K, Ruishalme I, Brännmark C, Franck N, Krook H, et al. Attenuated mTOR signaling and enhanced autophagy in adipocytes from obese patients with type 2 diabetes. Mol Med 2010; 16:235-46; PMID:20386866

210. Tang D, Kang R, Livesey KM, Cheh CW, Farkas A, Loughran P, et al. Endogenous HMGB1 regulates autophagy. J Cell Biol 2010; 190:881-92; PMID:20819940; http://dx.doi.org/10.1083/jcb.200911078

211. Gniadek TJ, Warren G. WatershedCounting3D: a new method for segmenting and counting punctate structures from confocal image data. Traffic 2007; 8:339-46; PMID:17319897; http://dx.doi.org/10.1111/j.1600-0854.2007.00538.x

212. Decuypere J-P, Welkenhuyzen K, Luyten T, Ponsaerts R, Dewaele M, Molgó J, et al. IP3 receptor-mediated Ca(2+) signaling and autophagy induction are interrelated. Autophagy 2011; 7:1472-89; PMID:22082873; http://dx.doi.org/10.4161/auto.7.12.17909

213. Amer AO, Swanson MS. Autophagy is an immediate macrophage response to *Legionella pneumophila*. Cell Microbiol 2005; 7:765-78; PMID:15888080; http://dx.doi.org/10.1111/j.1462-5822.2005.00509.x

214. Gutierrez MG, Master SS, Singh SB, Taylor GA, Colombo MI, Deretic V. Autophagy is a defense mechanism inhibiting BCG and *Mycobacterium tuberculosis* survival in infected macrophages. Cell 2004; 119:753-66; PMID:15607973; http://dx.doi.org/10.1016/j.cell.2004.11.038

215. Ogawa M, Sasakawa C. Intracellular survival of *Shigella*. Cell Microbiol 2006; 8:177-84; PMID:16441429; http://dx.doi.org/10.1111/j.1462-5822.2005.00652.x

216. Kamentsky L, Jones TR, Fraser A, Bray MA, Logan DJ, Madden KL, et al. Improved structure, function and compatibility for CellProfiler: modular high-throughput image analysis software. Bioinformatics 2011; 27:1179-80; PMID:21349861; http://dx.doi.org/10.1093/bioinformatics/btr095

217. Wu JQ, Pollard TD. Counting cytokinesis proteins globally and locally in fission yeast. Science 2005; 310:310-4; PMID:16224022; http://dx.doi.org/10.1126/science.1113230

218. Geng J, Baba M, Nair U, Klionsky DJ. Quantitative analysis of autophagy-related protein stoichiometry by fluorescence microscopy. J Cell Biol 2008; 182:129-40; PMID:18625846; http://dx.doi.org/10.1083/jcb.200711112

219. Brady NR, Hamacher-Brady A, Yuan H, Gottlieb RA. The autophagic response to nutrient deprivation in the hl-1 cardiac myocyte is modulated by Bcl-2 and sarco/endoplasmic reticulum calcium stores. FEBS J 2007; 274:3184-97; PMID:17540004; http://dx.doi.org/10.1111/j.1742-4658.2007.05849.x

220. Qadir MA, Kwok B, Dragowska WH, To KH, Le D, Bally MB, et al. Macroautophagy inhibition sensitizes tamoxifen-resistant breast cancer cells and enhances mitochondrial depolarization. Breast Cancer Res Treat 2008; 112:389-403; PMID:18172760; http://dx.doi.org/10.1007/s10549-007-9873-4

221. Dolloff NG, Ma X, Dicker DT, Humphreys RC, Li LZ, El-Deiry WS. Spectral imaging-based methods for quantifying autophagy and apoptosis. Cancer Biol Ther 2011; 12:349-56; PMID:21757995; http://dx.doi.org/10.4161/cbt.12.4.17175

222. Phadwal K, Alegre-Abarrategui J, Watson AS, Pike L, Anbalagan S, Hammond EM, et al. A novel method for autophagy detection in primary cells: Impaired levels of macroautophagy in immunosenescent T cells. Autophagy 2012; 8; In press; PMID:22302009

223. Lee HK, Lund JM, Ramanathan B, Mizushima N, Iwasaki A. Autophagy-dependent viral recognition by plasmacytoid dendritic cells. Science 2007; 315:1398-401; PMID:17272685; http://dx.doi.org/10.1126/science.1136880

224. Kuma A, Matsui M, Mizushima N. LC3, an autophagosome marker, can be incorporated into protein aggregates independent of autophagy: caution in the interpretation of LC3 localization. Autophagy 2007; 3:323-8; PMID:17387262

225. Szeto J, Kaniuk NA, Canadien V, Nisman R, Mizushima N, Yoshimori T, et al. ALIS are stress-induced protein storage compartments for substrates of the proteasome and autophagy. Autophagy 2006; 2:189-99; PMID:16874109

226. Kaniuk NA, Kiraly M, Bates H, Vranic M, Volchuk A, Brumell JH. Ubiquitinated-protein aggregates form in pancreatic beta-cells during diabetes-induced oxidative stress and are regulated by autophagy. Diabetes 2007; 56:930-9; PMID:17395740; http://dx.doi.org/10.2337/db06-1160

227. Fujita K, Maeda D, Xiao Q, Srinivasula SM. Nrf2-mediated induction of p62 controls Toll-like receptor-4-driven aggresome-like induced structure formation and autophagic degradation. Proc Natl Acad Sci U S A 2011; 108:1427-32; PMID:21220332; http://dx.doi.org/10.1073/pnas.1014156108

228. Pierre P. Dendritic cells, DRiPs, and DALIS in the control of antigen processing. Immunol Rev 2005; 207:184-90; PMID:16181336; http://dx.doi.org/10.1111/j.0105-2896.2005.00300.x

229. Pankiv S, Clausen TH, Lamark T, Brech A, Bruun JA, Outzen H, et al. p62/SQSTM1 binds directly to Atg8/LC3 to facilitate degradation of ubiquitinated protein aggregates by autophagy. J Biol Chem 2007; 282:24131-45; PMID:17580304; http://dx.doi.org/10.1074/jbc.M702824200

230. Hara T, Nakamura K, Matsui M, Yamamoto A, Nakahara Y, Suzuki-Migishima R, et al. Suppression of basal autophagy in neural cells causes neurodegenerative disease in mice. Nature 2006; 441:885-9; PMID:16625204; http://dx.doi.org/10.1038/nature04724

231. Komatsu M, Waguri S, Chiba T, Murata S, Iwata J, Tanida I, et al. Loss of autophagy in the central nervous system causes neurodegeneration in mice. Nature 2006; 441:880-4; PMID:16625205; http://dx.doi.org/10.1038/nature04723

232. Calvo-Garrido J, Escalante R. Autophagy dysfunction and ubiquitin-positive protein aggregates in Dictyostelium cells lacking Vmp1. Autophagy 2010; 6:100-9; PMID:20009561; http://dx.doi.org/10.4161/auto.6.1.10697

233. Bjørkøy G, Lamark T, Johansen T. p62/SQSTM1: a missing link between protein aggregates and the autophagy machinery. Autophagy 2006; 2:138-9; PMID:16874037

234. Matsumoto G, Wada K, Okuno M, Kurosawa M, Nukina N. Serine 403 phosphorylation of p62/SQSTM1 regulates selective autophagic clearance of ubiquitinated proteins. Mol Cell 2011; 44:279-89; PMID:22017874; http://dx.doi.org/10.1016/j.molcel.2011.07.039

235. Köchl R, Hu XW, Chan EYW, Tooze SA. Microtubules facilitate autophagosome formation and fusion of autophagosomes with endosomes. Traffic 2006; 7:129-45; PMID:16420522; http://dx.doi.org/10.1111/j.1600-0854.2005.00368.x

236. Eng KE, Panas MD, Hedestam GB, McInerney GM. A novel quantitative flow cytometry-based assay for autophagy. Autophagy 2010; 6:634-41; PMID:20458170; http://dx.doi.org/10.4161/auto.6.5.12112

237. Ciechomska IA, Tolkovsky AM. Non-autophagic GFP-LC3 puncta induced by saponin and other detergents. Autophagy 2007; 3:586-90; PMID:17786021

238. Tsvetkov AS, Miller J, Arrasate M, Wong JS, Pleiss MA, Finkbeiner S. A small-molecule scaffold induces autophagy in primary neurons and protects against toxicity in a Huntington disease model. Proc Natl Acad Sci U S A 2010; 107:16982-7; PMID:20833817; http://dx.doi.org/10.1073/pnas.1004498107

239. Joo JH, Dorsey FC, Joshi A, Hennessy-Walters KM, Rose KL, McCastlain K, et al. Hsp90-Cdc37 chaperone complex regulates Ulk1- and Atg13-mediated mitophagy. Mol Cell 2011; 43:572-85; PMID:21855797; http://dx.doi.org/10.1016/j.molcel.2011.06.018

240. Fujita N, Hayashi-Nishino M, Fukumoto H, Omori H, Yamamoto A, Noda T, et al. An Atg4B mutant hampers the lipidation of LC3 paralogues and causes defects in autophagosome closure. Mol Biol Cell 2008; 19:4651-9; PMID:18768752; http://dx.doi.org/10.1091/mbc.E08-03-0312

241. Decuypere JP, Bultynck G, Parys JB. A dual role for Ca^{2+} in autophagy regulation. Cell Calcium 2011; 50:242-50; PMID:21571367; http://dx.doi.org/10.1016/j.ceca.2011.04.001

242. Nyfeler B, Bergman P, Triantafellow E, Wilson CJ, Zhu Y, Radetich B, et al. Relieving autophagy and 4EBP1 from rapamycin resistance. Mol Cell Biol 2011; 31:2867-76; PMID:21576371; http://dx.doi.org/10.1128/MCB.05430-11

243. García-Martínez JM, Moran J, Clarke RG, Gray A, Cosulich SC, Chresta CM, et al. Ku-0063794 is a specific inhibitor of the mammalian target of rapamycin (mTOR). Biochem J 2009; 421:29-42; PMID:19402821; http://dx.doi.org/10.1042/BJ20090489

244. Pereira GJ, Hirata H, Fimia GM, do Carmo LG, Bincoletto C, Han SW, et al. Nicotinic acid adenine dinucleotide phosphate (NAADP) regulates autophagy in cultured astrocytes. J Biol Chem 2011; 286:27875-81; PMID:21610076; http://dx.doi.org/10.1074/jbc.C110.216580

245. Serra V, Markman B, Scaltriti M, Eichhorn PJ, Valero V, Guzman M, et al. NVP-BEZ235, a dual PI3K/mTOR inhibitor, prevents PI3K signaling and inhibits the growth of cancer cells with activating PI3K mutations. Cancer Res 2008; 68:8022-30; PMID:18829560; http://dx.doi.org/10.1158/0008-5472.CAN-08-1385

246. Liu TJ, Koul D, LaFortune T, Tiao N, Shen RJ, Maira SM, et al. NVP-BEZ235, a novel dual phosphatidylinositol 3-kinase/mammalian target of rapamycin inhibitor, elicits multifaceted antitumor activities in human gliomas. Mol Cancer Ther 2009; 8:2204-10; PMID:19671762; http://dx.doi.org/10.1158/1535-7163.MCT-09-0160

247. Vingtdeux V, Giliberto L, Zhao H, Chandakkar P, Wu Q, Simon JE, et al. AMP-activated protein kinase signaling activation by resveratrol modulates amyloid-beta peptide metabolism. J Biol Chem 2010; 285:9100-13; PMID:20080969; http://dx.doi.org/10.1074/jbc.M109.060061

248. Puissant A, Auberger P. AMPK- and p62/SQSTM1-dependent autophagy mediate Resveratrol-induced cell death in chronic myelogenous leukemia. Autophagy 2010; 6:655-7; PMID:20458181; http://dx.doi.org/10.4161/auto.6.5.12126

249. Vingtdeux V, Chandakkar P, Zhao H, d'Abramo C, Davies P, Marambaud P. Novel synthetic small-molecule activators of AMPK as enhancers of autophagy and amyloid-β peptide degradation. FASEB J 2011; 25:219-31; PMID:20852062; http://dx.doi.org/10.1096/fj.10-167361

250. Gordon PB, Holen I, Fosse M, Røtnes JS, Seglen PO. Dependence of hepatocytic autophagy on intracellularly sequestered calcium. J Biol Chem 1993; 268:26107-12; PMID:8253727

251. Ganley IG, Wong PM, Gammoh N, Jiang X. Distinct autophagosomal-lysosomal fusion mechanism revealed by thapsigargin-induced autophagy arrest. Mol Cell 2011; 42:731-43; PMID:21700220; http://dx.doi.org/10.1016/j.molcel.2011.04.024

252. Thoreen CC, Kang SA, Chang JW, Liu Q, Zhang J, Gao Y, et al. An ATP-competitive mammalian target of rapamycin inhibitor reveals rapamycin-resistant functions of mTORC1. J Biol Chem 2009; 284:8023-32; PMID:19150980; http://dx.doi.org/10.1074/jbc.M900301200

253. Sarkar S, Davies JE, Huang Z, Tunnacliffe A, Rubinsztein DC. Trehalose, a novel mTOR-independent autophagy enhancer, accelerates the clearance of mutant huntingtin and alpha-synuclein. J Biol Chem 2007; 282:5641-52; PMID:17182613; http://dx.doi.org/10.1074/jbc.M609532200

254. Casarejos MJ, Solano RM, Gómez A, Perucho J, de Yébenes JG, Mena MA. The accumulation of neurotoxic proteins, induced by proteasome inhibition, is reverted by trehalose, an enhancer of autophagy, in human neuroblastoma cells. Neurochem Int 2011; 58:512-20; PMID:21232572; http://dx.doi.org/10.1016/j.neuint.2011.01.008

255. Carpenter JE, Jackson W, Benetti L, Grose C. Autophagosome formation during varicella-zoster virus infection following endoplasmic reticulum stress and the unfolded protein response. J Virol 2011; 85:9414-24; PMID:21752906; http://dx.doi.org/10.1128/JVI.00281-11

256. Seglen PO, Gordon PB. 3-Methyladenine: specific inhibitor of autophagic/lysosomal protein degradation in isolated rat hepatocytes. Proc Natl Acad Sci U S A 1982; 79:1889-92; PMID:6952238; http://dx.doi.org/10.1073/pnas.79.6.1889

257. Wu YT, Tan HL, Shui G, Bauvy C, Huang Q, Wenk MR, et al. Dual role of 3-methyladenine in modulation of autophagy via different temporal patterns of inhibition on class I and III phosphoinositide 3-kinase. J Biol Chem 2010; 285:10850-61; PMID:20123989; http://dx.doi.org/10.1074/jbc.M109.080796

258. Bampton ET, Goemans CG, Niranjan D, Mizushima N, Tolkovsky AM. The dynamics of autophagy visualized in live cells from autophagosome formation to fusion with endo/lysosomes. Autophagy 2005; 1:23-36; PMID:16874023; http://dx.doi.org/10.4161/auto.1.1.1495

259. Tormo D, Checińska A, Alonso-Curbelo D, Pérez-Guijarro E, Cañón E, Riveiro-Falkenbach E, et al. Targeted activation of innate immunity for therapeutic induction of autophagy and apoptosis in melanoma cells. Cancer Cell 2009; 16:103-14; PMID:19647221; http://dx.doi.org/10.1016/j.ccr.2009.07.004

260. Lee HK, Mattei LM, Steinberg BE, Alberts P, Lee YH, Chervonsky A, et al. In vivo requirement for Atg5 in antigen presentation by dendritic cells. Immunity 2010; 32:227-39; PMID:20171125; http://dx.doi.org/10.1016/j.immuni.2009.12.006

261. Tamura N, Oku M, Sakai Y. Atg8 regulates vacuolar membrane dynamics in a lipidation-independent manner in *Pichia pastoris*. J Cell Sci 2010; 123:4107-16; PMID:21045113; http://dx.doi.org/10.1242/jcs.070045

262. Strømhaug PE, Reggiori F, Guan J, Wang C-W, Klionsky DJ. Atg21 is a phosphoinositide binding protein required for efficient lipidation and localization of Atg8 during uptake of aminopeptidase I by selective autophagy. Mol Biol Cell 2004; 15:3553-66; PMID:15155809; http://dx.doi.org/10.1091/mbc.E04-02-0147

263. Baens M, Noels H, Broeckx V, Hagens S, Fevery S, Billiau AD, et al. The dark side of EGFP: defective polyubiquitination. PLoS One 2006; 1:e54; PMID:17183684; http://dx.doi.org/10.1371/journal.pone.0000054

264. Cali T, Galli C, Olivari S, Molinari M. Segregation and rapid turnover of EDEM1 by an autophagy-like mechanism modulates standard ERAD and folding activities. Biochem Biophys Res Commun 2008; 371:405-10; PMID:18452703; http://dx.doi.org/10.1016/j.bbrc.2008.04.098

265. Al-Younes HM, Al-Zeer MA, Khalil H, Gussmann J, Karlas A, Machuy N, et al. Autophagy-independent function of MAP-LC3 during intracellular propagation of Chlamydia trachomatis. Autophagy 2011; 7:814-28; PMID:21464618; http://dx.doi.org/10.4161/auto.7.8.15597

266. Shroff H, Galbraith CG, Galbraith JA, White H, Gillette J, Olenych S, et al. Dual-color superresolution imaging of genetically expressed probes within individual adhesion complexes. Proc Natl Acad Sci U S A 2007; 104:20308-13; PMID:18077327; http://dx.doi.org/10.1073/pnas.0710517105

267. Nicklin P, Bergman P, Zhang B, Triantafellow E, Wang H, Nyfeler B, et al. Bidirectional transport of amino acids regulates mTOR and autophagy. Cell 2009; 136:521-34; PMID:19203585; http://dx.doi.org/10.1016/j.cell.2008.11.044

268. Cherra SJ, 3rd, Kulich SM, Uechi G, Balasubramani M, Mountzouris J, Day BW, et al. Regulation of the autophagy protein LC3 by phosphorylation. J Cell Biol 2010; 190:533-9; PMID:20713600; http://dx.doi.org/10.1083/jcb.201002108

269. Sarkar S, Korolchuk VI, Renna M, Imarisio S, Fleming A, Williams A, et al. Complex inhibitory effects of nitric oxide on autophagy. Mol Cell 2011; 43:19-32; PMID:21726807; http://dx.doi.org/10.1016/j.molcel.2011.04.029

270. Rosado CJ, Mijaljica D, Hatzinisiriou I, Prescott M, Devenish RJ. Rosella: a fluorescent pH-biosensor for reporting vacuolar turnover of cytosol and organelles in yeast. Autophagy 2008; 4:205-13; PMID:18094608

271. Mijaljica D, Rosado CJ, Devenish RJ, Prescott M. Biosensors for monitoring autophagy In: Serra PA, ed. Biosensors-Emerging Materials and Applications Croatia: InTech, 2011:383-400.

272. Chudakov DM, Matz MV, Lukyanov S, Lukyanov KA. Fluorescent proteins and their applications in imaging living cells and tissues. Physiol Rev 2010; 90:1103-63; PMID:20664080; http://dx.doi.org/10.1152/physrev.00038.2009

273. Zhou J, Lin J, Zhou C, Deng X, Xia B. Cytotoxicity of red fluorescent protein DsRed is associated with the suppression of Bcl-xL translation. FEBS Lett 2011; 585:821-7; PMID:21320495; http://dx.doi.org/10.1016/j.febslet.2011.02.013

274. Loos B, Genade S, Ellis B, Lochner A, Engelbrecht AM. At the core of survival: autophagy delays the onset of both apoptotic and necrotic cell death in a model of ischemic cell injury. Exp Cell Res 2011; 317:1437-53; PMID:21420401; http://dx.doi.org/10.1016/j.yexcr.2011.03.011

275. Shvets E, Fass E, Elazar Z. Utilizing flow cytometry to monitor autophagy in living mammalian cells. Autophagy 2008; 4:621-8; PMID:18376137

dc_840_14

©2012 Landes Bioscience. Do not distribute.

276. Hundeshagen P, Hamacher-Brady A, Eils R, Brady NR. Concurrent detection of autolysosome formation and lysosomal degradation by flow cytometry in a high-content screen for inducers of autophagy. BMC Biol 2011; 9:38; PMID:21635740; http://dx.doi.org/10.1186/1741-7007-9-38
277. de la Calle C, Joubert PE, Law HK, Hasan M, Albert ML. Simultaneous assessment of autophagy and apoptosis using multispectral imaging cytometry. Autophagy 2011; 7:1045-51; PMID:21606680; http://dx.doi.org/10.4161/auto.7.9.16252
278. Gannagé M, Dormann D, Albrecht R, Dengjel J, Torossi T, Rämer PC, et al. Matrix protein 2 of influenza A virus blocks autophagosome fusion with lysosomes. Cell Host Microbe 2009; 6:367-80; PMID:19837376; http://dx.doi.org/10.1016/j.chom.2009.09.005
279. Kaminskyy V, Abdi A, Zhivotovsky B. A quantitative assay for the monitoring of autophagosome accumulation in different phases of the cell cycle. Autophagy 2011; 7:83-90; PMID:20980814; http://dx.doi.org/10.4161/auto.7.1.13893
280. Kirkin V, Lamark T, Sou YS, Bjørkøy G, Nunn JL, Bruun JA, et al. A role for NBR1 in autophagosomal degradation of ubiquitinated substrates. Mol Cell 2009; 33:505-16; PMID:19250911; http://dx.doi.org/10.1016/j.molcel.2009.01.020
281. Larsen KB, Lamark T, Øvervatn A, Harneshaug I, Johansen T, Bjørkøy G. A reporter cell system to monitor autophagy based on p62/SQSTM1. Autophagy 2010; 6:784-93; PMID:20574168; http://dx.doi.org/10.4161/auto.6.6.12510
282. Huang JJ, Li HR, Huang Y, Jiang WQ, Xu RH, Huang HQ, et al. Beclin 1 expression: a predictor of prognosis in patients with extranodal natural killer/T-cell lymphoma, nasal type. Autophagy 2010; 6:777-83; PMID:20639699; http://dx.doi.org/10.4161/auto.6.6.12784
283. Sivridis E, Koukourakis MI, Zois CE, Ledaki I, Ferguson DJ, Harris AL, et al. LC3A-positive light microscopy detected patterns of autophagy and prognosis in operable breast carcinomas. Am J Pathol 2010; 176:2477-89; PMID:20382705; http://dx.doi.org/10.2353/ajpath.2010.090049
284. Sivridis E, Giatromanolaki A, Liberis V, Koukourakis MI. Autophagy in endometrial carcinomas and prognostic relevance of 'stone-like' structures (SLS): what is destined for the atypical endometrial hyperplasia? Autophagy 2011; 7:74-82; PMID:21099253; http://dx.doi.org/10.4161/auto.7.1.13947
285. Giatromanolaki A, Koukourakis MI, Koutsopoulos A, Chloropoulou P, Liberis V, Sivridis E. High Beclin 1 expression defines a poor prognosis in endometrial adenocarcinomas. Gynecol Oncol 2011; 123:147-51; PMID:21741077; http://dx.doi.org/10.1016/j.ygyno.2011.06.023
286. Chen Y, Lu Y, Lu C, Zhang L. Beclin-1 expression is a predictor of clinical outcome in patients with esophageal squamous cell carcinoma and correlated to hypoxia-inducible factor (HIF)-1alpha expression. Pathol Oncol Res 2009; 15:487-93; PMID:19130303; http://dx.doi.org/10.1007/s12253-008-9143-8
287. Wan XB, Fan XJ, Chen MY, Xiang J, Huang PY, Guo L, et al. Elevated Beclin 1 expression is correlated with HIF-1alpha in predicting poor prognosis of nasopharyngeal carcinoma. Autophagy 2010; 6:395-404; PMID: 20150769; http://dx.doi.org/10.4161/auto.6.3.11303
288. Shi YH, Ding ZB, Zhou J, Qiu SJ, Fan J. Prognostic significance of Beclin 1-dependent apoptotic activity in hepatocellular carcinoma. Autophagy 2009; 5:380-2; PMID:19145109; http://dx.doi.org/10.4161/auto.5.3.7658
289. Ding ZB, Shi YH, Zhou J, Qiu SJ, Xu Y, Dai Z, et al. Association of autophagy defect with a malignant phenotype and poor prognosis of hepatocellular carcinoma. Cancer Res 2008; 68:9167-75; PMID:19010888; http://dx.doi.org/10.1158/0008-5472.CAN-08-1573
290. Pirtoli L, Cevenini G, Tini P, Vannini M, Oliveri G, Marsili S, et al. The prognostic role of Beclin 1 protein expression in high-grade gliomas. Autophagy 2009; 5:930-6; PMID:19556884; http://dx.doi.org/10.4161/auto.5.7.9227
291. Karpathiou G, Sivridis E, Koukourakis MI, Mikroulis D, Bouros D, Froudarakis ME, et al. Light-chain 3A autophagic activity and prognostic significance in non-small cell lung carcinomas. Chest 2011; 140:127-34; PMID:21148243; http://dx.doi.org/10.1378/chest.10-1831
292. Fujii S, Mitsunaga S, Yamazaki M, Hasebe T, Ishii G, Kojima M, et al. Autophagy is activated in pancreatic cancer cells and correlates with poor patient outcome. Cancer Sci 2008; 99:1813-9; PMID:18616529
293. Li BX, Li CY, Peng RQ, Wu XJ, Wang HY, Wan DS, et al. The expression of beclin 1 is associated with favorable prognosis in stage IIIB colon cancers. Autophagy 2009; 5:303-6; PMID:19066461; http://dx.doi.org/10.4161/auto.5.3.7491
294. Koukourakis MI, Giatromanolaki A, Sivridis E, Pitiakoudis M, Gatter KC, Harris AL. Beclin 1 over- and underexpression in colorectal cancer: distinct patterns relate to prognosis and tumour hypoxia. Br J Cancer 2010; 103:1209-14; PMID:20842118; http://dx.doi.org/10.1038/sj.bjc.6605904
295. Giatromanolaki A, Koukourakis MI, Harris AL, Polychronidis A, Gatter KC, Sivridis E. Prognostic relevance of light chain 3 (LC3A) autophagy patterns in colorectal adenocarcinomas. J Clin Pathol 2010; 63:867-72; PMID:20876316; http://dx.doi.org/10.1136/jcp.2010.079525
296. Sivridis E, Koukourakis MI, Mendrinos SE, Karpouzis A, Fiska A, Kouskoukis C, et al. Beclin-1 and LC3A expression in cutaneous malignant melanomas: a biphasic survival pattern for beclin-1. Melanoma Res 2011; 21:188-95; PMID:21537144; http://dx.doi.org/10.1097/CMR.0b013e328346612c
297. Giatromanolaki AN, Charitoudis GS, Bechrakis NE, Kozobolis VP, Koukourakis MI, Foerster MH, et al. Autophagy patterns and prognosis in uveal melanomas. Mod Pathol 2011; 24:1036-45; PMID:21499230; http://dx.doi.org/10.1038/modpathol.2011.63
298. McShane LM, Altman DG, Sauerbrei W, Taube SE, Gion M, Clark GM & Statistics Subcommittee of the NCI-EORTC Working Group on Cancer Diagnostics. Reporting recommendations for tumor marker prognostic studies (REMARK). J Natl Cancer Inst 2005; 97:1180-4; PMID:16106022; http://dx.doi.org/10.1093/jnci/dji237
299. Kuwahara Y, Oikawa T, Ochiai Y, Roudkenar MH, Fukumoto M, Shimura T, et al. Enhancement of autophagy is a potential modality for tumors refractory to radiotherapy. Cell Death Dis 2011; 2:e177; PMID: 21716292; http://dx.doi.org/10.1038/cddis.2011.56
300. Hou YJ, Dong LW, Tan YX, Yang GZ, Pan YF, Li Z, et al. Inhibition of active autophagy induces apoptosis and increases chemosensitivity in cholangiocarcinoma. Lab Invest 2011; 91:1146-57; PMID:21647092; http://dx.doi.org/10.1038/labinvest.2011.97
301. O'Donovan TR, O'Sullivan GC, McKenna SL. Induction of autophagy by drug-resistant esophageal cancer cells promotes their survival and recovery following treatment with chemotherapeutics. Autophagy 2011; 7:509-24; PMID:21325880; http://dx.doi.org/10.4161/auto.7.5.15066
302. Yoshimura K, Shibata M, Koike M, Gotoh K, Fukaya M, Watanabe M, et al. Effects of RNA interference of Atg4B on the limited proteolysis of LC3 in PC12 cells and expression of Atg4B in various rat tissues. Autophagy 2006; 2:200-8; PMID:16874114
303. Tamura H, Shibata M, Koike M, Sasaki M, Uchiyama Y. Atg9A protein, an autophagy-related membrane protein, is localized in the neurons of mouse brains. J Histochem Cytochem 2010; 58:443-53; PMID: 20124090; http://dx.doi.org/10.1369/jhc.2010.955690
304. Cui J, Bai XY, Shi S, Cui S, Hong Q, Cai G, et al. Age-related changes in the function of autophagy in rat kidneys. Age (Dordr) 2011; In press; PMID:21455601; http://dx.doi.org/10.1007/s11357-011-9237-1
305. Mellén MA, de la Rosa EJ, Boya P. The autophagic machinery is necessary for removal of cell corpses from the developing retinal neuroepithelium. Cell Death Differ 2008; 15:1279-90; PMID:18369370; http://dx.doi.org/10.1038/cdd.2008.40
306. Mellén MA, de la Rosa EJ, Boya P. Autophagy is not universally required for phosphatidyl-serine exposure and apoptotic cell engulfment during neural development. Autophagy 2009; 5:964-72; PMID:19587526; http://dx.doi.org/10.4161/auto.5.7.9292
307. Shibata M, Yoshimura K, Furuya N, Koike M, Ueno T, Komatsu M, et al. The MAP1-LC3 conjugation system is involved in lipid droplet formation. Biochem Biophys Res Commun 2009; 382:419-23; PMID:19285958; http://dx.doi.org/10.1016/j.bbrc.2009.03.039
308. Komatsu M, Waguri S, Koike M, Sou YS, Ueno T, Hara T, et al. Homeostatic levels of p62 control cytoplasmic inclusion body formation in autophagy-deficient mice. Cell 2007; 131:1149-63; PMID:18083104; http://dx.doi.org/10.1016/j.cell.2007.10.035
309. Germain M, Nguyen AP, Le Grand JN, Arbour N, Vanderluit JL, Park DS, et al. MCL-1 is a stress sensor that regulates autophagy in a developmentally regulated manner. EMBO J 2011; 30:395-407; PMID: 21139567; http://dx.doi.org/10.1038/emboj.2010.327
310. Komatsu M, Wang QJ, Holstein GR, Friedrich VL, Jr., Iwata J, Kominami E, et al. Essential role for autophagy protein Atg7 in the maintenance of axonal homeostasis and the prevention of axonal degeneration. Proc Natl Acad Sci U S A 2007; 104:14489-94; PMID:17726112; http://dx.doi.org/10.1073/pnas.0701311104
311. Wang QJ, Ding Y, Kohtz DS, Mizushima N, Cristea IM, Rout MP, et al. Induction of autophagy in axonal dystrophy and degeneration. J Neurosci 2006; 26:8057-68; PMID:16885219; http://dx.doi.org/10.1523/JNEUROSCI.2261-06.2006
312. Nezis IP, Simonsen A, Sagona AP, Finley K, Gaumer S, Contamine D, et al. Ref(2)P, the *Drosophila melanogaster* homologue of mammalian p62, is required for the formation of protein aggregates in adult brain. J Cell Biol 2008; 180:1065-71; PMID: 18347073; http://dx.doi.org/10.1083/jcb.200711108
313. Bartlett BJ, Isakson P, Lewerenz J, Sanchez H, Kotzebue RW, Cumming RC, et al. p62, Ref(2)P and ubiquitinated proteins are conserved markers of neuronal aging, aggregate formation and progressive autophagic defects. Autophagy 2011; 7:572-83; PMID:21325881; http://dx.doi.org/10.4161/auto.7.6.14943
314. Lee JH, Yu WH, Kumar A, Lee S, Mohan PS, Peterhoff CM, et al. Lysosomal proteolysis and autophagy require presenilin 1 and are disrupted by Alzheimer-related PS1 mutations. Cell 2010; 141:1146-58; PMID:20541250; http://dx.doi.org/10.1016/j.cell.2010.05.008
315. Masiero E, Agatea L, Mammucari C, Blaauw B, Loro E, Komatsu M, et al. Autophagy is required to maintain muscle mass. Cell Metab 2009; 10:507-15; PMID:19945408; http://dx.doi.org/10.1016/j.cmet.2009.10.008
316. Moscat J, Diaz-Meco MT. p62 at the crossroads of autophagy, apoptosis, and cancer. Cell 2009; 137:1001-4; PMID:19524504; http://dx.doi.org/10.1016/j.cell.2009.05.023
317. Duran A, Amanchy R, Linares JF, Joshi J, Abu-Baker S, Porollo A, et al. p62 is a key regulator of nutrient sensing in the mTORC1 pathway. Mol Cell 2011; 44:134-46; PMID:21981924; http://dx.doi.org/10.1016/j.molcel.2011.06.038
318. Komatsu M, Kurokawa H, Waguri S, Taguchi K, Kobayashi A, Ichimura Y, et al. The selective autophagy substrate p62 activates the stress responsive transcription factor Nrf2 through inactivation of Keap1. Nat Cell Biol 2010; 12:213-23; PMID:20173742
319. Jain A, Lamark T, Sjøttem E, Larsen KB, Awuh JA, Øvervatn A, et al. p62/SQSTM1 is a target gene for transcription factor NRF2 and creates a positive feed-back loop by inducing antioxidant response element-driven gene transcription. J Biol Chem 2010; 285:22576-91; PMID:20452972; http://dx.doi.org/10.1074/jbc.M110.118976
320. Bardag-Gorce F, Francis T, Nan L, Li J, He Lue Y, French BA, et al. Modifications in P62 occur due to proteasome inhibition in alcoholic liver disease. Life Sci 2005; 77:2594-602; PMID:15964033; http://dx.doi.org/10.1016/j.lfs.2005.04.020
321. Myeku N, Figueiredo-Pereira ME. Dynamics of the degradation of ubiquitinated proteins by proteasomes and autophagy: association with sequestosome 1/p62. J Biol Chem 2011; 286:22426-40; PMID:21536669; http://dx.doi.org/10.1074/jbc.M110.149252
322. Norman JM, Cohen GM, Bampton ET. The in vitro cleavage of the hAtg proteins by cell death proteases. Autophagy 2010; 6:1042-56; PMID:21121091; http://dx.doi.org/10.4161/auto.6.8.13337
323. Lelouard H, Schmidt EK, Camosseto V, Clavarino G, Ceppi M, Hsu HT, et al. Regulation of translation is required for dendritic cell function and survival during activation. J Cell Biol 2007; 179:1427-39; PMID: 18166652; http://dx.doi.org/10.1083/jcb.200707166
324. Schmidt EK, Clavarino G, Ceppi M, Pierre P. SUnSET, a nonradioactive method to monitor protein synthesis. Nat Methods 2009; 6:275-7; PMID: 19305406; http://dx.doi.org/10.1038/nmeth.1314
325. Nakaso K, Yoshimoto Y, Nakano T, Takeshima T, Fukuhara Y, Yasui K, et al. Transcriptional activation of p62/A170/ZIP during the formation of the aggregates: possible mechanisms and the role in Lewy body formation in Parkinson's disease. Brain Res 2004; 1012:42-51; PMID:15158159; http://dx.doi.org/10.1016/j.brainres.2004.03.029
326. Zheng Q, Su H, Ranek MJ, Wang X. Autophagy and p62 in cardiac proteinopathy. Circ Res 2011; 109:296-308; PMID:21659648; http://dx.doi.org/10.1161/CIRCRESAHA.111.244707
327. Colosetti P, Puissant A, Robert G, Luciano F, Jacquel A, Gounon P, et al. Autophagy is an important event for megakaryocytic differentiation of the chronic myelogenous leukemia K562 cell line. Autophagy 2009; 5:1092-8; PMID:19786835; http://dx.doi.org/10.4161/auto.5.8.9889
328. Toepfer N, Childress C, Parikh A, Rukstalis D, Yang W. Atorvastatin induces autophagy in prostate cancer PC3 cells through activation of LC3 transcription. Cancer Biol Ther 2011; 12:691-9; PMID:21768780; http://dx.doi.org/10.4161/cbt.12.8.15978
329. BenYounès A, Tajeddine N, Tailler M, Malik SA, Shen S, Métivier D, et al. A fluorescence-microscopic and cytofluorometric system for monitoring the turnover of the autophagic substrate p62/SQSTM1. Autophagy 2011; 7:883-91; PMID:21460612; http://dx.doi.org/10.4161/auto.7.8.15538
330. Bjørkøy G, Lamark T, Pankiv S, Øvervatn A, Brech A, Johansen T. Monitoring autophagic degradation of p62/SQSTM1. Methods Enzymol 2009; 452:181-97; PMID:19200883; http://dx.doi.org/10.1016/S0076-6879(08)03612-4
331. Lim J, Kim HW, Youdim MB, Rhyu IJ, Choe KM, Oh YJ. Binding preference of p62 towards LC3-II during dopaminergic neurotoxin-induced impairment of autophagic flux. Autophagy 2011; 7:51-60; PMID: 21045561; http://dx.doi.org/10.4161/auto.7.1.13909
332. Waguri S, Komatsu M. Biochemical and morphological detection of inclusion bodies in autophagy-deficient mice. Methods Enzymol 2009; 453:181-96; PMID:19216907; http://dx.doi.org/10.1016/S0076-6879(08)04009-3
333. Hocking LJ, Lucas GJ, Daroszewska A, Mangion J, Olavesen M, Cundy T, et al. Domain-specific mutations in sequestosome 1 (SQSTM1) cause familial and sporadic Paget's disease. Hum Mol Genet 2002; 11:2735-9; PMID:12374763; http://dx.doi.org/10.1093/hmg/11.22.2735
334. Mizushima N, Levine B. Autophagy in mammalian development and differentiation. Nat Cell Biol 2010; 12:823-30; PMID:20811354; http://dx.doi.org/10.1038/ncb0910-823
335. Maloverjan A, Piirsoo M, Michelson P, Kogerman P, Osterlund T. Identification of a novel serine/threonine kinase ULK3 as a positive regulator of Hedgehog pathway. Exp Cell Res 2010; 316:627-37; PMID: 19878745; http://dx.doi.org/10.1016/j.yexcr.2009.10.018
336. Young ARJ, Narita M, Ferreira M, Kirschner K, Sadaie M, Darot JF, et al. Autophagy mediates the mitotic senescence transition. Genes Dev 2009; 23:798-803; PMID:19279323; http://dx.doi.org/10.1101/gad.519709
337. Chan EY, Tooze SA. Evolution of Atg1 function and regulation. Autophagy 2009; 5:758-65; PMID:19411825
338. Chan EY, Kir S, Tooze SA. siRNA screening of the kinome identifies ULK1 as a multidomain modulator of autophagy. J Biol Chem 2007; 282:25464-74; PMID:17595159; http://dx.doi.org/10.1074/jbc.M703663200
339. Hardie DG, AMP-activated protein kinase: an energy sensor that regulates all aspects of cell function. Genes Dev 2011; 25:1895-908; PMID:21937710; http://dx.doi.org/10.1101/gad.17420111
340. Carling D, Mayer FV, Sanders MJ, Gamblin SJ. AMP-activated protein kinase: nature's energy sensor. Nat Chem Biol 2011; 7:512-8; PMID:21769098; http://dx.doi.org/10.1038/nchembio.610
341. Samari HR, Møller MT, Holden L, Asmyhr T, Seglen PO. Stimulation of hepatocytic AMP-activated protein kinase by okadaic acid and other autophagy-suppressive toxins. Biochem J 2005; 386:237-44; PMID: 15461583; http://dx.doi.org/10.1042/BJ20040609
342. Behrends C, Sowa ME, Gygi SP, Harper JW. Network organization of the human autophagy system. Nature 2010; 466:68-76; PMID:20562859; http://dx.doi.org/10.1038/nature09204
343. Chiacchiera F, Matrone A, Ferrari E, Ingravallo G, Lo Sasso G, Murzilli S, et al. p38alpha blockade inhibits colorectal cancer growth in vivo by inducing a switch from HIF1alpha- to FoxO-dependent transcription. Cell Death Differ 2009; 16:1203-14; PMID: 19343039; http://dx.doi.org/10.1038/cdd.2009.36
344. Kovács AL, Seglen PO. Inhibition of hepatocytic protein degradation by methylaminopurines and inhibitors of protein synthesis. Biochim Biophys Acta 1981; 676:213-20; PMID:7260116; http://dx.doi.org/10.1016/0304-4165(81)90189-6
345. Liu HY, Han J, Cao SY, Hong T, Zhuo D, Shi J, et al. Hepatic autophagy is suppressed in the presence of insulin resistance and hyperinsulinemia: inhibition of FoxO1-dependent expression of key autophagy genes by insulin. J Biol Chem 2009; 284:31484-92; PMID: 19758991; http://dx.doi.org/10.1074/jbc.M109.033936
346. Mammucari C, Milan G, Romanello V, Masiero E, Rudolf R, Del Piccolo P, et al. FoxO3 controls autophagy in skeletal muscle in vivo. Cell Metab 2007; 6:458-71; PMID:18054315; http://dx.doi.org/10.1016/j.cmet.2007.11.001
347. Mihaylova MM, Vasquez DS, Ravnskjaer K, Denechaud PD, Yu RT, Alvarez JG, et al. Class IIa histone deacetylases are hormone-activated regulators of FOXO and mammalian glucose homeostasis. Cell 2011; 145:607-21; PMID:21565617; http://dx.doi.org/10.1016/j.cell.2011.03.043
348. Pfisterer SG, Mauthe M, Codogno P, Proikas-Cezanne T. Ca2+/calmodulin-dependent kinase (CaMK) signaling via CaMKI and AMP-activated protein kinase contributes to the regulation of WIPI-1 at the onset of autophagy. Mol Pharmacol 2011; 80:1066-75; PMID: 21896713; http://dx.doi.org/10.1124/mol.111.071761
349. Rodgers JT, Lerin C, Gerhart-Hines Z, Puigserver P. Metabolic adaptations through the PGC-1 alpha and SIRT1 pathways. FEBS Lett 2008; 582:46-53; PMID: 18036349; http://dx.doi.org/10.1016/j.febslet.2007.11.034
350. Samari HR, Seglen PO. Inhibition of hepatocytic autophagy by adenosine, aminoimidazole-4-carboxamide riboside, and N6-mercaptopurine riboside. Evidence for involvement of amp-activated protein kinase. J Biol Chem 1998; 273:23758-63; PMID: 9726984; http://dx.doi.org/10.1074/jbc.273.37.23758
351. Sanchez AM, Csibi A, Raibon A, Cornille K, Gay S, Bernardi H, et al. AMPK promotes skeletal muscle autophagy through activation of Forkhead FoxO3a and interaction with Ulk1. J Cell Biochem 2012; PMID: 22006269; http://dx.doi.org/10.1002/jcb.23399
352. Inoki K, Zhu T, Guan KL. TSC2 mediates cellular energy response to control cell growth and survival. Cell 2003; 115:577-90; PMID:14651849; http://dx.doi.org/10.1016/S0092-8674(03)00929-2
353. Gwinn DM, Shackelford DB, Egan DF, Mihaylova MM, Mery A, Vasquez DS, et al. AMPK phosphorylation of raptor mediates a metabolic checkpoint. Mol Cell 2008; 30:214-26; PMID:18439900; http://dx.doi.org/10.1016/j.molcel.2008.03.003
354. Egan D, Kim J, Shaw RJ, Guan K-L. The autophagy-initiating kinase ULK1 is regulated via opposing phosphorylation by AMPK and mTOR. Autophagy 2011; 7:643-4; PMID:21460621; http://dx.doi.org/10.4161/auto.7.6.15123
355. Egan DF, Shackelford DB, Mihaylova MM, Gelino S, Kohnz RA, Mair W, et al. Phosphorylation of ULK1 (hATG1) by AMP-activated protein kinase connects energy sensing to mitophagy. Science 2011; 331:456-61; PMID:21205641; http://dx.doi.org/10.1126/science.1196371
356. Kim J, Kundu M, Viollet B, Guan K-L. AMPK and mTOR regulate autophagy through direct phosphorylation of Ulk1. Nat Cell Biol 2011; 13:132-41; PMID: 21258367; http://dx.doi.org/10.1038/ncb2152
357. Zhou G, Myers R, Li Y, Chen Y, Shen X, Fenyk-Melody J, et al. Role of AMP-activated protein kinase in mechanism of metformin action. J Clin Invest 2001; 108:1167-74; PMID:11602624
358. Emerling BM, Viollet B, Tormos KV, Chandel NS. Compound C inhibits hypoxic activation of HIF-1 independent of AMPK. FEBS Lett 2007; 581:5727-31; PMID:18036344; http://dx.doi.org/10.1016/j.febslet.2007.11.038
359. Vucicevic L, Misirkic M, Janjetovic K, Vilimanovich U, Sudar E, Isenovic E, et al. Compound C induces protective autophagy in cancer cells through AMPK inhibition-independent blockade of Akt/mTOR pathway. Autophagy 2011; 7:40-50; PMID:20980833; http://dx.doi.org/10.4161/auto.7.1.13883
360. Meley D, Bauvy C, Houben-Weerts JH, Dubbelhuis PF, Helmond MT, Codogno P, et al. AMP-activated protein kinase and the regulation of autophagic proteolysis. J Biol Chem 2006; 281:34870-9; PMID: 16990266; http://dx.doi.org/10.1074/jbc.M605488200

dc_840_14
©Landes Bioscience. Do not distribute.

361. Groteneier A, Alers S, Pfisterer SG, Paasch F, Daubrawa M, Dieterle A, et al. AMPK-independent induction of autophagy by cytosolic Ca^{2+} increase. Cell Signal 2010; 22:914-25; PMID:20114074; http://dx.doi.org/10.1016/j.cellsig.2010.01.015
362. Williams T, Forsberg LJ, Viollet B, Brenman JE. Basal autophagy induction without AMP-activated protein kinase under low glucose conditions. Autophagy 2009; 5:1155-65; PMID:19844161; http://dx.doi.org/10.4161/auto.5.8.10090
363. Shang L, Chen S, Du F, Li S, Zhao L, Wang X. Nutrient starvation elicits an acute autophagic response mediated by Ulk1 dephosphorylation and its subsequent dissociation from AMPK. Proc Natl Acad Sci U S A 2011; 108:4788-93; PMID:21383122; http://dx.doi.org/10.1073/pnas.1100844108
364. Zoncu R, Bar-Peled L, Efeyan A, Wang S, Sancak Y, Sabatini DM. mTORC1 senses lysosomal amino acids through an inside-out mechanism that requires the vacuolar H(+)-ATPase. Science 2011; 334:678-83; PMID:22053050; http://dx.doi.org/10.1126/science.1207056
365. Di Bartolomeo S, Corazzari M, Nazio F, Oliverio S, Lisi G, Antonioli M, et al. The dynamic interaction of AMBRA1 with the dynein motor complex regulates mammalian autophagy. J Cell Biol 2010; 191:155-68; PMID:20921139; http://dx.doi.org/10.1083/jcb.201002100
366. Tang HW, Wang YB, Wang SL, Wu MH, Lin SY, Chen GC. Atg1-mediated myosin II activation regulates autophagosome formation during starvation-induced autophagy. EMBO J 2011; 30:636-51; PMID:21169990; http://dx.doi.org/10.1038/emboj.2010.338
367. Jung CH, Jun CB, Ro S-H, Kim Y-M, Otto NM, Cao J, et al. ULK-Atg13-FIP200 complexes mediate mTOR signaling to the autophagy machinery. Mol Biol Cell 2009; 20:1992-2003; PMID:19225151; http://dx.doi.org/10.1091/mbc.E08-12-1249
368. Chang Y-Y, Neufeld TP. An Atg1/Atg13 complex with multiple roles in TOR-mediated autophagy regulation. Mol Biol Cell 2009; 20:2004-14; PMID:19225150; http://dx.doi.org/10.1091/mbc.E08-12-1250
369. Hosokawa N, Hara T, Kaizuka T, Kishi C, Takamura A, Miura Y, et al. Nutrient-dependent mTORC1 association with the ULK1-Atg13-FIP200 complex required for autophagy. Mol Biol Cell 2009; 20:1981-91; PMID:19211835; http://dx.doi.org/10.1091/mbc.E08-12-1248
370. Chan EYW, Longatti A, McKnight NC, Tooze SA. Kinase-inactivated ULK proteins inhibit autophagy via their conserved C-terminal domains using an Atg13-independent mechanism. Mol Cell Biol 2009; 29:157-71; PMID:18936157; http://dx.doi.org/10.1128/MCB.01082-08
371. Jung CH, Seo M, Otto NM, Kim DH. ULK1 inhibits the kinase activity of mTORC1 and cell proliferation. Autophagy 2011; 7:1212-21; PMID:21795849; http://dx.doi.org/10.4161/auto.7.10.16660
372. Löffler AS, Alers S, Dieterle AM, Keppeler H, Franz-Wachtel M, Kundu M, et al. Ulk1-mediated phosphorylation of AMPK constitutes a negative regulatory feedback loop. Autophagy 2011; 7:696-706; PMID:21460634; http://dx.doi.org/10.4161/auto.7.7.15451
373. Erlich S, Alexandrovich A, Shohami E, Pinkas-Kramarski R. Rapamycin is a neuroprotective treatment for traumatic brain injury. Neurobiol Dis 2007; 26:86-93; PMID:17270455; http://dx.doi.org/10.1016/j.nbd.2006.12.003
374. Lavieu G, Scarlatti F, Sala G, Carpentier S, Levade T, Ghidoni R, et al. Regulation of autophagy by sphingosine kinase 1 and its role in cell survival during nutrient starvation. J Biol Chem 2006; 281:8518-27; PMID:16415355; http://dx.doi.org/10.1074/jbc.M506182200
375. Brunn GJ, Hudson CC, Sekulić A, Williams JM, Hosoi H, Houghton PJ, et al. Phosphorylation of the translational repressor PHAS-I by the mammalian target of rapamycin. Science 1997; 277:99-101; PMID:9204908; http://dx.doi.org/10.1126/science.277.5322.99
376. Yip CK, Murata K, Walz T, Sabatini DM, Kang SA. Structure of the human mTOR complex I and its implications for rapamycin inhibition. Mol Cell 2010; 38:768-74; PMID:20542007; http://dx.doi.org/10.1016/j.molcel.2010.05.017
377. Cheong H, Nair U, Geng J, Klionsky DJ. The Atg1 kinase complex is involved in the regulation of protein recruitment to initiate sequestering vesicle formation for nonspecific autophagy in *Saccharomyces cerevisiae*. Mol Biol Cell 2008; 19:668-81; PMID:18077553; http://dx.doi.org/10.1091/mbc.E07-08-0826
378. Kabeya Y, Kamada Y, Baba M, Takikawa H, Sasaki M, Ohsumi Y. Atg17 functions in cooperation with Atg1 and Atg13 in yeast autophagy. Mol Biol Cell 2005; 16:2544-53; PMID:15743910; http://dx.doi.org/10.1091/mbc.E04-08-0669
379. Kamada Y, Funakoshi T, Shintani T, Nagano K, Ohsumi M, Ohsumi Y. Tor-mediated induction of autophagy via an Apg1 protein kinase complex. J Cell Biol 2000; 150:1507-13; PMID:10995454; http://dx.doi.org/10.1083/jcb.150.6.1507
380. Scott SV, Nice DC, 3rd, Nau JJ, Weisman LS, Kamada Y, Keizer-Gunnink I, et al. Apg13p and Vac8p are part of a complex of phosphoproteins that are required for cytoplasm to vacuole targeting. J Biol Chem 2000; 275:25840-9; PMID:10837477; http://dx.doi.org/10.1074/jbc.M002813200
381. Mao K, Wang K, Zhao M, Xu T, Klionsky DJ. Two MAPK-signaling pathways are required for mitophagy in *Saccharomyces cerevisiae*. J Cell Biol 2011; 193:755-67; PMID:21576396; http://dx.doi.org/10.1083/jcb.201102092
382. Yeh YY, Wrasman K, Herman PK. Autophosphorylation within the Atg1 activation loop is required for both kinase activity and the induction of autophagy in Saccharomyces cerevisiae. Genetics 2010; 185:871-82; PMID:20439775; http://dx.doi.org/10.1534/genetics.110.116566
383. Singh K, Matsuyama S, Drazba JA, Almasan A. Autophagy-dependent senescence in response to DNA damage and chronic apoptotic stress. Autophagy 2012; 8; In press; PMID:22240589
384. Djavaheri-Mergny M, Amelotti M, Mathieu J, Besançon F, Bauvy C, Souquère S, et al. NF-kappaB activation represses tumor necrosis factor-alpha-induced autophagy. J Biol Chem 2006; 281:30373-82; PMID:16857678; http://dx.doi.org/10.1074/jbc.M602097200
385. Liu Z, Lenardo MJ. Reactive oxygen species regulate autophagy through redox-sensitive proteases. Dev Cell 2007; 12:484-5; PMID:17419989; http://dx.doi.org/10.1016/j.devcel.2007.03.016
386. Scarlatti F, Bauvy C, Ventruti A, Sala G, Cluzeaud F, Vandewalle A, et al. Ceramide-mediated macroautophagy involves inhibition of protein kinase B and up-regulation of beclin 1. J Biol Chem 2004; 279:18384-91; PMID:14970205; http://dx.doi.org/10.1074/jbc.M313561200
387. Scherz-Shouval R, Shvets E, Fass E, Shorer H, Gil L, Elazar Z. Reactive oxygen species are essential for autophagy and specifically regulate the activity of Atg4. EMBO J 2007; 26:1749-60; PMID:17347651; http://dx.doi.org/10.1038/sj.emboj.7601623
388. Zeng X, Kinsella TJ. Mammalian target of rapamycin and S6 kinase 1 positively regulate 6-thioguanine-induced autophagy. Cancer Res 2008; 68:2384-90; PMID:18381446; http://dx.doi.org/10.1158/0008-5472.CAN-07-6163
389. Yu L, McPhee CK, Zheng L, Mardones GA, Rong Y, Peng J, et al. Termination of autophagy and reformation of lysosomes regulated by mTOR. Nature 2010; 465:942-6; PMID:20526321; http://dx.doi.org/10.1038/nature09076
390. Mochizuki H, Toda H, Ando M, Kurusu M, Tomoda T, Furukubo-Tokunaga K. Unc-51/ATG1 controls axonal and dendritic development via kinesin-mediated vesicle transport in the Drosophila brain. PLoS One 2011; 6:e19632; PMID:21589871; http://dx.doi.org/10.1371/journal.pone.0019632
391. Wairkar YP, Toda H, Mochizuki H, Furukubo-Tokunaga K, Tomoda T, Diantonio A. Unc-51 controls active zone density and protein composition by downregulating ERK signaling. J Neurosci 2009; 29:517-28; PMID:19144852; http://dx.doi.org/10.1523/JNEUROSCI.3848-08.2009
392. Loh SH, Francescut L, Lingor P, Bähr M, Nicotera P. Identification of new kinase clusters required for neurite outgrowth and retraction by a loss-of-function RNA interference screen. Cell Death Differ 2008; 15:283-98; PMID:18007665; http://dx.doi.org/10.1038/sj.cdd.4402258
393. Zhou X, Babu JR, da Silva S, Shu Q, Graef IA, Oliver T, et al. Unc-51-like kinase 1/2-mediated endocytic processes regulate filopodia extension and branching of sensory axons. Proc Natl Acad Sci U S A 2007; 104:5842-7; PMID:17389358; http://dx.doi.org/10.1073/pnas.0701402104
394. Tomoda T, Kim JH, Zhan C, Hatten ME. Role of Unc51.1 and its binding partners in CNS axon outgrowth. Genes Dev 2004; 18:541-58; PMID:15014045; http://dx.doi.org/10.1101/gad.1151204
395. Okazaki N, Yan J, Yuasa S, Ueno T, Kominami E, Masuho Y, et al. Interaction of the Unc-51-like kinase and microtubule-associated protein light chain 3 related proteins in the brain: possible role of vesicular transport in axonal elongation. Brain Res Mol Brain Res 2000; 85:1-12; PMID:11146101; http://dx.doi.org/10.1016/S0169-328X(00)00218-7
396. Young ARJ, Chan EYW, Hu XW, Köchl R, Crawshaw SG, High S, et al. Starvation and ULK1-dependent cycling of mammalian Atg9 between the TGN and endosomes. J Cell Sci 2006; 119:3888-900; PMID:16940348; http://dx.doi.org/10.1242/jcs.03172
397. Reggiori F, Shintani T, Nair U, Klionsky DJ. Atg9 cycles between mitochondria and the pre-autophagosomal structure in yeasts. Autophagy 2005; 1:101-9; PMID:16874040; http://dx.doi.org/10.4161/auto.1.2.1840
398. Mari M, Griffith J, Rieter E, Krishnappa L, Klionsky DJ, Reggiori F. An Atg9-containing compartment that functions in the early steps of autophagosome biogenesis. J Cell Biol 2010; 190:1005-22; PMID:20855505; http://dx.doi.org/10.1083/jcb.200912089
399. Reggiori F, Tucker KA, Stromhaug PE, Klionsky DJ. The Atg1-Atg13 complex regulates Atg9 and Atg23 retrieval transport from the pre-autophagosomal structure. Dev Cell 2004; 6:79-90; PMID:14723849; http://dx.doi.org/10.1016/S1534-5807(03)00402-7
400. Mizushima N, Kuma A, Kobayashi Y, Yamamoto A, Matsubae M, Takao T, et al. Mouse Apg16L, a novel WD-repeat protein, targets to the autophagic isolation membrane with the Apg12-Apg5 conjugate. J Cell Sci 2003; 116:1679-88; PMID:12665549; http://dx.doi.org/10.1242/jcs.00381
401. Mizushima N, Yamamoto A, Hatano M, Kobayashi Y, Kabeya Y, Suzuki K, et al. Dissection of autophagosome formation using Apg5-deficient mouse embryonic stem cells. J Cell Biol 2001; 152:657-68; PMID:11266458; http://dx.doi.org/10.1083/jcb.152.4.657
402. Thompson AR, Doelling JH, Suttangkakul A, Vierstra RD. Autophagic nutrient recycling in Arabidopsis directed by the ATG8 and ATG12 conjugation pathways. Plant Physiol 2005; 138:2097-110; PMID:16040659; http://dx.doi.org/10.1104/pp.105.060673
403. Yousefi S, Perozzo R, Schmid I, Ziemiecki A, Schaffner T, Scapozza L, et al. Calpain-mediated cleavage of Atg5 switches autophagy to apoptosis. Nat Cell Biol 2006; 8:1124-32; PMID:16998475; http://dx.doi.org/10.1038/ncb1482
404. Kihara A, Noda T, Ishihara N, Ohsumi Y. Two distinct Vps34 phosphatidylinositol 3-kinase complexes function in autophagy and carboxypeptidase Y sorting in *Saccharomyces cerevisiae*. J Cell Biol 2001; 152:519-30; PMID:11157979; http://dx.doi.org/10.1083/jcb.152.3.519
405. Matsunaga K, Saitoh T, Tabata K, Omori H, Satoh T, Kurotori N, et al. Two Beclin 1-binding proteins, Atg14L and Rubicon, reciprocally regulate autophagy at different stages. Nat Cell Biol 2009; 11:385-96; PMID:19270696; http://dx.doi.org/10.1038/ncb1846
406. Zhong Y, Wang QJ, Li X, Yan Y, Backer JM, Chait BT, et al. Distinct regulation of autophagic activity by Atg14L and Rubicon associated with Beclin 1-phosphatidylinositol-3-kinase complex. Nat Cell Biol 2009; 11:468-76; PMID:19270693; http://dx.doi.org/10.1038/ncb1854
407. Sun Q, Fan W, Chen K, Ding X, Chen S, Zhong Q. Identification of Barkor as a mammalian autophagy-specific factor for Beclin 1 and class III phosphatidylinositol 3-kinase. Proc Natl Acad Sci U S A 2008; 105:19211-6; PMID:19050071; http://dx.doi.org/10.1073/pnas.0810452105
408. Itakura E, Kishi C, Inoue K, Mizushima N. Beclin 1 forms two distinct phosphatidylinositol 3-kinase complexes with mammalian Atg14 and UVRAG. Mol Biol Cell 2008; 19:5360-72; PMID:18843052; http://dx.doi.org/10.1091/mbc.E08-01-0080
409. Fan W, Nassiri A, Zhong Q. Autophagosome targeting and membrane curvature sensing by Barkor/Atg14(L). Proc Natl Acad Sci U S A 2011; 108:7769-74; PMID:21518905; http://dx.doi.org/10.1073/pnas.1016472108
410. Matsunaga K, Morita E, Saitoh T, Akira S, Kristakis NT, Izumi T, et al. Autophagy requires endoplasmic reticulum targeting of the PI3-kinase complex via Atg14L. J Cell Biol 2010; 190:511-21; PMID:20713597; http://dx.doi.org/10.1083/jcb.200911141
411. Ravikumar B, Moreau K, Jahreiss L, Puri C, Rubinsztein DC. Plasma membrane contributes to the formation of pre-autophagosomal structures. Nat Cell Biol 2010; 12:747-57; PMID:20639872; http://dx.doi.org/10.1038/ncb2078
412. Guan J, Stromhaug PE, George MD, Habibzadegah-Tari P, Bevan A, Dunn WA, Jr., et al. Cvt18/Gsa12 is required for cytoplasm-to-vacuole transport, pexophagy, and autophagy in *Saccharomyces cerevisiae* and *Pichia pastoris*. Mol Biol Cell 2001; 12:3821-38; PMID:11739783
413. Barth H, Meiling-Wesse K, Epple UD, Thumm M. Autophagy and the cytoplasm to vacuole targeting pathway both require Aut10p. FEBS Lett 2001; 508:23-8; PMID:11707261; http://dx.doi.org/10.1016/S0014-5793(01)03016-2
414. Proikas-Cezanne T, Waddell S, Gaugel A, Frickey T, Lupas A, Nordheim A. WIPI-1alpha (WIPI49), a member of the novel 7-bladed WIPI protein family, is aberrantly expressed in human cancer and is linked to starvation-induced autophagy. Oncogene 2004; 23:9314-25; PMID:15602573; http://dx.doi.org/10.1038/sj.onc.1208331
415. Monastyrska I, Klionsky DJ. Autophagy in organelle homeostasis: peroxisome turnover. Mol Aspects Med 2006; 27:483-94; PMID:16973210; http://dx.doi.org/10.1016/j.mam.2006.08.004
416. Nair U, Klionsky DJ. Molecular mechanisms and regulation of specific and nonspecific autophagy pathways in yeast. J Biol Chem 2005; 280:41785-8; PMID:16230342; http://dx.doi.org/10.1074/jbc.R500016200
417. Tallóczy Z, Virgin HW, 4th, Levine B. PKR-dependent autophagic degradation of herpes simplex virus type 1. Autophagy 2006; 2:24-9; PMID:16874088
418. Polson HE, de Lartigue J, Rigden DJ, Reedijk M, Urbé S, Clague MJ, et al. Mammalian Atg18 (WIPI2) localizes to omegasome-anchored phagophores and positively regulates LC3 lipidation. Autophagy 2010; 6:506-22; PMID:20505359; http://dx.doi.org/10.4161/auto.6.4.11863
419. Proikas-Cezanne T, Ruckerbauer S, Stierhof YD, Berg C, Nordheim A. Human WIPI-1 puncta-formation: a novel assay to assess mammalian autophagy. FEBS Lett 2007; 581:3396-404; PMID:17618624; http://dx.doi.org/10.1016/j.febslet.2007.06.040
420. Itakura E, Mizushima N. Characterization of autophagosome formation site by a hierarchical analysis of mammalian Atg proteins. Autophagy 2010; 6:764-76; PMID:20639694; http://dx.doi.org/10.4161/auto.6.6.12709
421. Mauthe M, Jacob A, Freiberger S, Hentschel K, Stierhof YD, Codogno P, et al. Resveratrol-mediated autophagy requires WIPI-1-regulated LC3 lipidation in the absence of induced phagophore formation. Autophagy 2011; 7:1448-61; PMID:22082875; http://dx.doi.org/10.4161/auto.7.12.17802
422. Lu Q, Yang P, Huang X, Hu W, Guo B, Wu F, et al. The WD40 repeat PtdIns(3)P-binding protein EPG-6 regulates progression of omegasomes to autophagosomes. Dev Cell 2011; 21:343-57; PMID:21802374; http://dx.doi.org/10.1016/j.devcel.2011.06.024
423. Yang Z, Klionsky DJ. Mammalian autophagy: core molecular machinery and signaling regulation. Curr Opin Cell Biol 2010; 22:124-31; PMID:20034776; http://dx.doi.org/10.1016/j.ceb.2009.11.014
424. Cao Y, Klionsky DJ. Physiological functions of Atg6/Beclin 1: a unique autophagy-related protein. Cell Res 2007; 17:839-49; PMID:17893711; http://dx.doi.org/10.1038/cr.2007.78
425. Pattingre S, Tassa A, Qu X, Garuti R, Liang XH, Mizushima N, et al. Bcl-2 antiapoptotic proteins inhibit Beclin 1-dependent autophagy. Cell 2005; 122:927-39; PMID:16179260; http://dx.doi.org/10.1016/j.cell.2005.07.002
426. Zalckvar E, Berissi H, Mizrachy L, Idelchuk Y, Koren I, Eisenstein M, et al. DAP-kinase-mediated phosphorylation on the BH3 domain of beclin 1 promotes dissociation of beclin 1 from Bcl-XL and induction of autophagy. EMBO Rep 2009; 10:285-92; PMID:19180116; http://dx.doi.org/10.1038/embor.2008.246
427. Wei Y, Sinha S, Levine B. Dual role of JNK1-mediated phosphorylation of Bcl-2 in autophagy and apoptosis regulation. Autophagy 2008; 4:949-51; PMID:18769111
428. Wei Y, Pattingre S, Sinha S, Bassik M, Levine B. JNK1-mediated phosphorylation of Bcl-2 regulates starvation-induced autophagy. Mol Cell 2008; 30:678-88; PMID:18570871; http://dx.doi.org/10.1016/j.molcel.2008.06.001
429. Lossi L, Gambino G, Ferrini F, Alasia S, Merighi A. Posttranslational regulation of BCL2 levels in cerebellar granule cells: A mechanism of neuronal survival. Dev Neurobiol 2009; 69:855-70; PMID:19672954; http://dx.doi.org/10.1002/dneu.20744
430. Lossi L, Gambino G, Salio C, Merighi A. Autophagy regulates the post-translational cleavage of BCL-2 and promotes neuronal survival. ScientificWorldJournal 2010; 10:924-9; PMID:20495771; http://dx.doi.org/10.1100/tsw.2010.82
431. Scarlatti F, Maffei R, Beau I, Codogno P, Ghidoni R. Role of non-canonical Beclin 1-independent autophagy in cell death induced by resveratrol in human breast cancer cells. Cell Death Differ 2008; 15:1318-29; PMID:18421301; http://dx.doi.org/10.1038/cdd.2008.51
432. Kang R, Zeh HJ, Lotze MT, Tang D. The Beclin 1 network regulates autophagy and apoptosis. Cell Death Differ 2011; 18:571-80; PMID:21311563; http://dx.doi.org/10.1038/cdd.2010.191
433. Kihara A, Kabeya Y, Ohsumi Y, Yoshimori T. Beclin-phosphatidylinositol 3-kinase complex functions at the trans-Golgi network. EMBO Rep 2001; 2:330-5; PMID:11306555; http://dx.doi.org/10.1093/embo-reports/kve061
434. Amritraj A, Peake K, Kodam A, Salio C, Merighi A, Vance JE, et al. Increased activity and altered subcellular distribution of lysosomal enzymes determine neuronal vulnerability in Niemann-Pick type C1-deficient mice. Am J Pathol 2009; 175:2540-56; PMID:19893049; http://dx.doi.org/10.2353/ajpath.2009.081096
435. Castino R, Bellio N, Follo C, Murphy D, Isidoro C. Inhibition of PI3k class III-dependent autophagy prevents apoptosis and necrosis by oxidative stress in dopaminergic neuroblastoma cells. Toxicol Sci 2010; 117:152-62; PMID:20525898; http://dx.doi.org/10.1093/toxsci/kfq170
436. Yue Z, Horton A, Bravin M, DeJager PL, Selimi F, Heintz N. A novel protein complex linking the delta 2 glutamate receptor and autophagy: implications for neurodegeneration in lurcher mice. Neuron 2002; 35:921-33; PMID:12372286; http://dx.doi.org/10.1016/S0896-6273(02)00861-9
437. Axe EL, Walker SA, Manifava M, Chandra P, Roderick HL, Habermann A, et al. Autophagosome formation from membrane compartments enriched in phosphatidylinositol 3-phosphate and dynamically connected to the endoplasmic reticulum. J Cell Biol 2008; 182:685-701; PMID:18725538; http://dx.doi.org/10.1083/jcb.200803137
438. Crighton D, Wilkinson S, O'Prey J, Syed N, Smith P, Harrison PR, et al. DRAM, a p53-induced modulator of autophagy, is critical for apoptosis. Cell 2006; 126:121-34; PMID:16839881; http://dx.doi.org/10.1016/j.cell.2006.05.034
439. Valbuena A, Castro-Obregón S, Lazo PA. Down-regulation of VRK1 by p53 in response to DNA damage is mediated by the autophagic pathway. PLoS One 2011; 6:e17320; PMID:21386980; http://dx.doi.org/10.1371/journal.pone.0017320
440. Lorin S, Pierron G, Ryan KM, Codogno P, Djavaheri-Mergny M. Evidence for the interplay between JNK and p53-DRAM signalling pathways in the regulation of autophagy. Autophagy 2010; 6:153-4; PMID:19949306; http://dx.doi.org/10.4161/auto.6.1.10537
441. Nara A, Mizushima N, Yamamoto A, Kabeya Y, Ohsumi Y, Yoshimori T. SKD1 AAA ATPase-dependent endosomal transport is involved in autolysosome formation. Cell Struct Funct 2002; 27:29-37; PMID:11937716; http://dx.doi.org/10.1247/csf.27.29
442. Kirisako T, Baba M, Ishihara N, Miyazawa K, Ohsumi M, Yoshimori T, et al. Formation process of autophagosome is traced with Apg8/Aut7p in yeast. J Cell Biol 1999; 147:435-46; PMID:10525546; http://dx.doi.org/10.1083/jcb.147.2.435
443. Kouroku Y, Fujita E, Tanida I, Ueno T, Isoai A, Kumagai H, et al. ER stress (PERK/eIF2alpha phosphorylation) mediates the polyglutamine-induced LC3 conversion, an essential step for autophagy formation. Cell Death Differ 2007; 14:230-9; PMID:16794605; http://dx.doi.org/10.1038/sj.cdd.4401984

dc 840.14

© Landes Bioscience. Do not distribute.

444. Moussay E, Kaoma T, Baginska J, Muller A, Van Moer K, Nicot N, et al. The acquisition of resistance to TNFα in breast cancer cells is associated with constitutive activation of autophagy as revealed by a transcriptome analysis using a custom microarray. Autophagy 2011; 7:760-70; PMID:21490427; http://dx.doi.org/10.4161/auto.7.7.15454
445. Mitroulis I, Kourtzelis I, Kambas K, Rafail S, Chrysanthopoulou A, Speletas M, et al. Regulation of the autophagic machinery in human neutrophils. Eur J Immunol 2010; 40:1461-72; PMID:20162553; http://dx.doi.org/10.1002/eji.200940025
446. Rodríguez-Muela N, Germain F, Mariño G, Fitze PS, Boya P. Autophagy promotes survival of retinal ganglion cells after optic nerve axotomy in mice. Cell Death Differ 2012; 19:162-9; PMID:21701497; http://dx.doi.org/10.1038/cdd.2011.88
447. Vázquez P, Arroba AI, Cecconi F, de la Rosa EJ, Boya P, De Pablo F. Atg5 and Ambra1 differentially modulate neurogenesis in neural stem cells. Autophagy 2012; 8; In press; PMID:22240590
448. Rouschop KM, van den Beucken T, Dubois L, Niessen H, Bussink J, Savelkouls K, et al. The unfolded protein response protects human tumor cells during hypoxia through regulation of the autophagy genes MAP1LC3B and ATG5. J Clin Invest 2010; 120:127-41; PMID:20038797; http://dx.doi.org/10.1172/JCI40027
449. Gorski SM, Chittaranjan S, Pleasance ED, Freeman JD, Anderson CL, Varhol RJ, et al. A SAGE approach to discovery of genes involved in autophagic cell death. Curr Biol 2003; 13:358-63; PMID:12593804; http://dx.doi.org/10.1016/S0960-9822(03)00082-4
450. Lee C-Y, Clough EA, Yellon P, Teslovich TM, Stephan DA, Baehrecke EH. Genome-wide analyses of steroid- and radiation-triggered programmed cell death in *Drosophila*. Curr Biol 2003; 13:350-7; PMID:12593803; http://dx.doi.org/10.1016/S0960-9822(03)00085-X
451. Denton D, Shravage B, Simin R, Baehrecke EH, Kumar S. Larval midgut destruction in Drosophila: not dependent on caspases but suppressed by the loss of autophagy. Autophagy 2010; 6:163-5; PMID:20009534; http://dx.doi.org/10.4161/auto.6.1.10601
452. Franzetti E, Huang ZJ, Shi YX, Xie K, Deng XJ, Li JP, et al. Erratum to: Autophagy precedes apoptosis during the remodeling of silkworm larval midgut. Apoptosis 2012; In press; PMID:22223360; http://dx.doi.org/10.1007/s10495-011-0693-y
453. Juhász G, Puskás LG, Komonyi O, Erdi B, Maróy P, Neufeld TP, et al. Gene expression profiling identifies FKBP39 as an inhibitor of autophagy in larval Drosophila fat body. Cell Death Differ 2007; 14:1181-90; PMID:17363962; http://dx.doi.org/10.1038/sj.cdd.4402123
454. Barth JM, Szabad J, Hafen E, Köhler K. Autophagy in Drosophila ovaries is induced by starvation and is required for oogenesis. Cell Death Differ 2011; 18:915-24; PMID:21151027; http://dx.doi.org/10.1038/cdd.2010.157
455. Lecker SH, Jagoe RT, Gilbert A, Gomes M, Baracos V, Bailey J, et al. Multiple types of skeletal muscle atrophy involve a common program of changes in gene expression. FASEB J 2004; 18:39-51; PMID:14718385; http://dx.doi.org/10.1096/fj.03-0610com
456. Phillips AR, Suttangkakul A, Vierstra RD. The ATG12-conjugating enzyme ATG10 Is essential for autophagic vesicle formation in Arabidopsis thaliana. Genetics 2008; 178:1339-53; PMID:18245858; http://dx.doi.org/10.1534/genetics.107.086199
457. Selliez I, Gutierrez J, Salmerón C, Skiba-Cassy S, Chauvin C, Dias K, et al. An in vivo and in vitro assessment of autophagy-related gene expression in muscle of rainbow trout (Oncorhynchus mykiss). Comp Biochem Physiol B Biochem Mol Biol 2010; 157:258-66; PMID:20601058; http://dx.doi.org/10.1016/j.cbpb.2010.06.011
458. Lapierre LR, Gelino S, Meléndez A, Hansen M. Autophagy and lipid metabolism coordinately modulate life span in germline-less *C. elegans*. Curr Biol 2011; 21:1507-14; PMID:21906946; http://dx.doi.org/10.1016/j.cub.2011.07.042
459. Sandri M. Autophagy in health and disease. 3. Involvement of autophagy in muscle atrophy. Am J Physiol Cell Physiol 2010; 298:C1291-7; PMID:20089936; http://dx.doi.org/10.1152/ajpcell.00531.2009
460. Eisenberg T, Knauer H, Schauer A, Büttner S, Ruckenstuhl C, Carmona-Gutierrez D, et al. Induction of autophagy by spermidine promotes longevity. Nat Cell Biol 2009; 11:1305-14; PMID:19801973; http://dx.doi.org/10.1038/ncb1975
461. Ropolo A, Grasso D, Pardo R, Sacchetti ML, Archange C, Lo Re A, et al. The pancreatitis-induced vacuole membrane protein 1 triggers autophagy in mammalian cells. J Biol Chem 2007; 282:37124-33; PMID:17940279; http://dx.doi.org/10.1074/jbc.M706956200
462. Tian Y, Li Z, Hu W, Ren H, Tian E, Zhao Y, et al. *C. elegans* screen identifies autophagy genes specific to multicellular organisms. Cell 2010; 141:1042-55; PMID:20550938; http://dx.doi.org/10.1016/j.cell.2010.04.034
463. Settembre C, Di Malta C, Polito VA, Garcia Arencibia M, Vetrini F, Erdin S, et al. TFEB links autophagy to lysosomal biogenesis. Science 2011; 332:1429-33; PMID:21617040; http://dx.doi.org/10.1126/science.1204592
464. Sardiello M, Palmieri M, di Ronza A, Medina DL, Valenza M, Gennarino VA, et al. A gene network regulating lysosomal biogenesis and function. Science 2009; 325:473-7; PMID:19556463
465. Palmieri M, Impey S, Kang H, di Ronza A, Pelz C, Sardiello M, et al. Characterization of the CLEAR network reveals an integrated control of cellular clearance pathways. Hum Mol Genet 2011; 20:3852-66; PMID:21752829; http://dx.doi.org/10.1093/hmg/ddr306
466. Kang YA, Sanalkumar R, O'Geen H, Linnemann AK, Chang CJ, Bouhassira EE, et al. Autophagy driven by a master regulator of hematopoiesis. Mol Cell Biol 2012; 32:226-39; PMID:22025678; http://dx.doi.org/10.1128/MCB.06166-11
467. Ma D, Panda S, Lin JD. Temporal orchestration of circadian autophagy rhythm by C/EBPβ. EMBO J 2011; 30:4642-51; PMID:21897364; http://dx.doi.org/10.1038/emboj.2011.322
468. Brest P, Lapaquette P, Souidi M, Lebrigand K, Cesaro A, Vouret-Craviari V, et al. A synonymous variant in IRGM alters a binding site for miR-196 and causes deregulation of IRGM-dependent xenophagy in Crohn's disease. Nat Genet 2011; 43:242-5; PMID:21278745; http://dx.doi.org/10.1038/ng.762
469. Meenhuis A, van Veelen PA, de Looper H, van Boxtel N, van den Berge IJ, Sun SM, et al. MiR-17/20/93/106 promote hematopoietic cell expansion by targeting sequestosome 1-regulated pathways in mice. Blood 2011; 118:916-25; PMID:21628417; http://dx.doi.org/10.1182/blood-2011-02-336487
470. Roccaro AM, Sacco A, Jia X, Azab AK, Maiso P, Ngo HT, et al. microRNA-dependent modulation of histone acetylation in Waldenstrom macroglobulinemia. Blood 2010; 116:1506-14; PMID:20519629; http://dx.doi.org/10.1182/blood-2010-01-265686
471. Martinet W, De Meyer GR, Andries L, Herman AG, Kockx MM. In situ detection of starvation-induced autophagy. J Histochem Cytochem 2006; 54:85-96; PMID:16148314; http://dx.doi.org/10.1369/jhc.5A6743.2005
472. Pattingre S, Petiot A, Codogno P. Analyses of Galpha-interacting protein and activator of G-protein-signaling-3 functions in macroautophagy. Methods Enzymol 2004; 390:17-31; PMID:15488168; http://dx.doi.org/10.1016/S0076-6879(04)90002-X
473. Bauvy C, Meijer AJ, Codogno P. Assaying of autophagic protein degradation. Methods Enzymol 2009; 452:47-61; PMID:19200875; http://dx.doi.org/10.1016/S0076-6879(08)03604-5
474. Ichimura Y, Kumanomidou T, Sou YS, Mizushima T, Ezaki J, Ueno T, et al. Structural basis for sorting mechanism of p62 in selective autophagy. J Biol Chem 2008; 283:22847-57; PMID:18524774; http://dx.doi.org/10.1074/jbc.M802182200
475. Kabuta T, Furuta A, Aoki S, Furuta K, Wada K. Aberrant interaction between Parkinson disease-associated mutant UCH-L1 and the lysosomal receptor for chaperone-mediated autophagy. J Biol Chem 2008; 283:23731-8; PMID:18550537; http://dx.doi.org/10.1074/jbc.M801918200
476. Ding WX, Ni HM, Gao W, Yoshimori T, Stolz DB, Ron D, et al. Linking of autophagy to ubiquitin-proteasome system is important for the regulation of endoplasmic reticulum stress and cell viability. Am J Pathol 2007; 171:513-24; PMID:17620365; http://dx.doi.org/10.2353/ajpath.2007.070188
477. Iwata A, Riley BE, Johnston JA, Kopito RR. HDAC6 and microtubules are required for autophagic degradation of aggregated huntingtin. J Biol Chem 2005; 280:40282-92; PMID:16192271; http://dx.doi.org/10.1074/jbc.M508786200
478. Pandey UB, Nie Z, Batlevi Y, McCray BA, Ritson GP, Nedelsky NB, et al. HDAC6 rescues neurodegeneration and provides an essential link between autophagy and the UPS. Nature 2007; 447:859-63; PMID:17568747; http://dx.doi.org/10.1038/nature05853
479. Tomek K, Wagner R, Varga F, Singer CF, Karlic H, Grunt TW. Blockade of fatty acid synthase induces ubiquitination and degradation of phosphoinositide-3-kinase signaling proteins in ovarian cancer. Mol Cancer Res 2011; 9:1767-79; PMID:21970855; http://dx.doi.org/10.1158/1541-7786.MCR-10-0467
480. Zimmermann AC, Zarei M, Eiselein S, Dengjel J. Quantitative proteomics for the analysis of spatio-temporal protein dynamics during autophagy. Autophagy 2010; 6:1009-16; PMID:20603599; http://dx.doi.org/10.4161/auto.6.8.12786
481. Kristensen AR, Schandorff S, Høyer-Hansen M, Nielsen MO, Jäättelä M, Dengjel J, et al. Ordered organelle degradation during starvation-induced autophagy. Mol Cell Proteomics 2008; 7:2419-28; PMID:18687634; http://dx.doi.org/10.1074/mcp.M800184-MCP200
482. Furuya N, Kanazawa T, Fujimura S, Ueno T, Kominami E, Kadowaki M. Leupeptin-induced appearance of partial fragment of betaine homocysteine methyltransferase during autophagic maturation in rat hepatocytes. J Biochem 2001; 129:313-20; PMID:11173534; http://dx.doi.org/10.1093/oxfordjournals.jbchem.a002859
483. Ueno T, Ishidoh K, Mineki R, Tanida I, Murayama K, Kadowaki M, et al. Autolysosomal membrane-associated betaine homocysteine methyltransferase. Limited degradation fragment of a sequestered cytosolic enzyme monitoring autophagy. J Biol Chem 1999; 274:15222-9; PMID:10329731; http://dx.doi.org/10.1074/jbc.274.21.15222
484. Øverbye A, Sætre F, Hagen LK, Johansen HT, Seglen PO. Autophagic activity measured in whole rat hepatocytes as the accumulation of a novel BHMT fragment (p10), generated in amphisomes by the asparaginyl proteinase, legumain. Autophagy 2011; 7:1011-27; PMID:21610319; http://dx.doi.org/10.4161/auto.7.9.16436
485. Seglen PO, Øverbye A, Sætre F. Sequestration assays for mammalian autophagy. Methods Enzymol 2009; 452:63-83; PMID:19200876; http://dx.doi.org/10.1016/S0076-6879(08)03605-7
486. Mercer CA, Kaliappan A, Dennis PB. Macroautophagy-dependent, intralysosomal cleavage of a betaine homocysteine methyltransferase fusion protein requires stable multimerization. Autophagy 2008; 4:185-94; PMID:18059170
487. Nimmerjahn F, Milosevic S, Behrends U, Jaffee EM, Pardoll DM, Bornkamm GW, et al. Major histocompatibility complex class II-restricted presentation of a cytosolic antigen by autophagy. Eur J Immunol 2003; 33:1250-9; PMID:12731050; http://dx.doi.org/10.1002/eji.200323730
488. Taylor GS, Long HM, Haigh TA, Larsen M, Brooks J, Rickinson AB. A role for intercellular antigen transfer in the recognition of EBV-transformed B cell lines by EBV nuclear antigen-specific CD4+ T cells. J Immunol 2006; 177:3746-56; PMID:16951335
489. Klionsky DJ, Emr SD. Membrane protein sorting: biosynthesis, transport and processing of yeast vacuolar alkaline phosphatase. EMBO J 1989; 8:2241-50; PMID:2676517
490. Venerando R, Miotto G, Kadowaki M, Siliprandi N, Mortimore GE. Multiphasic control of proteolysis by leucine and alanine in the isolated rat hepatocyte. Am J Physiol 1994; 266:C455-61; PMID:8141260
491. Häussinger D, Hallbrucker C, vom Dahl S, Lang F, Gerok W. Cell swelling inhibits proteolysis in perfused rat liver. Biochem J 1990; 272:239-42; PMID:2264828
492. vom Dahl S, Häussinger D. Cell hydration and proteolysis control in liver. Biochem J 1995; 312:988-9; PMID:8554549
493. Cuervo AM, Stefanis L, Fredenburg R, Lansbury PT, Sulzer D. Impaired degradation of mutant alpha-synuclein by chaperone-mediated autophagy. Science 2004; 305:1292-5; PMID:15333840; http://dx.doi.org/10.1126/science.1101738
494. Reggiori F, Monastyrska I, Shintani T, Klionsky DJ. The actin cytoskeleton is required for selective types of autophagy, but not nonspecific autophagy, in the yeast Saccharomyces cerevisiae. Mol Biol Cell 2005; 16:5843-56; PMID:16221887; http://dx.doi.org/10.1091/mbc.E05-07-0629
495. Manjithaya R, Jain S, Farré JC, Subramani S. A yeast MAPK cascade regulates pexophagy but not other autophagy pathways. J Cell Biol 2010; 189:303-10; PMID:20385774; http://dx.doi.org/10.1083/jcb.200909154
496. Journo D, Mor A, Abeliovich H. Aup1-mediated regulation of Rtg3 during mitophagy. J Biol Chem 2009; 284:35885-95; PMID:19840933; http://dx.doi.org/10.1074/jbc.M109.048140
497. Kanki T, Klionsky DJ. Mitophagy in yeast occurs through a selective mechanism. J Biol Chem 2008; 283:32386-93; PMID:18818209; http://dx.doi.org/10.1074/jbc.M802403200
498. Kanki T, Wang K, Baba M, Bartholomew CR, Lynch-Day MA, Du Z, et al. A genomic screen for yeast mutants defective in selective mitochondria autophagy. Mol Biol Cell 2009; 20:4730-8; PMID:19793921; http://dx.doi.org/10.1091/mbc.E09-03-0225
499. Kanki T, Wang K, Cao Y, Baba M, Klionsky DJ. Atg32 is a mitochondrial protein that confers selectivity during mitophagy. Dev Cell 2009; 17:98-109; PMID:19619495; http://dx.doi.org/10.1016/j.devcel.2009.06.014
500. Okamoto K, Kondo-Okamoto N, Ohsumi Y. Mitochondria-anchored receptor Atg32 mediates degradation of mitochondria via selective autophagy. Dev Cell 2009; 17:87-97; PMID:19619494; http://dx.doi.org/10.1016/j.devcel.2009.06.013
501. Sakai Y, Koller A, Rangell LK, Keller GA, Subramani S. Peroxisome degradation by microautophagy in Pichia pastoris: identification of specific steps and morphological intermediates. J Cell Biol 1998; 141:625-36; PMID:9566964; http://dx.doi.org/10.1083/jcb.141.3.625
502. Nazarko TY, Nicaud JM, Sibirny AA. Observation of the *Yarrowia lipolytica* peroxisome-vacuole dynamics by fluorescence microscopy with a single filter set. Cell Biol Int 2005; 29:65-70; PMID:15763501; http://dx.doi.org/10.1016/j.cellbi.2004.11.014
503. Roetzer A, Gratz N, Kovarik P, Schüller C. Autophagy supports *Candida glabrata* survival during phagocytosis. Cell Microbiol 2010; 12:199-216; PMID:19811500; http://dx.doi.org/10.1111/j.1462-5822.2009.01391.x
504. Bormann C, Sahm H. Degradation of microbodies in relation to activities of alcohol oxidase and catalase in *Candida boidinii*. Arch Microbiol 1978; 117:67-72; PMID:678013; http://dx.doi.org/10.1007/BF00689353
505. Stasyk OV, Nazarko TY, Sibirny AA. Methods of plate pexophagy monitoring and positive selection for ATG gene cloning in yeasts. Methods Enzymol 2008; 451:229-39; PMID:19185724; http://dx.doi.org/10.1016/S0076-6879(08)03216-3
506. Hutchins MU, Veenhuis M, Klionsky DJ. Peroxisome degradation in *Saccharomyces cerevisiae* is dependent on machinery of macroautophagy and the Cvt pathway. J Cell Sci 1999; 112:4079-87; PMID:10547367
507. Mukaiyama H, Oku M, Baba M, Samizo T, Hammond AT, Glick BS, et al. Paz2 and 13 other *PAZ* gene products regulate vacuolar engulfment of peroxisomes during micropexophagy. Genes Cells 2002; 7:75-90; PMID:11856375; http://dx.doi.org/10.1046/j.1356-9597.2001.00499.x
508. Tuttle DL, Dunn WA, Jr.. Divergent modes of autophagy in the methylotrophic yeast Pichia pastoris. J Cell Sci 1995; 108:25-35; PMID:7738102
509. Nazarko TY, Huang J, Nicaud JM, Klionsky DJ, Sibirny AA. Trs85 is required for macroautophagy, pexophagy and cytoplasm to vacuole targeting in *Yarrowia lipolytica* and *Saccharomyces cerevisiae*. Autophagy 2005; 1:37-45; PMID:16874038; http://dx.doi.org/10.4161/auto.1.1.1512
510. Veenhuis M, Douma A, Harder W, Osumi M. Degradation and turnover of peroxisomes in the yeast *Hansenula polymorpha* induced by selective inactivation of peroxisomal enzymes. Arch Microbiol 1983; 134:193-203; PMID:6351780; http://dx.doi.org/10.1007/BF00407757
511. Monosov EZ, Wenzel TJ, Lüers GH, Heyman JA, Subramani S. Labeling of peroxisomes with green fluorescent protein in living *P. pastoris* cells. J Histochem Cytochem 1996; 44:581-9; PMID:8666743; http://dx.doi.org/10.1177/44.6.8666743
512. Wiemer EA, Wenzel T, Deerinck TJ, Ellisman MH, Subramani S. Visualization of the peroxisomal compartment in living mammalian cells: dynamic behavior and association with microtubules. J Cell Biol 1997; 136:71-80; PMID:9008704; http://dx.doi.org/10.1083/jcb.136.1.71
513. Monastyrska I, van der Heide M, Kilkken AM, Kiel JAKW, van der Klei IJ, Veenhuis M. Atg8 is essential for macropexophagy in *Hansenula polymorpha*. Traffic 2005; 6:66-74; PMID:15569246; http://dx.doi.org/10.1111/j.1600-0854.2004.00252.x
514. Devenish RJ, Prescott M, Turcic K, Mijaljica D. Monitoring organelle turnover in yeast using fluorescent protein tags. Methods Enzymol 2008; 451:109-31; PMID:19185717; http://dx.doi.org/10.1016/S0076-6879(08)03209-6
515. Farré JC, Manjithaya R, Mathewson RD, Subramani S. PpAtg30 tags peroxisomes for turnover by selective autophagy. Dev Cell 2008; 14:365-76; PMID:18331717; http://dx.doi.org/10.1016/j.devcel.2007.12.011
516. Kanki T, Klionsky DJ. The molecular mechanism of mitochondria autophagy in yeast. Mol Microbiol 2010; 75:795-800; PMID:20487284; http://dx.doi.org/10.1111/j.1365-2958.2009.07035.x
517. Tal R, Winter G, Ecker N, Klionsky DJ, Abeliovich H. Aup1p, a yeast mitochondrial protein phosphatase homolog, is required for efficient stationary phase mitophagy and cell survival. J Biol Chem 2007; 282:5617-24; PMID:17166847; http://dx.doi.org/10.1074/jbc.M605940200
518. Abeliovich H. Stationary-phase mitophagy in respiring *Saccharomyces cerevisiae*. Antioxid Redox Signal 2011; 14:2003-11; PMID:21194383; http://dx.doi.org/10.1089/ars.2010.3807
519. Aksam EB, Koek A, Kiel JAKW, Jourdan S, Veenhuis M, van der Klei IJ. A peroxisomal lon protease and peroxisome degradation by autophagy play key roles in vitality of Hansenula polymorpha cells. Autophagy 2007; 3:96-105; PMID:17172804
520. Roberts P, Moshitch-Moshkovitz S, Kvam E, O'Toole E, Winey M, Goldfarb DS. Piecemeal microautophagy of nucleus in *Saccharomyces cerevisiae*. Mol Biol Cell 2003; 14:129-41; PMID:12529432; http://dx.doi.org/10.1091/mbc.E02-08-0483
521. Krick R, Muehe Y, Prick T, Bremer S, Schlotterhose P, Eskelinen E-L, et al. Piecemeal microautophagy of the nucleus requires the core macroautophagy genes. Mol Biol Cell 2008; 19:4492-505; PMID:18701704; http://dx.doi.org/10.1091/mbc.E08-04-0363
522. Farré JC, Krick R, Subramani S, Thumm M. Turnover of organelles by autophagy in yeast. Curr Opin Cell Biol 2009; 21:522-30; PMID:19515549; http://dx.doi.org/10.1016/j.ceb.2009.04.015
523. Kvam E, Goldfarb DS. Structure and function of nucleus-vacuole junctions: outer-nuclear-membrane targeting of Nvj1p and a role in tryptophan uptake. J Cell Sci 2006; 119:3622-33; PMID:16912077; http://dx.doi.org/10.1242/jcs.03093
524. Millen JI, Krick R, Prick T, Thumm M, Goldfarb DS. Measuring piecemeal microautophagy of the nucleus in *Saccharomyces cerevisiae*. Autophagy 2009; 5:75-81; PMID:18989095; http://dx.doi.org/10.4161/auto.5.7187181
525. Bernales S, McDonald KL, Walter P. Autophagy counterbalances endoplasmic reticulum expansion during the unfolded protein response. PLoS Biol 2006; 4:e423; PMID:17132049; http://dx.doi.org/10.1371/journal.pbio.0040423
526. Yorimitsu T, Nair U, Yang Z, Klionsky DJ. Endoplasmic reticulum stress triggers autophagy. J Biol Chem 2006; 281:30299-304; PMID:16901900; http://dx.doi.org/10.1074/jbc.M607007200
527. Klionsky DJ, Cuervo AM, Dunn WA, Jr., Levine B, van der Klei I, Seglen PO. How shall I eat thee? Autophagy 2007; 3:413-6; PMID:17568180
528. Fujita E, Kouroku Y, Isoai A, Kumagai H, Misutani A, Matsuda C, et al. Two endoplasmic reticulum-associated degradation (ERAD) systems for the novel variant of the mutant dysferlin: ubiquitin/proteasome ERAD(I) and autophagy/lysosome ERAD(II). Hum Mol Genet 2007; 16:618-29; PMID:17331981; http://dx.doi.org/10.1093/hmg/ddm002
529. Kraft C, Deplazes A, Sohrmann M, Peter M. Mature ribosomes are selectively degraded upon starvation by an autophagy pathway requiring the Ubp3p/Bre5p ubiquitin protease. Nat Cell Biol 2008; 10:602-10; PMID:18391941; http://dx.doi.org/10.1038/ncb1723
530. Yorimitsu T, Klionsky DJ. Atg11 links cargo to the vesicle-forming machinery in the cytoplasm to vacuole targeting pathway. Mol Biol Cell 2005; 16:1593-605; PMID:15659643; http://dx.doi.org/10.1091/mbc.E04-11-1035

dc_840_14
© Landes Bioscience. Do not distribute.

531. Shintani T, Huang W-P, Stromhaug PE, Klionsky DJ. Mechanism of cargo selection in the cytoplasm to vacuole targeting pathway. Dev Cell 2002; 3:825-37; PMID:12479808; http://dx.doi.org/10.1016/S1534-5807(02)00373-8
532. Abeliovich H, Darsow T, Emr SD. Cytoplasm to vacuole trafficking of aminopeptidase I requires a t-SNARE-Sec1p complex composed of Tlg2p and Vps45p. EMBO J 1999; 18:6005-16; PMID: 10545112; http://dx.doi.org/10.1093/emboj/18.21.6005
533. Brown CR, Chiang H-L. A selective autophagy pathway that degrades gluconeogenic enzymes during catabolite inactivation. Commun Integr Biol 2009; 2:177-83; PMID:19513275
534. Schüle T, Rose M, Entian KD, Thumm M, Wolf DH. Ubc8p functions in catabolite degradation of fructose-1, 6-bisphosphatase in yeast. EMBO J 2000; 19:2161-7; PMID:10811607; http://dx.doi.org/10.1093/emboj/19.10.2161
535. Schork SM, Thumm M, Wolf DH. Catabolite inactivation of fructose-1,6-bisphosphatase of *Saccharomyces cerevisiae*. Degradation occurs via the ubiquitin pathway. J Biol Chem 1995; 270:26446-50; PMID:7592860
536. Regelmann J, Schüle T, Josupeit FS, Horak J, Rose M, Entian KD, et al. Catabolite degradation of fructose-1,6-bisphosphatase in the yeast Saccharomyces cerevisiae: a genome-wide screen identifies eight novel GID genes and indicates the existence of two degradation pathways. Mol Biol Cell 2003; 14:1652-63; PMID: 12686616; http://dx.doi.org/10.1091/mbc.E02-08-0456
537. Hung GC, Brown CR, Wolfe AB, Liu J, Chiang HL. Degradation of the gluconeogenic enzymes fructose-1,6-bisphosphatase and malate dehydrogenase is mediated by distinct proteolytic pathways and signaling events. J Biol Chem 2004; 279:49138-50; PMID:15358789; http://dx.doi.org/10.1074/jbc.M404544200
538. Chiang H-L, Schekman R, Hamamoto S. Selective uptake of cytosolic, peroxisomal, and plasma membrane proteins into the yeast lysosome for degradation. J Biol Chem 1996; 271:9934-41; PMID:8626630; http://dx.doi.org/10.1074/jbc.271.17.9934
539. Huang PH, Chiang H-L. Identification of novel vesicles in the cytosol to vacuole protein degradation pathway. J Cell Biol 1997; 136:803-10; PMID: 9049246; http://dx.doi.org/10.1083/jcb.136.4.803
540. Alibhoy AA, Giardina BJ, Dunton DD, Chiang H-L. Vid30 is required for the association of Vid vesicles and actin patches in the vacuole import and degradation pathway. Autophagy 2012; 8; In press; PMID: 22082961; http://dx.doi.org/10.4161/auto.8.1.18104
541. Brown CR, Wolfe AB, Cui D, Chiang H-L. The vacuolar import and degradation pathway merges with the endocytic pathway to deliver fructose-1,6-bisphosphatase to the vacuole for degradation. J Biol Chem 2008; 283:26116-27; PMID:18660504; http://dx.doi.org/10.1074/jbc.M709922200
542. Chiang MC, Chiang H-L. Vid24p, a novel protein localized to the fructose-1, 6-bisphosphatase-containing vesicles, regulates targeting of fructose-1,6-bisphosphatase from the vesicles to the vacuole for degradation. J Cell Biol 1998; 140:1347-56; PMID:9508768; http://dx.doi.org/10.1083/jcb.140.6.1347
543. Brown CR, Dunton D, Chiang H-L. The vacuole import and degradation pathway utilizes early steps of endocytosis and actin polymerization to deliver cargo proteins to the vacuole for degradation. J Biol Chem 2010; 285:1516-28; PMID:19892709; http://dx.doi.org/10.1074/jbc.M109.028241
544. Vida TA, Emr SD. A new vital stain for visualizing vacuolar membrane dynamics and endocytosis in yeast. J Cell Biol 1995; 128:779-92; PMID:7533169; http://dx.doi.org/10.1083/jcb.128.5.779
545. Brown CR, Hung GC, Dunton D, Chiang H-L. The TOR complex 1 is distributed in endosomes and in retrograde vesicles that form from the vacuole membrane and plays an important role in the vacuole import and degradation pathway. J Biol Chem 2010; 285:23359-70; PMID:20457600; http://dx.doi.org/10.1074/jbc.M109.075143
546. Geisler S, Holmström KM, Treis A, Skujat D, Weber SS, Fiesel FC, et al. The PINK1/Parkin-mediated mitophagy is compromised by PD-associated mutations. Autophagy 2010; 6:871-8; PMID:20798600; http://dx.doi.org/10.4161/auto.6.7.13286
547. Geisler S, Holmström KM, Skujat D, Fiesel FC, Rothfuss OC, Kahle PJ, et al. PINK1/Parkin-mediated mitophagy is dependent on VDAC1 and p62/SQSTM1. Nat Cell Biol 2010; 12:119-31; PMID: 20098416; http://dx.doi.org/10.1038/ncb2012
548. Boya P, Gonzalez-Polo RA, Casares N, Perfettini JL, Dessen P, Larochette N, et al. Inhibition of macroautophagy triggers apoptosis. Mol Cell Biol 2005; 25:1025-40; PMID:15657430; http://dx.doi.org/10.1128/MCB.25.3.1025-1040.2005
549. Katayama H, Kogure T, Mizushima N, Yoshimori T, Miyawaki A. A sensitive and quantitative technique for detecting autophagic events based on lysosomal delivery. Chem Biol 2011; 18:1042-52; PMID:21867919; http://dx.doi.org/10.1016/j.chembiol.2011.05.013
550. Yang JY, Yang WY. Spatiotemporally controlled initiation of Parkin-mediated mitophagy within single cells. Autophagy 2011; 7:1230-8; PMID:22011618; http://dx.doi.org/10.4161/auto.7.10.16626
551. Luiken JJ, van den Berg M, Heikoop JC, Meijer AJ. Autophagic degradation of peroxisomes in isolated rat hepatocytes. FEBS Lett 1992; 304:93-7; PMID: 1618306; http://dx.doi.org/10.1016/0014-5793(92)80596-9
552. Yokota S. Formation of autophagosomes during degradation of excess peroxisomes induced by administration of dioctyl phthalate. Eur J Cell Biol 1993; 61:67-80; PMID:8223709
553. Huybrechts SJ, Van Veldhoven PP, Brees C, Mannaerts GP, Los GV, Fransen M. Peroxisome dynamics in cultured mammalian cells. Traffic 2009; 10:1722-33; PMID:19719477; http://dx.doi.org/10.1111/j.1600-0854.2009.00970.x
554. Lee JY, Nagano Y, Taylor JP, Lim KL, Yao TP. Disease-causing mutations in parkin impair mitochondrial ubiquitination, aggregation, and HDAC6-dependent mitophagy. J Cell Biol 2010; 189:671-9; PMID: 20457763; http://dx.doi.org/10.1083/jcb.201001039
555. Chan NC, Salazar AM, Pham AH, Sweredoski MJ, Kolawa NJ, Graham RL, et al. Broad activation of the ubiquitin-proteasome system by Parkin is critical for mitophagy. Hum Mol Genet 2011; 20:1726-37; PMID:21296869; http://dx.doi.org/10.1093/hmg/ddr048
556. Tanaka A, Cleland MM, Xu S, Narendra DP, Suen DF, Karbowski M, et al. Proteasome and p97 mediate mitophagy and degradation of mitofusins induced by Parkin. J Cell Biol 2010; 191:1367-80; PMID: 21173115; http://dx.doi.org/10.1083/jcb.201007013
557. Yoshii SR, Kishi C, Ishihara N, Mizushima N. Parkin mediates proteasome-dependent protein degradation and rupture of the outer mitochondrial membrane. J Biol Chem 2011; 286:19630-40; PMID:21454557; http://dx.doi.org/10.1074/jbc.M110.209338
558. Okatsu K, Saisho K, Shimanuki M, Nakada K, Shitara H, Sou YS, et al. p62/SQSTM1 cooperates with Parkin for perinuclear clustering of depolarized mitochondria. Genes Cells 2010; 15:887-900; PMID:20604804
559. Lyamzaev KG, Nepryakhina OK, Saprunova VB, Bakeeva LE, Pletjushkina OY, Chernyak BV, et al. Novel mechanism of elimination of malfunctioning mitochondria (mitoptosis): formation of mitoptotic bodies and extrusion of mitochondrial material from the cell. Biochim Biophys Acta 2008; 1777:817-25; PMID:18433711
560. Hara-Kuge S, Fujiki Y. The peroxin Pex14p is involved in LC3-dependent degradation of mammalian peroxisomes. Exp Cell Res 2008; 314:3531-41; PMID: 18848543; http://dx.doi.org/10.1016/j.yexcr.2008.09.015
561. Ezaki J, Kominami E, Ueno T. Peroxisome degradation in mammals. IUBMB Life 2011; 63:1001-8; PMID:21990012; http://dx.doi.org/10.1002/iub.537
562. Øverbye A, Fengsrud M, Seglen PO. Proteomic analysis of membrane-associated proteins from rat liver autophagosomes. Autophagy 2007; 3:300-22; PMID: 17377489
563. Ju JS, Miller SE, Jackson E, Cadwell K, Piwnica-Worms D, Weihl CC. Quantitation of selective autophagic protein aggregate degradation in vitro and in vivo using luciferase reporters. Autophagy 2009; 5:511-9; PMID:19305149; http://dx.doi.org/10.4161/auto.5.4.7761
564. Fuentealba RA, Marasa J, Diamond MI, Piwnica-Worms D, Weihl CC. An aggregation sensing reporter identifies leflunomide and teriflunomide as polyglutamine aggregate inhibitors. Hum Mol Genet 2012; 21:664-80; PMID:22052286; http://dx.doi.org/10.1093/hmg/ddr500
565. Webster P. Cytoplasmic bacteria and the autophagic pathway. Autophagy 2006; 2:159-61; PMID:16874112
566. Dubuisson JF, Swanson MS. Mouse infection by Legionella, a model to analyze autophagy. Autophagy 2006; 2:179-82; PMID:16874080
567. Jordan TX, Randall G. Manipulation or capitulation: virus interactions with autophagy. Microbes Infect 2012; PMID:22051604; http://dx.doi.org/10.1016/j.micinf.2011.09.007
568. Knodler LA, Celli J. Eating the strangers within: host control of intracellular bacteria via xenophagy. Cell Microbiol 2011; 13:1319-27; PMID:21740500; http://dx.doi.org/10.1111/j.1462-5822.2011.01632.x
569. Levine B, Mizushima N, Virgin HW. Autophagy in immunity and inflammation. Nature 2011; 469:323-35; PMID:21248839; http://dx.doi.org/10.1038/nature09782
570. Deretic V. Autophagy in immunity and cell-autonomous defense against intracellular microbes. Immunol Rev 2011; 240:92-104; PMID:21349088; http://dx.doi.org/10.1111/j.1600-065X.2010.00995.x
571. Kageyama S, Omori H, Saitoh T, Sone T, Guan JL, Akira S, et al. The LC3 recruitment mechanism is separate from Atg9L1-dependent membrane formation in the autophagic response against Salmonella. Mol Biol Cell 2011; 22:2290-300; PMID:21525242; http://dx.doi.org/10.1091/mbc.E10-11-0893
572. Zheng YT, Shahnazari S, Brech A, Lamark T, Johansen T, Brumell JH. The adaptor protein p62/SQSTM1 targets invading bacteria to the autophagy pathway. J Immunol 2009; 183:5909-16; PMID:19812211; http://dx.doi.org/10.4049/jimmunol.0904441
573. Thurston TL, Ryzhakov G, Bloor S, von Muhlinen N, Randow F. The TBK1 adaptor and autophagy receptor NDP52 restricts the proliferation of ubiquitin-coated bacteria. Nat Immunol 2009; 10:1215-21; PMID: 19820708; http://dx.doi.org/10.1038/ni.1800
574. Wild P, Farhan H, McEwan DG, Wagner S, Rogov VV, Brady NR, et al. Phosphorylation of the autophagy receptor optineurin restricts Salmonella growth. Science 2011; 333:228-33; PMID:21617041; http://dx.doi.org/10.1126/science.1205405
575. Huang J, Canadien V, Lam GY, Steinberg BE, Dinauer MC, Magalhaes MA, et al. Activation of antibacterial autophagy by NADPH oxidases. Proc Natl Acad Sci U S A 2009; 106:6226-31; PMID:19339495; http://dx.doi.org/10.1073/pnas.0811045106
576. Rich KA, Burkett C, Webster P. Cytoplasmic bacteria can be targets for autophagy. Cell Microbiol 2003; 5:455-68; PMID:12814436; http://dx.doi.org/10.1046/j.1462-5822.2003.00292.x
577. Shahnazari S, Brumell JH. Mechanisms and consequences of bacterial targeting by the autophagy pathway. Curr Opin Microbiol 2011; 14:68-75; PMID:21112809; http://dx.doi.org/10.1016/j.mib.2010.11.001
578. McLean JE, Wudzinska A, Datan E, Quaglino D, Zakeri Z. Flavivirus NS4A-induced autophagy protects cells against death and enhances virus replication. J Biol Chem 2011; 286:22147-59; PMID:21511946; http://dx.doi.org/10.1074/jbc.M110.192500
579. Mao Y, Da L, Tang H, Yang J, Lei Y, Tiollais P, et al. Hepatitis B virus X protein reduces starvation-induced cell death through activation of autophagy and inhibition of mitochondrial apoptotic pathway. Biochem Biophys Res Commun 2011; 415:68-74; PMID:22020078; http://dx.doi.org/10.1016/j.bbrc.2011.10.013
580. Orvedahl A, Alexander D, Tallóczy Z, Sun Q, Wei Y, Zhang W, et al. HSV-1 ICP34.5 confers neurovirulence by targeting the Beclin 1 autophagy protein. Cell Host Microbe 2007; 1:23-35; PMID:18005679; http://dx.doi.org/10.1016/j.chom.2006.12.001
581. Alexander DE, Ward SL, Mizushima N, Levine B, Leib DA. Analysis of the role of autophagy in replication of herpes simplex virus in cell culture. J Virol 2007; 81:12128-34; PMID:17855538; http://dx.doi.org/10.1128/JVI.01356-07
582. Leib DA, Alexander DE, Cox D, Yin J, Ferguson TA. Interaction of ICP34.5 with Beclin 1 modulates herpes simplex virus type 1 pathogenesis through control of CD4 T-cell responses. J Virol 2009; 83:12164-71; PMID:19759141; http://dx.doi.org/10.1128/JVI.01676-09
583. Zhang H, Monken CE, Zhang Y, Lenard J, Mizushima N, Lattime EC, et al. Cellular autophagy machinery is not required for vaccinia virus replication and maturation. Autophagy 2006; 2:91-5; PMID: 16874104
584. Heaton NS, Randall G. Dengue virus and autophagy. Viruses 2011; 3:1332-41; PMID:21994782; http://dx.doi.org/10.3390/v3081332
585. Dreux M, Gastaminza P, Wieland SF, Chisari FV. The autophagy machinery is required to initiate hepatitis C virus replication. Proc Natl Acad Sci U S A 2009; 106:14046-51; PMID:19666601; http://dx.doi.org/10.1073/pnas.0907344106
586. Collins CA, De Mazière A, van Dijk S, Carlsson F, Klumperman J, Brown EJ. Atg5-independent sequestration of ubiquitinated mycobacteria. PLoS Pathog 2009; 5:e1000430; PMID:19436699; http://dx.doi.org/10.1371/journal.ppat.1000430
587. Moreau K, Lacas-Gervais S, Fujita N, Sebbane F, Yoshimori T, Simonet M, et al. Autophagosomes can support *Yersinia pseudotuberculosis* replication in macrophages. Cell Microbiol 2010; 12:1108-23; PMID:20180800; http://dx.doi.org/10.1111/j.1462-5822.2010.01456.x
588. Singh R, Kaushik S, Wang Y, Xiang Y, Novak I, Komatsu M, et al. Autophagy regulates lipid metabolism. Nature 2009; 458:1131-5; PMID:19339967; http://dx.doi.org/10.1038/nature07976
589. Grasso D, Ropolo A, Lo Ré A, Boggio V, Molejón MI, Iovanna JL, et al. Zymophagy, a novel selective autophagy pathway mediated by VMP1-USP9x-p62, prevents pancreatic cell death. J Biol Chem 2011; 286:8308-24; PMID:21173155; http://dx.doi.org/10.1074/jbc.M110.197301
590. Al Rawi S, Louvet-Vallée S, Djeddi A, Sachse M, Culetto E, Hajjar C, et al. Allophagy: A macroautophagic process degrading spermatozoid-inherited organelles. Autophagy 2012; In press.
591. Sato M, Sato K. Maternal inheritance of mitochondrial DNA: Degradation of paternal mitochondria by allogeneic organelle autophagy, allophagy. Autophagy 2012; 8; In press; PMID:22302002
592. Al Rawi S, Louvet-Vallée S, Djeddi A, Sachse M, Culetto E, Hajjar C, et al. Postfertilization autophagy of sperm organelles prevents paternal mitochondrial DNA transmission. Science 2011; 334:1144-7; PMID:22033522; http://dx.doi.org/10.1126/science.1211878
593. Sato M, Sato K. Degradation of paternal mitochondria by fertilization-triggered autophagy in *C. elegans* embryos. Science 2011; 334:1141-4; PMID:21998252; http://dx.doi.org/10.1126/science.1210333
594. Seglen PO, Gordon PB, Tolleshaug H, Høyvik H. Use of [^{3}H]raffinose as a specific probe of autophagic sequestration. Exp Cell Res 1986; 162:273-7; PMID: 3940229; http://dx.doi.org/10.1016/0014-4827(86)90446-5
595. Kopitz J, Kisen GO, Gordon PB, Bohley P, Seglen PO. Nonselective autophagy of cytosolic enzymes by isolated rat hepatocytes. J Cell Biol 1990; 111:941-53; PMID:2391370; http://dx.doi.org/10.1083/jcb.111.3.941
596. Nair U, Thumm M, Klionsky DJ, Krick R. GFP-Atg8 protease protection as a tool to monitor autophagosome biogenesis. Autophagy 2011; 7:1546-50; PMID: 22108003; http://dx.doi.org/10.4161/auto.7.12.18424
597. Plomp PJ, Gordon PB, Meijer AJ, Høyvik H, Seglen PO. Energy dependence of different steps in the autophagic-lysosomal pathway. J Biol Chem 1989; 264:6699-704; PMID:2708336
598. Høyvik H, Gordon PB, Berg TO, Strømhaug PE, Seglen PO. Inhibition of autophagic-lysosomal delivery and autophagic lactolysis by asparagine. J Cell Biol 1991; 113:1305-12; PMID:1904444; http://dx.doi.org/10.1083/jcb.113.6.1305
599. Rodriguez-Enriquez S, Kim I, Currin RT, Lemasters JJ. Tracker dyes to probe mitochondrial autophagy (mitophagy) in rat hepatocytes. Autophagy 2006; 2:39-46; PMID:16874071
600. Lorenz H, Hailey DW, Lippincott-Schwartz J. Fluorescence protease protection of GFP chimeras to reveal protein topology and subcellular localization. Nat Methods 2006; 3:205-10; PMID:16489338; http://dx.doi.org/10.1038/nmeth857
601. Dagda RK, Zhu J, Kulich SM, Chu CT. Mitochondrially localized ERK2 regulates mitophagy and autophagic cell stress: implications for Parkinson's disease. Autophagy 2008; 4:770-82; PMID:18594108
602. McNeil PL, Murphy RF, Lanni F, Taylor DL. A method for incorporating macromolecules into adherent cells. J Cell Biol 1984; 98:1556-64; PMID:6201494; http://dx.doi.org/10.1083/jcb.98.4.1556
603. Kim J, Huang WP, Stromhaug PE, Klionsky DJ. Convergence of multiple autophagy and cytoplasm to vacuole targeting components to a perivacuolar membrane compartment prior to de novo vesicle formation. J Biol Chem 2002; 277:763-73; PMID:11675395; http://dx.doi.org/10.1074/jbc.M109134200
604. Kovács AL, László L, Kovács J. Effect of amino acids and cycloheximide on changes caused by vinblastine, leupeptin and methylamine in the autophagic/lysosomal system of mouse hepatocytes in vivo. Exp Cell Res 1985; 157:83-94; PMID:3972014; http://dx.doi.org/10.1016/0014-4827(85)90154-5
605. Swanson MS, Byrne BG, Dubuisson JF. Kinetic analysis of autophagosome formation and turnover in primary mouse macrophages. Methods Enzymol 2009; 452:383-402; PMID:19200894; http://dx.doi.org/10.1016/S0076-6879(08)03623-9
606. Beugnet A, Tee AR, Taylor PM, Proud CG. Regulation of targets of mTOR (mammalian target of rapamycin) signalling by intracellular amino acid availability. Biochem J 2003; 372:555-66; PMID: 12611592; http://dx.doi.org/10.1042/BJ20021266
607. Urban J, Soulard A, Huber A, Lippman S, Mukhopadhyay D, Deloche O, et al. Sch9 is a major target of TORC1 in *Saccharomyces cerevisiae*. Mol Cell 2007; 26:663-74; PMID:17560372; http://dx.doi.org/10.1016/j.molcel.2007.04.020
608. Jomain-Baum M, Garber AJ, Farber E, Hanson RW. The effect of cycloheximide on the interaction between mitochondrial respiration and gluconeogenesis in guinea pig and rat liver. J Biol Chem 1973; 248:1536-43; PMID:4348543
609. Garber AJ, Jomain-Baum M, Salganicoff L, Farber E, Hanson RW. The effects of cycloheximide on energy transfer in rat and guinea pig liver mitochondria. J Biol Chem 1973; 248:1530-5; PMID:4144389
610. Mora R, Dokic I, Kees T, Hüber CM, Keitel D, Geibig R, et al. Sphingolipid rheostat alterations related to transformation can be exploited for specific induction of lysosomal cell death in murine and human glioma. Glia 2010; 58:1364-83; PMID: 20607862
611. Bright NA, Lindsay MR, Stewart A, Luzio JP. The relationship between lumenal and limiting membrane in swollen late endocytic compartments formed after wortmannin treatment or sucrose accumulation. Traffic 2001; 2:631-42; PMID:11555417; http://dx.doi.org/10.1034/j.1600-0854.2001.20906.x
612. Deter RL. Quantitative characterization of dense body, autophagic vacuole, and acid phosphatase-bearing particle populations during the early phases of glucagon-induced autophagy in rat liver. J Cell Biol 1971; 48:473-89; PMID:4322760; http://dx.doi.org/10.1083/jcb.48.3.473
613. Deter RL. Analog modeling of glucagon-induced autophagy in rat liver. I. Conceptual and mathematical model of telolysosome-autophagosome-autolysosome interaction. Exp Cell Res 1975; 94:122-6; PMID: 1193121; http://dx.doi.org/10.1016/0014-4827(75)90538-8
614. Deter RL. Analog modeling of glucagon-induced autophagy in rat liver. II. Evaluation of iron labeling as a means for identifying telolysosome, autophagosome and autolysosome populations. Exp Cell Res 1975; 94:127-39; PMID:172336; http://dx.doi.org/10.1016/0014-4827(75)90539-X
615. Deter RL, Baudhuin P, De Duve C. Participation of lysosomes in cellular autophagy induced in rat liver by glucagon. J Cell Biol 1967; 35:C11-6; PMID: 6055998; http://dx.doi.org/10.1083/jcb.35.2.C11
616. Deter RL, De Duve C. Influence of glucagon, an inducer of cellular autophagy, on some physical properties of rat liver lysosomes. J Cell Biol 1967; 33:437-49; PMID:4292315; http://dx.doi.org/10.1083/jcb.33.2.437

dc_840_14
©Landes Bioscience. Do not distribute.

617. Strømhaug PE, Berg TO, Fengsrud M, Seglen PO. Purification and characterization of autophagosomes from rat hepatocytes. Biochem J 1998; 335:217-24; PMID:9761717
618. Deter RL. Electron microscopic evaluation of subcellular fractions obtained by ultracentrifugation. In: Hayat MA, ed. Principles and Techniques of Electron Microscopy. New York: Van Nostrand Reinhold Co., 1973:199-235.
619. Marzella L, Ahlberg J, Glaumann H. Isolation of autophagic vacuoles from rat liver: morphological and biochemical characterization. J Cell Biol 1982; 93:144-54; PMID:7068752; http://dx.doi.org/10.1083/jcb.93.1.144
620. Wattiaux R, Wattiaux-De Coninck S, Ronveaux-dupal M-F, Dubois F. Isolation of rat liver lysosomes by isopycnic centrifugation in a metrizamide gradient. J Cell Biol 1978; 78:349-68; PMID:211139; http://dx.doi.org/10.1083/jcb.78.2.349
621. Rodríguez-Navarro JA, Rodríguez L, Casarejos MJ, Solano RM, Gómez A, Perucho J, et al. Trehalose ameliorates dopaminergic and tau pathology in parkin deleted/tau overexpressing mice through autophagy activation. Neurobiol Dis 2010; 39:423-38; PMID: 20546895; http://dx.doi.org/10.1016/j.nbd.2010.05.014
622. Weibel ER, Bolender RP. Stereological techniques for electron microscopic morphometry. In: Hayat MA, ed. Principles and Techniques of Electron Microscopy. New York: Van Nostrand Reinhold Co., 1973:237-96.
623. Baudhuin P, Evrard P, Berthet J. Electron microscopic examination of subcellular fractions. I. The preparation of representative samples from suspensions of particles. J Cell Biol 1967; 32:181-91; PMID:10976209; http://dx.doi.org/10.1083/jcb.32.1.181
624. Baudhuin P, Berthet J. Electron microscopic examination of subcellular fractions. II. Quantitative analysis of the mitochondrial population isolated from rat liver. J Cell Biol 1967; 35:631-48; PMID: 4294244; http://dx.doi.org/10.1083/jcb.35.3.631
625. Storrie B, Madden EA. Isolation of subcellular organelles. Methods Enzymol 1990; 182:203-25; PMID:2156127; http://dx.doi.org/10.1016/0076-6879(90)82018-W
626. Balch WE, Rothman JE. Characterization of protein transport between successive compartments of the Golgi apparatus: asymmetric properties of donor and acceptor activities in a cell-free system. Arch Biochem Biophys 1985; 240:413-25; PMID:2990347; http://dx.doi.org/10.1016/0003-9861(85)90046-3
627. Graham JM. Isolation of lysosomes from tissues and cells by differential and density gradient centrifugation. In: Bonifacino JS, Dasso M, Harford JB, Lippincott-Schwartz J and Yamada KM, eds. Current Protocols in Cell Biology: John Wiley & Sons, Inc., 2000:Unit 3.6.
628. Cuervo AM, Dice JF, Knecht E. A population of rat liver lysosomes responsible for the selective uptake and degradation of cytosolic proteins. J Biol Chem 1997; 272:5606-15; PMID:9038169; http://dx.doi.org/10.1074/jbc.272.9.5606
629. Iwai-Kanai E, Yuan H, Huang C, Sayen MR, Perry-Garza CN, Kim L, et al. A method to measure cardiac autophagic flux in vivo. Autophagy 2008; 4:322-9; PMID:18216495
630. Zhu H, Tannous P, Johnstone JL, Kong Y, Shelton JM, Richardson JA, et al. Cardiac autophagy is a maladaptive response to hemodynamic stress. J Clin Invest 2007; 117:1782-93; PMID:17607355; http://dx.doi.org/10.1172/JCI27523
631. Ding WX, Li M, Chen X, Ni HM, Lin CW, Gao W, et al. Autophagy reduces acute ethanol-induced hepatotoxicity and steatosis in mice. Gastroenterology 2010; 139:1740-52; PMID:20659474; http://dx.doi.org/10.1053/j.gastro.2010.07.041
632. Chiarelli R, Agnello M, Roccheri MC. Sea urchin embryos as a model system for studying autophagy induced by cadmium stress. Autophagy 2011; 7:1028-34; PMID:21628995; http://dx.doi.org/10.4161/auto.7.9.16450
633. Morici G, Agnello M, Spagnolo F, Roccheri MC, Di Liegro CM, Rinaldi AM. Confocal microscopy study of the distribution, content and activity of mitochondria during Paracentrotus lividus development. J Microsc 2007; 228:165-73; PMID:17970916; http://dx.doi.org/10.1111/j.1365-2818.2007.01860.x
634. Martinet W, De Meyer GR, Andries L, Herman AG, Kockx MM. Detection of autophagy in tissue by standard immunohistochemistry: possibilities and limitations. Autophagy 2006; 2:55-7; PMID:16874065
635. Holt SV, Wyspianska B, Randall KJ, James D, Foster JR, Wilkinson RW. The development of an immunohistochemical method to detect the autophagy-associated protein LC3-II in human tumor xenografts. Toxicol Pathol 2011; 39:516-23; PMID:21441228; http://dx.doi.org/10.1177/0192623310396903
636. Kimura S, Fujita N, Noda T, Yoshimori T. Monitoring autophagy in mammalian cultured cells through the dynamics of LC3. Methods Enzymol 2009; 452:1-12; PMID:19200872; http://dx.doi.org/10.1016/S0076-6879(08)03601-X
637. Dehay B, Bové J, Rodríguez-Muela N, Perier C, Recasens A, Boya P, et al. Pathogenic lysosomal depletion in Parkinson's disease. J Neurosci 2010; 30:12535-44; PMID:20844148; http://dx.doi.org/10.1523/JNEUROSCI.1920-10.2010
638. Ouimet M, Franklin V, Mak E, Liao X, Tabas I, Marcel YL. Autophagy regulates cholesterol efflux from macrophage foam cells via lysosomal acid lipase. Cell Metab 2011; 13:655-67; PMID:21641547; http://dx.doi.org/10.1016/j.cmet.2011.03.023
639. Gomes LC, Di Benedetto G, Scorrano L. During autophagy mitochondria elongate, are spared from degradation and sustain cell viability. Nat Cell Biol 2011; 13:589-98; PMID:21478857; http://dx.doi.org/10.1038/ncb2220
640. Grumati P, Coletto L, Sabatelli P, Cescon M, Angelin A, Bertaggia E, et al. Autophagy is defective in collagen VI muscular dystrophies, and its reactivation rescues myofiber degeneration. Nat Med 2010; 16:1313-20; PMID:21037586; http://dx.doi.org/10.1038/nm.2247
641. Haspel J, Shaik RS, Ifedigbo E, Nakahira K, Dolinay T, Englert JA, et al. Characterization of macroautophagic flux in vivo using a leupeptin-based assay. Autophagy 2011; 7:629-42; PMID:21460622; http://dx.doi.org/10.4161/auto.7.6.15100
642. Uchiyama Y. Autophagic cell death and its execution by lysosomal cathepsins. Arch Histol Cytol 2001; 64:233-46; PMID:11575420; http://dx.doi.org/10.1679/aohc.64.233
643. Biolo G, Fleming RY, Maggi SP, Wolfe RR. Transmembrane transport and intracellular kinetics of amino acids in human skeletal muscle. Am J Physiol 1995; 268:E75-84; PMID:7840186
644. Svanberg E, Möller-Loswick AC, Matthews DE, Körner U, Andersson M, Lundholm K. The role of glucose, long-chain triglycerides and amino acids for promotion of amino acid balance across peripheral tissues in man. Clin Physiol 1999; 19:311-20; PMID: 10451792; http://dx.doi.org/10.1046/j.1365-2281.1999.00183.x
645. Volpi E, Ferrando AA, Yeckel CW, Tipton KD, Wolfe RR. Exogenous amino acids stimulate net muscle protein synthesis in the elderly. J Clin Invest 1998; 101:2000-7; PMID:9576765; http://dx.doi.org/10.1172/JCI939
646. Denne SC, Liechty EA, Liu YM, Brechtel G, Baron AD. Proteolysis in skeletal muscle and whole body in response to euglycemic hyperinsulinemia in normal adults. Am J Physiol 1991; 261:E809-14; PMID: 1767841
647. Fukagawa NK, Minaker KL, Young VR, Matthews DE, Bier DM, Rowe JW. Leucine metabolism in aging humans: effect of insulin and substrate availability. Am J Physiol 1989; 256:E288-94; PMID:2645788
648. Gelfand RA, Barrett EJ. Effect of physiologic hyperinsulinemia on skeletal muscle protein synthesis and breakdown in man. J Clin Invest 1987; 80:1-6; PMID: 3298320; http://dx.doi.org/10.1172/JCI113033
649. Mortimore GE, Pösö AR. Intracellular protein catabolism and its control during nutrient deprivation and supply. Annu Rev Nutr 1987; 7:539-64; PMID: 3300746; http://dx.doi.org/10.1146/annurev.nu.07.070187.002543
650. Pozefsky T, Felig P, Tobin JD, Soeldner JS, Cahill GF, Jr. Amino acid balance across tissues of the forearm in postabsorptive man. Effects of insulin at two dose levels. J Clin Invest 1969; 48:2273-82; PMID: 5355340; http://dx.doi.org/10.1172/JCI106193
651. Weber SM, Levitz SM. Chloroquine interferes with lipopolysaccharide-induced TNF-alpha gene expression by a nonlysosomotropic mechanism. J Immunol 2000; 165:1534-40; PMID:10903761
652. Paludan C, Schmid D, Landthaler M, Vockerodt M, Kube D, Tuschl T, et al. Endogenous MHC class II processing of a viral nuclear antigen after autophagy. Science 2005; 307:593-6; PMID:15591165; http://dx.doi.org/10.1126/science.1104904
653. Chotechuang N, Azzout-Marniche D, Bos C, Chaumontet C, Gaudichon C, Tomé D. Down-regulation of the ubiquitin-proteasome proteolysis system by amino acids and insulin involves the adenosine monophosphate-activated protein kinase and mammalian target of rapamycin pathways in rat hepatocytes. Amino Acids 2011; 41:457-68; PMID:20957397; http://dx.doi.org/10.1007/s00726-010-0765-2
654. Bedford L, Lowe J, Dick LR, Mayer RJ, Brownell JE. Ubiquitin-like protein conjugation and the ubiquitin-proteasome system as drug targets. Nat Rev Drug Discov 2011; 10:29-46; PMID:21151032; http://dx.doi.org/10.1038/nrd3321
655. Akagi Y, Isaka Y, Akagi A, Ikawa M, Takenaka M, Moriyama T, et al. Transcriptional activation of a hybrid promoter composed of cytomegalovirus enhancer and beta-actin/beta-globin gene in glomerular epithelial cells in vivo. Kidney Int 1997; 51:1265-9; PMID:9083295; http://dx.doi.org/10.1038/ki.1997.172
656. Kimura T, Takabatake Y, Takahashi A, Kaimori JY, Matsui I, Namba T, et al. Autophagy protects the proximal tubule from degeneration and acute ischemic injury. J Am Soc Nephrol 2011; 22:902-13; PMID: 21493778; http://dx.doi.org/10.1681/ASN.2010070705
657. Hartleben B, Gödel M, Meyer-Schwesinger C, Liu S, Ulrich T, Köbler S, et al. Autophagy influences glomerular disease susceptibility and maintains podocyte homeostasis in aging mice. J Clin Invest 2010; 120:1084-96; PMID:20200449; http://dx.doi.org/10.1172/JCI39492
658. Berry DL, Baehrecke EH. Growth arrest and autophagy are required for salivary gland cell degradation in Drosophila. Cell 2007; 131:1137-48; PMID: 18083103; http://dx.doi.org/10.1016/j.cell.2007.10.048
659. Aits S, Gustafsson L, Hallgren O, Brest P, Gustafsson M, Trulsson M, et al. HAMLET (human alpha-lactalbumin made lethal to tumor cells) triggers autophagic tumor cell death. Int J Cancer 2009; 124:1008-19; PMID:19048621; http://dx.doi.org/10.1002/ijc.24076
660. Koike M, Shibata M, Tadakoshi M, Gotoh K, Komatsu M, Waguri S, et al. Inhibition of autophagy prevents hippocampal pyramidal neuron death after hypoxic-ischemic injury. Am J Pathol 2008; 172:454-69; PMID:18187572; http://dx.doi.org/10.2353/ajpath.2008.070876
661. Hou YC, Hannigan AM, Gorski SM. An executioner caspase regulates autophagy. Autophagy 2009; 5:530-3; PMID:19242106; http://dx.doi.org/10.4161/auto.5.4.8061
662. Nezis IP, Shravage BV, Sagona AP, Lamark T, Bjørkøy G, Johansen T, et al. Autophagic degradation of dBruce controls DNA fragmentation in nurse cells during late Drosophila melanogaster oogenesis. J Cell Biol 2010; 190:523-31; PMID:20713604; http://dx.doi.org/10.1083/jcb.201002035
663. Piras A, Gianetto D, Conte D, Bosone A, Vercelli A. Activation of autophagy in a rat model of retinal ischemia following high intraocular pressure. PLoS One 2011; 6:e22514; PMID:21799881; http://dx.doi.org/10.1371/journal.pone.0022514
664. Schwarze PE, Seglen PO. Reduced autophagic activity, improved protein balance and enhanced in vitro survival of hepatocytes isolated from carcinogen-treated rats. Exp Cell Res 1985; 157:15-28; PMID:2857648; http://dx.doi.org/10.1016/0014-4827(85)90148-X
665. Russo R, Berliocchi L, Adornetto A, Varano GP, Cavaliere F, Nucci C, et al. Calpain-mediated cleavage of Beclin-1 and autophagy deregulation following retinal ischemic injury in vivo. Cell Death Dis 2011; 2:e144; PMID:21490676; http://dx.doi.org/10.1038/cddis.2011.29
666. Denton D, Nicolson S, Kumar S. Cell death by autophagy: facts and apparent artefacts. Cell Death Differ 2012; PMID:22052193; http://dx.doi.org/10.1038/cdd.2011.146
667. Beaulaton J, Lockshin RA. Ultrastructural study of the normal degeneration of the intersegmental muscles of *Antheraea polyphemus* and *Manduca sexta* (Insecta, Lepidoptera) with particular reference of cellular autophagy. J Morphol 1977; 154:39-57; PMID: 915948; http://dx.doi.org/10.1002/jmor.1051540104
668. Clarke PG. Developmental cell death: morphological diversity and multiple mechanisms. Anat Embryol (Berl) 1990; 181:195-213; PMID:2186664; http://dx.doi.org/10.1007/BF00174615
669. Galluzzi L, Vitale I, Abrams JM, Alnemri ES, Baehrecke EH, Blagosklonny MV, et al. Molecular definitions of cell death subroutines: recommendations of the Nomenclature Committee on Cell Death 2012. Cell Death Differ 2012; 19:107-20; PMID:21760595; http://dx.doi.org/10.1038/cdd.2011.96
670. Kroemer G, Levine B. Autophagic cell death: the story of a misnomer. Nat Rev Mol Cell Biol 2008; 9:1004-10; PMID:18971948; http://dx.doi.org/10.1038/nrm2529
671. van Doorn WG, Beers EP, Dangl JL, Franklin-Tong VE, Gallois P, Hara-Nishimura I, et al. Morphological classification of plant cell deaths. Cell Death Differ 2011; 18:1241-6; PMID:21494263; http://dx.doi.org/10.1038/cdd.2011.36
672. Giusti C, Tresse E, Luciani MF, Golstein P. Autophagic cell death: analysis in Dictyostelium. Biochim Biophys Acta 2009; 1793:1422-31; PMID:19133302
673. Luciani MF, Giusti C, Harms B, Oshima Y, Kikuchi H, Kubohara Y, et al. Atg1 allows second-signaled autophagic cell death in Dictyostelium. Autophagy 2011; 7:501-8; PMID:21301205; http://dx.doi.org/10.4161/auto.7.5.14957
674. Uchikawa T, Yamamoto A, Inouye K. Origin and function of the stalk-cell vacuole in Dictyostelium. Dev Biol 2011; 352:48-57; PMID:21256841; http://dx.doi.org/10.1016/j.ydbio.2011.01.014
675. Galluzzi L, Aaronson SA, Abrams J, Alnemri ES, Andrews DW, Baehrecke EH, et al. Guidelines for the use and interpretation of assays for monitoring cell death in higher eukaryotes. Cell Death Differ 2009; 16:1093-107; PMID:19373242; http://dx.doi.org/10.1038/cdd.2009.44
676. Guimarães CA, Benchimol M, Amarante-Mendes GP, Linden R. Alternative programs of cell death in developing retinal tissue. J Biol Chem 2003; 278:41938-46; PMID:12917395; http://dx.doi.org/10.1074/jbc.M306547200
677. Lossi L, Gambino G, Mioletti S, Merighi A. In vivo analysis reveals different apoptotic pathways in pre- and postmigratory cerebellar granule cells of rabbit. J Neurobiol 2004; 60:437-52; PMID:15307148; http://dx.doi.org/10.1002/neu.20032
678. Lossi L, Alasia S, Salio C, Merighi A. Cell death and proliferation in acute slices and organotypic cultures of mammalian CNS. Prog Neurobiol 2009; 88:221-45; PMID:19552996; http://dx.doi.org/10.1016/j.pneurobio.2009.01.002
679. Thorburn A. I think autophagy controls the death of my cells: what do I do to get my paper published? Autophagy 2011; 7:455-6; PMID:21270514; http://dx.doi.org/10.4161/auto.7.5.14797
680. Kaushik S, Bandyopadhyay U, Sridhar S, Kiffin R, Martinez-Vicente M, Kon M, et al. Chaperone-mediated autophagy at a glance. J Cell Sci 2011; 124:495-9; PMID:21282471; http://dx.doi.org/10.1242/jcs.073874
681. Arias E, Cuervo AM. Chaperone-mediated autophagy in protein quality control. Curr Opin Cell Biol 2011; 23:184-9; PMID:21094035; http://dx.doi.org/10.1016/j.ceb.2010.10.009
682. Kaushik S, Cuervo AM. Methods to monitor chaperone-mediated autophagy. Methods Enzymol 2009; 452:297-324; PMID:19200890; http://dx.doi.org/10.1016/S0076-6879(08)03619-7
683. Dice JF. Peptide sequences that target cytosolic proteins for lysosomal proteolysis. Trends Biochem Sci 1990; 15:305-9; PMID:2204156; http://dx.doi.org/10.1016/0968-0004(90)90019-8
684. Cuervo AM, Dice JF. A receptor for the selective uptake and degradation of proteins by lysosomes. Science 1996; 273:501-3; PMID:8662539; http://dx.doi.org/10.1126/science.273.5274.501
685. Cuervo AM, Dice JF. Unique properties of lamp2a compared to other lamp2 isoforms. J Cell Sci 2000; 113:4441-50; PMID:11082038
686. Finn PF, Mesires NT, Vine M, Dice JF. Effects of small molecules on chaperone-mediated autophagy. Autophagy 2005; 1:141-5; PMID:16874031; http://dx.doi.org/10.4161/auto.1.3.2000
687. Bandyopadhyay U, Kaushik S, Varticovski L, Cuervo AM. The chaperone-mediated autophagy receptor organizes in dynamic protein complexes at the lysosomal membrane. Mol Cell Biol 2008; 28:5747-63; PMID:18644871; http://dx.doi.org/10.1128/MCB.02070-07
688. Aniento F, Emans N, Griffiths G, Gruenberg J. Cytoplasmic dynein-dependent vesicular transport from early to late endosomes. J Cell Biol 1993; 123:1373-87; PMID:8253838; http://dx.doi.org/10.1083/jcb.123.6.1373
689. Salvador N, Aguado C, Horst M, Knecht E. Import of a cytosolic protein into lysosomes by chaperone-mediated autophagy depends on its folding state. J Biol Chem 2000; 275:27447-56; PMID:10862611
690. Koga H, Martinez-Vicente M, Macian F, Verkhusha VV, Cuervo AM. A photoconvertible fluorescent reporter to track chaperone-mediated autophagy. Nat Commun 2011; 2:386; PMID:21750540; http://dx.doi.org/10.1038/ncomms1393
691. Sahu R, Kaushik S, Clement CC, Cannizzo ES, Scharf B, Follenzi A, et al. Microautophagy of cytosolic proteins by late endosomes. Dev Cell 2011; 20:131-9; PMID:21238931; http://dx.doi.org/10.1016/j.devcel.2010.12.003
692. Arndt V, Dick N, Tawo R, Dreiseidler M, Wenzel D, Hesse M, et al. Chaperone-assisted selective autophagy is essential for muscle maintenance. Curr Biol 2010; 20:143-8; PMID:20060297; http://dx.doi.org/10.1016/j.cub.2009.11.022
693. Niemann A, Baltes J, Elsässer HP. Fluorescence properties and staining behavior of monodansylpentane, a structural homologue of the lysosomotropic agent monodansylcadaverine. J Histochem Cytochem 2001; 49:177-85; PMID:11156686; http://dx.doi.org/10.1177/002215540104900205
694. Paglin S, Hollister T, Delohery T, Hackett N, McMahill M, Sphicas E, et al. A novel response of cancer cells to radiation involves autophagy and formation of acidic vesicles. Cancer Res 2001; 61:439-44; PMID:11212227
695. Florez-McClure ML, Linseman DA, Chu CT, Barker PA, Bouchard RJ, Le SS, et al. The p75 neurotrophin receptor can induce autophagy and death of cerebellar Purkinje neurons. J Neurosci 2004; 24:4498-509; PMID:15140920; http://dx.doi.org/10.1523/JNEUROSCI.5744-03.2004
696. Moriyasu Y, Hattori M, Jauh G-Y, Rogers JC. Alpha tonoplast intrinsic protein is specifically associated with vacuole membrane involved in an autophagic process. Plant Cell Physiol 2003; 44:795-802; PMID: 12941871; http://dx.doi.org/10.1093/pcp/pcg100
697. Biederbick A, Kern HF, Elsässer HP. Monodansylcadaverine (MDC) is a specific in vivo marker for autophagic vacuoles. Eur J Cell Biol 1995; 66:3-14; PMID:7750517
698. Høyer-Hansen M, Bastholm L, Mathiasen IS, Elling F, Jäättelä M. Vitamin D analog EB1089 triggers dramatic lysosomal changes and Beclin 1-mediated autophagic cell death. Cell Death Differ 2005; 12:1297-309; PMID:15905882; http://dx.doi.org/10.1038/sj.cdd.4401651
699. Munafó DB, Colombo MI. A novel assay to study autophagy: regulation of autophagosome vacuole size by amino acid deprivation. J Cell Sci 2001; 114:3619-29; PMID:11707514
700. Gutierrez MG, Munafó DB, Berón W, Colombo MI. Rab7 is required for the normal progression of the autophagic pathway in mammalian cells. J Cell Sci 2004; 117:2687-97; PMID:15138286; http://dx.doi.org/10.1242/jcs.01114
701. Freundt EC, Czapiga M, Lenardo MJ. Photoconversion of Lysotracker Red to a green fluorescent molecule. Cell Res 2007; 17:956-8; PMID:17893709; http://dx.doi.org/10.1038/cr.2007.80
702. Rubinsztein DC, Gestwicki JE, Murphy LO, Klionsky DJ. Potential therapeutic applications of autophagy. Nat Rev Drug Discov 2007; 6:304-12; PMID: 17396135; http://dx.doi.org/10.1038/nrd2272
703. Funderburk SF, Wang QJ, Yue Z. The Beclin 1-VPS34 complex–at the crossroads of autophagy and beyond. Trends Cell Biol 2010; 20:355-62; PMID:20356743; http://dx.doi.org/10.1016/j.tcb.2010.03.002
704. Levine B, Sinha S, Kroemer G. Bcl-2 family members: dual regulators of apoptosis and autophagy. Autophagy 2008; 4:600-6; PMID:18497563

dc 840–14
© Landes Bioscience. Do not distribute.

705. Simonsen A, Tooze SA. Coordination of membrane events during autophagy by multiple class III PI3-kinase complexes. J Cell Biol 2009; 186:773-82; PMID: 19797076; http://dx.doi.org/10.1083/jcb.200907014

706. Pyo JO, Jang MH, Kwon YK, Lee HJ, Jun JI, Woo HN, et al. Essential roles of Atg5 and FADD in autophagic cell death: dissection of autophagic cell death into vacuole formation and cell death. J Biol Chem 2005; 280:20722-9; PMID:15778222; http://dx.doi.org/10.1074/jbc.M413934200

707. Petiot A, Ogier-Denis E, Blommaart EF, Meijer AJ, Codogno P. Distinct classes of phosphatidylinositol 3'-kinases are involved in signaling pathways that control macroautophagy in HT-29 cells. J Biol Chem 2000; 275:992-8; PMID:10625637; http://dx.doi.org/10.1074/jbc.275.2.992

708. Harris J, Hartman M, Roche C, Zeng SG, O'Shea A, Sharp FA, et al. Autophagy controls IL-1beta secretion by targeting pro-IL-1beta for degradation. J Biol Chem 2011; 286:9587-97; PMID:21228274; http://dx.doi.org/10.1074/jbc.M110.202911

709. Cişan TO, Plantinga TS, van de Veerdonk FL, Farcaş MF, Stoffels M, Kullberg BJ, et al. Inflammasome-independent modulation of cytokine response by autophagy in human cells. PLoS One 2011; 6:e18666; PMID:21490934; http://dx.doi.org/10.1371/journal.pone.0018666

710. Kleinnijenhuis J, Oosting M, Plantinga TS, van der Meer JW, Joosten LA, Crevel RV, et al. Autophagy modulates the Mycobacterium tuberculosis-induced cytokine response. Immunology 2011; 134:341-8; PMID:21978003; http://dx.doi.org/10.1111/j.1365-2567.2011.03494.x

711. Cantino D, Mosso R, Baccino FM. Changes induced by fasting and cycloheximide in the vacuolar apparatus of rat hepatocytes. A morphometric investigation. Boll Soc Ital Biol Sper 1979; 55:1884-9; PMID:553561

712. Kovács J. Morphometric study of the effect of leupeptin, vinblastine, estron acetate and cycloheximide on the autophagic vacuole-lysosomal compartments in mouse seminal vesicle cells. Virchows Arch B Cell Pathol Incl Mol Pathol 1983; 42:83-93; PMID: 6132491

713. Papadopoulos T, Pfeifer U. Regression of rat liver autophagic vacuoles by locally applied cycloheximide. Lab Invest 1986; 54:100-7; PMID:3941538

714. Rumpelt HJ, Albring M, Thoenes W. Prevention of D-galactosamine-induced hepatocellular autophagocytosis by cycloheximide. Virchows Arch B Cell Pathol 1974; 16:195-203; PMID:4216140; http://dx.doi.org/10.1007/BF02894074

715. Rumpelt HJ, Weisbach T. Effect of cycloheximide on glucagon-induced autophagy. Quantitative examinations on hepatocytes in the rat. Am J Pathol 1978; 91:49-56; PMID:645821

716. Kovács AL, Kovács J. Autophagocytosis in mouse seminal vesicle cells in vitro. Temperature dependence and effects of vinblastine and inhibitors of protein synthesis. Virchows Arch B Cell Pathol Incl Mol Pathol 1980; 32:97-104; PMID:6102826

717. Rodemann HP, Dittmann K, Toulany M. Radiation-induced EGFR-signaling and control of DNA-damage repair. Int J Radiat Biol 2007; 83:781-91; PMID:18058366; http://dx.doi.org/10.1080/09553000701769970

718. Chaachouay H, Ohneseit P, Toulany M, Kehlbach R, Multhoff G, Rodemann HP. Autophagy contributes to resistance of tumor cells to ionizing radiation. Radiother Oncol 2011; 99:287-92; PMID:21722986; http://dx.doi.org/10.1016/j.radonc.2011.06.002

719. Apel A, Herr I, Schwarz H, Rodemann HP, Mayer A. Blocked autophagy sensitizes resistant carcinoma cells to radiation therapy. Cancer Res 2008; 68:1485-94; PMID:18316613; http://dx.doi.org/10.1158/0008-5472.CAN-07-0562

720. Eng CH, Yu K, Lucas J, White E, Abraham RT. Ammonia derived from glutaminolysis is a diffusible regulator of autophagy. Sci Signal 2010; 3:ra31; PMID: 20424262; http://dx.doi.org/10.1126/scisignal.2000911

721. Seglen PO, Gordon PB. Effects of lysosomotropic monoamines, diamines, amino alcohols, and other amino compounds on protein degradation and protein synthesis in isolated rat hepatocytes. Mol Pharmacol 1980; 18:468-75; PMID:7464813

722. Cheong H, Lindsten T, Wu J, Lu C, Thompson CB. Ammonia-induced autophagy is independent of ULK1/ULK2 kinases. Proc Natl Acad Sci U S A 2011; 108:11121-6; PMID:21690395; http://dx.doi.org/10.1073/pnas.1107969108

723. Wei P, Zhang L, Lu Y, Man N, Wen L. C60(Nd) nanoparticles enhance chemotherapeutic susceptibility of cancer cells by modulation of autophagy. Nanotechnology 2010; 21:495101; PMID:21071824; http://dx.doi.org/10.1088/0957-4484/21/49/495101

724. Lee DH, Goldberg AL. Proteasome inhibitors: valuable new tools for cell biologists. Trends Cell Biol 1998; 8:397-403; PMID:9789328; http://dx.doi.org/10.1016/S0962-8924(98)01346-4

725. Mehdi S. Cell-penetrating inhibitors of calpain. Trends Biochem Sci 1991; 16:150-3; PMID:1877091; http://dx.doi.org/10.1016/0968-0004(91)90058-4

726. Holen I, Gordon PB, Seglen PO. Inhibition of hepatocytic autophagy by okadaic acid and other protein phosphatase inhibitors. Eur J Biochem 1993; 215:113-22; PMID:8393787; http://dx.doi.org/10.1111/j.1432-1033.1993.tb18013.x

727. Sasaki K, Murata M, Yasumoto T, Mieskes G, Takai A. Affinity of okadaic acid to type-1 and type-2A protein phosphatases is markedly reduced by oxidation of its 27-hydroxyl group. Biochem J 1994; 298:259-62; PMID:8135728

728. Robinson DG, Albrecht S, Moriysu Y. The V-ATPase inhibitors concanamycin A and bafilomycin A lead to Golgi swelling in tobacco BY-2 cells. Protoplasma 2004; 224:255-60; PMID:15614486; http://dx.doi.org/10.1007/s00709-004-0070-6

729. Wu YC, Wu WK, Li Y, Yu L, Li ZJ, Wong CC, et al. Inhibition of macroautophagy by bafilomycin A1 lowers proliferation and induces apoptosis in colon cancer cells. Biochem Biophys Res Commun 2009; 382:451-6; PMID:19289106; http://dx.doi.org/10.1016/j.bbrc.2009.03.051

730. Yamamoto A, Tagawa Y, Yoshimori T, Moriyama Y, Masaki R, Tashiro Y. Bafilomycin A1 prevents maturation of autophagic vacuoles by inhibiting fusion between autophagosomes and lysosomes in rat hepatoma cell line, H-4-II-E cells. Cell Struct Funct 1998; 23:33-42; PMID:9639028; http://dx.doi.org/10.1247/csf.23.33

731. Ostenfeld MS, Høyer-Hansen M, Bastholm L, Fehrenbacher N, Olsen OD, Groth-Pedersen L, et al. Anti-cancer agent siramesine is a lysosomotropic detergent that induces cytoprotective autophagosome accumulation. Autophagy 2008; 4:487-99; PMID: 18305408

732. Matsuoka K, Higuchi T, Maeshima M, Nakamura K. A vacuolar-type H +-ATPase in a nonvacuolar organelle is required for the sorting of soluble vacuolar protein precursors in tobacco cells. Plant Cell 1997; 9:533-46; PMID:12237363; http://dx.doi.org/10.1105/tpc.9.4.533

733. Arstila AU, Nuuja IJ, Trump BF. Studies on cellular autophagocytosis. Vinblastine-induced autophagy in the rat liver. Exp Cell Res 1974; 87:249-52; PMID: 4415937; http://dx.doi.org/10.1016/0014-4827(74)90477-7

734. Hirsimäki Y, Arstila AU, Trump BF. Autophagocytosis: in vitro induction by microtuble poisons. Exp Cell Res 1975; 92:11-4; PMID:1169154; http://dx.doi.org/10.1016/0014-4827(75)90630-8

735. Kominami E, Hashida S, Khairallah EA, Katunuma N. Sequestration of cytoplasmic enzymes in an autophagic vacuole-lysosomal system induced by injection of leupeptin. J Biol Chem 1983; 258:6093-100; PMID: 6133857

736. Réz G, Fellinger E, Réti M, Biczó I, Kovács AL. Time course of quantitative morphological changes of the autophagic-lysosomal compartment of murine seminal vesicle epithelial cells under the influence of vinblastine. J Submicrosc Cytol Pathol 1990; 22:529-34; PMID:2282639

737. Oliva O, Réz G, Pálfia Z, Fellinger E. Dynamics of vinblastine-induced autophagocytosis in murine pancreatic acinar cells: influence of cycloheximide post-treatments. Exp Mol Pathol 1992; 56:76-86; PMID: 1547871; http://dx.doi.org/10.1016/0014-4800(92)90025-7

738. von Haefen C, Sifringer M, Menk M, Spies CD. Ethanol enhances susceptibility to apoptotic cell death via down-regulation of autophagy-related proteins. Alcohol Clin Exp Res 2011; 35:1381-91; PMID: 21410490

739. Krüger U, Wang Y, Kumar S, Mandelkow EM. Autophagic degradation of tau in primary neurons and its enhancement by trehalose. Neurobiol Aging 2011; In press; PMID:22169203; http://dx.doi.org/10.1016/j.neurobiolaging.2011.11.009

740. Williams A, Sarkar S, Cuddon P, Trofi EK, Saiki S, Siddiqi FH, et al. Novel targets for Huntington's disease in an mTOR-independent autophagy pathway. Nat Chem Biol 2008; 4:295-305; PMID:18391949; http://dx.doi.org/10.1038/nchembio.79

741. Palomo GM, Cerrato T, Gargini R, Diaz-Nido J. Silencing of frataxin gene expression triggers p53-dependent apoptosis in human neuron-like cells. Hum Mol Genet 2011; 20:2807-22; PMID:21531789; http://dx.doi.org/10.1093/hmg/ddr187

742. Feldman ME, Apsel B, Uotila A, Loewith R, Knight ZA, Ruggero D, et al. Active-site inhibitors of mTOR target rapamycin-resistant outputs of mTORC1 and mTORC2. PLoS Biol 2009; 7:e38; PMID:19209957; http://dx.doi.org/10.1371/journal.pbio.1000038

743. Fleming A, Noda T, Yoshimori T, Rubinsztein DC. Chemical modulators of autophagy as biological probes and potential therapeutics. Nat Chem Biol 2011; 7:9-17; PMID:21164513; http://dx.doi.org/10.1038/nchembio.500

744. Yu K, Toral-Barza L, Shi C, Zhang WG, Lucas J, Shor B, et al. Biochemical, cellular, and in vivo activity of novel ATP-competitive and selective inhibitors of the mammalian target of rapamycin. Cancer Res 2009; 69:6232-40; PMID:19584280; http://dx.doi.org/10.1158/0008-5472.CAN-09-0299

745. Chresta CM, Davies BR, Hickson I, Harding T, Cosulich S, Critchlow SE, et al. AZD8055 is a potent, selective, and orally bioavailable ATP-competitive mammalian target of rapamycin kinase inhibitor with in vitro and in vivo antitumor activity. Cancer Res 2010; 70:288-98; PMID:20028854; http://dx.doi.org/10.1158/0008-5472.CAN-09-1751

746. Roscic A, Baldo B, Crochemore C, Marcellin D, Paganetti P. Induction of autophagy with catalytic mTOR inhibitors reduces huntingtin aggregates in a neuronal cell model. J Neurochem 2011; 119:398-407; PMID:21854390; http://dx.doi.org/10.1111/j.1471-4159.2011.07435.x

747. Fan QW, Cheng C, Hackett C, Feldman M, Houseman BT, Nicolaides T, et al. Akt and autophagy cooperate to promote survival of drug-resistant glioma. Sci Signal 2010; 3:ra81; PMID:21062993; http://dx.doi.org/10.1126/scisignal.2001017

748. Sakagami H, Kawase M, Wakabayashi H, Kurihara T. Factors that affect the type of cell death induced by chemicals. Autophagy 2007; 3:493-5; PMID:17611389

749. Doelling JH, Walker JM, Friedman EM, Thompson AR, Vierstra RD. The APG8/12-activating enzyme APG7 is required for proper nutrient recycling and senescence in Arabidopsis thaliana. J Biol Chem 2002; 277:33105-14; PMID:12070171; http://dx.doi.org/10.1074/jbc.M204630200

750. Fimia GM, Stoykova A, Romagnoli A, Giunta L, Di Bartolomeo S, Nardacci R, et al. Ambra1 regulates autophagy and development of the nervous system. Nature 2007; 447:1121-5; PMID:17589504

751. Kuma A, Hatano M, Matsui M, Yamamoto A, Nakaya H, Yoshimori T, et al. The role of autophagy during the early neonatal starvation period. Nature 2004; 432:1032-6; PMID:15525940; http://dx.doi.org/10.1038/nature03029

752. Zhu H, Wu H, Liu X, Li B, Chen Y, Ren X, et al. Regulation of autophagy by a beclin 1-targeted microRNA, miR-30a, in cancer cells. Autophagy 2009; 5:816-23; PMID:19535919

753. Hamacher-Brady A, Brady NR, Logue SE, Sayen MR, Jinno M, Kirshenbaum LA, et al. Response to myocardial ischemia/reperfusion injury involves Bnip3 and autophagy. Cell Death Differ 2007; 14:146-57; PMID:16645637; http://dx.doi.org/10.1038/sj.cdd.4401936

754. Yang L, Li P, Fu S, Calay ES, Hotamisligil GS. Defective hepatic autophagy in obesity promotes ER stress and causes insulin resistance. Cell Metab 2010; 11:467-78; PMID:20519119; http://dx.doi.org/10.1016/j.cmet.2010.04.005

755. Poeck H, Besch R, Maihoefer C, Renn M, Tormo D, Morskaya SS, et al. 5'-Triphosphate-siRNA: turning gene silencing and Rig-I activation against melanoma. Nat Med 2008; 14:1256-63; PMID:18978796; http://dx.doi.org/10.1038/nm.1887

756. Delgado MA, Elmaoued RA, Davis AS, Kyei G, Deretic V. Toll-like receptors control autophagy. EMBO J 2008; 27:1110-21; PMID:18337753; http://dx.doi.org/10.1038/emboj.2008.31

757. Pua HH, Dzhagalov I, Chuck M, Mizushima N, He YW. A critical role for the autophagy gene Atg5 in T cell survival and proliferation. J Exp Med 2007; 204:25-31; PMID:17190837; http://dx.doi.org/10.1084/jem.20061303

758. Miller BC, Zhao Z, Stephenson LM, Cadwell K, Pua HH, Lee HK, et al. The autophagy gene ATG5 plays an essential role in B lymphocyte development. Autophagy 2008; 4:309-14; PMID:18188005

759. Lee JS, Li Q, Lee JY, Lee SH, Jeong JH, Lee HR, et al. FLIP-mediated autophagy regulation in cell death control. Nat Cell Biol 2009; 11:1355-62; PMID: 19838173; http://dx.doi.org/10.1038/ncb1980

760. Kyei GB, Dinkins C, Davis AS, Roberts E, Singh SB, Dong C, et al. Autophagy pathway intersects with HIV-1 biosynthesis and regulates viral yields in macrophages. J Cell Biol 2009; 186:255-68; PMID: 19635843; http://dx.doi.org/10.1083/jcb.200903070

761. Kimball SR, Siegfried BA, Jefferson LS. Glucagon represses signaling through the mammalian target of rapamycin in rat liver by activating AMP-activated protein kinase. J Biol Chem 2004; 279:54103-9; PMID:15494402; http://dx.doi.org/10.1074/jbc.M410755200

762. Blommaart EF, Luiken JJ, Blommaart PJ, van Woerkom GM, Meijer AJ. Phosphorylation of ribosomal protein S6 is inhibitory for autophagy in isolated rat hepatocytes. J Biol Chem 1995; 270:2320-6; PMID:7836465; http://dx.doi.org/10.1074/jbc.270.5.2320

763. Klionsky DJ, Meijer AJ, Codogno P, Neufeld TP, Scott RC. Autophagy and p70S6 kinase. Autophagy 2005; 1:59-60, discussion 60-1; PMID:16874035; http://dx.doi.org/10.4161/auto.1.1.1536

764. Noda T, Ohsumi Y. Tor, a phosphatidylinositol kinase homologue, controls autophagy in yeast. J Biol Chem 1998; 273:3963-6; PMID:9461583; http://dx.doi.org/10.1074/jbc.273.7.3963

765. Sarkar S, Floto RA, Berger Z, Imarisio S, Cordenier A, Pasco M, et al. Lithium induces autophagy by inhibiting inositol monophosphatase. J Cell Biol 2005; 170:1101-11; PMID:16186256; http://dx.doi.org/10.1083/jcb.200504035

766. Høyer-Hansen M, Bastholm L, Szyniarowski P, Campanella M, Szabadkai G, Farkas T, et al. Control of macroautophagy by calcium, calmodulin-dependent kinase kinase-beta, and Bcl-2. Mol Cell 2007; 25:193-205; PMID:17244528; http://dx.doi.org/10.1016/j.molcel.2006.12.009

767. Furuya N, Liang XH, Levine B. Autophagy and cancer. In: Klionsky DJ, ed. Autophagy. Georgetown, TX: Landes Bioscience, 2004:241-55.

768. de Medina P, Paillasse MR, Segala G, Khallouki F, Brillouet S, Dalenc F, et al. Importance of cholesterol and oxysterols metabolism in the pharmacology of tamoxifen and other AEBS ligands. Chem Phys Lipids 2011; PMID:21641337; http://dx.doi.org/10.1016/j.chemphyslip.2011.05.005

769. de Medina P, Payré B, Boubekeur N, Bertrand-Michel J, Tercé F, Silvente-Poirot S, et al. Ligands of the antiestrogen-binding site induce active cell death and autophagy in human breast cancer cells through the modulation of cholesterol metabolism. Cell Death Differ 2009; 16:1372-84; PMID:19521424; http://dx.doi.org/10.1038/cdd.2009.62

770. Sarkar S, Perlstein EO, Imarisio S, Pineau S, Cordenier A, Maglathlin RL, et al. Small molecules enhance autophagy and reduce toxicity in Huntington's disease models. Nat Chem Biol 2007; 3:331-8; PMID: 17486044; http://dx.doi.org/10.1038/nchembio883

771. Zhang L, Yu J, Pan H, Hu P, Hao Y, Cai W, et al. Small molecule regulators of autophagy identified by an image-based high-throughput screen. Proc Natl Acad Sci U S A 2007; 104:19023-8; PMID:18024584; http://dx.doi.org/10.1073/pnas.0709695104

772. Cárdenas C, Miller RA, Smith I, Bui T, Molgó J, Müller M, et al. Essential regulation of cell bioenergetics by constitutive InsP3 receptor Ca^{2+} transfer to mitochondria. Cell 2010; 142:270-83; PMID:20655468; http://dx.doi.org/10.1016/j.cell.2010.06.007

773. Vicencio JM, Ortiz C, Criollo A, Jones AW, Kepp O, Galluzzi L, et al. The inositol 1,4,5-trisphosphate receptor regulates autophagy through its interaction with Beclin 1. Cell Death Differ 2009; 16:1006-17; PMID:19325567; http://dx.doi.org/10.1038/cdd.2009.34

774. Dayan F, Bilton RL, Lafermière J, Trottier E, Roux D, Pouysségur J, et al. Hypoxia-induced autophagy is mediated through hypoxia-inducible factor induction of BNIP3 and BNIP3L via their BH3 domains. Mol Cell Biol 2009; 29:2570-81; PMID: 19273585; http://dx.doi.org/10.1128/MCB.00166-09

775. Bellot G, Garcia-Medina R, Gounon P, Chiche J, Roux D, Pouysségur J, et al. Hypoxia-induced autophagy is mediated through hypoxia-inducible factor induction of BNIP3 and BNIP3L via their BH3 domains. Mol Cell Biol 2009; 29:2570-81; PMID: 19273585; http://dx.doi.org/10.1128/MCB.00166-09

776. Yamashita S, Yurimoto H, Murakami D, Yoshikawa M, Oku M, Sakai Y. Lag-phase autophagy in the methylotrophic yeast *Pichia pastoris*. Genes Cells 2009; 14:861-70; PMID:19549169; http://dx.doi.org/10.1111/j.1365-2443.2009.01316.x

777. van Zutphen T, Baerends RJ, Susanna KA, de Jong A, Kuipers OP, Veenhuis M, et al. Adaptation of *Hansenula polymorpha* to methanol: a transcriptome analysis. BMC Genomics 2010; 11:1; PMID:20044946; http://dx.doi.org/10.1186/1471-2164-11-1

778. Inoue Y, Suzuki T, Hattori M, Yoshimoto K, Ohsumi Y, Moriyasu Y. AtATG genes, homologs of yeast autophagy genes, are involved in constitutive autophagy in Arabidopsis root tip cells. Plant Cell Physiol 2006; 47:1641-52; PMID:17085765; http://dx.doi.org/10.1093/pcp/pcl031

779. Yano K, Suzuki T, Moriyasu Y. Constitutive autophagy in plant root cells. Autophagy 2007; 3:360-2; PMID:17426438

780. Gordon PB, Kisen GO, Kovács AL, Seglen PO. Experimental characterization of the autophagic-lysosomal pathway in isolated rat hepatocytes. Biochem Soc Symp 1989; 55:129-43; PMID:2619764

781. Poli A, Gordon PB, Schwarze PE, Grinde B, Seglen PO. Effects of insulin and anchorage on hepatocytic protein metabolism and amino acid transport. J Cell Sci 1981; 48:1-18; PMID:7024288

782. Schliess F, Reissmann R, Reinehr R, vom Dahl S, Häussinger D. Involvement of integrins and Src in insulin signaling toward autophagic proteolysis in rat liver. J Biol Chem 2004; 279:21294-301; PMID: 14985360; http://dx.doi.org/10.1074/jbc.M313901200

783. vom Dahl S, Dombrowski F, Schmitt M, Schliess F, Pfeifer U, Häussinger D. Cell hydration controls autophagosome formation in rat liver in a microtubule-dependent way downstream from p38 MAPK activation. Biochem J 2001; 354:31-6; PMID:11171076; http://dx.doi.org/10.1042/0264-6021:3540031

784. vom Dahl S, Stoll B, Gerok W, Häussinger D. Inhibition of proteolysis by cell swelling in the liver requires intact microtubular structures. Biochem J 1995; 308:529-36; PMID:7772037

785. Kovacs AL, Zhang H. Role of autophagy in *Caenorhabditis elegans*. FEBS Lett 2010; 584:1335-41; PMID:20138173; http://dx.doi.org/10.1016/j.febslet.2010.02.002

786. Zhang Y, Yan L, Zhou Z, Yang P, Tian E, Zhang K, et al. SEPA-1 mediates the specific recognition and degradation of P granule components by autophagy in *C. elegans*. Cell 2009; 136:308-21; PMID:19167335; http://dx.doi.org/10.1016/j.cell.2008.12.022

787. Morselli E, Maiuri MC, Markaki M, Megalou E, Pasparaki A, Palikaras K, et al. Caloric restriction and resveratrol promote longevity through the Sirtuin-1-dependent induction of autophagy. Cell Death Dis 2010; 1:e10; PMID:21364612; http://dx.doi.org/10.1038/cddis.2009.8

788. Samara C, Syntichaki P, Tavernarakis N. Autophagy is required for necrotic cell death in Caenorhabditis elegans. Cell Death Differ 2008; 15:105-12; PMID: 17901876; http://dx.doi.org/10.1038/sj.cdd.4402231

789. Alberti A, Michelet X, Djeddi A, Legouis R. The autophagosomal protein LGG-2 acts synergistically with LGG-1 in dauer formation and longevity in *C. elegans*. Autophagy 2010; 6:622-33; PMID: 20523114; http://dx.doi.org/10.4161/auto.6.5.12252

790. Kang C, You YJ, Avery L. Dual roles of autophagy in the survival of *Caenorhabditis elegans* during starvation. Genes Dev 2007; 21:2161-71; PMID:17785524; http://dx.doi.org/10.1101/gad.1573107

791. Willig KI, Kellner RR, Medda R, Hein B, Jakobs S, Hell SW. Nanoscale resolution in GFP-based microscopy. Nat Methods 2006; 3:721-3; PMID:16896340; http://dx.doi.org/10.1038/nmeth922

792. Huang B, Bates M, Zhuang X. Super-resolution fluorescence microscopy. Annu Rev Biochem 2009; 78:993-1016; PMID:19489737; http://dx.doi.org/10.1146/annurev.biochem.77.061906.092014

793. Alers S, Löffler AS, Paasch F, Dieterle AM, Keppler H, Lauber K, et al. Atg13 and FIP200 act independently of Ulk1 and Ulk2 in autophagy induction. Autophagy 2011; 7:1424-33; PMID:22024743; http://dx.doi.org/10.4161/auto.7.12.18027

794. Brown WR, Hubbard SJ, Tickle C, Wilson SA. The chicken as a model for large-scale analysis of vertebrate gene function. Nat Rev Genet 2003; 4:87-98; PMID: 12560806; http://dx.doi.org/10.1038/nrg998

dc 840 14

795. Baba TW, Giroir BP, Humphries EH. Cell lines derived from avian lymphomas exhibit two distinct phenotypes. Virology 1985; 144:139-51; PMID: 2998040; http://dx.doi.org/10.1016/0042-6822(85)90312-5

796. Shelly S, Lukinova N, Bambina S, Berman A, Cherry S. Autophagy is an essential component of Drosophila immunity against vesicular stomatitis virus. Immunity 2009; 30:588-98; PMID:19362021; http://dx.doi.org/10.1016/j.immuni.2009.02.009

797. Hou YC, Chittaranjan S, Barbosa SG, McCall K, Gorski SM. Effector caspase Dcp-1 and IAP protein Bruce regulate starvation-induced autophagy during *Drosophila melanogaster* oogenesis. J Cell Biol 2008; 182:1127-39; PMID:18794330; http://dx.doi.org/10.1083/jcb.200712091

798. Josefsen L, Droce A, Sondergaard TE, Sørensen JL, Bormann J, Schäfer W, et al. Autophagy provides nutrients for nonassimilating fungal structures and is necessary for plant colonization but not for infection in the necrotrophic plant pathogen Fusarium graminearum. Autophagy 2012; 8; In press; PMID:22240663

799. Nadal M, Gold SE. The autophagy genes *ATG8* and *ATG1* affect morphogenesis and pathogenicity in *Ustilago maydis*. Mol Plant Pathol 2010; 11:463-78; PMID:20618705; http://dx.doi.org/10.1111/j.1364-3703.2010.00620.x

800. Pollack JK, Harris SD, Marten MR. Autophagy in filamentous fungi. Fungal Genet Biol 2009; 46:1-8; PMID:19010432; http://dx.doi.org/10.1016/j.fgb.2008.10.010

801. Richie DL, Fuller KK, Fortwendel J, Miley MD, McCarthy JW, Feldmesser M, et al. Unexpected link between metal ion deficiency and autophagy in Aspergillus fumigatus. Eukaryot Cell 2007; 6:2437-47; PMID:17921348; http://dx.doi.org/10.1128/EC.00224-07

802. Pinan-Lucarré B, Balguerie A, Clavé C. Accelerated cell death in Podospora autophagy mutants. Eukaryot Cell 2005; 4:1765-74; PMID:16278443; http://dx.doi.org/10.1128/EC.4.11.1765-1774.2005

803. Asakura M, Ninomiya S, Sugimoto M, Oku M, Yamashita S, Okuno T, et al. Atg26-mediated pexophagy is required for host invasion by the plant pathogenic fungus *Colletotrichum orbiculare*. Plant Cell 2009; 21:1291-304; PMID:19363139; http://dx.doi.org/10.1105/tpc.108.060996

804. Liu X-H, Lu J-P, Zhang L, Dong B, Min H, Lin F-C. Involvement of a *Magnaporthe grisea* serine/threonine kinase gene, Mg*ATG1*, in appressorium turgor and pathogenesis. Eukaryot Cell 2007; 6:997-1005; PMID: 17416896; http://dx.doi.org/10.1128/EC.00011-07

805. Nguyen LN, Bormann J, Le GT, Stärkel C, Olsson S, Nosanchuk JD, et al. Autophagy-related lipase FgATG15 of Fusarium graminearum is important for lipid turnover and plant infection. Fungal Genet Biol 2011; 48:217-24; PMID:21094265; http://dx.doi.org/10.1016/j.fgb.2010.11.004

806. Deng YZ, Ramos-Pamplona M, Naqvi NI. Methods for functional analysis of macroautophagy in filamentous fungi. Methods Enzymol 2008; 451:295-310; PMID: 19185728; http://dx.doi.org/10.1016/S0076-6879(08)03220-5

807. Berger B, Abdalla FC, Cruz-Landim C. Effect of narcosis with CO2 on the ovarian development in queens of *Apis mellifera* (Hymenoptera, Apini). Sociobiology 2005; 45:261-70.

808. Silva-Zacarin ECM, Tomaino GA, Brocheto-Braga MR, Taboga SR, De Moraes RL. Programmed cell death in the larval salivary glands of *Apis mellifera* (Hymenoptera, Apidae). J Biosci 2007; 32:309-28; PMID:17435323; http://dx.doi.org/10.1007/s12038-007-0031-2

809. Gregorc A, Bowen ID. Programmed cell death in the honey-bee (*Apis mellifera* L.) larvae midgut. Cell Biol Int 1997; 21:151-8; PMID:9151991; http://dx.doi.org/10.1006/cbir.1997.0127

810. Navajas M, Migeon A, Alaux C, Martin-Magniette M, Robinson G, Evans J, et al. Differential gene expression of the honey bee *Apis mellifera* associated with *Varroa destructor* infection. BMC Genomics 2008; 9:301; PMID:18578863; http://dx.doi.org/10.1186/1471-2164-9-301

811. Spruessel A, Steimann G, Jung M, Lee SA, Carr T, Fentz AK, et al. Tissue ischemia time affects gene and protein expression patterns within minutes following surgical tumor excision. Biotechniques 2004; 36:1030-7; PMID:15211754

812. Espina V, Edmiston KH, Heiby M, Pierobon M, Sciro M, Merritt B, et al. A portrait of tissue phosphoprotein stability in the clinical tissue procurement process. Mol Cell Proteomics 2008; 7:1998-2018; PMID:18667411; http://dx.doi.org/10.1074/mcp.M700596-MCP200

813. Barth S, Glick D, Macleod KF. Autophagy: assays and artifacts. J Pathol 2010; 221:117-24; PMID: 20225337; http://dx.doi.org/10.1002/path.2694

814. Nixon RA, Wegiel J, Kumar A, Yu WH, Peterhoff C, Cataldo A, et al. Extensive involvement of autophagy in Alzheimer disease: an immuno-electron microscopy study. J Neuropathol Exp Neurol 2005; 64:113-22; PMID:15751225

815. Vanhorebeek I, Gunst J, Derde S, Derese I, Boussemaere M, Güiza F, et al. Insufficient activation of autophagy allows cellular damage to accumulate in critically ill patients. J Clin Endocrinol Metab 2011; 96:E633-45; PMID:21270330; http://dx.doi.org/10.1210/jc.2010-2563

816. Nyman E, Brännmark C, Palmér R, Brugård J, Nyström FH, Strålfors P, et al. A hierarchical whole-body modeling approach elucidates the link between in Vitro insulin signaling and in Vivo glucose homeostasis. J Biol Chem 2011; 286:26028-41; PMID:21572040; http://dx.doi.org/10.1074/jbc.M110.188987

817. Buzgariu W, Chera S, Galliot B. Methods to investigate autophagy during starvation and regeneration in hydra. Methods Enzymol 2008; 451:409-37; PMID:19185734; http://dx.doi.org/10.1016/S0076-6879(08)03226-6

818. Chera S, Buzgariu W, Ghila L, Galliot B. Autophagy in Hydra: a response to starvation and stress in early animal evolution. Biochim Biophys Acta 2009; 1793:1432-43; PMID:19362111

819. Chera S, de Rosa R, Miljkovic-Licina M, Dobretz K, Ghila L, Kaloulis K, et al. Silencing of the hydra serine protease inhibitor Kazal1 gene mimics the human SPINK1 pancreatic phenotype. J Cell Sci 2006; 119:846-57; PMID:16478786; http://dx.doi.org/10.1242/jcs.02807

820. Galliot B. Autophagy and self-preservation: a step ahead from cell plasticity? Autophagy 2006; 2:231-3; PMID:16874084

821. Galliot B, Miljkovic-Licina M, de Rosa R, Chera S. Hydra, a niche for cell and developmental plasticity. Semin Cell Dev Biol 2006; 17:492-502; PMID: 16807002; http://dx.doi.org/10.1016/j.semcdb.2006.05.005

822. Sala-Mercado JA, Wider J, Undyala VV, Jahania S, Yoo W, Mentzer RM, Jr., et al. Profound cardioprotection with chloramphenicol succinate in the swine model of myocardial ischemia-reperfusion injury. Circulation 2010; 122(Suppl):S179-84; PMID:20837911; http://dx.doi.org/10.1161/CIRCULATIONAHA.109.928242

823. Sobolewska A, Motyl T, Gajewska M. Role and regulation of autophagy in the development of acinar structures formed by bovine BME-UV1 mammary epithelial cells. Eur J Cell Biol 2011; 90:854-64; PMID:21868124; http://dx.doi.org/10.1016/j.ejcb.2011.06.007

824. Motyl T, Gajewska M, Zarzynska J, Sobolewska A, Gajkowska B. Regulation of autophagy in bovine mammary epithelial cells. Autophagy 2007; 3:484-6; PMID:17592247

825. Sobolewska A, Gajewska M, Zarzyńska J, Gajkowska B, Motyl T. IGF-I, EGF, and sex steroids regulate autophagy in bovine mammary epithelial cells via the mTOR pathway. Eur J Cell Biol 2009; 88:117-30; PMID:19013662; http://dx.doi.org/10.1016/j.ejcb.2008.09.004

826. Facey CO, Lockshin RA. The execution phase of autophagy associated PCD during insect metamorphosis. Apoptosis 2010; 15:639-52; PMID:20405221; http://dx.doi.org/10.1007/s10495-010-0499-3

827. Malagoli D, Abdalla FC, Cao Y, Feng Q, Fujisaki K, Gregorc A, et al. Autophagy and its physiological relevance in arthropods: Current knowledge and perspectives. Autophagy 2010; 6:575-88; PMID: 20458176; http://dx.doi.org/10.4161/auto.6.5.11962

828. Mpakou VE, Nezis IP, Stravopodis DJ, Margaritis LH, Papassideri IS. Programmed cell death of the ovarian nurse cells during oogenesis of the silkmoth *Bombyx mori*. Dev Growth Differ 2006; 48:419-28; PMID: 16961589; http://dx.doi.org/10.1111/j.1440-169X.2006.00878.x

829. Mpakou VE, Nezis IP, Stravopodis DJ, Margaritis LH, Papassideri IS. Different modes of programmed cell death during oogenesis of the silkmoth *Bombyx mori*. Autophagy 2008; 4:97-100; PMID:17986869

830. Sumithra P, Britto CP, Krishnan M. Modes of cell death in the pupal perivisceral fat body tissue of the silkworm *Bombyx mori* L. Cell Tissue Res 2010; 339:349-58; PMID:19949813; http://dx.doi.org/10.1007/s00441-009-0898-3

831. Tettamanti G, Grimaldi A, Casartelli M, Ambrosetti E, Ponti B, Congiu T, et al. Programmed cell death and stem cell differentiation are responsible for midgut replacement in *Heliothis virescens* during prepupal instar. Cell Tissue Res 2007; 330:345-59; PMID: 17661086; http://dx.doi.org/10.1007/s00441-007-0449-8

832. Gonciu E, Parlak O. Some autophagic and apoptotic features of programmed cell death in the anterior silk glands of the silkworm, *Bombyx mori*. Autophagy 2008; 4:1069-72; PMID:18838861

833. Zhou S, Zhou Q, Liu Y, Wang S, Wen D, He Q, et al. Two Tor genes in the silkworm *Bombyx mori*. Insect Mol Biol 2010; 19:727-35; PMID:20609020; http://dx.doi.org/10.1111/j.1365-2583.2010.01026.x

834. Zhang X, Hu ZY, Li WF, Li QR, Deng XJ, Yang WY, et al. Systematic cloning and analysis of autophagy-related genes from the silkworm *Bombyx mori*. BMC Mol Biol 2009; 10:50; PMID:19470186; http://dx.doi.org/10.1186/1471-2199-10-50

835. Li Q, Deng X, Huang Z, Zheng S, Tettamanti G, Cao Y, et al. Expression of autophagy-related genes in the anterior silk gland of the silkworm (*Bombyx mori*) during metamorphosis. Can J Zool 2011; 89:1019-26; http://dx.doi.org/10.1139/z11-075

836. Thomé RG, Santos HB, Arantes FP, Domingos FF, Bazzoli N, Rizzo E. Dual roles for autophagy during follicular atresia in fish ovary. Autophagy 2009; 5:117-9; PMID:19011378; http://dx.doi.org/10.4161/auto.5.1.7302

837. Santos HB, Thomé RG, Arantes FP, Sato Y, Bazzoli N, Rizzo E. Ovarian follicular atresia is mediated by heterophagy, autophagy, and apoptosis in *Prochilodus argenteus* and *Leporinus taeniatus* (Teleostei: Characiformes). Theriogenology 2008; 70:1449-60; PMID:18701155; http://dx.doi.org/10.1016/j.theriogenology.2008.06.091

838. Santos HB, Sato Y, Moro L, Bazzoli N, Rizzo E. Relationship among follicular apoptosis, integrin betal and collagen type IV during early ovarian regression in the teleost Prochilodus argenteus after induced spawning. Cell Tissue Res 2008; 332:159-70; PMID: 18193286; http://dx.doi.org/10.1007/s00441-007-0540-1

839. Santos HB, Rizzo E, Bazzoli N, Sato Y, Moro L. Ovarian regression and apoptosis in the South American teleost *Leporinus taeniatus* Lutken (Characiformes, Anostomidae) from the São Francisco Basin. J Fish Biol 2005; 67:1446-59; http://dx.doi.org/10.1111/j.1095-8649.2005.00854.x

840. Couve E, Schmachtenberg O. Autophagic activity and aging in human odontoblasts. J Dent Res 2011; 90:523-8; PMID:21212314; http://dx.doi.org/10.1177/0022034510393347

841. González-Estévez C. Autophagy in freshwater planarians. Methods Enzymol 2008; 451:439-65; PMID: 19185735; http://dx.doi.org/10.1016/S0076-6879(08)03227-8

842. González-Estévez C, Felix DA, Aboobaker AA, Saló E. Gtdap-1 promotes autophagy and is required for planarian remodeling during regeneration and starvation. Proc Natl Acad Sci U S A 2007; 104:13373-8; PMID:17686979; http://dx.doi.org/10.1073/pnas.0703588104

843. Toyooka K, Moriyasu Y, Goto Y, Takeuchi M, Fukuda H, Matsuoka K. Protein aggregates are transported to vacuoles by a macroautophagic mechanism in nutrient-starved plant cells. Autophagy 2006; 2:96-106; PMID:16874101

844. Svenning S, Lamark T, Krause K, Johansen T. Plant NBR1 is a selective autophagy substrate and a functional hybrid of the mammalian autophagic adapters NBR1 and p62/SQSTM1. Autophagy 2011; 7:993-1010; PMID:21606687; http://dx.doi.org/10.4161/auto.7.9.16389

845. Zientara-Rytter K, Lukomska J, Moniuszko G, Gwozdecki R, Surowiecki P, Lewandowska M, et al. Identification and functional analysis of Joka2, a tobacco member of the family of selective autophagy cargo receptors. Autophagy 2011; 7:1145-58; PMID: 21670587; http://dx.doi.org/10.4161/auto.7.10.16617

846. Takeshige K, Baba M, Tsuboi S, Noda T, Ohsumi Y. Autophagy in yeast demonstrated with proteinase-deficient mutants and conditions for its induction. J Cell Biol 1992; 119:301-11; PMID:1400575; http://dx.doi.org/10.1083/jcb.119.2.301

847. Moriyasu Y, Ohsumi Y. Autophagy in tobacco suspension-cultured cells in response to sucrose starvation. Plant Physiol 1996; 111:1233-41; PMID: 12226358

848. Calvo-Garrido J, Carilla-Latorre S, Kubohara Y, Santos-Rodrigo N, Mesquita A, Soldati T, et al. Autophagy in Dictyostelium: genes and pathways, cell death and infection. Autophagy 2010; 6:686-701; PMID:20603609; http://dx.doi.org/10.4161/auto.6.6.12513

849. Tung SM, Unal C, Ley A, Peña C, Tunggal B, Noegel AA, et al. Loss of Dictyostelium ATG9 results in a pleiotropic phenotype affecting growth, development, phagocytosis and clearance and replication of Legionella pneumophila. Cell Microbiol 2010; 12:765-80; PMID:20070309; http://dx.doi.org/10.1111/j.1462-5822.2010.01432.x

850. Bozzaro S, Eichinger L. The professional phagocyte *Dictyostelium discoideum* as a model host for bacterial pathogens. Curr Drug Targets 2011; 12:942-54; PMID:21366522; http://dx.doi.org/10.2174/138945011795677782

851. Duszenko M, Ginger ML, Brennand A, Gualdrón-López M, Colombo MI, Coombs GH, et al. Autophagy in protists. Autophagy 2011; 7:127-58; PMID:20962583; http://dx.doi.org/10.4161/auto.7.2.13310

852. Barquilla A, Crespo JL, Navarro M. Rapamycin inhibits trypanosome cell growth by preventing TOR complex 2 formation. Proc Natl Acad Sci U S A 2008; 105:14579-84; PMID:18796613; http://dx.doi.org/10.1073/pnas.0802668105

853. Morais P, Lamas J, Sanmartín ML, Orallo F, Leiro J. Resveratrol induces mitochondrial alterations, autophagy and a cryptobiosis-like state in scuticociliates. Protist 2009; 160:552-64; PMID:19640787; http://dx.doi.org/10.1016/j.protis.2009.04.004

854. Yakisich JS, Kapler GM. The effect of phosphoinositide 3-kinase inhibitors on programmed nuclear degradation in Tetrahymena and fate of surviving nuclei. Cell Death Differ 2004; 11:1146-9; PMID: 15257301; http://dx.doi.org/10.1038/sj.cdd.4401473

855. Akematsu T, Pearlman RE, Endoh H. Gigantic macroautophagy in programmed nuclear death of Tetrahymena thermophila. Autophagy 2010; 6:901-11; PMID:20798592; http://dx.doi.org/10.4161/auto.6.7.13287

856. Thorgaard GH, Bailey GS, Williams D, Buhler DR, Kaattari SL, Ristow SS, et al. Status and opportunities for genomics research with rainbow trout. Comp Biochem Physiol B Biochem Mol Biol 2002; 133:609-46; PMID:12470823; http://dx.doi.org/10.1016/S1096-4959(02)00167-7

857. Govoroun M, Le Gac F, Guiguen Y. Generation of a large scale repertoire of Expressed Sequence Tags (ESTs) from normalised rainbow trout cDNA libraries. BMC Genomics 2006; 7:196; PMID:16887034; http://dx.doi.org/10.1186/1471-2164-7-196

858. Rexroad CE, 3rd, Lee Y, Keele JW, Karamycheva S, Brown G, Koop B, et al. Sequence analysis of a rainbow trout cDNA library and creation of a gene index. Cytogenet Genome Res 2003; 102:347-54; PMID: 14970727; http://dx.doi.org/10.1159/000075773

859. Rise ML, von Schalburg KR, Brown GD, Mawer MA, Devlin RH, Kuipers N, et al. Development and application of a salmonid EST database and cDNA microarray: data mining and interspecific hybridization characteristics. Genome Res 2004; 14:478-90; PMID: 14962987; http://dx.doi.org/10.1101/gr.1687304

860. Salem M, Rexroad CE, 3rd, Wang J, Thorgaard GH, Yao J. Characterization of the rainbow trout transcriptome using Sanger and 454-pyrosequencing approaches. BMC Genomics 2010; 11:564; PMID: 20942956; http://dx.doi.org/10.1186/1471-2164-11-564

861. Polakof S, Panserat S, Craig PM, Martyres DJ, Plagnes-Juan E, Savari S, et al. The metabolic consequences of hepatic AMP-kinase phosphorylation in rainbow trout. PLoS One 2011; 6:e20228; PMID: 21625448; http://dx.doi.org/10.1371/journal.pone.0020228

862. Seiliez I, Gabillard JC, Skiba-Cassy S, Garcia-Serrana D, Gutiérrez J, Kaushik S, et al. An in vivo and in vitro assessment of TOR signaling cascade in rainbow trout (Oncorhynchus mykiss). Am J Physiol Regul Integr Comp Physiol 2008; 295:R329-35; PMID:18434442; http://dx.doi.org/10.1152/ajpregu.00146.2008

863. Seiliez I, Gabillard J-C, Riflade M, Sadoul B, Dias K, Avérous J, et al. Amino acids downregulate the expression of several autophagy-related genes in rainbow trout myoblasts. Autophagy 2012; 8; In press; PMID:22252009

864. Umemiya R, Matsuo T, Hatta T, Sakakibara S, Boldbaatar D, Fujisaki K. Cloning and characterization of an autophagy-related gene, *ATG12*, from the three-host tick *Haemaphysalis longicornis*. Insect Biochem Mol Biol 2007; 37:975-84; PMID:17681237; http://dx.doi.org/10.1016/j.ibmb.2007.05.006

865. Kawano S, Umemiya-Shirafuji R, Boldbaatar D, Matsuoka K, Tanaka T, Fujisaki K. Cloning and characterization of the autophagy-related gene 6 from the hard tick, *Haemaphysalis longicornis*. Parasitol Res 2011; 109:1341-9; PMID:21537978; http://dx.doi.org/10.1007/s00436-011-2429-x

866. Umemiya-Shirafuji R, Matsuo T, Liao M, Boldbaatar D, Battur B, Suzuki HI, et al. Increased expression of *ATG* genes during nonfeeding periods in the tick *Haemaphysalis longicornis*. Autophagy 2010; 6:473-81; PMID:20404490; http://dx.doi.org/10.4161/auto.6.4.11668

867. Piggott N, Cook MA, Tyers M, Measday V. Genome-wide fitness profiles reveal a requirement for autophagy during yeast fermentation. Genes Genomes Genetics 2011; 1:353-67.

868. Cebollero E, Gonzalez R. Induction of autophagy by second-fermentation yeasts during elaboration of sparkling wines. Appl Environ Microbiol 2006; 72:4121-7; PMID:16751523; http://dx.doi.org/10.1128/AEM.02920-05

869. Marks VD, Ho Sui SJ, Erasmus D, van der Merwe GK, Brumm J, Wasserman WW, et al. Dynamics of the yeast transcriptome during wine fermentation reveals a novel fermentation stress response. FEMS Yeast Res 2008; 8:35-52; PMID:18215224; http://dx.doi.org/10.1111/j.1567-1364.2007.00338.x

870. Mendes-Ferreira A, Sampaio-Marques B, Barbosa C, Rodrigues F, Costa V, Mendes-Faia A, et al. Accumulation of non-superoxide anion reactive oxygen species mediates nitrogen-limited alcoholic fermentation by Saccharomyces cerevisiae. Appl Environ Microbiol 2010; 76:7918-24; PMID:20952641; http://dx.doi.org/10.1128/AEM.01535-10

871. Rossignol T, Dulau L, Julien A, Blondin B. Genome-wide monitoring of wine yeast gene expression during alcoholic fermentation. Yeast 2003; 20:1369-85; PMID: 14663829; http://dx.doi.org/10.1002/yea.1046

872. Teixeira MC, Raposo LR, Mira NP, Lourenço AB, Sá-Correia I. Genome-wide identification of Saccharomyces cerevisiae genes required for maximal tolerance to ethanol. Appl Environ Microbiol 2009; 75:5761-72; PMID:19633105; http://dx.doi.org/10.1128/AEM.00845-09

873. Yoshikawa K, Tanaka T, Furusawa C, Nagahisa K, Hirasawa T, Shimizu H. Comprehensive phenotypic analysis for identification of genes affecting growth under ethanol stress in *Saccharomyces cerevisiae*. FEMS Yeast Res 2009; 9:32-44; PMID:19054128; http://dx.doi.org/10.1111/j.1567-1364.2008.00456.x

874. Hazan R, Levine A, Abeliovich H. Benzoic acid, a weak organic acid food preservative, exerts specific effects on intracellular membrane trafficking pathways in *Saccharomyces cerevisiae*. Appl Environ Microbiol 2004; 70:4449-57; PMID:15294772; http://dx.doi.org/10.1128/AEM.70.8.4449-4457.2004

875. Winter G, Hazan R, Bakalinsky AT, Abeliovich H. Caffeine induces macroautophagy and confers a cytocidal effect on food spoilage yeast in combination with benzoic acid. Autophagy 2008; 4:28-36; PMID: 17952024

876. Singletary K, Milner J. Diet, autophagy, and cancer: a review. Cancer Epidemiol Biomarkers Prev 2008; 17:1596-610; PMID:18628411; http://dx.doi.org/10.1158/1055-9965.EPI-07-2917

877. Su CL, Chen FN, Won SJ. Involvement of apoptosis and autophagy in reducing mouse hepatoma ML-1 cell growth in inbred BALB/c mice by bacterial fermented soybean products. Food Chem Toxicol 2011; 49:17-24; PMID:20732379; http://dx.doi.org/10.1016/j.fct.2010.08.017

878. Abeliovich H, Gonzalez R. Autophagy in food biotechnology. Autophagy 2009; 5:925-9; PMID: 19556866; http://dx.doi.org/10.4161/auto.5.7.9213

dc_840_14

© Landes Bioscience. Do not distribute. © Landes Bioscience. Do not distribute.

879. He C, Bartholomew CR, Zhou W, Klionsky DJ. Assaying autophagic activity in transgenic GFP-Lc3 and GFP-Gabarap zebrafish embryos. Autophagy 2009; 5:520-6; PMID:19221467; http://dx.doi.org/10.4161/auto.5.4.7768

880. Komoike Y, Shimojima K, Liang JS, Fujii H, Maegaki Y, Osawa M, et al. A functional analysis of GABARAP on 17p13.1 by knockdown zebrafish. J Hum Genet 2010; 55:155-62; PMID:20111057; http://dx.doi.org/10.1038/jhg.2010.1

881. Dowling JJ, Low SE, Busta AS, Feldman EL. Zebrafish MTMR14 is required for excitation-contraction coupling, developmental motor function and the regulation of autophagy. Hum Mol Genet 2010; 19:2668-81; PMID: 20400459; http://dx.doi.org/10.1093/hmg/ddq153

882. Makky K, Tekiela J, Mayer AN. Target of rapamycin (TOR) signaling controls epithelial morphogenesis in the vertebrate intestine. Dev Biol 2007; 303:501-13; PMID:17222402; http://dx.doi.org/10.1016/j.ydbio.2006.11.030

883. Klionsky DJ, Baehrecke EH, Brumell JH, Chu CT, Codogno P, Cuervo AM, et al. A comprehensive glossary of autophagy-related molecules and processes (2nd edition). Autophagy 2011; 7:1273-94; PMID: 21997368; http://dx.doi.org/10.4161/auto.7.11.17661

884. Klionsky DJ, Codogno P, Cuervo AM, Deretic V, Elazar Z, Fueyo-Margareto J, et al. A comprehensive glossary of autophagy-related molecules and processes. Autophagy 2010; 6:438-48; http://dx.doi.org/10.4161/auto.6.4.12244

Glossary

For a more complete listing of autophagy-related terms and definitions we refer readers to Klionsky DJ, Baehrecke EH, Brumell JH, Chu CT, Codogno P, Cuervo AM, etal. A comprehensive glossary of autophagy-related molecules and processes (2nd edition). Autophagy 2011; 7:1273–94.

Amphisome: Intermediate compartment formed by the fusion of an autophagosome with an endosome; this compartment has not yet fused with a lysosome (also referred to as an acidic late autophagosome).

Autolysosome: A degradative compartment formed by the fusion of an autophagosome or amphisome with a primary lysosome or telolysosome. Upon completion of degradation, or when degradation has reached an end point, this compartment (again) becomes a telolysosome (also referred to as a residual body).

Autophagosome: A cytosolic membrane-bound compartment typically denoted by a limiting double membrane. The early autophagosome in particular contains cytoplasmic components and organelles that are morphologically unchanged because the compartment has not fused with a lysosome and lacks proteolytic enzymes.

Autophagy: A collection of processes typically involving degradative delivery of a portion of the cytoplasm to lysosomes or the plant or fungal vacuole that does not involve direct transport through the endocytic or vacuolar protein sorting, Vps, pathways.

Chaperone-mediated autophagy (CMA): Import and degradation of soluble cytosolic proteins by chaperone-dependent, direct translocation across the lysosomal membrane.

Cytoplasm-to-vacuole targeting (Cvt): A biosynthetic pathway in fungi that transports resident hydrolases to the vacuole through a selective autophagy-related process.

Lysosome: A degradative organelle in higher eukaryotes that compartmentalizes a range of hydrolytic enzymes and maintains a highly acidic pH. A primary lysosome is a relatively small compartment that has not yet participated in a degradation process, whereas secondary lysosomes are sites of present or past digestive activity. The secondary lysosomes include autolysosomes and telolysosomes. Autolysosomes/early secondary lysosomes are larger compartments actively engaged in digestion, whereas telolysosomes/late secondary lysosomes do not have significant digestive activity and contain residues of previous digestions. Both may contain material of either autophagic or heterophagic origin.

Macroautophagy: The largely nonspecific autophagic sequestration of cytoplasm into a double- or multiple-membrane-delimited compartment (an autophagosome) of nonlysosomal/vacuolar origin and its subsequent degradation by the lysosomal system. Note that certain proteins and organelles may be selectively degraded via a macroautophagy-related process, and conversely, some cytosolic components such as cytoskeletal elements are selectively excluded.

Microautophagy: Uptake and degradation of cytoplasm by protrusion, invagination or septation of the lysosome or vacuole membrane.

Mitophagy: The selective autophagic sequestration and degradation of mitochondria.

Nucleophagy: The selective autophagic degradation of the nucleus.

Pexophagy: A selective type of autophagy involving the sequestration and degradation of peroxisomes; can occur by a micro- or macroautophagic process.

Phagophore: Membrane cisterna that has been implicated in an initial event during formation of the autophagosome. Previously referred to as the "isolation membrane."

Phagophore assembly site (PAS): A perivacuolar compartment or location that is involved in the formation of Cvt vesicles and autophagosomes in yeast. The PAS may supply membranes during the formation process or may be an organizing center where most of the autophagic machinery resides, at least transiently.

Phosphatidylinositol 3-kinase (PtdIns3K): A family of enzymes that add a phosphate group to the 3' hydroxyls on the inositol ring of phosphoinositides. The class III phosphatidylinositol 3-kinases are stimulatory for autophagy, whereas class I enzymes are inhibitory.

Reticulophagy: A type of selective macroautophagy of the ER. Autophagy counterbalances endoplasmic reticulum expansion during the unfolded protein response. Activation of the UPR in yeast induces reticulophagy.

Ribophagy: The selective autophagic sequestration and degradation of ribosomes.

Vacuole: The fungal and plant counterpart of the lysosome; this organelle also carries out storage and osmoregulatory functions. The plants' bona fide equivalent of the lysosome is the lytic vacuole.

Xenophagy: The selective degradation of microbes (e.g., bacteria, fungi, parasites and/or viruses) through an autophagy-related mechanism.

Index

A
Acridine Orange 63
Atg8–PE conjugation 18, 23, 24, 26, 27, 33, 69, 70, 73, 74
Atg12–Atg5 conjugation 43
Atg12–Atg5, Atg16 fluorescence 33, 43
ATG16L1 43, 44, 46, 60
Atg18 43, 44, 46, 70, 78, 88
Autophagic body accumulation 75
Autophagosome characteristics 16-23, 25-29, 32-36, 38, 39, 42-44, 47, 48, 50-52, 54-57, 59, 60, 63-66, 69-71, 73-78

B
BHMT 48, 89
Bovine mammary epithelial cells 72, 97

C
C. elegans 44, 46, 55, 68, 69
Calcium 27, 32, 34, 66
Cell death 16, 27, 31, 32, 36, 39, 46, 49, 58, 60, 64-66, 70, 73
Chicken DT40 cells 67, 68
Chlamydomonas 68
Chloroquine 23, 26-30, 34, 38, 40, 43, 58, 59, 64, 65, 72
Correlative light and electron microscopy (CLEM) 21, 33, 54

D
Degradation assays 47
Dictyostelium 28, 30, 33, 46, 48, 60, 75
DQ-BSA 56, 57

E
Electron microscopy 16, 18, 21, 22, 78
Endosomal-microautophagy 62
EPG proteins 44, 78

F
Flow cytometry 32, 36, 37, 48
Fluorescence microscopy 18, 21, 25, 28-33, 35, 36, 43, 44, 49-53, 55, 56, 58, 60, 68, 70, 72, 74, 75, 78

G
GFP-Atg8/LC3 processing 30, 49, 74
GFP-LC3 fluorescence microscopy 35

H
HIV Nef 34, 66
Honeybee 70
Hydra 72

I
ICP34.5 34, 54, 66
Influenza M2 34
Inhibitors 34, 36, 37, 39, 40-42, 44, 45, 47, 48, 51, 53, 55, 56, 58, 59, 61-69, 72, 75, 78

K
Keima 52, 56

L
Large animals 72, 73
LC3-I and LC3-II western blot 69, 70
LC3-IIs 27
LC3-associated phagocytosis (LAP) 25
Lipofuscin 53, 56, 70, 78
Long-lived protein degradation 18, 48, 61, 78
LysoTracker Red 61-63, 65, 72-74, 76, 77

M
3-methyladenine 34
Mitophagy 20, 23, 25, 34, 35, 40, 48-53, 71
Monodansylcadaverine, MDC 63
MTOR activity 68, 72

P
p62 western blot 16, 22-33, 40-42, 45, 47, 48, 50, 51, 53, 55, 58-60, 68-73
Pexophagy 20, 48-50, 53, 55, 67
Planarians 74
Plants 16, 17, 19, 21, 26, 33, 60, 65, 74, 75, 78
PolyQ protein turnover 53
Protists 21, 75

R
Rainbow trout 76
Reticulophagy 49, 50
RFP chimera processing 78
Rosella 35, 36, 78

S
Saponin 33, 36, 38
Sea Urchin 76
Sequestration assays 55-57, 78
SQSTM1 western blot 39, 54

T
TAKA assay 43
Tandem mRFP/mCherry-GFP-LC3 21, 35, 36, 68
Trehalose 34, 66

V
Viral Bcl-2 66
Viral FLIP 66

W
WIPI1 44, 45
WIPI2 44, 45
WIPI4 44
Wortmannin 34, 40, 44, 45, 56, 57, 63, 64, 72, 76

X
Xenophagy 20, 49, 54

Z
Zebrafish 76, 77
Zymophagy 55

dc_840_14
© 2012 Landes Bioscience. Do not distribute.

dc_840_14

BMC Cell Biology

RESEARCH ARTICLE Open Access

Impaired proteasomal degradation enhances autophagy via hypoxia signaling in Drosophila

Péter Lőw†, Ágnes Varga†, Karolina Pircs, Péter Nagy, Zsuzsanna Szatmári, Miklós Sass and Gábor Juhász*

Abstract

Background: Two pathways are responsible for the majority of regulated protein catabolism in eukaryotic cells: the ubiquitin-proteasome system (UPS) and lysosomal self-degradation through autophagy. Both processes are necessary for cellular homeostasis by ensuring continuous turnover and quality control of most intracellular proteins. Recent studies established that both UPS and autophagy are capable of selectively eliminating ubiquitinated proteins and that autophagy may partially compensate for the lack of proteasomal degradation, but the molecular links between these pathways are poorly characterized.

Results: Here we show that autophagy is enhanced by the silencing of genes encoding various proteasome subunits (α, β or regulatory) in larval fat body cells. Proteasome inactivation induces canonical autophagy, as it depends on core autophagy genes *Atg1*, *Vps34*, *Atg9*, *Atg4* and *Atg12*. Large-scale accumulation of aggregates containing p62 and ubiquitinated proteins is observed in proteasome RNAi cells. Importantly, overexpressed Atg8a reporters are captured into the cytoplasmic aggregates, but these do not represent autophagosomes. Loss of *p62* does not block autophagy upregulation upon proteasome impairment, suggesting that compensatory autophagy is not simply due to the buildup of excess cargo. One of the best characterized substrates of UPS is the α subunit of hypoxia-inducible transcription factor 1 (HIF-1α), which is continuously degraded by the proteasome during normoxic conditions. Hypoxia is a known trigger of autophagy in mammalian cells, and we show that genetic activation of hypoxia signaling also induces autophagy in Drosophila. Moreover, we find that proteasome inactivation-induced autophagy requires *sima*, the Drosophila ortholog of *HIF-1α*.

Conclusions: We have characterized proteasome inactivation- and hypoxia signaling-induced autophagy in the commonly used larval Drosophila fat body model. Activation of both autophagy and hypoxia signaling was implicated in various cancers, and mutations affecting genes encoding UPS enzymes have recently been suggested to cause renal cancer. Our studies identify a novel genetic link that may play an important role in that context, as HIF-1α/sima may contribute to upregulation of autophagy by impaired proteasomal activity.

Keywords: Autophagy, Drosophila, HIF-1α/sima, Hypoxia, p62/Ref2P, Proteasome

Background

The proteasome is a multi-subunit protease complex, consisting of a 20S core particle and a 19S regulatory particle. 20S contains predominantly structural α and catalytic β subunits. 19S contains non-ATPase subunits that are involved in the recognition of polyubiquitinated proteins, and ATPase subunits responsible for unfolding substrates and maintaining protease activity. The ubiquitin-proteasome system (UPS) is considered to be the main route for the degradation of short-lived proteins. Proteasomal activity is also essential for eliminating excess or unfolded proteins and thus contributes to establishing steady-state overall protein levels. The selective and often well-timed degradation of regulatory proteins by the proteasome orchestrates and modulates multiple biological processes such as transcription, metabolism, cell cycle progression and differentiation [1].

During the main pathway of autophagy, initially appearing membrane cisterns called phagophores capture portions of the cytoplasm in double-membrane autophagosomes. These vesicles then deliver cargo for lysosomal degradation [2,3]. Autophagy is thought to be

* Correspondence: szmrt@elte.hu
†Equal contributors
Department of Anatomy, Cell and Developmental Biology, Eötvös Loránd University, Pázmány P. s. 1/C, H-1117, Budapest, Hungary

BioMed Central

© 2013 Lőw et al.; licensee BioMed Central Ltd. This is an Open Access article distributed under the terms of the Creative Commons Attribution License (http://creativecommons.org/licenses/by/2.0), which permits unrestricted use, distribution, and reproduction in any medium, provided the original work is properly cited.

mainly responsible for degrading long-lived proteins and whole organelles, and stress-induced autophagy maintains the amino acid pool and energy production necessary for biosynthetic processes during chronic starvation [1,3].

UPS and autophagy were long considered as independent, parallel pathways. Recent observations challenged this view, suggesting interactions between these degradative routes [4,5]. First, autophagy also plays an important role in the degradation of ubiquitinated proteins. Loss of autophagy leads to neurodegeneration accompanied by the formation of pathological protein aggregates both in mice and flies [3,6,7]. These aggregates contain ubiquitinated proteins and p62 (also known as Ref2P in flies), an autophagy receptor. p62 facilitates selective autophagic removal of ubiquitinated cargo by binding to both ubiquitin and Atg8 that is covalently bound to phagophore and autophagosome membranes [8,9]. Second, protein degradation by the autophagy and UPS pathways is coordinately regulated by the evolutionarily conserved Foxo transcription factors in muscles [10,11]. In addition, we recently showed that genes encoding proteins of the UPS are upregulated in response to starvation in autophagy mutant Drosophila larvae compared to starved control animals [12]. Third, impairment of the UPS has been shown to enhance autophagy in various cells, but the molecular links are poorly characterized [4,5].

In this study, we investigated the consequences of proteasome inhibition on aggregate formation and autophagic activity in somatic clones of larval fat body cells in Drosophila. We showed that genetic activation of hypoxia signaling induces autophagy, and identified HIF-1α as a novel molecular link between UPS and autophagy.

Results

Depletion of genes encoding various proteasome subunits leads to impaired proteasomal degradation in vivo

We selected transgenic RNAi lines to mediate inducible silencing of 26 genes encoding different proteasome subunits in Drosophila. Expression of these UAS-proteasome RNAi constructs can be triggered in vivo in a tissue-specific manner by simply crossing these lines to another line that carries an appropriate promoter-Gal4 transgene (driver). As systemic RNAi mediated by an Actin-Gal4 driver resulted in developmental delays and lethality in case of the majority of RNAi lines, we used the standard mosaic approach to generate RNAi cells (marked by an appropriate fluorescent reporter such as GFP) in an otherwise wild-type background. To investigate proteasome activity in vivo, we analyzed transgenic flies expressing a fluorescent reporter of UPS function. GFP-CL1 is a fusion protein created by introducing a degradation signal to the otherwise stable green fluorescent protein (GFP) [13]. This protein is rapidly degraded by the UPS, and its steady state levels reflect the functional status of this pathway. In control animals, clones of fat body cells expressing GFP-CL1 were similar in size to neighboring cells and showed weak, diffuse GFP fluorescence (Figure 1A). Gal4-mediated expression of either one of 19 out of 26 different RNAi lines decreased cell size and led to the accumulation and large-scale aggregation of GFP-CL1, indicating impaired proteasomal degradation activity (Figure 1B, C, see also Additional file 1: Figure S1 for further images).

Proteasome maturation protein (Pomp) facilitates the main steps in 20S core complex formation at the ER by coordinating the assembly process, and it is necessary for the continuous supply of newly formed proteasomes. Similar to the above results, depletion of Pomp also resulted in accumulation of GFP-CL1 (Figure 1C).

We have also tested the level of p62, a well-characterized intracellular receptor for ubiquitinated proteins. As ubiquitin-containing proteins were shown to be captured into aggregates of p62 [9,14,15], inactivation of the proteasome was expected to increase p62 aggregation due to a block in ubiquitinated protein degradation. Note that in the various staining experiments in genetic mosaic animals, GFP-positive RNAi cells are always surrounded by control cells in the very same tissue, which serve as an internal control to directly compare phenotypes to (Figure 1D). Immunostainings indeed revealed large ubiquitin- and p62-positive aggregates in the cytoplasm of proteasome subunit RNAi cells compared to control non-GFP cells (Figure 1E, F, see also Additional file 2: Figure S2 for further images). Importantly, aggregates never colocalized with the lysosome marker Lamp1-GFP in these cells, suggesting that aggregated proteins are not accumulated inside lysosomes. Quantification of immunostainings revealed that 20 out of the 27 RNAi lines (targeting 26 different proteasome subunits and Pomp) led to large-scale accumulation of endogenous p62 aggregates (Figure 1G). Notably, exactly the same seven lines failed to trigger a statistically significant elevation of both p62 and GFP-CL1 aggregates. This may be due to that these RNAi lines did not work properly in fat body cells, although it cannot be excluded that some of the proteasome subunits targeted by these seven RNAi lines are dispensable for proteasome function. The transcription of p62 is also regulated during starvation and stress, both in Drosophila and mammalian cells [12,16,17]. RT-PCR experiments revealed that p62 transcription in proteasome depleted animals was also increased relative to controls (see Additional file 3: Figure S3).

It was obvious in these experiments that smaller fat body cells had higher GFP-CL1 levels (see Additional file 4: Figure S4). This suggested that proteasomal degradation is necessary for proper growth and endomitosis of larval fat body cells, and a more severe block of proteasome function likely produces smaller cells.

dc_840_14

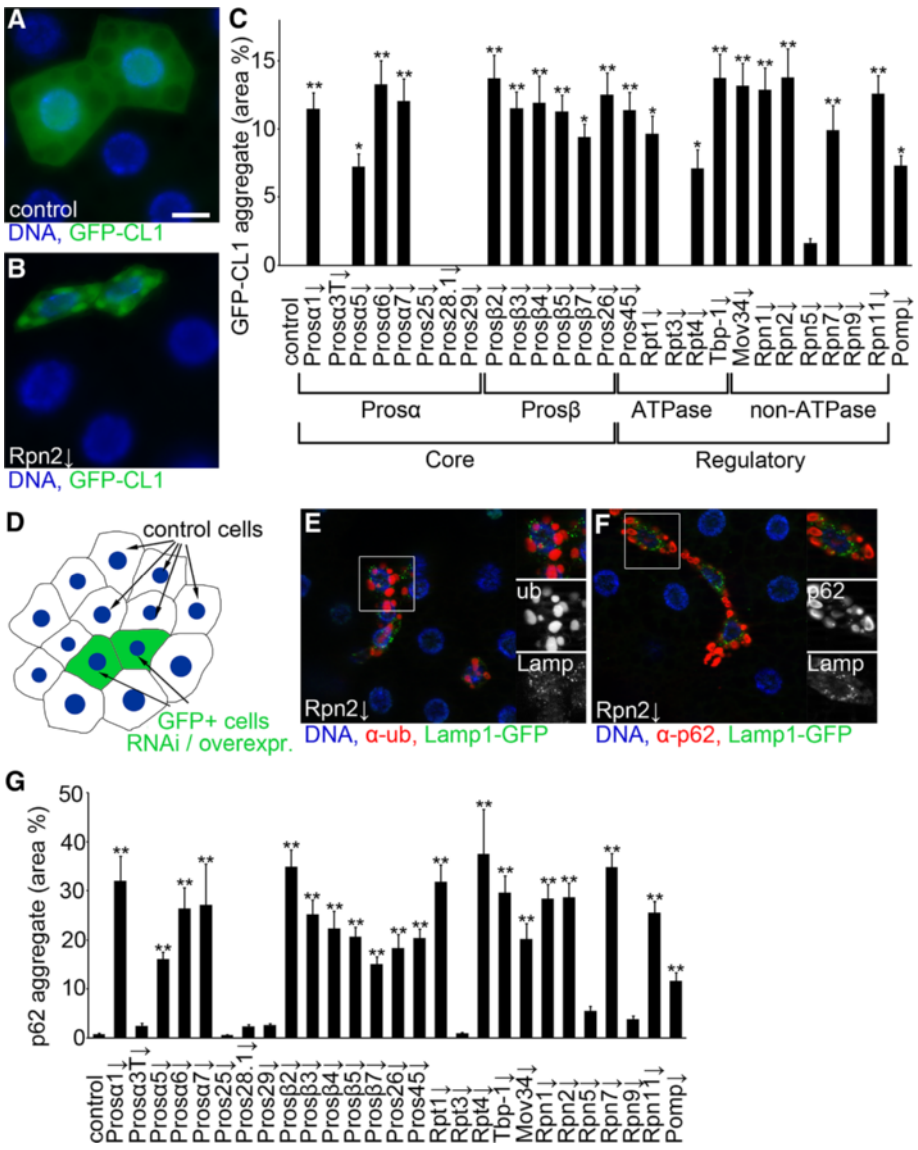


Figure 1 Depletion of genes encoding various proteasome subunits decreases proteasomal activity in vivo. A) Control cells expressing the proteasome degradation reporter GFP-CL1 are similarly sized as neighboring non-GFP control fat body cells and show diffuse fluorescence. Cell nuclei are labeled with DAPI (blue). **B)** *Rpn2* RNAi cells are smaller than control cells and accumulate large aggregates of GFP-CL1. **C)** Proteasome RNAi leads to accumulation of GFP-CL1 aggregates relative to control cells shown in panel **A**. Statistically significant differences are marked by asterisks (Kruskal-Wallis test, n = 5-6 per genotype, ** $P < 0.01$, * $P < 0.05$), and error bars denote standard error. The different types of subunits are indicated as 20S core subunits (α and β), and 19S regulatory particle subunits (ATPase and non-ATPase). Pomp is required for assembly of the 20S core. **D)** Schematic of the clonal expression system. GFP-positive cells of interest are surrounded by wild-type cells in the same tissue of mosaic animals, serving as an internal control in various staining experiments. **E)** Depletion of *Rpn2* leads to accumulation of ubiquitinated protein aggregates in Lamp1-GFP marked fat body cell clones. Note that the numerous small Lamp1-GFP dots representing lysosomes are not ubiquitin-positive. **F)** Similarly, silencing of *Rpn2* leads to cell-autonomous accumulation of p62 aggregates in Lamp1-GFP marked fat body cell clones. Note that Lamp1-GFP dots are not p62-positive either. **G)** Proteasome RNAi leads to accumulation of endogenous p62 aggregates relative to control cells. n = 5-6 per genotype. Statistically significant differences are marked by asterisks (Kruskal-Wallis test, n = 5-6 per genotype, ** $P < 0.01$, * $P < 0.05$), and error bars denote standard error. Boxed areas in **E** and **F** are shown enlarged. Scale bar in **A** equals 20 μm for **A**, **B**, **E**, **F**.

We selected five proteasome subunit RNAi lines for further experiments that all worked very well in both in vivo proteasome activity assays (that is, GFP-CL1 and p62 aggregation). These represent different subunit types: 20S core particle subunits Prosα1, Prosα5, Prosβ2, and 19S regulatory particle subunits Rpt1, Rpn2 (Figure 1C).

dc_840_14

Proteasome impairment enhances starvation-induced and basal autophagy

Lysotracker Red (LTR) staining is an established and widely used assay for detection of autolysosomes in Drosophila fat body and other tissues [6,11,12,18-25]. Inactivation of proteasome function increased autophagic activity in Lamp1-GFP-marked fat body cell clones of starved larvae, based on increased punctate LTR labeling compared to surrounding non-GFP control cells (Figure 2A, see also Additional file 5: Figure S5 for further images). LTR structures also colocalized with Lamp1-GFP in clone cells, an artificial reporter that labels late endosomes and all lysosomes in Drosophila cells [26]. Note that the colocalization is not complete, as LTR only stains acidic, actively digesting lysosomes, whereas primary lysosomes are also labeled by Lamp1-GFP. Moreover, Lamp1-GFP is continuously degraded in active lysosomes, so its levels are often strongly decreased in LTR structures (see Additional file 6: Figure S6 for colocalization of these markers in control fat body cells dissected from starved animals, and for colocalization data in control and proteasome RNAi cells).

These genetic manipulations also activated autophagy in a cell-autonomous manner in well-fed larvae, based on increased LTR and autophagosome-associated punctate anti-Atg8a immunostainings (Figure 2B-E, see also Additional file 7: Figure S7 for further images). Similarly, knockdown of genes encoding proteasome subunits led to elevated levels of autophagosome-associated, lipidated Atg8a-II in western blots of well-fed larvae (Figure 2F). Levels of the ubiquitin-binding selective autophagy cargo p62 also showed a marked increase in these samples (Figure 2F).

We found that upon proteasome RNAi, smaller cells always had increased normalized LTR dot number (see also Additional file 8: Figure S8). Thus, more severe proteasome inactivation seems to induce higher levels of autophagy and a stronger cell growth impairment.

Proteasome RNAi leads to accumulation of cytoplasmic aggregates and enhances autophagic flux

We have recently described that overexpressed p62 and Atg8a reporters bind each other to form large aggregates in Drosophila fat body cells [21]. Overexpressed GFP-tagged Atg8a, a routinely used marker of autophagosomes [6,18,23], not only labeled small structures likely representing genuine autophagosomes with a diameter of about 1 μm, but also colocalized with the large p62-positive aggregates (approximate diameter: 5 μm) that formed in proteasome RNAi cells (Figure 3A, see also Additional file 9: Figure S9 for further images). Importantly, small genuine

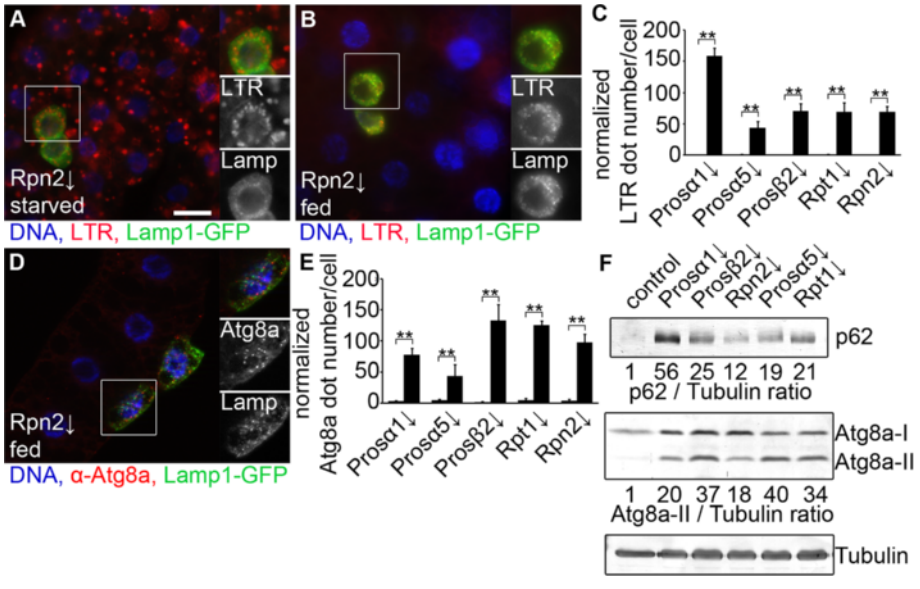


Figure 2 Proteasome impairment enhances autophagy in *Drosophila* larvae. A) Depletion of *Rpn2* increases punctate Lysotracker Red (LTR) staining in Lamp1-GFP marked larval fat body cell clones of starved animals relative to surrounding control cells. **B)** *Rpn2* knockdown induces autophagy in fat body cell clones of well fed larvae, as LTR dots are only observed in GFP-positive RNAi cells but not in control cells. **C)** Silencing of genes encoding different proteasome subunits results in a statistically significant induction of punctate LTR in well fed conditions (u test, n = 5-7 per genotype, ** $P < 0.01$), and error bars denote standard error. **D)** Immunostaining reveals cell-autonomous activation of punctate endogenous Atg8a labeling in *Rpn2* RNAi cells, representing autophagosomes. **E)** Statistical evaluation of the effect of proteasome subunit RNAi on punctate endogenous Atg8a. Statistically significant differences are marked (u or *t* test, n = 5 per genotype, ** $P < 0.01$), and error bars denote standard error. **(F)** Western blots show that RNAi knockdown of genes encoding different proteasome subunits greatly increases the levels of both the specific autophagy cargo p62 and autophagosome-associated lipidated Atg8a-II. Numbers refer to relative expression levels compared to Tubulin, as determined by densitometric evaluation. Boxed areas in **A**, **B** and **D** are shown enlarged. Scale bar in **A** equals 20 μm for **A**, **B**, **D**.

dc_840_14

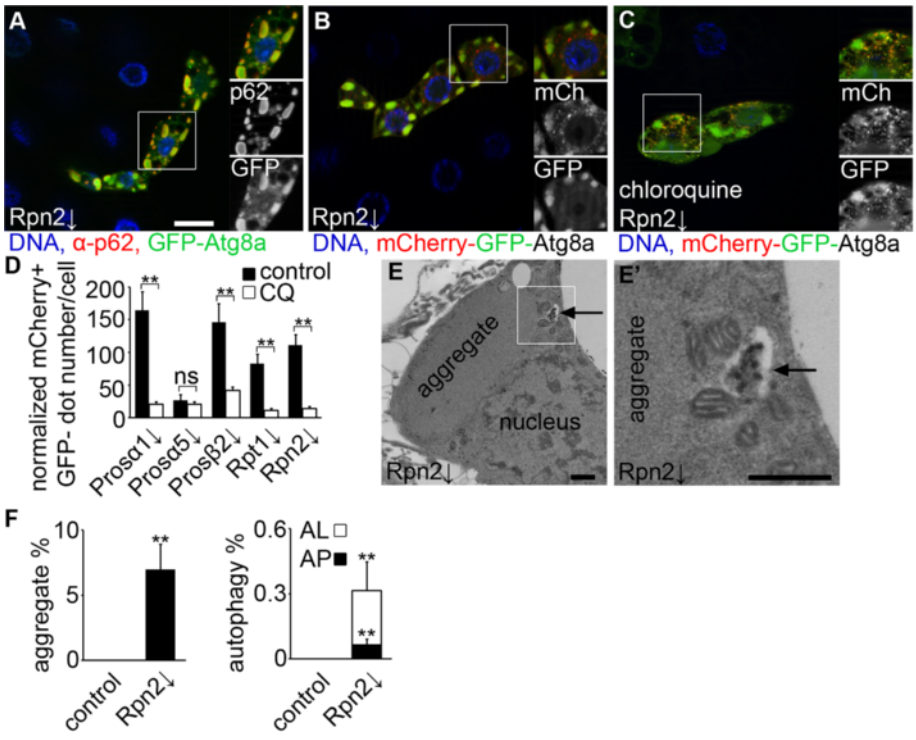


Figure 3 Proteasome impairment leads to accumulation of cytoplasmic aggregates and enhances autophagic flux. A) Overexpressed GFP-Atg8a reporter is incorporated into the large protein aggregates containing p62 in *Rpn2* RNAi cells. **B)** The tandemly tagged mCherry-GFP-Atg8a reporter forms numerous small mCherry-labeled autolysosomes, in addition to large aggregates positive for both mCherry and GFP in *Rpn2* RNAi cells. **C)** The lysosome inhibitor chloroquine blocks autophagy-dependent quenching of GFP, as now most puncta are positive for both mCherry and GFP. **D)** Quantification of data from panels **B** and **C** (u or t test, n = 5-8 per genotype, ** $P < 0.01$, * $P < 0.05$), and error bars denote standard error. **E)** Transmission electron microscopy reveals the presence of autolysosomes (arrow) and large protein aggregates in fat body cells with impaired proteasome function in well-fed larvae. The boxed area is shown enlarged in panel **E'**. **F)** Quantification of ultrastructural data. Protein aggregates occupy 7% of the total cytoplasm in *Rpn2* depleted fat body cells of well-fed larvae, and double-membrane autophagosomes (AP) and degrading autolysosomes (AL) take up 0.06% and 0.24% of the total cytoplasm, respectively. No such structures are recognized in fat body cells of well-fed control larvae (*u* test, n = 3 per genotype, ** $P < 0.01$), and error bars denote standard error. Boxed areas in **A**-**C** are shown enlarged. Scale bar in **A** equals 20 μm for **A**-**C**. Scale bars equal 1 μm in **E**, **E'**.

autophagosomes marked by endogenous anti-Atg8a staining [20,25] showed markedly different size and distribution from this overexpressed Atg8a reporter in proteasome RNAi cells (compare Figure 2D with Figure 3A). We next employed a tandemly tagged mCherry-GFP-Atg8a reporter, a standard assay to follow autophagic flux [25,27]. This reporter is selectively transported to autolysosomes, where GFP is quenched while mCherry remains fluorescent. In addition to small mCherry-positive autolysosomes in the perinuclear region of proteasome RNAi cells, large structures positive for both GFP and mCherry were also formed, with a size and localization again reminiscent of protein aggregates (Figure 3B). Treatment with the lysosome inhibitor chloroquine prevented the quenching of GFP in acidic autolysosomes in proteasome RNAi cells, greatly decreasing the number of structures that were positive for only mCherry (Figure 3C and D, see also Additional file 10: Figure S10 for further images).

We then carried out electron microscopy to completely rule out the possibility that these large aggregates were inside autophagosomes. Ultrastructural images of proteasome depleted fat bodies dissected from well-fed animals revealed the presence of large cytoplasmic protein aggregates that were never surrounded by membranes (Figure 3E, F). In addition, double-membrane autophagosomes and degrading autolysosomes were also readily detected in well-fed larval samples, consistent with autophagy induction in these cells (Figure 3E, F). See also Additional file 11: Figure S11 for further ultrastructural images.

It was striking that upon proteasome RNAi, smaller cells always had increased p62 accumulation (see Additional file 12: Figure S12). These results altogether indicated that even though autophagic activity is enhanced in these cells, it fails to remove the excess protein aggregates formed due to impaired proteasomal degradation.

As expected, LTR practically never colocalized with Atg8a or p62 reporters (see Additional file 13: Figure S13). Even the size of these structures was different: LTR-positive digesting lysosomes in fat body cells had an

approximate diameter of 1-3 μm, while p62 was present in the large protein aggregates (approximate diameter: 5 μm), and GFP-Atg8a labeled small autophagosomes (approximate diameter: 1 μm) in addition to being captured into the large p62 aggregates.

These data altogether suggest that p62 accumulation is due to both transcriptional and post-transcriptional mechanisms, that is, increased rate of transcription, and reduced protein turnover by autophagy due to large-scale aggregate formation.

Activation of hypoxia signaling induces autophagy in Drosophila

One of the best characterized substrates of UPS is the α subunit of hypoxia-inducible transcription factor HIF-1 [28]. HIF-1α is ubiquitinated by the tumor suppressor protein von Hippel-Lindau (VHL) under normoxic conditions, resulting in its proteasomal degradation. Decreased levels of oxygen lead to stabilization of HIF-1α by preventing its ubiquitination, and a concomitant upregulation of genes involved in the hypoxia response [28]. Hypoxia is a known trigger of autophagy in mammalian cells, but its role has not been characterized in Drosophila autophagy. The fly ortholog of the mammalian *HIF-1α* gene is *sima* (short for *similar*) [29]. Overexpression of sima, or depletion of *Vhl* led to the formation of LTR-positive autolysosomes in fat body cell clones of well-fed larvae (Figure 4A-C). Similarly, forced expression of sima or *Vhl* RNAi induced punctate mCherry-Atg8a representing autophagosomes and autolysosomes (Figure 4D-F). The mCherry-GFP-Atg8a reporter revealed that most of the punctate autophagic structures were positive for only mCherry in sima overexpressing and *Vhl* RNAi cells (Figure 4G, H). This indicated that GFP-Atg8a was delivered to autolysosomes and quenched. Chloroquine treatment again reduced the number of structures that were positive for only mCherry (Figure 4I-K), indicating that autophagic flux is enhanced in these cells.

We also carried out anti-active caspase 3 stainings to analyze cell death, but no apoptotic caspase activation was detected in cell clones undergoing proteasome or *Vhl* RNAi, or overexpressing sima in larval tissues (see Additional file 14: Figure S14).

Proteasome inactivation-induced autophagy requires Atg genes and sima/HIF-1α

Since genetic activation of hypoxia signaling increased autophagy, we first tested whether proteasome RNAi activates this pathway. BNIP3 (BCL2/adenovirus E1B 19 kDa protein-interacting protein 3) is a well-characterized transcriptional target of HIF1 in mammalian cells [30]. Our RT-PCR experiments revealed that transcription of Drosophila *BNIP3* (*CG5059*) is enhanced upon silencing of *Rpn2* to a similar extent as in *Vhl* RNAi animals (Figure 4L). Additionally, proteasome RNAi increased the expression level of an in vivo transcriptional reporter for hypoxia signaling (see Additional file 15: Figure S15).

These results suggested that hypoxia signaling may be involved in proteasome RNAi-induced autophagy. To evaluate the genetic pathways mediating compensatory autophagy upon proteasome impairment, we tested the potential role of *sima*, core *Atg* genes required for starvation-induced autophagy, and *p62*.

Clones of fat body cells showed LTR-positive autolysosome formation in well-fed animals upon silencing of *Prosβ2*, *Rpt1* and *Rpn2* (Figure 5A, G). We silenced *sima* using 3 independent transgenic constructs, each of which targeted different regions of this gene and achieved knockdown by distinct experimental approaches (long hairpin- versus microRNA-based, please see Methods). Depletion of *sima* significantly inhibited proteasome inactivation-induced punctate LTR staining in most combinations (Figure 5B, G). Depletion of *Atg1, Atg9* or *Atg12* also blocked compensatory autophagy, similar to expression of dominant-negative Atg1, Vps34 or Atg4 transgenes (Figure 5C, G). As a negative control we used an RNAi line for *Atg18b*, as this gene was shown to be dispensable for starvation-induced autophagy in Drosophila (Figure 5G) [23]. Finally, we tested the role of *p62* using previously characterized transgenic RNAi lines [21]. Depletion of *p62* by combining two indepedent RNAi lines targeting different regions of the gene, or using a third transgenic RNAi line failed to suppress proteasome inactivation-induced punctate LTR staining: the changes were not statistically significant (Figure 5D, E, G). As expected, depletion of *p62* completely prevented the formation of p62 aggregates in proteasome inactivated cells (Figure 5F).

As a final confirmation of our results, we also tested two additional proteasome RNAi lines for hypoxia and p62 signaling. Depletion of *sima*, but not *p62*, also reduced the number of LTR puncta in *Prosα1* and *Prosα5* RNAi cells (Figure 5H).

Discussion

Autophagy and UPS coordinately sustain cellular homeostasis through protein quality control and clearance. A wide range of neurodegenerative diseases (often described as proteinopathies) are characterized by accumulation of aggregate-prone proteins that are not efficiently removed by proteasome. Compensatory autophagy may alleviate disease pathology in these cases, as numerous studies showed that substrates of autophagy and UPS overlap [1,4,5]. Indeed, genetic or pharmacological activation of autophagy facilitates aggregate clearance and neuronal function in disease models [1,5]. Chronic block of proteasomal degradation also leads to toxicity, ER stress and cell death in various mammalian and Drosophila cells, and proteasome

dc_840_14

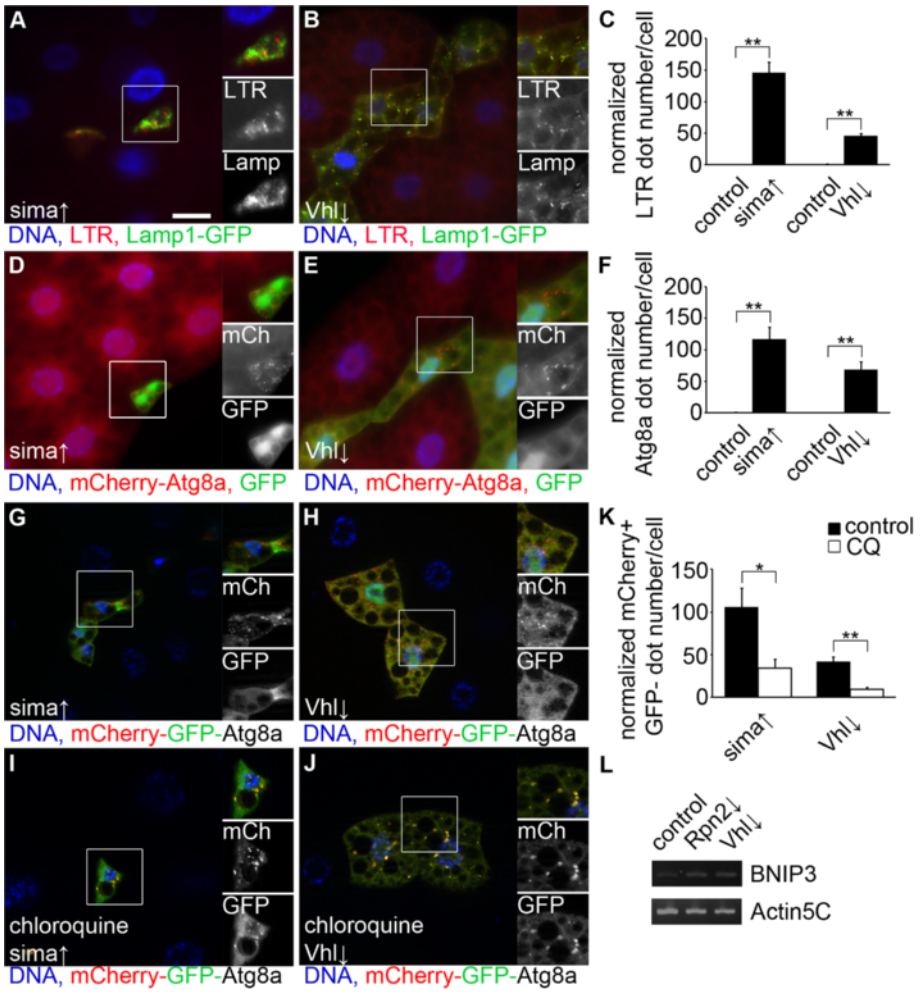


Figure 4 Activation of hypoxia signaling induces autophagy in *Drosophila*. A-C) Overexpression of the *Drosophila* HIF-1α ortholog sima **(A)** or depletion of *Vhl* **(B)** induces the formation of autolysosomes positive for both Lamp1-GFP and LTR in fat body cell clones in well-fed larvae. Quantification of data is shown in panel **C**. Statistically significant differences are marked (*u* test, n = 6 per genotype, ** P < 0.01), and error bars denote standard error. **D-F)** Overexpression of sima **(D)** or knockdown of *Vhl* **(E)** promotes the formation of punctate mCherry-Atg8a in fat body cell clones marked by GFP-nls (nuclear localization sequence) in well-fed larvae. Quantification of data is shown in panel **F**. Statistically significant differences are marked (u test, n = 6 per genotype, ** P < 0.01), and error bars denote standard error. **G-J)** Overexpression of sima **(G)** or depletion of *Vhl* **(H)** leads to formation of dots that are mostly positive for mCherry with the mCherry-GFP-Atg8a reporter. Chloroquine treatment blocks the autolysosomal quenching of GFP, as puncta are now positive for both mCherry and GFP in cells overexpressing sima **(I)** or *Vhl* RNAi **(J)**. **K)** Quantification of data from panels **G-J**. Statistically significant differences are marked (u or *t* test, n = 5-8 per genotype, ** P < 0.01, * P < 0.05), and error bars denote standard error. **L)** RT-PCR analyses show that the transcription of BNIP3 is upregulated in both *Vhl* and *Rpn2* RNAi samples relative to controls. Boxed areas in **A**, **B**, **D**, **E**, **G-J** are shown enlarged. Scale bar in **A** equals 20 μm for **A**, **B**, **D**, **E**, **G-J**.

inhibitors are in clinical use to trigger apoptosis of cancer cells in multiple myeloma patients [31-34]. While we found no evidence of cell death in larval Drosophila fat body upon silencing of genes encoding essential subunits of the proteasome or genetic activation of hypoxia signaling, these genetic manipulations strongly enhanced both basal and starvation-induced autophagy in these cells, and this effect was dependent on canonical autophagy genes *Atg1, Vps34, Atg9, Atg4* and *Atg12*.

An important aspect of our study is that overexpressed tagged Atg8 is not ideal for analyzing autophagy in proteasome RNAi cells, as excess p62-containing aggregates incorporate these reporter molecules, likely due to the physical interaction of p62 and Atg8. This artefact may then lead to false conclusions regarding autophagic activity, similar to the case of co-overexpressed p62 and Atg8 reporters [21].

How does proteasome impairment lead to compensatory autophagy? Multiple scenarios are possible, and these are not mutually exclusive. One hypothesis would be that accumulation of excess cargo triggers the formation of autophagosomes. However, overexpression of

dc_840_14

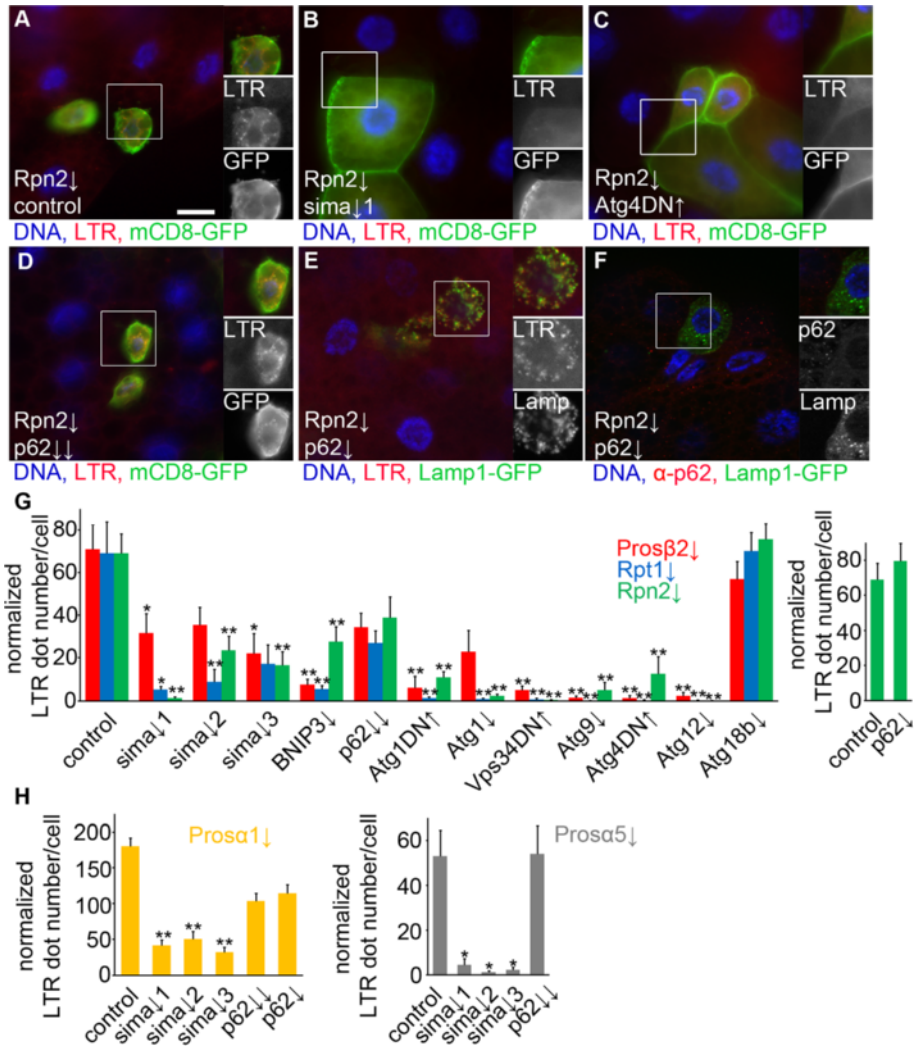


Figure 5 Proteasome inactivation-induced autophagy requires *Atg* genes and *sima/HIF-1α*. A) Depletion of *Rpn2* increases punctate LTR staining in larval fat body cell clones in fed animals, marked by membrane-associated mCD8-GFP. **B)** Simultaneous silencing of *Rpn2* and *sima* results in a block of punctate LTR staining. **C)** Overexpression of dominant-negative (DN) Atg4 inhibits LTR dot formation in *Rpn2* RNAi cells. **D**, **E)** Simultaneous silencing of *Rpn2* and *p62* using two independent RNAi lines combined **(D)** or a third independent single *p62* RNAi line **(E)** does not inhibit punctate LTR staining in larval fat body cell clones in fed animals. **F)** Depletion of *p62* blocks aggregate formation in *Rpn2* RNAi cells. **G)** Statistical evaluation of punctate staining in *Rpn2, Rpt1* and *Prosβ2* knockdown cells. Depletion of *sima* using 3 independent RNAi transgenes, silencing of *BNIP3, Atg1, Atg9, Atg12*, or overexpression of dominant-negative Atg1, Vps34, Atg4 inhibits proteasome inhibition-induced autophagy. Depletion of *p62* or *Atg18b* (which is dispensable for starvation-induced autophagy and used as a negative control here) does not block the autophagy-inducing effect of proteasome inactivation. Statistically significant differences are marked (Kruskal-Wallis test or ANOVA, n = 5-8 per genotype, * $P < 0.05$, ** $P < 0.01$), and error bars denote standard error. **H)** Similarly, silencing of *sima* but not *p62* attenuates LTR puncta formation in *Prosa1* and *Prosa5* RNAi cells. Statistically significant differences are marked (Kruskal-Wallis test or ANOVA, n = 5-8 per genotype, * $P < 0.05$, ** $P < 0.01$), and error bars denote standard error. Boxed areas in **A**-**F** are shown enlarged. Scale bar in **A** equals 20 μm for **A**-**F**.

specific autophagy substrates p62 or blue cheese (the fly homolog of human Alfy that is also involved in the clearance of ubiquitinated proteins) did not result in an obvious increase in autophagy in Drosophila, unlike proteasome impairment [21,35]. Moreover, p62 was found to be dispensable for both viability and starvation-induced autophagy in knockout mice [14]. Multiple selective autophagy receptors have been identified in mammalian cells, but these are relatively uncharacterized in Drosophila, as only HDAC6 and blue cheese have been analyzed so far besides p62 [13,35,36]. Further studies are necessary to find out whether any of the selective adaptors is involved in autophagy induced by proteasome inactivation, or by starvation. After all, autophagy is thought to be responsible for breakdown and recycling of bulk cytoplasm upon nutrient limitation [3], so it is possible that none of the receptors are actually required for these large-scale autolysosomal degradation processes.

A second hypothesis is that proteasomal degradation is essential to maintain free intracellular amino acid levels and compensatory autophagy is induced by amino acid shortage, as suggested in a recent publication [32]. In this paper, addition of exogenous amino acids was reported to attenuate proteasome inactivation-induced autophagy and partially rescue lifespan reduction in flies treated with a proteasome inhibitor [32]. In this scenario, loss of autophagy in cells with impaired proteasome activity would further reduce amino acid levels as both recycling pathways are inhibited, presumably resulting in a stronger block of cell growth. However, blocking the function of core autophagy genes did not further decrease the growth of proteasome RNAi cells in fat body clones, indicating that reduced amino acid levels are likely not the only link between these processes in this setting.

A third hypothesis is that stabilization of certain proteasome substrate(s) positively regulates autophagy. The levels of HIF-1α are normally kept low through ubiquitination mediated by VHL, which is followed by proteasomal degradation. Hypoxia leads to stabilization of HIF-1α, resulting in its translocation to the nucleus and upregulation of hypoxia-inducible genes that mediate survival at low oxygen concentrations [28]. Cytoprotective autophagy is also induced by hypoxia, and hypoxia-induced autophagy is necessary for survival of cancer cells in the central, poorly vascularized regions of solid tumors [30]. We found that genetic activation of hypoxia signaling induced autophagy in Drosophila, and silencing of the fly *HIF-1α* ortholog *sima* attenuated proteasome impairment-induced autophagy. These results suggest that autophagy is enhanced by proteasome inhibition at least in part through hypoxia signaling. A recent genome-wide association study identified mutations affecting the UPS pathway in renal cell carcinoma, which were associated with increased levels of HIF-1α in these tumors [37]. Interestingly, cells derived from many established cancers show elevated levels of autophagy, and multiple oncogenes and tumor suppressors (such as *VHL*) encode enzymes of the UPS involved in ubiquitin conjugation or deconjugation [38]. Thus, based on these and our results, activation of hypoxia signaling by UPS impairment may be responsible for increased autophagy in the absence of hypoxic conditions in a subset of established cancers.

Conclusions

Our work showed that genetic inactivation of proteasomal degradation induces compensatory autophagy in the widely used Drosophila fat body model, which requires core autophagy genes *Atg1, Vps34, Atg9, Atg4* and *Atg12*. Proteasome impairment leads to large-scale accumulation of aggregates containing ubiquitinated proteins and the selective autophagy cargo p62, but *p62* itself turned out to be largely dispensable for enhanced autophagy. Finally, we showed that genetic activation of hypoxia/HIF-1α signaling induces autophagy in Drosophila, and HIF-1α/sima, a well-characterized proteasome substrate, contributes to autophagy induced by proteasome impairment.

Methods

Drosophila stocks and culture

Flies were raised at 25°C on standard cornmeal/agar media, at 50% humidity and a 12-hour light/12-hour dark daily cycle. Fly stocks used in this study were obtained from the Vienna Drosophila RNAi Center, VDRC, Vienna, Austria and Bloomington Drosophila Stock Center, Bloomington, Indiana, USA, or kindly provided by Udai Pandey (*GFP-CL1*) [13] and Pablo Wappner (*LDH-GFP*) [29] (see Additional file 16: Figure S16 for a list of stocks). Note that KK, GD and JF lines are long hairpin-based RNAi transgenics, and HMS stocks contain short microRNA-based silencing constructs.

RT-PCR, western blots and immunostainings

Total RNA was isolated from L3 stage larvae using Purelink RNA Mini Kit (Ambion), followed by cDNA synthesis with Revertaid First Strand cDNA Synthesis Kit (Fermentas) and PCR amplification at 25 cycles. The following primers were used (designed to overlap exon-exon boundaries to prevent accidental amplification from genomic DNA): TACTCCTCCCGACACAAAGC, CTGGGT CATCTTCTCACGGT (Actin5C), TGGATCGACGCTG ATAAAGA, GTCTCCTGAAACGGGCAAT (p62), CTT GGATCGAACTCAGCACA, CAATGTTCCAGCTACT GGGTG (BNIP3).

Western blots were carried out as described [6,25], using primary antibodies: rabbit anti-p62 (1:5,000) [21], rabbit anti-Atg8a (1:5,000) [25] or mouse monoclonal anti-Tubulin AA4.3 (1:1,000, DSHB), followed by alkaline phosphatase conjugated goat anti-rabbit, anti-mouse secondary antibodies (1:5,000, Millipore). Immunostainings were done as before [21,25], using primary antibodies chicken anti-GFP (1:1,500, Invitrogen), rabbit anti-Atg8a (1:500, gift of Katja Köhler) [20], rabbit anti-p62 (1:2,000) [21], rabbit anti-ubiquitin (1:50, Dako), rabbit anti-active caspase 3 (1:500, Cell Signaling). Secondary antibodies were Alexa 488 anti-chicken, Alexa 546 anti-rabbit (1:1,500, Invitrogen).

Please see Additional file 17: Figure S17 for original images of RT-PCR gels and western blots.

Genetics and treatments

Clonal analysis in larval fat bodies was done as exhaustively described previously [6,18,19,21-25]. Briefly, cell clones were spontaneously generated by Flp-mediated excision of the FRT (Flp Recombination Target, >) cassette from Act > CD2 > Gal4 to activate UAS-dependent transcription of overexpression, dominant-negative and

dc_840_14

RNAi transgenes, together with the GFP reporters indicated in figure legends. Note that cell clones arose in embryos, and all of our analyses were carried out in L3 stage larvae at 84-90 hours after egg deposition. We also generated stable lines of *hsFlp[22], Act > CD2 > Gal4, UAS-mCD8-GFP* (all recombined together on chromosome X); *UAS-Rpn2* or *UAS-Rpt1* or *UAS-Prosβ2 RNAi* (located on autosomes). These lines were crossed to various *Atg*, *p62* and *sima* RNAi and dominant-negative lines in genetic interaction tests. RNAi was mediated in whole fat bodies by *cg-Gal4* for electron microscopy. As systemic knockdown of proteasomal genes resulted in early stage lethality, *hsFlp[22], Act > CD2 > Gal4, UAS-RNAi* stocks were heat shocked for 1 hour at 37 degrees at 48 hours after egg deposition to induce gene silencing in polyploid cells for western blots. Larvae of the age 60-66 hours after egg deposition were transferred to fresh medium containing 3 mg/ml chloroquine (Sigma) for a 24-hour treatment in autophagic flux experiments.

Histology and imaging

Lysotracker stainings were carried out as described [19,21-25]. Briefly, larvae were allowed to feed on food supplemented with plenty of yeast (fed) or floated in 20% sucrose solution for 3 hours (starved). Fat bodies were dissected, stained with Lysotracker Red (Invitrogen) and DAPI in PBS for 5 minutes, and photographed live. A Zeiss Axioimager M2 microscope equipped with an Apotome2 unit and a Plan-NeoFluar 40× 0.75 NA objective was used to capture images with Axiovision software. Primary images were processed in Adobe Photoshop to produce final figures. Tissues were processed for transmission electron microscopy analysis as described previously [6,18,25]. Images were captured on a Jeol JEM-1011 microscope using an Olympus Morada 11 megapixel camera and iTEM software (Olympus).

Statistics

Autophagic structures in ultrastructural images, Lyso tracker Red (LTR) and mCherry-Atg8a puncta were manually counted in Photoshop. Statistical evaluation of GFP-CL1, p62 and anti-Atg8a images was carried out using ImageJ (NIH) as described [21,25]. As proteasome RNAi and *sima* overexpressing cells were usually smaller than control cells, the numbers of dots per GFP-positive clone area or control tissue area were counted. To avoid errors owing to cell size differences, dot numbers shown in figures are normalized to control cells, that is, if the average size of GFP-positive cells was 10% of control cells and contained 5 dots on average, then the normalized number of dots per cell is 50 [21].

Images taken from multiple individual larvae per genotype (n) as indicated in figure legends were evaluated. Data were analyzed in PASW Statistics 18 (IBM). After testing for normality of data distribution, p values were calculated by Student's t tests or Mann-Whitney u tests in pairwise comparisons for normal or non-normal distribution data, respectively. We used ANOVA for multiple comparisons of normal distribution data and Kruskal-Wallis test for non-normal distribution data. Bar charts show average values and standard deviations. Regression analyses were also done in SPSS.

LDH-GFP fluorescence was detemined with ImageJ (NIH) software. Individual larvae were selected in the greyscale GFP channel, and the mean gray value was measured. Backgrund fluorescence from near each larva was subtracted from the mean gray value.

Additional files

Additional file 1: Figure S1. Aggregates of GFP-CL1 accumulate in proteasome RNAi cells. A-D) Expression of transgenic RNAi constructs in mosaic animals for *Prosa1* (A), *Prosa5* (B), *Prosβ2* (C), and *Rpt1* (D) results in accumulation of GFP-CL1 aggregates in larval fat body cells. Scale bar in A equals 20 μm for A-D.

Additional file 2: Figure S2. Aggregates of p62 and ubiquitinated proteins accumulate in proteasome RNAi cells. A-H) Knockdown of *Prosa1* (A, B), *Prosa5* (C, D), *Prosβ2* (E, F), and *Rpt1* (G, H) leads to the formation of large aggregates containing ubiquitinated proteins (A, C, E, G) and p62 (B, D, F, H). Boxed areas in A-H are shown enlarged. Scale bar in A equals 20 μm for A-H.

Additional file 3: Figure S3. Proteasome RNAi upregulates *p62* transcription. Systemic depletion of *Prosβ2* or *Rpt1* leads to increased transcription of *p62* relative to controls in RT-PCR experiments.

Additional file 4: Figure S4. Cell size decreases upon proteasome inactivation. Regression analysis reveals that GFP-CL1 level inversely changes with cell size in proteasome RNAi cells. Spearman's correlation coefficient = -0.728, $p < 0.001$, R^2 Linear = 0.332.

Additional file 5: Figure S5. Proteasome RNAi enhances starvation-induced autophagy. A-D) Knockdown of *Prosa1* (A), *Prosa5* (B), *Prosβ2* (C), and *Rpt1* (D) leads to increased punctate LTR staining in fat body cell clones of starved larvae compared to control non-GFP cells. Boxed areas in A-D are shown enlarged. Scale bar in A equals 20 μm for A-D.

Additional file 6: Figure S6. Lamp1-GFP partially colocalizes with LTR. Colocalization of the reporter Lamp1-GFP that labels primary lysosomes, late endosomes and digesting lysosomes is not complete with LTR, a dye that stains acidic structures only. Boxed area is shown enlarged. Scale bar equals 20 μm.

Additional file 7: Figure S7. Proteasome RNAi induces autophagy in well-fed cells. A-H) Knockdown of *Prosa1* (A, B), *Prosa5* (C, D), *Prosβ2* (E, F), and *Rpt1* (G, H) induces the formation of LTR-positive autolysosomes in fat body cell clones (marked by Lamp1-GFP expression) compared to surrounding non-GFP control cells in well fed larvae (A, C, E, G), and also leads to increased generation of Atg8a-positive autophagosomes (B, D, F, H) in fat body cell clones of well fed larvae. Boxed areas in A-H are shown enlarged. Scale bar in A equals 20 μm for A-H.

Additional file 8: Figure S8. Punctate LTR staining is increased by proteasome inactivation. Regression analysis reveals that punctate LTR staining inversely changes with cell size in proteasome RNAi cells. $R^2 = 0.101$, $P < 0.001$. The linearized equation of the curve is the following: $\ln(y) = \ln(a) + b*\ln(x)$, where $a = -0.012 \pm 0.002$; $p < 0.001$ and $b = 1.015 \pm 0.002$.

Additional file 9: Figure S9. Overexpressed Atg8a reporters are captured into p62 aggregates in proteasome RNAi cells. A-D) Overexpressed GFP-Atg8a is incorporated into large p62-positive aggregates in *Prosa1* (A), *Prosa5* (B), *Prosβ2* (C), and *Rpt1* (D) RNAi cells. Boxed areas in A-D are shown enlarged. Scale bar in A equals 20 μm for A-D.

Additional file 10: Figure S10. Autophagic flux is enhanced upon genetic inactivation of the proteasome. A-H) Knockdown of *Prosa1* (A, B), *Prosa5* (C, D), *Prosβ2* (E, F), and *Rpt1* (G, H) cells expressing the tandemly tagged mCherry-GFP-Atg8a reporter induces the formation of mCherry-labeled autolysosomes in fat body cell clones in well fed larvae (A, C, E, G). The lysosome inhibitor chloroquine blocks autophagy-dependent quenching of GFP, as now most puncta are positive for both mCherry and GFP (B, D, F, H). Boxed areas in A-H are shown enlarged. Scale bar in A equals 20 μm for A-H.

Additional file 11: Figure S11. Protein aggregates and autophagic structures form in fat body cells undergoing *Rpn2* RNAi. Depletion of *Rpn2* in whole fat bodies (mediated by the cg-Gal4 driver) results in the formation of protein aggregates (agg), double-membrane autophagosomes (arrow) and digesting autolysosomes (arrowhead) in cells. Scale bars equal 1 μm.

Additional file 12: Figure S12. Accumulation of p62 aggregates is increased by proteasome inactivation. Regression analysis reveals that accumulation of p62 aggregates inversely changes with cell size in proteasome RNAi cells. Spearman's correlation coefficient = -0.806, $P < 0.001$, R^2 Linear = 0.412.

Additional file 13: Figure S13. LTR-positive autolysosomes do not colocalize with p62 and Atg8a reporters. A, B) p62-GFP (A) and GFP-Atg8a (B) display practically no colocalization with the lysosome marker LTR. Boxed areas in A and B are shown enlarged. Scale bar in A equals 20 μm for A and B.

Additional file 14: Figure S14. Caspases are not activated in proteasome or *Vhl* RNAi or sima overexpressing cells. A-H) No active caspase 3 immunoreactivity is detected in *Prosa1* (A), *Prosa5* (B), *Prosβ2* (C), *Rpt1* (D) and *Rpn2* (E) RNAi fat body cells. (F) Similarly, no active caspase 3 immunolabeling is detected in *Rpt1* RNAi cells (marked by Lamp1-GFP) in brains. Note that several control cells positive for active caspase 3 (arrowheads) are seen in this panel. Similarly, overexpression of sima (G) or depletion of *Vhl* (H) does not lead to activation of caspase 3 in fat body cells either. Boxed areas in A-H are shown enlarged. Scale bar in A equals 20 μm for A-H.

Additional file 15: Figure S15. The hypoxia reporter LDH-GFP is activated in proteasome or *Vhl* RNAi animals. Systemic depletion of *Prosβ2*, *Rpn2*, *Rpt1* or *Vhl* all lead to a similar upregulation of the transcriptional hypoxia reporter transgene *LDH-GFP*, compared to control larvae. Per cent values refer to GFP fluorescence.

Additional file 16: Figure S16. List of Drosophila stocks used in this study.

Additional file 17: Figure S17. Original images for gels and western blots. Black boxes highlight cropped regions, which are shown in image panels as indicated.

Competing interests
The authors declare that they have no competing interests.

Authors' contributions
PL, AV, MS and GJ designed experiments. PL, AV, KP, PN, ZS, GJ carried out experiments. PL, AV, KP, ZS, GJ analyzed data. AV prepared figures. PL, GJ wrote the manuscript. All authors read and approved the final manuscript.

Acknowledgements
We would like to thank Zsófia Kováts and Sarolta Pálfia for technical assistance, and Pablo Wappner, Katja Köhler and public stock centers for providing reagents. This work was supported by grants from the Hungarian Scientific Research Fund (OTKA NK78012 for MS), and the Wellcome Trust (087518/Z/08/Z for GJ).

Received: 22 February 2013 Accepted: 21 June 2013
Published: 25 June 2013

References
1. Wong E, Cuervo AM: **Integration of clearance mechanisms: the proteasome and autophagy.** *Cold Spring Harb Perspect Biol* 2010, **2**(12):a006734.
2. Juhasz G, Neufeld TP: **Autophagy: a forty-year search for a missing membrane source.** *PLoS Biol* 2006, **4**(2):e36.
3. Mizushima N, Levine B, Cuervo AM, Klionsky DJ: **Autophagy fights disease through cellular self-digestion.** *Nature* 2008, **451**(7182):1069–1075.
4. Lamark T, Johansen T: **Autophagy: links with the proteasome.** *Curr Opin Cell Biol* 2010, **22**(2):192–198.
5. Korolchuk VI, Menzies FM, Rubinsztein DC: **Mechanisms of cross-talk between the ubiquitin-proteasome and autophagy-lysosome systems.** *FEBS Lett* 2010, **584**(7):1393–1398.
6. Juhasz G, Erdi B, Sass M, Neufeld TP: **Atg7-dependent autophagy promotes neuronal health, stress tolerance, and longevity but is dispensable for metamorphosis in Drosophila.** *Genes Dev* 2007, **21**(23):3061–3066.
7. Simonsen A, Cumming RC, Brech A, Isakson P, Schubert DR, Finley KD: **Promoting basal levels of autophagy in the nervous system enhances longevity and oxidant resistance in adult Drosophila.** *Autophagy* 2008, **4**(2):176–184.
8. Bjorkoy G, Lamark T, Brech A, Outzen H, Perander M, Overvatn A, Stenmark H, Johansen T: **p62/SQSTM1 forms protein aggregates degraded by autophagy and has a protective effect on huntingtin-induced cell death.** *J Cell Biol* 2005, **171**(4):603–614.
9. Nezis IP, Simonsen A, Sagona AP, Finley K, Gaumer S, Contamine D, Rusten TE, Stenmark H, Brech A: **Ref(2)P, the Drosophila melanogaster homologue of mammalian p62, is required for the formation of protein aggregates in adult brain.** *J Cell Biol* 2008, **180**(6):1065–1071.
10. Sandri M: **Autophagy in skeletal muscle.** *FEBS Lett* 2010, **584**(7):1411–1416.
11. Juhasz G, Puskas LG, Komonyi O, Erdi B, Maroy P, Neufeld TP, Sass M: **Gene expression profiling identifies FKBP39 as an inhibitor of autophagy in larval Drosophila fat body.** *Cell Death Differ* 2007, **14**(6):1181–1190.
12. Erdi B, Nagy P, Zvara A, Varga A, Pircs K, Menesi D, Puskas LG, Juhasz G: **Loss of the starvation-induced gene Rack1 leads to glycogen deficiency and impaired autophagic responses in Drosophila.** *Autophagy* 2012, **8**(7):1124–1135.
13. Pandey UB, Nie Z, Batlevi Y, McCray BA, Ritson GP, Nedelsky NB, Schwartz SL, DiProspero NA, Knight MA, Schuldiner O, Padmanabhan R, Hild M, Berry DL, Garza D, Hubbert CC, Yao TP, Baehrecke EH, Taylor JP: **HDAC6 rescues neurodegeneration and provides an essential link between autophagy and the UPS.** *Nature* 2007, **447**(7146):859–863.
14. Komatsu M, Waguri S, Koike M, Sou YS, Ueno T, Hara T, Mizushima N, Iwata J, Ezaki J, Murata S, Hamazaki J, Nishito Y, Iemura S, Natsume T, Yanagawa T, Uwayama J, Warabi E, Yoshida H, Ishii T, Kobayashi A, Yamamoto M, Yue Z, Uchiyama Y, Kominami E, Tanaka K: **Homeostatic levels of p62 control cytoplasmic inclusion body formation in autophagy-deficient mice.** *Cell* 2007, **131**(6):1149–1163.
15. Bartlett BJ, Isakson P, Lewerenz J, Sanchez H, Kotzebue RW, Cumming RC, Harris GL, Nezis IP, Schubert DR, Simonsen A, Finley KD: **p62, Ref(2)P and ubiquitinated proteins are conserved markers of neuronal aging, aggregate formation and progressive autophagic defects.** *Autophagy* 2011, **7**(6):572–583.
16. Liu XD, Ko S, Xu Y, Fattah EA, Xiang Q, Jagannath C, Ishii T, Komatsu M, Eissa NT: **Transient aggregation of ubiquitinated proteins is a cytosolic unfolded protein response to inflammation and endoplasmic reticulum stress.** *J Biol Chem* 2012, **287**(23):19687–19698.
17. Kuusisto E, Suuronen T, Salminen A: **Ubiquitin-binding protein p62 expression is induced during apoptosis and proteasomal inhibition in neuronal cells.** *Biochem Biophys Res Commun* 2001, **280**(1):223–228.
18. Juhasz G, Hill JH, Yan Y, Sass M, Baehrecke EH, Backer JM, Neufeld TP: **The class III PI(3)K Vps34 promotes autophagy and endocytosis but not TOR signaling in Drosophila.** *J Cell Biol* 2008, **181**(4):655–666.
19. Juhasz G, Neufeld TP: **Experimental control and characterization of autophagy in Drosophila.** *Methods Mol Biol* 2008, **445**:125–133.
20. Barth JM, Szabad J, Hafen E, Kohler K: **Autophagy in Drosophila ovaries is induced by starvation and is required for oogenesis.** *Cell Death Differ* 2011, **18**(6):915–924.
21. Pircs K, Nagy P, Varga A, Venkei Z, Erdi B, Hegedus K, Juhasz G: **Advantages and limitations of different p62-based assays for estimating autophagic activity in Drosophila.** *PLoS One* 2012, **7**(8):e44214.
22. Scott RC, Juhasz G, Neufeld TP: **Direct induction of autophagy by atg1 inhibits cell growth and induces apoptotic cell death.** *Curr Biol* 2007, **17**(1):1–11.
23. Scott RC, Schuldiner O, Neufeld TP: **Role and regulation of starvation-induced autophagy in the Drosophila fat body.** *Dev Cell* 2004, **7**(2):167–178.

24. Rusten TE, Lindmo K, Juhasz G, Sass M, Seglen PO, Brech A, Stenmark H: **Programmed autophagy in the Drosophila fat body is induced by ecdysone through regulation of the PI3K pathway.** *Dev Cell* 2004, **7**(2):179–192.
25. Takats S, Nagy P, Varga A, Pircs K, Karpati M, Varga K, Kovacs AL, Hegedus K, Juhasz G: **Autophagosomal Syntaxin17-dependent lysosomal degradation maintains neuronal function in Drosophila.** *J Cell Biol* 2013, **201**(4):531–539.
26. Pulipparacharuvil S, Akbar MA, Ray S, Sevrioukov EA, Haberman AS, Rohrer J, Kramer H: **Drosophila Vps16A is required for trafficking to lysosomes and biogenesis of pigment granules.** *J Cell Sci* 2005, **118**(Pt 16):3663–3673.
27. Klionsky DJ, Abdalla FC, Abeliovich H, Abraham RT, Acevedo-Arozena A, Adeli K, Agholme L, Agnello M, Agostinis P, Aguirre-Ghiso JA, Ahn HJ, Ait-Mohamed O, Ait-Si-Ali S, Akematsu T, Akira S, Al-Younes HM, Al-Zeer MA, Albert ML, Albin RL, Alegre-Abarrategui J, Aleo MF, Alirezaei M, Almasan A, Almonte-Becerril M, Amano A, Amaravadi R, Amarnath S, Amer AO, Andrieu-Abadie N, Anantharam V, *et al*: **Guidelines for the use and interpretation of assays for monitoring autophagy.** *Autophagy* 2012, **8**(4):445–544.
28. Nys K, Maes H, Dudek AM, Agostinis P: **Uncovering the role of hypoxia inducible factor-1alpha in skin carcinogenesis.** *Biochim Biophys Acta* 2011, **1816**(1):1–12.
29. Lavista-Llanos S, Centanin L, Irisarri M, Russo DM, Gleadle JM, Bocca SN, Muzzopappa M, Ratcliffe PJ, Wappner P: **Control of the hypoxic response in Drosophila melanogaster by the basic helix-loop-helix PAS protein similar.** *Mol Cell Biol* 2002, **22**(19):6842–6853.
30. Bellot G, Garcia-Medina R, Gounon P, Chiche J, Roux D, Pouyssegur J, Mazure NM: **Hypoxia-induced autophagy is mediated through hypoxia-inducible factor induction of BNIP3 and BNIP3L via their BH3 domains.** *Mol Cell Biol* 2009, **29**(10):2570–2581.
31. McPhee CK, Balgley BM, Nelson C, Hill JH, Batlevi Y, Fang X, Lee CS, Baehrecke EH: **Identification of factors that function in Drosophila salivary gland cell death during development using proteomics.** *Cell Death Differ* 2013, **20**(2):218–225.
32. Suraweera A, Munch C, Hanssum A, Bertolotti A: **Failure of amino acid homeostasis causes cell death following proteasome inhibition.** *Mol Cell* 2012, **48**(2):242–253.
33. Velentzas PD, Velentzas AD, Mpakou VE, Antonelou MH, Margaritis LH, Papassideri IS, Stravopodis DJ: **Detrimental effects of proteasome inhibition activity in Drosophila melanogaster: implication of ER stress, autophagy, and apoptosis.** *Cell Biol Toxicol* 2013, **29**(1):13–37.
34. Velentzas PD, Velentzas AD, Mpakou VE, Papassideri IS, Stravopodis DJ, Margaritis LH: **Proteasome inhibition induces developmentally deregulated programs of apoptotic and autophagic cell death during Drosophila melanogaster oogenesis.** *Cell Biol Int* 2011, **35**(1):15–27.
35. Simonsen A, Cumming RC, Lindmo K, Galaviz V, Cheng S, Rusten TE, Finley KD: **Genetic modifiers of the Drosophila blue cheese gene link defects in lysosomal transport with decreased life span and altered ubiquitinated-protein profiles.** *Genetics* 2007, **176**(2):1283–1297.
36. Johansen T, Lamark T: **Selective autophagy mediated by autophagic adapter proteins.** *Autophagy* 2011, **7**(3):279–296.
37. Guo G, Gui Y, Gao S, Tang A, Hu X, Huang Y, Jia W, Li Z, He M, Sun L, Song P, Sun X, Zhao X, Yang S, Liang C, Wan S, Zhou F, Chen C, Zhu J, Li X, Jian M, Zhou L, Ye R, Huang P, Chen J, Jiang T, Liu X, Wang Y, Zou J, Jiang Z, *et al*: **Frequent mutations of genes encoding ubiquitin-mediated proteolysis pathway components in clear cell renal cell carcinoma.** *Nat Genet* 2012, **44**(1):17–19.
38. Kirkin V, Dikic I: **Ubiquitin networks in cancer.** *Curr Opin Genet Dev* 2011, **21**(1):21–28.

doi:10.1186/1471-2121-14-29
Cite this article as: Lőw *et al.*: Impaired proteasomal degradation enhances autophagy via hypoxia signaling in Drosophila. *BMC Cell Biology* 2013 **14**:29.

Submit your next manuscript to BioMed Central and take full advantage of:

- **Convenient online submission**
- **Thorough peer review**
- **No space constraints or color figure charges**
- **Immediate publication on acceptance**
- **Inclusion in PubMed, CAS, Scopus and Google Scholar**
- **Research which is freely available for redistribution**

Submit your manuscript at
www.biomedcentral.com/submit

BioMed Central

OPEN ACCESS Freely available online

dc_840_14

PLOS | GENETICS

Myc-Driven Overgrowth Requires Unfolded Protein Response-Mediated Induction of Autophagy and Antioxidant Responses in *Drosophila melanogaster*

Péter Nagy, Ágnes Varga, Karolina Pircs, Krisztina Hegedűs, Gábor Juhász*

Department of Anatomy, Cell and Developmental Biology, Eötvös Loránd University, Budapest, Hungary

Abstract

Autophagy, a lysosomal self-degradation and recycling pathway, plays dual roles in tumorigenesis. Autophagy deficiency predisposes to cancer, at least in part, through accumulation of the selective autophagy cargo p62, leading to activation of antioxidant responses and tumor formation. While cell growth and autophagy are inversely regulated in most cells, elevated levels of autophagy are observed in many established tumors, presumably mediating survival of cancer cells. Still, the relationship of autophagy and oncogenic signaling is poorly characterized. Here we show that the evolutionarily conserved transcription factor Myc (dm), a proto-oncogene involved in cell growth and proliferation, is also a physiological regulator of autophagy in *Drosophila melanogaster*. Loss of Myc activity in null mutants or in somatic clones of cells inhibits autophagy. Forced expression of Myc results in cell-autonomous increases in cell growth, autophagy induction, and p62 (Ref2P)-mediated activation of Nrf2 (cnc), a transcription factor promoting antioxidant responses. Mechanistically, Myc overexpression increases unfolded protein response (UPR), which leads to PERK-dependent autophagy induction and may be responsible for p62 accumulation. Genetic or pharmacological inhibition of UPR, autophagy or p62/Nrf2 signaling prevents Myc-induced overgrowth, while these pathways are dispensable for proper growth of control cells. In addition, we show that the autophagy and antioxidant pathways are required in parallel for excess cell growth driven by Myc. Deregulated expression of Myc drives tumor progression in most human cancers, and UPR and autophagy have been implicated in the survival of Myc-dependent cancer cells. Our data obtained in a complete animal show that UPR, autophagy and p62/Nrf2 signaling are required for Myc-dependent cell growth. These novel results give additional support for finding future approaches to specifically inhibit the growth of cancer cells addicted to oncogenic Myc.

Citation: Nagy P, Varga Á, Pircs K, Hegedűs K, Juhász G (2013) Myc-Driven Overgrowth Requires Unfolded Protein Response-Mediated Induction of Autophagy and Antioxidant Responses in *Drosophila melanogaster*. PLoS Genet 9(8): e1003664. doi:10.1371/journal.pgen.1003664

Editor: Bruce Edgar, Zentrum für Molekulare Biologie der Universität Heidelberg, Germany

Received January 9, 2013; **Accepted** June 10, 2013; **Published** August 8, 2013

Copyright: © 2013 Nagy et al. This is an open-access article distributed under the terms of the Creative Commons Attribution License, which permits unrestricted use, distribution, and reproduction in any medium, provided the original author and source are credited.

Funding: The authors would like to thank the Wellcome Trust (087518/Z/08/Z), the Hungarian Scientific Research Fund (OTKA K83509) and the Hungarian Academy of Sciences (BO/00552/11) for support. The funders had no role in study design, data collection and analysis, decision to publish, or preparation of the manuscript.

Competing Interests: The authors have declared that no competing interests exist.

* E-mail: szmrt@elte.hu

Introduction

The balance of anabolic and catabolic processes determines net changes in cell size. An increased ratio of biosynthetic versus degradative activity results in cell growth. Activation of growth-promoting signaling pathways such as the class I PI3K (phosphatidylinositol 3-kinase), AKT and TOR (target of rapamycin) kinase systems increases protein translation and inhibits autophagy, an *Atg* gene dependent pathway in eukaryotic cells that captures proteins, lipids and organelles in double-membrane autophagosomes, followed by lysosomal degradation and recycling [1]. In addition, we and others have shown previously that genetic activation of autophagy reduces cell size in flies and mammals, and autophagy-deficient cells have a net growth advantage during long-term starvation in Drosophila melanogaster larvae [2,3].

However, the role of autophagy in cell growth and physiology is more complex. Low-level basal autophagy maintains protein and organelle quality control by selectively removing unfolded proteins and damaged or superfluous organelles. Loss of basal autophagy results in gradual accumulation of toxic protein aggregates and excess or non-functional organelles, leading to pathological consequences including neurodegeneration and decreased lifespan both in Drosophila and mice [4–6]. Autophagy deficiency is associated with increased production of reactive oxygen species, proteotoxicity and accelerated tumorigenesis [7]. Autophagy is upregulated in response to starvation and stress to promote survival by recycling dispensable intracellular components. Large-scale autolysosomal degradation provides building blocks that fuel biosynthetic and metabolic pathways under these conditions. Elevated levels of autophagy are also observed in many established cancers [6–8]. While the underlying genetic changes are still poorly characterized, autophagy induction has been suggested to sustain the altered metabolism and survival of various cancer cells. These reports altogether indicate that autophagy has a context-dependent role in the regulation of cell growth.

Myc is required for proper expression of genes involved in various processes including cell growth and proliferation [9–11]. It forms an evolutionarily conserved heterodimeric transcription factor with its binding partner Max. Myc-Max complexes show high affinity binding to E-box sequences in the promoters or introns of their target genes to increase their transcription rate. In addition, Myc exhibits lower affinity binding to additional

dc_840_14

Author Summary

The evolutionarily conserved transcription factor Myc promotes protein synthesis, cell growth and cancer progression through incompletely understood mechanisms. In this work, we show that forced expression of Myc induces the accumulation of abnormal proteins leading to unfolded protein responses (UPR), presumably by overloading the protein synthetic capacity of cells in Drosophila. UPR then results in autophagy-mediated breakdown and recycling of cytoplasmic material, and at the same time, to activation of antioxidant responses in these cells. Blocking the UPR stress signaling, autophagy and antioxidant pathways genetically, or by feeding larvae an autophagy-inhibiting drug, prevents overgrowth of Myc-expressing cells, but these treatments do not affect the growth of control cells in the same tissues. These results, together with recent reports in mammalian cancer models, suggest that drugs targeting UPR, autophagy and antioxidant responses may specifically inhibit cancer cell proliferation driven by oncogenic Myc.

promoter sequences to regulate a much larger set of genes. Myc is a classical oncogene deregulated in most tumors, although the mechanisms of how it promotes overgrowth of cancer cells are incompletely understood [9–12]. We decided to explore potential connections between Myc, autophagy, and Myc-induced overgrowth in the genetic model organism Drosophila.

Results

Depletion of *Myc* (also known as *dm*) by expression of a transgenic RNAi line, or overexpression of its antagonist Mad (also known as Mnt) in GFP-marked clones reduced the size of polyploid fat body cells in a cell-autonomous manner, as described earlier [13,14]. Lysotracker red is an acidophilic dye commonly used to label digesting autolysosomes in Drosophila [2,4,15–19]. Myc activity was required for starvation-induced formation of Lysotracker-positive punctae, as GFP-positive *Myc* RNAi or Mad overexpressing cells had fewer dots compared to surrounding control fat tissue (Figure 1A–C, see also Table S1 for statistical analyses of these and all subsequent data). Activated, lipidated Atg8a is covalently bound to autophagosomes, and is rapidly degraded upon their fusion with lysosomes, so analyzing endogenous Atg8a-positive puncta is widely used to follow the generation of early autophagic structures [16,19,20]. Silencing of *Myc* or overexpression of Mad in GFP-positive cell clones also interfered with starvation-induced punctate endogenous Atg8a labeling compared to control cells in starved larvae (Figure 1D–F). Similarly, *Myc* null mutant larvae showed impaired starvation-induced autophagy of the fat body and midgut, based on Lysotracker staining and transmission electron microscopy (Figure 1G–K). p62 (also known as Ref2P, for refractory to sigma P) is a constitutively expressed selective autophagic cargo. Impaired autophagy leads to stabilization of p62, so analyzing the levels of p62 aggregates is a standard assay for estimating autophagic degradation [16,17,19,21]. Loss of Myc activity in GFP-marked cells in well-fed larvae cell-autonomously increased both the number and size of p62 aggregates (Figure 1L–N), suggesting basal autophagy defects. These results established that *Myc* is a physiological regulator of autophagy.

Overexpression of Drosophila Myc in GFP-marked fat body cell clones increased cell growth compared to neighboring control cells, as described previously (Figure 2A) [14,22]. Myc overexpression activated autophagy in fat body cells of well-fed Drosophila larvae in a cell-autonomous manner, based on the induction of Lysotracker-positive autolysosomes, punctate mCherry-Atg8a that labels both autophagosomes and autolysosomes as mCherry remains fluorescent in lysosomes [16,17,19,20,23], and increased formation of endogenous Atg8a-positive autophagosomes in GFP-positive cells compared to neighboring control cells (Figure 2B–E). Determining the levels of autophagosome-associated, lipidated Atg8a-II relative to loading control in western blot experiments is a standard biochemical assay to analyze autophagy [16,19,24]. Myc overexpression in whole larval fat bodies indeed elevated the amounts of Atg8a-II relative to Tubulin (Figure 2F). Electron microscopy confirmed the presence of autolysosomes containing cytoplasmic material in various stages of degradation, and double-membrane autophagosomes containing undigested cargo in Myc overexpressing cells (Figure 2G, Figure S1). Similarly, forced expression of Myc in a stripe of cells in wing imaginal discs increased the size of this expression domain and enhanced mCherry-Atg8a dot formation (Figure 2H, I), indicating autophagy induction in these diploid cells.

To further characterize how Myc overexpression regulates the multi-step process of autophagy, we used a double tagged reporter transgene mCherry-GFP-Atg8a, a common tool for measuring autophagic flux (the rate of autophagic degradation) [16,19,25,26]. This reporter molecule is selectively bound to autophagosomes, followed by its transport to autolysosomes where GFP is quenched rapidly but mCherry fluorescence is retained. Autophagosomes are positive for both mCherry and GFP, while autolysosomes only show mCherry fluorescence in control cells undergoing autophagy [16,19,25,26]. Practically no dots were observed in control fat body cells of well-fed larvae using this reporter (Figure 3A), indicating normally low basal autophagy levels. The few dots we saw were mostly mCherry-positive (13% of mCherry dots were also positive for GFP, 10/77 dots counted). Overexpression of Myc led to the formation of numerous punctae that were also mostly positive for mCherry only (9.2% colocalization with GFP, 227/2,459 dots counted, Figure 3C).

Chloroquine is a small molecule drug that neutralizes the normally acidic lysosomal pH, and thus inhibits all lysosomal degradation routes including autophagy and endocytosis [8,16]. Chloroquine treatment is often used to distinguish autophagy induction from impaired autolysosomal degradation: both conditions can result in increased numbers of autophagic structures, but these numbers further increase in the presence of chloroquine if autophagic flux is normal, while chloroquine has no effect if degradation is already impaired [16]. Feeding larvae chloroquine led to the induction of dots in control cells that were positive for both mCherry and GFP (98.8% colocalization, 327/331 dots counted, Figure 3B, E), indicating that low-level basal autophagic degradation was inhibited by this treatment, and autolysosomes accumulated unable to digest their cargo. Chloroquine treatment of larvae with Myc-overexpressing fat body cell clones also increased mCherry dot numbers compared to non-treated cells overexpressing Myc, and punctate mCherry-positive structures this time also contained GFP (99.2% colocalization, 4,361/4,394 dots counted, Figure 3D, E). Importantly, the number of mCherry-GFP-Atg8a positive structures was also much higher in chloroquine-treated Myc overexpressing cells than in chloroquine-treated control cells (Figure 3E), altogether suggesting that Myc promotes both the induction and degradation steps of autophagy.

Autophagic flux can also be analyzed using these fluorescently tagged Atg8a reporters in western blots, as Atg8a itself is rapidly broken down in autolysosomes, resulting in autophagic degrada-

dc_840_14

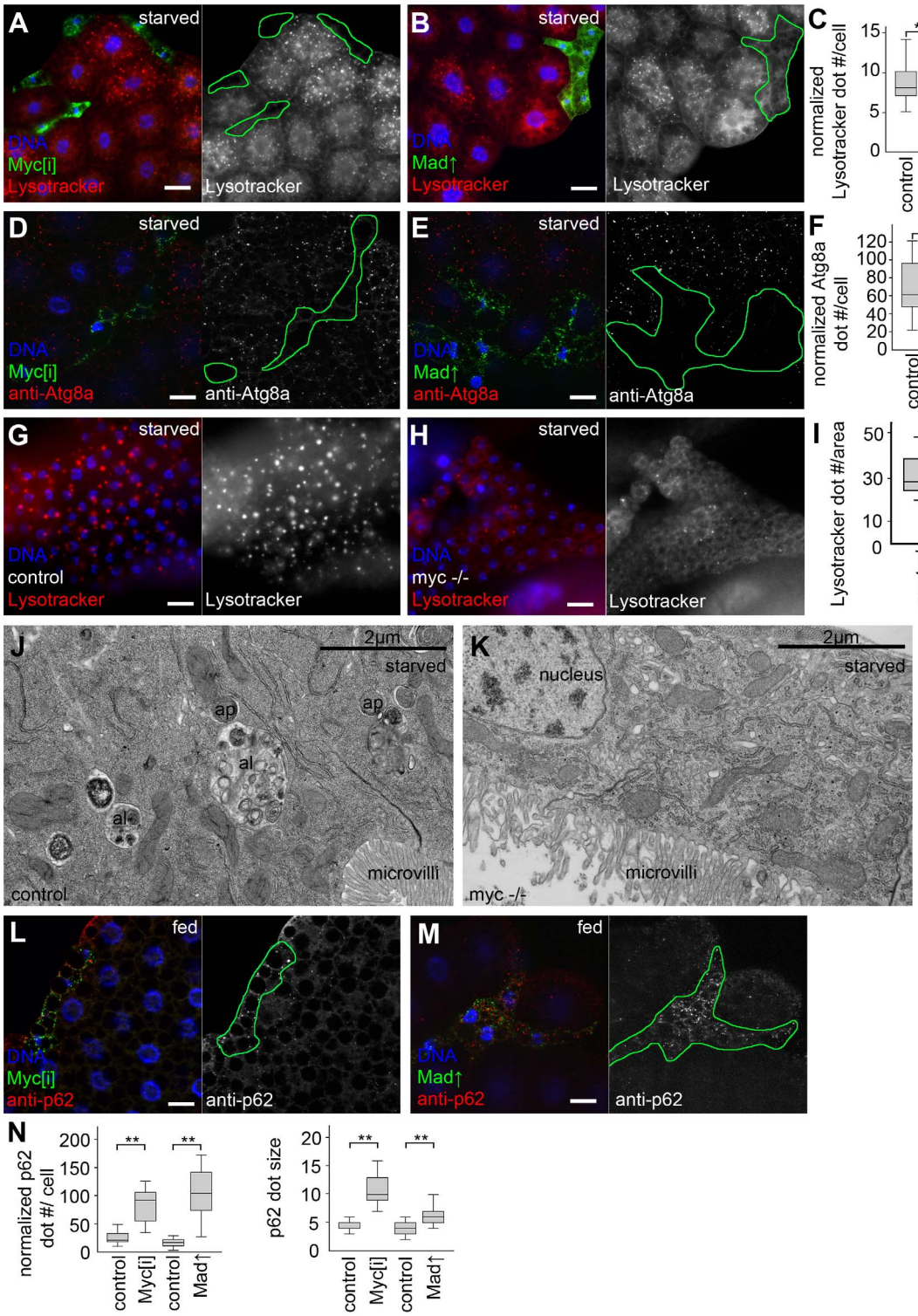


Figure 1. Myc is necessary for starvation-induced autophagy in Drosophila. (A) *Myc* depletion in LAMP1-GFP marked fat body cell clones inhibits starvation-induced punctate Lysotracker staining, compared to surrounding control cells that do not express GFP. Mid-L3 stage larvae were analyzed in all fat body experiments unless noted otherwise. (B) Overexpression of Mad also blocks Lysotracker dot formation in cells marked by LAMP1-GFP. (C) Quantification of data presented in panels A and B, n = 7 for all genotypes. (D) Starvation-induced punctate endogenous Atg8a staining is inhibited in *Myc* RNAi cells marked by LAMP1-GFP expression, compared to neighboring control tissue. (E) Forced expression of Mad also decreases Atg8a dot formation. (F) Quantification of data presented in panels D and E, n = 6 for all genotypes. (G) Starvation leads to the formation of Lysotracker-positive autolysosomes in fat body cells of control L1 stage larvae. (H) A near-complete block of Lysotracker puncta formation is seen in *Myc* null mutant L1 stage larvae. (I) Quantification of data presented in panels G and H. (J) Double-membrane autophagosomes (ap) and dense autolysosomes (al) degrading sequestered cytoplasmic cargo are observed in midgut cells of control L1 stage larvae. (K) No autophagic structures are seen in midgut cells of L1 stage *Myc* null mutant larvae. (L) The selective autophagy cargo p62 accumulates in *Myc* RNAi cells (marked by LAMP1-GFP

dc_840_14

expression) compared to surrounding control tissue in well-fed animals. (M) Mad overexpression also leads to large-scale accumulation of p62 aggregates. (N) Statistical evaluation of data presented in panels M and N, n = 7 for all genotypes. Scalebars in A, B, D, E, G, H, L, M equal 20 μm. Statistically significant differences are indicated, ** $p<0.01$.
doi:10.1371/journal.pgen.1003664.g001

tion-dependent generation of free mCherry or GFP [3,16]. Again, Myc overexpression in whole fat bodies strongly increased autolysosomal conversion of mCherry-GFP-Atg8a to free mCherry relative to the loading control Tubulin (Figure 3F).

We next evaluated the role of autophagy in supporting the increased growth of Myc-expressing cells. Myc-induced overgrowth of GFP-positive clones of fat body cells relative to neighboring control cells was completely suppressed by chloro-

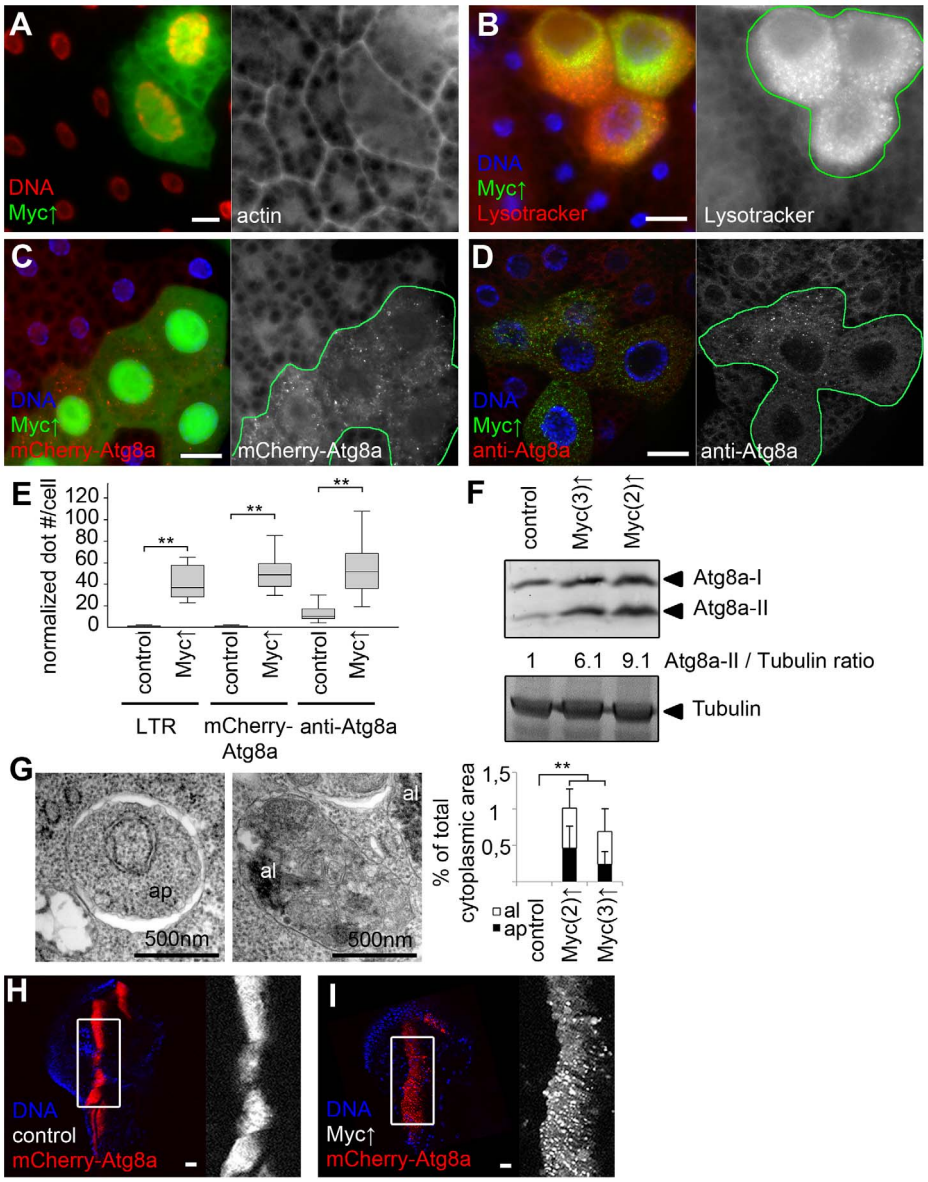


Figure 2. Myc overexpression induces autophagy in Drosophila. (A) Myc overexpression in GFP-marked fat body cell clones leads to cell-autonomous overgrowth. (B–D) Enhanced punctate Lysotracker staining (B), mCherry-Atg8a dot formation (C) and endogenous Atg8a labeling (D) is observed in Myc-overexpressing fat body cell clones (marked by expression of LAMP1-GFP in panels B and D and by GFP in panel C), when compared to surrounding control tissue in well-fed larvae. (E) Quantification of data presented in B–D, n = 7 for all genotypes. (F) Fat body-specific expression of Myc from transgenes located on chromosome 2 or 3 increase the amount of activated Atg8a-II compared to control fat bodies of well-fed larvae. Numbers indicate the level of lipidated Atg8a-II relative to the loading control Tubulin in different genotypes, as determined by densitometric evaluation. (G) Fat body-specific overexpression of Myc induces formation of typical double-membrane autophagosomes (ap) and autolysosomes that contain cytoplasmic material in various stages of degradation (al), n = 5 for all genotypes. (H, I) Myc overexpression leads to punctate mCherry-Atg8a labeling (I) and increased expression area in the *patched* domain of wing discs compared to control discs (H). Scalebars in A–D and H–I equal 20 μm. Statistically significant differences are indicated, ** $p<0.01$.
doi:10.1371/journal.pgen.1003664.g002

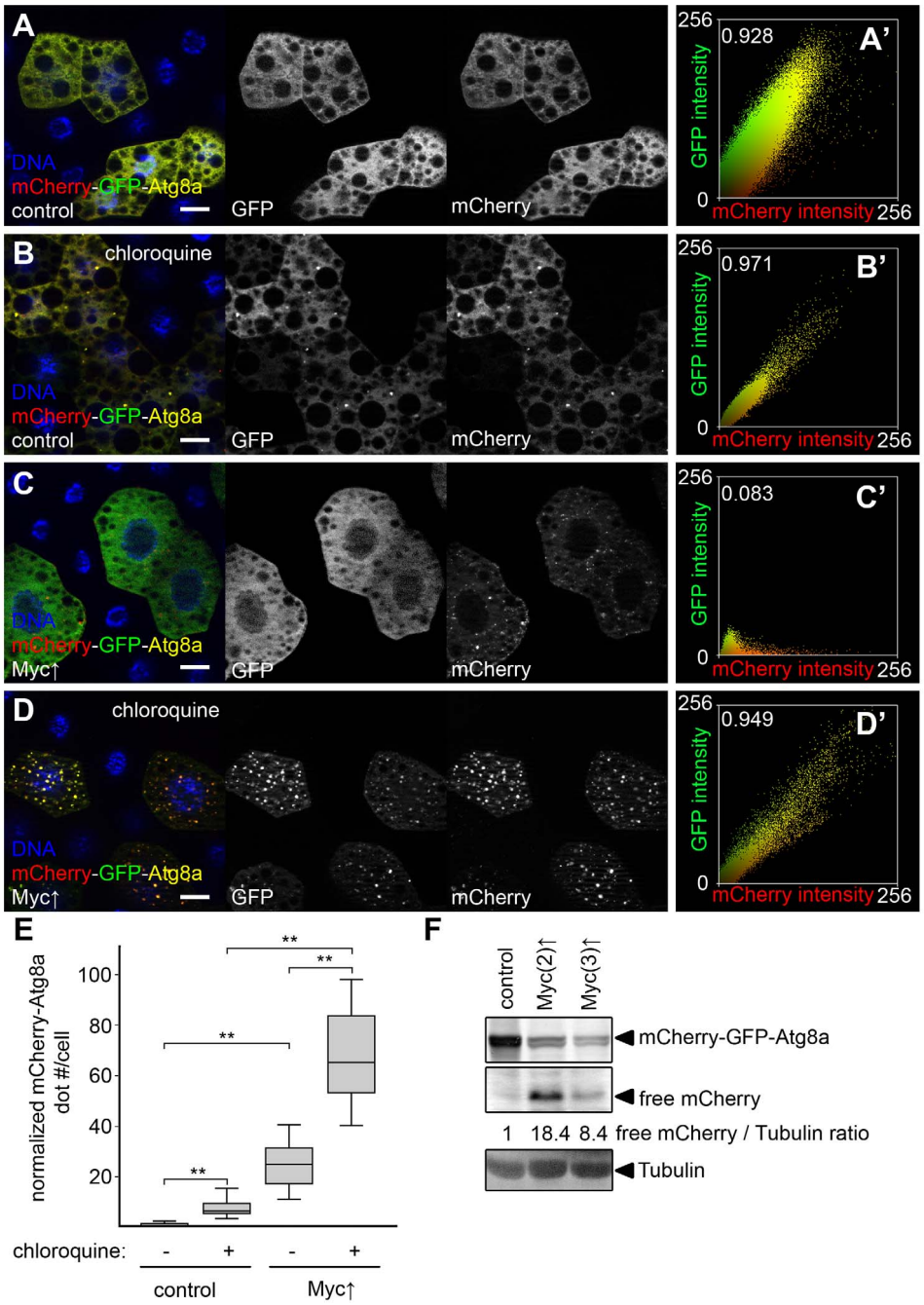


Figure 3. Myc increases autophagic flux. (A) Practically no mCherry-GFP-Atg8a dots are seen in control fat body cells of well-fed larvae. (B) Dots positive for both mCherry and GFP appear in control cells upon feeding larvae chloroquine, a drug that blocks lysosomal degradation. (C) Overexpression of Myc results in the formation of puncta that are mostly mCherry-positive. (D) Chloroquine treatment strongly increases the number of mCherry punctae in Myc overexpressing cells. Note that dots are now positive for GFP as well. (A′–D′) Fluorescent intensity and colocalization profiles of mCherry and GFP channels from panels A–D. Pearson correlation coefficients shown in A′–D′ indicate that the correlation of the mCherry and GFP pixel intensity is low in panel C but high in panels A, B, and D. (E) Quantification of data in panels A–D, n = 15–30 per genotype/treatment. Myc expression in fat body cells strongly induces mCherry puncta formation compared to control cells. Chloroquine treatment increases dot numbers both in control and Myc overexpressing cells. (F) Autophagic degradation-dependent conversion of mCherry-GFP-Atg8a to free mCherry is increased by overexpression of Myc in fat body cells. Numbers indicate the level of free mCherry relative to the loading control Tubulin in different genotypes, as determined by densitometric evaluation. Scalebars in A–D equal 20 μm. Statistically significant differences are indicated, ** $p<0.01$.
doi:10.1371/journal.pgen.1003664.g003

quine treatment (Figure 4A, C). Chloroquine was also able to suppress cellular overgrowth induced by two copies of overexpressed Myc (Figure S2A–C). Null mutation of *FIP200*, or blocking the function of other core *Atg* genes that specifically inhibit autophagic breakdown also completely suppressed the Myc-induced overgrowth of GFP-positive fat cells relative to neighboring control cells, similar to *Myc* RNAi or co-overexpression of Mad (Figure 4B, C, Figure S2D–K). Similarly, inhibition of

dc_840_14

autophagy blocked increases in Myc-overexpressing domain size and punctate mCherry-Atg8a labeling in wing imaginal discs (Figure 4D–F, Figure S2M–O). Myc expression in this domain of developing wing discs increased L3–L4 vein distance in adult wings, which was also suppressed by the silencing of *Atg1, FIP200, Atg18a*, or by blocking Vps34 (Figure 4G, Figure S2L). Importantly, Myc overexpression failed to increase L3–L4 vein distance in the absence of Atg8a, but it readily did so if mCherry-Atg8a was co-expressed in *Atg8a* null mutants (Figure 4G). Inhibition of autophagy did not reduce growth of fat body or wing intervein cells in the absence of forced Myc expression in well-fed animals (Figure S2P, Q), similar to our earlier reports [2,4,15]. Autophagy-dependent overgrowth of Myc expressing cells was also obvious using a different wing expression system (Figure S3) [27].

Human p62 (also known as SQSTM1 for sequestosome 1) is a multidomain adaptor protein involved in various diseases including cancer [28]. Drosophila p62 has a similar domain structure including an N-terminal PB1 (Phox and Bem1p) domain mediating its aggregation, an ubiquitin-binding UBA (ubiquitin-associated) domain, and an Atg8-interacting motif responsible for its selective degradation by autophagy [17,21]. Myc overexpression led to the accumulation of both p62 and ubiquitinated proteins in Drosophila fat body cells (Figure 5A, B). p62 was recently shown to be required for tumorigenesis in various cancer models, and mediate persistent activation of the transcription factor Nrf2 (nuclear factor erythroid-related factor 2) [29–32]. Mechanistically, human p62 binds to Keap1 (kelch-like ECH-associated protein 1) by disrupting the Keap1-Nrf2 interaction, resulting in stabilization of Nrf2 and induction of antioxidant responses [31,33]. Drosophila p62 also bound to Keap1 (Figure 5C). Consistent with these, overexpression of Myc activated the Nrf2-dependent transcriptional reporters *gstD-LacZ* and *gstD-GFP* in Drosophila fat body and wing disc cells, respectively (Figure 5D, Figure S4A, B). Knockdown of *p62* or the Drosophila *Nrf2* homologue *cnc* (cap and collar) prevented the activation of *gstD-GFP* by Myc (Figure S4C, D). This indicated that p62/Nrf2 signaling is required for Myc-induced activation of the antioxidant response reporter. Depletion of *p62* also blocked the overgrowth of Myc-expressing cell clones (marked by GFP) compared to surrounding control cells, similar to overexpression of Keap1, or silencing *cnc* or its binding partner *Maf* (Figure 5E, F, H, Figure S4E–K). Further activation of antioxidant responses by

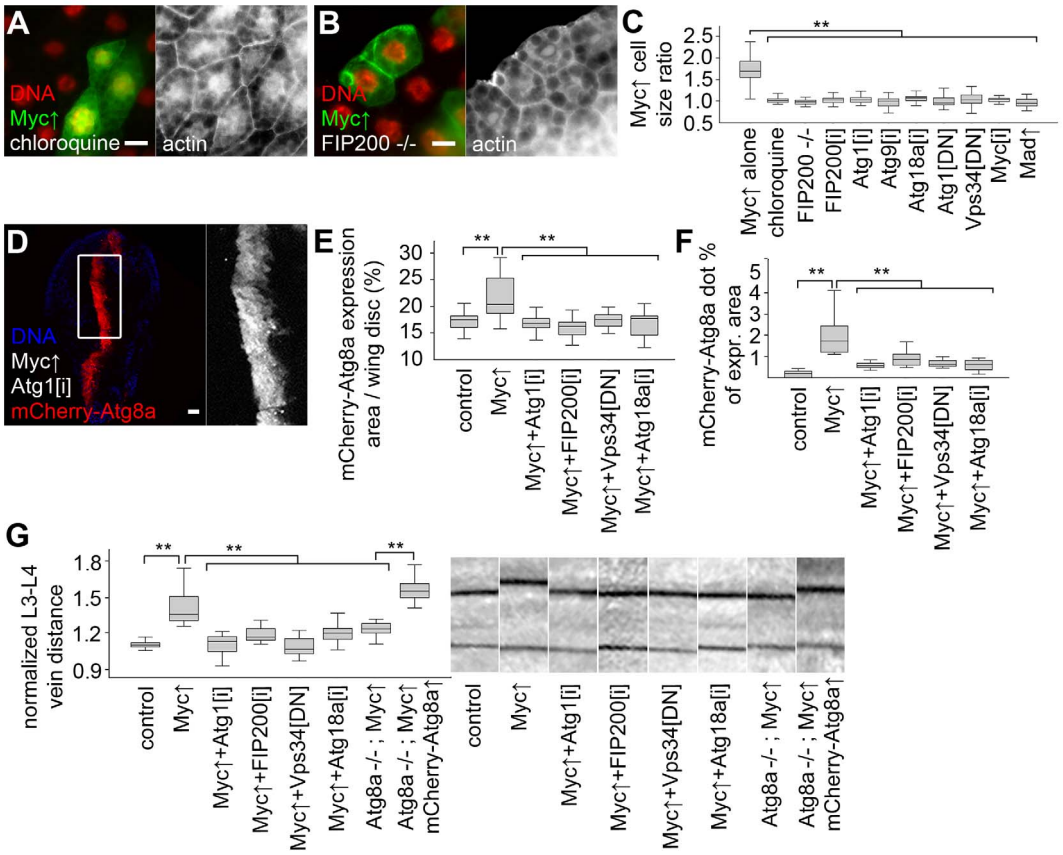


Figure 4. Autophagy is required for Myc-induced overgrowth. (A, B) Feeding larvae a chloroquine-containing diet (A) or null mutation of *FIP200* (B) blocks the increased growth of Myc overexpressing cells, as the size of these GFP-positive cells is now similar to neighboring control cells. (C) Statistical evaluation shows that chloroquine treatment or blocking autophagy by null mutation of *FIP200*, depletion of *FIP200, Atg1, Atg9, Atg18a*, and expression of dominant-negative (DN) Atg1 and Vps34 prevents overgrowth of Myc-expressing fat body cells compared to surrounding control cells to a similar extent as *Myc* RNAi or overexpression of Mad. n = 8–11 per genotype. (D) Knockdown of *Atg1* blocks Myc-induced overgrowth and punctate mCherry-Atg8a labeling in wing imaginal discs. (E, F) Quantification shows that inhibition of *Atg1*, *FIP200*, *Vps34* or *Atg18a* blocks Myc-induced increases of mCherry-Atg8a expression area (E; n = 10–25 per genotype) and Atg8a dot formation (F; n = 10–13 per genotype) in wing discs. (G) Myc expression in the *patched* domain increases L3–L4 wing vein distance relative to L4–L5 vein distance, which is inhibited by knockdown of *Atg1, FIP200, Atg18a*, expression of dominant-negative Vps34, or null mutation of *Atg8a*. Expression of mCherry-Atg8a restores Myc-induced increased vein distance in *Atg8a* mutants. n = 16–26 per genotype. Scalebars in A, B, D equal 20 μm. Statistically significant differences are indicated, ** $p<0.01$.
doi:10.1371/journal.pgen.1003664.g004

dc_840_14

overexpression of cnc or knockdown of *Keap1* did not have much influence on overgrowth of Myc-expressing cells relative to neighboring control cells, but these genetic manipulations restored Myc-driven increased cell growth in *p62* RNAi cells (Figure 5G, H, Figure S4L–N). In contrast, Myc-induced overgrowth of GFP-positive cells relative to neighboring control cells could not be restored in *FIP200* RNAi or dominant-negative Vps34 expressing cells by co-overexpression of cnc (Figure 5H, Figure S4O, P), suggesting that Nrf2 signaling acts parallel to autophagy. Inhibition of p62/Nrf2 signaling in wing imaginal discs reduced Myc-driven cell growth without affecting punctate mCherry-Atg8a labeling (Figure 5I–K, Figure S4S, T), indicating that p62/Nrf2 signaling is dispensable for Myc-induced autophagy. Blocking antioxidant responses by knockdown of *p62* or *cnc*, or overexpression of Keap1 inhibited Myc-induced vein distance increase as well (Figure 5L). Similar to fat bodies, activation of antioxidants by silencing *Keap1* or overexpression of cnc restored increased growth in *p62* RNAi wings expressing Myc (Figure 5L), suggesting that p62 acts upstream of Nrf2 signaling in Myc-induced cell growth. Fat body cell size and wing vein distance remained mostly similar to controls upon modulation of p62/Nrf2 signaling in the absence of Myc overexpression (Figure S4Q, R).

To gain insight into the temporal regulation of autophagy and antioxidant responses by Myc, we analyzed the activation of these processes in response to its transient overexpression. Upregulation of both autophagy and antioxidant reporters became obvious by 12 hours after heat shock-mediated induction of Myc in fat body cells (Figure S5), suggesting that Myc activates these processes with similar kinetics.

Increased levels of the specific autophagy cargo p62 in spite of elevated autophagy in Myc overexpressing cells suggested that p62 is also regulated independent of autophagy in this context. The unfolded protein response (UPR) in the ER and cytosol has been recently shown to upregulate p62 in cultured mammalian cells [34]. Increased ubiquitinated protein levels in Myc overexpressing fat bodies suggested that Myc induces UPR (Figure 5B). Accumulation of unfolded proteins in the ER leads to phosphorylation of eIF2α through activation of PERK (also known as PEK, for pancreatic eIF2α kinase) [35]. Indeed, Myc overexpressing fat bodies had increased levels of phosphorylated eIF2α (Figure 6A, B). Overexpression of Myc also activated the UPR-specific splicing of Xbp1, based on an in vivo reporter assay (Figure S6A, B) [36]. Genetic activation of ER stress signaling by overexpressing PERK in GFP-marked cell clones induced punctate mCherry-Atg8a and Lysotracker staining in a cell-autonomous manner in well-fed animals (Figure 6C–E), indicating that PERK activation promotes autophagy in Drosophila. Gadd34 associates with protein phosphatase 1 to dephosphorylate eIF2α, thereby antagonizing PERK signaling in Drosophila and mammals [35]. Depletion of *PERK* or overexpression of Gadd34 blocked Myc-induced overgrowth in GFP-marked fat body cell clones relative to neighboring control cells (Figure 6F–H). These genetic manipulations also prevented increases in the Myc-expressing area of wing discs, and attenuated Myc-induced autophagy based on decreased punctate mCherry-Atg8a labeling (Figure 6I–L). Silencing of *PERK* or overexpression of Gadd34 also blocked Myc-induced vein distance increase in adult wings (Figure 6M). *PERK* RNAi and Gadd34 overexpression had no effect on the growth of wild-type fat body cells, and only slightly influenced vein distance in control wings (Figure S6C, D).

Discussion

Previous genetic studies established that *Myc* is required for proper expression of hundreds of housekeeping genes and is therefore essential for cell growth and proliferation [9,11]. *Myc* is a typical example of a nuclear oncogene: a transcription factor that drives tumor progression if its expression is deregulated in mammalian cells [12]. Its mechanisms of promoting cell growth are likely different in many ways from that of cytoplasmic oncogenes such as kinases encoded by *PI3K* and *AKT* genes, also frequently activated in various cancers [12]. Overexpression of these drives cell growth in Drosophila as well, but Myc also increases the nuclear:cytoplasmic ratio in hypertrophic cells, unlike activation of PI3K/AKT signaling [14,22]. PI3K and AKT suppress basal and starvation-induced autophagy, while their inactivation strongly upregulates this process [18]. In contrast, here we showed that both basal and starvation-induced autophagy requires *Myc*, and that overexpression of Myc increases UPR, leading to PERK-dependent induction of autophagy, and presumably to accumulation of cytoplasmic p62 that activates antioxidant responses (Figure 7A, B). Autophagy deficiency predisposes to cancer at least in part through accumulation of the selective autophagy cargo p62, resulting in activation of antioxidant responses and tumor formation [32]. Our analyses show that both of these cytoprotective pathways can be activated simultaneously, and are required in parallel to sustain Myc-induced overgrowth in Drosophila cells (Figure 7C, D).

Autophagy and antioxidant responses have been considered to act as tumor suppressor pathways in normal cells and during early stages of tumorigenesis, while activation of these processes may also confer advantages for cancer cells [7,8]. Lack of proper vasculature in solid tumors causes hypoxia and nutrient limitation. These stresses in the tumor microenvironment were suggested to elevate UPR and autophagy to promote survival of cancer cells [37]. Our studies demonstrate that genetic alterations similar to those observed in cancer cells (that is, deregulated expression of Myc) can also activate the UPR, autophagy and antioxidant pathways in a cell-autonomous manner in Drosophila. These processes are likely also activated as a consequence of deregulated Myc expression in human cancer cells based on a number of recent reports, similar to our findings in Drosophila presented here. First, chloroquine treatment that impairs all lysosomal degradation pathways was sufficient to reduce tumor volume in Myc-dependent lymphoma models [38,39]. Second, a related study has been published while we were preparing this manuscript, showing that ER stress and autophagy induced by transient Myc expression increased survival of cultured cells, and PERK-dependent autophagy was necessary for tumor formation in a mouse model [40]. Our data suggest that UPR-mediated autophagy and antioxidant responses may also be necessary to sustain the increased cellular growth rate driven by deregulated expression of Myc.

Myc has proven difficult to target by drugs. Myc-driven cancer cell growth could also be selectively prevented by blocking cellular processes that are required in cancer cells but dispensable in normal cells, known as the largely unexplored non-oncogene addiction pathways [41]. Previous genetic studies established that autophagy is dispensable for the growth and development of mice, although knockout animals die soon after birth due to neonatal starvation after cessation of placental nutrition [6,42]. Tissue-specific *Atg* gene knockout mice survive and the animals are viable, with potential adverse effects only observed in aging animals [6,32,43]. Genetic deficiencies linked to *p62* are also implicated in certain diseases, but knockout mice grow and develop normally and are viable [28,44]. Similarly, *Nrf2* knockout mice are viable and adults exhibit no gross abnormalities, while these animals are hypersensitive to oxidants [45,46]. Mice lacking *PERK* also develop normally and are viable [47]. All these knockout studies

dc_840_14

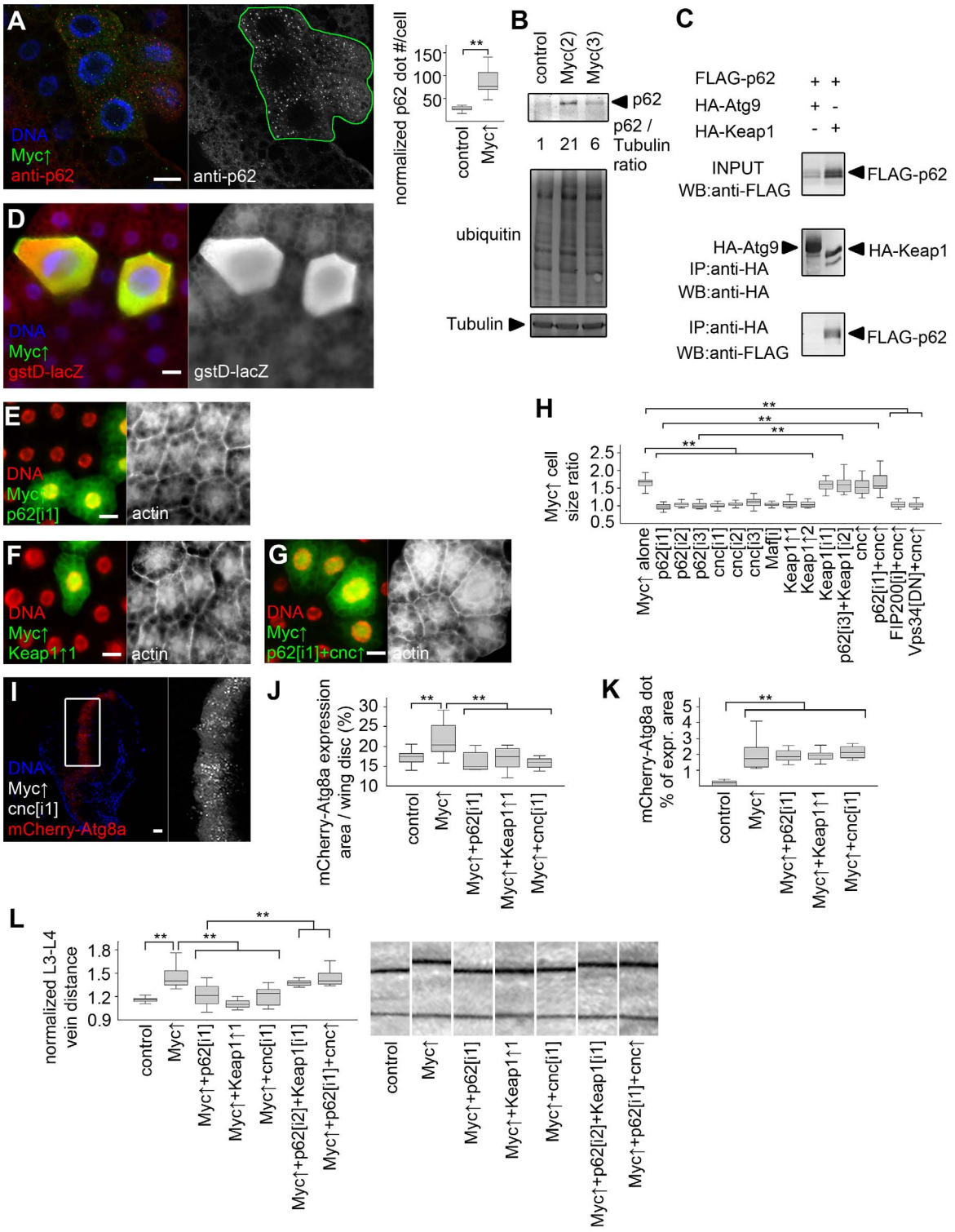


Figure 5. Activation of cnc/Nrf2 is required for Myc-induced overgrowth. (A) p62 aggregates accumulate in Myc-expressing cells (marked by LAMP1-GFP) relative to neighboring control cells, n = 7 for both genotypes. (B) Overexpression of Myc upregulates p62 and increases ubiquitinated protein profiles in fat bodies of well-fed larvae. Numbers indicate the level of p62 relative to Tubulin in different genotypes, as determined by densitometry. (C) HA-Keap1 strongly binds to FLAG-tagged Drosophila p62 in immunoprecipitation (IP) experiments in cultured cells, unlike HA-Atg9. WB, western blot. (D) Myc overexpression in GFP-positive cells activates the Nrf2/cnc-dependent transcriptional reporter gstD-LacZ. (E, F) Depletion of *p62* (E) or overexpression of Keap1 (F) inhibits Myc-induced overgrowth of GFP-positive cells relative to neighboring control cells. (G) Co-overexpression of cnc restores Myc-induced overgrowth of GFP-positive *p62* RNAi cells compared to surrounding cells. (H) Knockdown of *p62, cnc, Maf*, or overexpression of Keap1 prevents Myc-induced overgrowth relative to neighboring control cells. Co-overexpression of cnc or *Keap1* depletion has little effect on Myc-expressing cell size. Depletion of Keap1 restores Myc-induced overgrowth in *p62* RNAi cells, similar to overexpression of cnc. Myc-induced overgrowth is not restored by cnc overexpression in *FIP200* RNAi or dominant-negative Vps34 expressing cells.

dc_840_14

n = 8–11 per genotype. (I–K) Knockdown of *cnc* (I), *p62* or overexpression of Keap1 prevents Myc-induced increases in mCherry-Atg8a expression area of wing discs (quantifications shown in panel J; n = 10–25 per genotype) without affecting punctate mCherry-Atg8a labeling (K; n = 10–13 per genotype). (L) Myc overexpression in the *patched* domain increases L3–L4 vein distance, which is inhibited by knockdown of *p62* or *cnc*, or by co-overexpression of Keap1. *Keap1* depletion or cnc co-overexpression restores Myc-induced increased vein distance in *p62* RNAi wings. n = 8–25 per genotype. Scalebars in A, E–G, I equal 20 μm, and 40 μm in D. Statistically significant differences are indicated, ** $p<0.01$.
doi:10.1371/journal.pgen.1003664.g005

demonstrate that the above genes are largely dispensable for normal growth and development of mice, and that progressive development of certain diseases is only observed later during the life of these mutant animals. There are currently no data regarding the effects of transient inhibition of these processes, with the exception of the non-specific lysosomal degradation inhibitor chloroquine, originally approved for the treatment of malaria, which is already used in the clinic for certain types of cancer [8,16].

Based on these knockout mouse data, UPR, autophagy and antioxidant responses may be considered as potential non-oncogene addiction pathways: strictly required for Myc-dependent overgrowth (our study) and tumor formation [30,32,40], but dispensable for the growth and viability of normal cells, both in Drosophila and mammals. One can speculate that the transient inactivation of these pathways will have even more subtle effects than those observed in knockout mice, but this needs experimental testing. While it is difficult to extrapolate data obtained in Drosophila (or even mouse) studies to human patients, it is tempting to speculate that specific drugs targeting UPR, autophagy and antioxidant responses may prove effective against Myc-dependent human cancers, perhaps without causing adverse side-

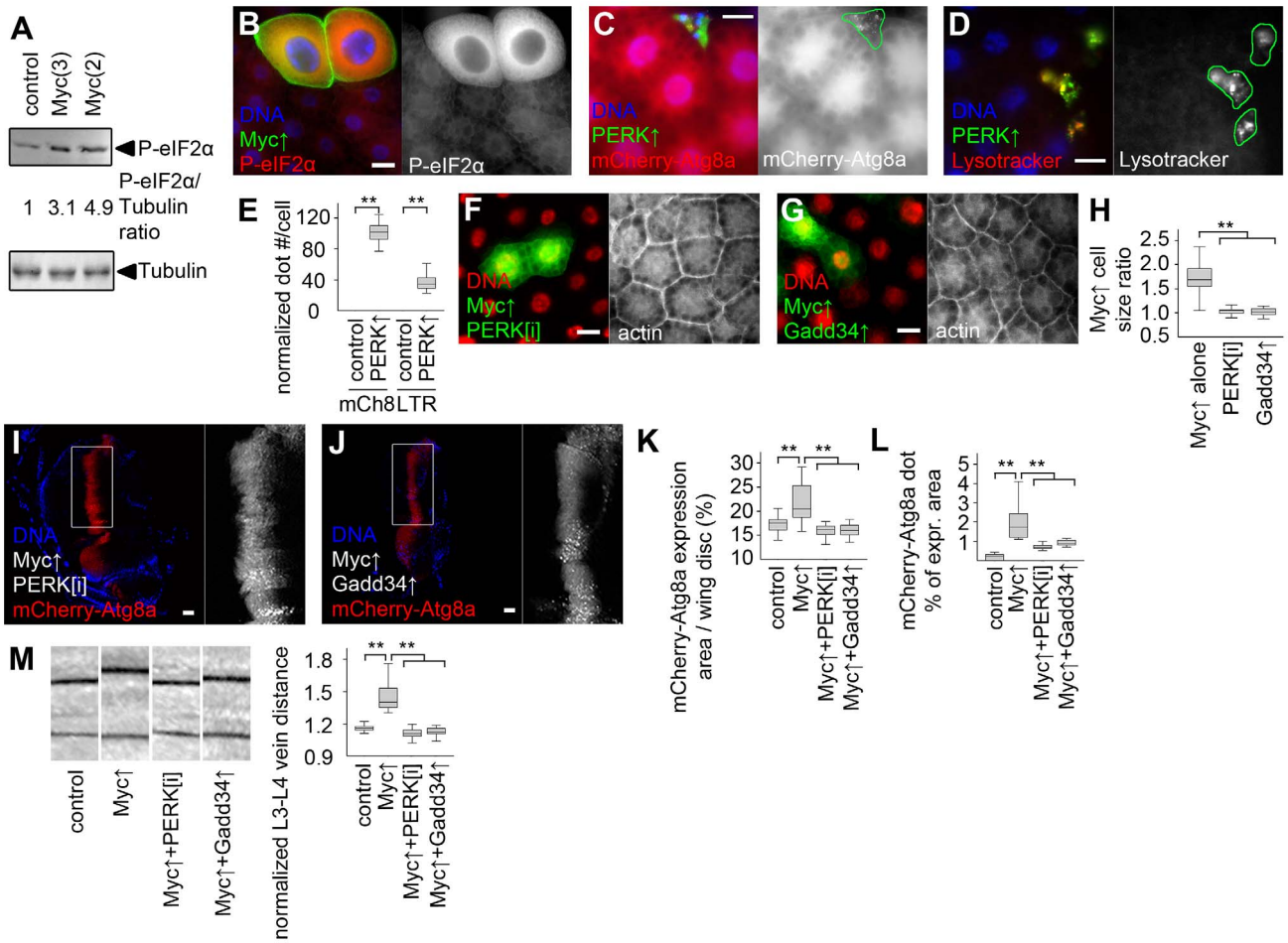


Figure 6. Myc-induced UPR is required for increased cell growth and autophagy. (A) Overexpression of Myc in larval fat bodies increases the level of phosphorylated eIF2α compared to controls. Numbers indicate the level of phospho- eIF2α relative to the loading control Tubulin in different genotypes, as determined by densitometric evaluation. (B) Forced expression of Myc in GFP-marked fat body cell clones increases the levels of phospho- eIF2α in a cell-autonomous manner. (C, D) Overexpression of PERK induces punctate mCherry-Atg8a (C) and Lysotracker (D) labeling in GFP-marked fat body cell clones of well-fed larvae. (E) Quantification of data presented in panels C and D, n = 7–8 per genotype. (F, G) Depletion of *PERK* (F) or co-overexpression of Gadd34 (G) prevents Myc-induced overgrowth of GFP-marked fat body cell clones relative to surrounding control cells. (H) Quantification of data presented in panels F and G, n = 9–11 per genotype. (I–L) Knockdown of *PERK* (I) or overexpression of Gadd34 (J) prevents Myc-induced increases in the mCherry-Atg8a expression area of wing discs (K; n = 10–25 per genotype) and inhibits punctate mCherry-Atg8a labeling (L; n = 10–13 per genotype). (M) Myc overexpression in the *patched* domain increases L3–L4 vein distance relative to L4–L5 vein distance in adult wings, which is inhibited by knockdown of *PERK* or by overexpression of Gadd34, n = 19–25 per genotype. Scalebars in B–D, F, G, I, J equal 20 μm. Statistically significant differences are indicated, ** $p<0.01$.
doi:10.1371/journal.pgen.1003664.g006

dc_840_14

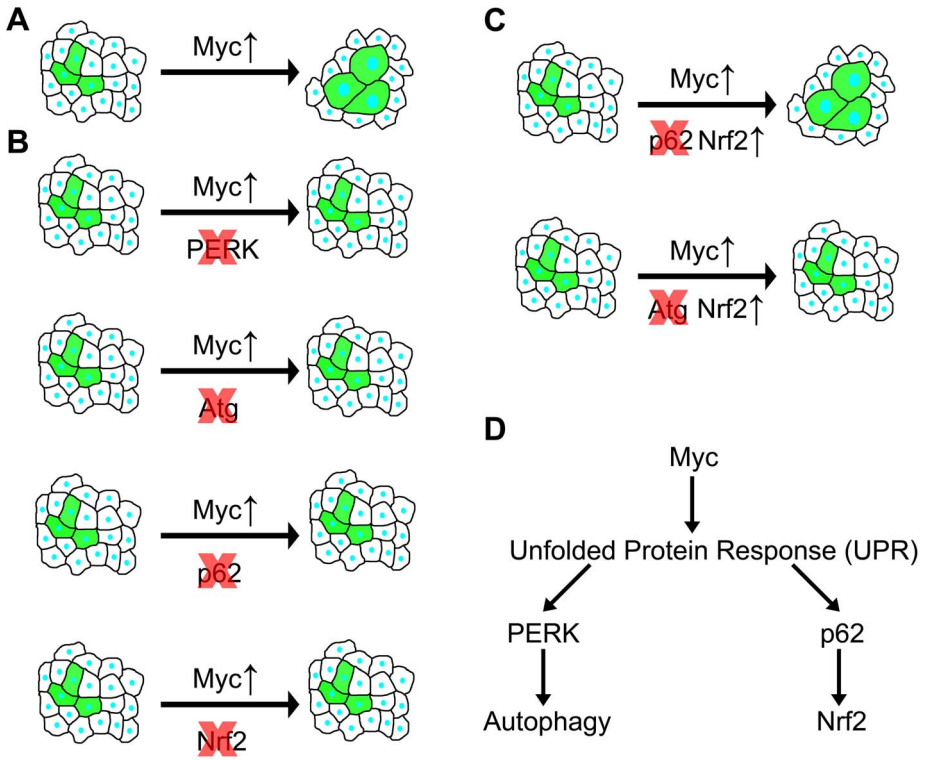


Figure 7. Summary of genetic interactions in the context of Myc-induced overgrowth. (A) Overexpression of Myc in GFP-positive cells leads to a cell-autonomous increase of size. (B) Genetic inhibition of PERK signaling, autophagy, p62 or Nrf2/cnc signaling prevents Myc-induced overgrowth, as GFP-positive cells are now unable to overgrow neighboring cells. (C) Overexpression of Nrf2 restores Myc-induced overgrowth in the absence of p62, while it has no effect in autophagy-deficient cells, indicating that Nrf2 acts downstream of p62 but in parallel to autophagy. (D) Overexpression of Myc induces UPR, leading to activation of PERK in the ER that triggers autophagy. At the same time, cytoplasmic UPR presumably results in accumulation of p62, which then activates Nrf2.
doi:10.1371/journal.pgen.1003664.g007

effects such as current, less specific therapeutic approaches. Notably, widely used anticancer chemotherapy treatments are known to greatly increase the risk that cancer survivors will develop secondary malignancies [48,49]. Moreover, the autophagy and antioxidant pathways appear to be required in parallel during Myc-induced overgrowth in Drosophila cells. If a similar genetic relationship exists in Myc-dependent human cancer cells, then increased efficacy may be predicted for the combined block of key enzymes acting in these processes.

Elucidation of the genetic alterations behind increased UPR, autophagy and antioxidant responses observed in many established human cancer cells may allow specific targeting of these pathways, and potentially have a tremendous benefit for personalized therapies. In addition to non-specific autophagy inhibitors such as chloroquine, new and more specific inhibitors of selected Atg proteins are being developed [8]. Given the dual roles of autophagy during cancer initiation and progression, a major question is how to identify patients who would likely benefit from taking these drugs. For example, no single test can reliably estimate autophagy levels in clinical samples, as increases in autophagosome generation or decreases in autophagosome maturation and autolysosome breakdown both result in accumulation of autophagic structures [16]. Based on our data and recent mammalian reports, elevated Myc levels may even turn out to be useful as a biomarker before therapeutic application of inhibitors for key autophagy, UPR or antioxidant proteins in cancer patients.

Materials and Methods

Drosophila genetics

Flies were maintained on standard cornmeal-yeast-agar medium. We mostly used clonal analysis throughout our work, which represents a very powerful technique, as genetically manipulated cells are surrounded by normal cells in the very same tissue that serve as an internal control, thus eliminating much of the variability that may arise from differences between individual animals. Fat body cell clones were spontaneously generated by Flp recombinase-mediated excision of the FRT cassette from *Actin>y+>Gal4* or *Actin>CD2>Gal4* to activate UAS (upstream activating sequence)-dependent transcription of overexpression, dominant-negative and RNAi transgenes. Myc overexpression was mediated in whole fat bodies by *collagen(cg)-Gal4* for western blots and electron microscopy and by *heat shock(hs)-Gal4* for measuring the time course of autophagy and antioxidant responses, by *patched(ptc)-Gal4* in a stripe of wing imaginal discs that gives rise to the L3–L4 intervein area of adult wings, and by *apterous(ap)-Gal4* in apical epithelial sheets of the developing wings. Fat bodies were dissected from L3 stage larvae 84–90 hours after egg laying, with the exception of Myc mutants and their heterozygous siblings (used as control) when L1 larvae were used as Myc mutants do not develop beyond this stage. Wing discs were dissected from wandering stage L3 larvae (108–120 hours after egg laying), and adult wings were evaluated in 3–7 day old imagoes. The following

dc_840_14

stocks were used in this study: *Keap1[i1, KK107052], p62[i1, KK108193], cnc[i1, KK108127], FIP200[i, KK104864], Atg18a[i, KK105366], Atg1[i, GD16133], PERK[i, GL00030]* (obtained from the Vienna Drosophila RNAi Center), *p62[i3, HMS00938], p62[i2, HMS00551], cnc[i2, JF02006], cnc[i3, HMS00650], Atg9[i, JF02891], Myc[i, JF01761], Maf[i, JF02008], UAS-Keap1[/2, EY15427], UAS-cnc[EY17502], UAS-Myc* (inserted on chromosome 2), *w[1118]* (control), *ap-Gal4, cg-Gal4,hs-Gal4* (obtained from the Bloomington Drosophila Stock Center), *Myc[4], UAS-Mad* (kindly provided by Peter Gallant) [14], *UAS-Keap1[/1], Keap1[i2, dsRNA], gstD-GFP, gstD-LacZ* (kindly provided by Dirk Bohmann) [50], *UAS-mGadd34, UAS-PERK* (kindly provided by Stefan Marciniak) [35], *ptc-Gal4* (kindly provided by József Mihály), *UAS-Myc* (inserted on chromosome 3, kindly provided by Tom Neufeld), *UAS-mCherry-GFP-Atg8a* [19], *UAS-Xbp1-GFP[HG]* (kindly provided by Hyung Don Ryoo) [36], *UAS-Atg1[DN]* [2], *UAS-Vps34[DN]* [15], *Atg8a[d4]* [17], *FIP200[d130]* (to be described elsewhere). Fat body cell clones expressing *UAS-Myc* were generated by *hs-Flp[22]; UAS-Dcr2; Actin>CD2>Gal4, UAS-GFPnls, r4-mCherry-Atg8a* [17] or by *hs-Flp[22]; UAS-LAMP1-GFP; Actin>CD2>Gal4, UAS-Dcr2* (for Lysotracker and anti-Atg8a stainings) [17]. For epistasis analyses, we used *hsFlp[22]; Actin>y+>Gal4, UAS-GFPnls; UAS-Myc* for all fat body clones with the exception of *FIP200* mutants for which we used *hs-Flp[22], Actin>CD2>Gal4, UAS-mCD8-GFP* (all recombined together on chromosome X), and *ptc-Gal4, UAS-mCherry-Atg8a, UAS-Myc* (all recombined together on chromosome 2) for wing experiments.

Molecular cloning, cell culture and immunoprecipitation

Coding sequences were PCR amplified for Drosophila p62 (lacking the PB1 domain to prevent self-aggregation), and cloned into pUAST-3×FLAG. Full-length Atg9 and Keap1 were amplified and cloned into pUAST-3×HA. D.Mel-2 cells were maintained in Express Five Serum-Free Medium with penicillin and streptomycin (Invitrogen). Cells were transfected with equal amounts of metallothionein-Gal4, UAS-FLAG-p62 and UAS-HA-Atg9 or UAS-HA-Keap1 plasmids using TransIT-2020 (Mirus). 48 h later, protein expression was induced by 1 mM $CuSO_4$ for overnight incubation. Cells were collected by centrifugation, washed twice in PBS and lysed on ice in lysis buffer (0.5% Triton-X100, 150 mM NaCl, 1 mM EDTA, 20 mM TRIS-HCl pH 8) with complete protease and phosphatase inhibitor cocktails (Sigma), spun for 10 min at 10,000 g in an Eppendorf 5430R at 4°C followed by the addition of 30 µl anti-FLAG slurry (Sigma) to the cleared supernatant. After incubation at 4°C for 2 h, beads were collected by centrifugation at 5,000 g for 30 sec at 4°C followed by extensive washes in lysis buffer, and finally boiled in 30 µl Laemmli sample buffer.

Western blots and immunostainings

50 larval fat bodies per genotype were dissected from well-fed L3 stage larvae, homogenized in Laemmli sample buffer (Sigma), boiled and equal amounts loaded on SDS-PAGE gels, followed by processing as described [4,17,19]. Phosphatase inhibitor cocktail PhosSTOP (Roche) was added to samples processed for phospho-eIF2α western blots. Immunostaining of dissected larvae was performed as before [2,15,17,19]. The following primary antibodies were used: rat anti-mCherry (WB 1:5,000), rat anti-Atg8a (IF 1:300) [19], rabbit anti-Atg8a (WB 1:5,000) [19], rabbit anti-p62 (IF 1:2,000, WB 1:5,000) [17], mouse anti-Tubulin (WB 1:1,000, clone AA4.3-s, DSHB), mouse anti-LacZ (IF 1:100, clone 40-1a-s, DSHB), chicken anti-GFP (IF 1:1,500, Invitrogen), rabbit anti-phospho-eIF2α (IF 1:100, WB 1:1,000, Cell Signaling Technologies), rabbit anti-ubiquitin (1:500, DAKO). Secondary antibodies were alkaline phosphatase-conjugated goat anti-mouse (WB 1: 5,000, Millipore), rabbit anti-rat (WB 1: 5,000, Sigma), and Alexa 488 goat anti-chicken, Alexa 546 goat anti-rabbit, Alexa 568 goat anti-rat, Alexa 568 goat anti-mouse (IF 1:1,500, Invitrogen).

Histology and microscopy

Approximately 20 larvae were allowed to feed on food supplemented with plenty of dry yeast until reaching the appropriate age. For drug treatment, L1 larvae were transferred to food containing 3 mg/ml chloroquine (Sigma). Starvations were carried out in 20% sucrose solution for 3 hours. Lysotracker and cortical actin Alexa 633-phalloidin (Invitrogen) stainings were carried out as described [2,15,17,19]. All preparations were mounted in 50% glycerol/PBS with 0.2 µM DAPI and viewed on a Zeiss Axioimager M2 equipped with an Apotome2 grid confocal unit, using Plan-NeoFluar 20× 0.5 NA and 40× 0.75 NA objectives, Axiocam Mrm camera, and Axiovision software. DAPI-stained DNA is pseudocoloured red to enhance visibility for actin stainings. Electron microscopy was carried out as before [4,15,17]. Adult wings were photographed on a Zeiss Lumar stereomicroscope with Axiocam Icc camera and Axiovision software.

Image analysis

Original, unmodified images were evaluated in ImageJ (NIH) as before [17,19]. For fat body measurements, we quantified cell size by manually encircling a GFP-marked cell in ImageJ (NIH) with its nucleus in the focal plane to ensure that the maximal diameter of the given cell is counted, and randomly selected a non-GFP control cell from the very same image (with its nucleus also in the focal plane) to compare it to. The ratio of the GFP-positive cell's size relative to its randomly selected neighbor is calculated as one data point. The only factor we considered was that cells situated at the edge of fat body are usually bigger, so when quantifying a GFP-positive cell at the edge of a fat body lobe we always selected a control cell from the edge as well. Dot number per randomly selected area (400×400 pixel) was measured in the case of Myc null mutant fat bodies and controls, or per whole wing discs, by setting the appropriate threshold in the relevant channel in ImageJ so that as many dots were selected as possible without selecting background fluorescence or merging adjacent separate dots. For clonal analyses, dot number per cell was quantified by first setting the threshold for the relevant channel, and then encircling a GFP-positive cell and recording dot number and size values, followed by evaluating a randomly selected neighboring control cell from the same image, similar to cell size measurements. Dot number per cell data points were corrected according to differences in cell size by normalizing each GFP-positive cell relative to the size of the neighboring control cell, as described [2,18]. That is, if a Mad overexpressing cell had 2 endogenous Atg8-positive puncta and the size of this cell was 25% of the control cell size, the normalized Atg8 dot number per cell would be 8. Note that inhibition of Myc signaling decreases both cell size and autophagy, meaning that the difference in autophagic dot number between Myc loss of function cells and control cells decreases during normalization (but remains statistically significant). On the other hand, Myc overexpression increases both cell size and autophagy in fat body cells, meaning that the difference in autophagic dot number between Myc gain of function cells and controls again decreases during normalization (but is still statistically very significant). In autophagic flux measurements with and without chloroquine, primary images from mCherry-GFP-Atg8a experiments were analyzed automatically in ImageJ (NIH) with the colocalization plugin using the intensity correlation function [19]. For quantifying *gstD-GFP*

dc_840_14

expression in fat bodies, the pixel intensity of the green channel was determined in images captured with the same exposure time throughout the experiments.

Western blots were digitized with an Epson Photo 4990 scanner at 600 dpi, by preserving the background. Densitometric evaluation of blots was carried out in ImageJ (NIH). After rectangular selection of individual lanes of interest, these were evaluated using Analyze>Gels>Plot lanes. Then, the peaks of interest were measured in plots by first setting the background with the straight line tool, and then measuring the area under the peak with the wand tool. Values were calculated relative to Tubulin, and fold changes relative to lanes with control lysates are shown in panels.

Statistics

Sample number (n) in figure legends and Table S1 refers to the number of individual animals analyzed per genotype. For mosaic experiments in fat body cells, 3 GFP versus non-GFP cell pairs were evaluated per animal, with each pair chosen from the same image as described in the image analysis section. For wing disc and adult wing measurements, one disc or wing per animal was quantified. Data were imported into SPSS Statistics version 20 (IBM) and analyzed as indicated in Table S1. For each figure, the table lists genotype for relevant panels, sample number (n), median (or mean), standard deviation, and p value calculated either by two-tailed two-sample unequal variance Student's t test for normal distribution data or by Mann-Whitney u test for non-normal distribution data in pairwise comparisons. We used ANOVA for multiple comparisons of normal distribution data and Kruskal-Wallis test for non-normal distribution data. $p<0.05$ is considered statistically significant (marked by *) and $p<0.01$ statistically highly significant (marked by **), and non-significant p values are highlighted by a grey background in the table. Boxplots in figures show median scores, 25% interquartiles, maximum and minimum values, and were also created using SPSS Statistics 20 (IBM). Bar charts for electron microscopy analysis and for time course experiments show average values and standard deviations.

Supporting Information

Figure S1 Myc overexpression induces autophagy in Drosophila. (A) No autophagy is detected in fat body cells of well-fed control larvae. (B) Myc expression leads to the appearance of double-membrane autophagosomes (ap) containing undigested cytoplasmic material, and dense autolysosomes (al) degrading sequestered cytoplasmic cargo.
(TIF)

Figure S2 Myc-induced overgrowth is suppressed by inhibition of autophagy. (A) Overexpressing two copies of *UAS-Myc* in fat body cell clones, marked by GFP, increases growth compared to neighboring control cells. (B) Chloroquine treatment prevents overgrowth driven by two copies of *UAS-Myc*.(C) Quantification of data in A and B, n = 10–15 per genotype. (D–K) Myc-driven overgrowth of GFP-positive fat cells compared to surrounding control cells is inhibited by *Atg1* RNAi (D), expression of dominant-negative Atg1 (E) or Vps34 (F), silencing of *Atg18a* (G), *Atg9* (H), *FIP200* (I), *Myc* (J), or overexpression of Mad (K). (L) In adult wings, the *patched* domain corresponds to the region between longitudinal veins L3 and L4 (marked by mCherry-Atg8a expression in lower panel). Wing vein distance was quantitated based on the ratio of L3–L4 distance (measured halfway between PCV and wing margin) to L4–L5 vein distance at the posterior crossvein (PCV) for each individual wing, as indicated in the upper panel. (M–O) Myc-induced punctate mCherry-Atg8a labeling and expansion of the patched expression domain is inhibited by depletion of *FIP200* (M) or *Atg18a* (N), or by expression of dominant-negative Vps34 (O). (P) Silencing of *FIP200, Atg1, Atg9, Atg18a* or expression of dominant-negative Vps34 has no effect on the growth of fat body cells. Expression of dominant-negative Atg1 reduces cell size, likely due to competition of the overexpressed catalitically inactive protein with other substrates of TOR kinase, such as the critical growth regulator S6K. Depletion of *Myc* or Mad overexpression also reduces cell size. n = 7 for all genotypes. (Q) L3–L4 wing vein distance is not reduced compared to control wings upon inhibition of *Atg1*, *FIP200*, *Vps34* or *Atg18a*, n = 13–21 per genotype. Scalebars in A, B, D–K, M–O equal 20 μm. Statistically significant differences are indicated, ** $p<0.01$.
(TIF)

Figure S3 Myc-induced overgrowth of the apical epithelial sheet in the wing is blocked by inhibition of autophagy or *p62*. (A) The wings of control flies are straight. (B) Myc overexpression in the *apterous* expression domain results in overgrowth of the apical epithelial layer, producing flies with downward curving wings. (C–F) The downward-curving phenotype of Myc overexpressing wings is suppressed by null mutation of *Atg8a* (C), expression of dominant-negative Vps34 (D), depletion of *Atg18a* (E) or *p62* (F).
(TIF)

Figure S4 Myc-induced overgrowth requires antioxidant responses. (A) No expression of the Nrf2/cnc-dependent transcriptional reporter gstD-GFP is seen in the *patched* expressing domain (marked by mCherry-Atg8a) in control wing imaginal discs. (B) Myc overexpression induces gstD-GFP expression in the mCherry-Atg8a expressing domain. (C, D) Knockdown of *p62* or *cnc* prevents activation of GstD-GFP by Myc. (E–K) Myc-induced overgrowth of GFP-positive cells compared to neighboring control cells is inhibited by depletion of *p62* (E, F), *cnc* (G–I), *Maf* (J), or overexpression of Keap1 (K). (L, M) GFP-positive cells overexpressing Myc remain much bigger than control cells upon *Keap1* depletion (L) or overexpression of cnc (M). (N) *Keap1* depletion restores Myc-induced overgrowth in *p62* RNAi cells. (O, P) Overexpression of cnc fails to restore Myc-induced overgrowth in *FIP200* RNAi (O) or dominant-negative Vps34 expressing cells (P). (Q) Modulation of p62/cnc signaling in GFP-positive cell clones has no effect on the size of these fat body cells relative to neighboring control cells. n = 7 for all genotypes. (R) Modulation of p62/cnc signaling has no or minor effects on L3–L4 wing vein distance in adult wings, n = 12–19 per genotype. (S, T) Depletion of *p62* (S) or overexpression of Keap1 (T) reduces the area of the Myc-expressing *patched* domain but does not block punctate mCherry-Atg8a labeling. Scalebars in A–P and S, T equal 20 μm. Statistically significant differences are indicated, * $p<0.05$ and ** $p<0.01$.
(TIF)

Figure S5 Temporal regulation of autophagy and Nrf2 activity by Myc. (A) Induction of Myc expression by a 2-hour heat shock results in the formation of numerous mCherry-GFP-Atg8a punctae by 12 and 18 hours after induction. Practically no dots are seen in fat body cells of control larvae upon heat shock-mediated expression of mCherry-GFP-Atg8a. n = 12 for each genotype/time point. (B) Expression of the Nrf2-dependent transcriptional reporter *gstD-GFP* is similar to basal fat body expression levels (not shown) at 4 hours after heat shock-mediated induction of Myc and in control larvae expressing only *hs-Gal4*. Upregulation of this reporter becomes obvious by 12 and 18 hours after induction of Myc. n = 10 for each genotype/time point. Scalebars equal 20 μm. Statistically significant differences are indicated, ** $p<0.01$.
(TIF)

dc_840_14

Figure S6 PERK signaling is largely dispensable for cell growth. (A) The unfolded protein response (UPR) reporter XBP1-GFP shows only diffuse fluorescnce in control wing discs that express mCherry-Atg8a in the *patched* domain. (B) Xbp1-GFP expression is enhanced by overexpression of Myc in the mCherry-Atg8a expression area. (C) Depletion of *PERK* or overexpression of its antagonist Gadd34 in GFP-positive cell clones has no effect on the size of these fat body cells relative to neighboring control cells. n = 7 for both genotypes. (D) *PERK* RNAi or Gadd34 overexpression only slightly reduces L3–L4 vein distance compared to L4–L5 vein distance in adult wings, n = 12–19 per genotype. Scalebars in A, B equal 20 μm. Statistically significant differences are indicated, ** $p<0.01$.
(TIF)

Table S1 Quantification of experimental data. The number of individual animals quantified (n) is indicated for all genotypes. Note that in mosaic analyses, clone and control cell pairs were always evaluated from the same image, same tissue, same animal. P values≥0.05 (considered not statistically significant) are highlighted by a grey background. Please see methods for further details.
(XLSX)

Acknowledgments

We thank Sarolta Pálfia for technical assistance, Dirk Bohmann, Peter Gallant, Stefan Marciniak, József Mihály, Tom Neufeld, Hyung Don Ryoo, public stock centers VDRC, BDSC and TRiP at Harvard Medical School for fly lines, Attila L. Kovacs for useful comments on the manuscript, and all members of our lab for help with experiments.

Author Contributions

Conceived and designed the experiments: PN GJ. Performed the experiments: PN AV KP KH GJ. Analyzed the data: PN KP GJ. Wrote the paper: PN GJ.

References

1. Neufeld TP (2010) TOR-dependent control of autophagy: biting the hand that feeds. Curr Opin Cell Biol 22: 157–168.
2. Scott RC, Juhasz G, Neufeld TP (2007) Direct induction of autophagy by atg1 inhibits cell growth and induces apoptotic cell death. Curr Biol 17: 1–11.
3. Hosokawa N, Hara Y, Mizushima N (2007) Generation of cell lines with tetracycline-regulated autophagy and a role for autophagy in controlling cell size. FEBS Lett 581: 2623–2629.
4. Juhasz G, Erdi B, Sass M, Neufeld TP (2007) Atg7-dependent autophagy promotes neuronal health, stress tolerance, and longevity but is dispensable for metamorphosis in Drosophila. Genes Dev 21: 3061–3066.
5. Simonsen A, Cumming RC, Brech A, Isakson P, Schubert DR, et al. (2008) Promoting basal levels of autophagy in the nervous system enhances longevity and oxidant resistance in adult Drosophila. Autophagy 4: 176–184.
6. Mizushima N, Levine B, Cuervo AM, Klionsky DJ (2008) Autophagy fights disease through cellular self-digestion. Nature 451: 1069–1075.
7. White E (2012) Deconvoluting the context-dependent role for autophagy in cancer. Nature Rev Cancer 12: 401–410.
8. Cheong H, Lu C, Lindsten T, Thompson CB (2012) Therapeutic targets in cancer cell metabolism and autophagy. Nat Biotechnol 30: 671–678.
9. Eilers M, Eisenman RN (2008) Myc's broad reach. Genes Dev 22: 2755–2766.
10. Littlewood TD, Kreuzaler P, Evan GI (2012) All things to all people. Cell 151: 11–13.
11. Soucek L, Evan GI (2010) The ups and downs of Myc biology. Curr Opin Genet Dev 20: 91–95.
12. Weinberg RA (2007) The Biology of Cancer. New York: Garland Science.
13. Johnston LA, Prober DA, Edgar BA, Eisenman RN, Gallant P (1999) Drosophila myc regulates cellular growth during development. Cell 98: 779–790.
14. Pierce SB, Yost C, Britton JS, Loo LW, Flynn EM, et al. (2004) dMyc is required for larval growth and endoreplication in Drosophila. Development 131: 2317–2327.
15. Juhasz G, Hill JH, Yan Y, Sass M, Baehrecke EH, et al. (2008) The class III PI(3)K Vps34 promotes autophagy and endocytosis but not TOR signaling in Drosophila. J Cell Biol 181: 655–666.
16. Klionsky DJ, Abdalla FC, Abeliovich H, Abraham RT, Acevedo-Arozena A, et al. (2012) Guidelines for the use and interpretation of assays for monitoring autophagy. Autophagy 8: 445–544.
17. Pircs K, Nagy P, Varga A, Venkei Z, Erdi B, et al. (2012) Advantages and limitations of different p62-based assays for estimating autophagic activity in Drosophila. PloS one 7: e44214.
18. Scott RC, Schuldiner O, Neufeld TP (2004) Role and regulation of starvation-induced autophagy in the Drosophila fat body. Dev Cell 7: 167–178.
19. Takats S, Nagy P, Varga A, Pircs K, Karpati M, et al. (2013) Autophagosomal Syntaxin17-dependent lysosomal degradation maintains neuronal function in Drosophila. J Cell Biol 201: 531–539.
20. Barth JM, Szabad J, Hafen E, Kohler K (2011) Autophagy in Drosophila ovaries is induced by starvation and is required for oogenesis. Cell Death Differ 18: 915–924.
21. Nezis IP, Simonsen A, Sagona AP, Finley K, Gaumer S, et al. (2008) Ref(2)P, the Drosophila melanogaster homologue of mammalian p62, is required for the formation of protein aggregates in adult brain. J Cell Biol 180: 1065–1071.
22. Saucedo LJ, Edgar BA (2002) Why size matters: altering cell size. Curr Opin Genet Dev 12: 565–571.
23. Chang YY, Neufeld TP (2009) An Atg1/Atg13 complex with multiple roles in TOR-mediated autophagy regulation. Mol Biol Cell 20: 2004–2014.
24. Mizushima N, Yoshimori T (2007) How to interpret LC3 immunoblotting. Autophagy 3: 542–545.
25. Nezis IP, Shravage BV, Sagona AP, Lamark T, Bjorkoy G, et al. (2010) Autophagic degradation of dBruce controls DNA fragmentation in nurse cells during late Drosophila melanogaster oogenesis. J Cell Biol 190: 523–531.
26. Kimura S, Noda T, Yoshimori T (2007) Dissection of the autophagosome maturation process by a novel reporter protein, tandem fluorescent-tagged LC3. Autophagy 3: 452–460.
27. Rintelen F, Stocker H, Thomas G, Hafen E (2001) PDK1 regulates growth through Akt and S6K in Drosophila. Proc Natl Acad Sci USA 98: 15020–15025.
28. Moscat J, Diaz-Meco MT (2012) p62: a versatile multitasker takes on cancer. Trends Biochem Sci 37: 230–236.
29. Mathew R, Karp CM, Beaudoin B, Vuong N, Chen G, et al. (2009) Autophagy suppresses tumorigenesis through elimination of p62. Cell 137: 1062–1075.
30. Inami Y, Waguri S, Sakamoto A, Kouno T, Nakada K, et al. (2011) Persistent activation of Nrf2 through p62 in hepatocellular carcinoma cells. J Cell Biol 193: 275–284.
31. Komatsu M, Kurokawa H, Waguri S, Taguchi K, Kobayashi A, et al. (2010) The selective autophagy substrate p62 activates the stress responsive transcription factor Nrf2 through inactivation of Keap1. Nat Cell Biol 12: 213–223.
32. Takamura A, Komatsu M, Hara T, Sakamoto A, Kishi C, et al. (2011) Autophagy-deficient mice develop multiple liver tumors. Genes Dev 25: 795–800.
33. Jain A, Lamark T, Sjottem E, Larsen KB, Awuh JA, et al. (2010) p62/SQSTM1 is a target gene for transcription factor NRF2 and creates a positive feedback loop by inducing antioxidant response element-driven gene transcription. J Biol Chem 285: 22576–22591.
34. Liu XD, Ko S, Xu Y, Fattah EA, Xiang Q, et al. (2012) Transient aggregation of ubiquitinated proteins is a cytosolic unfolded protein response to inflammation and endoplasmic reticulum stress. J Biol Chem 287: 19687–19698.
35. Malzer E, Daly ML, Moloney A, Sendall TJ, Thomas SE, et al. (2010) Impaired tissue growth is mediated by checkpoint kinase 1 (CHK1) in the integrated stress response. J Cell Sci 123: 2892–2900.
36. Sone M, Zeng X, Larese J, Ryoo HD (2013) A modified UPR stress sensing system reveals a novel tissue distribution of IRE1/XBP1 activity during normal Drosophila development. Cell Stress Chaperones 18: 307–319.
37. Wang S, Kaufman RJ (2012) The impact of the unfolded protein response on human disease. J Cell Biol 197: 857–867.
38. Amaravadi RK, Yu D, Lum JJ, Bui T, Christophorou MA, et al. (2007) Autophagy inhibition enhances therapy-induced apoptosis in a Myc-induced model of lymphoma. J Clin Invest 117: 326–336.
39. Maclean KH, Dorsey FC, Cleveland JL, Kastan MB (2008) Targeting lysosomal degradation induces p53-dependent cell death and prevents cancer in mouse models of lymphomagenesis. J Clin Invest 118: 79–88.
40. Hart LS, Cunningham JT, Datta T, Dey S, Tameire F, et al. (2012) ER stress-mediated autophagy promotes Myc-dependent transformation and tumor growth. J Clin Invest 122: 4621–4634.
41. Luo J, Solimini NL, Elledge SJ (2009) Principles of cancer therapy: oncogene and non-oncogene addiction. Cell 136: 823–837.
42. Kuma A, Hatano M, Matsui M, Yamamoto A, Nakaya H, et al. (2004) The role of autophagy during the early neonatal starvation period. Nature 432: 1032–1036.
43. Mizushima N, Komatsu M (2011) Autophagy: renovation of cells and tissues. Cell 147: 728–741.
44. Komatsu M, Waguri S, Koike M, Sou YS, Ueno T, et al. (2007) Homeostatic levels of p62 control cytoplasmic inclusion body formation in autophagy-deficient mice. Cell 131: 1149–1163.
45. Chan K, Lu R, Chang JC, Kan YW (1996) NRF2, a member of the NFE2 family of transcription factors, is not essential for murine erythropoiesis, growth, and development. Proc Natl Acad Sci USA 93: 13943–13948.

dc_840_14

46. Ishii T, Itoh K, Takahashi S, Sato H, Yanagawa T, et al. (2000) Transcription factor Nrf2 coordinately regulates a group of oxidative stress-inducible genes in macrophages. J Biol Chem 275: 16023–16029.
47. Harding HP, Zeng H, Zhang Y, Jungries R, Chung P, et al. (2001) Diabetes mellitus and exocrine pancreatic dysfunction in perk−/− mice reveals a role for translational control in secretory cell survival. Mol Cell 7: 1153–1163.
48. Vega-Stromberg T (2003) Chemotherapy-induced secondary malignancies. J Infus Nurs 26: 353–361.
49. Hijiya N, Ness KK, Ribeiro RC, Hudson MM (2009) Acute leukemia as a secondary malignancy in children and adolescents: current findings and issues. Cancer 115: 23–35.
50. Sykiotis GP, Bohmann D (2008) Keap1/Nrf2 signaling regulates oxidative stress tolerance and lifespan in Drosophila. Dev Cell 14: 76–85.

Published May 13, 2013

This article has original data in the JCB Data Viewer
http://jcb-dataviewer.rupress.org/jcb/browse/5905

dc_840_14

Autophagosomal Syntaxin17-dependent lysosomal degradation maintains neuronal function in *Drosophila*

Szabolcs Takáts, Péter Nagy, Ágnes Varga, Karolina Pircs, Manuéla Kárpáti, Kata Varga, Attila L. Kovács, Krisztina Hegedűs, and Gábor Juhász

Department of Anatomy, Cell and Developmental Biology, Eötvös Loránd University, H-1117 Budapest, Hungary

During autophagy, phagophores capture portions of cytoplasm and form double-membrane autophagosomes to deliver cargo for lysosomal degradation. How autophagosomes gain competence to fuse with late endosomes and lysosomes is not known. In this paper, we show that Syntaxin17 is recruited to the outer membrane of autophagosomes to mediate fusion through its interactions with ubisnap (SNAP-29) and VAMP7 in *Drosophila melanogaster*. Loss of these genes results in accumulation of autophagosomes and a block of autolysosomal degradation during basal, starvation-induced, and developmental autophagy. Viable *Syntaxin17* mutant adults show large-scale accumulation of autophagosomes in neurons, severe locomotion defects, and premature death. These mutant phenotypes cannot be rescued by neuron-specific inhibition of caspases, suggesting that caspase activation and cell death do not play a major role in brain dysfunction. Our findings reveal the molecular mechanism underlying autophagosomal fusion events and show that lysosomal degradation and recycling of sequestered autophagosome content is crucial to maintain proper functioning of the nervous system.

Introduction

Autophagy ensures degradation and recycling of intracellular material, including macromolecules and even whole organelles in eukaryotic cells. Autophagy has a role in a wide range of physiological and pathological settings, such as cellular adaptation to stress, starvation, and protection from aging, cancer, neurodegeneration, and invading pathogens (Mizushima et al., 2008). Cytoplasmic cargo sequestered into double-membrane autophagosomes by phagophore cisterns (also called isolation membranes) is transported to lysosomes for degradation and reuse to support biosynthetic and energy production pathways (Tooze and Yoshimori, 2010). Several different sources such as ER, Golgi, mitochondria, endosomes, and plasma membrane have been suggested to supply membranes for the phagophore (Axe et al., 2008; Tooze and Yoshimori, 2010). Regardless of the membrane source, all autophagosomes fuse with late endosomes and lysosomes to generate amphisomes and autolysosomes, respectively, whereas phagophores do not. Therefore, autophagosomes must gain competence for specific fusion through acquiring the required molecular machinery during their maturation process.

Vesicle fusion events are usually mediated by the action of different SNARE proteins that assemble into complexes in a combinatorial fashion. A SNARE complex contains four parallel SNARE helix bundles, supplied by a Qa SNARE and either separate Qb and Qc SNAREs or a SNAP protein that contains both Qb and Qc SNARE domains, all located on the membrane of the first vesicle, and an R SNARE anchored to the second vesicle (Hong, 2005). Yeast SNARE proteins Vam3, Vam7, Vti1, and Ykt6 have all been suggested to play a role in fusion of autophagosomes with the vacuole, the equivalent of metazoan lysosomes (Dilcher et al., 2001; Ishihara et al., 2001; Ohashi and Munro, 2010). Vam3 and Vam7 have no clear homologues in metazoa. Moreover, we and others showed that autophagosomes accumulate if formation of late endosomes is blocked in *Drosophila melanogaster* and mammals, indicating that amphisomes play a critical role in autophagosome clearance in these cells, unlike in yeast (Filimonenko et al., 2007; Rusten et al., 2007; Juhász et al., 2008). Mammalian VAMP7, VAMP8, and

Correspondence to Gábor Juhász: szmrt@elte.hu

Abbreviations used in this paper: LTR, LysoTracker red; UAS, upstream activation sequence.

© 2013 Takáts et al. This article is distributed under the terms of an Attribution–Noncommercial–Share Alike–No Mirror Sites license for the first six months after the publication date (see http://www.rupress.org/terms). After six months it is available under a Creative Commons License (Attribution–Noncommercial–Share Alike 3.0 Unported license, as described at http://creativecommons.org/licenses/by-nc-sa/3.0/).

Supplemental Material can be found at:
http://jcb.rupress.org/content/suppl/2013/05/08/jcb.201211160.DC1.html
Original image data can be found at:
http://jcb-dataviewer.rupress.org/jcb/browse/5905

The Rockefeller University Press $30.00
J. Cell Biol. Vol. 201 No. 4 531–539
www.jcb.org/cgi/doi/10.1083/jcb.201211160

THE JOURNAL OF CELL BIOLOGY

Downloaded from jcb.rupress.org on May 16, 2013

Published May 13, 2013

Vti1b were all suggested to be involved in autophagosomal fusion events (Fader et al., 2009; Furuta et al., 2010). The accumulation of both autophagosomes and autolysosomes in *Vti1b* knockout mice indicates that this gene product is likely to function in later steps of autophagy (Atlashkin et al., 2003). Ykt6 and VAMP7 have also been implicated in the formation of phagophores in yeast and mammalian cells, respectively (Moreau et al., 2011; Nair et al., 2011).

In a screen for SNAREs involved in autophagy, we identified Syx17 (Syntaxin17, Qa), the SNAP-29 homologue ubisnap (usnp, Qbc), and VAMP7 (CG1599, R) as required for autophagosome fusion events. We showed that Syx17 is recruited to the outer membrane of autophagosomes to acquire fusion competence, and loss of *Syx17* results in neuronal dysfunction, locomotion defects, and early death of adult flies.

Results and discussion

We performed a genetic screen for SNARE proteins involved in starvation-induced autophagy, by generating GFP-marked RNAi cell clones in mCherry-Atg8a–expressing *Drosophila* fat bodies. The mCherry-Atg8a reporter is bound to phagophores and autophagosomes through a lipid anchor on its C terminus. In addition, mCherry-Atg8a attached to the inner membrane of autophagosomes is selectively transported to autolysosomes, which are prominently labeled by this reporter as a result of large-scale accumulation of the protease- and low pH–resistant mCherry tag inside lysosomes (Kimura et al., 2007). *Syx17*, *usnp*, and *VAMP7* knockdown cells showed a similar and very characteristic phenotype: small mCherry-Atg8a dots accumulated in the perinuclear region, unlike the evenly distributed, bigger, and brighter dots observed in neighboring control cells (Fig. 1, A–C and P; and Table S1 shows the results of our screen).

Depletion of *Syx17*, *usnp*, or *VAMP7* resulted in a complete block of starvation-induced punctate LysoTracker staining, a dye commonly used to label autolysosomes in *Drosophila* fat body (Fig. 1, D–F and Q). Starvation-induced LysoTracker red (LTR) staining was also impaired in *Syx17[LL]* and *VAMP7[EP]* mutant larvae that carry transposon insertions in the coding sequences of these genes 22 and 24 nucleotides downstream of the translation start site, respectively (Fig. 1, G, H, J, and R), similar to an independent RNAi line targeting *usnp* (Fig. 1, K and Q). Transgenic expression of Syx17 restored punctate LysoTracker staining in *Syx17* mutants, confirming that loss of *Syx17* caused the mutant phenotype (Fig. 1, I and R). Tandem-tagged mCherry-GFP-Atg8a is commonly used for analyzing autophagic flux (Kimura et al., 2007). This reporter is normally transported to autolysosomes where GFP is rapidly quenched, but mCherry persists in control cells (Fig. 1, L and L′). In contrast, structures positive for both GFP and mCherry accumulated in the perinuclear region of *Syx17*, *usnp*, and *VAMP7* RNAi cells, indicating a block of GFP inactivation (Fig. 1, M–O′). Developmental autophagy of the fat body at the onset of metamorphosis was also impaired in *Syx17*, *usnp*, and *VAMP7* RNAi cells (Fig. S1, A–F, M, and N).

Immunostainings revealed accumulation of endogenous Atg8a-positive dots representing autophagosomes in *Syx17*, *usnp*, and *VAMP7* loss-of-function cells compared with adjacent control fat body cells, both in starved (Fig. 2, A–C and M) and well-fed larvae (Fig. S1, G–I and O). Levels of the specific cargo p62 inversely correlate with autophagic degradation in flies and mammals (Bjørkøy et al., 2009; Pircs et al., 2012). p62 aggregates accumulated in *Syx17*, *usnp*, and *VAMP7* loss-of-function cells both in starved (Fig. 2, D–F and N) and well-fed larvae (Fig. S1, J–L and P), indicating impaired autophagic breakdown. Western blots also revealed increased p62 and autophagosome-associated, lipidated Atg8a-II levels in starved *Syx17* and *VAMP7* mutant larvae compared with controls (Fig. 2 G). Larvae expressing *usnp* RNAi in all cells showed similar accumulation of Atg8a-II and p62 (Fig. S1 Q). *Syx17* mutants are viable despite profound autophagy defects, similar to *Atg7*- and *Atg8a*-null mutants (Juhász et al., 2007; Simonsen et al., 2008). Levels of p62 and lipidated Atg8a-II also increased in well-fed *Syx17* mutant adult flies compared with controls (Fig. 2 H). Western blots using our novel polyclonal rat and guinea pig anti-Syx17 antisera detected two bands near the predicted molecular weight of this protein, both of which were missing from *Syx17* mutants (Fig. 2, G and H; and Fig. S1 R). Faint bands were visible in the independent *Syx17* transposon insertion mutant line *Syx17[WH]* (Fig. 2 G). All these results indicated that autophagosomes cannot progress to autolysosomes in the absence of *Syx17*, *usnp*, and *VAMP7*. Ultrastructural analysis indeed revealed accumulation of double-membrane autophagosomes and impaired generation of autolysosomes in starved *Syx17* mutant, *usnp* RNAi, and *VAMP7* mutant fat body cells (Fig. 2, I–L and O).

Our loss-of-function data suggested that Syx17, usnp, and VAMP7 function as part of the same SNARE complex. Human STX17 (Syntaxin17) was previously shown to bind to SNAP-29, but the significance of this interaction remained unknown (Steegmaier et al., 1998). We found that both HA-tagged usnp and VAMP7 coimmunoprecipitated with FLAG-tagged Syx17 in cultured *Drosophila* cells (Fig. 3 A). The amount of VAMP7 bound to beads increased when all three proteins were co-expressed, suggesting that Syx17 and usnp together bind more efficiently to VAMP7 than Syx17 alone (Fig. 3 A). We also produced anti-usnp antisera to detect interactions of endogenous proteins. These polyclonal rat antibodies specifically recognized endogenous usnp as a single 36-kD band, which was reduced by systemic expression of *usnp* RNAi transgenes in larvae (Fig. S1 Q). We could readily detect endogenous usnp in anti-Syx17 immunoprecipitates from lysates of adult flies (Fig. 3 B). Vice versa, endogenous Syx17 could be immunoprecipitated with anti-usnp antibodies from cultured cell lysates (Fig. 3 C).

These results established the identity of autophagosome fusion-specific SNARE complex subunits but did not reveal which ones are present on autophagosomes. As ubisnap/SNAP-29 has both Qb and Qc SNARE domains but no transmembrane domain or lipidation site, it is likely recruited to its target membrane through interaction with Syx17, a Qa SNARE. *Drosophila* Syx17 localized to the ER (Fig. S2, A and B), similar to human STX17 (Hong, 2005). *Drosophila* VAMP7 is predicted to be present in late endosomes and lysosomes (Hong, 2005). We thus reasoned that Syx17 could also localize to autophagosomes to

Downloaded from jcb.rupress.org on May 16, 2013

Published May 13, 2013

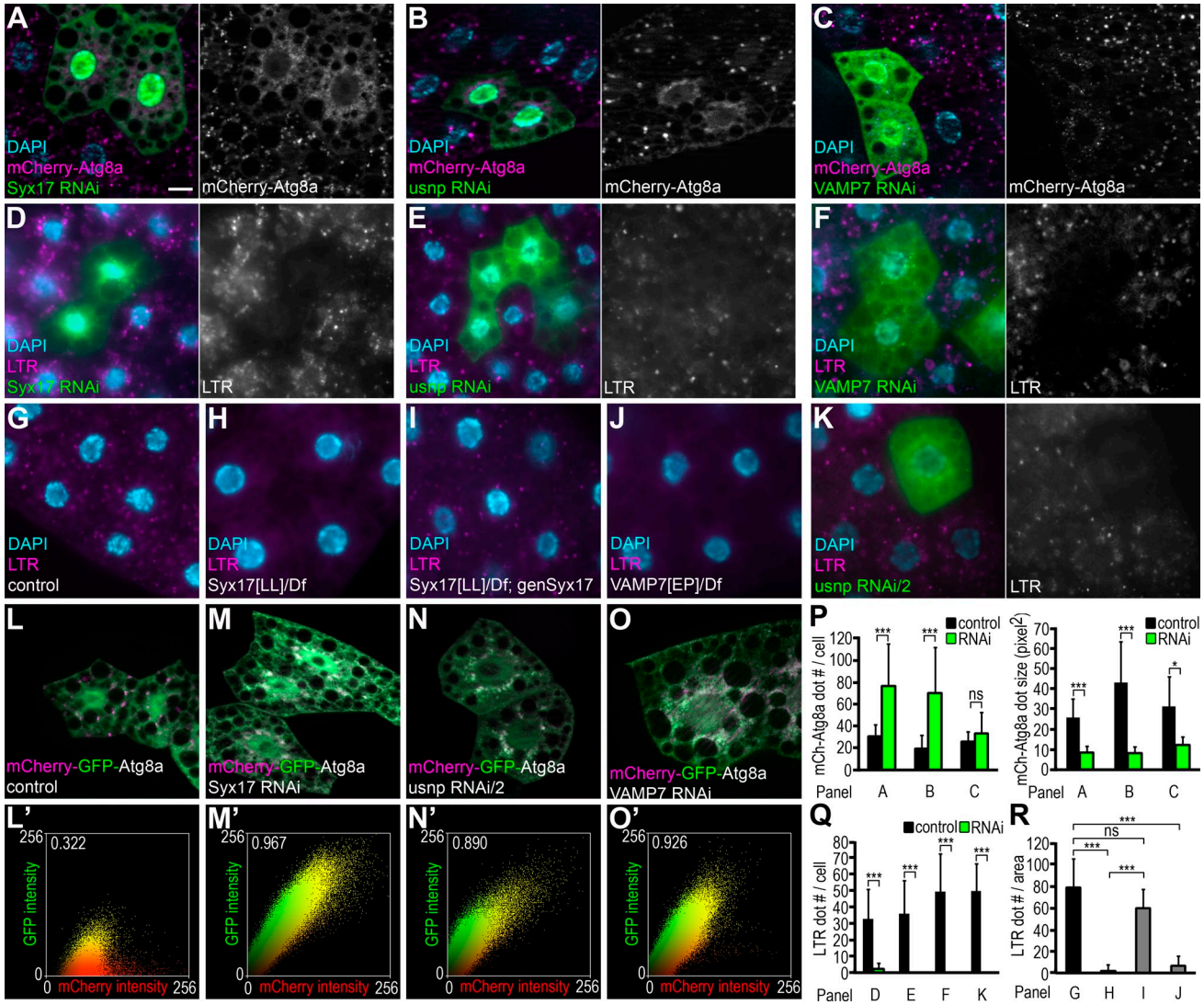


Figure 1. **Syx17, usnp, and VAMP7 are required for autophagy in *Drosophila*.** (A–C) *Syx17* (A), *usnp* (B), or *VAMP7* (C) depletion in GFP-marked fat cell clones leads to formation of numerous small, mostly perinuclear mCherry-Atg8a dots, unlike the larger, brighter, evenly distributed punctae in surrounding control cells of starved larvae. (D–F) Knockdown of *Syx17* (D), *usnp* (E), or *VAMP7* (F) in LAMP1-GFP–marked cells blocks starvation-induced punctate LysoTracker red (LTR) staining. (G–J) Starvation leads to formation of LTR dots in control larvae (G). No LTR punctae form in starved *Syx17* mutants (H), whereas LTR staining is restored in mutants expressing a *Syx17* transgene (I). No LTR dots appear in *VAMP7* mutants (J). (K) Expression of a second, independent *usnp* RNAi transgene also blocks LTR puncta formation. (L–O) Tandem-tagged mCherry-GFP-Atg8a is transported to autolysosomes that appear as mCherry-positive puncta (magenta in L) in control cells of starved larvae. Silencing of *Syx17* (M), *usnp* (N), or *VAMP7* (O) results in the formation of numerous dots positive for both mCherry and GFP (white). Dot plots in L′–O′ show intensity and colocalization profiles of mCherry and GFP dots. Pearson correlation coefficients shown at the top indicate strong colocalization of GFP and mCherry in M′–O′. (P–R) Quantification of data presented in A–C (P), D–F and K (Q), and G–J (R); $n = 10$ for all genotypes. mCh, mCherry. Error bars mark SDs. *, $P < 0.05$; ***, $P < 0.001$. Bar, 20 µm.

recruit usnp, and they mediate fusion of autophagosomes and endo/lysosomes by binding to VAMP7 located in the membranes of the degradative organelles. Endogenous Syx17 was indeed detected in 30.5% (61/200) of endogenous Atg8a-positive autophagosomes in starved animals and also colocalized with 43% (86/200) of GFP-Atg8a dots (Fig. 4, A and B). In contrast, Syx17 essentially did not colocalize with the phagophore marker Atg5 (2.5%, 5/200) or GFP-dLAMP–positive late endosomes and lysosomes (6.8%, 16/236; Fig. 4, C and D). Loss of *Atg2* results in accumulation of stalled phagophores that already contain Atg8 homologues in worms and mammals (Lu et al., 2011; Velikkakath et al., 2012). Accordingly, Atg8a and Syx17 did not colocalize in *Atg2* mutants (2.8%, 9/322; Fig. 4 E). Finally, immuno-EM showed the presence of endogenous Syx17 in the outer membrane of autophagosomes (Fig. 4 F). Thus, Syx17 is recruited to autophagosomes to promote their fusion with late endosomes and lysosomes through its interactions with usnp and VAMP7.

Two papers relying on siRNA depletion of human *STX17* were published while our manuscript was under review (Itakura et al., 2012; Hamasaki et al., 2013). Itakura et al. (2012) found that STX17, SNAP-29, and VAMP8 cooperate to mediate fusion of autophagosomes with late endosomes and lysosomes in mammalian cells. Also, GFP-STX17 localized to the outer membrane of autophagosomes. In contrast, Hamasaki et al. (2013) suggested that no autophagosomes form in *STX17* siRNA–treated

Downloaded from jcb.rupress.org on May 16, 2013

Published May 13, 2013

dc_840_14

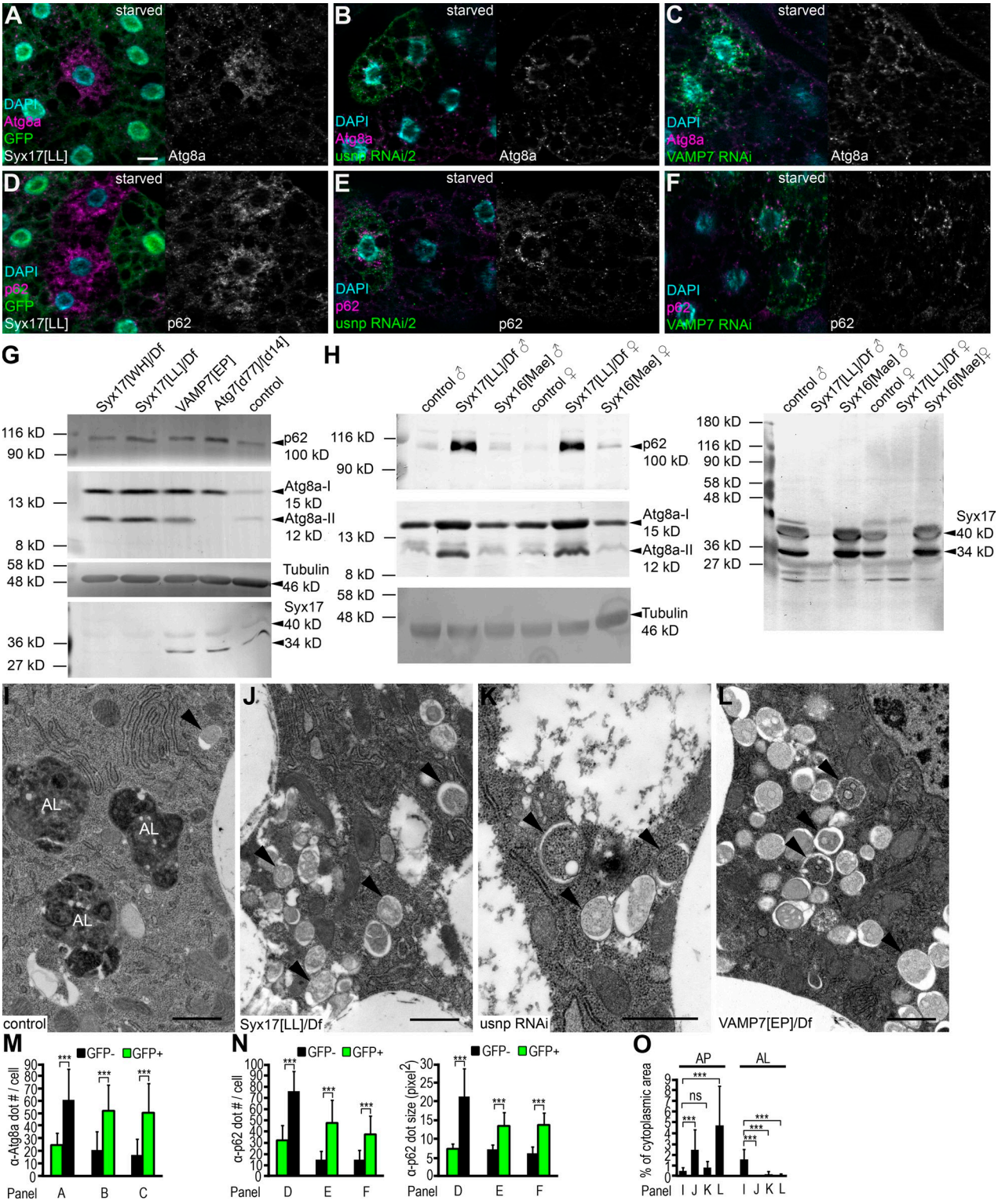


Figure 2. **Autophagosomes accumulate upon loss of *Syx17*, *usnp*, or *VAMP7*.** (A–C) Increased numbers of Atg8a-positive autophagosomes are seen in *Syx17* mutant (A), *usnp* (B), and *VAMP7* (C) RNAi cells in starved larvae. (D–F) p62 aggregates accumulate in *Syx17* mutant (D), *usnp* (E), and *VAMP7* (F) RNAi cells in starved larvae. Note that *Syx17* mutant cells are marked by lack of GFP expression in A and D, whereas RNAi cells express LAMP1-GFP in B, C, E, and F. (G) Western blots show increased autophagosome-associated, lipidated Atg8a-II levels in starved *Syx17* and *VAMP7* mutant larvae compared with controls. Accumulation of p62 in *Syx17* and *VAMP7* mutants is comparable to *Atg7* mutants that are unable to lipidate Atg8a. Both the 34- and 40-kD isoforms of Syx17 disappear in *Syx17[LL]* mutants based on rat anti-Syx17 immunoblots, whereas faint bands are visible in *Syx17[WH]* mutant larvae. (H) Atg8a-II and p62 accumulate in well-fed *Syx17* mutant adults compared with controls or *Syx16* mutants (an additional control). Both Syx17-specific bands are missing from *Syx17* mutant adults. (I–L) Numerous large autolysosomes (AL) and few double-membrane autophagosomes (arrowheads) are visible in ultrastructural images of control fat body cells from starved animals (I). Loss of *Syx17* (J), *usnp* (K), or *VAMP7* (L) function leads to accumulation of autophagosomes and lack of autolysosomes. (M–O) Quantification of data presented in A–C (M), D–F (N), and I–L (O). AP, autophagosome. $n = 10$ for A–F, and $n = 4$ for I–L. Error bars mark SDs. ***, $P < 0.001$. Bars: (A–F) 20 µm; (I–L) 1 µm.

Downloaded from jcb.rupress.org on May 16, 2013

Published May 13, 2013

dc_840_14

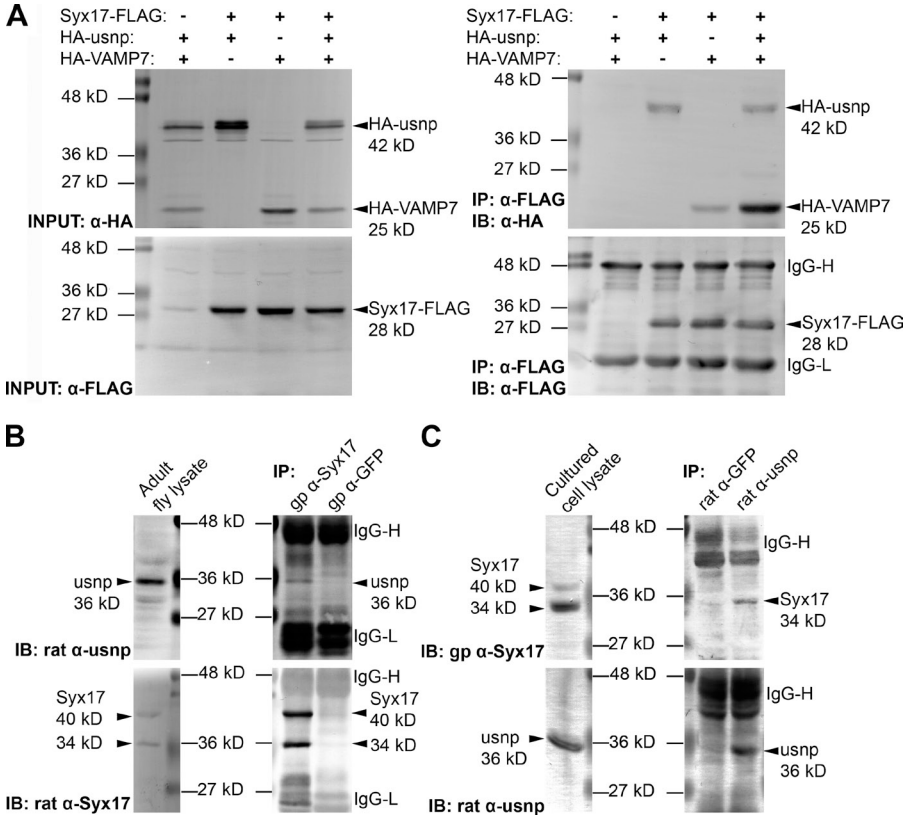


Figure 3. **Syx17 binds to usnp and VAMP7.** (A) Coimmunoprecipitation shows that Syx17-FLAG binds to both HA-usnp and HA-VAMP7 in cultured *Drosophila* cells. Note that usnp facilitates the interaction of overexpressed VAMP7 with Syx17 (both lacking transmembrane domains). (B) Endogenous usnp coimmunoprecipitates with endogenous Syx17. (C) Endogenous Syx17 coimmunoprecipitates with endogenous usnp. gp, guinea pig; IP, immunoprecipitation; IB, immunoblotting.

cells. Our results support the findings of the former work with the exception of VAMP8, but flies appear to have only VAMP7 and lack the closely related VAMP8. According to Itakura et al. (2012), a pool of free cytosolic STX17 may be directly inserted into the outer membrane of autophagosomes. This is likely mediated by its two glycine-rich transmembrane domains and the C-terminal region (Itakura et al., 2012). *Drosophila* Syx17 shows a similar domain structure to human STX17, so it may also be transported to autophagosomes by this pathway (Fig. S2 C).

Depletion of *syntaxin5* was recently shown to cause defects in autophagic protein degradation caused by impaired trafficking of hydrolases from ER to Golgi and thus lysosomes (Renna et al., 2011). Importantly, *syntaxin5* seemed to be dispensable for the fusion of autophagosomes with endosomes and lysosomes, indicating that it functions at a later step during autophagy than Syx17.

Continuous basal autophagy is critical for the homeostasis of quiescent, nondividing cells, such as neurons. We and others reported earlier that autophagy deficiency results in accumulation of protein aggregates and progressive neurodegeneration in flies and mice (Hara et al., 2006; Komatsu et al., 2006; Juhász et al., 2007). *Syx17* mutant adults were viable but unable to fly or climb properly, and all died within 4 d of eclosion (n = 351). We detected large-scale accumulation of Atg8a-positive autophagosomes and p62 aggregates in *Syx17* mutant brains (Fig. 5, A, B, and F). Neurons of well-fed *Syx17* mutant adult flies contained vast numbers of autophagosomes: on average, 20% of total cytoplasm was enclosed within them (Fig. 5, D and G). In contrast, autophagic structures were rarely observed in ultrastructural images of control brains or mutants rescued by transgenic expression of Syx17 (Fig. 5, C, E, and G). Altogether 86% of cells (201/234, n = 4) contained autophagosomes in ultrastructural sections of mutant brains, in contrast with 1% of neurons in control flies (3/270, n = 4) or 2% in rescued flies (6/327, n = 4).

2-d-old *Syx17* mutants performed poorly in a climbing test (Fig. 5 H), an established measure of nervous system function (Juhász et al., 2007). Again, transgenic expression of Syx17 rescued this locomotion defect (Fig. 5 H). We showed earlier that loss of *Atg7* leads to widespread apoptosis in brains of 30-d-old mutant adults (Juhász et al., 2007). On average, 25% of neurons were positive for active caspase 3 in the absence of Syx17 in mutant brains, unlike in similarly aged controls (Fig. S2, D–F). TUNEL assays showed that 20% of mutant cells contained fragmented DNA indicating cell death, whereas practically no TUNEL-positive neurons were identified in control or rescued 2-d-old adult brains (Fig. 5, I–K; and Fig. S2 G, quantification). This seemed specific to neurons, as no TUNEL-positive cells were detected in muscles of mutant adults (Fig. S2, H and I). Transgenic expression of the effector caspase inhibitor p35 in mutant neurons suppressed TUNEL staining (Fig. S2, G and J), but 85% of neurons (202/238, n = 3) still contained autophagosomes in brain sections similar to *Syx17* mutants (Fig. S2 K). The potential contribution of caspase activation to mutant phenotypes was tested in epistasis analyses. Neuron-specific expression of p35 or the pancaspase inhibitor DIAP1 (*Drosophila* inhibitor of apoptosis protein 1) failed to rescue locomotion defects in 2-d-old *Syx17* mutant adults (Fig. 5 H). In addition, although transgenic expression of Syx17 fully rescued the viability of *Syx17* mutant adults (174/175 adults alive on day 4),

Downloaded from jcb.rupress.org on May 16, 2013

Published May 13, 2013

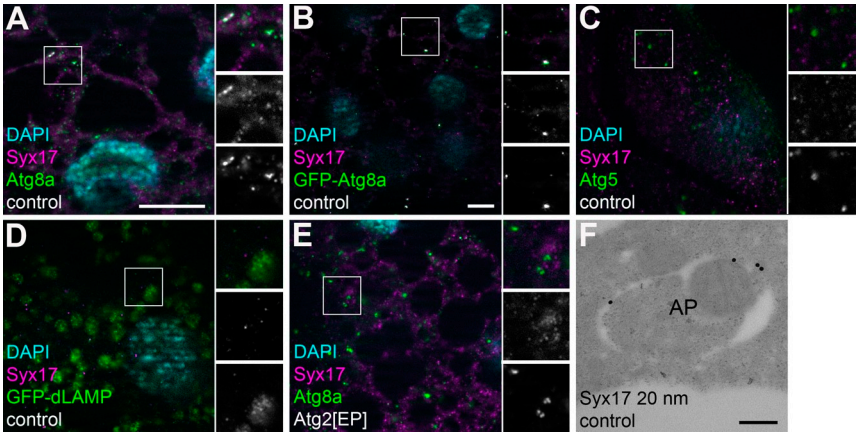


Figure 4. **Syx17 is recruited to completed autophagosomes.** (A and B) Endogenous Syx17 colocalizes with both endogenous (A) and GFP-tagged (B) Atg8a in starved fat body cells. (C and D) No colocalization is observed between Syx17 and the phagophore marker Atg5 (C) or late endosomes and lysosomes, labeled by GFP-dLAMP (D). (E) Syx17 and Atg8a do not colocalize in *Atg2* mutants that accumulate Atg8a-positive stalled phagophores. Insets show merged images (top), Syx17 channels (middle), and relevant green channels (bottom) enlarged from boxed areas in A–E. (F) Immunogold labeling reveals that Syx17 is associated with the outer membrane of autophagosomes (AP). Bars: (A and C–E) 20 µm; (B) 20 µm; (F) 100 nm.

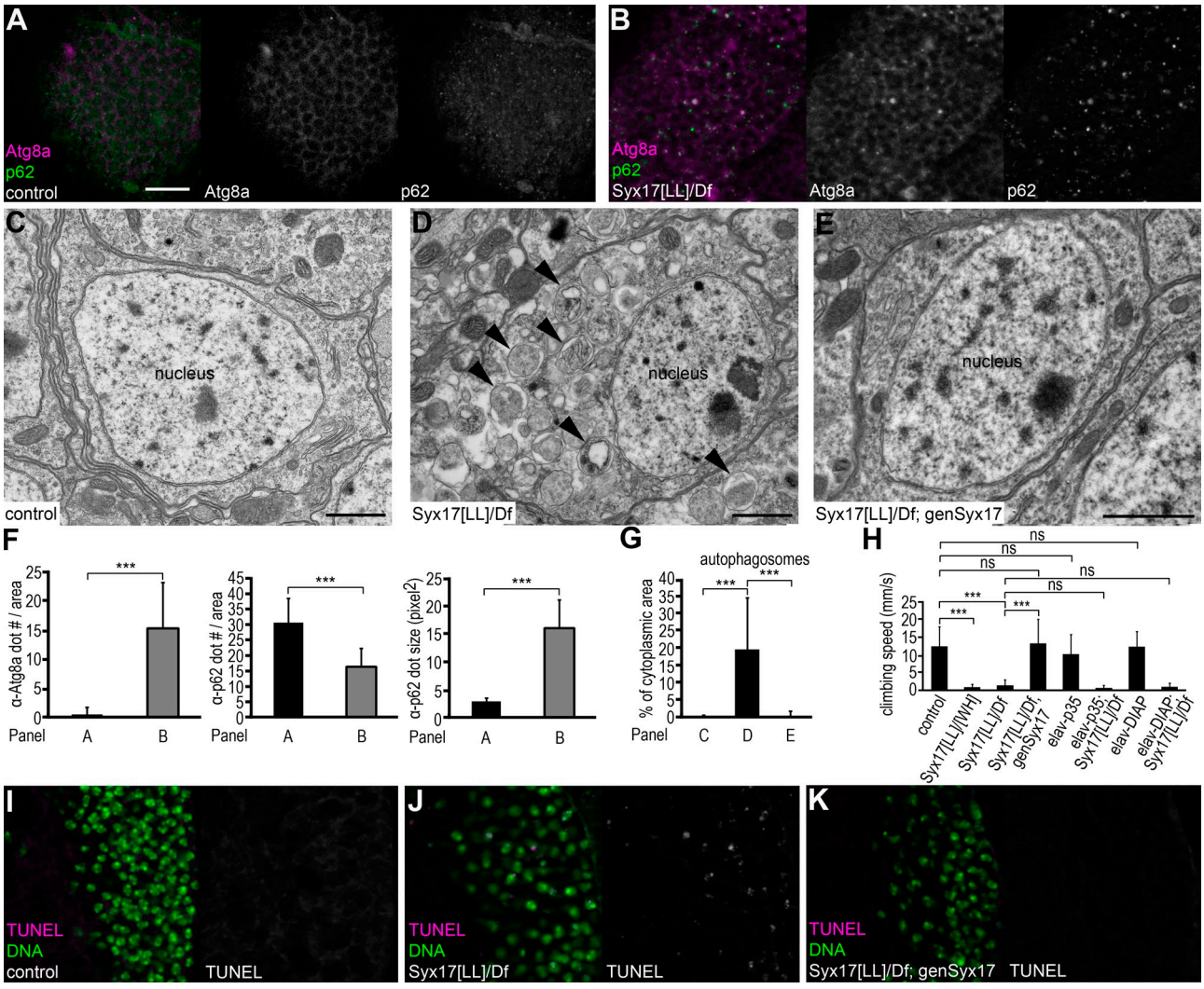


Figure 5. **Impaired autophagosome maturation leads to locomotion defects in 2-d-old adult flies.** (A and B) Atg8a-positive autophagosomes and p62 aggregates accumulate in *Syx17* mutant brains (B) compared with similarly aged controls (A). (C–E) No autophagosomes are found by EM in neurons of control adult flies (C). Large-scale accumulation of autophagosomes (arrowheads) is obvious in *Syx17* mutant neurons (D). Autophagosome accumulation is rescued in *Syx17* mutant neurons by transgenic expression of Syx17 (E). (F and G) Quantification of data presented in A and B (F) and C–E (G); $n = 9$ for A and B, and $n = 4$ for C–E. Error bars mark SDs. ***, $P < 0.001$. (H) *Syx17* mutant adults perform poor compared with controls in climbing tests. Expression of Syx17 in mutants rescues locomotion defects. Neuron-specific expression of caspase inhibitors p35 or DIAP1 have no influence on climbing performance of adult flies, and these do not rescue the defects of *Syx17* mutant adults. $n = 90$ for all genotypes. Error bars mark SDs. ***, $P < 0.001$. (I–K) TUNEL assays reveal apoptotic DNA fragmentation in *Syx17* mutant brains (J) compared with controls (I), which is rescued by expression of Syx17 (K). Bars: (A, B, and I–K) 20 µm; (C–E) 1 µm.

Downloaded from jcb.rupress.org on May 16, 2013

Published May 13, 2013

all mutant flies expressing either p35 or DIAP1 still died within 4 d of eclosion (n = 90 and 105, respectively). These results suggest that neuronal caspase activation may not be a major cause for the locomotion defects and premature death of *Syx17* mutant adult flies.

Collectively, we showed that a complex of SNARE proteins Syx17, usnp, and VAMP7 is required for autophagosome clearance and that autophagosomes gain competence to fuse with late endosomes and lysosomes by recruiting Syx17. The locomotion defects and early death of viable *Syx17* mutants indicate that lysosomal degradation and recycling of sequestered autophagosomal cargo is crucial to maintain organismal health and proper brain functions in *Drosophila*.

Materials and methods

Fly strains and genetics

Flies were maintained on standard yeast/cornmeal/agar media. In climbing tests, a total of 90 adults per genotype were recorded and scored in cohorts of three to six flies, after tapping them down in a plastic graduated cylinder (Juhász et al., 2007). In clonal analyses, RNAi cells were generated spontaneously in larvae carrying hs-Flp; upstream activation sequence (UAS)-Dcr2; Actin>CD2>Gal4 UAS-RNAi (and UAS-GFP or UAS-LAMP1-GFP as a knockdown cell marker), and mutant cell clones (marked by lack of GFP expression) were generated by heat shocking 2–4-h embryos of the genotype hs-Flp; ubi-GFP FRT2A/Syx17[LL] FRT2A in a 38°C water bath for 1 h (Juhász et al., 2007, 2008; Pircs et al., 2012). Expression of mCherry-Atg8a was driven by a fat body–specific r4 promoter in our screen (transgenic flies were provided by T. Neufeld, University of Minnesota, Minneapolis, MN; Pircs et al., 2012). We used the GFP knockin line dLAMP[CPTI001775] (Drosophila Genetic Resource Center) to label lysosomes, w[1118] as control, UAS-GFP-KDEL and Pdi[G00198] as ER reporters (Bloomington Drosophila Stock Center), Atg2[EP3697] (Berry and Baehrecke, 2007), Atg7[d77]/Atg7[d14] (Juhász et al., 2007) mutants, and SNARE loss-of-function strains listed in Table S1. Knockdown of usnp was induced by Actin-Gal4 for Western blots and collagen-Gal4 for EM in L3 stage larvae, and overexpression of UAS-p35 or UAS-DIAP1 in adult neurons was mediated by elav-Gal4 (all obtained from Bloomington Drosophila Stock Center).

Histology and imaging

LTR stainings were performed by incubating dissected L3 stage fat bodies in 100 nM LTR (Invitrogen) for 5 min. For immunofluorescent labeling, bisected larvae were fixed overnight in 3.7% paraformaldehyde at 4°C and blocked in PBS with 0.1% Triton X-100, 0.05% sodium deoxycholate, and 3% goat serum for 3 h followed by overnight incubations with primary and secondary antibodies in blocking buffer at 4°C (Juhász et al., 2008; Pircs et al., 2012). We used chicken anti-GFP (1:1,500; Invitrogen), rabbit anti-Atg5 (1:100; Sigma-Aldrich), rabbit anti-Atg8a (1:500; provided by K. Kohler, Eidgenössische Technische Hochschule Zürich, Zurich, Switzerland; Barth et al., 2011), rabbit anti-p62 (1:2,000; Pircs et al., 2012), rabbit anti–active caspase 3 (1:300; Cell Signaling Technology), rat anti-Atg8a (1:300), and rat anti-Syx17 (1:300; this study) primary and Alexa Fluor 488 anti–chicken, Alexa Fluor 488 anti–rabbit, Alexa Fluor 568 anti–rat, and Alexa Fluor 647 anti–rabbit (all 1:1,500; Invitrogen) secondary antibodies. For TUNEL stainings, adult heads and half-thoraces were fixed in 3.7% paraformaldehyde overnight at 4°C and embedded into paraffin following standard protocols. Sections were processed using In Situ Cell Death Detection Kit, tetramethylrhodamine red (Roche) with SYTOX green DNA stain (Juhász et al., 2007). Images were obtained on a microscope (Axio Imager.M2; Carl Zeiss) equipped with a grid confocal unit (ApoTome.2; Carl Zeiss) at room temperature, using Plan-Neofluar 20×, 0.5 NA (air), 40×, 0.75 NA (air), and 100×, 1.3 NA (oil) objectives, a camera (AxioCam MRm; Carl Zeiss), and AxioVision software (Carl Zeiss). Microscope settings were identical for experiments of the same kind. Primary images were processed in AxioVision and Photoshop (Adobe) to produce final figures. Note that Alexa Fluor 568 or 647 channels are pseudocolored magenta.

Image analysis and statistics

Colocalization of puncta was counted manually on a computer situated in a darkroom, only taking into account overlapping structures with a similar shape and size in relevant fluorescent channels. For statistical analyses, original, unmodified images were imported in ImageJ (National Institutes of Health), and the intensity threshold for the relevant channel was set so that as many dots as possible were selected without the merging of clearly separable adjacent dots. In clonal analyses, mutant or RNAi cells were then manually encircled based on the GFP channel, and the number and size of dots in the relevant channel within that area were recorded. Adjacent control cells were selected randomly from the same image and analyzed. When comparing images from different control and mutant animals, a 300 × 300–pixel area was randomly selected from each image and analyzed as in clonal experiments. Images taken from the number of animals (n) per genotype as indicated in figure legends were evaluated for all experiments. Data were then imported into SPSS Statistics (IBM) and tested for normality of data distribution, and then, p-values were calculated with the appropriate statistical tests: two-tailed, two-sample, unequal variance t test or U test for pairwise comparison of normal or nonnormal distribution data, respectively, and analysis of variance or nonparametric Kruskal-Wallis tests for multiple comparisons of normal or nonnormal distribution data, respectively. For autophagic flux measurements with mCherry-GFP-Atg8a, primary images were imported into ImageJ and analyzed automatically using the colocalization plugin with the intensity correlation tool. Clones from 5–10 animals per genotype were evaluated with similar results, and one representative dot plot is shown in Fig. 1 (L′–O′) for each.

Molecular cloning and generation of polyclonal antibodies

The genomic region containing *Drosophila* Syx17 was amplified using primers 5′-GGCGCGCCGCATGCGGCCGCTTAGACGTAAGCGCACCACCGC-3′ and 5′-GCATGCTAGCGGCCGCGTGACCAACGAGAACACGGGC-3′ and cloned into pCasper5 as an SphI fragment. Transgenic flies genSyx17 were generated following standard procedures (BestGene, Inc.). Syx17 coding sequences were amplified by PCR using primers 5′-ATGACGCGCGATGAGAAACTGCC-3′ and 5′-ATCCTTCTGGCTTCTCTTTTAGCTCCAGTCTCTC-3′, phosphorylated, blunt cloned into XmnI–EcoRV-digested dephosphorylated pENTR1A (Invitrogen), and subsequently recombined into pDEST17 (Invitrogen). N-terminally His-tagged protein was expressed in the *Escherichia coli* Rosetta strain (EMD Millipore) and purified using Ni-agarose beads (QIAGEN). Recombinant protein was used to immunize rats and guinea pigs following standard procedures with Freund's adjuvants (Sigma-Aldrich). Syx17 pENTR1A was recombined into pTWF (Drosophila Genomics Resource Center) to yield UAS-Syx17-FLAG, in which 3×FLAG replaces the two transmembrane domains and the extreme C-terminal region of Syx17. usnp and VAMP7 coding sequences were amplified using primers 5′-GTAGCGGCCGCGGGTACCGGAATGGCCCATAACTACCTGCAGC-3′/5′-TATGGTACCGCGGCCGCTACTTCTTCAGAAGCTTGCTCATGTCC-3′ and 5′-GTAGCGGCCGCGGGTACCGGACCGATACTATATAGTGTGATATCGCGGG-3′/5′-ATATGGTACCGCGGCCGCTAGACGCGGATGTTCTTCCAAAA-3′, respectively, and cloned into pUAST-3×HA to generate UAS-HA-usnp and UAS-HA-VAMP7. Note that the transmembrane domain is removed from tagged VAMP7. The aforementioned primers were used to blunt clone usnp coding sequences into pENTR1A followed by recombination of the resulting entry clone into pDEST17, expression and purification of the recombinant protein, and immunization of rats as for Syx17.

Cell culture and coimmunoprecipitations

Embryonic hemocyte-derived D.Mel-2 cells were maintained in Express-Five Serum-Free medium (Invitrogen) and transfected with UAS constructs and metallothionein-Gal4 plasmid using TransIT-2020 reagent (Mirus Bio LLC). 48 h later, protein expression was induced by adding 1 mM $CuSO_4$ for overnight incubation. Cultured cells were collected, washed twice in PBS, lysed on ice in lysis buffer (0.5% Triton X-100, 150 mM NaCl, 1 mM EDTA, and 20 mM Tris-HCl, pH 7.5) containing complete protease and phosphatase inhibitor cocktails (Sigma-Aldrich), and spun for 10 min at 10,000 *g* in a centrifuge (5430R; Eppendorf) at 4°C followed by the addition of anti-FLAG slurry (Sigma-Aldrich) to the cleared supernatant. After incubation at 4°C for 2 h, beads were collected by centrifugation at 5,000 *g* for 30 s at 4°C followed by extensive washes in lysis buffer and finally boiling in 30 µl Laemmli sample buffer. Coimmunoprecipitations were repeated using a different DNA clone for all constructs, with similar results. For endogenous interaction experiments, either 100 mg of adult flies was starved for 2 h or 150 mg of cultured cells was washed for 2 × 10 min in PBS and homogenized for 2 × 10 s on ice in 1 ml lysis buffer containing 1% Triton X-100, using an homogenizer (Ultra-Turret T10; IKA) equipped with a disperser (S10N-5G; IKA). Lysates were cleared by centrifugation at 30,130 *g* for 10 min at 4°C (adult supernatants were spun once more to completely

Downloaded from jcb.rupress.org on May 16, 2013

Published May 13, 2013

get rid of fat and unbroken cuticle pieces) followed by incubation with 3 µl rat anti-usnp (this study) or anti-GFP (Pircs et al., 2012), or guinea pig anti-Syx17 (this study) or anti-GFP (raised in collaboration with J. Mihály and I. Andó, Biological Research Center, Szeged, Hungary) antisera for 2 h at 4°C. Antibody–antigen complexes were collected by addition of 20 µl protein A (for guinea pig sera) or protein G (for rat sera) agarose 50% slurry for 1 h at 4°C and processed for Western blots as in co-overexpression experiments. Immunoprecipitations were performed from both cultured cells and adult flies, and representative examples are shown.

Transmission EM and immuno-EM

Dissected tissues were fixed in 3.2% paraformaldehyde, 0.5% glutaraldehyde, 1% sucrose, and 0.028% $CaCl_2$ in 0.1 N sodium cacodylate, pH 7.4, overnight at 4°C, postfixed in 0.5% osmium tetroxide for 1 h, and embedded into Durcupan (Fluka) according to the manufacturer's recommendations (Juhász et al., 2007, 2008). 70-nm sections were stained in Reynold's lead citrate and viewed on a transmission electron microscope (JEM-1011; JEOL) equipped with camera (Morada; Olympus) and iTEM software (Olympus). A total of 17–29 randomly taken 10,000× magnification images of sections from four animals were evaluated per genotype by manually encircling relevant structures in Photoshop and calculating their percentage of area relative to total cytoplasm. P-values were calculated as described in Image analysis and statistics. For immuno-EM, samples were fixed as for conventional EM and embedded in London Resin white resin (Sigma-Aldrich) without postfixation. 90-nm sections were cut and incubated with rat anti-Syx17 (1:30) in PBS with 3% milk overnight at 4°C followed by biotin-conjugated anti–rat (1:100; Jackson ImmunoResearch Laboratories, Inc.) for 1 h in PBS with 1.5% milk at 25°C and anti-biotin conjugated to 20-nm gold for 5 h in TBS with 1.5% milk and 0.25% Tween 20 at 4°C (1:100; British Biocell; Juhász et al., 2007, 2008).

Western blots

Equal amounts of proteins per sample were separated by denaturing SDS-PAGE and processed for Western blots as previously described (Juhász et al., 2007; Pircs et al., 2012). Mouse anti-tubulin (1:1,000; AA4.3-s; Developmental Studies Hybridoma Bank), mouse anti-FLAG (1:2,000; M2; Sigma-Aldrich), rabbit anti-HA (1:2,000; Sigma-Aldrich), rabbit anti-p62 (1:8,000; Pircs et al., 2012), rabbit anti-Atg8a (1:5,000), rat anti-Syx17 (1:5,000; this study), guinea pig anti-Syx17 (1:5,000; this study), rat anti-usnp (1:3,000; this study) primary and alkaline phosphatase–conjugated anti–guinea pig, anti–rat (1:5,000; Sigma-Aldrich), anti–rabbit, and anti–mouse (1:5,000; EMD Millipore) secondary antibodies were used in TBS, pH 7.4, with 0.1% Tween 20 and 0.25% casein followed by colorimetric detection with nitro-blue tetrazolium–5-bromo-4-chloro-3-indolyl phosphate (Sigma-Aldrich).

Online supplemental material

Fig. S1 shows that *Syx17*, *usnp*, and *VAMP7* are required for developmental and basal autophagy. Fig. S2 shows additional Syx17 localization, sequence alignment, and interaction data. Table S1 lists *Drosophila* homologues of human and yeast SNARE proteins, RNAi and mutant lines for these genes used in this study, and results of our small-scale RNAi screen. Online supplemental material is available at http://www.jcb.org/cgi/content/full/jcb.201211160/DC1. Additional data are available in the JCB DataViewer at http://dx.doi.org/10.1083/jcb.201211160.dv.

We thank Sarolta Pálfia, Zsófia Kováts, Eszter Papp, and Eszter Vágó for technical assistance, public repositories, and colleagues listed in the Materials and methods section for reagents,

We thank the Wellcome Trust (087518/Z/08/Z), the Hungarian Scientific Research Fund (K83509), and the Hungarian Academy of Sciences (BO/00552/11) for support.

Submitted: 28 November 2012
Accepted: 11 April 2013

References

Atlashkin, V., V. Kreykenbohm, E.L. Eskelinen, D. Wenzel, A. Fayyazi, and G. Fischer von Mollard. 2003. Deletion of the SNARE vti1b in mice results in the loss of a single SNARE partner, syntaxin 8. *Mol. Cell. Biol.* 23:5198–5207. http://dx.doi.org/10.1128/MCB.23.15.5198-5207.2003

Axe, E.L., S.A. Walker, M. Manifava, P. Chandra, H.L. Roderick, A. Habermann, G. Griffiths, and N.T. Ktistakis. 2008. Autophagosome formation from membrane compartments enriched in phosphatidylinositol 3-phosphate and dynamically connected to the endoplasmic reticulum. *J. Cell Biol.* 182:685–701. http://dx.doi.org/10.1083/jcb.200803137

Barth, J.M., J. Szabad, E. Hafen, and K. Köhler. 2011. Autophagy in *Drosophila* ovaries is induced by starvation and is required for oogenesis. *Cell Death Differ.* 18:915–924. http://dx.doi.org/10.1038/cdd.2010.157

Berry, D.L., and E.H. Baehrecke. 2007. Growth arrest and autophagy are required for salivary gland cell degradation in *Drosophila*. *Cell*. 131:1137–1148. http://dx.doi.org/10.1016/j.cell.2007.10.048

Bjørkøy, G., T. Lamark, S. Pankiv, A. Øvervatn, A. Brech, and T. Johansen. 2009. Monitoring autophagic degradation of p62/SQSTM1. *Methods Enzymol.* 452:181–197. http://dx.doi.org/10.1016/S0076-6879(08)03612-4

Dilcher, M., B. Köhler, and G.F. von Mollard. 2001. Genetic interactions with the yeast Q-SNARE VTI1 reveal novel functions for the R-SNARE YKT6. *J. Biol. Chem.* 276:34537–34544. http://dx.doi.org/10.1074/jbc.M101551200

Fader, C.M., D.G. Sánchez, M.B. Mestre, and M.I. Colombo. 2009. TI-VAMP/VAMP7 and VAMP3/cellubrevin: two v-SNARE proteins involved in specific steps of the autophagy/multivesicular body pathways. *Biochim. Biophys. Acta.* 1793:1901–1916. http://dx.doi.org/10.1016/j.bbamcr.2009.09.011

Filimonenko, M., S. Stuffers, C. Raiborg, A. Yamamoto, L. Malerød, E.M. Fisher, A. Isaacs, A. Brech, H. Stenmark, and A. Simonsen. 2007. Functional multivesicular bodies are required for autophagic clearance of protein aggregates associated with neurodegenerative disease. *J. Cell Biol.* 179:485–500. http://dx.doi.org/10.1083/jcb.200702115

Furuta, N., N. Fujita, T. Noda, T. Yoshimori, and A. Amano. 2010. Combinational soluble N-ethylmaleimide-sensitive factor attachment protein receptor proteins VAMP8 and Vti1b mediate fusion of antimicrobial and canonical autophagosomes with lysosomes. *Mol. Biol. Cell*. 21:1001–1010. http://dx.doi.org/10.1091/mbc.E09-08-0693

Hamasaki, M., N. Furuta, A. Matsuda, A. Nezu, A. Yamamoto, N. Fujita, H. Oomori, T. Noda, T. Haraguchi, Y. Hiraoka, et al. 2013. Autophagosomes form at ER-mitochondria contact sites. *Nature*. 495:389–393. http://dx.doi.org/10.1038/nature11910

Hara, T., K. Nakamura, M. Matsui, A. Yamamoto, Y. Nakahara, R. Suzuki-Migishima, M. Yokoyama, K. Mishima, I. Saito, H. Okano, and N. Mizushima. 2006. Suppression of basal autophagy in neural cells causes neurodegenerative disease in mice. *Nature*. 441:885–889. http://dx.doi.org/10.1038/nature04724

Hong, W. 2005. SNAREs and traffic. *Biochim. Biophys. Acta*. 1744:120–144. http://dx.doi.org/10.1016/j.bbamcr.2005.03.014

Ishihara, N., M. Hamasaki, S. Yokota, K. Suzuki, Y. Kamada, A. Kihara, T. Yoshimori, T. Noda, and Y. Ohsumi. 2001. Autophagosome requires specific early Sec proteins for its formation and NSF/SNARE for vacuolar fusion. *Mol. Biol. Cell*. 12:3690–3702.

Itakura, E., C. Kishi-Itakura, and N. Mizushima. 2012. The hairpin-type tail-anchored SNARE syntaxin 17 targets to autophagosomes for fusion with endosomes/lysosomes. *Cell*. 151:1256–1269. http://dx.doi.org/10.1016/j.cell.2012.11.001

Juhász, G., B. Erdi, M. Sass, and T.P. Neufeld. 2007. Atg7-dependent autophagy promotes neuronal health, stress tolerance, and longevity but is dispensable for metamorphosis in *Drosophila*. *Genes Dev.* 21:3061–3066. http://dx.doi.org/10.1101/gad.1600707

Juhász, G., J.H. Hill, Y. Yan, M. Sass, E.H. Baehrecke, J.M. Backer, and T.P. Neufeld. 2008. The class III PI(3)K Vps34 promotes autophagy and endocytosis but not TOR signaling in *Drosophila*. *J. Cell Biol.* 181:655–666. http://dx.doi.org/10.1083/jcb.200712051

Kimura, S., T. Noda, and T. Yoshimori. 2007. Dissection of the autophagosome maturation process by a novel reporter protein, tandem fluorescent-tagged LC3. *Autophagy*. 3:452–460.

Komatsu, M., S. Waguri, T. Chiba, S. Murata, J. Iwata, I. Tanida, T. Ueno, M. Koike, Y. Uchiyama, E. Kominami, and K. Tanaka. 2006. Loss of autophagy in the central nervous system causes neurodegeneration in mice. *Nature*. 441:880–884. http://dx.doi.org/10.1038/nature04723

Lu, Q., P. Yang, X. Huang, W. Hu, B. Guo, F. Wu, L. Lin, A.L. Kovács, L. Yu, and H. Zhang. 2011. The WD40 repeat PtdIns(3)P-binding protein EPG-6 regulates progression of omegasomes to autophagosomes. *Dev. Cell*. 21:343–357. http://dx.doi.org/10.1016/j.devcel.2011.06.024

Mizushima, N., B. Levine, A.M. Cuervo, and D.J. Klionsky. 2008. Autophagy fights disease through cellular self-digestion. *Nature*. 451:1069–1075. http://dx.doi.org/10.1038/nature06639

Moreau, K., B. Ravikumar, M. Renna, C. Puri, and D.C. Rubinsztein. 2011. Autophagosome precursor maturation requires homotypic fusion. *Cell*. 146:303–317. http://dx.doi.org/10.1016/j.cell.2011.06.023

Nair, U., A. Jotwani, J. Geng, N. Gammoh, D. Richerson, W.L. Yen, J. Griffith, S. Nag, K. Wang, T. Moss, et al. 2011. SNARE proteins are required for macroautophagy. *Cell*. 146:290–302. http://dx.doi.org/10.1016/j.cell.2011.06.022

Ohashi, Y., and S. Munro. 2010. Membrane delivery to the yeast autophagosome from the Golgi-endosomal system. *Mol. Biol. Cell*. 21:3998–4008. http://dx.doi.org/10.1091/mbc.E10-05-0457

Downloaded from jcb.rupress.org on May 16, 2013

Published May 13, 2013

dc_840_14

Pircs, K., P. Nagy, A. Varga, Z. Venkei, B. Erdi, K. Hegedus, and G. Juhasz. 2012. Advantages and limitations of different p62-based assays for estimating autophagic activity in *Drosophila*. *PLoS ONE*. 7:e44214. http://dx.doi.org/10.1371/journal.pone.0044214

Renna, M., C. Schaffner, A.R. Winslow, F.M. Menzies, A.A. Peden, R.A. Floto, and D.C. Rubinsztein. 2011. Autophagic substrate clearance requires activity of the syntaxin-5 SNARE complex. *J. Cell Sci.* 124:469–482. http://dx.doi.org/10.1242/jcs.076489

Rusten, T.E., T. Vaccari, K. Lindmo, L.M. Rodahl, I.P. Nezis, C. Sem-Jacobsen, F. Wendler, J.P. Vincent, A. Brech, D. Bilder, and H. Stenmark. 2007. ESCRTs and Fab1 regulate distinct steps of autophagy. *Curr. Biol.* 17:1817–1825. http://dx.doi.org/10.1016/j.cub.2007.09.032

Simonsen, A., R.C. Cumming, A. Brech, P. Isakson, D.R. Schubert, and K.D. Finley. 2008. Promoting basal levels of autophagy in the nervous system enhances longevity and oxidant resistance in adult *Drosophila*. *Autophagy*. 4:176–184.

Steegmaier, M., B. Yang, J.S. Yoo, B. Huang, M. Shen, S. Yu, Y. Luo, and R.H. Scheller. 1998. Three novel proteins of the syntaxin/SNAP-25 family. *J. Biol. Chem.* 273:34171–34179. http://dx.doi.org/10.1074/jbc.273.51.34171

Tooze, S.A., and T. Yoshimori. 2010. The origin of the autophagosomal membrane. *Nat. Cell Biol.* 12:831–835. http://dx.doi.org/10.1038/ncb0910-831

Velikkakath, A.K., T. Nishimura, E. Oita, N. Ishihara, and N. Mizushima. 2012. Mammalian Atg2 proteins are essential for autophagosome formation and important for regulation of size and distribution of lipid droplets. *Mol. Biol. Cell*. 23:896–909. http://dx.doi.org/10.1091/mbc.E11-09-0785

Downloaded from jcb.rupress.org on May 16, 2013

Autophagy 9:10, 1642–1646; October 2013; © 2013 Landes Bioscience
dc_840_14

Evolutionarily conserved role and physiological relevance of a STX17/Syx17 (syntaxin 17)-containing SNARE complex in autophagosome fusion with endosomes and lysosomes

Krisztina Hegedűs, Szabolcs Takáts, Attila L Kovács, and Gábor Juhász*
Department of Anatomy, Cell and Developmental Biology; Eötvös Loránd University; Budapest, Hungary

Keywords: autophagosome, autophagy, flux, fusion, lysosome, neurodegeneration, ubisnap/SNAP29, syntaxin 17, CG1599/Vamp7, VAMP8

Submitted: 05/17/2013

Revised: 06/24/2013

Accepted: 07/09/2013

http://dx.doi.org/10.4161/auto.25684

*Correspondence to: Gábor Juhász;
Email: szmrt@elte.hu

Commentary to: Takáts S, Nagy P, Varga A, Pircs K, Kárpáti M, Varga K, et al. Autophagosomal Syntaxin17-dependent lysosomal degradation maintains neuronal function in Drosophila. J Cell Biol 2013; 201:531–9; PMID:23671310; http://dx.doi.org/10.1083/jcb.201211160

Itakura E, Kishi-Itakura C, Mizushima N. The hairpin-type tail-anchored SNARE syntaxin 17 targets to autophagosomes for fusion with endosomes/lysosomes. Cell 2012; 151:1256–69; PMID:23217709; http://dx.doi.org/10.1016/j.cell.2012.11.001

Hamasaki M, Furuta N, Matsuda A, Nezu A, Yamamoto A, Fujita N, et al. Autophagosomes form at ER-mitochondria contact sites. Nature 2013; 495:389–93; PMID:23455425; http://dx.doi.org/10.1038/nature11910

Phagophores engulf cytoplasmic material and give rise to autophagosomes, double-membrane vesicles mediating cargo transport to lysosomes for degradation. The regulation of autophagosome fusion with endosomes and lysosomes during autophagy has remained poorly characterized. Two recent papers conclude that STX17/syntaxin 17 (Syx17 in *Drosophila*) has an evolutionarily conserved role in autophagosome fusion with endosomes and lysosomes, acting in one SNARE complex with SNAP29 (ubisnap in *Drosophila*) and the endosomal/lysosomal VAMP8 (CG1599/Vamp7 in *Drosophila*). Surprisingly, a third report suggests that STX17 might also contribute to proper phagophore assembly. Although several experiments presented in the two human cell culture studies yielded controversial results, the essential role of STX17 in autophagic flux is now firmly established, both in cultured cells and in an animal model. Based on these data, we propose that genetic inhibition of STX17/Syx17 may be a more specific tool in autophagic flux experiments than currently used drug treatments, which impair all lysosomal degradation routes and also inactivate MTOR (mechanistic target of rapamycin), a major negative regulator of autophagy. Finally, the neuronal dysfunction and locomotion defects observed in Syx17 mutant animals point to the possible contribution of defective autophagosome clearance to various human diseases.

During autophagy, phagophores capture cytoplasmic cargo and form double-membrane autophagosomes, which are transport vesicles required for degradation of sequestered material in lysosomes; fusion with the degradative organelle is followed by recycling of the breakdown products. Autophagy is clearly becoming one of the hottest topics in biomedical research. Our understanding of the molecular machinery underlying autophagy made tremendous advances during the past 20 years, thanks to the discovery of autophagy-related (Atg) gene products in yeast. These evolutionarily conserved proteins are required for efficient autophagosome formation in all metazoan cells.[1,2] Functional analyses of *ATG* genes revealed that autophagy has important roles in various developmental, physiological, and pathological processes.[1] Nevertheless, significant gaps have remained in our knowledge regarding autophagy. Among these are the process of autophagosome maturation, and the mechanisms that ensure timely and specific fusion with late endosomes and lysosomes.

SNAREs [soluble N-ethylmaleimide-sensitive factor (NSF) attachment protein receptor] are likely to be involved in autophagosome-lysosome fusion because the majority of vesicle fusion events are usually mediated by the action of these proteins. R SNAREs contribute an arginine (R) residue to the zero ionic layer of the assembled core complex, while Q SNAREs have a glutamine (Q) in the same position.[3] A trans-SNARE complex is formed by the binding of an R SNARE (associated with the first vesicle) to two or three proteins (located on the second

dc_840_14

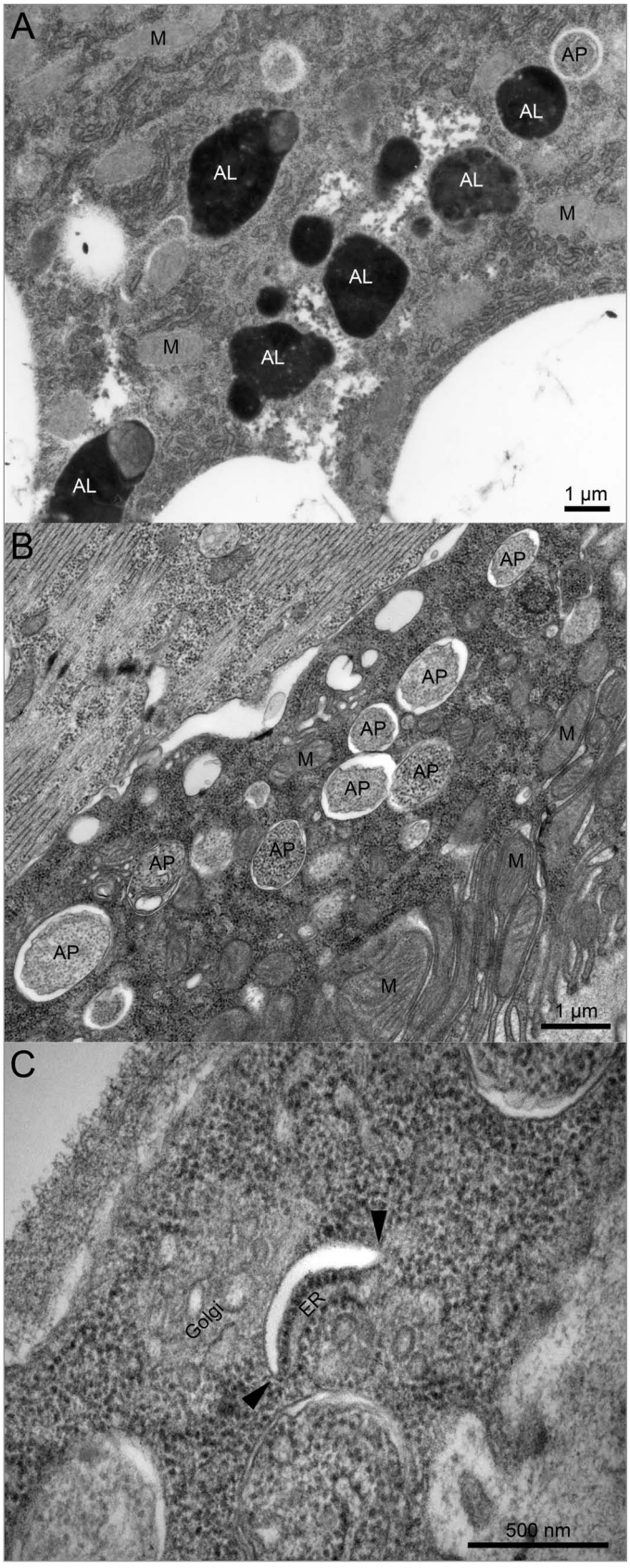


Figure 1. Ultrastructural images of wild-type and *Syx17* mutant *Drosophila* cells from early L3 stage larvae starved for 3 h. (**A**) Both autophagosomes (AP) and electron-dense autolysosomes (AL) can be observed in various tissues of starved control larvae, such as the fat body shown here. M, mitochondrion. (**B**) Typical double-membrane autophagosomes accumulate in large numbers in starved *Syx17* mutant larvae, illustrated by a Malpighian tubule cell in this image. (**C**) This panel shows a rarely observed phagophore in a *Syx17* mutant cell, which appears as a curved, nonbranching membrane cistern with a characteristic cleft between the two membranes after standard glutaraldehyde fixation. While the empty-looking space is an artifact, it greatly facilitates the identification of early autophagic structures. Arrowheads point to the edges of the phagophore, where the transitions of prospective outer and inner membrane layers are clearly visible.

compartment) that altogether supply three Q SNARE domains. After membrane fusion is accomplished, all four SNARE domains are bound to the same membrane and are referred to as a cis-SNARE complex. The approximately 30 SNARE proteins found in different organisms assemble in a combinatorial fashion, and the same protein is often incorporated in functionally distinct complexes, complicating mechanistic studies.[3] Clear loss-of-function phenotypes (ideally obtained with the use of null mutants and genetic rescue experiments), together with interaction and localization data for endogenous proteins, are key for proving the direct role of a given SNARE in autophagy.

In yeast cells, autophagosomes can directly fuse with the vacuole, the functional counterpart of lysosomes. In contrast, delivery of autophagosomal contents to lysosomes in metazoan cells appears to depend on late endosomes.[4-6] Furthermore, the SNAREs Vam3 and Vam7 that are required for autophagosome-vacuole fusion in yeast do not have clear homologs in animals, and no autophagosome-associated SNARE protein has been identified in metazoan cells until recently.[3,7,8] Two papers now reveal how the specificity of autophagosome fusion with endosomes and lysosomes is achieved.[9,10] In one of these papers, we presented the results of a systematic screen for SNARE proteins involved in starvation-induced autophagy, using genetic mosaics of *Drosophila*

larvae.[9] RNAi depletion of *Syx17*, *ubisnap* [the fly homolog of *SNAP29* (synaptosomal-associated protein, 29 kDa)], and *CG1599* [*Vamp7* (vesicle-associated membrane protein 7)] leads to a similar, very characteristic phenotype: autophagosomes positive for Atg8a accumulate in the perinuclear region of fat body cells (the fly equivalent of hepatocytes and adipocytes). Autophagic degradation is completely blocked in these cells, as no LysoTracker-positive acidic autolysosomes form, no autophagy-dependent lysosomal quenching of GFP-Atg8a fluorescence is observed, and selective autophagic degradation of ref(2)P (mammalian SQSTM1/p62) aggregates is impaired. More rigorous genetic tests of *Syx17* and *CG1599/Vamp7* mutants show large-scale accumulation of autophagosomes in larval and adult tissues, based on commonly used transgenic reporters, immunofluorescent staining, western blot and ultrastructural analyses. **Figure 1**. shows the morphology of typical double-membrane autophagosomes that abound in *Syx17* mutant larval tissues, and also illustrates a phagophore, which is a rarely observed structure likely to be short-lived both in control and mutant cells. Importantly, these autophagy defects could be rescued by transgenic expression of the wild-type protein in *Syx17* mutant backgrounds. In line with the results of our screen, Syx17 forms a complex with ubisnap and CG1599, the closest fly homolog of the mammalian VAMP7 and VAMP8 proteins. Finally, we showed that endogenous Syx17 is present in Atg8a-positive autophagosomes, based on immunofluorescence microscopy and immuno-electron microscopy (EM), but not in phagophores [marked by endogenous Atg5, or by Atg8a in *Atg2* mutants that accumulate stalled phagophore assembly sites (PASs)].

In the other study, siRNA silencing of *STX17* in cultured human cells was also found to result in the accumulation of autophagosomes positive for LC3 (a human homolog of Atg8), and this phenotype could be rescued by co-transfection with an RNAi-resistant transgene.[10] This paper also identified a SNARE complex of STX17 (Qa), SNAP29 that contains two SNARE domains (Qbc), but no membrane anchor, and lysosomal/endosomal VAMP8 (R). As expected from the interaction data, silencing of either *SNAP29* or *VAMP8* phenocopied the loss of STX17. Moreover, GFP-Syntaxin 17 could be detected in LC3-positive autophagosomes, but not in phagophores, and immuno-electron microscopy suggested that it is located in the outer membrane of double-membrane autophagosomes. These data support the following model for fusion: STX17 is first loaded onto the outer bordering membrane of autophagosomes and recruits SNAP29, which is followed by binding to VAMP8 (CG1599/Vamp7 in flies) located in endosomes and lysosomes. After fusion is completed, the cis-SNARE complex is presumably disassembled and recycled from the lysosomal membrane through the actions of NSF (N-ethylmaleimide-sensitive factor) and NAPA (NSF attachment protein, α, also known as α-SNAP), as usual.[3]

These two recent papers shed some light onto how autophagosomes gain competence for fusion with endosomes and lysosomes, as phagophores never participate in such events. A new question immediately arises: how is STX17/Syx17 transported to the outer membrane of autophagosomes? Itakura et al. found that a free cytoplasmic pool of STX17 exists, which is likely to be the result of its atypical structure.[10] Unique among SNARE proteins, it contains two transmembrane domains. These glycine-rich motifs were suggested to form a glycine zipper, mediating close packing of the two domains. Interestingly, replacement of selected glycines with leucines greatly reduces the autophagosomal localization of this protein without affecting its presence in the ER and mitochondria. The specific mechanism responsible for loading STX17 into the outer autophagosomal membrane only after sealing of the phagophore is not yet known. Future studies should provide further insights into this process, such as by proteomic identification of STX17 binding partners, or through the analysis of new hits from genetic screens that result in autophagosome accumulation by preventing STX17 recruitment to autophagosomes.

The number and size of autophagic structures at a given time point depends on two processes: the rate of autophagosome formation (incoming material), and degradation of sequestered cargo in lysosomes (outgoing material). Thus, experiments aimed at measuring autophagic flux have become an essential part of autophagy analyses. The most common test for this purpose is the application of bafilomycin, chloroquine, or similar drugs that block lysosomal breakdown.[11] Unfortunately, these treatments also impair degradation of endosomal cargo and interfere with lysosome-dependent activation of MTOR, a major regulator of cell growth and autophagy.[12,13] In addition, the use of bafilomycin is limited to cultured cells due to toxicity in complex multicellular organisms. Although a role of STX17 in endocytosis has not been excluded yet, we propose that mutation or RNAi knockdown of this gene may eventually turn out to be more specific than bafilomycin treatment in autophagic flux experiments. Importantly, it can also be used to determine autophagic flux in whole animals in addition to cultured cells.

A third recent study suggested that autophagosomes may often form in the vicinity of both the ER and mitochondria, and implicated a role for STX17 in phagophore closure based on limited analysis.[14] Many aspects of the two human cell culture reports match: STX17 was found on both mitochondria and the ER, LC3-positive dots accumulate in microscopy images of STX17-depleted cells, and the levels of lipidated LC3 and the selective autophagy cargo SQSTM1 increased in western blots of siRNA cell lysates.[10,14] It is important to highlight that these tests do not distinguish between accumulation of phagophores or autophagosomes. Unfortunately, multiple experiments performed in these different labs produced contradicting results.[10,14] First, Itakura et al. found no colocalization of STX17 with numerous markers of the PAS including ATG14, ATG16L1, ZFYVE1/DFCP1, ULK1 or WIPI1, whereas Hamasaki et al. reported its partial colocalization with ATG14, but they did not test other PAS markers. Second, Itakura et al. detected about half of the endogenous (or GFP-tagged) STX17 pool in the cytosolic fraction after ultracentrifugation, whereas Hamasaki et al. showed that endogenous STX17 is almost entirely

membrane-associated, and it is hardly detectable in the cytosol in fractionation experiments. Transmission EM is still one of the most informative autophagy tests, and helps to interpret results obtained by other methods. The prerequisite of reliable support by transmission EM is the exact and rigorous identification of the various autophagic structures. Itakura et al. detected and quantified the accumulation of typical double-membrane autophagosomes in *STX17* siRNA cells. In the ultrastructural images selected by Hamasaki et al., the identity of phagophores and autophagosomes is uncertain in many cases even in enlarged images due to low resolution, tangentional sectioning and discontinuity of the membranes at certain places.

Nevertheless, these studies are not entirely incompatible with each other. It could be possible that STX17 is also involved in autophagosome formation, although it is not clear why unsealed phagophores with a size of regular autophagosomes would accumulate if the allegedly critical membrane trafficking from ER and mitochondria was blocked with *STX17* siRNA. One may argue that the siRNA treatments by Hamasaki et al. were more potent than those of Itakura et al., and perhaps revealed an earlier function. Careful biochemical and cell biology analysis of chromosomally deleted alleles (knockouts) of *STX17* in mouse embryonic fibroblasts and in mice will be very important for resolving these discrepancies. Our *Drosophila* studies could also be complicated by the presence of maternally provided *Syx17* gene products: a 40-kDa isoform of unknown identity is still visible and only the main, 34-kDa isoform is missing in mutant larvae, although neither isoform can be detected in western blots of adult lysates. The large-scale accumulation of autophagosomes in neurons of *Syx17* mutant adults, occupying 20% of the cytoplasm in the perikaryon on average vs. 0% in control or genetically rescued animals, strongly suggests that Syx17 is dispensable for autophagosome formation in *Drosophila*. Still, mutants lacking both maternal and zygotic gene products can be analyzed to exclude maternal contribution in all developmental stages in flies.

In addition to serving cytoprotective roles during stress and starvation, autophagy is thought to be required for proper homeostasis under normal conditions.[1] This function seems to be especially critical in long-lived cells such as neurons. Supporting this view, we and others have reported that loss of basal autophagy leads to progressive accumulation of ubiquitinated protein aggregates and neurodegeneration, both in fly mutants of *Atg7* and in mice with neuron-specific deletion of *Atg5* or *Atg7*.[15-17] Different from these previous studies of *Atg* mutations that prevent autophagosome formation, *Syx17* mutation leads to large-scale accumulation of autophagosomes in neurons of adult flies.[9] These mutants perform very poorly in a climbing assay, a standard test for neuronal dysfunction, and all die within 4 d of eclosing from the pupal case, in contrast with normal flies that live for months. Since genetic suppression of cell death in neurons does not improve these mutant phenotypes, unlike transgenic expression of wild-type *Syx17*, it is likely the accumulation of autophagosomes that renders these neurons unable to perform their normal tasks.[9] The first animal model of genetically impaired autophagosome fusion clearly shows that in addition to the initial sequestration of cytoplasmic cargo, the final lysosomal breakdown is also essential. Numerous diseases are characterized by the accumulation of autophagosomes and autophagic vesicles, such as neurons in Alzheimer disease and muscles in vacuolar myopathy patients, respectively.[1] Therefore, it will be exciting to see whether future studies can link genetic defects of the STX17-dependent fusion machinery to certain human diseases.

Disclosure of Potential Conflicts of Interest

The authors declare that no financial or other conflicts exist.

Acknowledgments

Work in the Juhasz lab is funded by the Wellcome Trust (087518/Z/08/Z) and the Hungarian Scientific Research Fund (OTKA K83509).

References

1. Mizushima N, Levine B, Cuervo AM, Klionsky DJ. Autophagy fights disease through cellular self-digestion. Nature 2008; 451:1069-75; PMID:18305538; http://dx.doi.org/10.1038/nature06639
2. Mizushima N, Yoshimori T, Ohsumi Y. The role of Atg proteins in autophagosome formation. Annu Rev Cell Dev Biol 2011; 27:107-32; PMID:21801009; http://dx.doi.org/10.1146/annurev-cellbio-092910-154005
3. Hong W. SNAREs and traffic. Biochim Biophys Acta 2005; 1744:493-517; PMID:16038056; http://dx.doi.org/10.1016/j.bbamcr.2005.03.014
4. Filimonenko M, Stuffers S, Raiborg C, Yamamoto A, Malerød L, Fisher EM, et al. Functional multivesicular bodies are required for autophagic clearance of protein aggregates associated with neurodegenerative disease. J Cell Biol 2007; 179:485-500; PMID:17984323; http://dx.doi.org/10.1083/jcb.200702115
5. Rusten TE, Vaccari T, Lindmo K, Rodahl LM, Nezis IP, Sem-Jacobsen C, et al. ESCRTs and Fab1 regulate distinct steps of autophagy. Curr Biol 2007; 17:1817-25; PMID:17935992; http://dx.doi.org/10.1016/j.cub.2007.09.032
6. Juhász G, Hill JH, Yan Y, Sass M, Baehrecke EH, Backer JM, et al. The class III PI(3)K Vps34 promotes autophagy and endocytosis but not TOR signaling in Drosophila. J Cell Biol 2008; 181:655-66; PMID:18474623; http://dx.doi.org/10.1083/jcb.200712051
7. Moreau K, Renna M, Rubinsztein DC. Connections between SNAREs and autophagy. Trends Biochem Sci 2013; 38:57-63; PMID:23306003; http://dx.doi.org/10.1016/j.tibs.2012.11.004
8. Wang CW, Stromhaug PE, Shima J, Klionsky DJ. The Ccz1-Mon1 protein complex is required for the late step of multiple vacuole delivery pathways. J Biol Chem 2002; 277:47917-27; PMID:12364329; http://dx.doi.org/10.1074/jbc.M208191200
9. Takáts S, Nagy P, Varga A, Pircs K, Kárpáti M, Varga K, et al. Autophagosomal Syntaxin17-dependent lysosomal degradation maintains neuronal function in Drosophila. J Cell Biol 2013; 201:531-9; PMID:23671310; http://dx.doi.org/10.1083/jcb.201211160
10. Itakura E, Kishi-Itakura C, Mizushima N. The hairpin-type tail-anchored SNARE syntaxin 17 targets to autophagosomes for fusion with endosomes/lysosomes. Cell 2012; 151:1256-69; PMID:23217709; http://dx.doi.org/10.1016/j.cell.2012.11.001
11. Klionsky DJ, Abdalla FC, Abeliovich H, Abraham RT, Acevedo-Arozena A, Adeli K, et al. Guidelines for the use and interpretation of assays for monitoring autophagy. Autophagy 2012; 8:445-544; PMID:22966490; http://dx.doi.org/10.4161/auto.19496
12. Zoncu R, Bar-Peled L, Efeyan A, Wang S, Sancak Y, Sabatini DM. mTORC1 senses lysosomal amino acids through an inside-out mechanism that requires the vacuolar H(+)-ATPase. Science 2011; 334:678-83; PMID:22053050; http://dx.doi.org/10.1126/science.1207056
13. Juhász G. Interpretation of bafilomycin, pH neutralizing or protease inhibitor treatments in autophagic flux experiments: novel considerations. Autophagy 2012; 8:1875-6; PMID:22874642; http://dx.doi.org/10.4161/auto.21544
14. Hamasaki M, Furuta N, Matsuda A, Nezu A, Yamamoto A, Fujita N, et al. Autophagosomes form at ER-mitochondria contact sites. Nature 2013; 495:389-93; PMID:23455425; http://dx.doi.org/10.1038/nature11910
15. Juhász G, Erdi B, Sass M, Neufeld TP. Atg7-dependent autophagy promotes neuronal health, stress tolerance, and longevity but is dispensable for metamorphosis in Drosophila. Genes Dev 2007; 21:3061-6; PMID:18056421; http://dx.doi.org/10.1101/gad.1600707

16. Hara T, Nakamura K, Matsui M, Yamamoto A, Nakahara Y, Suzuki-Migishima R, et al. Suppression of basal autophagy in neural cells causes neurodegenerative disease in mice. Nature 2006; 441:885-9; PMID:16625204; http://dx.doi.org/10.1038/nature04724

17. Komatsu M, Waguri S, Chiba T, Murata S, Iwata J, Tanida I, et al. Loss of autophagy in the central nervous system causes neurodegeneration in mice. Nature 2006; 441:880-4; PMID:16625205; http://dx.doi.org/10.1038/nature04723

Cell Metabolism
Article

Nucleocytosolic Depletion of the Energy Metabolite Acetyl-Coenzyme A Stimulates Autophagy and Prolongs Lifespan

Tobias Eisenberg,[1,17] Sabrina Schroeder,[1,17] Aleksandra Andryushkova,[1,17] Tobias Pendl,[1] Victoria Küttner,[2,3] Anuradha Bhukel,[4,5] Guillermo Mariño,[6,7,8] Federico Pietrocola,[6,7,8] Alexandra Harger,[1,9] Andreas Zimmermann,[1] Tarek Moustafa,[1] Adrian Sprenger,[2,3] Evelyne Jany,[1] Sabrina Büttner,[1] Didac Carmona-Gutierrez,[1] Christoph Ruckenstuhl,[1] Julia Ring,[1] Wieland Reichelt,[1] Katharina Schimmel,[1] Tina Leeb,[1] Claudia Moser,[1] Stefanie Schatz,[1] Lars-Peter Kamolz,[10] Christoph Magnes,[11] Frank Sinner,[9,11] Simon Sedej,[12] Kai-Uwe Fröhlich,[1] Gabor Juhasz,[13] Thomas R. Pieber,[9,11] Jörn Dengjel,[2,3] Stephan J. Sigrist,[4,5] Guido Kroemer,[6,7,8,14,15,16,18,*] and Frank Madeo[1,18,*]

[1]Institute of Molecular Biosciences, University of Graz, Humboldtstrasse 50, 8010 Graz, Austria
[2]Freiburg Institute for Advanced Studies (FRIAS), University of Freiburg, Albertstrasse 19, 79104 Freiburg, Germany
[3]Department of Dermatology, University Freiburg Medical Center, Hauptstrasse 7, 79104 Freiburg, Germany
[4]Institute for Biology/Genetics, Freie Universität, Takustraße 6, 14195 Berlin, Germany
[5]NeuroCure, Charité, Charitéplatz 1, 10117 Berlin, Germany
[6]INSERM U848, Pavillon de Recherche 1, 94805 Villejuif, France
[7]Metabolomics and Cell Biology Platforms, Institut Gustave Roussy, Pavillon de Recherche 1, 94805 Villejuif, France
[8]Université Paris Sud, Faculté de Médecine, 63 Rue Gabriel Péri, 94270 Le Kremlin Bicêtre, France
[9]Division of Endocrinology and Metabolism, Department of Internal Medicine, Medical University of Graz, Auenbruggerplatz 15, 8036 Graz, Austria
[10]Division of Plastic, Aesthetic and Reconstructive Surgery, Department of Surgery, Medical University Graz, Auenbruggerplatz 29, 8036 Graz, Austria
[11]HEALTH–Institute for Biomedicine and Health Sciences, Joanneum Research Forschungsgesellschaft m.b.H., Leonhardstraße 59, 8010 Graz, Austria
[12]Department of Cardiology, Medical University of Graz, Auenbruggerplatz 15, 8036 Austria
[13]Department of Anatomy, Cell, and Developmental Biology, Eotvos Lorand University, Egyetem tér 1–3, 1053 Budapest, Hungary
[14]Equipe 11 Labellisée Ligue Contre le Cancer, INSERM U1138, Centre de Recherche des Cordeliers, 15 Rue de l'École de Médecine, 75006 Paris, France
[15]Pôle de Biologie, Hôpital Européen Georges Pompidou, AP-HP, 20 Rue Leblanc, 75908 Paris, France
[16]Université Paris Descartes, Sorbonne Paris Cité, 12 Rue de l'École de Médecine, 75006 Paris, France
[17]These authors contributed equally to this work
[18]Co-senior authors
*Correspondence: kroemer@orange.fr (G.K.), frank.madeo@uni-graz.at (F.M.)
http://dx.doi.org/10.1016/j.cmet.2014.02.010
This is an open access article under the CC BY license (http://creativecommons.org/licenses/by/3.0/).

SUMMARY

Healthy aging depends on removal of damaged cellular material that is in part mediated by autophagy. The nutritional status of cells affects both aging and autophagy through as-yet-elusive metabolic circuitries. Here, we show that nucleocytosolic acetyl-coenzyme A (AcCoA) production is a metabolic repressor of autophagy during aging in yeast. Blocking the mitochondrial route to AcCoA by deletion of the CoA-transferase *ACH1* caused cytosolic accumulation of the AcCoA precursor acetate. This led to hyperactivation of nucleocytosolic AcCoA-synthetase Acs2p, triggering histone acetylation, repression of autophagy genes, and an age-dependent defect in autophagic flux, culminating in a reduced lifespan. Inhibition of nutrient signaling failed to restore, while simultaneous knockdown of *ACS2* reinstated, autophagy and survival of *ach1* mutant. Brain-specific knockdown of *Drosophila* AcCoA synthetase was sufficient to enhance autophagic protein clearance and prolong lifespan. Since AcCoA integrates various nutrition pathways, our findings may explain diet-dependent lifespan and autophagy regulation.

INTRODUCTION

Aging is accompanied by accumulation of cellular damage, changes in the repair and detoxification processes, and a shifting homeostatic balance in conflicting lethal and vital signaling programs (Madeo et al., 2010a; Rubinstein and Kimchi, 2012). Macroautophagy (hereafter referred to as "autophagy") is a bulk degradation pathway in which parts of the cytosol or cytoplasmic organelles are encapsulated into double-membraned vesicles, so-called autophagosomes, which ultimately fuse with vacuoles/lysosomes where the cytoplasmic material becomes degraded (He and Klionsky, 2009). Autophagy plays a major role in the maintenance of cellular homeostasis, recycling

energy reserves in the context of dwindling external resources and contributing to the removal of damaged organelles and potentially harmful protein aggregates (Chen and White, 2011; Kroemer et al., 2010; Mizushima and Komatsu, 2011). Autophagy therefore has emerged as a pivotal cellular process that can delay the pathogenic manifestations of aging and age-associated disease (Gelino and Hansen, 2012; Madeo et al., 2010a; Rubinsztein et al., 2011). While regulation of autophagy during short-term induction conditions (up to several hours) is well-investigated, understanding the long-term regulation of autophagy during the process of aging remains a challenge.

Autophagy is profoundly influenced by nutrient-responsive kinases, including the target of rapamycin (TOR), protein kinase A (PKA), and AMP-activated protein kinase (AMPK), all of which are also well-known regulators of aging and lifespan (Fontana et al., 2010; He and Klionsky, 2009; Kenyon, 2010). However, recent studies suggest that protein acetylation, a process that is lately recognized as a posttranslational modification that rivals phosphorylation in importance (Choudhary et al., 2009; Guan and Xiong, 2011; Sadoul et al., 2011), may also regulate autophagy at targets distinct from that of known kinase regulators (Geeraert et al., 2010; Lee et al., 2008; Morselli et al., 2011; Xie et al., 2010; Yi et al., 2012). While acetylation of ATG3 and of tubulin is required for autophagy (Geeraert et al., 2010; Xie et al., 2010; Yi et al., 2012), ATG7 must be deacetylated by sirtuin 1 for the initiation of starvation-induced autophagy (Lee et al., 2008). Autophagy is in principle a cytoplasmic process that does not require a nuclear-localized transcriptional response for short-term activity, as demonstrated by the ability of cytoplasts (i.e., enucleated cells) to undergo starvation-induced autophagy (Morselli et al., 2011). Nevertheless, regulation of age-associated autophagy may depend on epigenetic processes (including that of histone acetylation) as well as on specific transcription factors such as FoxO3 that transactivate the autophagy-relevant transcriptome necessary for enduring autophagic activity that exceeds beyond a few hours (Eisenberg et al., 2009; Settembre et al., 2011; Zhao et al., 2007). Acetylation at lysine 16 of histone H4 has only recently been demonstrated to determine the outcome of autophagy (i.e., cytotoxic versus protective), possibly by influencing the transcriptional status of *ATG* genes (Füllgrabe et al., 2013), and the Ume6p transcription factor regulates the size of autophagosomes through control of *ATG8* expression levels (Bartholomew et al., 2012).

Acetyl-coenzyme A (AcCoA) serves as an acetyl-group donor for protein and histone acetylation in eukaryotic cells and at the same time represents a central metabolite of cellular energy metabolism. It has been proposed that metabolism may connect to various cellular functions by modulating intracellular metabolites (including that of AcCoA), which in turn act as cofactors for posttranslational modifications affecting enzyme function or epigenetic status of the chromatin (Kaelin and McKnight, 2013; Lu and Thompson, 2012). Given the increasingly recognized role of protein acetylation as well as histone acetylation in the regulation of autophagy, we therefore aimed at evaluating the hypothesis that AcCoA biosynthetic availability would affect autophagy in a long-term context, in chronological aging.

For more than a decade now, budding yeast has significantly contributed to our understanding of aging, unraveling mechanisms of cellular senescence and age-induced death of postmitotic cells in a model of chronological aging (Kaeberlein, 2010; Longo et al., 2012). In budding yeast, de novo synthesis of AcCoA is facilitated by two distinguishable metabolic routes, namely the mitochondrial (*ACS1*-, *ACH1*-, or *MPC1*-dependent) versus the nucleocytosolic (*ACS2*-dependent) pathways (Bricker et al., 2012; Fleck and Brock, 2009; Takahashi et al., 2006). Based on these premises, we determined the autophagy-modulatory effects of manipulating the de novo biosynthetic pathways of AcCoA generation in a model of chronological aging.

RESULTS

Knockdown of *ACS2* Is Sufficient to Promote Autophagy during Aging

To test if de novo AcCoA biosynthesis from acetate or pyruvate modulated the autophagic response during cellular aging, we screened deletion or knockdown mutants of genes encoding enzymes involved in AcCoA formation (see scheme in Figure 1A). To this end, we first assessed the potential influence of the AcCoA synthetases Acs1p and Acs2p that generate AcCoA through the ATP-dependent condensation of acetate and coenzyme A (CoA). We optimized the experimental conditions for knockdown of the growth essential *ACS2* gene using a doxycycline-repressible tetO7-promoter (*tet-ACS2*) so that cells would manifest a significant depletion of the Acs2 protein (Figure 1B) yet only partially reduce their growth during the logarithmic phase, yielding a rather modest reduction of cell densities upon entry into the stationary phase as compared to wild-type controls (tet-WT) (1 ng/ml doxycycline, Figure S1, available online). Knockdown of *ACS2* led to a strong induction of autophagy upon chronological aging, as monitored by assessing the autophagy-dependent translocation of a cytosolic green fluorescent protein (GFP)-Atg8p fusion to the vacuole (Figures 1C and 1D). Both the number of autophagic cells, defined as cells that displayed clearly vacuolar localization of GFP (Figure 1C; quantified in Figure 1D), and vacuolar GFP intensities increased upon knockdown of *ACS2*. To strengthen these findings, we used a complementary assay based on the immunoblot detection of *liberated* GFP that is generated upon the autophagy-associated delivery of GFP-Atg8p to the vacuole and subsequent proteolytic removal of Atg8p (Klionsky et al., 2007). This *GFP liberation assay* demonstrated enhanced autophagic flux with active vacuolar proteolysis in aged *tet-ACS2* cells compared to its wild-type (tet-WT) counterpart (Figure 1E). In contrast to knockdown of *ACS2*, age-associated autophagy was not affected by deletion of *ACS1* (Figures 1F–1H).

Thus, while deletion of *ACS1*, the gene which is known to be suppressed by glucose (van den Berg et al., 1996), was dispensable for age-dependent autophagic activity, knockdown of *ACS2*—the crucial gene for AcCoA production on glucose conditions (Takahashi et al., 2006)—was sufficient to enhance the autophagic response to aging.

Mitochondrial AcCoA Production Pathways Are Required for Age-Associated Autophagy

We next asked if blocking AcCoA synthesis through Ach1p, which transfers CoA from short-chain Acyl-CoAs to acetate generating AcCoA (Fleck and Brock, 2009), would also affect the autophagic response of aging cells. Remarkably, deletion of *ACH1* completely blocked the autophagic activity after

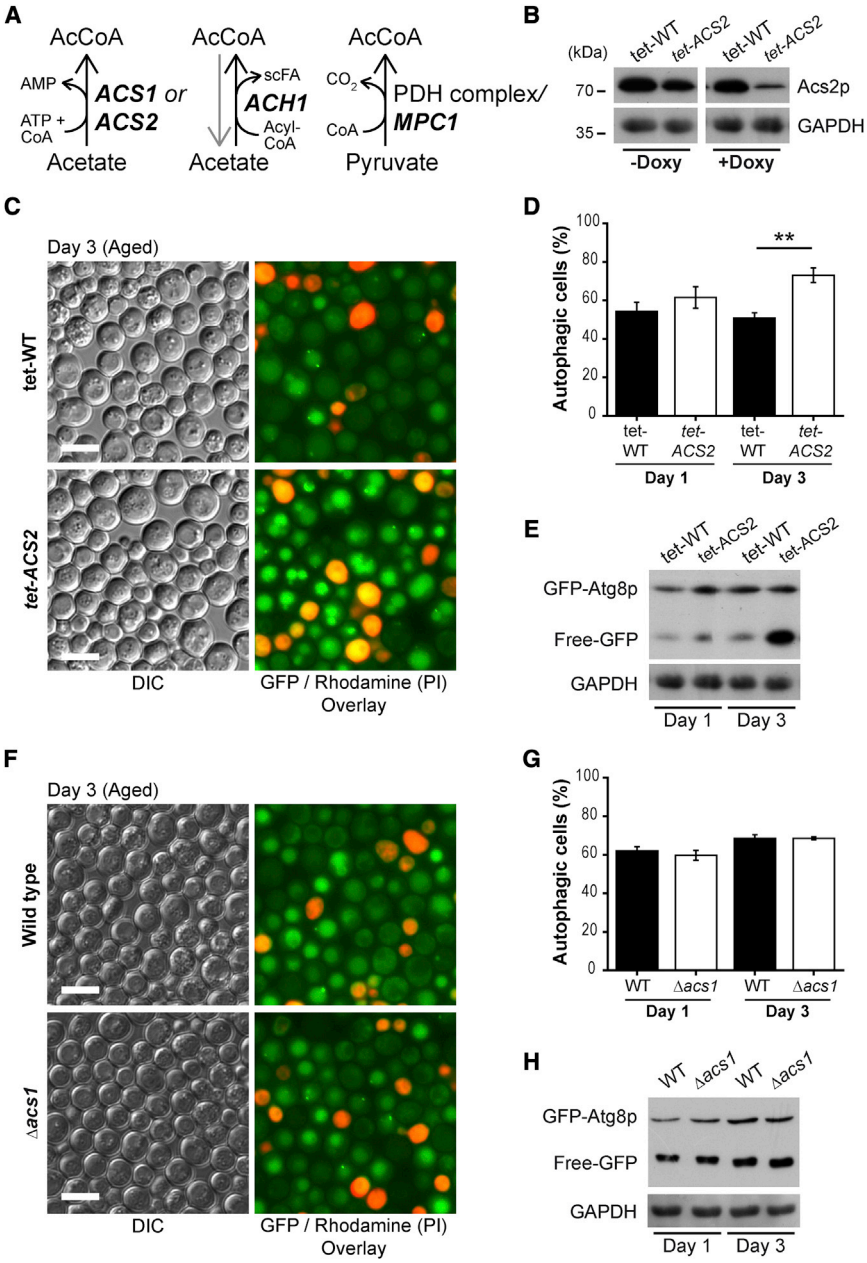


Figure 1. *ACS2* Depletion Ameliorates Age-Associated Autophagy in Yeast

(A) Scheme of known major acetyl-CoA (AcCoA)-producing enzymes (bold characters) modulated in this study.

(B) Representative immunoblot of GFP-Atg8p expressing yeast. Wild-type cells (tet-WT) were compared to strains carrying a doxycycline-repressible tet-O7 promoter controlling *ACS2* transcription (*tet-ACS2*). Cells were grown in SC 2% glucose medium for 24 hr (day 1 of aging) in the presence (+Doxy) or absence (−Doxy) of 1 ng/ml doxycycline to induce knockdown of *ACS2* (see also Figure S1).

(C) Fluorescence microscopy of GFP-Atg8p expressing (under control of its natural pATG8 promoter) wild-type (tet-WT) and *ACS2* knockdown (*tet-ACS*) cells grown in the presence of 1 ng/ml doxycycline (as shown in A) and chronologically aged for 3 days. Propidium iodide (PI) counterstaining served to visualize dead cells. Scale bars represent 5 μm.

(D) Quantification of cells depicted in (C) (day 3) and of young (day 1) cells with 150–300 counts (blinded) for each replicate. Autophagic cells were defined as cells with clear vacuolar GFP fluorescence. Data represent means ± SEM (n = 4). $^{**}p < 0.01$.

(E) Representative immunoblot analysis of day 1 (young controls) and day 3 (aged) cells shown in (C) and (D) using anti-GFP and anti-GAPDH (loading control) antibodies to detect "free-GFP" indicative of autophagic flux.

(F–H) Representative micrographs (F), respective quantification (G), and immunoblot analysis (H) of wild-type (WT) and *ACS1*-deleted (Δ*acs1*) yeast aged to day 3 compared to young (day 1) cells expressing GFP-Atg8p chimera as in (C)–(E). Data represent means ± SEM (n = 4).

3 days of aging, while young (day 1) cultures presented comparable levels of autophagy-competent cells (manifesting vacuolar localization of GFP-Atg8p as well as *GFP liberation* activity) in both wild-type and *ach1* mutant (Figures 2A–2C). In addition, we assessed the autophagic flux by measuring vacuolar alkaline phosphatase (vac. ALP) activity using yeast strains carrying an engineered form of *PHO8* (*pho8ΔN60*), encoding a cytosolically localized phosphatase, which becomes activated through autophagic delivery to the vacuole (Noda and Klionsky, 2008). While showing comparable levels of vac. ALP activity early during aging, *ach1* mutant cells developed a strong defect in vac. ALP activity after 3 days (>72 hr) of aging (Figure S2A). We also measured cell stress by assessing the fraction of cells staining positive upon incubation with dihydroethidine (DHE), which is converted into fluorescent ethidium in ROS-overproducing cells but also gives rise to strong fluorescence in cells that have lost their plasma membrane integrity. This assay revealed that Δ*ach1* cells lost their autophagic capacity before actual cell stress or death occurred (>88 hr; Figure S2A). These observations rule out that the autophagy defect was simply a result of the previously reported increase in cell death of *ach1* mutant cells (Orlandi et al., 2012). Since Ach1p has been suggested to function primarily in mitochondria (Fleck and Brock, 2009), we next assessed whether block of AcCoA production through mitochondrial pyruvate dehydrogenase (PDH) pathway would also impair autophagy of aging yeast. Deletion of *MPC1*, a recently identified transporter of pyruvate into mitochondria crucial for PDH-derived AcCoA formation (Bricker et al., 2012), indeed caused a comparable defect of age-associated autophagy as observed for Δ*ach1* (Figures 2D–2F). The combined deletion of *ACH1* and *MPC1* led to similar kinetics of the age-dependent loss of autophagy (Figure S2B). Together, this strongly suggests that neither the specific CoA-transferase function of Ach1p nor

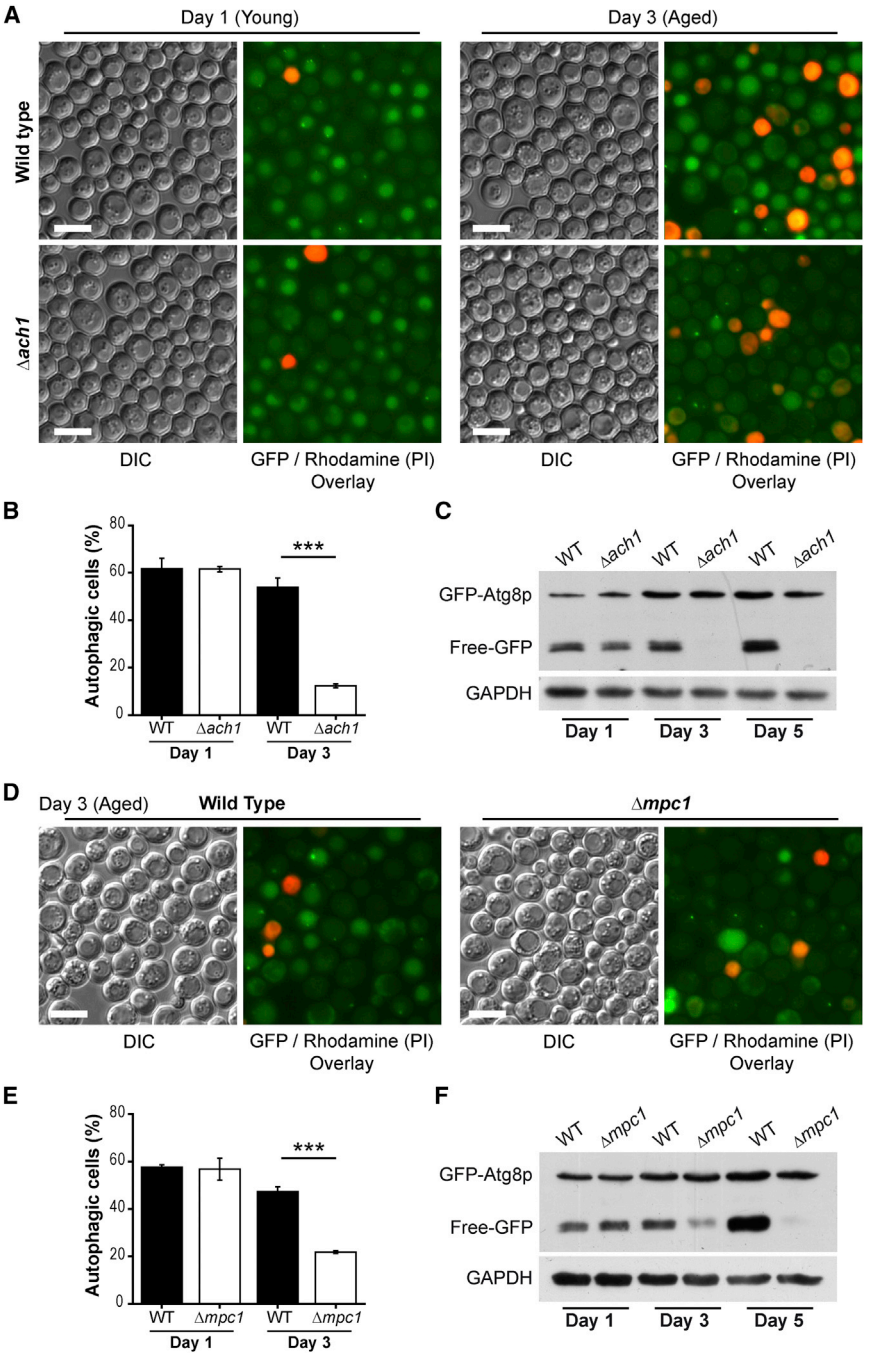


Figure 2. Mitochondrial AcCoA Production by Ach1p- or Mpc1p-Associated Pathways Is Required for Autophagy during Aging

(A) Fluorescence microscopy of GFP-Atg8p expressing wild-type (WT) and *ACH1*-deleted (Δ*ach1*) yeast grown to day 1 (young) and aged for 3 days in SC 2% glucose medium; propidium iodide (PI) counterstaining served to visualize dead cells. Scale bars represent 5 μm.

(B) Quantification of cells depicted in (A) with 150–300 counts (blinded) for each replicate. Autophagic cells were defined as cells with clear vacuolar GFP fluorescence. Data represent means ± SEM (n = 4). ***p < 0.001.

(C) Representative immunoblot analysis of cells shown in (A) and further aged to day 5 using anti-GFP and anti-GAPDH (loading control) antibodies to detect "free-GFP" indicative of autophagic flux (see also Figure S2).

(D–F) Representative micrographs (D), respective quantification (E), and immunoblot analysis (F) of wild-type (WT) and *MPC1* deleted (Δ*mpc1*) yeast expressing GFP-Atg8p chimera as in (A)–(C) and aged to indicated time points. Data represent means ± SEM (n = 4). ***p < 0.001.

mitochondrial pyruvate supply by Mpc1p was specifically responsible for the autophagic deficiency of *ach1* or *mpc1* mutant cells. Our data demonstrate a strict requirement of mitochondrial AcCoA production pathways for maintaining autophagic flux during aging.

Mitochondrial AcCoA Biosynthesis Pathways Are Required for Healthy Aging

We next asked if the repression of autophagy induced by blockade of the mitochondrial route to AcCoA biosynthesis would culminate in increased cell death and a reduced lifespan. While deletion or knockdown of *ACS1* or *ACS2*, respectively, barely affected yeast survival during chronological aging as measured by clonogenic assays (Figures 3A and S3A–S3D), deletion of either *ACH1* or *MPC1* dramatically reduced lifespan (Figures 3B and 3C). The frequency of cell death (as determined by propidium iodide-positive cells and further characterized to be of apoptotic and secondary necrotic morphology, see Figure S3I and respective legend for details) consistently increased in short-lived mutant conditions (Δ*ach1* and Δ*mpc1*) compared to wild-type cells and remained largely unchanged upon deletion or knockdown of *ACS1* or *ACS2*, respectively (Figures 3D–3F, S3E, and S3F). Similar to the comparable kinetics of age-associated autophagy impairment, the combined deletion of *ACH1* and *MPC1* showed an epistatic effect on lifespan and age-induced cell death (Figures S3G and S3H). Thus, the consequences of these mutations on lifespan and cell death correlate with the (in)ability to induce a permanently activated autophagy response during aging.

Accumulating extracellular acetate upon deletion of *ACH1* (Fleck and Brock, 2009; Orlandi et al., 2012) has been suggested to trigger the death of *ach1* mutant cells (Orlandi et al., 2012). Accordingly, both *ach1* and *mpc1* mutant cells exhibited an age-dependent and comparable increase in extracellular acetate (Figures 3H and 3I). Deletion of *ACS1* instead entailed rather minor changes in extracellular acetate concentration (Figure 3G), consistent with its lack of an effect on lifespan or autophagic activity.

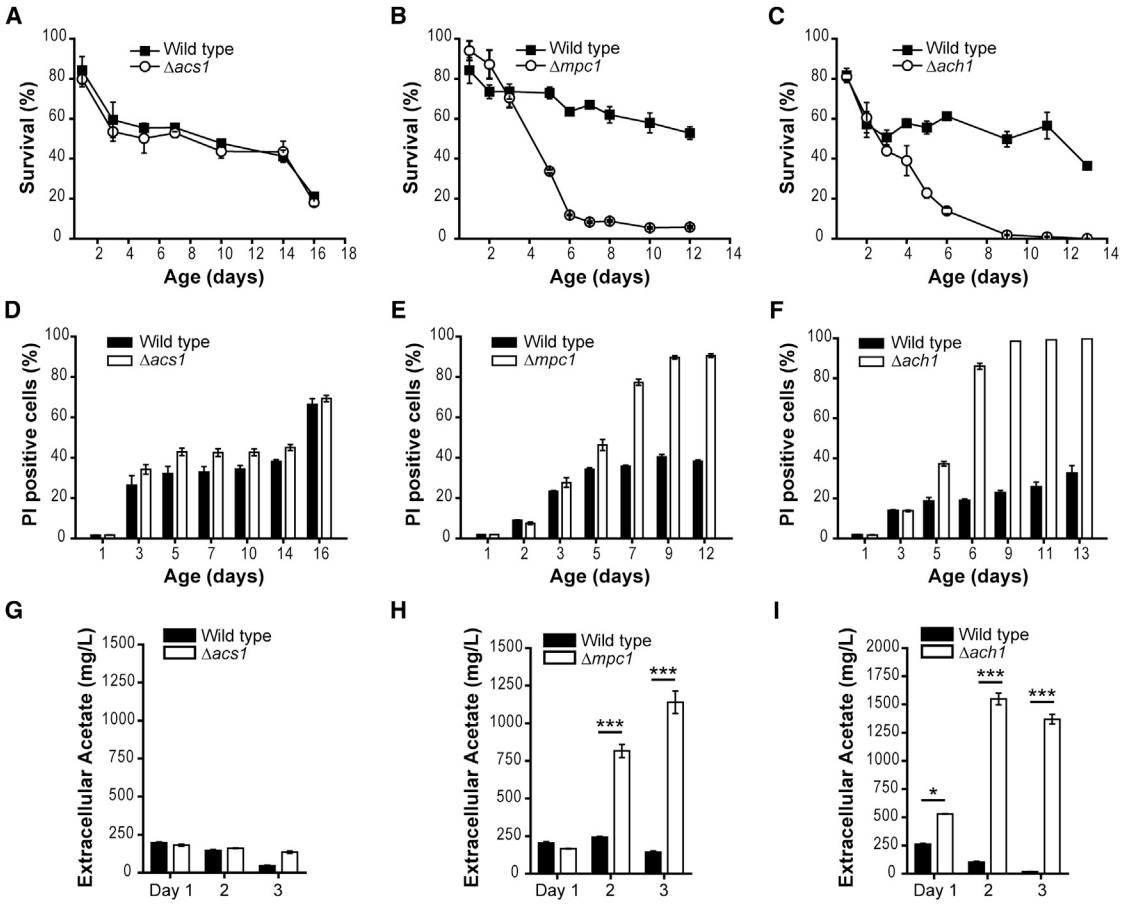


Figure 3. Deletion of *ACH1* or *MPC1* Shortens Chronological Lifespan and Leads to Excess Release of Cellular Acetate

(A–C) Chronological lifespan (CLS) analyses in SC 2% glucose medium of wild-type (WT) cells compared to Δ*acs1* (A), Δ*mpc1* (B), or Δ*ach1* (C) cells (see also Figure S3). Survival was determined by colony-forming capacity (clonogenicity). Data represent means ± SEM (n = 4) of a representative aging experiment.

(D–F) Propidium iodide (PI)-positive cells analyzed by flow cytometry to quantify age-induced cell death of experiments shown in (A)–(C). Data represent means ± SEM (n = 4) (see also Figure S4).

(G–I) Extracellular acetate assessed from crude culture supernatants obtained at indicated time points of experiments shown in (A)–(C). Data represent means ± SEM (n = 4).

*$p < 0.05$ and ***$p < 0.001$.

Deletion of *MPC1* or *ACH1* Causes Upregulation of the Nucleocytosolic, Acs2p-Mediated Pathway of AcCoA Production

Excess acetate released from cells most likely reflects an overflow of acetate within the cytosol, which may fuel and trigger a cytosolic acetate-metabolizing pathway. Since Acs2p, the nucleocytosolic acetate-converting AcCoA synthetase, appeared limiting for autophagy (remember knockdown provoked autophagy during aging; compare to Figure 1), we hypothesized that upregulation of the Acs2p pathway would mechanistically explain the autophagy defect of *ach1* and *mpc1* mutant cells.

To test this hypothesis, we first analyzed the protein level of Acs2p in these mutants. While the level of Acs2p decreased during aging in wild-type cells, deletion of *ACH1* or *MPC1* clearly increased the relative amount of Acs2p compared to wild-type cells, suggesting an upregulation of the nucleocytosolic AcCoA pathway under both conditions (Figures 4A, 4B, S4A, and S4B). Interestingly, the sole addition of acetate to aging cultures was similarly efficient in increasing Acs2p protein levels as well as in the inhibition of autophagy, suggesting that acetate may indeed represent the trigger of its downstream metabolic pathway (Figure S4C). To test if the increased protein level of Acs2p also resulted in higher enzyme activity, we determined the AcCoA synthetase (ACS) activity from crude protein extracts using an established biochemical enzyme assay (van den Berg et al., 1996), using Δ*acs1* background conditions to specifically address Acs2p activity (for details, see Supplemental Experimental Procedures and Figures S3J–S3L). In agreement with the idea that deletion of *ACH1* hyperactivates the nucleocytosolic AcCoA pathway, *ach1 acs1* double mutant cells developed an age-dependent increase in ACS activity compared to *acs1* control cells (Figure S4D).

Simple measurement of AcCoA levels is not applicable to our experimental question, as crude extracts reflect the total cellular content of AcCoA, not allowing for discrimination of the mitochondrial versus nuclear-cytosolic pools, which constitute two

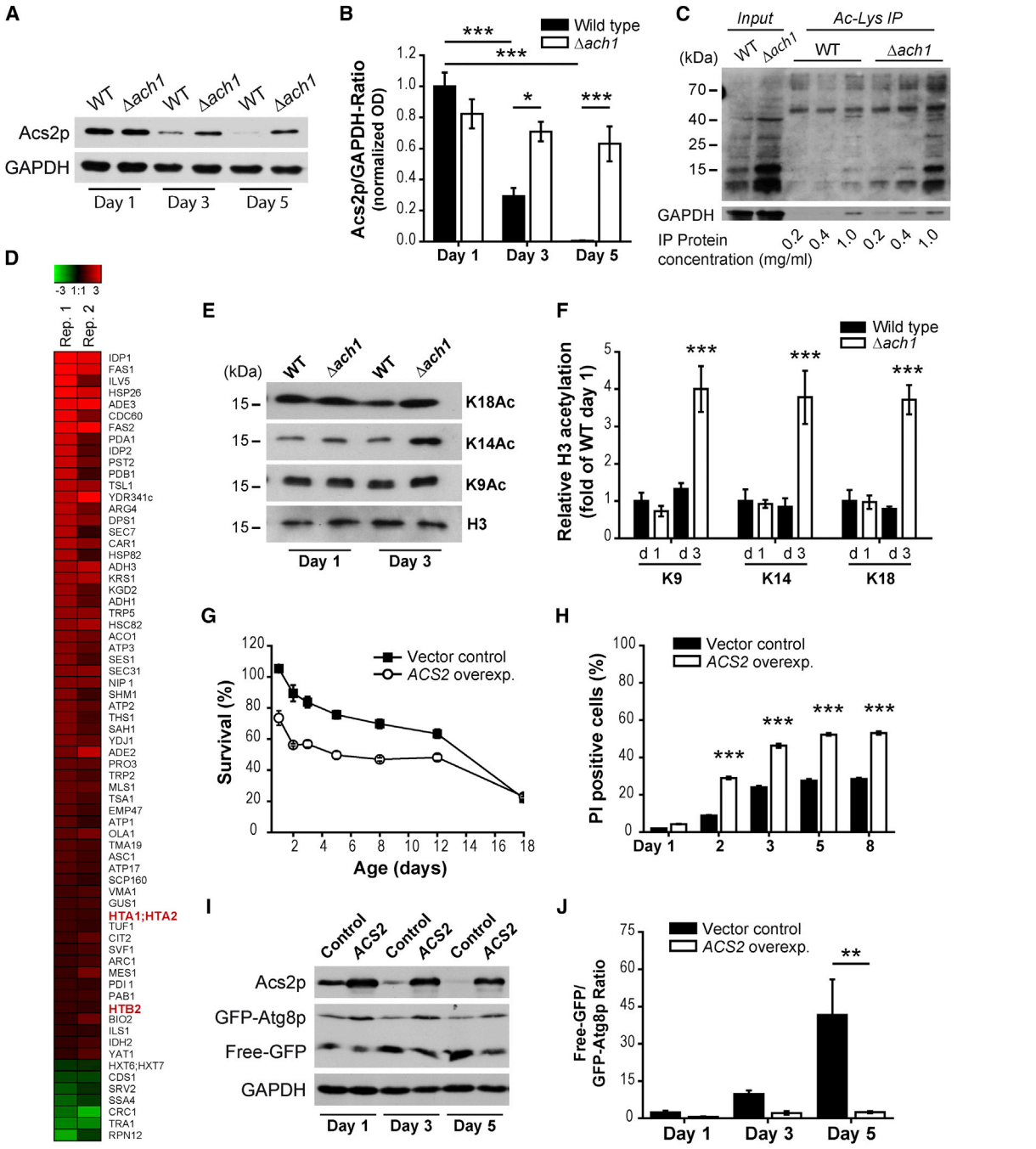


Figure 4. Deletion of *ACH1* or MPC1 Results in Upregulation of the Nucleocytosolic Acs2p Pathway, Causing Histone Hyperacetylation

(A and B) Representative immunoblot (A) and densitometric quantification expressed as normalized Acs2p/GAPDH ratios (B) of protein extracts from wild-type (WT) and Δ*ach1* yeast chronologically aged to indicated time points in SC 2% glucose medium (see also Figure S4).

(C) Representative immunoblot analysis of 3-day-old WT and Δ*ach1* cells similar to (A) using pan-acetyl-lysine antibodies. Crude protein extracts (*Input*) obtained in the presence of histone deacetylase and sirtuin inhibitors (see Supplemental Experimental Procedures) were subjected to immunoprecipitation (IP) at indicated protein concentrations using pan-acetyl-lysine antibodies to enrich acetylated proteins (*Ac-Lys IP*). GAPDH served as loading control.

(D) Heatmap of protein ratios (Δ*ach1* versus WT, log2 scale) corresponding to indicated genes. Data were obtained from mass spectrometric analyses of acetylated proteins enriched by IP similar to (C, 1 mg/ml protein). Extracts from stable-isotope (SILAC)-labeled cells were mixed prior to IP (prelysate), and mean SILAC-protein ratios after IP were normalized to ratios of prelysates to correct for changes in general protein abundance. Two biological replicates were performed (Rep. 1 and Rep. 2) with a regression coefficient of 0.76 of observed protein ratios. Heatmap represents identified proteins with reproducible 1.5-fold upregulation (red color) or downregulation (green color).

(E and F) Representative immunoblots of whole cell acid extracts of wild-type (WT) and Δ*ach1* (E) cells chronologically aged to designated time points. Blots were probed with antibodies against total histone H3 (loading control) or H3 acetylated lysines (K9Ac, K14Ac, K18Ac). Densitometric quantification (F)

(legend continued on next page)

separate subcellular sites of AcCoA generation in yeast (Takahashi et al., 2006). Therefore, we decided to investigate the changes in AcCoA metabolism by alternative technologies that were based on the consideration that AcCoA represents an important cofactor of protein acetylation in eukaryotic cells and may directly affect the level of protein acetylation, enzymatically or nonenzymatically (Guan and Xiong, 2011). Consistent with the increased Acs2p activity, *ach1* mutants exhibited increased overall acetylation based on immunoblot analysis using pan-acetyl-lysine antibodies (Figure 4C, Input). In a more sophisticated approach using SILAC-based proteomics of crude protein extracts that were enriched for acetylated proteins by means of immunoprecipitation (IP) (Figure 4C, *Ac-Lys IP*), we identified potential targets affected by deletion of *ACH1*. Under the selected cutoff conditions (reproducible 1.5-fold regulation; for details, see Experimental Procedures), 61 proteins were found to be hyperacetylated upon *ACH1* deletion, while only 7 proteins were hypoacetylated (Figure 4D). Among these hyperacetylated target proteins, we identified several histones (Figure 4D, red highlighted text), in line with the prior observation that histone acetylation is associated with cellular AcCoA fluctuations in yeast and mammals (Cai et al., 2011; Wellen et al., 2009) as well as to the activity of Acs2p (Takahashi et al., 2006). The most abundant immunoblot signals detected after IP using pan-acetyl-lysine antibodies indeed corresponded to the size of histones at about 10–15 kDa (Figure 4C).

Next, we directly assessed the levels of histone H3 acetylation by means of acetylation-site-specific antibodies (i.e., histone marks that we have previously connected to autophagy during aging of yeast; Eisenberg et al., 2009). In line with the mass spectrometry results, Δ*ach1* but also Δ*mpc1* cells exhibited consistent hyperacetylation of all tested N-terminally located lysine residues in histone H3 compared to wild-type cells (Figures 4E, 4F, S4E, and S4F). As identified by our mass spectrometry analysis, the histones H2A and H2B appeared similarly hyperacetylated (Figure 4D, *HTA1/2 and HTB2*), as observed for H3. Since acetylation of histone H4, in particular that of lysine 16, was only recently found to regulate the outcome of autophagy in yeast and mammals (Füllgrabe et al., 2013) and may determine yeast replicative lifespan (Dang et al., 2009), we asked whether this histone was also affected by deletion of *ACH1*. Interestingly, histone H4 acetylation was unaffected by deletion of *ACH1* after 3 days of aging (Figure S4G), pointing toward a role of histone H2A/B and H3 acetylation under conditions of chronological aging that is distinct from that of the control of replicative lifespan by acetylation targets at histone H4.

In conclusion, impaired mitochondrial AcCoA production resulting from deletion of *ACH1* or *MPC1* causes upregulation of the nucleocytosolic pathway of AcCoA biosynthesis, as indicated by a concomitant increase in the Acs2p substrate acetate, the expression of Acs2p protein, the enzymatic activity of Acs2p, and hyperacetylation of specific histones.

Episomal Overexpression of *ACS2* Mimics the Effects of *ACH1* Deletion

To exclude that the effects of *ACH1* or *MPC1* deletion were simply due to a general defect in mitochondrial AcCoA supply, we tested whether genetic overexpression of *ACS2* mimicked the effects of blocking mitochondrial AcCoA pathways. Indeed, Gal10p-driven overexpression of *ACS2* led to early onset cell death (Figures 4G and 4H) and limited the autophagic response during aging (Figures 4I and 4J). Importantly, ectopic expression of a mutant *acs2-Ts1* allele, which is stably expressed but shows reduced catalytic activity upon increased temperature (Takahashi et al., 2006), failed to induce cell death and caused reduced histone acetylation compared to expression of its wild-type counterpart that showed toxicity compared to BY4741 controls (Figures S4I–S4K). Of note, under our aging conditions (using only moderately increased permissive temperature to facilitate normal growth of the otherwise lethal *acs2-Ts* mutation), both the *ACS2* wild-type (Wt-ACS2) and the *Acs2-Ts1* mutant displayed a comparable increase in Acs2p levels compared to its BY4741 background strain (Figure S4H).

Histone Hyperacetylation Is Associated with Impaired Transcription of Autophagy-Essential Genes

We previously reported that histone hypoacetylation induced by supplementation of cultures with spermidine (an inhibitor of histone acetyl transferases) or simultaneous genetic inactivation of two histone acetyl transferase complexes correlates with enhanced expression of *ATG* genes and increased autophagy during aging (Eisenberg et al., 2009). Based on this premise, we hypothesized that histone hyperacetylation induced by upregulation of the Acs2p pathway could repress the transcription of autophagy-essential *ATG* genes. We therefore determined the relative mRNA abundance of five *ATG* transcripts (*ATG5*, *ATG7*, *ATG8*, *ATG11*, and *ATG14*) by quantitative reverse-transcriptase PCR. *ACH1* deletion significantly reduced the abundance of several *ATG* transcripts, including that of *ATG7*, whose mRNA level decreased to ~40% compared to the wild-type level (Figures 5A and S5A). In contrast, the *ATG8* mRNA level increased in Δ*ach1* cells (Figure S5A). The protein levels of Atg7p (assessed by immunoblotting of *pATG7-ATG7-6HA* fusion strains) consistently decreased upon deletion of *ACH1* during aging (Figure 5B), while Atg8p levels remained constant (compare immunoblots of *pATG8-EGFP-ATG8* in Figure 2C). The level of total Atg7p also decreased significantly in aged wild-type cells (Figure 5B), again in clear contrast to Atg8p

of relative acetylation was calculated as Ac-K/total H3 ratios normalized to ratios of WT at day 1. Data represent means ± SEM (n = 7–8) (see also Figure S5).

(G and H) Survival analyses in SC 1.25% galactose/0.75% glucose medium of wild-type cells ectopically overexpressing *ACS2* (*ACS2 overexp.*) compared to vector control cells (Vector control). Survival (I) was determined by colony-forming capacity (clonogenicity) and cell death (J) assessed by propidium iodide (PI)-positive cells analyzed by flow cytometry. Data represent means ± SEM (n = 4) of a representative aging experiment.

(I and J) Autophagic flux determination by vacuolar protease-dependent GFP liberation after *ACS2* overexpression compared to empty vector controls (Control) similar to (G) and (H). Representative immunoblots at indicated time points (G) and quantification by densitometry of free-GFP/GFP-Atg8p signal ratios (H) are shown. Data represent means ± SEM (n = 4).

*p < 0.05, **p < 0.01, and ***p < 0.001.

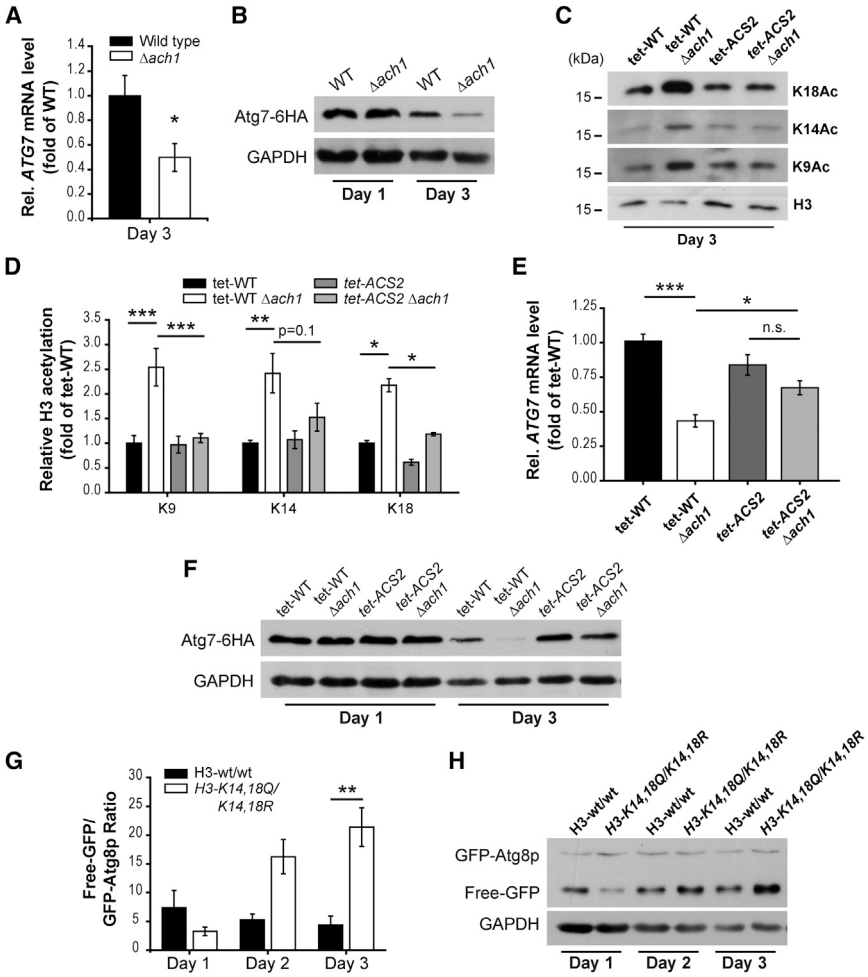


Figure 5. Acs2p Controls ATG7 Transcription through Epigenetic Histone Acetylation

(A) *ATG7* mRNA levels by quantitative reverse-transcriptase PCR (RT-qPCR) of wild-type and Δ*ach1* cells aged to day 3 (see also Figure S5). Rel. mRNA levels are expressed as ratios of 18S rRNA normalized to wild-type cells by ΔΔCt-method. Data represent means ± SEM (n = 8).

(B) Representative immunoblot analysis from wild-type (WT) and *ACH1*-deleted (Δ*ach1*) yeast expressing chromosomally tagged *ATG7* by C-terminal 6HA fusion aged to indicated time points. Blots were probed with anti-HA and anti-GAPDH (loading control) antibodies.

(C and D) Representative immunoblots (C) and densitometric quantification (D) of whole-cell acid extracts of wild-type and Δ*ach1* cells combined with or without knockdown of *ACS2* (*tet-ACS2*). Cells were chronologically aged to day 3 in the presence of 1 ng/ml doxycycline. Blots were probed with antibodies against total histone H3 (loading control) or H3 acetylated lysines (K9Ac, K14Ac, K18Ac). Data represent means ± SEM (n = 8).

(E and F) *ATG7* mRNA levels (E) by RT-qPCR and representative immunoblot analysis (F) of wild-type and Δ*ach1* cells with or without knockdown of *ACS2* (*tet-ACS2*) as in (C) and (E) aged to day 3. Rel. mRNA levels (E) are expressed as ratios to 18S rRNA normalized to wild-type cells by ΔΔCt method. Data represent means ± SEM (n = 7–8).

(G and H) Representative immunoblot (H) and densitometric quantification (G) of histone H3 wild-type (H3-wt/wt) and H3 mutated (*H3-K14,18Q/-K14,18R*) strains carrying the GFP-Atg8p fusion to calculate "free-GFP/GFP-Atg8p Ratio" indicative of autophagic flux.

Data represent means ± SEM (n = 4) (for strain details and supplemental data, see Figures S5D–S5F).

*p < 0.05, **p < 0.01, and ***p < 0.001; n.s., not significant.

(Figure 2C). Thus, as exemplified by Atg7p, transcriptional control of the autophagy-relevant proteome may be crucial for enduring autophagic activity during chronological aging.

ACS2 Depletion Reinstalls Histone Deacetylation and *ATG7* Transcription in *ach1* Mutants

In order to test if Acs2p-induced histone acetylation was indeed causally linked to the transcriptional repression of *ATG7*, we tested if knockdown of *ACS2* in the background of *ACH1* deletion would (1) reverse the observed histone hyperacetylation phenotype and (2) reinstate normal *ATG7* transcription. Using the conditions depicted in Figure 1, knockdown of *ACS2* almost completely restored physiological (wild-type-like) levels of histone acetylation in *ach1* mutant cells (*tet-ACS2* Δ*ach1*), while deletion of *ACH1* alone (tet-WT Δ*ach1*) again increased overall acetylation at lysines 9, 14, and 18 of histone H3 compared to tet-WT controls (Figures 5C and 5D). Consistently, knockdown of *ACS2* also partly recovered *ATG7* mRNA and protein levels (Figures 5E and 5F, respectively) and almost completely annihilated the transcriptional defect induced by *ACH1* deletion (*tet-ACS2* Δ*ach1* compared to *tet-ACS2*; Figure 5E).

Altogether our data are consistent with a causal inverse relationship of histone H3 acetylation with the transcriptional control of autophagy-essential genes, exemplified by *ATG7* that is profoundly influenced by the Acs2p-mediated AcCoA production pathway. In support of a deficiency in the Atg7p-dependent Atg8p lipidating machinery, *ach1* mutants failed to accumulate lipidated Atg8p normally evident from enlarged GFP-Atg8p punctuate structures that were observed in autophagy-deficient *atg1* mutants carrying functional *ATG7* (Figure S5C; see also Autophagy Measurements in the Supplemental Experimental Procedures for more details).

In order to demonstrate the principal requirement of histone acetylation in age-associated autophagy control, we created a panel of (nonacetylable) histone H3 lysyl point mutations, mimicking different states of acetylation and deacetylation. In addition to pure deacetylation-mimicking lysine to arginine (KR) mutations (that likely result in quite unphysiological situations), we also rendered mixed KQ/KR mutations introduced to either one of two histone copies present within the genome as a promising strategy to test for more physiological alterations that retain a certain opening of the chromatin. The triple K9,14,18R mutation indeed resulted in generally impaired survival during aging (for

summary of results and histone mutants tested, see Figure S5D), but strikingly we identified a mutant (H3-K14,18Q/K14,18R) that continuously enhanced autophagy during aging (Figures 5G, 5H, and S5D–S5F). Although such mutants are per se far away from the highly refined, time- and location-dependent chromatin modifications that occur in vivo, this finding demonstrates that epigenetic modifications by histone acetylation are in principle capable of modulating the cellular autophagic response during aging, and goes in line with our hypothesis that histone acetylation may represent a determining downstream event upon modulation of AcCoA availability.

Depletion of *ACS2*, but Not Inhibition of Tor or Sch9 Signaling, Restores Autophagy in *ach1* Mutants

As knockdown of *ACS2* in the background of Δ*ach1* almost completely abolished the transcriptional impairment of *ATG7*, we next asked whether *ACS2* knockdown would also be able to reinstate the autophagic activity of *ach1* mutant cells. Strikingly, knockdown of *ACS2* almost completely restored age-associated autophagy of *ach1* mutants (Figures 6A–6C and S6A), as determined by the frequency of cells with GFP-Atg8p-positive vacuoles (Figures 6A and 6B) and the levels of *liberated* GFP reflecting autophagic flux (Figures 6C and S6A). Autophagic activity of *tet-ACS2* Δ*ach1* cells approached that of the enhanced levels of the corresponding control strain without deletion of *ACH1* (*tet-ACS2*). Importantly, the knockdown of *ACS2* did not prevent extracellular accumulation of acetate induced by deletion of *ACH1*. The single deletion mutant (tet-WT Δ*ach1*), as well as *ACH1* deletion combined with the knockdown of *ACS2* (*tet-ACS2* Δ*ach1*), displayed almost comparable levels of excess acetate released from cells (Figure S6D). In addition, the autophagy-inhibitory effect of acetate supplementation to aging yeast cultures (compare Figure S4C) was annihilated and autophagic activity almost retained at wild-type levels in the *ACS2* knockdown condition (Figure S6E). This excludes a possible toxic effect of extracellular acetate on general cellular functions including autophagy and strongly argues for a specific role of the nucleocytosolic (Acs2p-mediated) pathway of acetate utilization that explains the inhibition of autophagy by *ACH1* deletion.

We next investigated whether the autophagy defect of cells lacking *ACH1* would be bypassed by inhibition of autophagy-regulatory kinases. Suppression of Tor- or Sch9-function by either genetic or pharmacological means induces autophagy and delays aging in yeast and other model organisms (He and Klionsky, 2009; Madeo et al., 2010a). Using previously reported conditions (Alvers et al., 2009), rapamycin, a potent inhibitor of TORC1, was able to induce autophagy during aging of BY4742 wild-type cells but completely failed to restore the age-induced autophagy defect of Δ*ach1* cells (Figures 6E and S6C). Rapamycin was well capable of inducing autophagy in young (day 1) Δ*ach1* cells (Figures 6E and S6C), excluding that rapamycin would simply fail to inhibit Tor in *ach1* mutant cells at the concentrations used for wild-type cells. Similarly, deletion of *SCH9*, which has been suggested to act in parallel to TORC1 as an autophagy suppressor (Yorimitsu et al., 2007) as well as in the same pathway with TORC1 during lifespan regulation (Wei et al., 2009), transiently amplified the autophagic response of aging wild-type but again failed to reinduce autophagy of aging *ach1* cells (Figures 6D and S6B). Thus, knockdown of *ACS2*—but not inhibition of Tor or Sch9—specifically reinstated autophagy of *ach1* mutants, strengthening our conclusion that upregulation of the Acs2p pathway is causally linked to the autophagy defect of Δ*ach1* cells.

Finally, we tested if ectopic overexpression of *ACS2* would also impair autophagy induced by nutrient depletion, a known autophagy trigger via nutrient-responsive signaling, including TORC1- or AMPK-dependent pathways (He and Klionsky, 2009). While the level of Acs2p decreased upon starvation (Figure 6H, compare empty vector controls, "*WT*"), *ACS2* overexpression profoundly inhibited autophagic flux after 12 hr of starvation, as evident from reduced vacuolar translocation of GFP-Atg8p (Figures 6F and 6G) as well as reduced amount of *liberated* GFP (Figure 6H, "Free-GFP"). Similar results were observed after autophagy induction by rapamycin treatment (data not shown).

In sum, enduring autophagic activity during aging (but also that of acute nutrient depletion conditions) is profoundly repressed by nucleocytosolic Acs2p, which appears dominant over autophagy regulation by known kinase regulators such as Sch9 or TORC1.

Reinstating Autophagy of Δ*ach1* Partly Restores Lifespan in an Autophagy-Dependent Manner

Given the crucial role of autophagy for healthy aging, reinstating autophagy in *ach1* mutants may recover survival of aging cells, which would hence argue in favor of a causal role of the autophagy deficit in the reduction of lifespan. Knockdown of *ACS2*, using the same conditions that reactivated autophagy of *ach1* cells, indeed significantly enhanced survival (Figure 7A) and reduced markers of cell death (Figure 7B) in aging *ach1* cells. Compared to that of wild-type cells, the strong lifespan-shortening effect of *ACH1* deletion (tet-WT versus tet-WT Δ*ach1*) was significantly inhibited by knockdown of *ACS2* (*tet-ACS2* versus *tet-ACS2* Δ*ach1*). Additional deletion of the autophagy-essential gene *ATG7* (known to completely abrogate autophagy in aging yeast) again revealed the full lifespan-compromising consequences of *ACH1* deletion, even when *ACS2* expression was suppressed (Figures 7C and 7D). Knockdown of *ACS2* even accelerated death of *ach1* mutants when autophagy was absent (compare *tet-ACS2* Δ*ach1* Δ*atg7* to tet-WT Δ*ach1* Δ*atg7*, Figures 7C and 7D). This strongly suggests that loss of autophagy is—at least in part—responsible for the detrimental effects of *ACH1* deletion.

Knockdown of Acetyl-CoA Synthetase Extends Mean and Maximum Lifespan of Flies

Finally, we tested if inhibition of the nucleocytosolic acetyl-CoA production pathway would affect autophagy and aging in a metazoan organism. In *Drosophila*, a renowned model of aging in a higher eukaryote, autophagic efficacy was shown to decline with brain aging, while activating the autophagic pathway by brain-specific overexpression of Atg8a using brain-specific appl-gal4 was previously shown to improve lifespan (Simonsen et al., 2008). Therefore, we addressed the effects of brain-specific RNAi-mediated knockdown of the fly acetyl-CoA synthetase gene (AcCoAS).

Remarkably, although initially with adverse effects in males, flies expressing RNAi specific for AcCoAS exhibited mean and

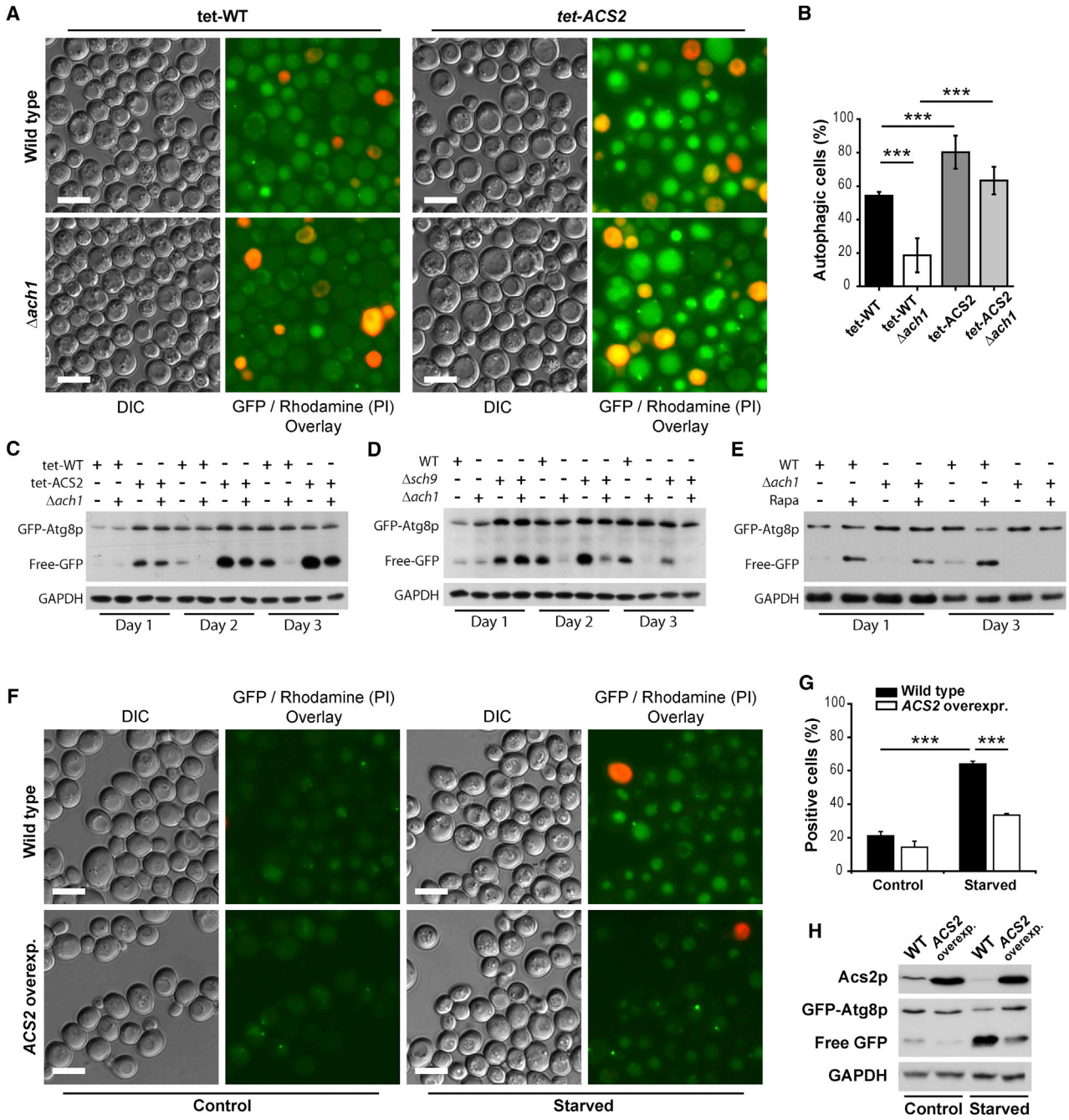


Figure 6. Knockdown of Acs2p Cures the Autophagy Defect in *ach1* Mutants

(A and B) Representative micrographs (A) and respective quantification (B) of wild-type and Δ*ach1* cells expressing GFP-Atg8p chimera combined with or without knockdown of *ACS2* (*tet-ACS2*). Cells were chronologically aged to day 3 in the presence of 1 ng/ml doxycycline and PI counterstained prior to epifluorescence microscopy (see also Figure S6).

(C) Representative immunoblot analysis of cells shown in (A) aged until days 1, 2, and 3 to detect "free-GFP" indicative of autophagic flux (see Figure S6A for quantification).

(D and E) Representative immunoblot analyses of GFP-Atg8p expressing wild-type (WT) and Δ*ach1* cells either combined with deletion of *SCH9* (D) or supplemented with or without 20 nM rapamycin (Rapa) (E) and aged until indicated time points. Blots were probed with anti-GFP and anti-GAPDH (loading control) antibodies to detect "free-GFP" indicative of autophagic flux (see Figures S6B and S6C for quantification).

(F and G) Representative micrographs (F) and respective quantification (G) of GFP-Atg8p expressing yeast cells ectopically overexpressing *ACS2 (ACS2 overexp.)* or carrying the empty vector (wild-type) during nutrient depletion (starved) compared to SC 2% galactose control conditions (control). Counterstaining of cells with propidium iodide was used to visualize dead cells.

(H) Representative immunoblot analyses of the experiment shown in (F) to detect "free-GFP" indicative of autophagic flux.

***$p < 0.001$.

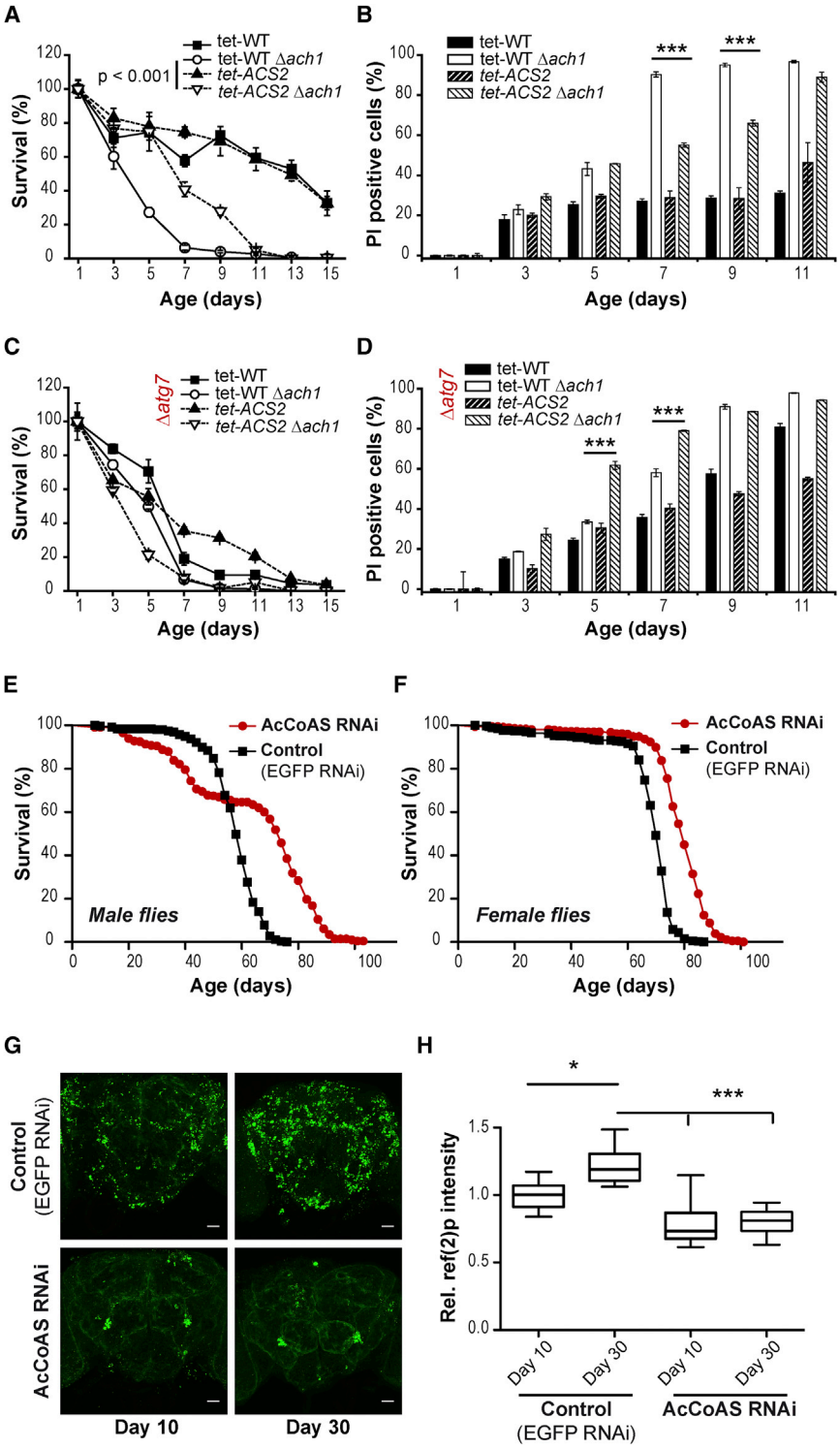


Figure 7. Knockdown of Acs2p Partly Restores Survival of *ach1* in an *ATG7*-Dependent Manner

(A and B) Chronological aging in SC 2% glucose medium supplemented with 1 ng/ml doxycycline of wild-type and Δ*ach1* cells combined with or without knockdown of *ACS2* (*tet-ACS2*). Survival (A) was determined by colony-forming capacity (clonogenicity). Age-associated cell death (B) was assessed through propidium iodide (PI) staining analyzed by flow cytometry. Data represent day 1 normalized means ± SEM (n = 4).

(C and D) Survival (C) and cell death (D) of chronological aging experiment similar to (A) and (B) but in the background of *ATG7*-deleted autophagy-incompetent cells (Δ*atg7*). Data represent day 1 normalized means ± SEM (n = 4).

(E and F) *Drosophila* lifespan analyses of male (E) and female (F) flies depleted for acetyl-CoA synthetase (AcCoAS) using RNAi-mediated knockdown (*AcCoAS RNAi*) compared to isogenized controls (*Control (EGFP RNAi)*). Log rank tests revealed $p < 0.0001$ for both sexes.

(G) Immunofluorescence specific to p62-homolog ref(2)p of adult brain sections from 10-day-old flies compared to 30-day-old flies as depicted in (E). Representative confocal micrographs are shown with scale bars representing 25 μm.

(H) Quantification of total ref(2)P intensity in the central brain region normalized to 10-day-old control flies (*Control (EGFP RNAi)*). Standard box plot represents data from seven to eight independent brains (whiskers indicate minimum and maximum values).

*$p < 0.05$, ***$p < 0.001$.

maximum lifespan extension in both sexes compared to isogenic control flies that expressed an unrelated RNAi specific for GFP not present in this organism (Figures 7E and 7F, $p < 0.0001$ for both sexes). We then assessed the levels of the p62-homolog ref(2)p, a protein known to increase with age and to decrease again when autophagy is activated (Gupta et al., 2013). In fact, while both the number of dot-like (aggregated) ref(2)p structures as determined by immunofluorescence (Figure 7G) and overall levels of ref(2)p as quantified by total pixel intensities (Figure 7H) increased in brains of aged (30 days) compared to young (10 days) control animals, this increase was largely abolished in the animals expressing the AcCoAS RNAi by appl-gal4. Thus, our data suggest that, indeed, knockdown of AcCoAS induced the autophagic pathway associated with its longevity-promoting effects.

DISCUSSION

In the present study we identified the nucleocytosolic (Acs2p-mediated) AcCoA production pathway as a suppressor of age-associated autophagy, conserved from yeast to flies. While upregulation of Acs2p activity as a consequence of impaired mitochondrial acetate or pyruvate utilization led to autophagy deficiency, reducing the protein level of Acs2p was sufficient to ameliorate the autophagic response to aging (see Figure S7 for an overview of the mechanistic model). In

agreement with this idea, hyperactivation of the Acs2p pathway observed in *ach1* or *mpc1* mutant cells hampered genetic or pharmacological means of autophagy induction, including deletion of *SCH9* or application of rapamycin, respectively. Ectopic overexpression of *ACS2* not only limited the autophagic response to aging but also strongly impaired autophagy induced by nutrient depletion, a scenario known to inhibit nutrient signaling. Thus, autophagy observed under distinct conditions is counteracted by a hyperactive Acs2p pathway, which may imply a general requirement of Acs2p inhibition for efficient induction of autophagy.

The activity of Acs2p culminates in its downstream target of histone acetylation. The mechanism by which Acs2p activity affects age-associated autophagy may thus include epigenetic control of *ATG* gene transcription, as exemplified in this study by regulation of *ATG7* mRNA and protein levels. *ATG7* mRNA and protein levels inversely correlated with the acetylation of N-terminally located lysyl residues of histone H3. However, regulation of autophagy by changes in the relevant transcriptome most likely involves more than just one *ATG* transcript. The precise mechanism of how global hyperacetylation modulates the autophagy-relevant transcriptome remains to be clarified but is in agreement with our previous finding that global hypoacetylation can induce *ATG7* transcription and autophagy upon treatment with the natural polyamine spermidine (Eisenberg et al., 2009; Madeo et al., 2010b). Our findings add evidence to a previously underestimated pathway of autophagy regulation that may particularly apply to enduring autophagic responses and that involves epigenetic and/or transcriptional alterations (Füllgrabe et al., 2014). Acetylation of histone H4 at lysine 16 has only recently been shown to direct the decision of whether or not autophagy can become toxic (Füllgrabe et al., 2013). The transcription factor FoxO3 controls the expression of autophagy-related genes, including that of LC3—the mammalian ortholog of yeast *ATG8*—and is required for autophagy induction of mammalian muscle cells with implications to muscle atrophy (Zhao et al., 2007). In yeast, *ATG8* transcription is regulated by the Ume3-Sin3-Rpd3-complex, which suppresses induction of *ATG8* under nonstarved conditions and modulates the size of autophagosomes during starvation-induced autophagy (Bartholomew et al., 2012).

In this line and as a proof of principle we introduced a histone point mutation that displayed enhanced autophagy during aging. However, we cannot exclude that in combination with transcriptomic alterations driven by epigenetic histone modifications also acetylation of nonhistone proteins may explain the observed phenotypes. This could, for instance, include the acetylation of Atg proteins or autophagy-relevant transcription factors that affect *ATG* gene transcription more directly. Apart from protein acetylation and/or histone acetylation, more indirect effects on metabolism downstream of AcCoA generation may also explain some of the consequences on autophagy and lifespan and need to be investigated in the future.

The connection of metabolism to posttranslational modifications of histones has been recognized and linked to disease-relevant situations (Kaelin and McKnight, 2013; Lu and Thompson, 2012). However, the connection of AcCoA metabolism to age-relevant autophagy has remained elusive. Here, we describe how energy metabolism controls autophagic activity during cellular aging through modulation of a central metabolite, AcCoA, presumably via its connection to epigenetic changes in chromatin.

The role of acetate in promoting yeast aging has been critically discussed recently (Burhans and Weinberger, 2009; Burtner et al., 2009; Longo et al., 2012). Our data strongly suggest that acetate exerts its proaging effects on yeast not only through rather unspecific events resulting from the primary toxic activity of extracellular acetate, but also through the Acs2p-mediated conversion of acetate to AcCoA. Importantly, acetate metabolism was proposed to contribute to aging in mammals, again via its impact on protein acetylation by generation of AcCoA and subsequent regulation of metabolism (Shimazu et al., 2010).

Interestingly, many lifespan-prolonging regimens (e.g., caloric restriction, rapamycin treatment) or age-associated disease-preventing supplements (e.g., resveratrol) that are known to induce autophagy were also reported to modulate mitochondrial function and respiration (Bonawitz et al., 2007; Houtkooper et al., 2010; Ocampo et al., 2012; Pan et al., 2011). Hence, it is tempting to speculate that efficient utilization of AcCoA by mitochondrial TCA cycle activity and oxidative phosphorylation prevents overflow of AcCoA into protein acetylation and/or histone acetylation pathways that would negatively influence autophagy and other prosurvival processes during aging and age-associated disease.

In summary, we propose that the nucleocytosolic acetyl-CoA pool functions as a crucial, evolutionary conserved, and dominant inhibitor of autophagy and healthy aging. Inhibition of major nutrient signaling pathways (i.e., TORC1 or Sch9) fails to induce autophagy when the Acs2p pathway is activated, arguing for a fundamental function of this pathway downstream of nutrient signaling. Since AcCoA integrates various nutrition pathways, our findings have implications for the understanding of lifespan and autophagy regulation in the context of excessive, restricted, or unbalanced feeding behaviors.

EXPERIMENTAL PROCEDURES

Yeast Strains, Molecular Biology, and Chronological Aging Experiments

Experiments were carried out in *S. cerevisiae* BY4741 or BY4742 wild-type yeast and respective mutant strains depicted in Table S1. Chronological aging experiments were performed in SC 2% glucose medium, survival determined by plating cells on YPD agar (clonogenicity), and cell death quantified by propidium iodide staining. For further details on yeast strains and genetics (Table S1), pharmacological treatments, cell death assays, and culture conditions, please refer to Supplemental Information.

Immunoblotting and Quantification of Histone Acetylation

Immunoblotting was performed using standard protocols. Details on antibodies and on quantification of histone acetylation by blotting serial dilutions of acid extracts are depicted in Supplemental Information.

Yeast Autophagy Measurements

Autophagy was measured either by monitoring the cytosol to vacuole translocation of Atg8p using fluorescence microscopy or immunoblotting (*GFP liberation assay*) of cells/cell extracts from strains carrying a GFP-Atg8p fusion protein (Kirisako et al., 1999; Klionsky et al., 2007) expressed from its endogenous promoter and natural chromosomal locus (*pATG8-EGFP-ATG8* strains) or by alkaline phosphatase (ALP) activity (Noda and Klionsky, 2008). Propidium iodide (PI) staining served to exclude analyses of dead, potentially

autofluorescent cells visualized by standard rhodamine filters. For more details also on quantification of results, refer to Supplemental Information.

Determination of Acetyl-Proteome from SILAC Yeast Cultures

To assess changes in the acetyl-proteome, yeast protein extracts were first enriched for acetylated proteins by IP. Stable isotope-labeled amino acid cell cultures (SILAC) from yeast (Lys0, Lys4, or Lys8 labeled) were subjected to cell disruption by glass beads in the presence of histone deacetylase (trichostatin A, 30 mM) and sirtuin (nicotinamid, 2 μM) inhibitors. Crude extracts from wild-type and Δ*ach1* cultures aged to day 3 were mixed in equal amounts of total protein (determined by Bio-Rad protein assay, Bio-Rad) and subjected to IP using pan-acetyl-lysine antibodies (1:100, Cell Signaling; an equal mix of Ac-K [#9441] and Ac-K^2 [#9814] antibodies was used) and subsequently analyzed by mass spectrometry. For details on IP procedure and on quantification and identification of SILAC ratios by mass spectrometry, see Supplemental Information.

Acetyl-CoA-Synthetase Activity

Acetyl-CoA synthetase (ACS) activity was determined using an established biochemical enzyme assay (van den Berg et al., 1996). For details, see Supplemental Information.

Acetic Acid Detection

Enzymatic measurement of acetic acid from crude culture supernatants (appropriately diluted with water) was conducted using the Acetic Acid (Acetate Kinase Manual Format) kit (Megazyme) following the manufacturer's protocol adapted to a volume of 100 μl for readout in a TECAN plate reader.

Quantitative Reverse-Transcriptase PCR

Target mRNA quantification by quantitative reverse-transcriptase PCR using ΔΔCt-method with 18S rRNA as an internal standard was performed on an ABI StepOnePlus using SYBR Select Master Mix (Life Tech, Invitrogen) ΔΔCt-method. Primers (Table S3) and details can be found in Supplemental Experimental Procedures.

Drosophila Lifespan Analyses and Brain Immunofluorescence

UAS-RNAi lines for acetyl-CoA Synthetase (P{TRiP.HMS02314}attP2) and EGFP (P{VALIUM20-EGFP.shRNA.1}attP2) serving as a background-matched control were obtained from Bloomington *Drosophila* Stock Center. Isogenized panneural driver line APPL-Gal4 was used to drive RNAi expression in fly brains. Details on housing, survival assessment, and ref(2)p-specific immunofluorescence can be found in Supplemental Information.

Statistical Analyses

One-factor analysis of variance (ANOVA) corrected by the post-hoc Bonferroni test was used for all experiments (multiple comparisons as appropriate) except for mass spectrometric and for chronological lifespan (CLS) analyses. If not otherwise stated, representative CLS experiments are shown with three to four biologically independent samples (as indicated) aged at the same time. CLS experiments have been performed at least three times with similar outcome. For comparison of CLS, a two-factor ANOVA with time and strain as independent factors was used. Log rank tests were performed for *Drosophila* lifespan analyses. Mass spectrometry was performed twice from two independent chronological aging experiments. Error bars represent SEM of biological replicates as indicated. Whiskers in box plots (Figure 7H) indicate minimum and maximum values.

SUPPLEMENTAL INFORMATION

Supplemental Information includes seven figures, four tables, and Supplemental Experimental Procedures and can be found with this article at http://dx.doi.org/10.1016/j.cmet.2014.02.010.

ACKNOWLEDGMENTS

We thank Drs. Jef D. Boeke, Daniel Klionsky, and Günther Daum for providing antibodies. We are also grateful for strains provided by Dr. Boeke. We thank Harald Hofbauer for support with quantitative PCR; and Lydia Opriessnig, Christian Pendl, and Birgit Michelitsch for assistance. This work was supported by the Austrian Science Fund FWF (grants T414-B09 and V235-B09 to S.B.; grants LIPOTOX, I1000, P23490-B12, and P24381-B20 to F.M.). T.E. is recipient of an APART fellowship of the Austrian Academy of Sciences at the Institute of Molecular Biosciences, University of Graz. This work was also supported by grants to G.K. from the Ligue Contre le Cancer (Équipe Labelisée), Agence National de la Recherche (ANR), Association Pour la Recherche sur le Cancer (ARC), Cancéropôle Ile-de-France; AXA Chair for Longevity Research, Institut National du Cancer (INCa), Fondation Bettencourt-Schueller, Fondation de France, Fondation pour la Recherche Médicale (FRM), the European Commission (ArtForce), the European Research Council (ERC), the LabEx Immuno-Oncology, the SIRIC Stratified Oncology Cell DNA Repair and Tumor Immune Elimination (SOCRATE), the SIRIC Cancer Research and Personalized Medicine (CARPEM), and the Paris Alliance of Cancer Research Institutes (PACRI).

Received: September 3, 2013
Revised: December 28, 2013
Accepted: February 12, 2014
Published: March 4, 2014

REFERENCES

Alvers, A.L., Wood, M.S., Hu, D., Kaywell, A.C., Dunn, W.A., Jr., and Aris, J.P. (2009). Autophagy is required for extension of yeast chronological life span by rapamycin. Autophagy *5*, 847–849.

Bartholomew, C.R., Suzuki, T., Du, Z., Backues, S.K., Jin, M., Lynch-Day, M.A., Umekawa, M., Kamath, A., Zhao, M., Xie, Z., et al. (2012). Ume6 transcription factor is part of a signaling cascade that regulates autophagy. Proc. Natl. Acad. Sci. USA *109*, 11206–11210.

Bonawitz, N.D., Chatenay-Lapointe, M., Pan, Y., and Shadel, G.S. (2007). Reduced TOR signaling extends chronological life span via increased respiration and upregulation of mitochondrial gene expression. Cell Metab. *5*, 265–277.

Bricker, D.K., Taylor, E.B., Schell, J.C., Orsak, T., Boutron, A., Chen, Y.-C., Cox, J.E., Cardon, C.M., Van Vranken, J.G., Dephoure, N., et al. (2012). A mitochondrial pyruvate carrier required for pyruvate uptake in yeast, Drosophila, and humans. Science *337*, 96–100.

Burhans, W.C., and Weinberger, M. (2009). Acetic acid effects on aging in budding yeast: are they relevant to aging in higher eukaryotes? Cell Cycle *8*, 2300–2302.

Burtner, C.R., Murakami, C.J., Kennedy, B.K., and Kaeberlein, M. (2009). A molecular mechanism of chronological aging in yeast. Cell Cycle *8*, 1256–1270.

Cai, L., Sutter, B.M., Li, B., and Tu, B.P. (2011). Acetyl-CoA induces cell growth and proliferation by promoting the acetylation of histones at growth genes. Mol. Cell *42*, 426–437.

Chen, H.-Y., and White, E. (2011). Role of autophagy in cancer prevention. Cancer Prev. Res. *4*, 973–983.

Choudhary, C., Kumar, C., Gnad, F., Nielsen, M.L., Rehman, M., Walther, T.C., Olsen, J.V., and Mann, M. (2009). Lysine acetylation targets protein complexes and co-regulates major cellular functions. Science *325*, 834–840.

Dang, W., Steffen, K.K., Perry, R., Dorsey, J.A., Johnson, F.B., Shilatifard, A., Kaeberlein, M., Kennedy, B.K., and Berger, S.L. (2009). Histone H4 lysine 16 acetylation regulates cellular lifespan. Nature *459*, 802–807.

Eisenberg, T., Knauer, H., Schauer, A., Büttner, S., Ruckenstuhl, C., Carmona-Gutierrez, D., Ring, J., Schroeder, S., Magnes, C., Antonacci, L., et al. (2009). Induction of autophagy by spermidine promotes longevity. Nat. Cell Biol. *11*, 1305–1314.

Fleck, C.B., and Brock, M. (2009). Re-characterisation of Saccharomyces cerevisiae Ach1p: fungal CoA-transferases are involved in acetic acid detoxification. Fungal Genet. Biol. *46*, 473–485.

Fontana, L., Partridge, L., and Longo, V.D. (2010). Extending healthy life span—from yeast to humans. Science *328*, 321–326.

Füllgrabe, J., Lynch-Day, M.A., Heldring, N., Li, W., Struijk, R.B., Ma, Q., Hermanson, O., Rosenfeld, M.G., Klionsky, D.J., and Joseph, B. (2013). The histone H4 lysine 16 acetyltransferase hMOF regulates the outcome of autophagy. Nature *500*, 468–471.

Füllgrabe, J., Klionsky, D.J., and Joseph, B. (2014). The return of the nucleus: transcriptional and epigenetic control of autophagy. Nat. Rev. Mol. Cell Biol. *15*, 65–74.

Geeraert, C., Ratier, A., Pfisterer, S.G., Perdiz, D., Cantaloube, I., Rouault, A., Pattingre, S., Proikas-Cezanne, T., Codogno, P., and Poüs, C. (2010). Starvation-induced hyperacetylation of tubulin is required for the stimulation of autophagy by nutrient deprivation. J. Biol. Chem. *285*, 24184–24194.

Gelino, S., and Hansen, M. (2012). Autophagy—an emerging anti-aging mechanism. J. Clin. Exp. Pathol. Suppl. *4*, 006.

Guan, K.-L., and Xiong, Y. (2011). Regulation of intermediary metabolism by protein acetylation. Trends Biochem. Sci. *36*, 108–116.

Gupta, V.K., Scheunemann, L., Eisenberg, T., Mertel, S., Bhukel, A., Koemans, T.S., Kramer, J.M., Liu, K.S.Y., Schroeder, S., Stunnenberg, H.G., et al. (2013). Restoring polyamines protects from age-induced memory impairment in an autophagy-dependent manner. Nat. Neurosci. *16*, 1453–1460.

He, C., and Klionsky, D.J. (2009). Regulation mechanisms and signaling pathways of autophagy. Annu. Rev. Genet. *43*, 67–93.

Houtkooper, R.H., Williams, R.W., and Auwerx, J. (2010). Metabolic networks of longevity. Cell *142*, 9–14.

Kaeberlein, M. (2010). Lessons on longevity from budding yeast. Nature *464*, 513–519.

Kaelin, W.G., Jr., and McKnight, S.L. (2013). Influence of metabolism on epigenetics and disease. Cell *153*, 56–69.

Kenyon, C.J. (2010). The genetics of ageing. Nature *464*, 504–512.

Kirisako, T., Baba, M., Ishihara, N., Miyazawa, K., Ohsumi, M., Yoshimori, T., Noda, T., and Ohsumi, Y. (1999). Formation process of autophagosome is traced with Apg8/Aut7p in yeast. J. Cell Biol. *147*, 435–446.

Klionsky, D.J., Cuervo, A.M., and Seglen, P.O. (2007). Methods for monitoring autophagy from yeast to human. Autophagy *3*, 181–206.

Kroemer, G., Mariño, G., and Levine, B. (2010). Autophagy and the integrated stress response. Mol. Cell *40*, 280–293.

Lee, I.H., Cao, L., Mostoslavsky, R., Lombard, D.B., Liu, J., Bruns, N.E., Tsokos, M., Alt, F.W., and Finkel, T. (2008). A role for the NAD-dependent deacetylase Sirt1 in the regulation of autophagy. Proc. Natl. Acad. Sci. USA *105*, 3374–3379.

Longo, V.D., Shadel, G.S., Kaeberlein, M., and Kennedy, B. (2012). Replicative and chronological aging in *Saccharomyces cerevisiae*. Cell Metab. *16*, 18–31.

Lu, C., and Thompson, C.B. (2012). Metabolic regulation of epigenetics. Cell Metab. *16*, 9–17.

Madeo, F., Tavernarakis, N., and Kroemer, G. (2010a). Can autophagy promote longevity? Nat. Cell Biol. *12*, 842–846.

Madeo, F., Eisenberg, T., Büttner, S., Ruckenstuhl, C., and Kroemer, G. (2010b). Spermidine: a novel autophagy inducer and longevity elixir. Autophagy *6*, 160–162.

Mizushima, N., and Komatsu, M. (2011). Autophagy: renovation of cells and tissues. Cell *147*, 728–741.

Morselli, E., Mariño, G., Bennetzen, M.V., Eisenberg, T., Megalou, E., Schroeder, S., Cabrera, S., Bénit, P., Rustin, P., Criollo, A., et al. (2011). Spermidine and resveratrol induce autophagy by distinct pathways converging on the acetylproteome. J. Cell Biol. *192*, 615–629.

Noda, T., and Klionsky, D.J. (2008). The quantitative Pho8Delta60 assay of nonspecific autophagy. Methods Enzymol. *451*, 33–42.

Ocampo, A., Liu, J., Schroeder, E.A., Shadel, G.S., and Barrientos, A. (2012). Mitochondrial respiratory thresholds regulate yeast chronological life span and its extension by caloric restriction. Cell Metab. *16*, 55–67.

Orlandi, I., Casatta, N., and Vai, M. (2012). Lack of Ach1 CoA-transferase triggers apoptosis and decreases chronological lifespan in yeast. Front. Oncol. *2*, 67.

Pan, Y., Schroeder, E.A., Ocampo, A., Barrientos, A., and Shadel, G.S. (2011). Regulation of yeast chronological life span by TORC1 via adaptive mitochondrial ROS signaling. Cell Metab. *13*, 668–678.

Rubinstein, A.D., and Kimchi, A. (2012). Life in the balance—a mechanistic view of the crosstalk between autophagy and apoptosis. J. Cell Sci. *125*, 5259–5268.

Rubinsztein, D.C., Mariño, G., and Kroemer, G. (2011). Autophagy and aging. Cell *146*, 682–695.

Sadoul, K., Wang, J., Diagouraga, B., and Khochbin, S. (2011). The tale of protein lysine acetylation in the cytoplasm. J. Biomed. Biotechnol. *2011*, 970382.

Settembre, C., Di Malta, C., Polito, V.A., Garcia Arencibia, M., Vetrini, F., Erdin, S., Erdin, S.U., Huynh, T., Medina, D., Colella, P., et al. (2011). TFEB links autophagy to lysosomal biogenesis. Science *332*, 1429–1433.

Shimazu, T., Hirschey, M.D., Huang, J.Y., Ho, L.T., and Verdin, E. (2010). Acetate metabolism and aging: an emerging connection. Mech. Ageing Dev. *131*, 511–516.

Simonsen, A., Cumming, R.C., Brech, A., Isakson, P., Schubert, D.R., and Finley, K.D. (2008). Promoting basal levels of autophagy in the nervous system enhances longevity and oxidant resistance in adult Drosophila. Autophagy *4*, 176–184.

Takahashi, H., McCaffery, J.M., Irizarry, R.A., and Boeke, J.D. (2006). Nucleocytosolic acetyl-coenzyme a synthetase is required for histone acetylation and global transcription. Mol. Cell *23*, 207–217.

van den Berg, M.A., de Jong-Gubbels, P., Kortland, C.J., van Dijken, J.P., Pronk, J.T., and Steensma, H.Y. (1996). The two acetyl-coenzyme A synthetases of Saccharomyces cerevisiae differ with respect to kinetic properties and transcriptional regulation. J. Biol. Chem. *271*, 28953–28959.

Wei, M., Fabrizio, P., Madia, F., Hu, J., Ge, H., Li, L.M., and Longo, V.D. (2009). Tor1/Sch9-regulated carbon source substitution is as effective as calorie restriction in life span extension. PLoS Genet. *5*, e1000467.

Wellen, K.E., Hatzivassiliou, G., Sachdeva, U.M., Bui, T.V., Cross, J.R., and Thompson, C.B. (2009). ATP-citrate lyase links cellular metabolism to histone acetylation. Science *324*, 1076–1080.

Xie, R., Nguyen, S., McKeehan, W.L., and Liu, L. (2010). Acetylated microtubules are required for fusion of autophagosomes with lysosomes. BMC Cell Biol. *11*, 89.

Yi, C., Ma, M., Ran, L., Zheng, J., Tong, J., Zhu, J., Ma, C., Sun, Y., Zhang, S., Feng, W., et al. (2012). Function and molecular mechanism of acetylation in autophagy regulation. Science *336*, 474–477.

Yorimitsu, T., Zaman, S., Broach, J.R., and Klionsky, D.J. (2007). Protein kinase A and Sch9 cooperatively regulate induction of autophagy in Saccharomyces cerevisiae. Mol. Biol. Cell *18*, 4180–4189.

Zhao, J., Brault, J.J., Schild, A., Cao, P., Sandri, M., Schiaffino, S., Lecker, S.H., and Goldberg, A.L. (2007). FoxO3 coordinately activates protein degradation by the autophagic/lysosomal and proteasomal pathways in atrophying muscle cells. Cell Metab. *6*, 472–483.

dc_840_14

Hindawi Publishing Corporation
BioMed Research International
Volume 2014, Article ID 470482, 13 pages
http://dx.doi.org/10.1155/2014/470482

Research Article

The Putative HORMA Domain Protein Atg101 Dimerizes and Is Required for Starvation-Induced and Selective Autophagy in *Drosophila*

Krisztina Hegedűs,[1] Péter Nagy,[1] Zoltán Gáspári,[2] and Gábor Juhász[1]

[1] *Department of Anatomy, Cell and Developmental Biology, Eötvös Loránd University, Budapest 1117, Hungary*
[2] *Faculty of Information Technology and Bionics, Pázmány Péter Catholic University, Budapest 1083, Hungary*

Correspondence should be addressed to Gábor Juhász; szmrt@elte.hu

Received 17 January 2014; Accepted 11 March 2014; Published 8 May 2014

Academic Editor: Ioannis P. Nezis

Copyright © 2014 Krisztina Hegedűs et al. This is an open access article distributed under the Creative Commons Attribution License, which permits unrestricted use, distribution, and reproduction in any medium, provided the original work is properly cited.

The large-scale turnover of intracellular material including organelles is achieved by autophagy-mediated degradation in lysosomes. Initiation of autophagy is controlled by a protein kinase complex consisting of an Atg1-family kinase, Atg13, FIP200/Atg17, and the metazoan-specific subunit Atg101. Here we show that loss of Atg101 impairs both starvation-induced and basal autophagy in *Drosophila*. This leads to accumulation of protein aggregates containing the selective autophagy cargo ref(2)P/p62. Mapping experiments suggest that Atg101 binds to the N-terminal HORMA domain of Atg13 and may also interact with two unstructured regions of Atg1. Another HORMA domain-containing protein, Mad2, forms a conformational homodimer. We show that *Drosophila* Atg101 also dimerizes, and it is predicted to fold into a HORMA domain. Atg101 interacts with ref(2)P as well, similar to Atg13, Atg8a, Atg16, Atg18, Keap1, and RagC, a known regulator of Tor kinase which coordinates cell growth and autophagy. These results raise the possibility that the interactions and dimerization of the putative HORMA domain protein Atg101 play critical roles in starvation-induced autophagy and proteostasis, by promoting the formation of protein aggregate-containing autophagosomes.

1. Introduction

Autophagy ensures the lysosome-mediated degradation and recycling of cytoplasmic components including organelles. During the main pathway, a phagophore cistern (also called an isolation membrane) forms and captures cargo destined for breakdown into a double-membrane autophagosome. This vesicle then fuses with a late endosome or lysosome containing acidic hydrolases. Assembly of the phagophore is achieved by the action of Atg proteins. *Atg* genes were originally discovered in yeast, and the majority of them have clear orthologs in higher eukaryotes including animals [1, 2].

Initiation of autophagy usually begins with the activation of an Atg1 protein kinase complex in animal cells, which contains the serine/threonine kinase Atg1 (its orthologs are called UNC51 in worms and ULK1 and 2 in mammals), Atg13, FIP200/Atg17, and the metazoan-specific subunit Atg101 [3]. This complex directly binds to Tor (target of rapamycin) kinase, which is active when bound to digesting lysosomes and promotes cell growth and inhibits autophagy by phosphorylating Atg1 [4, 5]. Autophagy-inducing stimuli such as starvation rapidly lead to inactivation of Tor and induction of Atg1-dependent autophagy [3, 6]. This results in the removal of inhibitory phosphogroups from Atg1 by poorly characterized phosphatases, which may potentially include PP2A [7]. Atg1 then undergoes autophosphorylation on residues separate from those phosphorylated by Tor and also phosphorylates downstream targets including Atg13 [3, 8, 9]. Overexpression of Atg1 strongly promotes autophagy in *Drosopohila*, while expression of a kinase dead form suppresses starvation-induced autophagy [10].

It is largely unknown how the Atg1 kinase complex transmits its autophagy-inducing signal to downstream components, which include an autophagy-specific lipid kinase complex, phospholipid effectors such as Atg18, the transmembrane protein Atg9, and two protein conjugation systems that

include the ubiquitin-like Atg8 family proteins [1, 3]. Atg8 is conjugated to phosphatidylethanolamine, and thus it is bound to phagophore and autophagosome membranes [11, 12]. Atg8, and its mammalian homologs such as LC3, binds to cargo receptors including p62 to mediate the selective autophagic breakdown of ubiquitinated protein aggregates [13, 14]. Ref(2)P, the fly homolog of p62, is required for the formation of these protein aggregates in *Drosopohila* [15].

FIP200/Atg17 is thought to act as a scaffold protein in the Atg1 kinase complex, whereas the role of the metazoan-specific subunit Atg101 is poorly characterized [3]. Atg101 (also known as C12orf44) is a subunit of the Atg1/ULK complex in human cells, and shRNA depletion of *Atg101* impairs autophagy in mammalian cells [16, 17]. Moreover, the *Atg101* ortholog *epg-9* has recently been shown to be required for degradation of P granule aggregates in worm embryos as well [18]. As the precise role of Atg101 in autophagy is unclear, we decided to analyze its function in *Drosopohila*.

2. Materials and Methods

2.1. Drosopohila Genetics. Flies were reared on standard yeast-cornmeal-agar medium (fed), and mid-L3 stage larvae were transferred to a 20% sucrose solution for 3 h for starvation experiments. Fat body cell clones expressing RNAi constructs *Atg101[KK106176]* and *Atg101[HMS01349]* were generated spontaneously, as described in detail previously [19–22].

2.2. Histology. Dissected larval carcasses were incubated in a solution of LysoTracker Red (LTR) and DAPI as before [19–23]. Fixed samples were processed for indirect immunofluorescence using rat anti-Atg8a [9] and rabbit anti-ref(2)P [22] and imaged as described in detail previously [19, 20, 22]. Dissected fat body lobes containing *Atg101* RNAi clones were attached to poly-L-lysine-coated coverslips in PBS, photographed live to record the position of GFP-positive cells, fixed and embedded into Durcupan (Fluka), and then sectioned and analyzed by transmission electron microscopy as described [19, 21]. Statistical analysis was carried out as described [19, 20]. *N* refers to the number of animals, and multiple cells were evaluated from each animal.

2.3. RT-PCR. Total RNA was isolated from starved L3 stage larvae of the genotypes *w[1118]* (used as wild type), *Atg101[KK106176]/+*, *Act-Gal4/+*, and *Atg101[HMS01349]/Act-Gal4* using PureLink RNA Mini Kit (Invitrogen), followed by preparation of cDNAs using RevertAid First Strand cDNA Synthesis Kit (Thermo) and RNase free DNase I (Sigma). PCR reactions on cDNA samples were performed with the following primers: TACTCCTCCCGACACAAAGC, CTGGGTCATCTTCTCACGGT for *Actin5C* (23 amplification cycles), and ATGAACGCGCGTTCGCAG, TCACATTGCGAGCGTTTCCT for *Atg101* (25 amplification cycles). Parallel reactions were performed without adding reverse transcriptase to control for DNA contamination. As expected, no PCR products were obtained in these experiments.

2.4. Cell Culture and Immunoprecipitations. *Drosopohila* D.Mel-2 cells (Invitrogen) were used for transfection and immunoprecipitation experiments as recently described elsewhere [9, 19, 20]. The following constructs were used in coimmunoprecipitation experiments: an N-terminally truncated 3xFLAG-ref(2)P lacking the PB1 domain mediating self-aggregation, 3xHA-Keap1 [20], 3xHA-Atg18 [24], 3xHA-Atg101, full-length 3xHA-Atg13 and its N-terminal, middle, and C-terminal fragments [9], and kinase dead myc-Atg1 [8]. 3xHA-Atg8a, 3xHA-Atg16, 3xHA-RagC, 3xFLAG-Atg101, and Atg101-3xFLAG were generated by PCR amplifying the full-length coding sequences from a cDNA sample and cloning these into appropriate UAS vectors, respectively. GST coding sequence was PCR amplified and cloned into a UAS-3xHA vector downstream of the HA tag. 3xHA-GST-Atg1 constructs were generated by PCR amplifying and cloning the appropriate Atg1 fragments downstream of GST.

2.5. Bioinformatics. Sequence analysis and motif search were performed using the NCBI BLAST service as well as the Pfam (version 27.0) and Prosite (release 20.97) databases and their associated search tools. Alignments of orthologous sequences were extracted from OMA groups as cross-linked to the corresponding SwissProt entries [25]. For structure prediction, the I-TASSER and Phyre2 servers were used [26, 27]. Pairwise and multiple structural alignments were done with DaliLite and MAMMOTH-Mult, respectively [28, 29]. The ANCHOR and IUPred servers were used to predict unstructured regions and potential binding sites within these regions in fly Atg1, Atg13, and Atg101 [30, 31]. Structure visualization was performed using UCSF Chimera [32] and the Prosite HORMA logo was reproduced with WebLogo [33]. The alignment of human, fly, and worm Atg101 was generated using CLUSTALW and colored with TEXSHADE at the Biology Workbench server [34].

3. Results and Discussion

3.1. Drosopohila Atg101 Is Required for Starvation-Induced Autophagy. BLAST searches reveal that *Drosopohila* Atg101 shares 51% amino acid identity (111/218) and 71% similarity (156/218) with human Atg101 and 33% amino acid identity (81/244) and 46% similarity (113/244) with isoform a of worm Atg101/EPG-9, respectively (Figure 1), suggesting that it is an ortholog of Atg101 proteins. Two separate transgenic RNAi lines are available from public stock centers that allow inducible silencing of *Drosopohila Atg101*, both integrated into specific, nonrandom landing sites in the genome. *Atg101[KK]* is based on a long hairpin, while *Atg101[HMS]* contains a short, microRNA-based duplex RNA that targets a 22-nucleotide sequence in the 3′ untranslated region of the endogenous mRNA. LysoTracker Red (LTR) is widely used for the labeling of acidic autolysosomes in the larval *Drosophila* fat body, as this vital dye shows little to no punctate staining in fat body cells of well-fed larvae [9, 19, 23, 35]. Expression of either of the *Atg101* RNAi constructs in GFP-marked cell clones prevents starvation-induced LysoTracker Red- (LTR-) positive autolysosome formation (Figures 2(a),

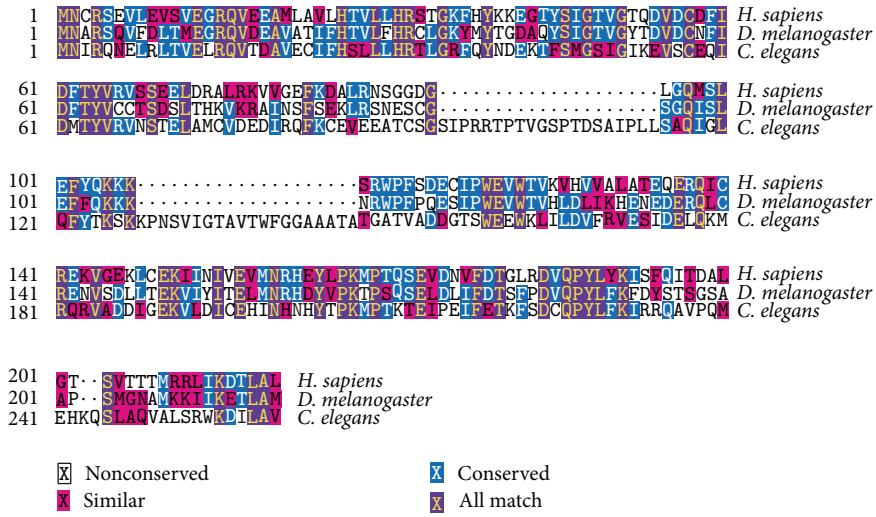


Figure 1: Multiple sequence alignments of human, fly, and worm Atg101 proteins.

2(b), and 2(c)). As expected, systemic expression of either of these transgenic RNAi lines strongly decreases endogenous *Atg101* mRNA levels (Figure 2(d)). Depletion of *Atg101* also impairs the distribution of endogenous Atg8a, as instead of the numerous small Atg8a-positive autophagosomes seen in control cells, fewer but larger Atg8a structures are observed in GFP-marked *Atg101* knockdown cells (Figures 3(a), 3(b), and 3(d)). This may not be simply due to incomplete gene silencing, as these aberrant Atg8a-positive structures are also seen upon simultaneous expression of both *Atg101* RNAi constructs (Figures 3(c) and 3(d)). This phenotype is very similar to the accumulation of Atg8/LGG-1 aggregates reported in *Atg101/epg-9* mutant worms [18]. The enlarged Atg8a structures observed in *Atg101* RNAi cells of starved animals colocalize with protein aggregates containing the specific autophagy cargo ref(2)P (Figure 3(e)). Although it is not possible to conclude that Atg101 is not required for Atg8a recruitment to ref(2)P aggregates solely based on RNAi experiments, this seems to be a possibility, which is also supported by data from mutant worms. Interestingly, of the core *Atg* genes, *Atg2* has also been shown to be dispensable for Atg8a recruitment to the phagophore assembly site and protein aggregates in worm, fly, and mammalian cells [19, 24, 36, 37]. To exclude the possibility that these Atg8a dots might represent autophagosomes, we carried out electron microscopy. Ultrastructural analysis indeed revealed that autophagosome formation is blocked in *Atg101* RNAi cells (Figure 4). A potential explanation for the presence of a few enlarged Atg8a-positive dots in *Atg101* loss-of-function cells but not in *FIP200* null mutants [9] may be that mammalian Atg8 homologs have been shown to directly bind to FIP200, Atg13, and Atg1/ULKs [38]. These Atg1 kinase subunits may facilitate the recruitment of Atg8a to aggregates containing ref(2)P and ubiquitinated proteins, which have been proposed to act as scaffolds for autophagosome biogenesis, both in mammals and *Drosophila* [9, 24, 39].

3.2. Drosopohila Atg101 Is Required for Selective Basal Autophagy of Ref(2)P-Containing Protein Aggregates. Ref(2)P appears to be selectively degraded by autophagy all the time, independent of the induction conditions such as starvation or developmental contexts, similar to its mammalian homolog p62 [24, 40]. Continuous basal autophagy is usually difficult to be visualized directly, due to its low levels. For this reason, assessing basal autophagic activity by looking at levels of ref(2)P has become a standard test, similar to mammals [14, 19, 22, 41, 42]. Expression of either of the two *Atg101* silencing constructs results in large-scale accumulation of ref(2)P aggregates in GFP-marked cells, when compared to surrounding wild-type tissue in well-fed larvae (Figures 5(a), 5(b), and 5(c)), indicating defects in selective basal autophagy.

3.3. Atg101 Interacts with Atg1. The Atg13, FIP200, and ULK1 subunits of the mammalian Atg1/ULK kinase complex have been shown to bind to Atg101 in coimmunoprecipitation experiments on the level of endogenous proteins [16]. Atg101 directly binds to Atg13 in mammals, and the Atg101 ortholog EPG-9 was recently proposed to directly interact with the Atg1 ortholog UNC-51 as well in *C. elegans* [16–18]. In line with these studies, we found that myc-tagged, kinase dead Atg1 coimmunoprecipitates with Atg101 in cultured *Drosopohila* cells (Figure 6(a)). We used the kinase dead form because wild-type Atg1 is expressed poorly in cultured cells, and it also reduces the expression of other transgenes, likely due to Atg1-mediated feedback inhibition of Tor-dependent translation [9, 10, 43]. To determine which regions of the 835 amino acid long Atg1 protein are involved in its interaction with Atg101, we generated four HA-GST-tagged constructs for different Atg1 fragments. The N-terminal kinase domain was not included in these experiments, as again it is expressed poorly and strongly impairs the expression of coexpressed constructs [9]. We decided to search for potential Atg101

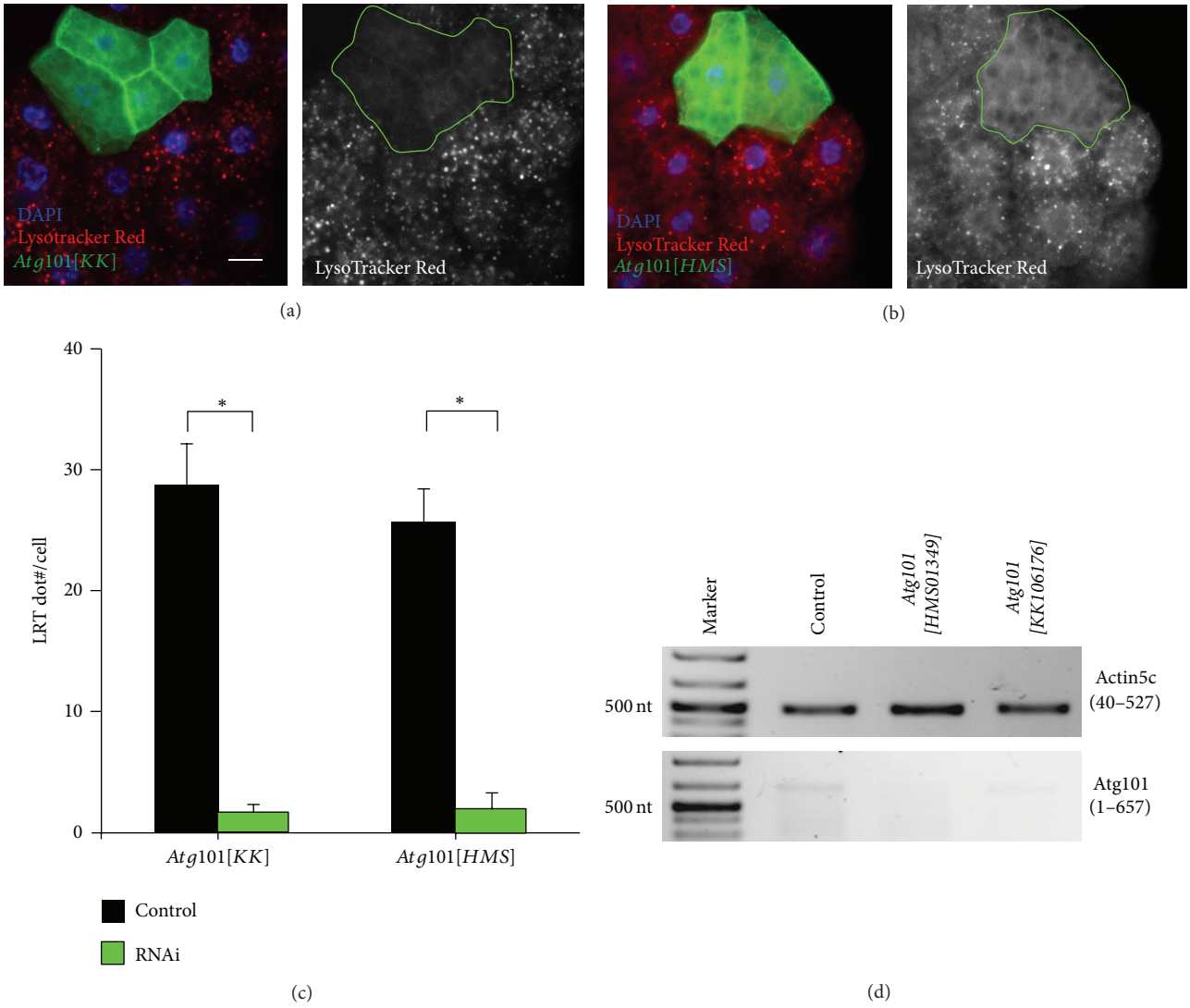


Figure 2: RNAi depletion of *Atg101* by expression of a long hairpin (a) or a microRNA-based silencing construct (b) in clones of cells marked by membrane-bound mCD8-GFP prevents starvation-induced punctate LysoTracker Red (LTR) staining, compared to surrounding control fat body cells of third instar larvae. (c) Quantification of data shown in (a) and (b), $N = 5$, $P < 0.001$, two-tailed, two-sample Student's *t*-tests. (d) Reverse Transcriptase-PCR analysis reveals that *Atg101* mRNA expression is strongly reduced upon expression of *Atg101[KK],* and it is undetectable in *Atg101[HMS]* expressing animals compared to wild type L3 stage larvae. Note that the expression level of *Atg101* is much lower than that of *Actin5C*, a commonly used control in such experiments. Numbers in parentheses indicate the amplified region of the coding sequence of these genes. Scalebar equals 20 μm for microscopic images.

binding sites in the middle region (amino acids 233–725) of Atg1, because the N-terminal kinase domain is the only known domain in this protein, and the C-terminal region is involved in its binding to Atg13 [44]. The rest of the protein is predicted to be mostly unstructured by the IUPRED server, and the ANCHOR method identifies numerous potential binding sites within these unstructured regions. We found that Atg101-FLAG coimmunoprecipitates with two Atg1 fragments containing either amino acids 233–360 or 565–725 but not with fragments containing amino acids 364–459 or 461–570 (Figures 6(b) and 6(c)). These results suggest that Atg101 interacts with multiple regions in Atg1 either directly or indirectly.

3.4. Atg101 Binds to the HORMA Domain of Atg13, and It Can Dimerize. Coimmunoprecipitations showed that full-length HA-Atg13 binds to Atg101-FLAG (Figure 7(b)), in line with data from mammals [16, 17]. Mapping experiments revealed that only those regions of Atg13 coprecipitate with Atg101 that contain amino acids 1–230, whereas the unstructured middle and C-terminal regions do not show binding (Figures 7(a) and 7(b)). The N-terminal part of Atg13 folds into a HORMA (Hop1, Rev1, and Mad2) domain similar to that of Mad2, a spindle checkpoint protein [45]. Mad2 forms a conformational homodimer, as its dimerization requires the binding of two different stable conformations to each other: open, O-Mad2, and closed, C-Mad2 [46]. Since the Atg13

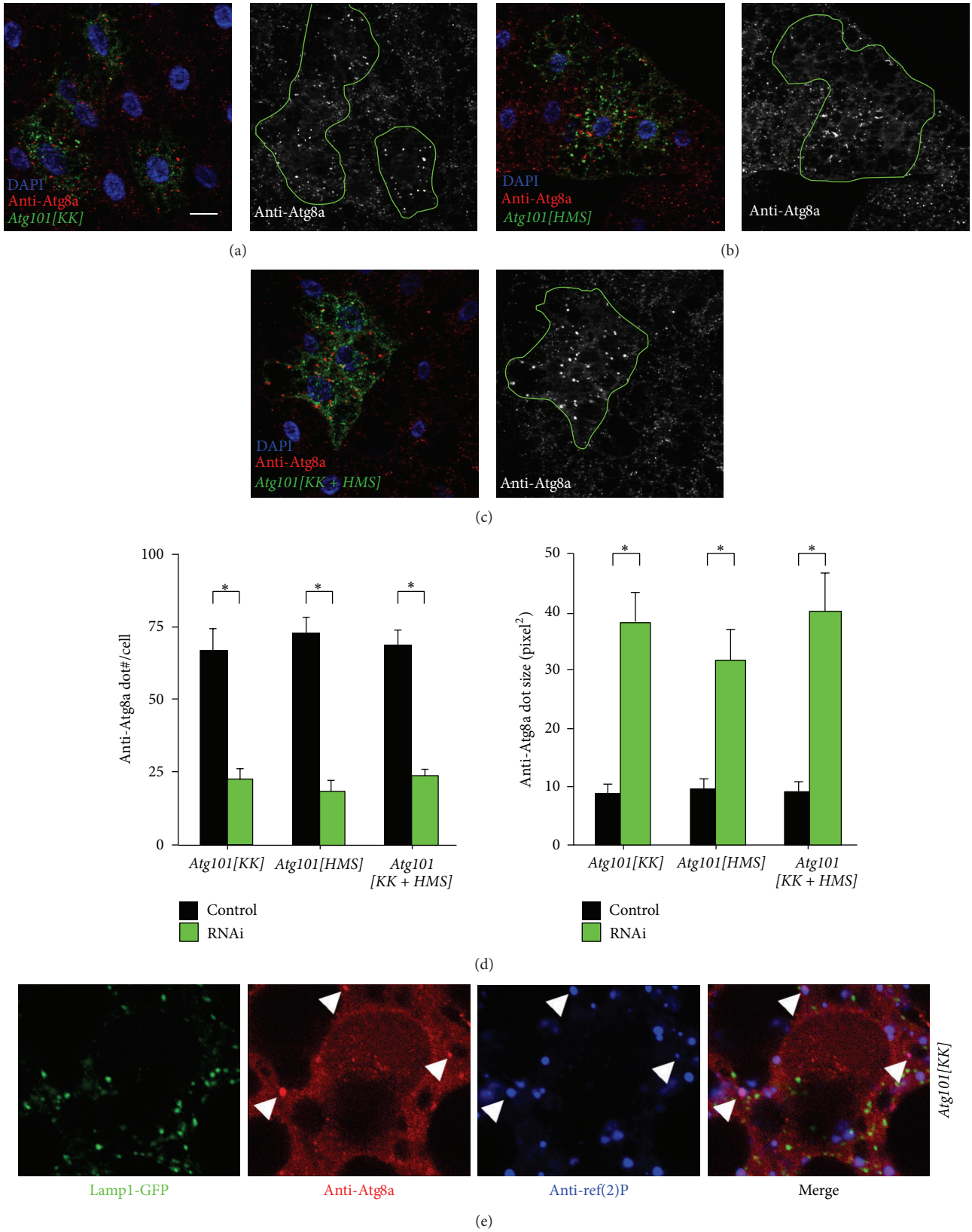


Figure 3: Knockdown of *Atg101* using separate RNAi lines ((a), (b)), or the combination of both (c), impairs the formation of Atg8a-positive autophagosomes upon starvation. Note that fewer but bigger Atg8a puncta are seen in Lamp1-GFP-marked RNAi cells than in neighboring control fat body cells. (d) Quantification of data shown in (a) to (c), $N = 5$, $P < 0.001$, two-tailed, two-sample Student's t-tests. (e) Overlapping Atg8a and ref(2)P structures are highlighted by arrowheads in *Atg101* depleted cells. Scalebar equals 20 μm.

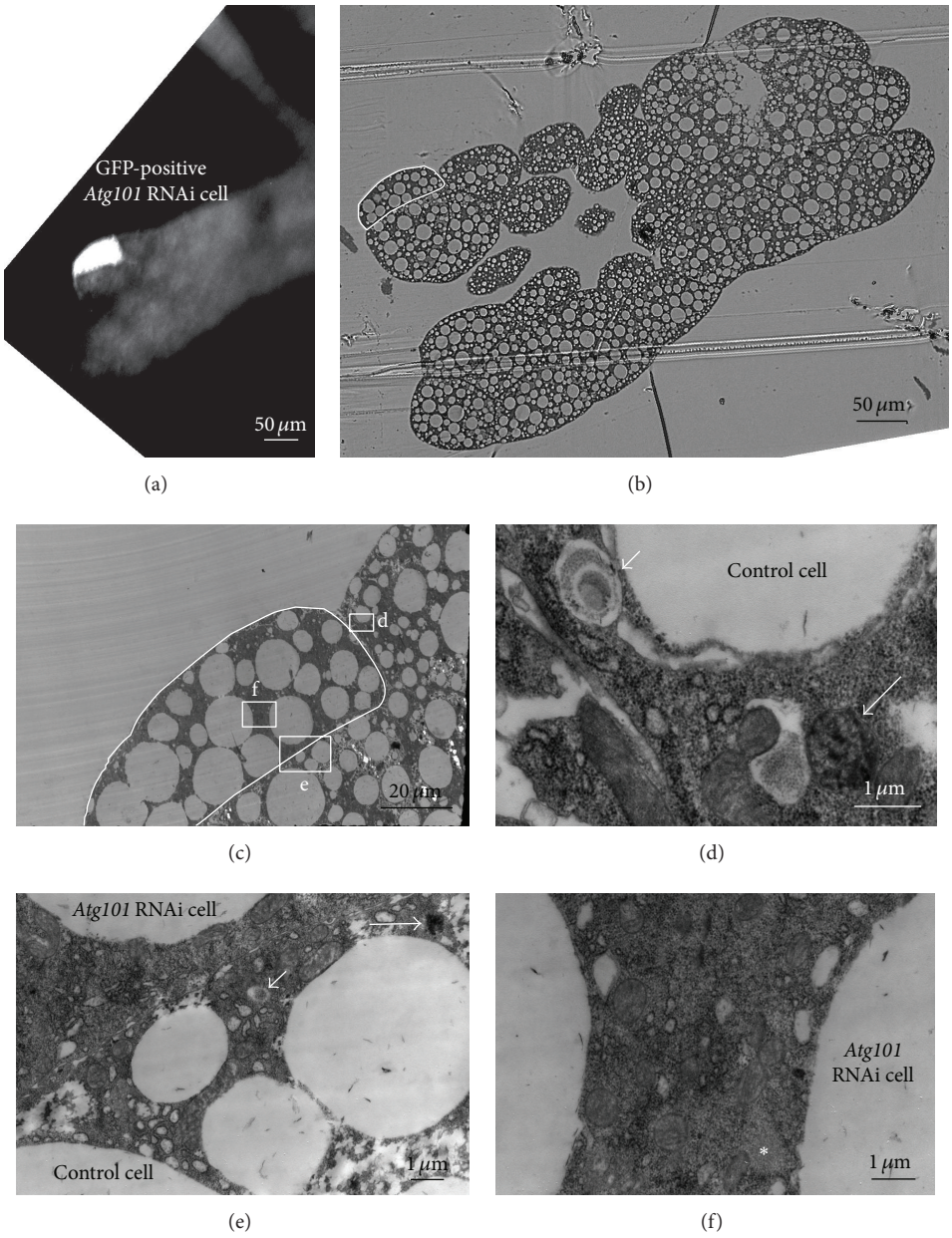


Figure 4: Ultrastructural analysis of *Atg101[KK+HMS]* RNAi cells. A fat body lobe containing a single GFP-marked RNAi cell (a) was embedded in plastic, and the same cell is highlighted in semithin (b) and low-magnification ultrastructural images (c). High magnification images show autophagosomes (short arrows) and autolysosomes (long arrows) in control cells ((d), and also in (e), bottom). The generation of such autophagic structures is inhibited in *Atg101* RNAi cells ((e), top, and (f)). Asterisk marks a potential cytoplasmic protein aggregate, which can be recognized by its homogenous appearance and exclusion of organelles and ribosomes.

HORMA domain is similar to C-Mad2 [45], we hypothesized that Atg101 may potentially be a HORMA domain protein as well, perhaps capable of forming either an O-Mad2 state or both O-Mad2 and C-Mad2 states. To study this model further, we first determined the interaction of Atg101 with itself. We found that Atg101-FLAG coprecipitates with HA-Atg101, and vice versa HA-Atg101 coprecipitates with Atg101 tagged by FLAG on either its N- or C-terminus (Figure 7(c)), suggesting that Atg101 dimerizes.

3.5. Atg101 Is Potentially a HORMA Domain Protein. Atg101 is classified as a single-domain protein with a domain of unknown function (DUF1649 in Pfam), with no trivially detectable relatives of known structure. Basic structural predictions suggest that it is a structured globular cytoplasmic protein. Results obtained with I-TASSER and Phyre2 indicate that the protein might have a HORMA domain fold. Both servers identified templates with HORMA fold and three of I-TASSER's 5 predicted structures have a fold similar to

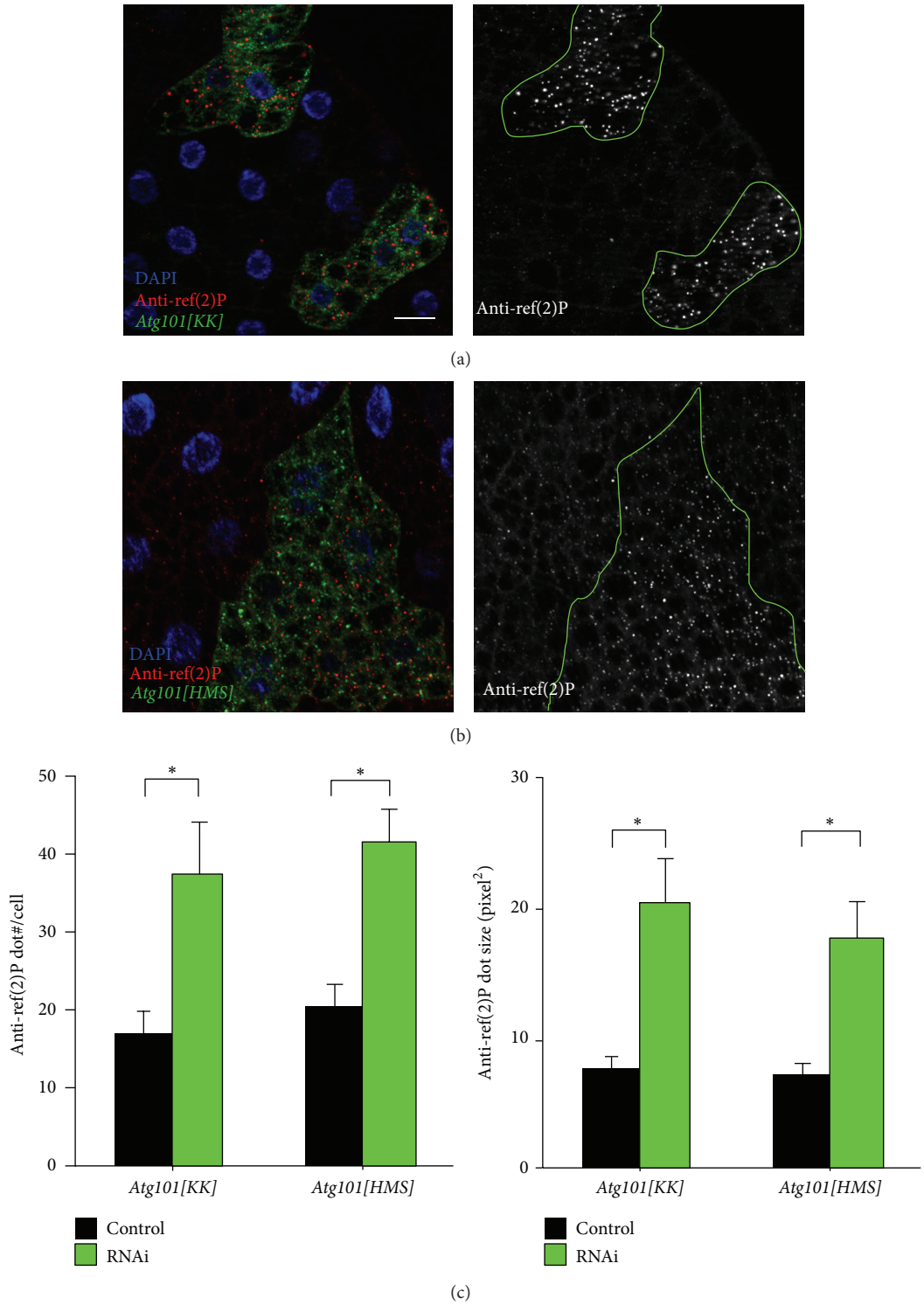


FIGURE 5: Depletion of *Atg101* in Lamp1-GFP-marked fat body cells of well-fed larvae results in the accumulation of ref(2)P aggregates ((a), (b)). (c) Quantification of data shown in (a) and (b), $N = 5$, $P < 0.001$, two-tailed, two-sample Student's t-tests. Scalebar equals 20 μm.

each other as well as the Atg13 and Mad2 HORMA domains (Figure 8). Moreover, the model predicted by Phyre2 also has a HORMA-like structural core (not shown). To assess the plausibility of this hypothesis, we created a multiple structure alignment of the best I-TASSER model of Atg101 with the known structures of human Mad2 [46] and yeast Atg13 [45], and manually compared it to the HORMA domain profile composed of 33 proteins in Prosite (entry PS50815). Our analysis reveals a number of corresponding sites showing conservation both in the HORMA domains in Prosite and

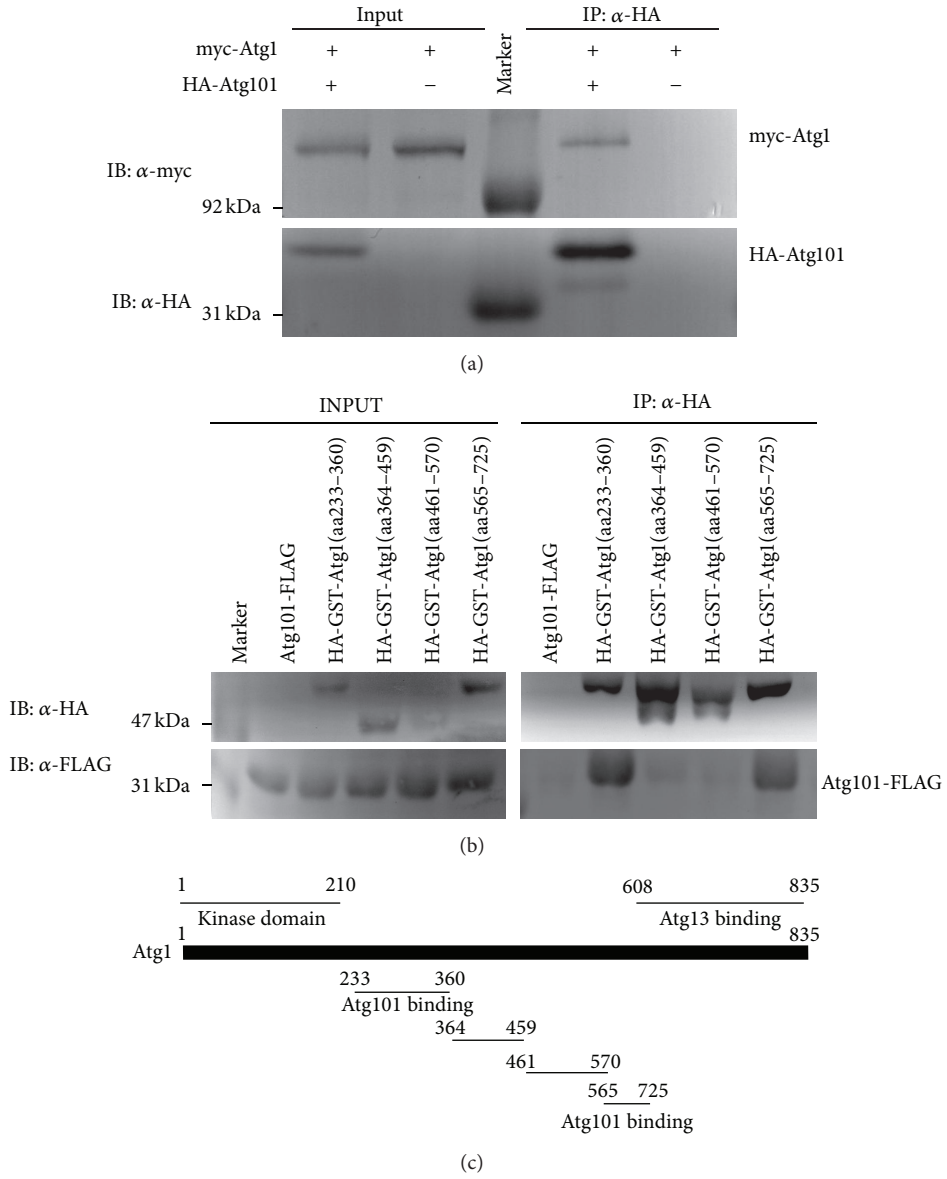


Figure 6: Full-length, kinase dead myc-Atg1 coprecipitates with HA-Atg101 but not with anti-HA beads (a). Atg101-FLAG coprecipitates with HA-GST-tagged Atg1 fragments 233–360 and 565–725 but not with 364–459 and 461–570 (b). Atg1 domain structure [9] and fragments used in mapping experiments (c).

within Atg101 homologs (OMA group 413828 containing Atg101 proteins from 66 different species). In addition, a characteristic pattern of largely conserved Leu/Ile/Val residues in Atg101 proteins and matching hydrophobic residues in the Prosite profile is apparent (Figure 9).

3.6. Atg101 Interacts with Ref(2)P/p62. *Drosopohila* Atg101 was suggested to bind to ref(2)P and also to several subunits of the lysosomal proton pump v-ATPase complex (Vha26, Vha36-1, Vha44, Vha55, and Vha68-2) in a large-scale proteomic study [47]. As we have recently found that the Atg1 kinase subunit FIP200 frequently localizes to ref(2)P aggregates near lysosomes [9], we wished to confirm the proposed interaction of Atg101 with ref(2)P. Indeed, FLAG-tagged ref(2)P coprecipitated with HA-Atg101 (Figure 10(a)). We used HA-Atg8a as a positive control in this experiment, as Atg8 homologs are established binding partners of p62 in mammalian cells, and fly Atg8a has been proposed to bind to ref(2)P through a conserved Atg8 interacting region as well [14, 15, 48]. These data raised the possibility that the entire Atg1 kinase complex may bind to aggregates of ref(2)P and ubiquitinated proteins. Indeed, we found that Atg13 also shows an interaction with ref(2)P, similar to Atg101 (Figure 10(b)). Positive controls that we used in these coimmunoprecipitations include Keap1 and Atg18, both of which have recently been shown to bind to ref(2)P [20, 24]. Ref(2)P coprecipitates with additional critical regulators

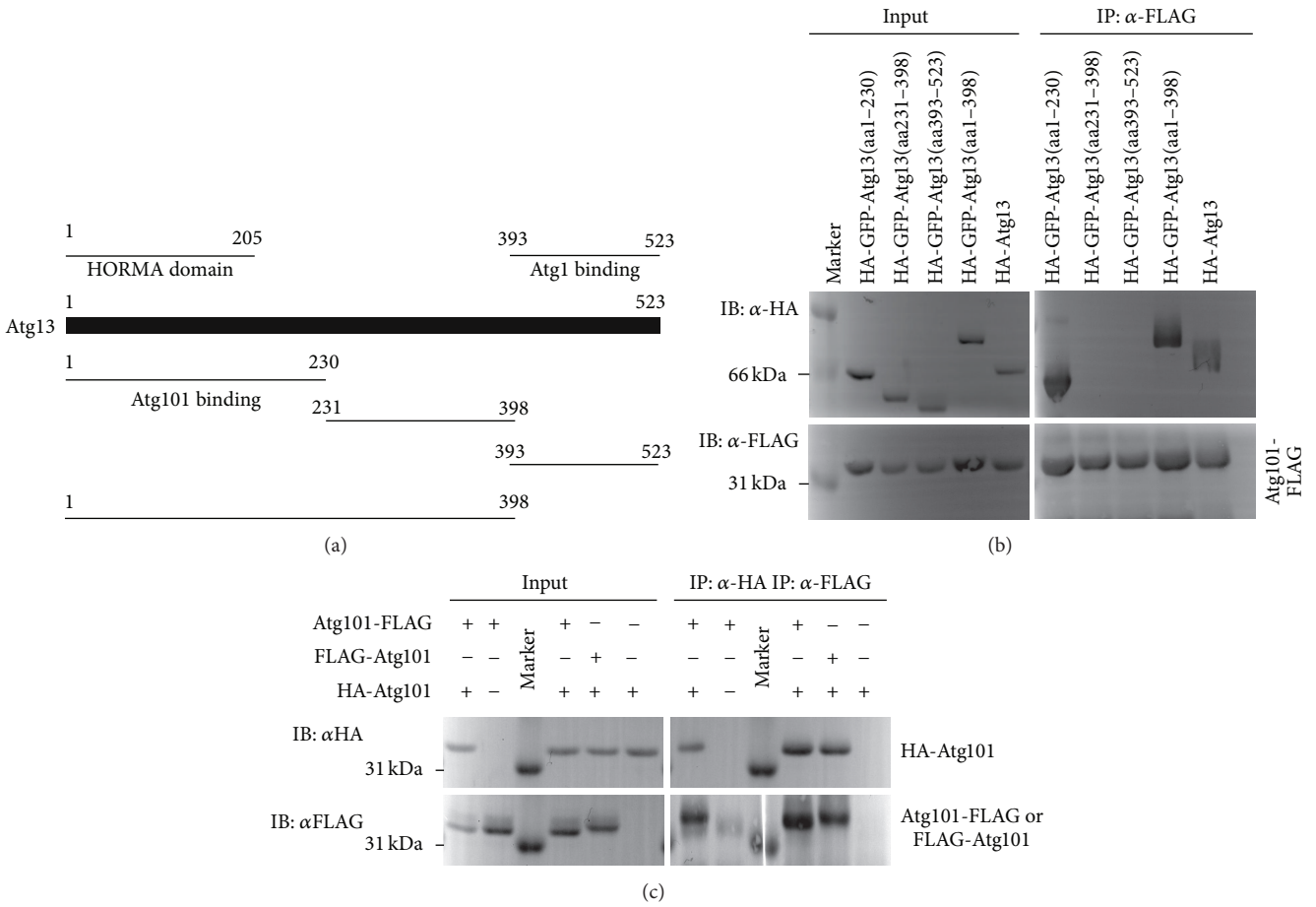


Figure 7: Atg13 domain structure and fragments used in mapping experiments [9] (a). Atg101-FLAG coprecipitates the full-length HA-Atg13, and also HA-GFP-Atg13 fragments containing the N-terminal HORMA domain: 1–230 and 1–398, but not the middle (231–398) or C-terminal (393–523) Atg13 fragments (b). Atg101-FLAG coprecipitates with HA-Atg101, and HA-Atg101 coprecipitates with both FLAG-Atg101 and Atg101-FLAG, but not with anti-HA or anti-FLAG beads alone, respectively (c).

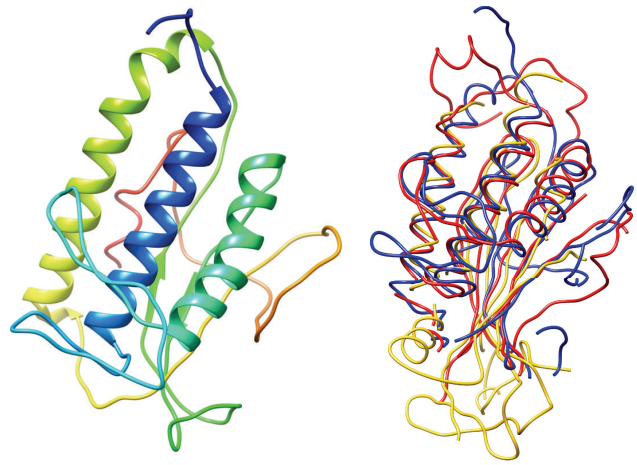


Figure 8: Ribbon representation of the best model of *Drosopohila* Atg101 obtained with I-TASSER (a). Atg101 structure alignment of the best model obtained with I-TASSER (blue), as well as human Mad2 (2V64, chain A, yellow) and Atg13 from the yeast *Lachancea thermotolerans* (4J2G, chain A, red) (b).

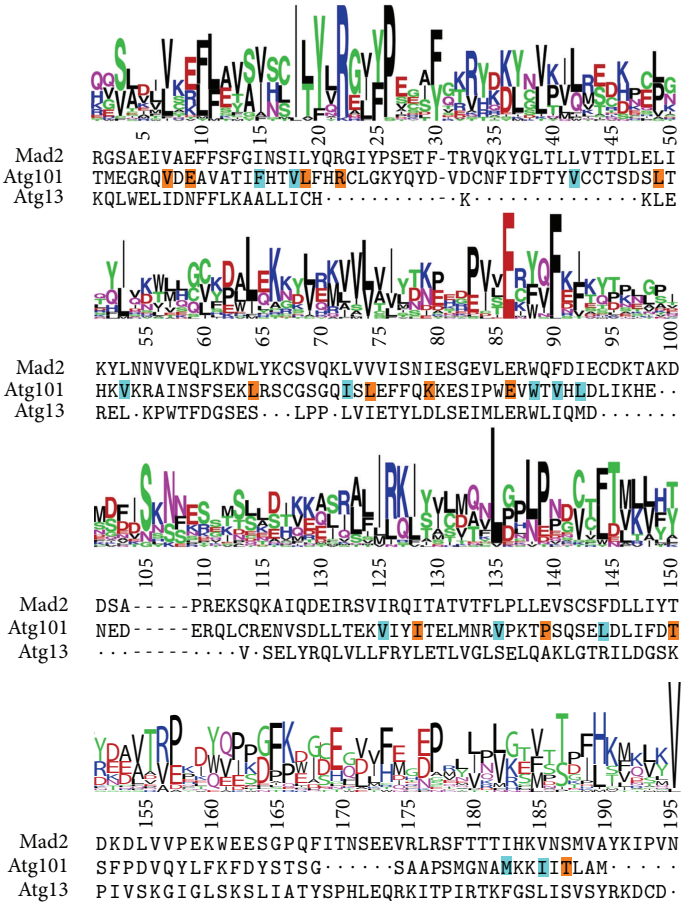


FIGURE 9: Comparison of the Prosite HORMA domain logo with the sequence alignment derived from the multiple structure alignment of the predicted Atg101 structure, Mad2 (2V64, chain A), and Atg13 (4J2G, chain A). Residues in *Drosopohila* Atg101 corresponding to the most frequent one in the Prosite logo and mostly conserved in other Atg101 proteins are highlighted with an orange background. Residues with a similar character to those in the logo and conserved in Atg101 proteins are highlighted with cyan background. Dots denote gaps arisen in the original structural alignment, dashes represent gaps relative to the Prosite logo. Note that the alignment is adjusted to match the full Prosite logo, so insertions relative to that have been removed from all sequences, and thus they do not correspond to the full native ones. In the Prosite logo, positively and negatively charged residues are colored blue and red, respectively; those with hydrophobic side chains are shown in black; Gln and Asn in magenta; other amino acids with hydrophilic side chains and glycine in green.

of autophagy as well: the ubiquitin-binding protein Atg16 [49] and the small GTPase RagC, a known Vha complex-associated regulator of Tor kinase [4], which shows a particularly strong interaction with ref(2)P as inferred from a large-scale proteomic study [47] (Figure 10(b)). These data are in line with the potential role of lysosome-associated protein aggregates as scaffolds for autophagosome biogenesis [9, 24, 39].

4. Conclusions

Our data establish that Atg101 is required for autophagy in *Drosopohila*, and that it is a subunit of the Atg1 kinase complex, similar to mammals and worms [16–18]. The potential binding of Atg101 to Atg1 may involve multiple regions in Atg1, whereas the HORMA domain of Atg13 appears to be the only region important for its interaction with Atg101. Atg101 is a small protein of 218 amino acids, and it is predicted to fold into a globular domain, potentially a HORMA domain. Proteins with such structure often have numerous binding partners, the identity of which determines the open or closed conformation in the case of Mad2 [46]. Our bioinformatics analysis predicts a possible HORMA domain structure for Atg101, and we show that it can indeed dimerize. If Atg101 functions similar to Mad2, then it may perhaps be capable of switching between open and closed conformations and form a conformational homodimer as well. This would represent an elegant way of determining which proteins can bind to Atg101 at one time. This model predicts that Atg101 binds to Atg13 through direct interaction of the two HORMA domains, whereas for some of its other partners (potentially including Atg1), certain oligopeptides located in unstructured regions may engage in an interaction with Atg101, as seen in the case of Mad2 as well [46].

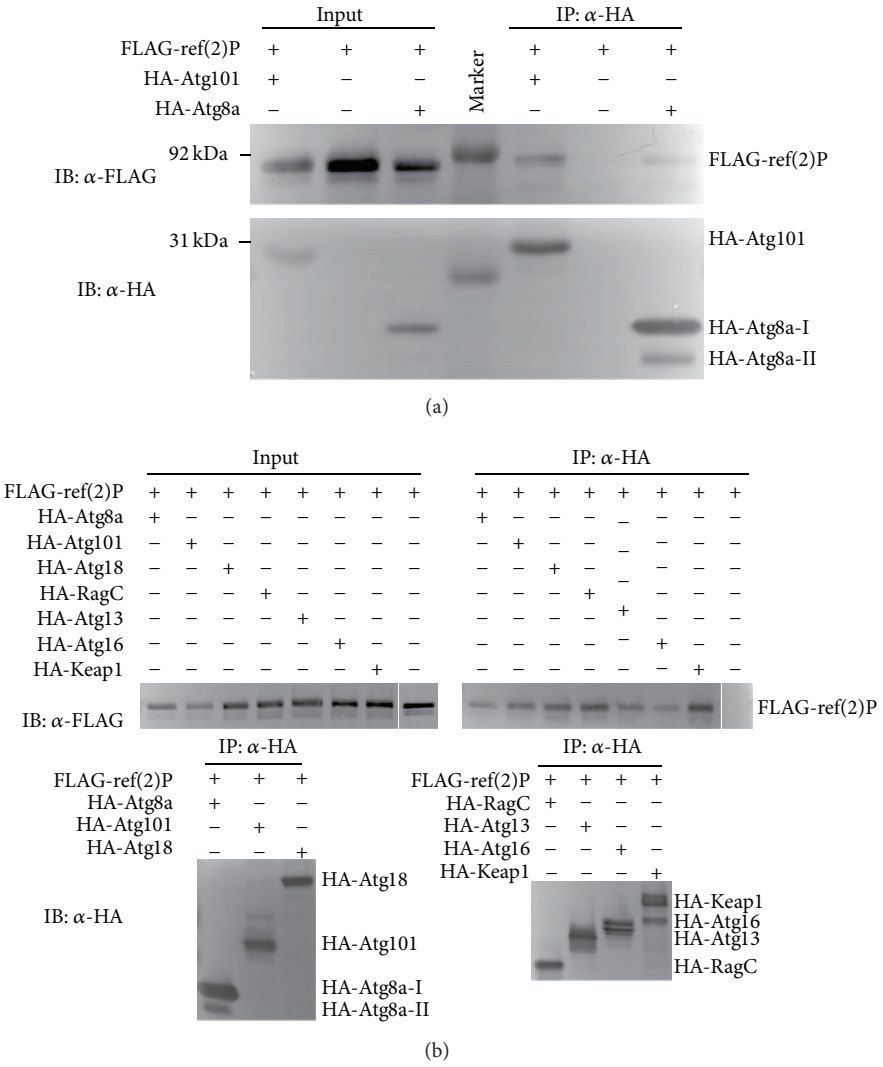


Figure 10: FLAG-tagged ref(2)P coprecipitates with both HA-Atg101 and HA-Atg8a, but not with anti-HA beads (a). Note that HA-Atg8a-II migrates faster than HA-Atg8a-I, due to the covalent attachment of the lipid moiety phosphatidylethanolamine to its C-terminus. (b) The selective autophagy cargo ref(2)P coprecipitates with Atg8a, Atg101, Atg18, RagC, Atg13, Atg16, and Keap1, but not with empty beads.

It is important to emphasize that the HORMA domain structure of Atg101 is not supported experimentally. Further analysis of Atg101 binding partners, fine mapping of the binding sites mediating the interaction of each partner with Atg101, and analysis of the Atg101 domain by structural biochemistry will be necessary to test our hypothetical model presented in this paper. This will be particularly important, as the absence of an Atg101 ortholog in yeast clearly indicates that a metazoan-specific regulatory mechanism has evolved to control the initiation step of autophagy in animal cells.

Conflict of Interests

The authors declare that there is no conflict of interests regarding the publication of this paper.

Acknowledgments

The authors thank Sarolta Pálfia for her excellent technical assistance, László Nyitray, Viktor Kis, and Rita Pancsa for helpful discussions, and stock centers BDSC and VDRC for providing *Atg101* RNAi lines. This work was supported by the Wellcome Trust (087518/Z/08/Z), the Hungarian Scientific Research Fund (OTKA K83509), the European Union (TÁMOP-4.2.1.B-11/2/KMR-2011-0002), and the Hungarian Academy of Sciences (BO/00552/11).

References

[1] D. J. Klionsky, J. M. Cregg, W. A. Dunn Jr. et al., "A unified nomenclature for yeast autophagy-related genes," *Developmental Cell*, vol. 5, no. 4, pp. 539–545, 2003.

[2] B. Erdi, P. Nagy, A. Zvara et al., "Loss of the starvation-induced gene Rack1 leads to glycogen deficiency and impaired autophagic responses in Drosophila," *Autophagy*, vol. 8, pp. 1124–1135, 2012.

[3] N. Mizushima, "The role of the Atg1/ULK1 complex in autophagy regulation," *Current Opinion in Cell Biology*, vol. 22, no. 2, pp. 132–139, 2010.

[4] R. Zoncu, L. Bar-Peled, A. Efeyan, S. Wang, Y. Sancak, and D. M. Sabatini, "mTORC1 senses lysosomal amino acids through an inside-out mechanism that requires the vacuolar H+-ATPase," *Science*, vol. 334, no. 6056, pp. 678–683, 2011.

[5] G. Juhasz, "Interpretation of bafilomycin, pH neutralizing or protease inhibitor treatments in autophagic flux experiments: novel considerations," *Autophagy*, vol. 8, pp. 1875–1876, 2012.

[6] N. Hosokawa, T. Hara, T. Kaizuka et al., "Nutrient-dependent mTORCl association with the ULK1-Atg13-FIP200 complex required for autophagy," *Molecular Biology of the Cell*, vol. 20, no. 7, pp. 1981–1991, 2009.

[7] A. Banreti, T. Lukacsovich, G. Csikos, M. Erdelyi, and M. Sass, "PP2A regulates autophagy in two alternative ways in Drosophila," *Autophagy*, vol. 8, pp. 623–636, 2012.

[8] Y.-Y. Chang and T. P. Neufeld, "An Atg1/Atg13 complex with multiple roles in TOR-mediated autophagy regulation," *Molecular Biology of the Cell*, vol. 20, no. 7, pp. 2004–2014, 2009.

[9] P. Nagy, M. Kárpáti, A. Varga et al., "Atg17/FIP200 localizes to perilysosomal Ref(2)P aggregates and promotes autophagy by activation of Atg1 in Drosophila," *Autophagy*, vol. 10, pp. 453–467, 2014.

[10] R. C. Scott, G. Juhász, and T. P. Neufeld, "Direct induction of autophagy by Atg1 inhibits cell growth and induces apoptotic cell death," *Current Biology*, vol. 17, no. 1, pp. 1–11, 2007.

[11] Y. Ichimura, T. Kirisako, T. Takao et al., "A ubiquitin-like system mediates protein lipidation," *Nature*, vol. 408, no. 6811, pp. 488–492, 2000.

[12] N. Mizushima, A. Yamamoto, M. Matsui, T. Yoshimori, and Y. Ohsumi, "In vivo analysis of autophagy in response to nutrient starvation using transgenic mice expressing a fluorescent autophagosome marker," *Molecular Biology of the Cell*, vol. 15, no. 3, pp. 1101–1111, 2004.

[13] T. Johansen and T. Lamark, "Selective autophagy mediated by autophagic adapter proteins," *Autophagy*, vol. 7, no. 3, pp. 279–296, 2011.

[14] S. Pankiv, T. H. Clausen, T. Lamark et al., "p62/SQSTM1 binds directly to Atg8/LC3 to facilitate degradation of ubiquitinated protein aggregates by autophagy," *Journal of Biological Chemistry*, vol. 282, no. 33, pp. 24131–24145, 2007.

[15] I. P. Nezis, A. Simonsen, A. P. Sagona et al., "Ref(2)P, the Drosophila melanogaster homologue of mammalian p62, is required for the formation of protein aggregates in adult brain," *Journal of Cell Biology*, vol. 180, no. 6, pp. 1065–1071, 2008.

[16] N. Hosokawa, T. Sasaki, S.-I. Iemura, T. Natsume, T. Hara, and N. Mizushima, "Atg101, a novel mammalian autophagy protein interacting with Atg13," *Autophagy*, vol. 5, no. 7, pp. 973–979, 2009.

[17] C. A. Mercer, A. Kaliappan, and P. B. Dennis, "A novel, human Atg13 binding protein, Atg101, interacts with ULK1 and is essential for macroautophagy," *Autophagy*, vol. 5, no. 5, pp. 649–662, 2009.

[18] Q. Liang, P. Yang, E. Tian, J. Han, and H. Zhang, "The C. elegans ATG101 homolog EPG-9 directly interacts with EPG-1/Atg13 and is essential for autophagy," *Autophagy*, vol. 8, pp. 1426–1433, 2012.

[19] S. Takats, P. Nagy, Á. Varga et al., "Autophagosomal syntaxin17-dependent lysosomal degradation maintains neuronal function in Drosophila," *The Journal of Cell Biology*, vol. 201, pp. 531–539, 2013.

[20] P. Nagy, A. Varga, K. Pircs, K. Hegedus, and G. Juhasz, "Myc-driven overgrowth requires unfolded protein response-mediated induction of autophagy and antioxidant responses in drosophila melanogaster," *PLOS Genetics*, vol. 9, Article ID e1003664, 2013.

[21] G. Juhász, B. Érdi, M. Sass, and T. P. Neufeld, "Atg7-dependent autophagy promotes neuronal health, stress tolerance, and longevity but is dispensable for metamorphosis in Drosophila," *Genes and Development*, vol. 21, no. 23, pp. 3061–3066, 2007.

[22] K. Pircs, P. Nagy, A. Varga et al., "Advantages and limitations of different p62-based assays for estimating autophagic activity in Drosophila," *PloS ONE*, vol. 7, Article ID e44214, 2012.

[23] G. Juhasz and T. P. Neufeld, "Experimental control and characterization of autophagy in drosophila," *Methods in Molecular Biology*, vol. 445, pp. 125–133, 2008.

[24] P. Nagy, K. Hegedus, K. Pircs, A. Varga, and G. Juhasz, "Different effects of Atg2 and Atg18 mutations on Atg8a and Atg9 trafficking during starvation in Drosophila," *FEBS Letters*, vol. 588, pp. 408–413, 2014.

[25] A. M. Altenhoff, A. Schneider, G. H. Gonnet, and C. Dessimoz, "OMA 2011: orthology inference among 1000 complete genomes," *Nucleic Acids Research*, vol. 39, no. 1, pp. D289–D294, 2011.

[26] A. Roy, A. Kucukural, and Y. Zhang, "I-TASSER: a unified platform for automated protein structure and function prediction," *Nature Protocols*, vol. 5, no. 4, pp. 725–738, 2010.

[27] L. A. Kelley and M. J. E. Sternberg, "Protein structure prediction on the Web: a case study using the Phyre server," *Nature Protocols*, vol. 4, no. 3, pp. 363–371, 2009.

[28] L. Holm and J. Park, "DaliLite workbench for protein structure comparison," *Bioinformatics*, vol. 16, no. 6, pp. 566–567, 2000.

[29] D. Lupyan, A. Leo-Macias, and A. R. Ortiz, "A new progressive-iterative algorithm for multiple structure alignment," *Bioinformatics*, vol. 21, no. 15, pp. 3255–3263, 2005.

[30] B. Meszaros, Z. Dosztanyi, and I. Simon, "Disordered binding regions and linear motifs—bridging the gap between two models of molecular recognition," *PloS ONE*, vol. 7, Article ID e46829, 2012.

[31] Z. Dosztányi, V. Csizmok, P. Tompa, and I. Simon, "IUPred: web server for the prediction of intrinsically unstructured regions of proteins based on estimated energy content," *Bioinformatics*, vol. 21, no. 16, pp. 3433–3434, 2005.

[32] E. F. Pettersen, T. D. Goddard, C. C. Huang et al., "UCSF Chimera—a visualization system for exploratory research and analysis," *Journal of Computational Chemistry*, vol. 25, no. 13, pp. 1605–1612, 2004.

[33] G. E. Crooks, G. Hon, J.-M. Chandonia, and S. E. Brenner, "WebLogo: a sequence logo generator," *Genome Research*, vol. 14, no. 6, pp. 1188–1190, 2004.

[34] S. Subramaniam, "The Biology Workbench—a seamless database and analysis environment for the biologist," *Proteins*, vol. 32, pp. 1–2, 1998.

[35] R. C. Scott, O. Schuldiner, and T. P. Neufeld, "Role and regulation of starvation-induced autophagy in the Drosophila fat body," *Developmental Cell*, vol. 7, no. 2, pp. 167–178, 2004.

[36] Q. Lu, P. Yang, X. Huang et al., "The WD40 repeat ptdIns(3)P-binding protein EPG-6 regulates progression of omegasomes to

autophagosomes," *Developmental Cell*, vol. 21, no. 2, pp. 343–357, 2011.

[37] A. K. G. Velikkakath, T. Nishimura, E. Oita, N. Ishihara, and N. Mizushima, "Mammalian Atg2 proteins are essential for autophagosome formation and important for regulation of size and distribution of lipid droplets," *Molecular Biology of the Cell*, vol. 23, no. 5, pp. 896–909, 2012.

[38] E. A. Alemu, T. Lamark, K. M. Torgersen et al., "ATG8 family proteins act as scaffolds for assembly of the ULK complex: sequence requirements for LC3-interacting region (LIR) motifs," *The Journal of Biological Chemistry*, vol. 287, pp. 39275–39290, 2012.

[39] V. Rogov, V. Dotsch, T. Johansen, and V. Kirkin, "Interactions between autophagy receptors and ubiquitin-like proteins form the molecular basis for selective autophagy," *Molecular Cell*, vol. 53, pp. 167–178, 2014.

[40] M. Komatsu, S. Waguri, M. Koike et al., "Homeostatic levels of p62 control cytoplasmic inclusion body formation in autophagy-deficient mice," *Cell*, vol. 131, no. 6, pp. 1149–1163, 2007.

[41] B. J. Bartlett, P. Isakson, J. Lewerenz et al., "p62, Ref(2)P and ubiquitinated proteins are conserved markers of neuronal aging, aggregate formation and progressive autophagic defects," *Autophagy*, vol. 7, no. 6, pp. 572–583, 2011.

[42] D. J. Klionsky, F. C. Abdalla, H. Abeliovich et al., "Guidelines for the use and interpretation of assays for monitoring autophagy," *Autophagy*, vol. 8, pp. 445–544, 2012.

[43] C. H. Jung, M. Seo, N. M. Otto, and D.-H. Kim, "ULK1 inhibits the kinase activity of mTORC1 and cell proliferation," *Autophagy*, vol. 7, no. 10, pp. 1212–1221, 2011.

[44] C. H. Jung, C. B. Jun, S.-H. Ro et al., "ULK-Atg13-FIP200 complexes mediate mTOR signaling to the autophagy machinery," *Molecular Biology of the Cell*, vol. 20, no. 7, pp. 1992–2003, 2009.

[45] C. C. Jao, M. J. Ragusa, R. E. Stanley, and J. H. Hurley, "A HORMA domain in Atg13 mediates PI 3-kinase recruitment in autophagy," *Proceedings of the National Academy of Sciences of the United States of America*, vol. 110, pp. 5486–5491, 2013.

[46] M. Mapelli, L. Massimiliano, S. Santaguida, and A. Musacchio, "The Mad2 conformational dimer: structure and implications for the spindle assembly checkpoint," *Cell*, vol. 131, no. 4, pp. 730–743, 2007.

[47] K. G. Guruharsha, J.-F. Rual, B. Zhai et al., "A protein complex network of Drosophila melanogaster," *Cell*, vol. 147, no. 3, pp. 690–703, 2011.

[48] I. P. Nezis, "Selective autophagy in Drosophila," *International Journal of Cell Biology*, vol. 2012, Article ID 146767, 9 pages, 2012.

[49] N. Fujita, E. Morita, T. Itoh et al., "Recruitment of the autophagic machinery to endosomes during infection is mediated by ubiquitin," *The Journal of Cell Biology*, vol. 203, pp. 115–128, 2013.

Autophagy 10:3, 453–467; March 2014; © 2014 Landes Bioscience

dc_840_14

Atg17/FIP200 localizes to perilysosomal Ref(2)P aggregates and promotes autophagy by activation of Atg1 in *Drosophila*

Péter Nagy,[†] Manuéla Kárpáti,[†] Ágnes Varga, Karolina Pircs, Zsolt Venkei,[‡] Szabolcs Takáts, Kata Varga, Balázs Érdi,[§] Krisztina Hegedűs, and Gábor Juhász*

Department of Anatomy, Cell and Developmental Biology; Eötvös Loránd University; Budapest, Hungary

[†]These authors contributed equally to this work.

Current affiliation: [‡]Center for Stem Cell Biology; Life Sciences Institute; University of Michigan; Ann Arbor, MI USA; [§]IMP–Research Institute of Molecular Pathology; Vienna, Austria

Keywords: Atg1, Atg13, autophagy, *Drosophila*, Atg17/FIP200, lysosome, Ref(2)P/p62, TOR

Abbreviations: Atg, autophagy-related; C12orf44, chromosome 12 open reading frame 44; Cp1, cysteine proteinase-1; Cvt, cytoplasm-to-vacuole targeting; DAPI, 4′,6-diamidino-2-phenylindole; DN, dominant-negative; FIP200, 200 kDa FAK family kinase-interacting protein; Gal4, galactose metabolism 4; Lamp1, lysosomal-associated membrane protein 1; LTR, LysoTracker Red; PAS, phagophore assembly site; MTOR, mechanistic target of rapamycin; PBS, phosphate-buffered saline; PBTX-DOC, PBS with Triton X-100 and sodium deoxycholate; QF, Q factor; QUAS, Q factor upstream activation sequence; RB1CC1, RB1-inducible coiled-coil 1; Ref(2)P, refractory to sigma P; SQSTM1, sequestosome 1; TBST, tris-buffered saline and Tween 20; TOR, target of rapamycin; Tsc, tuberous sclerosis complex; UAS, upstream activation sequence; ULK, unc-51 like autophagy activating kinase

Phagophore-derived autophagosomes deliver cytoplasmic material to lysosomes for degradation and reuse. Autophagy mediated by the incompletely characterized actions of Atg proteins is involved in numerous physiological and pathological settings including stress resistance, immunity, aging, cancer, and neurodegenerative diseases. Here we characterized Atg17/FIP200, the *Drosophila* ortholog of mammalian RB1CC1/FIP200, a proposed functional equivalent of yeast Atg17. *Atg17* disruption inhibits basal, starvation-induced and developmental autophagy, and interferes with the programmed elimination of larval salivary glands and midgut during metamorphosis. Upon starvation, Atg17-positive structures appear at aggregates of the selective cargo Ref(2)P/p62 near lysosomes. This location may be similar to the perivacuolar PAS (phagophore assembly site) described in yeast. *Drosophila* Atg17 is a member of the Atg1 kinase complex as in mammals, and we showed that it binds to the other subunits including Atg1, Atg13, and Atg101 (C12orf44 in humans, 9430023L20Rik in mice and RGD1359310 in rats). Atg17 is required for the kinase activity of endogenous Atg1 in vivo, as loss of *Atg17* prevents the Atg1-dependent shift of endogenous Atg13 to hyperphosphorylated forms, and also blocks punctate Atg1 localization during starvation. Finally, we found that Atg1 overexpression induces autophagy and reduces cell size in *Atg17*-null mutant fat body cells, and that overexpression of Atg17 promotes endogenous Atg13 phosphorylation and enhances autophagy in an Atg1-dependent manner in the fat body. We propose a model according to which the relative activity of Atg1, estimated by the ratio of hyper- to hypophosphorylated Atg13, contributes to setting low (basal) vs. high (starvation-induced) autophagy levels in *Drosophila*.

Introduction

During autophagy, cytoplasmic material including organelles is transported to lysosomes for degradation and recycling of building blocks. The main pathway, macroautophagy (simply referred to as autophagy hereafter) is characterized by the formation of double-membrane autophagosomes, which then fuse with lysosomes to deliver their contents for breakdown. Autophagy is an ancient starvation survival pathway promoting stress resistance and longevity in all eukaryotes. In addition, autophagy acquired numerous additional functions in multicellular organisms and protects from various diseases including cancer and neurodegeneration.[1]

*Correspondence to: Gábor Juhász; Email: szmrt@elte.hu
Submitted: 07/17/2013; Revised: 11/26/2013; Accepted: 12/05/2013
http://dx.doi.org/10.4161/auto.27442

The evolutionarily conserved MTOR (mechanistic target of rapamycin) kinase promotes cell growth in part by phosphorylating RPS6K (ribosomal protein S6 kinase) and EIF4EBP1 (eIF-4E binding protein 1) to enhance protein synthesis, and inhibits autophagy through direct phosphorylation of Atg1 (or its mammalian orthologs ULK [unc 51-like autophagy activating kinase] 1 and 2) when bound to actively digesting lysosomes.[2-4] Recent in vitro experiments suggest that MTOR activity depends on intralysosomal amino acids.[5] Starvation leads to dissociation of MTOR from lysosomes and autophagy induction, which has been suggested to be required for reactivation of MTOR, potentially by restoring the amino acid pool in lysosomes through the breakdown of autophagic cargo.[2,6] Thus, the regulation of cell growth and autophagy is integrated at the level of lysosomes.

Formation of autophagosomes is controlled by ~20 conserved autophagy-related (Atg) gene products, most of which were originally discovered in yeast.[7] Most of these proteins assemble into complexes to promote autophagosome formation at a site commonly referred to as the PAS (phagophore assembly site). Various potential sources including ER, mitochondria, Golgi, and plasma membrane have been suggested to contribute lipids to sustain the growth of initially appearing membrane cisterns (called phagophores), which engulf cytoplasmic material and give rise to autophagosomes after sealing of the edges.[8,9] It is widely accepted that initiation of autophagy is usually triggered by activation of an Atg1 kinase complex (consisting of Atg1, 13, 17, 29, and 31 in yeast), followed by phagophore nucleation and assembly steps that require an Atg14-containing autophagy-specific lipid kinase complex, the transmembrane protein Atg9, and 2 ubiquitin-like protein conjugation systems mediating the C-terminal lipidation of Atg8 family proteins. Atg7 acts as an E1-like enzyme for both Atg8 and Atg12, followed by actions of the E2-like enzymes Atg3 and Atg10, respectively. Atg12 is then covalently attached to Atg5 and subsequently assembles into a large complex that also contains Atg16. This complex facilitates Atg8 lipidation and anchoring into phagophore and autophagosome membranes through a phosphatidyl-ethanolamine tail. Atg8 is recycled from the outer membrane, while the pool bound to the inner membrane is degraded after fusion with a lysosome.[9]

Low-level, basal autophagic degradation contributes to the turnover of orgenelles and proteins in metazoan cells, thus maintaining cellular homeostasis. We and others have shown that ubiquitinated protein aggregates accumulate in autophagy gene mutant brains in fly and mouse models.[1,10,11] These aggregates also contain the multidomain protein SQSTM1/p62 (sequestosome 1) in mammals, or its fly ortholog Ref(2)P (refractory to sigma P). SQSTM1/Ref(2)P acts as a selective receptor for cargo recognition during autophagy. Binding of Atg8 homologs to SQSTM1/Ref(2)P ensures autophagic degradation of ubiquitinated protein aggregates, as SQSTM1/Ref(2)P contains an Atg8-interacting motif and a C-terminal ubiquitin-binding domain.[12-14] Consequently, SQSTM1/Ref(2)P is also degraded in autolysosomes.

Recent studies characterized the mammalian ULK complex in cultured cells, which contains the multidomain adaptor protein RB1CC1 (RB1-inducible coiled-coil 1)/FIP200 (200 kDa FAK family kinase-interacting protein), ATG13, the Atg1 orthologs ULK1 and ULK2, and the animal-specific subunit C12orf44 (chromosome 12 open reading frame 44)/ATG101.[3,15-18] As loss of RB1CC1 blocks autophagy, it has been suggested to play a role similar to Atg17, a scaffold protein required for starvation-induced autophagy as part of the yeast Atg1 complex. These studies revealed dynamic changes in the electrophoretic mobility of multiple subunits in nutrient-replete vs. autophagy-inducing conditions. In vitro kinase assays in these reports suggest that MTOR and ULK1/2 kinases are responsible for most of these phosphorylation events.[3,16] Importantly, cell type-specific differences have been seen, but overall the phosphorylation status of endogenous ATG13 decreases during starvation.[3] The regulation of the endogenous Atg1 kinase complex in an in vivo setting is still uncharacterized.

Here we explore the role of the single *Drosophila* ortholog of RB1CC1, Atg17/FIP200 in autophagy (also known by the annotation symbol CG1347).[19,20] It is referred to as Atg17 in Flybase, the *Drosophila* genome homepage, as Banreti et al. suggested this symbol even though they also show that this *Drosophila* protein is an ortholog of mammalian RB1CC1, and it is not homologous to yeast Atg17.[20] We use both loss- and gain-of-function studies to show that Atg17 activates endogenous Atg1 kinase to facilitate autophagy, and that Atg17 localizes to perilysosomal aggregates of the selective autophagy cargo Ref(2)P in polyploid larval *Drosophila* tissues.

Results

Generation of *Atg17*-null mutants, overexpression lines, and antibodies

Taking advantage of a transposon insertion (*EY03045*) in the first intron of *Atg17*, we generated a chromosomal deletion that removes practically the entire coding sequence (**Fig. 1A and B**). Loss of *Atg17* resulted in pharate adult lethality in homozygotes, and escapers were very rarely seen in hemizygotes (**Fig. S1A**), similar to previously described *Atg1* and *Atg13* mutants.[21,22] We generated polyclonal antibodies against Atg17, and used these to show that no protein product is detected in null mutants (**Fig. 1C**). We also established inducible transgenic Atg17 lines, the expression of which can be triggered by the presence of appropriate driver transgenes (**Fig. 1C**). Low-level expression of transgenic Atg17-GFP restored viability of *Atg17*-null mutant animals in genetic rescue experiments, confirming that lethality was due to loss of *Atg17* (**Fig. S1A**).

Atg17 is required for starvation-induced and basal autophagy upstream of Atg1

Starvation leads to the formation of autophagosomes and autolysosomes in fat bodies of control larvae. Both structures are labeled by mCherry-Atg8a, as this transgenic reporter is specifically bound to autophagosomes, and the mCherry tag remains fluorescent and accumulates in autolysosomes (**Fig. 2A**).[21,23] Loss of *Atg17* completely blocked the punctate mCherry-Atg8a response to starvation (**Fig. 2B and I**). LysoTracker Red (LTR) is a commonly used staining for autolysosomes in

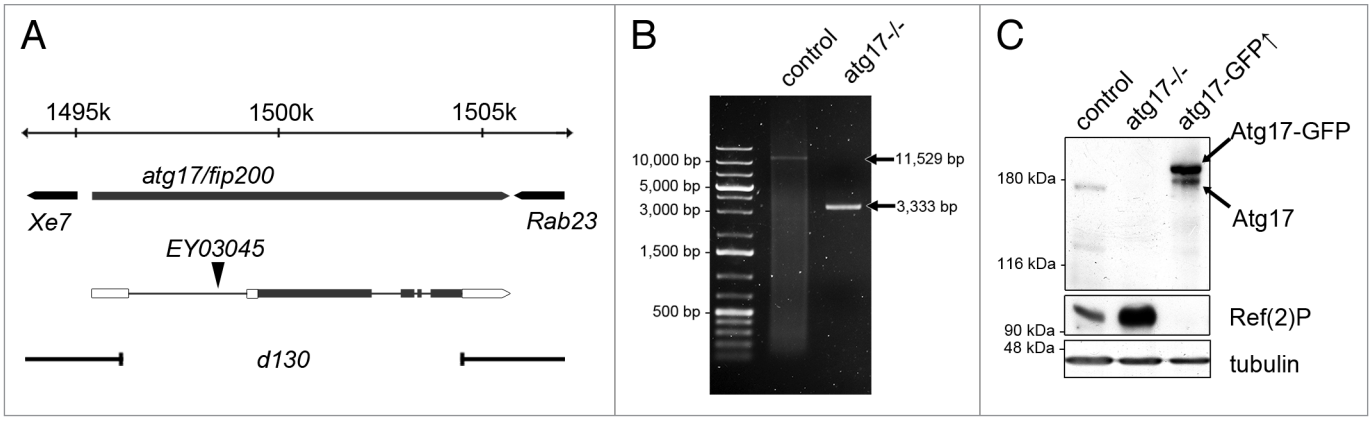


Figure 1. Generation of *atg17*-null mutants, overexpression lines, and antibodies. (**A**) *atg17[d130]*-null mutants harbor a 8,196 bp chromosomal deletion that leaves behind only the last 55 nucleotides of the 4,071-nucleotide open reading frame (black bars), after improper excision of the P element *EY03045* located in the first intron. Open bars: untranslated regions. (**B**) PCR using primers flanking the *atg17* locus demonstrates the extent of the genomic deletion in homozygous *atg17[d130]* mutant larvae compared with controls. (**C**) Western blots detect endogenous Atg17 of 170 kDa in control larvae, and also show the overexpressed protein in larvae expressing Atg17-GFP. No protein product is seen in mutants. The selective autophagy cargo Ref(2)P accumulates in *atg17*-null mutants and disappears in larvae constitutively overexpressing Atg17-GFP.

the larval fat body. *Atg17* was cell-autonomously required for starvation-induced formation of LTR-positive autolysosomes in fat body cell clones (**Fig. 2C and J**). We also raised polyclonal antibodies against Atg8a, enabling the identification of nascent autophagosomes in immunostaining experiments (**Fig. S1B, S1C, and S1E**). Anti-Atg8a staining revealed severely impaired autophagosome formation in *Atg17*-null mutant or RNAi cells in mosaic experiments, compared with neighboring control cells that contained numerous Atg8a-positive dots after starvation (**Fig. 2D and K**; **Fig. S1D and S1E**). Finally, ultrastructural analysis confirmed the absence of autophagosomes and autolysosomes in fat bodies of starved *Atg17*-null mutant larvae (**Fig. 2E, F, and L**).

Basal autophagic degradation occurs at a low level in many tissues, making it difficult to estimate by conventional autophagy reporters. As the specific autophagy cargo Ref(2)P accumulates upon reduction of basal autophagy, determining its levels is a common test in these experiments.[23-25] Indeed, loss of *Atg17* resulted in large-scale accumulation of endogenous Ref(2)P in western blots (**Fig. 1C**), and in null mutant and RNAi cells (**Fig. 2D, G, K, and M**).

The Atg1 kinase complex, and its subunit Atg17 in yeast and the corresponding proposed ortholog RB1CC1 in mammalian cells in particular, is suggested to act most upstream in the hierarchy of Atg protein complexes.[26,27] In line with that, we found that knockdown of *Atg17* prevented starvation-induced punctate mCherry-Atg1 localization (**Fig. 2H and N**). We and others have shown previously that overexpression of Atg1 activates autophagy, and also reduces cell size at least in part by negative feedback on TOR (target of rapamycin).[22,28,29] High-level expression of Atg1 could still trigger punctate Atg8a labeling in *Atg17*-null mutant fat body cells and reduced cell size in epistasis experiments (**Fig. S2A and S2B**).

Atg17 is required for developmental autophagy and programmed removal of salivary glands during metamorphosis

Increased level of the molting hormone ecdysone at a low juvenile hormone concentration leads to initiation of wandering behavior, when L3 stage larvae leave the food in search of an appropriate place for pupariation. At the same time, ecdysone triggers autophagy in polyploid larval tissues including fat body, presumably facilitating the removal of these organs which become obsolete during metamorphosis.[30] Loss of *Atg17* blocked developmental autophagy in fat body cells, based on lack of punctate LTR and mCherry-Atg8a signals (**Fig. 3A–E**). In addition, programmed elimination of larval salivary glands during metamorphosis was impaired in *Atg17*-null mutants (**Fig. 3F–I**), similar to previous observations in animals carrying mutations in genes that act downstream of the Atg1 kinase complex during autophagy.[31] The volume of prepupal midguts strongly decreases during the onset of metamorphosis in an autophagy-dependent manner.[10,32] Midgut shrinkage was also attenuated by loss of *Atg17* in our experiments (**Fig. S2C–S2F**).

Atg17 localizes to Ref(2)P aggregates near lysosomes

Atg17-GFP dots showed 52% colocalization with endogenous Atg8a, which is recruited to the PAS and remains bound to autophagosomes (n = 611 dots counted, **Fig. 4A**). Atg5 is a commonly used marker for PAS.[9,23,33] Stalled PASs containing upstream Atg proteins accumulate in yeast and mammalian cells lacking downstream *ATG* genes.[26,27] We used this strategy to analyze the colocalization of endogenous Atg17 and Atg5 in *Atg8a*-null mutants, in which PAS formation is stalled and no autophagosomes form.[22,26] We did not detect cytoplasmic dots positive for endogenous Atg17 or Atg5 in gastric ceca cells of well-fed larvae (**Fig. 4B**). Punctate structures appeared in response to starvation, and Atg17 showed 81% colocalization with Atg5 dots (n = 97, **Fig. 4C**). This colocalization experiment was performed in gastric ceca, a tissue that produces similar starvation-induced autophagic response to fat bodies,[10,30] because endogenous Atg5-positive structures were difficult to visualize in fat body cells of starved larvae. 89% of Atg17-GFP dots colocalized with

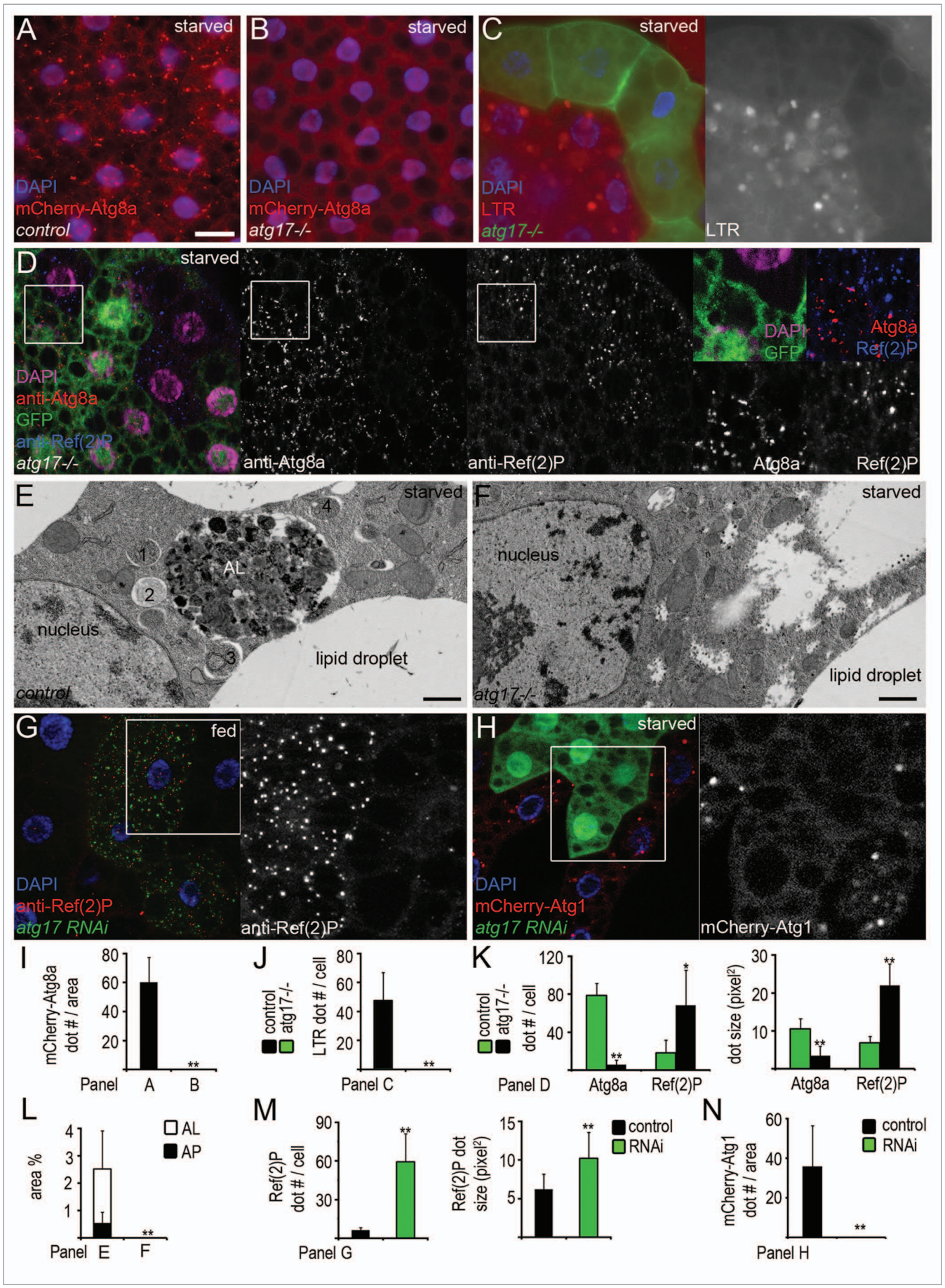

A
starved
DAPI
mCherry-Atg8a
control
B
starved
DAPI
mCherry-Atg8a
atg17-/-
C
starved
DAPI
LTR
atg17-/-
LTR
D
starved
DAPI
anti-Atg8a
GFP
anti-Ref(2)P
atg17-/-
anti-Atg8a
anti-Ref(2)P
DAPI
GFP
Atg8a
Ref(2)P
Atg8a
Ref(2)P
E
starved
1
2
3
4
AL
nucleus
lipid droplet
control
F
starved
nucleus
lipid droplet
atg17-/-
G
fed
DAPI
anti-Ref(2)P
atg17 RNAi
anti-Ref(2)P
H
starved
DAPI
mCherry-Atg1
atg17 RNAi
mCherry-Atg1
I
mCherry-Atg8a dot # / area
80
60
40
20
**
Panel A B
J
control
atg17-/-
LTR dot # / cell
80
60
40
20
**
Panel C
K
control
atg17-/-
dot # / cell
120
80
40
**
*
Panel D
Atg8a
Ref(2)P
dot size (pixel²)
30
20
10
**
**
Atg8a
Ref(2)P
L
area %
4
3
2
1
AL
AP
**
Panel E F
M
Ref(2)P dot # / cell
90
60
30
**
Panel G
Ref(2)P dot size (pixel²)
15
10
5
**
control
RNAi
N
mCherry-Atg1 dot # / area
60
40
20
control
RNAi
**
Panel H

Figure 2 (See opposite page). *atg17* is required for starvation-induced and basal autophagy. (**A and B**) mCherry-Atg8a-positive autophagosomes and autolysosomes form in fat body cells of starved control (**A**) but not in *atg17*-null mutant larvae (**B**). (**C**) No LTR (LysoTracker Red)-positive autolysosomes form in GFP-positive *atg17*-null mutant cells, compared with surrounding control cells in the same fat body tissue in starved animals. (**D**) Endogenous Atg8a-positive autophagosomes are missing and Ref(2)P aggregates accumulate in starved *atg17*-null mutant cells (these are marked by the lack of GFP in this image, unlike in **C**), compared with neighboring control cells. (**E and F**) Electron microscopy shows that autophagosomes (1–4) and autolysosomes (AL) form in fat body cells of control (**E**) but not in *atg17*-null mutant larvae during starvation (**F**). (**G**) Depletion of *atg17* in GFP-positive cells results in large-scale accumulation of Ref(2)P in fat bodies of well-fed larvae. (**H**) Depletion of *atg17* prevents starvation-induced mCherry-Atg1 dot formation. (**I–N**) Quantification of data from (**A and B**) (**I**, n = 12/genotype), (**C**) (**J**, n = 14), (**D**) (**K**, n = 18), (**E and F**), showing the ratio of autophagosomes and autolysosomes relative to total cytoplasm (**L**, n = 4/genotype), (**G**) (**M**, n = 10), (**H**) (**N**, n = 10). Scale bar: (**A–D, G, and H**) 20 μm; (**E and F**) 1 μm. Error bars: s.d., $^{*}P < 0.05$, $^{**}P < 0.01$.

the selective cargo Ref(2)P in control fat cells, and 93% of endogenous Atg17 colocalized with Ref(2)P aggregates in *Atg7*-null mutants (n = 391 and 148, respectively, **Fig. 4D and E**). As expected, no cytoplasmic Atg17 dots were seen in starved *Atg17*-null mutants, whereas most likely nonspecific nuclear staining remained (**Fig. 4F**).

In genetic rescue experiments, transient expression of Atg17-GFP fully rescued the autophagy defect of *Atg17*-null mutants (**Fig. 4G**). We noticed that Atg17-GFP exhibited a punctate pattern, and practically all dots clustered around LTR- and mCherry-Atg8a-positive autolysosomes (**Fig. 4G**; **Fig. S3A**). Moreover, Venus-tagged Atg1 also formed punctate structures closely associated with LTR-positive autolysosomes (**Fig. S3B**). In line with these, endogenous Atg17 dots closely associated with, but did not colocalize with the resident lysosomal hydrolase Cp1 (Cysteine proteinase-1)/cathepsin L, both in *Atg7* or *Atg8a*-null mutant fat body or gastric ceca cells of starved larvae (**Fig. 4H**; **Fig. S3C**).

Previous studies in yeast showed that phagophores assemble at cytoplasmic areas excluding ribosomes and organelles.[34] We were able to identify ribosome-free areas with associated 40- to 60-nm vesicles, which is the reported size of Atg9 vesicles in yeast,[35] and these structures could be observed next to autolysosomes in ultrastructural images (**Fig. S3D and S3E**). We speculate that these may represent the phagophore formation site in *Drosophila*, although alternative interpretations are also possible.

Aggregates of the specific autophagy cargo Ref(2)P-GFP also frequently clustered around LTR-positive autolysosomes in starved *Drosophila* larvae (**Fig. 4I**). MTOR, an upstream negative regulator of autophagy, is bound to lysosomes in growing cells, and starvation results in dispersion of MTOR and its dissociation from lysosomes. SQSTM1 is associated with MTOR complex 1.[12] We found that FLAG-TOR displayed a punctate distribution in fat bodies of well-fed *Drosophila* larvae that showed 95% overlap with Ref(2)P dots (n = 77), and starvation led to a complete dispersion of FLAG-TOR but not Ref(2)P (**Fig. S3F and S3G**).

Overexpression of Atg17 enhances autophagy in an Atg1-dependent manner

Constitutive expression of Atg17-GFP dramatically reduced the levels of endogenous Ref(2)P in well-fed larvae, indicating enhanced autophagic degradation (**Fig. 1C**). Similarly, overexpression of Atg17 in GFP-marked fat cells led to the formation of mCherry-Atg8a and mCherry-Atg1 positive autophagic structures in well-fed mosaic animals (**Fig. 5A, B, J, and K**). Heat shock-mediated transient expression of Atg17-GFP also induced punctate LTR staining (**Fig. 5C, D, and L**). Coexpression of a kinase-dead, dominant-negative (DN) Atg1 attenuated Atg17-induced LTR staining, but not punctate Atg17 localization (**Fig. 5E and L**). Similarly, overexpression of Atg17 increased the number of Atg8a-positive autophagosomes in an Atg1-dependent manner in fat bodies of well-fed larvae (**Fig. 5F–I, and M**). These results suggest that Atg17-induced autophagy requires Atg1.

Atg17 is a subunit of the Atg1 kinase complex

To further characterize the role of *Drosophila* Atg17, we performed coimmunoprecipitations with Atg1 kinase complex subunits in cultured *Drosophila* cells. Atg17-GFP readily coprecipitated with FLAG-tagged Atg13 and FLAG-tagged Atg101 (**Fig. 6A**). Atg17-GFP was clearly detectable in precipitates of kinase-dead or wild-type myc-Atg1, although in lower amounts than in case of Atg13 or Atg101 (**Fig. 6B**). Note that overexpression of wild-type Atg1 strongly reduces the expression of tagged proteins including its own expression, which is likely due to inhibition of TOR-dependent translation by Atg1.[29] In these experiments, coexpression of myc-Atg1 but not kinase-dead myc-Atg1 also decreased the electrophoretic mobility of Atg17-GFP. This is consistent with mammalian studies showing that ULK1/2 can phosphorylate RB1CC1, which is facilitated by ATG13.[16] Tagged overexpressed proteins also coprecipitated from larval extracts (**Fig. S4A**).

ATG13 has been reported to directly bind to both RB1CC1 and the Atg1 orthologs ULK1 and ULK2 in mammalian cells, which prompted us to map the regions involved in these interactions in *Drosophila*.[3,16,17] All Atg13 homologs share an N-terminal domain, followed by poorly conserved regions (**Fig. S5**).[17,36] We generated HA-GFP-tagged truncated fragments of Atg13 for interaction studies (**Fig. 6C**). The highest amount of Atg17-GFP was observed in precipitates of the putative unstructured regions (amino acids 231 to 523) of Atg13 (**Fig. 6C**). *Drosophila* Atg13 has recently been shown to interact with Atg1, but the region involved has remained unknown.[21] We found that Atg1 was coprecipitated with the C-terminal region (amino acids 393 to 523) of Atg13 (**Fig. 6D**). Although our data do not rule out the possibility that the observed interactions reflect indirect binding, these results are consistent with previous mammalian reports, which show the direct binding of ATG13 to both ULK1/2 and RB1CC1.[16,17]

Atg17 activates Atg1 in vivo

Atg13 phosphorylation levels are influenced by TOR and Atg1 kinases in yeast, flies, and mammals.[17] In agreement with these, coexpression of Atg1 strongly increased, while an N-terminally truncated active fragment of TOR appeared to slightly reduce the

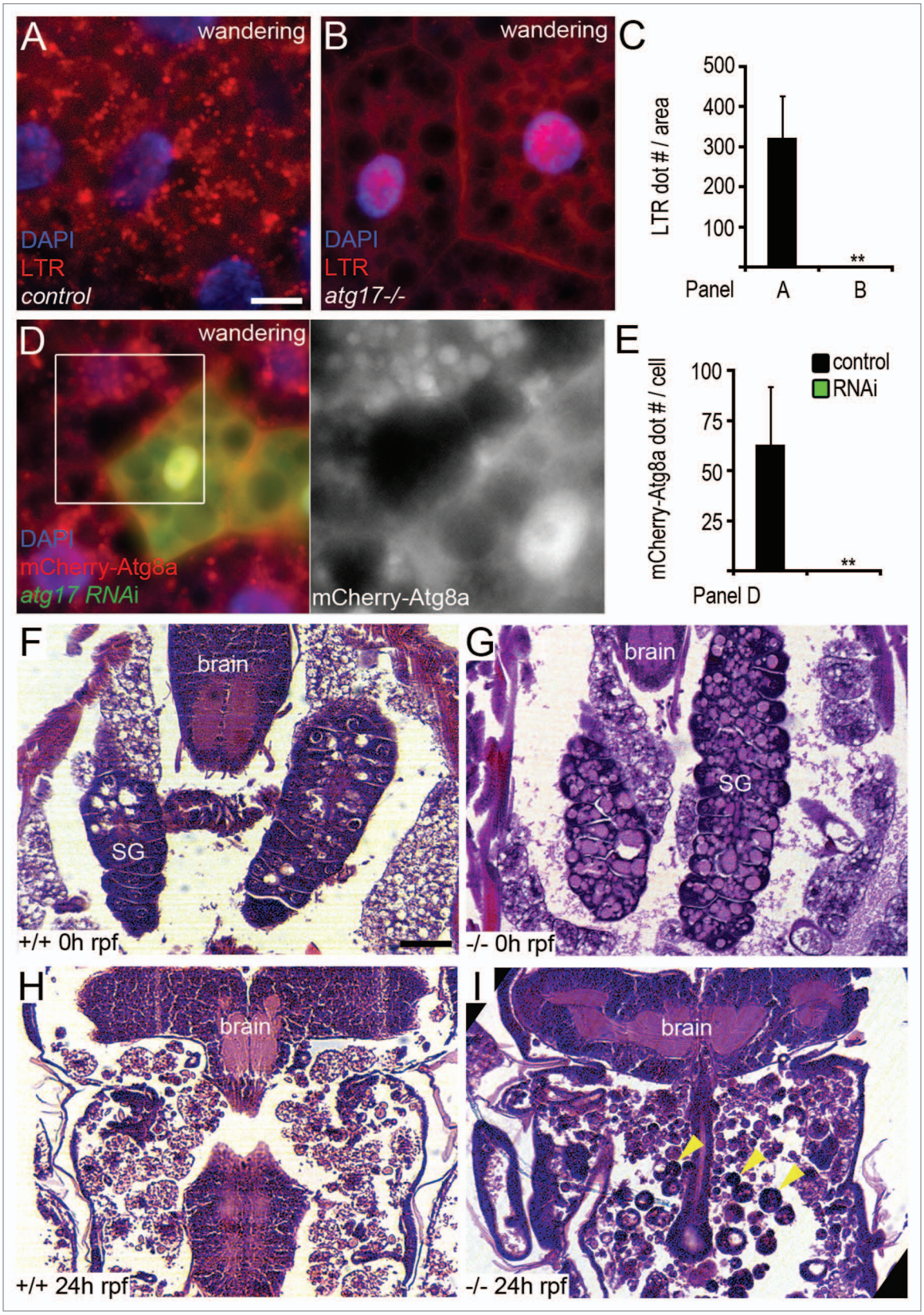


Figure 3. For figure legend, see page 459.

Figure 3 (See opposite page). *atg17* is necessary for developmental autophagy and proper salivary gland histolysis. (**A and B**) Punctate LTR staining is observed in controls (**A**), but not in *atg17*-null mutant fat bodies of L3 stage wandering larvae prior to metamorphosis (**B**). (**C**) Quantification of data from (**A and B**); n = 20/genotype. (**D**) Depletion of *atg17* in GFP-positive cells blocks the formation of mCherry-Atg8a positive autophagosomes and autolysosomes in fat bodies of wandering larvae. (**E**) Quantification of data from (**D**); n = 26. (**F–I**) Larval salivary glands (SG) are visible in hematoxylin-eosin stained paraffin sections of both control (**F**, n = 3) and *atg17*-null mutant (**G**, n = 5) white prepupae (0 h relative to puparium formation, rpf). Salivary gland histolysis is completed by 24 h rpf in controls (**H**, n = 7), but numerous large, persisting salivary gland cells (arrowheads) are visible in all similarly aged *atg17*-null mutant pupae (**I**, n = 9). Scale bars: (**A, B, and D**) 20 μm, (**F–I**) 60 μm. Error bars: s.d., $^{**}P < 0.01$.

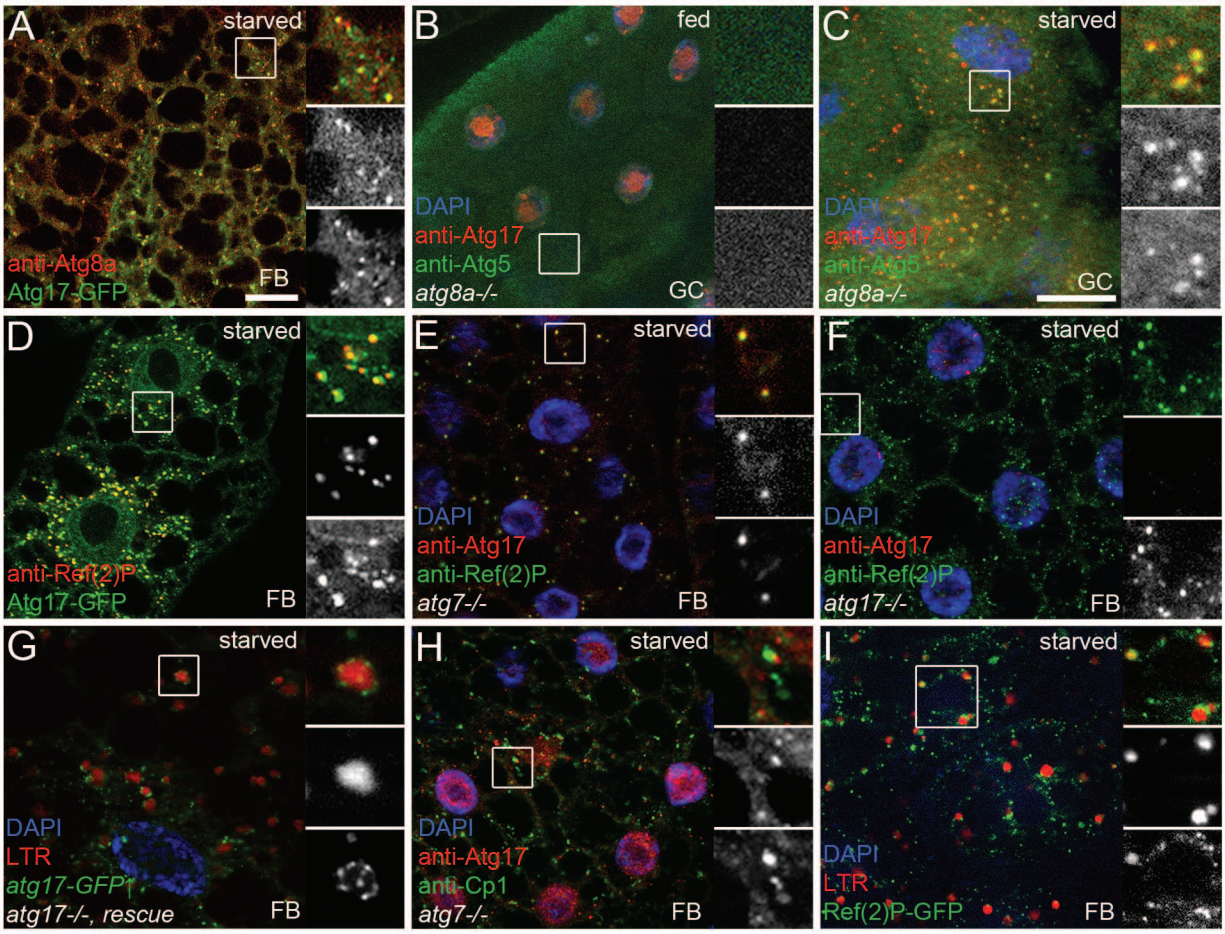


Figure 4. Atg17 is associated with lysosomes and colocalizes with Atg8a, Atg5, and Ref(2)P. (**A**) Atg17-GFP colocalizes with endogenous Atg8a in fat cells of starved larvae. (**B**) No punctate Atg17 or Atg5 structures are seen in well-fed *Atg8a*-null mutant gastric ceca. (**C**) Endogenous Atg17 colocalizes with Atg5-positive PAS in starved *Atg8a*-null mutant gastric ceca. (**D**) Atg17-GFP localizes to Ref(2)P aggregates in control larvae. (**E**) Endogenous Atg17 colocalizes with endogenous Ref(2)P in *Atg7*-null mutants. (**F**) No cytoplasmic Atg17 dots are seen in starved *atg17*-null mutants, while nonspecific nuclear staining is observed. (**G**) Transient expression of Atg17-GFP rescues punctate LTR staining in fat body cells of starved *atg17*-null mutants. Note that Atg17 dots are tightly associated with LTR-positive autolysosomes. (**H**) Endogenous Atg17 accumulates near Cp1-positive lysosomes in *Atg7*-null mutant fat cells. (**I**) Punctate Ref(2)P-GFP structures are observed near LTR-positive autolysosomes. Scale bar in (**A**): 20 μm for (**A, B, E, F, H, and I**); in (**C**): 20 μm for (**C, D, and G**). Boxed areas are shown enlarged with merged image (top), red channel in grayscale (middle) and green channel in grayscale (bottom). FB, fat body; GC, gastric ceca.

overall phosphorylation level of HA-Atg13 in cultured *Drosophila* cells (**Fig. 6E**). In line with our interaction data, co-expression of Atg1 decreased the mobility of Atg13 fragments containing the C-terminus (**Fig. 6F**), suggesting that Atg1phosphorylated these fragments.

To gain more insight into the regulation of endogenous Atg1 kinase complex, we raised polyclonal antisera against *Drosophila* Atg13 and Atg1, which specifically recognized endogenous proteins in western blots (**Fig. 7A**; **Fig. S4B**). It was striking that endogenous Atg13 appeared as multiple bands in fat body extracts prepared from well-fed animals, and starving larvae for 3 or 24 h strongly increased the ratio of slower mobility to faster mobility bands ($Atg13^{high}/Atg13^{low}$, **Fig. 7B**). Endogenous Atg1 was difficult to visualize using our antibody in fat body extracts of well-fed animals, although the bands became clearly visible upon starvation (**Fig. S4C**). Epitope mapping suggested that this antibody may recognize the middle region of Atg1, which is rich in prolines and serines (**Fig. S4D**). As the sites phosphorylated

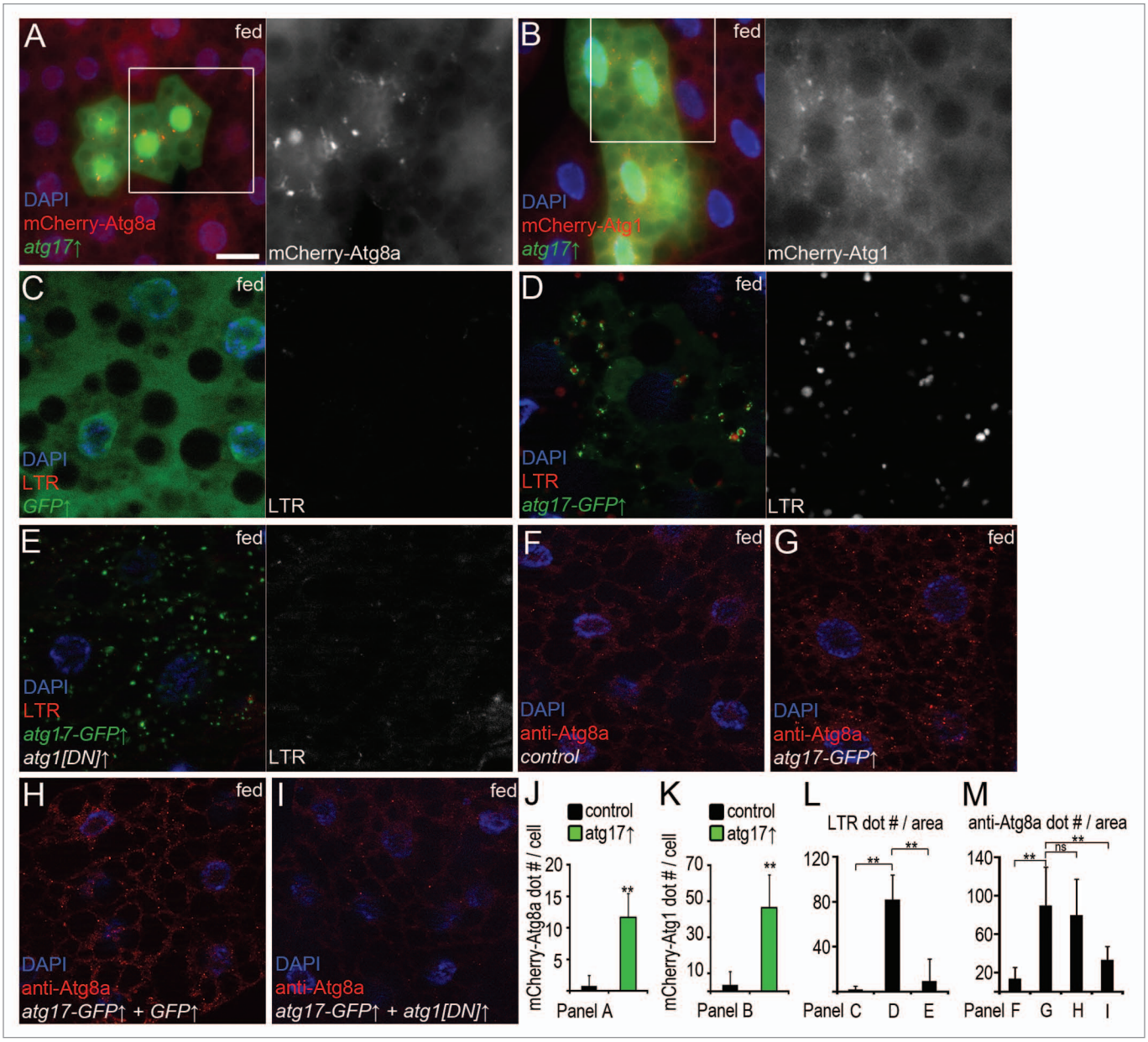


Figure 5. Overexpression of Atg17 enhances autophagy in well-fed larvae. (**A and B**) Overexpression of Atg17 in GFP-positive cells promotes mCherry-Atg8a (**A**) and mCherry-Atg1 (**B**) puncta formation. (**C**) Practically no LTR dots are seen in fat body cells of well-fed control larvae expressing GFP. (**D**) Transient expression of Atg17-GFP induces punctate LTR staining. (**E**) Coexpression of dominant-negative Atg1 blocks Atg17-induced LTR staining. (**F**) Only a few Atg8a puncta are seen in heat-shocked control larvae. (**G**) Heat shock-induced transient expression of Atg17-GFP enhances autophagosome-associated Atg8a dot formation. (**H**) Coexpression of GFP has no effect on punctate Atg8a staining induced by Atg17-GFP. (**I**) Coexpression of dominant-negative Atg1 prevents Atg17-induced Atg8a dot formation. (**J–M**) Quantification of data from (**A**) (**J**, n = 22), (**B**) (**K**, n = 18) and (**C–E**) (**L**, n = 14/genotype), (**F–I**) (**M**, n = 10/genotype). Scale bar: (**A–I**) 20 μm. Error bars: s.d., $^{**}P < 0.01$.

by TOR (a proline-directed Ser/Thr kinase) are found in this region of Atg1 homologs,[37] TOR-mediated phosphorylation may be responsible for the reduced affinity of our antibody in nutrient-replete fat body extracts. The usefulness of this reagent is thus limited, therefore anti-Atg1 counterparts of western blots are shown in supplemental data.

Phosphatase treatment practically reduced both Atg13 and Atg1 to single bands, suggesting that these endogenous proteins are phosphorylated (**Fig. 7C**; **Fig. S4E**). In agreement with that, overexpression of Atg1 led to a shift of endogenous Atg13 to slower mobility forms in fat bodies of well-fed animals, similar to genetic suppression of TOR by co-overexpressing Tsc1 and Tsc2 (**Fig. 7D**; **Fig. S4F**). Expression of dominant-negative Atg1 in fat bodies of fed larvae reduced the amount of slower mobility forms of endogenous Atg13, and in starved larvae practically eliminated all $Atg13^{high}$ forms (**Fig. 7E**; **Fig. S4G**). Thus, Atg1 kinase appears to be responsible for starvation-induced hyperphosphorylation of Atg13, and likely

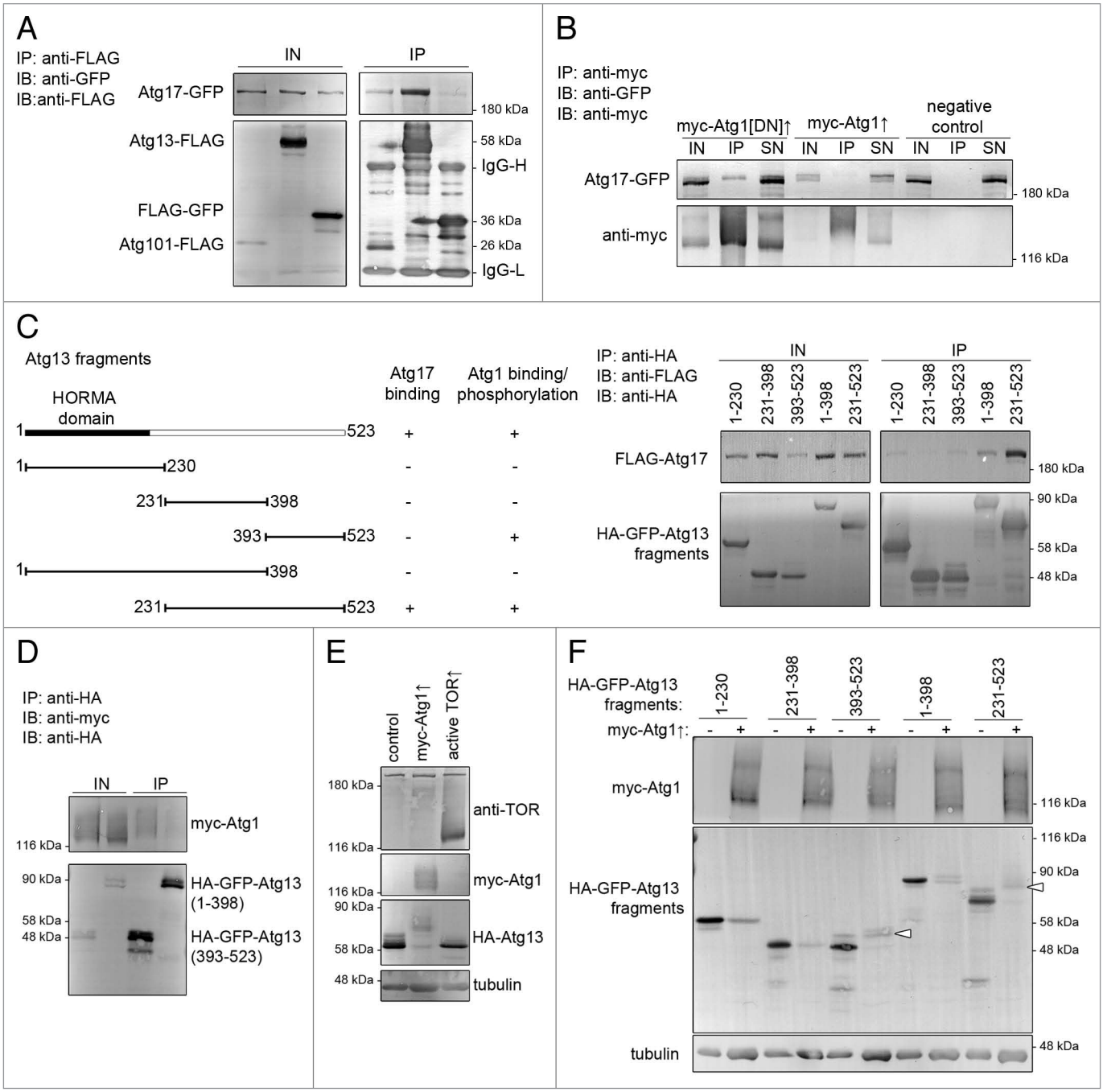


Figure 6. Interactions of Atg17, Atg1 and Atg13. (**A and B**) Immunoprecipitation experiments in cultured *Drosophila* cells. Atg17-GFP coprecipitates with Atg13-FLAG and Atg101-FLAG, but not with FLAG-GFP (**A**). Atg17-GFP binds weakly to kinase-dead and wild-type myc-Atg1, but not to anti-myc beads (**B**). Note the decreased mobility of Atg17-GFP upon coexpression of myc-Atg1. (**C**) Of the truncated Atg13 constructs (see left panel), a fragment containing the putative unstructured regions (231 to 523) binds strongly to Atg17-GFP. (**D**) Myc-Atg1 binds to the C-terminus (393 to 523) of Atg13. (**E**) Expression of myc-Atg1 strongly decreases and active TOR (amino acids 1333 to 2470) slightly increases the mobility of HA-Atg13 in cultured cells. (**F**) Expression of myc-Atg1 results in a shift (indicated by arrowheads) of Atg13 fragments containing the C terminus (393 to 523 and 231 to 523). IN, input, IP, immunoprecipitation, SN, supernatant.

also contributes to phosphorylation of Atg13 in nutrient-replete conditions in vivo.

In line with the essential role of *Atg17* in autophagy, the starvation-induced shift from $Atg13^{low}$ to $Atg13^{high}$ forms was blocked in *Atg17*-null mutants (**Fig. 7F**). Constitutive or transient expression of Atg17-GFP increased the $Atg13^{high}/Atg13^{low}$ ratio even in well-fed larvae (**Fig. 7F**; **Fig. S4H**). In agreement with our microscopy data that Atg17-induced autophagy requires Atg1, coexpression of kinase-dead Atg1 blocked Atg17-induced Atg13 hyperphosphorylation in fat bodies of well-fed larvae

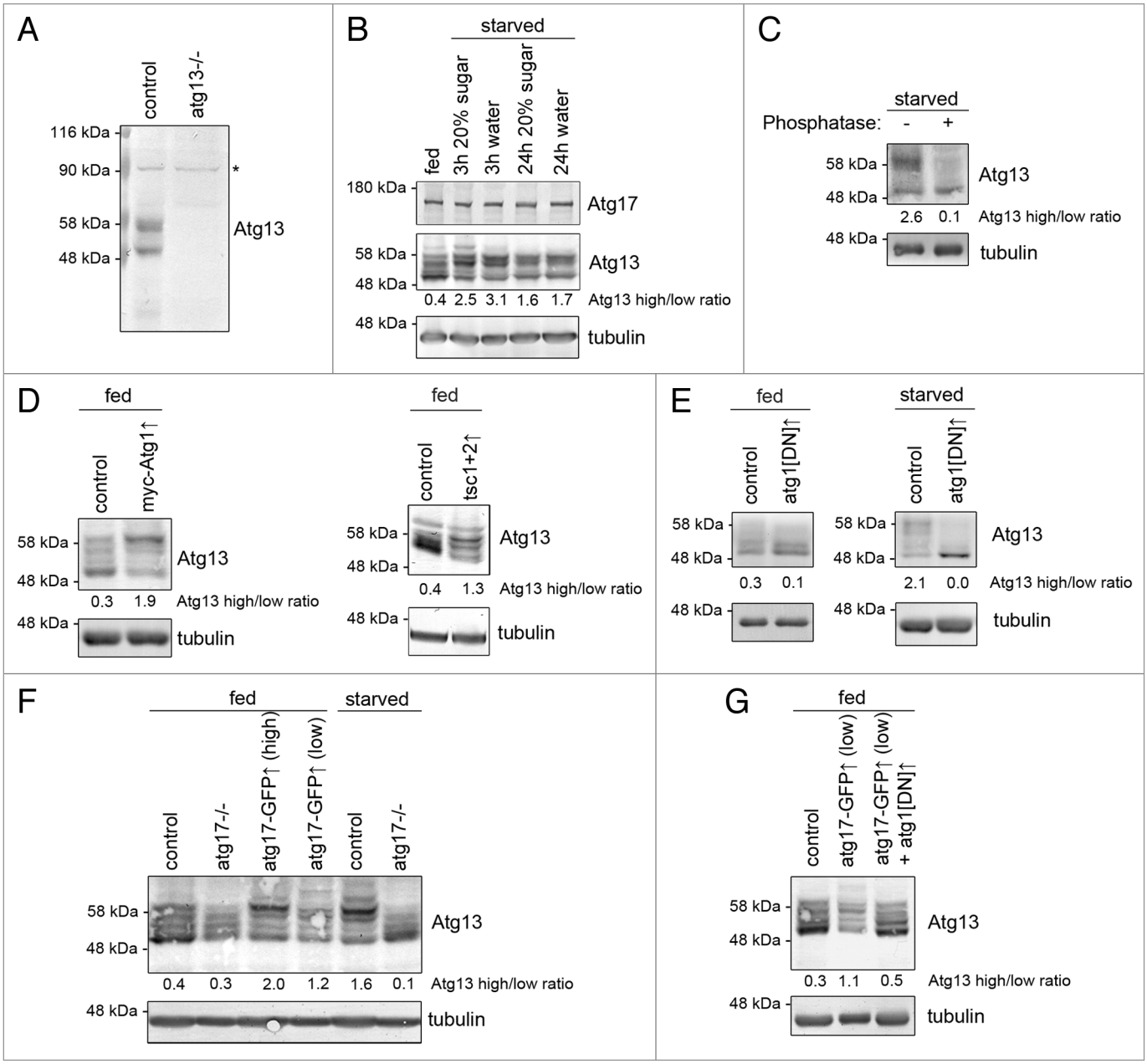


Figure 7. Atg17 regulates Atg13 phosphorylation in vivo. (**A**) Western blots using our novel antibody recognize endogenous Atg13, which is absent from a*tg13*-null mutant larvae. Asterisk denotes a nonspecific band that serves as loading control. (**B**) Starvation strongly decreases the mobility of Atg13 in larval fat body extracts. (**C**) Phosphatase treatment of starved fat body lysates demonstrates that Atg13 is phosphorylated in vivo. (**D**) Transient overexpression of myc-Atg1, or Tsc1 and Tsc2 decreases Atg13 mobility in fat bodies of fed larvae. (**E**) Transient overexpression of dominant-negative Atg1 reduces the ratio of slower mobility Atg13 forms relative to higher mobility forms in fat bodies of well-fed larvae. Dominant-negative Atg1 expression practically eliminates all Atg13 phospho-forms in starved fat bodies. (**F**) Transient (low) or constitutive (high) expression of Atg17-GFP decreases Atg13 mobility in fat bodies of well-fed animals. The starvation-induced shift of Atg13 to slower mobility forms is lost in *atg17*-null mutants. (**G**) Coexpression of dominant-negative Atg1 prevents Atg17-induced shift of Atg13 to slower mobility forms in fat body extracts of well-fed larvae. Numbers indicating Atg13 high/low ratio are calculated by densitometric evaluation of blots as described in Materials and Methods.

(**Fig. 7G**; **Fig. S4I**), suggesting that Atg17 induces autophagy at least in part by activating Atg1.

Discussion

Basal autophagy primarily functions as a housekeeping mechanism, ensuring proper turnover and quality control of macromolecules and organelles. High levels of autophagy are induced by starvation, and degradation of dispensable cellular constituents provides nutrients and building blocks for synthetic and energy producing reactions. This prosurvival function of autophagy is conserved in all eukaryotes including yeast, and probably represents its most ancient role. In contrast, autophagy was found to promote cell death during metamorphosis, as

proper programmed elimination of polyploid larval salivary glands and midguts is suggested to depend on autophagy.[31,32] All 3 pathways (basal, starvation-induced, and developmental autophagy) serving various cellular and organismal functions require *Atg17,* indicating that its protein product plays an equally critical role in autophagy in these different contexts. A related study published while our manuscript was in preparation also reports that *Drosophila Atg17* is required for starvation-induced and developmental autophagy.[38]

Previous reports establish that RB1CC1 is an essential subunit of the Atg1/ULK kinase complex in mammalian cells.[3,15,16] RB1CC1 directly binds the C-terminal region of human ATG13, which facilitates its interaction with, and phosphorylation by, ULK1 and ULK2.[16] ULK1 and ULK2 also bind to the C-terminal region of ATG13, and phosphorylate multiple serine and threonine residues during autophagy induction. In addition, mammalian ATG13 is phosphorylated by MTOR in vitro in kinase assays.[16] Thus, a model was proposed, according to which ATG13 is inhibited by MTOR-mediated phosphorylation under basal conditions. Starvation results in activation of ULK1/2, and then it directly phosphorylates mammalian ATG13, which is thought to be important for the induction of autophagy. The Atg1 mammalian orthologs ULK1 and ULK2 are inhibited at least in part by direct MTOR-mediated phosphorylation and undergo autophosphorylation during autophagy induction.[17] Interestingly, the Atg1 complex appears to be regulated differently in yeast: Atg13 is phosphorylated by TOR in up to 8 different residues in well-fed cells, and Atg13 undergoes practically complete dephosphorylation during autophagy induction.[39] Six of these phosphorylation events occur in or near the central region of yeast Atg13, and are thought to destabilize the Atg1 complex. An unphosphorylatable Atg13 mutant triggers autophagy in nutrient-replete conditions independent of TOR in yeast.[39] A recent paper shows that the assembled Atg1 kinase complex can be detected in yeast cells under nutrient-replete conditions as well.[40] This pool may be important to sustain the Cvt (cytoplasm-to-vacuole targeting) pathway, an *ATG* gene-dependent vesicular route transporting certain hydrolases to the vacuole in well-fed yeast cells. The Cvt pathway shares certain similarities with basal autophagy observed in metazoan cells, such as specific recognition of aggregated cargo proteins. In fact, a double-membrane Cvt vesicle resembles a small autophagosome, which only contains specific cargo and no bulk cytosol.[41]

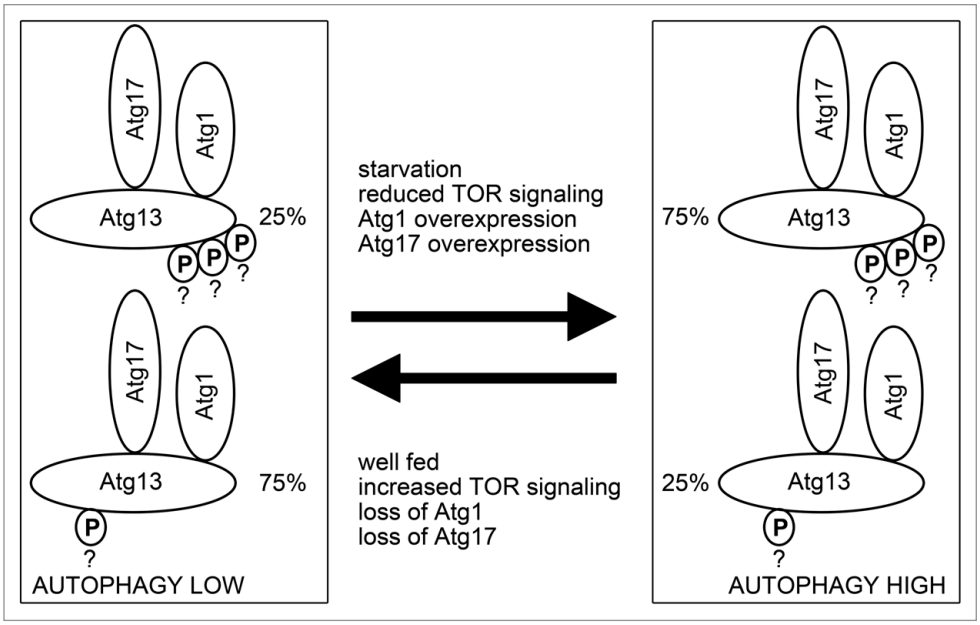


Figure 8. A hypothetical model of Atg13 function during basal and induced autophagy. Based on correlation of overall Atg13 phosphorylation level with autophagic status, Atg13 is likely activated at least in part by Atg1-mediated phosphorylation on multiple residues. Question marks near phosphogroups of Atg13 highlight the fact that the number and exact sites of these phosphorylation events is currently unknown. The ratio of this active Atg13 appears to be lower during nutrient-replete conditions relative to the inactive form, which is potentially phosphorylated by TOR or other kinases, or not phosphorylated at all. The presence of the active form at a lower level under basal conditions may be necessary to support low-level autophagic activity. Starvation, genetic inactivation of TOR, and overexpression of Atg1 or Atg17 appear to increase the ratio of active Atg13, which may contribute to increased autophagosome formation observed in response to these autophagy-inducing treatments.

Atg1 and Atg17 have been suggested to bind to more central regions of yeast Atg13, unlike in mammals.[36] These differences are reflected at the sequence level as well: only the N-terminal domain appears to be conserved, although the double arginine motifs thought to function as a phosphorylation sensor in yeast Atg13 are missing in higher eukaryotes (**Fig. S5**). *Drosophila* Atg13 has also been reported to bind to Atg1, but the region involved has not been determined.[21] We found that Atg1 interacts with the C-terminal part of Atg13, similar to mammals. Our results also reveal that the interaction of Atg13 and RB1CC1 is conserved, but the C-terminal region may not be sufficient: only a fragment containing both the middle and C-terminus of Atg13 elicited strong binding to Atg17, although we did not test whether this interaction is also direct in *Drosophila*.

There are striking differences between yeast, fly, and mammalian cells in the overall phosphorylation status of Atg13 during autophagy induction. The phosphorylation level of yeast Atg13 strongly decreases upon starvation, it does not change much in mammalian cells, whereas it strongly increases in polyploid larval fat bodies in starved *Drosophila* larvae. The shift of Atg13 to more phosphorylated forms during starvation agrees with the findings of a recent report that relied on cooverexpressed proteins.[21] Although other kinases may also

phosphorylate and thus modulate endogenous Atg13, our data strongly suggest that Atg1 is mostly responsible for starvation-induced hyperphosphorylation of Atg13 in *Drosophila*. First, overexpression of Atg1 results in a remarkable decrease in the mobility of both tagged and endogenous Atg13, both in cultured cells and in well-fed larvae. Second, overexpression of dominant-negative Atg1 leads to a near-complete block of starvation-induced Atg13 phosphorylation in vivo, practically eliminating all slower mobility bands in fat body lysates. *Drosophila* Atg17 appears to be necessary for starvation-induced phosphorylation of endogenous Atg13, similar to its mammalian ortholog RB1CC1.[3] Finally, transient or constitutive overexpression of Atg17 induces autophagy and also shifts Atg13 to slower mobility forms, both in an Atg1-dependent manner. Thus, endogenous Atg17 appears to be required for the Atg1-mediated hyperphosphorylation of Atg13 during starvation in vivo, and its overexpression likely enhances basal autophagy at least in part by promoting Atg1 kinase activity toward Atg13.

We recently reported that *Atg* genes including *Atg1* and *Atg13* are required for basal autophagy in *Drosophila*.[24] Therefore, Atg1 must have some residual kinase activity in nutrient-replete conditions as well. A pool of active Atg13 (phosphorylated by Atg1) likely exists even in well-fed cells, which may be important for sustaining basal autophagy. In line with these, we found that overexpression of dominant-negative Atg1 reduces the amount of hyperphosphorylated Atg13 observed in well-fed cells. Based on the correlation of changes in Atg13 phosphorylation patterns with autophagic status, we propose a model according to which the ratio, and not simply the presence or absence of different pools of Atg1 complexes may regulate the level of autophagy in *Drosophila* (**Fig. 8**). Currently there is no evidence for the number and exact sites of Atg13 phosphorylation events in *Drosophila*. Thus, our model will need to be tested by the identification of all phosphosites in Atg13 and determination of the percentage of phosphorylated vs. nonphosphorylated states for each site in different conditions, followed by functional analysis of phospho-mimetic and nonphosphorylatable mutant forms of Atg13 in vivo.

Previous reports propose that Atg17 and its proposed functional counterpart RB1CC1 acts most upstream of all Atg/ATG proteins in yeast and mammals, respectively.[26,27] Our genetic epistasis results also support the upstream role of Atg17 in autophagy in *Drosophila*. In contrast, a recent report suggests that *Drosophila* Atg17 functions downstream of Atg1.[38] This conclusion was based on: i) failure of overexpressed Atg17 to influence the mobility of overexpressed Atg1 in western blots of cultured cell lysates, ii) Atg1 phosphorylation level remained responsive to cellular energy status in cultured *atg17* siRNA cells and starved hypomorphic *Atg17* mutants, iii) *Atg17* RNAi reduced myc-Atg1 overexpression-induced LTR and acridin-orange staining in eye disks, and iv. coexpression of Atg17 with Atg1 did not induce eye degeneration. Importantly, no loss-of-function tests were performed in *Atg17*-null mutants, so interpretation of the above phenotypes may be complicated by the presence of residual protein. Another potential explanation is that Atg17 and Atg1 are subunits of the same complex and appear to function together during autophagy induction, which makes it difficult to clearly establish their hierarchical relationship.

Atg17 colocalizes with markers of early autophagic structures both in controls and *atg7* and *Atg8a*-null mutants, in which autophagosome formation is impaired and stalled PAS dots accumulate. The aggregate-forming protein SQSTM1 is a specific cargo for autophagy and is recruited to the PAS in cultured cells and mouse tissues.[14,25] SQSTM1 interacts with MTOR complex 1, which is found on lysosomes in growing mammalian cells. This localization is facilitated by the binding of MTOR to RRAG (Ras-related GTP binding) proteins and the Ragulator complex. These latter components are anchored to lysosomes partly through their physical interaction with subunits of the lysosomal proton pump v-ATPase complex.[5] Ref(2)P aggregates also colocalize with TOR in fat body cells of well-fed *Drosophila* larvae, and starvation results in dispersion of TOR. As Ref(2)P puncta appear to remain associated with lysosomes and colocalize with Atg17 during starvation, these protein aggregates near lysosomes may be specifically captured into forming autophagosomes after TOR is inactivated. To our knowledge, this localization has not been reported in animal models or cells yet, so it remains to be seen if it is a characteristic of these large polyploid cells and tissues, which primarily function as nutrient storing and metabolic organs in the fly larva. It is important to note that the PAS always assembles at aggregates of the selective cargo prApe1 (precursor aminopeptidase I) near the vacuole, the equivalent of the metazoan lysosomal network in yeast.[42] The functional significance of this location is not known yet. A recent report argues that vesicles containing the transmembrane protein Atg9 may be recycled from vacuole/autolysosome membranes to fuel ongoing cycles of autophagosome generation in yeast.[35] If Atg9 plays similar roles in *Drosophila*, then the putative perilysosomal localization of early autophagic structures may give instant access to these membrane-recycling vesicles. The perilysosomal localization of PAS suggested by our data may also couple upstream signals such as TOR with robust induction of autophagy at lysosome-associated Ref(2)P aggregates in polyploid larval *Drosophila* cells. It will be interesting to see if the association of SQSTM1 and Atg proteins near lysosomes is also observed in a mammalian tissue in future studies.

Materials and Methods

Fly strains and genetics

Flies were maintained on standard yeast/cornmeal/agar media. P element excisions and fat body cell clones were generated as described earlier in detail.[10,22,23,33] Briefly, RNAi cell clones were generated spontaneously in larvae carrying *hs-Flp, Act > CD2 > Gal4* and *UAS-RNAi* (and *UAS-GFPnls* as a knockdown cell marker). For mutant cell clones, 2 to 4 h embryos were heat shocked in a 38 °C water bath for 1 h to generate loss-of-function cells (marked either by lack of GFP expression, or vice versa, by GFP expression in case of the positively marked mutant clone generation system).[10,23,33,43] Overexpression experiments were routinely performed using standard binary

expression systems. In these, Gal4 and QF transcription factors drive expression of transgenes under the influence of UAS or QUAS promoters, respectively.[43] For transient expression, *UAS-Atg17-GFP* was induced by *hs-Gal4* and a 30 to 60 min heat shock at 37 °C, followed by 3 h of recovery before analysis. For constitutive expression, *QUAS-Atg17-GFP* was driven by *ET49-QF*.[43] The following stocks were used in this study: *atg17[KK104864], atg8a[KK109654]* (both obtained from the Vienna *Drosophila* RNAi Center), *atg12[JF02704]*,[24] *UAS-Atg17[EY03045], w[1118]* used as control, *FRT82B, Ubi-GFP, UAS-GFP, cg-Gal4, ET49-QF, QUAS-GFP, tub-QS, Df(3R) BSC464* (all obtained from the Bloomington *Drosophila* Stock Center), *atg17[d130]* (referred to as $atg17^{-/-}$ or null mutant throughout the paper), *UAS-Atg17-GFP, QUAS-Atg17-GFP, r4-mCherry-Atg1* (all described in this study), *UAS-Atg1[6B], UAS-Atg1[DN]*,[22] *UAS-Lamp1-GFP*, *hsFlp[22], Atg13[d81], r4-mCherry-Atg8a, UAS-myc-Atg1, UAS-Atg13-FLAG, UAS-FLAG-tor, UAS-Ref(2)P-GFP, r4-Gal4, UAS-Tsc1, UAS-Tsc2* (kindly provided by Tom Neufeld),[21] *UAS-Venus-Atg1* (kindly provided by Toshifumi Tomoda),[44] *atg7[d77], atg7[d14]*,[10] *atg8a[d4]*,[24] *atg1[KG07993]* (obtained from the *Drosophila* Genetic Resource Center).

Generation of polyclonal antibodies

Full-length Atg8a and partial Atg17 (amino acids 1 to 420) coding sequences were amplified by PCR and cloned into pEV (kindly provided by Peter Rapali) as NdeI-XhoI fragments. The full Atg1 and partial TOR (amino acids 2,345–2,470) coding regions were PCR amplified, blunt cloned into XmnI-EcoRV-digested pENTR1A (Invitrogen, 11813011) and subsequently recombined into pDEST17 (Invitrogen, 11803012). The Atg13 entry clone (kindly provided by Tom Neufeld) was also recombined into pDEST17. All these N-terminally His-tagged proteins were expressed in *E. coli* Rosetta strain and purified using Ni-NTA agarose beads (Qiagen/Biomarker, 30210). Recombinant proteins were used to immunize rats in-house following standard procedures with Freund's adjuvants (Sigma, F5881 and F5506, respectively). Recombinant Atg8a was also used to immunize rabbits (Immunogenes).

Generation of transgenic lines

Coding sequences were amplified with specific primers from cDNA and cloned into pR4-*mCherry-Atg8a* (kindly provided by Tom Neufeld) by replacing the BsrGI fragment (Atg8a coding region) to generate pR4-*mCherry-Atg1*. An 1xHA-*EGFP-Sirup* coding sequence was chemically synthesized (Genscript) and cloned into pUAST (DGRC 1000) with EcoRI and XhoI to generate pUAS-*GFP-Sirup*. A pUAS-C-*GFP* plasmid was generated by amplifying the HA-*EGFP* sequence from pUAS-*GFP-Sirup* and cloning it as an XbaI-NheI fragment into the XbaI site of pUAST. This vector was subsequently used to generate pUAS-*Atg17-GFP* by cloning the *Atg17* coding region amplified from cDNA as an XbaI fragment upstream of *GFP*. *Atg17-GFP* sequences were amplified from this plasmid and cloned into pQUAST[43] as a NotI fragment to generate pQUAS-*Atg17-GFP*. Coding sequences for pUAS-3xHA-*Atg101* were chemically synthesized (Genscript). Transgenic flies were established by standard embryo injection techniques (Bestgene).

Cell culture

D.Mel-2 cells (a serum-independent S2 line) were maintained in Express Five Serum-Free Medium with penicillin and streptomycin (Invitrogen, 10486025 and 15140122, respectively). Cells were transfected with UAS constructs and metallothionein-Gal4 plasmid using TransIT-2020 reagent (Mirus/BioTec, MIR5405) according to the manufacturer's recommendations. 48 h later, protein expression was induced by adding 1mM $CuSO_4$ for overnight incubation. The following DNA constructs were used in cell culture experiments: pUAS-*atg17-GFP*, pUAS-myc-*atg1* (generated by recombination of the Atg1 entry clone into pTMW [DGRC 1107]), pUAS-*atg13*-FLAG (generated by recombination of the Atg13 entry clone into pTWF [DGRC 1116]), pUAS-FLAG-*tor*, pUAS-myc-*atg1[KD]* (kindly provided by Tom Neufeld), pUAS-*Atg101*-FLAG (generated by PCR amplifying and blunt cloning the Atg101 coding region into XmnI-EcoRV-digested pENTR1A, followed by recombination into pTWF). Atg101 coding sequences were replaced with GFP in pUAS-3xHA-*Atg101*, and PCR amplified Atg13 and Atg1 fragments were cloned into this pUAS-3xHA-*GFP* plasmid using NotI-Acc65I to generate the various truncated forms. An active TOR fragment (amino acids 1333 to 2470)[16] was amplified from pUAS-FLAG-*tor* and ligated as an XbaI fragment into pUAST. Gateway vectors and ESTs used for cloning were obtained from the *Drosophila* Genomics Resource Center (DGRC). Primer and synthetic gene sequences used in molecular cloning experiments are available on request.

Histology and imaging

For starvation treatments, early L3 larvae were floated in 20% sucrose for 3 h, dissected and mounted in 50% glycerol/PBS (phosphate-buffered saline) with 1 μg/μl DAPI (4',6-diamidino-2-phenylindole, Sigma, D9542) for transgenic reporters or stained in 100 μM LTR (Invitrogen, L7528) in PBS before mounting. Images were obtained on a fluorescent microscope (Carl Zeiss, Axioimager M2) equipped with a grid confocal unit (Carl Zeiss, Apotome2) using Plan-NeoFluar 40× 0.75 NA air or 100× 1.30 NA oil immersion objectives (Carl Zeiss), Axiocam Mrm camera (Carl Zeiss) and Axiovision software (Carl Zeiss), or an laser scanning microscope (Olympus, FV500) with a 63× 1.45 NA oil immersion objective (Olympus) in sequential scanning mode. Primary images were processed in Photoshop (Adobe) to produce final figures. Tissues were processed for conventional electron microscopy as described previously.[10,23]

Statistics

For statistical analyses, either 300 × 300 pixel areas were selected randomly from different genotypes, or randomly selected GFP-positive cells together with neighboring control cells from the same images were evaluated in clonal studies. Dot number and size data was extracted by setting an appropriate threshold for the relevant channel in ImageJ (National Institutes of Health). Data were imported into SPSS Statistics version 20 (IBM), which was used to test for normality and calculate *P* values. In pairwise comparisons, normal distribution data were analyzed with 2-tailed, 2-sample Student *t* test, whereas Mann-Whitney u-tests

were used when one or both data sets showed a non-normal distribution, respectively.[23,45]

Primary antibodies

The following primary antibodies were used in this study: rat anti-Atg8a (IF 1:300, this study), rat anti-GFP (WB 1:5,000),[24] mouse anti-FLAG (IF 1:100, WB 1:2,000, Sigma, F1804), mouse anti-myc (WB 1:5,000, Sigma, M4439), rabbit anti-HA (WB 1:2,000, Sigma, H6908), rat anti-Atg17 (IF 1:100, WB 1:5,000, this study), rabbit anti-Ref(2)P/p62 (IF 1:2,000, WB 1:5,000),[24] mouse anti-tubulin (WB 1:1,000, DSHB AA4.3 s), rat anti-Atg1 (WB 1:5,000, this study), rat anti-Atg13 (WB 1:5,000, this study), rat anti-TOR (WB 1:5,000, this study), rabbit anti-Atg5 (IF 1:100, Sigma, A0856), rabbit anti-cathepsin L/Cp1 (IF 1:150, Abcam, ab58991), chicken anti-GFP (IF 1:1,500, Invitrogen, A10262). Note that the specificity of our rat and rabbit anti-Atg8a antisera described here has recently been shown elsewhere as well.[23,45]

Immunostaining of whole-mount larval tissues

Bisected third instar larvae were inverted and fixed with 3.7% paraformaldehyde in PBS overnight at 4 °C. Next, samples were rinsed twice and washed for 2 h in PBS, permeabilized for 15 min in PBTX-DOC (PBS with 0.1% Triton X-100 and 0.05% sodium deoxycholate) and blocked for 3 h in 3% goat serum in PBTX-DOC. Samples were then incubated overnight at 4 °C with primary antibodies in 1% goat serum in PBTX-DOC. After 3 × 30 min washes in PBTX-DOC, samples were incubated with secondary antibodies diluted 1:1,500 in 1% goat serum in PBTX-DOC for 4 h at room temperature. Finally, after 3 × 15 min washes in PBTX-DOC and 1 × 15 min in PBS, fat bodies and midguts were dissected and mounted in 50% glycerol/PBS with 0.2 μM DAPI. The following secondary antibodies were used: Alexa 488 anti-chicken, Alexa 488 anti-rabbit, Alexa 546 anti-rabbit, Alexa 568 anti-rat, Alexa 568 anti-mouse, Alexa 647 anti-rabbit (all used in 1:1,500, Invitrogen A11039, A11034, A11035, A11077, A1104, A21245, respectively).

Immunoprecipitation

Cultured cells were collected by centrifugation, washed twice in PBS and lysed on ice in lysis buffer (0.5% Triton-X100, 150 mM NaCl, 1 mM EDTA, 20 mM TRIS-HCl pH 8) containing complete protease and phosphatase inhibitor cocktails (Sigma P8340 and Roche 04906845001, respectively), spun for 10 min at 10,000 g in an Eppendorf 5430R at 4 °C, followed by the addition of 20 μl anti-HA or anti-FLAG slurry (Sigma A2095 and A2220, respectively) to the cleared supernatant fraction. After incubation at 4 °C for 2 h, beads were collected by centrifugation at 5,000 g for 30 s at 4 °C followed by extensive washes in lysis buffer, and finally boiled in 20 μl 2× Laemmli sample buffer (Sigma S3401).

Western blots and densitometry

Equal amounts of proteins were loaded and separated by denaturing SDS-PAGE and transferred to Immobilon-P PVDF membrane (Millipore/Biocenter IPVH00010) in transfer buffer (0.025 M Trizma base, 0.2 M glycine, 10% methanol). Membranes were blocked in CBB (casein blocking buffer, 0.5% casein [Sigma C3400] dissolved in 0.1 M Trizma base, followed by adjusting pH to 7.5 with HCl) for 1 h at room temperature, washed 3 × 5 min in TBST (0.025 M Trizma base pH adjusted to 7.5 with HCl, 0.9% NaCl, 0.1% Tween 20), incubated with primary antibodies in 1:1 CBB (casein blocking buffer)/TBST for 1 h at room temperature, followed by 3 × 10 min washes in TBST. Blots were then incubated with AP (alkaline phosphatase) conjugated goat anti-mouse, anti-rabbit (Millipore/Biocenter, AP124A and AP132A, respectively) or rabbit anti-rat (Sigma, A6066) secondary antibodies diluted 1:5,000 in 1:1 CBB (casein blocking buffer)/TBST for 1 h at room temperature. Blots were washed 3 × 10 min in TBST and 1 × 5 min in AP (alkaline phosphatase) buffer (100 mM Trizma base, 100 mM NaCl, 5 mM $MgCl_2$, 0,05% Tween 20, pH adjusted to 9.5 with HCl) and then developed using NBT-BCIP (Sigma, 72091) diluted 1:50 in AP (alkaline phosphatase) buffer.

All western blots were repeated on independent biological samples with similar results, and representative examples are shown. For fat body lysates, 25 to 30 fat bodies were dissected and pooled per genotype. The ratio of slower vs. faster mobility Atg13 forms (upper bands vs. lowest band) was calculated by densitometry using ImageJ (National Institutes of Health). Briefly, lanes were selected using the Rectangular Selection tool, and plots were drawn using Plot Lanes. A Straight Line tool was used to enclose the peak corresponding to the bands of interest, peaks were highlighted by the Wand tool, and Label Peaks was used to collect data.

Disclosure of Potential Conflicts of Interest

No potential conflicts of interest were disclosed.

Acknowledgments

We thank Sarolta Pálfia, Zsófia Kováts, Eszter Papp, and Eszter Vágó for technical assistance, Attila L Kovács for comments on the manuscript, colleagues and public repositories listed in the methods section for reagents, and the Hungarian Scientific Research Fund (OTKA K83509), Wellcome Trust (087518/Z/08/Z) and Hungarian Academy of Sciences (BO/00552/11) for support.

Supplemental Materials

Supplemental materials may be found here:
www.landesbioscience.com/journals/autophagy/article/27442

References

1. Mizushima N, Levine B, Cuervo AM, Klionsky DJ. Autophagy fights disease through cellular self-digestion. Nature 2008; 451:1069-75; PMID:18305538; http://dx.doi.org/10.1038/nature06639
2. Juhász G. Interpretation of bafilomycin, pH neutralizing or protease inhibitor treatments in autophagic flux experiments: novel considerations. Autophagy 2012; 8:1875-6; PMID:22874642; http://dx.doi.org/10.4161/auto.21544
3. Hosokawa N, Hara T, Kaizuka T, Kishi C, Takamura A, Miura Y, Iemura S, Natsume T, Takehana K, Yamada N, et al. Nutrient-dependent mTORC1 association with the ULK1-Atg13-FIP200 complex required for autophagy. Mol Biol Cell 2009; 20:1981-91; PMID:19211835; http://dx.doi.org/10.1091/mbc.E08-12-1248

4. Korolchuk VI, Saiki S, Lichtenberg M, Siddiqi FH, Roberts EA, Imarisio S, Jahreiss L, Sarkar S, Futter M, Menzies FM, et al. Lysosomal positioning coordinates cellular nutrient responses. Nat Cell Biol 2011; 13:453-60; PMID:21394080; http://dx.doi.org/10.1038/ncb2204
5. Zoncu R, Bar-Peled L, Efeyan A, Wang S, Sancak Y, Sabatini DM. mTORC1 senses lysosomal amino acids through an inside-out mechanism that requires the vacuolar H(+)-ATPase. Science 2011; 334:678-83; PMID:22053050; http://dx.doi.org/10.1126/science.1207056
6. Yu L, McPhee CK, Zheng L, Mardones GA, Rong Y, Peng J, Mi N, Zhao Y, Liu Z, Wan F, et al. Termination of autophagy and reformation of lysosomes regulated by mTOR. Nature 2010; 465:942-6; PMID:20526321; http://dx.doi.org/10.1038/nature09076
7. Klionsky DJ, Cregg JM, Dunn WA Jr., Emr SD, Sakai Y, Sandoval IV, Sibirny A, Subramani S, Thumm M, Veenhuis M, et al. A unified nomenclature for yeast autophagy-related genes. Dev Cell 2003; 5:539-45; PMID:14536056; http://dx.doi.org/10.1016/S1534-5807(03)00296-X
8. Mizushima N, Komatsu M. Autophagy: renovation of cells and tissues. Cell 2011; 147:728-41; PMID:22078875; http://dx.doi.org/10.1016/j.cell.2011.10.026
9. Chen Y, Klionsky DJ. The regulation of autophagy - unanswered questions. J Cell Sci 2011; 124:161-70; PMID:21187343; http://dx.doi.org/10.1242/jcs.064576
10. Juhász G, Erdi B, Sass M, Neufeld TP. Atg7-dependent autophagy promotes neuronal health, stress tolerance, and longevity but is dispensable for metamorphosis in Drosophila. Genes Dev 2007; 21:3061-6; PMID:18056421; http://dx.doi.org/10.1101/gad.1600707
11. Simonsen A, Cumming RC, Brech A, Isakson P, Schubert DR, Finley KD. Promoting basal levels of autophagy in the nervous system enhances longevity and oxidant resistance in adult Drosophila. Autophagy 2008; 4:176-84; PMID:18059160
12. Moscat J, Diaz-Meco MT. p62: a versatile multitasker takes on cancer. Trends Biochem Sci 2012; 37:230-6; PMID:22424619; http://dx.doi.org/10.1016/j.tibs.2012.02.008
13. Nezis IP, Simonsen A, Sagona AP, Finley K, Gaumer S, Contamine D, Rusten TE, Stenmark H, Brech A. Ref(2)P, the Drosophila melanogaster homologue of mammalian p62, is required for the formation of protein aggregates in adult brain. J Cell Biol 2008; 180:1065-71; PMID:18347073; http://dx.doi.org/10.1083/jcb.200711108
14. Komatsu M, Waguri S, Koike M, Sou YS, Ueno T, Hara T, Mizushima N, Iwata J, Ezaki J, Murata S, et al. Homeostatic levels of p62 control cytoplasmic inclusion body formation in autophagy-deficient mice. Cell 2007; 131:1149-63; PMID:18083104; http://dx.doi.org/10.1016/j.cell.2007.10.035
15. Hara T, Takamura A, Kishi C, Iemura S, Natsume T, Guan JL, Mizushima N. FIP200, a ULK-interacting protein, is required for autophagosome formation in mammalian cells. J Cell Biol 2008; 181:497-510; PMID:18443221; http://dx.doi.org/10.1083/jcb.200712064
16. Jung CH, Jun CB, Ro SH, Kim YM, Otto NM, Cao J, Kundu M, Kim DH. ULK-Atg13-FIP200 complexes mediate mTOR signaling to the autophagy machinery. Mol Biol Cell 2009; 20:1992-2003; PMID:19225151; http://dx.doi.org/10.1091/mbc.E08-12-1249
17. Mizushima N. The role of the Atg1/ULK1 complex in autophagy regulation. Curr Opin Cell Biol 2010; 22:132-9; PMID:20056399; http://dx.doi.org/10.1016/j.ceb.2009.12.004
18. Chan EY, Longatti A, McKnight NC, Tooze SA. Kinase-inactivated ULK proteins inhibit autophagy via their conserved C-terminal domains using an Atg13-independent mechanism. Mol Cell Biol 2009; 29:157-71; PMID:18936157; http://dx.doi.org/10.1128/MCB.01082-08
19. Erdi B, Nagy P, Zvara A, Varga A, Pircs K, Ménesi D, Puskás LG, Juhász G. Loss of the starvation-induced gene Rack1 leads to glycogen deficiency and impaired autophagic responses in Drosophila. Autophagy 2012; 8:1124-35; PMID:22562043; http://dx.doi.org/10.4161/auto.20069
20. Bánréti Á, Lukácsovich T, Csikós G, Erdélyi M, Sass M. PP2A regulates autophagy in two alternative ways in Drosophila. Autophagy 2012; 8:623-36; PMID:22330894; http://dx.doi.org/10.4161/auto.19081
21. Chang YY, Neufeld TP. An Atg1/Atg13 complex with multiple roles in TOR-mediated autophagy regulation. Mol Biol Cell 2009; 20:2004-14; PMID:19225150; http://dx.doi.org/10.1091/mbc.E08-12-1250
22. Scott RC, Juhász G, Neufeld TP. Direct induction of autophagy by Atg1 inhibits cell growth and induces apoptotic cell death. Curr Biol 2007; 17:1-11; PMID:17208179; http://dx.doi.org/10.1016/j.cub.2006.10.053
23. Takáts S, Nagy P, Varga Á, Pircs K, Kárpáti M, Varga K, Kovács AL, Hegedűs K, Juhász G. Autophagosomal Syntaxin17-dependent lysosomal degradation maintains neuronal function in Drosophila. J Cell Biol 2013; 201:531-9; PMID:23671310; http://dx.doi.org/10.1083/jcb.201211160
24. Pircs K, Nagy P, Varga A, Venkei Z, Erdi B, Hegedus K, Juhasz G. Advantages and limitations of different p62-based assays for estimating autophagic activity in Drosophila. PLoS One 2012; 7:e44214; PMID:22952930; http://dx.doi.org/10.1371/journal.pone.0044214
25. Itakura E, Mizushima N. p62 Targeting to the autophagosome formation site requires self-oligomerization but not LC3 binding. J Cell Biol 2011; 192:17-27; PMID:21220506; http://dx.doi.org/10.1083/jcb.201009067
26. Suzuki K, Kubota Y, Sekito T, Ohsumi Y. Hierarchy of Atg proteins in pre-autophagosomal structure organization. Genes Cells 2007; 12:209-18; PMID:17295840; http://dx.doi.org/10.1111/j.1365-2443.2007.01050.x
27. Itakura E, Mizushima N. Characterization of autophagosome formation site by a hierarchical analysis of mammalian Atg proteins. Autophagy 2010; 6:764-76; PMID:20639694; http://dx.doi.org/10.4161/auto.6.6.12709
28. Lee SB, Kim S, Lee J, Park J, Lee G, Kim Y, Kim JM, Chung J. ATG1, an autophagy regulator, inhibits cell growth by negatively regulating S6 kinase. EMBO Rep 2007; 8:360-5; PMID:17347671; http://dx.doi.org/10.1038/sj.embor.7400917
29. Jung CH, Seo M, Otto NM, Kim DH. ULK1 inhibits the kinase activity of mTORC1 and cell proliferation. Autophagy 2011; 7:1212-21; PMID:21795849; http://dx.doi.org/10.4161/auto.7.10.16660
30. Rusten TE, Lindmo K, Juhász G, Sass M, Seglen PO, Brech A, Stenmark H. Programmed autophagy in the Drosophila fat body is induced by ecdysone through regulation of the PI3K pathway. Dev Cell 2004; 7:179-92; PMID:15296715; http://dx.doi.org/10.1016/j.devcel.2004.07.005
31. Berry DL, Baehrecke EH. Growth arrest and autophagy are required for salivary gland cell degradation in Drosophila. Cell 2007; 131:1137-48; PMID:18083103; http://dx.doi.org/10.1016/j.cell.2007.10.048
32. Denton D, Shravage B, Simin R, Mills K, Berry DL, Baehrecke EH, Kumar S. Autophagy, not apoptosis, is essential for midgut cell death in Drosophila. Curr Biol 2009; 19:1741-6; PMID:19818615; http://dx.doi.org/10.1016/j.cub.2009.08.042
33. Juhász G, Hill JH, Yan Y, Sass M, Baehrecke EH, Backer JM, Neufeld TP. The class III PI(3)K Vps34 promotes autophagy and endocytosis but not TOR signaling in Drosophila. J Cell Biol 2008; 181:655-66; PMID:18474623; http://dx.doi.org/10.1083/jcb.200712051
34. Kirisako T, Baba M, Ishihara N, Miyazawa K, Ohsumi M, Yoshimori T, Noda T, Ohsumi Y. Formation process of autophagosome is traced with Apg8/Aut7p in yeast. J Cell Biol 1999; 147:435-46; PMID:10525546; http://dx.doi.org/10.1083/jcb.147.2.435
35. Yamamoto H, Kakuta S, Watanabe TM, Kitamura A, Sekito T, Kondo-Kakuta C, Ichikawa R, Kinjo M, Ohsumi Y. Atg9 vesicles are an important membrane source during early steps of autophagosome formation. J Cell Biol 2012; 198:219-33; PMID:22826123; http://dx.doi.org/10.1083/jcb.201202061
36. Jao CC, Ragusa MJ, Stanley RE, Hurley JH. A HORMA domain in Atg13 mediates PI 3-kinase recruitment in autophagy. Proc Natl Acad Sci U S A 2013; 110:5486-91; PMID:23509291; http://dx.doi.org/10.1073/pnas.1220306110
37. Dorsey FC, Rose KL, Coenen S, Prater SM, Cavett V, Cleveland JL, Caldwell-Busby J. Mapping the phosphorylation sites of Ulk1. J Proteome Res 2009; 8:5253-63; PMID:19807128; http://dx.doi.org/10.1021/pr900583m
38. Kim M, Park HL, Park HW, Ro SH, Nam SG, Reed JM, Guan JL, Lee JH. Drosophila Fip200 is an essential regulator of autophagy that attenuates both growth and aging. Autophagy 2013; 9:1201-13; PMID:23819996; http://dx.doi.org/10.4161/auto.24811
39. Kamada Y, Yoshino K, Kondo C, Kawamata T, Oshiro N, Yonezawa K, Ohsumi Y. Tor directly controls the Atg1 kinase complex to regulate autophagy. Mol Cell Biol 2010; 30:1049-58; PMID:19995911; http://dx.doi.org/10.1128/MCB.01344-09
40. Kraft C, Kijanska M, Kalie E, Siergiejuk E, Lee SS, Semplicio G, Stoffel I, Brezovich A, Verma M, Hansmann I, et al. Binding of the Atg1/ULK1 kinase to the ubiquitin-like protein Atg8 regulates autophagy. EMBO J 2012; 31:3691-703; PMID:22885598; http://dx.doi.org/10.1038/emboj.2012.225
41. Suzuki K. Selective autophagy in budding yeast. Cell Death Differ 2013; 20:43-8; PMID:22705847; http://dx.doi.org/10.1038/cdd.2012.73
42. Scott SV, Nice DC 3rd, Nau JJ, Weisman LS, Kamada Y, Keizer-Gunnink I, Funakoshi T, Veenhuis M, Ohsumi Y, Klionsky DJ. Apg13p and Vac8p are part of a complex of phosphoproteins that are required for cytoplasm to vacuole targeting. J Biol Chem 2000; 275:25840-9; PMID:10837477; http://dx.doi.org/10.1074/jbc.M002813200
43. Potter CJ, Tasic B, Russler EV, Liang L, Luo L. The Q system: a repressible binary system for transgene expression, lineage tracing, and mosaic analysis. Cell 2010; 141:536-48; PMID:20434990; http://dx.doi.org/10.1016/j.cell.2010.02.025
44. Toda H, Mochizuki H, Flores R 3rd, Josowitz R, Krasieva TB, Lamorte VJ, Suzuki E, Gindhart JG, Furukubo-Tokunaga K, Tomoda T. UNC-51/ATG1 kinase regulates axonal transport by mediating motor-cargo assembly. Genes Dev 2008; 22:3292-307; PMID:19056884; http://dx.doi.org/10.1101/gad.1734608
45. Nagy P, Varga A, Pircs K, Hegedűs K, Juhász G. Myc-driven overgrowth requires unfolded protein response-mediated induction of autophagy and antioxidant responses in Drosophila melanogaster. PLoS Genet 2013; 9:e1003664; PMID:23950728; http://dx.doi.org/10.1371/journal.pgen.1003664

dc_840_14

FEBS Letters 588 (2014) 408–413

journal homepage: www.FEBSLetters.org

Different effects of *Atg2* and *Atg18* mutations on Atg8a and Atg9 trafficking during starvation in Drosophila ☆

Péter Nagy, Krisztina Hegedűs, Karolina Pircs, Ágnes Varga, Gábor Juhász *

Department of Anatomy, Cell and Developmental Biology, Eötvös Loránd University, Budapest H-1117, Hungary

ARTICLE INFO

Article history:
Received 17 October 2013
Revised 6 December 2013
Accepted 10 December 2013
Available online 24 December 2013

Edited by Noboru Mizushima

Keywords:
Atg2
Atg7
Atg8a
Atg9
Atg18
Ref(2)P/p62

ABSTRACT

The Atg2–Atg18 complex acts in parallel to Atg8 and regulates Atg9 recycling from phagophore assembly site (PAS) during autophagy in yeast. Here we show that in Drosophila, both Atg9 and Atg18 are required for Atg8a puncta formation, unlike Atg2. Selective autophagic degradation of ubiquitinated proteins is mediated by Ref(2)P/p62. The transmembrane protein Atg9 accumulates on refractory to Sigma P (Ref(2)P) aggregates in *Atg7*, *Atg8a* and *Atg2* mutants. No accumulation of Atg9 is seen on Ref(2)P in cells lacking Atg18 or Vps34 lipid kinase function, while the Atg1 complex subunit FIP200 is recruited. The simultaneous interaction of Atg18 with both Atg9 and Ref(2)P raises the possibility that Atg18 may facilitate selective degradation of ubiquitinated protein aggregates by autophagy.

Structured summary of protein interactions:
Ref(2)P physically interacts with **Atg18** by anti tag coimmunoprecipitation (View interaction) **Atg18** physically interacts with **Atg2** by anti tag coimmunoprecipitation (View interaction) **CG8678** physically interacts with **Atg2** by anti tag coimmunoprecipitation (View interaction) **Atg18** physically interacts with **atg9** by anti tag coimmunoprecipitation (View interaction)

© 2013 The Authors. Published by Elsevier B.V. All rights reserved.

1. Introduction

Autophagy is a major catabolic pathway capable of degrading all kinds of intracellular material including proteins, lipids, polysaccharides, and nucleic acids. During its main pathway, phagophores capture cytosol and organelles to form autophagosomes, followed by the fusion of these double-membrane vesicles with lysosomes [1]. Autophagy was initially considered to be a non-specific, bulk degradation system, in contrast with the ubiquitin–proteasome pathway, in which individual polyubiquitinated proteins are recognized, unfolded and degraded in the inner proteolytic chamber of proteasomes. More recently, multiple studies showed that ubiquitination also signals for selective autophagic degradation, and characterization of ubiquitin-specific autophagy receptors revealed the molecular mechanism involved [2,3]. Proteins such as p62 contain distinct domains mediating multimerization, ubiquitin binding and interaction with Atg8 family proteins. Atg8 is a ubiquitin-like protein bound to phagophores and autophagosomes through a lipid anchor [1,4,5]. Ubiquitinated proteins are captured into aggregates by binding to p62 multimers, and the interaction of p62 with Atg8-positive phagophores is considered to be responsible for their elimination by autophagy [2,3,6–8]. In contrast with this simple model, p62 was found to colocalize with proteins involved in the initiation of phagophores independent of the presence of mammalian Atg8 homologs such as LC3 [9]. These results suggest that additional factors also contribute to the recognition of p62 aggregates by phagophores.

Atg9 is the only transmembrane protein of core autophagy factors, and it likely supplies initial vesicles for phagophore nucleation from multiple membrane sources including endosomes, plasma membrane and Golgi [10–12]. Atg9 is considered to be an upstream factor in the hierarchy of autophagy-related (Atg) proteins in yeast, but the molecular determinants of Atg9

Abbreviations: Atg, autophagy-related; PAS, phagophore assembly site; PI3P, phosphatidylinositol 3-phosphate; Ref(2)P, refractory to Sigma P; ULK, uncoordinated-51 like autophagy kinase; Vps, vacuolar protein sorting; WIPI, WD40 repeat domain phosphoinositide-interacting protein

☆ This is an open-access article distributed under the terms of the Creative Commons Attribution License, which permits unrestricted use, distribution, and reproduction in any medium, provided the original author and source are credited.

* Corresponding author. Address: Department of Anatomy, Cell and Developmental Biology, Eötvös Loránd University, Pázmány s. 1/C. 6.520., Budapest H-1117, Hungary. Fax: +36 1 3812184.
E-mail address: szmrt@elte.hu (G. Juhász).

0014-5793/$36.00 © 2013 The Authors. Published by Elsevier B.V. All rights reserved.
http://dx.doi.org/10.1016/j.febslet.2013.12.012

recruitment to the phagophore assembly site (PAS) are incompletely characterized [13]. A recent study shows that mammalian Atg9 is recruited to damaged mitochondria independent of lipidated Atg8 homologs and the upstream kinase Atg1/ULK1 during selective autophagic degradation of mitochondria [14]. In yeast, the Atg2–Atg18 protein complex is thought to act in parallel to the Atg8 system, and regulates Atg9 recycling from PAS [13,15]. Diverse Atg18-like proteins are found in eukaryotes. The four mammalian homologs fall into two groups based on bioinformatic analysis: WIPI1/2 and WIPI3/4 [16,17]. Of these, both WIPI2 and WIPI4 were suggested to promote autophagosome formation based on siRNA experiments in cultured cells [16,18]. Yeast Atg18 and its paralog Atg21 belong to the WIPI1/2 group [16,17]. Atg21 only functions in an autophagy-related biosynthetic pathway called cytoplasm to vacuole targeting (cvt) which delivers a subset of hydrolases to the vacuole under growth conditions, whereas Atg18 is required for both autophagy and cvt in yeast [19]. Ygr223c, the third Atg18 family protein in yeast, belongs to the WIPI3/4 group and regulates micronucleophagy, a selective autophagy pathway for degradation of nuclear components [16,20].

Clear orthologs of most Atg proteins are found in the popular metazoan model Drosophila, and the p62 ortholog refractory to Sigma P (Ref(2)P) also promotes ubiquitinated protein aggregation [21,22]. Single genes code for Atg9 and Atg2, and the WIPI1/2 homolog CG7986 is referred to as Atg18, as it is required for autophagy in Drosophila [23–26]. The roles of another WIPI1/2 family Drosophila protein, CG8678, and of the WIPI3/4-like CG11975 are unknown [16,17].

Here we show that loss of Atg2 or Atg18 have different consequences on Atg8a puncta formation and Atg9 recruitment to Ref(2)P aggregates during starvation in Drosophila, raising the possibility that these proteins act differently during autophagosome formation in Drosophila.

2. Materials and methods

2.1. Molecular cloning, immunoprecipitation and antibody production

Atg18 coding sequences were PCR amplified from LD38705 (DGRC), and cloned into appropriate vectors to generate R4-mCherry-Atg18, UAS-3xHA-Atg18, and UAS-3xFLAG-Atg18, respectively. Coding sequences were amplified from genomic DNA or GH07816 (DGRC) to generate UAS-3xFLAG-Atg2 or UAS-3xHA-CG8678, respectively. These UAS plasmids, together with UAS-3xHA-Atg9, UAS-3xFLAG-Ref(2)P and mt-Gal4, were used to transfect D.Mel-2 cells (Invitrogen), followed by processing for immunoprecipitation as described [25,27]. His-tagged recombinant Atg9 protein fragment (amino acids 541–845) was purified from bacteria and used for immunization of rats as before [27].

2.2. Drosophila genetics

Flies were reared on standard cornmeal-yeast-agar diet, and well-fed mid-third instar larvae were floated in a 20% sucrose solution for 3 h in starvation experiments. Genotypes used in this study are RNAi lines *Atg9*^{GD10045} (VDRC), *Atg9*^{HMS01246}, *Atg9*^{JF02891}, *Atg18*^{JF02898}, *Atg8a*^{KK109654}, *Atg2*^{JF02786}, and *w*^{1118} used as wild type (all from BDSC) [26], mutants *Atg7*^{d77} [28], *Atg2*^{EP3697}*/Df(3L)BSC119*, *Atg18*^{KG03090}*/Df(3L)Exel6112*, *Atg8a*^{d4} [23,26], *cg-Gal4, UAS-Vps34*^{KD} [29], and stocks for clonal analysis *hs-Flp; UAS-Dcr2; Act > CD2 > Gal4, UAS-GFPnls, R4-mCherry-Atg8a* and *hs-Flp; UAS-Lamp1-GFP; Act > CD2 > Gal4, UAS-Dcr2* [25–27]. *R4-mCherry-Atg18* transgenics were generated by Bestgene.

2.3. Western blots and histology

Western blots were carried out as described previously [25–27]. Dissected larval carcasses were processed for LysoTracker Red (Invitrogen) or immunostaining as before, using rabbit anti-Ref(2)P (1:2000), rat anti-Atg8a (1:300), rat anti-Atg9 (1:300), rat anti-FIP200 (1:300) and rat anti-mCherry (1:300) primary antibodies [25–27]. Preparations were photographed on an Axioimager M2 with Apotome2 (Zeiss), and original unmodified images were processed for statistical evaluation using ImageJ (NIH) and SPSS Statistics (IBM), as described [25–27]. Colocalizations were calculated either by the colocalization tool in ImageJ to obtain Mander's colocalization coefficients for Atg8a-Ref(2)P, or by manual counting for Atg9-Ref(2)P. Immunogold labeling for ubiquitin was done as described [28]. Anti-Atg9 (1:30) and anti-Ref(2)P (1:60) double immunogold labeling was carried out on adult brains embedded into LR White resin (Sigma) to increase antigenicity, using secondary antibodies anti-rat conjugated to 10 nm gold (1:20, Sigma) and anti-rabbit conjugated to 18 nm gold particles (1:60, Jackson Immunoresearch).

3. Results

p62 aggregates are selectively captured into autophagosomes under both basal or starvation conditions in mammalian cells, as more than 90% of LC3-positive autophagosomes are also positive for p62 [6]. In line with that, most Atg8a-positive autophagosomes colocalized with Ref(2)P in fat bodies of well-fed, starved or wandering Drosophila larvae, respectively (Figs. 1A and S1). As expected, the number of Atg8a dots increased in response to autophagy induction (Fig. 1B). Strikingly, larger Ref(2)P aggregates seen under low autophagy level in fed cells disappeared during

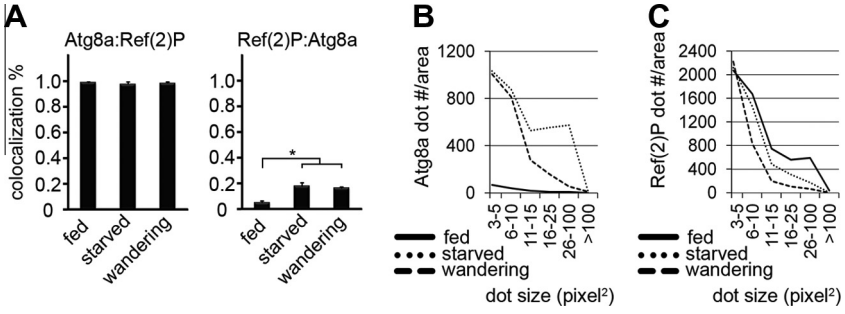


Fig. 1. (A) Atg8a colocalizes with Ref(2)P in Drosophila fat body cells of fed, starved and wandering wild type L3 larvae. The colocalization of Ref(2)P with Atg8a increases during starvation or developmental autophagy, as much more autophagosomes are generated under these circumstances. $N = 6–15$ per stage, $^{*}P < 0.001$, ANOVA, errors bars: S.D. (B) Atg8a-positive autophagosomes are induced by starvation or during the wandering stage. (C) Larger Ref(2)P aggregates observed in fat body cells of well-fed animals are eliminated during starvation or wandering.

starvation-induced or developmental autophagy (Fig. 1C). Thus, Ref(2)P aggregates are selectively eliminated by autophagy in Drosophila.

Atg2 and Atg18 act in parallel to Atg8 in yeast, whereas Atg2 appears to function downstream of Atg8 family proteins in worms and mammals, respectively [18,30]. We also found that punctate Atg8a structures form in fat bodies of starved *Atg2* mutants previously shown to be defective in autophagic degradation (Fig. 2A, B and E) [23,26]. In contrast, Atg8a dots were rarely detected in starved *Atg18* mutants, and they were restored by expression of mCherry-Atg18 (Fig. 2C–E). Similarly, RNAi depletion of *Atg2* failed to block the formation of Atg8a-positive structures, while *Atg18* knockdown inhibited punctate Atg8a in GFP-marked RNAi cells (Fig. 2F–H). Immunoprecipitation experiments suggested that Atg2 may interact with Drosophila Atg18, and more efficiently with its paralog CG8678 (Fig. S2).

We have recently shown that Drosophila Atg9 is required for basal, Myc-induced or proteasome inactivation-induced autophagy, respectively [24–26]. Atg9 is also necessary for the starvation response, as expression of either one of three independent RNAi lines in GFP-marked cell clones prevented punctate LysoTracker staining, a commonly used marker of autolysosomes in the fat body (Fig. S3A–C and J). Moreover, formation of mCherry-Atg8a positive autophagosomes and autolysosomes were also blocked in knockdown cells, and the selective cargo Ref(2)P accumulated upon *Atg9* RNAi during starvation (Fig. S3D–I, K and L).

We raised polyclonal antibodies against Drosophila Atg9, which specifically recognized Atg9 dots and clusters in starved fat body cells (Fig. S3M). Phagophores assemble at aggregates of the selective cargo pro-aminopeptidase I in yeast, and p62-positive aggregates may play similar roles in metazoans [3]. In wild type cells, the overlap of Atg9 with Ref(2)P was low (Fig. 3A and G), in line with the transient localization of Atg9 to forming phagophores described in mammalian cells [10,31]. Loss of downstream Atg genes results in the accumulation of upstream factors in stalled PAS, both in yeast and mammals [13,32]. We therefore carried out similar analyses for Atg9 and Ref(2)P. Nearly all Ref(2)P aggregates colocalized with Atg9 in null mutants of *Atg7* encoding the E1-like enzyme required for Atg8a lipidation and membrane association, and in *Atg8a* nulls (Fig. 3B, C and G).

Aggregates of Ref(2)P also overlapped with Atg9 in *Atg2* mutant fat cells in starved fly larvae (Fig. 3D and G), consistent with the role of Atg2 downstream of (or parallel to) Atg8a. Strikingly, colocalization of these two proteins was low in *Atg18* mutants (Fig. 3E and G). Atg18 is a phosphatidylinositol 3-phosphate (PI3P) effector [33], which prompted us to test whether Vps34, the lipid kinase producing this phospholipid, is involved in Atg9 recruitment to Ref(2)P. Colocalization of Atg9 with Ref(2)P was again low in fat bodies expressing dominant-negative Vps34 (Fig. 3F and G). These data suggested that either Atg9 or Ref(2)P is not recruited to the PAS in the absence of Atg18 or Vps34 function. To distinguish between these possibilities, we looked at the localization of FIP200/Atg17. FIP200 is a subunit of the Atg1 kinase complex, and it accumulates on Ref(2)P aggregates in fat body cells of starved *Atg7* null mutant larvae [34]. FIP200 was also enriched on Ref(2)P aggregates in cells lacking Atg2, Atg18 or Vps34 function (Fig. 3H–J), suggesting that Atg9 recruitment to PAS may specifically be affected by the absence of Atg18 or Vps34. Moreover, overlapping mCherry-Atg18 and Ref(2)P structures were readily observed in *Atg2* and *Atg8a* RNAi cells (Figs. 3K and S3N).

These data suggested that Ref(2)P aggregates with associated upstream Atg proteins may represent stalled PAS in *Atg* mutants. The ultrastructure of protein inclusions is well-characterized in *Atg* mutant neurons of adult flies and mice, respectively [28,35,36]. These aggregates contain ubiquitinated protein, and are often surrounded by small vesicles (Fig. 3L). Double immunolabeling experiments revealed that at least a subset of vesicles associated with Ref(2)P-positive inclusions are positive for endogenous Atg9 in neurons of *Atg7* and *Atg8a* null mutant adult brains (Fig. 3M and N).

The lack of Atg9 accumulation on Ref(2)P aggregates in *Atg18* mutants raised the possibility that Atg18 may facilitate Atg9 recruitment to Ref(2)P. Indeed, HA-Atg18 coprecipitated with FLAG-Ref(2)P in cultured cells (Fig. 4A). HA-Atg9 showed strong binding to FLAG-Atg18, but not to FLAG-Ref(2)P (Fig. 4B), suggesting that the colocalization of Atg9 with Ref(2)P may not map a direct physical interaction. We hypothesized that Atg18 may potentially facilitate Atg9 recruitment to Ref(2)P aggregates by simultaneously binding to both proteins. In line with this model, coexpression of HA-Atg18 resulted in coprecipitation of HA-Atg9 with FLAG-Ref(2)P (Fig. 4B).

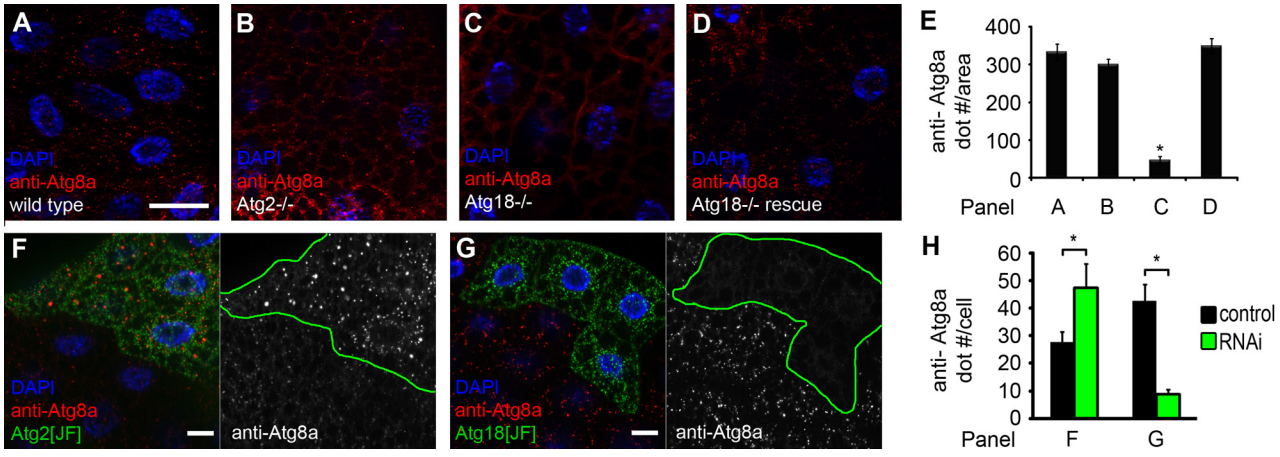


Fig. 2. (A–D) Punctate endogenous Atg8a staining is seen in fat body cells of wild type (A) and *Atg2* mutant (B) starved larvae. The Atg8a dot formation defect of *Atg18* mutants (C) is rescued by transgenic expression of Atg18 (D). Note that Atg8a is pseudocolored red in panel D, as Alexa 488 was used to avoid bleedthrough from the mCherry channel. (E) Quantification of data shown in (A–D). $N = 5$/genotype, $^{*}P < 0.001$, ANOVA, errors bars: S.D. (F) *Atg2* RNAi in GFP-positive cells does not block Atg8a puncta formation. Note that Atg8a structures in RNAi cells appear brighter, and a fraction of these are also bigger than Atg8a dots observed in surrounding control cells lacking GFP. (G) RNAi knockdown of *Atg18* in GFP-marked cell clones blocks Atg8a puncta formation. Note that the Atg8a dots that do form in RNAi cells appear smaller and are much less bright than those observed in neighboring control cells. (H) Quantification of data shown in F, G. $N = 5$/genotype, $^{*}P < 0.001$, two-tailed, two-sample Student's T test, errors bars: S.D. Bar in A equals 20 μm for A–D, F, G, and the relevant channels are shown in grayscale as indicated.

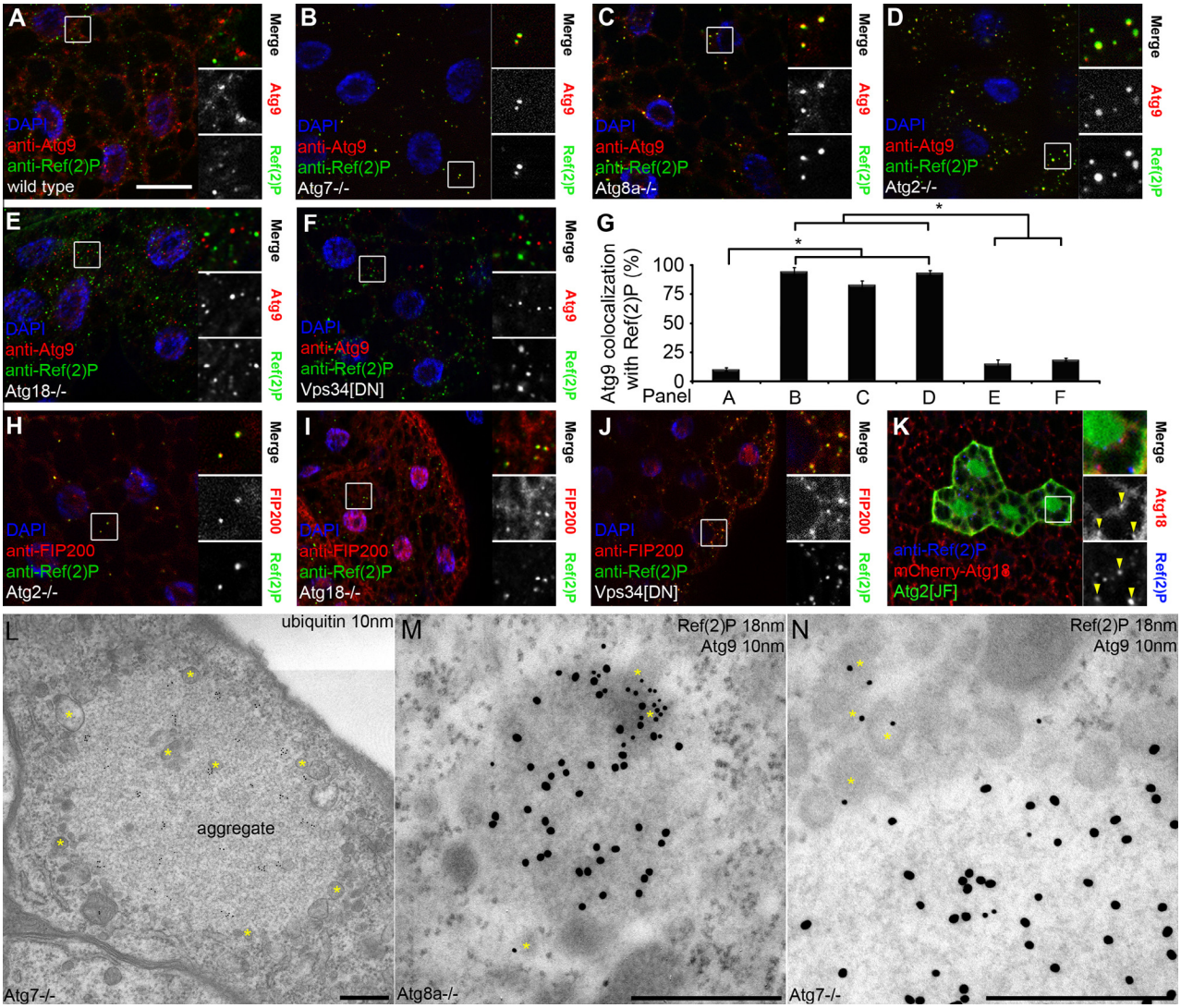


Fig. 3. (A) Atg9 rarely colocalizes with Ref(2)P in wild type larvae. (B–D) A near-complete overlap of Atg9 and Ref(2)P is seen in *Atg7* (B), *Atg8a* (C) and *Atg2* (D) mutants. (E, F) Atg9 and Ref(2)P rarely colocalize in *Atg18* mutants (E) or in fat bodies expressing dominant-negative Vps34 (F). (G) Quantification of data from A–F. $N = 5$/genotype, $^{*}P < 0.001$, ANOVA, errors bars: S.D. (H–J) FIP200 accumulates on Ref(2)P aggregates in starved *Atg2* (H) and *Atg18* mutants (I), and in larvae expressing dominant-negative Vps34 in fat bodies (J). (K) mCherry-Atg18 colocalizes with Ref(2)P in GFP-marked *Atg2* RNAi cells. (L) Immunogold labeling shows accumulation of numerous vesicles (some of which are indicated by asterisks) around and occasionally also inside aggregates containing ubiquitinated proteins in *Atg7* mutant neurons. (M, N) Double immunogold labeling shows endogenous Atg9-positive vesicles (asterisks) accumulating at the periphery of Ref(2)P aggregates in *Atg8a* (M) and *Atg7* (N) mutant neurons. Bar in A equals 20 μm for A–F, H–K, and boxed areas are shown enlarged as indicated. Bars equal 300 nm in L–N.

4. Discussion

Previous studies established the importance of the interaction between p62 and Atg8 family proteins (such as LC3) during selective autophagy in mammalian cells [2,3,6]. A recent live imaging-based report shows that these two proteins are recruited together to the PAS, but later than the Atg1/ULK kinase complex, the Vps34 lipid kinase complex and its effectors such as WIPI1 [31]. How p62 and LC3 are recruited to the PAS is still not understood completely. Several interactions have been recently described between Atg proteins belonging to distinct functional groups and complexes, which likely cooperately coordinate the recruitment of downstream factors. For instance, LC3-interacting regions have been characterized in ULK1/Atg1 and its binding partners Atg13 and FIP200, which may facilitate LC3 recruitment to PAS [37].

Atg9 likely supplies lipids in the form of small vesicles to initiate phagophore formation, and most of it is normally recycled from phagophores [10,31]. Atg18 is a phospholipid effector, and its complex with Atg2 regulates Atg9 recycling from phagophores in yeast [15]. Atg18 and Atg2 are considered to function together, genetically in parallel to Atg8 in yeast [13]. A recent paper shows that Atg18 recruitment to PAS requires PI3P and Atg2, and the Atg18-related protein Atg21 also appears to facilitate its localization to pro-aminopeptidase I aggregates in yeast [38]. Loss of Atg2 leads to formation of stalled phagophores in worms and mammalian cells, and it does not block the recruitment of worm Atg18 to protein aggregates [18,30], which are entirely consistent with our findings in Drosophila. Loss of Atg18 suppressed Atg8a puncta formation unlike the lack of Atg2 function, indicating that Atg18 acts upstream of Atg8a in Drosophila. Similar to our findings, RNAi depletion of the *Atg18* homolog *WIPI2* was found to prevent LC3 puncta formation in cultured mammalian cells, and mutation of *Atg18* attenuates efficient Atg8 puncta formation in the 50 cell stage worm embryo [16,18]. Interestingly, Atg18 and Atg21 were

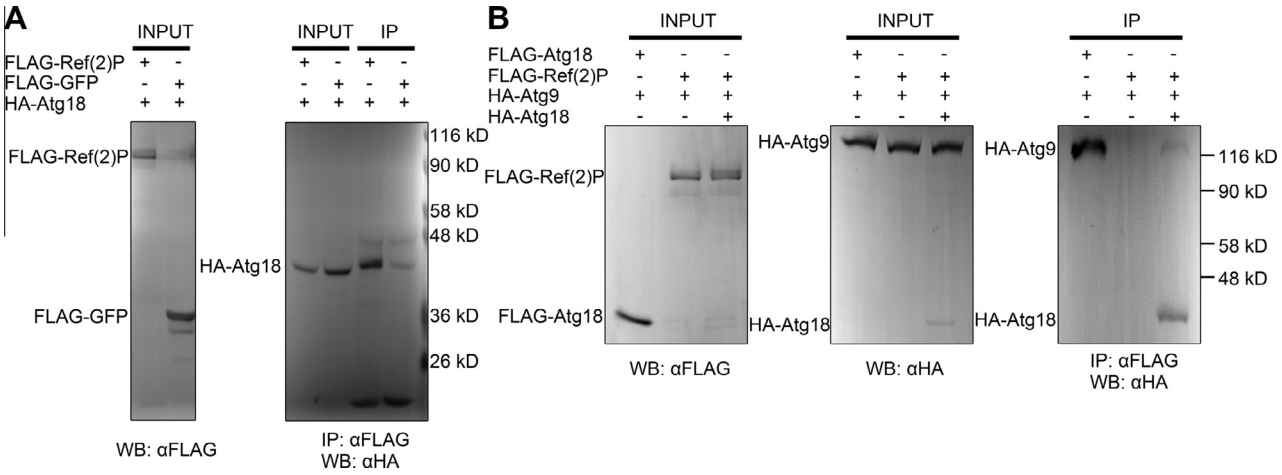


Fig. 4. (A, B) Analysis of protein interactions in cultured cells. (A) HA-Atg18 coprecipitates FLAG-Ref(2)P. FLAG-GFP is shown as negative control. (B) HA-Atg9 coprecipitates with FLAG-Atg18, but not with FLAG-Ref(2)P. Coexpression of HA-Atg18 results in coprecipitation of HA-Atg9 with FLAG-Ref(2)P. IP: immunoprecipitation, WB: western blot.

also suggested to promote the recruitment of lipidated Atg8 to the PAS in yeast, based on experiments carried out in a multiple knockout strain which contains only a subset of *Atg* genes [19].

Our data raise the possibility that the selective autophagy cargo Ref(2)P may be used as a potential PAS marker in *Atg* mutant Drosophila cells, as most Ref(2)P aggregates become positive for upstream Atg proteins. The Atg1 complex subunit FIP200 is enriched on Ref(2)P aggregates in the absence of Atg7, Atg2, Atg18 or Vps34 function. Atg9 also accumulates on Ref(2)P aggregates in *Atg7*, *Atg8a* and *Atg2* mutants, but not in *Atg18* mutants. Atg18 family proteins contain a WD40 domain with 7 beta-propellers. This structure likely enables the binding of Atg18 to multiple targets simultaneously, including the autophagy proteins Atg2 and Atg9 that we also show here, and PI3P on autophagic membranes [15,19,33,38]. In line with the interaction of Atg18 with this phospholipid, accumulation of Atg9 on Ref(2)P aggregates also requires the lipid kinase Vps34. Our data suggest that Atg18 may play an important role in phagophore nucleation, potentially by facilitating the recruitment of Atg9-containing vesicles to Ref(2)P for selective capture and degradation of ubiquitinated protein aggregates through autophagy in Drosophila.

Acknowledgements

We thank Sarolta Pálfia and Eszter Papp for technical assistance, Zsolt Venkei for purifying recombinant Atg9, and the Wellcome Trust (087518/Z/08/Z), the Hungarian Scientific Research Fund (OTKA K83509), and Hungarian Academy of Sciences (BO/00552/11) for support.

Appendix A. Supplementary data

Supplementary data associated with this article can be found, in the online version, at http://dx.doi.org/10.1016/j.febslet.2013.12.012.

References

[1] Mizushima, N., Levine, B., Cuervo, A.M. and Klionsky, D.J. (2008) Autophagy fights disease through cellular self-digestion. Nature 451, 1069–1075.
[2] Shaid, S., Brandts, C.H., Serve, H. and Dikic, I. (2013) Ubiquitination and selective autophagy. Cell Death Differ. 20, 21–30.
[3] Johansen, T. and Lamark, T. (2011) Selective autophagy mediated by autophagic adapter proteins. Autophagy 7, 279–296.
[4] Ichimura, Y. et al. (2000) A ubiquitin-like system mediates protein lipidation. Nature 408, 488–492.
[5] Mizushima, N., Yamamoto, A., Matsui, M., Yoshimori, T. and Ohsumi, Y. (2004) In vivo analysis of autophagy in response to nutrient starvation using transgenic mice expressing a fluorescent autophagosome marker. Mol. Biol. Cell 15, 1101–1111.
[6] Komatsu, M. et al. (2007) Homeostatic levels of p62 control cytoplasmic inclusion body formation in autophagy-deficient mice. Cell 131, 1149–1163.
[7] Bjorkoy, G., Lamark, T., Brech, A., Outzen, H., Perander, M., Overvatn, A., Stenmark, H. and Johansen, T. (2005) P62/SQSTM1 forms protein aggregates degraded by autophagy and has a protective effect on huntingtin-induced cell death. J. Cell Biol. 171, 603–614.
[8] Pankiv, S. et al. (2007) P62/SQSTM1 binds directly to Atg8/LC3 to facilitate degradation of ubiquitinated protein aggregates by autophagy. J. Biol. Chem. 282, 24131–24145.
[9] Itakura, E. and Mizushima, N. (2011) P62 targeting to the autophagosome formation site requires self-oligomerization but not LC3 binding. J. Cell Biol. 192, 17–27.
[10] Orsi, A., Razi, M., Dooley, H., Robinson, D., Weston, A., Collinson, L. and Tooze, S. (2012) Dynamic and transient interactions of Atg9 with autophagosomes, but not membrane integration, is required for autophagy. Mol. Biol. Cell 23, 1860–1873.
[11] Yamamoto, H. et al. (2012) Atg9 vesicles are an important membrane source during early steps of autophagosome formation. J. Cell Biol. 198, 219–233.
[12] Puri, C., Renna, M., Bento, C.F., Moreau, K. and Rubinsztein, D.C. (2013) Diverse autophagosome membrane sources coalesce in recycling endosomes. Cell 154, 1285–1299.
[13] Suzuki, K., Kubota, Y., Sekito, T. and Ohsumi, Y. (2007) Hierarchy of Atg proteins in pre-autophagosomal structure organization. Genes Cells 12, 209–218.
[14] Itakura, E., Kishi-Itakura, C., Koyama-Honda, I. and Mizushima, N. (2012) Structures containing Atg9A and the ULK1 complex independently target depolarized mitochondria at initial stages of Parkin-mediated mitophagy. J. Cell Sci. 125, 1488–1499.
[15] Reggiori, F., Tucker, K.A., Stromhaug, P.E. and Klionsky, D.J. (2004) The Atg1–Atg13 complex regulates Atg9 and Atg23 retrieval transport from the pre-autophagosomal structure. Dev. Cell 6, 79–90.
[16] Polson, H.E., de Lartigue, J., Rigden, D.J., Reedijk, M., Urbe, S., Clague, M.J. and Tooze, S.A. (2010) Mammalian Atg18 (WIPI2) localizes to omegasome-anchored phagophores and positively regulates LC3 lipidation. Autophagy 6, 506–522.
[17] Proikas-Cezanne, T., Waddell, S., Gaugel, A., Frickey, T., Lupas, A. and Nordheim, A. (2004) WIPI-1alpha (WIPI49), a member of the novel 7-bladed WIPI protein family, is aberrantly expressed in human cancer and is linked to starvation-induced autophagy. Oncogene 23, 9314–9325.
[18] Lu, Q. et al. (2011) The WD40 repeat PtdIns(3)P-binding protein EPG-6 regulates progression of omegasomes to autophagosomes. Dev. Cell 21, 343–357.
[19] Nair, U., Cao, Y., Xie, Z. and Klionsky, D.J. (2010) Roles of the lipid-binding motifs of Atg18 and Atg21 in the cytoplasm to vacuole targeting pathway and autophagy. J. Biol. Chem. 285, 11476–11488.
[20] Krick, R., Henke, S., Tolstrup, J. and Thumm, M. (2008) Dissecting the localization and function of Atg18, Atg21 and Ygr223c. Autophagy 4, 896–910.
[21] Erdi, B., Nagy, P., Zvara, A., Varga, A., Pircs, K., Menesi, D., Puskas, L.G. and Juhasz, G. (2012) Loss of the starvation-induced gene Rack1 leads to glycogen deficiency and impaired autophagic responses in Drosophila. Autophagy 8, 1124–1135.
[22] Nezis, I.P. et al. (2008) Ref(2)P, the *Drosophila melanogaster* homologue of mammalian p62, is required for the formation of protein aggregates in adult brain. J. Cell Biol. 180, 1065–1071.

dc_840_14

[23] Scott, R.C., Schuldiner, O. and Neufeld, T.P. (2004) Role and regulation of starvation-induced autophagy in the Drosophila fat body. Dev. Cell 7, 167–178.
[24] Low, P., Varga, A., Pircs, K., Nagy, P., Szatmari, Z., Sass, M. and Juhasz, G. (2013) Impaired proteasomal degradation enhances autophagy via hypoxia signaling in Drosophila. BMC Cell Biol. 14, 29.
[25] Nagy, P., Varga, A., Pircs, K., Hegedus, K. and Juhasz, G. (2013) Myc-driven overgrowth requires unfolded protein response-mediated induction of autophagy and antioxidant responses in *Drosophila melanogaster*. PLOS Genet. 9, e1003664.
[26] Pircs, K., Nagy, P., Varga, A., Venkei, Z., Erdi, B., Hegedus, K. and Juhasz, G. (2012) Advantages and limitations of different p62-based assays for estimating autophagic activity in Drosophila. PLoS One 7, e44214.
[27] Takats, S. et al. (2013) Autophagosomal Syntaxin17-dependent lysosomal degradation maintains neuronal function in Drosophila. J. Cell Biol. 201, 531–539.
[28] Juhasz, G., Erdi, B., Sass, M. and Neufeld, T.P. (2007) Atg7-dependent autophagy promotes neuronal health, stress tolerance, and longevity but is dispensable for metamorphosis in Drosophila. Genes Dev. 21, 3061–3066.
[29] Juhasz, G., Hill, J.H., Yan, Y., Sass, M., Baehrecke, E.H., Backer, J.M. and Neufeld, T.P. (2008) The class III PI(3)K Vps34 promotes autophagy and endocytosis but not TOR signaling in Drosophila. J. Cell Biol. 181, 655–666.
[30] Velikkakath, A.K., Nishimura, T., Oita, E., Ishihara, N. and Mizushima, N. (2012) Mammalian Atg2 proteins are essential for autophagosome formation and important for regulation of size and distribution of lipid droplets. Mol. Biol. Cell 23, 896–909.
[31] Koyama-Honda, I., Itakura, E., Fujiwara, T.K. and Mizushima, N. (2013) Temporal analysis of recruitment of mammalian ATG proteins to the autophagosome formation site. Autophagy 9, 1491–1499.
[32] Itakura, E. and Mizushima, N. (2010) Characterization of autophagosome formation site by a hierarchical analysis of mammalian Atg proteins. Autophagy 6, 764–776.
[33] Obara, K., Sekito, T., Niimi, K. and Ohsumi, Y. (2008) The Atg18–Atg2 complex is recruited to autophagic membranes via phosphatidylinositol 3-phosphate and exerts an essential function. J. Biol. Chem. 283, 23972–23980.
[34] Nagy, P. et al. (2014) Atg17/FIP200 localizes to perilysosomal Ref(2)P aggregates and promotes autophagy by activation of Atg1 in Drosophila. Autophagy 10 (3) (in press).
[35] Hara, T. et al. (2006) Suppression of basal autophagy in neural cells causes neurodegenerative disease in mice. Nature 441, 885–889.
[36] Komatsu, M. et al. (2006) Loss of autophagy in the central nervous system causes neurodegeneration in mice. Nature 441, 880–884.
[37] Alemu, E.A. et al. (2012) ATG8 family proteins act as scaffolds for assembly of the ULK complex: sequence requirements for LC3-interacting region (LIR) motifs. J. Biol. Chem. 287, 39275–39290.
[38] Rieter, E., Vinke, F., Bakula, D., Cebollero, E., Ungermann, C., Proikas-Cezanne, T. and Reggiori, F. (2013) Atg18 function in autophagy is regulated by specific sites within its beta-propeller. J. Cell Sci. 126, 593–604.

MBoC | ARTICLE

Rab11 facilitates cross-talk between autophagy and endosomal pathway through regulation of Hook localization

Zsuzsanna Szatmári[a], Viktor Kis[a], Mónika Lippai[a], Krisztina Hegedűs[a], Tamás Faragó[b], Péter Lőrincz[a], Tsubasa Tanaka[c], Gábor Juhász[a], and Miklós Sass[a]

[a]Department of Anatomy, Cell, and Developmental Biology, Eötvös Loránd University, Budapest 1117, Hungary; [b]MTA-ELTE Comparative Ethology Research Group, Budapest 1117, Hungary; [c]Department of Germline Development, Kumamoto University, 2-2-1 Honjo, Kumamoto 860-0811, Japan

ABSTRACT **During autophagy, double-membrane autophagosomes deliver sequestered cytoplasmic content to late endosomes and lysosomes for degradation. The molecular mechanism of autophagosome maturation is still poorly characterized. The small GTPase Rab11 regulates endosomal traffic and is thought to function at the level of recycling endosomes. We show that loss of Rab11 leads to accumulation of autophagosomes and late endosomes in *Drosophila melanogaster*. Rab11 translocates from recycling endosomes to autophagosomes in response to autophagy induction and physically interacts with Hook, a negative regulator of endosome maturation. Hook anchors endosomes to microtubules, and we show that Rab11 facilitates the fusion of endosomes and autophagosomes by removing Hook from mature late endosomes and inhibiting its homodimerization. Thus induction of autophagy appears to promote autophagic flux by increased convergence with the endosomal pathway.**

Monitoring Editor
Tamotsu Yoshimori
Osaka University

Received: Oct 4, 2013
Revised: Dec 10, 2013
Accepted: Dec 12, 2013

INTRODUCTION

Macroautophagy (hereafter autophagy) is an evolutionarily conserved bulk degradation process of eukaryotic cells. The regulation of this process was originally described in yeast (*Saccharomyces cerevisiae*) but even has a key role in multicellular organisms as a cytoprotective response to stress and pathological conditions (Levine and Kroemer, 2008; Mizushima *et al.*, 2008). Autophagy has the capacity to engulf large portions of the cytoplasm through the formation of double-membrane vesicles, called *autophagosomes*. These vesicles arise from preautophagosomal structures (PAS), which are defined sites of cytoplasm, marked by a subset of autophagy-related (*Atg*) proteins (Mizushima *et al.*, 2011). Closed autophagosomes undergo a maturation process, as they subsequently fuse with endosomes and lysosomes.

On autophagy induction, the Atg1 kinase complex (ULK1/2 in mammals) localizes to the PAS (Chan and Tooze, 2009; Mizushima, 2010) and together with the class III phosphatidylinositol-3-kinase (Vps34) complex initiates the phagophore nucleation and expansion (Funderburk *et al.*, 2010). After these events, the members of two ubiquitin-like conjugation systems are recruited to the phagophore membrane: the Atg5-12-16 complex and the phosphatidylethanolamine-conjugated Atg8a (LC3 in mammals; Geng and Klionsky, 2008). The lipid-conjugated form of Atg8a (Atg8a-II) is located on both sides of the membrane of the phagophore and autophagosomes as well. While the Atg8a located on the outer membrane is routed for recyclization, the other portion of Atg8a becomes trapped in the autolysosomal lumen and is degraded by lysosomal hydrolases. Thus Atg8a is a widely used marker of autophagic structures (Klionsky *et al.*, 2012).

This article was published online ahead of print in MBoC in Press (http://www.molbiolcell.org/cgi/doi/10.1091/mbc.E13-10-0574) on December 19, 2013.

The authors declare they have no conflict of interest.

Address correspondence to: Zsuzsanna Szatmári (zsuzs.szatmari@gmail.com).

Abbreviations used: *Atg*, autophagy-related gene; BDSC, Bloomington Drosophila Stock Center; BSA, bovine serum albumin; CQ, chloroquine; DAPI, 4′,6-diamidino-2-phenylindole; DGRC, Drosophila Genomics Resource Center; GFP, green fluorescent protein; HA, hemagglutinin; LTR, LysoTracker Red; PAS, preautophagosomal structures; PBS, phosphate-buffered saline; pMT, metallothionein promoter; RE, recycling endosome; RNAi, RNA interference; TBST, Tween-20/TBS; TfR, transferrin receptor; TRA, Texas Red Avidin; VDRC, Vienna Drosophila RNAi Center; YFP, yellow fluorescent protein.

© 2014 Szatmári *et al.* This article is distributed by The American Society for Cell Biology under license from the author(s). Two months after publication it is available to the public under an Attribution–Noncommercial–Share Alike 3.0 Unported Creative Commons License (http://creativecommons.org/licenses/by-nc-sa/3.0).

"ASCB®," "The American Society for Cell Biology®," and "Molecular Biology of the Cell®" are registered trademarks of The American Society of Cell Biology.

Supplemental Material can be found at:
http://www.molbiolcell.org/content/suppl/2013/12/16/mbc.E13-10-0574v1.DC1.html

After completion, autophagosomes can fuse with lysosomes. However, there is also growing evidence about the convergence of the autophagic route with the earlier stages of endosomal pathways. Recent studies show that autophagosomes can fuse with different populations of both early (Tooze *et al.*, 1990; Razi *et al.*, 2009) and late (Lucocq and Walker, 1997; Köchl *et al.*, 2006; Filimonenko *et al.*, 2007) endosomes to form hybrid organelles called *amphisomes* (Gordon and Seglen, 1988).

In spite of numerous studies, many questions remained open concerning the spatial and temporal regulation of autophagosome maturation, amphisome formation, and the exact molecular mechanisms of the fusion events. As a recent review discussed, a cross-talk may exist between autophagic and endosomal processes, which likely plays an important role in the regulation of both degradative pathways (Lamb *et al.*, 2013).

The members of the Rab small GTPase protein family are the main regulators of membrane trafficking and fusion events (Stenmark, 2009). The active, GTP-bound Rab proteins recruit several specific effectors to the membrane in which they are associated, thereby determining the membrane's identity, traffic, and fusion ability. Recent studies revealed a role for a subset of Rab proteins in autophagy (Chua *et al.*, 2011). Rab11 was indicated to play an important role both at the early and late stages of autophagy. Recent studies found that Rab11 is involved in vesicle trafficking events from recycling endosomes (REs) to the phagophore during autophagosome formation (Longatti *et al.*, 2012; Knævelsrud *et al.*, 2013). Meanwhile, previous studies suggested a role for Rab11 in the maturation of autophagosomes (Fader *et al.*, 2008; Richards *et al.*, 2011).

RESULTS

Rab11 is required for amphisome formation

Rab11 was previously described as a potent regulator of autophagosome maturation in cultured mammalian cells (Fader *et al.*, 2008). To better understand the role of Rab11 in autophagy, we examined the functions of this protein in *Drosophila melanogaster*. We analyzed whether the decrease in the level of functional Rab11 protein causes any defect upon autophagy. Using three independent RNA interference (RNAi) lines, we observed the accumulation of small-sized Atg8a-positive dots in Rab11-depleted cells under both fed and starved conditions (Figure 1A and Supplemental Figure S1, A, B, E, and F). Fat body cells overexpressing the GDP-locked dominant-negative form of Rab11 or Rab11 hypomorphic mutant clone cells showed the same phenotype (Figure S1, C, D, and F).

Accumulation of autophagic structures can be caused both by increased induction of autophagy and by failures in the autophagosome maturation. For monitoring autophagic flux, we used tandem-tagged mCherry–green fluorescent protein–Atg8a reporter (mCherry-GFP-Atg8a; Kimura *et al.*, 2007). In Rab11 RNAi cells, we observed double-labeled immature autophagic structures, suggesting depletion of Rab11 blocks the autophagic flux (Figure 1B). Furthermore, our Western blot and immunostaining experiments showed the accumulation of p62, a well-known target of autophagic degradation due to Rab11 silencing (Figure 1, C and D). Rab11 depletion resulted in the accumulation of GFP-Atg8a–positive puncta both in presence and in absence of chloroquine (CQ), an inhibitor of lysosomal acidification. However, CQ treatment did not cause a further increase in the number of autophagic structures (Figure S1, G and H). The GFP-Atg8 processing assay is also suitable for investigating autophagic degradation (Klionsky *et al.*, 2012). Using this tool, we found significantly less free GFP in Rab11-depleted larvae compared with control larvae (Figures 1E and S1I). Moreover, our ultrastructural studies also suggest that Rab11 RNAi leads to the accumulation of abnormal autophagic vacuoles (Figure 1F).

Surprisingly, when we examined the influence of Rab11 depletion on the pattern of LysoTracker Red (LTR), a marker of acidic structures, we observed an accumulation of LTR-positive dots under both fed and starved conditions, compared with control cells (Figures 2A and S2, A and D). However, we found a decrease in the colocalization frequency of GFP-Atg8a with LTR (from 43 ± 1.6 to 8 ± 0.8%), indicating that a drop in Rab11 protein levels results in a reduced number of late autophagic structures (Figure S2, E and F). Next we tested whether LTR colocalizes with any marker of the endolysosomal system. Using Lamp1-GFP, a marker of late endosomes and lysosomes (Schwake *et al.*, 2013), we observed an increased number of Lamp1-positive dots and 90 ± 1.4% of LTR-positive dots colocalized with them in Rab11 RNAi cells (Figures 2A and S2, B–D). Moreover, we found the accumulation of the late endosomal marker Rab7 (Wang *et al.*, 2011), but not that of the early endosomal marker Rabenosyn-5 (de Renzis *et al.*, 2002; Figures 2B and S2G).

Because our results showed the accumulation of both autophagosomes and late endosomes, we tested whether Rab11 depletion affects amphisome formation. Colocalization of Atg8a with different endosomal markers was studied both in the presence and absence of Rab11 during starvation-induced autophagy. We found a significant decrease in colocalization of the endocytic tracer Texas Red Avidin (TRA) with GFP-Atg8a due to Rab11-depletion (from 43 ± 0.9 to 8 ± 0.2%; Figure 2, C and C'). Silencing of Rab11 decreased the colocalization of mCherry-Atg8a with the endosomal markers Rab7 (from 20±1.6% to 1.8±0.3%) and Lamp1 (from 75 ± 1.7 to 32 ± 1.6%) as well (Figures 2C and S2, H and I). Supporting these findings, our electron microscopic analysis showed acidic late endosomes often located in proximity to autophagosomes, but we could not detect any acidic autophagic vacuoles (Figure S2J).

These findings suggest that Rab11 is required for amphisome formation and lack of Rab11 results in the accumulation of abnormal autophagosomes and late endosomes.

Rab11 localizes to autophagosomes

As our results suggest, Rab11 presumably plays an important role in the fusion of autophagosomes with late endosomes. Therefore our aim was to verify whether Rab11 indeed localizes to autophagic structures. At first, we investigated the colocalization of Rab11 with Atg8a. We found that 40 ± 0.4% of ectopically expressed Rab11-GFP–positive puncta colocalized with mCherry-Atg8a under starved conditions (Figure S3A). Supporting this result, mCherry-Atg8a was also found to colocalize with endogenous Rab11 (Figure 3B).

These findings raised the question of whether there is an autophagy induction–dependent change in the colocalization of endogenous Rab11 with mCherry-Atg8a. We observed that only 0.46 ± 0.1% of Rab11-positive dots colocalized with mCherry-Atg8a under fed conditions, while amino acid starvation significantly increased the colocalization frequency to 18 ± 1.5% (Figure 3, A, B, and F). However, autophagy induction did not affect the number of Rab11-positive structures in fat body cells (Figure S3B). This suggests that Rab11, besides being found in REs, can be also found on autophagic structures.

Vps32/Snf7 is a member of the ESCRT-III complex, playing a key role in the maturation of endosomes (Williams and Urbé, 2007; Hanson *et al.*, 2008; Raiborg and Stenmark, 2009). It was previously described that ESCRT proteins are required for amphisome formation and that immature autophagosomes accumulate due to the lack of ESCRT components (Filimonenko *et al.*, 2007; Lee *et al.*, 2007). We detected a moderate increase in the frequency of

dc_840_14

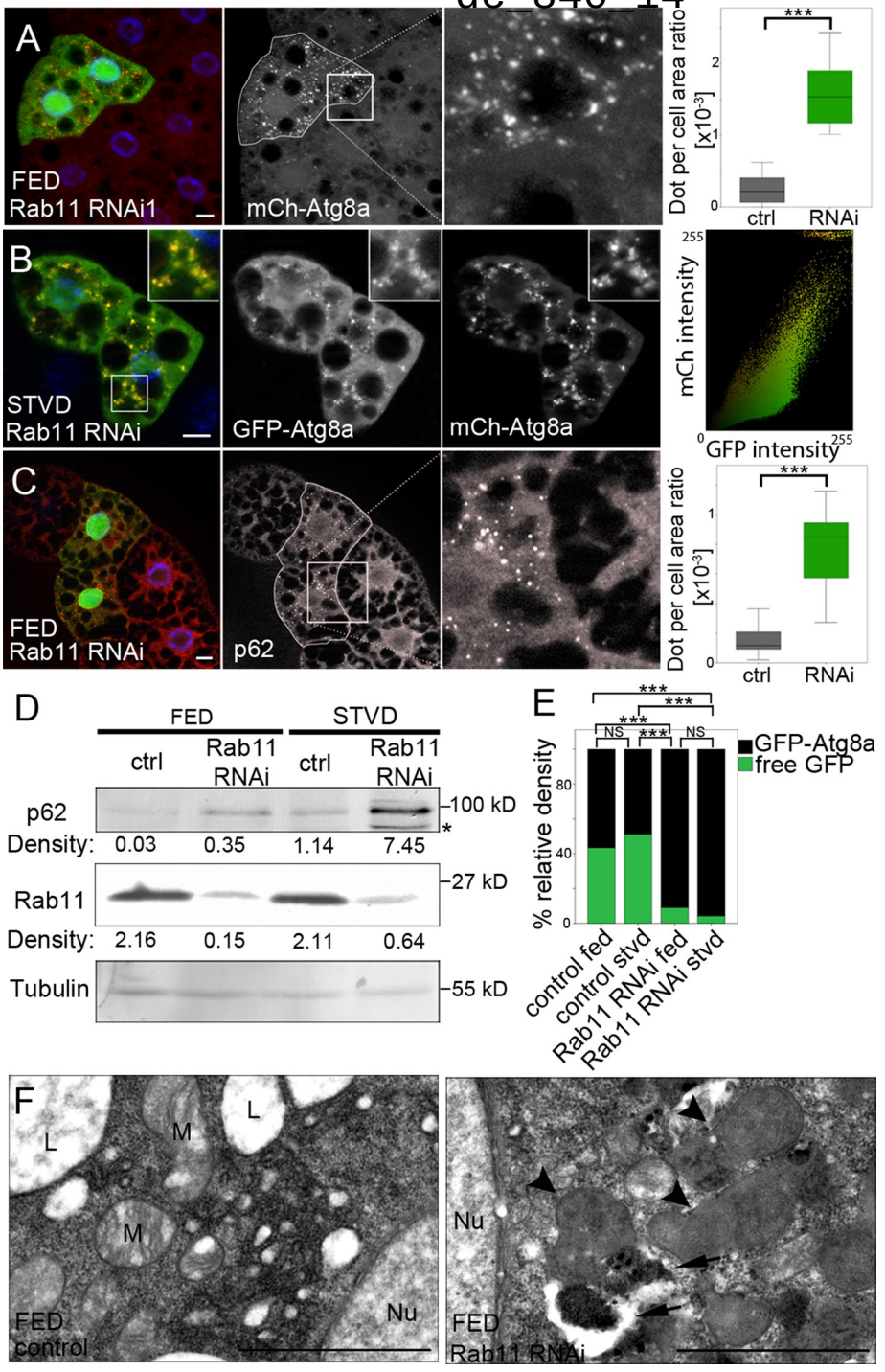


FIGURE 1: Rab11 is required for autophagosome maturation. (A) Control and Rab11-depleted (green) fat body cells of L3 fed *Drosophila* larvae expressing mCherry-Atg8a (red). Nuclei were stained using 4′,6-diamidino-2-phenylindole (DAPI, blue). The mCherry-Atg8a–positive dot per cell area ratio was calculated as described and compared between Rab11 RNAi and neighboring control cells using Wilcoxon's signed-rank test ($n = 21$, $p < 0.0001$). (B) Fat body cells of starved Rab11-depleted L3 starved larvae clonally expressing the mCherry-GFP-Atg8a autophagic flux marker. Nuclei were stained using DAPI (blue). Dot plot shows fluorescence intensity and colocalization profiles of mCherry and GFP channels of the main image. (C) Control and Rab11 RNAi (green) fat body cells of L3 fed larvae were stained with anti-p62 antibody (red). Nuclei were stained using DAPI (blue). P62-positive dot per cell area ratio was calculated and compared between the two groups using Wilcoxon's signed-rank test ($n = 22$, $p < 0.0001$). (D) Representative Western blot showing p62, Rab11, and α-tubulin levels (relative density) in fed and starved control and Rab11-depleted larvae. Asterisk marks aspecific band. (E) Western blots of the GFP-Atg8a processing assay in fed and starved control and Rab11-depleted larvae were measured as described and compared between groups using GLMM ($n = 4$, $p < 0.0001$). The differently colored sections of bars show the relative amounts of free GFP (green) and GFP-Atg8a (black) in the samples. (F) Ultrastructure of Rab11-depleted clone cells and neighboring control cells. Rab11-depletion results in the accumulation of immature (arrows) and abnormal (arrowheads) autophagosomes compared with the control cells. Nu, nuclei; M, mitochondria; L, lipid droplets. Scale bars: (A–C) 10 μm; (F) 1 μm. On box-and-whisker plots, bars (gray, control; green, Rab11 RNAi) show the data lying between the upper and lower quartiles; the median is indicated as a horizontal line within the box. Whiskers plot the smallest and largest observations. ***, $p < 0.001$.

colocalization between Rab11 and mCherry-Atg8a in Vps32-silenced cells. This observation also provides further evidence that Rab11 localizes to immature autophagosomes (Figure 3, C and F).

Rab11 is a widely used marker of REs (Hsu and Prekeris, 2010). Thus we examined whether autophagy induction affects the colocalization of Rab11 with GFP-labeled transferrin receptor (TfR), a well-known cargo of the Rab11-dependent recycling pathway (Maxfield and McGraw, 2004). Starvation-induced autophagy caused significant decrease in colocalization of Rab11 with TfR compared with control cells, while the amount of TfR-positive dots did not change (Figures 3, D, E, and G, and S3C).

These results suggest that, upon autophagy induction, Rab11 translocates from REs to autophagosomes.

Rab11 supports endosome maturation by regulating Hook

A recent study in cultured HEK293T cells showed that Rab11 can bind to Hook, a protein playing a role in the maturation of endosomes (Luiro *et al.*, 2004). We also found a strong interaction between transgenic Hook and Rab11 in cultured *Drosophila* D. Mel-2 cells, while Rab11 did not bind to another late endosomal protein, Lamp1 (Figure S3, D and D′). Confirming these results, we could detect in vivo interaction of Hook-FLAG with endogenous Rab11 (Figure 4A), and we found that Rab11 interacts with Hook in a GTP-dependent manner (Figure S3E). Moreover, the strength of this interaction increased due to autophagy induction by starvation (Figure 4A). Finally, our coimmunoprecipitation experiments showed that Rab11 binds to the central coiled-coil

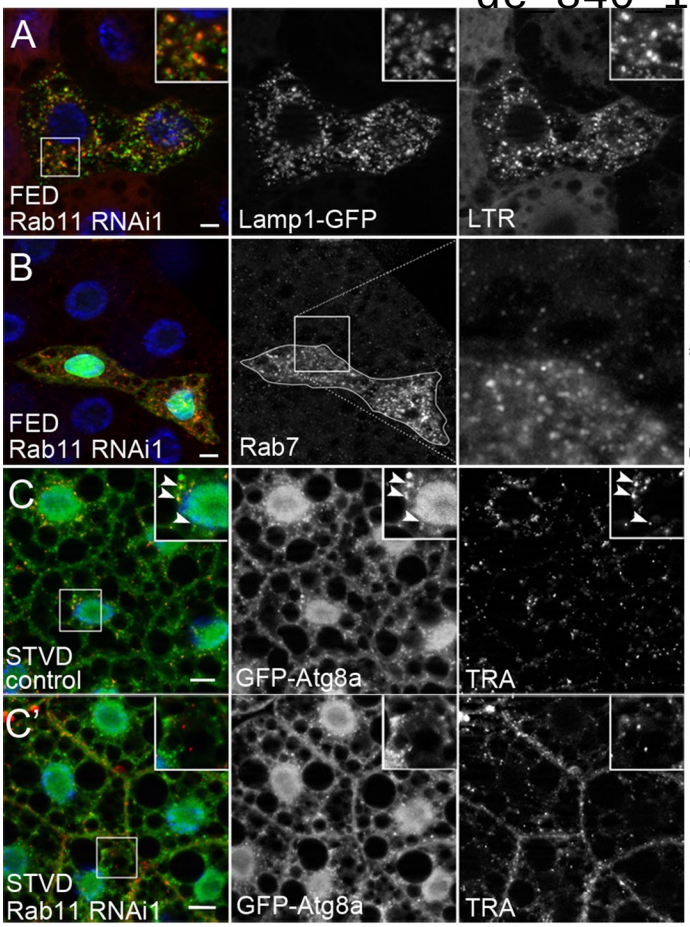


FIGURE 2: Rab11 is required for amphisome formation. (A) Fat body cells of Rab11-depleted fed L3 larvae clonally expressing Lamp1-GFP (green) were stained with LTR (red). Nuclei were stained using DAPI (blue). The LTR-positive dot per cell area ratio was calculated and compared between clone and neighboring control cells using Wilcoxon's signed-rank test ($n = 21$, $p < 0.0001$). Lamp1-GFP–positive dot per cell area ratio was also calculated and compared between control (see Figure S2C) and Rab11-depleted groups using the Mann-Whitney test ($n_{ctrl} = 34$, $n_{RNAi} = 27$, $p < 0.0001$). (B) Control and green, Rab11-depleted fat body cells of fed L3 larvae were stained with anti-Rab7 antibody (red). Nuclei were stained using DAPI (blue). Dot per cell area ratio was calculated and compared between the groups using Wilcoxon's signed-rank test (Rab7: $n = 28$, $p < 0.0001$; Rbsn5: $n = 15$, $p = 0.8647$). (C–C') Colocalization between GFP-Atg8a (green) and TRA (red) decreased due to Rab11 depletion. Nuclei were stained with DAPI (blue). Colocalization between GFP-Atg8a and TRA, mCh-Atg8a and anti-Rab7, and mCh-Atg8a and Lamp1-GFP was quantified and compared between the groups using the Mann-Whitney test (Atg8-TRA: $n_{ctrl} = 100$, $n_{RNAi} = 190$, $p = 0.0002$; Atg8-Rab7: $n_{ctrl} = 41$, $n_{RNAi} = 39$, $p = 0.0008$; Atg8-Lamp1: $n_{ctrl} = 57$, $n_{RNAi} = 57$, $p < 0.0001$). On box-and-whisker plots, bars (gray, control; green, Rab11 RNAi) show the data lying between the upper and lower quartiles; the median is indicated as a horizontal line within the box. Whiskers plot the smallest and largest observations. NS, $p > 0.05$; ***, $p < 0.001$. Scale bars: 10 μm.

domain of Hook, which was previously found to be responsible for homodimerization (Krämer and Phistry, 1999; Figure S3, F–K).

Furthermore, we found a 21 ± 1.5% colocalization ratio between Hook and Rab11 in fat body cells of fed larvae. This ratio increased to 45 ± 2.2% upon autophagy induction by starvation (Figure 4, B–D), while the number of Hook-positive structures and the level of Hook protein remained unaffected (Figure S4, A and B).

Our further experiments showed that 4 ± 0.4% of Hook-positive puncta colocalizes with mCherry-Atg8a under fed conditions, and this ratio increased to 16 ± 1% after autophagy induction (Figure 4, E–G). Parallel with these results, we could observe a decrease (from 48 ± 0.9 to 13 ± 0.6%) in colocalization between Hook and the late endosomal marker Rab7 after autophagy induction (Figure 4, H, I, and K). Meanwhile, no changes were detected in the number of Rab7-positive structures (Figure S4C). Similarly, induction of autophagy did not significantly increase the colocalization between Rab11 and Rab7 (Figure S4, D–F). This suggests that the increased colocalization of Hook with mCherry-Atg8a is not due to the increased convergence of autophagic and endosomal pathways. Furthermore, we could not detect any changes in the frequency of Hook-Rab7 colocalization upon amino acid starvation in cells lacking Atg1 protein, which is required for autophagy induction (Chan and Tooze, 2009; Figure S4, G–I). These results suggest that autophagy induction by starvation results in the translocation of Hook from Rab7-positive endosomes to autophagic structures.

We investigated whether Rab11 is required for the altered Hook localization. We found that silencing of Rab11 in fed larvae resulted in the accumulation of Hook on Rab7-positive late endosomes, indicated by an increased colocalization (65 ± 1.3% compared with 48 ± 0.9% in control cells; Figure 4, J and K). Moreover, we could not detect any changes in the frequency of colocalization between Hook and mCherry-Atg8a upon autophagy induction in Rab11-depleted cells (Figure S4, J–L). In addition to these results in fat body cells overexpressing wild-type Rab11, we observed an increase in the colocalization of Hook with mCherry-Atg8a (from 4 ± 4 to 52 ± 8.1%) and a decrease in the frequency of Hook-Rab7 colocalization (from 42 ± 7.9 to 16 ± 5.1%) due to amino acid starvation, whereas overexpression of GDP-locked Rab11 did not result in any changes in the colocalization of Hook with mCherry-Atg8a or Rab7–yellow fluorescent protein (Rab7-YFP; Figures 4L and S4, M–T).

Next we examined whether Rab11 has any effect on heterodimerization of endogenous Hook with transgenic Hook-FLAG. Our coimmunoprecipitation studies showed that starvation resulted in a decrease in heterodimer formation of Hook with Hook-FLAG in the presence of Rab11. However, we could not detect any changes in Hook heterodimerization in Rab11 RNAi larvae (Figure 4M).

A previous study showed that Hook has a negative regulatory role in the process of endosome maturation (Narayanan *et al.*, 2000). Supporting this result, we found that overexpression of full-length Hook in fat body cells results in the accumulation of Rab7-positive structures (Figure 4, N and P). Moreover, we observed a moderate accumulation of mCherry-Atg8a–positive puncta in cells overexpressing Hook (Figures 4P and S4U).

It was previously described that the N-terminal domain of Hook is responsible for microtubule binding (Krämer and Phistry, 1999). We also could detect the interaction of the Hook N-terminus with

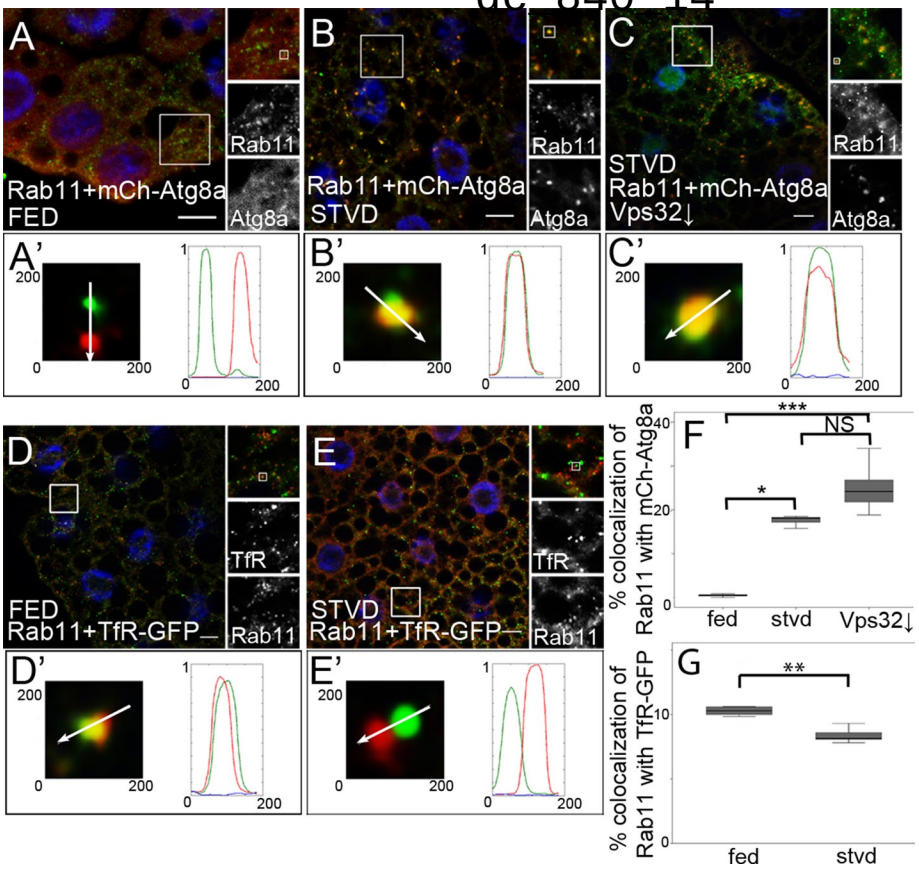


FIGURE 3: Rab11 localizes to autophagosomes. Fat body cells of fed (A) and starved (B) L3 larvae expressing mCherry-Atg8a (red) were stained with anti-Rab11 antibody (green). Nuclei were stained using DAPI (blue). (C) Fat body cells of starved larvae expressing mCherry-Atg8a (red) were stained with anti-Rab11 antibody (green). Vps32 is depleted (↓) in GFP-expressing cells. Nuclei were stained using DAPI (blue). Fat body cells of a fed (D) and starved (E) L3 larva expressing TfR-GFP (green) were stained with anti-Rab11 antibody (red). Nuclei were stained using DAPI (blue). (A′–E′) show the indicated single dots from their main images. Arrows indicate the direction of scanning intensity. Diagrams show the intensity of red, green, and blue channels. (F) Autophagy induction increases the colocalization of Rab11 with mCherry-Atg8a. Colocalization was calculated and compared between the groups using the Kruskal-Wallis test ($n_{fed} = 72$, $n_{stvd} = 143$, $n_{Vps32} = 20$, $p < 0.0001$; fed-starved: $p = 0.0140$; fed-Vsp32↓: $p < 0.0001$; starved-Vps32 ↓: $p = 0.1840$). (G) Colocalization of Rab11 with TfR-GFP was calculated and compared between cell groups described in (D and E) using the Mann-Whitney test ($n_{fed} = 35$, $n_{stvd} = 34$, $p < 0.0017$). On box-and-whisker plots, bars show the data lying between the upper and lower quartiles; the median is indicated as a horizontal line within the box. Whiskers plot the smallest and largest observations. NS, $p > 0.05$; *, $p < 0.05$; **, $p < 0.001$; ***, $p < 0.001$. Scale bars: 10 μm.

α-tubulin (Figure 4, R and S). Furthermore, we found that overexpression of N-terminally truncated Hook in fat body cells does not result in accumulation of autophagic or Rab7-positive endosomal structures (Figures 4, O and Q, and S4V).

All of these data suggest that autophagy induction results in a Rab11-dependent translocation of Hook from late endosomes to autophagic structures. Through their interaction, Rab11 can inhibit the negative regulatory role of Hook on late endosomal development; therefore the presence of Rab11 allows the endosomes to mature.

DISCUSSION

Former work suggested a role for Rab11 in the maturation process of autophagosomes (Fader *et al.*, 2008; Richards *et al.*, 2011). In this in vivo study, we identified novel key functions of Rab11 in this process in *Drosophila melanogaster*. Loss of Rab11 leads to the accumulation of abnormal autophagosomes and acidic late endosomes, which is probably a consequence of impaired amphisome formation.

Furthermore, we observed autophagy induction–dependent translocation of Rab11 from TfR-positive REs to autophagosomes. This finding supports previous reports, which revealed REs as a possible membrane source for autophagosome formation and a role for Rab11 in vesicle trafficking from REs to the sites of autophagosome formation in cultured mammalian cells (Longatti *et al.*, 2012; Puri *et al.*, 2013). In line with these findings, a recent study of Knævelsrud and colleagues showed that Rab11 participates in membrane traffic from REs to the autophagosome precursors together with the *Drosophila* homologue of SNX18 (Knævelsrud *et al.*, 2013). This study suggests that Rab11 has a similar role in *Drosophila melanogaster* and a role in providing an RE-derived membrane source for phagophore expansion. However, we did not observe any defect in autophagosome formation in the absence of functional Rab11 protein.

The molecular mechanism of autophagosome formation is a poorly understood process. Recently several organelles were implicated as possible membrane sources for autophagosomes (Mari *et al.*, 2011). Many studies suggest that the possible origin of the autophagosomal membrane might vary, even in different mammalian cell types (Hayashi-Nishino *et al.*, 2009; Hailey *et al.*, 2010; Ravikumar *et al.*, 2010; Yamamoto *et al.*, 2012; Hamasaki *et al.*, 2013), and this question needs further investigation in *Drosophila melanogaster* as well. Presumably, although REs contribute to the formation of autophagic membrane in flies, they are not likely to be the main membrane source. This could explain why the loss of Rab11 did not block autophagosome formation in our experiments.

We demonstrated the interaction of both transgenic and endogenous Rab11 with Hook protein in *Drosophila* cell culture and even in the whole organism. These results confirm a former study that showed the same phenomenon using COS-1 cells cotransfected with tagged Hook and Rab11 constructs (Luiro *et al.*, 2004). Furthermore, we found an autophagy induction–dependent increase in the strength of this physical interaction.

In addition to these findings, our results provide mechanistic insights into the maturation of endosomes and autophagosomes: the interaction between Rab11 and Hook is crucial for the maturation of these structures. Autophagy induction by amino acid starvation increased the colocalization of Rab11 with Hook and Hook with Atg8a. In line with that, we found a significant decrease in Hook-Rab7 colocalization during starvation-induced autophagy. Our data suggest a Rab11-dependent translocation of Hook from Rab7-labeled late endosomes to autophagic structures. This idea is supported by the

finding that lack of Rab11 causes the accumulation of Hook on Rab7-positive late endosomes.

Previously Hook was found to be a negative regulator of endosome maturation in *Drosophila* (Narayanan *et al.*, 2000) and the Hook-like protein Acinus was described as an important regulator of endosome maturation and autophagic processes (Haberman *et al.*, 2010). In line with these findings, we found that overexpression of full-length Hook protein mimics the effects of Rab11 depletion on the maturation of autophagosomes and endosomes. Moreover, we show that the N-terminal microtubule-binding domain of Hook is required for its negative regulatory role. Our latter results reveal a key mechanistic role for Rab11 in removal of Hook from late endosomes, which allows termination of endosome maturation and subsequent fusion with lysosomes. As was demonstrated in previous work, mature late endosomes can undergo fusion with nascent autophagosomes and promote their maturation (Lucocq and Walker, 1997; Köchl *et al.*, 2006; Filimonenko *et al.*, 2007). On the basis of these findings, we developed a model representing a mode of cross-talk between the autophagic and endosomal pathways (Figure 5). On starvation, the enhanced autophagic activity requires an increased input from the endolysosomal system. For this purpose, Rab11 removes Hook from the late endosomes, thereby allowing subsequent fusion of these compartments with immature autophagosomes as well.

Why Hook does not inhibit the maturation of autophagosomes once it localizes to these organelles is still an open question. We mapped the Hook interaction surface with Rab11 to residues 180–530, which represents the coiled-coil domain of Hook. This domain was previously found to be responsible for homodimerization of Hook (Krämer and Phistry, 1999). Conceivably, homodimerization and Rab11 binding are distinct and separable functions of the Hook coiled-coil domain, as was shown in the case of the FIP2 coiled-coil domain, which also interacts with Rab11 (Wei *et al.*, 2006). Our further experiments showed that Rab11 binding prevents Hook from homodimerization. Thus our results suggest that Rab11 promotes autophagic flux by decreasing Hook homodimerization and inhibiting its negative regulatory role on endosome maturation.

MATERIALS AND METHODS

Drosophila stocks and culture

Fly stocks used in this study (derived from the Vienna Drosophila RNAi Center [referred to as VDRC; Vienna, Austria] and Bloomington Drosophila Stock Center [referred to as BDSC; Bloomington, IN]) are listed in Supplemental Table S1. UAS-Hook-FLAG, UAS–ΔN-Hook–hemagglutinin (UAS-ΔN-Hook-HA), and UAS-Rab11-HA stocks were generated by BestGene, using constructs described below. Flies were raised on standard yeast/cornmeal/agar media at 25°C, 50% humidity and a 12-h light/12-h dark daily cycle, under uncrowded conditions. During amino acid starvation, well-fed 72–86 h AEL (after egg laying) larvae were floated in 20% sucrose solution in a microfuge tube for 3 h at room temperature.

Cell culture and constructs

Drosophila D.Mel-2 cells were cultured in Express Five Serum-Free Medium (Invitrogen). Transfections were performed with TransIT-2020 reagent (Mirus) according to the manufacturer's recommendations. HA2-679hook, HA248-679hook (ΔN-Hook), and hook1-551MYC (ΔC-Hook) constructs controlled by inducible metallothionein promoter (hereafter pMT) were kind gifts of Helmut Krämer (Krämer and Phistry, 1999). Full-length Hook and the coiled-coil domain, N-terminus, and C-terminus of Hook, Rab11, and Lamp1 were amplified from the *Drosophila* cDNA clones LD05265, GM06568, and RE72002 (provided by Drosophila Genomics Resource Center [DGRC]). UAS constructs were cotransfected into *Drosophila* D.Mel-2 cells with pMT-GAL4 vector (provided by DGRC, ID 1042). Cells were transfected with 2500 ng of plasmids in each case, and protein expression was induced 24–48 h later by overnight incubation with 1 mM $CuSO_4$. Primers for amplification were as follows: full-length Hook, 5′-ATGTCCGCGCCCAAGAACGA-3′ and 5′-ATCCCTTTGATTTCATTGCA-3′; Rab11, 5′-ATGGGTGCAAGAGAAGACGA-3′ and 5′-ATCCCTGACAGCACTGTTTG-3′; Lamp1, 5′-ATGTTCGCCAACAAATTGTT-3′ and 5′-ATCCGAAGCTCATGTAACCG-3′. All these PCR products were inserted into *Xmn*I/*Eco*RV-digested pENTR1A Gateway vector (Invitrogen). Entry clones were recombined with the destination vector pTWF in case of C-terminally FLAG-tagged proteins or pTWH in case of C-terminally HA-tagged protein using LR Clonase II Enzyme Mix (Invitrogen). For mapping, the Rab11-binding site Hook coiled-coil domain (180–530 aa), N-terminus, and C-terminus of Hook were amplified from the LD05265 clone using the following primers: coiled-coil domain, 5′-CTGGACAGCAAGGCAGTTCAG-3′ and 5′-CTATTGTTTACCAAACTCGCTCTC-3′; N-terminus of Hook, 5′-TCCGCGCCCAAGAACGAGATG-3′ and 5′-TTGTTTACCAAACTCGCTCTC-3′; C-terminus of Hook, 5′-ATCAAACAGTTAATGGAGCTA-3′ and 5′-CTTTGATTTCATTGCACTTAG-3′. All of these oligonucleotides included a 5′ *Not*I restriction site and a 3′ *Acc*65I restriction site. Resulting products were inserted into *Not*I/*Acc*65I-digested UAS-3×HA vector. For all PCR amplifications, we used Phusion DNA Polymerase (Finnzymes). For the UAS-ΔN-Hook construct, HA248-679hook construct from Helmut Krämer was cloned into pENTR1A Gateway vector (Invitrogen) using *Acc*65I and *Not*I restriction sites. Entry clones were recombined with the destination vector pTWH using LR Clonase II Enzyme Mix (Invitrogen).

Immunoprecipitation

Transfected cells were harvested, pelleted (1000 × *g* for 3 min), and washed twice with phosphate-buffered saline (PBS). All steps of the following procedure were performed on ice or at 4°C. Cells were lysed in 500 µl lysis buffer (0.5% Triton-X100, 150 mM NaCl, 1 mM EDTA, 20 mM Tris-HCl, pH 7.5, and complete protease inhibitor cocktail [Sigma-Aldrich]). Lysate was cleared by centrifugation at 10,000 × *g* for 10 min in an Eppendorf 5430R microcentrifuge. Before incubation, beads were washed three times with lysis buffer. Two hours later, beads were pelleted (8000 × *g* for 30 s), thoroughly washed five times with lysis buffer, and finally boiled in 30 µl Laemmli sample buffer (Sigma-Aldrich) for 5 min. Cell lysates were incubated with 30 µl anti-FLAG– or anti-HA–conjugated agarose beads (Sigma-Aldrich) for 2 h at 4°C. For immunoprecipitation studies carried out in whole organisms, expression of Hook-FLAG was induced by heat shocking well-fed L3 larvae for 1 h at 37°C. After this procedure, larvae were kept at 25°C for a 2-h recovery incubation, which was followed by 2 h of starvation. Larvae (100 mg) were washed twice and homogenized in 1 ml RIPA buffer (Sigma-Aldrich) containing protease inhibitor cocktail (Sigma-Aldrich). Detritus was pelleted (10,000 × *g* for 10 min), and the middle fraction was incubated with 30 µl anti-FLAG–conjugated agarose beads (Sigma-Aldrich) for 2 h at 4°C. Beads were collected by centrifugation for 30 s at 8000 × *g*, washed extensively, and boiled in 30 µl Laemmli sample buffer. Bound proteins were detected by Western blotting.

Western blots and immunostainings

Larvae (10–15 mg) were washed twice with PBS, and each mg of larvae was homogenized in 20 µl Laemmli sample buffer (Sigma-Aldrich). Homogenate was boiled for 5 min and pelleted at 10,000 × *g* for 10 min at 4°C, and the middle fraction was

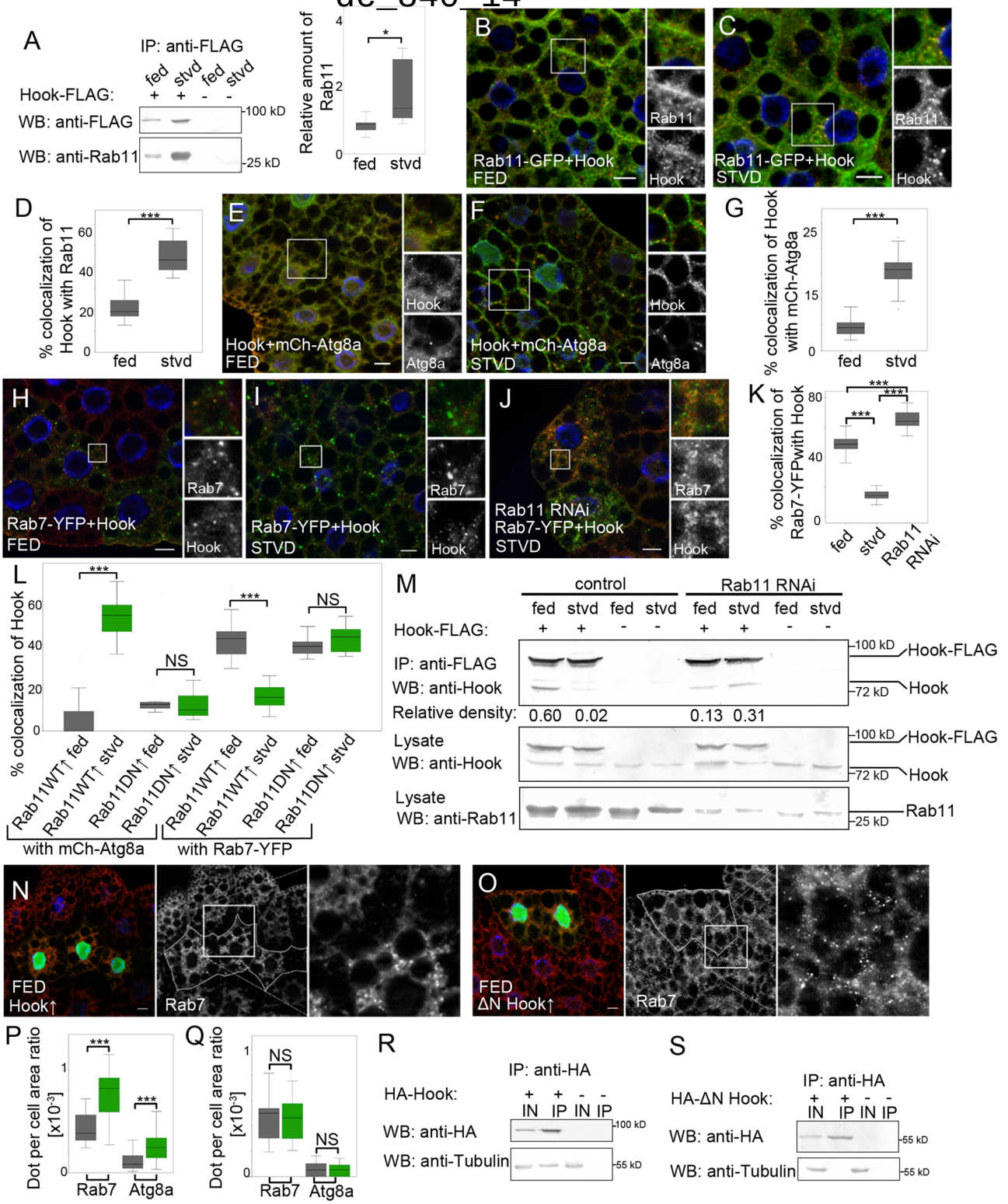


FIGURE 4: Rab11 facilitates endosome maturation by regulating Hook localization. (A) Lysates of Hook-FLAG–expressing and control fed and starved L3 *Drosophila* larvae were incubated with anti-FLAG antibody–conjugated agarose beads, and bound proteins were detected by Western blotting. The relative density of Rab11 bands compared with Hook-FLAG bands was measured as described and compared between fed and starved groups using Wilcoxon's signed-rank test ($n = 5$, $p = 0.0431$). Rab11-GFP–expressing (green) fat body cells of fed (B) and starved (C) L3 larvae were stained with anti-Hook antibody (red). Nuclei were stained using DAPI (blue). (D) Colocalization of Hook with Rab11 was calculated and compared between fed and starved groups using the Mann-Whitney test ($n_{fed} = 132$, $n_{stvd} = 64$, $p < 0.0001$). Fat body cells of fed (E) and starved (F) larvae expressing mCherry-Atg8a (red) were stained with anti-Hook antibody (green). Nuclei were stained using DAPI (blue). (G) Colocalization of Hook with mCherry-Atg8a was calculated and compared between two groups using the Mann-Whitney test ($n_{fed} = 20$, $n_{stvd} = 20$, $p < 0.0001$). Fat body

collected. Protein samples were separated on 8–12% polyacrylamide gel and were transferred to nitrocellulose membrane (Bio-Rad). After incubation in blocking solution (3% bovine serum albumin [BSA] in Tween-20/TBS [TBST]) for 1 h at room temperature, membranes were incubated with primary antibody in antibody solution (1% BSA in TBST) for 1 h at room temperature; this was followed by three 10-min washes in TBST. Signals were detected using alkaline phosphatase–coupled secondary antibodies diluted in antibody solution. Finally, membranes were developed by BCIP/NBT solution (Sigma-Aldrich). For immunostaining studies, we used larvae in the nutrient conditions and at the ages indicated above. The larval cuticle was opened, and tissue was fixed with 4% formaldehyde freshly depolymerized from paraformaldehyde in PBS overnight at 4°C. After fixation, larvae were washed three times for 30 min each time in PBST (0.1% Triton X-100 in PBS) and incubated in blocking solution (5% normal goat serum in PBST) for 2 h at room temperature. Larvae were incubated in primary antibody in PBST overnight at 4°C; this was followed by three 30-min washes in PBST. Afterward, larvae were incubated with fluorescent dye–conjugated secondary antibody; this was followed by three 30-min washes. Finally, fat bodies were dissected and analyzed by microscopy.

Antibodies

Antibodies used in this study are listed in Table S2. The EGFP gene was amplified from the pIRES2-EGFP vector (Clontech) and directly cloned into the pQE-UA bacterial expression vector (Qiagen). Recombinant protein encoding the full-length EGFP fused to an N-terminal hexahistidine tag was expressed in *Escherichia coli* M15 cells. Protein purification was performed using the QIAexpressionist kit (Qiagen). Mice were immunized with the fusion protein, and the resulting polyclonal antisera were used for further investigation.

Histology and imaging

Fat bodies from well-fed or amino acid–starved larvae were dissected in PBS and incubated for 2 min in 50 nM LTR (Invitrogen) and 1 µM Hoechst in PBS at room temperature. Stained fat bodies were washed with PBS, covered, and immediately analyzed by microscopy. For TRA uptake assay, larvae were dissected in M3 medium containing

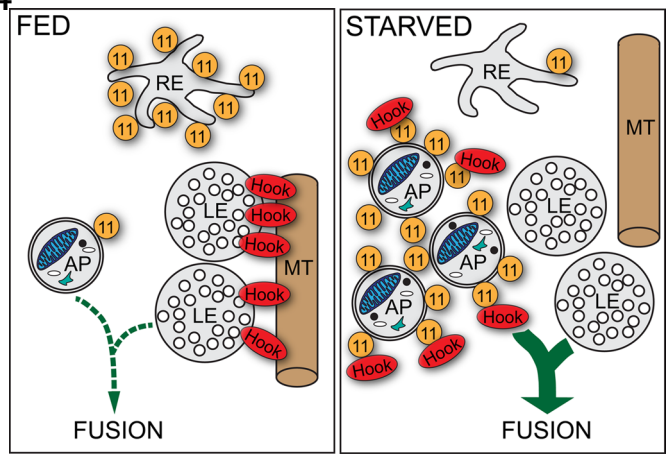


FIGURE 5: Model for the role of Rab11-Hook interaction in autophagosome maturation. Under fed conditions, Rab11 (11) localizes to REs, and Hook anchors late endosomes (LE) to microtubules (MT), thereby suppressing endosome maturation and fusion events. Autophagy induction by starvation results in the translocation of Rab11 from REs to autophagosomes (AP). Meanwhile, Rab11 removes Hook from LEs, allowing subsequent fusion of LEs with APs.

Insect Medium Supplement (Sigma-Aldrich). A 30-min incubation in pulse solution (TRA [Invitrogen] 1:25 in 5% fetal calf serum [FCS] in M3/IMS medium) was followed by a 10-min chase (5% FCS in M3/IMS medium). Larvae were washed three times with 5% BSA in PBS at 4°C and fixed in 4% paraformaldehyde solution. Fixed larvae were washed with PBS, and nuclei were stained with 1 µM Hoechst in PBS. Prepared tissues were covered in a solution containing 75% glycerol and 25% PBS. Primary images were edited using Adobe Photoshop CS5 software: area of interest was cropped, and brightness and contrast adjustments were modified, if it was necessary. To capture images, we used a Zeiss Axio Imager Z1 microscope equipped with an ApoTome unit and a Plan-Neofluar 40 × 0.75 numerical aperture objective using AxioCam MRm camera with AxioVision 4.82 software.

cells of fed (H) and starved (I) Rab7-YFP–expressing (green) larvae were stained with anti-Hook antibody (red). Nuclei were stained with DAPI (blue). (J) Starved Rab7-YFP–expressing (green) Rab11 RNAi cells (marked by GFP expression) were stained with anti-Hook antibody (red). Nuclei were stained with DAPI (blue). (K) Colocalization of Rab7-YFP with Hook was calculated and compared between the groups using the Kruskal-Wallis test ($p < 0.0001$; $n_{fed} = 40$, $n_{stvd} = 35$, $n_{RNAi} = 24$, in all pairwise comparisons $p < 0.0001$). (L) Colocalization of Hook with mCh-Atg8a or Rab7-YFP was measured in the fat body cells of fed and starved larvae overexpressing wild-type (Rab11WT↑) or GDP-locked form (Rab11DN↑) of Rab11. Data were compared between fed and starved groups using the Mann-Whitney test (Hook-Atg8a: Rab11WT↑: $n_{fed} = 33$, $n_{stvd} = 30$, $p < 0.0001$; Rab11DN↑: $n_{fed} = 10$, $n_{stvd} = 14$, $p = 0.7252$; Hook-Rab7: Rab11WT↑: $n_{fed} = 49$, $n_{stvd} = 36$, $p < 0.0001$; Rab11DN↑: $n_{fed} = 13$, $n_{stvd} = 16$, $p = 0.2729$). Green bars, starved groups; gray bars, fed groups. (M) Lysates of Hook-FLAG expressing and lacking fed and starved control and Rab11 RNAi L3 *Drosophila* larvae were incubated with anti-FLAG antibody–conjugated agarose beads. Bound proteins and Rab11, Hook, and Hook-FLAG levels of lysates were detected by Western blotting. (N) Control and full-length Hook overexpressing (green) fat body cells of fed L3 larvae were stained with anti-Rab7 antibody (red). Nuclei were stained using DAPI (blue). (O) Control and ΔN-Hook overexpressing (green) fat body cells of fed L3 larvae were stained with anti-Rab7 antibody (red). Nuclei were stained with DAPI (blue). (P) Rab7 and mCh-Atg8a–positive dot per cell area ratio was calculated and compared between the groups indicated on (N) image using Wilcoxon's signed-rank test (Rab7: $n = 18$, $p = 0.0002$; Atg8: $n = 29$, $p < 0.0001$). Green bars, Rab11 RNAi; gray bars, control groups. (Q) Rab7 and mCh-Atg8a–positive dot per cell area ratio was calculated and compared between the groups indicated on (O) image using Wilcoxon's signed-rank test (Rab7: $n = 22$, $p = 0.8838$; Atg8: $n = 20$, $p = 0.4955$). Green bars, Rab11 RNAi; gray bars, control groups. D.Mel-2 cells were transfected with HA-tagged full-length Hook (R) or ΔN-Hook (S) constructs. Lysates were incubated with anti-HA antibody–conjugated agarose beads, and bound proteins were detected by Western blotting. IN, 1% input; IP, anti-HA bound protein samples. On box-and-whisker plots, bars show the data lying between the upper and lower quartiles; the median is indicated as a horizontal line within the box. Whiskers plot the smallest and largest observations. NS, $p > 0.05$; *, $p < 0.05$; ***, $p < 0.001$. Scale bars: 10 µm.

Quantification and statistical analysis

We determined the number of dots in the cells of interest using ImageJ software. These data were weighted for the cell area to exclude unwanted biases, which could derive from variations in age or size of larvae. Cell area was measured using ImageJ software. In this way, we generated dot per cell area ratio data. For colocalization analyses, the number of double- and single-labeled dots was measured using the Red and Green Puncta Colocalization Macro of ImageJ software. We calculated their percentage ([double-labeled/single-labeled dots] × 100). When using a clonal analysis system during a study, we tried to choose the nearest neighbor of the clone cell in the same location (inside or on the periphery of the tissue) for control. If that was not possible, we took the next neighboring cell in a clockwise direction. When analyzing whole fat bodies, we measured the number of dots in 8–10 cells per larva and calculated an average value for each animal. Blots were quantified using ImageJ software. Density of P62, Rab11, GFP-Atg8, and free GFP bands were measured using ImageJ and weighted with the relative protein amount of the protein samples (density of tubulin bands). Statistical analysis of the GFP-Atg8a processing assay was performed using general linear mixed models (GLMM). We applied linear modeling for analysis, but the normal distribution is a strong requirement for this process, so we applied square-root transformation to normalize data distribution. Three main effects were investigated: two groups (Rab11 RNAi and control), two measurements (relative density of GFP-Atg8a and free GFP bands), and two treatments (fed and starved), respectively the two- and three-way interaction of these. The model showed the following results: there is significant difference between the two groups ($F(1,24) = 37.426$; $p < 0.001$) and the two measurements ($F(1,24) = 7.336$; $p = 0.012$), and these two are in significant interaction with each other ($F(1,24) = 8.552$; $p = 0.007$). The different treatments do not result in significant difference ($F(1,24) = 0.235$; $p = 0.632$). The post hoc test shows there is less free GFP in Rab11 RNAi larvae ($t(24) = 5.603$; $p < 0.001$), while there is no difference ($t(24) = -0.125$; $p = 0.902$) in the control. Density of Rab11 and Hook bands was measured and weighed with the density of Hook-FLAG bands. Statistical analysis was performed using the indicated tests in IBM SPSS Statistics software. Box-and-whisker plot figures were generated using the same software. On box-and-whisker plots, bars show the data lying between the upper and lower quartiles; the median is indicated as a horizontal line within the box. Whiskers plot the smallest and largest observations, while dots and asterisks indicate outliers. A p value of less than 0.05 was considered to be significant; * means $p < 0.05$; ** means $p < 0.01$; *** means $p < 0.001$. For details and results of statistical analyses, see Table S3. Analysis of colocalizing dots was performed using Matlab (R2012b) software.

Ultrastructural analysis

Transmission electron microscopy. Larvae were dissected in ice-cold PBS, and fat bodies were fixed in a solution containing 2% formaldehyde, 0.5% glutaraldehyde, 3 mM $CaCl_2$, and 1% sucrose in 0.1 M Na-cacodylate (pH 7.4; 30 min at room temperature); postfixed in 0.5% osmium tetroxide (45 min at room temperature) and in half-saturated aqueous uranyl acetate (30 min at room temperature); dehydrated in graded series of ethanol; embedded in LR White according to the manufacturer's instructions; and cured for 36 h at 60°C. Ultrathin sections were stained with lead citrate for 5 min. Grids were analyzed in a JEOL JEM 1011 transmission electron microscope operating at 60 kV. Images were taken using an Olympus Morada 11 megapixel camera and iTEM software (Olympus). All reagents and materials used for electron microscopy were obtained from Sigma-Aldrich.

Acid phosphatase cytochemistry. Fat body lobes were fixed as described above and washed in 0.05M Na-acetate buffer (pH 5.0; three times for 5 min each time at room temperature), incubated in Gömöri's medium (5 mM β-glycerophosphate and 4 mM lead nitrate dissolved in 0.05M acetate buffer) for 30 min at room temperature, and then washed in acetate buffer (three times for 5 min each time) and processed for electron microscopy as described above. Substrate-free medium was used for control experiments.

ACKNOWLEDGMENTS

This work was supported by a grant from the Hungarian Scientific Research Funds (NK78012) provided to M.S. The European Union and the European Social Fund have provided financial support to this project under grant agreement no. TAMOP 4.2.1./B-09/KMR-2010-0003. T.F. was supported by the Hungarian Academy of Sciences (F01/031). We address special thanks to Helmut Krämer for the indicated antibodies, stocks, and constructs. We are thankful to János Elek for the colocalization analysis script in Matlab software.

REFERENCES

Chan EYW, Tooze SA (2009). Evolution of Atg1 function and regulation. Autophagy 5, 758–765.

Chua CEL, Gan BQ, Tang BL (2011). Involvement of members of the Rab family and related small GTPases in autophagosome formation and maturation. Cell Mol Life Sci 68, 3349–3358.

De Renzis S, Sönnichsen B, Zerial M (2002). Divalent Rab effectors regulate the sub-compartmental organization and sorting of early endosomes. Nat Cell Biol 4, 124–133.

Fader CM, Sánchez DG, Furlán M, Colombo MI (2008). Induction of autophagy promotes fusion of multivesicular bodies with autophagic vacuoles in k562 cells. Traffic 9, 230–250.

Filimonenko M, Stuffers S, Raiborg C, Yamamoto A, Malerød L, Fisher EMC, Isaacs AM, Brech A, Stenmark H, Simonsen A (2007). Functional multivesicular bodies are required for autophagic clearance of protein aggregates associated with neurodegenerative disease. J Cell Biol 179, 485–500.

Funderburk SF, Wang QJ, Yue Z (2010). The Beclin 1-VPS34 complex–at the crossroads of autophagy and beyond. Trends Cell Biol 20, 355–362.

Geng J, Klionsky DJ (2008). The Atg8 and Atg12 ubiquitin-like conjugation systems in macroautophagy. "Protein modifications: beyond the usual suspects" review series. EMBO Rep 9, 859–864.

Gordon PB, Seglen PO (1988). Prelysosomal convergence of autophagic and endocytic pathways. Biochem Biophys Res Commun 151, 40–47.

Haberman AS, Akbar MA, Ray S, Krämer H (2010). *Drosophila acinus* encodes a novel regulator of endocytic and autophagic trafficking. Development 137, 2157–2166.

Hailey DW, Rambold AS, Satpute-Krishnan P, Mitra K, Sougrat R, Kim PK, Lippincott-Schwartz J (2010). Mitochondria supply membranes for autophagosome biogenesis during starvation. Cell 141, 656–667.

Hamasaki M *et al.* (2013). Autophagosomes form at ER–mitochondria contact sites. Nature 495, 389–393.

Hanson PI, Roth R, Lin Y, Heuser JE (2008). Plasma membrane deformation by circular arrays of ESCRT-III protein filaments. J Cell Biol 180, 389–402.

Hayashi-Nishino M, Fujita N, Noda T, Yamaguchi A, Yoshimori T, Yamamoto A (2009). A subdomain of the endoplasmic reticulum forms a cradle for autophagosome formation. Nat Cell Biol 11, 1433–1437.

Hsu VW, Prekeris R (2010). Transport at the recycling endosome. Curr Opin Cell Biol 22, 528–534.

Kimura S, Noda T, Yoshimori T (2007). Dissection of the autophagosome maturation process by a novel reporter protein, tandem fluorescent-tagged LC3. Autophagy 3, 452–460.

Klionsky DJ *et al.* (2012). Guidelines for the use and interpretation of assays for monitoring autophagy. Autophagy 8, 445–544.

Knævelsrud H *et al.* (2013). Membrane remodeling by the PX-BAR protein SNX18 promotes autophagosome formation. J Cell Biol 202, 331–349.

Köchl R, Hu XW, Chan EYW, Tooze SA (2006). Microtubules facilitate autophagosome formation and fusion of autophagosomes with endosomes. Traffic 7, 129–145.

dc_840_14

Krämer H, Phistry M (1999). Genetic analysis of *hook*, a gene required for endocytic trafficking in *Drosophila*. Genetics 151, 675–684.
Lamb CA, Dooley HC, Tooze SA (2013). Endocytosis and autophagy: shared machinery for degradation. Bioessays 35, 34–45.
Lee J-A, Beigneux A, Ahmad ST, Young SG, Gao F-B (2007). ESCRT-III dysfunction causes autophagosome accumulation and neurodegeneration. Curr Biol 17, 1561–1567.
Levine B, Kroemer G (2008). Autophagy in the pathogenesis of disease. Cell 132, 27–42.
Longatti A, Lamb CA, Razi M, Yoshimura S, Barr FA, Tooze SA (2012). TBC1D14 regulates autophagosome formation via Rab11- and ULK1-positive recycling endosomes. J Cell Biol 197, 659–675.
Lucocq J, Walker D (1997). Evidence for fusion between multilamellar endosomes and autophagosomes in HeLa cells. Eur J Cell Biol 72, 307–313.
Luiro K, Yliannala K, Ahtiainen L, Maunu H, Järvelä I, Kyttälä A, Jalanko A (2004). Interconnections of CLN3, Hook1 and Rab proteins link Batten disease to defects in the endocytic pathway. Hum Mol Genet 13, 3017–3027.
Mari M, Tooze SA, Reggiori F (2011). The puzzling origin of the autophagosomal membrane. F1000 Biol Rep 3, 25.
Maxfield FR, McGraw TE (2004). Endocytic recycling. Nat Rev Mol Cell Biol 5, 121–132.
Mizushima N (2010). The role of the Atg1/ULK1 complex in autophagy regulation. Curr Opin Cell Biol 22, 132–139.
Mizushima N, Levine B, Cuervo AM, Klionsky DJ (2008). Autophagy fights disease through cellular self-digestion. Nature 451, 1069–1075.
Mizushima N, Yoshimori T, Ohsumi Y (2011). The role of Atg proteins in autophagosome formation. Annu Rev Cell Dev Biol 27, 107–132.
Narayanan R, Krämer H, Ramaswami M (2000). *Drosophila* endosomal proteins hook and deep orange regulate synapse size but not synaptic vesicle recycling. J Neurobiol 45, 105–119.
Puri C, Renna M, Bento CF, Moreau K, Rubinsztein DC (2013). Diverse autophagosome membrane sources coalesce in recycling endosomes. Cell 154, 1285–1299.
Raiborg C, Stenmark H (2009). The ESCRT machinery in endosomal sorting of ubiquitylated membrane proteins. Nature 458, 445–452.
Ravikumar B, Moreau K, Jahreiss L, Puri C, Rubinsztein DC (2010). Plasma membrane contributes to the formation of pre-autophagosomal structures. Nat Cell Biol 12, 747–757.
Razi M, Chan EYW, Tooze SA (2009). Early endosomes and endosomal coatomer are required for autophagy. J Cell Biol 185, 305–321.
Richards P *et al*. (2011). Dendritic spine loss and neurodegeneration is rescued by Rab11 in models of Huntington's disease. Cell Death Differ 18, 191–200.
Schwake M, Schröder B, Saftig P (2013). Lysosomal membrane proteins and their central role in physiology. Traffic 14, 739–748.
Stenmark H (2009). Rab GTPases as coordinators of vesicle traffic. Nat Rev Mol Cell Biol 10, 513–525.
Tooze J, Hollinshead M, Ludwig T, Howell K, Hoflack B, Kern H (1990). In exocrine pancreas, the basolateral endocytic pathway converges with the autophagic pathway immediately after the early endosome. J Cell Biol 111, 329–345.
Wang T, Ming Z, Xiaochun W, Hong W (2011). Rab7: role of its protein interaction cascades in endo-lysosomal traffic. Cell Signal 23, 516–521.
Wei J, Fain S, Harrison C, Feig LA, Baleja JD (2006). Molecular dissection of Rab11 binding from coiled-coil formation in the Rab11-FIP2 C-terminal domain. Biochemistry 45, 6826–6834.
Williams RL, Urbé S (2007). The emerging shape of the ESCRT machinery. Nat Rev Mol Cell Biol 8, 355–368.
Yamamoto H, Kakuta S, Watanabe TM, Kitamura A, Sekito T, Kondo-Kakuta C, Ichikawa R, Kinjo M, Ohsumi Y (2012). Atg9 vesicles are an important membrane source during early steps of autophagosome formation. J Cell Biol 198, 219–233.

dc_840_14

Hindawi Publishing Corporation
BioMed Research International
Volume 2014, Article ID 273473, 24 pages
http://dx.doi.org/10.1155/2014/273473

Review Article

Autophagy in *Drosophila*: From Historical Studies to Current Knowledge

Nitha C. Mulakkal,[1] Peter Nagy,[2] Szabolcs Takats,[2] Radu Tusco,[1] Gábor Juhász,[2] and Ioannis P. Nezis[1]

[1] *School of Life Sciences, University of Warwick, Coventry CV4 7AL, UK*
[2] *Department of Anatomy, Cell and Developmental Biology, Eötvös Loránd University, Budapest H-1117, Hungary*

Correspondence should be addressed to Gábor Juhász; szmrt@elte.hu and Ioannis P. Nezis; I.Nezis@warwick.ac.uk

Received 23 January 2014; Accepted 17 April 2014; Published 18 May 2014

Academic Editor: Rodney J. Devenish

Copyright © 2014 Nitha C. Mulakkal et al. This is an open access article distributed under the Creative Commons Attribution License, which permits unrestricted use, distribution, and reproduction in any medium, provided the original work is properly cited.

The discovery of evolutionarily conserved Atg genes required for autophagy in yeast truly revolutionized this research field and made it possible to carry out functional studies on model organisms. Insects including *Drosophila* are classical and still popular models to study autophagy, starting from the 1960s. This review aims to summarize past achievements and our current knowledge about the role and regulation of autophagy in *Drosophila*, with an outlook to yeast and mammals. The basic mechanisms of autophagy in fruit fly cells appear to be quite similar to other eukaryotes, and the role that this lysosomal self-degradation process plays in *Drosophila* models of various diseases already made it possible to recognize certain aspects of human pathologies. Future studies in this complete animal hold great promise for the better understanding of such processes and may also help finding new research avenues for the treatment of disorders with misregulated autophagy.

1. Introduction

Autophagy collectively refers to a group of intracellular degradation pathways that mediate the breakdown of intracellular material in lysosomes. This definition could as well include the endocytic downregulation of transmembrane proteins in the plasma membrane, but for historical and mechanistic reasons, that pathway is not considered to be part of autophagy. Different routes have evolved to solve the same topological issue; that is, cytoplasmic material including proteins, lipids, nucleic acids, and whole organelles including ER and mitochondria needs to be transported into the lumen of lysosomes. Three main subtypes are usually distinguished based on how cargo reaches the lysosome.

(A) During chaperone-mediated autophagy, a subset of individual proteins bearing a KFERQ amino acid sequence are unfolded and translocated across the lysosomal membrane through a channel consisting of LAMP2A proteins [1]. This pathway was described in cell-free systems and in cultured mammalian cells and its existence has not been shown in invertebrates yet.

(B) During microautophagy, invaginations of the lysosomal membrane pinch off portions of the cytoplasm. The resulting intraluminal vesicles are then broken down inside lysosomes. While the topology of this pathway resembles multivesicular endosome formation, genetic studies in yeast revealed that it requires a subset of the same genes that mediate the main, macroautophagic pathway. Although a morphological account of microautophagy is already found in a 1965 paper on the premetamorphotic insect fat body [2], this process is still difficult to study in metazoans, as no specific genes and reporters have been described yet. Thus, it is not discussed further here, and interested readers are suggested to consult a recent review on this topic [3].

(C) During macroautophagy, membrane cisterns called phagophores (also known as isolation membranes)

assemble and capture cargo to be degraded. The resulting double-membrane autophagosomes then fuse with endosomes or lysosomes to give rise to amphisomes or autolysosomes, respectively. Autophagosome formation is enhanced in response to certain stress conditions such as starvation or during physiological changes triggered by hormonal cues [4, 5]. Thus, the degradative capacity of macroautophagy is the highest of the three pathways. As it is also the best studied route, it is usually simply referred to as autophagy, including the rest of this review.

2. Historical Early Studies

During the first 35–40 years of autophagy research, only a very limited methodological repertoire was available to study this process. The most commonly used technique was transmission electron microscopy (TEM), sometimes used together with cytochemical detection or biochemical measurement of lysosomal enzyme activities, and classical histological staining methods for light microscopy.

The first report with properly interpreted ultrastructural images of autophagic structures dates back to 1959 by Novikoff [6]. In the epithelial cells of proximal convolutions of kidneys in experimental hydronephrosis (caused by ligation of the ureter), mitochondria could be found in dense bodies that were positive for acidic phosphatase, a typical lysosomal enzyme [6, 7]. In 1962, Ashford and Porter published ultrastructural images of vesicles observed in hepatic cells of rats treated with glucagon, which obviously contained cytoplasmic material in various stages of degradation [8]. Subsequently, work in the laboratory of Christian de Duve, the biochemist famous for identifying and naming lysosomes, revealed that glucagon induced the relocalization of lysosomes to mediate glucagon-induced autophagy in rat liver [9]. Pfeifer published complementary studies on suppression of liver autophagy by insulin [10, 11]. Furthermore, starvation was already reported to be a strong enhancer of autophagy in rat liver back in 1964 [12]. It was de Duve who recommended to refer to the process of progressive degeneration of mitochondria and other organelles in cytolysosomes as autophagy (literally meaning "self-eating" in Greek), at a scientific meeting held in 1963 [13], and later described it in a widely cited review article [14]. It is worth noting that he also coined the names for processes now known as endocytosis (or heterophagy, which means "different eating" in Greek) and exocytosis in his lecture. A variety of terms were used initially for vesicles involved in autophagy, including initial and degrading autophagic vacuoles; these structures are now usually referred to as autophagosomes and autolysosomes, respectively.

Many of the pioneering early studies were carried out on insects other than *Drosophila*, as the fruit fly was not as popular before the revolution of molecular genetics as it is today. It was already shown in 1899 that in certain insects, the larval fat body (an organ with metabolic and storage functions similar to our liver and fat tissues) contains storage granules of proteins [15], and it was later described that honey bee larvae accumulated such granules just prior to pupation [16, 17]. The first recognition of autophagy in *Drosophila* melanogaster was published in 1963, showing TEM images of large autolysosomes containing ER and mitochondria in fat body cells of larvae approaching the time of puparium formation [18]. This programmed wave of autophagy in the larval fat body of holometabolous insects (those undergoing complete metamorphosis) is now known as an example of developmental autophagy.

In 1965, Locke and Collins provided a very detailed ultrastructural description of this process in the larva of the butterfly *Calpodes ethlius* [2]. Similar to the above examples, a large number of granules (which are essentially vesicles with a high protein content) form prior to metamorphosis in these animals. Three types could be distinguished: granules composed almost entirely of densely packed proteins that often form crystals, granules containing isolated regions of ER and mitochondria, and granules of a mixed type. This pioneering study published ultrastructural images that beautifully demonstrate phagophores in the process of capturing cytoplasmic contents such as a mitochondrion, double-membrane autophagosomes containing ER and mitochondria, and autolysosomes within which organelles are seen in various stages of degradation. Moreover, the authors properly recognized that the outer membrane of autophagosomes is involved in fusion with lysosomes (or first with each other), and after loss of the internal membrane, ER and mitochondria coalesce due to degradation by lysosomal enzymes. It is important to emphasize that the densely packed protein granules generated during this period originate in large part from the endocytic uptake of blood proteins when such holometabolous insect larvae (including *Drosophila*) are preparing for metamorphosis and that the heterophagy and autophagy pathways converge at the level of lysosomes [19–21]. It became clear that increases in the steroid hormone ecdysone trigger larval molts in these insects at a high concentration of juvenile hormone, and the drop in juvenile hormone concentration allows for the larval-pupal molt [22]. Note that in flies including *Drosophila*, first the larval cuticle hardens during puparium formation, and the actual molt only happens 5-6 h later, when the adult appendages such as legs and wings are everted from their primordia found as imaginal disks within the larval body. As early as in 1969, ligation and decapitation experiments (separating the ecdysone-producing endocrine organ from the larval fat body) were shown to prevent storage granule formation in *Calpodes*, and this effect could be rescued by injection of ecdysone [23]. In this report, Janet Collins already correctly hypothesized that ecdysone triggers autophagy only when juvenile hormone concentration is low, which was later confirmed in other insects including *Drosophila* [21, 24, 25].

Autolysosomes were also observed in ultrastructural images of *Rhodnius* larval fat body cells during prolonged starvation, published in 1967 by Wigglesworth [26]. Two years earlier, Francis Butterworth and colleagues reported that a 3-day starvation of early third instar *Drosophila* larvae induced massive granule formation in the fat body based on light microscopy [27], although this effect may have been due to the fact that once larvae reach the so-called 72 h checkpoint

counted from the time of egg laying, they are able to initiate metamorphosis (and thus turn on developmental autophagy and heterophagy in the fat body) following acute starvation [28].

These early studies were not limited to the insect fat body. An ultrastructural analysis of eye development of wild-type and eye color mutants of *Drosophila* was published in 1966, demonstrating that the so-called type IV granules form in the pigment cells of various colorless mutants [29]. These granules are essentially autolysosomes as they were found to be positive for acid phosphatase and contained ribosomes, myelin-like membranes, glycogen, and ferritin [29]. In 1965, Lockshin and Williams showed that during the elimination of intersegmental muscles following adult ecdysis in silkmoths, increased activity of lysosomal cathepsins and acid phosphatases can be detected biochemically, and lysosome-like organelles abound which were later found to contain mitochondria [30–32]. These findings led to the morphological classification of this histolysis as a type II (or autophagic) cell death, to distinguish it from type I cell death events, which are characterized by the classical apoptotic morphology such as chromatin condensation, cell shrinkage, and blebbing [33].

3. Genetic Control of Autophagy in *Drosophila*

Multiple genetic screens carried out in the 1990's identified a core set of about 20 evolutionarily conserved genes required for autophagy in yeast [34–36]. Since different names were proposed often for the same genes in each screen, a consensus nomenclature for these *Atg* (autophagy-related) genes was adopted in late 2003 [37]. Note that the first study to demonstrate that an *Atg* gene homolog is also required for autophagy in a complete animal was published in *Drosophila* earlier that year, that is why it did not follow the agreed-upon naming conventions and referred to the fly homolog of *Atg3* as *Drosophila Aut1* [38]. It is commonly accepted that Atg gene products assemble into functional protein complexes, and several attempts have been made to establish their hierarchy during autophagosome formation in various models [39–41]. Such genetic epistasis analyses have proven difficult based on data from yeast and cultured mammalian cells, which is likely explained by the emerging connections between Atg proteins that were originally grouped into separate complexes, by temporal differences in the recruitment of various Atg proteins to phagophore assembly sites (PAS), and by differences in the localization of proteins thought to act as part of the same complex [4, 42, 43]. Nevertheless, we will discuss the role of these proteins according to the canonical classification in this review for clarity (please see also Figure 1).

The Atg1 complex is usually considered to act most upstream in the hierarchy of Atg gene products in all eukaryotic cells and contains the serine/threonine kinase Atg1 (the homolog of mammalian ULK1 and ULK2 proteins), Atg13, Atg101, and FIP200 (also known as RB1CC1 in mammals and Atg17 in flies) in metazoans. Of these, neither Atg101 nor FIP200 has clear homologs in yeast based on sequence

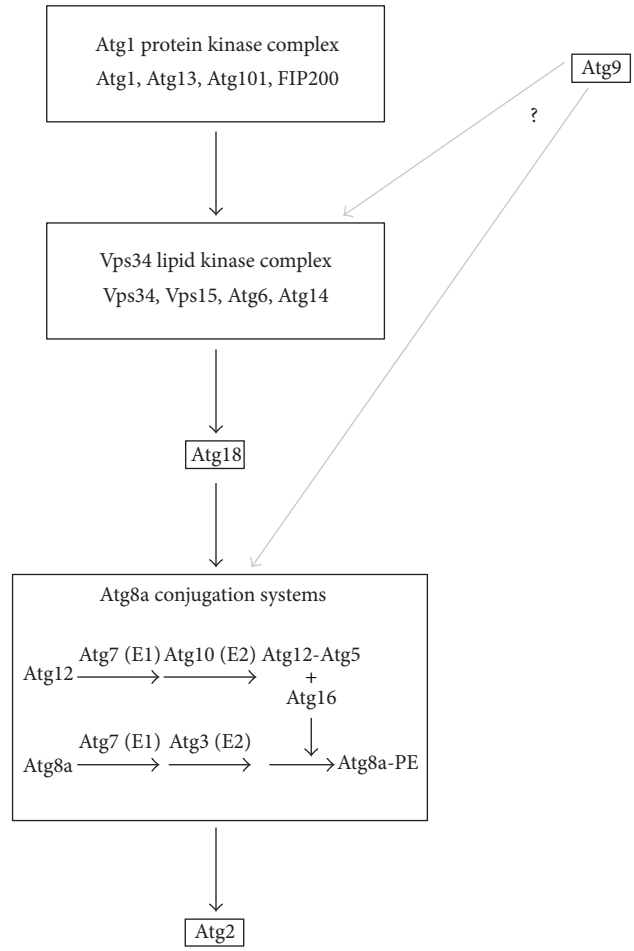


Figure 1: A model for the hierarchical relationships of Atg proteins in *Drosophila*. PE: phosphatidyl-ethanolamine. See text for details.

comparisons, although FIP200 is thought to act similar to the scaffold protein Atg17 [44]. Biochemical studies in flies and mammals show that Atg13 directly binds to the other three subunits, and that it undergoes Atg1-mediated hyperphosphorylation upon starvation in *Drosophila* [44–46]. The catalytic activity of Atg1 seems to be especially important for autophagy induction. First, expression of kinase dead Atg1 inhibits autophagy in a dominant-negative fashion [47]. Second, overexpression of Atg1 strongly induces autophagy, which eventually culminates in cell death due to activation of caspases [47]. Third, Atg1 undergoes limited autophosphorylation during starvation, which is thought to increase its activity [44]. Interestingly, expression of dominant-negative, kinase dead Atg1 still shows a low-level rescue of the lethality of Atg1 null mutants [47]. Moreover, Atg1 was found to localize to the whole phagophore in yeast while all other subunits of this complex remain restricted to the initially appearing PAS area, indicating that Atg1 may also function independent of its canonical binding partners [43].

Both autophagosome and endosome membranes are positive for phosphatidylinositol 3-phosphate (PI3P), a phospholipid generated by the action of similar lipid kinase complexes. The core complex contains Atg6 (known as

Beclin-1 in mammals), the catalytically active class III phosphatidylinositol 3-kinase (PI3K) Vps34, and its regulatory subunit Vps15, which has a serine/threonine kinase domain. A catalytically inactive point mutant of Vps15 was shown to lose Vps34 binding in yeast [48], but the significance of its putative protein kinase activity is poorly understood. The identity of the fourth subunit is critical: Atg14 is present in the autophagy-specific complex while the other complex involved in endocytosis contains UVRAG/Vps38, and the binding of these subunits to the core complex has been shown to be mutually exclusive in mammalian cells [49, 50]. Starvation-induced autophagy is severely impaired in Vps34 null mutant or dominant-negative Vps34 overexpressing cells, although some autophagosomes form at a reduced rate [51]. This may be explained by the activity of the class II PI3K, which was suggested to partially compensate for the loss of Vps34 during autophagy in mammalian cells [52, 53]. Similarly, deletion of *Drosophila* Vps15 or Atg6 results in a block of starvation-induced autophagy [54, 55]. In line with the distinct roles of different Vps34 complexes in mammals and yeast, it has been shown that *Drosophila* UVRAG is involved in endolysosome maturation and is dispensable for autophagosome formation or fusion with lysosomes, whereas studies using RNAi or hypomorphic mutants suggested that Atg14 is required for autophagy in larval fat body cells [56–59].

It is commonly accepted that PI3P found on phagophore and autophagosomal membranes recruits and activates phospholipid effectors. One class of such proteins includes the metazoan homologs of the yeast WD40 domain protein Atg18, which are called WIPI1-4 in mammals [60, 61]. In *Drosophila*, Atg18 has been shown to be required for autophagy, whereas the function of its closely related paralog CG8678 (also known as Atg18b) is not known [62]. DFCP1 (double FYVE containing protein 1) was characterized as another phospholipid effector, and it translocates to a putative subdomain of the ER during autophagy induction [63]. This structure is called the omegasome, and it is also positive for VMP1 (vacuole membrane protein 1), an ER-localized, six transmembrane domain containing protein of poorly characterized function [40, 64]. Interestingly, VMP1 has been found to interact with Beclin-1, suggesting that it may modulate phospholipid production [65]. The fly homolog of VMP1 is called Tango5 (Transport and Golgi organization 5), as it was recovered in a cell culture-based RNAi screen as required for ER to Golgi trafficking in the secretory pathway [66]. Interestingly, the gene encoding DFCP1 has been lost multiple times during evolution as it is missing from all *Caenorhabditis* and most *Drosophila* species including *Drosophila melanogaster*, but its homolog can be clearly identified in *Drosophila willistoni* and the *virilis* subgroup using bioinformatic searches, in addition to more ancient species such as *Trichoplax* and *Hydra*. The role of DFCP1 is also unknown in mammals, and it is mostly used as a marker along with VMP1 for the PAS [40, 42].

Atg9 is the only transmembrane protein among the Atg gene products identified in yeast, and it likely plays a critical role in the membrane transport events during phagophore assembly in all eukaryotes studied so far [42, 67–69]. The source of autophagic membranes has been debated since the discovery of this process, and practically all membrane compartments were suggested to contribute, including endosomes, ER, Golgi, mitochondria, and plasma membrane [70–72]. *Drosophila* Atg9 is still largely uncharacterized, with only a few RNAi studies showing that it is also required for autophagy in various settings [57, 73–75]. Yeast Atg9 physically binds to Atg18 and Atg2, and these proteins are required for the retrograde traffic of Atg9 from the PAS in yeast [76]. Atg9 also binds to fly Atg18, and it has recently been shown that Atg9 accumulates on protein aggregates containing the autophagy cargo Ref(2)P (also known as p62/SQSTM1) in starved Atg7, Atg8a, and Atg2 mutants, but not in Atg18 mutants [75].

Structural studies of Atg8 and Atg12 revealed that these proteins belong to the family of ubiquitin-like modifiers, and these are involved in two related ubiquitin-like conjugation systems [77]. First, the C-terminal amino acid(s) following a glycine residue of Atg8 and its homologs are cleaved by the Atg4 family of cystein proteases. Subsequently, the exposed glycine is conjugated to the E1-like enzyme Atg7, followed by its transfer to the E2-like Atg3 (also known as Aut1 in flies). In parallel, Atg12 is activated by Atg7 as well, and then the E2-like Atg10 catalyzes the formation of an Atg5-Atg12 conjugate [77]. Atg5 contains two ubiquitin-related domains flanking a helical region [78]. Then, a multimeric complex of Atg5-Atg12 and Atg16 forms, which enhances the covalent conjugation of Atg8 to the membrane lipid phosphatidylethanolamine (PE) [78]. Atg8 and its homologs (Atg8a and Atg8b in flies, and LC3 and GABARAP family proteins in mammals) are the most commonly used markers in autophagy studies [40, 79]. First, Atg8 is covalently bound to phagophore and autophagosome membranes, making it possible to visualize these structures using tagged reporters or by immunostaining using antibodies against endogenous proteins (Figure 2). Second, the processing of Atg8 can be followed by Western blots, as unconjugated Atg8 (usually referred to as Atg8-I or LC3-I) migrates slower than the lipid-bound form (Atg8-II or LC3-II). Autophagy induction usually increases the amount of the processed form relative to tubulin or actin, which becomes even more obvious if the fusion of autophagosomes with lysosomes is blocked by bafilomycin, or genetically by loss of the autophagosomal SNARE Syntaxin 17 [79–82].

It is clearly established that Atg2 and Atg18 function together in yeast, acting most likely in parallel to the Atg8 and Atg12 conjugation systems [39, 83]. In mammals, depletion of the Atg18 homolog WIPI2 suppressed LC3 puncta formation [61]. In contrast, its putative binding partner Atg2 appears to function most downstream of the core Atg genes in mammals and worms, similar to VMP1 homologs, as Atg8-positive structures with some characteristics of phagophores form in cells upon silencing of these genes [40, 41, 64, 84]. Atg18 also shows an interaction with Atg2 in *Drosophila*, although it is weaker than that observed between its paralog CG8678 and Atg2 [75]. Interestingly, *Drosophila* Atg2 acts downstream of, or parallel to, the Atg8 systems in *Drosophila* as well, as it is dispensable for Atg8a dot formation in the fat body [75, 80]. In contrast, no GFP-Atg8a puncta were seen in Atg2 mutant

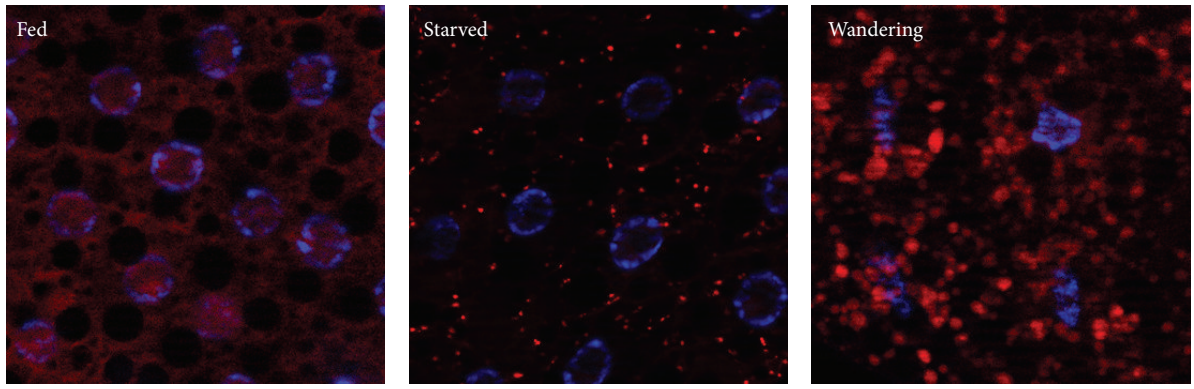


Figure 2: Autophagy induction in the larval *Drosophila* fat body. Dots positive for mCherry-Atg8a (red), representing autophagosomes and autolysosomes, are rarely seen in fat body cells of well-fed larvae (a). Punctate mCherry-Atg8a structures form in response to starvation (b) or during the wandering period (c). DNA is stained blue.

prepupal midguts [85], suggesting that either tissue-specific differences exist, or that a GFP-Atg8a reporter expressed at very low levels is not as potent as anti-Atg8a immunolabeling for the visualization of these aberrant structures that are apparently seen in most metazoan cells. This issue clearly warrants further studies.

Drosophila Atg18 appears to function upstream of Atg8 recruitment during phagophore formation similar to worms and mammals, as punctate Atg8a localization is lost in Atg18 mutant or RNAi cells [41, 61, 75, 84]. Interestingly, protein aggregates positive for ubiquitin and Ref(2)P show a near complete colocalization with FIP200 and Atg9 in *Drosophila* mutants lacking more downstream players, raising the possibility that such protein aggregates may serve as an organizing centre during autophagosome formation [46, 75]. This hypothesis will need further testing.

A complicated network of core Atg proteins coordinates the process of autophagosome formation, a process that is still not completely understood. Autophagosomes must fuse with lysosomes and endosomes to deliver their cargo for degradation. In yeast, direct fusion of the autophagosome with the vacuole is achieved by a tethering factor called HOPS (homotypic fusion and vacuole protein sorting) complex, which facilitates membrane fusion catalyzed by SNARE proteins Vam3, Vam7, and Vti1 [86]. Interestingly, autophagosome fusion in *Drosophila* appears to depend on the amphisome pathway, as a genetic block of multivesicular endosome formation results in large-scale accumulation of autophagosomes [51, 87]. Recent studies identified Syntaxin 17 as the autophagosomal SNARE protein, both in flies and mammals [80, 81]. Syntaxin 17 binds to ubisnap, an ortholog of mammalian SNAP-29, to mediate fusion by forming a ternary complex with late endosomal/lysosomal VAMP7 (VAMP8 in mammals) [80, 81]. Fusion is facilitated by the binding of HOPS to this SNARE complex, both in *Drosophila* and mammalian cells [58, 88]. In the final steps following fusion, cargo is degraded inside acidic autolysosomes by the action of hydrolases such as cathepsins, and the breakdown products are recycled back to the cytosol to fuel synthetic and energy producing pathways.

4. Regulation of Autophagy during *Drosophila* Development

The best known examples for stimulus-induced autophagy in *Drosophila* larvae are the starvation response during the feeding stages and developmental autophagy triggered by hormonal cues around the start of metamorphosis in polyploid tissues. The role and regulation of autophagy have also been studied in a developmental context in adult ovaries and in the extraembryonic tissue called amnioserosa during early embryogenesis. The following paragraphs summarize the major regulatory pathways regulating autophagy in these settings.

Autophagy is controlled by the main nutrient and energy sensor in all eukaryotic cells, a serine/threonine kinase called TOR (target of rapamycin) [89]. TOR activity is increased by the presence of nutrients and growth factors and promotes cell growth in part through the phosphorylation and activation of S6k (RPS6-p70-protein kinase) and phosphorylation and inactivation of Thor (also known as 4E-BP for Eukaryotic translation initiation factor 4E binding) [90]. TOR not only enhances general protein synthesis this way, but it may also increase net cell growth by actively repressing autophagy through the direct phosphorylation and inhibition of Atg1 in metazoans [45, 91–93]. Inactivation of TOR during starvation, growth factor withdrawal, or impaired lysosomal function rapidly results in the shutdown of cap-dependent translation and in the activation of autophagy, which is likely also facilitated by the poorly characterized action of phosphatases such as PP2A that may antagonize TOR [52, 56, 62, 91–94]. Interestingly, the serine/threonine kinase Atg1 and its mammalian homologs are able to directly phosphorylate TOR, which may act as a feedback mechanism to inhibit cell growth and further enhance autophagy induction [47, 95].

Growth signaling pathways are remarkably active in the larva, a specialized life stage of holometabolous insects. Larvae basically just eat and grow throughout the feeding stages to acquire and store as many nutrients as possible in a relatively short time, mostly in the form of polyploid cells and tissues besides the hemolymph. Notably, the size of the larval fat body (a metabolic organ similar to our liver and white fat tissues) increases more than 200-fold between the first and mid-third instar stages in *Drosophila*. This process generates polyploid cells of enormous size, reaching a ploidy level of 256–512 n for fat cells and 1,024 n for salivary glands. As expected, autophagic activity is very low during these stages (Figure 2). Initiation of wandering behavior, when larvae crawl out of the food in search of a dry place to pupariate around 108 h after egg laying (AEL), or starvation before this time results in a remarkable induction of autophagy in polyploid tissues (Figure 2), but not in diploid cells. This response is thought to serve as a nutrient reallocation mechanism, as breakdown products released from polyploid cells likely feed diploid tissues that will give rise to the adult fly by the end of metamorphosis. Mechanistically, growth signaling mediated by the insulin-like receptor is rapidly inactivated during starvation or at the beginning of metamorphosis in polyploid tissues [62, 96]. Diploid tissues such as the brain and wing disc appear to be able to grow and proliferate thanks to maintained activation of TOR signaling by sustained receptor Tyrosine kinase signaling, originating from Alk in neurons and Stit in future wing cells, respectively [97, 98]. In addition, the larval fat body secretes an insulin-like peptide (dilp6) during nonfeeding stages to maintain insulin signaling in diploid tissues [99].

As described briefly in the chapter on historical early studies, autophagy of the polyploid tissues including fat body and midgut cells is induced by a small peak of the molting hormone ecdysone towards the end of the last larval instar [20, 96]. Interestingly, there is a preprogrammed anterior-posterior gradient in the magnitude of autophagy in the fat body [100]. This is also observed for the separation of fat cells and kynurenine synthesis during metamorphosis, potentially due to the extremely low blood circulation in sessile prepupae and pupae, which necessitates the coordination of all these responses with respect to the location of nearby imaginal organs [100, 101]. Autophagy is induced in fat body cells as a cell-autonomous response, as overexpression of dominant-negative forms of the ecdysone receptor in mosaic animals maintains insulin signaling and blocks developmental autophagy in these cells [96]. Massive induction of autophagy is not seen during earlier ecdysone peaks that trigger larval molts, because high concentration of the juvenile hormone during the first and second larval stages inhibits autophagy. It is not known yet how juvenile hormone may inhibit autophagy. One candidate mechanism involves the peptidyl-prolyl cis-trans isomerase FKBP39. FKBP39 is a juvenile hormone target gene, and it has been shown to inhibit autophagy likely by preventing the translocation of the transcription factor FOXO into the nucleus [102, 103]. The presence of FOXO in the nucleus during starvation or at the beginning of metamorphosis likely promotes transcription of genes involved in autophagy, and its loss strongly impairs autophagic responses [103, 104]. It is worth mentioning that metamorphosis is not the only developmentally programmed starvation period in *Drosophila*, as larvae are also essentially immobile and do not feed during periods of molting that separate L1/L2 and L2/L3 stages, leading to increased autophagy in fat body (Gábor Juhász, unpublished data). This response is similar to the induction of autophagy observed during molting in worms [105].

Polyploid cells that account for the majority of larval masses undergo programmed cell death during metamorphosis. Initially, the larval fat body disintegrates into individual trophocytes following puparium formation, which is triggered by a prominent ecdysone peak at the end of the last larval instar [106]. Interestingly, approximately half of the larval fat cells survive until eclosion of adult flies and are only eliminated by caspase-dependent cell death during the first two days of adult life, promoting the survival of starved young adults [107, 108]. Salivary glands are also almost entirely composed of polyploid cells in the larva, with the exception of a ring of diploid imaginal cells surrounding the ducts of the paired glands. Larval gland cells are eliminated around 13–18 h after puparium formation, and both autophagy and activation of apoptotic caspases have been shown to facilitate histolysis, although the relative importance of each pathway is not fully understood [109–114]. A wave of autophagy is also seen in larval midgut cells of wandering larvae, but their elimination begins only after puparium formation, and it is not completed until after adult flies eclose [96, 115]. Groups of diploid imaginal cells (scattered throughout the larval gut) proliferate and replace polyploid cells during this process. Thus, polyploid cells are extruded into the lumen of the future adult gut, which is accompanied by caspase activation, DNA fragmentation, and autophagy-mediated shrinkage of these larval cells [85, 110, 112, 113, 115]. Remnants of the larval midgut form the meconium, the waste product that adult flies get rid of during the first defecation.

There is some discrepancy regarding the role of the apoptotic and autophagic pathways during larval *Drosophila* midgut degeneration. Two papers suggested that midgut shrinkage is blocked by expression of the caspase inhibitor p35, or by simultaneous loss of two proapoptotic genes Rpr and Hid [110, 112]. Importantly, RNAi depletion of the caspase inhibitor DIAP1 leads to premature caspase activation and death of larval midguts and salivary glands [110]. In contrast, midgut shrinkage was suggested to proceed largely independent of caspase activation based on experiments carried out on animals with a combination of mutations for certain caspases, whereas midgut cells fail to shrink properly if certain *Atg* genes are silenced or mutated [85, 115]. Interestingly, overexpression of Hid in *Drosophila* larvae triggers apoptosis in diploid cells of the developing eye and brain, but it leads to the induction of autophagy in polyploid cells of the fat body, salivary glands, and midguts [116], also indicating tissue-specific differences in the mechanism of action of certain proapoptotic genes.

In contrast to ecdysone-mediated shutdown of insulin signaling, which is responsible for the initial wave of autophagy in wandering animals, death of polyploid cells in salivary glands and midguts appears to be regulated by

a complex transcriptional cascade. As mentioned earlier, the elimination of about half of the fat body cells takes place in the pupa in a seemingly random manner, and surviving cells only die in young adults [108]. In prepupal midguts and pupal salivary glands, binding of ecdysone (or more likely its active form 20-hydroxyecdysone) activates the heterodimeric steroid receptor complex consisting of EcR and USP (the homolog of mammalian retinoid X receptor). Activation of this complex by ecdysone is necessary to trigger salivary gland cell death by inducing transcription of insect-specific target genes such as E93, E74A, and BR-C, but this process also requires a competence factor: the nuclear receptor βFTZ-F1 [117]. E93 is a transcription factor acting as a master regulator of the complex genetic programme involved in the death of both larval salivary glands and midgut in *Drosophila* [114, 118]. The role of autophagy in dying salivary gland and midgut cells may not be restricted to the recycling of building blocks to support diploid cells. Autophagy in dying mammalian cells is known to promote the release of so-called "eat me" and "come get me" signals to attract engulfing macrophages [119]. While larval midgut cells are situated inside the adult gut and are therefore protected from hemocytes, clearance of salivary gland cell fragments may be facilitated by macrophages in the pupa. This hypothetical scenario would explain why salivary glands undergo complete histolysis, whereas midgut cell remnants remain in the lumen of the adult gut until excreted.

Given the seemingly important role of autophagy during *Drosophila* development, it is surprising that null mutants for different genes show large differences regarding viability. Null mutants of *Atg1*, *Atg13*, and *FIP200* display a highly penetrant pharate adult lethality: adult flies form completely inside the pupal case, but almost all of them fail to eclose [45–47, 120]. The lipid kinase complex subunit null mutants (*Atg6, Vps34*, and *Vps15*) die much earlier (as L3 stage larvae), and only a few *Atg6* mutants are able to initiate pupariation [51, 54, 55]. This is not surprising considering that these gene products are involved in endosome maturation and biosynthetic transport to lysosomes acting in a complex with UVRAG. It is worth noting that UVRAG null mutants also die as late L3 stage larvae, even though UVRAG is dispensable for autophagosome formation or fusion with lysosomes [58, 121]. It will be interesting to see the phenotype of flies null mutant for *Atg14*, which encodes the autophagy-specific subunit of this complex, as these should behave similar to Atg1 kinase complex subunits in showing pharate adult lethality. Similarly, both *Atg2* and *Atg18* mutants are late pupal/pharate adult lethal. In contrast, all null mutants identified so far in genes encoding proteins involved in the ubiquitin-like conjugation systems are viable, including *Atg7* [113], *Atg8a* [57, 122], and *Atg16* (Gábor Juhász, unpublished data). Moreover, these null mutants can be maintained as viable stocks over multiple generations despite their shorter lifespan and increased stress sensitivity. The reason why null mutations affecting conjugation system components are viable in *Drosophila* is not known. A recent paper showed that prepupal midgut shrinkage requires Atg8a and Atg16, but not Atg3 or Atg7 [115], suggesting that Atg8a promotes cell shrinkage in a lipidation-independent manner. Still, these results do not explain the lethality data described above. Potential explanations can be that certain *Atg* genes are not required for autophagy in certain key developmental settings (such as *Atg3* and *Atg7* in midgut shrinkage), or that the ones that are lethal also have important roles independent of autophagic degradation (similar to *Vps34*, *Vps15,* and *Atg6*). It is important to note that *Atg3, Atg5, Atg7, Atg9,* and *Atg16L1* knockout mice complete embryonic development and are born at expected Mendelian ratios and only die due to suckling defects, whereas the loss of beclin *1/Atg6* leads to lethality during early embryogenesis [4].

Another role of autophagy has been described in the *Drosophila* ovary. During oogenesis, 15 nurse cells transfer a large part of their cytoplasm to the single oocyte through interconnecting cytoplasmic bridges called ring canals. Nurse cells die after the oocyte has matured, which is accompanied by caspase activation and DNA fragmentation. Caspase activation is reduced in nurse cells lacking Atg1, Atg13, or Vps34, and both DNA fragmentation and cell elimination are reduced [123]. Interestingly, the antiapoptotic protein Bruce accumulates in these mutant cells. Bruce colocalizes with GFP-Atg8a in wild-type ovaries, and loss of Bruce restores nurse cell death in autophagy mutants [123]. These observations suggest that autophagic elimination of Bruce may contribute to caspase activation and cell death in late stage *Drosophila* ovaries. However, mutation of either core autophagy genes or caspases, or the simultaneous loss of both autophagy and caspases still results in only a partial inhibition of developmental nurse cell death [124]. In contrast, hypomorphic mutation of dor/Vps18, a subunit of the HOPS complex, blocks nurse cell elimination much more efficiently, suggesting that lysosomes or endocytosis may play a more important role in developmental nurse cell death than autophagy or caspases [124, 125].

Autophagy can also be induced in the ovary during two earlier nutrient status checkpoints in germarium and mid-oogenesis stages, both in nurse cells and follicle cells, somatic epithelium surrounding germ cells [126–128]. This autophagic response requires core Atg genes and the caspase Dcp-1, and it can be suppressed by overexpression of Bruce [126, 127]. Interestingly, oogenesis is impaired in chimeric ovaries lacking autophagy in a subset of follicle cells but not in the germline, which may be caused at least in part by precocious activation of Notch signaling in mutant follicle cells [127, 129].

Another example for developmentally programmed autophagy is seen in the amnioserosa, a polyploid extraembryonic tissue of the developing embryo. Autophagy is induced prior to, and independent of, the activation of a caspase-dependent cell death programme in these cells [130]. Autophagy is also activated in a subset of amnioserosa cells that undergo extrusion during dorsal closure, but it is not required for the death of these cells [131].

In contrast with the paradigm of the inverse regulation of cell growth and autophagy by TOR signaling, autophagy has been shown to be required for cellular overgrowth driven by the evolutionarily conserved transcription factor Myc. Myc is required for autophagy, both in *Drosophila* and mammalian cells [73, 132]. Conversely, overexpression of this well-known

oncogene not only enhances cell growth, but it also leads to autophagy induction through activation of PERK, an ER-associated kinase involved in the unfolded protein response (UPR). Importantly, blocking PERK or autophagy prevents Myc-induced overgrowth in *Drosophila* and inhibits Myc-induced tumorigenesis in mouse models [73, 133]. These results suggest that inhibition of PERK or autophagy may be a potential therapeutic strategy in the context of Myc-dependent cancers.

5. Autophagy Implication in the Immune Response, Aging, and Neurodegeneration

Autophagy plays an important role in development, cellular differentiation, and homeostasis. Defects in autophagy are associated with many diseases including neurodegeneration, ageing, pathogenic infection, and cancer [5]. *Drosophila* melanogaster has been shown to be an excellent model system to study such cellular processes. The key advantages of using *Drosophila* as a disease model organism are short life cycle, small body size, ability to produce large number of progeny, availability of powerful genetic tools, and less redundant genome than that of mammals. Moreover, more than 70% of human disease genes have orthologues in *Drosophila* [134].

Autophagy has also been proposed to play a role in the removal of pathogens, given that it is the only degradative system in the cell which is able to handle cargo that is too large for proteasomal degradation. Evidence shows that autophagy is able to capture and degrade multiple categories of pathogens, including bacteria, viruses, and parasites [135]. This is not, however, a universally effective defence system, as some pathogens have developed resistance against it, or even learnt how to use autophagy in order to enhance their own replication [135, 136]. This interplay between host defences and infective agents suggests that autophagy, as an intracellular immune response, has exerted strong selective pressure on pathogens over the course of a long evolutionary time [137]. Flies lack an adaptive immune system, which facilitates the study of autophagy-derived innate immunity at the cellular level, without added complexity [138].

Drosophila has also been used successfully to study of the effects of pharmacological modulators of autophagy in neurodegenerative disease models. The available *Drosophila* disease models successfully recapitulate many of the symptoms associated with human diseases, and these can be used to identify new factors with a role in diseases [134].

5.1. Autophagy-Derived Innate Immunity. In mammals, pathogen recognition activates the antimicrobial response of the host, using transcription level regulators [137]. So far, two well-characterised nuclear factor-κB (NF-κB) pathways are known in flies: the Toll and immune deficiency (IMD) pathways, which are key to regulating the immune response against bacterial and fungal infections, by means such as the secretion of antimicrobial peptides (AMPs) [138, 139]. The Jak-Stat pathway, native to higher organisms, also plays a role in the immune defence response in flies, and all of the aforementioned pathways have been observed to mediate antiviral responses at the level of transcription [140, 141]. There are many aspects of the innate immune response in insects which are yet to be elucidated, and the role of autophagy in the antimicrobial response is only beginning to be deciphered. Striking parallels were observed between flies and mammals in terms of antimicrobial functions of autophagy [137]. A new aspect in mammalian antimicrobial autophagy, which is quickly gaining visibility, is the role of pattern recognition receptors (PRRs) in the activation of autophagy [135, 142]. These receptors work by recognising well-conserved molecular signature sequences, called pathogen-associated molecular patterns (PAMPs) [143]. The *Drosophila* protein Toll was first used to pinpoint the mammalian Toll-like receptors (TLRs) by virtue of homology, which make up the canonical pattern recognition system [137, 138]. These membrane receptors can induce autophagy upon binding to a cognate ligand [144]. Their cytoplasmic counterparts, the NOD-like receptors (NLRs), can activate autophagy as well [145, 146]. The importance of autophagy control by PRRs in mammalian host defence is certainly an interesting research avenue, despite the difficulty of assessing its *in vivo* potential during infection in mice. *Drosophila*, on the other hand, offers a much more genetically malleable system for such studies. The relationship between autophagy and PRRs has been found to be critical in preventing the host from succumbing to viral and bacterial infections [137]. Hence, it is likely that antimicrobial autophagy is an ancient cellular response to invading pathogens.

Autophagy genes have been shown to confer resistance to parasites (*Toxoplasma gondii*), bacteria (*Staphylococcus aureus*, *Listeria monocytogenes*, *Salmonella enterica*, *Typhimurium,* and *Mycobacterium tuberculosis*), and viruses (Sindbis virus, vesicular stomatitis virus (VSV), and herpes simplex type 1) [147–154]. Importantly, a landmark study recently showed that parkin, a gene implicated in the pathogenesis of Parkinson disease by promoting the selective autophagic elimination of mitochondria, is also important for the recognition and subsequent autophagic degradation of infecting intracellular bacteria in mice and *Drosophila* [155].

In terms of bacterial resistance, the *Drosophila* immunity comes equipped with two previously mentioned major response pathways: the Toll pathway, which is usually activated by Gram-positive bacteria, and the IMD pathway, which mainly handles Gram-negative bacteria [138]. Activation of either of these systems depends on the receptors' ability to detect PAMPs, such as the bacterial cell wall component peptidoglycan (PGN) [138]. This process and the subsequent release of AMPs are vital given that flies that are deficient in either the IMD or Toll pathway display hypersusceptibility to bacterial infection [156].

There are, however, species that show resistance to such a host response. Both the IMD and Toll signalling pathways are dispensable for controlling intracellular *L. monocytogenes* in flies. Instead, once bacteria have escaped to the cytoplasm, autophagy restricts their replication. *L. monocytogenes* replication takes place in the cytoplasm of *Drosophila* blood cells, termed "haemocytes" [157]. It has been observed that *L. monocytogenes* induces autophagy, which was visualised by the appearance of GFP-fused LC3 puncta that colocalised

with internalised bacteria [157]. This study showed that RNAi-mediated silencing of core autophagy genes causes increased bacterial replication and reduces fly life expectancy in infected adultsvspace2pt

In mammalian cells, autophagy can also degrade *L. monocytogenes*, but this process is normally blocked by the release of ActA, which inhibits the host's ability to ubiquitinate the pathogen and target it for autophagosomal degradation [153]. A similar autophagy evading behaviour has been independently observed in conjunction with protein InlK, although the mechanism is yet unexplained [158]. Failure to successfully resist the host's response, such as in the unnatural host *Drosophila*, reveals restrictive pathways that the *L. monocytogenes* cannot evade and highlights the constant adaptations that the bacterium must undergo in order to effectively counteract the immune responses of the host [137]. Upstream of the IMD pathway is the PGN recognition protein (PGRP) family receptors, which recognize bacterial PGN structures. PGRP-LC is a transmembrane sensor, which recognises monomeric and polymeric diaminopimelic acid-(DAP-) type PGN at the cell surface. PGRP-LE comes in two forms that have both cell-autonomous and non-cell-autonomous functions [159]. It is constitutively secreted into the open circulatory system, where it activates the IMD pathway [160]; it is also found within immune cells and acts as an intracellular receptor for the detection of the PAMP tracheal cytotoxin, a monomeric DAP-type PGN, initiating the release of the listericin AMP [161, 162]. Loss of either of the two receptors confers susceptibility to infection by *L. monocytogenes*, but only PGRP-LE initiates autophagy as an immune response. Unexpectedly, PGRP-LE can signal via the IMD pathway, components of which are not required either for autophagy induction or intracellular bacterial sequestration, suggesting that an unknown signalling pathway links PRR engagement to antimicrobial autophagy in *Drosophila*. Autophagy is observed to play an important regulatory role against a variety of bacterial invaders. Multiple hosts have been found to utilise autophagy to control the growth of *Wolbachia*, a common endosymbiotic bacterium, found in arthropods and filarial nematodes. Activation of autophagy by starvation or rapamycin treatment was found to reduce the rate of bacterial replication; conversely, siRNA-mediated depletion of Atg1 in flies was associated with enhanced bacterial replication [163].

In addition to controlling bacterial infection, autophagy was found to impact viral replication and pathogenesis in some mammalian infections [137]. Overexpression of beclin-1 (mammalian homologue of Atg6) in neonatal mice protects neurons against Sindbis virus infection-induced pathogenesis [164]. Loss of Atg5 expression accelerates the development of Sindbis-associated symptoms, due to failed viral capsid clearance, even though autophagy does not appear to affect viral replication proper [150]. A range of other viral agents are ostensibly managed by autophagy, such as HIV, encephalomyocarditis virus, and human papilloma virus in mammalian cells, although the *in vivo* significance has not been weighed [165, 166].

Recent data demonstrates that autophagy is a key element of the innate antiviral response against (−) ssRNA Rhabdovirus VSV in flies [151]. Negative sense viral RNAs must be first converted into mRNA-like positive-sense strands by an RNA polymerase, before they can be translated. Depletion of core autophagic machinery genes in *Drosophila* S2 cells leads to increased viral replication. Along the same lines, RNAi silencing of autophagy genes was associated with increased viral replication and mortality after infection of flies, directly linking autophagy with an important antiviral role *in vivo* [151]. VSV was observed to induce PI3 K-Akt regulated autophagy in primary haemocytes and in adult flies [151]. Similar to the immune response against *L. monocytogenes* infection, antiviral protection is also initiated by the recognition of PAMPs [151]. An active response against UV-inactivated VSV suggested that nucleic acids are not the targeted markers; rather, the viral glycoprotein VSV-G was sufficient to induce autophagy. Eventually, the *Drosophila* Toll-7 receptor was identified as the PRR, which identifies VSV as a trigger for an autophagic response [167]. Toll-7 is localised to the plasma membrane in order to interact with the virions, suggesting that the roles of Toll-7 and the mammalian TLRs are similar. Toll-7 restricts VSV replication in cells as well as in adult flies, as deficiency of Toll-7 leads to significantly increased mortality after infection [167]. Recent work has drawn in other Toll receptors as likely participants in the host's immune response. Tollo (Toll-8) has been shown to negatively regulate AMP expression in *Drosophila* respiratory epithelium [168]. Many antiviral factors are upregulated during infection; given that *Drosophila* Toll and Toll-7 receptors have been recently shown to be transcriptionally induced upon infection, it is possible that the other less characterised Toll receptors may also play a role in antiviral defences (Figure 3).

There is an overlap in the mode of action of Toll receptors and mammalian TLRs in triggering autophagy. A number of studies using model ligands and in vitro systems have shown autophagy induction via the TLR pathway (such as lipopolysaccharide, a ligand for TLR4, by looking at the colocalisation of autophagosome markers and intracellular bacteria) [169]. Autophagic activation can be observed using canonical ligands for TLR1, TLR3, TLR5, TLR6, and TLR7 [144, 170]. TLR8 was revealed in a recent study to activate vitamin D-dependent autophagy in human macrophages, in order to restrict HIV replication [137, 171].

5.2. Autophagy in Ageing and Life Span Extension. Ageing is a complex process that involves a progressive decline in physiological functions of an organism, eventually causing disease and death [172]. During this decline, cellular and molecular damage accumulates such as deleterious mutations, shortening of telomeres, accumulation of ROS, damaged organelles, and misfolded proteins. Aged individuals have increased sensitivity to environmental stress and a decreased capacity to maintain cell and tissue homeostasis. Prevalence of many diseases such as neurodegeneration, cardiovascular dysfunction, and cancer increases with age [173].

Autophagy maintains cellular homeostasis by targeting unwanted and deleterious intracellular materials to the lysosome for degradation. Autophagy has been implicated

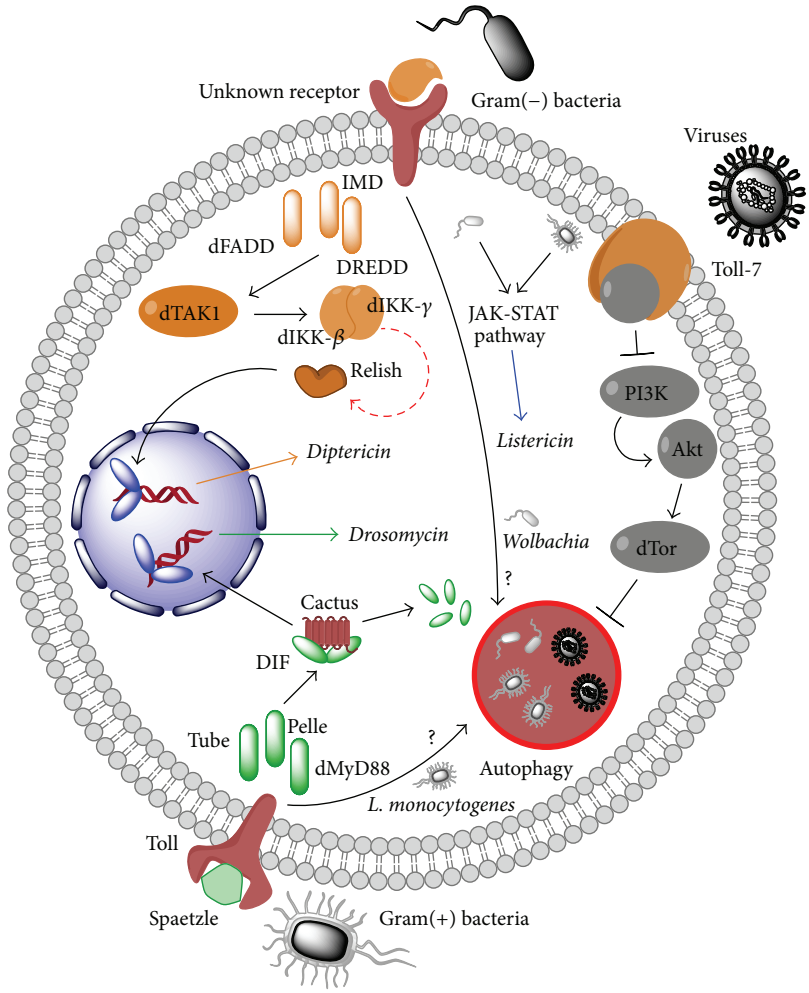


Figure 3: *Drosophila* immunity response pathways. A robust innate immunity system confers *Drosophila* protection against a variety of pathogens. Autophagy has been suggested to play a role in restricting infections, but the exact pathway of this response has yet to be deciphered. In addition there have been observations of a number of antimicrobial peptides (e.g., Diptericin) being expressed in response to immunological challenge.

in numerous diseases [5]. Accumulating evidence indicates that the efficiency of autophagy decreases with age, and the induction of autophagy delays aging-associated symptoms and extends life span [172]. In addition to the direct effect of autophagy on ageing, cellular pathways with a role in regulating ageing are shown to induce autophagy as their downstream targets [174–176]. These highly conserved pathways are insulin/insulin like growth factor (Igf) (ISS) pathway, the TOR pathway, c-Jun N-terminal kinase (JNK) signaling, and histone deacetylation [174, 177].

During ageing, the expression levels of several autophagy genes are downregulated in mammals. Autophagy mutants often exhibit phenotypes such as the accumulation of ubiquitinated protein aggregates, damaged organelles, increased sensitivity to oxidative stress, abnormal motor function, and short life span that are similar to those observed during ageing [172]. The expression level of Atg5, Atg7, and Beclin-1 is downregulated in human brains during ageing [178, 179]. Furthermore, a decrease in Beclin-1 expression has been reported in the brains of patients with Alzheimer's disease (AD) and Huntington's disease (HD) [179, 180]. Disruption of autophagy by reducing Beclin-1 expression enhances the severity of neurodegenerative phenotypes in transgenic APP (amyloid precursor protein) mice, and overexpression of Beclin-1 was sufficient to rescue the adverse effects in APP transgenic mice [180]. Suppression of basal autophagy in the central nervous system causes neurodegenerative phenotypes in mice even in the absence of a toxic protein: mice lacking Atg5 or Atg7 specifically in the central nervous system exhibit behavioural defects, motor dysfunction, accumulation of protein aggregates, and reduced life span [181, 182]. Chaperone-mediated autophagy (CMA) has been shown to be downregulated in rat livers during ageing as well. Restoring the level of chaperone-mediated autophagy by overexpressing LAMP2a, a CMA receptor, decreased the accumulation of damaged proteins and increased organ function [183]. A reduction in autophagy levels is also observed in mice during ageing. The heart-specific deletion of Atg5 causes abnormal heart morphology and the accumulation of

abnormal protein aggregates and damaged mitochondria in mice [184].

Similar to these observations in mammals, the expression of several autophagy genes (Atg2, Atg8a, Atg18, and bchs) is reduced in *Drosophila* during ageing. This correlates with an increase in accumulation of insoluble ubiquitinated protein aggregates (IUP) in the ageing brain [122]. *Drosophila* Atg8a mutants exhibit reduced autophagy, increased accumulation of IUP, increased sensitivity to oxidative stress, and reduced life span. Overexpression of Atg8a in adult brains decreased the incidence of IUP and increased oxidative stress tolerance and life span [122]. Similarly, *Drosophila* Atg7 null mutants are hypersensitive to nutrient and oxidative stress. Atg7 null mutants exhibit reduced life span and progressive neurodegeneration, which is characterized by the accumulation of ubiquitinated proteins [113]. Overexpression of Atg7 increases life span in wild-type flies and also rescues the age-related phenotypes caused by the knockdown of Hsp27 chaperone in *Drosophila*. Interestingly, overexpression of Hsp27 also extends life span in wild-type flies and rescues the neurodegenerative phenotypes caused by mild polyQ toxicity. The Hsp27-mediated rescue effect is abolished in flies lacking Atg7 [185]. Loss of the autophagosomal SNARE Syntaxin 17 has severe consequences: young mutant adults perform extremely poor in standard climbing tests that measure neuromuscular function and die within 3-4 days of eclosion. This is potentially due to large-scale accumulation of autophagosomes in neurons which causes neuronal dysfunction, rather than to cell death, as the lethality and behavior defects cannot be rescued by genetic inhibition of caspases in Syntaxin 17 mutant brains [80].

The insulin/insulin-like growth factor (Igf) pathway modulates longevity in multiple species [177]. The first insights into the role of the insulin pathway in longevity came from *C. elegans*. Mutant worms with reduced insulin signaling (mutation in insulin/insulin like receptor (igf), *daf2*) live twice as long as wild-type ones [186]. The longevity effect of the daf2 gene mutation is mediated through *daf16*, the *C. elegans* homologue of transcriptional factor FOXO. The Igf pathway negatively regulates the downstream acting FOXO transcriptional factor [187]. Knocking down the expression of autophagy genes (atg5, atg12, or bec1) abolishes the longevity effect of reduced insulin signaling in *daf2* mutants. It is worth noting that deletion of bec1 also reduces life span in wild-type worms [188].

Drosophila mutants with decreased insulin signaling (mutation in Insulin like receptor (InR) or in insulin receptor substrate *chico*) exhibit slow ageing and increased life span [189, 190]. Similar to *C. elegans* Igf mutants, these mutants also require FOXO for life span extension [191, 192]. Phosphorylation of FOXO by activated Igf prevents its nuclear localization and leads to the transcriptional downregulation of FOXO target genes. FOXO mediates the activation of pathways that inhibit growth and promote stress response [193]. It has been shown that FOXO induces autophagy in *Drosophila* larvae [103]. Furthermore, specific activation of FOXO in head fat body increases life span and oxidative stress tolerance. This localized overexpression of FOXO decreases systemic insulin signaling and it is correlated with a decrease in expression of dilp 2 (insulin-like peptide 2) in neurons [193]. Further studies show that reduced insulin signaling causes transcriptional repression of dawdle, an activin-like ligand in the TGF-beta super family, through FOXO, which in turn activates autophagy, thereby maintaining protein homeostasis. This study also shows that overexpression of Atg8a in muscle is also sufficient for life span extension in *Drosophila* [194].

Progressive muscle degeneration is associated with ageing and this precedes other age-related pathologies across species. However, the mechanism underlying muscle ageing is not completely understood. Muscle degeneration is associated with the accumulation of ubiquitinated protein aggregates, which are also positive for Ref(2)P in *Drosophila*. Overexpression of FOXO, or its target 4E-BP, in muscle prevents protein accumulation and increases muscle function via autophagy in *Drosophila*. Overexpression of FOXO increases Atg gene expression in muscle. RNAi-mediated knockdown of Atg7 to about half in FOXO overexpression backgrounds partially increases protein accumulation, suggesting that the effects of FOXO overexpression require autophagy. Moreover, the increase in muscle function by FOXO/4E-BP overexpression is sufficient to extend life span. FOXO/4E-BP overexpression in muscles regulates organism-wide protein homeostasis by reducing feeding and also by decreasing the release of insulin-like growth factors from neurosecretory cells in the brain [195].

JNK signaling plays a major role in regulating ageing in *Drosophila*. Activation of JNK signaling increases tolerance to oxidative stress and extends life span [196]. Life span extension upon JNK activation is also mediated through FOXO. Flies with reduced FOXO activity fail to extend life span and exhibit reduced tolerance to oxidative stress even upon JNK activation. The JNK pathway antagonizes the ISS pathway and promotes the translocation of FOXO to the nucleus [197]. Nuclear translocation of FOXO results in the transcription of autophagy genes [103]. JNK/FOXO reduces Igf activity systemically by reducing dilp2 expression in neuroendocrine cells [197]. JNK-mediated protection from oxidative stress is abolished in flies with compromised autophagy, and the induction of JNK signaling may activate autophagy through FOXO [198].

Spermidine, a naturally occurring polyamine, increases life span in multiple species. Levels of polyamines have been shown to decrease during ageing [199]. Dietary supplementation of spermidine induces autophagy and extends life span in *Drosophila*, and spermidine-mediated longevity is abrogated in flies which lack Atg7 [199]. Moreover, spermidine triggered autophagy inhibits the age-associated cognitive impairment in *Drosophila* [200]. Spermidine regulates ageing most likely by epigenetically regulating autophagy. Spermidine inhibits histone acetyltransferases (HAT), which in turn cause a global deacetylation of histone H3 and activation of autophagy in yeast [199]. Interestingly, spermidine treatment may confer oxidative stress resistance both in autophagy-dependent and autophagy-independent ways in *Drosophila* [201].

The TOR pathway modulates ageing in multiple species. Decreased TOR signaling is associated with an increase in life span and increased tolerance to stress. Treatment of

Drosophila with rapamycin (an inhibitor of TOR) increases life span and tolerance to both nutrient starvation and oxidative stress. Rapamycin-mediated life span extension is abrogated in flies undergoing Atg5 RNAi [202]. Genetic inhibition of TOR also increases life span in flies [203]. This is likely due to the fact that TOR inhibition activates autophagy [5].

Dietary restriction (reduced food intake without malnutrition) has been shown to be an effective intervention to expand lifespan in multiple species, including *Drosophila* [174, 204]. Cellular pathways that mediate the longevity effect of dietary restriction are not fully understood. Studies in *C. elegans* show that autophagy is required for the longevity effect of dietary restriction. When autophagy is compromised (by deleting bec-1 and ce-atg7) in *eat-2* mutants (a genetic model for dietary restriction in *C. elegans*), longevity is blocked [205]. In fact, most longevity pathways have been suggested to converge on autophagy genes in worms [206].

5.3. Autophagy and Neurodegeneration. Neurodegenerative diseases encompass a group of progressive disorders characterised by memory loss, cognitive impartment, loss of sensation, and motor dysfunctions. The cellular hallmark of neurodegenerative disease is the presence of ubiquitinated protein aggregates and neuronal cell death [207]. Several lines of evidence connect autophagy with neurodegeneration. Autophagy maintains cellular homeostasis by removing aggregated proteins and damaged organelles. This process is the most critical in neurons, because neurons do not divide and cannot get rid of protein aggregates through self-replication or self-renewal [208].

One of the risk factors for neurodegenerative diseases is ageing. Ageing is associated with decreased autophagy [208]. The connection between autophagy, ageing, and neurodegeneration is described in detail in Section 5.2.

Several neurodegenerative disease models have been developed in *Drosophila*, based on overexpressing wild type or mutant versions of human disease proteins. These disease models also provide insights into the role of autophagy in the context of neurodegeneration [207].

The overexpression of a human huntingtin protein containing a 120-amino acid long polyQ expansion causes age-dependent degeneration in *Drosophila* compound eye [209]. Treatment of these flies with rapamycin reduces retinal degeneration in an autophagy-dependent manner, similar to results observed in mouse and cell culture models of HD [210]. Further studies showed that the beneficial effect of rapamycin was not restricted to huntingtin disease. Rapamycin treatment alleviates neurodegenerative phenotypes in *Drosophila* nonhuntingtin polyglutamine, polyalanine, and tau disease models [211]. Induction of autophagy by rapamycin is conserved from yeast to mammals. A high-throughput drug screen identified three novel drugs, which induce autophagy independent of TOR. These small molecules reduce the number of protein aggregates and cytotoxicity, both in cellular and *Drosophila* models of neurodegenerative disease [212, 213]. Overexpression of Rab5 also ameliorates huntingtin-induced cell death in *Drosophila*, potentially by the formation of a Rab5 complex with Beclin-1 and Vps34, leading to enhanced autophagosome formation [214].

An independent study documented that hyperactivation of the TOR pathway suppresses autophagy and leads to neuronal cell death. Overexpression of Rheb, an activator of TOR, causes age- and light-dependent degeneration in the *Drosophila* retina. This was likely due to autophagy suppression, as autophagy induction by Atg1 was sufficient to rescue retinal degeneration. Similarly, overexpression of Atg1 or genetic inhibition of TOR by overexpressing TSC1/2 alleviates the neurodegenerative phenotype in *Drosophila* HD and phospholipase C- (norpA-) mediated retinal degeneration models. This study suggests that neurodegenerative symptoms observed in these flies are due to TOR-dependent suppression of autophagy, and not due to the effect of TOR on cell growth [215].

Puromycin-sensitive aminopeptidase (PSA) is the only cytosolic enzyme capable of degrading polyQ sequences. PSA has been shown to be involved in neurodegeneration in *Drosophila*, mice, and cell culture models of poly Q diseases. Overexpression of PSA inhibits polyQ toxicity, whereas inhibiting PSA expression enhances poly Q toxicity in *Drosophila* models of poly Q diseases. PSA was suggested to reduce polyQ toxicity by activating autophagy and subsequent clearance of toxic aggregates, but how it may promote autophagy is still unknown [216].

Results of a genetic modifier screen aimed at the identification of genes involved in Ataxin3 toxicity in *Drosophila* found numerous candidates. A subset of the suppressors was proposed to act either by enhancing autophagy-mediated clearance of protein aggregates or by inhibiting autophagy to prevent autophagy-mediated cell loss. This study also pointed out that only the pathogenic form of ataxin3, and not wild type ataxin, induces autophagy [217].

Induction of autophagy does not rescue neurodegeneration caused by the polyglutamine-containing atrophin in *Drosophila* DRPLA (dentatorubropallidoluysian atrophy) model. The neurodegenerative phenotype is characterized by the accumulation of autophagic vacuoles in degenerating neurons and glia. Inhibiting autophagy by Atg5 RNAi or using an Atg1 null mutant enhances neurodegenerative phenotypes. However, both pharmaceutical and genetic inductions of autophagy failed to rescue neurodegeneration. Ultrastructural analysis showed the presence of abnormally large autolysosomes with impaired degradation of the contents. Thus, the beneficial effect of autophagy may be suppressed by lysosomal dysfunction in this case [218]. Transcriptional profiling identified that atrophin reduces the expression of fat, a tumor suppressor protein. Fat, and Hippo kinase acting downstream of it, may protect the neuron by activating autophagy [219]. Although the exact mechanisms of neuroprotection by the Fat/Hippo pathway are not fully understood, authors of these studies suggested two plausible mechanisms: (1) Hippo may activate autophagy by inhibiting TOR, or (2) Hippo might enhance autophagy through its interaction with Atg8a [220].

An immunoelectron microscopy study identified the accumulation of abnormal autophagic vacuoles (AV) in

human AD brain [221]. In line with that, overexpression of Aβ42 (the byproduct of APP proteolysis, a major component of Abeta inclusion in AD) results in age-dependent dysfunction of autophagy at a lysosomal stage in *Drosophila* [222]. This is characterised by the accumulation of abnormal autophagic vacuoles in the brain. The leakage of these vacuoles causes the acidification of cytosol, and further damage to membranes and organelles eventually leads to neuronal cell death. In contrast, overexpression of Aβ40, another byproduct of APP proteolysis, does not cause autophagy dysfunction or neuronal abnormality. This differential neurotoxicity raises the possibility that Aβ40 is degraded by autophagy. Interestingly, inhibition of autophagy partially rescues the neurodegenerative phenotype and activation of autophagy exuberates symptoms in Aβ42 *Drosophila* models. The authors of this study suggest that autophagy may act as a prosurvival pathway in early stages of the disease, and as a prodeath pathway in later stages [222].

Studies in *Drosophila* provide potential mechanistic links between UPS and autophagy. Autophagy is induced as a compensatory mechanism during proteasome dysfunction. This compensatory induction is dependent on histone deacetylase 6 (HDAC6), a microtubule-associated deacetylase that interacts with polyubiquitinated proteins. Autophagy is induced in temperature sensitive proteasome mutant flies, and also in response to UPS impairment in *Drosophila* SBMA (spinobulbar muscular atrophy (SBMA)) models. Overexpression of HDAC6 was shown to rescue degenerative phenotypes associated with UPS dysfunction in an autophagy-dependent manner in these flies. Furthermore, HDAC6 overexpression rescues neurodegenerative phenotypes observed in *Drosophila* Ataxia and Abeta models. The rescuing effect of HDAC was again abolished in flies with impaired autophagy [223].

Studies in *Drosophila* have also contributed to our understanding of the link between endocytosis and neurodegeneration and its relation to autophagy. Mutations in the Endosomal Sorting Complex Required for Transport- (ESCRT-) III subunit CHMP2B are associated with FTD (frontotemporal dementia) and ALS (amyotrophic lateral sclerosis). These diseases are characterized by the presence of ubiquitinated protein aggregates, which are positive for p62/SQSTM1. The ESCRT complex is involved in the recognition and sorting of ubiquitinated endocytosed integral membrane proteins into the intraluminal vesicles of the multivesicular body (MVB) and is required for their subsequent degradation in lysosomes. Autophagic degradation is inhibited in cells overexpressing CHMP2B and in cells or *Drosophila* lacking ESCRT function. Reduced ESCRT function impairs the clearance of mutant huntingtin protein in cell and *Drosophila* models of HD diseases. These studies show that the functional MVB pathway is important for proper autophagic function [51, 224, 225].

6. Selective Autophagy in *Drosophila*

The Atg8 family proteins are required for the expansion of the phagophore membrane and also participate in cargo recognition and recruitment to the forming autophagosome. These ubiquitin-like (UBL) proteins are conjugated to phosphatidylethanolamine (PE) and are found both on the inner and outer sides of the autophagosome membrane. The Atg8 family proteins including LC3 (microtubule-associated protein 1 light chain 3) lie at the heart of selective autophagy, through their binding to selective autophagy receptors. Six receptors have been identified in mammals so far: p62/SQSTM1/SQSTM1, NBR1, NDP52, Nix, optineurin, and Stbd1 [226–228]. These proteins contain a LIR/LRS (LC3-interacting region/LC3 recognition sequence) motif and have been shown to interact with LC3 family proteins [198, 199].

6.1. Selective Autophagy Receptors in Drosophila. In *Drosophila*, only two selective autophagy receptors have been described so far: Ref(2)P, the homologue of mammalian p62/SQSTM1/SQSTM1, and blue cheese, the homologue of mammalian Alfy. p62/SQSTM1/SQSTM1 is the first and best understood selective autophagy cargo receptor. It is a multifunctional protein, performing a variety of functions in the cell [229, 230]. Human p62/SQSTM1 is 440 amino acids long and contains several functional motifs [229]. A Phox and Bemlp (PB1) domain is located at the N-terminus and is necessary for the multimerisation of the protein, as well as its interaction with a range of kinases (MEKK3, MEK5, ERK, PKCζ, PKCλ/t, and another autophagy receptor, NBR1) [229]. Following the PB1 domain is a ZZ zinc-finger domain, which interacts with the serine-threonine kinase receptor-interacting protein 1 (RIP1) [230]. Importantly, p62/SQSTM1 contains an LC3 interacting LIR/LRS motif, and a kelch-like ECH-associated protein 1 (KEAP1) interacting region (KIR) motif, which interacts with KEAP1 [231–233]. At its C-terminus, p62/SQSTM1 retains an ubiquitin-associated (UBA) domain, required for binding monomeric and multimeric ubiquitin [229].

p62/SQSTM1 binds to polyubiquitinated proteins and crosslinks these to the growing phagophore via Atg8/LC3 binding. A reduction in p62/SQSTM1 expression increases huntingtin-induced cell death in HD cell culture models [231, 234]. Autophagy deficient mice lacking p62/SQSTM1 failed to form ubiquitin positive aggregates, indicating that p62/SQSTM1 is important for aggregate formation [235]. The *Drosophila* p62/SQSTM1 homologue, Refractory to Sigma P (Ref(2)P), is 599 amino acids long and also contains an N-terminal PB1 domain, a ZZ-type zinc-finger domain, and a C-terminal UBA domain [236]. Similar to p62/SQSTM1, Ref(2)P is accumulated when autophagy is impaired and it has been found within protein aggregates in autophagy deficient *Drosophila* and in *Drosophila* neurodegenerative models [236] (Figure 4). It makes use of its PB1 domain to multimerise and is able to bind ubiquitin molecules via its UBA domain [237]. Ref(2)P also harbours a LIR motif between residues 451–458 (DPEWQLID) [237, 238], which fits well with the revised LIR motif sequence, proposed by Johansen and Lamark, which could be written as D/E-D/E-D/E-W/F/Y-X-X-L/I/V [229]. Ref(2)P has recently been established as a selective autophagy substrate in *Drosophila* as well [75]. Moreover, it has a putative KIR motif and

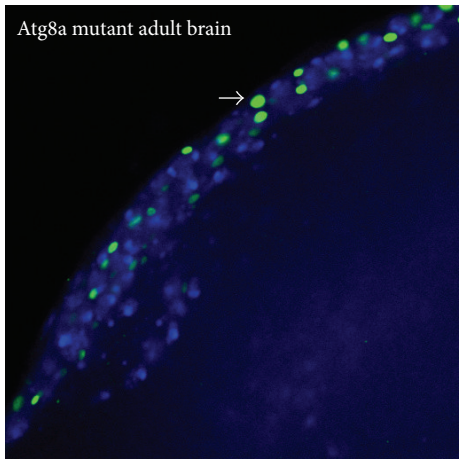


Figure 4: Ref(2)P accumulates in the brain of Atg8a mutant adult flies. Confocal micrograph of a mid-section of the optic lobe in the brain of an Atg8a mutant adult fly. The tissue is stained for Ref(2)P (green, arrow highlights an aggregate) and DNA (blue).

its interaction with both Keap1 and Atg8a appears to be conserved, too [73, 238, 239].

S6 kinase is a central regulator of autophagy and cell growth. TOR activation suppresses autophagy and leads to the phosphorylation of S6K. S6K was long considered as an autophagy inhibitor, a fact now contested, as S6K is found to be required for starvation-induced autophagy [62, 240]. Consistent with these observations, loss in S6K significantly increased the number (but not the size) of Ref(2)P aggregates in *Drosophila* larval fat body cells [57].

A novel role of Ref(2)P was reported in *Drosophila* haemocytes. Alongside Atg1, Ref(2)P-mediated selective autophagy was shown to be indispensable for cellular remodelling of the haemocyte cortex [241, 242]. Arresting autophagy with 3-methyladenine (3MA) or knocking down other Atg genes (Atg4, Atg6, Atg7, Atg8a, and Atg9) all produced a similar phenotype. Taken together, the above information demonstrates that Ref(2)P has a wide spectrum of cellular functions, like its human p62/SQSTM1 homologue, whose functions require further elucidation.

Loss of function mutation in *Drosophila* blue cheese gene (bchs) results in an age-dependent accumulation of ubiquitinated protein aggregates and amyloid precursor-like proteins and reduces life span. Abnormal central nervous system morphology and size were also documented in bchs mutants [243]. The ubiquitinated protein aggregates in bchs mutants are positive for Ref(2)P [244]. Alfy, the human homologue of *Drosophila* blue cheese, is involved in the selective disposal of ubiquitinated protein aggregates. Alfy is a large, 3527 amino acid long protein, which contains a variety of functional domains, including a FYVE domain suggesting an affinity for PI(3)-P rich endosomes. Instead, Alfy has been found to localise mostly to the nuclear envelope, but it translocates to autophagic membranes and ubiquitin-rich aggregates under strenuous cellular conditions [245]. Alfy-mediated aggrephagy makes use of p62/SQSTM1, the human homologue of *Drosophila* Ref(2)P. Alfy, together with p62/SQSTM1, may crosslink ubiquitinated protein aggregates with the core autophagy machinery for disposal, highlighting the importance of this so-called aggrephagy in neuronal homeostasis [246]. A genetic modifier screen based on the overexpression of blue cheese in *Drosophila* eye has linked lysosomal dysfunction to altered ubiquitin profiles and reduced life span and shows the genetic interaction between certain genes and blue cheese [247, 248]. Alfy has been shown to play a role in the removal of high polyQ-containing mutant huntingtin [246]. Blue cheese overexpression has been observed to rescue morphological and functional qualities in fly eyes expressing a polyQ127 transgene. Recent work by the Simonsen and Finley groups has established a link between overexpression of blue cheese C-terminal region and a general improvement of neurodegenerative phenotypes *in vivo* [246].

6.2. Selective Autophagy and Chaperone Assisted Autophagy. Chaperone-assisted autophagy (CAA) differs from macroautophagy in the method of cargo transport, which is mediated by chaperones in CAA, rather than via autophagosomes. However, there is a level of interplay between CAA chaperones and selective autophagy adaptor proteins, which uncovers a hybrid degradative solution, termed Chaperone-assisted selective autophagy (CASA). The *Drosophila* melanogaster cochaperone Starvin (Stv) interacts with ubiquitin adaptor Ref(2)P and ubiquitin ligase CHIP in order to coordinate the activity of Hsc70 and HspB8. This CASA complex is behind the selective degradation of damaged components in muscle Z disks. Loss of CASA function has been associated with progressive muscle weakness and general myopathies in flies, mice, and men [249, 250]. High molecular mass ubiquitin conjugates have been observed in mouse muscle tissue with a concomitant increase in the level of BAG-3 (mammalian ortholog of Starvin), as a result of repetitive tetanic contraction. These conjugates were observed to form microaggregates, which partially colocalised with LC3, suggesting an involvement of autophagosomal engulfment, as part of muscle protein degradation [249]. It is possible that selective macroautophagy and selective chaperone-assisted autophagy cooperate, in order to maintain a healthy protein landscape at tissue level.

6.3. Mitophagy. Mitophagy (selective autophagic degradation of damage impaired mitochondria) has been recently described in yeast and mammals [251]. Atg8/LC3 was observed to interact with mitochondrial membrane proteins via its LIR motif, such as the yeast Atg32 [252] and the mammalian NIP3-like protein NIX [253, 254]. The mechanism behind mitophagy is tightly connected to the fusion/fission behaviour of the mitochondrial network. A bioenergetically impaired mitochondrion is prevented from fusing back into the network, by the proteasomal degradation of the profusion factor mitofusin, Mfn, also known as marf in *Drosophila*. This behaviour is facilitated by the E3 ligase Parkin, recruited to the outer mitochondrial membrane (OMM) by PTEN-induced putative kinase protein I (PINK1) as a result of a loss in membrane potential [255, 256]. Parkin is thought to

target various OMM substrates such as Mfn: ubiquitinating them and targeting them for proteasomal degradation [257]. Fusion incompetent mitochondrial organelles are then removed by selective autophagy [251]. Mutations of Parkin and Pink1 are associated with familial forms of Parkinson's disease (PD). Most of our understanding of Pink1 and Parkin function comes from *Drosophila*. Pink1 or Parkin null mutants exhibit muscle degeneration, male sterility, reduced life span, and an abnormal mitochondrial morphology [258–260]. Overexpression of the mitochondrial fission inducer Drp1, or knocking down the expression of mitochondrial fusion inducers mfn or opa1 rescues the degenerative phenotypes in Pink1 and Parkin mutants. This suggests that Pink1 and Parkin maintain mitochondrial morphology at least in part by preventing mitochondrial fusion or by enhancing mitochondrial fission [261]. Pink1 and Parkin have been shown to be involved in mitophagy in mammalian cells [255]. Genetic analysis in *Drosophila* showed that Pink1 acts upstream of Parkin [258]. Recruitment of Parkin to mitochondria causes the ubiquitination of mfn in a Pink1-dependent manner. These studies indicate that both Pink1 and Parkin are involved in the removal of dysfunctional mitochondria, and loss of Pink1 or Parkin led to the accumulation of abnormal mitochondria, which causes oxidative stress and neurodegeneration [262, 263].

Recent work by Vincow et al. and colleagues suggests that mitophagy may be the result of an interplay between several processes [264]. Overall mitochondrial protein turnover in parkin null *Drosophila* was similar to that in Atg7 deficient mutants. By contrast, the turnover of respiratory chain (RC) subunits showed greater impairment with relation to parkin loss, than in Atg7 mutants. RC subunit turnover was also selectively impaired in PINK1 mutants [264]. Given the various degrees of mitochondrial protein turnover impairment in response to a deficit in either proteasom- associated factors or selective autophagy regulators, two theories attempt to pinpoint the pathways involved in mitophagy. One model revolves around the chaperone-mediated extraction of mitochondrial proteins [265]. Another possible model involves mitochondria-derived vesicles, which carry selected cargo directly to the lysosome, in an autophagy-independent manner [266]. The latter model has been observed experimentally, whereby vesicles were found to transport a membrane-bound complex IV subunit and contain inner mitochondrial membrane [267].

6.4. Novel Selective Autophagy Regulators. Protein ubiquitination is a widespread method for targeting molecules for selective autophagy, including bacteria, mitochondria, and aggregated proteins. As such, ubiquitinating proteins, such as the E1 Atg7, E2 Atg3, and E3 Atg12-Atg5-Atg16 are key regulators of autophagy [226]. Recent work has uncovered the first deubiquitinating enzyme of regulatory importance towards selective autophagy, Usp36 [268]. This protein inhibits selective autophagy in both *Drosophila* and in human cells, while promoting cell growth [269]. Despite phenotypic similarity, Usp36 is not actually part of the TOR pathway [268]. Loss of *Drosophila* Usp36 (*dUsp36*) accompanied the accumulation of aggregated histone H2B (known substrate of Usp36) in cell nuclei, reflecting profound defects of chromatin structure in *dUsp36* mutant cells. Knockdown of dUsp36 led to the accumulation of GFP-LC3 positive vesicles. Anti-LC3B antibody testing revealed an increase in both autophagosome and lysosome formation, inferring total autophagy flux activation in mutant cells and suggesting that USP36 inhibits upstream events of autophagosome initiation [268]. A link was established between p62/SQSTM1-mediated accumulation of ubiquitinated substrates following USP36 inactivation and subsequent induction of autophagy, providing a final piece of evidence that USP36 regulates selective autophagy by inactivating its cognate cargo via deubiquitination [268]. So far, USP36 is the only characterised deubiquitinating enzyme which has been linked to autophagy regulation. Recent studies have identified another two deubiquitinating enzymes, USP19 and USP24, both of which exert negative control on autophagy under normal nutritional conditions [270].

7. Conclusion and Future Direction

Studies on morphological aspects and the hormonal regulation of autophagy in insects including *Drosophila* have a long and successful history. More recently, molecular genetics has enabled the functional analysis of autophagy in this complete animal, in which all major tissue types and organs are found and function in many ways similar to our own body. Autophagy studies in *Drosophila* melanogaster have revealed that it has wide-ranging implications in sustaining homeostasis, with possible links to organism development, the immune response, and the removal of cellular damage and waste often associated with ageing and age-related diseases. From the presented literature, it is apparent that there are many unexplored avenues in the mechanisms and regulation of autophagic degradation in *Drosophila*. To better understand its molecular mechanisms, more efforts should be taken to identify selective autophagy receptors which are thought to govern the remarkable degradation specificity seen in certain settings. These studies will be facilitated by recently developed computer software to predict Atg8-family interacting proteins [271]. Manipulating selective autophagy influences the phenotype in a range of neurodegenerative disease models, such as Alzheimer's [272], Huntington's [273], and Parkinson's [274] diseases, which often revolves around the removal of molecules damaged by reactive oxygen species (ROS), or eliminating ROS synthesis sites such as impaired mitochondria. It would therefore be interesting to test whether upregulating autophagy can facilitate effective removal of proteins associated with neurodegenerative pathologies caused by the expression of hyperphosphorylated tau or high polyglutamine length huntingtin. It might be worth investigating the importance of mitophagy in maintaining a healthy cellular environment and resisting stress, particularly with regard to age-related myocardial degeneration, as this is a vastly underexamined area. Finally, the recent discovery of deubiquitinating enzymes as negative regulators of autophagy lays the ground for further study of a novel class of autophagy regulators.

Conflict of Interests

The authors declare that there is no conflict of interests regarding the publication of this paper.

Authors' Contribution

Nitha C. Mulakkal, Peter Nagy, Szabolcs Takats and Radu Tusco are shared first authors. Gábor Juhász and Ioannis P. Nezis are shared senior authors.

References

[1] S. Kaushik and A. M. Cuervo, "Chaperone-mediated autophagy: a unique way to enter the lysosome world," *Trends in Cell Biology*, vol. 22, no. 8, pp. 407–417, 2012.

[2] M. Locke and J. V. Collins, "The structure and formation of protein granules in the fat body of an insect," *The Journal of Cell Biology*, vol. 26, no. 3, pp. 857–884, 1965.

[3] D. Mijaljica, M. Prescott, and R. J. Devenish, "Microautophagy in mammalian cells: revisiting a 40-year-old conundrum," *Autophagy*, vol. 7, no. 7, pp. 673–682, 2011.

[4] N. Mizushima and M. Komatsu, "Autophagy: renovation of cells and tissues," *Cell*, vol. 147, no. 4, pp. 728–741, 2011.

[5] Z. Yang and D. J. Klionsky, "Eaten alive: a history of macroautophagy," *Nature Cell Biology*, vol. 12, no. 9, pp. 814–822, 2010.

[6] A. B. Novikoff, "The proximal tubule cell in experimental hydronephrosis," *The Journal of Biophysical and Biochemical Cytology*, vol. 6, no. 1, pp. 136–138, 1959.

[7] A. B. Novikoff and E. Essner, "Cytolysomes and mitochondrial degeneration," *The Journal of Cell Biology*, vol. 15, pp. 140–146, 1962.

[8] T. P. Ashford and K. R. Porter, "Cytoplasmic components in hepatic cell lysosomes," *The Journal of Cell Biology*, vol. 12, pp. 198–202, 1962.

[9] R. L. Deter, P. Baudhuin, and C. De Duve, "Participation of lysosomes in cellular autophagy induced in rat liver by glucagon," *The Journal of Cell Biology*, vol. 35, no. 2, pp. C11–C16, 1967.

[10] U. Pfeifer, "Inhibition by insulin of the formation of autophagic vacuoles in rat liver. A morphometric approach to the kinetics of intracellular degradation by autophagy," *The Journal of Cell Biology*, vol. 78, no. 1, pp. 152–167, 1978.

[11] U. Pfeifer, "Inhibition by insulin of the physiological autophagic breakdown of cell organelles," *Acta Biologica et Medica Germanica*, vol. 36, no. 11-12, pp. 1691–1694, 1977.

[12] A. B. Novikoff, E. Essner, and N. Quintana, "Golgi apparatus and lysosomes," *Federation Proceedings*, vol. 23, pp. 1010–1022, 1964.

[13] A. V. S. de Reuck and M. P. Cameron, *Ciba Foundation Symposium on Lysosomes*, J.A. Churchill, London, UK, 1963.

[14] C. De Duve and R. Wattiaux, "Functions of lysosomes," *Annual Review of Physiology*, vol. 28, pp. 435–492, 1966.

[15] A. Berlese, "Osservazioni su fenomeni che avvengono durante la ninfosi insetti metabolici," *Rivista dì Patologia Vegetale*, vol. 8, no. 1, 1899.

[16] G. H. Bishop, "Cell metabolism in the insect fat-body-I. Cytological changes accompanying growth and histolysis of the fat-body of Apis mellifica," *Journal of Morphology*, vol. 36, pp. 567–601, 1922.

[17] G. H. Bishop, "Cell metabolism in the insect fat-body-II. A functional interpretation of the changes in structure in the fat-body cells of the honey bee," *Journal of Morphology*, vol. 37, pp. 533–553, 1923.

[18] B. von Gaudecker, "Uber den Formwechsel einiger Zellorganelle bei der Bildung der Reservestoffe in Fettkorper von Drosophila-larven," *Zeitschrift für Zellforschung und Mikroskopische Anatomie*, vol. 61, no. 1, pp. 56–95, 1963.

[19] M. Locke and J. V. Collins, "Protein uptake into multivesicular bodies and storage granules in the fat body of an insect," *The Journal of Cell Biology*, vol. 36, no. 3, pp. 453–483, 1968.

[20] F. M. Butterworth and E. C. Forrest, "Ultrastructure of the preparative phase of cell death in the larval fat body of Drosophila melanogaster," *Tissue and Cell*, vol. 16, no. 2, pp. 237–250, 1984.

[21] W. A. Thomasson and H. K. Mitchell, "Hormonal control of protein granule accumulation in fat bodies of Drosophila melanogaster larvae," *Journal of Insect Physiology*, vol. 18, no. 10, pp. 1885–1899, 1972.

[22] L. M. Riddiford, "Hormone receptors and the regulation of insect metamorphosis," *Receptor*, vol. 3, no. 3, pp. 203–209, 1993.

[23] J. V. Collins, "The hormonal control of fat body development in Calpodes ethlius (Lepidoptera, Hesperiidae)," *Journal of Insect Physiology*, vol. 15, no. 2, pp. 341–352, 1969.

[24] M. Sass and J. Kovacs, "Ecdysterone and an analogue of juvenile hormone on the autophagy in the cells of fat body of Mamestra brassicae," *Acta Biologica Academiae Scientiarum Hungaricae*, vol. 26, no. 3-4, pp. 189–196, 1975.

[25] M. Sass and J. Kovacs, "The effect of ecdysone on the fat body cells of the penultimate larvae of Mamestra brassicae," *Cell and Tissue Research*, vol. 180, no. 3, pp. 403–409, 1977.

[26] V. B. Wigglesworth, "Cytological changes in the fat body of Rhodnius during starvation, feeding and oxygen want," *Journal of Cell Science*, vol. 2, no. 2, pp. 243–256, 1967.

[27] F. M. Butterworth, D. Bodenstein, and R. C. King, "Adipose tissue of Drosophila melanogaster. I. An experimental study of larval fat body," *The Journal of Experimental Zoology*, vol. 158, pp. 141–153, 1965.

[28] G. Beadle, E. L. Tatum, and C. W. Clancy, "Food level in relation to rate of development and eye pigmentation in Drosophila melanogaster," *The Biological Bulletin*, vol. 75, pp. 447–462, 1938.

[29] J. R. Shoup, "The development of pigment granules in the eyes of wild type and mutant Drosophila melanogaster," *The Journal of Cell Biology*, vol. 29, no. 2, pp. 223–249, 1966.

[30] R. A. Lockshin and C. M. Williams, "Programmed cell death-I. Cytology of degeneration in the intersegmental muscles of the Pernyi silkmoth," *Journal of Insect Physiology*, vol. 11, no. 2, pp. 123–133, 1965.

[31] R. A. Lockshin and C. M. Williams, "Programmed cell death-V. Cytolytic enzymes in relation to the breakdown of the intersegmental muscles of silkmoths," *Journal of Insect Physiology*, vol. 11, no. 7, pp. 831–844, 1965.

[32] J. Beaulaton and R. A. Lockshin, "Ultrastructural study of the normal degeneration of the intersegmental muscles of Antheraea polyphemus and Manduca sexta (Insecta, Lepidoptera) with particular reference to cellular autophagy," *Journal of Morphology*, vol. 154, no. 1, pp. 39–57, 1977.

[33] P. G. H. Clarke, "Developmental cell death: morphological diversity and multiple mechanisms," *Anatomy and Embryology*, vol. 181, no. 3, pp. 195–213, 1990.

[34] M. Tsukada and Y. Ohsumi, "Isolation and characterization of autophagy-defective mutants of Saccharomyces cerevisiae," *FEBS Letters*, vol. 333, no. 1-2, pp. 169–174, 1993.

[35] M. Thumm, R. Egner, B. Koch et al., "Isolation of autophagocytosis mutants of Saccharomyces cerevisiae," *FEBS Letters*, vol. 349, no. 2, pp. 275–280, 1994.

[36] T. M. Harding, K. A. Morano, S. V. Scott, and D. J. Klionsky, "Isolation and characterization of yeast mutants in the cytoplasm to vacuole protein targeting pathway," *The Journal of Cell Biology*, vol. 131, no. 3, pp. 591–602, 1995.

[37] D. J. Klionsky, J. M. Cregg, W. A. Dunn Jr. et al., "A unified nomenclature for yeast autophagy-related genes," *Developmental Cell*, vol. 5, no. 4, pp. 539–545, 2003.

[38] G. Juhász, G. Csikós, R. Sinka, M. Erdélyi, and M. Sass, "The Drosophila homolog of Aut1 is essential for autophagy and development," *FEBS Letters*, vol. 543, no. 1–3, pp. 154–158, 2003.

[39] K. Suzuki, Y. Kubota, T. Sekito, and Y. Ohsumi, "Hierarchy of Atg proteins in pre-autophagosomal structure organization," *Genes to Cells*, vol. 12, no. 2, pp. 209–218, 2007.

[40] E. Itakura and N. Mizushima, "Characterization of autophagosome formation site by a hierarchical analysis of mammalian Atg proteins," *Autophagy*, vol. 6, no. 6, pp. 764–776, 2010.

[41] Q. Lu, P. Yang, X. Huang et al., "The WD40 repeat PtdIns(3)P-binding protein EPG-6 regulates progression of omegasomes to autophagosomes," *Developmental Cell*, vol. 21, no. 2, pp. 343–357, 2011.

[42] I. Koyama-Honda, E. Itakura, T. K. Fujiwara, and N. Mizushima, "Temporal analysis of recruitment of mammalian ATG proteins to the autophagosome formation site," *Autophagy*, vol. 9, no. 10, pp. 1491–1499, 2013.

[43] K. Suzuki, M. Akioka, C. Kondo-Kakuta, H. Yamamoto, and Y. Ohsumi, "Fine mapping of autophagy-related proteins during autophagosome formation in Saccharomyces cerevisiae," *Journal of Cell Science*, vol. 126, part 11, pp. 2534–2544, 2013.

[44] N. Mizushima, "The role of the Atg1/ULK1 complex in autophagy regulation," *Current Opinion in Cell Biology*, vol. 22, no. 2, pp. 132–139, 2010.

[45] Y.-Y. Chang and T. P. Neufeld, "An Atg1/Atg13 complex with multiple roles in TOR-mediated autophagy regulation," *Molecular Biology of the Cell*, vol. 20, no. 7, pp. 2004–2014, 2009.

[46] P. Nagy, M. Karpati, A. Varga et al., "Atg17/FIP200 localizes to perilysosomal Ref(2)P aggregates and promotes autophagy by activation of Atg1 in Drosophila," *Autophagy*, vol. 10, no. 3, pp. 453–467, 2014.

[47] R. C. Scott, G. Juhász, and T. P. Neufeld, "Direct induction of autophagy by atg1 inhibits cell growth and induces apoptotic cell death," *Current Biology*, vol. 17, no. 1, pp. 1–11, 2007.

[48] J. H. Stack, D. B. DeWald, K. Takegawa, and S. D. Emr, "Vesicle-mediated protein transport: regulatory interactions between the Vps15 protein kinase and the Vps34 PtdIns 3-kinase essential for protein sorting to the vacuole in yeast," *The Journal of Cell Biology*, vol. 129, no. 2, pp. 321–334, 1995.

[49] E. Itakura, C. Kishi, K. Inoue, and N. Mizushima, "Beclin 1 forms two distinct phosphatidylinositol 3-kinase complexes with mammalian Atg14 and UVRAG," *Molecular Biology of the Cell*, vol. 19, no. 12, pp. 5360–5372, 2008.

[50] X. Li, L. He, K. H. Che et al., "Imperfect interface of Beclin1 coiled-coil domain regulates homodimer and heterodimer formation with Atg14L and UVRAG," *Nature Communications*, vol. 3, article 662, 2012.

[51] G. Juhász, J. H. Hill, Y. Yan et al., "The class III PI(3)K Vps34 promotes autophagy and endocytosis but not TOR signaling in Drosophila," *The Journal of Cell Biology*, vol. 181, no. 4, pp. 655–666, 2008.

[52] P. Musiwaro, M. Smith, M. Manifava, S. A. Walker, and N. T. Ktistakis, "Characteristics and requirements of basal autophagy in HEK 293 cells," *Autophagy*, vol. 9, no. 9, pp. 1407–1417, 2013.

[53] K. Devereaux, C. Dall'armi, A. Alcazar-Roman et al., "Regulation of mammalian autophagy by class II and III PI 3-kinases through PI3P synthesis," *PloS ONE*, vol. 8, no. 10, Article ID e76405, 2013.

[54] K. Lindmo, A. Brech, K. D. Finley et al., "The PI 3-kinase regulator Vps15 is required for autophagic clearance of protein aggregates," *Autophagy*, vol. 4, no. 4, pp. 500–506, 2008.

[55] B. V. Shravage, J. H. Hill, C. M. Powers, L. Wu, and E. H. Baehrecke, "Atg6 is required for multiple vesicle trafficking pathways and hematopoiesis in Drosophila," *Development*, vol. 140, no. 6, pp. 1321–1329, 2013.

[56] A. Banreti, T. Lukacsovich, G. Csikos, M. Erdelyi, and M. Sass, "PP2A regulates autophagy in two alternative ways in Drosophila," *Autophagy*, vol. 8, no. 4, pp. 623–636, 2012.

[57] K. Pircs, P. Nagy, A. Varga et al., "Advantages and limitations of different p62-based assays for estimating autophagic activity in Drosophila," *PloS ONE*, vol. 7, no. 8, Article ID e44214, 2012.

[58] S. Takats, K. Pircs, P. Nagy et al., "Interaction of the HOPS complex with Syntaxin 17 mediates autophagosome clearance in Drosophila," *Molecular Biology of the Cell*, vol. 25, no. 8, pp. 1338–1354, 2014.

[59] P. Lorincz, Z. Lakatos, T. Maruzs, Z. Szatmari, V. Kis, and M. Sass, "Atg6/UVRAG/Vps34-containing lipid kinase complex is required for receptor downregulation through endolysosomal degradation and epithelial polarity during Drosophila wing development," *BioMed Research International*. In press.

[60] T. Proikas-Cezanne, S. Ruckerbauer, Y.-D. Stierhof, C. Berg, and A. Nordheim, "Human WIPI-1 puncta-formation: a novel assay to assess mammalian autophagy," *FEBS Letters*, vol. 581, no. 18, pp. 3396–3404, 2007.

[61] H. E. J. Polson, J. De Lartigue, D. J. Rigden et al., "Mammalian Atg18 (WIPI2) localizes to omegasome-anchored phagophores and positively regulates LC3 lipidation," *Autophagy*, vol. 6, no. 4, pp. 506–522, 2010.

[62] R. C. Scott, O. Schuldiner, and T. P. Neufeld, "Role and regulation of starvation-induced autophagy in the Drosophila fat body," *Developmental Cell*, vol. 7, no. 2, pp. 167–178, 2004.

[63] E. L. Axe, S. A. Walker, M. Manifava et al., "Autophagosome formation from membrane compartments enriched in phosphatidylinositol 3-phosphate and dynamically connected to the endoplasmic reticulum," *The Journal of Cell Biology*, vol. 182, no. 4, pp. 685–701, 2008.

[64] Y. Tian, Z. Li, W. Hu et al., "C. elegans screen identifies autophagy genes specific to multicellular organisms," *Cell*, vol. 141, no. 6, pp. 1042–1055, 2010.

[65] M. I. Molejon, A. Ropolo, A. L. Re, V. Boggio, and M. I. Vaccaro, "The VMP1-Beclin 1 interaction regulates autophagy induction," *Scientific Reports*, vol. 3, article 1055, 2013.

[66] F. Bard, L. Casano, A. Mallabiabarrena et al., "Functional genomics reveals genes involved in protein secretion and Golgi organization," *Nature*, vol. 439, no. 7076, pp. 604–607, 2006.

[67] H. Yamamoto, S. Kakuta, T. M. Watanabe et al., "Atg9 vesicles are an important membrane source during early steps of autophagosome formation," *The Journal of Cell Biology*, vol. 198, no. 2, pp. 219–233, 2012.

[68] A. Orsi, M. Razi, H. Dooley et al., "Dynamic and transient interactions of Atg9 with autophagosomes, but not membrane integration, is required for autophagy," *Molecular Biology of the Cell*, vol. 23, no. 10, pp. 1860–1873, 2012.

[69] C. Puri, M. Renna, C. F. Bento, K. Moreau, and D. C. Rubinsztein, "Diverse autophagosome membrane sources coalesce in recycling endosomes," *Cell*, vol. 154, no. 6, pp. 1285–1299, 2013.

[70] S. A. Tooze, "Current views on the source of the autophagosome membrane," *Essays in Biochemistry*, vol. 55, pp. 29–38, 2013.

[71] G. Juhasz and T. P. Neufeld, "Autophagy: a forty-year search for a missing membrane source," *PLoS Biology*, vol. 4, no. 2, p. e36, 2006.

[72] A. L. Kovács, Z. Pálfia, G. Réz, T. Vellai, and J. Kovács, "Sequestration revisited: integrating traditional electron microscopy, de novo assembly and new results," *Autophagy*, vol. 3, no. 6, pp. 655–662, 2007.

[73] P. Nagy, A. Varga, K. Pircs, K. Hegedus, and G. Juhasz, "Myc-driven overgrowth requires unfolded protein response-mediated induction of autophagy and antioxidant responses in Drosophila melanogaster," *PLoS Genetics*, vol. 9, no. 8, Article ID e1003664, 2013.

[74] P. Low, A. Varga, K. Pircs et al., "Impaired proteasomal degradation enhances autophagy via hypoxia signaling in Drosophila," *BMC Cell Biology*, vol. 14, no. 1, article 29, 2013.

[75] P. Nagy, K. Hegedus, K. Pircs, A. Varga, and G. Juhasz, "Different effects of Atg2 and Atg18 mutations on Atg8a and Atg9 trafficking during starvation in Drosophila," *FEBS Letters*, vol. 588, no. 3, pp. 408–413, 2014.

[76] F. Reggiori, K. A. Tucker, P. E. Stromhaug, and D. J. Klionsky, "The Atg1-Atg13 complex regulates Atg9 and Atg23 retrieval transport from the pre-autophagosomal structure," *Developmental Cell*, vol. 6, no. 1, pp. 79–90, 2004.

[77] Y. Ichimura, T. Kirisako, T. Takao et al., "A ubiquitin-like system mediates protein lipidation," *Nature*, vol. 408, no. 6811, pp. 488–492, 2000.

[78] M. Matsushita, N. N. Suzuki, K. Obara, Y. Fujioka, Y. Ohsumi, and F. Inagaki, "Structure of Atg5·Atg16, a complex essential for autophagy," *Journal of Biological Chemistry*, vol. 282, no. 9, pp. 6763–6772, 2007.

[79] D. J. Klionsky, F. C. Abdalla, H. Abeliovich et al., "Guidelines for the use and interpretation of assays for monitoring autophagy," *Autophagy*, vol. 8, no. 4, pp. 445–544, 2012.

[80] S. Takats, P. Nagy, A. Varga et al., "Autophagosomal Syntaxin17-dependent lysosomal degradation maintains neuronal function in Drosophila," *The Journal of Cell Biology*, vol. 201, no. 4, pp. 531–539, 2013.

[81] E. Itakura, C. Kishi-Itakura, and N. Mizushima, "The hairpin-type tail-anchored SNARE syntaxin 17 targets to autophagosomes for fusion with endosomes/lysosomes," *Cell*, vol. 151, no. 6, pp. 1256–1269, 2012.

[82] K. Hegedus, S. Takats, A. L. Kovacs, and G. Juhasz, "Evolutionarily conserved role and physiological relevance of a STX17/Syx17 (syntaxin 17)-containing SNARE complex in autophagosome fusion with endosomes and lysosomes," *Autophagy*, vol. 9, no. 10, pp. 1642–1646, 2013.

[83] T. Kobayashi, K. Suzuki, and Y. Ohsumi, "Autophagosome formation can be achieved in the absence of Atg18 by expressing engineered PAS-targeted Atg2," *FEBS Letters*, vol. 586, no. 16, pp. 2473–2478, 2012.

[84] A. K. G. Velikkakath, T. Nishimura, E. Oita, N. Ishihara, and N. Mizushima, "Mammalian Atg2 proteins are essential for autophagosome formation and important for regulation of size and distribution of lipid droplets," *Molecular Biology of the Cell*, vol. 23, no. 5, pp. 896–909, 2012.

[85] D. Denton, B. Shravage, R. Simin et al., "Autophagy, not apoptosis, is essential for midgut cell death in Drosophila," *Current Biology*, vol. 19, no. 20, pp. 1741–1746, 2009.

[86] C.-W. Wang, P. E. Stromhaug, J. Shima, and D. J. Klionsky, "The Ccz1-Mon1 protein complex is required for the late step of multiple vacuole delivery pathways," *Journal of Biological Chemistry*, vol. 277, no. 49, pp. 47917–47927, 2002.

[87] T. E. Rusten, T. Vaccari, K. Lindmo et al., "ESCRTs and Fab1 regulate distinct steps of autophagy," *Current Biology*, vol. 17, no. 20, pp. 1817–1825, 2007.

[88] P. Jiang, T. Nishimura, Y. Sakamaki et al., "The HOPS complex mediates autophagosome-lysosome fusion through interaction with syntaxin 17," *Molecular Biology of the Cell*, vol. 25, no. 8, pp. 1327–1337, 2014.

[89] T. Noda and Y. Ohsumi, "Tor, a phosphatidylinositol kinase homologue, controls autophagy in yeast," *Journal of Biological Chemistry*, vol. 273, no. 7, pp. 3963–3966, 1998.

[90] T. P. Neufeld, "TOR-dependent control of autophagy: biting the hand that feeds," *Current Opinion in Cell Biology*, vol. 22, no. 2, pp. 157–168, 2010.

[91] N. Hosokawa, T. Hara, T. Kaizuka et al., "Nutrient-dependent mTORCl association with the ULK1-Atg13-FIP200 complex required for autophagy," *Molecular Biology of the Cell*, vol. 20, no. 7, pp. 1981–1991, 2009.

[92] C. H. Jung, C. B. Jun, S.-H. Ro et al., "ULK-Atg13-FIP200 complexes mediate mTOR signaling to the autophagy machinery," *Molecular Biology of the Cell*, vol. 20, no. 7, pp. 1992–2003, 2009.

[93] G. Juhasz, "Interpretation of bafilomycin, pH neutralizing or protease inhibitor treatments in autophagic flux experiments: novel considerations," *Autophagy*, vol. 8, no. 12, pp. 1875–1876, 2012.

[94] M. Li, B. Khambu, H. Zhang et al., "Suppression of lysosome function induces autophagy via a feedback down-regulation of MTOR complex 1 (MTORC1) activity," *The Journal of Biological Chemistry*, vol. 288, no. 50, pp. 35769–35780, 2013.

[95] C. H. Jung, M. Seo, N. M. Otto, and D.-H. Kim, "ULK1 inhibits the kinase activity of mTORC1 and cell proliferation," *Autophagy*, vol. 7, no. 10, pp. 1212–1221, 2011.

[96] T. E. Rusten, K. Lindmo, G. Juhász et al., "Programmed autophagy in the Drosophila fat body is induced by ecdysone through regulation of the PI3K Pathway," *Developmental Cell*, vol. 7, no. 2, pp. 179–192, 2004.

[97] L. Y. Cheng, A. P. Bailey, S. J. Leevers, T. J. Ragan, P. C. Driscoll, and A. P. Gould, "Anaplastic lymphoma kinase spares organ growth during nutrient restriction in drosophila," *Cell*, vol. 146, no. 3, pp. 435–447, 2011.

[98] F. O'Farrell, S. Wang, N. Katheder, T. E. Rusten, and C. Samakovlis, "Two-tiered control of epithelial growth and autophagy by the insulin receptor and the ret-like receptor, stitcher," *PLoS Biology*, vol. 11, no. 7, Article ID e1001612, 2013.

[99] M. Slaidina, R. Delanoue, S. Gronke, L. Partridge, and P. Léopold, "A Drosophila insulin-like peptide promotes growth during nonfeeding states," *Developmental Cell*, vol. 17, no. 6, pp. 874–884, 2009.

[100] B. Tysell and F. M. Butterworth, "Different rate of protein granule formation in the larval fat body of Drosophila melanogaster," *Journal of Insect Physiology*, vol. 24, no. 3, pp. 201–206, 1978.

[101] T. M. Rizki and R. M. Rizki, "Developmental biology and genetics of adipose tissue of the Drosophila larva," *Egyptian Journal of Genetics and Cytology*, vol. 1, pp. 173–184, 1972.

[102] M. Jindra, S. R. Palli, and L. M. Riddiford, "The juvenile hormone signaling pathway in insect development," *Annual Review of Entomology*, vol. 58, pp. 181–204, 2013.

[103] G. Juhász, L. G. Puskás, O. Komonyi et al., "Gene expression profiling identifies FKBP39 as an inhibitor of autophagy in larval Drosophila fat body," *Cell Death and Differentiation*, vol. 14, no. 6, pp. 1181–1190, 2007.

[104] B. Erdi, P. Nagy, A. Zvara et al., "Loss of the starvation-induced gene Rack1 leads to glycogen deficiency and impaired autophagic responses in Drosophila," *Autophagy*, vol. 8, no. 7, pp. 1124–1135, 2012.

[105] T. Sigmond, J. Fehér, A. Baksa et al., "Qualitative and quantitative characterization of autophagy in Caenorhabditis elegans by electron microscopy," *Methods in Enzymology*, vol. 451, pp. 467–491, 2008.

[106] L. Cherbas, X. Hu, I. Zhimulev, E. Belyaeva, and P. Cherbas, "EcR isoforms in Drosophila: testing tissue-specific requirements by targeted blockade and rescue," *Development*, vol. 130, no. 2, pp. 271–284, 2003.

[107] J. R. Aguila, J. Suszko, A. G. Gibbs, and D. K. Hoshizaki, "The role of larval fat cells in adult Drosophila melanogaster," *Journal of Experimental Biology*, vol. 210, no. 6, pp. 956–963, 2007.

[108] F. M. Butterworth, L. Emerson, and E. M. Rasch, "Maturation and degeneration of the fat body in the Drosophila larva and pupa as revealed by morphometric analysis," *Tissue and Cell*, vol. 20, no. 2, pp. 255–268, 1988.

[109] F. Akdemir, R. Farkaš, P. Chen et al., "Autophagy occurs upstream or parallel to the apoptosome during histolytic cell death," *Development*, vol. 133, no. 8, pp. 1457–1465, 2006.

[110] V. P. Yin and C. S. Thummel, "A balance between the diap1 death inhibitor and reaper and hid death inducers controls steroid-triggered cell death in Drosophila," *Proceedings of the National Academy of Sciences of the United States of America*, vol. 101, no. 21, pp. 8022–8027, 2004.

[111] D. L. Berry and E. H. Baehrecke, "Growth arrest and autophagy are required for salivary gland cell degradation in Drosophila," *Cell*, vol. 131, no. 6, pp. 1137–1148, 2007.

[112] C. Jiang, E. H. Baehrecke, and C. S. Thummel, "Steroid regulated programmed cell death during Drosophila metamorphosis," *Development*, vol. 124, no. 22, pp. 4673–4683, 1997.

[113] G. Juhász, B. Érdi, M. Sass, and T. P. Neufeld, "Atg7-dependent autophagy promotes neuronal health, stress tolerance, and longevity but is dispensable for metamorphosis in Drosophila," *Genes and Development*, vol. 21, no. 23, pp. 3061–3066, 2007.

[114] C.-Y. Lee and E. H. Baehrecke, "Steroid regulation of autophagic programmed cell death during development," *Development*, vol. 128, no. 8, pp. 1443–1445, 2001.

[115] T. K. Chang, B. V. Shravage, S. D. Hayes et al., "Uba1 functions in Atg7- and Atg3-independent autophagy," *Nature Cell Biology*, vol. 15, no. 9, pp. 1067–1078, 2013.

[116] G. Juhász and M. Sass, "Hid can induce, but is not required for autophagy in polyploid larval Drosophila tissues," *European Journal of Cell Biology*, vol. 84, no. 4, pp. 491–502, 2005.

[117] J. Broadus, J. R. McCabe, B. Endrizzi, C. S. Thummel, and C. T. Woodard, "The Drosophila βFTZ-F1 orphan nuclear receptor provides competence for stage-specific responses to the steroid hormone ecdysone," *Molecular Cell*, vol. 3, no. 2, pp. 143–149, 1999.

[118] C.-Y. Lee, B. A. K. Cooksey, and E. H. Baehrecke, "Steroid regulation of midgut cell death during Drosophila development," *Developmental Biology*, vol. 250, no. 1, pp. 101–111, 2002.

[119] X. Qu, Z. Zou, Q. Sun et al., "Autophagy gene-dependent clearance of apoptotic cells during embryonic development," *Cell*, vol. 128, no. 5, pp. 931–946, 2007.

[120] M. Kim, H. L. Park, H. W. Park et al., "Drosophila Fip200 is an essential regulator of autophagy that attenuates both growth and aging," *Autophagy*, vol. 9, no. 8, 2013.

[121] G. Lee, C. Liang, G. Park, C. Jang, J. U. Jung, and J. Chung, "UVRAG is required for organ rotation by regulating Notch endocytosis in Drosophila," *Developmental Biology*, vol. 356, no. 2, pp. 588–597, 2011.

[122] A. Simonsen, R. C. Cumming, A. Brech, P. Isakson, D. R. Schubert, and K. D. Finley, "Promoting basal levels of autophagy in the nervous system enhances longevity and oxidant resistance in adult Drosophila," *Autophagy*, vol. 4, no. 2, pp. 176–184, 2008.

[123] I. P. Nezis, B. V. Shravage, A. P. Sagona et al., "Autophagic degradation of dBruce controls DNA fragmentation in nurse cells during late Drosophila melanogaster oogenesis," *The Journal of Cell Biology*, vol. 190, no. 4, pp. 523–531, 2010.

[124] J. S. Peterson and K. McCall, "Combined inhibition of autophagy and caspases fails to prevent developmental nurse cell death in the Drosophila melanogaster ovary," *PloS ONE*, vol. 8, no. 9, Article ID e76046, 2013.

[125] B. P. Bass, E. A. Tanner, D. Mateos San Martín et al., "Cell-autonomous requirement for DNaseII in nonapoptotic cell death," *Cell Death and Differentiation*, vol. 16, no. 10, pp. 1362–1371, 2009.

[126] Y.-C. C. Hou, S. Chittaranjan, S. G. Barbosa, K. McCall, and S. M. Gorski, "Effector caspase Dcp-1 and IAP protein Bruce regulate starvation-induced autophagy during Drosophila melanogaster oogenesis," *The Journal of Cell Biology*, vol. 182, no. 6, pp. 1127–1139, 2008.

[127] J. M. I. Barth, J. Szabad, E. Hafen, and K. Köhler, "Autophagy in Drosophila ovaries is induced by starvation and is required for oogenesis," *Cell Death and Differentiation*, vol. 18, no. 6, pp. 915–924, 2011.

[128] L. P. Nezis, T. Lamark, A. D. Velentzas et al., "Cell death during Drosophila melanogaster early oogenesis is mediated through autophagy," *Autophagy*, vol. 5, no. 3, pp. 298–302, 2009.

[129] J. M. Barth, E. Hafen, and K. Kohler, "The lack of autophagy triggers precocious activation of Notch signaling during Drosophila oogenesis," *BMC Developmental Biology*, vol. 12, article 35, 2012.

[130] N. Mohseni, S. C. McMillan, R. Chaudhary, J. Mok, and B. H. Reed, "Autophagy promotes caspase-dependent cell death during Drosophila development," *Autophagy*, vol. 5, no. 3, pp. 329–338, 2009.

[131] O. Cormier, N. Mohseni, I. Voytyuk, and B. H. Reed, "Autophagy can promote but is not required for epithelial cell extrusion in the amnioserosa of the Drosophila embryo," *Autophagy*, vol. 8, no. 2, pp. 252–264, 2012.

[132] P. P. Toh, S. Luo, F. M. Menzies, T. Rasko, E. E. Wanker, and D. C. Rubinsztein, "Myc inhibition impairs autophagosome formation," *Human Molecular Genetics*, vol. 22, no. 25, pp. 5237–5248, 2013.

[133] L. S. Hart, J. T. Cunningham, T. Datta et al., "ER stress-mediated autophagy promotes Myc-dependent transformation and tumor growth," *The Journal of Clinical Investigation*, vol. 122, no. 12, pp. 4621–4634, 2012.

[134] E. Bier, "Drosophila, the golden bug, emerges as a tool for human genetics," *Nature Reviews Genetics*, vol. 6, no. 1, pp. 9–23, 2005.

[135] V. Deretic and B. Levine, "Autophagy, immunity, and microbial adaptations," *Cell Host and Microbe*, vol. 5, no. 6, pp. 527–549, 2009.

[136] K. Kirkegaard, M. P. Taylor, and W. T. Jackson, "Cellular autophagy: surrender, avoidance and subversion by microorganisms," *Nature Reviews Microbiology*, vol. 2, no. 4, pp. 301–314, 2004.

[137] R. H. Moy and S. Cherry, "Antimicrobial autophagy: a conserved innate immune response in Drosophila," *Journal of Innate Immunity*, vol. 5, no. 5, pp. 444–455, 2013.

[138] B. Lemaitre and J. Hoffmann, "The host defense of Drosophila melanogaster," *Annual Review of Immunology*, vol. 25, pp. 697–743, 2007.

[139] D. Ferrandon, J.-L. Imler, C. Hetru, and J. A. Hoffmann, "The Drosophila systemic immune response: sensing and signalling during bacterial and fungal infections," *Nature Reviews Immunology*, vol. 7, no. 11, pp. 862–874, 2007.

[140] H. Agaisse and N. Perrimon, "The roles of JAK/STAT signaling in Drosophila immune responses," *Immunological Reviews*, vol. 198, pp. 72–82, 2004.

[141] J. Xu, G. Grant, L. R. Sabin et al., "Transcriptional pausing controls a rapid antiviral innate immune response in Drosophila," *Cell Host & Microbe*, vol. 12, no. 4, pp. 531–543, 2012.

[142] V. Deretic, "Autophagy as an innate immunity paradigm: expanding the scope and repertoire of pattern recognition receptors," *Current Opinion in Immunology*, vol. 24, no. 1, pp. 21–31, 2012.

[143] S. Akira, S. Uematsu, and O. Takeuchi, "Pathogen recognition and innate immunity," *Cell*, vol. 124, no. 4, pp. 783–801, 2006.

[144] M. A. Delgado, R. A. Elmaoued, A. S. Davis, G. Kyei, and V. Deretic, "Toll-like receptors control autophagy," *The EMBO Journal*, vol. 27, no. 7, pp. 1110–1121, 2008.

[145] S. Kurata, "Peptidoglycan recognition proteins in Drosophila immunity," *Developmental and Comparative Immunology*, vol. 42, no. 1, pp. 36–41, 2014.

[146] J. Royet, "Drosophila melanogaster innate immunity: an emerging role for peptidoglycan recognition proteins in bacteria detection," *Cellular and Molecular Life Sciences*, vol. 61, no. 5, pp. 537–546, 2004.

[147] M. G. Gutierrez, S. S. Master, S. B. Singh, G. A. Taylor, M. I. Colombo, and V. Deretic, "Autophagy is a defense mechanism inhibiting BCG and Mycobacterium tuberculosis survival in infected macrophages," *Cell*, vol. 119, no. 6, pp. 753–766, 2004.

[148] Y. M. Ling, M. H. Shaw, C. Ayala et al., "Vacuolar and plasma membrane stripping and autophagic elimination of Toxoplasma gondii in primed effector macrophages," *The Journal of Experimental Medicine*, vol. 203, no. 9, pp. 2063–2071, 2006.

[149] I. Nakagawa, A. Amano, N. Mizushima et al., "Autophagy defends cells against invading group A Streptococcus," *Science*, vol. 306, no. 5698, pp. 1037–1040, 2004.

[150] A. Orvedahl, S. MacPherson, R. Sumpter Jr., Z. Tallóczy, Z. Zou, and B. Levine, "Autophagy protects against Sindbis virus infection of the central nervous system," *Cell Host and Microbe*, vol. 7, no. 2, pp. 115–127, 2010.

[151] S. Shelly, N. Lukinova, S. Bambina, A. Berman, and S. Cherry, "Autophagy is an essential component of Drosophila immunity against vesicular stomatitis virus," *Immunity*, vol. 30, no. 4, pp. 588–598, 2009.

[152] B. Yordy and A. Iwasaki, "Cell type-dependent requirement of autophagy in HSV-1 antiviral defense," *Autophagy*, vol. 9, no. 2, pp. 236–238, 2013.

[153] Y. Yoshikawa, M. Ogawa, T. Hain et al., "Listeria monocytogenes ActA-mediated escape from autophagic recognition," *Nature Cell Biology*, vol. 11, no. 10, pp. 1233–1240, 2009.

[154] Y. T. Zheng, S. Shahnazari, A. Brech, T. Lamark, T. Johansen, and J. H. Brumell, "The adaptor protein p62/SQSTM1 targets invading bacteria to the autophagy pathway," *Journal of Immunology*, vol. 183, no. 9, pp. 5909–5916, 2009.

[155] P. S. Manzanillo, J. S. Ayres, R. O. Watson et al., "The ubiquitin ligase parkin mediates resistance to intracellular pathogens," *Nature*, vol. 501, no. 7468, pp. 512–516, 2013.

[156] B. E. Mansfield, M. S. Dionne, D. S. Schneider, and N. E. Freitag, "Exploration of host-pathogen interactions using Listeria monocytogenes and Drosophila melanogaster," *Cellular Microbiology*, vol. 5, no. 12, pp. 901–911, 2003.

[157] T. Yano, S. Mita, H. Ohmori et al., "Autophagic control of listeria through intracellular innate immune recognition in drosophila," *Nature Immunology*, vol. 9, no. 8, pp. 908–916, 2008.

[158] L. Dortet, S. Mostowy, A. S. Louaka et al., "Recruitment of the major vault protein by inlk: a listeria monocytogenes strategy to avoid autophagy," *PLoS Pathogens*, vol. 7, no. 8, Article ID e1002168, 2011.

[159] S. Kurata, "Extracellular and intracellular pathogen recognition by Drosophila PGRP-LE and PGRP-LC," *International Immunology*, vol. 22, no. 3, Article ID dxp128, pp. 143–148, 2010.

[160] A. Takehana, T. Yano, S. Mita, A. Kotani, Y. Oshima, and S. Kurata, "Peptidoglycan recognition protein (PGRP)-LE and PGRP-LC act synergistically in Drosophila immunity," *EMBO Journal*, vol. 23, no. 23, pp. 4690–4700, 2004.

[161] T. Kaneko, T. Yano, K. Aggarwal et al., "PGRP-LC and PGRP-LE have essential yet distinct functions in the drosophila immune response to monomeric DAP-type peptidoglycan," *Nature Immunology*, vol. 7, no. 7, pp. 715–723, 2006.

[162] A. Goto, T. Yano, J. Terashima, S. Iwashita, Y. Oshima, and S. Kurata, "Cooperative regulation of the induction of the novel antibacterial listericin by peptidoglycan recognition protein LE and the JAK-STAT pathway," *Journal of Biological Chemistry*, vol. 285, no. 21, pp. 15731–15738, 2010.

[163] D. Voronin, D. A. Cook, A. Steven, and M. J. Taylor, "Autophagy regulates Wolbachia populations across diverse symbiotic associations," *Proceedings of the National Academy of Sciences of the United States of America*, vol. 109, no. 25, pp. E1638–E1646, 2012.

[164] X. H. Liang, L. K. Kleeman, H. H. Jiang et al., "Protection against fatal sindbis virus encephalitis by Beclin, a novel Bcl-2-interacting protein," *Journal of Virology*, vol. 72, no. 11, pp. 8586–8596, 1998.

[165] Z. Surviladze, R. T. Sterk, S. A. DeHaro, and M. A. Ozbun, "Cellular entry of human papillomavirus type 16 involves activation of the phosphatidylinositol 3-kinase/Akt/mTOR pathway and inhibition of autophagy," *Journal of Virology*, vol. 87, no. 5, pp. 2508–2517, 2013.

[166] G. R. Campbell and S. A. Spector, "Vitamin D inhibits human immunodeficiency virus type 1 and Mycobacterium tuberculosis infection in macrophages through the induction of autophagy," *PLoS Pathogens*, vol. 8, no. 5, Article ID e1002689, 2012.

[167] M. Nakamoto, R. H. Moy, J. Xu et al., "Virus recognition by Toll-7 activates antiviral autophagy in Drosophila," *Immunity*, vol. 36, no. 4, pp. 658–667, 2012.

[168] F. Leulier and B. Lemaitre, "Toll-like receptors—taking an evolutionary approach," *Nature Reviews Genetics*, vol. 9, no. 3, pp. 165–178, 2008.

[169] Y. Xu, C. Jagannath, X.-D. Liu, A. Sharafkhaneh, K. E. Kolodziejska, and N. T. Eissa, "Toll-like receptor 4 is a sensor for autophagy associated with innate immunity," *Immunity*, vol. 27, no. 1, pp. 135–144, 2007.

[170] C.-S. Shi and J. H. Kehrl, "MyD88 and Trif target Beclin 1 to trigger autophagy in macrophages," *Journal of Biological Chemistry*, vol. 283, no. 48, pp. 33175–33182, 2008.

[171] G. R. Campbell and S. A. Spector, "Toll-like receptor 8 ligands activate a vitamin D mediated autophagic response that inhibits human immunodeficiency virus type 1," *PLoS Pathogens*, vol. 8, no. 11, Article ID e1003017, 2012.

[172] Y. S. Rajawat and I. Bossis, "Autophagy in aging and in neurodegenerative disorders," *Hormones*, vol. 7, no. 1, pp. 46–61, 2008.

[173] C. Lopez-Otin, M. A. Blasco, L. Partridge, M. Serrano, and G. Kroemer, "The hallmarks of aging," *Cell*, vol. 153, no. 6, pp. 1194–1217, 2013.

[174] F. Madeo, N. Tavernarakis, and G. Kroemer, "Can autophagy promote longevity?" *Nature Cell Biology*, vol. 12, no. 9, pp. 842–846, 2010.

[175] D. C. Rubinsztein, G. Mariño, and G. Kroemer, "Autophagy and aging," *Cell*, vol. 146, no. 5, pp. 682–695, 2011.

[176] T. Vellai, K. Takács-Vellai, M. Sass, and D. J. Klionsky, "The regulation of aging: does autophagy underlie longevity?" *Trends in Cell Biology*, vol. 19, no. 10, pp. 487–494, 2009.

[177] L. Partridge, N. Alic, I. Bjedov, and M. D. W. Piper, "Ageing in Drosophila: the role of the insulin/Igf and TOR signalling network," *Experimental Gerontology*, vol. 46, no. 5, pp. 376–381, 2011.

[178] M. M. Lipinski, B. Zheng, T. Lu et al., "Genome-wide analysis reveals mechanisms modulating autophagy in normal brain aging and in Alzheimer's disease," *Proceedings of the National Academy of Sciences of the United States of America*, vol. 107, no. 32, pp. 14164–14169, 2010.

[179] M. Shibata, T. Lu, T. Furuya et al., "Regulation of intracellular accumulation of mutant huntingtin by beclin 1," *Journal of Biological Chemistry*, vol. 281, no. 20, pp. 14474–14485, 2006.

[180] F. Pickford, E. Masliah, M. Britschgi et al., "The autophagy-related protein beclin 1 shows reduced expression in early Alzheimer disease and regulates amyloid β accumulation in mice," *Journal of Clinical Investigation*, vol. 118, no. 6, pp. 2190–2199, 2008.

[181] T. Hara, K. Nakamura, M. Matsui et al., "Suppression of basal autophagy in neural cells causes neurodegenerative disease in mice," *Nature*, vol. 441, no. 7095, pp. 885–889, 2006.

[182] M. Komatsu, S. Waguri, T. Chiba et al., "Loss of autophagy in the central nervous system causes neurodegeneration in mice," *Nature*, vol. 441, no. 7095, pp. 880–884, 2006.

[183] C. Zhang and A. M. Cuervo, "Restoration of chaperone-mediated autophagy in aging liver improves cellular maintenance and hepatic function," *Nature Medicine*, vol. 14, no. 9, pp. 959–965, 2008.

[184] M. Taneike, O. Yamaguchi, A. Nakai et al., "Inhibition of autophagy in the heart induces age-related cardiomyopathy," *Autophagy*, vol. 6, no. 5, pp. 600–606, 2010.

[185] S. F. Chen, M. L. Kang, Y. C. Chen et al., "Autophagy-related gene 7 is downstream of heat shock protein 27 in the regulation of eye morphology, polyglutamine toxicity, and lifespan in Drosophila," *Journal of Biomedical Science*, vol. 19, article 52, 2012.

[186] C. Kenyon, J. Chang, E. Gensch, A. Rudner, and R. Tabtiang, "A C. elegans mutant that lives twice as long as wild type," *Nature*, vol. 366, no. 6454, pp. 461–464, 1993.

[187] K. Lin, J. B. Dorman, A. Rodan, and C. Kenyon, "daf-16: an HNF-3/forkhead family member that can function to double the life-span of Caenorhabditis elegans," *Science*, vol. 278, no. 5341, pp. 1319–1322, 1997.

[188] A. Meléndez, Z. Tallóczy, M. Seaman, E.-L. Eskelinen, D. H. Hall, and B. Levine, "Autophagy genes are essential for dauer development and life-span extension in C. elegans," *Science*, vol. 301, no. 5638, pp. 1387–1391, 2003.

[189] M. Tatar, A. Kopelman, D. Epstein, M.-P. Tu, C.-M. Yin, and R. S. Garofalo, "A mutant Drosophila insulin receptor homolog that extends life-span and impairs neuroendocrine function," *Science*, vol. 292, no. 5514, pp. 107–110, 2001.

[190] D. J. Clancy, D. Gems, L. G. Harshman et al., "Extension of life-span by loss of CHICO, a Drosophila insulin receptor substrate protein," *Science*, vol. 292, no. 5514, pp. 104–106, 2001.

[191] R. Yamamoto and M. Tatar, "Insulin receptor substrate chico acts with the transcription factor FOXO to extend Drosophila lifespan," *Aging Cell*, vol. 10, no. 4, pp. 729–732, 2011.

[192] C. Slack, M. E. Giannakou, A. Foley, M. Goss, and L. Partridge, "dFOXO-independent effects of reduced insulin-like signaling in Drosophila," *Aging Cell*, vol. 10, no. 5, pp. 735–748, 2011.

[193] D. S. Hwangbo, B. Gershman, M.-P. Tu, M. Palmer, and M. Tatar, "Drosophila dFOXO controls lifespan and regulates insulin signalling in brain and fat body," *Nature*, vol. 429, no. 6991, pp. 562–566, 2004.

[194] H. Bai, P. Kang, A. M. Hernandez, and M. Tatar, "Activin signaling targeted by insulin/dFOXO regulates aging and muscle proteostasis in Drosophila," *PLoS Genetics*, vol. 9, no. 11, Article ID e1003941, 2013.

[195] F. Demontis and N. Perrimon, "FOXO/4E-BP signaling in Drosophila muscles regulates organism-wide proteostasis during aging," *Cell*, vol. 143, no. 5, pp. 813–825, 2010.

[196] M. C. Wang, D. Bohmann, and H. Jasper, "JNK signaling confers tolerance to oxidative stress and extends lifespan in Drosophila," *Developmental Cell*, vol. 5, no. 5, pp. 811–816, 2003.

[197] M. C. Wang, D. Bohmann, and H. Jasper, "JNK extends life span and limits growth by antagonizing cellular and organism-wide responses to insulin signaling," *Cell*, vol. 121, no. 1, pp. 115–125, 2005.

[198] H. Wu, M. C. Wang, and D. Bohmann, "JNK protects Drosophila from oxidative stress by trancriptionally activating autophagy," *Mechanisms of Development*, vol. 126, no. 8-9, pp. 624–637, 2009.

[199] T. Eisenberg, H. Knauer, A. Schauer et al., "Induction of autophagy by spermidine promotes longevity," *Nature Cell Biology*, vol. 11, no. 11, pp. 1305–1314, 2009.

[200] V. K. Gupta, L. Scheunemann, T. Eisenberg et al., "Restoring polyamines protects from age-induced memory impairment in an autophagy-dependent manner," *Nature Neuroscience*, vol. 16, no. 10, pp. 1453–1460, 2013.

[201] N. Minois, D. Carmona-Gutierrez, M. A. Bauer et al., "Spermidine promotes stress resistance in Drosophila melanogaster through autophagy-dependent and -independent pathways," *Cell Death & Disease*, vol. 3, p. e401, 2012.

[202] I. Bjedov, J. M. Toivonen, F. Kerr et al., "Mechanisms of life span extension by rapamycin in the fruit fly Drosophila melanogaster," *Cell Metabolism*, vol. 11, no. 1, pp. 35–46, 2010.

[203] P. Kapahi, B. M. Zid, T. Harper, D. Koslover, V. Sapin, and S. Benzer, "Regulation of lifespan in Drosophila by modulation of genes in the TOR signaling pathway," *Current Biology*, vol. 14, no. 10, pp. 885–890, 2004.

[204] M. D. W. Piper and L. Partridge, "Dietary restriction in Drosophila: delayed aging or experimental artefact?" *PLoS Genetics*, vol. 3, no. 4, p. e57, 2007.

[205] K. Jia and B. Levine, "Autophagy is required for dietary restriction-mediated life span extension in C. elegans," *Autophagy*, vol. 3, no. 6, pp. 597–599, 2007.

[206] M. L. Tóth, T. Sigmond, É. Borsos et al., "Longevity pathways converge on autophagy genes to regulate life span in Caenorhabditis elegans," *Autophagy*, vol. 4, no. 3, pp. 330–338, 2008.

[207] M. Jaiswal, H. Sandoval, K. Zhang, V. Bayat, and H. J. Bellen, "Probing mechanisms that underlie human neurodegenerative diseases in Drosophila," *Annual Review of Genetics*, vol. 46, pp. 371–396, 2012.

[208] J. H. Son, J. H. Shim, K.-H. Kim, J.-Y. Ha, and J. Y. Han, "Neuronal autophagy and neurodegenerative diseases," *Experimental and Molecular Medicine*, vol. 44, no. 2, pp. 89–98, 2012.

[209] G. R. Jackson, I. Salecker, X. Dong et al., "Polyglutamine-expanded human huntingtin transgenes induce degeneration of Drosophila photoreceptor neurons," *Neuron*, vol. 21, no. 3, pp. 633–642, 1998.

[210] B. Ravikumar, C. Vacher, Z. Berger et al., "Inhibition of mTOR induces autophagy and reduces toxicity of polyglutamine expansions in fly and mouse models of Huntington disease," *Nature Genetics*, vol. 36, no. 6, pp. 585–595, 2004.

[211] Z. Berger, B. Ravikumar, F. M. Menzies et al., "Rapamycin alleviates toxicity of different aggregate-prone proteins," *Human Molecular Genetics*, vol. 15, no. 3, pp. 433–442, 2006.

[212] S. Sarkar, E. O. Perlstein, S. Imarisio et al., "Small molecules enhance autophagy and reduce toxicity in Huntington's disease models," *Nature Chemical Biology*, vol. 3, no. 6, pp. 331–338, 2007.

[213] R. A. Floto, S. Sarkar, E. O. Perlstein, B. Kampmann, S. L. Schreiber, and D. C. Rubinsztein, "Small molecule enhancers of rapamycin-induced TOR inhibition promote autophagy, reduce toxicity in Huntington's disease models and enhance killing of mycobacteria by macrophages," *Autophagy*, vol. 3, no. 6, pp. 620–622, 2007.

[214] B. Ravikumar, S. Imarisio, S. Sarkar, C. J. O'Kane, and D. C. Rubinsztein, "Rab5 modulates aggregation and toxicity of mutant huntingtin through macroautophagy in cell and fly models of Huntington disease," *Journal of Cell Science*, vol. 121, no. 10, pp. 1649–1660, 2008.

[215] T. Wang, U. Lao, and B. A. Edgar, "TOR-mediated autophagy regulates cell death in Drosophila neurodegenerative disease," *The Journal of Cell Biology*, vol. 186, no. 5, pp. 703–711, 2009.

[216] F. M. Menzies, R. Hourez, S. Imarisio et al., "Puromycin-sensitive aminopeptidase protects against aggregation-prone proteins via autophagy," *Human Molecular Genetics*, vol. 19, no. 23, pp. 4573–4586, 2010.

[217] J. Bilen and N. M. Bonini, "Genome-wide screen for modifiers of ataxin-3 neurodegeneration in Drosophila," *PLoS Genetics*, vol. 3, no. 10, pp. 1950–1964, 2007.

[218] I. Nisoli, J. P. Chauvin, F. Napoletano et al., "Neurodegeneration by polyglutamine Atrophin is not rescued by induction of autophagy," *Cell Death and Differentiation*, vol. 17, no. 10, pp. 1577–1587, 2010.

[219] F. Napoletano, S. Occhi, P. Calamita et al., "Polyglutamine Atrophin provokes neurodegeneration in Drosophila by repressing fat," *EMBO Journal*, vol. 30, no. 5, pp. 945–958, 2011.

[220] P. Calamita and M. Fanto, "Slimming down fat makes neuropathic hippo: the fat/hippo tumor suppressor pathway protects adult neurons through regulation of autophagy," *Autophagy*, vol. 7, no. 8, pp. 907–909, 2011.

[221] R. A. Nixon, J. Wegiel, A. Kumar et al., "Extensive involvement of autophagy in Alzheimer disease: an immuno-electron microscopy study," *Journal of Neuropathology and Experimental Neurology*, vol. 64, no. 2, pp. 113–122, 2005.

[222] D. Ling, H.-J. Song, D. Garza, T. P. Neufeld, and P. M. Salvaterra, "Abeta42-induced neurodegeneration via an age-dependent autophagic-lysosomal injury in Drosophila," *PLoS ONE*, vol. 4, no. 1, Article ID e4201, 2009.

[223] U. B. Pandey, Y. Batlevi, E. H. Baehrecke, and J. P. Taylor, "HDAC6 at the intersection of autophagy, the ubiquitin-proteasome system and neurodegeneration," *Autophagy*, vol. 3, no. 6, pp. 643–645, 2007.

[224] M. Filimonenko, S. Stuffers, C. Raiborg et al., "Functional multivesicular bodies are required for autophagic clearance of protein aggregates associated with neurodegenerative disease," *The Journal of Cell Biology*, vol. 179, no. 3, pp. 485–500, 2007.

[225] T. E. Rusten, M. Filimonenko, L. M. Rodahl, H. Stenmark, and A. Simonsen, "ESCRTing autophagic clearance of aggregating proteins," *Autophagy*, vol. 4, no. 2, pp. 233–236, 2008.

[226] A. B. Birgisdottir, T. Lamark, and T. Johansen, "The LIR motif—crucial for selective autophagy," *Journal of Cell Science*, vol. 126, part 15, pp. 3237–3247, 2013.

[227] P. Wild, H. Farhan, D. G. McEwan et al., "Phosphorylation of the autophagy receptor optineurin restricts Salmonella growth," *Science*, vol. 333, no. 6039, pp. 228–233, 2011.

[228] S. Jiang, C. D. Wells, and P. J. Roach, "Starch-binding domain-containing protein 1 (Stbd1) and glycogen metabolism: identification of the Atg8 family interacting motif (AIM) in Stbd1 required for interaction with GABARAPL1," *Biochemical and Biophysical Research Communications*, vol. 413, no. 3, pp. 420–425, 2011.

[229] T. Johansen and T. Lamark, "Selective autophagy mediated by autophagic adapter proteins," *Autophagy*, vol. 7, no. 3, pp. 279–296, 2011.

[230] J. Moscat and M. T. Diaz-Meco, "p62 at the crossroads of autophagy, apoptosis, and cancer," *Cell*, vol. 137, no. 6, pp. 1001–1004, 2009.

[231] S. Pankiv, T. H. Clausen, T. Lamark et al., "p62/SQSTM1 binds directly to Atg8/LC3 to facilitate degradation of ubiquitinated protein aggregates by autophagy," *Journal of Biological Chemistry*, vol. 282, no. 33, pp. 24131–24145, 2007.

[232] M. Komatsu, H. Kurokawa, S. Waguri et al., "The selective autophagy substrate p62 activates the stress responsive transcription factor Nrf2 through inactivation of Keap1," *Nature Cell Biology*, vol. 12, no. 3, pp. 213–223, 2010.

[233] A. Jain, T. Lamark, E. Sjøttem et al., "p62/SQSTM1 is a target gene for transcription factor NRF2 and creates a positive feedback loop by inducing antioxidant response element-driven gene transcription," *Journal of Biological Chemistry*, vol. 285, no. 29, pp. 22576–22591, 2010.

[234] G. Bjørkøy, T. Lamark, A. Brech et al., "p62/SQSTM1 forms protein aggregates degraded by autophagy and has a protective effect on huntingtin-induced cell death," *The Journal of Cell Biology*, vol. 171, no. 4, pp. 603–614, 2005.

[235] M. Komatsu, S. Waguri, M. Koike et al., "Homeostatic levels of p62 control cytoplasmic inclusion body formation in autophagy-deficient mice," *Cell*, vol. 131, no. 6, pp. 1149–1163, 2007.

[236] I. P. Nezis, A. Simonsen, A. P. Sagona et al., "Ref(2)P, the Drosophila melanogaster homologue of mammalian p62, is required for the formation of protein aggregates in adult brain," *The Journal of Cell Biology*, vol. 180, no. 6, pp. 1065–1071, 2008.

[237] I. P. Nezis, "Selective autophagy in Drosophila," *International Journal of Cell Biology*, vol. 2012, Article ID 146767, 9 pages, 2012.

[238] I. P. Nezis and H. Stenmark, "p62 at the interface of autophagy, oxidative stress signaling, and cancer," *Antioxidants & Redox Signaling*, vol. 17, no. 5, pp. 786–793, 2012.

[239] K. Hegedus, P. Nagy, Z. Gaspari, and G. Juhasz, "The putative HORMA domain protein Atg101 dimerizes and is required for starvation-induced and selective autophagy in Drosophila," *BioMed Research International*, vol. 2014, Article ID 470482, 13 pages, 2014.

[240] D. J. Klionsky, A. J. Meijer, and P. Codogno, "Autophagy and p70S6 kinase," *Autophagy*, vol. 1, no. 1, pp. 59–61, 2005.

[241] P. Kadandale and A. A. Kiger, "Role of selective autophagy in cellular remodeling: "Self-eating" into shape," *Autophagy*, vol. 6, no. 8, pp. 1194–1195, 2010.

[242] P. Kadandale, J. D. Stender, C. K. Glass, and A. A. Kiger, "Conserved role for autophagy in Rhol-mediated cortical remodeling and blood cell recruitment," *Proceedings of the National Academy of Sciences of the United States of America*, vol. 107, no. 23, pp. 10502–10507, 2010.

[243] K. D. Finley, P. T. Edeen, R. C. Cumming et al., "Blue cheese mutations define a novel, conserved gene involved in progressive neural degeneration," *Journal of Neuroscience*, vol. 23, no. 4, pp. 1254–1264, 2003.

[244] T. H. Clausen, T. Lamark, P. Isakson et al., "p62/SQSTM1 and ALFY interact to facilitate the formation of p62 bodies/ALIS and their degradation by autophagy," *Autophagy*, vol. 6, no. 3, pp. 330–344, 2010.

[245] A. Simonsen, H. C. G. Birkeland, D. J. Gillooly et al., "Alfy, a novel FYVE-domain-containing protein associated with protein granules and autophagic membranes," *Journal of Cell Science*, vol. 117, no. 18, pp. 4239–4251, 2004.

[246] M. Filimonenko, P. Isakson, K. D. Finley et al., "The selective macroautophagic degradation of aggregated proteins requires the PI3P-binding protein Alfy," *Molecular Cell*, vol. 38, no. 2, pp. 265–279, 2010.

[247] A. Simonsen, R. C. Cumming, and K. D. Finley, "Linking lysosomal trafficking defects with changes in aging and stress response in Drosophila," *Autophagy*, vol. 3, no. 5, pp. 499–501, 2007.

[248] A. Simonsen, R. C. Cumming, K. Lindmo et al., "Genetic modifiers of the drosophila blue cheese gene link defects in lysosomal transport with decreased life span and altered ubiquitinated-protein profiles," *Genetics*, vol. 176, no. 2, pp. 1283–1297, 2007.

[249] V. Arndt, N. Dick, R. Tawo et al., "Chaperone-assisted selective autophagy is essential for muscle maintenance," *Current Biology*, vol. 20, no. 2, pp. 143–148, 2010.

[250] A. C. Massey, C. Zhang, and A. M. Cuervo, "Chaperone-mediated autophagy in aging and disease," *Current Topics in Developmental Biology*, vol. 73, pp. 205–235, 2006.

[251] R. J. Youle and D. P. Narendra, "Mechanisms of mitophagy," *Nature Reviews Molecular Cell Biology*, vol. 12, no. 1, pp. 9–14, 2011.

[252] T. Kanki, K. Wang, Y. Cao, M. Baba, and D. J. Klionsky, "Atg32 is a mitochondrial protein that confers selectivity during mitophagy," *Developmental Cell*, vol. 17, no. 1, pp. 98–109, 2009.

[253] I. Novak, V. Kirkin, D. G. McEwan et al., "Nix is a selective autophagy receptor for mitochondrial clearance," *EMBO Reports*, vol. 11, no. 1, pp. 45–51, 2010.

[254] R. L. Schweers, J. Zhang, M. S. Randall et al., "NIX is required for programmed mitochondrial clearance during reticulocyte maturation," *Proceedings of the National Academy of Sciences of the United States of America*, vol. 104, no. 49, pp. 19500–19505, 2007.

[255] D. Narendra, A. Tanaka, D.-F. Suen, and R. J. Youle, "Parkin is recruited selectively to impaired mitochondria and promotes their autophagy," *The Journal of Cell Biology*, vol. 183, no. 5, pp. 795–803, 2008.

[256] D. P. Narendra, S. M. Jin, A. Tanaka et al., "PINK1 is selectively stabilized on impaired mitochondria to activate Parkin," *PLoS Biology*, vol. 8, no. 1, Article ID e1000298, 2010.

[257] S. A. Sarraf, M. Raman, V. Guarani-Pereira et al., "Landscape of the PARKIN-dependent ubiquitylome in response to mitochondrial depolarization," *Nature*, vol. 496, no. 7445, pp. 372–376, 2013.

[258] I. E. Clark, M. W. Dodson, C. Jiang et al., "Drosophila pink1 is required for mitochondrial function and interacts genetically with parkin," *Nature*, vol. 441, no. 7097, pp. 1162–1166, 2006.

[259] J. C. Greene, A. J. Whitworth, I. Kuo, L. A. Andrews, M. B. Feany, and L. J. Pallanck, "Mitochondrial pathology and apoptotic muscle degeneration in Drosophila parkin mutants," *Proceedings of the National Academy of Sciences of the United States of America*, vol. 100, no. 7, pp. 4078–4083, 2003.

[260] Y. Pesah, T. Pham, H. Burgess et al., "Drosophila parkin mutants have decreased mass and cell size and increased sensitivity to oxygen radical stress," *Development*, vol. 131, no. 9, pp. 2183–2194, 2004.

[261] H. Deng, M. W. Dodson, H. Huang, and M. Guo, "The Parkinson's disease genes pink1 and parkin promote mitochondrial fission and/or inhibit fusion in Drosophila," *Proceedings of the National Academy of Sciences of the United States of America*, vol. 105, no. 38, pp. 14503–14508, 2008.

[262] A. C. Poole, R. E. Thomas, S. Yu, E. S. Vincow, and L. Pallanck, "The mitochondrial fusion-promoting factor mitofusin is a substrate of the PINK1/parkin pathway," *PLoS ONE*, vol. 5, no. 4, Article ID e10054, 2010.

[263] E. Ziviani, R. N. Tao, and A. J. Whitworth, "Drosophila Parkin requires PINK1 for mitochondrial translocation and ubiquitinates Mitofusin," *Proceedings of the National Academy of Sciences of the United States of America*, vol. 107, no. 11, pp. 5018–5023, 2010.

[264] E. S. Vincow, G. Merrihew, R. E. Thomas et al., "The PINK1-Parkin pathway promotes both mitophagy and selective respiratory chain turnover in vivo," *Proceedings of the National Academy of Sciences of the United States of America*, vol. 110, no. 16, pp. 6400–6405, 2013.

[265] D. H. Margineantu, C. B. Emerson, D. Diaz, and D. M. Hockenbery, "Hsp90 inhibition decreases mitochondrial protein turnover," *PLoS ONE*, vol. 2, no. 10, Article ID e1066, 2007.

[266] V. Soubannier, G.-L. McLelland, R. Zunino et al., "A vesicular transport pathway shuttles cargo from mitochondria to lysosomes," *Current Biology*, vol. 22, no. 2, pp. 135–141, 2012.

[267] M. Neuspiel, A. C. Schauss, E. Braschi et al., "Cargo-selected transport from the mitochondria to peroxisomes is mediated

by vesicular carriers," *Current Biology*, vol. 18, no. 2, pp. 102–108, 2008.

[268] E. Taillebourg, I. Gregoire, P. Viargues et al., "The deubiquitinating enzyme USP36 controls selective autophagy activation by ubiquitinated proteins," *Autophagy*, vol. 8, no. 5, pp. 767–779, 2012.

[269] H. Zhang, J. P. Stallock, J. C. Ng, C. Reinhard, and T. P. Neufeld, "Regulation of cellular growth by the Drosophila target of rapamycin dTOR," *Genes and Development*, vol. 14, no. 21, pp. 2712–2724, 2000.

[270] M. M. Lipinski, G. Hoffman, A. Ng et al., "A genome-wide siRNA screen reveals multiple mTORC1 independent signaling pathways regulating autophagy under normal nutritional conditions," *Developmental Cell*, vol. 18, no. 6, pp. 1041–1052, 2010.

[271] I. Kalvari, S. Tsompanis, N. C. Mulakkal et al., "iLIR: a web resource for prediction of Atg8-family interacting proteins," *Autophagy*, vol. 10, no. 5, 2014.

[272] Y. Tian, J. C. Chang, E. Y. Fan, M. Flajolet, and P. Greengard, "Adaptor complex AP2/PICALM, through interaction with LC3, targets Alzheimer's APP-CTF for terminal degradation via autophagy," *Proceedings of the National Academy of Sciences of the United States of America*, vol. 110, no. 42, pp. 17071–17076, 2013.

[273] S. E. Samaraweera, L. V. O'Keefe, G. R. Price, D. J. Venter, and R. I. Richards, "Distinct roles for Toll and autophagy pathways in double-stranded RNA toxicity in a Drosophila model of expanded repeat neurodegenerative diseases," *Human Molecular Genetics*, vol. 22, no. 14, pp. 2811–2819, 2013.

[274] S. Batelli, E. Peverelli, S. Rodilossi, G. Forloni, and D. Albani, "Macroautophagy and the proteasome are differently involved in the degradation of alpha-synuclein wild type and mutated A30P in an in vitro inducible model (PC12/TetOn)," *Neuroscience*, vol. 195, pp. 128–137, 2011.

MBoC | ARTICLE

Interaction of the HOPS complex with Syntaxin 17 mediates autophagosome clearance in *Drosophila*

Szabolcs Takáts[a,*], Karolina Pircs[a,*], Péter Nagy[a], Ágnes Varga[a], Manuéla Kárpáti[a], Krisztina Hegedűs[a], Helmut Kramer[b], Attila L. Kovács[a], Miklós Sass[a], and Gábor Juhász[a]

[a]Department of Anatomy, Cell and Developmental Biology, Eötvös Loránd University, Pazmany s. 1/C, H-1117 Budapest, Hungary; [b]Department of Neuroscience, Department of Cell Biology, University of Texas Southwestern Medical School, Dallas, TX 75390-9111

ABSTRACT **Homotypic fusion and vacuole protein sorting (HOPS) is a tethering complex required for trafficking to the vacuole/lysosome in yeast. Specific interaction of HOPS with certain SNARE (soluble NSF attachment protein receptor) proteins ensures the fusion of appropriate vesicles. HOPS function is less well characterized in metazoans. We show that all six HOPS subunits (Vps11 [vacuolar protein sorting 11]/CG32350, Vps18/Dor, Vps16A, Vps33A/Car, Vps39/CG7146, and Vps41/Lt) are required for fusion of autophagosomes with lysosomes in *Drosophila*. Loss of these genes results in large-scale accumulation of autophagosomes and blocks autophagic degradation under basal, starvation-induced, and developmental conditions. We find that HOPS colocalizes and interacts with Syntaxin 17 (Syx17), the recently identified autophagosomal SNARE required for fusion in *Drosophila* and mammals, suggesting their association is critical during tethering and fusion of autophagosomes with lysosomes. HOPS, but not Syx17, is also required for endocytic down-regulation of Notch and Boss in developing eyes and for proper trafficking to lysosomes and eye pigment granules. We also show that the formation of autophagosomes and their fusion with lysosomes is largely unaffected in null mutants of Vps38/UVRAG (UV radiation resistance associated), a suggested binding partner of HOPS in mammals, while endocytic breakdown and lysosome biogenesis is perturbed. Our results establish the role of HOPS and its likely mechanism of action during autophagy in metazoans.**

Monitoring Editor
Tamotsu Yoshimori
Osaka University

Received: Aug 8, 2013
Revised: Feb 5, 2014
Accepted: Feb 10, 2014

INTRODUCTION

Eukaryotic cells have developed distinct membrane-bound compartments with specific functions. Trafficking from one compartment to the other is usually achieved by the fusion of transport vesicles with their target. This process is mediated by complex molecular machineries that ensure proper movement, tethering, and specific fusion of various vesicles. A combination of signals establishes vesicle identity, including the lipid content of the limiting membrane (such as the presence of various phospholipids) and members of the Rab family of small GTPases (Stenmark, 2009). Tethering factors are involved in vesicle docking, and fusion of the vesicle with the appropriate target membrane is usually mediated by SNARE (soluble NSF attachment protein receptor) protein complexes, formed by four (Qa, Qb, Qc, and R) SNARE domains (Hong, 2005).

Much of our understanding of these processes comes from yeast studies. Genetic screens carried out in the 1980s identified the first set of genes required for transport from the Golgi to the vacuole, the yeast equivalent of the lysosomal system (Bankaitis *et al.*, 1986; Rothman and Stevens, 1986; Bowers and Stevens, 2005). All these vacuolar protein sorting (*VPS*) mutants secrete

This article was published online ahead of print in MBoC in Press (http://www.molbiolcell.org/cgi/doi/10.1091/mbc.E13-08-0449) on February 19, 2014.

*Co–first author.

Address correspondence to: Gábor Juhász (szmrt@elte.hu).

Abbreviations used: Atg, autophagy-related; CORVET, class C core vacuole/endosome tethering; HOPS, homotypic fusion and vacuole protein sorting; Lamp, lysosome-associated membrane protein; LTR, LysoTracker Red; Q and R SNARE, soluble NSF attachment protein receptor, contributing either a glutamine (Q) or an arginine (R) residue to the central layer of the assembled complex, respectively; UVRAG, UV radiation resistance associated; Vps, vacuolar protein sorting.

© 2014 Takáts *et al*. This article is distributed by The American Society for Cell Biology under license from the author(s). Two months after publication it is available to the public under an Attribution–Noncommercial–Share Alike 3.0 Unported Creative Commons License (http://creativecommons.org/licenses/by-nc-sa/3.0).

"ASCB®," "The American Society for Cell Biology®," and "Molecular Biology of the Cell®" are registered trademarks of The American Society of Cell Biology.

Supplemental Material can be found at:
http://www.molbiolcell.org/content/suppl/2014/02/17/mbc.E13-08-0449v1.DC1.html

dc_840_14

carboxypeptidase Y (CPY), which is a soluble vacuolar hydrolase in wild-type cells. *VPS* genes were classified based on the morphology of vacuoles in mutant cells (Bowers and Stevens, 2005). The class C group is characterized by the lack of a coherent vacuole and includes the genes *VPS11*, *VPS16*, *VPS18*, and *VPS33*. Mutants that belong to the class B group show numerous, small, fragmented vacuoles, and include *VPS39* and *VPS41*, among other genes. Biochemical studies established that these six gene products form a protein complex, which was named HOPS for homotypic fusion and vacuole protein sorting. A separate complex termed CORVET (for class C core vacuole/endosome tethering) was also described, which contains Vps3 and Vps8 instead of Vp39 and Vps41 (Balderhaar and Ungermann, 2013; Solinger and Spang, 2013). These complexes act as tethering factors by cross-linking two membranes, and also facilitate the formation of a SNARE complex during fusion. HOPS is not only required for the delivery of vacuolar proteins and homotypic fusion of vacuoles, but also appears to control the clearance of late endosomes and autophagosomes during heterophagy and autophagy through promoting fusion of these vesicles with the vacuole in yeast (Rieder and Emr, 1997). These pathways mediate the uptake and degradation of endocytosed extracellular material and receptor-ligand complexes, and the delivery of dispensable cytoplasmic material for breakdown, respectively. In contrast, CORVET was suggested to be involved in the maturation of early endosomes to late endosomes (Balderhaar and Ungermann, 2013; Solinger and Spang, 2013).

The function of these complexes is less well characterized in metazoan cells (Balderhaar and Ungermann, 2013; Solinger and Spang, 2013). Although clear homologues of *VPS8* are found, *VPS3* is not conserved. Studies in animals are also complicated by gene redundancy, as two homologues of *VPS16* and *VPS33* are found in worms, flies, and mammals. A complex containing VPS16A and VPS33A has been proposed to function similarly to HOPS in yeast, while a complex containing VPS16B and VPS33B has been speculated to play a role similar to that of CORVET (Balderhaar and Ungermann, 2013). These complexes play important roles in numerous biological processes in mammals, including antigen presentation and elimination of microbes in immune cells, and protection from various diseases causing neurodegeneration and multiorgan pathologies (Balderhaar and Ungermann, 2013; Solinger and Spang, 2013).

Several classical eye color mutant phenotypes in *Drosophila* turned out to be the result of mutations in genes encoding HOPS subunits (Lloyd *et al.*, 1998). These genes were named according to the phenotypes of mutant adult flies: *Vps18* is known as *dor* (*deep orange*), *Vps33A* as *car* (*carnation*), and *Vps41* as *lt* (*light*) in flies. These hypomorphic mutations perturb the biogenesis of eye pigment granules at the end of metamorphosis, whereas stronger mutations in these genes lead to lethality during earlier developmental stages. Loss of *dor* or *car* or hypomorphic mutation of *lt* also leads to defects in endocytosis, and similar phenotypes have been reported based on RNA interference (RNAi) analysis of *Vps16A* (Sevrioukov *et al.*, 1999; Pulipparacharuvil *et al.*, 2005; Akbar *et al.*, 2009; Swetha *et al.*, 2011). In contrast, *Vps16B/fob* (*full of bacteria*) appears to regulate the maturation of phagosomes containing endocytosed bacteria, and it is dispensable for receptor down-regulation (Akbar *et al.*, 2011). These studies suggest that distinct HOPS complexes may be responsible for different functions in animals.

During autophagy, fusion of double-membrane autophagosomes with lysosomes is required to deliver the sequestered cytoplasmic cargo for degradation. Autophagy has been implicated in a wide variety of physiological and pathological conditions (Mizushima *et al.*, 2008). In yeast, the SNARE proteins Vam3, Vti1, and Vam7 are involved in the direct fusion of autophagosomes with the vacuole (Darsow *et al.*, 1997; Wang *et al.*, 2002). Interestingly, metazoan cells seem to rely on a different trafficking route that appears to be critical: the fusion of autophagosomes with late endosomes to form intermediate vesicles called amphisomes, which then fuse with lysosomes (Filimonenko *et al.*, 2007; Rusten *et al.*, 2007; Juhasz *et al.*, 2008). In addition, among the SNAREs required for autophagosome clearance in yeast, only Vti1 has a clear homologue in animal cells, but not Vam3 or Vam7. We and others have recently identified Syntaxin 17 (Syx17 in *Drosophila* and STX17 in mammals) as the autophagosomal SNARE in metazoans, which forms a complex with ubisnap (Qbc, SNAP29 in mammals) and Vamp7 (R, VAMP8 in mammals) located on late endosomes and lysosomes (Itakura *et al.*, 2012; Takats *et al.*, 2013).

Whether and how HOPS is involved in autophagy in metazoans is not entirely clear, given that the SNAREs required for autophagosome-lysosome fusion are different from those in yeast. The possible involvement of HOPS in mammalian autophagy is controversial. Neuron-specific deletion of Vps18 was recently shown to cause neurodegeneration due to impaired biosynthetic, endocytic, and autophagic transport to lysosomes (Peng *et al.*, 2012). In contrast, Vps16 depletion by short hairpin RNA in mouse embryonic fibroblasts was found to delay the degradation of epidermal growth factor receptor (EGFR), a widely used endosomal cargo, but did not affect green fluorescent protein (GFP)-LC3 lipidation or puncta formation (Ganley *et al.*, 2011). In *Drosophila*, it was shown that *Vps16A* RNAi induced in the developing eye results in retinal degeneration, and ultrastructural images of dying photoreceptor cells in these animals revealed various vacuoles, including double-membrane autophagosomes, but the identity of these organelles was not further characterized (Pulipparacharuvil *et al.*, 2005). Another report showed that in viable *dor[1]* hypomorphic mutants, the size of LysoTracker Red (LTR)- and lysosome-associated membrane protein (Lamp1)-positive autolysosomes is decreased and the number of autophagosomes is increased during developmental autophagy of the fat body (Lindmo *et al.*, 2006). Interestingly, insulin signaling was up-regulated in those larvae, and levels of the molting hormone ecdysone, which is responsible for inducing developmental autophagy (Rusten *et al.*, 2004), remained low in wandering animals. These results suggest that systemic hormonal defects may contribute to autophagy phenotypes in these mutant animals (Lindmo *et al.*, 2006). The autophagic cargo p62/Ref2P was also found to be up-regulated in *dor[1]* but not in *car[1]* mutant adult heads (Bartlett *et al.*, 2011). Importantly, mutations used in these studies are hypomorphic alleles: *dor[1]* carries a C979Y amino acid change, while *car[1]* has L26V and G249V changes. Thus these point mutations may interfere with some but not all functions of these genes. This is further indicated by the lethality of *car* and *dor* null mutants during the first and second larval stages (Sevrioukov *et al.*, 1999; Akbar *et al.*, 2009).

In this work, we analyze the role of HOPS in autophagosome-lysosome fusion in *Drosophila*. Our results help in resolving the conflicting and inconsistent reports on the potential involvement of this complex in autophagy in the cells of a metazoan organism.

RESULTS

Novel mutations of *Vps16A* reveal its role in autophagosome clearance

We screened a collection of P element–bearing larval-lethal *Drosophila* strains for mutants with defects in developmental autophagy, and recently published the characterization of two hits

dc_840_14

from our screen (Lippai *et al.*, 2008; Csikos *et al.*, 2009). In these papers, we showed that loss of AMPK (AMP-activated kinase) or epsin interferes with the formation of autophagosomes. Homozygous mutants of another candidate line, *l(3)S007902* (later named *Vps16A[FUD]*, see below), showed a complete block of punctate LTR staining in fat body cells of wandering L3-stage animals (Figure 1, A, B, and K). It is important to emphasize that the LTR dots appear only in response to starvation or in wandering larvae, and no such LTR-positive structures are detected in fat bodies of well-fed *Drosophila* larvae; therefore LTR staining is commonly used as a marker for autolysosomes in this tissue (Scott *et al.*, 2004; Takats *et al.*, 2013). Transmission electron microscopy revealed that the cytoplasm of these cells is filled with typical double-membrane autophagosomes (Figure 1, C and D). This very characteristic phenotype raised the possibility of a specific impairment of autophagosome fusion with late endosomes and lysosomes in mutant larvae.

Transposase-mediated excision of the inserted P element in *l(3)S007902* failed to restore wild-type autophagy, and these revertant lines still died as late L3 larvae, similar to the original mutants. Furthermore, the mutation causing autophagy defects and larval lethality could be separated from the P element insertion by recombination. These genetic tests indicated that impaired autophagy and larval lethality are due to the presence of a background mutation on the P element–bearing chromosome. We thus named this unknown mutation *FUD* (*FUsion Defective*). Recombination and deletion mapping placed this mutation to the 85D7 region on the third chromosome, based on its failure to complement the deficiency lines *Df(3R)ED5339* and *Df(3R)BSC507*. One of the genes located in the overlapping region of these deficiencies, *Vps16A*, encoding a subunit of HOPS complex, seemed to be the most likely candidate potentially involved in autophagosome fusion events. Sequencing the locus identified a mutation at the 3′ end of the third intron in *FUD* mutants, changing the last three nucleotides from CAG to GAG (Figure 1E), which likely interferes with the proper splicing of *Vps16A*. To confirm the role of *Vps16A* in autophagy, we generated targeted deletions by improper excision of the P element *GS5053*, inserted in the 5′ untranslated region of the gene, 64 nucleotides upstream of the translational start site ATG. The new alleles remove 926 (*d116*) and 1105 (*d32*) nucleotides starting from the P element insertion site, deleting the protein-coding sequences in exons 1–3 and parts of exon 4 (Figure 1E). Animals transheterozygous for these alleles and a large chromosomal deficiency also die as late L3 stage larvae.

All three *Vps16A* alleles prevented LTR puncta formation in fat bodies of starved mutants (Figure 1, F–H, J, and L). As transgenic expression of wild-type *Vps16A* completely restored viability and starvation-induced LTR dot formation in $Vps16A^{d32}$ mutant animals (Figure 1, I and L), we concluded that the loss of *Vps16A* is responsible for these mutant phenotypes. In line with that, no Vps16A protein could be detected in $Vps16A^{d32}$ or $Vps16A^{d116}$ mutants, while a faint band was visible in $Vps16A^{FUD}$ (Figure 1M), suggesting these deletions represent null alleles and $Vps16A^{FUD}$ is a strong hypomorphic mutation. Levels of the selective autophagy cargo p62 (also known as Ref2P in flies) are widely used for monitoring autophagy (Pircs *et al.*, 2012). Accumulation of p62 was obvious in Western blots of all three *Vps16A* mutants, similar to highly increased levels of autophagosome-associated, lipidated Atg8a-II (autophagy-related 8a; Figure 1M), in line with impaired autophagosome clearance. As expected, transgenic expression of wild-type *Vps16A* restored normal levels of Vps16A, p62, and Atg8a-II in all three mutant lines (Figure 1M).

All six subunits of the HOPS complex are required for autophagosome clearance

These data prompted us to systematically analyze the role of individual HOPS subunits in autophagy. We generated RNAi-expressing somatic cell clones (marked by coexpression of GFP) in starved larvae expressing mCherry-Atg8a in the fat body. This reporter labels autophagosomes as well as autolysosomes due to persisting fluorescence of the mCherry tag inside acidic lysosomes. Knockdown of *Vps16A*, *car*, *dor*, *Vps39/CG7146*, *Vps11/CG32350*, or *lt* produced a very similar phenotype: faint, small, mCherry-positive dots accumulated in the perinuclear region of cells, unlike the brighter and bigger puncta observed in the cytoplasm of neighboring control cells (Figure 2, A and B, and Supplemental Figure S1, A–E). The variability seen in the number and size of mCherry-Atg8a structures in control cells among different genotypes is likely due to biological variability, which affects different animals or cohorts of animals. Some of these discrepancies may also be caused by slight differences in setting the appropriate signal intensity threshold when extracting dot size and number data during image analysis. Note that, in these and all subsequent mosaic experiments, genetically manipulated cells are compared with their neighboring cells in the same tissue of the same animal, which serve as a built-in control, so the control and RNAi (or mutant) data pairs are essentially linked together.

In cell clones marked by Lamp1-GFP, which also express RNAi transgenes to silence the genes encoding HOPS subunits, starvation failed to induce discernible dots of LTR (Figures 2, C and F, and S1, F–J). Similar to *Vps16A* mutants, punctate LTR staining was inhibited in a *Vps11* mutant line that harbors a transposon insertion in the 5′ untranslated region of this gene and in *lt* mutant larvae (Figure 2, D, E, and G). To further characterize these loss-of-function phenotypes, we used a tandem mCherry- and GFP-tagged Atg8a reporter of autophagic flux (Kimura *et al.*, 2007; Takats *et al.*, 2013). In control cells of starved larvae, these reporter molecules are transported by autophagy to lysosomes in which GFP is rapidly quenched but mCherry fluorescence persists (Figure 2H). Knockdown of *Vps16A*, *car*, *dor*, *Vps39/CG7146*, *Vps11/CG32350*, or *lt* strongly interfered with autophagic flux: although a large number of mCherry-GFP-positive dots were formed, these remained double positive (Figures 2I and S2), suggesting autophagosomes are unable to mature into autolysosomes in these cells. Immunofluorescence labeling of endogenous Atg8a revealed large-scale accumulation of autophagosomes in *Vps16A*, *dor*, or *car* mutant fat body cell clones of starved larvae (Figure 3, A, C, E, and G). Furthermore, both the number and size of endogenous p62 aggregates increased in these cells (Figure 3, B, D, F, and H). A similar accumulation of punctate Atg8a and p62 was detected in *Vps11* or *lt* mutants and in *Vps39* RNAi cells (Figure S3). Western blots confirmed the accumulation of lipidated Atg8a-II and p62 in starved *Vps11* and *lt* mutant L3 stage larvae, similar to *Vps16A* null mutants (Figure 3I). Punctate Atg8a and p62 structures also accumulated in cells lacking HOPS in well-fed larvae (Figure S4), and RNAi depletion of genes encoding HOPS subunits prevented the formation of mCherry-Atg8a– or LTR-positive, large autolysosomes in fat body cells of wandering larvae (Figure S5). These data suggested that the loss of any one of the subunits of this complex results in accumulation of autophagosomes due to impaired maturation into autolysosomes under basal, starvation-induced, or developmental autophagy. In line with these data, ultrastructural analyses detected large numbers of autophagosomes in fat bodies of starved *Vps16A*, *Vps11*, and *lt* mutants, unlike in control larvae (Figure 4, A, C, E, and G). Interestingly, small dense vesicles were also observed in all three mutants, the contents of which sometimes

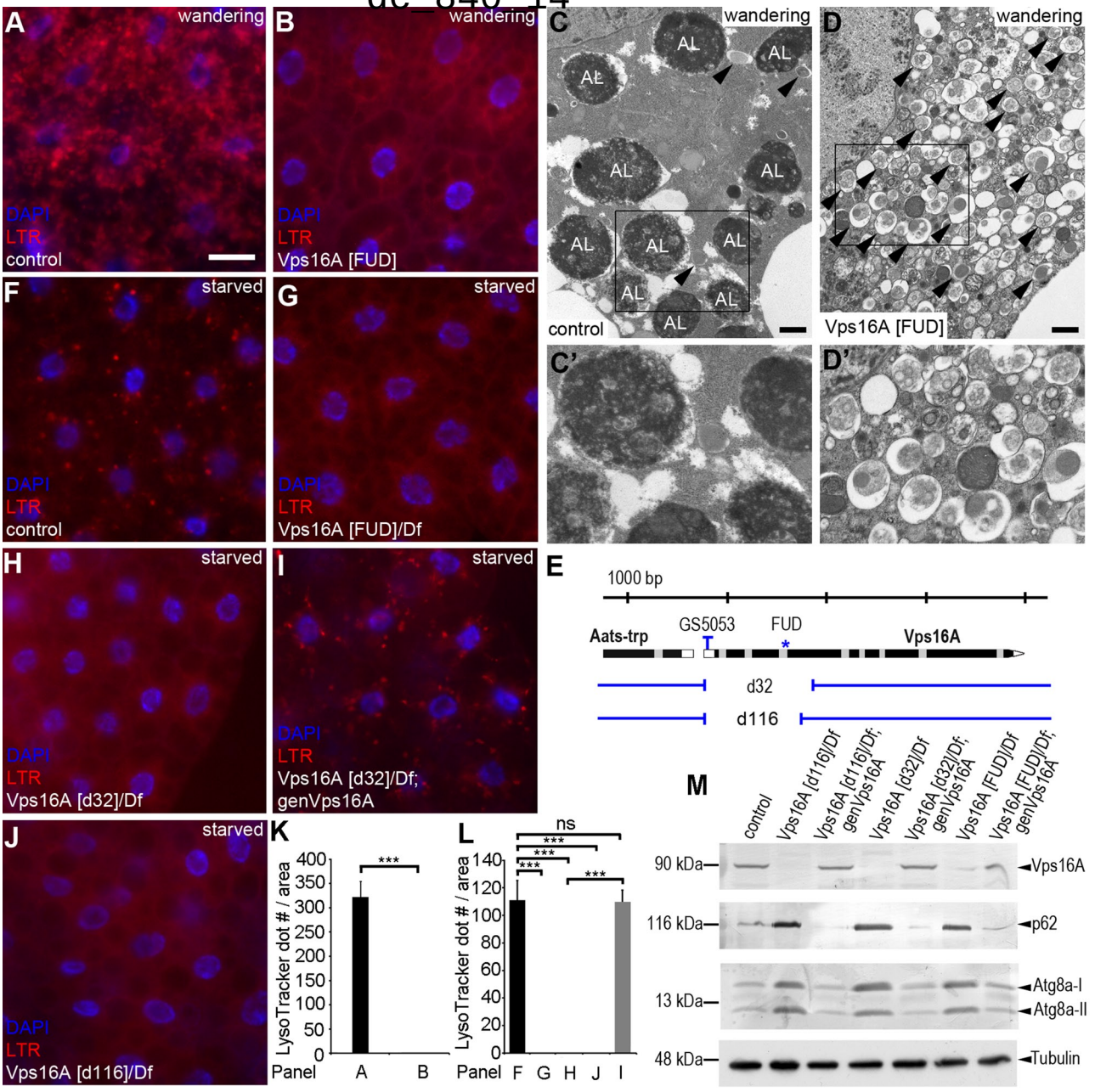


FIGURE 1: Autophagosomes accumulate in *Vps16A* mutants. (A) Large numbers of LTR-positive dots are seen in fat body cells of wandering larvae. (B) No discernible LTR dots are seen in homozygous *l(3)S007902* (*FUD*) mutant fat bodies of the same developmental stage. (C) Large-scale generation of autolysosomes (AL) is observed in fat body cells of wandering larvae. (D) Autolysosome formation is inhibited and autophagosomes (arrowheads) accumulate in large numbers in *FUD* mutant fat body cells of wandering larvae. Boxed areas in (C) and (D) are shown enlarged in (C′) and (D′). (E) Genomic map of the *Vps16A* locus. *FUD* mutants carry a point mutation at the 3′ end of the third intron (blue asterisk). The null alleles *d32* and *d116* were generated from the P element insertion *GS5053* (located in the 5′ untranslated region of *Vps16A*), and carry 1105– and 926–base pair deletions extending into the coding sequence starting from the original P element insertion site, respectively. (F–J) Three-hour starvation in a 20% sucrose solution induces punctate LTR staining in control larvae (F), unlike in hemizygous *Vps16A[FUD]* (G), *Vps16A[d32]* (H), or *Vps16A[d116]* (J) mutants. Transgenic expression of *Vps16A* restores starvation-induced LTR dot formation in *Vps16A[d32]* mutants (I). (K) Quantification of data shown in (A) and (B); $n = 10$/genotype. (L) Quantification of data shown in (F)–(J); $n = 10$/genotype. (M) Western blots reveal that Vps16A protein cannot be detected in lysates of starved *Vps16A[d32]* and *Vps16A[d116]* mutant larvae, and its level is strongly reduced in *Vps16A[FUD]* mutants. The autophagic cargo p62 and autophagosome-associated Atg8a-II accumulate to similar levels in all three mutants. Transgenic expression of *Vps16A* restores wild-type protein levels for Vps16A, p62, and Atg8a in all three mutant backgrounds. Scale bar in (A) = 20 μm for (A), (B), and (F)–(J); scale bars = 1 μm in (C) and (D). Error bars denote SE in (K) and (L); ns, not significant; ***, $p < 0.001$.

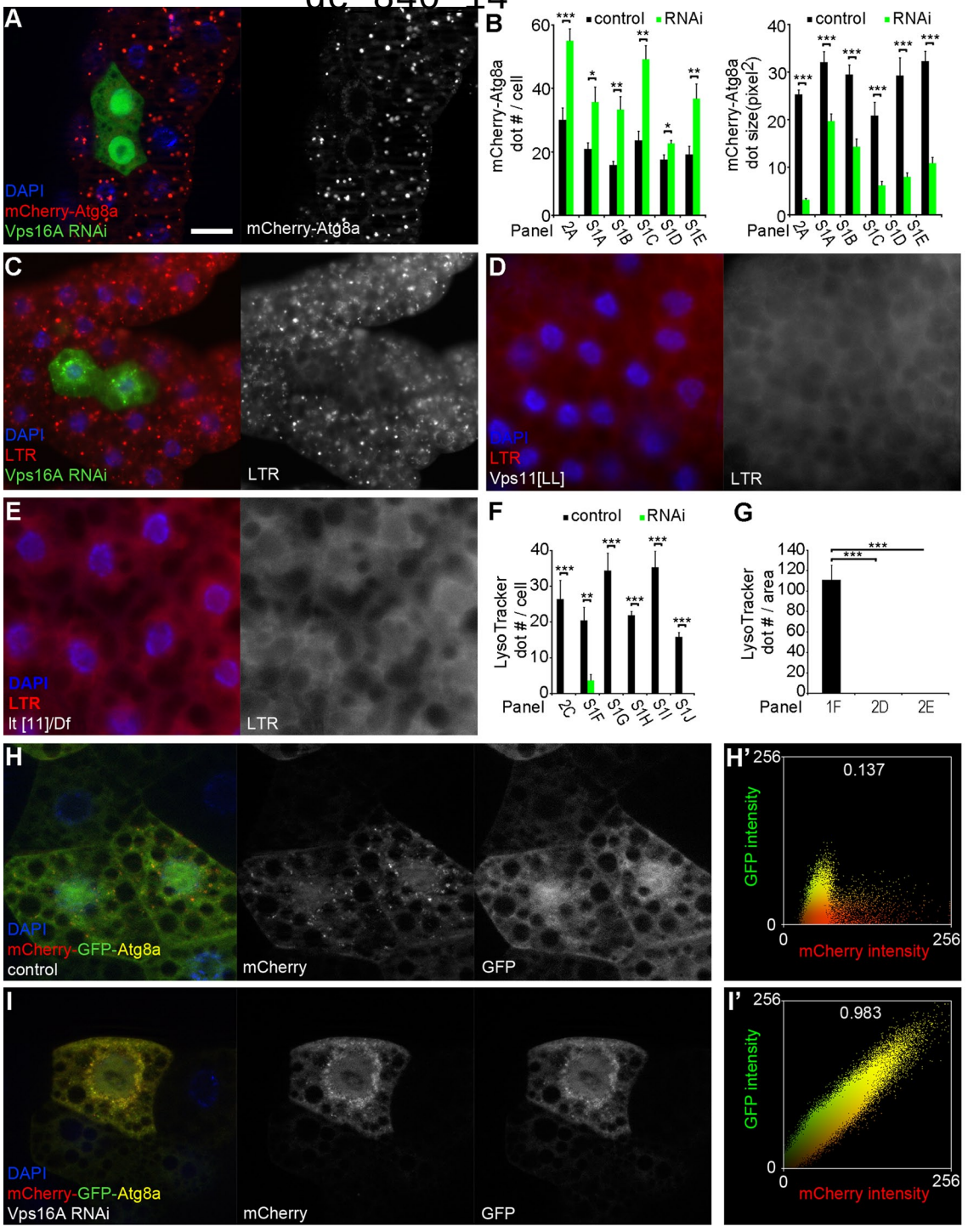


FIGURE 2: Loss of HOPS complex function leads to impaired starvation-induced autophagy. (A) Expression of a transgenic RNAi construct targeting *Vps16A* in GFP-marked clones of fat body cells causes the accumulation of small, faint, perinuclear mCherry-Atg8a dots, which are very different from the bigger, brighter puncta observed in neighboring control cells. (B) Quantification of data shown in (A) and in Figure S1, A–E; $n = 10$/genotype. (C–E) Depletion of *Vps16A* in cell clones marked by Lamp1-GFP prevents punctate LTR staining (C), compared with neighboring controls cells. Similarly, no discernible LTR structures are seen in starved *Vps11[LL]* (D) or *lt[11]* (E) mutant fat cells. (F) Quantification of data shown in (C) and Figure S1, F–J; $n = 9$/genotype for (F); $n = 10$/genotype for others. (G) Quantification of data shown in (D), (E), and Figure 1F; $n = 10$/genotype. (H and I) The double-tagged mCherry-GFP-Atg8a reporter is transported to autolysosomes, which are seen as mCherry-positive dots due to quenching of GFP in starved control cells (H). Silencing of *Vps16A* (I) results in a block of GFP quenching; thus dots appear yellow in merged images. (H') and (I') depict dot plots of intensity and colocalization profiles for the mCherry and GFP channels from (H) and (I). Numbers on top show Pearson correlation coefficients, indicating increased colocalization of GFP and mCherry in (I) compared with (H). Scale bar in (A) = 20 μm for (A), (C), (D), and (E); scale bar = 40 μm for (H) and (I). Error bars denote SE in (B), (F), and (G); ***, $p < 0.001$, **, $p < 0.01$, *, $p < 0.05$.

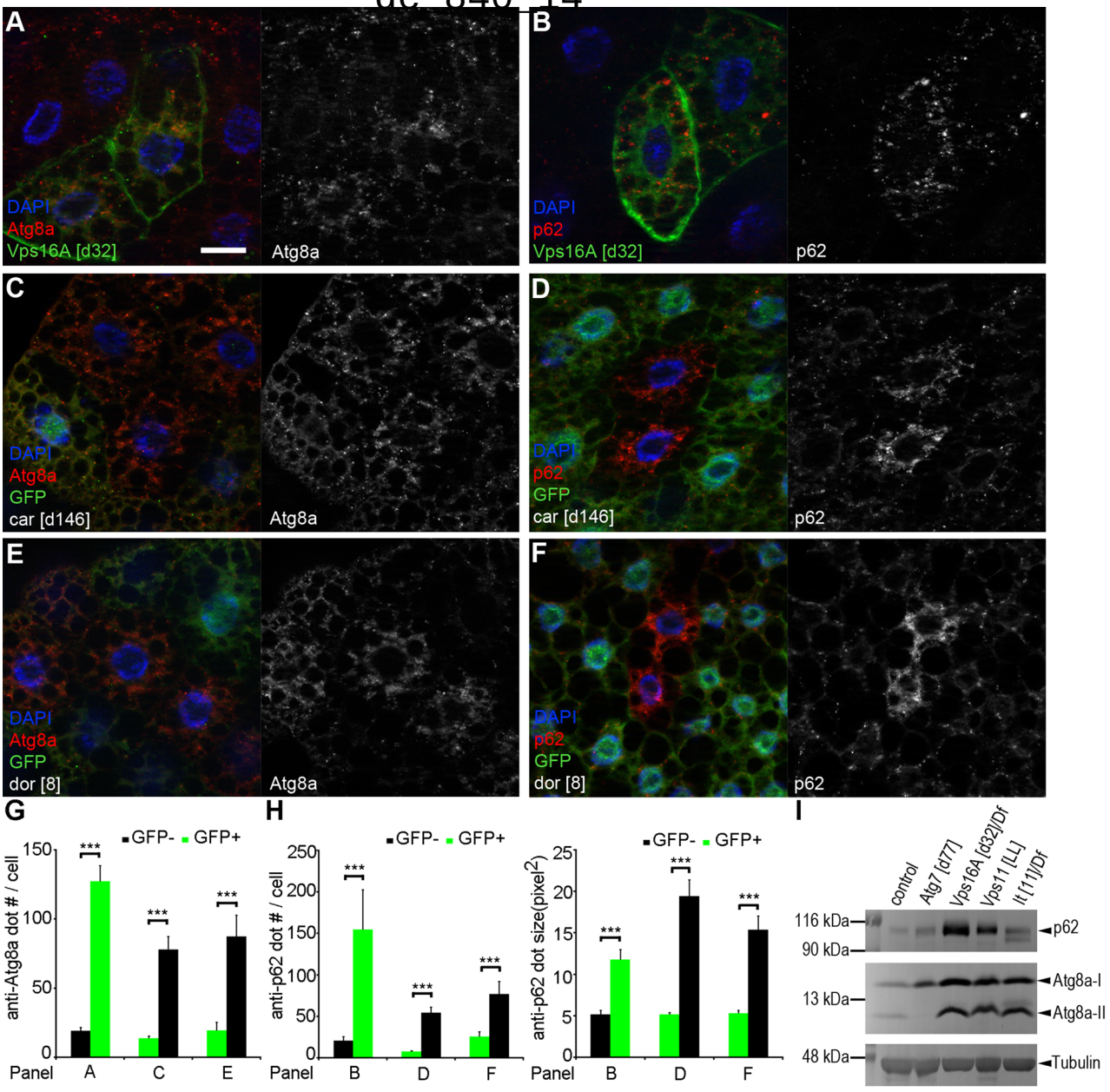


FIGURE 3: The autophagic cargo p62 and Atg8a-positive autophagosomes accumulate in starved HOPS mutants. (A–F) Endogenous Atg8a-positive autophagosomes (A, C, and E) and endogenous p62 (B, D, and F) aggregates accumulate in *Vps16A* (A and B), *car* (C and D), or *dor* (E and F) null mutant cells, compared with surrounding control fat cells in starved mosaic larvae. Note that *Vps16A* mutant cells are marked by GFP in (A) and (B), whereas *car* or *dor* mutant cells can be recognized by the lack of GFP in (C)–(F). (G) Quantification of data shown in (A), (C), and (E); $n = 10$/genotype. (H) Quantification of data shown in (B), (D), and (F); $n = 10$/genotype. (I) Western blots show that p62 and Atg8a-II are up-regulated in starved *Vps16A*, *Vps11*, and *lt* mutants compared with wild-type controls. *Atg7* mutants are used as an additional control. Scale bar in (A) = 20 µm for (A–F). Error bars denote SE in (G) and (H); ***, $p < 0.001$.

seemed to originate from sequestered cytoplasmic material (Figure 4, D, F, and H). While some of these structures likely represent aberrant autolysosomes, their size and morphology was profoundly different from autolysosomes observed in control cells, which also indicates the inefficient fusion of autophagosomes with lysosomes. Autolysosomes in control cells are much bigger and often have an irregular shape due to multiple autophagosomal fusion events, which is also evident from the heterogenity of the contents reflecting different stages of degradation within the same lytic organelle (Figure 4B).

Vps16A colocalizes with Syx17, Atg8a, and Lamp1-GFP

We and others have recently reported that Syx17, a Qa SNARE protein located on autophagosomes, is required for the fusion of these vesicles with late endosomes and lysosomes (Itakura *et al.*, 2012; Takats *et al.*, 2013). Thus we reasoned that Syx17 may cooperate with HOPS for autophagosome clearance. In line with this hypothesis, the colocalization of endogenous Vps16A with endogenous Syx17 could clearly be demonstrated in fat body cells of both control and *Vamp7* mutant larvae (Figure 5, A and B). Vps16A also localized to Atg8a-positive puncta in fat body cells of both

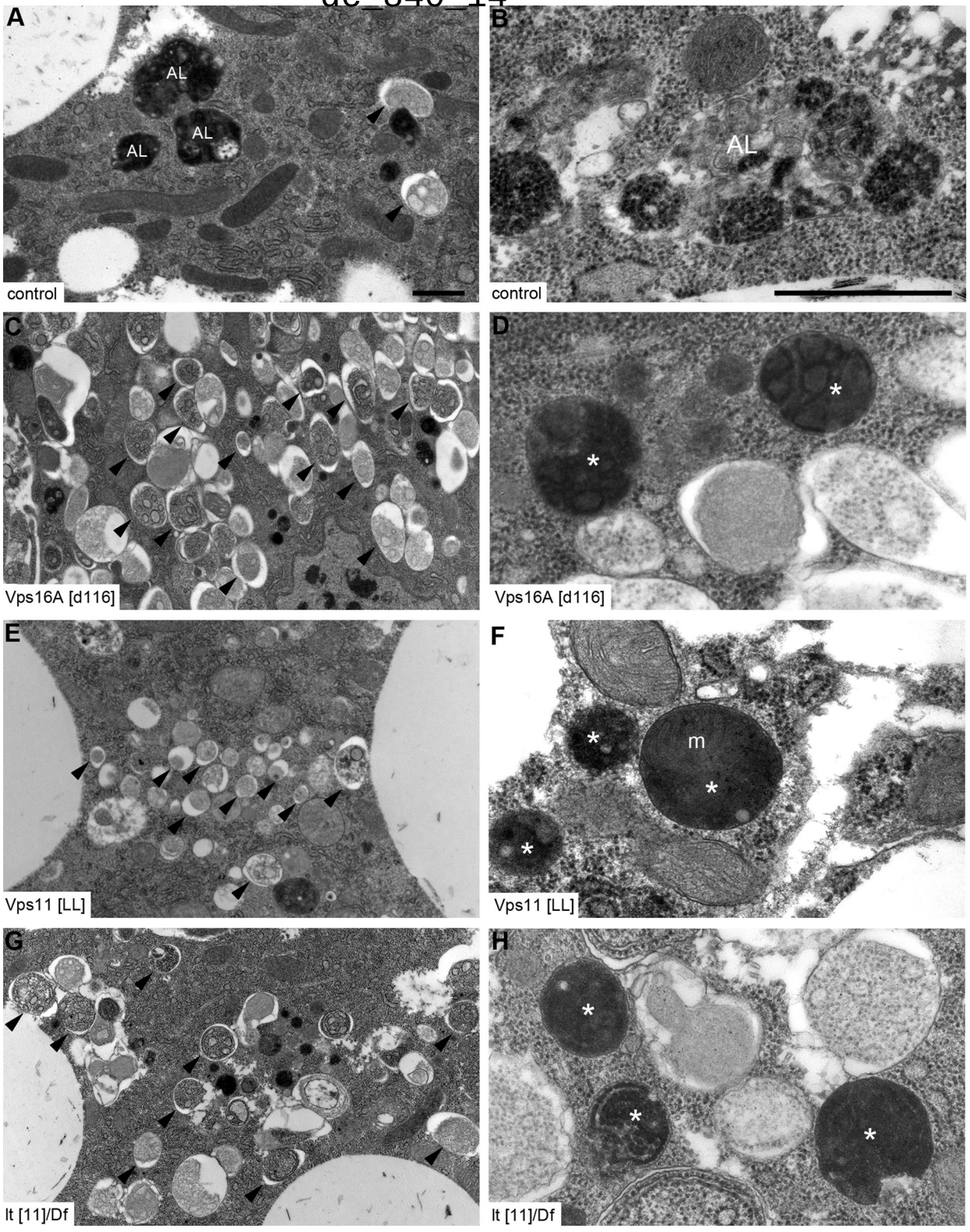


FIGURE 4: Ultrastructural analysis of starved HOPS mutants. (A) Starvation leads to the formation of autophagosomes (arrowheads) and autolysosomes (AL) in fat body cells of control larvae. (B) This panel illustrates a representative autolysosome containing heterogenous material due to different stages of degradation. Note that distinct parts within this irregularly shaped organelle can be seen, corresponding to multiple autophagosome-lysosome fusion events. (C–H) Autophagosomes accumulate in large numbers in *Vps16A* (C), *Vps11* (E), or *lt* (G) mutant cells. In addition, numerous dense organelles are seen, which are usually round and smaller than the autolysosomes observed in controls. High-magnification images reveal that a subset of these presumably lytic vesicles (marked by asterisks) in *Vps16A* (D), *Vps11* (F), or *lt* (H) mutant cells contain recognizable remnants of cytoplasmic material, such as a mitochondrion (m) in (F). Scale bar in (A) = 1 μm for (A), (C), (E), and (G); scale bar in (B) = 1 μm for (B), (D), (F), and (H).

dc_840_14

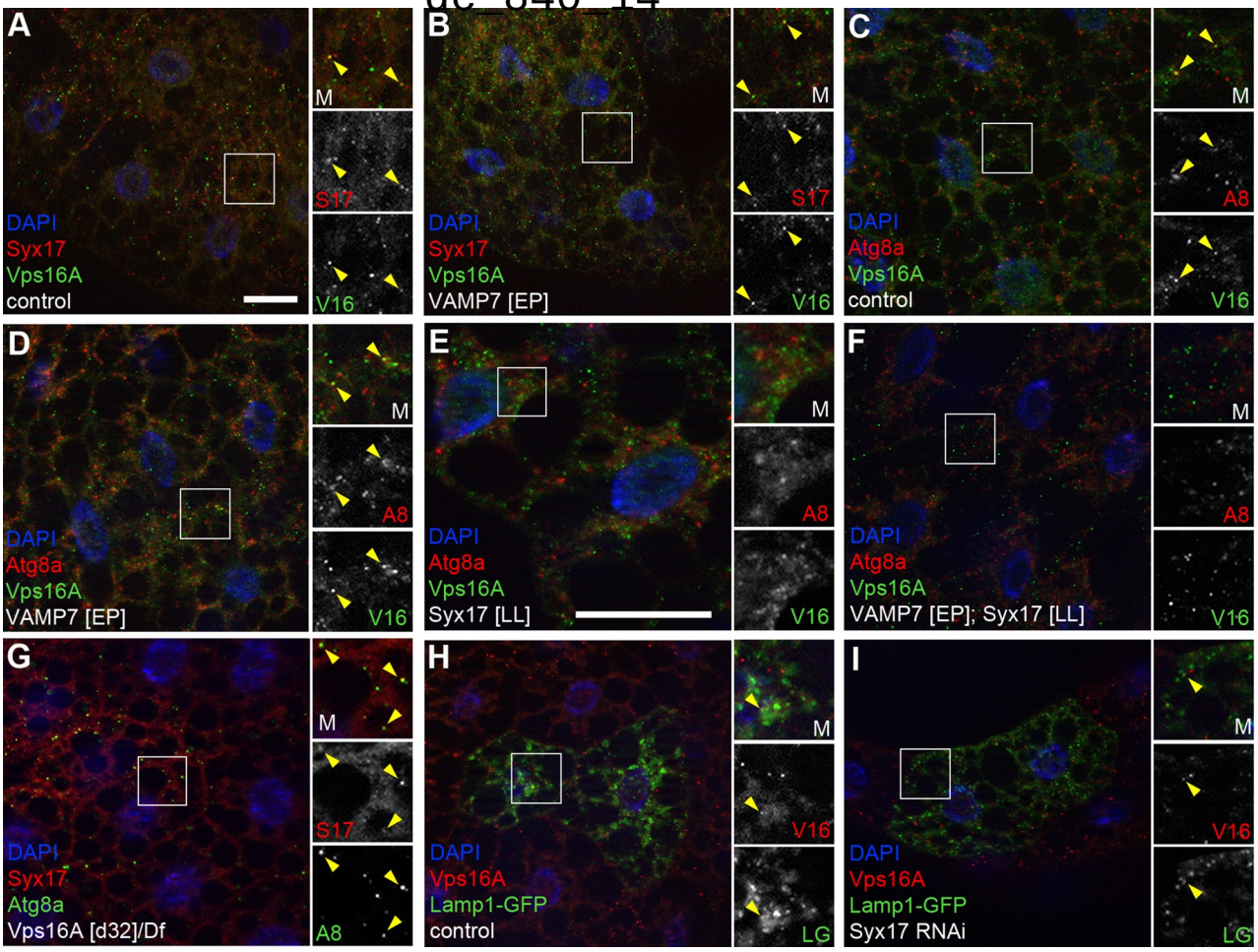


FIGURE 5: Vps16A colocalizes with the autophagosomal SNARE Syx17, the autophagosome marker Atg8a, and the lysosome reporter Lamp1-GFP in fat body cells of starved larvae. (A and B) Endogenous Syx17 colocalizes with endogenous Vps16A in starved control (A) and *Vamp7* mutant (B) fat body cells. (C–F) Vps16A localizes to endogenous Atg8a-positive structures in starved control (C) and *Vamp7* mutant (D) fat body cells. Colocalization of Vps16A with Atg8a is not seen in *Syx17* mutants (E) and *Vamp7, Syx17* double mutants (F). (G) Syx17 colocalizes with Atg8a in *Vps16A* mutants. (H and I) Vps16A colocalizes with the lysosome marker Lamp1-GFP in both starved control (H) and *Syx17* RNAi (I) fat body cells. Boxed areas are shown enlarged as indicated, with representative colocalizations highlighted by yellow arrowheads. M, merged; S17, Syx17; V16, Vps16A; A8, Atg8a; LG, Lamp1-GFP. Scale bar in (A) = 20 µm for (A)–(D) and (F)–(I); scale bar in (E) = 20 µm.

control and *Vamp7* mutant larvae (Figure 5, C and D). Vps16A colocalization with Atg8a was almost never seen in *Syx17* mutants and in *Vamp7, Syx17* double mutants (Figure 5, E and F), raising the possibility that Syx17 may have a role in the association of Vps16A with autophagosomes. Syx17 still colocalized with Atg8a in *Vps16A* mutants (Figure 5G), similar to the situation described for wild-type cells (Takats *et al.*, 2013). These data suggested that HOPS is dispensable for Syx17 loading onto autophagosomes. HOPS is also involved in homotypic vacuole/lysosome fusion in yeast, and may fulfill its function during autophagosome-lysosome fusion while associated with the surface of lysosomes. This prompted us to carry out further localization experiments. Indeed, colocalization of Vps16A with the lysosome reporter Lamp1-GFP, and with the resident lysosomal hydrolase reporter cathepsin D-mCherry could be detected in both control and *Syx17* RNAi or mutant cells (Figures 5, H and I, and S6, A and B). As expected, RNAi silencing of *Vps39* prevented the colocalization of endogenous Atg8a or Syx17 with Lamp1-GFP (Figure S6, C–F), indicating that HOPS-mediated tethering is important for the fusion of Atg8a- and Syx17-positive autophagosomes with lysosomes.

HOPS interacts with Syx17

The similar mutant phenotypes and our colocalization experiments suggested that HOPS may bind to Syx17. Indeed, hemagglutinin (HA)-Car, Myc-Dor, and HA-Vps16A were readily coimmunoprecipitated with FLAG-Syx17 from cultured insect cells (Figure 6A). The strength of interactions seen between these overexpressed proteins was very similar, suggesting that the HOPS complex as a whole may interact with Syx17. We next tested whether the interaction of Syx17 with HOPS is enhanced by starvation, because this treatment induces autophagosome formation, and as a consequence, it also increases the number of autophagosomal fusion events. In line with this model, the interaction of endogenous Syx17 with transiently expressed Myc-Dor appeared to increase in response to starvation in adult flies (Figure 6B). A previous report showed that in yeast, the Vps33-Vam3 interaction requires Vps18 (Sato *et al.*, 2000), raising

dc_840_14

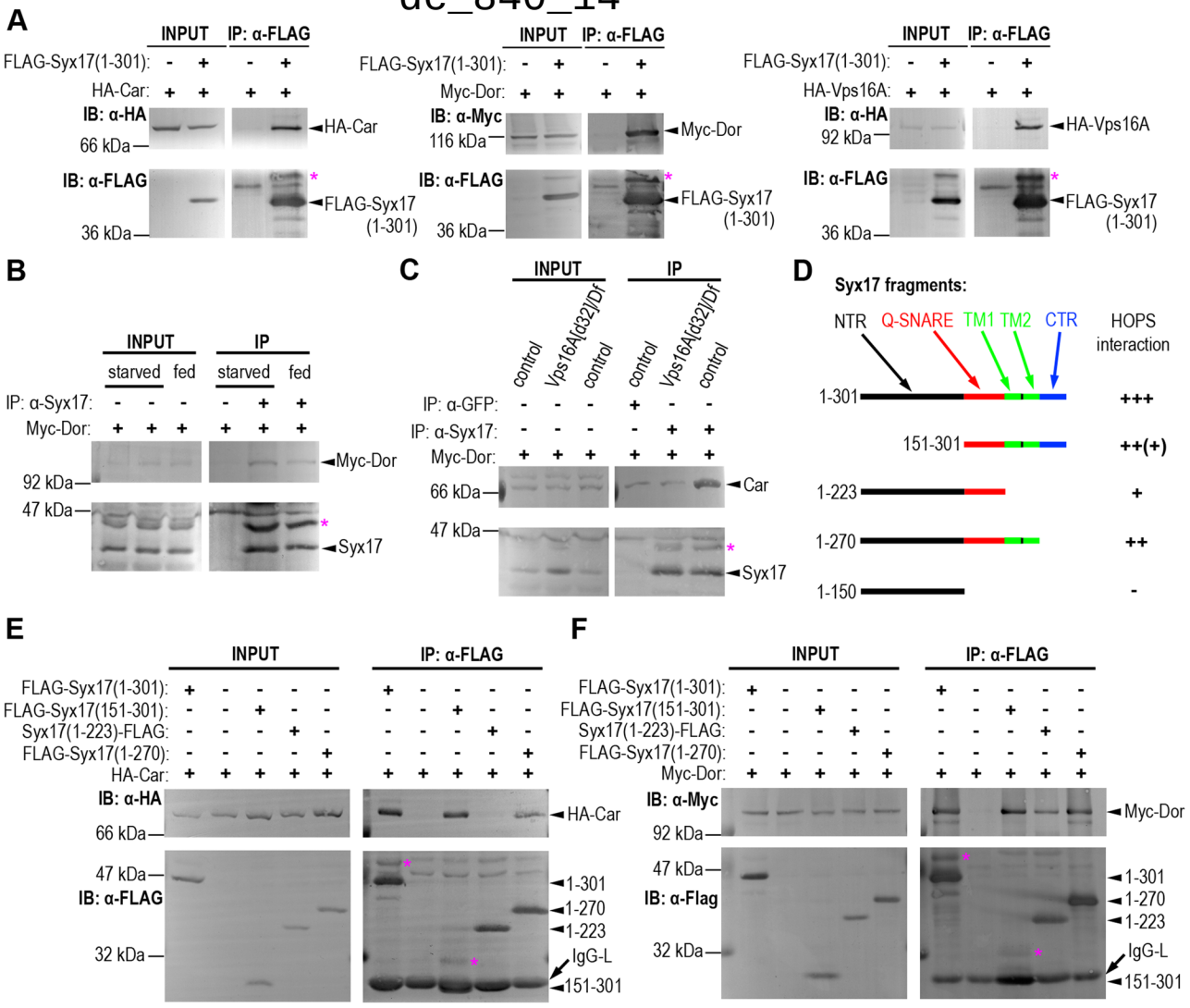


FIGURE 6: Multiple HOPS subunits interact with Syx17. (A) HA-Car, Myc-Dor, and HA-Vps16A coprecipitate with full-length FLAG-Syx17 in cultured *Drosophila* cells. (B) The interaction of transiently expressed Myc-Dor increases with endogenous Syx17 in response to starvation in immunoprecipitation experiments from adult flies. (C) Endogenous Car coprecipitates with endogenous Syx17 in starved control larvae, but not in starved *Vps16A* mutants. (D) An illustration of the truncated Syx17 fragments used in mapping experiments, together with the summary of their interactions with HOPS subunits based on experiments shown in (E), (F), and Figure S6, I and J. Abbreviations are as follows: NTR, N-terminal region; Q-SNARE, Q-SNARE domain; TM1 and 2, transmembrane domains 1 and 2, respectively; CTR, C-terminal region. Numbers refer to amino acid positions in full-length Syx17. (E and F) Immunoprecipitation analysis of HA-Car (E) and Myc-Dor (F) with FLAG-tagged Syx17 constructs shown in (D). Asterisks mark a higher-molecular-weight isoform of endogenous Syx17 in (B) and (C), which likely represents a C-terminally extended 346–amino acid protein isoform as a result of stop codon readthrough (Dunn *et al.*, 2013). Note that a higher-molecular-weight isoform (also marked by asterisks in A, E, and F) is seen in the case of tagged constructs expressing full-length and N-terminally truncated Syx17, both of which contain the full 3′ untranslated region of this gene, but not in the case of C-terminally truncated versions. IP, immunoprecipitate; IgG-L, immunoglobulin light chain.

the possibility that the HOPS complex as a whole may interact with its partner SNAREs. As Vps16 is the only subunit of HOPS that binds to Vps33 in yeast (Lobingier and Merz, 2012; Solinger and Spang, 2013), we tested whether the binding of Car/Vps33A to Syx17 depends on Vps16A in *Drosophila*. Endogenous Car coprecipitated with endogenous Syx17 in starved larvae, but this specific interaction was abolished in *Vps16A* mutants (Figure 6C), supporting the hypothesis that multiple interactions between the assembled HOPS complex and Syx17 may be required for efficient binding. RNAi depletion of *car* in cultured cells appeared to destabilize the Syx17-Vamp7 complex (Figure S6G). Furthermore, the interaction of endogenous Syx17 with endogenous usnp (ubisnap) was decreased in hypomorphic *dor* mutant adult flies (Figure S6H), suggesting that HOPS promotes proper assembly of the Syx17/usnp/Vamp7 *trans*-SNARE complex.

In yeast, biochemical studies suggested that the Vps11, Vps16, and Vps18 subunits of HOPS in combination bind to the N-terminal region of Vam3, a Qa SNARE, whereas Vps33 was found to interact with the SNARE domains of Vam3 (Qa), Vam7 (Qc), and Nyv1 (R), but not with Vti1 (Qb) of the quaternary SNARE complex involved in

dc_840_14

homotypic vacuole fusion (Lobingier and Merz, 2012). Given that metazoan cells rely on different SNAREs during autophagosome fusion and that sequence similarity between the Qa SNAREs Vam3 and Syx17 is limited to the SNARE domains, we attempted to map the region of Syx17 involved in binding to HOPS, using various truncated fragments expressed in cultured cells (Figure 6D). In these coimmunoprecipitation experiments, full-length FLAG-Syx17 bound slightly more effectively to HA-Car than an N-terminally truncated protein (containing the Q SNARE domains, both transmembrane regions and the C-terminus; Figure 6, D and E). This is in line with the fact that Car belongs to the Sec1/Munc18-like protein family, whose members may bind to the N-terminal region of syntaxins as well (Akbar *et al.*, 2009). Full-length and N-terminally truncated Syx17 appeared to bind equally well to Myc-Dor and HA-Vps16A, respectively (Figures 6, D and F, and S6I). Removing the C-terminal region of Syx17 seemed to slightly reduce its interaction with these HOPS subunits, whereas a C-terminally truncated fragment lacking both transmembrane domains showed strongly reduced binding to HA-Car, Myc-Dor, and HA-Vps16A (Figures 6, D–F, and S6I). Finally, we could not detect an obvious interaction between the N-terminal region of Syx17 and HA-Car, Myc-Dor, or HA-Vps16A (Figures 6D and S6J). These results raise the possibility that both the SNARE domain and membrane association of Syx17 may be required for effective interaction with HOPS.

We have recently shown that loss of Syx17 impairs starvation-induced LysoTracker staining in larval fat body cells, results in the accumulation of p62 and lipidated Atg8a, and leads to climbing defects indicating neuromuscular dysfunction in adult flies (Takats *et al.*, 2013). In line with the above mapping data, transgenic expression of Syx17 lacking its extreme C-terminal region rescued these phenotypes of *Syx17* mutants similar to full-length transgenes, unlike a Syx17 transgene missing the second transmembrane domain, which is required for its membrane association (Figure 7, A–J; Itakura *et al.*, 2012).

HOPS, but not Syx17, is required for endocytic degradation

Mutations of the HOPS complex subunits *car* or *dor* have been shown to interfere with the degradation of multiple endocytic cargo molecules in vivo, including the transmembrane proteins Bride of sevenless (Boss) and Notch in developing eyes (Sevrioukov *et al.*, 1999; Akbar *et al.*, 2009). Boss is produced by the R8 photoreceptor neuron and binds to Sevenless, a receptor tyrosine kinase located on the surface of a neighboring cell, to induce its differentiation into an R7 neuron. In control larvae, anti-Boss immunostaining shows pairs of large and small dots corresponding to the R8 apical surface and endosomes in R7 cells, respectively (Figure 8A; see also the schematic in Figure 8G). *Vps16A* and *lt* mutants accumulated large amounts of Boss, just like *car* and *dor* mutant eye disks (Figure 8, B–E). In contrast, Boss staining in *Syx17* mutant eye disks was similar to controls (Figure 8F). Our immunolabeling experiments also revealed large-scale accumulation of Notch in developing eyes lacking *Vps16A*, *lt*, *car*, or *dor*, while *Syx17* mutants were again similar to controls (Figure 8, H–M). These results suggest that Syx17 is dispensable for endocytic down-regulation of Boss and Notch in vivo.

HOPS, but not Syx17, is involved in biosynthetic transport to lysosomes

Car, *dor*, and *lt* were named after the eye color phenotypes caused by hypomorphic mutations in these genes (Lloyd *et al.*, 1998). In these mutants, the formation of lysosome-related eye pigment granules is defective compared with wild-type flies that have bright red eyes. We found that eyes composed of entirely null mutant cells for *Vps16A* had a light orange color similar to *dor* null mutant eyes (Figure 9, A–C), while the eye color of viable *Syx17* null mutants were indistinguishable from wild-type eyes (Figure 9D). These data prompted us to further analyze the biogenesis of lysosomes in the absence of HOPS or Syx17. Lamp family proteins are heavily glycosylated and protect the lysosomal membrane from digestion by resident acidic hydrolases. As a result, Lamp proteins are continuously turned over in lysosomes (Pulipparacharuvil *et al.*, 2005). With a GFP insertion in the endogenous locus, accumulation of dLamp in Western blots of *Vps16A* mutants was evident compared with control or *Syx17* mutant larvae (Figure 9E). Cathepsin L is a resident lysosomal protease synthesized as an inactive proenzyme, and it is activated by limited proteolysis in lysosomes, during which an N-terminal portion is cleaved and degraded. Endogenous pro–cathepsin L immunoreactivity was normally very low, and practically only the mature form could be seen in Western blots of control larvae, similar to *Atg7*, *Syx17*, or *Vamp7* mutants (Figure 9F). In contrast, mutation of *Vps16A* or *Vps11* resulted in large-scale accumulation of the proenzyme (Figure 9F). Taken together, these results suggest that the HOPS complex, but not Syx17, is required for proper trafficking to and biogenesis of lysosomes.

We have also tested the role of *fob/Vps16B* (encoding a subunit of an alternative HOPS complex) in biosynthetic and autophagic transport to lysosomes, using a recently published knockout line (Akbar *et al.*, 2011). Western blots did not reveal any defects in the maturation of cathepsin L in these mutants (Figure S7A). Moreover, the levels of p62 and Atg8a-II were also similar to those of controls in lysates prepared from starved *fob* mutant larvae, suggesting proper autophagic degradation (Figure S7A).

Loss of UVRAG perturbs biosynthetic transport to lysosomes, but not autophagosome formation and fusion

It has been suggested that UVRAG, the mammalian homologue of Vps38, binds to the HOPS complex to promote both autophagy and heterophagy (Liang *et al.*, 2008). Thus we decided to extend our analysis to its *Drosophila* homologue. *UVRAG* mutants have recently been described in flies: *UVRAG[GS]*, carrying a transposon insertion in the 5′ untranslated region of the gene; and two deletion alleles, *UVRAG[B7]*, removing the first exon and a small part of the second one; and *UVRAG[B21]*, removing the first exon and most of the second one (Lee *et al.*, 2011). In addition, we identified another transposon-bearing line, *UVRAG[LL]*, which is inserted at nucleotide 66 of the protein-coding sequence downstream of the translation start site ATG. In our initial genetic characterization, *UVRAG[B21]* and *UVRAG[LL]* mutants died as L3-stage larvae in *trans* with a large deficiency for this region or when crossed to each other, suggesting these alleles represent genetic nulls (Figure S7B). Hemizygous *UVRAG[B7]* larvae also died in the L3 stage, while some of the homozygotes survived until puparium formation, and *UVRAG[GS]* mutants died as pupae, indicating these alleles are strong hypomorphs (Figure S7B). *UVRAG* was recently reported to be required for endocytic degradation of multiple receptors in developing eyes (Lee *et al.*, 2011), which we also confirmed for Notch (Figure S7C). We then generated null mutant fat-cell clones for *UVRAG[B21]* and *UVRAG[LL]* and carried out standard tests for autophagy. No statistically significant alterations were detected in starvation-induced LTR or anti-Atg8a staining in these mutant cells compared with surrounding wild-type tissue (Figures 10, A–D, and S7, D and E). In the case of p62, the number of aggregates was similar in mutant and control cells, while their size was increased in mutant cells (Figures 10, E and F, and S7F). In line with these, Western blots showed that the level of lipidated Atg8a was slightly elevated in *UVRAG* mutants

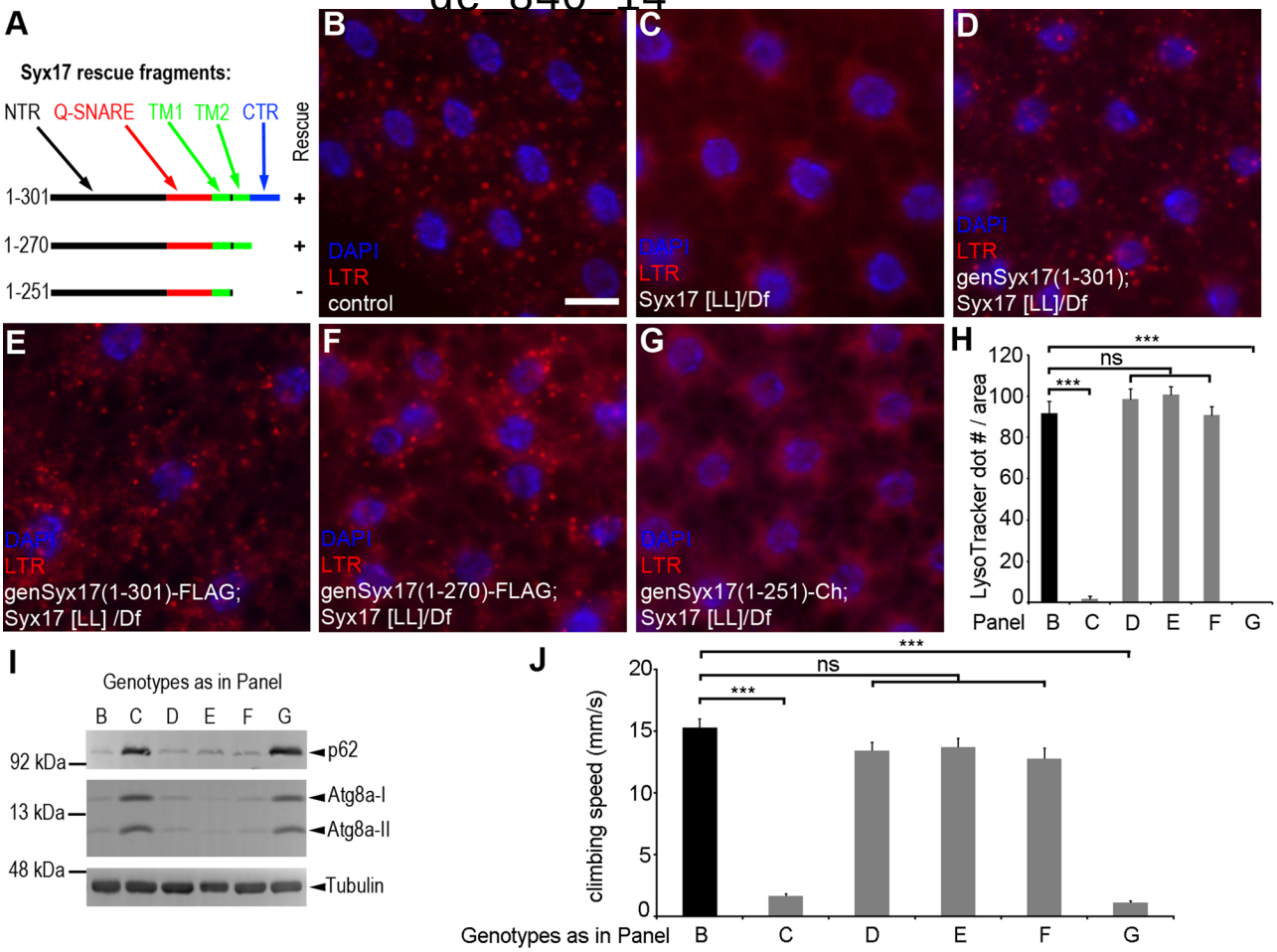


FIGURE 7: Genetic rescue experiments using truncated Syx17 fragments. (A) An illustration of the various Syx17 transgenes used in genetic rescue experiments. Please see Figure 6D for abbreviations. (B–G) LTR staining of fat body cells dissected from starved larvae. Punctate LTR staining seen in control cells (B) is missing from *Syx17* mutants (C). Both untagged (D) and C-terminally FLAG-tagged (E) full-length transgenes restore LTR dot formation in *Syx17* mutants, similar to a Syx17 fragment lacking the C-terminal region (F). A Syx17 construct lacking the second transmembrane region and C-terminus is unable to restore punctate LTR in *Syx17* mutants (G). Please note that the C-terminus of this last construct is tagged with mCherry, but the expression of this transgene is under direct control of the *Syx17* promoter, similar to the other constructs. This results in a very low expression level; therefore its fluorescence does not interfere with LTR staining. (H) Quantification of data shown in (B)–(G); $n = 10$/genotype. (I) Western blots of well-fed adult flies also show that a Syx17 fragment lacking the C-terminal region fully rescues the p62 and Atg8a-II accumulation phenotypes of well-fed *Syx17* mutant adult flies, similar to full-length transgenes. Truncating Syx17 after the first transmembrane domain prevents the rescue of these defects. (J) Negative geotaxis assays of adult flies reveal that both full-length transgenes and a Syx17 fragment lacking the C-terminal region fully rescue the climbing defects of *Syx17* mutant adult flies. Again, truncating the second transmembrane domain and C-terminus of Syx17 prevents rescue; $n = 90$ for all genotypes. Scale bar in (B) = 20 μm for (B)–(G). Error bars denote SE in (H) and (J); ns, not significant; ***, $p < 0.001$.

compared with controls, and p62 was up-regulated (Figure 10G). Ultrastructural analyses showed no accumulation of autophagosomes in *UVRAG[LL]* or *UVRAG[B21]* mutants (Figure 10, H and I). Autolysosomes were formed in these cells and had an irregular shape similar to those observed in control cells, indicating that multiple autophagosome-lysosome fusions have occurred. Interestingly, autolysosomal contents showed homogenous density, and more advanced stages of degradation were never seen in *UVRAG* mutants after 3 h of starvation, unlike in control cells. On the basis of these morphological analyses, we hypothesized that lysosomal function may be perturbed by loss of UVRAG. Indeed, pro-cathepsin L could be readily detected in Western blots of larval lysates, although its level was much lower than that observed in *Vps16A* null mutants (Figure 10G). Moreover, the lysosome reporter Lamp1-GFP accumulated in *UVRAG* mutant cells (Figures 10J and S7G). Finally, eyes composed entirely of *UVRAG* mutant tissue showed a color different from wild-type flies, although again it was not as severe as seen in cases of *Vps16A* or *dor* mutant eyes (Figure 10, K and L). The eye color defect of *UVRAG[LL]* mutants was even more obvious in the presence of a *white[+mC]* transgene in a *white* null mutant background, which creates a hypomorphic condition regarding eye color. In these experiments, the eye color of control flies was orange, and *UVRAG* mutants had a lighter eye color (Figure 10M). These results support a conclusion that *UVRAG* plays a role in heterophagy and

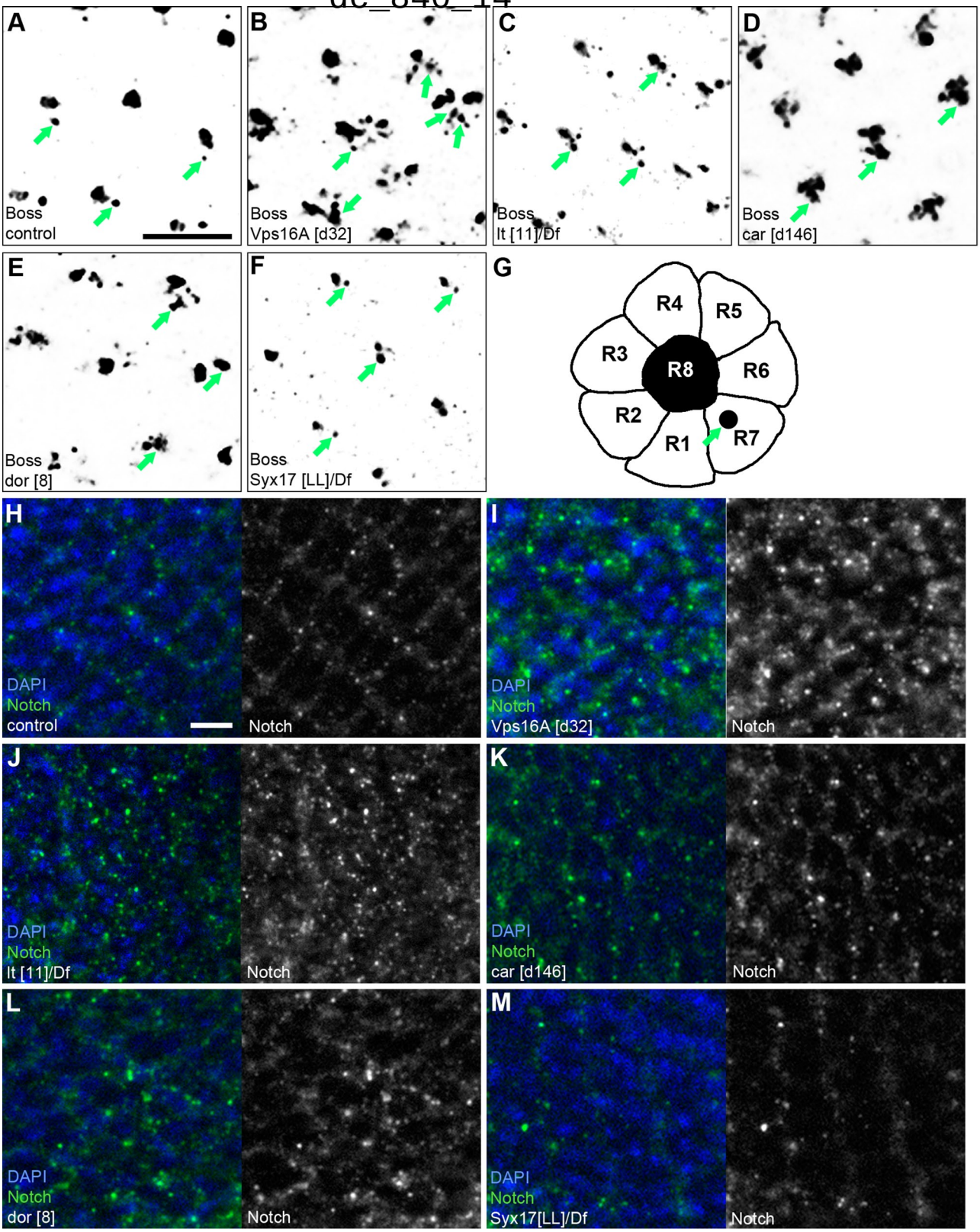


FIGURE 8: HOPS, but not Syx17, is required for endocytic down-regulation of Notch and Boss in developing eyes. (A–F) Anti-Boss staining reveals pairs of bigger and smaller dots corresponding to R8 and R7 photoreceptor neurons in the differentiating retina in control larvae (A), as indicated in the schematic (G). Accumulation of Boss is obvious in *Vps16A* (B) and *lt* (C) mutants, and also in developing eyes entirely composed of *car* (D) and *dor* (E) null mutant cells. Boss distribution in *Syx17* mutants (F) is similar to controls. (H–M) Punctate anti-Notch immunolabeling reveals a regular pattern of developing ommatidia in eye disks of control larvae (H). Mutation of *Vps16A* (I), *lt* (J), *car* (K), or *dor* (L) leads to large-scale accumulation of Notch. The level and localization of Notch in *Syx17* mutants (M) is similar to controls. Scale bar in (A) = 20 μm for (A)–(F); scale bar in (H) = 20 μm for (H)–(M).

dc_840_14

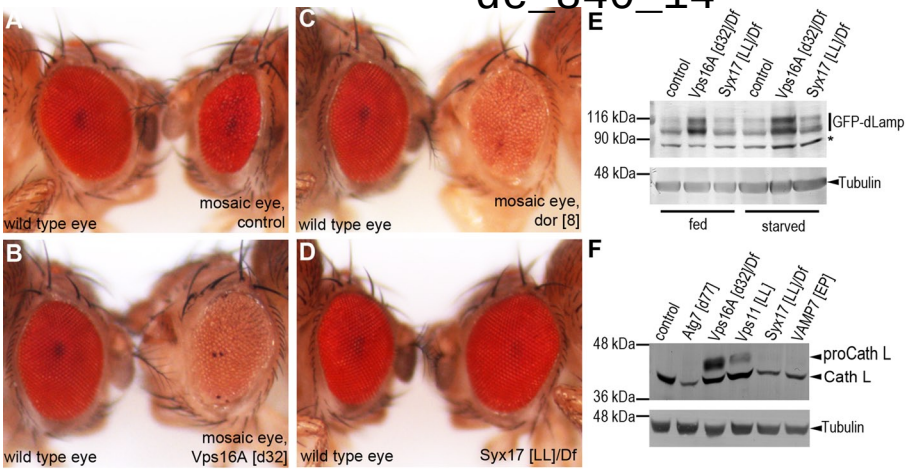


FIGURE 9: HOPS, but not Syx17, is required for biosynthetic transport to lysosomes and pigment granules. (A–D) Eye pigment granules, a type of lysosome-related organelle, are responsible for the bright red color of wild-type eyes (A). Eye tissue homozygous for one chromosome arm can be generated with the GMR-Hid method by eliminating nonhomozygous tissue due to eye-specific expression of the proapoptotic gene *Hid* in mosaic eyes. The right side (A) shows the eyes of flies entirely homozygous for a chromosome arm bearing a GFP insertion, which serves as an additional control for mosaic eye experiments. Note that the GMR-Hid method results in a rough eye phenotype, but it does not affect eye color. Eyes composed of entirely mutant cells for *Vps16A* (B) or *dor* (C) have a much lighter, orange color. The eye color of homozygous, viable *Syx17* mutants (D) is similar to that of wild-type flies. (E) Western blot using a GFP knock-in line of endogenous dLamp reveals that this lysosomal membrane protein accumulates in *Vps16A* mutant larvae, whereas no difference is seen between *Syx17* mutant and control larvae. Asterisk indicates a nonspecific band that serves as an additional loading control. (F) The proform of the resident lysosomal hydrolase cathepsin L accumulates in *Vps16A* and *Vps11* mutant larvae compared with controls, but not in *Atg7*, *Syx17*, or *Vamp7* mutants.

proper biogenesis of lysosomes. As a result, its loss likely causes a delay in autolysosomal degradation without affecting earlier steps of autophagy.

DISCUSSION

Our data presented here clearly show that all six subunits of the HOPS complex are important for the clearance of autophagosomes, acting in a cell-autonomous manner in *Drosophila*. HOPS likely promotes the fusion of autophagosomes with late endosomes and lysosomes through its interaction with Syx17, the autophagosomal SNARE. The HOPS subunit Vps16A colocalizes with Syx17 in both control and *Vamp7* mutant cells, suggesting the interaction of HOPS with Syx17 may not necessarily require formation of the Syx17-usnp-Vamp7 *trans*-SNARE complex. Supporting this hypothesis, Vps16A colocalized with Atg8a not only in control cells but also in *Vamp7* mutants, in which the fusion of autophagosomes with lysosomes is inhibited (Takats *et al.*, 2013). The presence of Vps16A on lysosomes appears to be independent of Syx17, consistent with the known roles of HOPS during homotypic fusion of vacuoles/lysosomes. Our data are compatible with the model in which HOPS is associated with the lysosome and tethers an autophagosome moving into proximity. Interestingly, HOPS was also shown to bind various phospholipids with high affinity, including the autophagosome- and endosome-specific phosphatidylinositol 3-phosphate (Stroupe *et al.*, 2006). This is in line with our results, which suggest that the membrane association of Syx17 may increase its interaction with HOPS. Tethering is followed by formation of the *trans*-SNARE complex, which may be stabilized by HOPS during vacuole fusion in yeast as has been proposed by Starai *et al.* (2008). Finally, following fusion of the vesicles, Syx17 is rapidly recycled from the autolysosome, as suggested by the low level of Syx17 localization to lysosomes in fly and mammalian cells (Itakura *et al.*, 2012; Takats *et al.*, 2013).

Supporting our results and conclusions, a study related to ours shows that small interfering RNA (siRNA) silencing of *Vps33A*, *Vps16*, or *Vps39* in cultured human cells results in the accumulation of autophagosomes due to impaired fusion of these vesicles with late endosomes and lysosomes. Subunits of the HOPS complex have also been found to interact with STX17, the mammalian homologue of Syx17 in that study, suggesting a similar HOPS-dependent fusion mechanism facilitates the clearance of autophagosomes in *Drosophila* and mammals.

Unlike HOPS, which is involved in homo- and heterotypic vacuole fusion, CORVET is thought to function at the level of early endosomes in yeast, but the existence of this complex has not been verified in metazoans yet. The putative alternative HOPS complex found in animal cells, which contains Vps16B and Vps33B, has been speculated to play a role similar to that of CORVET (Balderhaar and Ungermann, 2013). Recently the *Drosophila Vps16B* homologue *fob* has been shown to be required for the maturation of bacteria-containing phagosomes but not for general endocytosis or starvation-induced LTR staining (Akbar *et al.*, 2011). Accordingly, we found no defects in lysosomal processing of cathepsin L, or in the degradation of Atg8a and p62 during autophagy in *fob* mutants. These results further confirm the distinct and specific roles of a Vps16A- and Car-containing HOPS complex in heterophagy, autophagy, and lysosome biogenesis.

The role of UVRAG in autophagy has been controversial. The yeast homologue of this gene, *VPS38*, is classified as a member of the class A *VPS* group (Bowers and Stevens, 2005). Its mutation leads to secretion of CPY without affecting vacuolar morphology, suggesting that the effect on vacuolar protein sorting may be relatively mild. Vps38/UVRAG is a subunit of a Vps34-containing lipid kinase complex both in yeast and mammals (Kihara *et al.*, 2001; Itakura *et al.*, 2008; Matsunaga *et al.*, 2009; Farre *et al.*, 2010). These studies showed that the mutually exclusive presence of Atg14 or UVRAG in distinct Vps34 complexes specifies a role in autophagosome formation or endocytosis, respectively. UVRAG has also been identified as a potential binding partner of HOPS, and based on overexpression experiments, it has been suggested as a promoter of both autophagic and endocytic degradation (Liang *et al.*, 2008). Recently *Drosophila* UVRAG was found to be required for the degradation of multiple receptors during eye development (Lee *et al.*, 2011), which we also confirmed. However, we found no defects in the formation of autophagosomes and their fusion with lysosomes in two independent cases of *UVRAG* null mutant alleles, based on multiple standard autophagy assays. The accumulation of both procathepsin L and the lysosomal membrane protein Lamp1, and defective eye pigment granule formation in *UVRAG* mutants are similar to but weaker than the phenotypes observed with HOPS mutants.

In fact, all the phenotypes of *Drosophila UVRAG* mutants may be explained by the role of this protein as a Vps34 lipid kinase subunit, which is important for endocytosis and biosynthetic transport to lysosomes (Juhasz *et al.*, 2008). Our findings are consistent with yeast studies that documented vacuolar protein–sorting defects but found no perturbation of autophagosome formation or clearance in *UVRAG* mutants (Farre *et al.*, 2010). Our data also suggest that the loss of UVRAG only influences a late step of autophagy by delaying the degradation of sequestered cargo in autolysosomes. Similarly, siRNA depletion of UVRAG blocked endocytic degradation of EGFR, but it did not affect autophagosome formation or fusion in cultured mammalian cells (Knaevelsrud *et al.*, 2010; Jiang *et al.*, 2014).

Taken together, our studies clearly establish the role of HOPS in facilitating the Syx17-dependent fusion of autophagosomes with endosomes and lysosomes in *Drosophila*, and clarify that the effect of UVRAG on autophagic degradation is likely due to perturbed biosynthetic transport of hydrolases to lysosomes.

MATERIALS AND METHODS

Drosophila genetics, treatments, and climbing tests

Flies were reared on standard yeast/cornmeal medium, and L3 stage larvae of the age 80–88 h after egg laying were transferred to a 20% sucrose solution for 3 h in starvation experiments. *Drosophila* mutants and transgenics used in this study are *l(3)S007902* bearing the *Vps16A[FUD]* allele (Szeged Stock Center, Hungary); Gal4-responsive transgenic UAS-RNAi lines for *Vps16A[GD13782]*, *car[GD1397]*, *dor[KK102176]*, and *Vps39[GD12152]*, *Vps11[KK102566]* (all obtained from the Vienna Drosophila RNAi Center, Vienna, Austria); *car[12230R-1]* (referred to as RNAi/2, obtained from the National Institute of Genetics, Mishima, Japan); and *lt[HMS00190]* (obtained from the Bloomington Drosophila Stock Center *[*BDSC*]*, Indiana University, Bloomington, IN; and generated by the Transgenic RNAi Project, Harvard Medical School, Boston, MA). Mosaic eyes composed of entirely mutant tissue for *car*, *dor*,*Vps16A*, and *UVRAG* were generated with the help of *GMR-Hid, FRT19A*; *ey-Gal4, UAS-Flp* or *GMR-Hid, FRT40A*; *ey-Gal4, UAS-Flp* or *ey-Gal4, UAS-Flp*; *FRT82B, GMR-Hid* (BDSC), as previously described (Rusten *et al.*, 2007; Juhasz *et al.*, 2008). Mutant and deficiency lines used were *car[d146]* on *FRT19A* (Akbar *et al.*, 2009); *dor[4], dor[8]* on *FRT19A* (Sevrioukov *et al.*, 1999); *lt[11]* (Wakimoto and Hearn, 1990); *Df(2L)lt45*, *Df(3L)Exel8098*, *Df(3R)BSC507*, and *Df(3R)ED5339* (all obtained from BDSC); *Df(2L)ED784, UVRAG[GS17330]* (Lee *et al.*, 2011); *dLAMP[CPTI001775]*, *Syx17[LL06330]* on *FRT2A* (Takats *et al.*, 2013); *Vps11[LL06553], UVRAG[LL03097]* on *FRT40A* (Schuldiner *et al.*, 2008) (all obtained from the Drosophila Genetic Resource Center [DGRC], Kyoto, Japan); *Atg7[d77]* (Juhasz *et al.*, 2007); *fob[1]* (Akbar *et al.*, 2011); and *UVRAG[B7], UVRAG[B21]* on *FRT40A* (Lee *et al.*, 2011) (kindly provided by Sekyu Choi). *Vps16A[d32]* and *Vps16A[d116]* were generated by imprecise excision of *Vps16A[GS5053]* (obtained from DGRC) and recombined onto *FRT82B* for generation of mutant clones. New transgenic flies were generated by standard embryo injection technique (BestGene, Chino Hills, CA). Transgenic animals for full-length, untagged genomic Syx17 have been described (Takats *et al.*, 2013). LTR and 4′,6-diamidino-2-phenylindole staining, autophagy reporter lines, and the generation of mosaic animals were described previously (Rusten *et al.*, 2004, 2007; Scott *et al.*, 2004; Juhasz *et al.*, 2007, 2008; Erdi *et al.*, 2012; Pircs *et al.*, 2012; Takats *et al.*, 2013), with the exception of positively marked (by expression of GFP) mutant clones. For these experiments, we recombined the *Vps16A[d32]* mutation onto an *FRT82B* chromosome, and also established a stock with the following genotype: *hsFlp[22]; QUAS-mCD8-GFP[5J]; ET49-QF, FRT82B, tub-QS[21]/TM6B, Tb* (Potter *et al.*, 2010). After crossing these two lines, we generated mosaic clones by heat shocking 0- to 4-h-old embryos in a 37°C water bath, similar to generation of negatively marked (by lack of GFP or dsRed expression) mutant clones described previously (Rusten *et al.*, 2007; Juhasz *et al.*, 2008). Climbing tests were carried out on cohorts of six 2-d-old adult flies, as described previously (Juhasz *et al.*, 2007; Takats *et al.*, 2013).

Molecular cloning

The genomic rescue construct for *Vps16A* was made by cloning a 10.5-kb *Asp*718-*Bgl*II fragment containing the *Vps16A* locus into Casper4. For tagged transgenes expressed by their endogenous promoters, we generated genCherry and gen3×FLAG cloning vectors. First, a fragment containing UAS sequences, the minimal Hsp70 promoter, and multiple cloning site of UAST was removed by *Sph*I-*Xba*I digestion and replaced with a PCR-amplified *Sph*I-*Nhe*I fragment in which *Sph*I, *Not*I, *Asc*I, *Xba*I, and *Acc*65I restriction sites are upstream of an mCherry coding sequence and an *Eco*RI site is downstream of the stop codon of mCherry. Two PCR-amplified genomic fragments (*Sph*I-*Nhe*I) were cloned into *Sph*I-*Xba*I–digested genCherry vector: a 2001–base pair fragment for full-length cathepsin D containing the promoter, two exons, and the intron, and lacking the stop codon; and a 1649–base pair fragment of the genomic region of Syx17 truncated after the first transmembrane domain. The gen3×FLAG vector was generated by replacing the *Acc*65I-*Eco*RI mCherry coding fragment of genCherry with 3×FLAG, using annealed synthetic oligos. A 1799–base pair fragment of the genomic region encoding full-length Syx17 lacking the stop codon and a 1706–base pair fragment encoding Syx17 truncated after the second transmembrane domain were cloned as *Not*I-*Acc*65I fragments into gen3×FLAG digested with *Not*I-*Acc*65I. N-terminally tagged Syx17 expressing UAS constructs was generated by cloning PCR-amplified Syx17 coding sequences into UAS-3×FLAG; and N-terminally HA-tagged Vps16A-, Car-, and Vamp7-expressing constructs were generated by cloning the PCR-amplified cDNA fragments encoding full-length proteins into UAS-3×HA.

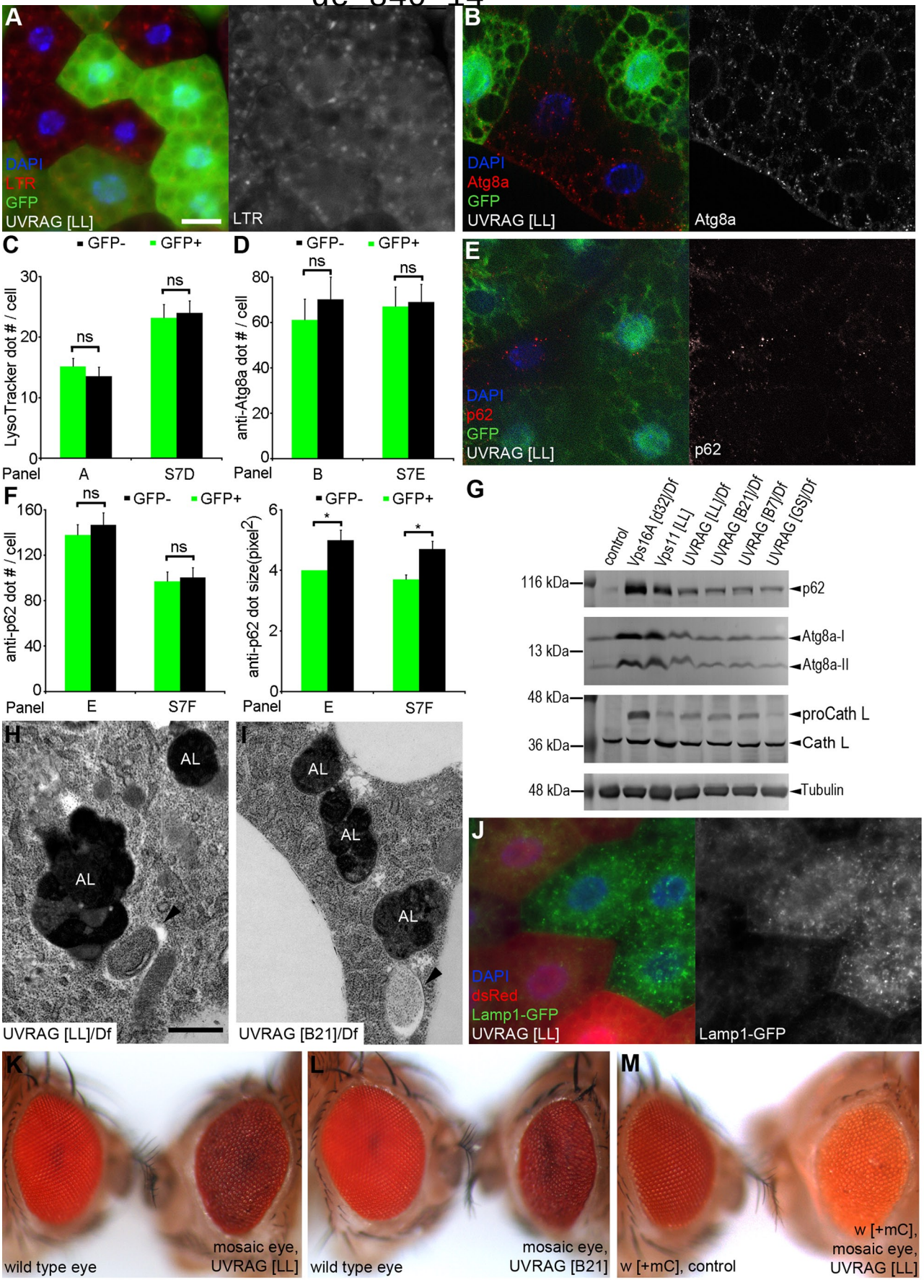
Cell culture and immunoprecipitation

Transfections and immunoprecipitations were carried out in D.mel-2 cells exactly as previously described (Takats *et al.*, 2013), using the plasmids MT-Gal4, UAS-Syx17(1-223)-FLAG (Takats *et al.*, 2013); UAS-Myc-Dor (Sevrioukov *et al.*, 1999); and N-terminally FLAG-tagged Syx17 and HA-tagged Vps16A, Car, and Vamp7 constructs described above. RNAi depletion of *car* was induced by adding 10 µg dsRNA to cultured cells in one well of a six-well plate 3 d before transfection with tagged Syx17 and Vamp7 plasmids. The dsRNA was synthesized by PCR amplification of the same region that is used in *car[12230R-1]* with specific primers containing a T7 promoter, and using the PCR fragment for in vitro transcription with the Megascript T7 kit (Life Technologies, Budapest, Hungary) followed by a clean-up reaction with the Megaclear kit (Life Technologies) and agarose gel electrophoresis to determine dsRNA integrity and quantity. Immunoprecipitations using guinea pig antisera against endogenous Syx17 (or GFP) were carried out from larval or adult fly lysates as previously described (Takats *et al.*, 2013).

Antibodies, immunolabeling, and Western blots

Indirect immunofluorescence labeling and Western blots were carried out as described (Nagy *et al.*, 2013; Takats *et al.*, 2013), using dissected fed or starved L3 larvae for fat body experiments and wandering L3 animals for eye disk experiments. The following antibodies were used: rabbit anti-Vps16A (IF [immunofluorescence]

dc_840_14


A
DAPI
LTR
GFP
UVRAG [LL]
LTR
B
DAPI
Atg8a
GFP
UVRAG [LL]
Atg8a
C
GFP-
GFP+
LysoTracker dot # / cell
ns
Panel
A
S7D
D
anti-Atg8a dot # / cell
Panel
B
S7E
E
DAPI
p62
GFP
UVRAG [LL]
p62
F
anti-p62 dot # / cell
anti-p62 dot size(pixel2)
Panel
E
S7F
G
control
Vps16A [d32]/Df
Vps11 [LL]
UVRAG [LL]/Df
UVRAG [B21]/Df
UVRAG [B7]/Df
UVRAG [GS]/Df
116 kDa
p62
13 kDa
Atg8a-I
Atg8a-II
48 kDa
proCath L
36 kDa
Cath L
48 kDa
Tubulin
H
AL
UVRAG [LL]/Df
I
UVRAG [B21]/Df
J
DAPI
dsRed
Lamp1-GFP
UVRAG [LL]
Lamp1-GFP
K
wild type eye
mosaic eye,
UVRAG [LL]
L
wild type eye
mosaic eye,
UVRAG [B21]
M
w [+mC], control
w [+mC],
mosaic eye,
UVRAG [LL]

dc_840_14

FIGURE 10: Null mutation of UVRAG has no effect on autophagosome formation and fusion, while it perturbs biosynthetic transport to lysosomes. (A) Starvation-induced punctate LTR staining in *UVRAG[LL]* mutant fat cells (marked by the lack of GFP) is similar to neighboring heterozygous (marked by expression of one copy of GFP) and homozygous (marked by two copies of GFP) control cells. (B) Atg8a-positive autophagosome numbers are similar in *UVRAG[LL]* mutant and control cells of starved larvae. (C) Quantification of data shown in (A) and Figure S7D; $n = 10$/genotype. (D) Quantification of data shown in (B) and Figure S7E; $n = 10$/genotype. (E) The autophagic cargo p62 is up-regulated in *UVRAG[LL]* mutant cells compared with surrounding control cells. (F) Quantification of data shown in (E) and Figure S7F; $n = 10$/genotype. (G) Western blots show that the levels of Atg8a-II are slightly higher in the lysates of different *UVRAG* mutant larvae than those seen in controls but are much lower than the levels seen in *Vps16A* or *Vps11* mutants. Similarly, p62 is up-regulated in *UVRAG* mutants relative to controls, but its levels do not reach those observed in *Vps16A* or *Vps11* mutants. Pro-cathepsin L accumulates in *UVRAG* mutants. (H and I) Ultrastructural analysis reveals a regular number of autophagosomes and autolysosomes in *UVRAG[LL]* (H) and *UVRAG[B21]* (I) mutant larvae in response to starvation. Note that the contents and the irregular shape of autolysosomes indicate that several autophagosomal fusion events have occurred, whereas all autolysosomes appear to contain homogenously dark material, suggesting defects in autolysosomal degradation. (J) Turnover of Lamp1-GFP (expressed in all cells) is perturbed in *UVRAG[LL]* mutant cells (marked by lack of dsRed expression), which accumulate high levels of this lysosomal reporter. (K and L) Formation of the bright red eye color observed in control flies is perturbed in animals with eyes composed of entirely *UVRAG[LL]* (K) or *UVRAG[B21]* (L) mutant tissue. (M) The dark orange eye color of flies expressing lower levels of the pigment transporter white (w) is much lighter in *UVRAG[LL]* mutant eyes. Scale bar in (A) = 20 μm for (A), (B), (E), and (J); scale bar in (H) = 1 μm for (H) and (I). Error bars denote SE in (C), (D), and (F); ns, not significant; *, $p < 0.05$.

1:300; WB [Western blot] 1:2000; Pulipparacharuvil *et al.*, 2005), rabbit anti-p62 (IF 1:2000; WB 1:5000; Pircs *et al.*, 2012), rabbit anti-Atg8a (IF: 1:500; Barth *et al.*, 2011), rabbit anti-Atg8a (WB 1:5000), rat anti-Atg8a (IF: 1:300; Takats *et al.*, 2013), mouse anti-tubulin (WB 1:1000; DSHB [Developmental Studies Hybridoma Bank, Iowa City, IA] AA4.3-s), mouse anti-FLAG M2 (WB 1:2000; Sigma-Aldrich, St. Louis, MO), mouse anti-Myc (WB 1:2000; Sigma-Aldrich), rabbit anti-HA (WB 1:2000, Sigma-Aldrich), rat anti-Syx17 (IF 1:300, WB 1:5000; Takats *et al.*, 2013), rabbit anti-Car (WB 1:1000; Akbar *et al.*, 2009), mouse anti-Notch (IF 1:50, DSHB C458.2H-c), rabbit anti-Boss (IF 1:1000; Sevrioukov *et al.*, 1999; Akbar *et al.*, 2009), rat anti-mCherry (IF 1:300), rat anti-GFP (WB 1:5000; Pircs *et al.*, 2012), chicken anti-GFP (IF 1:1500; Invitrogen, Carlsbad, CA), and rabbit anti-cathepsin L (WB 1:500; ab58991; Abcam, Cambridge, MA). Secondary antibodies were Alexa Fluor 488 goat anti-rabbit, Alexa Fluor 488 goat anti-chicken, Alexa Fluor 568 goat anti-rat, Alexa Fluor 647 goat anti-rabbit (all IF 1:1500; Invitrogen), and alkaline phosphatase–conjugated goat anti-rabbit, anti-rat and anti-mouse (both WB 1:5000; Millipore/Biocenter, Szeged, Hungary). Blots were developed using the NBT/BCIP colorimetric substrate (Sigma-Aldrich).

Microscopy and statistics

Images of dissected fat bodies were taken on an Axio Imager M2 equipped with Apotome2 and AxioCam Mrm (Zeiss, Jena, Germany), as before (Nagy *et al.*, 2013; Takats *et al.*, 2013). Autophagic structures were quantified from original, unmodified images in ImageJ (National Institutes of Health), and statistical significance was calculated with an appropriate test in SPSS Statistics (IBM, Armonk, NY), as described in detail previously (Nagy *et al.*, 2013; Takats *et al.*, 2013). Eyes of 2-d-old adults were photographed on a Lumar V12 stereomicroscope equipped with AxioCam ICc camera (Zeiss). Samples were processed for ultrastructural analysis as previously described (Erdi *et al.*, 2012; Takats *et al.*, 2013). Ultrathin sections from three individual larvae were evaluated per genotype.

ACKNOWLEDGMENTS

We thank Sarolta Pálfia and Zsófia Kováts for excellent technical assistance and public repositories and Sekyu Choi for providing fly stocks and reagents. This work was supported by the National Institutes of Health (NIH EY10199 to H.K.), the Hungarian Scientific Research Fund (OTKA K83509 to G.J.), and the Wellcome Trust (087518/Z/08/Z to G.J.).

REFERENCES

Akbar MA, Ray S, Kramer H (2009). The SM protein Car/Vps33A regulates SNARE-mediated trafficking to lysosomes and lysosome-related organelles. Mol Biol Cell 20, 1705–1714.

Akbar MA, Tracy C, Kahr WH, Kramer H (2011). The *full-of-bacteria* gene is required for phagosome maturation during immune defense in *Drosophila*. J Cell Biol 192, 383–390.

Balderhaar HJ, Ungermann C (2013). CORVET and HOPS tethering complexes—coordinators of endosome and lysosome fusion. J Cell Sci 126, 1307–1316.

Bankaitis VA, Johnson LM, Emr SD (1986). Isolation of yeast mutants defective in protein targeting to the vacuole. Proc Natl Acad Sci USA 83, 9075–9079.

Barth JM, Szabad J, Hafen E, Kohler K (2011). Autophagy in *Drosophila* ovaries is induced by starvation and is required for oogenesis. Cell Death Differ 18, 915–924.

Bartlett BJ *et al.* (2011). p62, Ref(2)P and ubiquitinated proteins are conserved markers of neuronal aging, aggregate formation and progressive autophagic defects. Autophagy 7, 572–583.

Bowers K, Stevens TH (2005). Protein transport from the late Golgi to the vacuole in the yeast *Saccharomyces cerevisiae*. Biochim Biophys Acta 1744, 438–454.

Csikos G, Lippai M, Lukacsovich T, Juhasz G, Henn L, Erdelyi M, Maroy P, Sass M (2009). A novel role for the Drosophila epsin (lqf): involvement in autophagy. Autophagy 5, 636–648.

Darsow T, Rieder SE, Emr SD (1997). A multispecificity syntaxin homologue, Vam3p, essential for autophagic and biosynthetic protein transport to the vacuole. J Cell Biol 138, 517–529.

Dunn JG, Foo CK, Belletier NG, Gavis ER, Weissman JS (2013). Ribosome profiling reveals pervasive and regulated stop codon readthrough in *Drosophila melanogaster*. Elife 2, e01179.

Erdi B, Nagy P, Zvara A, Varga A, Pircs K, Menesi D, Puskas LG, Juhasz G (2012). Loss of the starvation-induced gene Rack1 leads to glycogen deficiency and impaired autophagic responses in Drosophila. Autophagy 8, 1124–1135.

Farre JC, Mathewson RD, Manjithaya R, Subramani S (2010). Roles of *Pichia pastoris* Uvrag in vacuolar protein sorting and the phosphatidylinositol 3-kinase complex in phagophore elongation in autophagy pathways. Autophagy 6, 86–99.

Filimonenko M, Stuffers S, Raiborg C, Yamamoto A, Malerod L, Fisher EM, Isaacs A, Brech A, Stenmark H, Simonsen A (2007). Functional multivesicular bodies are required for autophagic clearance of protein aggregates associated with neurodegenerative disease. J Cell Biol 179, 485–500.

Ganley IG, Wong PM, Gammoh N, Jiang X (2011). Distinct autophagosomal-lysosomal fusion mechanism revealed by thapsigargin-induced autophagy arrest. Mol Cell 42, 731–743.

Hong W (2005). SNAREs and traffic. Biochim Biophys Acta 1744, 493–517.

Itakura E, Kishi C, Inoue K, Mizushima N (2008). Beclin 1 forms two distinct phosphatidylinositol 3-kinase complexes with mammalian Atg14 and UVRAG. Mol Biol Cell 19, 5360–5372.

dc_840_14

Itakura E, Kishi-Itakura C, Mizushima N (2012). The hairpin-type tail-anchored SNARE syntaxin 17 targets to autophagosomes for fusion with endosomes/lysosomes. Cell 151, 1256–1269.

Jiang P, Nishimura T, Sakamaki Y, Itakura E, Hatta T, Natsume T, Mizushima N (2014). The HOPS complex mediates autophagosome–lysosome fusion through interaction with syntaxin 17. Mol Biol Cell 25, 1327–1337.

Juhasz G, Erdi B, Sass M, Neufeld TP (2007). Atg7-dependent autophagy promotes neuronal health, stress tolerance, and longevity but is dispensable for metamorphosis in *Drosophila*. Genes Dev 21, 3061–3066.

Juhasz G, Hill JH, Yan Y, Sass M, Baehrecke EH, Backer JM, Neufeld TP (2008). The class III PI(3)K Vps34 promotes autophagy and endocytosis but not TOR signaling in *Drosophila*. J Cell Biol 181, 655–666.

Kihara A, Noda T, Ishihara N, Ohsumi Y (2001). Two distinct Vps34 phosphatidylinositol 3-kinase complexes function in autophagy and carboxypeptidase Y sorting in *Saccharomyces cerevisiae*. J Cell Biol 152, 519–530.

Kimura S, Noda T, Yoshimori T (2007). Dissection of the autophagosome maturation process by a novel reporter protein, tandem fluorescent-tagged LC3. Autophagy 3, 452–460.

Knaevelsrud H, Ahlquist T, Merok MA, Nesbakken A, Stenmark H, Lothe RA, Simonsen A (2010). UVRAG mutations associated with microsatellite unstable colon cancer do not affect autophagy. Autophagy 6, 863–870.

Lee G, Liang C, Park G, Jang C, Jung JU, Chung J (2011). UVRAG is required for organ rotation by regulating Notch endocytosis in *Drosophila*. Dev Biol 356, 588–597.

Liang C *et al*. (2008). Beclin1-binding UVRAG targets the class C Vps complex to coordinate autophagosome maturation and endocytic trafficking. Nat Cell Biol 10, 776–787.

Lindmo K, Simonsen A, Brech A, Finley K, Rusten TE, Stenmark H (2006). A dual function for Deep orange in programmed autophagy in the *Drosophila melanogaster* fat body. Exp Cell Res 312, 2018–2027.

Lippai M, Csikos G, Maroy P, Lukacsovich T, Juhasz G, Sass M (2008). SNF4Aγ, the Drosophila AMPK γ subunit is required for regulation of developmental and stress-induced autophagy. Autophagy 4, 476–486.

Lloyd V, Ramaswami M, Kramer H (1998). Not just pretty eyes: *Drosophila* eye-colour mutations and lysosomal delivery. Trends Cell Biol 8, 257–259.

Lobingier BT, Merz AJ (2012). Sec1/Munc18 protein Vps33 binds to SNARE domains and the quaternary SNARE complex. Mol Biol Cell 23, 4611–4622.

Matsunaga K *et al*. (2009). Two Beclin 1-binding proteins, Atg14L and Rubicon, reciprocally regulate autophagy at different stages. Nat Cell Biol 11, 385–396.

Mizushima N, Levine B, Cuervo AM, Klionsky DJ (2008). Autophagy fights disease through cellular self-digestion. Nature 451, 1069–1075.

Nagy P, Varga A, Pircs K, Hegedus K, Juhasz G (2013). Myc-driven overgrowth requires unfolded protein response-mediated induction of autophagy and antioxidant responses in *Drosophila melanogaster*. PLoS Genetics 9, e1003664.

Peng C *et al*. (2012). Ablation of vacuole protein sorting 18 (*Vps18*) gene leads to neurodegeneration and impaired neuronal migration by disrupting multiple vesicle transport pathways to lysosomes. J Biol Chem 287, 32861–32873.

Pircs K, Nagy P, Varga A, Venkei Z, Erdi B, Hegedus K, Juhasz G (2012). Advantages and limitations of different p62-based assays for estimating autophagic activity in *Drosophila*. PLoS One 7, e44214.

Potter CJ, Tasic B, Russler EV, Liang L, Luo L (2010). The Q system: a repressible binary system for transgene expression, lineage tracing, and mosaic analysis. Cell 141, 536–548.

Pulipparacharuvil S, Akbar MA, Ray S, Sevrioukov EA, Haberman AS, Rohrer J, Kramer H (2005). *Drosophila* Vps16A is required for trafficking to lysosomes and biogenesis of pigment granules. J Cell Sci 118, 3663–3673.

Rieder SE, Emr SD (1997). A novel RING finger protein complex essential for a late step in protein transport to the yeast vacuole. Mol Biol Cell 8, 2307–2327.

Rothman JH, Stevens TH (1986). Protein sorting in yeast: mutants defective in vacuole biogenesis mislocalize vacuolar proteins into the late secretory pathway. Cell 47, 1041–1051.

Rusten TE, Lindmo K, Juhasz G, Sass M, Seglen PO, Brech A, Stenmark H (2004). Programmed autophagy in the *Drosophila* fat body is induced by ecdysone through regulation of the PI3K pathway. Dev Cell 7, 179–192.

Rusten TE *et al*. (2007). ESCRTs and Fab1 regulate distinct steps of autophagy. Curr Biol 17, 1817–1825.

Sato TK, Rehling P, Peterson MR, Emr SD (2000). Class C Vps protein complex regulates vacuolar SNARE pairing and is required for vesicle docking/fusion. Mol Cell 6, 661–671.

Schuldiner O, Berdnik D, Levy JM, Wu JS, Luginbuhl D, Gontang AC, Luo L (2008). piggyBac-based mosaic screen identifies a postmitotic function for cohesin in regulating developmental axon pruning. Dev Cell 14, 227–238.

Scott RC, Schuldiner O, Neufeld TP (2004). Role and regulation of starvation-induced autophagy in the *Drosophila* fat body. Dev Cell 7, 167–178.

Sevrioukov EA, He JP, Moghrabi N, Sunio A, Kramer H (1999). A role for the *deep orange* and *carnation* eye color genes in lysosomal delivery in *Drosophila*. Mol Cell 4, 479–486.

Solinger JA, Spang A (2013). Tethering complexes in the endocytic pathway: CORVET and HOPS. FEBS J 280, 2743–2757.

Starai VJ, Hickey CM, Wickner W (2008). HOPS proofreads the *trans*-SNARE complex for yeast vacuole fusion. Mol Biol Cell 19, 2500–2508.

Stenmark H (2009). Rab GTPases as coordinators of vesicle traffic. Nat Rev Mol Cell Biol 10, 513–525.

Stroupe C, Collins KM, Fratti RA, Wickner W (2006). Purification of active HOPS complex reveals its affinities for phosphoinositides and the SNARE Vam7p. EMBO J 25, 1579–1589.

Swetha MG, Sriram V, Krishnan KS, Oorschot VM, ten Brink C, Klumperman J, Mayor S (2011). Lysosomal membrane protein composition, acidic pH and sterol content are regulated via a light-dependent pathway in metazoan cells. Traffic 12, 1037–1055.

Takats S, Nagy P, Varga A, Pircs K, Karpati M, Varga K, Kovacs AL, Hegedus K, Juhasz G (2013). Autophagosomal Syntaxin17-dependent lysosomal degradation maintains neuronal function in *Drosophila*. J Cell Biol 201, 531–539.

Wakimoto BT, Hearn MG (1990). The effects of chromosome rearrangements on the expression of heterochromatic genes in chromosome 2L of *Drosophila melanogaster*. Genetics 125, 141–154.

Wang CW, Stromhaug PE, Shima J, Klionsky DJ (2002). The Ccz1-Mon1 protein complex is required for the late step of multiple vacuole delivery pathways. J Biol Chem 277, 47917–47927.